



INTERNATIONAL SERIES IN PURE AND APPLIED PHYSICS

LEONARD I. SCHIFF, *Consulting Editor*

---

**MICROWAVE SPECTROSCOPY**

# INTERNATIONAL SERIES IN PURE AND APPLIED PHYSICS

LEONARD I. SCHIFF, *Consulting Editor*

---

- Becker* Introduction to Theoretical Mechanics  
*Clark* Applied X-rays  
*Edwards* Analytic and Vector Mechanics  
*Finkelburg* Atomic Physics  
*Green* Nuclear Physics  
*Gurney* Introduction to Statistical Mechanics  
*Hall* Introduction to Electron Microscopy  
*Hardy and Perrin* The Principles of Optics  
*Harnwell* Electricity and Electromagnetism  
*Harnwell and Livingood* Experimental Atomic Physics  
*Harnwell and Stephens* Atomic Physics  
*Houston* Principles of Mathematical Physics  
*Houston* Principles of Quantum Mechanics  
*Hughes and DuBridge* Photoelectric Phenomena  
*Hund* High-frequency Measurements  
*Kemble* The Fundamental Principles of Quantum Mechanics  
*Kennard* Kinetic Theory of Gases  
*Marshak* Meson Physics  
*Morse* Vibration and Sound  
*Morse and Feshbach* Methods of Theoretical Physics  
*Muskat* Physical Principles of Oil Production  
*Read* Dislocations in Crystals  
*Richtmyer, Kennard, and Lauritsen* Introduction to Modern Physics  
*Schiff* Quantum Mechanics  
*Seitz* The Modern Theory of Solids  
*Slater* Introduction to Chemical Physics  
*Slater* Microwave Transmission  
*Slater* Quantum Theory of Matter  
*Slater and Frank* Electromagnetism  
*Slater and Frank* Introduction to Theoretical Physics  
*Slater and Frank* Mechanics  
*Smythe* Static and Dynamic Electricity  
*Squire* Low Temperature Physics  
*Stratton* Electromagnetic Theory  
*Thorndike* Mesons: A Summary of Experimental Facts  
*Townes and Schawlow* Microwave Spectroscopy  
*White* Introduction to Atomic Spectra
- 

The late F. K. Richtmyer was Consulting Editor of the series from its inception in 1929 to his death in 1939. Lee A. DuBridge was Consulting Editor from 1939 to 1946; and G. P. Harnwell from 1947 to 1954.

# MICROWAVE SPECTROSCOPY

**C. H. TOWNES**

*Professor of Physics  
Columbia University*

**A. L. SCHAWLOW**

*Bell Telephone Laboratories*

525-55  
92-2-51  
McGRAW-HILL BOOK COMPANY, INC.

New York      Toronto      London

1955



## MICROWAVE SPECTROSCOPY

Copyright © 1955 by the McGraw-Hill Book Company, Inc. Printed in the United States of America. All rights reserved. This book, or parts thereof, may not be reproduced in any form without permission of the publishers.

*Library of Congress Catalog Card Number 54-9703*

CHECKED

*2*

*catalogued*

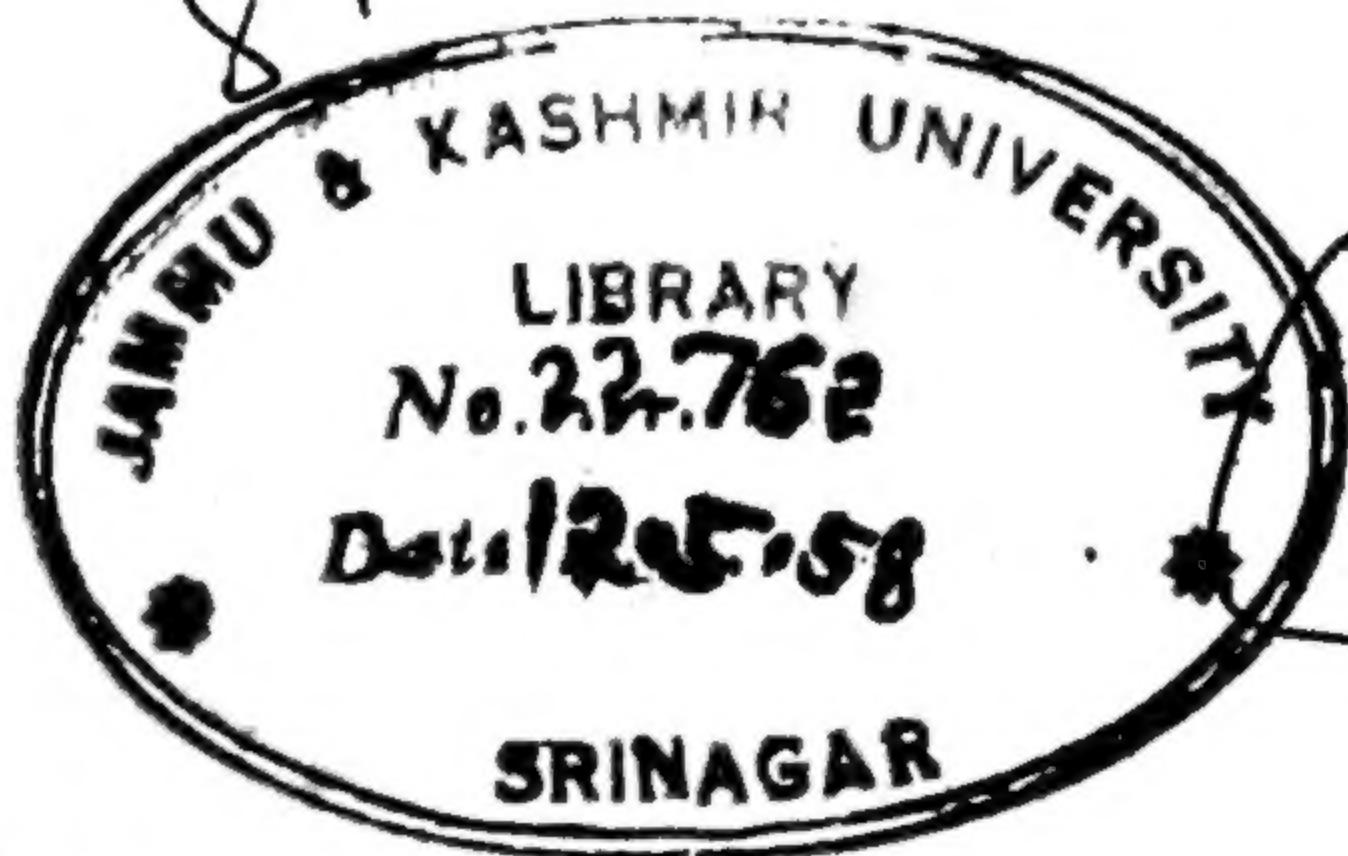


*537.12*

*T66 L N*

CHECK

*8A-282*



*70*

*103*



## PREFACE

This volume is concerned primarily with a relatively new field, the microwave spectroscopy of gases. The origins of microwave spectroscopy might be said to lie in the early high-frequency measurements of dielectric constants, or much more directly in the 1933 experiment of Cleeton and Williams on absorption of centimeter radiation by ammonia gas. However, a generally useful and accurate spectroscopy in the microwave region has come only after development of microwave oscillators and techniques and after demonstration in 1946 of the high resolution obtainable with low-pressure gases. Since 1946 microwave spectroscopy of gases has developed very rapidly and yielded a wide range of useful information in fields as far separated as nuclear physics, molecular structure, chemical kinetics, quantum electrodynamics, and astronomy. The purpose of this book is to present a systematic and fairly complete account of the large amount of theory, experimental data, and experimental know-how which has been developed, and to make this information more available to students, prospective research workers, and those interested in the many practical problems to which microwave spectroscopy may be applied.

The furious activity in microwave spectroscopy has made a book in this field both very desirable, because of the plethora of research work and results which need digestion and coordination, and at the same time very difficult because of the rapid development of ideas and outmoding of techniques. It is only now that microwave spectroscopy appears to have matured to the point where one can attempt a book of some perspective and lasting value.

Most microwave spectra are associated with molecules, although some important atomic microwave spectra occur and are treated here. Molecular spectra have previously been well described from the point of view of infrared spectroscopy; but the different frequency range, higher resolution, and greater accuracy of microwave spectroscopy makes available for study rather different types of phenomena such as hyperfine structure, pressure broadening, and Stark and Zeeman effects. The discussion is particularly full for those phases of the theory of molecular spectra which older types of spectroscopy have not been able to test adequately or which have been developed by persons interested in micro-



wave spectra. In addition, some attention is directed toward obtaining information about nuclear and molecular properties from the interpretation of molecular spectra.

Although a fairly complete account of microwave techniques is included, only those parts which are especially useful or somewhat peculiar to microwave spectroscopy are discussed in detail. The reader can obtain further elaboration on standard microwave techniques from the large number of excellent books on microwaves which have been published in the last few years. An attempt has been made to present not only the basic theory and properties of various types of microwave spectrometers, but also some details of construction and specific operating characteristics which would be useful to the person faced with the problem of making and operating this type of instrument.

This volume is not primarily intended as a text, but rather as a readable reference which can be used both by students interested in one of the many aspects of microwave spectroscopy, and by those interested in research in this field. The authors have endeavored to discuss the material critically, systematically, and in the simplest way consistent with some completeness in a single volume. It is hoped that the simplicity of wording and mathematics (no group theory, as such, is used) will allow most of the discussion to be profitably read by those with a very elementary knowledge of quantum mechanics and atomic physics.

Considerable effort has been directed at making this volume valuable as a reference to a variety of users. Although the treatment is a continuously developed one, attention has been directed at making each chapter and section as independent of other sections as is practical. For example, certain expressions and definitions of symbols are often repeated in order to reduce the need for reference to other parts of the book. Appendixes give most of the tables and information needed in doing research and in interpreting microwave spectra. They also contain extensive data on nuclear and molecular constants, including essentially all those determined by microwave techniques. A complete list of publications concerning microwave spectroscopy and a subject index are included. The tables and appendixes include material published up to January 1, 1955.

Microwave spectra of solids and other closely related types of spectroscopy are not discussed because it appeared that justice to such a wide variety of fields could hardly be done in one volume. However, much of the material will be of use to those interested in types of microwave and radio-frequency spectroscopy not specifically discussed here.

The authors are grateful to their many colleagues in microwave physics who have provided information, criticism, and encouragement for this volume. These include the following, who have given helpful comments on certain sections of the manuscript:



P. W. Anderson, T. S. Benedict, R. Beringer, D. G. Burkhard, D. K. Coles, B. P. Dailey, H. M. Foley, R. A. Frosch, R. H. Hughes, C. K. Jen, C. M. Johnson, W. C. King, D. R. Lide, H. Lyons, A. H. Nethercot, R. Novick, W. V. Smith, M. W. P. Strandberg, and E. B. Wilson, Jr. In addition, they wish to thank the many students and members of the Columbia Radiation Laboratory who have uncovered errors and provided valuable discussion.

The appendixes and tables have profited from the cooperation and assistance of a number of others whose help it is a pleasure to acknowledge. Inclusion of the extensive table in Appendix IV was made both possible and convenient through the efforts of T. E. Turner and G. Reitwiesner. J. A. Klein and G. C. Dousmanis did a major part of the work involved in compiling the bibliography and Appendix VI, respectively. L. C. Aamodt, J. F. Lotspeich, M. McDermott, and B. Herzog performed many of the computations necessary for the appendixes. J. Kraitchman assisted with Appendix III, in addition to checking many of the formulas and derivations.

One of the authors (C.H.T.) would like to thank Columbia University for grant of the E. K. Adams Fellowship which assisted in preparation of this work. The other (A.L.S.) would also like to thank this University for its hospitality during the time when much of the book was written.

CHARLES H. TOWNES  
ARTHUR L. SCHAWLOW





# CONTENTS

PREFACE . . . . .	v
LIST OF SYMBOLS . . . . .	xv
INTRODUCTION . . . . .	1
CHAPTER 1. ROTATIONAL SPECTRA OF DIATOMIC MOLECULES . . . . .	3
1-1. The Rigid Rotor . . . . .	3
1-2. <del>Energy Levels of the Diatomic Molecule</del> . . . . .	5
1-3. Mass Measurements . . . . .	14
1-4. Absorption Intensities and Selection Rules . . . . .	18
CHAPTER 2. LINEAR POLYATOMIC MOLECULES . . . . .	25
2-1. Pure Rotational Spectra—General Considerations . . . . .	25
2-2. <i>l</i> -Type Doubling . . . . .	31
2-3. Perturbations between Vibrational States—Fermi Reso- nance . . . . .	35
2-4. Moments of Inertia and Internuclear Distances . . . . .	40
2-5. Determination of Nuclear Masses . . . . .	42
CHAPTER 3. SYMMETRIC-TOP MOLECULES . . . . .	48
3-1. Introduction and General Features of Rotational Spectra . . . . .	48
3-2. Symmetric-top Wave Functions . . . . .	60
3-3. Symmetry and Inversion . . . . .	62
3-4. Effects of Nuclear Spins and Statistics . . . . .	69
3-5. Intensities of Symmetric-top Transitions . . . . .	73
3-6. Centrifugal Stretching in Symmetric Tops . . . . .	77
3-7. <u>Rotation-Vibration Interactions and <i>l</i>-Type Doubling in</u> Symmetric Tops . . . . .	79
3-8. Dipole Moment Due to Degenerate Vibrations . . . . .	82
CHAPTER 4. ASYMMETRIC-TOP MOLECULES . . . . .	83
4-1. Energy Levels of Asymmetric and Slightly Asymmetric Rotors . . . . .	83
4-2. Symmetry Considerations and Intensities . . . . .	92
4-3. Centrifugal Distortion . . . . .	105
4-4. <u>Structures of Asymmetric Rotors</u> . . . . .	109
CHAPTER 5. ATOMIC SPECTRA . . . . .	115
5-1. The Hydrogen Atom . . . . .	115
5-2. Atoms with More Than One Electron . . . . .	118
5-3. Fine Structure, Electron Spin, and the Vector Model . . . . .	120

5-4.	Atoms with More Than One Valence Electron . . . . .	123
5-5.	Selection Rules and Intensities . . . . .	124
5-6.	Fine Structure—More Exact Treatment . . . . .	126
5-7.	Hyperfine Structure . . . . .	130
5-8.	Penetrating Orbits . . . . .	143
5-9.	Zeeman Effects for Atoms . . . . .	143
5-10.	Microwave Studies of Atomic Hyperfine Structure . . . . .	145
5-11.	Microwave Spectra from Astronomical Sources . . . . .	146
CHAPTER 6.	QUADRUPOLE HYPERFINE STRUCTURE IN MOLECULES . . . . .	149
6-1.	Introduction . . . . .	149
6-2.	Quadrupole Hyperfine Structure in Linear Molecules . . . . .	150
6-3.	Quadrupole Hyperfine Structure in Symmetric Tops . . . . .	154
6-4.	Second-order Quadrupole Effects . . . . .	155
6-5.	Asymmetric Tops . . . . .	159
6-6.	Hyperfine Structure from Two or More Nuclei in the Same Molecule . . . . .	164
CHAPTER 7.	MOLECULES WITH ELECTRONIC ANGULAR MOMENTUM . . . . .	174
7-1.	Introduction . . . . .	174
7-2.	Hund's Coupling Cases . . . . .	177
7-3.	Rotational Energies . . . . .	180
7-4.	Spin Uncoupling . . . . .	185
7-5.	$\Lambda$ -Type Doubling . . . . .	188
7-6.	Nonlinear Molecules . . . . .	192
CHAPTER 8.	MAGNETIC HYPERFINE STRUCTURE IN MOLECULAR SPECTRA . . . . .	194
8-1.	Introduction . . . . .	194
8-2.	Coupling Schemes for Magnetic Hyperfine Structure . . . . .	196
8-3.	Examples of Magnetic Hyperfine Structure in Molecules with Electronic Angular Momentum . . . . .	199
8-4.	Nonlinear Molecules . . . . .	200
8-5.	Spin-spin Interaction between Nuclei . . . . .	202
8-6.	Effect of Hyperfine Structure on Doubling—Hyperfine Doubling . . . . .	203
8-7.	Electronic Angular Momentum in $^1\Sigma$ Molecules and Its Contributions to Molecular Energy. . . . .	207
8-8.	Effect of Electronic Motion on Rotational Energy . . . . .	212
8-9.	Magnetic Hyperfine Interaction ( $\mathbf{I} \cdot \mathbf{J}$ ) in $^1\Sigma$ Molecules . . . . .	215
8-10.	Magnetic Hyperfine Structure of Nonlinear Molecules in $^1\Sigma$ States . . . . .	219
CHAPTER 9.	INTERPRETATION OF HYPERFINE COUPLING CONSTANTS IN TERMS OF MOLECULAR STRUCTURE AND NUCLEAR MOMENTS . . . . .	225
9-1.	Introductory Remarks on Quadrupole Coupling . . . . .	225
9-2.	Quadrupole Coupling in Atoms . . . . .	226
9-3.	Quadrupole Coupling in Molecules—General Considera- tions . . . . .	228
9-4.	Procedure for Calculating $q$ in a Molecule . . . . .	234
9-5.	Quadrupole Coupling in Asymmetric Molecules . . . . .	241
9-6.	Interpretation of Magnetic Hyperfine Coupling Constants . . . . .	245



CHAPTER 10.	STARK EFFECTS IN MOLECULAR SPECTRA . . . . .	248
10-1.	Introduction . . . . .	248
10-2.	Quantum-mechanical Calculation of Stark Energy for Static Fields . . . . .	250
10-3.	Relative Intensities of Stark Components and Identification of Transitions from Their Stark Patterns . . . . .	255
10-4.	Stark Effect When Hyperfine Structure Is Present . . . . .	258
10-5.	Determination of Molecular Dipole Moments. . . . .	264
10-6.	Forbidden Lines and Change of Intensity Due to Stark Effect . . . . .	269
10-7.	Polarization of Molecules by Electric Fields . . . . .	270
10-8.	Stark Effects in Rapidly Varying Fields—Nonresonant Case . . . . .	273
10-9.	Stark Effects in Rapidly Varying Fields—Resonant Modulation . . . . .	279
CHAPTER 11.	ZEEMAN EFFECTS IN MOLECULAR SPECTRA. . . . .	284
11-1.	Introduction . . . . .	284
11-2.	Zeeman Effect in Weak Fields for Molecules Having Electronic Angular Momentum . . . . .	284
11-3.	Characteristics of Zeeman Splitting of Spectral Lines . . . . .	286
11-4.	Intermediate Coupling and Intermediate Fields . . . . .	289
11-5.	Zeeman Effect with Hyperfine Structure . . . . .	289
11-6.	Zeeman Effects in Ordinary Molecules ( $^1\Sigma$ States) . . . . .	290
11-7.	Combined Zeeman-Stark Effects . . . . .	296
11-8.	Transitions between Zeeman Components . . . . .	296
CHAPTER 12.	THE AMMONIA SPECTRUM AND HINDERED MOTIONS . . . . .	300
12-1.	Introduction . . . . .	300
12-2.	Inversion Frequency of $\text{NH}_3$ . . . . .	302
12-3.	Inversion of Other Symmetric Hydrides . . . . .	307
12-4.	Fine Structure of the Ammonia Inversion Spectrum—Rotation-Vibration Interactions. . . . .	307
12-5.	Asymmetric Forms of Ammonia . . . . .	314
12-6.	Hindered Torsional Motions in Symmetric Rotors . . . . .	315
12-7.	Heights of Hindering Barriers . . . . .	322
12-8.	Hindered Torsional Motions in Asymmetric Rotors . . . . .	324
12-9.	Selection Rules . . . . .	331
12-10.	Examples of Hindered Torsional Motion in Asymmetric Rotors . . . . .	333
CHAPTER 13.	SHAPES AND WIDTHS OF SPECTRAL LINES . . . . .	336
13-1.	Natural Line Breadth . . . . .	336
13-2.	Doppler Effect. . . . .	337
13-3.	Pressure Broadening . . . . .	338
13-4.	Absolute or Integrated Line Intensity . . . . .	343
13-5.	Comparison of the Van Vleck—Weisskopf Line Shape with Experiment . . . . .	344
13-6.	Pressure Broadening and Intermolecular Forces . . . . .	347
13-7.	Comparison of Methods of Treating Pressure Broadening. . . . .	348
13-8.	Impact Theory—Anderson's Treatment . . . . .	355
13-9.	Comparison of Theories with Experiment . . . . .	361

13-10.	Self-broadening of Linear Molecules . . . . .	366
13-11.	Oxygen Line Breadths . . . . .	368
13-12.	Temperature Dependence of Line Widths . . . . .	368
13-13.	Effect of Temperature on Intensities . . . . .	369
13-14.	High Pressures . . . . .	370
13-15.	Saturation Effects. . . . .	371
13-16.	Broadening by Collisions with Walls . . . . .	374
13-17.	Microwave Absorption in Nonpolar Gases. . . . .	375
CHAPTER 14.	MICROWAVE CIRCUIT ELEMENTS AND TECHNIQUES . . . . .	376
14-1.	Introduction. Electromagnetic Fields and Waves . . . . .	376
14-2.	Waveguides . . . . .	379
14-3.	Attenuation . . . . .	383
14-4.	Reflections in Waveguides . . . . .	386
14-5.	Cavity Resonators . . . . .	390
14-6.	Coupling of Cavities to Waveguide . . . . .	392
14-7.	Directional Couplers . . . . .	394
14-8.	Attenuators . . . . .	397
14-9.	Joints in Waveguide Systems . . . . .	397
14-10.	Waveguide Windows . . . . .	398
14-11.	Plungers . . . . .	399
14-12.	Other Types of Guided Waves . . . . .	399
14-13.	Microwave Applications of Ferrites . . . . .	400
14-14.	Microwave Generators . . . . .	401
14-15.	Klystrons . . . . .	402
14-16.	Magnetrons . . . . .	405
14-17.	Traveling-wave and Backward-wave Tubes . . . . .	405
14-18.	Detectors . . . . .	407
CHAPTER 15.	MICROWAVE SPECTROGRAPHS . . . . .	411
15-1.	General Principles and Ultimate Sensitivity . . . . .	411
15-2.	Source Modulation . . . . .	416
15-3.	Stark Modulation . . . . .	418
15-4.	Modulation-frequency Signal Amplifiers . . . . .	420
15-5.	Zeeman Modulation Spectrographs . . . . .	424
15-6.	Choice of Modulation Frequency for Spectrographs . . . . .	425
15-7.	Superheterodyne Detection . . . . .	425
15-8.	Bridge Spectrographs . . . . .	425
15-9.	High-resolution Spectrometers . . . . .	427
15-10.	Some High-resolution Spectrometers . . . . .	428
15-11.	Cavity Spectrographs . . . . .	435
15-12.	Large Untuned Cavity . . . . .	439
15-13.	Spectrographs for Measurements of Zeeman Effect . . . . .	441
15-14.	Spectrometers for High and Low Temperatures . . . . .	443
15-15.	Spectrographs for Intensity and Line-Shape Measure- ments . . . . .	445
15-16.	Gas Handling for Microwave Spectrographs . . . . .	446
15-17.	Spectrometers for Free Radicals . . . . .	447
15-18.	Microwave Radiometers . . . . .	448
CHAPTER 16.	MILLIMETER WAVES . . . . .	451
16-1.	Introduction . . . . .	451
16-2.	Spark Oscillators for Millimeter Waves . . . . .	451

# CONTENTS

xiii

16-3.	Vacuum-tube Generators . . . . .	452
16-4.	Harmonics from Vacuum Tubes . . . . .	454
16-5.	Detection of Millimeter Waves . . . . .	455
16-6.	Semi-conducting Crystal Harmonic Generators . . . . .	458
16-7.	Propagation of Millimeter Waves . . . . .	462
16-8.	Frequency Measurement . . . . .	463
16-9.	Absorption Spectrographs for the Millimeter Region. . . . .	464
CHAPTER 17.	FREQUENCY MEASUREMENT AND CONTROL . . . . .	466
17-1.	Wavemeters . . . . .	466
17-2.	Quartz-crystal-controlled Frequency Standards . . . . .	468
17-3.	Measurement of Frequency Differences . . . . .	473
17-4.	Frequency Stabilization of Microwave Oscillators . . . . .	474
17-5.	Control of Frequency by a Resonant Cavity . . . . .	475
17-6.	Stabilization of Microwave Oscillators by Absorption Lines . . . . .	477
17-7.	The Molecular-beam Maser . . . . .	482
17-8.	Realization of Atomic Frequency and Time Standards . . . . .	483
CHAPTER 18.	THE USE OF MICROWAVE SPECTROSCOPY FOR CHEMICAL ANAL- YSIS . . . . .	486
18-1.	Microwave Spectroscopy for Analysis . . . . .	486
18-2.	Qualitative Analysis . . . . .	488
18-3.	Quantitative Analysis . . . . .	492
18-4.	Special Equipment and Techniques for Spectroscopic Analysis . . . . .	497
APPENDIX	I. Intensities of Hyperfine Structure Components and Energies Due to Nuclear Quadrupole Interactions . . . . .	499
	II. Second-order Energies Due to Nuclear Quadrupole Interac- tions in Linear Molecules and Symmetric Tops. . . . .	517
	III. Coefficients for Energy Levels of a Slightly Asymmetric Top. . . . .	522
	IV. Energy Levels of a Rigid Rotor . . . . .	527
	V. Transition Strengths for Rotational Transitions . . . . .	557
	VI. Molecular Constants Involved in Microwave Spectra . . . . .	613
	VII. Properties of the Stable Nuclei (Abundance, Mass, and Mo- ments) . . . . .	643
BIBLIOGRAPHY	. . . . .	649
AUTHOR INDEX	. . . . .	683
SUBJECT INDEX	. . . . .	689
FUNDAMENTAL CONSTANTS AND CONVERSION FACTORS	. . . . . Inside back cover	





## LIST OF SYMBOLS

### *English letters*

- $a$  magnetic hyperfine-structure interval factor
- $a_0$   $a_0 = h^2/4\pi^2\mu e^2$  = radius of first Bohr orbit for hydrogen
- $A$  largest rotational constant of an asymmetric rotor
- $\mathfrak{A}$  dyadic (tensor) connecting angular momentum and magnetic hyperfine structure
- $b$  impact parameter, distance of closest approach of molecules
- $B$  rotational constant; intermediate rotational constant (usually in cycles/sec.)
- $B_0$  rotational constant in ground vibrational state
- $B_e$  rotational constant in absence of zero-point vibrations
- $B$  magnetic induction
- $c$  velocity of light
- $C$  smallest rotational constant of an asymmetric rotor
- $C$   $C = F(F + 1) - I(I + 1) - J(J + 1)$
- $D$  dissociation energy
- $D_0, D_J, D_{JK}$  centrifugal distortion constants
- $D$  spectroscopic symbol for state with  $l = 2$
- $D$  electric displacement
- $e$  electron charge or, in some cases, the proton charge
- $e$  subscript indicating equilibrium distance or conditions
- $E$  electric field intensity
- $E$  electric field
- $f$  fraction of molecules in state of interest
- $f_v$  fraction of molecules in vibrational state of interest
- $F$  quantum number for total angular momentum including nuclear spin
- $g$   $g$  factor = magnetic moment (in Bohr magnetons or sometimes in nuclear magnetons) divided by angular momentum (in units  $h/2\pi$ ). This is negative for electron spin or orbital motion
- $g_I$  nuclear  $g$  factor = nuclear magnetic moment (in nuclear magnetons) divided by angular momentum (in units  $h/2\pi$ )
- $h$  Planck's constant

$\hbar$	$\hbar = h/2\pi$ , where $h$ is Planck's constant
<b>H</b>	magnetic field intensity
$H$	Hamiltonian
$i$	electric current
$I$	moment of inertia of molecule
$I$	spin of nucleus in units of $\hbar/2\pi$
$J$	rotational quantum number
<b>J</b>	total angular momentum excluding nuclear spin
$k$	Boltzmann constant
$K$	quantum number of component of angular momentum along molecular axis
$l$	angular-momentum quantum number for polyatomic molecule with excited degenerate vibration
$l$	electronic orbital angular-momentum quantum number for a single electron
<b>L</b>	electronic orbital angular momentum of an entire atom or molecule
$m$	mass of electron
$m$	atomic magnetic quantum number
$M$	mass of nucleus
$M$	projection of <b>J</b> on fixed direction, magnetic quantum number
$M$	molecular weight
$M_F$	projection of total angular momentum, including nuclear spin, on space-fixed axis
$M_I$	projection of nuclear spin angular momentum on space-fixed axis
$M_J$	projection of total angular momentum, excluding nuclear spin, on space-fixed axis
$M_L$	projection of electronic orbital angular momentum on space-fixed axis
$M_S$	projection of electron spin on space-fixed axis
$\mathfrak{M}$	dyadic (tensor) connecting angular momentum and magnetic moment
$n$	atomic principal quantum number
$N$	number of molecules per cubic centimeter
<b>N</b>	total orbital angular momentum including rotation of molecule
$N_0$	Avogadro's number; number of molecules in one molecular weight
<b>O</b>	orbital angular momentum due to rotation of molecule
$P$	associated Legendre function
<b>P</b>	total angular momentum
$P$	spectroscopic symbol for state with $l = 1$

$q$	negative electric field gradient at nucleus = $\partial^2 V / \partial z^2$
$q_J$	negative electric field gradient in the direction of $J$ , or $(\partial^2 V / \partial z_J^2)_{av}$
$q_l$	$l$ -type doubling constant
$q_\Lambda$	$\Lambda$ -type doubling constant
$Q$	nuclear quadrupole moment
$Q$	resonator figure of merit
$r$	internuclear distance
$r$	intermolecular distance
$r_e$	equilibrium distance between nuclei
$R$	dipole moment matrix element
$R$	Rydberg constant
$s$	electron spin quantum number
$s$	quantum number for internal torsional states
$S$	degree of degeneracy for a symmetric top
$S$	transition strength
$S$	spectroscopic symbol for state with $l = 0$
$S$	electron spin angular momentum
$T$	absolute temperature
$U$	potential energy
$U_P$	number of unbalanced $P$ electrons oriented along the bond
$v$	vibrational quantum number
$v$	linear velocity of molecule
$V$	potential energy
$W$	energy
$x$	fractional importance of covalent bond
$x_e$	anharmonicity vibrational constant
$Y$	Dunham's molecular energy constant
$Z$	nuclear charge, in units of the proton charge
$Z$	characteristic impedance of a transmission line
$Z_i$	effective nuclear charge

*Greek letters*

$\alpha$	attenuation constant
$\alpha$	rotation-vibration interaction constant
$\alpha$	fine-structure constant $2\pi e^2 / hc$
$\alpha$	torsion angle of one part of a molecule with respect to another part
$\gamma$	absorption coefficient
$\gamma$	propagation constant
$\delta$	skin depth
$\Delta\nu$	line-breadth parameter
$\Delta\nu$	frequency bandwidth from which noise is passed by amplifier
$\epsilon$	dielectric constant

$\lambda_g$	wavelength in waveguide
$\lambda_0$	wavelength in free space
$\eta$	field gradient asymmetry
$\theta$	coordinate polar angle
$\kappa$	Ray's asymmetry parameter = $(2B - A - C)/(A - C)$
$\Lambda$	projection of electronic angular momentum on molecular axis
$\mu$	reduced mass
$\mu$	molecular electric dipole moment, or in some cases molecular magnetic dipole moment
$\mu$	magnetic permeability
$ \mu_{ij} ^2$	square of dipole moment matrix element, summed over directions
$\mu_n$	nuclear magneton = $hc/4\pi Mc$ , where $M$ is proton mass
$\mu_0$	Bohr magneton = $hc/4\pi mc$ , where $m$ is electron mass
$\nu$	frequency
$\nu_0$	resonant frequency; frequency absorbed by undisturbed molecule = $\omega_0/2\pi$
$\nu_1, \nu_2, \nu_3$	frequencies of vibration of polyatomic molecule
$\pi$	Zeeman components of line for transitions with $\Delta M = 0$
$\Pi$	molecular state having one unit of electronic orbital angular momentum
$\rho$	electric charge density
$\sigma$	effective cross section area of molecule
$\sigma$	Zeeman components of line for transitions with $\Delta M = \pm 1$
$\Sigma$	molecular state having zero electronic orbital angular momentum
$\Sigma$	projection of total electron spin on molecular axis
$\tau$	volume of space
$\tau$	integer used in specifying levels of asymmetric rotor
$\tau$	mean lifetime between collisions
$\tau$	resistivity
$\psi$	wave function
$\omega$	angular frequency = $2\pi\nu$
$\omega_e$	vibrational frequency (at equilibrium)
$\omega_0$	$2\pi$ times the natural molecular frequency = $2\pi\nu_0$
$\Omega$	projection of total angular momentum, excluding nuclear spin, on molecular axis (absolute value)
$\Omega_I$	projection of nuclear spin angular momentum on molecular axis
$\Omega_F$	projection of total angular momentum, including nuclear spin, on molecular axis



## INTRODUCTION

Some low-pressure gases selectively absorb electromagnetic radiation of particular wavelengths in the millimeter and centimeter range. This type of absorption can be observed in an experiment broadly represented by Fig. 1.

The source of microwaves (electromagnetic radiation of wavelength between 1 and 1000 mm) is usually an electronic tube, which emits radiation through a hollow metal pipe called a waveguide. The microwaves are detected after passage through a region of low-pressure gas (10 mm to  $10^{-4}$  mm Hg pressure) by a silicon "crystal" or other detecting device. This detector produces an electrical signal proportional to the

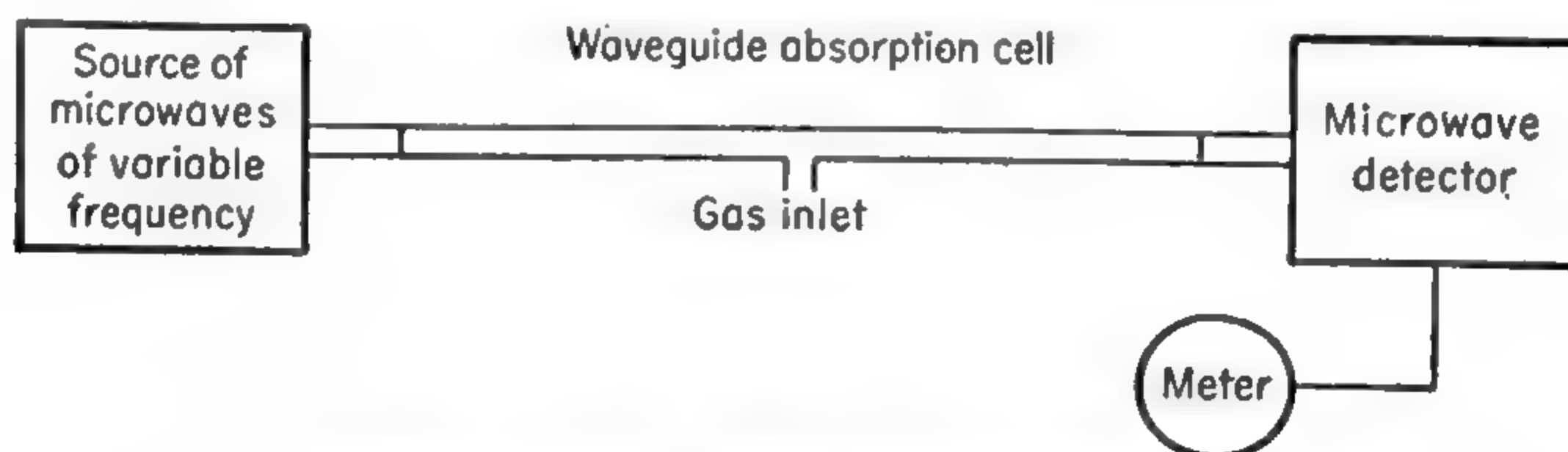


FIG. 1. Experiment for measuring microwave absorption.

microwave power which, after possible amplification, is observed on a meter or oscilloscope. As the frequency of the microwaves is varied, absorption appears as a sudden decrease in the voltage output of the detector.

Electronic techniques are characteristic of microwave spectroscopy, being involved in the production, detection, and amplification of microwaves. In some cases very sensitive electronic circuits are needed for proper detection and amplification, since the fractional power decrease may be quite small—as small as one part in  $10^8$  in an absorption path of 1 meter. In a few cases the absorption may be as much as 90 per cent in 1 meter path, and very easily detectable.

At gas pressures near 1 atm, a small microwave absorption may occur over a wide range of frequency. As the pressure is lowered, the range of frequency absorbed decreases proportionally down to pressures near  $10^{-3}$  mm Hg, where the range is so small that the term absorption "line" is well merited. Very significantly, and contrary to experience in most

other types of spectroscopy, the intensity of absorption in the center of the line does not appreciably decrease with this enormous decrease in pressure.

Because of the narrowness of absorption lines at low pressures, and the flexibility and sensitivity of electronic techniques, this type of experiment and its many refinements and ramifications form a basis for the precise, widely applicable microwave spectroscopy of gases which is the subject of this volume.

Consider now the frequencies absorbed. These must be interpretable in terms of the structure and behavior of the absorbing molecules. The motions (or transitions) of electrons in atoms and molecules are known to produce characteristically spectra in the optical and ultraviolet region. The slower vibrational motions of atoms in molecules are primarily responsible for the rich infrared spectra. It is the still slower end-over-end rotation of molecules which have characteristic frequencies so low that they lie in the microwave range and dominate microwave spectra.

Discussion of the interpretation of microwave spectra will begin with the rather simple diatomic molecules and progress in following chapters to successively more complex cases of linear polyatomic molecules, symmetric-top molecules, and asymmetric-top molecules.

Superimposed on the frequencies associated with molecular rotation are many interesting fine and hyperfine effects, some of which have been observed clearly for the first time by microwave techniques. These will be discussed after the broader outlines of rotational spectra have been treated.

## CHAPTER 1

### ROTATIONAL SPECTRA OF DIATOMIC MOLECULES

**1-1. The Rigid Rotor.** If the distance between nuclei in a diatomic molecule is considered fixed, the possible frequencies of the end-over-end rotation of this "rigid rotor" can be rather simply obtained. Using assumptions of the "old" quantum mechanics, the angular momentum must be some integral multiple of  $h/2\pi$ , so that

$$2\pi\nu I = \frac{Jh}{2\pi}$$

where  $h$  is Planck's constant,  $I$  is the molecular moment of inertia about axes perpendicular to the internuclear axis,  $\nu$  is the frequency of rotation, and  $J$  is a positive integer giving the angular momentum in units of  $h/2\pi$ . Hence the frequencies expected from such a system are

$$\nu = \frac{Jh}{4\pi^2 I} \quad (1-1)$$

The moment of inertia  $I$  comes largely from the nuclei, where most of the molecular mass is concentrated, and for diatomic molecules of ordinary masses is of such size that for small integral values of  $J$ , the frequency  $\nu$  is of the order 10,000 to 100,000 Mc, or the wavelength in the region 3 cm to 3 mm.

On this simple basis one might expect a rotation about the molecular axis to occur also and to have characteristic frequencies a few thousand times greater because the moment of inertia about this axis is produced by electrons, which are very much lighter than the nuclei. These frequencies lie then near the optical region, and in a very rough way the electronic frequencies may be regarded as due to this type of rotation about the molecular axis. Since these frequencies are very high, they lie far beyond the microwave range and are not ordinarily excited at room temperature. They will therefore be neglected in most of the following treatment. A somewhat more sophisticated and rigorous determination of the frequencies produced by a rigid diatomic molecule can be obtained by finding the permitted energy levels from wave mechanics (see [62], p. 271, or [305], p. 60). As the molecule rotates about its center of gravity, its orientation in space may be specified by the spherical



polar coordinates  $\theta$  and  $\phi$ . The wave equation may then be written

$$\frac{h^2}{8\pi^2 I} \left[ \frac{1}{\sin \theta} \frac{\partial}{\partial \theta} \left( \sin \theta \frac{\partial \psi}{\partial \theta} \right) + \frac{1}{\sin^2 \theta} \frac{\partial^2 \psi}{\partial \phi^2} \right] + W\psi = 0 \quad (1-2)$$

where  $\psi$  is the wave function and  $W$  the rotational energy of the molecule. The variables  $\theta$  and  $\phi$  may be separated by substituting

$$\psi = \Theta(\theta)\Phi(\phi)$$

which gives

$$\frac{d^2 \Phi}{d\phi^2} = -M^2 \Phi \quad (1-3)$$

and

$$\frac{h^2}{8\pi^2 I} \left[ \frac{1}{\sin \theta} \frac{d}{d\theta} \left( \sin \theta \frac{d\Theta}{d\theta} \right) - \frac{M^2 \Theta}{\sin^2 \theta} \right] + W\Theta = 0 \quad (1-4)$$

where  $M^2$  is an arbitrary constant.

Solutions of these equations which are single-valued and normalized can be obtained only when

$$W = \frac{h^2}{8\pi^2 I} J(J + 1)$$

where  $J$  is a positive integer and  $M$  is an integer such that  $|M| \leq J$ . Such solutions are

$$\Phi_M = \frac{1}{\sqrt{2\pi}} e^{iM\phi} \quad (1-5)$$

$$\Theta_{MJ} = \left[ \frac{(2J + 1)(J - |M|)!}{2(J + |M|)!} \right]^{\frac{1}{2}} P_J^{|M|}(\cos \theta) \quad (1-6)$$

where  $P_J^{|M|}(\cos \theta)$  is an associated Legendre function.  $[J(J + 1)](h^2/4\pi^2)$  is the square of the total angular momentum, so that the angular momentum may for convenience be designated by  $J$ . Similarly the projection of the angular momentum on the polar axis is given by  $M(h/2\pi)$ , or simply by the integer  $M$ .

The frequency observed when the molecule makes a transition between a lower state of energy  $W_1$  and an upper state of energy  $W_2$  is given by

$$\nu = \frac{W_2 - W_1}{h} = \frac{h}{8\pi^2 I} [J_2(J_2 + 1) - J_1(J_1 + 1)] \quad (1-7)$$

From the correspondence principle, these frequencies may be expected to approximately equal the frequencies given by expression (1-1); hence  $J_2$  should equal  $J_1 + 1$ , and

$$\nu = 2B(J + 1) \quad (1-8)$$

where  $J$  is the angular-momentum quantum number for the lower state ( $J_1$ ), and  $B = (h/8\pi^2 I)$  is called the rotational constant. The quantity

$B$  is often expressed in units of  $\text{cm}^{-1}$  for infrared spectroscopy. In that case  $B = (h/8\pi^2 Ic)$ . For microwave spectroscopy,  $B$  will generally be given in cycles per second, or  $B = h/8\pi^2 I$ . However, numerical values will usually be quoted in megacycles, or  $10^6$  cycles/sec. The selection rule that  $J_2 = J_1 + 1$  or  $\Delta J = \pm 1$  for dipole radiation of a diatomic molecule will be more rigorously demonstrated in the discussion of intensities later in this chapter.

**1-2. Energy Levels of the Diatomic Molecule.** From Eq. (1-8) it is seen that the spectrum of a rigid rotor consists of absorption lines equally spaced in frequency with an interval  $2B$ . Although the rigid rotor is an idealization to which actual molecules conform to a good approximation, accurate spectroscopic measurement reveals many deviations from this approximation. As  $J$  increases and the molecule rotates faster, it stretches so that the moment of inertia increases. Moreover, the nuclei vibrate back and forth along the line joining them even in the lowest vibrational state. A much greater difficulty from the point of view of obtaining a complete theoretical treatment is that the entire molecular system, composed of interacting electrons as well as nuclei, is so complicated that an exact quantum-mechanical solution is impossible.

However, since the electrons are very much lighter than the nuclei and move in electric fields of approximately the same intensity, the electron motion is very much faster than that of the nuclei; *i.e.*, many cycles of the electronic motion occur during a small portion of a cycle of the nuclear motion. It is therefore reasonable to treat first the electronic motion, considering the nuclei as fixed. Then the internuclear distance  $r$  appears as a parameter. In this way the electrons are found to be capable of occupying several states, each giving the molecule a particular value of the energy  $U$ , for each internuclear distance. Generally in microwave spectroscopy only the lowest of these electronic states is important.

As the internuclear distance is slowly varied, the electronic energy varies. Because the electronic motion is so fast in comparison with the nuclear motion, at each instant the electronic energy may be considered to have reached its equilibrium value corresponding to that distance. Thus we are justified in treating the vibration and rotation of the nuclei separately from the electronic motion. In this treatment  $U(r)$ , which is the sum of the electron energy plus energy of electrostatic interaction between the two nuclei, appears as the potential energy. The validity of this approximation was discussed by Born and Oppenheimer ([8]; see also [62], pp. 259–274, and [21], Chap. I). They showed that the entire molecular energy, including that due to electronic motion, can be expanded in powers of  $(m/M)^{1/2}$ , where  $m$  is the electronic mass and  $M$  an average nuclear mass. Separation of nuclear and electronic motions hence corresponds to selecting the larger terms of the series expansion



and neglecting those which are smaller by  $(m/M)^{1/2}$  or more. In some cases the neglected terms lead to observable effects, but they can only with difficulty be taken into account.

Using the approximation that the variation in electron energy with nuclear motion may be included in the potential  $U(r)$ , the wave equation for vibration and rotation of a diatomic molecule becomes

$$\frac{1}{M_1} \nabla_1^2 \psi + \frac{1}{M_2} \nabla_2^2 \psi + \frac{8\pi^2}{h^2} [W - U(r)] \psi = 0 \quad (1-9)$$

in which  $\psi$  is the wave function for the nuclear motion,  $M_1$  and  $M_2$  are the nuclear masses, and

$$\nabla_i^2 = \frac{\partial^2}{\partial x_i^2} + \frac{\partial^2}{\partial y_i^2} + \frac{\partial^2}{\partial z_i^2} \quad \text{where } i = 1 \text{ or } 2 \quad (1-10)$$

$x_i$ ,  $y_i$ , and  $z_i$  being Cartesian coordinates of the  $i$ th nucleus relative to axes fixed in space.

Transforming to spherical polar coordinates  $r$ ,  $\theta$ ,  $\phi$  of the second nucleus relative to the first as origin (*cf.* [62], p. 264),

$$\begin{aligned} \frac{1}{r^2} \frac{\partial}{\partial r} \left( r^2 \frac{\partial \psi}{\partial r} \right) + \frac{1}{r^2 \sin \theta} \frac{\partial}{\partial \theta} \left( \sin \theta \frac{\partial \psi}{\partial \theta} \right) + \frac{1}{r^2 \sin^2 \theta} \frac{\partial^2 \psi}{\partial \phi^2} \\ + \frac{8\pi^2 \mu}{h^2} [W - U(r)] \psi = 0 \end{aligned} \quad (1-11)$$

where  $\mu$  is the reduced mass,  $M_1 M_2 / (M_1 + M_2)$ . The variables may be separated by the substitution

$$\Psi = R(r) \Theta(\theta) \Phi(\phi) \quad (1-12)$$

$\Theta(\theta)$  and  $\Phi(\phi)$  turn out to be the same as the wave functions found above for the rigid rotor.

The radial wave function  $R(r)$  obtained by the separation process is given by

$$\frac{1}{r^2} \frac{d}{dr} \left( r^2 \frac{dR}{dr} \right) + \left\{ \frac{8\pi^2 \mu}{h^2} [W - U(r)] - \frac{J(J+1)}{r^2} \right\} R = 0 \quad (1-13)$$

The term  $J(J+1)/r^2$  may be regarded as a potential energy associated with the centrifugal force due to the rotational angular momentum  $J$ . Substituting the expression

$$R(r) = \frac{1}{r} S(r) \quad (1-14)$$

we get

$$\frac{d^2 S}{dr^2} + \left\{ -\frac{J(J+1)}{r^2} + \frac{8\pi^2 \mu}{h^2} [W - U(r)] \right\} S = 0 \quad (1-15)$$

The solutions of Eq. (1-15) will obviously depend on the form of  $U(r)$ . Since it is seldom possible actually to solve the electronic wave equation, it is customary to use an empirical expression for  $U(r)$ .

From experimental studies of molecular spectra and from calculations on simple molecules, the general form of  $U(r)$  is known to be that of Fig. 1-1 (see [471]). At large distances the atoms are independent, and the force between them is negligible. Their energy is then just the sum of the energies of the individual atoms. At very small distances, when the atoms are "in contact," they must repel each other. At some intermediate distance there must be a potential minimum, corresponding to the equilibrium distance of the atoms.

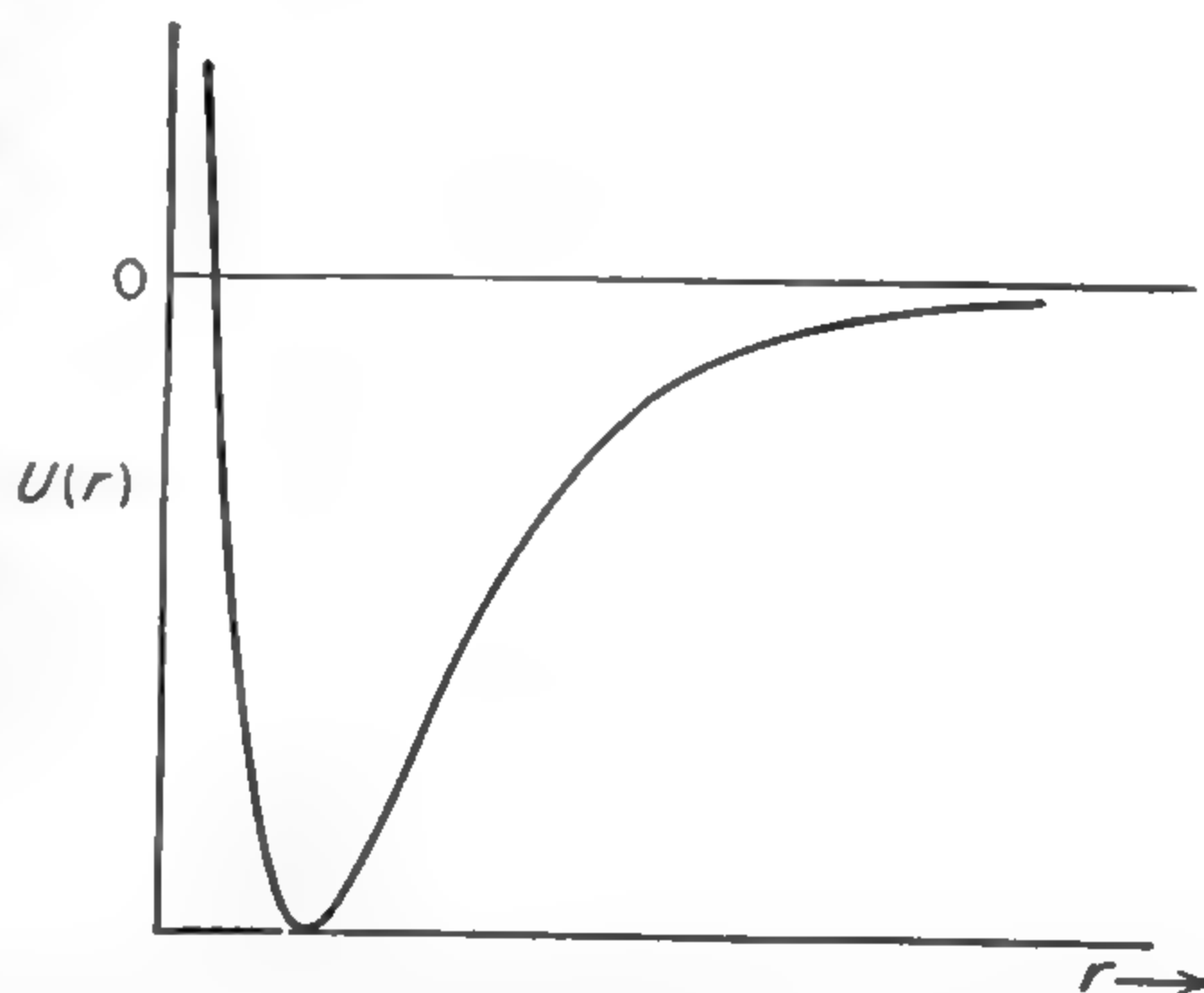


FIG. 1-1. Variation of molecular potential energy  $U(r)$  with internuclear distance  $r$ .

*Solution for Morse Potential.* A potential which fulfills these requirements is the Morse function [16]

$$U(r) = D(1 - e^{-a(r-r_e)})^2 \quad (1-16)$$

where  $D$  = dissociation energy of the molecule

$r_e$  = equilibrium distance between nuclei

$a$  = a constant

The Morse function differs from the true potential at  $r = 0$ , where the actual potential would be extremely large. However, the Morse potential is also quite large at  $r = 0$  and this is a region where the wave function of the vibrating rotor is expected to be small so that the discrepancy is not serious.

Using the Morse potential function, the radial equation (1-15) becomes

$$\frac{d^2S}{dr^2} + \left[ -\frac{J(J+1)}{r^2} + \frac{8\pi^2\mu}{h^2} (W - D - De^{-2a(r-r_e)} + 2De^{-a(r-r_e)}) \right] S = 0 \quad (1-17)$$

The solution of this equation for  $J = 0$  has been given by Morse [16] and for any  $J$  by Pekeris [52]. Substituting

$$y = e^{-a(r-r_e)} \quad \text{and} \quad A = J(J+1) \frac{h^2}{8\pi^2\mu r_e^2} \quad (1-18)$$

in Eq. (1-17), we obtain

$$\frac{d^2S}{dy^2} + \frac{1}{y} \frac{dS}{dy} + \frac{8\pi^2\mu}{a^2 h^2} \left( \frac{W - D}{y^2} + \frac{2D}{y} - D - \frac{Ar_e^2}{y^2 r^2} \right) S = 0 \quad (1-19)$$

For  $A \neq 0$ , it is necessary to expand  $r_e^2/r^2$  in terms of  $y$ :

$$\frac{r_e^2}{r^2} = \frac{1}{[1 - (\ln y)/ar_e]^2} = 1 + \frac{2}{ar_e}(y - 1) + \left(-\frac{1}{ar_e} + \frac{3}{a^2r_e^2}\right)(y - 1)^2 + \dots \quad (1-20)$$

If the first three terms of this Taylor expansion are retained, Eq. (1-19) becomes

$$\frac{d^2S}{dy^2} + \frac{1}{y} \frac{dS}{dy} + \frac{8\pi^2\mu}{a^2h^2} \left( \frac{W - D - c_0}{y^2} + \frac{2D - c_1}{y} - D - c_2 \right) S = 0 \quad (1-21)$$

in which

$$\begin{aligned} c_0 &= A \left( 1 - \frac{3}{ar_e} + \frac{3}{a^2r_e^2} \right) \\ c_1 &= A \left( \frac{4}{ar_e} - \frac{6}{a^2r_e^2} \right) \\ c_2 &= A \left( -\frac{1}{ar_e} + \frac{3}{a^2r_e^2} \right) \end{aligned} \quad (1-22)$$

Eq. (1-21) can be further simplified by the substitutions

$$\begin{aligned} S(y) &= e^{-z/2} z^{b/2} F(z) & z &= 2dy \\ d^2 &= \frac{8\pi^2\mu}{a^2h^2} (D + c_2) & b^2 &= -\frac{32\pi^2\mu}{a^2h^2} (W - D - c_0) \end{aligned} \quad (1-23)$$

so that it becomes

$$\frac{d^2F}{dz^2} + \left( \frac{b+1}{z} - 1 \right) \frac{dF}{dz} + \frac{v}{z} F = 0 \quad (1-24)$$

where

$$v = \frac{4\pi^2\mu}{a^2h^2d} (2D - c_1) - \frac{1}{2}(b+1) \quad (1-25)$$

As in the usual quantum-mechanical treatment of the simple harmonic oscillator or of the hydrogen atom (*cf.* [62]), for the solution of Eq. (1-24) to be finite and vanish at the ends of its range, it must be given by a terminating series, *i.e.*, a polynomial. In fact, Eq. (1-24) is identical in form with the equation for Laguerre polynomials found in the solution of the hydrogen atom. This requirement can be shown to restrict  $v$  to the values 0, 1, 2, . . . . Strictly speaking, the solutions thus obtained satisfy the boundary condition  $S \rightarrow 0$  as  $r \rightarrow -\infty$  rather than the proper condition  $S \rightarrow 0$  as  $r \rightarrow 0$ . Ter Haar [156] has examined this approximation and shown that it is usually a good one.

It is possible to solve for  $W$  using Eqs. (1-25), (1-23), (1-22), and



(1-18), which give

$$W_{Jv} = D + c_0 - \frac{(D - \frac{1}{2}c_1)^2}{D + c_2} + \frac{ah(D - \frac{1}{2}c_1)}{\pi \sqrt{2\mu} \sqrt{D + c_2}} \left(v + \frac{1}{2}\right) - \frac{a^2h^2}{8\pi^2\mu} \left(v + \frac{1}{2}\right)^2 \quad (1-26)$$

Expanding Eq. (1-26) in powers of  $c_1/D$  and  $c_2/D$ , it takes the form:

$$\frac{W_{Jv}}{h} = \omega_e(v + \frac{1}{2}) - x_e\omega_e(v + \frac{1}{2})^2 + J(J + 1)B_e - D_eJ^2(J + 1)^2 - \alpha_e(v + \frac{1}{2})J(J + 1) \quad (1-27)$$

where

$$\begin{aligned} \omega_e &= \frac{a}{2\pi} \sqrt{\frac{2D}{\mu}} & x_e &= \frac{h\omega_e}{4D} & B_e &= \frac{h}{8\pi^2I_e} \\ D_e &= \frac{h^3}{128\pi^6\mu^3\omega_e^2r_e^6} = \frac{4B_e^3}{\omega_e^2} \\ \alpha_e &= \frac{3h^2\omega_e}{16\pi^2\mu r_e^2D} \left(\frac{1}{ar_e} - \frac{1}{a^2r_e^2}\right) = 6 \sqrt{\frac{x_e B_e^3}{\omega_e}} - \frac{6B_e^2}{\omega_e} \end{aligned} \quad (1-28)$$

$\omega_e$ ,  $\alpha_e$ ,  $B_e$  in (1-27) and (1-28) are expressed in cycles per second. The terms in Eq. (1-27) can be identified with the solutions of more specialized problems, so that each can be given a physical significance. Thus the first term involving  $(v + \frac{1}{2})$  has the form of the solution of the wave equation of a pure vibrator with a harmonic potential. The second term is obtained when the vibrator potential is made anharmonic by the addition of a cubic term in the potential energy. A term of the form  $BJ(J + 1)$  is just that obtained in Eq. (1-4), the solution of the rigid rotor problem, while the next to last term comes from centrifugal stretching of the rotating molecule. The last term allows for the change in average moment of inertia due to vibration and the consequent change in rotational energy.

*Dunham's Solution for Energy Levels.* Some other more refined potentials have been used for problems in optical spectra involving excited rotational or vibrational states ([471], pp. 102, 108). Dunham [34] has calculated the energy levels of a vibrating rotor, by a Wentzel-Kramers-Brillouin method, for any potential which can be expanded as a series of powers of  $(r - r_e)$  in the neighborhood of the potential minimum. This treatment shows that the energy levels can be written in the form

$$F_{vJ} = \sum_{l,j} Y_{lj}(v + \frac{1}{2})^l J^j(J + 1)^j \quad (1-29)$$

where  $l$  and  $j$  are summation indices,  $v$  and  $J$  are, respectively, vibrational and rotational quantum numbers, and  $Y_{lj}$  are coefficients which depend on molecular constants. The effective potential function of the vibrating

rotor may be written in the form

$$U = a_0 \xi^2 (1 + a_1 \xi + a_2 \xi^2 + \dots) + B_e J(J+1) (1 - 2\xi + 3\xi^2 - 4\xi^3 + \dots) \quad (1-30)$$

where  $\xi = (r - r_e)/r_e$ ,  $B_e = h/8\pi^2 \mu r_e^2$ . The term involving  $B_e J(J+1)$  allows for the influence of the rotation on the effective potential.

Dunham [34] shows that the first 15  $Y_{ij}$ 's are

$$\left. \begin{aligned} Y_{00} &= B_e/8(3a_2 - 7a_1^2/4) \\ Y_{10} &= \omega_e[1 + (B_e^2/4\omega_e^2)(25a_4 - 95a_1a_3/2 - 67a_2^2/4 \\ &\quad + 459a_1^2a_2/8 - 1155a_1^4/64)] \\ Y_{20} &= (B_e/2)[3(a_2 - 5a_1^2/4) + (B_e^2/2\omega_e^2)(245a_6 - 1365a_1a_5/2 \\ &\quad - 885a_2a_4/2 - 1085a_3^2/4 + 8535a_1^2a_4/8 + 1707a_2^3/8 \\ &\quad + 7335a_1a_2a_3/4 - 23,865a_1^3a_3/16 - 62,013a_1^2a_2^2/32 \\ &\quad + 239,985a_1^4a_2/128 - 209,055a_1^6/512)] \\ Y_{30} &= (B_e^2/2\omega_e)(10a_4 - 35a_1a_3 - 17a_2^2/2 + 225a_1^2a_2/4 \\ &\quad - 705a_1^4/32) \\ Y_{40} &= (5B_e^3/\omega_e^2)(7a_6/2 - 63a_1a_5/4 - 33a_2a_4/4 - 63a_3^2/8 \\ &\quad + 543a_1^2a_4/16 + 75a_2^3/16 + 483a_1a_2a_3/8 - 1953a_1^3a_3/32 \\ &\quad - 4989a_1^2a_2^2/64 + 23,265a_1^4a_2/256 - 23,151a_1^6/1024) \end{aligned} \right\} \quad (1-31)$$

$$\left. \begin{aligned} Y_{01} &= B_e\{1 + (B_e^2/2\omega_e^2)[15 + 14a_1 - 9a_2 + 15a_3 - 23a_1a_2 \\ &\quad + 21(a_1^2 + a_1^3)/2]\} \\ Y_{11} &= (B_e^2/\omega_e)\{6(1 + a_1) + (B_e^2/\omega_e^2)[175 + 285a_1 - 335a_2/2 \\ &\quad + 190a_3 - 225a_4/2 + 175a_5 + 2295a_1^2/8 - 459a_1a_2 \\ &\quad + 1425a_1a_3/4 - 795a_1a_4/2 + 1005a_2^2/8 - 715a_2a_3/2 \\ &\quad + 1155a_1^3/4 - 9639a_1^2a_2/16 + 5145a_1^2a_3/8 \\ &\quad + 4677a_1a_2^2/8 - 14,259a_1^3a_2/16 \\ &\quad + 31,185(a_1^4 + a_1^5)/128]\} \\ Y_{21} &= (6B_e^3/\omega_e^2)[5 + 10a_1 - 3a_2 + 5a_3 - 13a_1a_2 \\ &\quad + 15(a_1^2 + a_1^3)/2] \\ Y_{31} &= (20B_e^4/\omega_e^3)[7 + 21a_1 - 17a_2/2 + 14a_3 - 9a_4/2 + 7a_5 \\ &\quad + 225a_1^2/8 - 45a_1a_2 + 105a_1a_3/4 - 51a_1a_4/2 + 51a_2^2/8 \\ &\quad - 45a_2a_3/2 + 141a_1^3/4 - 945a_1^2a_2/16 + 435a_1^2a_3/8 \\ &\quad + 411a_1a_2^2/8 - 1509a_1^3a_2/16 + 3807(a_1^4 + a_1^5)/128] \end{aligned} \right\} \quad (1-32)$$

$$\left. \begin{aligned} Y_{02} &= -(4B_e^3/\omega_e^2)\{1 + (B_e^2/2\omega_e^2)[163 + 199a_1 - 119a_2 + 90a_3 \\ &\quad - 45a_4 - 207a_1a_2 + 205a_1a_3/2 - 333a_1^2a_2/2 + 693a_1^2/4 \\ &\quad + 46a_2^2 + 126(a_1^3 + a_1^4/2)]\} \\ Y_{12} &= -(12B_e^4/\omega_e^3)(\frac{1}{2} + 9a_1 + 9a_1^2/2 - 4a_2) \\ Y_{22} &= -(24B_e^5/\omega_e^4)[65 + 125a_1 - 61a_2 + 30a_3 - 15a_4 \\ &\quad + 495a_1^2/4 - 117a_1a_2 + 26a_2^2 + 95a_1a_3/2 - 207a_1^2a_2/2 \\ &\quad + 90(a_1^3 + a_1^4/2)] \end{aligned} \right\} \quad (1-33)$$



$$\left. \begin{aligned} Y_{03} &= 16B_e^5(3 + a_1)/\omega_e^4 \\ Y_{13} &= (12B_e^6/\omega_e^5)(233 + 279a_1 + 189a_1^2 + 63a_1^3 - 88a_1a_2 \\ &\quad - 120a_2 + 80a_3/3) \\ Y_{04} &= -(64B_e^7/\omega_e^6)(13 + 9a_1 - a_2 + 9a_1^2/4) \end{aligned} \right\} \quad (1-34)$$

It should be noted that  $B_e$  is generally much smaller than  $\omega_e$ . For most molecules the ratio  $B_e^2/\omega_e^2$  is of the order of  $10^{-6}$ , although for light molecules such as  $H_2$  it approaches more nearly to  $10^{-3}$ . In such cases more terms are required in the expressions for the various coefficients.

If  $B_e/\omega_e$  is small, the  $Y$ 's can be related to the ordinary band spectrum constants as follows:

$$\begin{aligned} Y_{10} &\approx \omega_e & Y_{20} &\approx -\omega_e x_e & Y_{30} &\approx \omega_e y_e \\ Y_{01} &\approx B_e & Y_{11} &\approx -\alpha_e & Y_{21} &\approx \gamma_e \\ Y_{02} &\approx -D_e & Y_{12} &\approx \beta_e & Y_{40} &\approx \omega_e z_e \\ Y_{03} &\approx H_e \end{aligned} \quad (1-35)$$

where these symbols refer to the coefficients in the Bohr theory expansion for the molecular energy levels:

$$F_{vJ} = \omega_e(v + \frac{1}{2}) - \omega_e x_e(v + \frac{1}{2})^2 + \omega_e y_e(v + \frac{1}{2})^3 + \omega_e z_e(v + \frac{1}{2})^4 \\ + B_v J(J + 1) - D_e J^2(J + 1)^2 + H_e J^3(J + 1)^3 + \dots \quad (1-36)$$

where  $B_v = B_e - \alpha_e(v + \frac{1}{2}) + \gamma_e(v + \frac{1}{2})^2 \dots$  (cf. [471], p. 92, pp. 107-108).

Sandeman [103] has extended Dunham's treatment to include other terms of the same order of magnitude which involve higher powers of the vibrational quantum number.

For the special case of the Morse potential function, Dunham shows that all the  $Y_{10}$ 's except  $Y_{10}$  and  $Y_{20}$  vanish and all but the first terms in the expressions for  $Y_{10}$  and  $Y_{20}$  are zero. Because of the simplicity of the expressions obtained with the Morse function, and because it does give a quite good fit to the actual potential in the region of  $r = r_e$ , the Morse function has been widely used.

*Dependence of Energy on Isotopic Masses.* Since the frequencies of lines in microwave spectra can be measured with great precision, and since they can be used to evaluate the molecular moment of inertia, they permit an accurate evaluation of atomic or nuclear masses, or rather the mass ratios of isotopic nuclei.

To a good approximation we can use the Morse potential solution. The usual expansion for energy levels, appropriate to the Morse potential or other similar potentials, is given by (1-27), from which the frequency of a microwave rotational transition, where  $J$  changes by one unit, is easily shown to be

$$\nu = \frac{W_{J+1} - W_J}{h} = 2B_e(J + 1) - 2\alpha_e(v + \frac{1}{2})(J + 1) - 4D_e(J + 1)^3 \\ = 2B_v(J + 1) + 4D_e(J + 1)^3 \quad (1-37)$$

The constants  $B_e$ ,  $\alpha_e$ , and  $D_e$  are usually expressed in  $\text{cm}^{-1}$  in optical work. In the above formula they, and therefore the frequency, are in cycles per second, which may be divided by  $10^6$  to convert to megacycles, the most usual unit for microwave work.

$B_e$  and  $\alpha_e$  can be evaluated directly from microwave spectra if two lines can be measured with different values of  $v$ ; for instance, the same rotational transition in the ground vibrational state and the first excited vibrational state. The term in  $(J+1)^3$  is often negligible because  $D_e = (4B_e^3/\omega_e^2)$  is smaller in magnitude than  $B_e$  by  $4(B_e/\omega_e)^2$ , or approximately  $10^{-5}$  for most molecules. However, for very light molecules or large  $J$  this term may be rather prominent. When required it can be calculated with sufficient accuracy from  $B_0 \approx B_e$  and  $\omega_e$ , which is usually obtainable from optical spectra.

If the nuclear masses are known from mass spectrographic or other measurements, a determination of  $B_e$  allows an evaluation of the internuclear distance  $r_e$ , since  $B_e$  is related to the moment of inertia  $I_e$ .

$$r_e = \sqrt{\frac{I_e}{\mu}} = \sqrt{\frac{h}{8\pi^2 B_e \mu}} \quad (1-38)$$

where  $\mu = M_1 M_2 / (M_1 + M_2)$  is the reduced mass. The accuracy with which  $r_e$  can be determined for a diatomic molecule is limited mainly by the error in Planck's constant  $h$ , which is required to calculate  $I_e$  from  $B_e$ . The best available value of this constant is

$$h = (6.6252 \pm 0.0005) \times 10^{-27} \text{ erg-sec}$$

[795] so that  $r_e$  can be determined to an accuracy of about 1 part in 6000. It is often convenient to have  $B_e$  in megacycles,  $r_e$  in angstroms, and  $\mu$  in atomic mass units. In these units

$$I_e = \frac{5.055 \times 10^5}{B_e} = \frac{I_e \text{ in cgs units}}{1.6598 \times 10^{-40}} \quad (1-39)$$

and

$$r_e = \sqrt{\frac{5.055 \times 10^5}{\mu B_e}} \quad \text{angstrom units} \quad (1-40)$$

Table 1a gives the constants of a number of representative diatomic molecules. Table 1b lists certain constants of one isotopic species of all diatomic molecules whose microwave rotational spectrum have been studied.

If the spectroscopic constants have been measured for one isotopic species of a molecule, their values for other species may be found from the following relations which are deducible from Eq. (1-28):

$$\omega_e \propto \frac{1}{\sqrt{\mu}} \quad B_e \propto \frac{1}{\mu} \quad \alpha_e \propto \frac{1}{\mu^{3/2}} \quad D_e \propto \frac{1}{\mu^2} \quad (1-41)$$

The values in Table 1a have been calculated with the aid of these relations in some cases.

TABLE 1-1a. MOLECULAR CONSTANTS OF SOME REPRESENTATIVE DIATOMIC MOLECULES

Mole- cule	$Y_{01}$ (approx. $B_0$ ), Mc	$Y_{01}$ (approx. $B_0$ ), cm <sup>-1</sup>	$\alpha_0$ , Mc	$I_e$ , A <sup>2</sup> × atomic mass units	$r_e$ , Å	$\omega_e$ , cm <sup>-1</sup>	$D_e = \frac{4B_e^3}{\omega_e^2}$ , Mc	$\mu$ , debyes	Reference
H <sup>1</sup> Cl <sup>35</sup>	317,510	10,591	9050	1.592	1.275	2989.74	15.94	1.18	[336a] [471]
DI <sup>127</sup>	( $B_0 = 97,537.2$ )	( $B_0 = 3.25348$ )	1840	( $I_0 = 5.183$ )	1.604	1630	1.56	0.38	[755a] [827a] [782b]
C <sup>12</sup> O <sup>16</sup>	57,897.5	1.93124	524.0	8.731	1.128	2170.21	0.1834	0.10	[336a] [457]
C <sup>13</sup> O <sup>16</sup>	55,344.9	1.84610	488.3	9.134	1.128	2074.81	0.1753	0.10	[457]
Cl <sup>36</sup> F <sup>19</sup>	15,483.69	0.516479	130.67	32.65	1.628	793.2	0.02626	0.88	[366]
Cl <sup>37</sup> F <sup>19</sup>	15,189.22	0.506657	126.96	33.28	1.628	778.6	0.02527	0.88	[366]
Br <sup>79</sup> F <sup>19</sup>	10,706.9	0.357143	156.3	47.21	1.759	671	0.0121	1.29	[534]
Br <sup>81</sup> F <sup>19</sup>	10,655.7	0.355435	155.8	47.44	1.759	670	0.0121	1.29	[534]
K <sup>41</sup> Cl <sup>35</sup>	3,767.394	0.125667	22.865	134.2	2.667	300	0.003	10.48	[835] [938]
K <sup>39</sup> Cl <sup>35</sup>	3,856.370	0.128634	23.680	131.1	2.667	300	0.003	10.48	[835] [938]
K <sup>39</sup> Cl <sup>37</sup>	3,746.583	0.124972	22.676	134.9	2.667	300	0.003	10.48	[835] [938]
I <sup>127</sup> Cl <sup>35</sup>	3,422.300	0.114155	16.06	147.7	2.321	384.2	0.00121	0.65	[330]
I <sup>127</sup> Cl <sup>37</sup>	3,277.365	0.109320	15.05	154.2	2.321	376	0.00111	0.65	[330]



TABLE 1-1b. MOLECULAR CONSTANTS OF DIATOMIC MOLECULES WHOSE ROTATIONAL SPECTRA HAVE BEEN MEASURED IN THE MICROWAVE REGION

Molecule	$Y_{01}$ (approx $B_e$ ), Mc	$\alpha_e$ , Mc	$r_e$ , $10^{-8}$ cm or angstroms	$\mu$ , $10^{-18}$ esu or debyes	Reference
D <sup>79</sup> Br	( $B_0 = 127,358.2$ )	2500	1.414	0.79	[336a] [676c] [927]
DI	( $B_0 = 97,537.2$ )	1840	1.604	0.38	[755a] [782b] [827a]
FCl <sup>35</sup>	15,483.69	130.67	1.628	0.881	[366]
Br <sup>79</sup> Cl <sup>35</sup>	4,570.92	23.22	2.138	0.57	[535]
ICl <sup>35</sup>	3,422.300	16.06	2.321	0.65	[330]
FBr <sup>79</sup>	10,706.9	156.3	1.759	1.29	[534]
C <sup>12</sup> O <sup>16</sup>	57,897.5	524.0	1.128	0.10	[336a] [457]
C <sup>12</sup> S <sup>32</sup>	24,584.352	177.544	1.535	2.0	[777]
N <sup>14</sup> O <sup>16</sup>	51,084.5	534	1.151	0.16	[336a] [782b] [924]
Li <sup>6</sup> Br <sup>79</sup>	19,161.51	208.8	2.170	6.19	[938]
Li <sup>6</sup> I	15,381.45	152.6	2.392	6.25	[938]
NaCl <sup>35</sup>	6,536.86	48.28	2.361	8.5	[751] [987]
NaBr <sup>79</sup>	4,534.51	28.25	2.502	.....	[938]
NaI	3,531.76	19.44	2.712	.....	[938]
K <sup>39</sup> Cl <sup>35</sup>	3,856.370	23.680	2.667	10.48	[835] [987]
K <sup>39</sup> Br <sup>79</sup>	2,434.947	12.136	2.821	10.41	[799]
K <sup>39</sup> I	1,825.01	8.034	3.048	11.05	[938]
Rb <sup>85</sup> Cl <sup>35</sup>	2,627.400	13.601	2.787	.....	[938]
Rb <sup>85</sup> Br <sup>79</sup>	1,424.83	5.578	2.945	.....	[938]
Rb <sup>85</sup> I	984.31	3.281	3.177	.....	[938]
CsF	5,527.27	33.13	2.345	7.874	[423a] [938]
CsCl <sup>35</sup>	2,161.20	10.085	2.906	10.40	[751] [606a] [938]
CsBr <sup>79</sup>	1,081.34	3.718	3.072	.....	[938]
CsI	708.36	2.044	3.315	12.1	[938]

1-3. Mass Measurements. Once  $B_e$  has been measured for two isotopic species of a molecule, the reduced mass ratio is given directly by the ratio of the  $B_e$ 's. That is,

$$\frac{\mu^{(1)}}{\mu^{(2)}} = \frac{B_e^{(2)}}{B_e^{(1)}} = \frac{M_1(M + M_2)}{M_2(M + M_1)}$$

(1-42)

or

$$\frac{M_1}{M_2} = \frac{(M/M_2)(B_e^{(2)}/B_e^{(1)})}{1 + M/M_2 - B_e^{(2)}/B_e^{(1)}}$$

(1-43)

where  $M_1$  and  $M_2$  are the masses of the two isotopes;  $M$  is the mass of the other nucleus in the molecule. From (1-43) and microwave measurements of  $B_e^{(2)}/B_e^{(1)}$ , the mass ratio  $M_1/M_2$  can be obtained with great precision. The mass ratio  $M/M_2$  need be known only moderately accurately since it enters into both the numerator and denominator. Planck's constant and the other constants required to compute  $r_e$  from  $B_e$  do not enter at all. By this procedure the mass ratio of the chlorine 35 to the

chlorine 37 isotope has been found from the spectra of ICl and FCl. The values obtained are compared in Table 1-2 with another microwave measurement in the triatomic molecule ClCN and with values from mass-spectroscopic and nuclear-disintegration work. It may be seen from this table that they agree well with other determinations and represent very accurate determinations of the  $\text{Cl}^{35}/\text{Cl}^{37}$  mass ratio.

 TABLE 1-2. VALUE OF  $\text{Cl}^{35}/\text{Cl}^{37}$  MASS RATIO

Method	Value	Reference
Mass spectroscopy.....	$0.9459777 \pm 20$	[562a]
Nuclear reaction.....	$0.9459893 \pm 110$	[110a]
Microwave (ICl).....	$0.9459801 \pm 50$	[330]
Microwave (FCl).....	$0.9459775 \pm 40$	[366]
Microwave-molecular beam (KCl).....	$0.9459803 \pm 15$	[835]
Microwave (CsCl).....	$0.9459781 \pm 30$	[938]
Microwave (ClCN).....	$0.9459906 \pm 120$	[490]

Within the limits of error given in Table 1-2 for the microwave measurements, there seem to be no theoretical uncertainties which should affect mass ratios. However, microwave measurements can be made considerably more precise, so that it is important to examine even small effects which might possibly cause errors. Such effects have been observed in optical spectra of hydrides where the large mass ratio between  $\text{H}^1$  and  $\text{H}^2$ , the rapid rotation, and vibration with large amplitudes make them unusually large (see, for example, [57], [58], and [71]).

The more important errors in measuring mass ratios from rotational spectra of diatomic molecules (other than simply inaccurate measurements of  $B_e$ ) may be grouped under three causes:

1. Anharmonicity of the potential function
2. Uncertainties in electronic behavior, including  $L$  uncoupling
3. Inaccurate knowledge of the mass of the other atom in the molecule, or in  $M/M_2$

Anharmonicity has been partly taken into account by the use of the Morse function, but if this is not a sufficiently good approximation to the potential curve, Dunham's method must be used.

The Dunham coefficient corresponding most nearly to  $B_e$  is  $Y_{01}$ , but actually

$$Y_{01} = B_e \{ 1 + B_e^2 / 2\omega_e^2 [15 + 14a_1 - 9a_2 + 15a_3 - 23a_1a_2 + 21(a_1^2 + a_1^3)/2] \} \quad (1-31)$$

where  $a_1, a_2, \dots$  are the coefficients in the expansion for the potential curve in terms of powers of  $(r - r_e)/r_e$  [cf. (1-30)]. Then

$$Y_{01} = B_e [1 + (B_e^2 / \omega_e^2) \beta_{01}] \quad (1-44)$$

where  $\beta_{01}$  does not depend on  $M_1, M_2$

$$Y_{01}(\mu_1)/Y_{01}(\mu_2) = \mu_2/\mu_1 \left[ 1 + \beta_{01} \left( \frac{B_e^2}{\omega_e^2} \right) \left( \frac{\mu_2 - \mu_1}{\mu_2} \right) \right] \quad (1-45)$$

$\beta_{01}$  can be calculated from spectroscopically observable quantities, as Dunham shows.

$$\begin{aligned} \beta_{01} &= Y_{10}^2 Y_{21}/4Y_{01}^3 + 16a_1 Y_{20}/3Y_{01} - 8a_1 - 6a_1^2 + 4a_1^3 \quad (1-46) \\ a_1 &= Y_{11} Y_{10}/6Y_{01}^2 - 1 \end{aligned}$$

Since  $\beta_{01}$  is multiplied by  $B_e^2/\omega_e^2$  in the expression for  $Y_{01}$ , it will enter as a small correction, and it is sufficiently accurate to replace the coefficients entering into it by their approximate values from (1-35), *i.e.*,

$$\begin{aligned} Y_{10} &\approx \omega_e & Y_{01} &\approx B_e & Y_{21} &\approx \gamma_e & Y_{20} &\approx -\omega_e x_e & Y_{11} &\approx -\alpha_e \\ & & & & & & & & a_1 &\approx (-\alpha_e \omega_e/6B_e^2) - 1 \end{aligned}$$

For example, in the case of ICl,  $\beta_{01}$  is approximately 50, so that the fractional correction to the mass ratio deduced from the microwave measurements is  $50(B_e^2/\omega_e^2)[(\mu^{37} - \mu^{35})/\mu^{35}] = 2 \times 10^{-7}$ . Since the accuracy of the present measurements is about  $2 \times 10^{-6}$ , an improvement by a factor of 10 would make this correction appreciable.

It is customary in calculating the moment of inertia of a molecule to assume each atom has the proper number of electrons to make it neutral, and that the entire mass of the atom is concentrated at a point. Thus for diatomic molecules the moment of inertia is generally written  $I_e = [M_1 M_2 / (M_1 + M_2)] r_e^2$ , where  $M_1$  and  $M_2$  are the masses of neutral atoms. Such an approximation is good only because the electrons are very light compared with the atomic nuclei which are, indeed, concentrated within a very small radius. However, uncertainties in the location and behavior of electrons in a rotating molecule do appreciably affect the moment of inertia. In NaCl, for example, it would be more correct to associate with Cl the mass of one electron more than the neutral atom and with Na one electron less since the molecule is largely ionic or  $\text{Na}^+ \text{Cl}^-$ . In the case of LiBr and LiI, it has been shown [938] that the rotational spectrum gives a mass ratio for the two Li isotopes which is in agreement with other measurements of this ratio only if the Li is assumed to have lost one electron and be  $\text{Li}^+$ .

Electrons are certainly not concentrated at the nuclei, but are arranged more or less spherically about their respective nuclei. Hence the moments of inertia might be expected to be greater than those calculated from the point mass assumption by an amount approximately equal to the moments of inertia of the electrons about their respective nuclei. This last contribution to the moment of inertia would be rather large, but fortunately it is not really present because a completely spherical shell



of electrons around an atom would not, in fact, rotate as the molecule rotates. This is known as the "slip effect," for the spherical shells of electrons appear to remain fixed in orientation or slip as the molecule rotates (*cf.* [339] and discussion of this effect in Chap. 8). The valence shell of electrons, however, is not completely spherical, and part of it must be considered to rotate with the molecule, giving a contribution of approximately  $nmr^2$ , where  $n$  is the number of rotating valence electrons,  $m$  the electron mass, and  $r$  some average of their distance from the nuclei with which they are supposed to be associated. This is of approximately the same magnitude as the uncertainty in moment of inertia due to an uncertainty of the position in the molecule of one electron. If  $n$  is taken as 1 and  $r = r_e$ , the error in moment of inertia is of the order  $mr_e^2$ , or a fractional error of  $m(M_1 + M)/M_1M$ . This is less than 1 part in 10,000 for almost all atoms, and hence would not affect a calculation of  $r_e$  from  $B_e$ . On the other hand, it does affect a determination of mass ratios, giving a fractional error in the mass ratio  $M_1/M_2$  of  $m(M_1 - M_2)/M_1M_2$ . For ICl, this fractional error is  $8 \times 10^{-7}$ , which is of the same general magnitude as the other errors discussed above. However, for the light nucleus of Li in LiI, such an effect would be as large as  $10^{-5}$ , and easily detectable.

$L$  uncoupling also involves the behavior of electrons during rotation and is very closely related to the above effects, although it may be described in somewhat different language. The rotational momentum of the molecule can to a very small extent be transferred to the molecular electrons. Rotation tends to excite the valence electrons from their normal  $^1\Sigma$  state of zero angular momentum to excited  $^1\Pi$  states, which have unit angular momentum, and hence slightly change the rotational energy. This process, known as  $L$  uncoupling, is very difficult to evaluate quantitatively from theory, since little exact knowledge of the electronic wave functions and excited states is available. However, it can be approximately evaluated from experimental results. Since a  $\Pi$  state has an electronic angular momentum and magnetic moment, even a small excitation of this state contributes a considerable part of the magnetic moment of the rotating molecule, which is of the order of a nuclear magneton, or one two-thousandth that of an electron. Hence a measurement of the molecular magnetic moment allows a rough estimate of the extent of  $L$  uncoupling or of its effect on the rotational energy.

Electrons in a  $\Pi$  state also produce a large magnetic field at the positions of the nuclei and hence a magnetic hyperfine interaction with the nuclei. Although this is not the only source of magnetic hyperfine interactions in a rotating molecule, it is probably a major contributor, so that measurement of the magnetic hyperfine interactions allow an estimate of the  $L$  uncoupling.

It is estimated that  $L$  uncoupling in ICl or FCl produces uncertain-

ties in the mass ratio  $\text{Cl}^{35}/\text{Cl}^{37}$  of about 1 part in  $10^6$ . This is again large enough to be of importance in accurate microwave measurements. Lighter molecules, which rotate faster, would in general involve larger errors from  $L$  uncoupling.

These electronic effects and their interrelations will be discussed in some detail in Chap. 8. That chapter shows that the entire contribution of electrons to the kinetic energy of rotation of a  $^1\Sigma$  molecule can be evaluated by a measurement of the rotational magnetic moment of the molecule. The magnetic moment of a  $^1\Sigma$  molecule is due to the rotation of both nuclear and electronic charges. The nuclear effect can be calculated by assuming that the nuclei form a rigid rotating frame. If their effect is subtracted from the measured magnetic moment, the electronic contribution to the moment can be determined. The change in rotational energy due to electron motion is, from (8-29) and (11-15),

$$W_R = g_e J(J + 1)hB_e \quad (1-47)$$

where  $g_e J$  is the magnetic moment in Bohr magnetons due to the motion of all the electrons. This expression allows the possibility of precise corrections for all effects due to electron motion [type (2) above].

Finally, it is of interest to examine how accurately the mass  $M$  must be known for the atom whose mass is not being measured. In determining the ratio  $M_1/M_2$ , it may be seen from Eq. (1-42) that  $M/M_2$  is assumed known. A fractional error  $\epsilon$  in this ratio will give a fractional error  $\delta$  in the determination of  $M_1/M_2$  which is

$$\delta = \frac{(M_2 - M_1)\epsilon}{M + M_2} \quad (1-48)$$

It is evident that, when the fractional change in weight of the molecule,  $(M_2 - M_1)/(M + M_2)$ , is small, the ratio  $M/M_2$  need not be known with high accuracy. The error produced by uncertainties in  $M/M_2$  is not, of course, due to theoretical uncertainties in the behavior of the molecule as are errors (1) and (2) on page 15. However, inaccurate knowledge of  $M/M_2$  may often give errors in  $M_1/M_2$  of the same order as those of type (1) and (2).

So far microwave mass measurements are just at the threshold of difficulties of the types discussed here. Since the measurements of  $B_e$  with microwaves can be rather easily improved by another factor of 10, these difficulties will provide an ultimate limit to the accuracy of most mass ratio measurements of about 1 part in  $10^6$ . This limit, of course, represents a very good accuracy and one which cannot always be obtained by other methods, *i.e.*, an error of  $10^{-4}$  mass unit for nuclei of atomic mass 100.

**1-4. Absorption Intensities and Selection Rules.** A molecule interacts appreciably with a microwave electromagnetic field to emit or absorb



radiation only if it has an electric or magnetic dipole moment  $\mu$ . Usually the dipole is an electric moment due to the positive and negative charges in the molecule. In the ICl molecule, for example, the Cl has an excess negative charge and the I an excess positive charge, so that the molecule is a small rotating dipole which acts in many ways like a small antenna in radiating or receiving electromagnetic waves whose frequency coincides with its frequency of rotation. The rate of radiation is small because the molecule is so small (approximately  $10^{-8}$  cm) compared with the wavelengths radiated (approximately 1 cm).

As will be discussed in some detail in Chap. 13, the intensity of a narrow microwave absorption line in a gas may usually be written

$$\gamma = \frac{8\pi^2 N f |\mu_{ij}|^2 \nu^2 \Delta\nu}{3ckT[(\nu - \nu_0)^2 + (\Delta\nu)^2]} \quad (1-49)$$

where  $N$  = the number of molecules per cc in absorption cell

$f$  = fraction of these molecules in the lower of the two states involved in the transition

$|\mu_{ij}|^2$  = square of the dipole moment matrix element for the transition, summed over the three perpendicular directions in space

$\nu$  = frequency

$\nu_0$  = resonant frequency or, to a good approximation, the center frequency of the absorption line

$\Delta\nu$  = half width of the line at half maximum, or line-breadth parameter

$c$  = velocity of light

$k$  = Boltzmann constant

$T$  = absolute temperature

The peak absorption of the line occurs very near to  $\nu = \nu_0$ , and is

$$\gamma_{\max} = \frac{8\pi^2 N f |\mu_{ij}|^2 \nu_0^2}{3ckT \Delta\nu} \quad (1-50)$$

The fraction of molecules in a particular vibrational state of energy  $h\omega_e(v + \frac{1}{2})$  is given by

$$f_v = \frac{e^{-h\omega_e(v+\frac{1}{2})/kT}}{\sum_{n=0}^{\infty} e^{(h\omega_e/kT)(n+\frac{1}{2})}} = e^{-vh\omega_e/kT} (1 - e^{-h\omega_e/kT}) \quad (1-51)$$

since

$$1 + e^{-h\omega_e/kT} + e^{-2h\omega_e/kT} + e^{-3h\omega_e/kT} + \dots = \frac{1}{1 - e^{-h\omega_e/kT}} \quad (1-52)$$

Of the molecules in a particular vibrational state, we must find the fraction  $f_J$  in a particular rotational state  $J$  in order to obtain the fraction  $f = f_v f_J$  in the particular state of interest for expression (1-50). The



angular momentum  $J$  may be oriented in space  $2J + 1$  different ways, corresponding to the different values of the magnetic quantum number  $M = J, J - 1, J - 2, \dots, -J$ . The fraction having angular momentum  $J$  is then

$$f_J = \frac{(2J + 1)e^{-hBJ(J+1)/kT}}{\sum_{n=0}^{\infty} (2n + 1)e^{-hBn(n+1)/kT}} \quad (1-53)$$

If  $B/kT$  is sufficiently small, the sum, often called the partition function, may be replaced by an integral,

$$\sum_{n=0}^{\infty} (2n + 1)e^{-hBn(n+1)/kT} = \int_0^{\infty} (2x + 1)e^{-hBx(x+1)/kT} dx = \frac{kT}{hB} \quad (1-54)$$

In case  $B/kT$  is large enough that a more accurate value of the rotational partition function is needed, it may be written as an expansion

$$\begin{aligned} \sum_{n=0}^{\infty} (2n + 1)e^{-hBn(n+1)/kT} &= \frac{kT}{hB} + \frac{1}{3} + \frac{1}{15} \frac{hB}{kT} + \frac{4}{315} \left(\frac{hB}{kT}\right)^2 \\ &+ \frac{1}{315} \left(\frac{hB}{kT}\right)^3 + \dots \end{aligned} \quad (1-55)$$

Using only the first term of this expansion,

$$f_J = \frac{(2J + 1)hBe^{-hBJ(J+1)/kT}}{kT} \quad (1-56)$$

In most cases of microwave rotational spectra,  $hB/kT \approx \frac{1}{200}$  at room temperature, so that not only is  $hB/kT$  small, but  $e^{-hBJ(J+1)/kT}$  can usually be approximated as unity for low values of  $J$ . Hence

$$f = (2J + 1) \frac{hB}{kT} e^{-h\omega_0/kT} (1 - e^{-h\omega_0/kT}) \quad (1-57)$$

*Dipole Moment Matrix Elements.* The dipole moment of a macroscopic linear array of charges oriented along the  $z$  axis would be defined as

$$\mu = \sum_i e_i z_i \text{ or } \int \rho(z) z dz \quad (1-58)$$

where  $e_i$  is the size of the  $i$ th charge and  $z_i$  is its coordinate. In the integral form,  $\rho(z)$  is the charge density per unit length. A linear molecule may be thought of as having an inherent or permanent dipole moment of the same type oriented along its axis. However, the molecular orientation is not fixed in space, so that its average dipole moment in any one direction is zero unless it is subjected to external electric fields or other constraining forces.

A measure of the effectiveness of an electric field along the  $z$  axis in exerting a torque on a rotating molecule, or in inducing a transition between states  $JM$  and  $J'M'$  is given by the dipole moment matrix elements

$$\mu_z(JMJ'M') = \int \psi_{JM}^* \mu_z \psi_{J'M'} d\tau \quad (1-59)$$

where  $\mu_z$  is the projection of the molecular dipole moment on the  $z$  axis.  $\psi_{JM}$  represents the molecular wave function for a total angular momentum  $J$  and magnetic quantum number  $M$ . Similarly, for electric fields in the  $x$  or  $y$  directions the dipole matrix elements

$$\mu_x(JMJ'M') = \int \psi_{JM}^* \mu_x \psi_{J'M'} d\tau \quad (1-60)$$

$$\mu_y(JMJ'M') = \int \psi_{JM}^* \mu_y \psi_{J'M'} d\tau \quad (1-61)$$

are important. The intensity of absorption or emission of radiation polarized with the electric vector in  $x$ ,  $y$ , or  $z$  directions due to a transition between the states  $JM$  and  $J'M'$ , is just proportional to  $|\mu_x(JMJ'M')|^2$ ,  $|\mu_y(JMJ'M')|^2$ , and  $|\mu_z(JMJ'M')|^2$ , respectively. In expression (1-50) giving the intensity of an absorption line, in which either the radiation is unpolarized or the molecules are randomly distributed in various  $M$  states, the quantity  $|\mu_{ij}|^2$  is given by

$$|\mu_{ij}|^2 = \sum_{M'} |\mu_x(JMJ'M')|^2 + |\mu_y(JMJ'M')|^2 + |\mu_z(JMJ'M')|^2 \quad (1-62)$$

In terms of spherical polar coordinates fixed in space, the components of the dipole moment are

$$\mu_x = \mu \sin \theta \cos \phi \quad \mu_y = \mu \sin \theta \sin \phi \quad \mu_z = \mu \cos \theta \quad (1-63)$$

In these coordinates the matrix elements become:

$$\begin{aligned} \mu_x(JMJ'M') &= \mu \int \psi_{JM}^* \sin \theta \cos \phi \psi_{J'M'} d\tau \\ \mu_y(JMJ'M') &= \mu \int \psi_{JM}^* \sin \theta \sin \phi \psi_{J'M'} d\tau \\ \mu_z(JMJ'M') &= \mu \int \psi_{JM}^* \cos \theta \psi_{J'M'} d\tau \end{aligned} \quad (1-64)$$

where  $\psi_{JM}$  is an eigenfunction for the rotating molecule.

For the rigid rotator, on substituting the eigenfunctions from (1-5) and (1-6) and using  $d\tau = \sin \theta d\phi d\theta$ , we get

$$\mu_z(JMJ'M') = \mu N_{JM} N_{J'M'} \int_0^\pi P_J^{(M)}(\cos \theta) \cos \theta P_{J'}^{(M')}(\cos \theta) \sin \theta d\theta \int_0^{2\pi} e^{-iM\phi} e^{iM'\phi} d\phi \quad (1-65)$$

where  $N_{JM}$  and  $N_{J'M'}$  are the normalization factors for  $\psi_{JM}$  and  $\psi_{J'M'}$ , or

$$N_{JM} = \frac{1}{\sqrt{2\pi}} \left[ \frac{(2J+1)(J-|M|)!}{2(J+|M|)!} \right]^{\frac{1}{2}} \quad (1-66)$$

The second integral in (1-65) has the value of  $2\pi$  if  $M = M'$ ; otherwise it is zero. The first integral may be obtained from the properties of the

Legendre polynomials ([471], p. 73; [62], p. 307; [537], p. 136)

$$\begin{aligned} \cos \theta P_J^{|M|}(\cos \theta) &= \frac{J + |M|}{2J + 1} P_{J-1}^{|M|}(\cos \theta) \\ &+ \frac{J - |M| + 1}{2J + 1} P_{J+1}^{|M|}(\cos \theta) \end{aligned} \quad (1-67)$$

so that, remembering that  $M$  must equal  $M'$ ,

$$\begin{aligned} \mu_z(JMJ'M) &= 2\pi\mu N_{JM} N_{J'M} \left[ \frac{J + M}{2J + 1} \int P_{J-1}^{|M|}(\cos \theta) P_J^{|M|}(\cos \theta) \sin \theta d\theta \right. \\ &\quad \left. + \frac{J - |M| + 1}{2J + 1} \int P_{J+1}^{|M|}(\cos \theta) P_J^{|M|}(\cos \theta) \sin \theta d\theta \right] \end{aligned} \quad (1-68)$$

These integrals vanish unless  $J' = J \pm 1$ , giving the selection rule that for a transition  $\Delta J = \pm 1$ . Taking  $J$  as the lower state so that

$$J' = J + 1$$

the first integral vanishes and

$$\begin{aligned} \mu_z(JMJ'M) &= 2\pi\mu \frac{N_{JM}}{N_{J+1,M}} \frac{J - |M| + 1}{2J + 1} \\ &\quad \int N_{J+1,M}^2 [P_{J+1}^{|M|}(\cos \theta)]^2 \sin \theta d\theta \end{aligned} \quad (1-69)$$

The integral remaining is just the normalization integral and equals  $1/2\pi$  with our choice of normalization factor. Putting in values of  $N_{JM}$  and  $N_{J+1,M}$ ,

$$\mu_z(J, M, J + 1, M) = \mu \sqrt{\frac{(J + 1)^2 - M^2}{(2J + 1)(2J + 3)}} \quad (1-70)$$

Similarly,  $\mu_x$  and  $\mu_y$  are zero unless  $J = J' \pm 1$  and  $M = M' \pm 1$ . Then

$$\begin{aligned} \mu_x(J, M, J + 1, M + 1) &= -i\mu_y(J, M, J + 1, M + 1) \\ &= \frac{-\mu}{2} \sqrt{\frac{(J + M + 2)(J + M + 1)}{(2J + 1)(2J + 3)}} \end{aligned} \quad (1-71)$$

$$\begin{aligned} \mu_x(J, M, J + 1, M - 1) &= i\mu_y(J, M, J + 1, M - 1) \\ &= \frac{\mu}{2} \sqrt{\frac{(J - M + 1)(J - M + 2)}{(2J + 1)(2J + 3)}} \end{aligned} \quad (1-72)$$

The signs or "phases" of the matrix elements (1-71) and (1-72) are usually not important and may be positive or negative according to one's definition of  $P_J^M(\cos \theta)$ . The signs given are those adopted by Condon and Shortley [56] but are not used by all authors.

The probability of inducing an absorption in a particular molecule in a state  $JM$  by radiation with the electric field in the  $z$  direction is then



proportional to

$$|\mu_z|^2 = \mu^2 \frac{(J+1)^2 - M^2}{(2J+1)(2J+3)} \quad (1-73)$$

and only the transition  $J+1, M \leftarrow JM$  can occur. Here the arrow indicates that the absorption process produces a transition from the state  $JM$  to the state  $J+1, M$ .<sup>\*</sup> Probability of emission of radiation of the same polarization due to the transition  $J+1, M \rightarrow JM$  is proportional to the same quantity. For radiation with the electric vector in the  $x$  or  $y$  direction, the absorption probability is proportional to

$$|\mu_x|^2 = \frac{\mu^2}{4} \frac{(J+M+2)(J+M+1)}{(2J+1)(2J+3)} \quad (1-74)$$

for a transition  $J+1, M+1 \leftarrow JM$  and

$$|\mu_x|^2 = \frac{\mu^2}{4} \frac{(J-M+1)(J-M+2)}{(2J+1)(2J+3)} \quad (1-75)$$

for  $J+1, M-1 \leftarrow JM$ .

For an electric vector in the  $z$  direction, the result that  $M$ , the angular momentum about the  $z$  axis, cannot change is easily understood because there can then be no torque on the molecule about the  $z$  axis. For electric fields in the  $x$  or  $y$  directions, however, there is a torque about the  $z$  axis and  $M$  changes by one unit.

For any particular initial state  $JM$ , it can be shown from (1-73), (1-74), and (1-75) that

$$\begin{aligned} |\mu_{ij}|^2 &= \sum_{M'} |\mu_x(JMJ'M')|^2 + |\mu_y(JMJ'M')|^2 + |\mu_z(JMJ'M')|^2 \\ &= \mu^2 \frac{(J+1)}{2J+1} \quad \text{for the transition } J+1 \leftarrow J \\ &= \mu^2 \frac{J+1}{2J+3} \quad \text{for the transition } J+1 \rightarrow J \end{aligned} \quad (1-76)$$

The expression is independent of  $M$ , as it should be since it represents the probability of absorption of unpolarized radiation, which should be independent of molecular orientation.

It should be noted that, although the individual matrix elements are identical for reverse transitions  $J'M' \leftarrow JM$  and  $JM \leftarrow J'M'$ , the average matrix element given by (1-76) for a transition  $J+1 \leftarrow J$  is greater than that for the reverse transition  $J+1 \rightarrow J$ . This must be true in

<sup>\*</sup> In spectroscopy it is conventional to denote transitions by writing first the state having higher energy. For an absorption process, which is the common type of transition in microwave work, this involves writing the final state before the initial one. We follow the common convention for the sake of uniformity with other branches of spectroscopy, although the lower state is written first in much of the previous microwave literature.

order to maintain thermal equilibrium when transitions take place, since there are  $2J + 3$  states of angular momentum  $J + 1$ , but only  $2J + 1$  states of the lower angular momentum  $J$ .

*Peak Intensities of Absorption Lines.* Combining (1-57) and (1-76) for an absorption in which  $J + 1 \leftarrow J$

$$|\mu_{ij}|^2 f = \mu^2 \frac{hB(J + 1)}{kT} f_v = \frac{\mu^2 f_v}{2kT} h\nu_0$$

where  $f_v$  is the fraction of molecules in the vibrational state being considered. The peak intensity of an absorption line of a diatomic molecule given by (1-50) becomes

$$\gamma_{\max} = \frac{4\pi^2 h N f_v \mu^2 \nu_0^3}{3c(kT)^2 \Delta\nu} \quad (1-77)$$

Since the line-breadth parameter  $\Delta\nu$  is proportional to the molecular density  $N$  at low pressures,  $N/\Delta\nu$  and therefore  $\gamma_{\max}$  is quite constant for pressures from about 1 to  $10^5$  microns or  $10^{-3}$  to 100 mm Hg. As a standard procedure, the value  $\Delta\nu$  is often given for 1 mm Hg pressure. Then the universal constants of (1-77) may be evaluated and rewritten

$$\gamma_{\max} = 5.48 \times 10^{-17} f_v \frac{\mu^2 \nu_0^3}{\Delta\nu} \quad (1-78)$$

where  $\mu$  is measured in debye units, or  $10^{-18}$  esu,  $\nu_0$  and  $\Delta\nu$  are measured in megacycles and  $T$  is taken as  $300^\circ\text{K}$ . Typical values would be  $f_v \approx 1$ ,  $\mu = 1$ ,  $\nu_0 = 30,000$  ( $\lambda = 1$  cm),  $\Delta\nu = 15$ , giving  $\gamma_{\max} = 10^{-4}/\text{cm}$ . This value of  $\gamma_{\max}$  represents a conveniently strong absorption for microwave spectroscopic work, *i.e.*, 1 per cent absorption in one meter path length. Because of the rapid variation of intensity with  $\nu_0$ , absorption-line intensities for wavelengths longer than 10 cm are usually too weak to be readily observed, while those for wavelengths as short as 1 mm are quite intense.

Measurements of intensity, combined with expression (1-78), can be used in some cases to evaluate  $\Delta\nu$  if  $\mu$  is known. Although dipole moments are usually measured most accurately by Stark effects (Chap. 10), they may be determined to an accuracy of a few per cent from (1-78) by a measurement of both intensity  $\gamma_{\max}$  and the half width of the line  $\Delta\nu$ .

Expression (1-77) indicates that the absorption intensity  $\gamma_{\max}$  increases rapidly with decreasing temperature  $T$ . For this reason it is often advantageous to strengthen absorption lines by decreasing the temperature of the gas to  $-78^\circ\text{C}$  (dry ice) or lower if there is sufficient vapor pressure. The exact dependence of  $\gamma_{\max}$  on  $T$  depends on how  $\Delta\nu$  varies with  $T$ .  $\Delta\nu$  will be shown in Chap. 13 to vary as  $T^n$ , where  $-1 \leq n \leq -\frac{1}{2}$ . Even when  $n = -1$ ,  $\gamma_{\max}$  can be increased by decreasing the gas temperature  $T$ .

## CHAPTER 2

### LINEAR POLYATOMIC MOLECULES

**2-1. Pure Rotational Spectra—General Considerations.** Except for the complication of more possible modes of vibration, the spectrum of a linear polyatomic molecule is much like that of a diatomic molecule. There is a very small moment of inertia about the molecular axis, and hence angular momentum about this axis is not easily excited, and the linear molecule rotates end over end with energies of the same form as for a diatomic molecule

$$W = \frac{h^2}{8\pi^2 I} J(J + 1)$$

where  $I$  is the moment of inertia and vibrations are neglected. Wave functions and intensities for linear molecules are also similar to those for a diatomic molecule [Eqs. (1-5), (1-6), and (1-77)] if vibrations are neglected. Vibrations do, however, add considerably to the actual complexity of the spectra as well as introduce some new phenomena.

As an obvious extension of the effects of vibrations seen in diatomic molecules, the rotational constant  $B = h/8\pi^2 I$  for a polyatomic linear molecule should be written

$$B = B_e - \sum_i \alpha_i (v_i + \frac{1}{2}) - J(J + 1)D \quad (2-1)$$

where  $-\alpha_i$  represents the change in the equilibrium value  $B_e$  due to excitation of the  $i$ th vibration,  $D$  the change due to centrifugal stretching, and  $v_i$  is the quantum number for the vibrational excitation. Even in the ground state, where all  $v_i$  are zero, the zero-point vibrations change the rotational constant by  $-\sum_i \alpha_i/2$ . A linear molecule has one or more degenerate modes of vibration, *i.e.*, modes which have the same frequency  $\omega_i$  and the same value of  $\alpha_i$ . If these are counted as a single vibration, then (2-1) is written:

$$B = B_e - \sum_i \alpha_i \left( v_i + \frac{d_i}{2} \right) - J(J + 1)D$$

where  $d_i$  is the degree of the degeneracy, or the number of degenerate modes with the same value  $\alpha_i$ . For the diatomic molecule where there



is only one vibrational mode,  $\alpha$  can be fairly simply treated. We shall see that the addition of just one more atom to the diatomic molecule very greatly complicates the vibrational effects.

The commonest type of linear polyatomic molecule is triatomic, such as carbonyl sulfide or OCS, where in equilibrium the atoms are arranged in a straight line in the order of this chemical formula. Any arbitrary relative vibration of the atoms in OCS may be described as a sum of four types or normal modes of vibrations. For each normal mode, the displacement of each atom is periodic with a definite frequency and proportional to a variable called the normal coordinate  $q_i$ . Then the general motion of one atom, which we shall label  $s$ , is given by

$$x_s = \sum_i l_{is} q_i \quad y_s = \sum_i m_{is} q_i \quad z_s = \sum_i n_{is} q_i \quad (2-2)$$

Two of these normal modes are degenerate, or are similar and have the same frequency. The three different vibrations are shown in Fig. 2-1, where the arrows indicate the relative directions and magnitudes of the

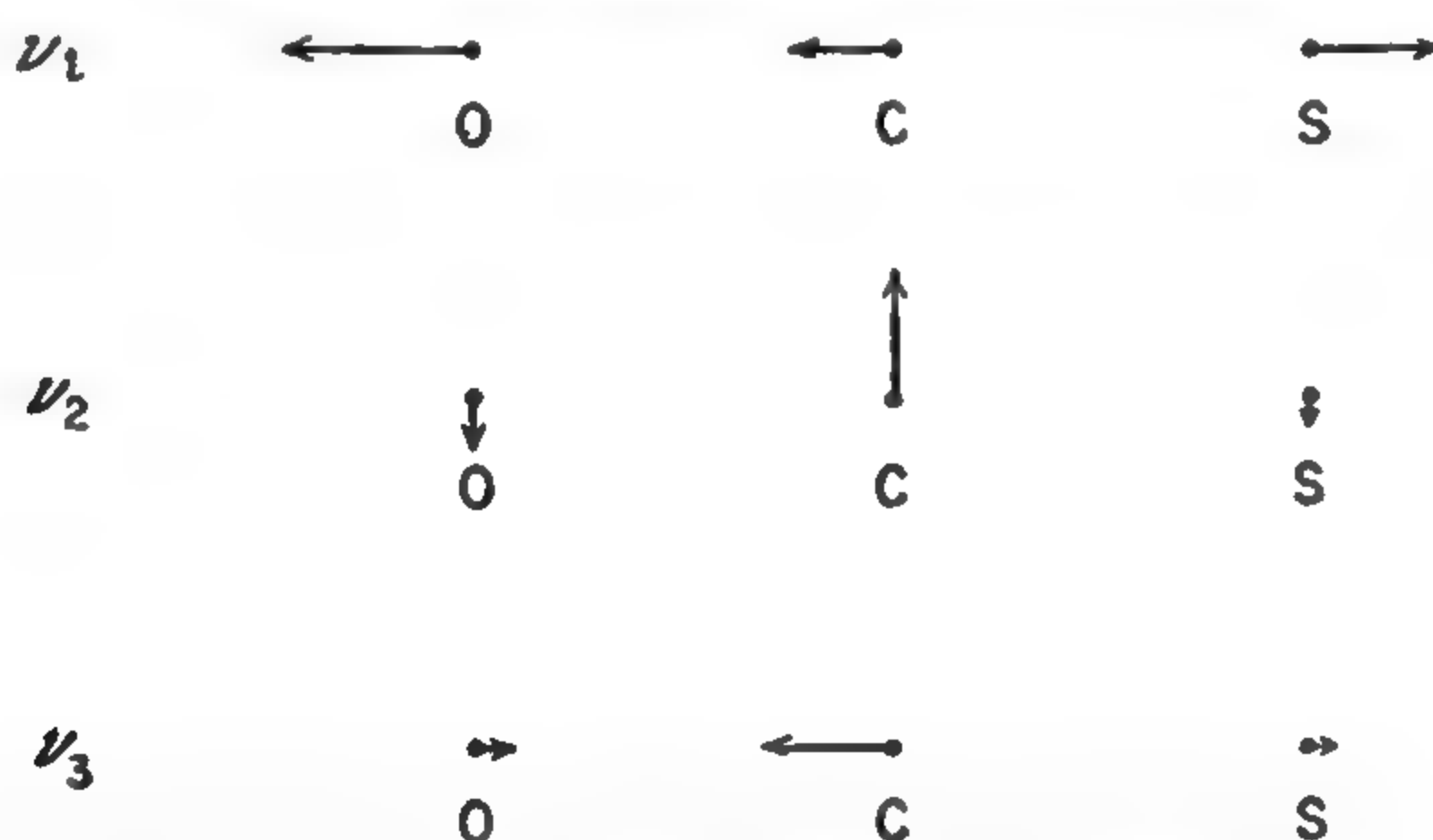


FIG. 2-1. The normal modes of the linear triatomic molecule OCS. Directions and lengths of arrows indicate relative motions of the three nuclei for the three different vibrations. The mode  $\nu_2$  is degenerate, a vibration of the same frequency with displacements perpendicular to the page being also possible.

displacements of each atom. The lowest frequency of vibration, which is indicated by  $\nu_2$ , corresponds to a bending of the molecule. This bending can take place in either of two perpendicular planes, corresponding to the two degenerate modes of oscillation of this type. Of the two stretching modes, by convention the one of lower frequency in which the two outer atoms move in opposite directions is called  $\nu_1$  and the higher-frequency vibration in which these atoms move in the same direction is  $\nu_3$ .

Allowing for the four modes of vibration, two of which are degenerate,

$$B_v = B_e - \alpha_1(v_1 + \tfrac{1}{2}) - \alpha_2(v_2 + 1) - \alpha_3(v_3 + \tfrac{1}{2}) \quad (2-3)$$

The  $\alpha$ 's as before must be evaluated from the molecular potential function. The potential function for a linear triatomic molecule is consider-

ably more complex than that for a diatomic molecule. Taking a coordinate system with origin at the center of mass and for which the  $z$  axis lies along the molecular axis, the potential for small displacements of the atoms may be written

$$V = \frac{K_1}{2} (z_2 - z_1)^2 + \frac{K_2}{2} (z_3 - z_2)^2 + \frac{K_3}{2} (z_3 - z_1)^2 \\ + K_{12}(z_2 - z_1)(z_3 - z_2) + K_{13}(z_2 - z_1)(z_3 - z_1) \\ + K_{23}(z_3 - z_2)(z_3 - z_1) + \frac{K_4}{2} (x^2 + y^2) \quad (2-4)$$

where the subscripts 1, 2, 3 refer to changes of the coordinates of the first, second, and third atoms from the equilibrium values. The  $K$ 's are potential constants, and

$$x = (2m_2x_2 - m_1x_1 - m_3x_3) \frac{m_1 + m_2 + m_3}{3m_2(m_1 + m_3)} \\ y = (2m_2y_2 - m_1y_1 - m_3y_3) \frac{m_1 + m_2 + m_3}{3m_2(m_1 + m_3)}$$

which represent relative displacements of the central and two end atoms perpendicular to the molecular axis. Here  $m_1$ ,  $m_2$ , and  $m_3$  are the masses of the three atoms. This potential is so complex that frequently it is simplified by assuming that forces occur only through the conventionally recognized molecular bonds corresponding to their stretching or bending. This "valence bond" approximation, which makes all constants in  $V$  zero except  $K_1$ ,  $K_2$ , and  $K_4$ , is usually a moderately good approximation. It tends to be rather poor if a stretching of one bond tends to affect the nature of a second bond as in bonds said to be "conjugated."

Evaluation of the  $\alpha$ 's involves not only the terms in the potential given above, but also the anharmonic potential constants. These anharmonic constants are most conveniently expressed if the potential is written in terms of the normal coordinates (see [130], p. 70)

$$V_{\text{anharmonic}} = k_{111}q_1^3 + k_{113}q_1^2q_3 + k_{133}q_1q_3^2 + k_{122}q_1q_2^2 + k_{322}q_3q_2^2 + k_{333}q_3^3 \quad (2-5)$$

For these normal coordinates  $q_i$ , the constants  $l_{is}$ ,  $m_{is}$ , and  $n_{is}$  of (2-2) have been chosen so that the kinetic energy due to vibration comes out simply

$$\text{KE} = \frac{1}{2} \sum_i \left( \frac{dq_i}{dt} \right)^2$$

Because of symmetry about the molecular axis, odd powers of  $q_2$  do not appear in (2-5). A. H. Nielsen [119] has obtained for the  $\alpha$ 's

$$\begin{aligned}
\alpha_1 &= \frac{2B_e^2}{c\omega_1} \left( 1 - 4\xi_{21}^2 \frac{\omega_1^2}{\omega_1^2 - \omega_2^2} - 4\xi_{23}^2 + 6I_e^{\frac{1}{2}} \frac{\xi_{23}k_{111}}{4\pi^2c^2\omega_1^2} + 2I_e^{\frac{1}{2}} \frac{\xi_{21}k_{113}}{4\pi^2c^2\omega_3^2} \right) \\
\alpha_2 &= \frac{B_e^2}{c\omega_2} \left[ -4I_e^{\frac{1}{2}} \frac{\xi_{21}k_{223}}{4\pi^2c^2\omega_3^2} + 4I_e^{\frac{1}{2}} \frac{\xi_{23}k_{122}}{4\pi^2c^2\omega_1^2} - (3\omega_2^2 + \omega_1^2) \frac{\xi_{21}^2}{\omega_2^2 - \omega_1^2} \right. \\
&\quad \left. - (3\omega_2^2 + \omega_3^2) \frac{\xi_{23}^2}{\omega_2^2 - \omega_3^2} \right]
\end{aligned} \tag{2-6}$$

$\alpha_3$  is similar to  $\alpha_1$  but with the indices 1 and 3 interchanged throughout. Even though these expressions appear somewhat complex, they have been abbreviated by using the quantities

$$\begin{aligned}
\xi_{21} &= \left[ \frac{m_1m_3}{(m_1 + m_3)I_e} \right]^{\frac{1}{2}} (z_{e1} - z_{e3}) \cos \gamma \\
&\quad + \left[ \frac{m_2(m_1 + m_2 + m_3)}{(m_1 + m_3)I_e} \right]^{\frac{1}{2}} z_{e2} \sin \gamma \\
\xi_{23} &= \left[ -\frac{m_1m_3}{(m_1 + m_3)I_e} \right]^{\frac{1}{2}} (z_{e1} - z_{e3}) \sin \gamma \\
&\quad + \left[ \frac{m_2(m_1 + m_2 + m_3)}{(m_1 + m_3)I_e} \right]^{\frac{1}{2}} z_{e2} \cos \gamma
\end{aligned} \tag{2-7}$$

$$\sin \gamma = \frac{1}{\sqrt{2}} \left[ 1 + \frac{(k'_1 - k'_3)^2}{4(k'_4)^2 + (k'_1 - k'_3)^2} \right]^{\frac{1}{2}}$$

The subscript  $e$  in  $z_{e1}$ ,  $z_{e2}$ , and  $z_{e3}$  indicates the equilibrium value of  $z_1$ ,  $z_2$ , and  $z_3$ .

$$\begin{aligned}
k'_1 &= \frac{m_1 + m_3}{m_1m_3} \left[ \frac{K_1m_3^2}{(m_1 + m_3)^2} + \frac{K_2m_1^2}{(m_1 + m_3)^2} + K_3 + \frac{2K_{12}m_1m_3}{(m_1 + m_3)^2} \right. \\
&\quad \left. + \frac{2K_{13}m_3}{m_1 + m_3} + \frac{2K_{23}m_1}{m_1 + m_3} \right]
\end{aligned}$$

$$k'_3 = \frac{m_1 + m_2 + m_3}{m_2(m_1 + m_3)} (K_1 + K_2 - 2K_{12})$$

$$\begin{aligned}
k'_4 &= \left( \frac{m_1 + m_2 + m_3}{m_1m_2m_3} \right)^{\frac{1}{2}} \left[ -\frac{K_1m_3}{m_1 + m_3} + \frac{K_2m_1}{m_1 + m_3} - \frac{K_{12}(m_1 - m_3)}{m_1 + m_3} \right. \\
&\quad \left. - K_{13} + K_{23} \right]
\end{aligned}$$

The frequencies are written as  $\omega_1$ ,  $\omega_2$ , and  $\omega_3$  to indicate as usual the ideal frequencies for infinitesimal vibrations. These do not in fact differ significantly from the observed frequencies of the lowest vibrational states,  $\nu_1$ ,  $\nu_2$ , and  $\nu_3$ . The frequencies  $\omega$  are all expressed in  $\text{cm}^{-1}$ , and  $B_e$  and the  $\alpha$ 's are in cycles per second.

There are so many potential constants involved in (2-6) that for no molecule of the form XYZ (such as OCS) have they yet been all evaluated so that the  $\alpha$ 's can be theoretically determined. However, if the tri-



atomic molecule is symmetric such as OCO (CO<sub>2</sub>), the potential constants and formulas simplify considerably [119], and one or two cases have been completely worked out from infrared measurements. There is, of course, no pure rotational spectrum for these symmetric linear molecules because the dipole moment is zero.

As in the case of diatomic molecules, the contributions to  $\alpha$  from the anharmonic force constants are usually larger than those from the harmonic potential terms. Thus the experimental values of  $\alpha_1$  and  $\alpha_3$  in all known cases are positive as a result of anharmonicities instead of negative as would be expected from a purely harmonic potential. From Table 2-1 it may be seen that  $\alpha_2$  is negative in cases which have been measured.

TABLE 2-1. MOLECULAR DIMENSIONS AND VIBRATION PARAMETERS OF SOME LINEAR TRIATOMIC MOLECULES\*

$l_1$  is the distance between the first two atoms and  $l_2$  that between the last two in the chemical formula.  $K_1$  and  $K_2$ , the force constants corresponding to stretching  $l_1$  or  $l_2$ , respectively, are evaluated under the assumption of valence forces only.

Molecule	$l_1$ , 10 <sup>-8</sup> cm	$l_2$ , 10 <sup>-8</sup> cm	$K_1$ , 10 <sup>5</sup> dynes/cm	$K_2$ , 10 <sup>5</sup> dynes/cm	$\nu_1$ , cm <sup>-1</sup>	$\nu_2$ , cm <sup>-1</sup>	$\nu_3$ , cm <sup>-1</sup>
H <sup>1</sup> C <sup>12</sup> N <sup>14</sup>	1.068	1.156	5.8	17.9	2089	712	3312
Cl <sup>35</sup> C <sup>12</sup> N <sup>14</sup>	1.629	1.163	5.2	16.7	729	397	2201
Br <sup>79</sup> C <sup>12</sup> N <sup>14</sup>	1.789	1.160	4.2	16.9	580	368	2187
I <sup>127</sup> C <sup>12</sup> N <sup>14</sup>	1.995	1.159	3.0	16.7	470	321	2158
O <sup>16</sup> C <sup>12</sup> S <sup>32</sup>	1.161	1.561	14.2	8.0	859	527	2079
N <sup>14</sup> N <sup>14</sup> O <sup>16</sup>	1.126	1.191	14.6	13.7	1285	589	2224

\* All data on force constants and frequencies are from Herzberg [130]. Internuclear distances come from microwave work (see Appendix VI).

The centrifugal stretching constant  $D$  has also been evaluated by Nielsen [119] as

$$D = 4B_e^3 \left( \frac{\xi_{21}^2}{c^2\omega_3^2} + \frac{\xi_{23}^2}{c^2\omega_1^2} \right) \quad (2-8)$$

where the  $\xi$ 's are defined in (2-7),  $\omega_1$  and  $\omega_3$  are in cm<sup>-1</sup>,  $B_e$  and  $D$  are in cycles per second. The centrifugal stretching of linear molecules is very small for most rotational lines in the microwave region, but not too small to be detected and measured. The calculated values of  $D$  assuming valence bond forces for several linear molecules are listed in Table 2-2 and compared with measured values.

*Coriolis Forces.* It may be at first surprising to note from (2-6) some terms which are "resonant." For example, the term in  $\alpha_2$  which is

$$- \frac{B_e^2(3\omega_2^2 + \omega_3^2)}{c\omega_2(\omega_2^2 - \omega_3^2)} \xi_{23}^2$$

would become very large if  $\omega_2$  were close to  $\omega_3$ . These terms are generally thought of as due to Coriolis forces, and represent a coupling of the modes of vibration  $\omega_2$  and  $\omega_3$  by Coriolis forces in the rotating molecule. The Coriolis force is a fictitious force which must be introduced if mechanical motion is studied in a rotating coordinate system and the rotation is otherwise overlooked. It has a value  $\mathbf{F} = 2\mathbf{v} \times \boldsymbol{\omega}$ , where  $\boldsymbol{\omega}$  is the vector angular velocity of rotation of the coordinate system and  $\mathbf{v}$  is the vector velocity of motion through the coordinate system.

A Coriolis force occurs in the case of a rotating and vibrating diatomic molecule as well as in the more complex case discussed here. As the rotating diatomic molecule stretches, its rotation is slowed down and as the molecule contracts its rotation is speeded up by Coriolis forces. Such changes in rotational velocity are often attributed simply to the law of conservation of angular momentum—as the molecule expands its moment of inertia increases and hence it must slow down in order to conserve angular momentum. This is not all, but it is a part of the origin of Coriolis forces, and the diatomic molecule may be regarded as subject to Coriolis forces which slightly change its rotation and give the “harmonic” contribution to the rotation-vibration interaction  $\alpha_e$  which is  $-6B_e^2/\omega_e$  [Eq. (1-28)].

TABLE 2-2. ROTATIONAL CONSTANTS AND DIPOLE MOMENTS OF SOME LINEAR POLYATOMIC MOLECULES

All rotational constants are given in megacycles.

Molecule	$B_0$	$\alpha_1$	$\alpha_2$	$\alpha_3$	$D$		$q_1$	$\mu$ , debyes or $10^{-18}$ esu	Reference
					Calcu- lated	Ob- served			
$\text{H}^{13}\text{C}^{12}\text{N}^{14}$	44,315.80	279	-21	324	0.065	0.10	224.47	3.00	[130] [532] [733] [803] [911] [997]
$\text{Cl}^{35}\text{C}^{12}\text{N}^{14}$	5,970.82	.....	-16.39	.....	0.00159	.....	7.50	2.80	[329] [528]
$\text{Br}^{79}\text{C}^{12}\text{N}^{14}$	4,120.19	15.54	-11.49	.....	0.000842	0.00091	3.91	2.94	[329] [531]
$\text{I}^{127}\text{C}^{12}\text{N}^{14}$	3,225.53	9.33	-9.50	.....	0.000626	0.00088	2.69	3.72	[329] [531]
$\text{O}^{16}\text{C}^{12}\text{S}^{32}$	6,081.48	20.5	-10.59	36.4	0.00128	0.00131	6.39	0.709	[329] [530] [946] [968]
$\text{O}^{16}\text{C}^{12}\text{Se}^{80}$	4,017.68	13.27	-6.92	.....	.....	0.00076	3.15	0.754	[418]
$\text{S}^{32}\text{C}^{12}\text{Se}^{80}$	2,017(?)	.....	.....	.....	.....	.....	.....	.....	[432]
$\text{S}^{32}\text{C}^{12}\text{Te}^{130}$	1,559.93	.....	-3.245	.....	.....	.....	0.660	0.17	[932]
$\text{N}^{14}\text{N}^{14}\text{O}^{16}$	12,561.64	51.6	-12.6	104	0.00524	0.0057	.....	0.166	[184] [528] [755] [915]
$\text{H}^{13}\text{C}^{12}\text{C}^{12}\text{C}^{135}$	5,684.24	.....	.....	.....	.....	.....	.....	0.44	[425]
$\text{H}^{13}\text{C}^{12}\text{C}^{12}\text{C}^{13}\text{N}^{14}$	4,549.07	.....	.....	.....	.....	.....	.....	3.6	[548]

For diatomic molecules, introduction of Coriolis forces seems an unnecessary complication. It is only for polyatomic molecules that the Coriolis-force approach is generally used, for there it is of real value in simplifying one's view of rotation-vibration interactions. Figure 2-2



shows the effect of Coriolis forces on a rotating linear triatomic molecule. It is evident that the vibration  $\omega_3$  excites some motion of the type  $\omega_2$ , and vice versa. This is the reason the resonance-type terms involving the difference between two frequencies are often called Coriolis terms. The other terms not involving anharmonic force constants or resonance denominators may also properly be called Coriolis terms, although they may be just as simply and correctly regarded as due to effects of harmonic vibration on the moment of inertia.

**2-2. *l*-Type Doubling.** Bending or perpendicular modes of oscillation in a linear polyatomic molecule are rather different from anything that occurs in a diatomic molecule, and they introduce a new phenomenon known as *l*-type doubling. If the molecule is not rotating, then it may bend in two perpendicular planes, say the  $xz$  plane and the  $yz$  plane, with exactly the same frequencies of oscillation. These are the two degenerate modes which have been considered to have the same rotation-vibration constant  $\alpha$ . However, if the molecule is rotating about the  $x$  axis, then bending in the  $xz$  plane is not quite equivalent to bending in the  $yz$  plane, the effective moments of inertia about the axis of rotation being different for the two cases. In addition it may be seen from Fig. 2-2

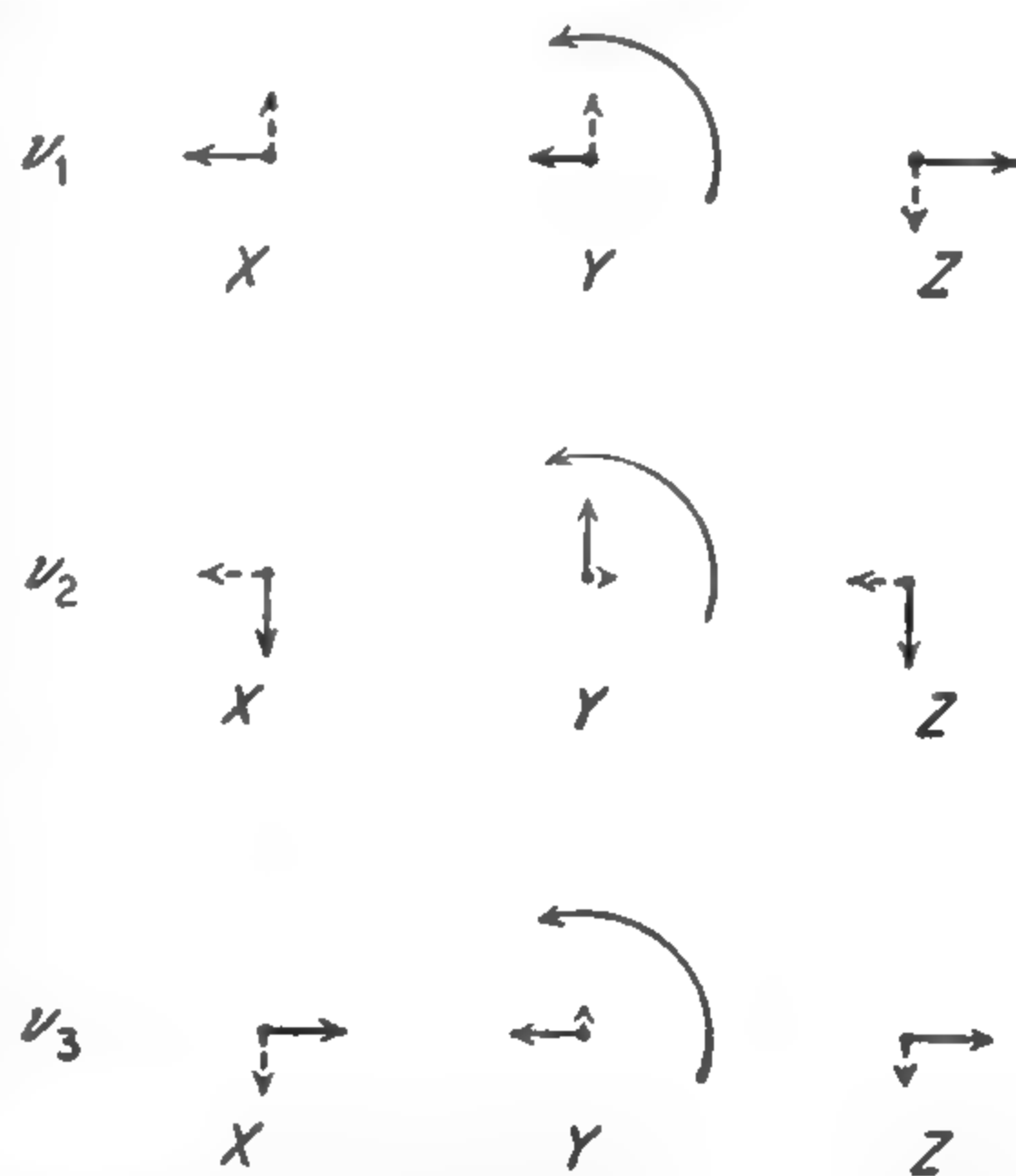


FIG. 2-2. Coriolis forces in a linear XYZ molecule. The curved arrows indicate direction of rotation. Solid straight arrows give the normal motion of the different modes of vibration, and dashed arrows indicate the Coriolis forces.

that, when the bending vibration is perpendicular to the angular momentum  $J$  of the molecule, the vibrational frequencies  $\nu_1$  and  $\nu_3$  are excited by Coriolis forces. However, when the bending motion is parallel to  $J$ , the Coriolis force  $2\mathbf{v} \times \boldsymbol{\omega}$  is zero and other vibration modes are not excited. Hence the two directions of vibration coupled with rotation give different energies also because of the different Coriolis forces. As a result of this vibration-rotation interaction, the two degenerate energy levels are slightly split, the splitting being called *l*-type doubling.

A more accurate description of *l*-type doubling and a calculation of the magnitude of the splitting must come from a quantum-mechanical treatment [120]. We start by considering a two-dimensional simple harmonic oscillator in the  $xy$  plane representing the two bending modes of equal frequency  $\omega$ . The oscillator may be studied in Cartesian coordinates and found to have various allowed energy levels  $(n_x + \frac{1}{2})h\nu$  for vibration along the  $x$  axis and similarly allowed energies  $(n_y + \frac{1}{2})h\nu$



for vibrations along the  $y$  axis. Here  $n_x$  and  $n_y$  are, of course, positive integers. The total energy  $W = (n_x + n_y + 1)h\nu$  does not uniquely determine the state of the oscillator since various combinations of  $n_x$  and  $n_y$  can give the same energy.

Considering the oscillator from a classical point of view, a proper phasing of the  $x$  and  $y$  motions will make the oscillator travel in a circle or ellipse and hence have an angular momentum. To discuss this angular momentum quantum-mechanically, it is appropriate to use cylindrical coordinates, specifying the state of the oscillator by its distance from the origin  $r$  and the angle  $\chi$  between  $r$  and the  $x$  axis. The wave equation may be solved in these coordinates, giving wave functions

$$\psi_{vl} = N_{vl} \rho^{|l|} e^{-\rho^2/2 + il\chi} F_{\frac{1}{2}(v+|l|)}^{(|l|)}(\rho^2) \quad (2-9)$$

$$\text{where } N_{vl} = 2 \frac{\left[ \left( \frac{v - |l|}{2} \right)! \right]^{\frac{1}{2}}}{\left[ \left( \frac{v + |l|}{2} \right)! \right]^{\frac{1}{2}}} \left( \frac{\pi m \nu}{h} \right)^{\frac{1}{2}}$$

$F_{\frac{1}{2}(v+|l|)}^{(|l|)}$  = an associated Laguerre polynomial

$$\rho = 2\pi \sqrt{m\nu/h} r$$

$m$  = mass of oscillator

The energy is given by  $h\nu(v + 1)$ , and the angular momentum  $l$  (in units of  $h/2\pi$ ) can take on only the values  $v, v - 2, v - 4, \dots, -v$ .

Similarly the linear molecule may have angular momentum about its axis as a result of vibration in one or more degenerate modes. This angular momentum affects the energies of rotation, making the molecule very similar to the symmetric-top molecules described in the next chapter with angular momentum about the symmetry axis. For a linear triatomic molecule where there is only one degenerate mode of vibration, the wave function for the molecule becomes

$$\psi_{vIJ} = \psi_{vl}(\rho, \chi) R_{Jl}(\theta, \phi) \quad (2-10)$$

where  $R_{Jl}$  = symmetric-top wave function discussed in Chap. 3

$$\rho = 2\pi \sqrt{\nu/h} (q_x^2 + q_y^2)^{\frac{1}{2}}, \text{ where } q_x \text{ and } q_y \text{ are normal coordinates for the two degenerate vibrations}$$

$$l = v, v - 2, v - 4, \dots, -v$$

The total angular momentum  $J$  cannot be less than the angular momentum  $l$  about the axis, or  $J \geq |l|$ . Except for the  $l$ -type doubling energy, the rotational energy is very similar to that for a symmetric top. However, the energy associated with rotation around the symmetry axis is normally attributed to vibration in this case,

$$W = h\nu_2(v + 1) + B_v[J(J + 1) - l^2] - D_v[J(J + 1) - l^2]^2 \quad (2-11)$$

Rotational frequencies are, according to (2-11),

$$\nu = 2B_v(J + 1) - 4D_v(J + 1)[(J + 1)^2 - l^2] \quad (2-12)$$

The energies given by (2-11), which are similar to those of a symmetric top, still do not include  $l$ -type doubling, but indicate a degeneracy between  $+l$  and  $-l$ . The  $l$ -type doubling is in many ways similar to the splitting of the symmetric-top energy levels by a slight asymmetry. Behavior of the vibrating linear molecule's wave functions and energy levels is exactly parallel to that of the slightly asymmetric rotor to be discussed in Chap. 4. The magnitude of splitting may even be approximately calculated from the crude model that the molecule is permanently bent by an amount equal to its average vibrational displacement, and by then treating it as an asymmetric rotor. The rather complete treatment of H. H. Nielsen ([402] and [624]) gives for the energy-level splitting when  $|l| = 1$

$$\frac{B_e^2}{\omega_2} \left( 1 + 4 \sum_i \xi_{2i}^2 \frac{\omega_2^2}{\omega_i^2 - \omega_2^2} \right) (v_2 + 1)J(J + 1) \quad (2-13)$$

where  $v_2$  = the quantum number for the degenerate vibration  $\omega_2$

$\omega_i'$  = a molecular vibrational frequency other than  $\omega_2$

$\xi_{2i}$  = certain Coriolis parameters of the molecule which are dependent on the masses, dimensions, and harmonic force constants of the molecule. For a linear triatomic molecule, they are given by (2-7).

The quantity

$$2 \frac{B_e^2}{\omega_2} \left( 1 + 4 \sum_i \xi_{2i}^2 \frac{\omega_2^2}{\omega_i^2 - \omega_2^2} \right)$$

may be abbreviated by  $q_l$ , the  $l$ -type doubling constant. In most cases  $4 \sum_i \xi_{2i}^2 [\omega_2^2 / (\omega_i^2 - \omega_2^2)]$  is near 0.3; so  $q_l$  is very approximately  $2.6B_e^2/\omega_2$ .

In the few cases where  $q$  has been fairly accurately calculated from the above expression, the values agree within a few per cent with measured values [505]. For  $l = 2$  or greater, the splitting is usually too small to observe, being of the order  $B(B/\omega_2)^l$ .

Allowing for the above splitting, expression (2-12) for the rotational frequencies is modified to

$$\nu = \left[ 2B_v \pm \frac{q_l}{2} (v_2 + 1) \right] (J + 1) - 4D(J + 1)[(J + 1)^2 - l^2] \quad (2-14)$$

where, of course,

$$B_v = B_e - \alpha_1(v_1 + \frac{1}{2}) - \alpha_2(v_2 + 1) - \alpha_3(v_3 + \frac{1}{2})$$

The above discussion may be readily extended to linear molecules involving more than three atoms, and hence more than one pair of degenerate vibrations.

Introduction of an angular momentum  $l$  about the molecular axis due to vibration affects not only the energy levels but also the intensities.

The dipole matrix elements are similar to those for symmetric and slightly asymmetric rotors to be discussed in following chapters. For any value of  $J$ , the energy level of these degenerate states may be specified by  $l$  and a subscript 1 or 2 indicating, respectively, the lower or upper of the two split states. Allowed transitions of the following types occur

$$\left. \begin{array}{l} J + 1, l_1 \leftarrow J, l_1 \\ J + 1, l_2 \leftarrow J, l_2 \end{array} \right\} |\mu_{ij}|^2 = \mu^2 \frac{(J + 1)^2 - l^2}{(J + 1)(2J + 1)} \quad (2-15)$$

$$J, l_2 \leftarrow J, l_1 \quad |\mu_{ij}|^2 = \mu^2 \frac{l^2}{(J + 1)(2J + 1)} \quad (2-16)$$

where  $\mu_{ij}$  is the dipole matrix element between the two states from which intensities may be computed according to (1-49) and  $\mu$  is the molecular dipole moment. If the molecular states are designated by asymmetric-top rotation (Chap. 4), the state  $J, l_1$  becomes  $J_{|l|, J+1-|l|}$  and  $J, l_2$  is  $J_{|l|, J-|l|}$ . The dipole matrix elements for transitions between these levels are identical with those for a slightly asymmetric top.

A type of transition with  $\Delta J = 0$  is indicated by (2-16) which cannot occur when  $l = 0$ . The frequency of such transitions, from (2-13), is

$$\nu = \frac{q_l}{2} (v_2 + 1) J(J + 1) \quad (2-17)$$

which is a rather low frequency for many molecules unless  $J$  is very large. However, Shulman and Townes [505] showed that for HCN  $q_l$  is so large that these transitions occur in the microwave region for moderate values of  $J$ . The observed frequencies for a series of these lines are given in Table 2-3. It may be noted that  $q_l$  is not accurately

TABLE 2-3. OBSERVED LINES IN HCN AND VALUES OF  $l$ -TYPE DOUBLING CONSTANT  $q_l$   
(After Westerkamp [997])

$J$	Frequency, Mc	$q_l = \text{frequency}/J(J + 1)$ , Mc
6	9,423.3	224.365
8	16,147.8	224.274
9	20,181.4	224.238
10	24,660.4	224.185
11	29,585.1	224.129
12	34,953.5	224.061

constant but decreases with increasing  $J$  by an amount which is of the order  $q_l(B/\omega_2)^2 J(J + 1)$  ([529], [547], [997]). A small variation in  $q_l$  of this type may be expected in analogy with the expansion of all rotational constants in powers of  $B/\omega$ , and has been justified by H. H. Nielsen [505].

Major features of the rotation-vibration spectrum of a linear molecule have now been described. They are illustrated in Fig. 2-3, which is the



$J = 2 \leftarrow 1$  transition of OCS. Each vibrational mode produces a series of lines of exponentially decreasing intensity. The degenerate mode shows  $l$ -type doubling when  $|l| = 1$ . Larger values of  $|l|$  cannot occur in this transition, since  $|l|$  must be less than  $J$ .

**2-3. Perturbations between Vibrational States—Fermi Resonance.** Ordinarily, the values of  $\alpha$  may be determined from the separation between lines of two adjacent vibrational states. Thus the frequency difference between the ground state (000) and the excited state (100) in the  $J = 2 \leftarrow 1$  transition shown in Fig. 2-3 should equal  $4\alpha_1$ . Similarly

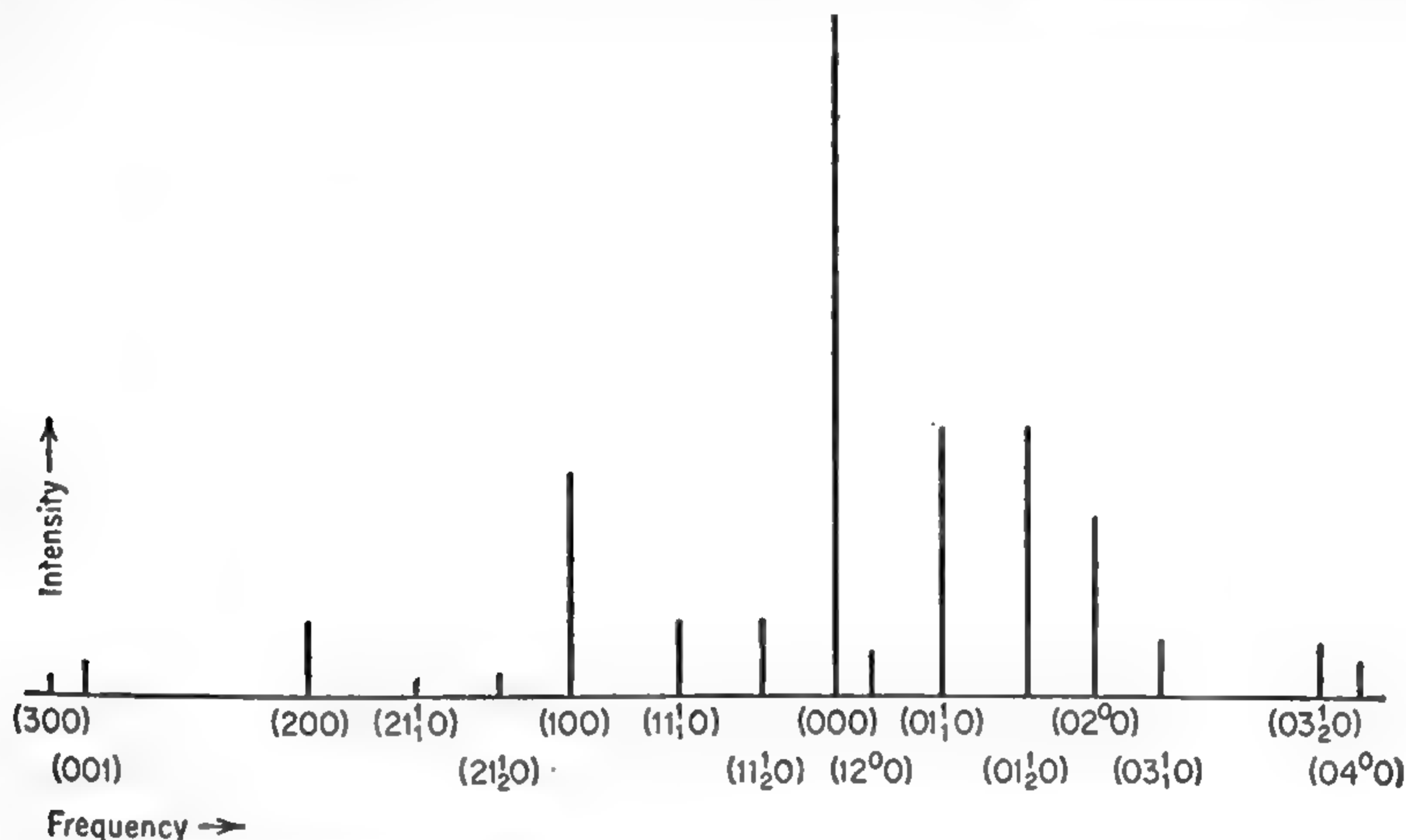


FIG. 2-3. Rotational transition  $J = 2 \leftarrow 1$  in OCS showing excited vibrational states and  $l$ -type doubling. The vibrational state is given by vibrational quantum numbers in brackets ( $v_1 v_2 v_3$ ),  $v_2$  having a superscript  $|l|$ . In case  $|l| = 1$ , a subscript 1 is applied to the lower-frequency component of the  $l$ -type doublet, and 2 to the higher-frequency component. Intensities of excited states in this figure are much larger than normal, being appropriate for a temperature of  $800^\circ\text{C}$ .

the frequency difference between (000) and the center of the two  $l$ -type doublets ( $01_1^1 0$ ) and ( $01_2^1 0$ ) should equal  $4\alpha_2$ . In most cases this is a satisfactory method of determining the  $\alpha$ 's. If higher excited vibrational states are observed, they also allow determination of the  $\alpha$ 's. The frequency difference between (000) and ( $02^0 0$ ) for a  $J = 2 \leftarrow 1$  transition should according to (2-14) give  $8\alpha_2$ , except for very small correction terms similar to  $Y_{21}$  in (1-29) or (1-32). However, in all polyatomic molecules there are perturbations between vibrational states which shift the energy levels, destroy the regularity predicted by (2-14), and make somewhat inaccurate the values of the  $\alpha$ 's obtained from simple application of this formula. Perturbations between vibrational states were first noticed in  $\text{CO}_2$ , and are generally called "Fermi resonance" effects because they were explained by Fermi as due to interaction between two states of nearly the same energy.

“Fermi resonance” effects on the rotational spectrum of OCS are rather prominent, and may be seen from Fig. 2-4, which illustrates the  $J = 3 \leftarrow 2$  transition. In this figure, the  $(02^00)$  line is displaced from the ground state  $(000)$  less than twice as much as the center of the two lines  $(01\frac{1}{2}0)$  and  $(01\frac{1}{2}0)$ . In addition, the  $(02^00)$  line does not coincide with the center of the unsplit doublet  $(02^20)$ . According to (2-14), these should differ only by the very small quantity  $16D(J+1)$ . Separation between  $(02^00)$  and  $(02^20)$  illustrates the fact that these perturbation interactions depend not just on the energies of vibration, but also on symmetry properties.

The lower vibrational levels of OCS are shown in Fig. 2-5 with possible interactions between adjacent vibrational levels. If the molecular potential were purely harmonic, then it could be written in normal coordinates

$$V = \frac{k_1}{2} q_1^2 + \frac{k_2}{2} q_2^2 + \frac{k_3}{2} q_3^2$$

and there would be no interaction between the various normal coordinates or vibrations. However, there are anharmonic terms in the potential (2-5) which couple the various normal modes. Thus a term such as  $k_{122}q_1q_2^2$  from (2-5) allows a variation of  $q_1$  to affect the behavior of  $q_2$  or vice versa.

Let  $\psi_n^0$  represent the molecular wave function for a vibrational level with quantum numbers  $v_1, v_2, v_3$ , and  $|l|$  when the anharmonic potential terms causing interactions between modes are omitted. Then these interactions may be taken into account by the usual quantum-mechanical perturbation theory. If the initial energies are  $W_n^0$ , the perturbed energies  $W$  are found by solving a determinant of the form:

$$\begin{vmatrix} W_1^0 - W & W_{21} & W_{31} & \dots \\ W_{12} & W_2^0 - W & W_{32} & \dots \\ W_{13} & W_{23} & W_3^0 - W & \dots \\ \dots & \dots & \dots & \dots \end{vmatrix} = 0 \quad (2-18)$$

where  $W_{ni} = \int \psi_n^* V_{\text{anh}} \psi_i d\tau$

$$V_{\text{anh}} = k_{113}q_1^2q_3 + k_{133}q_1q_3^2 + k_{122}q_1q_2^2 + k_{322}q_3q_2^2 + \dots$$

is the anharmonic perturbing potential. Since  $V_{\text{anh}}$  does not contain any of the angular coordinates  $\theta, \phi$ , or  $\chi$  indicating the molecular orientation,  $W_{ni}$  will be zero unless states  $n$  and  $i$  have the same dependence on  $\theta, \phi$ , and  $\chi$ , or hence have the same angular-momenta quantum numbers. This is connected with the fact that internal motions of the molecule cannot change its angular momentum. For a given vibrational state, any arbitrary total angular momentum  $J$  and magnetic quantum number  $M$  may be found (unless  $J < |l|$ ). However, any value of  $|l|$  cannot be

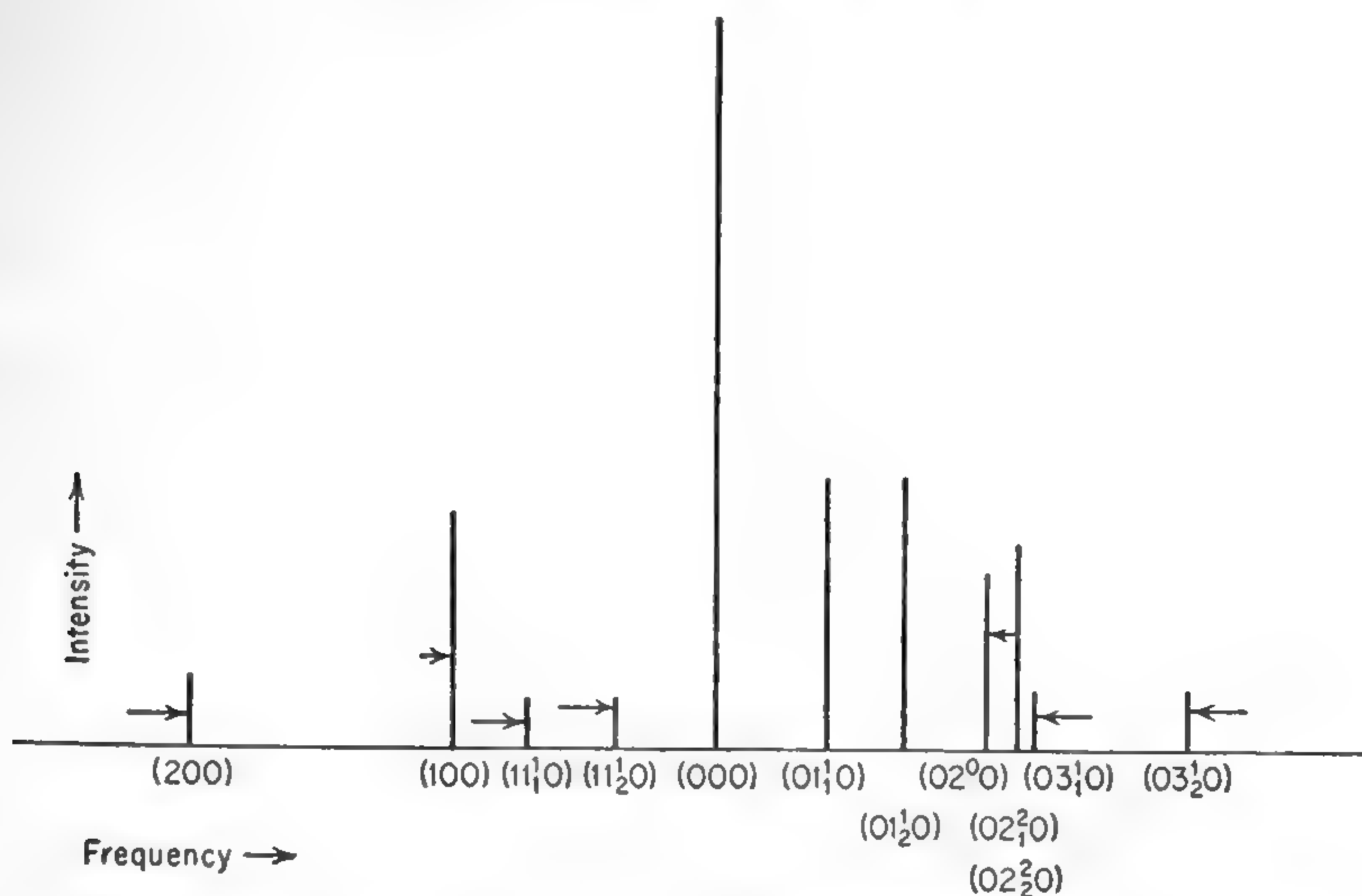


FIG. 2-4. Rotational transition  $J = 3 \leftarrow 2$  of OCS showing shifts in rotational frequencies due to perturbations. The arrows indicate the effects of "Fermi resonance" perturbations. Notation is the same as for Fig. 2-3.

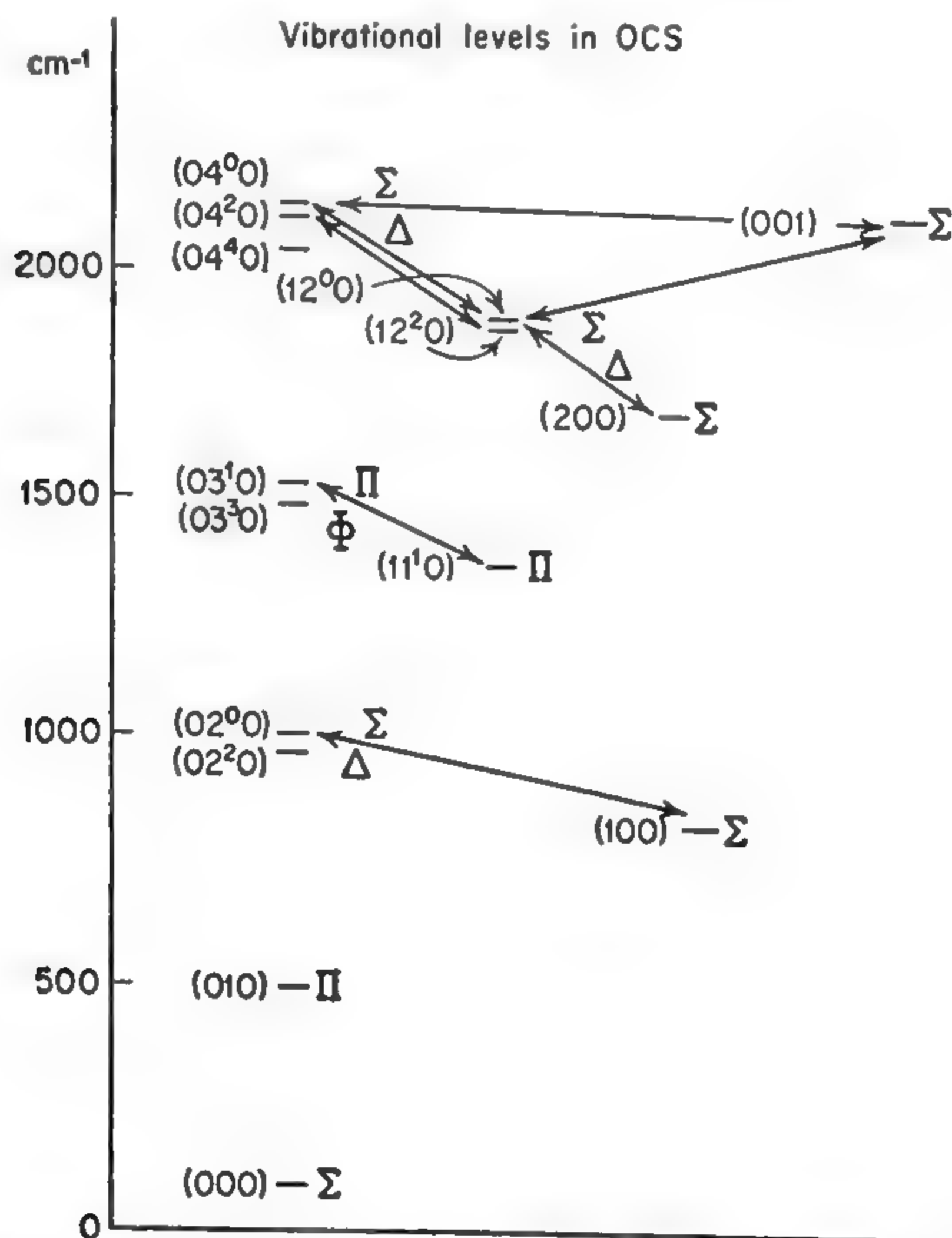


FIG. 2-5. Vibrational levels in OCS. Lines indicate possible interaction between nearby vibrational levels.



found, since a vibrational state is characterized by a particular value  $|l|$  of the angular momentum about the symmetry axis. The value of  $|l|$  is indicated in Fig. 2-5 by superscripts. It is also given in standard molecular notation by Greek letters, where  $\Sigma$ ,  $\Pi$ ,  $\Delta$ ,  $\Phi$ , and  $\Gamma$  represent values of  $|l| = 0, 1, 2, 3, 4$ , respectively. Only states of the same  $l$  can perturb each other, since otherwise  $W_{ni}$  is zero.

The perturbations which are most effective in changing the energies and wave functions are those between states which have nearly the same energy. The arrows in Fig. 2-5 indicate such nearby vibrational states which may perturb each other. These are mostly pairs of levels of the type  $(v_1, v_2^{||}, v_3)$  and  $(v_1 - 1, v_2 + 2^{||}, v_3)$ . Indicating such a pair of states by subscripts 1 and 2, respectively, the determinant (2-18) may be factored into a number of determinants of the type

$$\begin{vmatrix} W_1^0 - W & W_{21} \\ W_{12} & W_2^0 - W \end{vmatrix} \quad (2-19)$$

where  $W_{12} = \int \psi_{v_1 v_2 v_3}^* V_{\text{anh}} \psi_{v_1-1, v_2+2, v_3} d\tau$

The only nonvanishing term of  $V_{\text{anh}}$  after integration is

$$W_{12} = k_{122} \int \psi_{v_1 v_2 v_3}^* q_1 q_2^2 \psi_{v_1-1, v_2+2, v_3} d\tau \quad (2-20)$$

Since vibrational wave functions for simple harmonic motion are well known ([62], p. 74), (2-20) may be evaluated as

$$W_{12} = - \frac{h^{\frac{1}{2}} v_1^{\frac{1}{2}} [(v_2 + 2)^2 - l^2]^{\frac{1}{2}}}{16 \sqrt{2} \pi^{\frac{1}{2}} c^{\frac{1}{2}} \omega_1^{\frac{1}{2}} \omega_2^{\frac{1}{2}}} k_{122} \quad (2-21)$$

The perturbed energies are, from (2-19),

$$W = \frac{W_1^0 + W_2^0 \pm \sqrt{\delta^2 + 4|W_{12}|^2}}{2} \quad (2-22)$$

where  $\delta = W_1^0 - W_2^0$ . The perturbed wave functions  $\psi_1$  and  $\psi_2$  are combinations of the unperturbed wave functions  $\psi_1^0$  and  $\psi_2^0$

$$\psi_1 = a\psi_1^0 - b\psi_2^0 \quad \psi_2 = b\psi_1^0 + a\psi_2^0 \quad (2-23)$$

where

$$\begin{aligned} a &= \left( \frac{\sqrt{\delta^2 + 4|W_{12}|^2} + \delta}{2 \sqrt{\delta^2 + 4|W_{12}|^2}} \right)^{\frac{1}{2}} \\ b &= \left( \frac{\sqrt{\delta^2 + 4|W_{12}|^2} - \delta}{2 \sqrt{\delta^2 + 4|W_{12}|^2}} \right)^{\frac{1}{2}} \end{aligned} \quad (2-24)$$

If the rotational constant is expressed as an expansion in the normal coordinates,

$$B = B_0 + \sum_i q_i B'_i + \sum_{i,j} q_i q_j B''_{ij} + \dots$$

The effective value of  $B$  for a particular vibrational state  $(v_1 v_2 v_3)$  may be evaluated as

$$B_v = \int \psi_{v_1 v_2 v_3}^* B \psi_{v_1 v_2 v_3} d\tau = B_e + B_{11}'' \int \psi_{v_1 v_2 v_3}^* q_1^2 \psi_{v_1 v_2 v_3} d\tau + B_{22}'' \int \psi_{v_1 v_2 v_3}^* q_2^2 \psi_{v_1 v_2 v_3} d\tau + B_{33}'' \int \psi_{v_1 v_2 v_3}^* q_3^2 \psi_{v_1 v_2 v_3} d\tau$$

since all other terms of second or lower order in the  $q$ 's are identically zero. Now  $\int \psi_{v_1 v_2 v_3}^* q_i^2 \psi_{v_1 v_2 v_3} d\tau$  is proportional to the energy of oscillation of the  $i$ th mode; hence one may also write

$$B_v = B_e - \alpha_1(v_1 + \frac{1}{2}) - \alpha_2(v_2 + 1) - \alpha_3(v_3 + \frac{1}{2})$$

where, for example,

$$-\alpha_1(v_1 + \frac{1}{2}) = B_{11}'' \int \psi_{v_1 v_2 v_3}^* q_1^2 \psi_{v_1 v_2 v_3} d\tau$$

The effective value of  $B$  may be similarly evaluated for the perturbed wave function  $\psi_1 = a\psi_1^0 + b\psi_2^0$  and shown to be

$$B_1 = a^2 B_1^0 + b^2 B_2^0 = B_e + a^2(B_1^0 - B_e) + b^2(B_2^0 - B_e) \quad (2-25)$$

where  $B_1^0$  and  $B_2^0$  are the appropriate values of  $B$  for the unperturbed states  $\psi_1^0$  and  $\psi_2^0$ , respectively. The deviation of  $B$  from the equilibrium value  $B_e$  due to vibrations is thus intermediate between the deviation for the two unperturbed states. The sum of the  $B$  values for the two states does not change, that is,

$$B_1 + B_2 = B_1^0 + B_2^0 \quad (2-26)$$

since  $a^2 + b^2 = 1$ .

For various excited vibrational levels of OCS, Table 2-3 indicates the importance of perturbations in the rotational transitions  $J = 2 \leftarrow 1$  and  $J = 3 \leftarrow 2$ . Since  $\alpha_1$  and  $\alpha_2$  are rather different, even a small perturbation between pairs of vibrational states  $(v_1, v_2^{||}, v_3)$  and  $(v_1 - 1, v_2 + 2^{||}, v_3)$  can appreciably affect the rotational frequencies. From infrared measurements of vibrational frequencies [54] the separation between the ideal unperturbed states (100) and (020) may be determined as  $165 \text{ cm}^{-1}$ . The unperturbed value of  $\alpha_2$  may be obtained from the separation between rotational levels for the (000) and (01<sup>1</sup>0) states in Table 2-3. The frequency change due to perturbation of the (02<sup>0</sup>0) state may be then obtained from the known value of  $\alpha_2$ . The frequency change of the (10<sup>0</sup>0) state must be just equal to this but of opposite sign to satisfy (2-26) so that the unperturbed value of  $\alpha_1$  may be determined. From (2-25) the value of  $a^2$  and  $b^2$  for the (10<sup>0</sup>0) state can then be obtained as 0.944 and 0.056, respectively. The interaction energy  $W_{12}(v_1 = 1, v_2 = 0)$  is then evaluated from (2-24) as  $43 \text{ cm}^{-1}$ . This quantity, combined with  $\delta$ ,

$\alpha_1$ , and  $\alpha_2$ , allows prediction of the shift for all other excited states listed in Table 2-3.

Perturbation effects have also been found in  $\text{CO}_2$ ,  $\text{OCSe}$ , and  $\text{BrCN}$ , for which  $W_{12}(v_1 = 1, v_2 = 0)$  is 50.4, 46, and 60.5  $\text{cm}^{-1}$ , respectively.

TABLE 2-4. "FERMI RESONANCE" PERTURBATIONS IN THE ROTATIONAL SPECTRUM OF OCS

Perturbation corrections are calculated from the values  $\delta = 165 \text{ cm}^{-1}$ ,

$$W_{12}(v_1 = 1, v_2 = 0) = 43 \text{ cm}^{-1},$$

$\alpha_1 = 20.5 \text{ Mc}$ ,  $\alpha_2 = -10.59 \text{ Mc}$ . Pairs of interacting vibrational states are bracketed.

Rotational transition	Vibrational state $v_1 v_2^{l_1} v_3$	Observed frequency (center of $l$ -type doublets where doubling is present), Mc	Correction for perturbations, Mc
$J = 2 \leftarrow 1$	0 0 <sup>0</sup> 0	24,325.92	0
	0 1 <sup>1</sup> 0	24,368.17	0
	{ 1 0 <sup>0</sup> 0	24,253.44	-9.42
	{ 0 2 <sup>0</sup> 0	24,401.0	+9.42
	{ 2 0 <sup>0</sup> 0	24,179.62	-17.54
	{ 1 2 <sup>0</sup> 0	.....	+17.54
	{ 1 1 <sup>1</sup> 0	24,303.4	-17.15
	{ 0 3 <sup>1</sup> 0	24,435	+17.15
$J = 3 \leftarrow 2$	0 0 <sup>0</sup> 0	36,488.82	0
	0 1 <sup>1</sup> 0	36,551.7	0
	0 2 <sup>2</sup> 0	36,615.3	0
	{ 1 0 <sup>0</sup> 0	.....	-14.83
	{ 0 2 <sup>0</sup> 0	36,600.8	+14.83

2-4. Moments of Inertia and Internuclear Distances. The most obvious quantity determined by measurement of the rotational spectrum of a linear molecule is its rotational constant  $B$ , and consequently its effective moment of inertia  $J = h/8\pi^2 B$ . If vibrational motions of the molecule are negligible, as they are to a certain approximation in the ground vibrational state, and if all atomic masses are considered as concentrated at the atomic nuclei, then the molecular moment of inertia is dependent only on internuclear distances and atomic masses. A linear molecule of three atoms with masses  $m_1$ ,  $m_2$ , and  $m_3$  has a moment of inertia about its center of mass

$$I = \frac{m_1 m_2 l_{12}^2 + m_1 m_3 l_{13}^2 + m_2 m_3 l_{23}^2}{m_1 + m_2 + m_3} \tag{2-27}$$

where  $l_{ij}$  represents the distance between masses  $m_i$  and  $m_j$ . Moments of inertia of the more general linear molecule of an arbitrary number of



point masses may be found from a similar formula

$$I = \frac{\frac{1}{2} \sum_j \sum_i m_i m_j l_{ij}^2}{\sum_i m_i} \quad (2-28)$$

Expression (2-28) is correct, in fact, for the moment of inertia of any planar molecule about an axis through its center of mass and perpendicular to the plane of the molecule.

If the atomic masses are assumed known, the moment of inertia of a linear molecule of  $n$  atoms contains  $n - 1$  unknown distances (there are obvious relations between some of the  $l_{ij}$ 's for a linear molecule). For a diatomic molecule, a measurement of  $I$  would immediately allow determination of the one unknown distance. In the case of a linear molecule of  $n$  atoms, rotational spectra from  $n - 1$  different isotopic species, giving values of  $I$  for which the known masses are different but the unknown distances are not varied, are needed to determine all the internuclear distances.

Fortunately, it is usually easy to obtain moments of inertia of several isotopic species of polyatomic molecules. Measurements of effective moments of inertia can be made to very high precision, so that the measurements themselves usually offer no bar to very accurate determination of internuclear distances. The one serious limitation to easy attainment of extremely accurate internuclear distances for polyatomic molecules from microwave measurements is the occurrence of rotation-vibration interactions which were provisionally neglected above. Expressions (2-27) and (2-28) apply simply to the molecule if all atoms are at rest in their equilibrium positions, in which case they give the equilibrium moments of inertia  $I_e$ . What is actually measured is a reciprocal of the moment of inertia averaged over the ground vibrational state, or  $B_0$ .  $B_0$  differs from the equilibrium value  $B_e$  by  $-\frac{1}{2} \sum_i \alpha_i$ . The  $\alpha_i$  may depend in a rather complex way on the potential constants and masses, as is evident for the triatomic molecule from (2-6).

Although for the diatomic molecule evaluation of  $\alpha$  and allowance for it are easily made, in polyatomic molecules it is rarely practical to measure all the  $\alpha$ 's and determine their dependence on the various isotopic masses. Usually various isotopic values of  $B_0$  are measured and assumed to be equivalent to values of  $B_e$ , so that internuclear distances may be evaluated from (2-28). The errors resulting from neglect of the  $\alpha$ 's, or zero-point vibration, must be accepted as the primary limit on the accuracy of distances obtained. In the case of OCS, a large number of isotopic species have been measured, so that the two internuclear distances may be determined from various pairs of isotopic combinations.

The results of this procedure are shown in Table 2-5. Discrepancies between the various determinations in Table 2-5 are due primarily to the neglected zero-point vibrations.

Although Table 2-5 illustrates the usual size of errors due to neglect of zero-point vibrations, they can in some cases be considerably larger or considerably smaller. The linear molecule NNO affords an example where serious errors in internuclear distances can be made if the wrong isotopic species are used for their determination. The central nitrogen is very near the center of gravity of the molecule, and hence changing its mass from  $N^{14}$  to  $N^{15}$  might be expected to have a very small effect on the moment of inertia about the center of mass, or on  $B_e$ . However, a change in mass of the central nitrogen can rather markedly affect the vibrational frequencies and hence change the rotation-vibration interaction  $-\frac{1}{2} \sum_i \alpha_i$ . In fact, experimentally the rotational transitions of  $N^{14}N^{15}O^{16}$  are found to occur at higher frequencies than those for  $N^{14}N^{14}O^{16}$  [357]. If rotation-vibration interactions are neglected, this would indicate that an increase in mass of the central nitrogen had decreased the moment of inertia, which is clearly impossible from (2-27). A solution for the internuclear distances from the measured frequencies for  $N^{14}N^{15}O^{16}$  and  $N^{14}N^{14}O^{16}$  yields the interesting result that one of the internuclear distances is imaginary. This is obviously an extreme case, and one which can be remedied by using isotopic species involving a change of mass of the end nitrogen or of the oxygen. Then, even though the rotation-vibration interactions are changed by these isotopic substitutions, the equilibrium moment of inertia is changed appreciably and the effects of vibrations represent only small fractional errors in the observed isotopic effects. The internuclear distances given for  $N_2O$  in Table 2-1 were obtained from the pair  $N^{14}N^{14}O^{16}$  and  $N^{15}N^{14}O^{16}$ .

TABLE 2-5. INTERNUCLEAR DISTANCES IN OCS CALCULATED FROM VARIOUS ISOTOPIC PAIRS [329]

Zero-point vibrations are neglected, and are the main source of discrepancies between the different values.

Pair of isotopic molecules used	O—C distance, angstroms	C—S distance, angstroms
$O^{16}C^{12}S^{32}$ , $O^{16}C^{12}S^{34}$	1.1647	1.5576
$O^{16}C^{12}S^{32}$ , $O^{16}C^{13}S^{32}$	1.1629	1.5591
$O^{16}C^{12}S^{34}$ , $O^{16}C^{13}S^{34}$	1.1625	1.5594
$O^{16}C^{12}S^{32}$ , $O^{18}C^{12}S^{32}$	1.1552	1.5653

**2-5. Determination of Nuclear Masses.** For a polyatomic linear molecule of  $n$  atoms,  $n - 1$  isotopic species must be measured to determine the internuclear distances. If additional isotopic species are measured,



the measurements should allow accurate determination of mass ratios, assuming zero-point vibrations can be neglected. In OCS, for example, at least 11 different isotopic species have been measured.

It might at first be thought that two different sulfur isotopes can be used to determine the two unknown distances and that then measurement of moments of inertia for more than one C or O isotope should allow their mass ratios to be determined. Since frequency changes due to isotopic substitution are characteristically of the order of a few hundred megacycles, and frequencies can be measured to an accuracy of a few kilocycles, an accuracy of approximately  $10^{-5}$  mass unit might be expected. A look at Table 2-4, however, provides a quick disillusionment. Because of zero-point vibrations, the internuclear distances are not known to better than 1 part in  $10^3$ , so that the accuracy in mass ratios obtainable by this general method would not be very worthwhile.

In spite of the inaccurate determination of internuclear distances, there is a fairly general way of using the very accurate measurements of microwave spectroscopy to obtain accurate mass information. If rotational frequencies for three isotopes of the same element in one molecule are measured, and if masses of two of these isotopes are known, then the mass of the third isotope can usually be determined with an accuracy comparable with or better than that achieved by more standard methods. Use of two isotopes of known masses might be regarded as a "calibration" of the isotopic shift in the molecule and the effect of zero-point vibrations so that the mass of a third isotope may be determined.

This process of "calibration" with two known isotopic masses can be made exact if zero-point vibrations are negligible, without requiring detailed knowledge of the structure and internuclear distances of the molecule.

The moment of inertia through the center of gravity of a molecule and along a particular direction defined as the  $z$  axis of the molecule may be written

$$I_0 = \sum_i m_i(x_i^2 + y_i^2) \quad (2-29)$$

where  $m_i$  is the mass of the  $i$ th atom, and  $x_i^2 + y_i^2$  is the square of its distance from the axis. If the mass of the  $n$ th atom is changed an amount  $\Delta m$ , by making an isotopic substitution, the new moment of inertia through the new center of mass about an axis parallel to  $z$  is

$$I_1 = I_0 + \frac{\Delta m_1 M_0 (x_n^2 + y_n^2)}{\Delta m_1 + M_0} \quad (2-30)$$

where  $M_0$  is  $\sum_i m_i$ , the total mass of the original molecule before isotopic substitution and  $x_n^2 + y_n^2$  is the square of the distance from the  $n$ th atom to the center of mass of the original molecule. Equation (2-30) results



from the fact that the moment of inertia of an extended body about any axis is the sum of its moment of inertia about a parallel axis through the center of gravity and the moment of inertia of a point mass of equal magnitude placed at its center of gravity. If the mass of the  $n$ th atom had been changed by an amount  $\Delta m_2$ , the new moment of inertia would have been

$$I_2 = I_0 + \frac{\Delta m_2 M_0}{\Delta m_2 + M_0} (x_n^2 + y_n^2) \quad (2-31)$$

Combining (2-29), (2-30), and (2-31),

$$\frac{I_1 - I_0}{I_2 - I_0} = \frac{M_2}{M_1} \left( \frac{\Delta m_1}{\Delta m_2} \right) \quad (2-32)$$

where  $M_1$  and  $M_2$  are the total masses  $\Delta m_1 + M_0$  and  $\Delta m_2 + M_0$ , respectively, for the two isotopic substitutions. Since the moments of inertia are inversely proportional to the rotational constants, which are the quantities actually measured, (2-32) may more conveniently be written

$$\frac{\Delta m_1}{\Delta m_2} = \frac{m_1 - m_0}{m_2 - m_0} = \frac{M_1 B^{(2)} (B^{(0)} - B^{(1)})}{M_2 B^{(1)} (B^{(0)} - B^{(2)})} \quad (2-33)$$

Here  $m_0$  represents the original mass of the elements being isotopically replaced,  $m_1$  and  $m_2$  the first and second replacements,  $B^{(0)}$ ,  $B^{(1)}$  and  $B^{(2)}$  the corresponding values of the rotational constants. Evidently if  $m_1$  and  $m_2$  are known,  $m_0$  may be determined from a measurement of the rotational frequencies. About all that need be known of the molecule is the total mass of other atoms which it contains. It should be clear from the derivation that (2-32) or (2-33) holds not only for linear molecules, but for any type as long as the moments of inertia or rotational constants are appropriate for an axis fixed in direction with respect to the molecule. If two isotopic masses are not accurately known, but their mass difference is known, then mass differences between them and other isotopes may be obtained from (2-33).

Expression (2-33) is strictly correct only if the equilibrium values of the  $B$ 's are used. However, if the rotational constants  $B_0$  for the ground state are used in (2-33), it still gives the mass difference ratios to very good accuracy. Since the equilibrium values for  $B$  are seldom obtainable, masses are generally obtained from (2-33) by using the ground-state rotational constants. Various mass difference ratios obtained from (2-33) are compared with those obtained by other methods in Table 2-5. The errors listed for the microwave data are primarily due to zero-point vibrations or to the use of  $B_0$  rather than  $B_e$ , and their magnitudes will be discussed below [456]. Figure 2-6 shows a curve of Se masses found by microwave measurements, and calculated by assuming values for the two masses,  $\text{Se}^{76}$  and  $\text{Se}^{80}$ . This curve shows quite clearly the odd-even mass

variation, or the difference in nuclear mass behavior between odd and even isotopes. Although some errors may occur in the shape of the curve due to zero-point vibrations, these errors are unimportant in determining the odd-even mass variation. The even masses establish a smooth curve, and the odd-even mass variation is obtained simply by observing how far off of this curve the odd isotopes  $\text{Se}^{75}$ ,  $\text{Se}^{77}$ , and  $\text{Se}^{79}$  occur.

We turn now to an examination of the errors in mass determinations caused by zero-point vibrations. The rotational constants usually

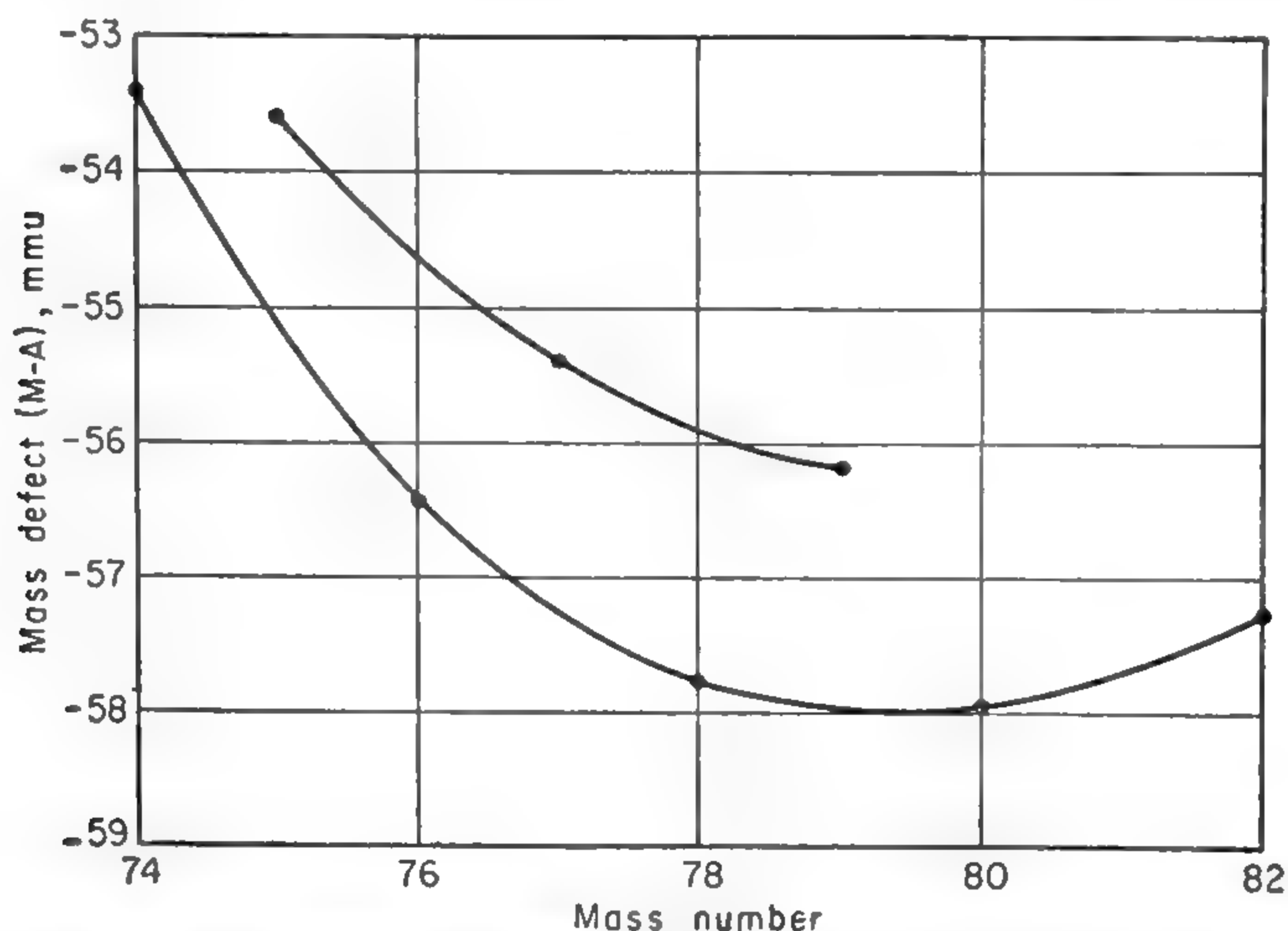


FIG. 2-6. Variation of masses of the stable Se isotopes as a function of mass number. The experimental masses are determined after assuming values for the two masses  $\text{Se}^{76}$  and  $\text{Se}^{80}$ . Note that  $\text{Se}^{75}$ ,  $\text{Se}^{77}$ , and  $\text{Se}^{79}$ , having odd mass numbers, fall considerably above the curve established by the even isotopes. (From Geschwind, Gunther-Mohr, and Townes [924a].)

inserted in (2-33) are those for the ground vibrational state. For a particular isotopic species, this corresponds to  $B_0 = B_e - \frac{1}{2} \sum_i \alpha_i$ , where  $\alpha_i$  is the rotation-vibration interaction for the  $i$ th vibrational mode. This sum is abbreviated in the subsequent discussion to  $\alpha = \sum_i \alpha_i$ .

From (2-33) it is evident that, if  $\alpha$  has the same dependence on mass variation as does  $B_e$ , then no error is introduced in the mass difference ratio  $(m_1 - m_0)/(m_2 - m_0)$ , for then the ratios of  $B$ 's are the same regardless of whether the  $B_e$ 's or the  $B_0$ 's are used. Since  $\alpha$  and  $B_e$  both vary in an approximately linear way for small fractional changes in mass, and since  $\alpha$  is much smaller than  $B_e$  in any case, the error introduced by  $\alpha$  is usually not large. If  $B_e$  is changed an amount  $\Delta\nu$  due to an isotopic change, then the zero-point vibration effects will be changed by an amount roughly proportional, or  $\alpha\Delta\nu/2B$ . As long as this change

is linearly proportional to  $\Delta\nu$  or to the change in mass  $\Delta m$ , no great errors will result. However, an error due to nonlinear dependence of  $\alpha$  on  $\Delta m$  will occur of magnitude approximately  $\delta = (\alpha_e/2B) \Delta\nu (\Delta m/m)$ . The fractional error which this will produce in the mass difference ratio is simply  $\delta/\Delta\nu$ , or

$$\frac{\delta}{\Delta\nu} = \frac{\alpha_e}{2B} \frac{\Delta m}{m} \tag{2-34}$$

This expression represents, of course, only a very rough estimate. For the sulfur masses in OCS,  $\Delta m/m \approx \frac{1}{16}$  and  $\alpha_e/2B \approx \frac{1}{16000}$ , so that the error in mass ratio would be of the order 1/16,000.

TABLE 2-6. SOME MASS DIFFERENCE RATIOS OBTAINED FROM ROTATIONAL SPECTRA OF POLYATOMIC MOLECULES AND A COMPARISON WITH OTHER DETERMINATIONS

Ratio of mass differences	Molecule	Microwave measurement	Reference	Other measurements	Method
$\frac{S^{32} - S^{32}}{S^{34} - S^{32}}$	OCS	$0.500714 \pm 0.00003$	[574]	$0.500727 \pm 0.00002$	Mass spectra [855a]
$\frac{Se^{77} - Se^{76}}{Se^{80} - Se^{77}}$	OCSe	$0.33395 \pm 0.00002$	[456]	$0.33394 \pm 0.00003$	Mass spectra [911a]
$\frac{Si^{28} - Si^{29}}{Si^{30} - Si^{28}}$	SiD <sub>3</sub> F	$0.49938 \pm 0.00003$	[574] [888]	$0.49943 \pm 0.00001$	Mass spectra [855a]
$\frac{O^{17} - O^{16}}{O^{18} - O^{16}}$	OCS	$0.501042 \pm 0.00008$	[924a]	$0.501044 \pm 0.00007$	Nuclear reaction [924a]
$\frac{Cl^{36} - Cl^{35}}{Cl^{37} - Cl^{35}}$	CH <sub>3</sub> Cl	$1.0018 \pm 0.0004$	[924a]	$1.00179 \pm 0.00007$	Nuclear reaction [924a]

A more exact expression may be obtained for the error due to neglect of zero-point vibration by expanding  $\alpha$  and  $B_e$  about their values when  $m = m_0$  in powers of the change in isotopic mass  $\Delta m$

$$\begin{aligned} \alpha &= \alpha^{(0)} + \alpha' \Delta m + \alpha'' \frac{(\Delta m)^2}{2} + \dots \\ B_e &= B_e^{(0)} + B' \Delta m + B'' \frac{(\Delta m)^2}{2} + \dots \end{aligned} \tag{2-35}$$

The “experimental” value of the ratio of mass differences obtained by using (2-33) and neglecting vibrational effects can then be related to the “true” value which would be obtained by using equilibrium rotational constants as follows:

$$\begin{aligned} \left(\frac{m_1 - m_0}{m_2 - m_0}\right)_{\text{exp}} &= \left(\frac{m_1 - m_0}{m_2 - m_0}\right)_{\text{true}} \left[ 1 - \frac{1}{4} \frac{\alpha'}{B'} \left(\frac{B''}{B'} - \frac{\alpha''}{\alpha'}\right) (m_2 - m_1) \right. \\ &\quad \left. + \frac{1}{2} \frac{\alpha}{B} \left(\frac{B'}{B} - \frac{\alpha'}{\alpha}\right) (m_2 - m_1) + \dots \right] \end{aligned} \tag{2-36}$$

This expression is not a final answer because usually an evaluation of  $\alpha'$  and  $\alpha''$  is very difficult. In fact, if they could be properly evaluated,



then corrections could be applied to eliminate these particular errors. However, it does allow an estimation of errors.

$B$  and  $\alpha$  are positive in all known cases,  $B'$  and  $\alpha'$  are negative, and  $B''$  and  $\alpha''$  positive. In this respect  $\alpha$  and  $B$  are similar, if not identical, functions of  $m$ . Hence the two terms in each bracket,  $(B''/B' - \alpha''/\alpha')$  and  $(B'/B - \alpha'/\alpha)$ , tend to cancel. In addition, the two error terms

$$\frac{1}{4} \frac{\alpha'}{B'} \left( \frac{B''}{B'} - \frac{\alpha''}{\alpha'} \right) (m_2 - m_1) \quad \text{and} \quad - \frac{1}{2} \frac{\alpha}{B} \left( \frac{B'}{B} - \frac{\alpha'}{\alpha} \right) (m_2 - m_1)$$

may be expected to be of opposite sign and to cancel partially. Hence an upper limit for the fractional error in  $(m_1 - m_0)/(m_2 - m_0)$  may be taken as the biggest of the four terms which multiply  $m_2 - m_1$ . However, the actual error to be expected should be considerably less than this upper limit. Detailed estimates [573][924a] indicate that errors of the type given by (2-36) in the ratio  $\frac{S^{33} - S^{32}}{S^{34} - S^{32}}$  obtained from the spectrum of OCS are less than 1 part in 15,000. This corresponds to an uncertainty of about 0.03 millimass unit in determining the mass of  $S^{33}$  if masses of  $S^{32}$  and  $S^{34}$  are assumed to be known.

It is, of course, possible to find cases for which the errors given by (2-36) would be very serious. These would be primarily cases where the masses being measured are located near the center of gravity of the molecule—such as the central nitrogen in NNO. Location near the center of gravity would make  $B'$  very small, but  $\alpha'$  and  $\alpha''$  would not necessarily be small, so that the error terms of (2-36) may be large. However, if these unfavorable cases are avoided, nuclear masses of the medium and heavy atoms may be measured in polyatomic molecules to an accuracy of one or two ten-thousandths of a mass unit. Perhaps the best assurance that the zero-point vibration errors are usually not serious and that no unforeseen errors are present is given by comparing the ratios in Table 2-5 which have been measured both by microwave spectroscopy and by other well-accepted techniques. Where accurate ratios are available from other techniques, they usually agree with microwave results very well and indicate that the errors due to zero-point vibrations are no larger than those which have been estimated.

## CHAPTER 3

### SYMMETRIC-TOP MOLECULES

**3-1. Introduction and General Features of Rotational Spectra.** For the normal rotation of a linear molecule, no angular momentum occurs in the direction of the molecular axis because the moment of inertia about this axis is so small that one quantum of angular momentum represents a large excitation energy. For a more general type of molecule, however, there is no axis about which the moment of inertia is extremely small, and the normal rotational states of nonlinear molecules may involve rotation about any molecular axis.

The moments of inertia of a molecule (or of any system of masses) may be represented by an ellipsoid whose orientation is fixed in the molecule and whose center coincides with the center of mass. The shape of the ellipsoid is such that the molecular moment of inertia about any axis through the center of mass is just equal to half the distance between intersections of this axis and the ellipsoid. Every ellipsoid has three perpendicular principal axes, and if the coordinate system is oriented so that  $x$ ,  $y$ , and  $z$  are along the principal axes of the ellipsoid of inertia, then the equation of the ellipsoid of inertia may be written simply

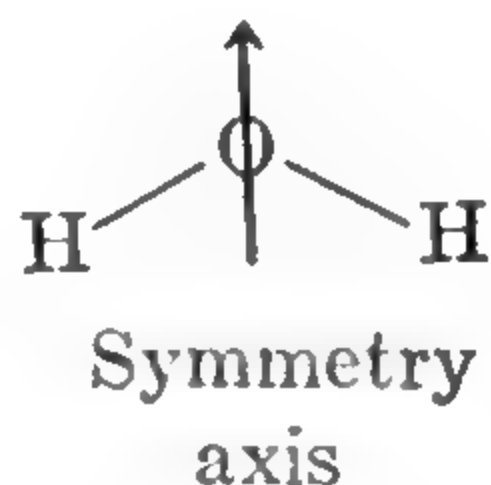
$$\frac{x^2}{I_x^2} + \frac{y^2}{I_y^2} + \frac{z^2}{I_z^2} = 1 \quad (3-1)$$

where  $I_x$ ,  $I_y$ , and  $I_z$  are the moments of inertia along the directions of the principal axes, and are hence called the principal moments of inertia.

A molecular rotation can usually most simply be described in terms of motions about the principal axes. The special case of a linear molecule has an ellipsoid of inertia which is a flat disk, since the moment of inertia along the molecular axis, which we shall take as the  $z$  direction, is very small, and the other two principal moments of inertia are equal. The general rotating body where all three principal moments of inertia are different is called an asymmetric rotor or asymmetric top, and usually the principal moments of inertia are indicated by  $I_A$ ,  $I_B$ , and  $I_C$  in increasing order of size. For some molecules, two moments of inertia, such as  $I_A$  and  $I_B$  or  $I_B$  and  $I_C$ , may be equal, in which case the molecule is called a symmetric rotor or symmetric top. The linear molecule is a special case of a symmetric rotor, since for it the two largest moments of inertia  $I_B$  and  $I_C$  are equal.



In many cases it is very easy to pick out the principal axes of a molecule and to see whether or not two principal moments of inertia are equal. If the molecule has an axis of symmetry, then this is always a principal axis of the molecule. An axis of symmetry is recognized if the distribution of atoms in space is unchanged when the molecule is rotated about some axis by an angle of  $2\pi/n$ , in which case the molecule is said to have an  $n$ -fold axis. For example, the water molecule,  $\text{H}_2\text{O}$ , has a configuration as follows



An axis in the plane of all three nuclei, passing through the oxygen nucleus lying halfway between the two hydrogens, is a twofold axis of symmetry, since the molecule will have just the same arrangement of atoms if it is rotated by  $\pi$  radians, or  $180^\circ$ , about this axis. Since the orientation of the ellipsoid of inertia must also remain unchanged as a result of this rotation, it is easy to see that this symmetry axis is a principal axis of inertia. The water molecule is not, however, a symmetric top, because its three principal moments of inertia are all different. If a molecule has an axis of three- or more fold symmetry, then it is always a symmetric top. An example would be  $\text{NH}_3$ , which is a pyramid-shaped molecule with the N at the apex and the three hydrogens equidistant from the nitrogen. An axis through the N and midway between the three hydrogens is a threefold axis of symmetry. It is also from the above discussion a principal axis of the ellipsoid of inertia and is usually taken as the  $z$  axis. If the molecule is rotated through an angle of  $2\pi/3$  radians, or  $120^\circ$ , the ellipsoid of inertia must be unchanged. This is possible only if  $I_x$  and  $I_y$  are equal, so that the cross section of the ellipsoid of inertia in a plane perpendicular to the axis of symmetry  $z$  degenerates into a circle. The same argument would hold for any axis of symmetry greater than threefold. A linear molecule, for example, has an infinityfold axis of symmetry.

By far the most common varieties of symmetric tops are linear molecules, which have already been treated, and those with a threefold axis of symmetry. It can conceivably happen that a molecule with less symmetry than a threefold axis is a symmetric top, which would be called an "accidental" symmetric top. Since the high resolution and accuracy of microwave spectroscopy can detect even a very slight deviation from equality of two moments of inertia, it is extremely unlikely that two moments of inertia would be nearly enough equal by "acci-



dent" to make the molecule appear to be a symmetric top. Hence this variety of symmetric top with less than a threefold axis of symmetry will be ignored. Cases of this type which are almost symmetric will be treated in Chap. 4 as "slightly asymmetric" rotors.

*Symmetric-rotor Spectra—Semiclassical Discussion.* Much of the

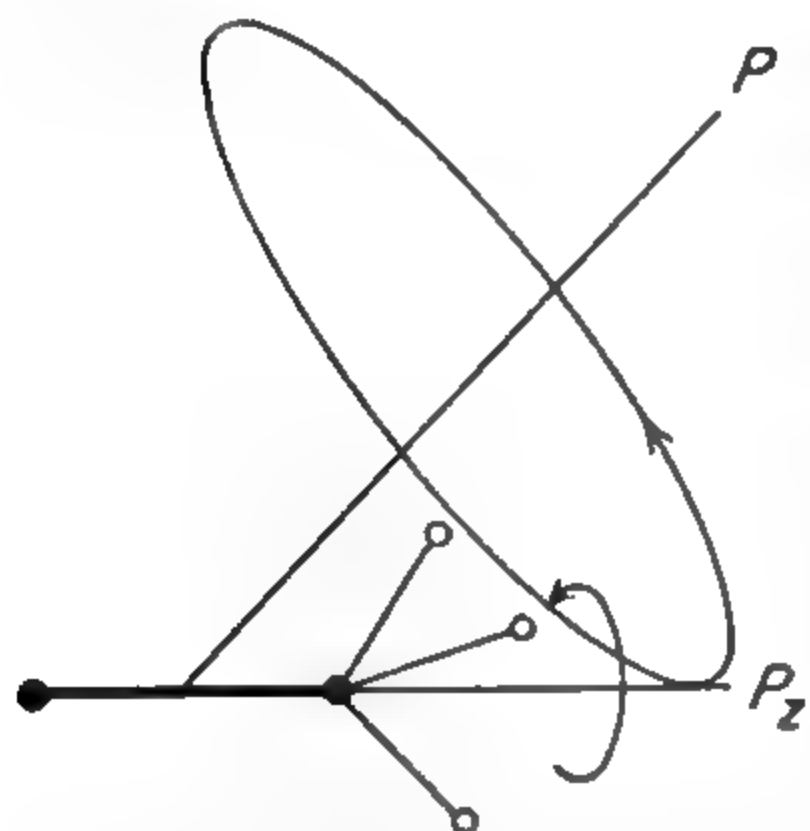
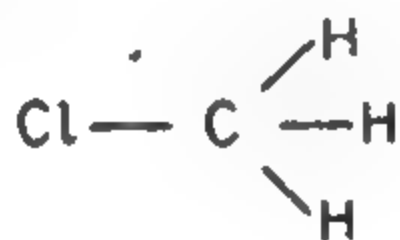


FIG. 3-1. Classical motion of a symmetric top. This is a combined rotation around the molecular axis associated with  $P_z$  and a precession of this axis around the total angular momentum  $P$ . The molecule represented is methyl chloride,



behavior—energy levels and selection rules—of a symmetric top can be deduced from classical mechanics and the correspondence principle. Figure 3-1 illustrates this classical motion. The axis of the molecule precesses around the total angular momentum  $P$  with a frequency that can be shown to be  $P/2\pi I_B$ . At the same time it may spin about its axis (see [130], p. 22). The energy of rotation would be given by

$$W = \frac{1}{2}I_x\omega_x^2 + \frac{1}{2}I_y\omega_y^2 + \frac{1}{2}I_z\omega_z^2 = \frac{P_x^2}{2I_x} + \frac{P_y^2}{2I_y} + \frac{P_z^2}{2I_z} \quad (3-2)$$

where  $x$ ,  $y$ , and  $z$  are directions along the principal axes of inertia,  $z$  being the symmetry axis of the molecule. Now since the molecule is a symmetric top,  $I_x$  and  $I_y$  are equal and will be both called  $I_B$ , which is the normal symbol for the moment of inertia of intermediate size.  $I_z$  will be properly designated either  $I_A$  or  $I_C$  according to whether it is smaller or larger than  $I_B$ . If the relative sizes of the moments of inertia are unknown or unimportant,

then  $I_z$  will always be designated as  $I_C$ . Using the fact that  $I_x = I_y = I_B$  and that  $P^2 = P_x^2 + P_y^2 + P_z^2$ , (3-2) becomes

$$W = \frac{P^2}{2I_B} + P_z^2 \left( \frac{1}{2I_C} - \frac{1}{2I_B} \right) \quad (3-3)$$

The square of the total angular momentum  $P^2$  is quantized and must equal  $J(J+1)h^2/4\pi^2$ , where  $J$  is an integer. Similarly, the component of the angular momentum along some direction, say the  $z$  axis, is quantized, so that  $P_z^2 = K^2h^2/4\pi^2$ , where  $K$  is an integer. Hence (3-3) becomes

$$W = \frac{J(J+1)h^2}{8\pi^2I_B} + \left( \frac{h^2}{8\pi^2I_C} - \frac{h^2}{8\pi^2I_B} \right) K^2$$

or, defining the rotational constants

$$A = \frac{h}{8\pi^2I_A} \quad B = \frac{h}{8\pi^2I_B} \quad C = \frac{h}{8\pi^2I_C} \quad (3-4)$$

$$\frac{W}{h} = BJ(J+1) + (C-B)K^2 \quad (3-5)$$

The expression (3-5) gives the correct allowed energy levels for a symmetric top, which are illustrated in Fig. 3-2. If  $K$  is zero, the energy levels are just those previously found for a linear molecule. For a given value of  $J$ , however,  $K$  may have a number of values.  $K$  cannot, of course, be larger than  $J$  since  $K$  represents a component of  $J$ . It can therefore be one of the integers

$$K = J, J - 1, \dots, -J \quad (3-6)$$

or have  $2J + 1$  different values. Since the energy is independent of the sign of  $K$ , levels with the same absolute magnitude of  $K$  coincide, so that all levels for which  $K$  is greater than zero are doubly degenerate, and there

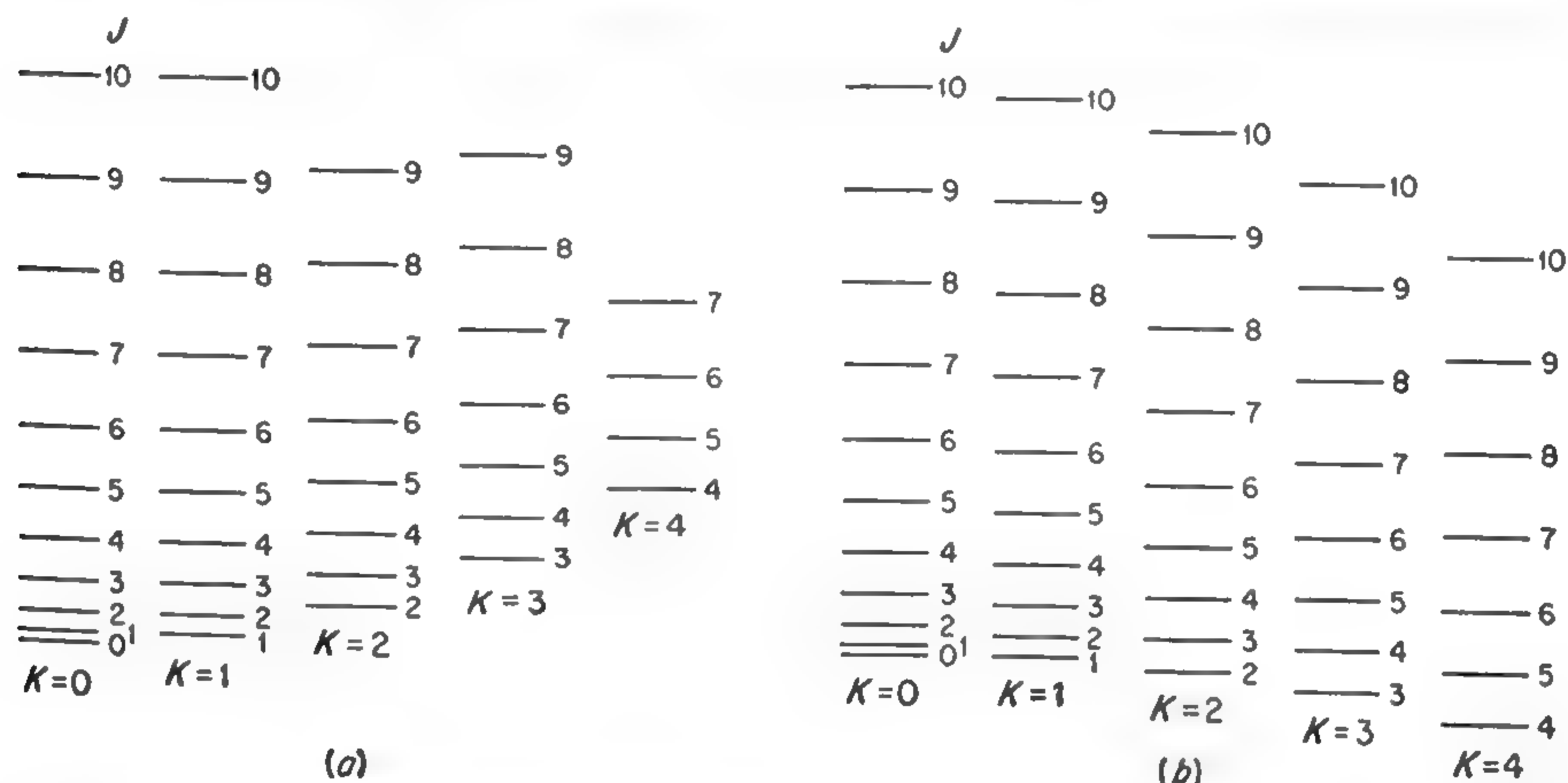


FIG. 3-2. Energy levels of typical symmetric-top molecules. (a) prolate; (b) oblate symmetric top.

are only  $J + 1$  different energy values for each possible value of  $J$ . For each particular  $K$ , there is an infinite series of levels with different values of  $J$ . These are identical in relative spacing with the linear molecule levels except that the series must start with  $J = K$  rather than  $J = 0$ .

A prolate symmetric top is one in which the molecule is more or less elongated like a cigar, and for which the moment of inertia about the symmetry axis  $I_z$  is smaller than the moment of inertia about the other principal axes. In that case  $h/8\pi^2 I_z - h/8\pi^2 I_B$ , which is the coefficient of  $K^2$  in (3-5), is positive, so that the energy levels for the same  $J$  increase with increasing  $K$  as in Fig. 3-2a. An oblate symmetric top, which might be represented by a pancake shape, would have  $I_z$  larger than  $I_B$ , and hence the coefficient of  $K^2$  in (3-5) would be negative. In this case energy levels for the same  $J$  decrease in energy with increasing  $K$  as in Fig. 3-2b. For a spherical top, with all moments of inertia equal, the coefficient of  $K^2$  in (3-5) is zero and the energy depends only on the total angular momentum  $J$ .

In order to determine the spectrum to be expected, the selection rules in addition to the energy levels are needed. Because of the symmetry, there can be no dipole moment perpendicular to the axis of a symmetric top, and hence no torque along the axis due to electric fields associated with radiation. This indicates from the correspondence principle that the angular momentum along the molecular axis cannot change due to radiation, or  $\Delta K = 0$ . The dipole moment lies along the molecular axis and this axis precesses around the total angular momentum, which is fixed in direction, with a frequency  $P/2\pi I_B$  as mentioned above. Hence the frequency to be expected classically is just  $P/2\pi I_B$ , which is identical with what would be expected from a linear molecule. This frequency can be obtained approximately with the selection rule  $\Delta J = \pm 1$ , which is identical with the rigorous result of a quantum-mechanical calculation.

It is important to note that, because of the above selection rules, as long as centrifugal stretching and other small effects are neglected, the frequencies observed for a symmetric top do not depend in any way on  $K$  or the moment of inertia about the symmetry axis. They are given simply by

$$\nu = \frac{2h(J + 1)}{8\pi^2 I_B} = 2B(J + 1) \quad (3-7)$$

The fact that the frequencies observed do not depend on  $I_A$  is an advantage in simplifying the spectrum; it is a disadvantage, however, in preventing any direct determination

from the spectrum of the moment of inertia about the axis of a symmetric top.

The simplest type of symmetric top (other than a linear molecule or an "accidental" symmetric top, which never is exactly symmetric) is composed of three identical atoms arranged in an equilateral triangle,

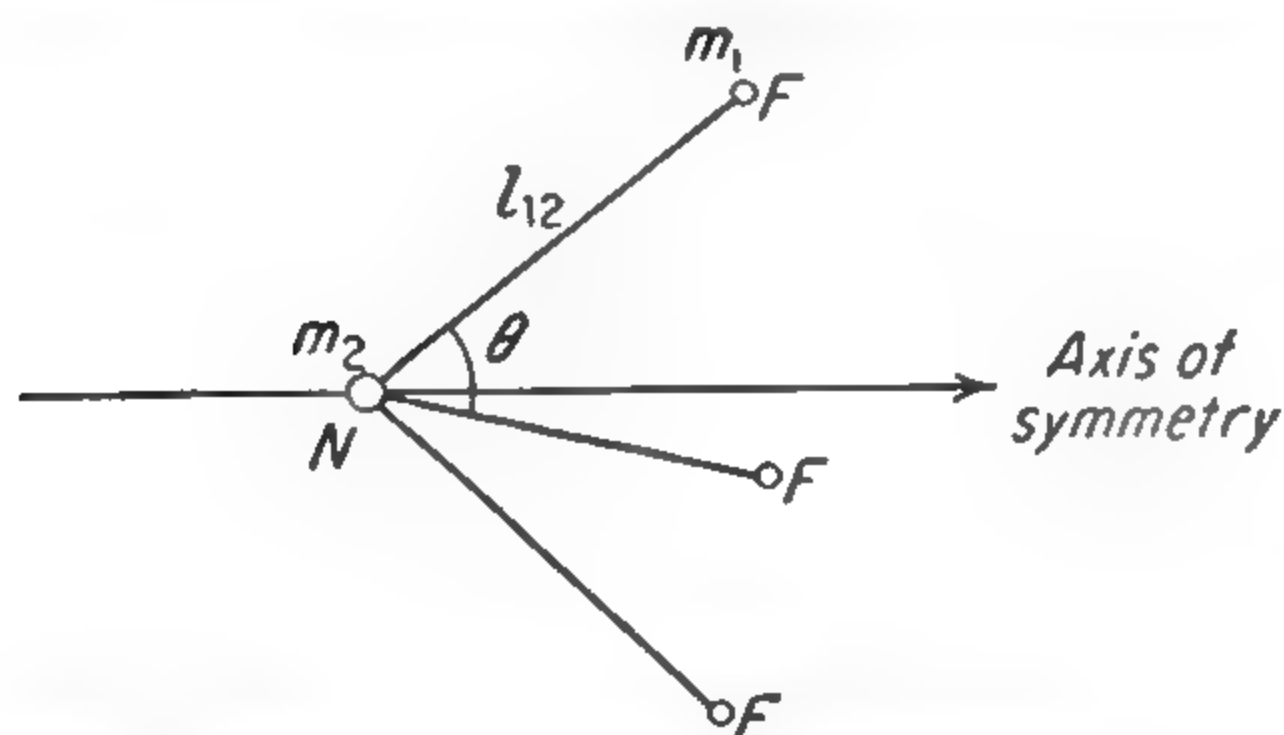


FIG. 3-3. A simple pyramidal symmetric-top molecule,  $\text{NF}_3$ .

and another atom equidistant from these three. The fourth atom may be in the plane of the three identical atoms, or out of this plane so that the molecule is pyramidal. Planar molecules of this type include the trihalides of elements of the third column of the periodic table such as  $\text{BF}_3$ ,  $\text{BCl}_3$ , and  $\text{AlCl}_3$ . Symmetric planar molecules give no pure rotational spectrum because they have no permanent dipole moment. Simple pyramidal symmetric molecules include the trihydrides and trihalides of the fifth-column elements such as  $\text{NH}_3$ ,  $\text{NF}_3$ ,  $\text{PH}_3$ ,  $\text{PCl}_3$ , or  $\text{AsF}_3$  (see Fig. 3-3). In order for these molecules to be symmetric rotors, the three like atoms must of course be of the same isotopic mass— $\text{NH}_2\text{D}$ , where one hydrogen has been replaced with deuterium, is by no means a symmetric rotor.



*Moments of Inertia.* The moment of inertia about the symmetry axis is given by

$$I_C = 2m_1l_{12}^2(1 - \cos \theta) \quad (3-8)$$

where  $m$  is the mass of one of the three identical atoms,  $l_{12}$  the distance from one of them to the fourth atom, and  $\theta$  is the angle between two lines joining the fourth atom with two of the other atoms, *i.e.*, the angle of one face of the pyramid at its apex. The angle  $\theta$  is usually called the bond

TABLE 3-1. ROTATIONAL CONSTANT AND STRUCTURE OF SYMMETRIC PYRAMIDAL MOLECULES

$l_{12}$  and  $\theta$  are defined as in Fig. 3-2. Where errors in  $l_{12}$  and  $\theta$  are not listed, the errors have not been estimated.

Molecule	$B_0$ , Mc	$l_{12}$ , angstroms	$\theta$	Reference
NH <sub>3</sub>	298,000	1.014	106°47'	[130] [662]
NF <sub>3</sub>	10,680.96	1.371	102°9'	[527]
PH <sub>3</sub>	133,478.3	1.421	93°27'	[606] [736] [866] [909]
PF <sub>3</sub>	7,819.90	1.55	102°	[367] [947]
PCl <sub>3</sub> <sup>35</sup>	2,617.1	2.043 ± 0.003	100°6' ± 20'	[481]
PBr <sub>3</sub> <sup>79</sup>	996.8	.....	.....	[551]
AsH <sub>3</sub>	111,620	1.523	92°0'	[606] [735]
AsF <sub>3</sub>	5,878.971	1.712 ± 0.006	102° ± 2°	[266] [824]
AsCl <sub>3</sub> <sup>35</sup>	2,147.2	2.161 ± 0.004	98°25' ± 30'	[481]
Sb <sup>121</sup> H <sub>3</sub>	88,000	1.712	91°30'	[606] [736]
Sb <sup>121</sup> Cl <sub>3</sub> <sup>35</sup>	1,754	2.325 ± 0.005	99°30' ± 1°30'	[597] [947]

angle because the chemical bonds are represented as straight lines between each of the three identical atoms and the fourth atom. The two equal moments of inertia perpendicular to the axis of symmetry are given by

$$I_B = m_1l_{12}^2(1 - \cos \theta) + \frac{m_1m_2l_{12}^2}{3m_1 + m_2}(1 + 2 \cos \theta) \quad (3-9)$$

Since the frequencies of allowed rotational transitions depend only on  $I_B$ , observation of the rotational spectrum of this type of molecule does not allow determination of both parameters  $l_{12}$  or  $\theta$ , which give the complete molecular configuration. If, however, spectra of two different isotopic species of the same molecule are observed, such as N<sup>14</sup>F<sub>3</sub> and N<sup>16</sup>F<sub>3</sub>, then two different moments  $I_B$  are measured giving two equations of the type (3-9), and both molecular parameters  $l_{12}$  and  $\theta$  may be determined. Structural information about these molecules may also be obtained from their nonsymmetric isotopic forms, *i.e.*, NH<sub>2</sub>D, AsCl<sub>2</sub><sup>35</sup>Cl<sup>37</sup>, etc. These asymmetric molecules will be discussed in Chap. 4. Table 3-1 includes the best data available on the structure of symmetric

pyramidal molecules. The internuclear distances and angles are subject to the same type of uncertainties due to zero-point vibrations as are the internuclear distances in linear molecules. Where estimates of these or other errors have been made, they are included in Table 3-1.

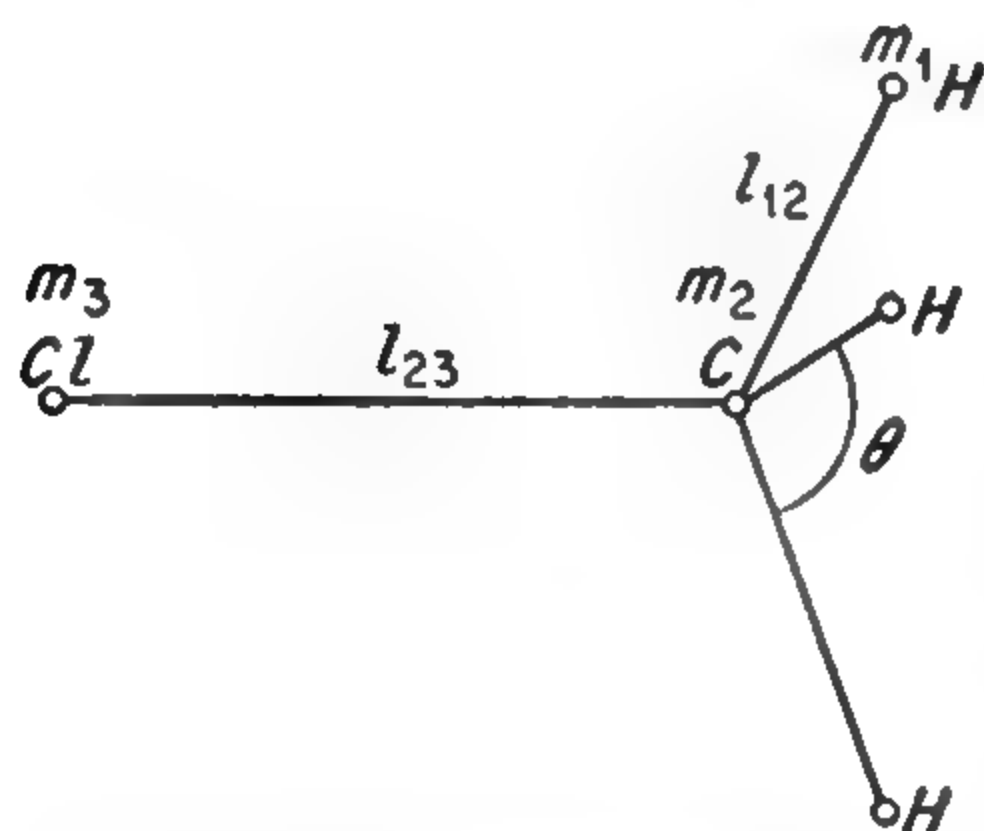


FIG. 3-4. A common type of symmetric-top molecule illustrated by methyl chloride.

Another common type of symmetric-top molecule involves elements of the fourth column of the periodic table bonded to three like atoms and a fourth different atom or group of atoms. Methyl chloride, an example of this type, is shown in Fig. 3-4. The moment of inertia  $I_c$  for this type of molecule

is of course also given by (3-8), and the moment of inertia perpendicular to the axis of symmetry is

$$I_B = m_1 l_{12}^2 (1 - \cos \theta) + \frac{m_1(m_2 + m_3)l_{12}^2}{3m_1 + m_2 + m_3} (1 + 2 \cos \theta) + \frac{m_3 l_{23}^2}{3m_1 + m_2 + m_3} \times \left[ (3m_1 + m_2)l_{23} + 6m_1 l_{12} \left( \frac{1 + 2 \cos \theta}{3} \right)^{\frac{1}{2}} \right] \quad (3-10)$$

For these molecules three isotopic species must be measured in order to determine the three structural parameters  $l_{12}$ ,  $l_{23}$ , and  $\theta$ . In the rather

TABLE 3-2. AN EXAMPLE OF SERIOUS VARIATIONS IN STRUCTURAL PARAMETERS FROM VARIOUS ISOTOPIC COMBINATIONS AS A RESULT OF ZERO-POINT VIBRATIONS

The best values are those in the last row obtained by using the asymmetric species  $\text{CHD}_2\text{Cl}$ . (Data from Miller *et al.* [729].)

Isotopic species used	Molecular parameters obtained		
	$l_{12}$ (CH)	$l_{23}$ (CCl)	$\theta$ (HCH)
$\text{C}^{12}\text{H}_3\text{Cl}^{35}$ , $\text{C}^{12}\text{H}_3\text{Cl}^{37}$ , $\text{C}^{13}\text{H}_3\text{Cl}^{37}$	1.123	1.7813	110°57'
$\text{C}^{12}\text{H}_3\text{Cl}^{35}$ , $\text{C}^{12}\text{H}_3\text{Cl}^{37}$ , $\text{C}^{12}\text{D}_3\text{Cl}^{37}$	1.128	1.7872	112°31'
$\text{C}^{12}\text{H}_3\text{Cl}^{37}$ , $\text{C}^{13}\text{H}_3\text{Cl}^{37}$ , $\text{C}^{12}\text{D}_3\text{Cl}^{37}$	0.949	1.7850	104°09'
$\text{C}^{12}\text{H}_3\text{Cl}^{35}$ , $\text{C}^{13}\text{H}_3\text{Cl}^{35}$ , $\text{C}^{12}\text{HD}_2\text{Cl}^{35}$	1.101	1.7815	110°13'

common case where the three identical atoms of mass  $m$  are hydrogen, effects of zero-point vibrations can give rather large uncertainties in the positions of these hydrogens ( $l_{12}$  and  $\theta$ ). Variations in structural parameters of  $\text{CH}_3\text{Cl}$  as a result of using various combinations of effective moments of inertia of three isotopic species are indicated in Table 3-2. In this case variations in the hydrogen positions obtained are especially large. It has been shown that for methyl chloride the average C—H distance appears to be 0.009 Å greater than the average C—D distance

of the deuterated compound, and that the HCH angle is smaller than the DCD angle by about  $\frac{1}{3}^\circ$  [729]. Symmetric-top molecules of the methyl chloride type (containing five atoms) which have so far been measured are listed in Table 3-3. In some cases all structural parameters have not been determined from microwave measurements because a sufficient

TABLE 3-3. SYMMETRIC TOPS OF FIVE ATOMS FOR WHICH MICROWAVE SPECTRA ARE KNOWN

For definition of  $l_{12}$ ,  $l_{23}$ , and  $\theta$  see Fig. 3-4.

Molecule	$B_0$ , Mc	$l_{12}$ , angstroms	$l_{23}$ , angstroms	$\theta$	Reference
CH <sub>3</sub> F	25,536.12	1.11	1.39	110°	[367] [946]
CH <sub>3</sub> Cl <sup>35</sup>	13,292.95	1.113	1.781	110°31'	[280] [412]
					[496] [729]
CH <sub>3</sub> Br <sup>79</sup>	9,568.19	1.113	1.939	111°14'	[280] [531]
					[533] [729]
CH <sub>3</sub> I	7,501.31	1.113	2.1392	111°25'	[531] [729]
Si <sup>28</sup> H <sub>3</sub> F	14,327.9	1.46	1.5946	109°20'	[522] [772]
Si <sup>28</sup> H <sub>3</sub> Cl <sup>35</sup>	6,673.8	1.44	2.050	110°	[315] [362]
					[727] [772]
Si <sup>28</sup> H <sub>3</sub> Br <sup>79</sup>	4,321.72	1.57 ± 0.03	2.209 ± 0.001	111°20' ± 1°	[409] [521]
Ge <sup>74</sup> H <sub>3</sub> Cl <sup>35</sup>	4,333.91	1.52	2.148	111°	[362] [727]
Ge <sup>74</sup> H <sub>3</sub> Br <sup>79</sup>	2,375.88	1.55 ± 0.05	2.297 ± 0.001	112° ± 1°	[521]
CF <sub>3</sub> H	10,348.74	1.332	1.098	108°48'	[367] [690]
CF <sub>3</sub> Cl <sup>35</sup>	3,335.56	1.32	1.77	109°	[358]
CF <sub>3</sub> Br <sup>79</sup>	2,098.06	1.33	1.91	108°	[520] [743]
CF <sub>3</sub> I	1,523.23	1.33	2.13	108°	[743]
CCl <sub>3</sub> <sup>35</sup> H	3,301.94	1.767	1.073	110°24'	[545] [690]
CBr <sub>3</sub> <sup>79</sup> H	1,247.61	1.930 ± 0.003	1.07	110°48' ± 16'	[764]
SiF <sub>3</sub> H	7,207.98	1.46	1.565	108°17'	[525]
Si <sup>28</sup> F <sub>3</sub> Cl <sup>35</sup>	2,477.7	1.560	1.989	108°30'	[525] [641]
Si <sup>28</sup> F <sub>3</sub> Br <sup>79</sup>	1,549.9	1.56	2.15	109°	[525] [641]
Ge <sup>74</sup> F <sub>3</sub> Cl <sup>35</sup>	2,166.60	1.69 ± 0.02	2.067 ± 0.005	107°40' ± 1°30'	[555]
PF <sub>3</sub> O	4,594.25	1.52	1.45 ± 0.03	102°30' ± 2°	[518] [765]
PF <sub>3</sub> S	2,657.63	1.53	1.87	100°20'	[686] [765]
PCl <sub>3</sub> <sup>35</sup> O	2,015.20	1.99	1.45 ± 0.03	103°30' ± 2°	[765]
PCl <sub>3</sub> <sup>35</sup> S	1,402.64	2.02	1.85 ± 0.02	100°30' ± 2°	[765]
MnO <sub>3</sub> F	4,129.11	1.586 ± 0.005	1.724 ± 0.005	108°27' ± 7'	[943a]
ReO <sub>3</sub> F	3,566.75	.....	.....	.....	[943a]
ReO <sub>3</sub> Cl <sup>35</sup>	2,094.20	1.761	2.230	108°20' ± 1°	[665] [943a]

number of isotopic species were not measured. In these cases one or two structural parameters have been estimated by other means.

More complex symmetric tops which have been studied in the microwaves are listed in Table 3-4. In many of these cases some structural parameters are estimated.

Isotopic mass ratios may be determined from microwave measurements on the moments of inertia of symmetric-top molecules. As in



TABLE 3-4. SYMMETRIC-TOP MOLECULES OF MORE THAN FIVE ATOMS

Molecule	$B_0$	Structure	Reference
$\text{CH}_3\text{CN}$	9,198.83		[446] [480] [543]
$\text{CH}_3\text{NC}$	10,052.90		[480] [543]
$\text{CH}_3\text{CCH}$	8,545.84		[544]
$\text{CH}_3\text{CCBr}^{79}$	1,561.11		[744]
$\text{CH}_3\text{CCI}$	1,259.02		[744]
$\text{CH}_3\text{Hg}^{202}\text{Cl}^{35}$	2,076.20		[462] [928]
$\text{CH}_3\text{Hg}^{202}\text{Br}^{79}$	1,139.88		[462] [928]
$\text{CH}_3\text{Hg}^{202}\text{I}$	788.0		[462]

TABLE 3-4. SYMMETRIC-TOP MOLECULES OF MORE THAN FIVE ATOMS  
(Continued)

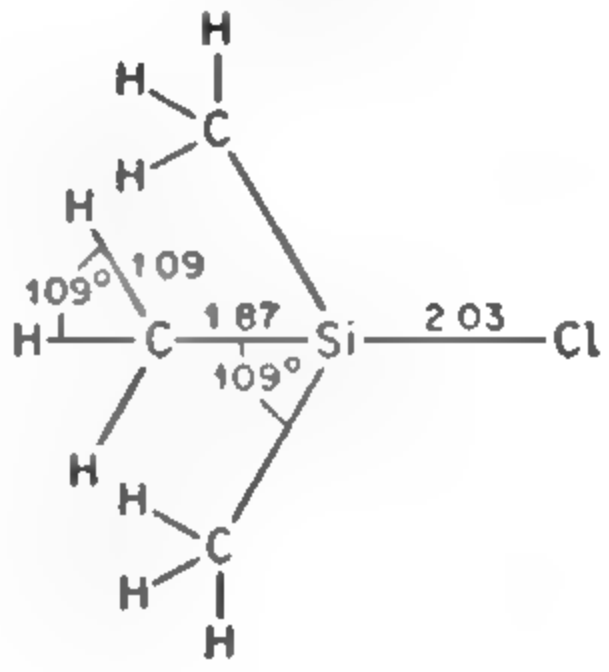
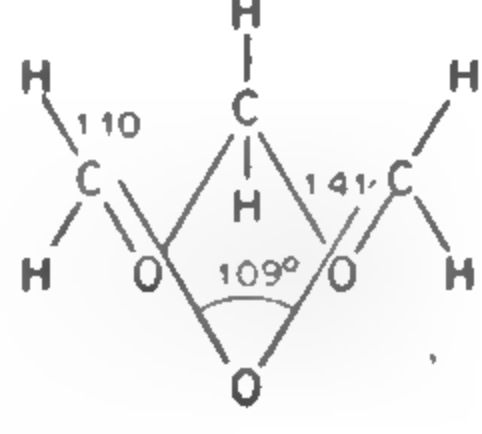
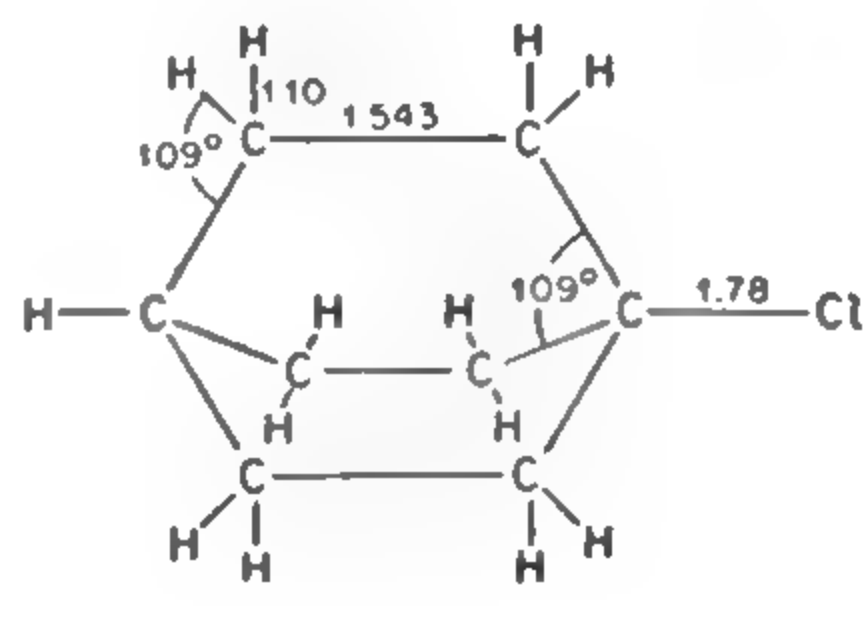
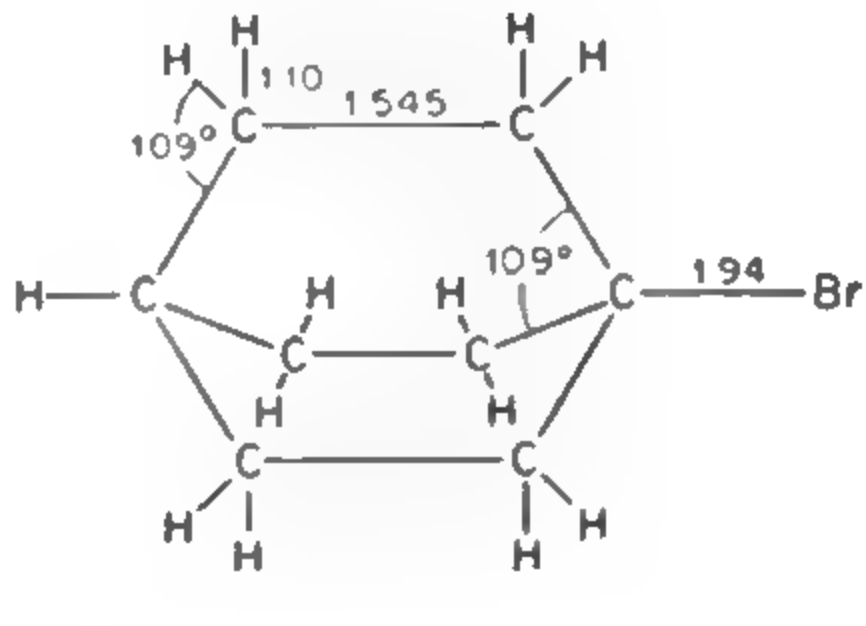
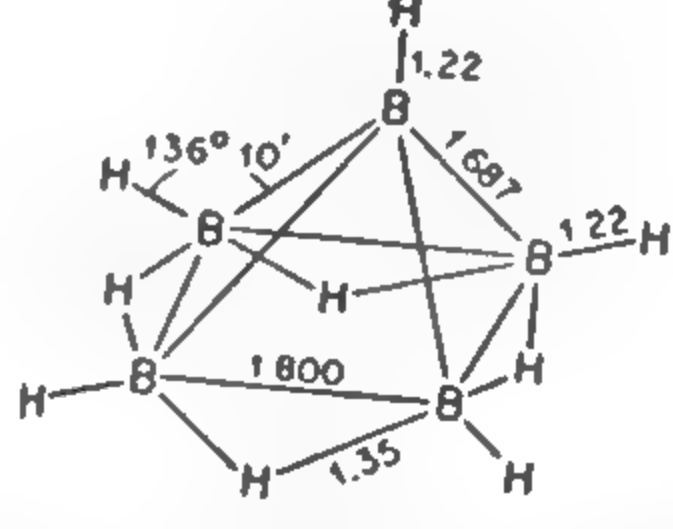
Molecule	$B_0$	Structure	Reference
$\text{CH}_3\text{Hg}^{202}\text{CN}$	1,747		[712b]
$\text{CH}_3\text{CF}_3$	5,185		[268]
$\text{CH}_3\text{SiH}_3$	10,968.96		[604]
$\text{CH}_3\text{SiF}_3$	3,715.63		[498] [641]
$\text{CH}_3\text{SiCl}_3^{35}$	1,769.84		[847]
$\text{CH}_3\text{Sn}^{120}\text{H}_3$	6,890.2		[603]
$\text{CF}_3\text{CN}$	2,945.54		[743]
$\text{CF}_3\text{CCH}$	2,877.95		[557]

TABLE 3-4. SYMMETRIC-TOP MOLECULES OF MORE THAN FIVE ATOMS  
(Continued)

Molecule	$B_0$	Structure	Reference
$\text{CF}_3\text{SF}_6$	1,097.6		[713]
$\text{B}^{11}\text{H}_3\text{CO}$	8,657.22		[461]
$(\text{CN})_3\text{P}$	2,326		[712b]
$(\text{CH}_3)_3\text{CCl}^{35}$	3,016		[550]
$(\text{CH}_3)_3\text{CBr}^{79}$	2,044		[550]
$(\text{CH}_3)_3\text{CI}$	1,562		[550]



TABLE 3-4. SYMMETRIC-TOP MOLECULES OF MORE THAN FIVE ATOMS  
(Continued)

Molecule	$B_0$	Structure	Reference
$(\text{CH}_3)_3\text{SiCl}^{35}$	2,197.44		[847]
$\text{C}_3\text{H}_6\text{O}_3$	5,273.6		[553]
$\text{C}_6\text{H}_{11}\text{Cl}^{35}$	1,090.90		[851]
$\text{C}_6\text{H}_{11}\text{Br}^{79}$	725.9		[851]
$\text{B}_6^{11}\text{H}_9^*$	7,002.85		[939]

\* Angle between plane containing two equivalent borons and the apical boron, and that containing the same equivalent borons and the hydrogen bonded to them is  $196^\circ$ .

polyatomic linear molecules, accurate determination of all the rotation-vibration effects and their dependence on mass is almost impossible, but mass difference ratios as given by (2-32) may be obtained

$$\frac{m_1 - m_0}{m_2 - m_0} = \frac{M_1 I_1 - I_0}{M_2 I_2 - I_0} \tag{2-32}$$

It was shown in Chap. 2 that this expression is valid for any type of molecule as long as the moments of inertia  $I$  represent the various values for an axis of fixed orientation with respect to the molecule and for the several isotopic masses  $m_0$ ,  $m_1$ , and  $m_2$ . If a molecule is to be a symmetric top with changes of the mass of one atom, this atom must necessarily be on the molecular axis, and hence the desired moments of inertia are simply given by the measured values of  $B$ , so that (2-32) becomes

$$\frac{m_1 - m_0}{m_2 - m_0} = \frac{M_1 B^{(2)} (B^{(0)} - B^{(1)})}{M_2 B^{(1)} (B^{(0)} - B^{(2)})} \tag{3-11}$$

Zero-point vibrations may be expected to give approximately the same types and magnitudes of errors in evaluation of masses from (3-11) as in the case of linear molecules. Mass difference ratios which have been measured from observations on symmetric tops are listed in Table 3-5.

TABLE 3-5. MASS-RATIO DETERMINATIONS FROM MEASUREMENTS OF  
ROTATIONAL CONSTANTS OF SYMMETRIC TOPS  
(From Geschwind, Gunther-Mohr, and Townes [924a])

Molecule	Ratio of mass differences	Other determinations
GeH <sub>3</sub> Cl <sup>35</sup>	$\frac{\text{Ge}^{72} - \text{Ge}^{70}}{\text{Ge}^{74} - \text{Ge}^{70}} = 0.49985 \pm 0.00003$	0.49978 $\pm$ 0.00002
	$\frac{\text{Ge}^{76} - \text{Ge}^{74}}{\text{Ge}^{74} - \text{Ge}^{70}} = 0.50013 \pm 0.00003$	0.50011 $\pm$ 0.00002
SiH <sub>3</sub> Cl <sup>35</sup>	$\frac{\text{Si}^{30} - \text{Si}^{29}}{\text{Si}^{30} - \text{Si}^{28}} = 0.49941 \pm 0.00005$	0.49934 $\pm$ 0.00020
		0.49943 $\pm$ 0.00003
SiD <sub>3</sub> F	$\frac{\text{Si}^{30} - \text{Si}^{29}}{\text{Si}^{30} - \text{Si}^{28}} = 0.49934 \pm 0.00003$	

**3-2. Symmetric-top Wave Functions.** Discussion of energy levels and selection rules has been so far on a semiclassical basis. A quantum-mechanical treatment of course starts with the Hamiltonian and hence the wave equation for a symmetric top. The motion of a top is usually described in terms of Euler's angles, which are illustrated in Fig. 3-5.  $\theta$  and  $\phi$  are equivalent to the usual polar angles between an axis fixed in space and some axis fixed in the molecule, and  $\chi$  (often designated  $\psi$  where there is no chance of confusion with the wave function) is the angle of rotation around the axis fixed in the molecule. For a symmetric top, this chosen axis is naturally the molecular or symmetry axis. Eulerian

angles are specified in several ways by various authors. Here they are defined as follows in agreement with Casimir [24]. Axes  $x$ ,  $y$ , and  $z$  are fixed in the body;  $X$ ,  $Y$ , and  $Z$  in space. The position of the body is specified from a starting position in which the two sets of axes coincide. The body is first rotated an angle  $\phi$  about the  $Z$  axis, then through an angle  $\theta$  about the  $x$  axis, and finally through an angle  $\chi$  about the  $z$  axis. It can be shown ([81], p. 230) that the wave equation can be written in the above coordinates

$$\begin{aligned} \frac{1}{\sin \theta} \frac{\partial}{\partial \theta} \left( \sin \theta \frac{\partial \psi}{\partial \theta} \right) + \frac{1}{\sin^2 \theta} \frac{\partial^2 \psi}{\partial \phi^2} \\ + \left( \frac{\cos^2 \theta}{\sin^2 \theta} + \frac{C}{B} \right) \frac{\partial^2 \psi}{\partial \chi^2} - \frac{2 \cos \theta}{\sin^2 \theta} \frac{\partial^2 \psi}{\partial \chi \partial \phi} \\ + \frac{W}{hB} \psi = 0 \quad (3-12) \end{aligned}$$

where  $C$  is the rotational constant for the symmetry axis and  $B$  is the rotational constant  $h/8\pi^2 I_B$  for an axis perpendicular to the symmetry axis. The variables in (3-12) may be separated, and the solutions written in the form

$$\psi = \Theta(\theta) e^{iM\phi} e^{iK\chi} \quad (3-12a)$$

where  $M$  and  $K$  must be integers  $0, \pm 1, \pm 2, \dots$  in order to make the wave function single-valued.  $\Theta$  satisfies the equation

$$\begin{aligned} \frac{1}{\sin \theta} \frac{d}{d\theta} \left( \sin \theta \frac{\partial \Theta}{\partial \theta} \right) - \left[ \frac{M^2}{\sin^2 \theta} + \left( \frac{\cos^2 \theta}{\sin^2 \theta} + \frac{C}{B} \right) K^2 \right. \\ \left. - 2 \frac{\cos \theta}{\sin^2 \theta} KM - \frac{W}{hB} \right] \Theta = 0 \quad (3-13) \end{aligned}$$

by introducing the variables

$$x = \frac{1}{2}(1 - \cos \theta) \quad (3-14)$$

and letting

$$\Theta(\theta) = x^{\frac{1}{2}|K-M|} (1-x)^{\frac{1}{2}|K+M|} F(x) \quad (3-15)$$

the equation for  $F$  may be found to be

$$x(1-x) \frac{d^2 F}{dx^2} + (\alpha - \beta x) \frac{dF}{dx} + \gamma F = 0 \quad (3-16)$$

where

$$\alpha = |K - M| + 1$$

$$\beta = |K + M| + |K - M| + 2$$

$$\begin{aligned} \gamma = \frac{W}{hB} - \frac{CK^2}{B} + K^2 - \left( \frac{1}{2}|K + M| + \frac{1}{2}|K - M| \right) \\ \times \left( \frac{1}{2}|K + M| + \frac{1}{2}|K - M| + 1 \right) \end{aligned} \quad (3-17)$$

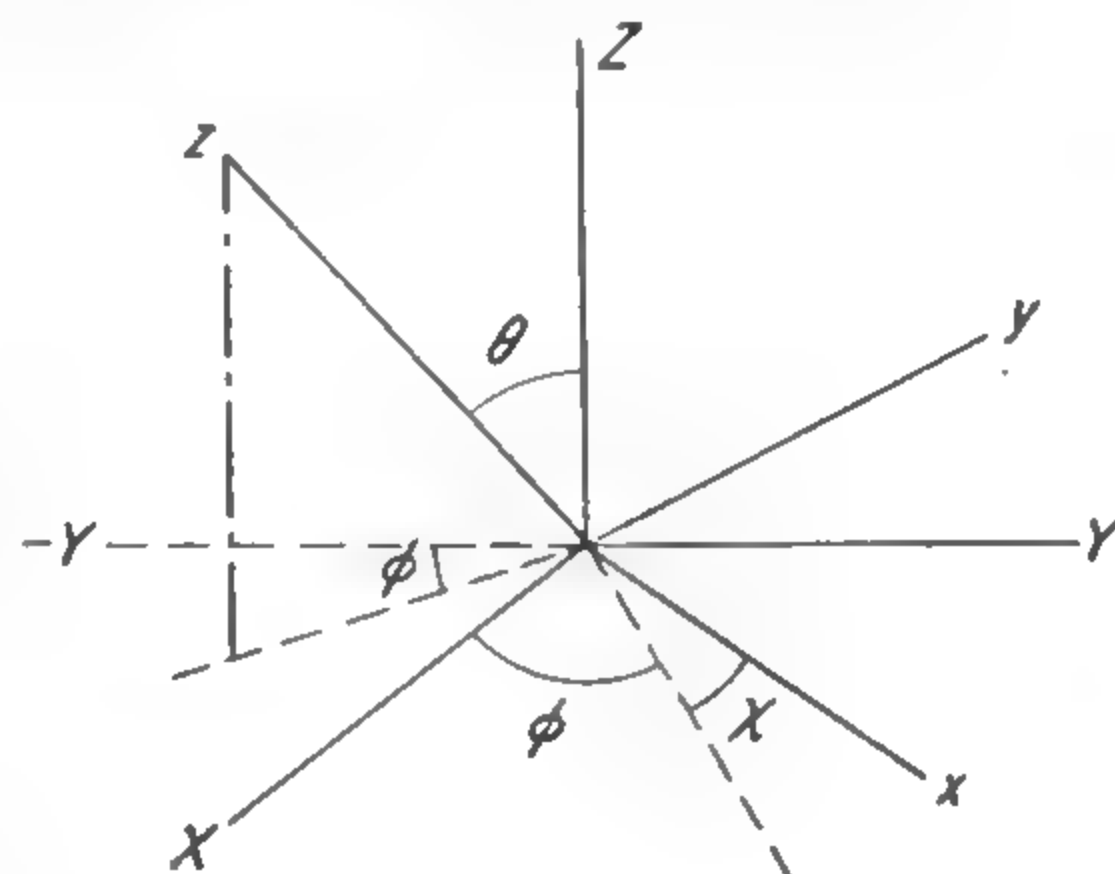


FIG. 3-5. Diagram showing Euler's angles for specifying the position of a rotating body. One dashed line is the line of nodes, or intersection between the  $xy$  and  $XY$  planes. Another is the projection of the  $z$  axis on the  $XY$  plane.



This is a well-known form of equation called the hypergeometric equation. Its solution, known as a hypergeometric function, can be obtained as a power series

$$F(x) = \sum_{n=0}^{\infty} a_n x^n \quad (3-18)$$

where

$$a_{n+1} = \frac{n(n-1) + \beta n - \gamma}{(n+1)(n+\alpha)} a_n \quad (3-19)$$

For  $\psi$  to be a satisfactory normalizable wave function, the series must terminate and become just a polynomial, which requires that the energy  $W$  is

$$\frac{W}{h} = BJ(J+1) + (C-B)K^2 \quad (3-20)$$

with

$$J = n_{\max} + \frac{1}{2}|K+M| + \frac{1}{2}|K-M| \quad (3-21)$$

$n_{\max}$  = the largest value of  $n$  in Eq. (3-18) for which  $a_n$  does not vanish.

In order for  $\psi$  to be normalized and to give matrix elements with signs or "phases" consistent with those of Condon and Shortley [56], the first term  $a_0$  of the series (3-18) for  $F(x)$  must be taken as (cf. [931])

$$e^{\frac{i\pi}{2}|K-M|} \left[ \frac{(2J+1)(J+\frac{1}{2}|K+M|+\frac{1}{2}|K-M|)!(J-\frac{1}{2}|K+M|+\frac{1}{2}|K-M|)^{\frac{1}{2}}}{8\pi^2(J-\frac{1}{2}|K+M|+\frac{1}{2}|K-M|)!|K-M|!(J+\frac{1}{2}|K+M|-\frac{1}{2}|K-M|)^{\frac{1}{2}}} \right]^{\frac{1}{2}} \quad (3-22)$$

This expression may be regarded as a normalization and phase factor for  $\psi$ .

From (3-21)  $J$  must be a positive integer which is equal to or larger than  $|K|$  or  $|M|$ , so that

$$\begin{aligned} J &= 0, 1, 2, \dots \\ K &= 0, \pm 1, \pm 2, \dots, \pm J \\ M &= 0, \pm 1, \pm 2, \dots, \pm J \end{aligned} \quad (3-23)$$

As the reader may suspect,  $J(J+1)h^2/4\pi^2$  can be shown to be the square of the total angular momentum;  $Kh/2\pi$  is its projection on the molecular axis, and  $Mh/2\pi$  its projection on the polar axis fixed in space. The energy (3-20) can be seen to be identical with Eq. (3-5) which was obtained from a semiclassical approach.

**3-3. Symmetry and Inversion.** The energy or behavior of a rotating molecule remains unchanged after certain types of changes of coordinates or symmetry operations, and hence the quantum-mechanical wave functions describing the molecule might be expected to remain unchanged. The wave equation may be written

$$H_{op}\psi = W\psi \quad (3-24)$$

where  $H_{op}$  represents the Hamiltonian operator for the energy which, for a symmetric top, takes the form (3-12) if Eulerian angles are used as coordinates. If Cartesian coordinates are used,  $H_{op}$  is easily seen to be unchanged when the coordinate system is inverted about the origin, *i.e.*, when  $x$  is replaced by  $-x$ ,  $y$  by  $-y$ , and  $z$  by  $-z$ . This is shown by the fact that terms in  $H_{op}$  do not involve odd powers of the coordinates, but only terms of the type  $\partial^2/\partial x^2$ ,  $x(\partial/\partial y)$ , etc.

If the coordinate change  $x \rightarrow -x'$ ,  $y \rightarrow -y'$ , and  $z \rightarrow -z'$  is made on (3-24), then  $H_{op}$  is unchanged, and the new  $\psi'$  must be a solution of (3-24), for the same energy  $W$ . If this energy does not represent a degenerate level, for which there are several different solutions of (3-24), then the new  $\psi'$  must be the same as the old  $\psi$ , or differ only by a multiplicative constant. Let this constant be  $c$ . If now another such transformation is made,  $x' \rightarrow -x''$ ,  $y' \rightarrow -y''$ ,  $z' \rightarrow -z''$ , the new  $\psi''$  is  $\psi'' = c\psi' = c^2\psi$ , but it also must be identical with  $\psi$  since this is just the reverse of the original transformation. Hence  $c^2 = 1$ , or  $c = \pm 1$ . If  $c = +1$ ,  $\psi$  is unchanged by inversion about the origin, is said to be symmetric with respect to this operation, and is designated as an even (+) level. If  $c = -1$ ,  $\psi$  simply changes sign on inversion, is said to be antisymmetric, and is designated as an odd (−) level.

One reason for the importance of the symmetry of the wave function with respect to inversion is its connection with the dipole matrix elements which determine the intensities of transitions. These have the form

$$\int \psi_1 x \psi_2 d\tau, \int \psi_1 y \psi_2 d\tau, \text{ and } \int \psi_1 z \psi_2 d\tau \quad (3-25)$$

where  $\psi_1$  and  $\psi_2$  are wave functions for the two states between which transitions occur and  $d\tau$  is a volume element.

The integrals are to be taken over all values of the coordinates. Each integral may be equated to the sum of two integrals, the first over all positive values of  $x$ ,  $y$ ,  $z$  and the second over all negative values. The second integral is obtained from the first by the transformation  $x \rightarrow -x'$ ,  $y \rightarrow -y'$ , and  $z \rightarrow -z'$ . In this transformation, the integrals will not of course change value, but may be seen to change sign unless  $\psi_1$  and  $\psi_2$  have opposite symmetries. Thus if  $\psi_1$  and  $\psi_2$  have the same symmetry, the integral over all space is the sum of two integrals which are equal in magnitude and opposite in sign, and so is zero. This establishes the selection rule

$$+ \longleftrightarrow - \quad + \leftrightarrow + \quad - \leftrightarrow -$$

The transitions of a diatomic molecule, for which the matrix elements vanish unless  $J \pm 1 \leftarrow J$  (page 22), must of course obey the above selection rule and will be found to do so. We shall examine the symmetry of symmetric-top wave functions, but before doing so, the coordinate system for a symmetric top must be more completely described.

Consider a planar symmetric top such as  $\text{BF}_3$  with three like atoms and a fourth atom equidistant from them. The orientation of this molecule can be specified in terms of an axis through the center of mass and perpendicular to the plane of the molecule. In order to define the positive direction of this axis, the three like (fluorine) atoms must be labeled with the numbers 1, 2, 3. The positive direction is then taken as the direction

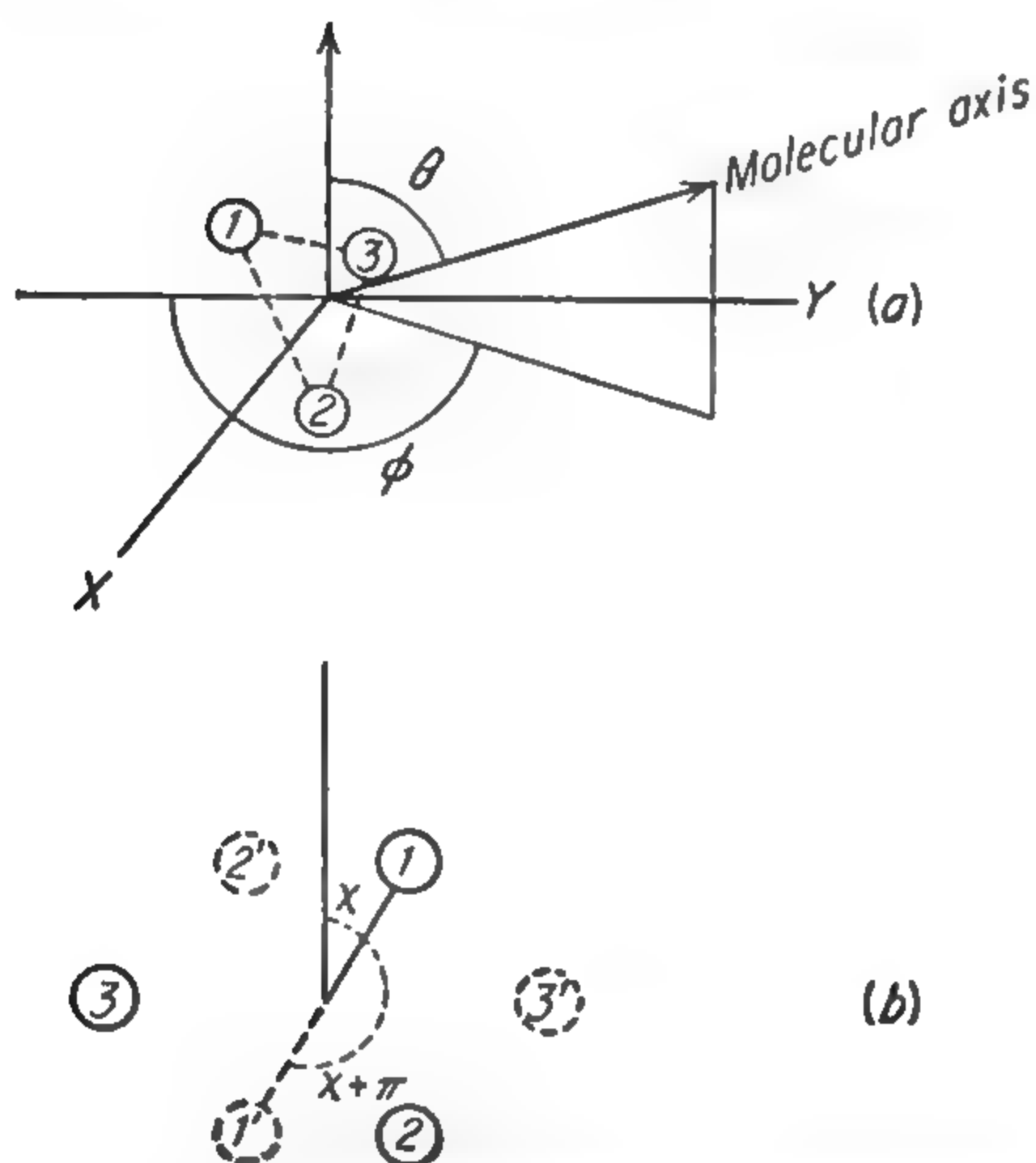


FIG. 3-6. Coordinates for a symmetric-top molecule. (a) The positive direction of the molecular axis of a symmetric-top molecule (e.g.,  $\text{BF}_3$ ) and the polar angles  $\theta$  and  $\phi$ . The three identical nuclei are labeled 1, 2, and 3. (b) A symmetric-top molecule viewed along the positive direction of the molecular axis showing the angle  $\chi$  which indicates rotation around the molecular axis. The vertical line is the "line of nodes." The solid circles represent the nuclear positions before an inversion through the origin, and the dotted circles are their positions after such an inversion.

inversion according to whether  $K$  is even or odd.

In addition to the rotational part of the wave function, the electronic, vibrational, and spin coordinates must be considered. The complete wave function may be indicated by a product

$$\psi_{\text{total}} = \psi_e \psi_v \psi_R \psi_I \quad (3-28)$$

where  $\psi_e$ ,  $\psi_v$ ,  $\psi_R$ , and  $\psi_I$  represent the parts of the wave function dependent, respectively, on electronic, vibrational, rotational, and spin coordinates. The behavior of  $\psi_{\text{total}}$  with respect to any symmetry operation

of advance of a right-handed screw rotated in the direction of successive nuclei 1, 2, 3. This is illustrated in Fig. 3-6a, or in Fig. 3-6b where the positive direction is into the page.  $\theta$  and  $\phi$  are the usual polar angles between the molecular axis and a fixed polar axis ( $z$ ), and  $\chi$ , illustrated in Fig. 3-6b, is the angle of rotation around the molecular axis. If the coordinates of each atom in the molecule are inverted about the origin, then Fig. 3-6b shows that the positive direction of the molecular axis does not change, so that  $\theta$  and  $\phi$  are unaffected. However,  $\chi$  is changed into  $\chi + \pi$ .

The rotational wave functions for a symmetric top are from (3-12a), of the form

$$\psi_{JKM} = e^{iM\phi} e^{iK\chi} \Theta_{JKM}(\theta) \quad (3-26)$$

so that when the coordinates undergo an inversion about the origin, the new wave function becomes

$$\psi = \psi e^{iK\pi} = (-1)^K \psi \quad (3-27)$$

Hence the rotational wave function is even (+) or odd (−) with respect to



depends on the behavior of each of these four parts. The electronic wave functions for almost all polyatomic molecules in the ground state are symmetric, so they may be neglected in considering the symmetry of  $\psi_{\text{total}}$ . The spin wave functions  $\psi_I$  may usually be either symmetric or antisymmetric, but consideration of them will be postponed until later.

The vibrational wave function for a molecule in the ground vibrational state is always symmetric, so in this case the symmetry of  $\psi_{\text{total}}$  depends only on  $\psi_R$  (if  $\psi_I$  is neglected). Consider excited states of the vibration for which the central boron atom in the symmetric top illustrated by Fig. 3-6 moves perpendicularly to the plane of the three fluorines. The coordinate for this motion will be called  $h$ . It indicates the distance moved by the boron from the center of mass and will be called positive when the boron has moved along the positive direction of the molecular axis, negative if the boron moves in the opposite direction. The wave functions for a harmonic vibration of this type are ([62], p. 74)

$$\psi_v(h) = c_1 e^{-c_2^2 h^2 / 2} H_v(c_2 h) \quad (3-29)$$

where  $c_1$  and  $c_2$  are constants, and  $H_v$  is a Hermite polynomial of order  $n$ . The lowest energy level corresponds to  $v = 0$ , with higher integral values  $v = 1, 2, \dots$  being successively higher in energy.  $H_v$  involves only odd or even powers of  $h$  according to whether  $v$  is odd or even. Hence when an inversion about the origin occurs, which changes  $h$  into  $-h'$ , the new vibrational wave function is

$$\psi'_v = (-1)^v \psi_v \quad (3-30)$$

The rotation-vibration wave functions hence have symmetries with respect to inversion as shown in Fig. 3-7, where the ground and first excited vibration states are indicated.

There are many symmetric tops such as  $\text{CH}_3\text{Cl}$  or  $\text{NH}_3$  which are not normally considered planar molecules, but which have the same symmetry with respect to inversion as  $\text{BF}_3$ .  $\text{NH}_3$  may actually be considered planar, but with a potential function which differs so much from a simple harmonic potential that as a result of vibration the nitrogen spends most of its time some distance from the plane of the three hydrogens. The energy levels of a particle moving in a parabolic potential are equally spaced as on the left side of Fig. 3-8. If the potential is distorted by a hill being gradually raised in the center, the energy levels approach each other in pairs as shown in Fig. 3-8. For a very high potential hill, the particle again has equally spaced energy levels, but two sets of them corresponding to oscillations on either one side of the hill or the other. However, even when the hill is so high that the particle does not have enough energy to go to its top, a quantum-mechanical "tunnel effect" occurs which allows the particle to oscillate slowly from one side of the potential barrier to the other. (This will be discussed more fully in

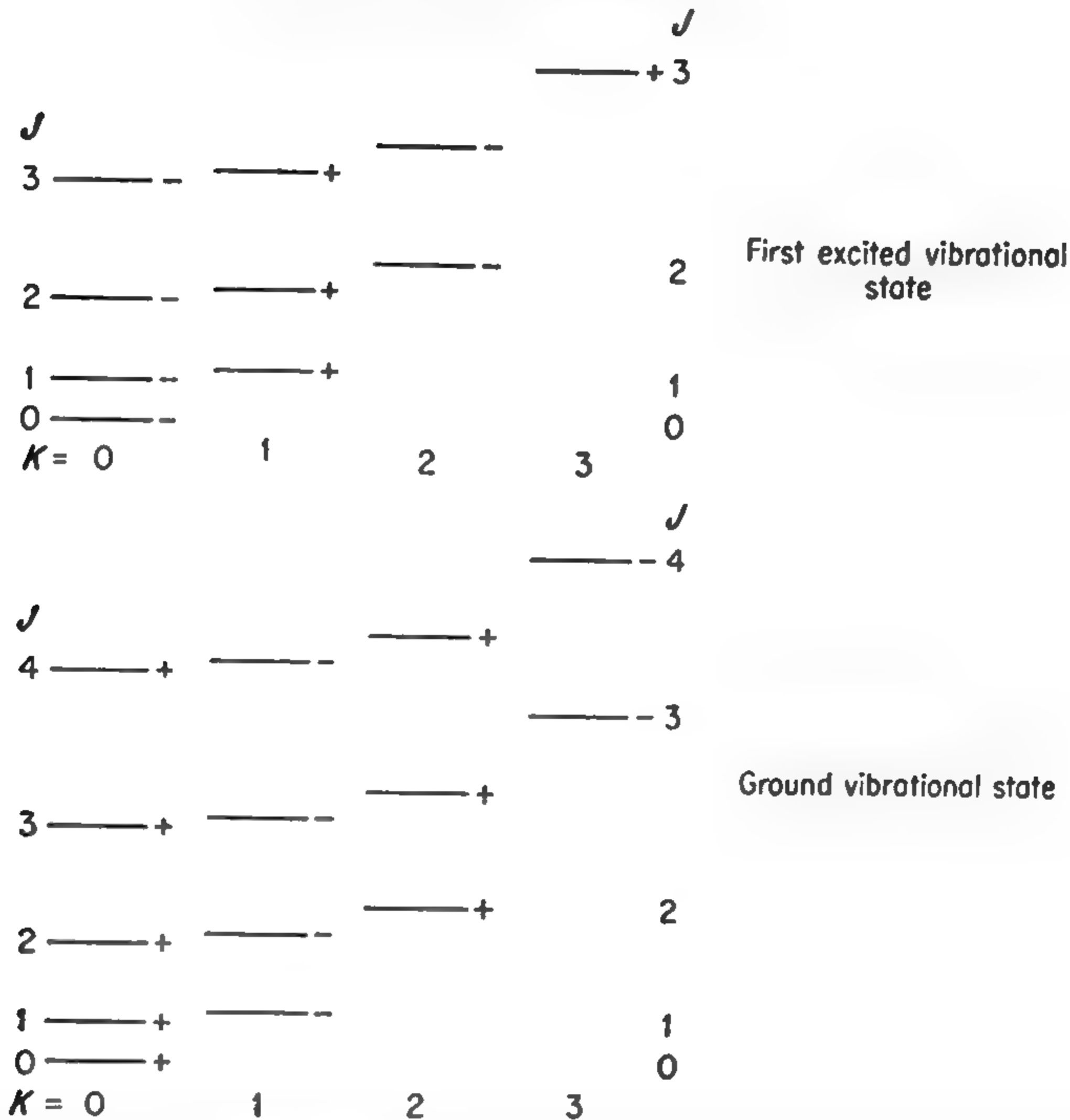


FIG. 3-7. Levels of a symmetric top and their symmetry with respect to inversion. The vibration is a nondegenerate mode in which atoms on the molecular axis move parallel to this axis.

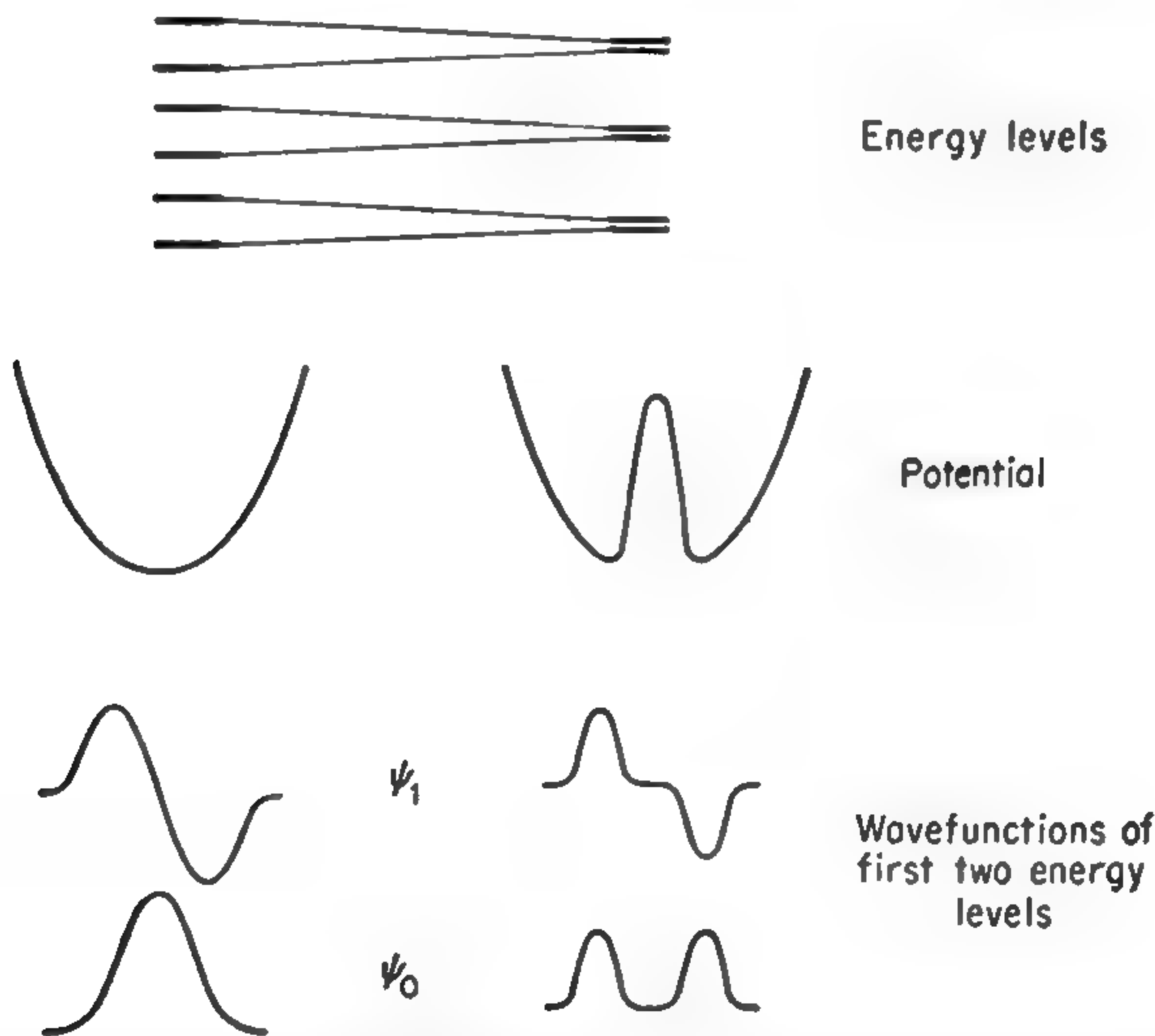


FIG. 3-8. Behavior of a vibration with introduction of a potential barrier.

Chap. 12 on the ammonia spectrum.) The rise of the central potential hill modifies the wave functions as is shown in Fig. 3-8, but does not destroy their symmetry. For  $\text{BF}_3$  there is no potential hill and the potential minimum occurs when the boron is in the plane of the fluorines, so the energy levels are those on the left of Fig. 3-8.  $\text{NH}_3$ , on the other hand, is a pyramidal molecule. Potential minima occur when the nitrogen is on either side of the plane of the hydrogens, and the energy levels correspond to those on the right-hand side of Fig. 3-8. In  $\text{NH}_3$ , the central potential hill is only moderately high, and the two lowest vibrational levels are separated by an energy gap such that a transition between them falls in the microwave region. In the case of  $\text{NF}_3$ ,  $\text{CH}_3\text{Cl}$ , or almost any other nonplanar top, the potential hill is so high that the two lowest vibrational levels have almost coalesced, their separation corresponding to frequencies which are so low that usually many years are required for an oscillation period.

For nonplanar symmetric tops, the transition between these two lowest levels is often referred to as inversion, for the classical motion corresponds to the molecule being turned inside out. This is not identical, however, with inversion of the molecule about the center of mass. Let the position of nitrogen with respect to the plane of the hydrogens in  $\text{NH}_3$  be given by wave functions  $\psi_0$  and  $\psi_1$  as shown on the right side of Fig. 3-8. The energy for  $\psi_0$  is  $W_0$ , so that it varies with time as  $\psi_0 e^{2\pi i W_0 t/h}$ , and similarly  $\psi_1$  varies as

$$\psi_1 e^{2\pi i (W_0 + \Delta) t/h}$$

where  $\Delta$  is the energy separating the two lowest levels. If at time  $t = 0$  the nitrogen is on the negative side of the hydrogens, then the wave function for the system may be written

$$\psi = \frac{1}{\sqrt{2}} (\psi_0 + \psi_1 e^{2\pi i \Delta t/h}) e^{2\pi i W_0 t/h} \quad (3-31)$$

which at time  $t = 0$  is  $(\psi_0 + \psi_1)/\sqrt{2}$ , and at time  $h/2\Delta$  is  $(\psi_0 - \psi_1)/\sqrt{2}$ , corresponding to the nitrogen being on the positive side. Hence the  $\text{NH}_3$  molecule inverts itself with a frequency (for a complete cycle)  $\nu = \Delta/h$ , which happens to be about  $2.4 \times 10^{10}$  times per second.  $\text{CH}_3\text{Cl}$ , on the other hand, exists for some time with Cl on one particular side of the molecular axis, and inverts only very slowly.

Symmetry and spacing of the rotation and inversion levels of  $\text{NH}_3$  are indicated in Fig. 3-9. Possible transitions, allowed by the rules  $+\longleftrightarrow-$ ,  $\Delta J = 0, \pm 1$ ,  $\Delta K = 0$ , are also shown. Figure 3-10 shows the same things for  $\text{CH}_3\text{Cl}$ , where the inversion levels are so close together as to be indistinguishable, and the rule  $+\longleftrightarrow-$  is no longer of importance since  $+$  and  $-$  levels coincide in pairs. Some levels in Fig. 3-9 for which  $K = 0$  are drawn as dashed lines. These levels cannot occur



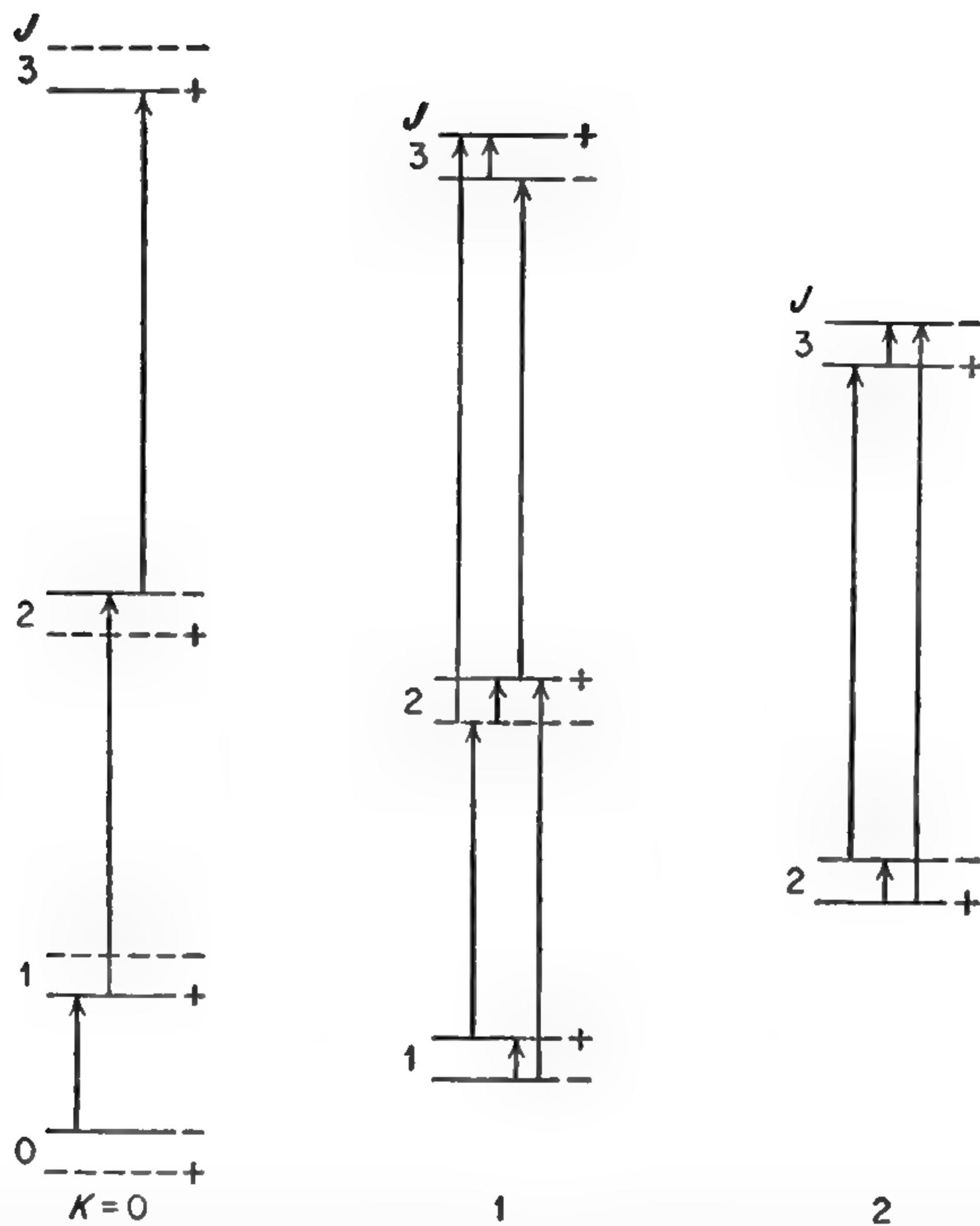


FIG. 3-9. Levels and possible transitions in the rotation-inversion spectrum of  $\text{NH}_3$ . The dotted levels for  $K = 0$  are forbidden by the exclusion principle.

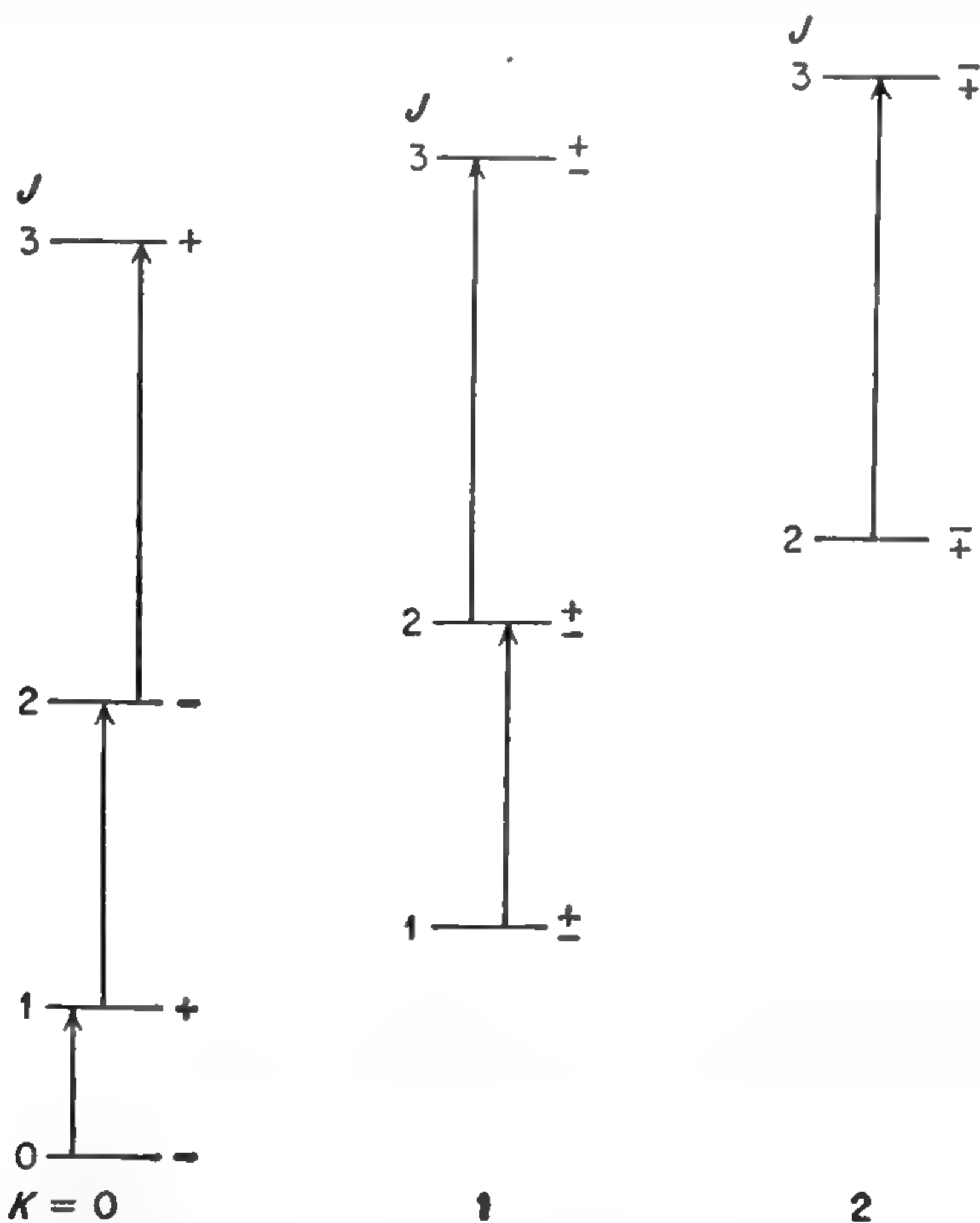


FIG. 3-10. Levels and possible transitions in the rotation-inversion spectrum of  $\text{CH}_2\text{Cl}$ , where the inversion frequency is negligibly small.

because of certain properties of the spin wave functions to be discussed below.

For  $\text{NH}_3$ , the doubling of each level due to inversion produces a doubling of the rotational lines with a separation between doublet components of twice the inversion frequency. This rotational spectrum lies in the infrared region. In addition, transitions between inversion levels with  $\Delta J = 0$ ,  $\Delta K = 0$  occur and produce lines which occur in the normal microwave range near 1 cm. In the case of  $\text{CH}_3\text{Cl}$ , the pure rotational spectrum is observed in the microwave range, and although each rotational line is split by twice the inversion frequency, this splitting is so small that it is completely unobservable even with the high resolution of microwave spectroscopy.

**3-4. Effects of Nuclear Spins and Statistics.** Other types of symmetry operations in addition to inversion about the center of mass may also be considered. For a symmetric top with a threefold axis of symmetry such as  $\text{NH}_3$  or  $\text{BF}_3$ , a rotation of  $120^\circ$  about the symmetry axis should leave the molecule essentially unchanged, and reasoning similar to that applied above to inversion about the origin shows that this rotation must either leave the wave function unchanged or change only its sign if the state is not degenerate. Similarly an interchange of two H nuclei in  $\text{NH}_3$  or two F nuclei in  $\text{BF}_3$  is another permissible symmetry operation which must affect the wave function in the same way.

Symmetry considerations may also be applied to the case of interchanging two identical particles in any type of system. It is found experimentally that  $\text{H}^1$ ,  $\text{F}^{19}$ , and any other nucleus of odd nuclear mass always occur in antisymmetric wave functions. These nuclei are said to obey Fermi-Dirac statistics. Nuclei of even mass always occur in symmetric wave functions and are said to obey Einstein-Bose statistics. Hence it is essential that any true and permissible wave function for  $\text{NH}_3$  changes sign when two H nuclei are exchanged.

Consider just rotation of  $120^\circ$  around the symmetry axis of  $\text{NH}_3$ . This is equivalent to exchanging two pairs of H nuclei, say first numbers 1 and 2, then 2 and 3. Since there are two exchanges, the wave function must be unchanged by a rotation of  $120^\circ$  if H obeys either Fermi-Dirac or Bose-Einstein statistics. The only one of Euler's angles which changes with such a rotation is  $\chi$ , which enters the wave function as  $e^{iK\chi}$  or  $e^{-iK\chi}$ . Hence after a  $120^\circ$ , or  $2\pi/3$ , rotation,

$$\psi' = \psi e^{\pm(2\pi/3)Ki} \quad (3-32)$$

If  $K$  is a multiple of 3, then the exponential in (3-32) equals 1, and  $\psi' = \psi$ , so that the wave function is symmetric. If  $K$  is not a multiple of 3, then  $\psi$  is neither symmetric nor antisymmetric. This indicates that the state is degenerate, which is true since the same energy is obtained for  $+K$  as for  $-K$ . In order to make wave functions of the

correct symmetry when  $K$  is not a multiple of 3, the spin wave function  $\psi_I$  must be considered, for when nuclei are exchanged not only their spatial coordinates are changed, but also their spins.

Before discussing spin wave functions, consider the symmetry operation of exchanging only one pair of nuclei, *e.g.*, 2 and 3. An interchange of these two nuclei changes the positive direction of the molecular axis as defined above, since it changes the relative order of the nuclei. The molecular variables are transformed as follows:

$$\begin{aligned}\theta' &\rightarrow \pi - \theta & \phi' &\rightarrow \phi + \pi \\ \chi' &\rightarrow \pi - \chi & h' &\rightarrow -h\end{aligned}\quad (3-33)$$

Detailed examination of the wave functions given by (3-12a) shows that for  $\theta \rightarrow \theta' - \pi$ ,  $\chi \rightarrow \pi - \chi'$ , and  $\phi \rightarrow \phi' - \pi$ , the wave function changes as

$$\psi_{JKM} \rightarrow (-1)^J \psi_{J,-K,M} \quad (3-34)$$

For this change of variables,  $\psi$  is neither symmetric nor antisymmetric but the wave functions are degenerate. They can be put in symmetric or antisymmetric form by choosing a wave function  $\psi_{JKM} + \psi_{J,-K,M}$  or  $\psi_{JKM} - \psi_{J,-K,M}$ . In exchanging nuclei 2 and 3,  $\chi$  changed to  $\pi - \chi$ . If, instead of interchanging 2 and 3, 1 and 3 had been interchanged, then the variables would have transformed as

$$\begin{aligned}\theta' &\rightarrow \pi - \theta & \phi' &\rightarrow \phi + \pi \\ \chi' &\rightarrow \pi - \chi + \frac{2\pi}{3} & h' &\rightarrow -h\end{aligned}\quad (3-35)$$

The new symmetrized forms  $e^{iKx} \pm e^{-iKx}$  would then for this exchange no longer be symmetric or antisymmetric unless  $K$  is a multiple of 3. Spin wave functions are needed to produce  $\psi_{\text{total}}$  which has the correct type of symmetry for all possible interchanges of nuclei.

*Spin Wave Functions.* The spin wave function for a nucleus needs to tell the projection of the spin on some fixed direction, which in the case of hydrogen can take on only two values,  $+\frac{1}{2}$  and  $-\frac{1}{2}$ . The  $+\frac{1}{2}$  value will be indicated graphically by a vector pointed up, and  $-\frac{1}{2}$  by a vector pointed down. Various possible spin functions which exactly specify the spin orientation of three H nuclei are then represented by Fig. 3-11.

The spin wave functions I and VIII of Fig. 3-11 are clearly symmetric with respect to interchange of any two nuclei, since they do not change. Spin function II, however, is symmetric with respect to interchange of 2 and 3, but it changes into III if 1 and 2 are interchanged, or into IV if 1 and 3 are interchanged. All spin functions shown in Fig. 3-11 are of this type except I and VIII, and hence are degenerate. Functions which are symmetric or antisymmetric with respect to interchange of any nuclei can be formed by combining the variation with  $\chi$  and spin. Such functions automatically are symmetric for a  $120^\circ$  rotation, which corresponds to successive interchange of two pairs of nuclei. If  $K$  is not a



multiple of 3, they are

$$\begin{aligned} & \psi_{JKM}(\text{II} + e^{2\pi Ki/3}\text{III} + e^{4\pi Ki/3}\text{IV}) \pm \psi_{J,-K,M}(\text{II} + e^{-2\pi Ki/3}\text{III} + e^{-4\pi Ki/3}\text{IV}) \\ & \psi_{JKM}(\text{V} + e^{2\pi Ki/3}\text{VI} + e^{4\pi Ki/3}\text{VII}) \\ & \pm \psi_{J,-K,M}(\text{V} + e^{-2\pi Ki/3}\text{VI} + e^{-4\pi Ki/3}\text{VII}) \end{aligned} \quad (3-36)$$

If  $K$  is a multiple of 3, these reduce to

$$\begin{aligned} & (\psi_{JKM} \pm \psi_{J,-K,M})(\text{II} + \text{III} + \text{IV}) \\ & (\psi_{JKM} \pm \psi_{J,-K,M})(\text{V} + \text{VI} + \text{VII}) \end{aligned} \quad (3-37)$$

and two additional functions have the correct symmetry,

$$\begin{aligned} & (\psi_{JKM} \pm \psi_{J,-K,M})\text{I} \\ & (\psi_{JKM} \pm \psi_{J,-K,M})\text{VIII} \end{aligned} \quad (3-38)$$

In all these expressions, when  $J$  is even the  $+$  sign produces a function which is symmetric with respect to interchange of two identical nuclei, and the  $-$  sign gives an antisymmetric function [cf. Eq. (3-34)]. When  $J$  is odd, the symmetries are reversed.

Not all the functions (3-36) or (3-37) and (3-38) are permitted for a particular rotation-inversion state. In the lowest inversion state, the vibrational (inversion) part of the wave function does not change sign for a transformation of the type (3-33) or (3-35), which reverses the sign of  $h$ . The parts of the wave function involving  $h$ ,  $\theta$ , and  $\phi$  are symmetric with respect to interchange of two nuclei if  $J + K$  is even [cf. (3-34)]. For these cases antisymmetric forms, with the  $-$  sign, must be chosen from (3-36), or (3-37) and (3-38) to make the total wave function change sign with exchange of two nuclei, i.e., if  $J$  is odd, the  $-$  sign is chosen in these equations, or if  $J$  is even, the  $+$  sign is needed. In the upper inversion state, the vibrational part of the wave function is antisymmetric for interchange of two nuclei, and the choice of  $+$  or  $-$  signs in (3-36), or (3-37) and (3-38) must be just reversed.

When  $K = 0$ , the functions of the form (3-37) or (3-38) become zero when the  $-$  sign is used, and hence no such wave function exists. This is the reason why half the levels are nonexistent when  $K = 0$  as indicated in Fig. 3-9. In the lowest inversion state, when  $K = 0$  and  $J = 0$ , a  $-$  sign in (3-37) or (3-38) would be called for, but this makes the wave function zero. In the upper inversion state, however, when  $K = 0$  and  $J = 0$ , a  $+$  sign is called for and such a wave function is not zero. When  $K = 0$  and  $J$  is odd, however, the ground inversion level requires the  $+$  sign and hence is the state in which molecules can exist.

Nucleus	1	2	3
I	↑	↑	↑
II	↓	↑	↑
III	↑	↓	↑
IV	↑	↑	↓
V	↑	↓	↓
VI	↓	↑	↓
VII	↓	↓	↑
VIII	↓	↓	↓

FIG. 3-11. The eight possible spin states for three nuclei with spin  $\frac{1}{2}$ .

*Statistical Weights.* It is evident that, with the exception of the case  $K = 0$ , there are twice as many acceptable wave functions from (3-37) and (3-38) for the case where  $K$  is a multiple of 3 as can be obtained from (3-36) for the cases where  $K$  is not a multiple of 3. This gives the states for which  $K$  is a multiple of 3 twice the statistical weight and hence approximately twice the population of otherwise similar states for which  $K$  is not a multiple of 3.

The above discussion has been specialized to the case of three identical atoms with spins  $\frac{1}{2}$ , which is by far the most common case. If there are three identical atoms with spin  $I$ , the statistical weights are given by Table 3-6 [25], [43]. Regardless of the type of statistics, the levels with  $K$  a multiple of 3 always have a greater weight, the ratio between these and other values of  $K$  being 2:1 in the case of spin  $\frac{1}{2}$  as was found above.

If  $K = 0$ , we have seen that alternate inversion levels on the level diagram of Fig. 3-9 are missing, beginning with the lowest inversion level for  $J = 0$ . If the spin  $I$  of the identical nuclei had been zero, Bose-Einstein statistics would apply instead of Fermi-Dirac, and for  $K = 0$  the role of permitted and forbidden levels on Fig. 3-9 would be just

TABLE 3-6. STATISTICAL WEIGHTS

Statistical weights due to nuclear spin for rotational levels of a symmetric-top molecule with three identical nuclei of spin  $I$ . These apply to molecules in a non-degenerate vibrational state. For a degenerate vibrational state,  $K$  should be replaced by  $K - l$ .

	Statistical weights	Nuclear spin, $I$
$K$ a multiple 3, but not 0	$\frac{1}{3}(2I + 1)(4I^2 + 4I + 3)$	0 $\frac{1}{2}$ 1 $\frac{3}{2}$
$K$ not a multiple of 3	$\frac{1}{3}(2I + 1)(4I^2 + 4I)$	
Ratio	$\frac{4I^2 + 4I + 3}{4I^2 + 4I}$	$\infty$ $\frac{2}{1}$ $\frac{11}{8}$ $\frac{6}{5}$
$K = 0$ , $J$ even lower inversion level or $J$ odd upper inversion level, Fermi-Dirac statistics	$\frac{1}{3}(2I + 1)(2I - 1)I$	
$K = 0$ , $J$ odd, lower inversion level or $J$ even, upper inversion level, Fermi-Dirac statistics	$\frac{1}{3}(2I + 1)(2I + 3)(I + 1)$	
Ratio Fermi-Dirac statistics	$\frac{(2I - 1)I}{(2I + 3)(I + 1)}$	0 $\frac{1}{5}$
Ratio Bose-Einstein statistics	$\frac{(2I + 3)(I + 1)}{(2I - 1)I}$	$\infty$ $\frac{10}{1}$

reversed. If the spin is greater than  $\frac{1}{2}$ , none of these  $K = 0$  levels is forbidden: their statistical weights for the case of Fermi-Dirac statistics are given in Table 3-6. For Bose-Einstein statistics, these formulas for statistical weights of alternate levels are just reversed.

For symmetric-top molecules with four identical nuclei equidistant around the axis, the statistical weights are as follows [43]:

For  $K \neq 0$ :

$$(I + 1)(2I + 1)(2I^2 + I + 1)$$

for  $K$  a multiple of 4, Bose-Einstein statistics or for  $K$  even, not a multiple of 4 and Fermi-Dirac statistics.

$$I(2I + 1)(2I^2 + 3I + 2)$$

for  $K$  a multiple of 4, Fermi-Dirac statistics or for  $K$  even, not a multiple of 4 and Bose-Einstein statistics.

$$I(I + 1)(2I + 1)^2$$

for  $K$  odd.

For  $K = 0$ :

$$\frac{1}{2}(I + 1)(2I + 1)(2I^2 + 3I + 2)$$

for  $J$  even, Bose-Einstein statistics.

$$\frac{1}{2}I(I + 1)(2I - 1)(2I + 1)$$

for  $J$  odd, Bose-Einstein statistics.

$$\frac{1}{2}I(2I + 1)(2I^2 + I + 1)$$

for  $J$  even, Fermi-Dirac statistics.

$$\frac{1}{2}I(I + 1)(2I + 1)(2I + 3)$$

for  $J$  odd, Fermi-Dirac statistics.

In this case, the inversion levels are considered to coincide, so statistical weights of the  $K = 0$  levels refer to the sum of both inversion levels.

The above considerations about statistical weights apply only to molecules in nondegenerate vibrational states. When a degenerate vibrational mode is excited, a new angular momentum  $l$  is introduced (*cf.*  $l$ -type doubling in Chap. 2 and below). In this case similar statistical weights apply, but with  $K$  replaced by  $K - l$  [943a]. Thus levels with  $K - l$  a multiple of 3 have greater statistical weights than do other levels for molecules with a threefold axis.

Nuclear spins are important in a wide variety of other types of molecules. Some of these are discussed by Placzek and Teller [43], Wilson ([64] and [90]), and Minden [730].

**3-5. Intensities of Symmetric-top Transitions.** Intensities of symmetric-top absorption lines may be calculated from the basic formula (1-49). Some of the quantities in this expression, however, such as the matrix element  $\mu$  and the fraction of molecules  $f$  in a given state, must be evaluated for the symmetric-top case.

Selection rules for dipole radiation of a nonplanar symmetric top (dipole moment taken only along the molecular axis since it is a truly symmetric top) are

$$\Delta J = 0, \pm 1 \quad \Delta K = 0 \quad + \rightarrow - \quad (3-39)$$

The last selection rule, taken from symmetry considerations above, is needed to specify the inversion levels involved in a transition, and may be



applied by referring to Fig. 3-9. Matrix elements may be calculated as indicated in (1-59), (1-60), and (1-61). However, since wave functions for a symmetric top are considerably more complex than those for a linear molecule, actual evaluation of these integrals is more difficult. The matrix elements are of course nonzero only for transitions given by the selection rules (3-39). The nonzero matrix elements are as follows:

$J + 1 \leftarrow J, K \leftarrow K$ :

$$|\mu_{ij}|^2 = \mu^2 \frac{(J + 1)^2 - K^2}{(J + 1)(2J + 1)} \quad (3-40)$$

$J \leftarrow J, K \leftarrow K$ :

$$|\mu_{ij}|^2 = \frac{\mu^2 K^2}{J(J + 1)} \quad (3-41)$$

$J - 1 \leftarrow J, K \leftarrow K$ :

$$|\mu_{ij}|^2 = \mu^2 \frac{J^2 - K^2}{J(2J + 1)} \quad (3-42)$$

These are the matrix elements appropriate for substitution into (1-49), and represent the sum of the components  $|R_x|^2$ ,  $|R_y|^2$ , and  $|R_z|^2$  for a particular molecule orientation specified by  $M$ , the projection of  $J$  on the  $z$  axis, to all possible final  $M$  states. The components  $|R_x|^2$ ,  $|R_y|^2$ , and  $|R_z|^2$  and their dependence on  $M$  are given in Table 4-4.

The quantity  $\mu$  in the above equations is the usual dipole moment of the molecule. One might question whether a symmetric top has a dipole moment, since we have been considering inversion as a type of vibration and even a pyramidal molecule as an oscillating planar molecule. This dipole moment  $\mu$ , however, is to be evaluated without considering inversion, but taking the symmetric top in its normal pyramidal configuration. Thus although  $\text{NH}_3$  is inverting approximately  $3 \times 10^{10}$  times per second,  $\mu$  is called a "permanent" dipole moment and is to be calculated when N is on one side only of the three hydrogens. This is the  $\text{NH}_3$  dipole moment which commonly enters into other physical and chemical measurements. Quantum-mechanically,  $\mu$  should be evaluated in the state  $(\psi_0 + \psi_1)/\sqrt{2}$ , where  $\psi_0$  and  $\psi_1$  represent wave functions for the two inversion levels.

The fraction of molecules  $f$  in a particular initial state is also needed to calculate absorption intensities from (1-49). This fraction  $f$  is the product of the fraction  $f_v$  in the vibrational state of interest and the fraction of these  $f_{JK}$  in a particular rotational state. If statistical weight due to nuclear spin is neglected, the probability of a molecule's being in a state  $J, K$  is proportional to

$$(2J + 1)e^{-[BJ(J+1) + (C-B)K^2]h/kT} \quad (3-43)$$

$2J + 1$  is the statistical weight due to the different orientations of  $J$ .

The fraction of molecules in this rotational state would be

$$f_{JK} = \frac{(2J + 1)e^{-[BJ(J+1)+(C-B)K^2]h/kT}}{\sum_{J=0}^{\infty} \sum_{K=-J}^J (2J + 1)e^{-[BJ(J+1)+(C-B)K^2]h/kT}} \quad (3-44)$$

Here  $B$  and  $C$  are in cycles per second as in (3-4). When  $Bh$  and  $Ch$  are small compared with  $kT$  the sums may be replaced by integrals, giving

$$f_{JK} = (2J + 1)e^{-[BJ(J+1)+(C-B)K^2]h/kT} \sqrt{\frac{B^2Ch^3}{\pi(kT)^3}} \quad (3-45)$$

It should be noted that (3-45) applies to one particular value of  $K$ , and does not allow for  $K$  degeneracy. A more accurate evaluation of the sum has been made ([130], p. 506) but is not of much interest to us because the error in approximating the sum as an integral is usually very small and in addition (3-44) does not allow for the statistical weights introduced by the spins of the like particles which must always be considered in a symmetric top.

The usual type of symmetric top has threefold symmetry about the axis and the separation between inversion levels is negligible. In that case, from Table 3-6 the degeneracy due to spin and inversion levels (or spin and  $K$  degeneracy) for each value of  $J$  and  $K$  is proportional to (omitting a constant factor  $(2I + 1)/3$ ):

For  $K$  a multiple of 3, but not 0,

$$S(I, K) = 2(4I^2 + 4I + 3) \quad (3-46a)$$

For  $K = 0$ ,

$$S(I, K) = (4I^2 + 4I + 3) \quad (3-46b)$$

For  $K$  not a multiple of 3,

$$S(I, K) = 2(4I^2 + 4I) \quad (3-46c)$$

Allowing for this degeneracy, (3-44) becomes

$$f_{JK} = \frac{S(I, K)(2J + 1)e^{-[BJ(J+1)+(C-B)K^2]h/kT}}{\sum_{J=0}^{\infty} \sum_{K=0}^J S(I, K)(2J + 1)e^{-[BJ(J+1)+(C-B)K^2]h/kT}} \quad (3-47)$$

It is evident that (3-47) is unaffected by the omission of a constant factor  $(2I + 1)/3$  in the degeneracy  $S(I, K)$  associated with spin and inversion as given in (3-46). Again assuming  $B$  and  $C$  to be much smaller than  $kT$ , the sums in (3-47) may be changed to integrals, so that one obtains

$$f_{JK} = \frac{S(I, K)(2J + 1)}{4I^2 + 4I + 1} \sqrt{\frac{B^2Ch^3}{\pi(kT)^3}} e^{-[BJ(J+1)+(C-B)K^2]h/kT} \quad (3-48)$$

For low values of  $J$  and  $K$ , the exponential in (3-48) is very close to 1, so that

$$f_{JK} = \frac{S(I,K)(2J+1)}{4I^2 + 4I + 1} \sqrt{\frac{B^2Ch^3}{\pi(kT)^3}} \quad (3-49)$$

The fraction of molecules in a given vibrational state may be obtained analogously to (1-51) as

$$f_v = e^{-W_v/kT} \prod_n (1 - e^{-h\omega_n/kT})^{d_n} \quad (3-50)$$

where  $d_n$  is the degeneracy of a vibrational mode of frequency  $\omega_n$  and  $\prod_n$  represents the product

$$(1 - e^{-h\omega_1/kT})^{d_1}(1 - e^{-h\omega_2/kT})^{d_2}(1 - e^{-h\omega_3/kT})^{d_3} \dots$$

for all vibrational modes. Since a symmetric top has a number of vibrational modes, the product  $\prod_n$  is sometimes appreciably less than 1, but in simple symmetric tops not usually less than about 0.5. Substituting (3-49) and (3-40) into (1-49), and setting  $2B(J+1) = h\nu_0$ , the intensity for a transition  $J+1 \leftarrow J, K \leftarrow K$  is

$$\gamma = \frac{4\pi h N f_v S(I,K)}{(4I^2 + 4I + 1)3c(kT)^2} \sqrt{\frac{\pi Ch}{kT}} \mu^2 \left[ 1 - \frac{K^2}{(J+1)^2} \right] \frac{\nu_0 \nu^2 \Delta \nu}{(\nu - \nu_0)^2 + (\Delta \nu)^2} \quad (3-51)$$

It may be seen that  $\gamma$  increases, as in a linear molecule, approximately as  $\nu^3$ . However, for a symmetric top  $\gamma$  is more strongly dependent on the temperature  $T$  than it is for the linear molecule. The expression (3-51) might be summed over all possible  $K$  for a particular  $J$  transition, since transitions for the various values of  $K$  coincide in frequency (approximately—see discussion of centrifugal distortions in Sec. 3-6).

Summing over the  $K$  values, assuming  $J$  is large, and letting  $\frac{S(I,K)}{4I^2 + 4I + 1}$  be approximately 2,

$$\gamma_{\text{total}} = \frac{2\pi h^2 N f_v}{9c(kT)^2 B} \sqrt{\frac{\pi Ch}{kT}} \mu^2 \frac{(4J+3)(J+2)}{(J+1)^2} \frac{\nu_0^2 \nu^2 \Delta \nu}{(\nu - \nu_0)^2 + (\Delta \nu)^2} \quad (3-52)$$

This shows that the entire intensity for a transition  $J+1 \leftarrow J$  summed over all  $K$  increases approximately as  $\nu^4$ , even more rapidly than intensities of transitions for linear molecules.

The maximum absorption coefficient of a symmetric-top transition  $J+1 \leftarrow J$  may also be written from (3-51), after some numerical



evaluation,

$$\gamma_{\max} = \frac{1.23 \times 10^{-20} f_v S(I, K) \sqrt{C}}{4I^2 + 4I + 1} \mu^2 \left[ 1 - \frac{K^2}{(J + 1)^2} \right] \frac{\nu_0^3}{\Delta\nu} \quad \text{cm}^{-1} \quad (3-53)$$

where  $C$  = rotational constant about the symmetry axis, Mc

$\mu$  = dipole moment, debye units ( $10^{-18}$  esu)

$\Delta\nu$  = half width at half maximum at a pressure of 1 mm Hg, Mc

$\nu_0$  = resonant frequency, Mc

the temperature is assumed to be 300°K

For symmetric tops with more than three identical nuclei, the statistical

weight factor  $\frac{S(I, K)}{4I^2 + 4I + 1}$  in (3-53) must be adjusted, but this factor

is of the order of 1 and may be set equal to 2 if an approximate evaluation of  $\gamma_{\max}$  is all that is required. The only other type of transition,  $J \leftarrow J$ , which occurs for a symmetric top is rather rarely of interest since it is a transition between inversion levels which usually corresponds to a negligibly small frequency. However, these inversion transitions are important in the case of  $\text{NH}_3$  and will be discussed in more detail in Chap. 13-

It may be noted that (3-51) or (3-53) does not reduce to the corresponding expression for a linear molecule when  $K = 0$  and  $C$  is infinite. This is because  $C$  has been assumed much smaller than  $kT$  in deriving these expressions, and hence they are no longer valid when  $C$  is allowed to be large. Because of the additional possible rotation around the symmetry axis, symmetric-top molecules are generally distributed throughout more states than are linear molecules and individual transitions are usually less intense by a factor of approximately 10. Typical intensity of a symmetric-top absorption at 1 cm wavelength is  $\gamma_{\max} = 10^{-6} \text{ cm}^{-1}$ .

Since variations in intensity with  $K$  depend on the nuclear spins (*cf.* [3-53] and Table 3-6), they may be used as a means of determining nuclear spins when several identical nuclei occur in the same molecule. This method of spin measurement has very limited utility, however, since molecules of this type are normally found only for abundant isotopes of common elements such as H and the halogens whose spins are already well known [233].

**3-6. Centrifugal Stretching in Symmetric Tops.** The discussion so far has assumed a rigid symmetric top, with no effects of vibration or centrifugal distortion. Centrifugal stretching of symmetric tops is somewhat more complicated than that for linear molecules because it involves both angular momentum quantum numbers  $J$  and  $K$ . It is fairly obvious that the amount of centrifugal distortion of the molecule cannot depend on the sign of the angular rotation (*e.g.*, whether it is clockwise or counterclockwise). Hence the change in rotational energy must involve only even powers of the momentum, such as the square of the total angular momentum  $J(J + 1)$  or of the component of momentum along the sym-

metry axis  $K^2$ . The rotational energy  $W$  including centrifugal effects may therefore be written

$$W(J, K) = BJ(J + 1) + (C - B)K^2 - D_J J^2(J + 1)^2 - D_{JK} J(J + 1)K^2 - D_K K^4 \quad (3-54)$$

plus terms of higher order in  $J(J + 1)$  and  $K^2$  where the centrifugal distortion constants  $D_J$ ,  $D_{JK}$ , and  $D_K$  are of the order of  $B^2/\omega$ ,  $\omega$  being a molecular vibrational frequency. The distortion constants are hence very small compared with the rotational constants  $B$  and  $C$ . The frequency due to a rotational transition  $J + 1 \leftarrow J$ ,  $\Delta K = 0$  is, from (3-54),

$$\nu = 2(J + 1)(B - D_{JK}K^2) - 4D_J(J + 1)^3 \quad (3-55)$$

Without centrifugal distortion, the rotational transitions for a symmetric top are all equally spaced, and for a given transition of  $J$ , the various possible values of  $K$  all give identical frequencies. From expression (3-55), it may be seen that centrifugal distortion destroys both these simple relations, although the previous approximation of a rigid rotor is still an extremely good one. Because of the term  $D_{JK}$ , molecules with different values of  $K$  have effectively slightly different values of the rotational constant  $B$ , so that their rotational transitions are not precisely superimposed. A high-resolution microwave spectroscope usually resolves separate rotational lines due to molecules with different values of  $K$ , so that  $D_{JK}$  is easily evaluated.

Centrifugal distortion for molecules of this type was first observed in the infrared rotational spectrum of  $\text{NH}_3$  and  $\text{PH}_3$  [44a]. In this case the lines due to different values of  $K$  were not resolved, but the center of gravity of successive  $J$  transitions could be fitted by an expression of the form

$$\nu = 2(J + 1)B - 4D(J + 1)^3$$

The constants  $D_J$ ,  $D_{JK}$ , and  $D_K$  depend of course on the various molecular force constants and the moments of inertia. The calculation from observed vibrational frequencies and rotational constants is both tedious and uncertain, since some of the force constants needed cannot always be accurately determined. However, Slawsky and Dennison [94a] obtained theoretical values of the centrifugal distortion constants of  $\text{NH}_3$ ,  $\text{ND}_3$ , and  $\text{PH}_3$  which fit experimental measurements of infrared spectra. These values are listed in Table 3-7. Chang and Dennison [783a] have succeeded in calculating  $D_J$  and  $D_{JK}$  for  $\text{CH}_3\text{Cl}$  to an accuracy of a few per cent. Nielsen [624] has given general expressions for the centrifugal stretching constants of symmetric molecules of the type  $\text{XY}_3$ . Appropriate force constants must be evaluated, however, before numerical results can be obtained from these expressions.

Values of  $D_J$  and  $D_{JK}$  for a number of molecules are given in Table 3-7.



It can be expected that  $D_J$  will always be positive as is illustrated in the table, since centrifugal forces due to rotation about any given axis will always tend to increase the moment of inertia about that axis or decrease the effective rotational constant. The sign of  $D_{JK}$  may in principle be either positive or negative. It is striking that all molecules of the type  $XY_3$  which have so far been examined have  $D_{JK}$  negative, while molecules involving a methyl group or its derivatives have a positive  $D_{JK}$ .

TABLE 3-7. VALUES OF CENTRIFUGAL STRETCHING CONSTANTS FOR REPRESENTATIVE SYMMETRIC-TOP MOLECULES

Molecule	$D_J$ , Mc	$D_{JK}$ , Mc	Reference
NH <sub>3</sub>	19	-28	[94a]
ND <sub>3</sub>	5.2	- 7.8	[94a]
PH <sub>3</sub>	3.7	- 4.6	[94a]
AsF <sub>3</sub>	.....	0.009 ± 0.002	[824]
CH <sub>3</sub> Cl <sup>35</sup>	0.0181	0.189	[531] [913]
CH <sub>3</sub> I	0.0080	0.0994	[531]
H <sub>3</sub> CCCI	.....	0.0072	[744]
F <sub>3</sub> CCCH	0.00024	0.0063	[557]
F <sub>3</sub> GeCl	~0.0006	$D_{JK}$   < 0.001	[555]
H <sub>3</sub> B <sup>11</sup> CO	.....	0.00036	[461]

**3-7. Rotation-Vibration Interactions and  $l$ -Type Doubling in Symmetric Tops.** The rotation-vibration constants  $\alpha$  for symmetric tops have been discussed theoretically by Shaffer [109a] and an extensive and systematic treatment has been given by Nielsen [624]. However, theoretical evaluation of these rotation-vibration constants involves knowing so many different force constants that as yet essentially no comparison between theory and experimental values of  $\alpha$  has been possible. There are a number of experimentally determined values of the  $\alpha$ 's in various symmetric tops. In many cases, however, the multiplicity of vibrational modes makes it difficult to assign uniquely a given observed rotational line due to an excited state to a particular vibrational mode, and hence to assign uniquely measured values of  $\alpha$ .

There are always a number of degenerate vibrational modes in symmetric tops. Even the simplest types (of the form  $XY_3$ ) have two sets of doubly degenerate vibrational modes, and each of these modes can produce an angular momentum which reacts in an interesting way with the angular momentum of rotation. If a degenerate vibrational mode involves only motion perpendicular to the molecular axis, then as in the case of the degenerate modes of a linear molecule, the vibration produces an angular momentum  $l\hbar$  about the molecular axis, where  $l$  is an integer and  $\hbar = h/2\pi$ . In general, the vibrational motion may not be entirely perpendicular to the axis, and it produces angular momentum  $\zeta l\hbar$  about



the axis of symmetry, where  $|\zeta| \leq 1$  (cf. [130]). The molecule may at the same time be rotating about the axis of symmetry, and it is the sum of the vibrational angular momentum plus that due to rotation of the molecular frame which is quantized and equal to  $K\hbar$ , where  $K$  is an integer. These two types of motions are illustrated in Fig. 3-12.

A given value of the angular momentum may be produced in a variety of ways. For example, if the molecule is excited to the first excited state of a degenerate mode for which  $\zeta = 1$ , then a momentum  $K = 1$  may be formed entirely of vibrational momentum ( $l = 1$ ) or it may be a combination of vibrational momentum  $l = -1$  and an angular momentum of the molecular frame of two units in the positive direction.

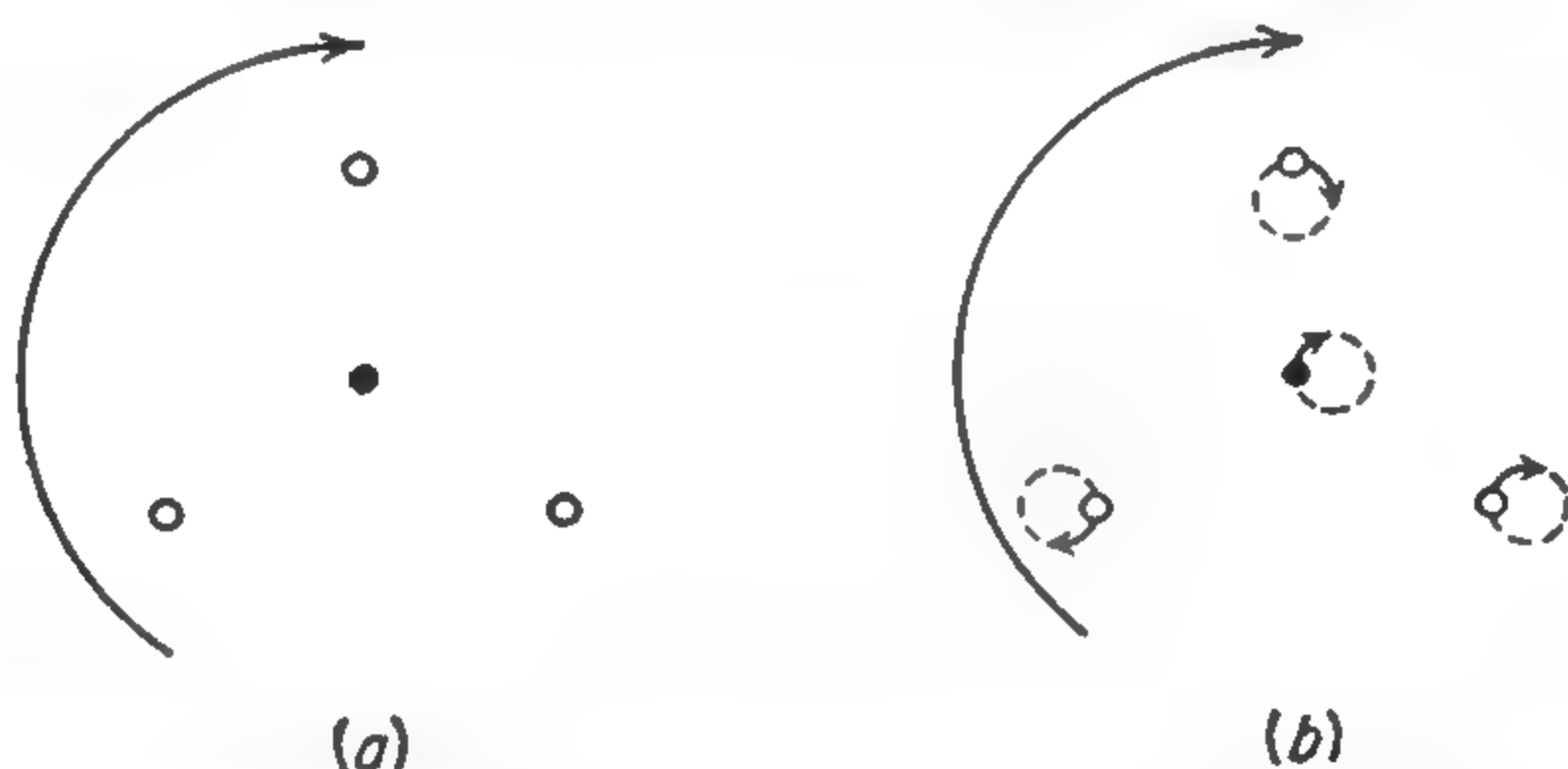


FIG. 3-12. Angular momentum along symmetry axis of  $XY_3$  molecule. (a) Rotation of molecular frame only; (b) rotation of molecular frame plus angular momentum produced by degenerate vibration.

Similarly  $K = -1$  can be formed in two ways. The angular momentum due to rotation of the molecular frame is  $K - \zeta l$ , and the energy associated with this momentum is hence not  $CK^2$ , but  $C(K - \zeta l)^2$  or

$$C(K^2 - 2\zeta lK + \zeta^2 l^2)$$

Since  $\zeta^2 l^2$  does not vary with rotational state, it may be omitted so that the rotational energy is written

$$W_R = BJ(J + 1) + (C - B)K^2 - 2K\zeta lC \quad (3-56)$$

The energy levels with  $l = \pm 1$  are compared in Fig. 3-13 with those for  $l = 0$ , assuming  $\zeta = 1$ .

When  $K = l = \pm 1$ , the molecule may be regarded as having no overall rotational motion about the symmetry axis. This is strictly true only if  $\zeta = 1$ , when the entire angular momentum  $K$  is provided by vibrational motion very much as in the case of a linear molecule with an angular momentum  $l = \pm 1$  due to a degenerate vibration. In this case, it is not hard to understand why  $l$ -type doubling occurs just as in a linear molecule [503], [624].

If the symmetric top is the common variety with a threefold symmetry axis, then levels for which  $K = -l = \pm 1$  are not split, nor is there appreciable splitting when  $|K| > 1$ . Since these cases correspond to the

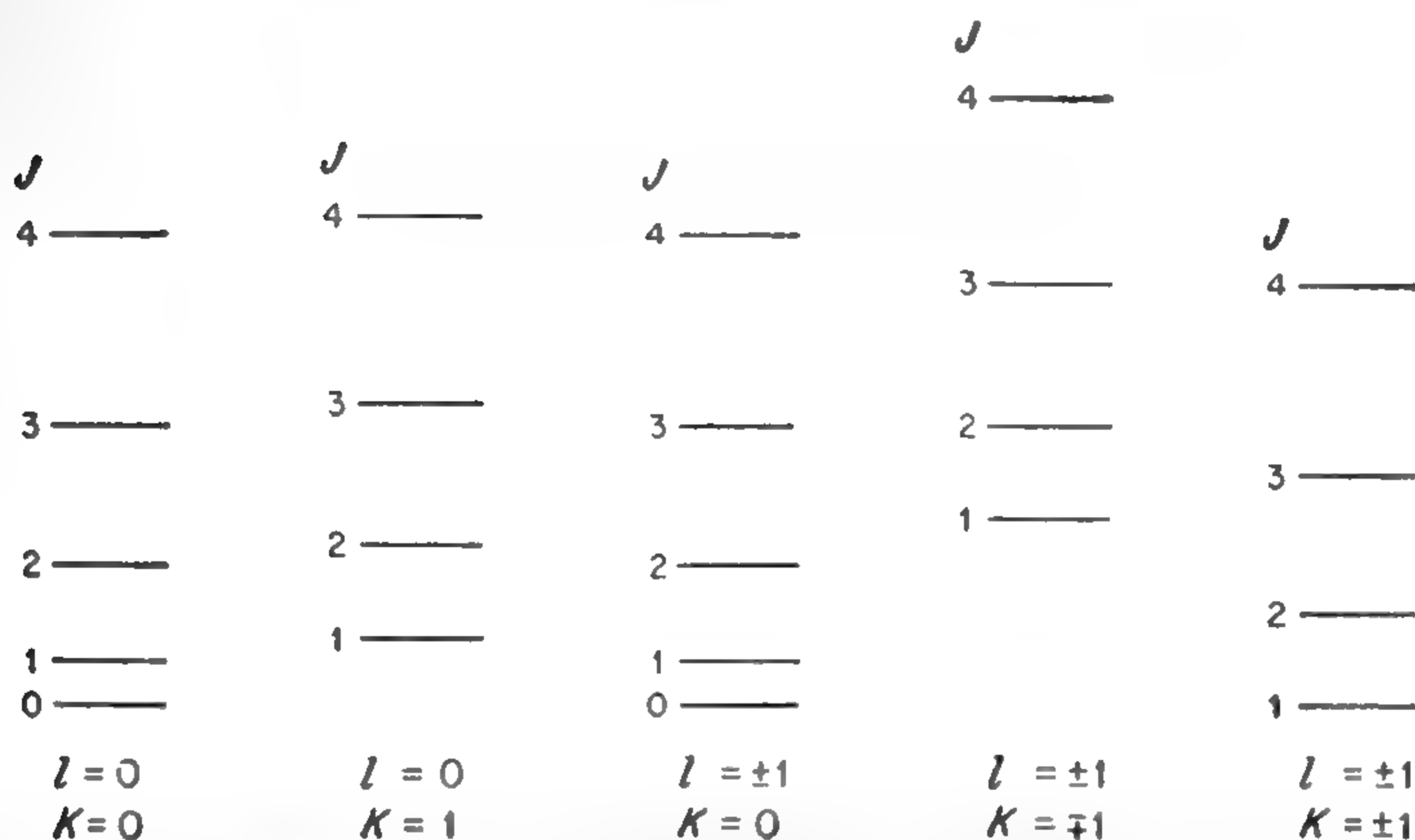


FIG. 3-13. Comparison of rotational energy levels for a symmetric top in the ground state with  $l = 0$  and those for an excited degenerate vibrational mode with  $l = \pm 1$ . The vibrational energy has been disregarded. Each level indicated by  $l = \pm 1$  is actually two which may be slightly different in energy due to  $l$ -type doubling.  $\zeta$  is assumed to be positive.

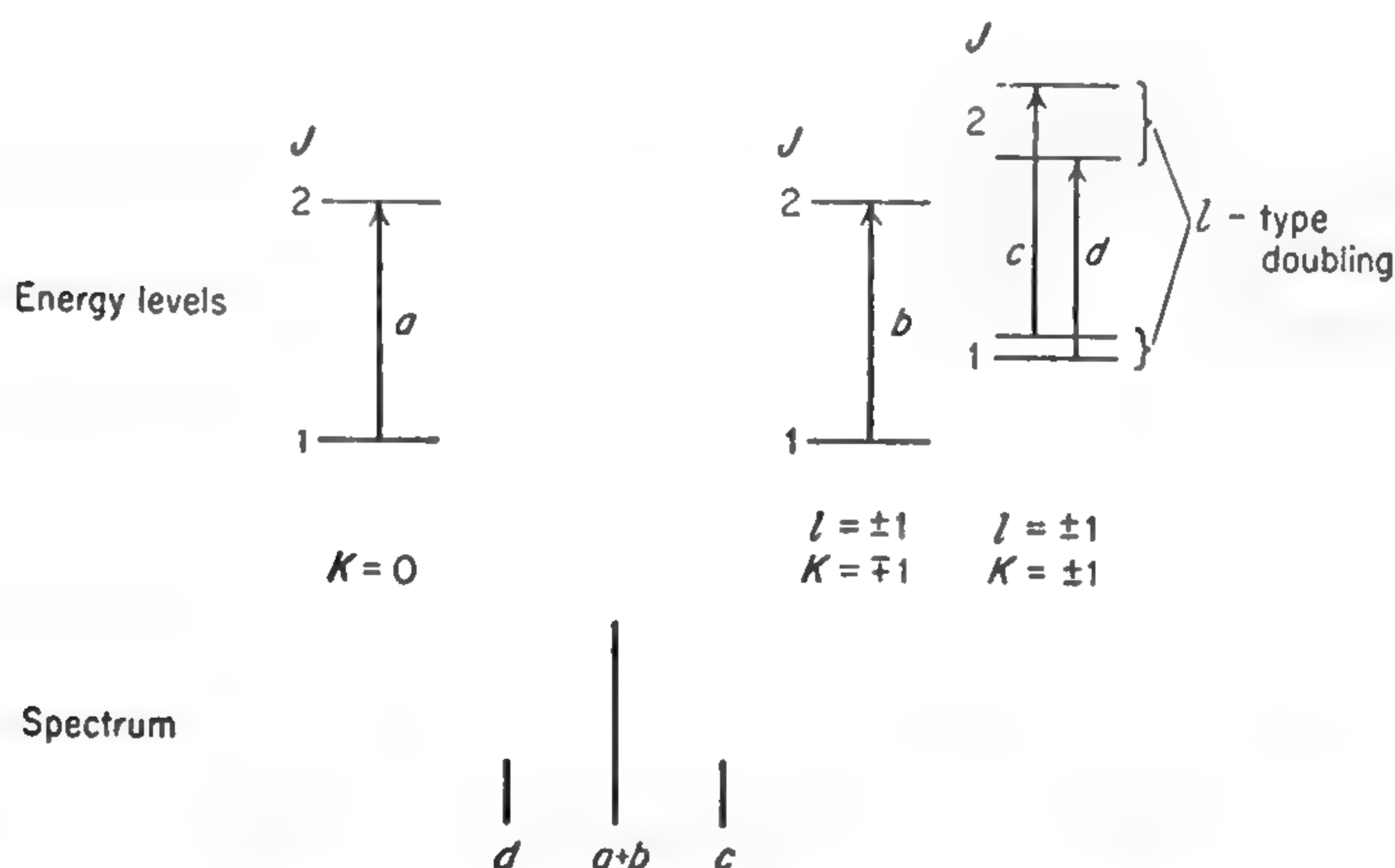


FIG. 3-14.  $l$ -type doubling in a symmetric rotator with three-fold symmetry axis. Energy levels and allowed transitions are shown above, and the resulting spectrum below.  $\zeta$  is assumed to be negative. Note that the transitions  $a$  and  $b$  are between doubly degenerate levels and are superimposed to a good approximation, although some splitting due to centrifugal distortion may occasionally be observed.

framework of the molecule rotating as a whole, any change in the effective values of  $B$  due to vibration may be thought of as equivalent for all orientations of the angular momentum  $J$  because of the averaging effect of the rotation. However, this qualitative explanation cannot be taken too seriously, since de Heer has shown [568] that, for a molecule with a fourfold axis of symmetry, the levels  $K = -l = \mp 1$  are split by an amount similar to those for which  $K = l = \pm 1$ .

Energy levels and allowed transitions for a  $J = 2 \leftarrow 1$  rotational line of a symmetric top with an excited degenerate vibration are shown in Fig. 3-14. The resulting spectrum is also shown.

**3-8. Dipole Moment Due to Degenerate Vibrations.** There are many symmetric molecules which have zero dipole moment because of their symmetry and hence one would not normally expect microwave absorption due to pure rotational transitions of these molecules. Mizushima and Venkateswarlu [846] have shown, however, that if certain types of symmetric molecules with zero dipole moment are excited to degenerate vibrational states, it is possible to observe pure rotational transitions due to an effective dipole moment resulting from the vibrations. Such an effect should occur in molecules like allene,  $C_3H_4$ , or spherical tops such as  $CF_4$ .



## CHAPTER 4

### ASYMMETRIC-TOP MOLECULES

An asymmetric top is a rotor with no two principal moments of inertia equal. General principles involved in the motion of such rotors are of course the same as for symmetric tops, but the details turn out to be much more complex. This complexity shows up not only in the quantum-mechanical behavior of an asymmetric top, but also in its classical motion. The classical motion is well known and closely parallels the quantum-mechanical behavior; but it is not simple enough to afford any generally useful model for the quantum-mechanical case. For this reason the discussion below will begin immediately with a quantum-mechanical approach. Much of the discussion follows the recent extensive work of King, Hainer, and Cross on asymmetric rotors [118], [122], [215], [372].

**4-1. Energy Levels of Asymmetric and Slightly Asymmetric Rotors.** A general picture of the behavior of the energy levels of an asymmetric top may be had from examining their behavior as the rotor begins to deviate from the two simple extremes, the prolate and the oblate symmetric top. As in (3-2), the energy is

$$W = \frac{P_x^2}{2I_x} + \frac{P_y^2}{2I_y} + \frac{P_z^2}{2I_z} = \frac{4\pi^2 A}{h} P_x^2 + \frac{4\pi^2 B}{h} P_y^2 + \frac{4\pi^2 C}{h} P_z^2$$

where for an asymmetric rotor the constants  $A$ ,  $B$ , and  $C$  are all different. If the three rotational constants are, in decreasing order of size,  $A$ ,  $B$ , and  $C$ , a prolate symmetric top corresponds to  $B = C$ , and an oblate symmetric top to  $B = A$ . The range of values of  $B$  between  $A$  and  $C$  correspond to various conditions of asymmetry. If  $B$  differs from  $A$  or from  $C$  by only a small amount, the rotor may be called a slightly asymmetric top. Figure 4-1 shows in a qualitative way how the energy levels vary as  $B$  varies from  $C$  to  $A$  so that on the left-hand side the levels are just those of a prolate symmetric top ( $B = C$ ) and on the right they correspond to an oblate symmetric top ( $B = A$ ). A slight asymmetry splits the levels  $\pm K$  which are degenerate for symmetric tops. Note that, as the value of  $B$  changes, no two levels of the same  $J$  cross. Levels of different  $J$  values may cross, however.

Various parameters may be used to indicate the degree of asymmetry.

Ray's asymmetry parameter [37] is

$$\kappa = \frac{2B - A - C}{A - C} \quad (4-1)$$

which becomes  $-1$  for a prolate symmetric top ( $B = C$ ) and  $1$  for an oblate symmetric top ( $B = A$ ), varying between these two values for asymmetric cases. Another parameter, especially appropriate for a slightly asymmetric prolate top, is

$$b_P = \frac{C - B}{2A - B - C} = \frac{\kappa + 1}{\kappa - 3} \quad (4-2)$$

$b_P$  is zero for a prolate symmetric top, and increases in size as the top becomes more asymmetric. The analogous asymmetry parameter for a slightly asymmetric oblate top is

$$b_O = \frac{A - B}{2C - B - A} = \frac{\kappa - 1}{\kappa + 3} \quad (4-3)$$

For an asymmetric top, the total angular momentum  $J$  and its projection  $M$  on an axis fixed in space are constants of the motion and "good" quantum numbers which can be used to specify the state of the rotor. However, neither in the classical motion (see [130], p. 42) nor for the quantum-mechanical solution is the component of the angular momentum constant along any direction in the rotating asymmetric molecule. This means that the quantum number  $K$ , which in a symmetric top is the projection of  $J$  on the symmetry axis, is no longer a "good" quantum number and cannot very well be used to specify the rotational state. In fact there is no set of convenient quantum numbers which can specify the state and also have simple physical meaning. Regardless of the fact that  $K$  is not a good quantum number for an asymmetric top, the energy levels may be specified by giving the value of  $J$ , and the value of  $K_{-1}$  for the limiting prolate and  $K_1$  for the limiting oblate symmetric top. The subscripts  $-1$  and  $1$  used here are the asymmetry parameter  $\kappa$ . Thus a level may be designated as  $J_{K_{-1}K_1}$  or  $5_{32}$ , indicating a  $J$  of 5 and a level which in the limiting cases connects on the left-hand side of Fig. 4-1 with a  $K$  of 3, and on the right-hand side with a  $K$  of 2. Another method of designating the levels is by  $J_\tau$ , where  $J$  is the total angular momentum and  $\tau$  is an integer between  $-J$  and  $J$  which indicates simply the order of the energy levels of a given  $J$ . Thus  $J_{-J}$  represents the lowest energy state of total angular momentum,  $J_{-J+1}$  the next, and  $J_J$  the highest. It may be seen from Fig. 4-1 that  $\tau = K_{-1} - K_1$ , so that these two common ways of designating the states are easily related.

If a molecule is a slightly asymmetric prolate top, the energy may be

conveniently written in the form

$$\frac{W}{h} = \frac{B + C}{2} J(J + 1) + \left( A - \frac{B + C}{2} \right) w \quad (4-4)$$

It may be seen by comparison with the energy of a prolate symmetric top that, since  $B \approx C$ ,  $w$  must approximately equal  $K^2$ . Exact expressions for the various possible values of  $w$ , regardless of the size of the asymmetry parameter  $b$ , are as follows:

$$\begin{aligned} J = 0: & \quad w = 0 \\ \\ J = 1: & \quad w = 0 \\ & \quad w - 1 - b = 0 \\ & \quad w - 1 + b = 0 \\ \\ J = 2: & \quad w - 4 = 0 \\ & \quad w - 1 + 3b = 0 \\ & \quad w - 1 - 3b = 0 \\ & \quad w^2 - 4w - 12b^2 = 0 \\ \\ J = 3: & \quad w - 4 = 0 \\ & \quad w^2 - 4w - 60b^2 = 0 \\ & \quad w^2 - (10 - 6b)w + (9 - 54b - 15b^2) = 0 \\ & \quad w^2 - (10 + 6b)w + (9 + 54b - 15b^2) = 0 \\ \\ J = 4: & \quad w^2 - 10(1 - b)w + (9 - 90b - 63b^2) = 0 \\ & \quad w^2 - 10(1 + b)w + (9 + 90b - 63b^2) = 0 \\ & \quad w^2 - 20w + (64 - 28b^2) = 0 \\ & \quad w^3 - 20w^2 + (64 - 208b^2)w + 2880b^2 = 0 \\ \\ J = 5: & \quad w^2 - 20w + 64 - 108b^2 = 0 \\ & \quad w^3 - 20w^2 + (64 - 528b^2)w + 6720b^2 = 0 \\ & \quad w^3 - w^2(35 - 15b) + w(259 - 510b - 213b^2) \\ & \quad \quad - (225 - 3375b - 4245b^2 + 675b^3) = 0 \\ & \quad w^3 - w^2(35 + 15b) + w(259 + 510b - 213b^2) \\ & \quad \quad - (225 + 3375b - 4245b^2 - 675b^3) = 0 \\ \\ J = 6: & \quad w^3 - w^2(35 - 21b) + w(259 - 714b - 525b^2) \\ & \quad \quad - 225 + 4725b + 9165b^2 - 3465b^3 = 0 \\ & \quad w^3 - w^2(35 + 21b) + w(259 + 714b - 525b^2) \\ & \quad \quad - 225 - 4725b + 9165b^2 + 3465b^3 = 0 \\ & \quad w^3 - 56w^2 + w(784 - 336b^2) - 2304 + 9984b^2 = 0 \\ & \quad w^4 - 56w^3 + w^2(784 - 1176b^2) \\ & \quad \quad - w(2304 - 53,664b^2) - 483,840b^2 + 55,440b^4 = 0 \end{aligned} \quad (4-5)$$



Similar expressions for  $J$  up to 11 have been developed by Randall, Dennison, Ginsburg, and Weber [84] and equations for still higher values of  $J$  may be derived from Wang's general expressions [18]. If the molecule is only slightly asymmetric,  $w$  may conveniently be expanded

$$w = K^2 + c_1 b_P + c_2 b_P^2 + c_3 b_P^3 + \dots \quad (4-6)$$

where  $b_P$  is the asymmetry parameter for a prolate top, which is given

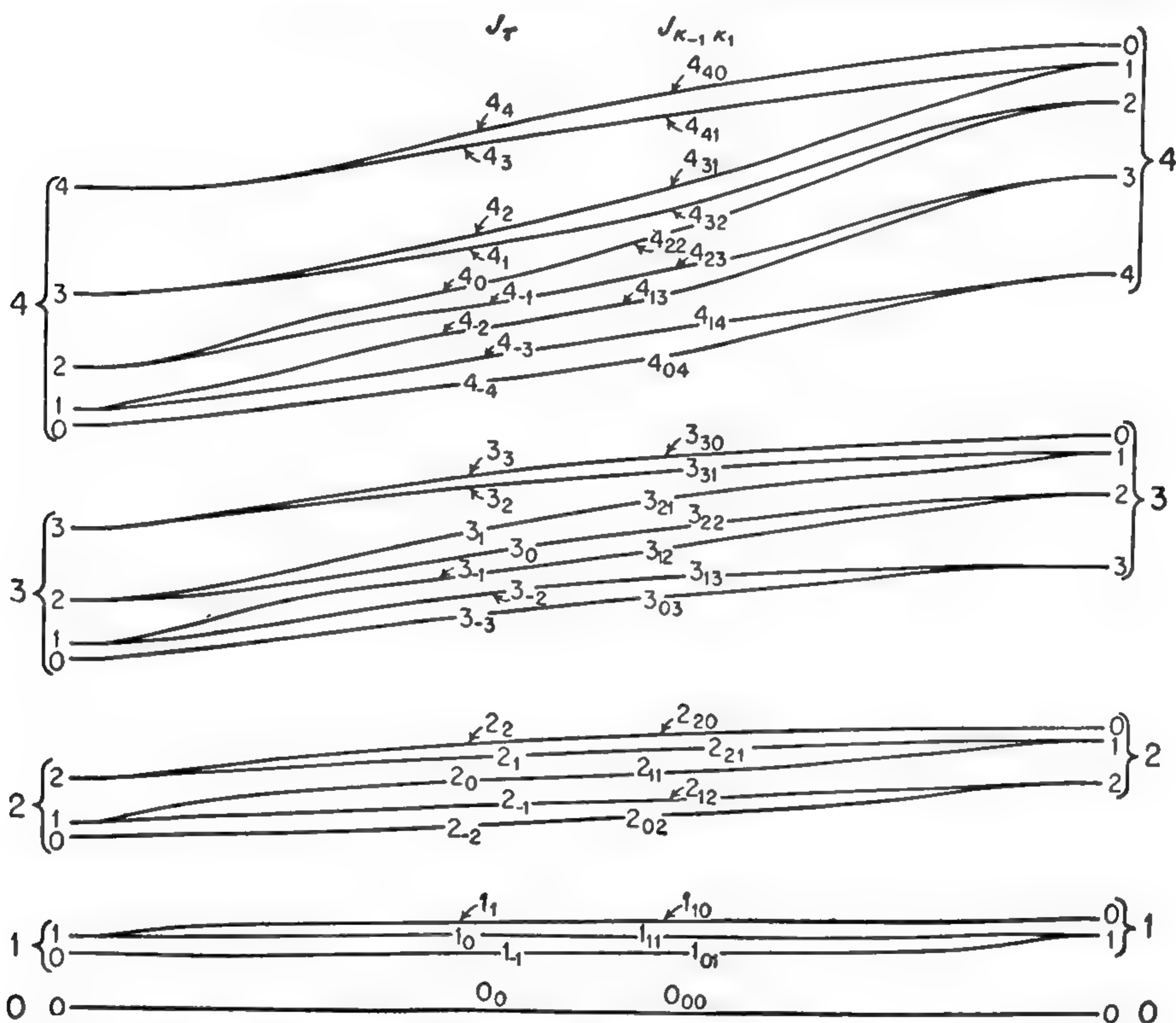


FIG. 4-1. Qualitative behavior of the asymmetric-top energy levels. The rotational constant  $B$  varies from left to right, equaling  $C$  and giving a prolate symmetric top on the left, and equaling  $A$  to give an oblate symmetric top on the right.

by (4-2). The coefficients  $c_1$ ,  $c_2$ , and  $c_3$  are given in Appendix III for a slightly asymmetric prolate top.

For the oblate case, similar formulas are good. The energy is

$$\frac{W}{h} = \frac{A+B}{2} J(J+1) + \left( C - \frac{A+B}{2} \right) w \quad (4-7)$$

with

$$w = K^2 + c_1 b_O + c_2 b_O^2 + c_3 b_O^3 + \dots \quad (4-8)$$

and  $b_O$  is defined by (4-3).  $K$  is now the appropriate value for an oblate

rotor, and  $c_1, c_2, c_3$  may be obtained from the table in Appendix III used for the prolate case if the values of  $K_{-1}$  and  $K_1$  are interchanged or the sign of  $\tau$  reversed.

It may be noted from Eqs. (4-5) or Appendix III that levels with  $K = 1$  which are degenerate for the symmetric case are split an amount proportional to the asymmetry  $b$  and to  $J(J + 1)$ . For levels with

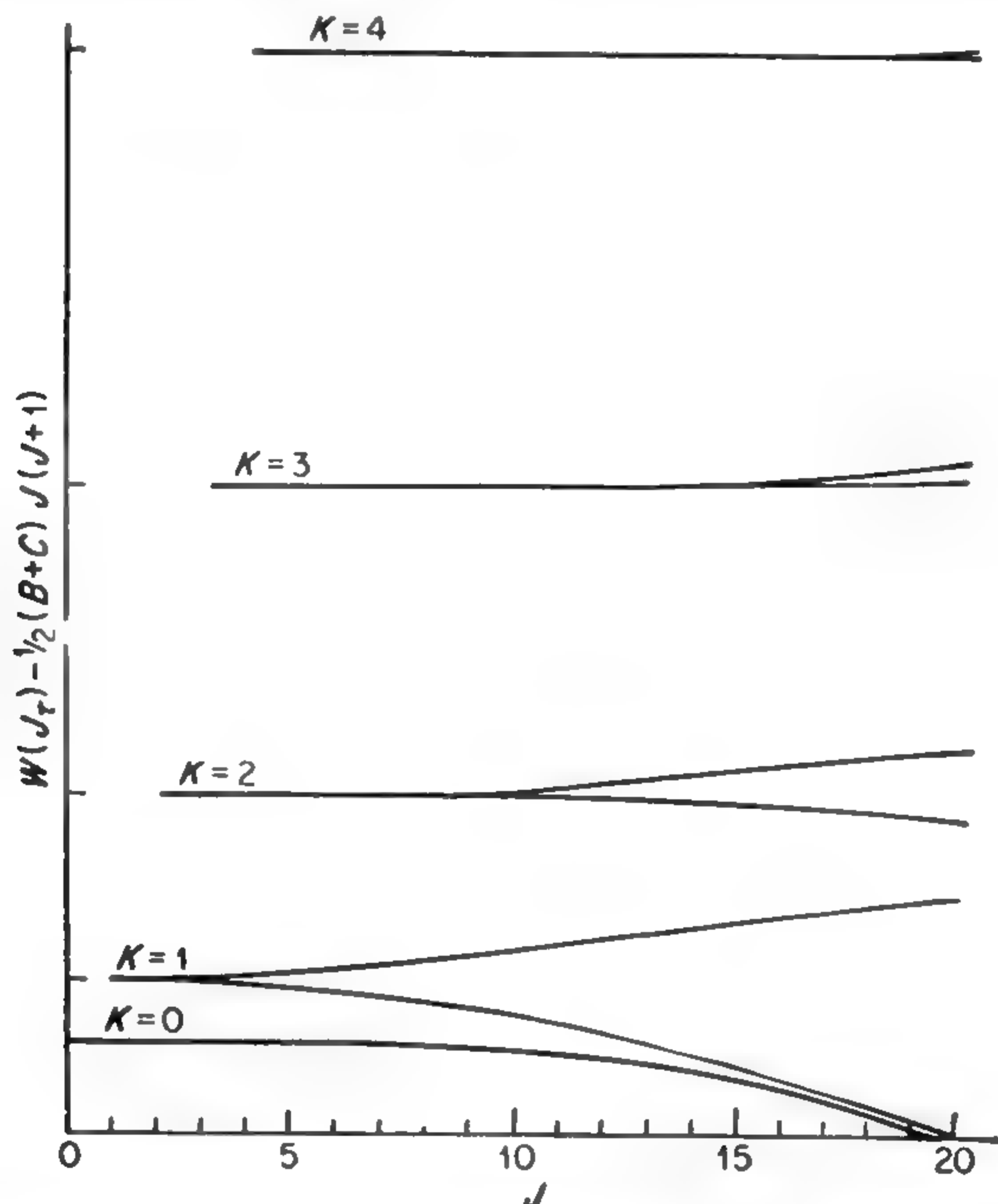


FIG. 4-2. Rotational energy of a slightly asymmetric top ( $b$  about 0.01) as a function of  $J$ . [The term  $\frac{1}{2}(B + C)J(J + 1)$  is subtracted from the energy, *i.e.*, the deviations of the curves from horizontal lines represent the deviations from the levels of the symmetric top.] (From Dieke and Kistiakowsky [47a].)

higher  $K$ , the splitting due to asymmetry is very much less and proportional to  $b^K$ , which is just analogous to the case of  $l$ -type doubling described in Chap. 2 for linear molecules. Wang [18] has shown that for small asymmetries the splitting of these levels which are degenerate in the symmetric case is given approximately by

$$\Delta w = \frac{b^K(J + K)!}{8^{K-1}(J - K)![(K - 1)!]^2} \quad (4-9)$$

where  $b$  and  $K$  are the appropriate prolate- or oblate-top values.

The variation of energy levels with  $J$  and  $K$  for a molecule of slight asymmetry is shown in Fig. 4-2. In addition to a splitting of the degenerate levels which increases with  $J$ , there is in most cases a deviation of the

center of the two degenerate levels from their symmetric-top values. This deviation is usually proportional to  $b^2$ . An approximation for the splitting which is good to the  $(K + 2)$ nd power of the asymmetry  $b$  has been given by Kivelson [825]. He showed that (4-9) should be multiplied by a factor of the form  $\{1 + [C_1 + C_2J(J + 1) + C_3J^2(J + 1)^2]b^2\}$ , where the constants  $C_1$ ,  $C_2$ , and  $C_3$  are tabulated [825] for various values of  $K$ .

The molecule  $\text{PCl}_3$  might ordinarily be classed as a symmetric top, as it is when all three chlorines are of the same isotopic species,  $\text{Cl}^{35}$  or  $\text{Cl}^{37}$ . However, common species of this molecule contain two atoms of  $\text{Cl}^{35}$  and one of  $\text{Cl}^{37}$ , or one of  $\text{Cl}^{35}$  and two of  $\text{Cl}^{37}$ , making them slightly

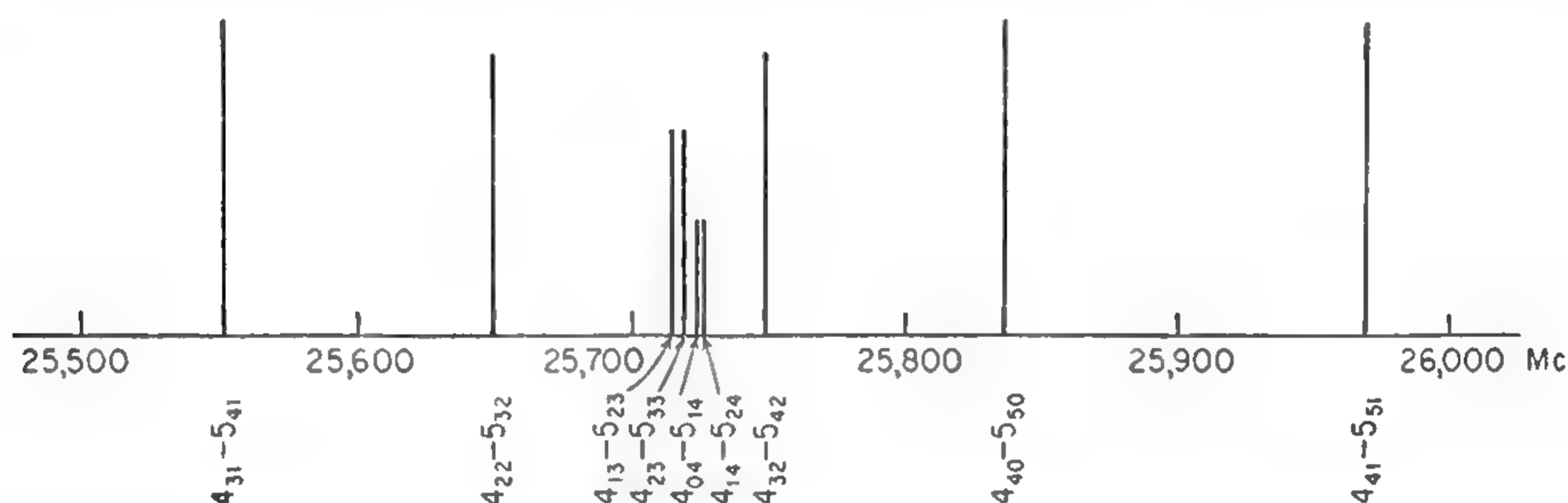


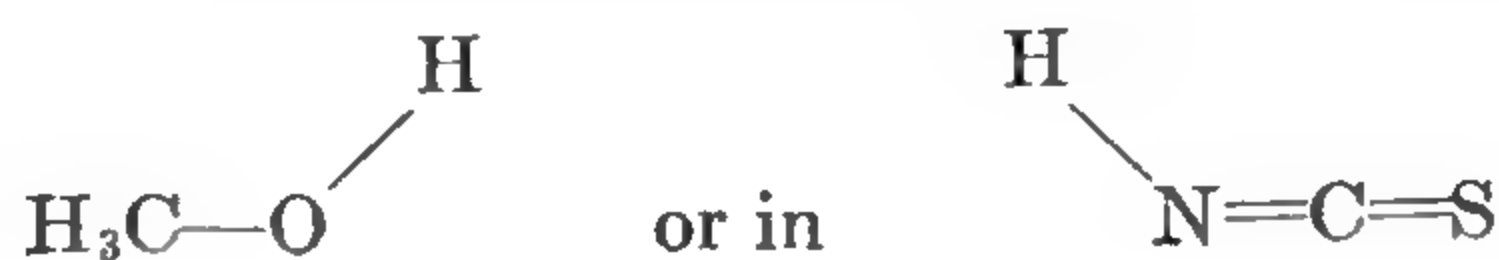
FIG. 4-3. The  $5 \leftarrow 4$  transition of a slightly asymmetric rotor  $\text{PCl}^{35}\text{Cl}_2^{37}$ . ( $b_0 = 0.037$ .)

asymmetric. This asymmetry affects the energy levels in a very noticeable way, since the observed frequencies are measured accurately. However, the effect of a slight asymmetry on the selection rules and intensities of transitions is generally negligible since intensities are not usually measured to high accuracy. The matrix elements and intensity relations given in Chap. 3 for a symmetric top may therefore be applied. The spectrum of the  $J = 5 \leftarrow 4$  transition of  $\text{PCl}_2^{35}\text{Cl}^{37}$  is shown in Fig. 4-3. Even though the asymmetry parameter

$$b_0 = \frac{A - B}{2C - B - A}$$

is only  $-0.037$ , most of the lines which would coincide for the symmetric molecule  $\text{PCl}_3^{35}$  are split by the asymmetry.

Slightly asymmetric tops are commonly and naturally formed by a mixture of isotopes as in  $\text{PCl}_2^{35}\text{Cl}^{37}$  or asymmetric methyl chloride  $\text{CH}_2\text{DCl}$ , and by adding a light off-axis atom to an otherwise symmetric structure as in methyl alcohol





Even the molecule  $\text{O}=\text{N}-\text{Cl}$  is approximately a prolate symmetric top

with an asymmetry parameter  $b$  as small as  $-0.0002$  [632]. Slight asymmetries may also occur in what may seem more accidental ways. For any bent triatomic molecule (as  $\text{NOCl}$ ), there is some value of the bond angle which makes the molecule an oblate symmetric top, and therefore a range of bond angles (in addition to those near  $0$  and  $180^\circ$ ) for which the molecule is only slightly asymmetric.

In case a molecule is very asymmetric and the asymmetry parameter  $b$  is large, an expansion for the energy of the type (4-6) or (4-8) is no longer appropriate. Equations (4-5) may of course be solved completely for any arbitrary value of  $b$  and hence the energies obtained from (4-4). However, it is generally better to express the energy in the form

$$\frac{W}{h} = \frac{1}{2}(A + C)J(J + 1) + \frac{1}{2}(A - C)E_\tau \quad (4-10)$$

where  $E_\tau$  has replaced  $w$  in (4-4) as a numeric to be evaluated for the particular case and amount of asymmetry.  $\tau$  is the integer used above to specify the order of the energy among the different levels of the same  $J$ . Certain values of  $E_\tau$  or  $E_{K_{-1}K_1}$  may be evaluated explicitly by solution of linear or quadratic equations. They are given in Table 4-1.

The quantity  $E_\tau$  in (4-10) is a function only of the asymmetry parameter, and if Ray's asymmetry parameter  $\kappa = (2B - A - C)/(A - C)$  is used, then

$$E_\tau(\kappa) = -E_{-\tau}(-\kappa) \quad (4-11a)$$

or in the  $J_{K_{-1}K_1}$  notation,

$$E_{mn}(\kappa) = -E_{nm}(-\kappa) \quad (4-11b)$$

Since  $E_\tau$  is a complicated function which must be computed and tabulated, relations (4-11) are of real value. Only positive or only negative values of  $\kappa$  need be tabulated, and from these the other values may be obtained from (4-11). The table in Appendix IV, computed by Turner, Hicks, and Reitwiesner [877a], gives values of  $E_\tau$  for all levels with  $J$  less than 13, and for values of  $\kappa$  from 0 to  $-1$  in steps of 0.01. These values of  $\kappa$  are not so closely spaced as might be desired for microwave work but, with care in interpolation between tabulated values of  $\kappa$ , energies may be obtained for any  $\kappa$  with sufficient accuracy for most microwave work.

It may also be noted that when  $\kappa = 0$ , which is sometimes called the most asymmetric case, (4-11) leads to the equation  $E_\tau(0) = E_{-\tau}(0)$ , so that the energy levels are symmetrically spaced [about  $E_0(0)$ ] when  $\kappa$  is zero. This relation might be guessed from examination of Fig. 4-1, since  $\kappa = 0$  is just halfway between the two limiting types of symmetric tops.

A number of sum rules for energy levels have been found by Mecke ([130], p. 50). They are of help in checking the correctness of energy-level computations. The most easily interpreted of these sum rules is

$$\frac{\sum_{\tau} \frac{W_{J\tau}}{h}}{2J + 1} = \frac{1}{3}(A + B + C)J(J + 1) \quad (4-12)$$

which states that the average rotational energy of all levels of a particular  $J$  is given by  $J(J + 1)$  times a rotational constant which is the average of  $A$ ,  $B$ , and  $C$ .

TABLE 4-1. SOLUTIONS OF  $E(\kappa)$ , THE ENERGY PARAMETER FOR ASYMMETRIC ROTORS [cf. Eq. (4-10)] FROM LINEAR OR QUADRATIC EQUATIONS

$J_{K_{-1}K_1}$	$E_{K_{-1}K_1}$
0 <sub>00</sub>	0
1 <sub>10</sub>	$\kappa + 1$
1 <sub>11</sub>	0
1 <sub>01</sub>	$\kappa - 1$
2 <sub>20</sub>	$2[\kappa + (\kappa^2 + 3)^{\frac{1}{2}}]$
2 <sub>21</sub>	$\kappa + 3$
2 <sub>11</sub>	$4\kappa$
2 <sub>12</sub>	$\kappa - 3$
2 <sub>02</sub>	$2[\kappa - (\kappa^2 + 3)^{\frac{1}{2}}]$
3 <sub>30</sub>	$5\kappa + 3 + 2(4\kappa^2 - 6\kappa + 6)^{\frac{1}{2}}$
3 <sub>31</sub>	$2[\kappa + (\kappa^2 + 15)^{\frac{1}{2}}]$
3 <sub>21</sub>	$5\kappa - 3 + 2(4\kappa^2 + 6\kappa + 6)^{\frac{1}{2}}$
3 <sub>22</sub>	$4\kappa$
3 <sub>12</sub>	$5\kappa + 3 - 2(4\kappa^2 - 6\kappa + 6)^{\frac{1}{2}}$
3 <sub>13</sub>	$2[\kappa - (\kappa^2 + 15)^{\frac{1}{2}}]$
3 <sub>03</sub>	$5\kappa - 3 - 2(4\kappa^2 + 6\kappa + 6)^{\frac{1}{2}}$
4 <sub>40</sub>	...
4 <sub>41</sub>	$5\kappa + 5 + 2(4\kappa^2 - 10\kappa + 22)^{\frac{1}{2}}$
4 <sub>31</sub>	$10\kappa + 2(9\kappa^2 + 7)^{\frac{1}{2}}$
4 <sub>32</sub>	$5\kappa - 5 + 2(4\kappa^2 + 10\kappa + 22)^{\frac{1}{2}}$
4 <sub>22</sub>	...
4 <sub>23</sub>	$5\kappa + 5 - 2(4\kappa^2 - 10\kappa + 22)^{\frac{1}{2}}$
4 <sub>13</sub>	$10\kappa - 2(9\kappa^2 + 7)^{\frac{1}{2}}$
4 <sub>14</sub>	$5\kappa - 5 - 2(4\kappa^2 + 10\kappa + 22)^{\frac{1}{2}}$
4 <sub>04</sub>	...
5 <sub>42</sub>	$10\kappa + 6(\kappa^2 + 3)^{\frac{1}{2}}$
5 <sub>24</sub>	$10\kappa - 6(\kappa^2 + 3)^{\frac{1}{2}}$

*Applicability of Various Approximate Methods.* Many useful methods for approximate evaluation of the rotational energy of asymmetric rotors have been developed. The discussion below is largely concerned with the applicability or range of usefulness of approximate methods. The reader is advised to consult original papers for detailed descriptions of the actual methods of computation (cf. also [872]).

Approximations are of most interest for large values of  $J$ , since many

of the equations (4-5) for small  $J$ 's are easily solved, and tabulations (Appendix IV) are available for  $J$ 's up to 12. For any large  $J$ , the various types of solutions for energy levels needed may be indicated on the two-dimensional diagram of Fig. 4-4. Various approximations are applicable in various parts of this diagram, but unfortunately in the

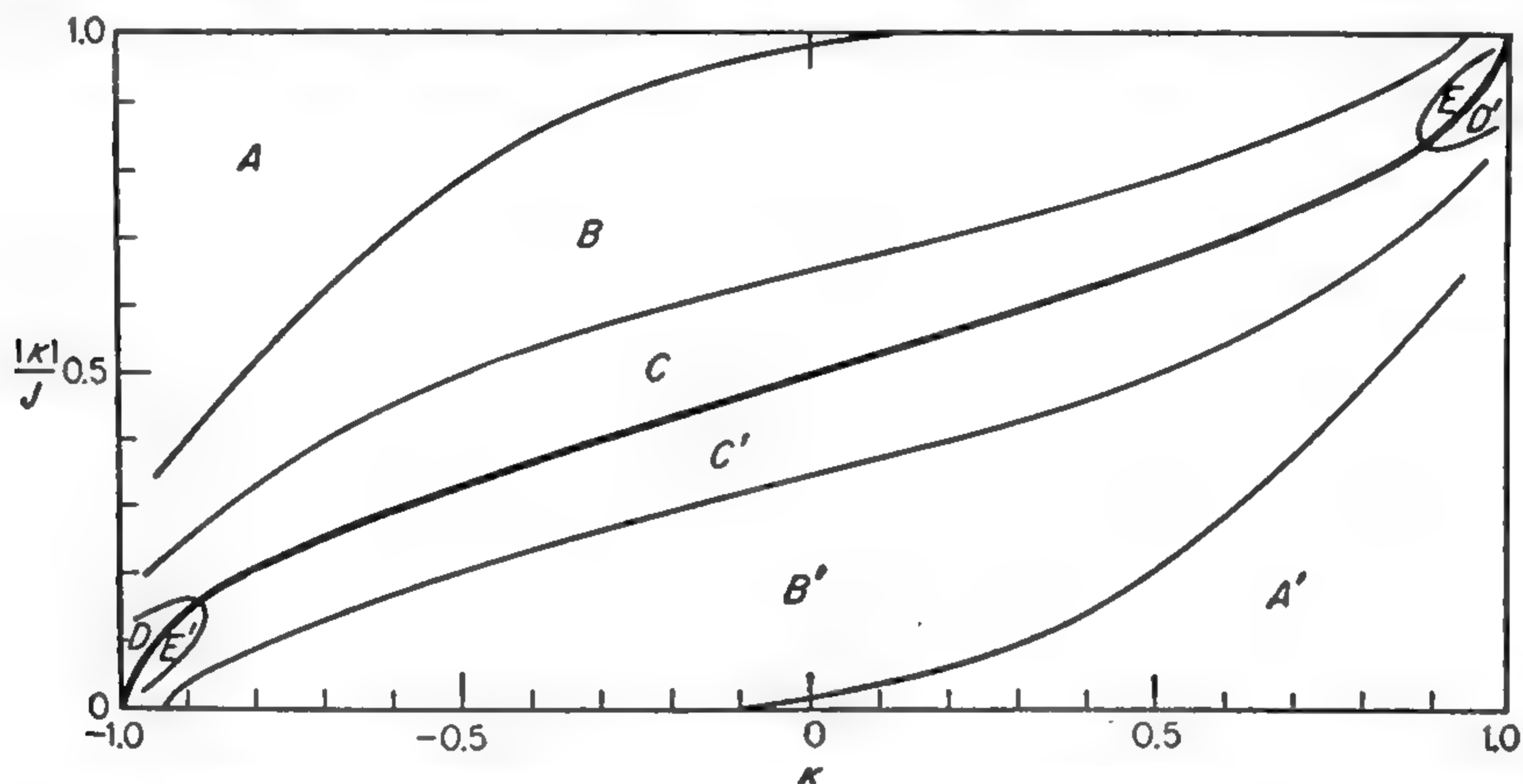


FIG. 4-4. Sketch of the regions of error expected in approximating  $E_\tau$ . (From Hainer, Cross, and King [372].)

regions  $C$  and  $C'$ , no known approximate method is very good because the energy levels change very rapidly across the heavy line

$$\frac{E_\tau(\kappa)}{J(J+1)} = \kappa$$

shown in this figure.

One type of approximation already discussed is a power-series expansion in the asymmetry parameter  $b$  [cf. (4-6) and (4-8)]. This expansion yields good results in the regions  $A$  and  $A'$ , that is, when  $|K|/J \approx 1$ . In the regions  $D$  and  $D'$ , that is, when  $|K|/J$  is small, the expansion is good only for very small asymmetries. Inaccuracy of such an expansion in these regions may be guessed from the very large size of the coefficients given in Appendix III when  $|K|/J$  is small, indicating the rapid change in energy near the line  $[E_\tau(\kappa)]/[J(J+1)] = \kappa$ .

Another power-series expansion about  $\kappa = 0$  of the form

$$E_\tau = a_0 + a_1\kappa + a_2\kappa^2 + \dots \quad (4-13)$$

has been used by King, Hainer, and Cross [118]. The coefficients  $a_0$ ,  $a_1$ , and  $a_2$  are tabulated for all levels with  $J$  less than 13. This expansion tends to be poor where the  $\kappa = 0$  line crosses the  $[E_\tau(\kappa)]/[J(J+1)] = \kappa$  line in Fig. 4-4, or hence for small  $E_\tau$ .

The "correspondence principle approximation" [215] uses the techniques of early quantum mechanics by setting the integrals of angular



momentum components for each of the Eulerian angles integrated over a complete cycle of the angle equal to some simple numerical multiple of  $h/2\pi$ . This leads to elliptic integrals which must be solved to obtain  $E_r$ . This approximation allows no difference in the energy between the two levels which are degenerate in the symmetric-top cases, and in general a good estimate of its error is the amount of actual splitting of these levels as given in (4-9). Hence for large values of  $J$  it yields very good results in regions  $A$  and  $A'$  of Fig. 4-4, is considerably worse in  $B$  and  $B'$ , bad in  $C$  and  $C'$ , and very bad in  $D$ ,  $D'$ ,  $E$ , and  $E'$  (for numerical illustrations of the errors due to this and the following approximation, see [372]).

Another method of approximating energy levels for large  $J$  takes advantage of the similarity between the matrix for the energy of an asymmetric rotor and a matrix arising from Mathieu's differential equation [274]. Characteristic values from Mathieu's equation with some corrections by perturbation methods may hence be used to approximate the asymmetric rotor energies. This "Mathieu's equation approximation" supplements the "correspondence principle approximation" by yielding good values for the energy in regions  $D$  and  $D'$  in Fig. 4-4 where the latter method is very poor. Elsewhere it is not appreciably better than the "correspondence principle approximation" and is less convenient because the amount of computation is somewhat greater. This approximation is therefore particularly useful when  $|K|/J \ll 1$ .

A similar type of approach may be used when  $|K|/J \approx 1$ . In this case, the energy matrix for large  $J$  becomes similar to one obtained from a harmonic oscillator. This "harmonic oscillator approximation" [369] is similar to the "correspondence principle approximation" in giving no splitting between the levels which are degenerate in the symmetric-rotor case. These two approximate methods are good in the same regions, that is,  $A$  and  $A'$ .

**4-2. Symmetry Considerations and Intensities.** The spectrum of an asymmetric rotor is complicated not only by the irregular distribution of energy levels, but also because the selection rules and transition probabilities between these levels are more complex than in the symmetric case. The selection rules are complicated partly by the increased number of separate levels, and partly because of the arbitrary direction of the dipole moment. It may be remembered that the dipole moment for a symmetric rotor must lie along the symmetry axis (if the possible, but nonexistent, accidentally symmetric rotor is excluded). In an asymmetric rotor the dipole moment may lie in any arbitrary direction with respect to the principal axes of inertia. However, the dipole moment is not uncommonly parallel to one of the three principal axes, and selection rules in such cases will be considered first.

General selection rules are usually the result of some symmetry prop-

erty, so we turn to an examination of symmetry relations. The rotational behavior of a molecule can be deduced from its ellipsoid of inertia, which is symmetric with respect to a rotation of  $180^\circ$  about any principal axis even though the molecule itself may not be symmetric with respect to such a rotation. Hence the wave function  $\psi$  must be either symmetric, antisymmetric, or degenerate with respect to such a rotation. Since degeneracy of the pure rotational energy levels is usually removed by asymmetry of the rotor, the only cases which need be considered are when  $\psi$  is symmetric (+) or antisymmetric (−).

For the limiting case of a symmetric prolate rotor, symmetry of the wave functions with respect to a rotation of  $180^\circ$  around the axis of least moment of inertia, which is the molecular axis, is easily determined. Since the wave function depends on this angle  $\chi$  as  $e^{\pm iK_{-1}\chi}$ , it is symmetric when  $K_{-1}$  is even, antisymmetric when  $K_{-1}$  is odd. Now this symmetry property of the wave function is not changed as a result of a perturbation of the same symmetry as the initial Hamiltonian; *i.e.*, although the wave function changes somewhat, it maintains the same symmetry or antisymmetry when the moments of inertia are slightly changed and the molecule becomes asymmetric. Hence any asymmetric wave function  $\psi_{J_{K_{-1}K_1}}$  is symmetric with respect to rotation of  $180^\circ$  around the axis of smallest moment of inertia when  $K_{-1}$  is even, antisymmetric when  $K_{-1}$  is odd. Similar consideration of the limiting oblate symmetric rotor shows that  $\psi_{J_{K_{-1}K_1}}$  is symmetric with respect to rotation around the axis of greatest moment of inertia when  $K_1$  is even, antisymmetric when  $K_1$  is odd.

Suppose the axes are labeled  $a$ ,  $b$ , and  $c$  in increasing order of size of the moments of inertia. The symmetry for axes  $a$  and  $c$  has already been determined. The symmetry for the intermediate axis  $b$  is derivable from them. Since successive rotations of  $180^\circ$  about each of the three axes brings the molecule back to its original orientation and the coordinates back to their original values, the symmetry for the rotation about  $b$  must be just such that it will counteract the effect of rotations about  $a$  and  $c$ . Hence the wave function is symmetric for a  $180^\circ$  rotation about  $b$  if  $K_{-1}$  and  $K_1$  are both odd or both even; otherwise it is antisymmetric.

If the dipole moment lies along the  $a$  axis, the dipole moment will reverse direction because of a rotation of  $180^\circ$  about either  $b$  or  $c$ . The matrix element, on which intensities depend, is of the form

$$\mu_0 = \int \psi_{J_{K_{-1}K_1}M} \mu \cos(ag) \psi_{J'_{K'_{-1}K'_1}M'} d\tau \quad (4-14)$$

where  $J_{K_{-1}K_1}M$  and  $J'_{K'_{-1}K'_1}M'$  represent the quantum numbers of initial and final states, and  $\cos(ag)$  is the cosine of the angle between  $a$  and some axis fixed in space. If  $\cos(ag)$  changes sign for a rotation of  $180^\circ$  around  $c$ , the  $\psi_{J_{K_{-1}K_1}}\psi_{J'_{K'_{-1}K'_1}}$  must also change sign if  $\mu_0$  is not zero. Otherwise

$\mu_a$  would appear to change sign, and since the matrix element  $\mu_a$  cannot change with this symmetry operation on the coordinates, it would have to equal zero. Hence transitions can occur only when  $K_1$  and  $K'_1$  are of different parity (one even and the other odd). A similar argument for rotation around  $b$  shows that  $K_{-1}$  and  $K'_{-1}$  must be of the same parity. This type of procedure may be applied to a molecule with dipole moment along the  $b$  or  $c$  direction to establish selection rules for these cases.

Wave-function symmetries are summarized in Table 4-2 and selection rules in Table 4-3.

TABLE 4-2. SYMMETRY PROPERTIES OF ASYMMETRIC-TOP WAVE FUNCTIONS

Designation		Behavior with 180° rotation about principal axes		
Cross, Hainer, and King $K_{-1}$ $K_1$	Dennison $c$ $a$	$a$ (least moment)	$b$ (intermediate moment)	$c$ (greatest moment)
$e$ $e$	$+$ $+$	$+$	$+$	$+$
$e$ $o$	$-$ $+$	$+$	$-$	$-$
$o$ $o$	$-$ $-$	$-$	$+$	$-$
$o$ $e$	$+$ $-$	$-$	$-$	$+$

TABLE 4-3. SELECTION RULES FOR ASYMMETRIC TOPS  
In all cases  $\Delta J = 0, \pm 1$ .

Axes parallel to dipole moment	Allowed transitions	
	Cross, Hainer, and King	Dennison
$a$ (least)	$ee \longleftrightarrow eo$ $oo \longleftrightarrow oe$	$++ \longleftrightarrow --$ $-- \longleftrightarrow +-$
$b$ (intermediate)	$ee \longleftrightarrow oo$ $eo \longleftrightarrow oe$	$++ \longleftrightarrow --$ $-+ \longleftrightarrow +-$
$c$ (greatest)	$ee \longleftrightarrow oe$ $oo \longleftrightarrow eo$	$++ \longleftrightarrow +-$ $-- \longleftrightarrow -+$

Symmetry properties have been discussed in terms of the evenness or oddness of  $K_{-1}$  and  $K_1$ , which are indicated by  $e$  or  $o$  in the tables. Since the symmetries for all three axes are not independent, it is sufficient to give the symmetry for the two axes only, and in the  $K$  notation they are given in the order  $a, c$ , the letters  $e$  and  $o$  being used for even and odd, respectively. The symmetry or antisymmetry of the wave func-



tion may also be indicated by  $+$  or  $-$ . When this notation is used, the two axes are designated in the order  $c, a$ . This is the older notation, and unfortunately the notation  $e, o$  above uses just the reverse order of axes. The usual selection rules  $\Delta J = 0, \pm 1$  for dipole radiation of a rotating body also apply to asymmetric rotors.

If the molecular dipole moment does not lie along any principal axis, it may be resolved into components along the three axes and the allowed transitions are the sum of all those allowed by Table 4-3 for each component. Thus if the dipole moment has nonzero components along all three axes, all possible transitions consistent with the general selection rule  $\Delta J = 0, \pm 1$  are allowed.

*Dipole Matrix Elements.* In order to evaluate intensities, the dipole matrix elements must be obtained. The  $z$  component of the matrix element for a transition  $j \leftarrow i$  is

$$\mu_z = \mu_a \int \cos(az) \psi_i \psi_j^* d\tau + \mu_b \int \cos(bz) \psi_i \psi_j^* d\tau + \mu_c \int \cos(cz) \psi_i \psi_j^* d\tau \quad (4-15)$$

where  $\mu_a, \mu_b, \mu_c$  are the components of the dipole moment along the three principal axes of the molecule and  $\cos(az), \cos(bz), \cos(cz)$  represent the cosines of angles between the principal axes and the  $z$  axis fixed in space. To obtain the integrals in (4-15), the wave functions for an asymmetric rotor are needed. The general form of these wave functions is discussed below, although the functions are not explicitly given.

The wave functions  $\psi_{JKM}$  for either a prolate or an oblate symmetric top form a complete set of functions in terms of which the wave functions for an asymmetric rotor may be expanded as follows:

$$\psi_{J_{K-1}K_1M} = \sum_{J'} \sum_K \sum_{M'} a_{J'KM'} \psi_{J'KM'} \quad (4-16)$$

where  $a_{J'KM'}$  is an appropriate numerical coefficient. Since the total angular momentum  $J$  and its projection  $M$  on a fixed axis are good quantum numbers for any asymmetry and more than one value cannot be involved in a given state,  $J' = J$  and  $M' = M$ , so that (4-16) reduces to

$$\psi_{J_{K-1}K_1M} = \sum_K a_{JKM} \psi_{JKM} \quad (4-17)$$

Prolate symmetric-top wave functions are, of course, most appropriate when the rotor approximates a prolate symmetric top, and oblate top functions when it is nearly an oblate symmetric top.

Since the function  $\psi_{J_{K-1}K_1M}$  must be either symmetric or antisymmetric with respect to a  $180^\circ$  rotation as pointed out above, only odd or only even  $K$  will appear in the sum; hence for an expansion in prolate wave

functions,

$$\psi_{J K_{-1} K_1 M} = \sum_{K=K_{-1} \pm 2n} a_{JKM} \psi_{JKM} \quad (4-18)$$

where  $n$  is an integer. The energy depends on the  $a_{JKM}$ , since they give the probability of rotation with the particular angular momenta  $J$  and  $K$ . However, since the energy cannot depend on  $M$ , the projection of  $J$  on some arbitrary direction in space, the  $a_{JKM}$  must be independent of the quantum number  $M$ . The  $a_{JKM}$  in (4-17) or (4-18) may hence be indicated simply by  $a_{JK}$ .

The coefficients  $a_{JK}$  can be evaluated (see, for example, [379]), but no simple closed expression may be found for them, except in special cases.

From (4-18) it may be seen that the matrix elements for an asymmetric rotor can be derived from those for a symmetric rotor. In cases of slightly asymmetric rotors, a sum of type (4-18) reduces to essentially one term, and matrix elements are, to good accuracy, the same as those for symmetric tops.

The dipole matrix elements for a symmetric top may be broken up into several factors [355]

$$\mu_{\theta} = \mu \phi_{JJ'} \phi_{JKJ'K'} \phi_{JMJ'M'} \quad (4-19)$$

where  $\mu$  is the molecular dipole moment, or its component along some principal axis. The  $\phi$ 's, which might be called factors of the direction-cosine matrix from (4-15), are each dependent on the rotational quantum numbers indicated by subscripts. The  $\phi$ 's are also dependent on the particular component  $\mu_{\theta}$  which is being evaluated and on the molecular axis along which the dipole moment  $\mu$  lies. Table 4-4 gives expressions for the various  $\phi$ 's.

From Table 4-4 the dipole matrix elements of symmetric tops for

TABLE 4-4. VALUES OF FACTORS OF THE DIRECTION-COSINE MATRIX ELEMENTS

The dipole moment matrix element is  $\mu \phi_{JJ'} \phi_{JKJ'K'} \phi_{JMJ'M'}$ . Subscript  $a$  applies to cases where  $\mu$  is along the molecular axis,  $b$  or  $c$  to cases where  $\mu$  is perpendicular to this axis. Subscripts  $x$ ,  $y$ , or  $z$  apply for  $\mu_x$ ,  $\mu_y$ , or  $\mu_z$ , which are the appropriate elements for polarization along the  $x$ ,  $y$ , or  $z$  directions, respectively. The phases chosen are consistent with reference [56]. Matrix elements listed are appropriate for a prolate symmetric top (with  $a$  the symmetry axis). For an oblate symmetric top,  $\phi_a$  should be replaced by  $\phi_c$ ,  $\phi_c$  by  $\phi_b$ , and  $\phi_b$  by  $\phi_a$ .

Matrix element factor	Value of $J'$		
	$J + 1$	$J$	$J - 1$
$\phi_{JJ'}$	$[4(J+1)\sqrt{(2J+1)(2J+3)}]^{-1}$	$[4J(J+1)]^{-1}$	$[4J\sqrt{4J^2-1}]^{-1}$
$(\phi_a)_{JKJ'K}$	$2\sqrt{(J+1)^2-K^2}$	$2K$	$-2\sqrt{J^2-K^2}$
$(\phi_b \text{ or } \pm i\phi_c)_{J,K,J',K \pm 1}$	$\mp \sqrt{(J \pm K + 1)(J \pm K + 2)}$	$\sqrt{(J \mp K)(J \pm K + 1)}$	$\pm \sqrt{(J \mp K)(J \mp K - 1)}$
$(\phi_c)_{JMJ'M}$	$2\sqrt{(J+1)^2-M^2}$	$2M$	$-2\sqrt{J^2-M^2}$
$(\phi_x \text{ or } -i\phi_y)_{J,M,J',M \pm 1}$	$\mp \sqrt{(J \pm M + 1)(J \pm M + 2)}$	$\sqrt{(J \mp M)(J \pm M + 1)}$	$\pm \sqrt{(J \mp M)(J \mp M - 1)}$

transitions between individual  $M$  values may be obtained, and from these the average square of the matrix element, or  $|\mu_{ij}|^2$  as given in (3-40),

(3-41), and (3-42). A rather unreliable, but sometimes useful, estimate of the transition intensity for an asymmetric rotor may be made by interpolating between the intensities of the corresponding transitions for a prolate and an oblate symmetric top. For slightly asymmetric rotors, Lide [720] has given the dipole matrix elements as those of the symmetric rotors plus a correction term proportional to the asymmetry. Numerical values for the intensities of the more important transitions involving levels with  $J$  less than 13 may be obtained as a function of asymmetry in Appendix V [122].

A general view of the many transitions which can occur in an asymmetric rotor is given by Table 4-5. The changes in pseudo quantum numbers  $K_{-1}$  and  $K_1$  are indicated by numbers, a minus sign being put before the numbers when a change in  $K_{-1}$  or  $K_1$  is negative. Superscripts  $a$ ,  $b$ , and  $c$  indicate components of the molecular dipole moment along directions of the least, intermediate, and greatest principal moments of inertia, respectively. For an arbitrary direction of the dipole moment, all possible changes  $\Delta K_{-1}$  and  $\Delta K_1$  are allowed except that both these changes cannot be even (cf. Table 4-3). Any particular transition is due to only one of the components of the dipole moment, that is,  $\mu_a$ ,  $\mu_b$ , or  $\mu_c$ .

Intensities of absorption lines of asymmetric rotors are given by the basic formula (1-59) or (13-19). The matrix element  $|\mu_{ij}|^2$  used in these expressions is the sum  $\sum_{M'} (\mu_x^2 + \mu_y^2 + \mu_z^2)$  for any arbitrary orientation of the molecule indicated by  $M$ , the projection of  $J$  on a fixed axis. As was found in Chap. I, this quantity is independent of  $M$ , and furthermore the sum of  $|\mu_{ij}|^2$  for all states  $M$  of the transition  $J' \leftarrow J$ , must just equal the sum for all states  $M'$  of the transition  $J' \rightarrow J$  in order to maintain thermal equilibrium. Since there are  $2J + 1$  different  $M$  states,

$$(2J + 1)|\mu_{J' \leftarrow J}|^2 = (2J' + 1)|\mu_{J' \rightarrow J}|^2 \quad (4-20)$$

Here states designated properly by  $J_{K_{-1}K_1}$  and  $J'_{K'_{-1}K'_1}$  have been indicated more briefly by  $J$  and  $J'$ . The quantity tabulated in Appendix V is what may be called the transition strength

$$^x S_{JJ'} = (2J + 1) \frac{|\mu_{J' \leftarrow J}|^2}{\mu^2} \quad (4-21)$$

The superscript  $x$  indicates the principal axis parallel to the dipole moment  $\mu$  which produces the transition, and hence takes on the values  $a$ ,  $b$ , or  $c$ . The quantity  $|\mu_{ij}|^2$  which is needed to obtain the absorption coefficient of a microwave line from expression (13-19) can hence be easily obtained from the entries in Appendix V, since

$$|\mu_{ij}|^2 = \frac{\mu^2 S}{2J + 1} \quad (4-22)$$



TABLE 4-5. PERMITTED TRANSITIONS BETWEEN ASYMMETRIC ROTOR LEVELS OF LOW  $J$  VALUES

Numbers indicate changes in  $K_{-1}$  and  $K_1$ ; the letter superscript indicates the axis along which the molecular dipole moment must have a nonzero component for the transition to occur. Thus  $a2, -1$  indicates a dipole moment component along the principal axis of smallest moment of inertia and  $\Delta K_{-1} = 2, \Delta K_1 = -1$ .

	$0_{0,0}$	$1_{0,1}$	$1_{1,1}$	$1_{1,0}$	$2_{0,2}$	$2_{1,2}$	$2_{1,1}$	$2_{2,1}$	$2_{2,0}$	$3_{0,3}$	$3_{1,3}$	$3_{1,2}$	$3_{2,2}$	$3_{2,1}$	$3_{3,1}$	$3_{3,0}$
$0_{0,0}$	—	$a0,1$	$b1,1$	$c1,0$												
$1_{0,1}$	$a0, -1$	—	$c1,0$	$b1, -1$	$a0,1$	$b1,1$	$c1,0$	—	$a2, -1$							
$1_{1,1}$	$b-1, -1$	$c-1,0$	—	$a0, -1$	$b-1,1$	$a0,1$	—	$c1,0$	$b1, -1$							
$1_{1,0}$	$c-1,0$	$b-1,1$	$a0,1$	—	$c-1,2$	—	$a0,1$	$b1,1$	$c1,0$							
$2_{0,2}$		$a0, -1$	$b1, -1$	$c1, -2$	—	$c1,0$	$b1, -1$	$a2, -1$	—	$a0,1$	$b1,1$	$c1,0$	—	$a2, -1$	$b3, -1$	$c3, -2$
$2_{1,2}$		$b-1, -1$	$a0, -1$	—	$c-1,0$	—	$a0, -1$	$b1, -1$	$c1, -2$	$b-1,1$	$a0,1$	—	$c1,0$	$b1, -1$	$a2, -1$	—
$2_{2,1}$		$c-1,0$	—	$a0, -1$	$b-1,1$	$a0,1$	—	$c1,0$	$b1, -1$	$c-1,2$	—	$a0,1$	$b1,1$	$c1,0$	—	$a2, -1$
$2_{2,1}$		—	$c-1,0$	$b-1, -1$	$a-2,1$	$b-1,1$	$c-1,0$	—	$a0, -1$	—	$c-1,2$	$b-1,1$	$a0,1$	—	$c1,0$	$b1, -1$
$2_{2,0}$		$c-2,1$	$b-1,1$	$c-1,0$	—	$c-1,2$	$b-1,1$	$a0,1$	—	$a-2,3$	$b-1,3$	$c-1,2$	—	$a0,1$	$b1,1$	$c1,0$
$3_{0,3}$					$a0, -1$	$b1, -1$	$c1, -2$	—	$a2, -3$	—	$c1,0$	$b1, -1$	$a2, -1$	—	$c3, -2$	$b3, -3$
$3_{1,3}$					$b-1, -1$	$a0, -1$	—	$c1, -2$	$b1, -3$	$c-1,0$	—	$a0, -1$	$b1, -1$	$c1, -2$	—	$a2, -3$
$3_{1,2}$					$c-1,0$	—	$a0, -1$	$b1, -1$	$c1, -2$	$b-1,1$	$a0,1$	—	$c1,0$	$b1, -1$	$a2, -1$	—
$3_{2,2}$					—	$c-1,0$	$b-1, -1$	$a0, -1$	—	$a-2,1$	$b-1,1$	$c-1,0$	—	$a0, -1$	$b1, -1$	$c1, -2$
$3_{2,1}$					$a-2,1$	$b-1,1$	$c-1,0$	—	$a0, -1$	—	$c-1,2$	$b-1,1$	$a0,1$	—	$c1,0$	$b1, -1$
$3_{3,1}$					$b-3,1$	$a-2,1$	—	$c-1,0$	$b-1, -1$	$c-3,2$	—	$a-2,1$	$b-1,1$	$c-1,0$	—	$a0, -1$
$3_{3,0}$					$c-3,2$	—	$a-2,1$	$b-1,1$	$c-1,0$	$b-3,3$	$a-2,3$	—	$c-1,2$	$b-1,1$	$a0,1$	—

where  $\mu$  is the component of the dipole moment responsible for the transition and  $J$  refers to the lower state.

Because of relation (4-20) if  ${}^xS_{JJ'}$  for the transition  $J_{K_{-1}K_1} \leftarrow J'_{K'_{-1}K'_1}$  is tabulated, the similar quantity for the reverse transition is immediately available, since it has the same value.

$${}^xS_{J_{kl}J'_{mn}}(\kappa) = {}^xS_{J'_{mn}J_{kl}}(\kappa) \quad (4-23)$$

where  $k, l, m$ , and  $n$  represent the values of  $K_{-1}$  and  $K_1$ , and the dependence of  $S$  on the asymmetry parameter  $\kappa$  is indicated. In addition, it can be shown that

$${}^xS_{J_{kl}J'_{mn}}(\kappa) = {}^{x'}S_{J_{lk}J'_{nm}}(-\kappa) \quad (4-24)$$

or that the strength of a transition  $J'_{mn} \leftarrow J_{kl}$  for a rotor with asymmetry parameter  $\kappa$  is just equal to that of what might be called the "inverse" transition  $J'_{nm} \leftarrow J_{lk}$  of a rotor with an equal and opposite asymmetry parameter. The relation (4-23) is rather similar and closely related to Eqs. (4-11) connecting energies for positive and negative values of  $\kappa$ . Note that in (4-24) the component of the dipole moment involved may be different for the inverse transitions. If the component is required to be along  $a$  in the first transition, it will be along  $c$  in the inverse transition, and vice versa. However, if the dipole moment required for the first transition lies along the  $b$  axis, it will also lie along the  $b$  axis for the inverse transition.

For rotation-vibration spectra, which occur in the infrared region, the groups of transitions of types  $J - 1 \leftarrow J$ ,  $J \leftarrow J$ , and  $J + 1 \leftarrow J$  often give somewhat separate parts or branches of the spectra, and are called the  $P$ ,  $Q$ , and  $R$  branches, respectively. These three types of transitions are intermingled in the pure rotational spectra which occur in the microwave region. However, the designation of branches  $P$ ,  $Q$ , and  $R$  for transitions with  $\Delta J = -1, 0$ , and  $+1$ , respectively, is still useful as an aid in classifying transitions. Types of transitions, approximately in order of intensity, are listed in Table 4-6. Transitions called "forbidden" are forbidden only for symmetric rotors but tend to be weak even in the asymmetric cases. Still weaker or more highly "forbidden" transitions occur, involving larger changes in  $K_{-1}$  or  $K_1$ , but they are not included in Table 4-6.

Appendix V lists transition strengths for the various types of transitions shown in Table 4-6, and in the same order. Because of relations (4-23) and (4-24), strengths of four types of transitions are given by the same entry in the table, *i.e.*,

$${}^xS_{J_{kl}J'_{mn}}(\kappa), \quad {}^xS_{J'_{mn}J_{kl}}(\kappa), \quad {}^{x'}S_{J_{lk}J'_{nm}}(-\kappa), \quad {}^{x'}S_{J'_{nm}J_{lk}}(-\kappa)$$

TABLE 4-6. SUMMARY OF THE STRONGER TRANSITIONS IN AN ASYMMETRIC ROTOR SPECTRUM

“Branches” or groups of transitions indicated by  $P$ ,  $Q$ , and  $R$  involve absorption transitions  $J - 1 \leftarrow J$ ,  $J \leftarrow J$ , or  $J + 1 \leftarrow J$ , respectively. Notation such as  ${}^cP_{1,-2}$  indicates a transition for which  $\Delta J = -1$ ,  $\Delta K_{-1} = 1$ ,  $\Delta K_1 = -2$ . The superscript, which in this case is  $c$ , indicates the principal axis along which a component of the dipole moment must lie in order for such a transition to occur. The forbidden transitions cannot occur in symmetric rotors and tend to be weak in asymmetric rotors. (After Cross, Hainer, and King [122].)

“Symmetric-rotor” subbranches			
$a$ and $c$ subbranches			
Prolate and oblate			
${}^cQ_{1,0}$	${}^cQ_{-1,0}$	${}^aQ_{0,1}$	${}^aQ_{0,-1}$
${}^cR_{1,0}$	${}^cP_{-1,0}$	${}^aR_{0,1}$	${}^aP_{0,-1}$
Prolate only ( $c$ )		Oblate only ( $a$ )	
${}^cQ_{-1,2}$	${}^cQ_{1,-2}$	${}^aQ_{2,-1}$	${}^aQ_{-2,1}$
${}^cR_{-1,2}$	${}^cP_{1,-2}$	${}^aR_{2,-1}$	${}^aP_{-2,1}$
$b$ subbranches			
${}^bQ_{-1,1}$	${}^bQ_{1,-1}$	${}^bQ_{1,-1}$	${}^bQ_{-1,1}$
${}^bR_{1,1}$	${}^bP_{-1,-1}$	${}^bR_{1,1}$	${}^bP_{-1,-1}$
Prolate only		Oblate only	
${}^bR_{-1,3}$	${}^bP_{1,-3}$	${}^bR_{3,-1}$	${}^bP_{-3,1}$
First-order forbidden subbranches			
$a$ and $c$ subbranches			
${}^cQ_{-3,2}$	${}^cQ_{3,-2}$	${}^aQ_{2,-3}$	${}^aQ_{-2,3}$
${}^cQ_{-3,4}$	${}^cQ_{3,-4}$	${}^aQ_{4,-3}$	${}^aQ_{-4,3}$
${}^cR_{3,-2}$	${}^cP_{-3,2}$	${}^aR_{-2,3}$	${}^aP_{2,-3}$
${}^cR_{-3,4}$	${}^cP_{3,-4}$	${}^aR_{4,-3}$	${}^aP_{-4,3}$
${}^cR_{-3,4}$	${}^cP_{3,-4}$	${}^aR_{4,-3}$	${}^aP_{-4,3}$
$b$ subbranches			
${}^bQ_{-3,3}$	${}^bQ_{3,-3}$	${}^bQ_{3,-3}$	${}^bQ_{-3,3}$
${}^bR_{-3,3}$	${}^bP_{3,-3}$	${}^bR_{3,-3}$	${}^bP_{-3,3}$
${}^bR_{-3,5}$	${}^bP_{3,-5}$	${}^bR_{5,-3}$	${}^bP_{-5,3}$

Transition strengths are listed for  $\kappa$  values of 1, 0.5, 0,  $-0.5$ , and  $-1$ . Strengths for intermediate values of  $\kappa$  must be obtained by interpolation.

*Intensities of Absorption Lines.* Absorption intensities involve not only  $|\mu_{ij}|^2$  but also the fraction  $f$  of molecules in the ground state of the transition. Neglecting the effects of nuclear spin,  $f$  may be written as previously (pages 19 and 20)

$$f = f_{J\kappa-1\kappa_1}f_v$$



where

$$f_{J_{K-1}K_1} = \frac{(2J+1)e^{-\frac{W_{J_{K-1}K_1}}{kT}}}{\sum_J (2J+1)e^{-\frac{W_{J_{K-1}K_1}}{kT}}} \quad (4-25)$$

$$f_v = e^{-W_v/kT} \prod_n (1 - e^{-h\omega_n/kT})^{d_n} \quad (4-26)$$

where  $W_{J_{K-1}K_1}$  is the rotational energy and  $W_v$  the vibrational energy. If the temperature is high enough so that  $kT/h \gg A$ ,

$$\sum_J (2J+1)e^{-\frac{W_{J_{K-1}K_1}}{kT}} = \sqrt{\frac{\pi}{ABC}} \left(\frac{kT}{h}\right)^3 \quad (4-27)$$

where  $A$ ,  $B$ , and  $C$  are the rotational constants in cycles per second. Better approximations for the partition function may be found [48]. However, when  $T$  is greater than 100°K, the approximation (4-27) for the partition function has an error less than 2 per cent for all known cases.

In the discussion of asymmetric rotors thus far, centrifugal stretching effects have been neglected. A precise evaluation of the partition function must take such effects into account. Their contribution to the partition function may in some cases be as large as 1 per cent. Hence if more accuracy than that given by (4-27) is needed, a rather detailed evaluation of the partition function must be made, taking into account centrifugal distortion.

Although the high-temperature approximation may be used for the denominator of (4-25), it cannot always be assumed that the exponential in the denominator of (4-25) is approximately equal to 1. For a symmetric molecule, only the lower rotation states give transitions in the microwave region,  $W_{JK} \ll kT$ , and the Boltzmann factor  $e^{-W_{JK}/kT}$  may usually be safely set equal to unity. For asymmetric rotors, however, microwave transitions may occur between states each of which has a very large rotational energy, so that the corresponding factor is sometimes considerably smaller than 1 and must be retained.

Assuming no effect of nuclear spins, the maximum absorption coefficient for an asymmetric transition in the microwave region from (4-25), (4-27), and (13-19), is

$$\gamma_{\max} = \frac{8\pi h N f_v}{3c(kT)^2} \sqrt{\frac{\pi h ABC}{kT}} e^{-\frac{W_{J_{K-1}K_1}}{kT}} (2J+1) |\mu_{ij}|^2 \frac{\nu^2}{\Delta\nu} \quad (4-28)$$

where all quantities are in cgs or electrostatic units.  $(2J+1)|\mu_{ij}|^2$  is just  $\mu_x^2 {}^xS_{J_{kl}J'_{mn}}$ , the square of the appropriate component of the dipole moment times the number tabulated in Appendix V. Letting  $T = 300^\circ\text{K}$

and substituting values for the universal constants,

$$\gamma_{\max} = 2.46 \times 10^{-20} f_v \sqrt{ABC} e^{-\frac{W_{J_{K-1}K_1}}{kT}} (2J + 1) |\mu_{ij}|^2 \frac{\nu^2}{\Delta\nu} \quad (4-29)$$

*The Effects of Nuclear Spins and Statistics.* If there are two equivalent nuclei in a molecule, *i.e.*, identical isotopes of the same element which have exactly the same molecular environment, the nuclear spins and statistics will affect the population of molecular states and hence the transition intensities. If two equivalent nuclei occur, the molecule has a twofold axis of symmetry, and coordinates of the two equivalent nuclei may be interchanged by a  $180^\circ$  rotation about this symmetry axis, or by combinations of inversion and  $180^\circ$  rotations about various axes. In an asymmetric rotor, there cannot be more than two equivalent nuclei, because if there were, the molecule would have at least a threefold axis and would be a symmetric top (*cf.* Sec. 3-1). However, there may be more than one pair of equivalent nuclei.

In order to avoid the complication of possible inversion of the molecule, we consider first a planar molecule. The molecules  $\text{H}_2\text{O}$ ,  $\text{NO}_2$ , and  $\text{H}_2\text{CO}$  are examples of this type. If a planar molecule has two equivalent nuclei, it has a symmetry axis which is the intersection between the plane in which the molecule lies and the perpendicular bisector of the line joining the two equivalent nuclei. This symmetry axis must be a principal axis of the ellipsoid of inertia (Sec. 3-1) and a rotation of  $180^\circ$  about this axis interchanges the positions of the two equivalent nuclei. If the nuclei obey Bose-Einstein statistics, an interchange of both the position and spin coordinates must leave the wave function unchanged; if they obey Fermi-Dirac statistics, the wave function must change sign (*cf.* page 69).

The wave function can be written as a product of rotational and nuclear spin functions

$$\psi = \psi_{J_{K-1}K_1} \psi_N \quad (4-30)$$

The symmetry of the rotational function has already been discussed.

Let the spin function of the first nucleus of spin  $I$  be written  $\sigma_m(1)$ , where  $m$  is the projection of  $I$  on an axis fixed in space, and may have the  $2I + 1$  values  $I, I - 1, I - 2, \dots, -I$ . Similarly, the spin functions for the second nucleus may be written  $\sigma_{m'}(2)$ , and spin functions for the two nuclei  $\sigma_m(1)\sigma_{m'}(2)$ . There are in all  $(2I + 1)^2$  such combinations. For the  $2I + 1$  cases when  $m = m'$ , the function  $\sigma_m(1)\sigma_{m'}(2)$  is clearly symmetric with respect to an interchange of the spin coordinates of nucleus 1 and 2. If  $m \neq m'$ , then this function is neither symmetric nor antisymmetric, but equal numbers of symmetric and antisymmetric combinations can be formed from these of the type

$$\begin{aligned} \sigma_m(1)\sigma_{m'}(2) + \sigma_m(2)\sigma_{m'}(1) & \quad (\text{symmetric}) \\ \sigma_m(1)\sigma_{m'}(2) - \sigma_m(2)\sigma_{m'}(1) & \quad (\text{antisymmetric}) \end{aligned}$$



There are  $[(2I + 1)^2 - (2I + 1)]/2$  of each of these types, so the total number of symmetric spin functions becomes

$$n_{\text{sym}} = (2I + 1)(I + 1) \quad (4-31a)$$

and of antisymmetric spin functions

$$n_{\text{antisym}} = (2I + 1)I \quad (4-31b)$$

A molecular rotation of  $180^\circ$  about the symmetry axis and an exchange of spin coordinates of the two equivalent nuclei amounts to an exchange of all coordinates of these two nuclei. Hence if Bose-Einstein statistics apply to the two nuclei, the symmetric spin functions must be used with rotational functions which are symmetric with respect to a rotation around the symmetry axis, and antisymmetric spin functions with antisymmetric rotational functions. The ratio of the number of spin states or the statistical weights of the levels which are symmetric to those which are antisymmetric with respect to a  $180^\circ$  rotation about the symmetry axis is then, from (4-31),

$$\text{For Bose-Einstein statistics: } \frac{I + 1}{I} \quad (4-32a)$$

$$\text{For Fermi-Dirac statistics: } \frac{I}{I + 1} \quad (4-32b)$$

Since the molecular symmetry axis in question is a principal axis of inertia, Table 4-2 gives the behavior of  $\psi_{J_K-K_1}$  with respect to  $180^\circ$  rotations about this axis. Statistical weights due to nuclear spins for a number of cases are given in Table 4-7. Expression (4-25) giving the fraction of molecules in a given rotational state must accordingly be modified for molecules with two equivalent atoms by multiplying the probability for each state by the nuclear spin statistical weight factor from (4-31) or Table 4-7. Actually only the ratio of statistical weights for the two types of states is of importance. The statistical weight due to nuclear spins may be considered unity for the more populated states and  $I/(I + 1)$  for the others. If this is done, the partition function [the denominator of (4-25)] is multiplied by  $(2I + 1)/[2(I + 1)]$ .

If there are more than one pair of equivalent nuclei in a molecule, the symmetry properties of each pair may be taken into account. An example is  $\text{CH}_2\text{Cl}_2$ , which is not planar, but the inversion, which will be discussed below, may be neglected. This molecule has a twofold axis of symmetry which exchanges the positions of the two hydrogens and the two chlorines at the same time. Let the hydrogens have  $S_1$  symmetric spin functions and  $A_1$  antisymmetric spin functions. Similarly the chlorines will have  $S_2$  symmetric and  $A_2$  antisymmetric spin functions. The product of hydrogen and chlorine functions will give  $S_1S_2 + A_1A_2$  symmetric and  $S_1A_2 + S_2A_1$  antisymmetric total spin functions. Hence from (4-31), letting the spins of the two different types of nuclei be  $I_1$



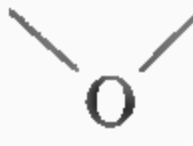

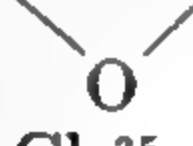
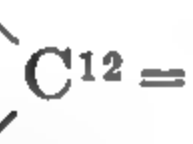
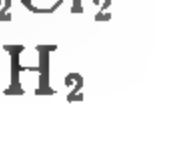


and  $I_2$ ,

$$n_{\text{sym}} = (2I_1 + 1)(2I_2 + 1)(2I_1I_2 + I_1 + I_2 + 1) \quad (4-33a)$$

$$n_{\text{antisym}} = (2I_1 + 1)(2I_2 + 1)(2I_1I_2 + I_1 + I_2) \quad (4-33b)$$

Both H and  $\text{Cl}^{35}$  obey Fermi-Dirac statistics, so that an interchange of both pairs of nuclei must leave the wave function unchanged, and symmetric total spin functions must be paired with symmetric rotational functions. The resulting statistical weights are given in Table 4-7.

TABLE 4-7. EXAMPLES OF STATISTICAL WEIGHTS DUE TO SPINS OF EQUIVALENT NUCLEI

Molecule	Symmetric levels*	Statistical weight	Antisymmetric levels*	Statistical weight
$\text{H}_2\text{O}$	$ee, oo$	1	$eo, oe$	3
$\text{D}_2\text{O}$	$ee, oo$	6	$eo, oe$	3
$\text{H}_2\text{CO}, \text{H}_2\text{C}_2\text{O}$	$ee, eo$	1	$oe, oo$	3
$\text{D}_2\text{CO}, \text{D}_2\text{C}_2\text{O}$	$ee, eo$	6	$oe, oo$	3
$\text{NO}_2^{16}, \text{SO}_2^{16}$	$ee, oo$	1	$eo, oe$	0
$\text{H}_2\text{C}^{12}-\text{C}^{12}\text{H}_2$ 	$ee, oo$	10	$eo, oe$	6
$\text{CH}_2\text{F}_2, \text{H}_2\text{C} = \text{CF}_2$ $\text{D}_2\text{C}^{12}-\text{C}^{12}\text{D}_2$ 	$ee, eo$	10	$oe, oo$	6
$\text{CD}_2\text{F}_2, \text{D}_2\text{C} = \text{CF}_2$ $\text{H}_2\text{C}^{13}-\text{C}^{13}\text{H}_2$ 	$ee, oo$	45	$eo, oe$	36
$\text{CD}_2\text{F}_2, \text{D}_2\text{C} = \text{CF}_2$ $\text{H}_2\text{C}^{13}-\text{C}^{13}\text{H}_2$ 	$ee, eo$	15	$oe, oo$	21
$\text{CH}_2\text{Cl}_2^{35}$ 	$ee, oo$	28	$eo, oe$	36
$\text{Cl}^{35}$ 	$ee, oo$	36	$eo, oe$	28
$\text{C}^{12} = \text{C}^{12}$ 	$ee, oo$	36	$eo, oe$	28
$\text{H}$ $\text{CD}_2\text{Cl}_2^{35}$	$ee, oo$	66	$eo, oe$	78
$\text{NDH}_2$	$ee, oo$	1	$eo, oe$	3
	(lower inversion level) or $eo, oe$ (upper inversion level)		(lower inversion level) or $ee, oo$ (upper inversion level)	

\* Rotational levels specified by evenness or oddness of  $K_{-1}K_1$ .

Other cases of more than one pair of equivalent nuclei may be similarly treated. In general for a molecule with  $n$  pairs of identical nuclei, the number of symmetric spin functions which can be formed is

$$n_{\text{sym}} = \frac{1}{2} \left[ \prod_{i=1}^n (2I_i + 1) \right] \left[ \prod_{i=1}^n (2I_i + 1) + 1 \right] \quad (4-34a)$$

and the number of antisymmetric functions

$$n_{\text{antisym}} = \frac{1}{2} \left[ \prod_{i=1}^n (2I_i + 1) \right] \left[ \prod_{i=1}^n (2I_i + 1) - 1 \right] \quad (4-34b)$$

If the molecule has a twofold axis of symmetry and the  $n$  pairs of nuclei are interchanged by a  $180^\circ$  rotation around this axis, the ratio of intensities of rotation levels of odd and even  $K$  is given by Eqs. (4-34).

**4-3. Centrifugal Distortion.** Centrifugal distortion is enormously more important in the microwave spectra of asymmetric rotors than in the spectra of symmetric tops. In the latter it produces very small shifts of the order of 1 Mc or less, whereas in the microwave spectra of some asymmetric rotors, centrifugal distortions change the rotational frequencies many hundreds of megacycles. This is because microwave transitions may occur in asymmetric rotors between states of rather large angular momentum and of very large rotational energies. In light symmetric tops, transitions between states of rather small  $J$  are generally observed. Furthermore, in the heavier symmetric molecules which give microwave spectra for transitions between states of larger  $J$ , the moment of inertia is so large that rotational energies in these states are still rather small.

Consider as an example the asymmetric rotor  $\text{SO}_2$ , whose rotational constants lie between 8000 and 80,000 Mc. If this molecule were linear, a transition involving  $J$  as small as 2 would fall in the “ $K$ -band” region near 24,000 Mc. However, in the actual spectrum between 20,000 and 30,000 Mc transitions involving  $J$  values from 3 to 35 have been identified [647]. Many other transitions occur in this region which are thought to involve still higher values of  $J$ . The rotational energy for  $J = 35$  is of the order of  $1000 \text{ cm}^{-1}$ , or  $3 \times 10^7 \text{ Mc}$ . Although the centrifugal distortion is a small fraction of the rotational energy, for  $J = 35$  it is as large as about  $0.3 \text{ cm}^{-1}$ , or  $10^4 \text{ Mc}$ , and hence corresponds to an enormous shift of the observed microwave lines. Hence for an accurate understanding of the microwave spectrum of  $\text{SO}_2$ , rather accurate knowledge of centrifugal effects is necessary.

Still more extreme cases are the light molecules  $\text{H}_2\text{O}$  and  $\text{HDO}$ . The  $6_{-5} \leftarrow 5_{-1}$  transition of  $\text{H}_2\text{O}$  which lies at 22,235 Mc involves levels with rotational energies near  $500 \text{ cm}^{-1}$ , or  $1.5 \times 10^7 \text{ Mc}$ , even though  $J$  is only 5 or 6. For  $J = 11$  states of  $\text{H}_2\text{O}$ , centrifugal distortion corrections occur which are as large as 9 per cent of the entire rotational energy, or  $280 \text{ cm}^{-1}$  [84]. Transitions involving these particular states of  $\text{H}_2\text{O}$  lie in the infrared region, however.

Lest the reader infer that centrifugal distortions produce even more difficulties in the interpretation of microwave spectra than they really do, it should be pointed out that, for all but the lightest molecules, it is

usually possible to find rotational transitions in the microwave region of low angular momentum  $J$  which are not shifted by centrifugal effects more than a few megacycles. Hence moments of inertia and parameters for asymmetric rotors may often be obtained with sufficient accuracy without allowing for centrifugal distortion. Furthermore, in some cases where centrifugal distortion is large, microwave transitions occur between states of rather similar angular momentum, so that the net shift in frequency due to centrifugal distortion is not so large.

In order to understand qualitatively what variables are important to centrifugal distortion, consider first a molecule which rotates about only one axis, so that classically the energy of rotation may be written

$$W = \frac{1}{2I} P^2 \quad (4-35)$$

where  $I$  is the moment of inertia and  $P$  the angular momentum. Assume now that  $I$  depends on one coordinate  $R$ . Then the centrifugal force tending to increase  $R$  is

$$F = - \frac{\partial W}{\partial R} = -\frac{1}{2}P^2 \frac{\partial(1/I)}{\partial R} \quad (4-36)$$

Because of this force,  $R$  is modified by a small amount  $\Delta R$  such that the restoring force  $k \Delta R$  equals  $F$ . Hence

$$\Delta R = -\frac{1}{2} \frac{P^2}{k} \frac{\partial(1/I)}{\partial R} \quad (4-37)$$

There is a consequent change in the energy of rotation

$$\Delta W_P = \frac{1}{2}P^2 \frac{\partial(1/I)}{\partial R} \Delta R = -\frac{1}{4} \frac{P^4}{k} \left[ \frac{\partial(1/I)}{\partial R} \right]^2 \quad (4-38)$$

In addition, the potential energy stored as a result of the displacement  $\Delta R$  is

$$\Delta W_k = \frac{1}{2}k(\Delta R)^2 = \frac{1}{8} \frac{P^4}{k} \left[ \frac{\partial(1/I)}{\partial R} \right]^2 \quad (4-39)$$

Combining (4-38) and (4-39), the total energy change due to centrifugal distortion is

$$\Delta W = -\frac{1}{8} \frac{P^4}{k} \left[ \frac{\partial(1/I)}{\partial R} \right]^2 \quad (4-40)$$

From (4-40) it may be seen that centrifugal distortion always decreases the energy by an amount dependent on the fourth power of the angular momentum, and the inverse of a molecular force-constant.

In the general case, angular momenta about all three principal axes of the molecule will be involved, and the energy due to centrifugal distortion must be written in the more general form (4-41) given by Wilson and Howard [76], [715].

$$\partial W = \frac{1}{4} \sum_{\alpha\beta\gamma\delta} \tau_{\alpha\beta\gamma\delta} P_\alpha P_\beta P_\gamma P_\delta \quad (4-41)$$



where  $P_\alpha$ ,  $P_\beta$ , etc., is each an angular momentum about some principal axis of the molecule (they are not all different, and all may be the same). The molecular constant  $\tau_{\alpha\beta\gamma\delta}$  is

$$\tau_{\alpha\beta\gamma\delta} = -\frac{1}{2} \sum_{ij} \frac{\partial \mu_{\alpha\beta}}{\partial R_i} \frac{\partial \mu_{\gamma\delta}}{\partial R_j} (k^{-1})_{ij} \quad (4-42)$$

Here  $\mu_{\alpha\beta}$  and  $\mu_{\gamma\delta}$  correspond to  $1/I$  in (4-40). In this generalized form, they are elements of the matrix which is inverse to the inertia matrix or dyadic. Before displacements  $\delta R_i$  and  $\delta R_j$  are made, the moments of inertia are with respect to principal axes, so that this matrix is simply

$$(\mu) = \begin{pmatrix} 1/I_{xx} & 0 & 0 \\ 0 & 1/I_{yy} & 0 \\ 0 & 0 & 1/I_{zz} \end{pmatrix} \quad (4-43)$$

The derivative  $\partial \mu_{\alpha\beta} / \partial R_i$  is more complicated. The matrix element  $(k^{-1})_{ij}$  replaces the factor  $1/k$  in (4-40). It is an element of the matrix which is inverse to the matrix of force constants  $k_{ij}$  obtained from the potential energy

$$V = \frac{1}{2} \sum_{ij} k_{ij} R_i R_j \quad (4-44)$$

The above expressions assume that the potential may be taken as harmonic, *i.e.*, of the form (4-44). This is probably a sufficiently good approximation since the effects of centrifugal distortion are usually not extremely large, and if they are very large the potential constants are not usually known so well that anharmonic terms in the potential would greatly improve the accuracy. However, it is possible that in the future the effects of anharmonic potential constants on centrifugal distortion may be determined and used as a method of evaluating these constants. An additional approximation is involved in omitting from (4-42) terms proportional to the sixth power of momenta and higher. These may be of importance in some extreme cases [346].

If  $R_i$ ,  $R_j$  are taken as normal coordinates  $Q_i$ ,  $Q_j$ , then by definition of normal coordinates the potential has the particularly simple form

$$V = \frac{1}{2} \sum_i k_{ii} Q_i^2 \quad (4-45)$$

The coordinates  $Q_i$  are usually taken such that the vibrating mass associated with each coordinate may be assumed to be unity, and the molecular vibrational frequency  $\nu_i = \left( \frac{1}{2\pi} \right) \sqrt{k_{ii}}$ . Hence (4-42) becomes

$$\tau_{\alpha\beta\gamma\delta} = -\frac{1}{2} \sum_i \frac{\partial \mu_{\alpha\beta}}{\partial Q_i} \frac{\partial \mu_{\gamma\delta}}{\partial Q_i} \left( \frac{1}{4\pi^2 \nu_i^2} \right) \quad (4-46)$$

Fortunately, many of the total of 81 constants  $\tau_{\alpha\beta\gamma\delta}$  are usually zero, and others are not independent. In a molecule such as  $\text{H}_2\text{O}$ , there are only four independent coefficients of this type. They can often be evaluated empirically by fitting the observed spectra. However, in some cases it is important to calculate the constants from the known geometry and force constants of the molecule.

The coefficients  $\tau_{\alpha\beta\gamma\delta}$  are probably most easily calculated by using expression (4-42), although this depends of course on what information about the molecule is available. If  $\alpha$ ,  $\beta$ ,  $\gamma$ , and  $\delta$  are directions of principal axes of inertia as assumed above,

$$\frac{\partial \mu_{\alpha\beta}}{\partial R_i} = - \frac{1}{I_{\alpha\alpha} I_{\beta\beta}} \frac{\partial I_{\alpha\beta}}{\partial R_i} \quad (4-47)$$

where  $I_{\alpha\beta}$  represents an element of the moment of inertia matrix or dyadic. In obtaining the derivatives  $\partial \mu_{\alpha\beta} / \partial R_i$ , the variation in the coordinates  $R_i$  must be taken in such a way that the center of gravity of the molecule is not changed, nor the orientation of its principal axes (*cf.* "Eckart conditions" [715]). If small variations  $\Delta\alpha_j$ ,  $\Delta\beta_j$ , etc., are found for the Cartesian coordinates  $\alpha_j$ ,  $\beta_j$  of each atom  $j$  of the molecule such that  $R_i$  is changed by  $\Delta R_i$ , and other internal molecular coordinates remain unchanged, then the above requirements give [826]

$$\frac{\partial I_{\alpha\beta}}{\partial R_i} = \frac{\Delta I_{\alpha\beta}}{\Delta R_i} = \frac{-2}{I_{\gamma\gamma} \Delta R_i} \left( \sum_l m_l \alpha_l^2 \sum_j m_j \beta_j \Delta\alpha_j + \sum_l m_l \beta_l^2 \sum_j m_j \alpha_j \Delta\beta_j \right) \quad (4-48)$$

Kivelson and Wilson [826] have given sample calculations of this type and formulas for several common cases.

A calculation of the effects of centrifugal distortion on the frequencies of rotational spectra depends on evaluation not only of the constants  $\tau_{\alpha\beta\gamma\delta}$ , but also of the effect of the operators  $P_\alpha$ ,  $P_\beta$ ,  $P_\gamma$ , and  $P_\delta$ . A closed general expression for the effect of such operators is not possible. However, since the energy due to centrifugal distortion is almost always a small part of the total rotational energy, the energy contributions due to it may usually be treated with sufficient accuracy by first-order perturbation theory. The Hamiltonian for the rotational energy without centrifugal distortion is as in (3-2)

$$H_0 = \frac{P_x^2}{2I_{xx}} + \frac{P_y^2}{2I_{yy}} + \frac{P_z^2}{2I_{zz}} \quad (4-49)$$

The perturbing centrifugal terms may be taken as

$$H^1 = \frac{1}{4} \sum_{\alpha\beta} \tau_{\alpha\alpha\beta\beta} P_\alpha^2 P_\beta^2 \quad (4-50)$$

Matrix elements for a Hamiltonian of the form (4-50) are given by Nielsen [108]. The technique of first-order perturbation theory may be described

as that of obtaining wave functions appropriate to the large part  $H_0$  of the Hamiltonian, and then averaging the perturbing energy  $H^1$  over these states. All terms involving odd powers of any component of  $P$  have been omitted from (4-50), since they are zero for a large class of molecules and in any case their average is zero so that they contribute nothing in this first-order approximation.

It can be shown [715] that the energy resulting from  $H_0$  and the first-order effects of  $H^1$  is

$$W = W_0 + A_1 W_0^2 + A_2 W_0 J(J+1) + A_3 J^2(J+1)^2 + A_4 J(J+1)(P_z^2)_{av} + A_5 (P_z^4)_{av} + A_6 W_0 (P_z^2)_{av} \quad (4-51)$$

where the  $A$ 's are constants of the molecule which are given explicitly in terms of the moments of inertia and the  $\tau_{\alpha\alpha\beta\beta}$  by Kivelson and Wilson [715],  $W_0$  is the rotational energy assuming no centrifugal distortion, and  $(P_z^2)_{av}$  represents the average or expectation value of  $P_z^2$ .

For a symmetric or nearly symmetric rotor,  $(P_z^2)_{av} = K^2$  and  $(P_z^4)_{av} = K^4$  so that (4-51) reduces to a form similar to that given for a symmetric rotor in (3-54). In other cases,  $(P_z^2)_{av}$  may be obtained from the relation [352]

$$(P_z^2)_{av} = \frac{\partial W_0}{\partial (1/I_{zz})} \quad (4-52)$$

The quantity  $\partial W_0 / \partial (1/I_{zz})$  may be evaluated by methods given in the earlier part of this chapter for obtaining the rotational energy of a rigid rotor. Evaluation of  $(P_z^4)_{av}$  is a bit complex when the approximation  $(P_z^4)_{av} \approx (P_z^2)_{av}^2$  is not sufficiently accurate. A method for its evaluation is discussed by Kivelson and Wilson [715] (*cf.* also [59] and [601]).

Lawrance and Strandberg ([601]; *cf.* also [59]) have developed an expression similar to (4-51) and applied it to  $H_2CO$  by evaluating the constants empirically from the observed spectral frequencies. Certain transitions were observed involving values of  $J$  as high as 31 and centrifugal distortion corrections as large as 600 Mc. These fitted the expected form (4-51) within a few megacycles.

A rather complete calculation of centrifugal distortion effects from molecular geometry and force constants has been carried out for  $SO_2$  [647], for  $PH_2D$  and  $PHD_2$  [866], and for HDS [587]. Matrix elements and helpful details of this type of calculation are included in the discussion of HDS by Hillger and Strandberg [587]. In each of the above cases the fit to experimental data obtained by the calculation of centrifugal distortion from known force constants appears to be satisfactory, although there is some minor disagreement in the case of HDS.

**4-4. Structures of Asymmetric Rotors.** Because of the complexities of the spectra of asymmetric rotors, the rotational structure of the spectra of only two ( $H_2O$  and  $HDO$ ) had been fairly completely solved before the



TABLE 4-8. STRUCTURES OF ASYMMETRIC ROTORS WHICH HAVE BEEN OBTAINED FROM MICROWAVE SPECTRA

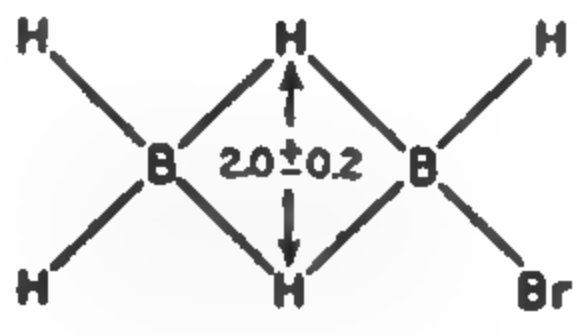
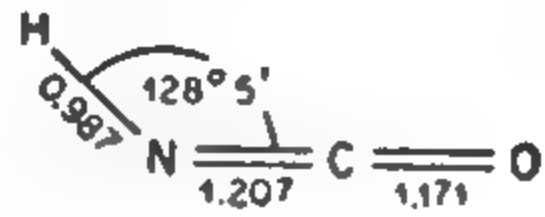
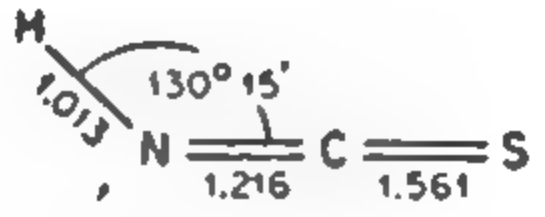
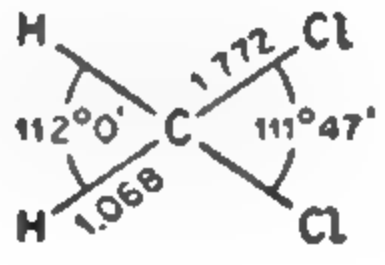
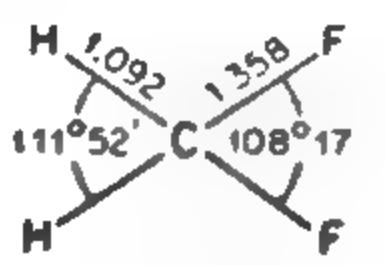
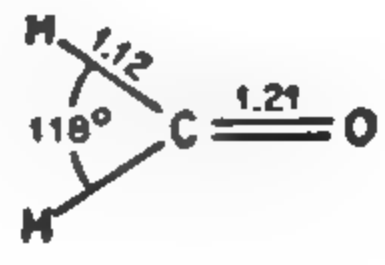
Molecule	Structure	Reference
$B_2BrH_5$		[447]
$CHNO$ (HNCO)		[479]
$CHNS$ (HNCS)		[434] [794]
$CH_2Cl_2$		[732]
$CH_2F_2$		[722]
$CH_2O$		[353] [601]

TABLE 4-8. STRUCTURES OF ASYMMETRIC ROTORS WHICH HAVE BEEN OBTAINED FROM MICROWAVE SPECTRA (*Continued*)

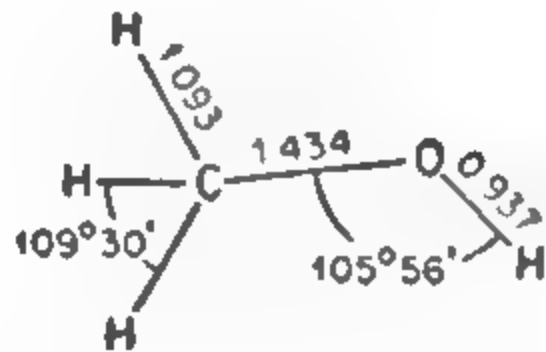
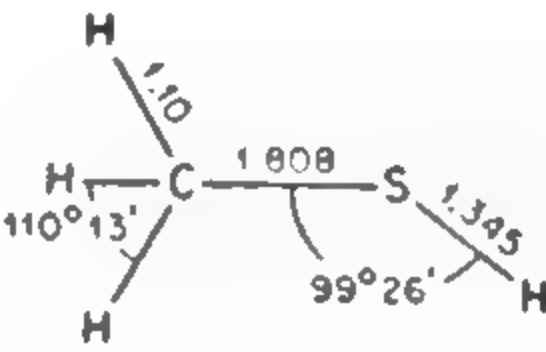
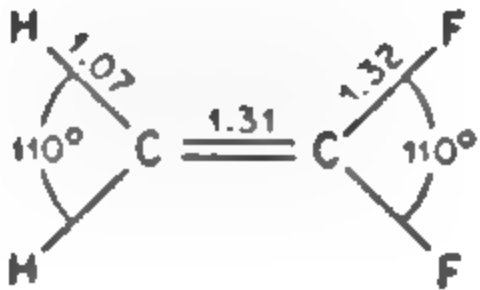
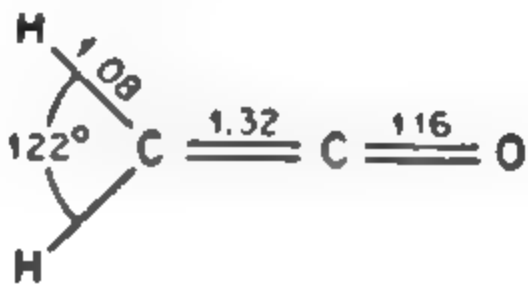
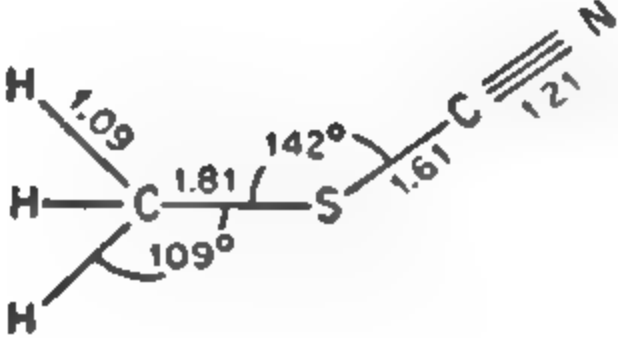
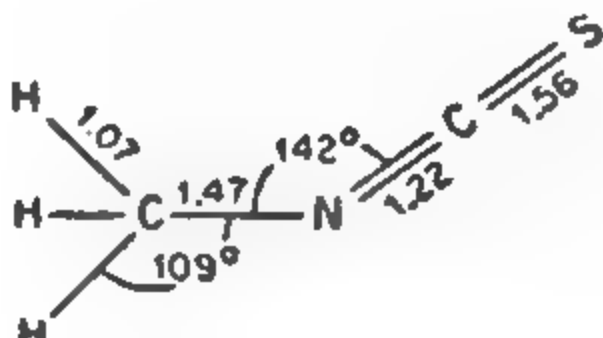
Molecule	Structure	Reference
$\text{CH}_3\text{O}$ ( $\text{CH}_3\text{COH}$ )	 <p>(Oxygen lies 0.079 Å above symmetry axis of methyl group)</p>	[817]
$\text{CH}_3\text{S}$ ( $\text{CH}_3\text{SH}$ )		[640] [870]
$\text{C}_2\text{H}_2\text{F}_2$ ( $\text{CH}_2\text{CF}_2$ )		[406]
$\text{C}_2\text{H}_2\text{O}$ ( $\text{H}_2\text{C}_2\text{O}$ )		[708]
$\text{C}_2\text{H}_3\text{NS}$ ( $\text{CH}_3\text{SCN}$ )		[345]
$\text{C}_2\text{H}_3\text{NS}$ ( $\text{CH}_3\text{NCS}$ )		[345]

TABLE 4-8. STRUCTURES OF ASYMMETRIC ROTORS WHICH HAVE BEEN OBTAINED FROM MICROWAVE SPECTRA (*Continued*)

Molecule	Structure	Reference
$C_2H_4O$	<p>(Angle between C—C bond and plane containing carbon and its two hydrogens is <math>159^\circ 25'</math>)</p>	[316] [566]
$C_2H_4S$	<p>(Angle between C—C bond and plane containing carbon and its two hydrogens is <math>151^\circ 43'</math>)</p>	[566]
$C_2H_5N$ (ethylenimine)	<p>(Angle between N—H bond and CCN plane is <math>112^\circ</math>. Angle between C—C bond and <math>CH_2</math> plane is <math>159^\circ 25'</math>)</p>	[877]
$C_3H_3N$ (vinyl cyanide)		[763a]
$C_4H_5N$ (pyrrole)	<p>(Molecule is entirely planar)</p>	[763]
$C_5H_5N$ (pyridine)		[893] [914]



TABLE 4-8. STRUCTURES OF ASYMMETRIC ROTORS WHICH HAVE BEEN OBTAINED FROM MICROWAVE SPECTRA (*Continued*)

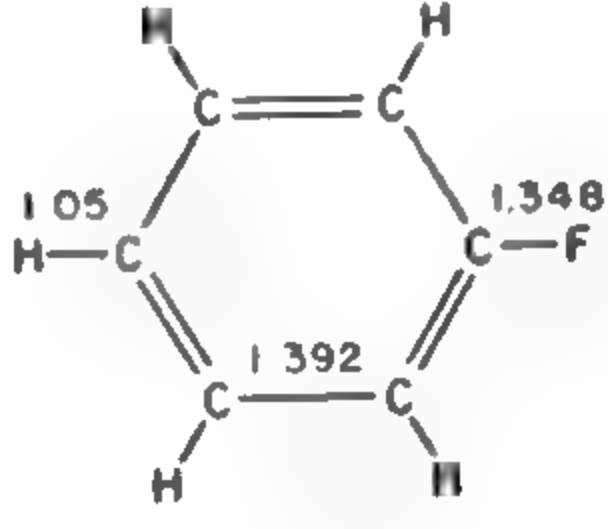
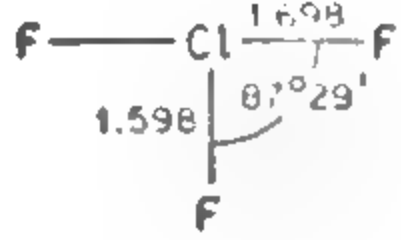
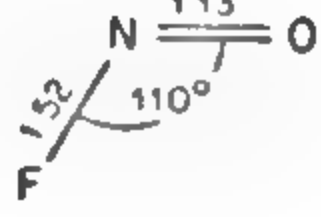
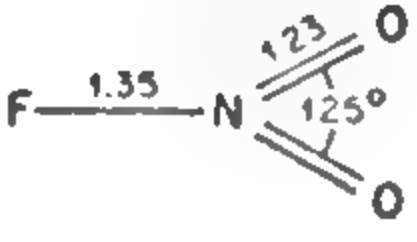
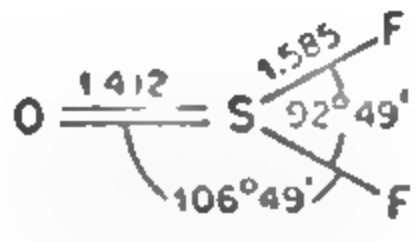
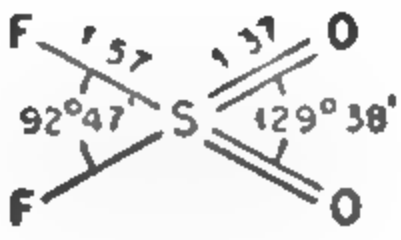
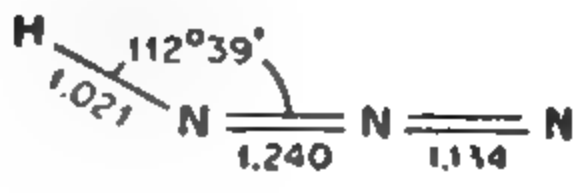
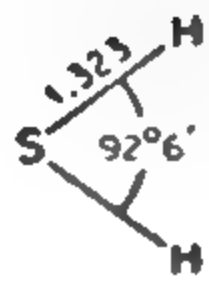
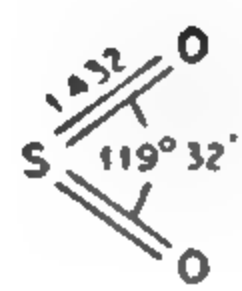
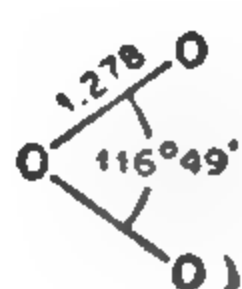
Molecule	Structure	Reference
$C_6H_5F$ (fluorobenzene)		[796]
$ClF_3$		[867]
$FNO$ (NOF)		[609]
$FNO_2$ ( $NO_2F$ )		[748]
$F_2OS$		[802] [922]
$F_2SO_2$		[684]

TABLE 4-8. STRUCTURES OF ASYMMETRIC ROTORS WHICH HAVE BEEN OBTAINED FROM MICROWAVE SPECTRA (*Concluded*)

Molecule	Structure	Reference
$\text{HN}_3$		[427]
$\text{H}_2\text{S}$		[783]
$\text{O}_2\text{S}$ ( $\text{SO}_2$ )		[647] [565]
$\text{O}_3$		[875]

advent of high-resolution microwave spectroscopy. A large number have now been worked out by microwave techniques, and it seems feasible to solve the rotational spectrum of any asymmetric rotor which does not have serious complications due to internal motions (*cf.* Chap. 12) or an exceptionally complex hyperfine structure (*cf.* Chap. 6). The Stark effect has been extremely valuable in identifying and working out this type of spectrum (*cf.* Chap. 10). The structures of asymmetric rotors which have been obtained from microwave results are given in Table 4-8.

## CHAPTER 5

### ATOMIC SPECTRA

While most microwave spectra have their origin in absorption by molecules, certain types of atomic spectra may fall in the microwave region. Atomic theory is important even for molecular spectroscopy because it is often convenient to consider a molecule as being composed of atoms whose properties are not too greatly different from their properties in the free state. Moreover, many molecular phenomena are sufficiently analogous to phenomena in atoms so that it is worthwhile to study first the simpler atomic case.

This chapter will present a summary of those parts of the theory of atomic spectra which are needed for microwave spectroscopy. More extensive treatments are given in the several books devoted to the subject (*e.g.*, A. C. Candler [79], G. Herzberg [124], L. Pauling and S. Goudsmit [23], H. E. White [53], and for a more advanced, quantum-mechanical treatment, E. U. Condon and G. H. Shortley [56]).

**5-1. The Hydrogen Atom.** The simplest atom is that of hydrogen, consisting of a single proton and an electron. It is described by the wave equation

$$\nabla^2\psi + \frac{8\pi^2\mu}{h^2} (W - V)\psi = 0$$

or, in spherical coordinates,

$$\begin{aligned} \frac{1}{r^2} \frac{\partial}{\partial r} \left( r^2 \frac{\partial \psi}{\partial r} \right) + \frac{1}{r^2 \sin^2 \theta} \frac{\partial^2 \psi}{\partial \phi^2} + \frac{1}{r^2 \sin \theta} \frac{\partial}{\partial \theta} \left( \sin \theta \frac{\partial \psi}{\partial \theta} \right) \\ + \frac{8\pi^2\mu}{h^2} (W - V)\psi = 0 \end{aligned} \quad (5-1)$$

where the nucleus, or more exactly the center of mass of the electron and nucleus, is taken as the origin of coordinates, and  $\mu = mM/(M + m)$  is the reduced mass of the atom.  $W$  is the total energy of the atom,  $V = -Ze^2/r$  is the potential energy,  $Z$  is the nuclear charge in units of the proton charge, and  $e$  is the proton charge.

By a process of separating the variables similar to that used for the diatomic molecule (Chap. 1), the wave equation may be solved [62], giving

$$\psi = R(r)\Theta(\theta)\Phi_m(\phi) \quad (5-2)$$



where

$$\Phi_M = \frac{1}{\sqrt{2\pi}} e^{im\phi} \quad (5-3)$$

$$\Theta_{Ml} = \left[ \frac{(2l+1)(l-|m|)!}{2(l+|m|)!} \right]^{\frac{1}{2}} P_{l|m|}(\cos \theta) \quad (5-4)$$

$$R_{nl} = \sqrt{\frac{4(n-l-1)!Z^3}{[(n+l)!]^3 n^4 a_1^3}} \left( \frac{2Zr}{na_0} \right)^l e^{-Zr/na_0} L_{n+l}^{2l+1} \left( \frac{2Zr}{na_0} \right) \quad (5-5)$$

and where  $n = 1, 2, \dots$  is the principal quantum number

$l = 0, 1, 2, \dots, (n-1)$  is the orbital quantum number

$m = -l, -l+1, \dots, l-1, l$  is the magnetic quantum number and should not be confused with the same symbol used for the mass of the electron

$P_{l|m|}$  = associated Legendre polynomial

$L_{n+l}^{2l+1}$  = associated Laguerre polynomial

$a_0 = h^2/4\pi^2\mu c^2$  is the radius of the first orbit of the hydrogen atom in the Bohr theory

It may be observed that Eq. (5-1) for the hydrogen atom is exactly the same as the wave equation (1-11) for a diatomic molecule with the potential  $V(r)$  replacing the molecular potential  $U(r)$ . The hydrogen atom may, in fact, be regarded as a diatomic molecule with the proton and electron as the two atoms. The parts of the wave function (5-3) and (5-4) which depend on angle are identical with those for a diatomic or linear molecule (1-5) and (1-6). They are the same for any spherically symmetric potential, since these functions represent conservation of total angular momentum ( $l$  or  $J$ ) and of the projection of the angular momentum ( $m$  or  $M$ ) on a chosen axis. Unlike the diatomic molecule, the dependence of the potential on  $r$  in this atomic case is very simple and the radial wave function (5-5) can be determined. In more complex atoms, the potential for a single electron may often be considered spherically symmetric, so that the angular parts of the wave function are unchanged. However, the dependence of the potential on  $r$  is usually very difficult to determine, so that the radial wave function and energy cannot be exactly obtained.

Figures 5-1, 5-2, and 5-3 show the radial and angular distribution of the electrons. The  $s$  electron wave function is seen to be the only one which does not vanish at the center of the nucleus. The  $s$  electron is also the only one which has a spherical charge distribution.

The allowed energy levels for the hydrogen atom are given by

$$W = -\frac{2\pi^2\mu e^4 Z^2}{n^2 h^2} = -Rhc \frac{Z^2}{n^2} \quad (5-6)$$

where  $R = 2\pi^2\mu e^4/ch^3$  is the Rydberg constant in  $\text{cm}^{-1}$ .  $W$  is in ergs; to convert to  $\text{cm}^{-1}$ , divide by  $hc$ . On this model of the hydrogen atom,

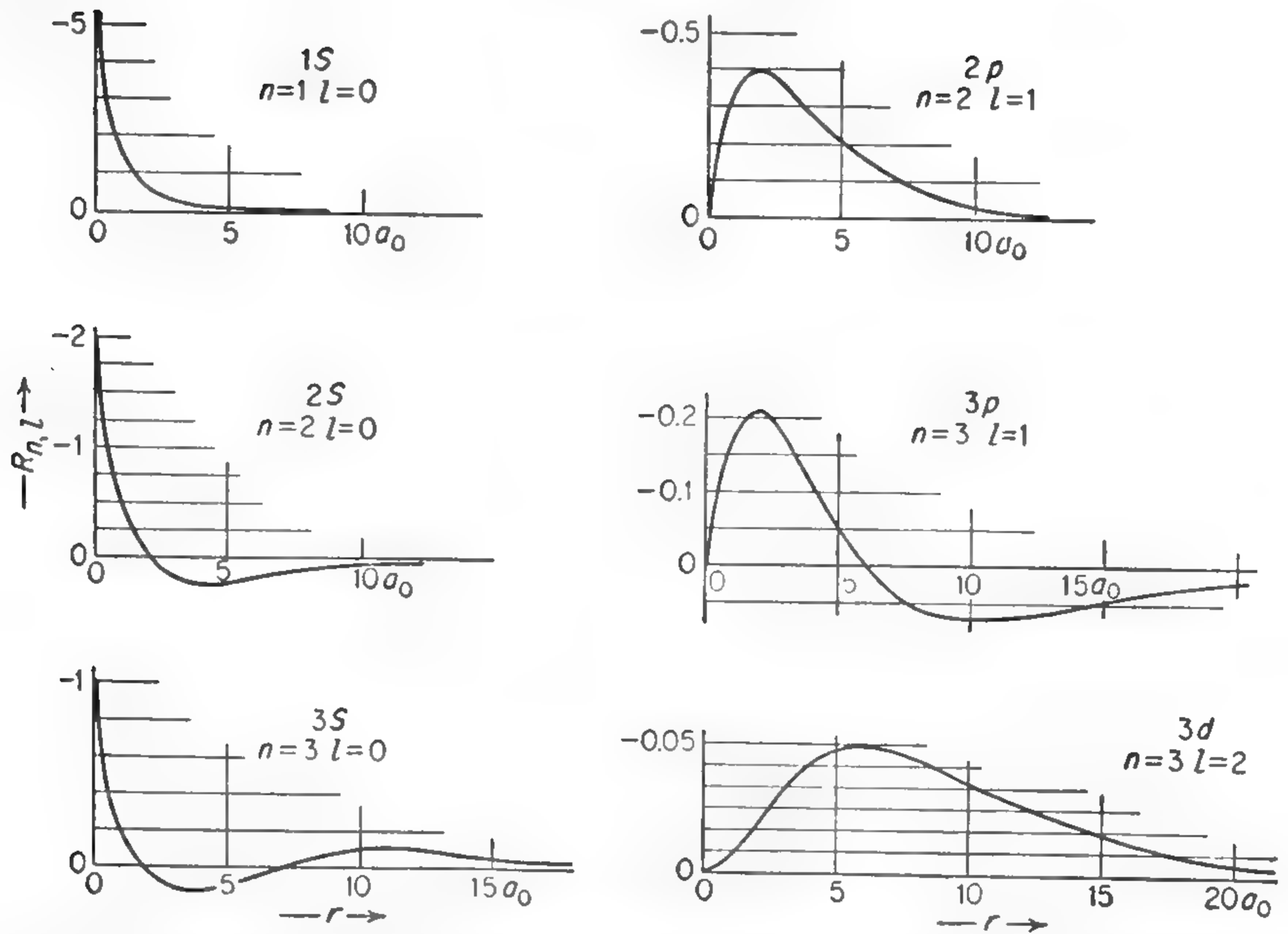


FIG. 5-1. The radial part of the hydrogen electronic wave function  $R_{n,l}$  plotted as a function of the distance between the electron and the nucleus.

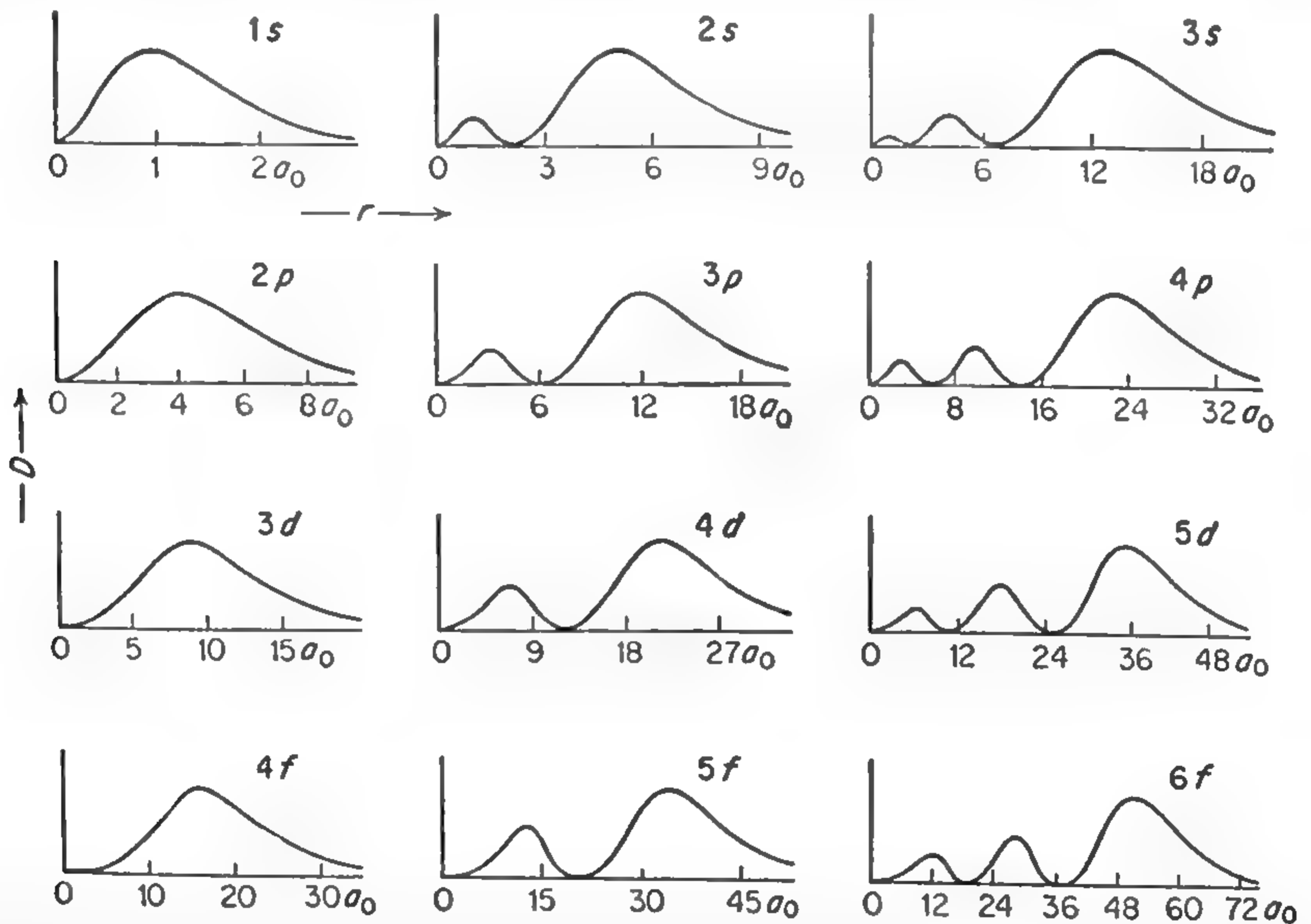


FIG. 5-2. The electronic density distribution  $r^2(R_{n,l})^2$  is plotted as a function of the electron-nuclear distance for several states of the hydrogen atom. The ordinate shows the probability of finding the electron between spherical shells of radii  $r$  and  $r + dr$ .

which neglects electron spin and relativistic effects, the energy is independent of  $l$  and  $m$ , and depends only on the principal quantum number  $n$ .

Since the angular dependence of the wave functions is the same as for the diatomic molecule, the selection rules and intensity relations which depend on angular momentum are identical. As in Chap. 1, it can be shown that transitions occur between energy levels such that

$$l' = l \pm 1 \quad \text{and} \quad m' = m, m \pm 1$$

A state with  $l = 0$  is called an  $S$  state; states for which  $l = 1, 2, 3, \dots$  are, respectively,  $P, D, F, G, H, \dots$  states.

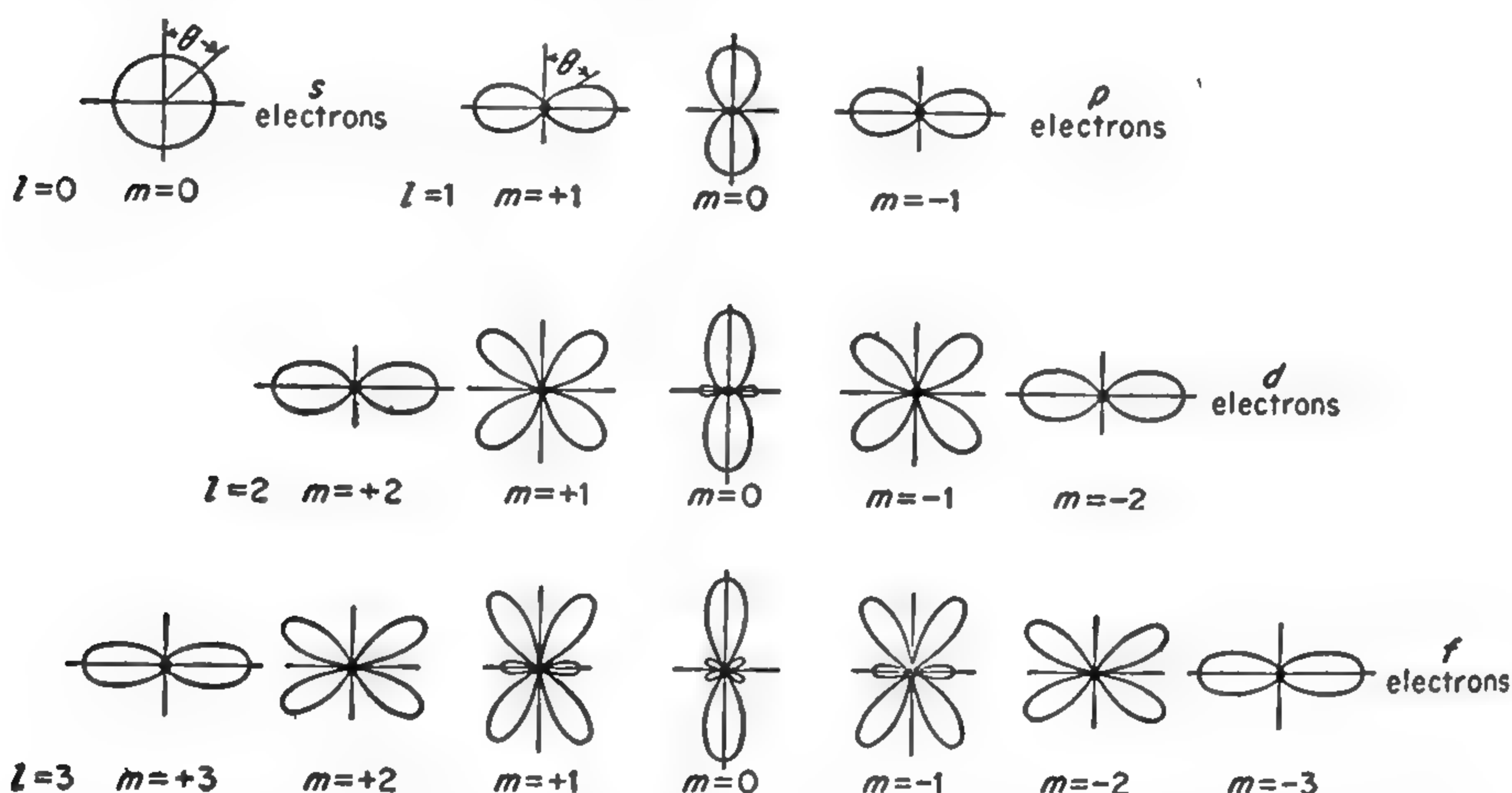


FIG. 5-3. The probability-density distribution factor  $\Theta^2$  plotted as a function of  $\theta$  for  $s, p, d, f$  electrons. For states with  $m = 0$  the scale is approximately  $l(l + 1)$  times that of the other states having the same value of  $l$ . (After White [53].)

**5-2. Atoms with More Than One Electron.** While a wave equation can be written for many-electron atoms, it is not possible to solve it exactly. To a good approximation, however, each electron may be considered to move in a spherically symmetrical field produced by the nucleus and all the other electrons. Then the angular part of the solution will be just the same as for the hydrogen atom, and the electron can be characterized by quantum numbers  $l$  and  $m$  as before.

The radial part of the wave function can only be approximated. Some useful methods of making the approximation and obtaining numerical or sometimes analytical wave functions have been discussed by Hartree, Fock, Fermi, Thomas, Slater, and others [305].

Particularly simple are the alkali-type atoms which have one electron outside a spherically symmetrical core of "closed electron shells." As



long as the valence electron stays out beyond all other electrons in the atom, it moves in a Coulomb field with  $Z_{\text{eff}} = 1$ . To this extent the wave functions and energy levels resemble those of the hydrogen atom, and each state is characterized by quantum numbers  $n$ ,  $l$ ,  $m$ . The energy is still independent of  $m$  and for large values of  $l$  does not depend greatly on  $l$ . But for small values of  $l$ , especially for  $S$  states where  $l = 0$ , the wave functions (Figs. 5-1 and 5-2) show a relatively large probability of the electron's being near the nucleus. In these states, the electron

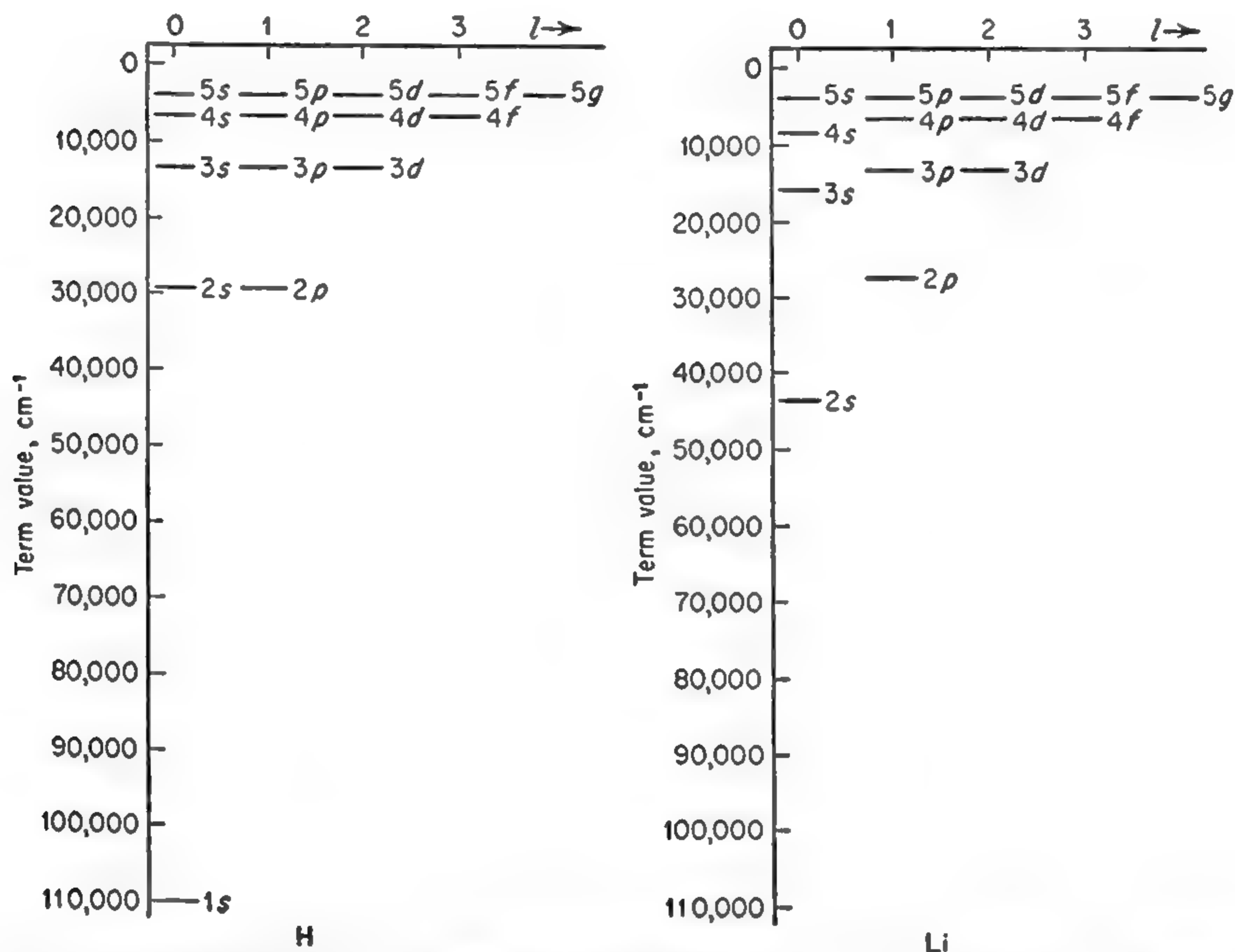


FIG. 5-4. Energy levels of hydrogen and an alkali atom. The term value, or energy, of the atom is referred to a zero which represents the energy after the valence electron has been completely removed or the atom ionized.

spends considerable time inside the closed electron shells, in a region of larger  $Z_{\text{eff}}$ , so that its binding energy is increased. Figure 5-4 shows the energy levels of a hydrogen atom and those of an alkali atom.

The energies for levels in a complex atom are often given by a formula analogous to Eq. (5-6) for the hydrogenic case. However, since Eq. (5-6) no longer applies exactly, it can be made to agree with the observed energies only by modifying the value of  $n$  or the value of  $Z$ , or both. Thus for the first case,

$$W = -\frac{RhcZ_o^2}{n^{*2}} = -\frac{RhcZ_o^2}{(n - \sigma)^2} \quad (5-7)$$

where  $R$  = Rydberg constant

$Z_o$  = effective nuclear charge in the outer region of the atom.

$Z_o = 1$  for alkali atoms, but may be 2, 3, 4, . . . for ionized alkalilike atoms such as  $\text{Be}^+$ ,  $\text{B}^{++}$ ,  $\text{C}^{+++}$ , etc.

$n^*$  = effective principal quantum number; not an integer

$n$  = principal quantum number, and is an integer

$\sigma$  = quantum defect

From Eq. (5-7) it is seen that

$$n^* = n - \sigma \quad (5-8)$$

If  $n$  is retained and  $Z$  is modified, the term value or energy depends on an effective  $Z$ ,  $Z_{\text{eff}}$ , such that

$$W = - \frac{RhcZ_{\text{eff}}^2}{n^2} \quad (5-9)$$

Equations (5-7) and (5-9) are written down by purely formal analogy with the expression which applies to a hydrogenic atom. Since  $n^*$  in Eq. (5-7) or  $Z_{\text{eff}}$  in Eq. (5-9) are not integers but are empirical constants, these equations are useful only when the same constant can be used for several purposes. Equation (5-7) is quite useful for describing the term values of alkalilike atoms because the quantum defect,  $\sigma = n - n^*$ , varies only slowly with  $n$  and  $l$ . Thus if  $n^*$  is known for one level, its value, and hence the term value for another level, can be found at least approximately.

An effective value of  $Z$  is often used in connection with atomic fine structure, or for the energy levels of different atoms in an isoelectronic sequence. It is then sometimes convenient to express  $Z_{\text{eff}}$  in terms of  $Z_{\text{inner}}$  and  $Z_{\text{outer}}$ , which are effective nuclear charges in the inner and outer region of the atom.

**5-3. Fine Structure, Electron Spin, and the Vector Model.** When spectral lines are examined with instruments of moderate resolving power, they are found to have a structure, *i.e.*, to consist of several components. This "fine structure" is explained by attributing to the electron a spin angular momentum and a magnetic moment. The angular momentum is related to a spin quantum number  $s$ , and its magnitude is given by  $\sqrt{s(s+1)}$  in units  $h/2\pi$ . For a single electron  $s$  always has the value  $\frac{1}{2}$ . This  $s$  should not be confused with the same letter used to denote a state with  $l = 0$ . The corresponding spin magnetic moment is  $1 + (\alpha/2\pi)$ , in units of the Bohr magneton\*  $he/4\pi mc$ , where  $m$  is the electron mass. The fine structure constant  $\alpha$  is  $2\pi e^2/hc$  and approximately equals  $\frac{1}{137}$ . A further quantum number  $m_s = \pm \frac{1}{2}$  is required to describe the projec-

\* The Bohr magneton is usually taken as a positive quantity even though the electron charge is negative. Regardless of this convention, it should be remembered that the electron magnetic moment is opposite to the direction of its spin.

tion of  $s$  on some fixed direction, just as  $m_l$  gives the projection of the orbital angular momentum on a fixed direction.

The electron's orbital angular momentum and spin angular momentum are vectors and will therefore add in some way similar to the ordinary rules of vector addition to form a resultant denoted by  $j$ . The magnitude of  $j$  is also quantized. It is specified by the total-angular-momentum quantum number  $j$  which has the values  $j = l + s$  and  $j = |l - s|$  (when  $s = \frac{1}{2}$ ). The corresponding vector equation is

$$\mathbf{j} = \mathbf{l} + \mathbf{s} \quad (5-10)$$

where the two possible values of  $j$  correspond to  $\mathbf{l}$  and  $\mathbf{s}$  being nearly parallel or nearly antiparallel.

The magnitudes of  $\mathbf{j}$ ,  $\mathbf{l}$ , and  $\mathbf{s}$  are, respectively,  $\sqrt{j(j+1)}$ ,  $\sqrt{l(l+1)}$ , and  $\sqrt{s(s+1)}$ . However, sometimes equations are written as if the magnitudes were  $j$ ,  $l$ , and  $s$ . This convention is frequently employed because of its conciseness (cf. [23]). Using it, one may speak of  $\mathbf{l}$  and  $\mathbf{s}$  being parallel or antiparallel for then the magnitude of their resultant would just be  $l + s$  or  $|l - s|$ . The method leads to equations which must finally be corrected by replacing  $j^2$  by  $j(j+1)$ ,  $l^2$  by  $l(l+1)$ , and  $s^2$  by  $s(s+1)$ .

The two orientations of  $\mathbf{s}$  relative to  $\mathbf{l}$  produce levels with slightly different energies. They are distinguished by appending the value of  $j$  as a subscript to the term symbol, for example,  $S_{\frac{1}{2}}$ ,  $P_{\frac{3}{2}}$ ,  $P_{\frac{1}{2}}$ ,  $D_{\frac{5}{2}}$ ,  $D_{\frac{3}{2}}$ . Since there are in general two possible orientations of  $\mathbf{s}$  relative to  $\mathbf{l}$ , for any given  $l$  there are two possible  $j$  values. The *multiplicity* of the term is therefore said to be 2, and this is denoted by a superscript 2 to the left of the term symbol. The doublet symbol is used even for  $S$  states where only one value of  $j$  is possible. Some typical states in a one-electron (hydrogenic or alkalilike) spectrum are  $^2S_{\frac{1}{2}}$ ,  $^2P_{\frac{3}{2}}$ ,  $^2P_{\frac{1}{2}}$ ,  $^2D_{\frac{5}{2}}$ ,  $^2D_{\frac{3}{2}}$ , . . . . The two levels  $^2P_{\frac{3}{2}}$  and  $^2P_{\frac{1}{2}}$  form a fine-structure doublet term.

The splitting between the two levels with different values of  $j$  which occurs when  $l$  is not zero is caused primarily by the magnetic interaction between the electron spin and electron orbital magnetic moments. This interaction can be derived from the magnitude of the magnetic field at the electron caused by the relative motion of the nucleus with respect to the electron. The splitting, however, is reduced by another contribution to the energy exactly half as large and in the opposite direction which is connected with a precession of the electron axis due to relativistic effects [7]. When both are taken into account, the energy level for a hydrogenic atom with nuclear charge  $Z$  is displaced by an amount

$$W_s = \frac{1}{2} \frac{e^2 h^2 Z}{4\pi^2 m^2 c^2} \left( \frac{1}{r^3} \right)_{av} s l \cos(\mathbf{s}, \mathbf{l}) \quad (5-11)$$



where  $e$  = electron charge

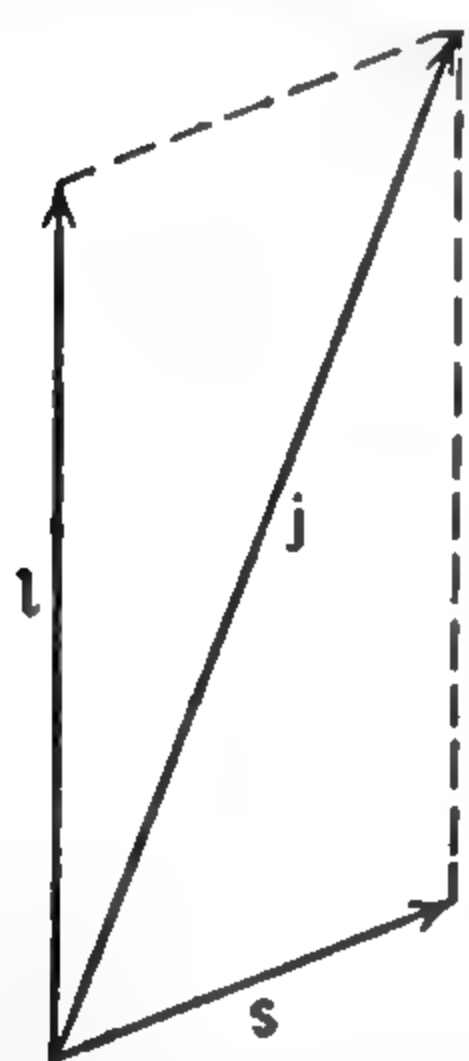
$m$  = mass of the electron

$c$  = velocity of light

$h$  = Planck's constant

$(1/r^3)_{av}$  = average of the inverse cube of the distance between nucleus of charge  $Z$  and the electron.

Two values of  $\cos(\mathbf{s}, \mathbf{l})$  are possible corresponding to  $\mathbf{l}$  and  $\mathbf{s}$  being "parallel" or "antiparallel"; *i.e.*, the quantum number  $j$  can equal  $l + s$  or  $l - s$ . The quantity  $sl \cos(\mathbf{s}, \mathbf{l})$  appearing in (5-11) can be evaluated from the vector model. Figure 5-5 shows how the vectors  $\mathbf{l}$  and  $\mathbf{s}$  combine to form a resultant  $\mathbf{j}$ . From the trigonometric relation between the sides and angles of a triangle in the diagram



combine to form a resultant  $\mathbf{j}$ . From the trigonometric relation between the sides and angles of a triangle in the diagram

$$sl \cos(\mathbf{s}, \mathbf{l}) = \frac{|\mathbf{j}|^2 - |\mathbf{s}|^2 - |\mathbf{l}|^2}{2}$$

where  $|\mathbf{j}|^2$ ,  $|\mathbf{s}|^2$ , and  $|\mathbf{l}|^2$  represent, respectively, squares of the magnitudes of the vectors  $\mathbf{j}$ ,  $\mathbf{s}$ , and  $\mathbf{l}$ . From quantum mechanics, these are to be replaced by  $j(j + 1)$ ,  $s(s + 1)$ , and  $l(l + 1)$ , so that

$$sl \cos(\mathbf{s}, \mathbf{l}) = \frac{j(j + 1) - s(s + 1) - l(l + 1)}{2} \quad (5-12)$$

FIG. 5-5. Vector addition of  $\mathbf{l}$  and  $\mathbf{s}$  to form resultant  $\mathbf{j}$ .

This method of adding vectors trigonometrically and then correcting the square of their magnitudes can be applied to any quantum vectors. It will be found useful for the addition of nuclear angular momenta to atomic or molecular angular momenta.

The vector model, which treats angular momenta as classical vectors except for quantum conditions imposed on their magnitudes, is very helpful because it permits easy calculation and visualization of many quantum-mechanical results. It always gives correctly the results of a true quantum-mechanical calculation if only the cosines between vectors or their projections on arbitrary directions are of importance. It is not directly applicable, however, when more complicated functions are required, such as the squares of cosines of angles between vectors.

Substituting the expression (5-12) or  $sl \cos(\mathbf{s}, \mathbf{l})$  into (5-11), the displacements of the two levels  $j = l \pm s = l \pm \frac{1}{2}$  are given by

$$W_{\pm} = \frac{1}{2} \frac{e^2 h^2}{4\pi^2 m^2 c^2} \left( \frac{Z}{r^3} \right)_{av} \frac{\pm (l + \frac{1}{2}) - \frac{1}{2}}{2}$$

The  $+$  sign corresponds to  $j = l + \frac{1}{2}$ . The splitting or energy difference between the two levels is then

$$\Delta\nu = R\alpha^2 a_0^3 \left( \frac{Z}{r^3} \right)_{av} (l + \frac{1}{2}) \quad \text{cm}^{-1} \quad (5-13a)$$

For a hydrogenic orbit,  $Z$  is constant and

$$\left(\frac{1}{r^3}\right)_{av} = \frac{Z^3}{n^3 a_0^3 l(l + \frac{1}{2})(l + 1)} \quad (5-13b)$$

so that

$$\Delta\nu = \frac{R\alpha^2 Z^4}{n^3 l(l + 1)} \quad (5-13c)$$

where  $R = 2\pi^2 me^4 / ch^3 \text{ cm}^{-1}$  [Eq. (5-6)]

$\alpha = 2\pi e^2 / hc$  is the fine-structure constant

$a_0 = h^2 / 4\pi^2 me^2$  is the Bohr radius of hydrogen

For an alkali-type atom a similar formula might be expected to hold approximately. The quantum number  $n$  in (5-13) must again be modified to an effective value  $n^* = n - \sigma$ . In addition, the  $Z^4$  is not a simply determinable quantity since the electron is affected by  $Z_o$ , or  $Z_{outer}$ , when it is very far from the nucleus, and  $Z_i$ , or  $Z_{inner}$ , when it is inside the shells of other electrons and close to the nucleus. A good empirical expression, which can also be justified theoretically, is

$$\Delta\nu = \frac{R\alpha^2 Z_i^2 Z_o^2}{n^* l(l + 1)} = \frac{5.83 Z_i^2 Z_o^2}{n^* l(l + 1)} \text{ cm}^{-1} \quad (5-14)$$

$n^*$  is the effective principal quantum number which may be evaluated from the term energy and from (5-7).  $Z_o$  is the same  $Z_o$  as in (5-7), which is the net charge on the atom after removing the valence electron.  $Z_i$ , the effective value of  $Z$  near the nucleus, may be taken as approximately 4 less than the nuclear charge  $Z$  for  $p$  electrons. Methods of approximating  $\Delta\nu$  and appropriate values of  $Z_i$  are discussed by White [53].

Although (5-14) represents as accurate an expression as can usually be obtained for many-electron atoms, the hydrogen case can be treated much more completely. A more exact theory for the hydrogenic case will be discussed below.

**5-4. Atoms with More Than One Valence Electron.** Many atoms have more than one valence electron, each one of which is characterized by quantum numbers  $n$ ,  $l$ , and  $s$ . The angular momenta  $l$  and  $s$  may be coupled in several different ways by the interactions between the electrons. The most common coupling scheme, and one that applies for all light atoms, is known as  $LS$  or Russell-Saunders coupling. For this scheme the individual  $l$ 's are coupled so that they add vectorially to form a resultant  $L$ , and the spins couple to form a resultant  $S$ . Finally  $L$  and  $S$  add vectorially to form a total angular momentum  $J$ . To the vectors  $L$ ,  $S$ , and  $J$  correspond quantum numbers  $L$ ,  $S$ , and  $J$ , while their magnitudes are, respectively,  $\sqrt{L(L + 1)}$ ,  $\sqrt{S(S + 1)}$ , and  $\sqrt{J(J + 1)}$ . The state of the atom as a whole is represented by a term symbol quite analogous to that used for the hydrogen atom. In fact the hydrogenlike atoms may be regarded as especially simple cases of  $LS$  coupling. A

capital letter  $S, P, D, F, \dots$  gives the value of  $L$ , corresponding, respectively, to  $L = 0, 1, 2, 3, \dots$ . A subscript to the right gives the value of  $J$ , while  $2S + 1$  is given by a superscript to the left.  $2S + 1$  is called the "multiplicity" of the state. This is because, as long as  $L \geq S$ ,  $J$  may assume any of the values  $L + S, L + S - 1, \dots, L - S$ , or  $2S + 1$  different  $J$  states are possible. For example, the states  $^3P_2, ^3P_1, ^3P_0$  have the same  $L$  and  $S$ , but different  $J$ 's; they constitute a triplet.

In compounding the angular momenta of the individual electrons, it is usually necessary to consider only those electrons outside closed shells, because for all closed shells  $L, S$ , and  $J$  are zero. The number of electrons in a closed shell is governed by the Pauli exclusion principle.

In a strong electric or magnetic field, the interactions of the individual electrons with the field are stronger than their interactions with each other. Then in addition to  $n, l$ , and  $s$ , each electron has quantum numbers  $m_l$  and  $m_s$  which are, respectively, the projections of  $l$  and  $s$  on the field direction.  $m_l$  can have the values  $l, l - 1, \dots, -l$ , while  $m_s = +\frac{1}{2}, -\frac{1}{2}$ . Pauli's exclusion principle states that only one electron in any one atom can have a given set of the five quantum numbers  $n, l, s, m_l, m_s$ . From this it follows that  $2(2l + 1)$  electrons may have a given  $n$  and  $l$ . They form a closed subshell, with zero angular momentum and a spherical distribution of charge. For a given value of  $n$ ,  $l$  may assume the values  $0, 1, 2, \dots, n - 1$ . Including all these possible values of  $l$ ,  $2n^2$  electrons have the same value of  $n$ , and they constitute a closed shell.

**5-5. Selection Rules and Intensities.** The intensity of a transition between two states of an atom is proportional to the square of the matrix element of the electric dipole moments between the states, that is,

$$I \propto |\int \psi_2^* e z \psi_1 d\tau|^2 \quad (5-15)$$

and to the population of the initial state.

The value of the matrix element involves both the radial and the angular parts of the wave function. The radial part of the wave function depends on the quantum numbers  $n$  and  $l$  and on the particular atom in question. It is usually difficult to evaluate exactly. However, the angular part of the wave function depends only on the angular momentum quantum numbers and not on the details of the particular atom as long as the electron can be considered to move in a spherical potential. General selection rules may hence be found for the changes in angular momentum quantum numbers allowed during a radiative transition. They are very similar to the selection rules of Sec. 1-4 and may be written

$$\begin{aligned} L' &= L \pm 1, L \\ J' &= J \pm 1, J \text{ (but } J' \text{ and } J \text{ cannot both be zero)} \\ \Sigma l_i &\text{ changes from odd to even or vice versa} \\ \Delta m_J &= 0, \pm 1 \end{aligned} \quad (5-16)$$



Although these selection rules are very useful in predicting which transitions may occur, they give little information about the absolute or relative intensities of transitions, which often depend on the radial parts of the wave function.

In cases involving a group of transitions with the various initial states and the various final states differing among themselves only in the relative orientation of the angular momentum vectors  $\mathbf{L}$ ,  $\mathbf{S}$ , and  $\mathbf{J}$ , the radial part of the matrix element (5-15) is constant. The relative intensities of such transitions then depend only on the angular momentum quantum numbers. A typical example of this type of case is a group of fine-structure components of "one" transition. Their relative intensities are given by [23], [53]:

For transitions  $L \leftarrow L - 1$ :

$$\begin{aligned} J \leftarrow J - 1, I &= \frac{B(L + J + S + 1)(L + J + S)(L + J - S)(L + J - S - 1)}{J} \\ J \leftarrow J, I &= - \frac{B(L + J + S + 1)(L + J - S)(L - J + S)(L - J - S - 1)(2J + 1)}{J(J + 1)} \\ J \leftarrow J + 1, I &= \frac{B(L - J + S)(L - J + S - 1)(L - J - S - 1)(L - J - S - 2)}{(J + 1)} \end{aligned} \quad (5-17)$$

For transitions  $L \leftarrow L$ :

$$\begin{aligned} J \leftarrow J - 1, I &= - \frac{A(L + J + S + 1)(L + J - S)(L - J + S + 1)(L - J - S)}{J} \\ J \leftarrow J, I &= \frac{A[L(L + 1) + J(J + 1) - S(S + 1)]^2(2J + 1)}{J(J + 1)} \\ J \leftarrow J + 1, I &= - \frac{A(L + J + S + 2)(L + J - S + 1)(L - J + S)(L - J - S - 1)}{(J + 1)} \end{aligned} \quad (5-18)$$

Expressions (5-17) and (5-18) for the relative intensities take into account both the squares of the matrix element (5-15) and the relative populations of the different levels, assuming that the populations are proportional to the statistical weights or  $M$  degeneracy.

In Appendix I, these relative intensities have been tabulated. It should be noted that the lines whose intensities are to be compared must be close together in frequency for Eqs. (5-17) and (5-18) to apply. Otherwise the intensity should be multiplied by a frequency factor which is  $\nu^4$  for optical emission lines, or  $\nu^2$  for microwave absorption.

These formulas and tables depend only on the magnitude and direc-

tions of the vectors which have been added, and not on the specific form of interaction between the vectors. They may therefore be used for transitions in which angular momentum vectors other than  $L$ ,  $S$ , and  $J$  are involved if appropriate changes are made in the symbols.

For example, if the nucleus has an angular momentum  $I$ , it can interact with the electronic angular momentum  $J$  to give a new total angular momentum quantum number  $F$ . The energy separations between levels with different values of  $F$  give rise to hyperfine structure, which will be considered shortly. Then the relative intensities of different transitions in a hyperfine-structure pattern are given by the same equations (5-17) and (5-18), provided we replace  $J$  by  $F$ ,  $L$  by  $J$ , and  $S$  by  $I$ . Here the symbol  $I$  should not be confused with the same letter used to denote intensity in Eqs. (5-17) and (5-18).

The general behavior of the relative intensities of fine-structure components may be readily understood. The radiation fields act primarily on the orbital angular momentum and change  $L$  by one unit without changing  $S$ . This is because the force of the electric component of the field on the electron charge is much greater than magnetic forces acting on the electron spin. If  $L$  is increased during the transition to  $L + 1$  and  $S$  is unaffected in magnitude or direction, then  $J$  would be expected to change in approximately the same way as  $L$ , or to increase to  $J + 1$ . It will be observed that the stronger transitions in Appendix I tend to be those for which the change in  $J$  has the same value as the change in  $L$ . This is most notably true for large values of  $L$ , where quantum-mechanical results most closely approximate classical expectations.

**5-6. Fine Structure—More Exact Treatment.** Although most atoms are so complex that a theoretical calculation of fine structure which is much more exact than the expressions (5-13) and (5-14) given above is very difficult and even uncertain, the hydrogen atom and hydrogenlike one-electron ions are sufficiently simple to allow a considerably more exact treatment. Because of this simplicity, the hydrogen spectrum, and the hydrogen fine structure in particular, has been much used as a testing ground for atomic theory. Several different treatments of the hydrogen fine structure have met with temporary success, but each in turn has required modification as experimental techniques and theoretical knowledge advanced. The basis of the modern treatment of the hydrogen atom and its fine structure was given in 1928 by Dirac. He proposed a relativistic form of quantum mechanics which inherently provides the electron with the properties previously postulated separately as a spin and magnetic moment.

According to the Dirac theory, the energy levels of a hydrogenlike atom are given by

$$W = mc^2 \left( \left\{ 1 + (\alpha Z)^2 [n - |K| + (K^2 - \alpha^2 Z^2)^{1/2}]^{-2} \right\}^{-1/2} - 1 \right) \quad (5-19)$$

where  $|K| = j + \frac{1}{2}$ . It may be seen from Eq. (5-19) that the levels with the same value of  $n$  and  $j$  are degenerate. If this equation is expanded in powers of  $\alpha Z$ , it gives

$$\frac{W_{nj}}{hc} = -\frac{Z^2 R}{n^2} - \frac{\alpha^2 Z^4 R}{n^3} \left[ (j + \frac{1}{2})^{-1} - \left( \frac{3}{4n} \right) \right] + \dots \quad (5-20)$$

so that the fine-structure doublet separation between the  $^2P_{3/2}$  and  $^2P_{1/2}$  levels is

$$\Delta\nu = \frac{R\alpha^2 Z^4}{n^3 l(l+1)} \quad (5-21)$$

which agrees with the previous result [Eq. (5-13)], although here it is evident that terms in higher orders of  $\alpha Z$  have been neglected. Figure

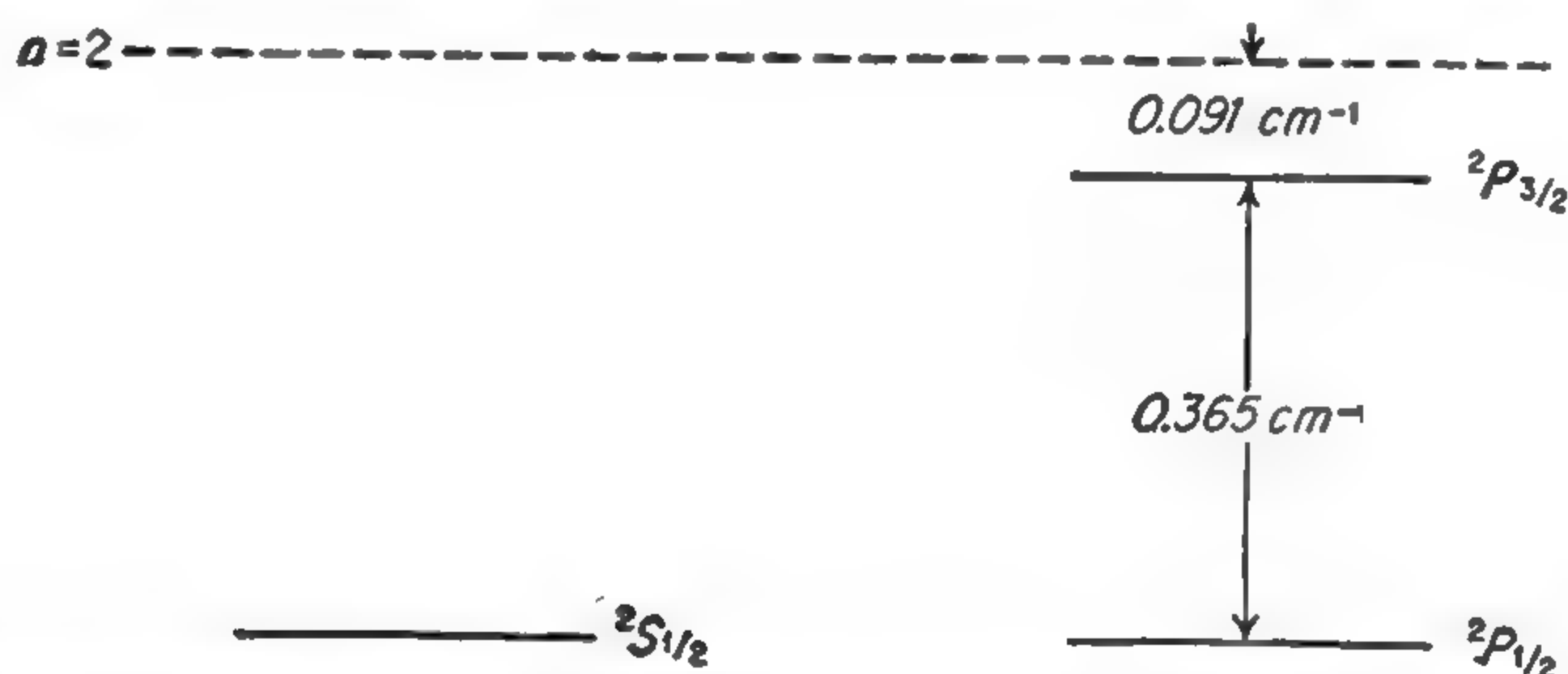


FIG. 5-6. Fine structure of  $n = 2$  levels of hydrogen (Dirac theory). The dotted line indicates the position the levels would have according to the Bohr theory, which does not consider fine structure.

5-6 shows the  $n = 2$  levels of the hydrogen atom according to the Dirac theory.

Optical spectroscopic measurements of the fine structure of the hydrogen  $H_\alpha$  line ( $n = 3$  to  $n = 2$ ), indicated that the structure of the  $n = 2$  level of hydrogen was in reasonable, although not precise, agreement with the predictions of the Dirac theory. However, because hydrogen is such a light gas, the atoms have large thermal velocities which, through the Doppler effect, cause considerable broadening of the lines. The resultant blurring of the pattern was sufficient even at liquid-air temperatures to make the disagreement uncertain. There was some indication that the  $^2S_{1/2}$  level was displaced upward with respect to the  $P$  levels by about  $0.03 \text{ cm}^{-1}$ , or 1000 Mc [80], [88], [89]. On the other hand, the apparent shifts were attributed by some [97] to impurities in the light source.

As early as 1928 Grotrian [9] had pointed out that the selection rules permitted transitions between states with the same value of  $n$ , and that radio waves might be used to induce such transitions. Several attempts were made [31], [60] to observe transitions between the  $2s \ ^2S_{1/2}$  and  $2p \ ^2P_{1/2}$  levels which on the Dirac theory should be separated by  $\Delta\nu = 0.365 \text{ cm}^{-1}$ ,



or 10,950 Mc. Spark-gap oscillators were used, and the radiation was passed through a hydrogen gas discharge tube. Betz reported absorptions of about 25 per cent at wavelengths of 3, 9, and 27 cm, but these absorptions seem to be impossibly large. Haase [60] found no resonant absorption at all.

It does appear possible to detect this fine-structure splitting by direct microwave absorption. Hydrogen atoms may be excited to the  $2s\ ^2S_{\frac{1}{2}}$  or  $2p\ ^2P_{\frac{1}{2}}$  states in an electrical discharge in wet hydrogen. From the  $^2P_{\frac{1}{2}}$  state they decay rapidly, since this state has a natural lifetime  $\tau_P$  of only  $1.6 \times 10^{-9}$  sec. The  $2s\ ^2S_{\frac{1}{2}}$  state is metastable, however, so that atoms tend to accumulate in it and they may absorb microwave energy by making a transition to the  $2p\ ^2P_{\frac{1}{2}}$  state. On the other hand, a relatively small electric field may be expected to produce a Stark effect in the  $^2S_{\frac{1}{2}}$  state which would make transitions to the ground state possible and drastically reduce its lifetime. Reesor [631] has looked for direct microwave absorption due to the  $2p \leftarrow 2s$  transition in a discharge tube and failed to find it.

The expression (1-49) giving the absorption coefficient in a gas for which both the upper and lower states are populated according to the Boltzmann distribution law needs only a slight modification to apply to this case where all the atoms considered are in the lower state of the transition. It becomes

$$\gamma = \frac{8\pi^2 N}{3hc} \frac{|e\mathbf{r}|^2 \nu \Delta\nu}{(\nu - \nu_0)^2 + (\Delta\nu)^2} \quad (5-22)$$

where  $\gamma$  is the absorption coefficient for microwave radiation of frequency  $\nu$ ,  $\nu_0$  is the resonant frequency, and  $|e\mathbf{r}|$  is the dipole moment matrix element, or  $e$  times the matrix element of the coordinate vector  $\mathbf{r}$  of the atomic electron for the transition  $2s\ ^2S_{\frac{1}{2}} \rightarrow 2p\ ^2P_{\frac{1}{2}}$ . The square of the matrix element  $|e\mathbf{r}|^2$  for the transition can be calculated as  $6a_0^2$ , where  $a_0 = h^2/4\pi^2 me^2$  is the radius of the first Bohr orbit for hydrogen. If broadening of the resonance absorption due to collisions can be ignored then there is no appreciable broadening of the  $^2S_{\frac{1}{2}}$  state and the half width is just  $1/(4\pi\tau_P)$ , where  $\tau_P$  is the natural lifetime of the  $^2P_{\frac{1}{2}}$  state,  $1.6 \times 10^{-9}$  sec. This short lifetime gives a half width of about 50 Mc. The number of atoms  $N$  in the  $2s\ ^2S_{\frac{1}{2}}$  state is very difficult to calculate. However, a rough estimate gives  $N = 5 \times 10^{10}$  atoms/cm<sup>3</sup> under optimum conditions [484], so that the absorption coefficient becomes, from (5-22),

$$\gamma = 1.6 \times 10^{-4} \text{ cm}^{-1} \quad (5-23)$$

This is a large absorption coefficient by microwave spectroscopic standards, but its detection would be made more difficult by the large half width of the line, which is  $1/(4\pi\tau_P) \approx 50$  Mc. The effective absorption might be reduced by transitions in the reverse direction if the  $^2P_{\frac{1}{2}}$  state is appreciably populated. A further complication is the back-

ground of continuous absorption by free electrons in the discharge tube. This might be of the order of  $10^{-4} \text{ cm}^{-1}$  in a typical case.

While it seems that the hydrogen fine structure could probably be detected by direct absorption, no experiment of this type has yet been done. An alternative experiment, which is very suitable for an accurate measurement of this resonance, is the atomic-beam method of Lamb and Retherford [484]. Figure 5-7 is a block diagram of their apparatus.

Hydrogen was dissociated in an oven, and collimated by slits to form an atomic beam. Some of the atoms were excited to the metastable  $2s \ ^2S_{1/2}$  state by an electron bombarder. Then the beam passed through a region in which a radio-frequency field was applied and finally hit a



FIG. 5-7. Block diagram of Lamb and Retherford's apparatus for measurement of hydrogen fine structure.

detector. This detector was a tungsten ribbon, from which metastable atoms can eject electrons by giving up their excitation energy. Atoms in the ground state are not detected at all.

When the radio-frequency field of the proper frequency is applied, transitions are induced from the  $2s \ ^2S_{1/2}$  to the  $2p \ ^2P_{1/2}$  state. From there the atoms quickly decay to the ground state. Since the density in the beam is low there is little imprisonment of resonance radiation to increase the  $2p \ ^2P_{1/2}$  population.

To avoid the necessity for varying the radio frequency over a wide range which would make difficult the maintenance of constant radio-frequency power, the transition region was placed in a variable magnetic field. Then the Zeeman effect of the transition was observed and the frequency for zero field was found by extrapolation.

The fine structure of singly ionized helium was also studied by Lamb and Skinner [381], [485]. In this case the decay of the metastable atoms on application of the microwave field was detected by observation of the ultraviolet photons emitted in the transition to the ground state.

In both hydrogen and helium the  $2s \ ^2S_{1/2}$  level was found to be higher than the  $2p \ ^2P_{1/2}$ . However the separation between the levels  $2p \ ^2P_{1/2}$  and  $2p \ ^2P_{3/2}$  in hydrogen was found to agree with expression (5-22) [790]. For hydrogen the measured separation between  $2s \ ^2S_{1/2}$  and  $2p \ ^2P_{1/2}$  was  $1057.777 \pm 0.10 \text{ Mc}$  [876]; while in ionized helium the shift was  $14,020 \pm 100 \text{ Mc}$  for the corresponding level [485]. To achieve this precision in the measurement of the center frequency of a broad line requires a careful consideration of the factors affecting the shape and position of the line [790], [876].

The apparent upward shifts of the  $2s \ ^2S_{1/2}$  levels are now explained fairly



well by the interaction between the atomic electron and its radiation field [177]. The calculation is very difficult to carry out accurately, but the calculated shift for hydrogen agrees within about 0.5 Mc with the observed shift [876].

Probably the simplest atom from the theoretical point of view is positronium. It consists of a positron and electron only, so that there is no complication from the short-range forces associated with heavy nucleons. This atom is not stable, decaying in about  $10^{-8}$  sec with the annihilation of the particles and emission of either two or three  $\gamma$  rays. Consequently, it is not easy to study experimentally, and was discovered only recently by Deutsch [568a]. Two  $\gamma$  rays are emitted in opposite directions from states with  $J = 0$ . States with  $J = 1$  must emit three photons to conserve angular momentum, and hence have a longer lifetime. If transitions could be induced by a radio-frequency field from the  $J = 1$  to the  $J = 0$  states, triplet positronium would be converted to singlet, and the transition detected by the increase in double quantum annihilation. For this direct experiment, a frequency near  $2 \times 10^5$  Mc would be needed.

However, lower frequencies can be used to measure the fine structure of positronium with the aid of the Zeeman effect. In a magnetic field the  $J = 1$  state is split into  $M = 0$  and  $M = \pm 1$  components. The  $M = 0$  state acquires some singlet character, so that double quantum annihilation can occur from it. Weinstein, Deutsch, and Brown [997a] have used the annihilation radiation to detect microwave induced transitions from the  $J = 1, M = \pm 1$  to the  $J = 0$  levels. Since this Zeeman splitting depends in part on the ratio of magnetic field to the singlet-triplet separation, this measurement determined the fine structure splitting between the  $J = 0$  and 1 states as  $(2.0338 \pm 0.0004) \times 10^5$  Mc. The calculated value of  $2.0337 \times 10^5$  Mc [712a] is in excellent agreement.

A few other fine-structure splittings in atoms can probably be studied by microwave techniques. However, in many cases the fine structure is so large that transition frequencies do not lie in the microwave region, or in other cases the lifetimes of both states are so small that application of microwave techniques is difficult.

**5-7. Hyperfine Structure.** Atomic nuclei have radii near  $10^{-12}$  cm, and hence are very small compared with the size of electron orbits, which are approximately  $10^{-8}$  cm. Nuclei are also some  $10^4$  times heavier than electrons. To a good approximation electronic energies can therefore be obtained by considering nuclei to be positive point charges of infinite mass. However, effects on electronic energy levels due to the finite size and mass of nuclei, although small, often appear on careful observation of atomic spectra. They are called hyperfine structure because they produce a very small splitting of atomic lines, usually much smaller than the fine structure.



If the nucleus is to be considered other than a point charge, it must be recognized that the nucleus involves a charge distribution and that this charge distribution may be in motion, producing magnetic fields and giving the nucleus an angular momentum. As for an atom or any other quantum-mechanical system, the angular momentum of the nucleus must be  $Ih/2\pi$ , where  $I$  is an integer or half integer and is usually called the nuclear spin.

A number of types of hyperfine interactions between nuclei and electrons are independent of the relative orientation of nuclear spin  $I$  and electronic angular momentum  $J$ . These include the small shifts due to the finite nuclear mass, variation of the electron potential from a coulomb potential when electrons are within the nuclear radius, and isotropic (*i.e.*, independent of nuclear orientation) polarization of the nucleus by electron fields. These effects slightly change each electronic energy level but can usually be detected only by examining their variation between two or more isotopes, and hence are called "isotope effects." Thus a given chemical element may produce a number of slightly different superimposed spectra, each associated with a particular isotope of the element. Since the "isotope effects" do not represent small splittings of the energy levels of any one atomic system, but rather small differences between the spectra of different systems, they are not generally observed by microwave spectroscopy.

On the other hand, hyperfine interactions which vary with nuclear orientation give small splittings of electronic energy levels and are often observed with microwave or radio-frequency techniques. These effects may be either electric or magnetic in origin. Although the magnetic effects are usually most prominent in atoms, electric effects predominate in molecules. The electric interactions will be discussed first.

*Hyperfine Structure Due to Electric Charge Distribution in the Nucleus.* Motion of the center of mass of the nucleus is unchanged for the various possible nuclear orientations; hence it is the natural origin in considering a nucleus of finite size. Let  $V_0$  be the electrostatic potential produced at the nuclear center of mass by all electronic charges in the atom, and  $\partial V_0/\partial x$  represent its derivative evaluated at the same point. The electrostatic energy of a charge  $\rho(x,y,z) \Delta x \Delta y \Delta z$ , where  $\rho$  represents the nuclear charge density, is  $\Delta W = \rho \Delta x \Delta y \Delta z V(x,y,z)$ .

Expanding  $V$  as a series and writing the volume element  $\Delta x \Delta y \Delta z = \Delta \tau$

$$\begin{aligned} \Delta W = \rho \Delta \tau \left[ V_0 + x \frac{\partial V_0}{\partial x} + y \frac{\partial V_0}{\partial y} + z \frac{\partial V_0}{\partial z} + \frac{1}{2} x^2 \frac{\partial^2 V_0}{\partial x^2} + \frac{1}{2} y^2 \frac{\partial^2 V_0}{\partial y^2} \right. \\ \left. + \frac{1}{2} z^2 \frac{\partial^2 V_0}{\partial z^2} + xy \frac{\partial^2 V_0}{\partial x \partial y} + yz \frac{\partial^2 V_0}{\partial y \partial z} + zx \frac{\partial^2 V_0}{\partial x \partial z} \right. \\ \left. + \dots + \frac{x^n y^m z^p}{n! m! p!} \frac{\partial^{n+m+p} V_0}{\partial x^n \partial y^m \partial z^p} + \dots \right] \quad (5-24) \end{aligned}$$

Integrating over the entire nuclear volume,

$$W = \int \rho(x,y,z) \left[ V_0 + x \frac{\partial V_0}{\partial x} + y \frac{\partial V_0}{\partial y} + z \frac{\partial V_0}{\partial z} + \frac{1}{2}x^2 \frac{\partial^2 V_0}{\partial x^2} + \frac{1}{2}y^2 \frac{\partial^2 V_0}{\partial y^2} + \frac{1}{2}z^2 \frac{\partial^2 V_0}{\partial z^2} + xy \frac{\partial^2 V_0}{\partial x \partial y} + yz \frac{\partial^2 V_0}{\partial y \partial z} + zx \frac{\partial^2 V_0}{\partial z \partial x} + \dots \right] dv \quad (5-25)$$

The first term may be easily integrated to give  $ZeV_0$ , where  $Z$  is the atomic number of the nucleus and  $Ze$  its total charge. This is the term which is independent of nuclear size or shape. The second term may be written

$$\frac{\partial V_0}{\partial x} \int \rho(x,y,z)x dv$$

where the integral is the nuclear dipole moment in the  $x$  direction. If this nuclear dipole is not produced by an external field, such as that of the electrons, but is a property only of the nucleus, it can be shown to be zero except in very rare cases. Suppose the wave function and hence the charge distribution for a nucleus is known and the dipole moment in the  $x$  direction,  $\int \rho x dx dy dz$ , has the value  $\mu_x$ . If the positive directions of the nuclear coordinates  $x$ ,  $y$ , and  $z$  are now reversed, a new wave function can be found and a new charge density which is just the same function of the new coordinates  $x'$ ,  $y'$ ,  $z'$  as it was of the old coordinates  $x$ ,  $y$ ,  $z$ . This is possible because, for all known forces within the nucleus, the Hamiltonian or wave equation turns out to depend only on even powers of the coordinates and hence remains unchanged when the signs of all coordinates are reversed. The charge density at  $x$  will be replaced by a similar charge density at  $x'$  or  $-x$ . However, the direction of the angular momentum does not change on reversing all coordinates. In the new coordinate system, the dipole moment  $\mu_{x'}$  has the same value as before but is oppositely directed, that is,  $\mu_{x'} = -\mu_x$ . Other nuclear properties, however, including the nuclear angular momentum, will have remained unchanged. We must conclude, therefore, that if the nucleus has a dipole moment in one direction with respect to its angular momentum, there must be a degenerate nuclear state, or one of the same energy, with an oppositely directed dipole. Normally, such identical or degenerate states of the nucleus are not encountered, and hence the nucleus has no inherent dipole moment.\* If a nucleus has angular momentum  $I$ , there are

\* A similar proof may be applied to any system, showing that no dipole moments may exist in nature without degeneracy. What is ordinarily referred to as the permanent dipole moment of a molecule in fact does not give a molecule an average dipole moment in one direction unless there is degeneracy or an external field. The dipole moment of a large macroscopic collection of charges may be regarded as existing only because of the very close spacing, and hence effective degeneracy, of the rotational energy levels of such a large system.



$2I + 1$  different possible states having the same energy, corresponding to the different values of  $M_I$ , the projection of  $I$  on a fixed direction. It might be thought that this is a degeneracy which allows a dipole moment. However, since the angular momentum operator is similar to the Hamiltonian in that it does not change sign when all coordinates are reversed, an argument similar to that above shows that no dipole moment can exist unless the system has two states of the same energy and the same value of  $M_I$ . It can thus be shown that all terms of (5-25) involving odd powers of the coordinates will normally be zero. However, terms such as  $\int \frac{1}{2}\rho x^2 dv$  and  $\int \rho xy dv$  are not necessarily zero because they do not change sign with reversal of direction of all coordinates. These terms are associated with the quadrupole moment of the nucleus.

Before reexpressing these terms in a more convenient form, it is interesting to note their approximate magnitude. The potential  $V$  produced by the electron is  $e/r_e$ , where  $r_e$  is the distance between electron and nucleus. Hence  $\partial^2 V / \partial x^2$  is roughly  $e/r_e^3$ . The integral  $\int \frac{1}{2}\rho x^2 dv$  is of the order  $\int \rho r_n^2 dv = Ze r_n^2$ , where  $r_n$  is the nuclear radius. Hence the term  $\partial^2 V / \partial x^2 \int \frac{1}{2}\rho x^2 dv \approx Ze^2 r_n^2 / r_e^3$ . This might be compared with the first term in our expansion,  $ZeV = Ze^2 / r_e$ , giving the electrostatic energy for a point nucleus. The ratio of the two is  $r_n^2 / r_e^2$ , or  $10^{-8}$  if  $r_n$  is  $10^{-12}$  cm and an average value of  $10^{-8}$  cm is taken for  $r_e$ . The usual electrostatic energy is of the order  $10^5 \text{ cm}^{-1}$ , so the energy associated with the small correction terms of this type is expected to be  $0.001 \text{ cm}^{-1}$ , or 30 Mc. Still higher-order terms in the expansion (5-24) which are nonzero involve fourth powers of the coordinates [that is,  $x^4(\partial^4 V / \partial x^4)$ , etc.] They are associated with the nuclear hexadecapole (16-pole) and are expected to be still smaller than the quadrupole terms by a factor of roughly  $10^8$ . In most cases this makes them only a few cycles per second, and too small for present experimental accuracy to detect.

Part of the energy due to terms of (5-25) containing second derivatives of the potential does not vary with nuclear orientation. To eliminate this part we subtract

$$\int \frac{1}{6}\rho(x^2 + y^2 + z^2) \left( \frac{\partial^2 V}{\partial x^2} + \frac{\partial^2 V}{\partial y^2} + \frac{\partial^2 V}{\partial z^2} \right) dv \text{ or } \nabla^2 V \int \frac{1}{6}\rho r^2 dv$$

If electrons do not penetrate the nucleus, then  $\nabla^2 V$  is zero everywhere  $\rho$  is not zero, and this energy integral vanishes. If the electrons do penetrate the nucleus, then this energy represents a deviation from a Coulomb field within the nuclear radius, and is an important part of the atomic isotope shift.

*The Electric Quadrupole Moment.* Eliminating then the parts of (5-25) which are independent of nuclear orientation and the dipole terms, which have been shown to vanish, the remaining terms are attributable to a



nuclear electric quadrupole and may be written

$$W_Q = \frac{1}{6} \int \rho \left[ (3x^2 - r^2) \frac{\partial^2 V}{\partial x^2} + (3y^2 - r^2) \frac{\partial^2 V}{\partial y^2} + (3z^2 - r^2) \frac{\partial^2 V}{\partial z^2} + 6xy \frac{\partial^2 V}{\partial x \partial y} + 6yz \frac{\partial^2 V}{\partial y \partial z} + 6zx \frac{\partial^2 V}{\partial z \partial x} \right] dv \quad (5-26)$$

or

$$W_Q = -\frac{1}{6} \mathbf{Q} : \nabla \mathbf{E} \quad (5-27)$$

which is the inner product between the quadrupole moment dyadic

$$\mathbf{Q} = \int (3\mathbf{r}\mathbf{r} - r^2 \mathbf{1}) \rho \, dx \, dy \, dz \quad (5-28)$$

and the gradient of the electric field due to the electrons.

The properties of dyadics may be found in [105] or [63]. A dyadic  $\mathbf{AB}$  is formed from the two vectors  $\mathbf{A} = A_x \mathbf{i} + A_y \mathbf{j} + A_z \mathbf{k} = \sum_n A_n \mathbf{e}_n$ .

$\mathbf{B} = B_x \mathbf{i} + B_y \mathbf{j} + B_z \mathbf{k} = \sum_n B_n \mathbf{e}_n$ , where  $\mathbf{e}_n$  represents one of the three unit vectors  $\mathbf{i}$ ,  $\mathbf{j}$ , or  $\mathbf{k}$ . The dyadic has nine components and may be written  $\sum_{nm} A_n B_m \mathbf{e}_n \mathbf{e}_m$ . The unit dyadic  $\mathbf{1}$  is  $\mathbf{ii} + \mathbf{jj} + \mathbf{kk}$ , and is said to be diagonal because no "cross terms" of the type  $\mathbf{ij}$  or  $\mathbf{jk}$  occur.

The inner product of two dyadics  $\mathbf{AB} : \mathbf{CD}$  is the scalar quantity  $\sum_{nm} A_n B_m C_n D_m$ ,

which is analogous to the scalar product of two vectors.

By a proper choice of axes any symmetric dyadic such as the quadrupole moment dyadic may be diagonalized. This eliminates all terms except those multiplying  $\mathbf{ii}$ ,  $\mathbf{jj}$ , or  $\mathbf{kk}$ .

The charges in the nucleus are rotating very rapidly about the direction of the nuclear spin. If an average is made over a time long enough for the nuclear particles to rotate many times, but so short that the electrons or charges outside the nucleus have not appreciably changed position, the electric field gradient may be considered constant and the nuclear charge distribution cylindrical. Using a new coordinate system with  $z_n$  in the direction of the nuclear spin, all nondiagonal terms of  $\mathbf{Q}$  become zero, and the diagonal terms are simply related;

$$\int \rho (3x_n^2 - r^2) \, dv = \int \rho (3y_n^2 - r^2) \, dv = -\frac{1}{2} \int \rho (3z_n^2 - r^2) \, dv \quad (5-29)$$

The entire quadrupole moment dyadic may hence be expressed in terms of one constant, called "the" nuclear quadrupole moment

$$\mathbf{Q} = \frac{1}{e} \int \rho (3z_n^2 - r^2) \, dx \, dy \, dz \quad (5-30)$$

where  $e$  is the charge of one proton. From (5-30) it can be seen that a nucleus whose charge distribution is spherical has zero quadrupole

moment, for then the average value of  $3z_n^2$  is just equal to the average value of  $r^2 = x_n^2 + y_n^2 + z_n^2$ . The quadrupole moment may be considered then a measure of the deviation of the nuclear charge from spherical shape. If the charge distribution is somewhat elongated along the nuclear axis  $z_n$ , then  $Q$  is positive; if it is flattened along the nuclear axis,  $Q$  is negative. From (5-26) the quadrupole energy becomes

$$W_Q = \frac{e}{6} Q \left[ \frac{\partial^2 V}{\partial z_n^2} - \frac{1}{2} \left( \frac{\partial^2 V}{\partial x_n^2} + \frac{\partial^2 V}{\partial y_n^2} \right) \right] \quad (5-31)$$

If the potential  $V$  is due entirely to charges outside the nucleus, then

$$\frac{\partial^2 V}{\partial x_n^2} + \frac{\partial^2 V}{\partial y_n^2} = - \frac{\partial^2 V}{\partial z_n^2}$$

from Laplace's equation, and

$$W_Q = \frac{e}{4} Q \frac{\partial^2 V}{\partial z_n^2} \quad (5-32)$$

The potential  $V$  is produced by electrons which are in rapid motion, so rapid that the nuclear axis  $z_n$  may be considered stationary during the time that the electrons traverse their entire orbits, or take up all possible positions. Hence, (5-31) may be averaged over all possible electron positions

$$W_Q = \frac{e}{6} Q \left[ \frac{\partial^2 V}{\partial z_n^2} - \frac{1}{2} \left( \frac{\partial^2 V}{\partial x_n^2} + \frac{\partial^2 V}{\partial y_n^2} \right) \right]_{av} \quad (5-33)$$

or, using Laplace's equation again

$$W_Q = \frac{e}{4} Q \left( \frac{\partial^2 V}{\partial z_n^2} \right)_{av} \quad (5-34)$$

If the average electron charge density is spherical, then

$$\frac{\partial^2 V}{\partial x_n^2} = \frac{\partial^2 V}{\partial y_n^2} = \frac{\partial^2 V}{\partial z_n^2} \quad \text{and} \quad W_Q = 0$$

Since only  $s$  electrons, which have spherically symmetric distributions, have large probabilities of being found within the nucleus, it is customary to set

$$W_Q = \frac{e}{4} Q \left( \frac{\partial^2 V'}{\partial z_n^2} \right)_{av} \quad (5-35)$$

where  $V'$  is the potential due only to the electronic distribution outside a small sphere surrounding the nucleus. This gives a small error, because  $p$  or  $d$  electrons, which are not spherically distributed, have a finite, though small, probability of being inside the nucleus. The density of a nonspherically distributed  $p$  electron must, however, be zero at the center of the nucleus, and its average density within the

nucleus is given in order of magnitude by  $e(r^2/r_e^5)$ , where  $r$  is the distance from the center of the nucleus and  $r_e$  is the radius of the electron orbit. Hence from Poisson's equation  $(\partial^2 V/\partial x_n^2)$  or  $(\partial^2 V/\partial y_n^2)$  due to this  $p$  electron cannot be much greater than  $e(r_n^2/r_e^5)$ . The neglected contribution to the energy is therefore of the order

$$eQ \frac{er_n^2}{r_e^5} \approx \frac{e^2 r_n^4}{r_e^5}$$

which is of the size of the hexadecapole energy discussed above and usually unobservably small. We shall henceforth define the quadrupole energy without this small contribution as

$$\frac{eQ}{4} \left( \frac{\partial^2 V'}{\partial z_n^2} \right)_{av}$$

or, omitting the prime,

$$\frac{eQ}{4} \left( \frac{\partial^2 V}{\partial z_n^2} \right)_{av}$$

We turn now to an examination of the gradient of the electric field,  $(\partial^2 V/\partial z_n^2)_{av}$ , along the nuclear axis produced by the electrons. About an axis parallel to the electronic angular momentum,  $J(h/2\pi)$  or  $J$ , the average electric field is cylindrically symmetric, and the dyadic or tensor  $(-\nabla \mathbf{E})_{av}$  is hence diagonal with components

$$\left( \frac{\partial^2 V}{\partial x_1^2} \right)_{av} = \left( \frac{\partial^2 V}{\partial y_1^2} \right)_{av} = \left( -\frac{1}{2} \frac{\partial^2 V}{\partial z_1^2} \right)_{av}$$

Here  $z_1$  is along the axis of electronic angular momentum. These quantities, which are elements of a tensor, can easily be transformed to the nuclear coordinate system. If  $\theta$  is the angle between  $I$  and  $J$  or  $z_n$  and  $z_1$ , and if  $x_1$  and  $x_n$  are chosen parallel to each other,

$$\begin{aligned} \left( \frac{\partial^2 V}{\partial z_n^2} \right)_{av} &= \sin^2 \theta \left( \frac{\partial^2 V}{\partial y_1^2} \right)_{av} + \cos^2 \theta \left( \frac{\partial^2 V}{\partial z_1^2} \right)_{av} \\ &= \frac{3 \cos^2 \theta - 1}{2} \left( \frac{\partial^2 V}{\partial z_1^2} \right)_{av} \end{aligned} \quad (5-36)$$

defining  $(\partial^2 V/\partial z_1^2)_{av} \equiv q_J$ , the quadrupole energy becomes

$$W_Q = \frac{eq_J Q}{4} \frac{3 \cos^2 \theta - 1}{2} \quad (5-37)$$

Expression (5-37) is the correct classical expression for quadrupole energy, but since the quantum numbers  $I$  and  $J$  are usually small, only a quantum-mechanical derivation, first given by Casimir [70], can be relied on for an accurate expression. To treat the energy quantum-mechanically, the Hamiltonian may be taken from Eq. (5-27) as

$$H = -\frac{1}{6} \mathbf{Q} : \nabla \mathbf{E}$$



$\mathcal{Q}$  and  $\nabla\mathbf{E}$  can be replaced by operators having known eigenvalues for the usual nuclear and electronic wave functions by the following method. The operator  $\frac{3}{2}(\mathbf{II} + \tilde{\mathbf{II}} - I^2\mathbf{I})$  has the same angular dependence with respect to nuclear orientation as  $\mathcal{Q}$ , which is proportional to  $3\mathbf{r}\mathbf{r} - r^2\mathbf{I}$ . Hence its matrix elements between states of various orientations must be identical with  $Q$  except for a proportionality constant.\*

$$(Im_I|\mathcal{Q}|Im_I) = \text{const} [Im_I|\frac{3}{2}(\mathbf{II} + \tilde{\mathbf{II}}) - I^2\mathbf{I}|Im_I] \quad (5-38)$$

where  $I, m_I$  are quantum numbers for the nuclear spin and the component of the nuclear spin in a direction  $z$  fixed in space. The symmetrized expression  $\frac{3}{2}(\mathbf{II} + \tilde{\mathbf{II}})$ , where  $\tilde{\mathbf{II}}$  indicates the transpose of  $\mathbf{II}$ , is used because  $\mathcal{Q}$  is a symmetric operator. To evaluate the proportionality constant, consider the  $zz$  component for the state  $m_I = I$

$$\begin{aligned} (II|Q_{zz}|II) &= \text{const} (II|3I_z^2 - I^2|II) \\ &= \text{const} [3I^2 - I(I+1)] \end{aligned} \quad (5-39)$$

from the known expectation values for  $I_z^2$  and  $I^2$ . The quantity

$$(II|Q_{zz}|II)$$

corresponds at least approximately to the classical quadrupole moment  $eQ$ , and will be so defined. Hence  $eQ = \text{const} I(2I-1)$ , or

$$Q_{op} = \frac{eQ}{I(2I-1)} [\frac{3}{2}(\mathbf{II} + \tilde{\mathbf{II}}) - I^2\mathbf{I}] \quad (5-40)$$

Similarly, it can be shown that

$$(\nabla\mathbf{E})_{op} = \frac{q_J}{J(2J-1)} [\frac{3}{2}(\mathbf{JJ} + \tilde{\mathbf{JJ}}) - J^2\mathbf{I}] \quad (5-41)$$

where  $q_J = \left( JJ \left| \frac{\partial^2 V}{\partial z^2} \right| JJ \right)$ . Expression (5-41) applies only to the common case where  $J$  is a "good" quantum number.

Since the electronic potential at the nucleus due to charge  $e$  is

$$\frac{e}{r} = \frac{e}{\sqrt{x^2 + y^2 + z^2}}$$

where  $r$  is the distance from nucleus to charge,

$$\frac{\partial^2 V}{\partial z^2} = e \frac{3z^2 - r^2}{r^5} = e \frac{3 \cos^2 \theta - 1}{r^3}$$

where  $\theta$  is the angle between the  $z$  axis fixed in space and the radius vector  $\mathbf{r}$ . This gives

$$q_J = \int \rho_{JJ} \frac{3 \cos^2 \theta - 1}{r^3} d\tau = \left( \frac{\partial^2 V}{\partial z^2} \right)_{av} \quad (5-42)$$

\* For a more complete discussion, see [969a], p. 16.

where  $\rho_{JJ}$  indicates the electron charge density for a state  $m_J = J$ . If only one electron of wave function  $\psi$  is included,

$$q_J = e \int \psi_{JJ}^* \frac{3 \cos^2 \theta - 1}{r^3} \psi_{JJ} d\tau \quad (5-43)$$

The operator for the quadrupole energy is  $W_{op} = -\frac{1}{6}Q_{op}:(\nabla E)_{op}$ . In case  $J$  is a constant or "good" quantum number, this becomes from (5-40) and (5-41) and use of the commutation rules for the components of angular momenta

$$\frac{1}{2} \frac{eq_J Q}{I(2I-1)J(2J-1)} [3(\mathbf{I} \cdot \mathbf{J})^2 + \frac{3}{2}(\mathbf{I} \cdot \mathbf{J}) - I^2 J^2] \quad (5-44)$$

If terms off diagonal in  $J$  must be considered, the basic form of  $W_{op}$  above must be used. It is easily shown that, if  $I$  and  $J$  are allowed to be very large, (5-44) becomes equivalent to the classical expression (5-37), since  $\mathbf{I} \cdot \mathbf{J}$  becomes  $IJ \cos \theta$ .

The total angular momentum of the system in units  $h/2\pi$  may be written  $\mathbf{F} = \mathbf{I} + \mathbf{J}$  and is of course constant, as is its projection

$$m_F = m_I + m_J$$

on the fixed axis. A representation  $F, m_F$  is hence appropriate, and in this representation  $I^2$ ,  $J^2$ , and  $\mathbf{I} \cdot \mathbf{J}$  are diagonal so that the expectation values of (5-44) can be easily determined. The diagonal elements for these operators are  $I(I+1)$ ,  $J(J+1)$ , and  $C/2$ , respectively, where

$$C = F(F+1) - I(I+1) - J(J+1)$$

Hence

$$W_Q = \frac{1}{2} \frac{eq_J Q}{I(2I-1)J(2J-1)} [\frac{3}{4}C(C+1) - I(I+1)J(J+1)] \quad (5-45)$$

From expression (5-45) hyperfine splitting of energy levels due to nuclear quadrupole effects may be calculated. The magnitude of the quadrupole effects determined by the quadrupole coupling constant  $eqQ$ , which involves both the nuclear quadrupole moment  $Q$ , and  $q_J$ , the second derivative of the potential along the axis of electronic angular momentum. This coupling constant may vary from zero to a few tenths of a wave number, or thousands of megacycles, and of course can be either positive or negative. Evaluation of the quantity  $q_J$  will be discussed at some length in Chap. 9. If  $q_J$  is known, then determination of the quadrupole coupling constant allows a determination of the nuclear constant  $Q$ .

*Nuclear Polarizability.* Another type of electrostatic interaction is an electric polarization of the nucleus. The strong electrostatic fields due to atomic electrons induce a small electric dipole moment on the nucleus which slightly increases the force of attraction between electron and

nucleus, thus lowering the electronic energy levels by an amount which depends on the nuclear polarizability and the square of the electric field strength.

The nuclear polarizability  $\alpha_z$  along the spin axis is not necessarily the same as its polarizability  $\alpha_x$  perpendicular to this axis. Hence the energy depends on the orientation of the spin with respect to the electric field. Since the polarizability is a symmetric tensor just as is the quadrupole moment, it is not difficult to show that the energy of polarization has the same dependence on nuclear orientation as that due to a quadrupole moment. Gunther-Mohr, Geschwind, and Townes [583] have given the variation of energy of polarization with angle as

$$W_A = \frac{e}{3} \frac{(\alpha_z - \alpha_x)p_J}{I(2I - 1)J(2J - 1)} [\frac{3}{4}C(C + 1) - I(I + 1)J(J + 1)] \quad (5-46)$$

This expression is very similar to the energy (5-45) due to a quadrupole moment. Here  $p_J$  corresponds to  $q_J$ , and is defined in analogy with (5-42) as

$$p_J = \int \rho_{JJ} \frac{3 \cos^2 \theta - 1}{r^4} d\tau = \frac{2}{e} (E_z^2 - E_x^2)_{av} \quad (5-47)$$

The coupling constant  $ep_J(\alpha_z - \alpha_x)$  is equivalent to  $\frac{3}{2}eq_JQ$ , and in many cases these two are experimentally indistinguishable. The difference  $\alpha_z - \alpha_x$  in classical polarizabilities can be expressed quantum-mechanically as

$$\alpha_z - \alpha_x = \frac{2I(I + 1)}{2I - 1} \sum_n \frac{|\mu_{0n}|_{M=I}^2 - |\mu_{0n}|_{M=I-1}^2}{W_n - W_0} \quad (5-48)$$

where  $|\mu_{0n}|$  is the  $z$  component of the electric dipole matrix element between the ground state of energy  $W_0$  and an excited state of energy  $W_n$ . Subscripts  $M = I$  and  $M = I - 1$  indicate that the matrix elements are states with the projection  $M$  of  $I$  on the  $z$  direction equal to  $I$  and  $I - 1$ , respectively.

If the nuclear matrix elements and energy levels were known, the polarizabilities could be easily calculated. However, generally only rough magnitudes for these quantities are known.  $|\mu_{0n}|$  may be taken approximately equal to one protonic charge times one nuclear radius, and  $W_n - W_0$  as 1 Mev to roughly evaluate  $\alpha_z - \alpha_x$ . The quantity  $\alpha_z - \alpha_x$  may also be taken as approximately equal to the nuclear volume. From such estimates and evaluation of  $p$  from Hartree wave functions, it may be shown that the anisotropic polarization effects are usually about 1 per cent of the nuclear quadrupole effects, hence generally not larger than a few megacycles. They can be experimentally distinguished from nuclear quadrupole effects only because they depend in a different way on the electron-nuclear distance  $r$ . Thus the relative size of quadrupole coupling and polarization energy will be different in different electronic



states. If precision measurements of hyperfine-structure splittings could be made in several electronic states of an atom with two isotopes, the ratio of the splittings for the two isotopes would vary from state to state. Because it is not usually possible to measure precisely the hyperfine structure of excited states, this method is not very practical.

However, in different types of molecules the electronic configuration about a given atom may be quite different. Then if nuclear polarization is appreciable the apparent quadrupole coupling ratio between two isotopes would depend on the molecule in which it is measured. Certain variations in the ratios of quadrupole moments for  $\text{Cl}^{35}$  and  $\text{Cl}^{37}$  have been observed but cannot clearly be attributed to nuclear polarizability ([575], [760]).

*Magnetic Hyperfine Structure.* Another type of hyperfine structure which depends on the nuclear orientation is connected with magnetic interactions between the nucleus and atomic electrons. If the structure of the nucleus and the possibility of having circulating charges within the nucleus is considered, it is not surprising that this magnetic hyperfine structure shows that a magnetic dipole moment  $\mu$  must be attributed to the nucleus. Each possible orientation of the nuclear spin has a slightly different energy due to interaction between the nuclear magnetic moment and the magnetic field at the nucleus produced by the spins and orbital motions of surrounding electrons.

The electrons precess about their total angular momentum  $\mathbf{J}$  so that the currents and magnetic fields must on the average be cylindrically symmetric about the direction of  $\mathbf{J}$ , and hence the magnetic field they produce at the nucleus is parallel to  $\mathbf{J}$ . For similar reasons the magnetic moment  $\mu_I$  of the nucleus is parallel to its spin  $\mathbf{I}$ . The energy of interaction is  $\mu_I H \cos \theta$  or  $\mu_I \cdot \mathbf{H}$ , which may be written

$$W = a\mathbf{I} \cdot \mathbf{J} \quad (5-49)$$

since  $\mu_I$  is parallel to  $\mathbf{I}$  and  $\mathbf{H}$  to  $\mathbf{J}$ . The quantity  $a$  is a constant for a given electronic state and nucleus, and is known as the interval factor.

The quantity  $\mathbf{I} \cdot \mathbf{J}$  involves the cosine of the angle between  $\mathbf{I}$  and  $\mathbf{J}$ , and can easily be obtained from the vector model [cf. Eq. (5-12)], so that

$$W = \frac{a}{2} [F(F + 1) - J(J + 1) - I(I + 1)] \quad (5-50)$$

where  $F$  is the magnitude of the vector  $\mathbf{F} = \mathbf{I} + \mathbf{J}$ .  $F$  may take on the values  $I + J, I + J - 1, \dots, |I - J|$ . The total number of different values of  $F$  is  $2I + 1$  if  $I < J$ , or otherwise  $2J + 1$ .

If the angular momenta of a number of electrons add up vectorially to a resultant angular momentum of zero, as in the case of a closed shell of electrons, then the average magnetic field at the nucleus is zero. Hence in evaluating the constant  $a$ , it is necessary to take into account

only the unfilled shell of electrons, which in many common cases may consist of only one electron, or a closed shell minus one electron. Although a nonrelativistic treatment of the magnetic field  $H$  at the nucleus gives a good approximation for hyperfine structure produced by electrons with orbital angular momentum, for  $s$  electrons relativistic theory (summarized in [67]) is necessary. Hyperfine structure is particularly important and large for  $s$  electrons, since they penetrate most closely to the nucleus.

For non- $s$  electrons (*i.e.*, with  $l > 0$ ) in a hydrogenic atom,

$$a = \frac{2\mu_I\mu_o}{I} \left( \frac{1}{r^3} \right)_{av} \frac{l(l+1)}{j(j+1)} = \frac{g(I)}{1836} \frac{e^2\hbar^2}{8\pi^2 m^2 c^2} \left( \frac{1}{r^3} \right)_{av} \frac{l(l+1)}{j(j+1)} \quad (5-51)$$

where  $g(I)$  is the "nuclear  $g$  factor," *i.e.*, the ratio of the nuclear magnetic moment in nuclear magnetons to its angular momentum in units of  $\hbar/2\pi$ . One nuclear magneton  $= \hbar e_P/4\pi M_P c$ , where  $M_P$  is the mass of the proton and  $e_P$  its charge. Since  $M_P$  is 1836 times the mass of the electron, the nuclear magneton is 1836 times smaller than the Bohr magneton.

Substituting the quantum-mechanical value of  $\left( \frac{1}{r^3} \right)_{av}$  [Eq. 5-12)]

$$\begin{aligned} a &= \frac{g(I)}{1836} \frac{R\alpha^2 Z^3}{n^3(l + \frac{1}{2})(l+1)j(j+1)} \\ &= \frac{g(I)}{1836} \frac{\Delta\nu l(l+1)}{Z(l + \frac{1}{2})j(j+1)} \end{aligned} \quad (5-52)$$

where  $\Delta\nu$  is the fine-structure doublet splitting given by Eq. (5-13c).

Expression (5-52) follows either from a nonrelativistic calculation which treats the electrons as point particles with electric charge and a magnetic dipole moment, or from a semirelativistic calculation which neglects the electron's binding energy in comparison with its rest mass. A more exact relativistic treatment [19], [28] gives

$$a = \frac{g(I)}{1836} \frac{\Delta\nu l(l+1)}{Z(l + \frac{1}{2})j(j+1)} \frac{\kappa}{\lambda} \quad (5-53)$$

$$\text{where } \kappa = \frac{4j(j + \frac{1}{2})(j+1)}{(4\rho^2 - 1)\rho}$$

$$\rho = \sqrt{(j + \frac{1}{2})^2 - (\alpha Z_i)^2}$$

$$\lambda = \left[ \frac{2l(l+1)}{(\alpha Z_i)^2} \right] \{ [(l+1)^2 - (\alpha Z_i)^2]^{\frac{1}{2}} - 1 - [l^2 - (\alpha Z_i)^2]^{\frac{1}{2}} \}$$

The values of  $\lambda$  and  $\kappa$  are tabulated by Goudsmit [41].

Since  $\rho$  depends on  $j$ ,  $\kappa$  is quite different for  $p_{\frac{1}{2}}$  and  $p_{\frac{3}{2}}$  states. Thus the relativistic correction makes the constant larger for a  $p_{\frac{1}{2}}$  electron than for a  $p_{\frac{3}{2}}$  electron. This is because, in a relativistic treatment, spin and orbital angular momentum are not sharply separated. Thus a  $p_{\frac{1}{2}}$  electron has some of the character of an  $s_{\frac{1}{2}}$  electron (the only other type for which

$j = \frac{1}{2}$ ). We shall see that an  $s_{\frac{1}{2}}$  electron has a large interaction constant. The relativistic theory shows that for an  $s$  electron

$$a = \frac{g(I)}{1836} \frac{e^2 h^2}{3\pi m^2 c^2} \psi^2(0)_\kappa \quad (5-54)$$

$\psi^2(0)$  is the electron density at the nucleus, or the square of the non-relativistic Schrödinger wave function at  $r = 0$ , the center of the nucleus.

For a hydrogenic atom  $\psi^2(0) = Z^3/\pi a_H^3 n^3$ , so that

$$a = \frac{g(I)}{1836} \frac{e^2 h^2 Z^3 \kappa}{3\pi^2 m^2 c^2 a_H^3 n^3} \quad (5-55)$$

$$a = \frac{g(I)}{1836} \frac{8R\alpha^2 Z^3 \kappa}{3n^3} \quad (5-56)$$

It is interesting that this expression for an  $s$  electron is just what would be obtained by more or less arbitrarily using expression (5-52) for  $a$  and setting  $l = 0, j = \frac{1}{2}$ .

Interaction between atomic magnetic fields and a nuclear magnetic octupole moment has recently been detected by Jaccarino, King, Satten, and Stroke [942]. A rough estimate of the magnitude of magnetic octupole interaction would indicate that it is smaller than the dipole interaction by the square of the ratio of nuclear radius to the distance between nucleus and electron [cf. discussion of hexadecapole moment above]. However, the magnetic octupole actually gives effects somewhat larger than such an estimate. In the case of atomic I and In the effects are many kilocycles in size and have been detected by molecular beam techniques [942] [953].

*General Considerations about the Existence of Nuclear Moments.* If a nucleus has spin  $I$ , the pole of highest order which can occur is given by  $2^I$ . Thus, for  $I = 0$ , no dipole or quadrupole moment may exist, but only a monopole (charge). If  $I = \frac{1}{2}$ , a dipole moment may exist, but not a quadrupole moment, which occurs only if  $I \geq 1$ . This limit to the order of poles which may occur can be proved quite generally, but we shall only attempt an indication of why it occurs. In an external field, a nucleus of spin  $I$  can have  $2I + 1$  different orientations or states and hence  $2I + 1$  different energies. In order to specify these energies completely, only  $2I + 1$  different constants of the nucleus need be given. Thus, if  $I = 0$ , there is no need for more than one constant, the monopole strength or electric charge (no magnetic "charge" exists). If  $I = \frac{1}{2}$ , two states occur, and one need specify only the monopole and dipole strength. When  $I \geq 1$ , a quadrupole moment is needed, etc. Additional discussion of this limit can be found in [969a].

Poles of various orders alternate between electric and magnetic type for reasons of symmetry. Thus, as shown above, electric monopoles and quadrupoles exist, but ordinarily electric dipoles do not occur. However, magnetic dipoles and octupoles are permitted.



**5-8. Penetrating Orbits.** If the state of an electron is not well approximated by a hydrogenlike wave function, as in the cases of valence electrons which penetrate a closed shell of electrons around the nucleus, an exact expression for the interval factor  $a$  is very difficult to calculate. However, on the basis of some approximate models, the following expressions for  $a$  may be obtained for these cases.

For a non- $s$  electron [41]:

$$a = \frac{g(I)}{1836} \frac{\Delta\nu}{Z_i} \frac{l(l+1)\kappa}{(l+\frac{1}{2})j(j+1)\lambda} \quad (5-57)$$

and for an  $s$  electron [40]

$$a = \frac{g(I)}{1836} \frac{8R\alpha^2 Z_i Z_0^2}{3n^{*3}} \kappa \left( 1 - \frac{d\sigma}{dn} \right) \quad (5-58)$$

where  $n^*$  is the effective principal quantum number and  $\sigma = n - n^*$  is the quantum defect. If the energy levels of the atom satisfy a Rydberg-Ritz equation,

$$T = \frac{RZ_0^2}{(n - \alpha - \beta T)^2} \quad (5-59)$$

where  $\alpha$  and  $\beta$  are constants,  $T$  is the term value, and  $R$  is the Rydberg constant, then [359]

$$\frac{d\sigma}{dn} = \frac{\beta}{\beta - n^*/2T} \quad (5-60)$$

In the above equations, for  $s$  electrons  $Z_i = Z$ , the nuclear charge. The equation then works well for elements of medium weight but gives values of  $a$  which may be 10 to 20 per cent high for very light or very heavy elements. For heavy elements an additional correction for the finite radius of the nucleus should be made, and with this addition the formula is quite accurate [359].

For  $p$  electrons, it is usual to put  $Z_i = Z - 4$  in place of  $Z$  in (5-52). This works well in the equation for  $\Delta\nu$ , the fine-structure splitting, but is not so good for hyperfine structure where the average of a different power of  $Z$  is involved (cf. [364]). If the nuclear moment and so  $g(I)$  is known, it is also possible to use the observed hyperfine-structure interval factor,  $a$ , to evaluate  $(1/r^3)_{av}$  [67]. For a non- $s$  electron, from Eq. (5-53), with relativistic corrections,

$$\left( \frac{1}{r^3} \right)_{av} = \frac{1836}{g(I)} \frac{8\pi^2 m^2 c^2}{e^2 h^2} \frac{j(j+1)\lambda}{l(l+1)} \frac{1}{\kappa} a \quad (5-61)$$

This value of  $(1/r^3)_{av}$  may then be used in evaluation of nuclear quadrupole moments from observed quadrupole coupling energies.

**5-9. Zeeman Effects for Atoms.** When an atom is placed in a magnetic field, the energy levels undergo a splitting known as the Zeeman

effect (*cf.* Chap. 11 for Zeeman effects on molecules). It is convenient to distinguish three cases: (a) a weak magnetic field, where this splitting is considerably less than the hyperfine structure, (b) a strong field, where the splitting is much larger than the hyperfine structure, and (c) intermediate fields.

In the weak-field case, the nuclear spin  $\mathbf{I}$  remains coupled to the electronic angular momentum  $\mathbf{J}$ , and their resultant  $\mathbf{F}$  has  $2F + 1$  possible values of the component,  $M_F$ , along the field direction. Then the energy due to magnetic hyperfine structure and interactions with the magnetic field is [*cf.* (11-13)]

$$W(F, M_F) = \frac{a}{2} [F(F + 1) - I(I + 1) - J(J + 1)] \\ - \left\{ \frac{\mu_I}{I} [I(I + 1) + F(F + 1) - J(J + 1)] \right. \\ \left. + \frac{\mu_J}{J} [F(F + 1) + J(J + 1) - I(I + 1)] \right\} \frac{M_F H}{2F(F + 1)} \quad (5-62)$$

where  $a$  is a constant which gives the strength of the magnetic hyperfine structure,  $\mu$  is the nuclear magnetic moment,  $\mu_J$  the atomic (electron spin and orbital combined) magnetic moment, and  $H$  the applied magnetic field.

In a very strong field,  $I$  and  $J$  interact more strongly with the field than with each other. Then

$$W(I, J, M_I, M_J) = a M_I M_J - \frac{\mu_J}{J} H M_J - \frac{\mu_I}{I} H M_I \quad (5-63)$$

where  $M_I$  and  $M_J$  are the quantum numbers for the projection of  $\mathbf{I}$  and  $\mathbf{J}$ , respectively, on  $H$ . The intermediate field case is generally more complicated. For the important special case of  $J = \frac{1}{2}$  (*e.g.*, hydrogen, the alkalis, silver, gold, indium, thallium) the energies are given by Breit and Rabi [19a]

$$W(F, M_F) = - \frac{\Delta W}{2(2I + 1)} - \frac{\mu_I}{I} H M_F \pm \frac{\Delta W}{2} \sqrt{1 + \frac{4M_F}{2I + 1} x + x^2} \quad (5-64)$$

where  $\Delta W \equiv (a/2)(2I + 1) \equiv h \Delta\nu$ , and  $\Delta\nu$  is the zero-field hyperfine structure splitting

$$x = \frac{(-\mu_J/J + \mu_I/I) H}{\Delta W}$$

Zeeman effects in atoms are often relatively large (several megacycles per gauss). It is then possible to measure transitions between Zeeman components of several hyperfine levels by varying the applied magnetic field until the transitions coincide with a given microwave frequency.

When a resonant cavity spectrograph is employed, this possibility is especially useful.

Beringer and Heald [898] obtained an accurate measurement of the Zeeman splitting in atomic hydrogen, using a frequency near 9500 Mc and a variable magnetic field. The hydrogen was dissociated by a discharge just before passing through the cavity resonator. From their measurements, and the molecular-beam measurement of the zero field hyperfine structure splitting [737a], the electron-spin magnetic moment  $g$  factor is found to be  $g_s = -2(1.001148 \pm 0.000006)$ . The precision of this value was not limited by the microwave spectrum, but by the absolute calibration of magnetic fields in terms of proton resonance frequencies. A similar technique has been applied to the atoms O [739a], N [932a], and P [913b].

**5-10. Microwave Studies of Atomic Hyperfine Structure.** Since the separations between hyperfine-structure levels often lie in the microwave range, it is possible to use microwaves to induce transitions between these levels. The electric dipole matrix element between these states vanishes because they belong to the same electronic configuration. However, the magnetic dipole matrix element is not zero and it permits the transition to take place. The peak intensity for a transition in which  $\Delta F = \pm 1$  is then given by Eq. (1-50), where in this case  $\mu_{ij}$  is the appropriate matrix element for the magnetic dipole moment of the atom.

The transitions are most likely to be found in the microwave region for an atom in a  $^2S_{1/2}$  ground state, because the largest number of atoms would occur in the ground state, and a  $^2S_{1/2}$  state has a relatively large hyperfine structure. In that case, the matrix elements are ([56], pp. 64-72), for  $F = I + \frac{1}{2} \leftarrow F = I - \frac{1}{2}$ ,

$$|\mu_{ij}|^2 = \frac{[(I + \frac{1}{2})^2 - m_F^2]}{(2I + 1)^2} \mu_0^2 \quad \text{when } \Delta m_F = 0 \quad (5-65)$$

$$|\mu_{ij}|^2 = \frac{(I + \frac{1}{2} \mp m_F)(I - \frac{1}{2} \mp m_F)}{2(2I + 1)^2} \mu_0^2 \quad \text{when } \Delta m_F = \pm 1 \quad (5-66)$$

where  $m_F$  = projection of the total angular momentum,  $F$ , on a fixed direction

$\mu_0$  = the Bohr magneton,  $he/4\pi mc$ .

The transitions with  $\Delta m_F = 0$  are polarized so that the electric vector is perpendicular to the fixed direction and those with  $\Delta m_F = \pm 1$  are polarized with the electric vector parallel to the fixed direction.

If the above matrix elements are substituted into (1-50) to obtain the absorption coefficient for each component of the transition ( $\Delta m_F = 0$ ,  $\Delta m_F = +1$ , or  $\Delta m_F = -1$ ), then  $Nf/3$  in this formula must be interpreted as the number of atoms in the ground state of each component. In case the atom is in an external magnetic field, each value of  $m_F$  has a slightly different energy, and the intensity of individual components is



needed. If, however, there is no external magnetic field for one polarization of the incident radiation, then what is wanted is the average of all transitions for which  $\Delta m_F = 0$  or  $\Delta m_F = \pm 1$ . This average, after multiplication by 3 to obtain the sum of the squares of the dipole matrix elements for all three directions of polarization, is

$$|\mu_{ij}|_{\text{av}}^2 = \frac{4I}{2I+1} \mu_0^2 \quad (5-67)$$

Expression (5-67) is the appropriate quantity to insert in the customary way into (1-50) if  $Nf$  is taken to be the fraction of atoms in the state  $F = I - \frac{1}{2}$ .

The hyperfine structure of the  $^2S_{\frac{1}{2}}$  ground state of cesium was investigated by Roberts, Beers, and Hill [405]. In that case, using the notation of Eq. (1-50) and calculating the intensity of the entire transition,

$$Nf = 2.5 \times 10^{14} \text{ atoms/cm}^3 \text{ corresponding to a pressure of } 3 \times 10^{-2} \text{ mm}$$

$$T = 500^\circ\text{K}$$

$$\Delta\nu = 1.5 \times 10^5 \text{ cycles/sec (estimated roughly from kinetic theory)}$$

$$\nu_0 = 9.2 \times 10^9 \text{ cycles/sec}$$

$$I = \frac{7}{2}$$

$$|\mu_{ij}|_{\text{av}}^2 = \frac{7}{16} \mu_0^2$$

so that  $\gamma_{\text{max}} = 3.1 \times 10^{-9} \text{ cm}^{-1}$  for an average component. The cesium was placed in a microwave resonant cavity which was used to control the frequency of a klystron oscillator. The cavity was in a variable magnetic field so that each component could be brought in turn to the resonant frequency of the cavity. As the magnetic field was varied to make a component of the line approach the resonant frequency of the cavity, this resonant frequency was slightly changed by the anomalous dispersion associated with the cesium resonance, and the consequent variation in frequency of the controlled oscillator was detected.

Few other atoms have been investigated by microwave absorption spectroscopy because of the relatively weak absorptions and the difficulty of obtaining many materials in atomic form. However, Shimoda and Nishikawa [642] obtained a measurement of transitions between hyperfine components of  $\text{Na}^{23}$  at 1772 Mc. Hyperfine interactions in H [737a], N [932a], and P [913b] have been obtained from microwave transitions between Zeeman components (see Sec. 5.9). A large number of atoms have been investigated by molecular-beam techniques (see [969a]), which are particularly suited for this purpose.

**5-11. Microwave Spectra from Astronomical Sources.** Microwave radiation due to transitions between the hyperfine components of atomic hydrogen in interstellar space was first detected by Ewen and Purcell [571] and independently discovered by Muller and Oort [621]. This radiation has a wavelength near 21 cm and penetrates the earth's iono-

sphere and gas and dust particles in interstellar space rather readily. The frequency corresponding to the transition between hyperfine components of hydrogen has been measured in the laboratory as 1420.405 Mc [737a]. Near this frequency, hydrogen gas has a large enough absorption coefficient to be opaque for certain directions through our own galaxy, the Milky Way. Hence it also radiates an intensity corresponding to a black body at about 100°K, which is the effective temperature for the hyperfine levels of H in interstellar space.

In interstellar space, hydrogen atoms occur with a density near 1 atom/cm<sup>3</sup>, or a pressure of less than 10<sup>-19</sup> atm. Since a collision between atoms is very rare, occurring only once in a number of years, the dominating source of broadening is the Doppler effect. The various parts of the Milky Way have random velocities as large as about  $\pm 10$  km/sec with respect to each other so that the Doppler effect gives a line-width parameter  $\Delta\nu$  of about  $\frac{\nu}{3 \times 10^4}$ , or 50 kc, for  $\nu = 1420$  Mc.

The total amount of power received by an antenna from the radiation by interstellar hydrogen is approximately  $kT \Delta\nu$ , where  $T$  is the temperature 100°K, and  $\Delta\nu$  the line width of 50 kc. This amounts to slightly less than 10<sup>-16</sup> watt but is enough to give a signal which is a few hundred times background noise in a carefully constructed radiometer of the type described in Chap. 15.

If the temperature of an object is measured by the intensity of radiation at a given frequency, the apparent temperature is given by

$$T = T_o(1 - e^{-\gamma L}) \quad (5-68)$$

where  $T_o$  = temperature of the object

$L$  = thickness of the object

$\gamma$  = absorption coefficient at the frequency of measurement

For an opaque object,  $T = T_o$ . For less opaque material the apparent temperature  $T$  of emission is reduced. It must be at least as large as about 1° for an emission line to be detectable. Temperature changes which are this small correspond to observation of a gas which is almost transparent, that is,  $\gamma L \ll 1$ . In this case the observed temperature is, from (5-65),

$$T \approx T_o \gamma L \quad (5-69)$$

Now the absorption coefficient  $\gamma$  for a gas is given by Eq. (1-50). For the ground atomic state of hydrogen,  $f = 1$  and  $\mu$  is approximately one Bohr magneton, since the transition involves a magnetic rather than an electric dipole moment. Inserting values of the constants, expression (5-66) becomes

$$T \approx 5 \times 10^{-19} \frac{NL}{\lambda} \quad (5-70)$$

Here  $\nu/\Delta\nu = 3 \times 10^4$  due to Doppler effect has been used and  $\lambda$  is the wavelength. For a temperature change as large as  $1^\circ\text{C}$ , the number of molecules  $NL$  which must be in the path of observation is

$$NL = 2 \times 10^{18}\lambda \quad (5-71)$$

Since the longest dimension of the Milky Way is approximately  $10^{23}$  cm, an interstellar gas must have a density as high as about  $N = 2 \times 10^{-5}\lambda$  to be detected by microwave emission if the transition involved is due to a magnetic dipole moment. Since hydrogen has a density of approximately 1 atom/cm<sup>3</sup> in interstellar space, its radiation is clearly observable. In fact, in this case  $\gamma L$  is larger than unity in most directions through our galaxy, and the galaxy is opaque at the center of the hydrogen line. On the other hand, deuterium would be very difficult to observe, since it probably has a density of only  $10^{-3}$  or  $10^{-4}$  atom/cm<sup>3</sup>, and the transition between hyperfine levels falls at longer wavelengths.

If the transition is due to an electric dipole moment, then the dipole matrix element is approximately 1 debye, which is 100 times larger than the matrix element due to a magnetic dipole transition, and the minimum observable density of interstellar gas would be approximately

$$N = 2 \times 10^{-9}\lambda$$

A few molecules with dipole moments, such as the radical OH, are thought to have densities as high as  $N = 10^{-6}$ , and hence their spectra may possibly be observed.

Transitions between several other hyperfine levels in atoms may eventually be observed from astronomical objects. The hyperfine structure of  $\text{N}^{14}$  in several states of ionization may be sufficiently intense for observation since the density of nitrogen in interstellar gas is approximately  $10^{-3}$  atom/cm<sup>3</sup>. However, frequencies for the hyperfine structure of  $\text{N}^{14}$  are known experimentally only for the ground state of the neutral atom. The hyperfine structure of  $\text{N}^{14}$  in high states of ionization may possibly also be observed in the sun's atmosphere.

The microwave line emitted by interstellar hydrogen has been particularly valuable for astronomy. For example, its observation has shown that, in certain directions through our galaxy, there are several strips of gas each moving systematically at velocities appropriate to the successive arms of a rotating spiral nebula. This seems to give the clearest evidence so far available that our galaxy is a spiral nebula.



## CHAPTER 6

# QUADRUPOLE HYPERFINE STRUCTURE IN MOLECULES

**6-1. Introduction.** In most atoms, the predominant hyperfine structure is due to interaction between a nuclear magnetic moment and magnetic fields of the atomic electrons. Effects of a nuclear quadrupole moment are smaller and give small deviations from the expected magnetic hyperfine intervals. However, for most molecules in the ground state, the magnetic fields due to various electrons almost completely cancel, giving zero or only very small magnetic fields at the nucleus. Electric quadrupole effects in molecules may still be sizable, however, and they become the dominating source of hyperfine structure.

The cancellation of magnetic fields in molecules due to electronic motions is simply because the electrons are paired; *i.e.*, for each electron with an angular momentum and hence magnetic field, there is another electron in a similar state but with oppositely directed angular momentum. The net electronic angular momentum for the electrons in the ground state of most molecules is indicated by the spectroscopic term  $^1\Sigma_0$ , which signifies that the net electronic spin and orbital angular momentum are both zero. It is not surprising that electronic momenta are paired off in a molecule if the nature of molecular bonds is considered. Generally an atom forms chemical bonds with each of its unpaired electrons, each one pairing with an electron from another atom in the molecule to give a net zero angular momentum. For the rare molecules such as NO, ClO<sub>2</sub> and NO<sub>2</sub> having an odd number of electrons, a complete pairing of electron spins is impossible. These molecules are hence paramagnetic and have large magnetic hyperfine structures. There are in addition a few cases of molecules having an even number of electrons in which the chemical bonds are unusual and the electron spins are not paired. The most notable example of this case is O<sub>2</sub>, which is in a  $^3\Sigma_1$  state, having two parallel electron spins.

For the overwhelming majority of molecules, however, magnetic hyperfine effects are extremely small, and it is electric quadrupole hyperfine structure that is evident when molecular spectra are examined with high resolution.

The discussion given in the preceding chapter of interaction between a nuclear electric quadrupole moment and a surrounding charge distribution is of course as valid for a molecular system as for an atomic system

since the charge distribution assumed is a general one. Expression (5-45), which is

$$W_q = \frac{1}{2} \frac{eq_J Q}{I(2I-1)J(2J-1)} [\frac{3}{4}C(C+1) - I(I+1)J(J+1)] \quad (6-1)$$

may be applied to the molecular case if  $J$  is taken as the angular momentum of the molecule, and  $q_J$ , given by (5-42), is

$$q_J = \int \rho_{JJ} \frac{(3 \cos^2 \theta - 1)}{r^3} d\tau = \left( \frac{\partial^2 V}{\partial z_J^2} \right)_{av}$$

where the charge density  $\rho$  applies to all charges in the molecule outside of a small sphere around the nucleus considered. It may be seen that the integral is just the average value of the second derivative of the potential at the nucleus due to all extranuclear charges  $\rho_{JJ}$ , taken along the direction of  $J$ , which is fixed in space and labeled  $z_J$ . The only problem peculiar to the molecular case is the particular evaluation of  $q_J$ , which will depend not only on the charge distribution in the molecule, but also on an average of the orientation of the molecule with respect to  $J$ . For a molecule of little symmetry, such as an asymmetric top, evaluation of  $q_J$  in terms of the various molecular axes and rotational quantum numbers can be rather tedious. We therefore begin by considering the much simpler and fortunately common case of a linear molecule.

**6-2. Quadrupole Hyperfine Structure in Linear Molecules.** In a linear molecule, the charge distribution is symmetric around the molecular axis, and hence if  $z_m$  indicates the direction of the molecular axis,

$$\frac{\partial^2 V}{\partial x_m^2} = \frac{\partial^2 V}{\partial y_m^2} = -\frac{1}{2} \frac{\partial^2 V}{\partial z_m^2}$$

using Laplace's equation and the equivalence of the  $x$  and  $y$  directions. A transformation of coordinates allows a reexpression of  $q_J$ .

$$\begin{aligned} q_J &= \left( \frac{\partial^2 V}{\partial z_J^2} \right)_{av} = \left( \frac{\partial^2 V}{\partial z_m^2} \cos^2 \theta_{mJ} + \frac{\partial^2 V}{\partial x_m^2} \sin^2 \theta_{mJ} \right)_{av} \\ &= \frac{\partial^2 V}{\partial z_m^2} \left( \frac{3 \cos^2 \theta_{mJ} - 1}{2} \right)_{av} \end{aligned} \quad (6-2)$$

where  $\theta_{mJ}$  is the angle between the molecular axis and  $J$ . The quantity  $\partial^2 V / \partial z_m^2$  is the second derivative of the potential at the nucleus under discussion along the direction of the molecular axis due to all charges outside a small sphere surrounding the nucleus. It is a property of the molecule independent of the rotational state of the molecule, and will be designated as  $q_m$  or simply  $q$  in analogy to  $q_J$  which is a similar quantity referred to the direction of  $J$ , and hence dependent on the rotational state.

In order to evaluate  $[(3 \cos^2 \theta_{mJ} - 1)/2]_{\text{av}}$  we must use the molecular wave functions which have already been given in Chap. 1 as

$$\psi_{J,M=J} = \sqrt{\frac{2J+1}{4\pi(2J)!}} P_J^J(\cos \theta) e^{iJ\phi}$$

then

$$\begin{aligned} \left( \frac{3 \cos^2 \theta_{mJ} - 1}{2} \right)_{\text{av}} &= \frac{2J+1}{4\pi(2J)!} \int_0^\pi \int_0^{2\pi} [P_J^J(\cos \theta)]^2 \frac{(3 \cos^2 \theta - 1)}{2} \sin \theta d\theta d\phi \\ &= \frac{-J}{2J+3} \end{aligned} \quad (6-3)$$

If  $J$  becomes very large, this result approaches the classical expectation that  $[(3 \cos^2 \theta_{mJ} - 1)/2]_{\text{av}} = -\frac{1}{2}$ , since classically the molecular axis should be perpendicular to the angular momentum and  $\cos \theta_{mJ} = 0$ . Hence from (6-1), (6-2), and (6-3), the quadrupole energy is

$$W_Q = - \frac{eq_m Q}{2I(2I-1)(2J-1)(2J+3)} \left[ \frac{3}{4} C(C+1) - I(I+1)J(J+1) \right] \quad (6-4)$$

where  $C = F(F+1) - I(I+1) - J(J+1)$ .  $F$  is the quantum number for the total angular momentum, which takes on the values  $I+J$ ,  $I+J-1$ , . . . ,  $|I-J|$ .

The expression (6-4) gives the quadrupole energy for a single nucleus in a linear molecule in terms of the molecular constant  $q_m$ , the nuclear constant  $Q$ , and angular momentum quantum numbers  $I$ ,  $J$ ,  $F$ . It might be written  $W = -eq_m Q f(I, J, F)$ , where  $eq_m Q$  or simply  $eqQ$  is called the quadrupole coupling constant and  $f(I, J, F)$  might be called Casimir's function since it comes rather directly from theory developed by Casimir. This function is given in Appendix I for all values of  $I$  up to  $\frac{11}{2}$  (excluding 0 and  $\frac{1}{2}$ , for which  $Q$  is necessarily zero) and for values of  $J$  up to 10. It may be noted that, when  $F$  has its maximum or minimum values, corresponding to  $I$  and  $J$  parallel or antiparallel, respectively, Casimir's function is positive, whereas for intermediate values of  $F$ , the function is negative. This behavior corresponds roughly to the classically expected variation of  $3 \cos^2 \theta_{IJ} - 1$ .

From Appendix I and a knowledge of the quadrupole coupling constant  $eqQ$  the hyperfine energy levels can be easily determined. The constant  $eqQ$  may have an extremely wide range of values, but a representative value would be 100 Mc. To predict the hyperfine structure of a molecular transition, we need in addition some information about the selection rules and intensities. Selection rules for hyperfine structure are exactly the same as for fine structure assuming either type of inter-



action is very small compared with the separation between major energy levels. Thus if a microwave tends to change the angular momentum  $J$  of rotation of a molecule without acting on the nuclear spin  $I$ , this is an exact parallel to a light wave changing the orbital momentum  $L$  of electrons in an atom without acting on the electron spins  $S$ . The selection rules of Chap. 5 for fine structure then become for hyperfine structure

$$\Delta J = 0, \pm 1 \quad \Delta F = 0, \pm 1 \quad \Delta I = 0 \quad (6-5)$$

Relative intensities for the different possibilities are given by appropriate substitution of quantum numbers in expression (5-17) and (5-18).

For transitions  $J \leftarrow J - 1$ :

$$\begin{aligned} F \leftarrow F - 1: & \frac{B(J + F + I + 1)(J + F + I)(J + F - I)(J + F - I - 1)}{F} \\ F \leftarrow F: & - \frac{B(J + F + I + 1)(J + F - I)(J - F + 1)(J - F - I - 1)(2F + 1)}{F(F + 1)} \\ F \leftarrow F + 1: & \frac{B(J - F + I)(J - F + I - 1)(J - F - I - 1)(J - F - I - 2)}{F + 1} \end{aligned} \quad (6-6a)$$

For transitions  $J \leftarrow J$ :

$$\begin{aligned} F \leftarrow F - 1: & - \frac{A(J + F + I + 1)(J + F - I)(J - F + I + 1)(J - F - I)}{F} \\ F \leftarrow F: & \frac{A[J(J + 1) + F(F + 1) - I(I + 1)]^2(2F + 1)}{F(F + 1)} \\ F \leftarrow F + 1: & - \frac{A(J + F + I + 2)(J + F - I + 1)(J - F + I)(J - F - I - 1)}{F + 1} \end{aligned} \quad (6-6b)$$

Since the probability of exciting a transition between two states is independent of the direction of the transition, relative intensities for the components of the transition  $J - 1 \leftarrow J$  may be obtained simply by reversing all arrows in the first group of three equations.

Appendix I gives relative intensities of the various possible hyperfine component transitions for low values of  $J$  and  $I$  up to  $\frac{11}{2}$ . Values given in this appendix are simply calculated from the formulas above, with their absolute values adjusted so that the sum of all hyperfine components of a particular  $J$  transition is unity. This is convenient because the sum of the intensities of hyperfine components of a transition should just equal the intensity of the transition if it had not been split.

Only very rarely is the hyperfine structure of rotational lines involving  $J$  greater than 10 of interest, since it is usually not prominent enough to be observed. For such large values of  $J$ , the more intense components of the hyperfine structure are always those for which  $F$  changes in the same way as  $J$  ( $\Delta F = \Delta J$ ), and for these the hyperfine splitting is very small. Relative intensities of these components of a transition involving large  $J$  are approximately proportional to the statistical weights  $2F + 1$  or, therefore, to  $F$ . For each of the weaker components, when  $J$  is larger than 10 the intensity is a small fraction of that of the entire transition. This fraction is given within a factor of about 2 by the following expressions:

When  $J + 1 \leftarrow J$ ,  $F \leftarrow F$ , fraction of intensity  $\approx 1/2J^2$

$J + 1 \leftarrow J$ ,  $F - 1 \leftarrow F$ , fraction of intensity  $\approx 1/10J^4$

$J \leftarrow J$ ,  $F \pm 1 \leftarrow F$ , fraction of intensity  $\approx 1/2J^2$

Changes in quadrupolar energies may be similarly approximated for large  $J$ . For the stronger components of the transition where  $\Delta F = \Delta J$ , the change in quadrupole energy is a small fraction of the quadrupole coupling constant, being in almost all cases smaller in size than  $eqQ/4J^2$ . For the other, very much weaker, components, the change in energy is larger and can be approximated by

$$\Delta W_q(\Delta F = \Delta J \pm 1) = \mp \frac{3[2(F - J) \pm 1]eqQ}{8I(2I - 1)} + \text{terms of order } \frac{eqQ}{2J}$$

The quantities given in Appendix I allow a ready calculation of quadrupole hyperfine structure such as is shown in Fig. 6-1. In this figure the

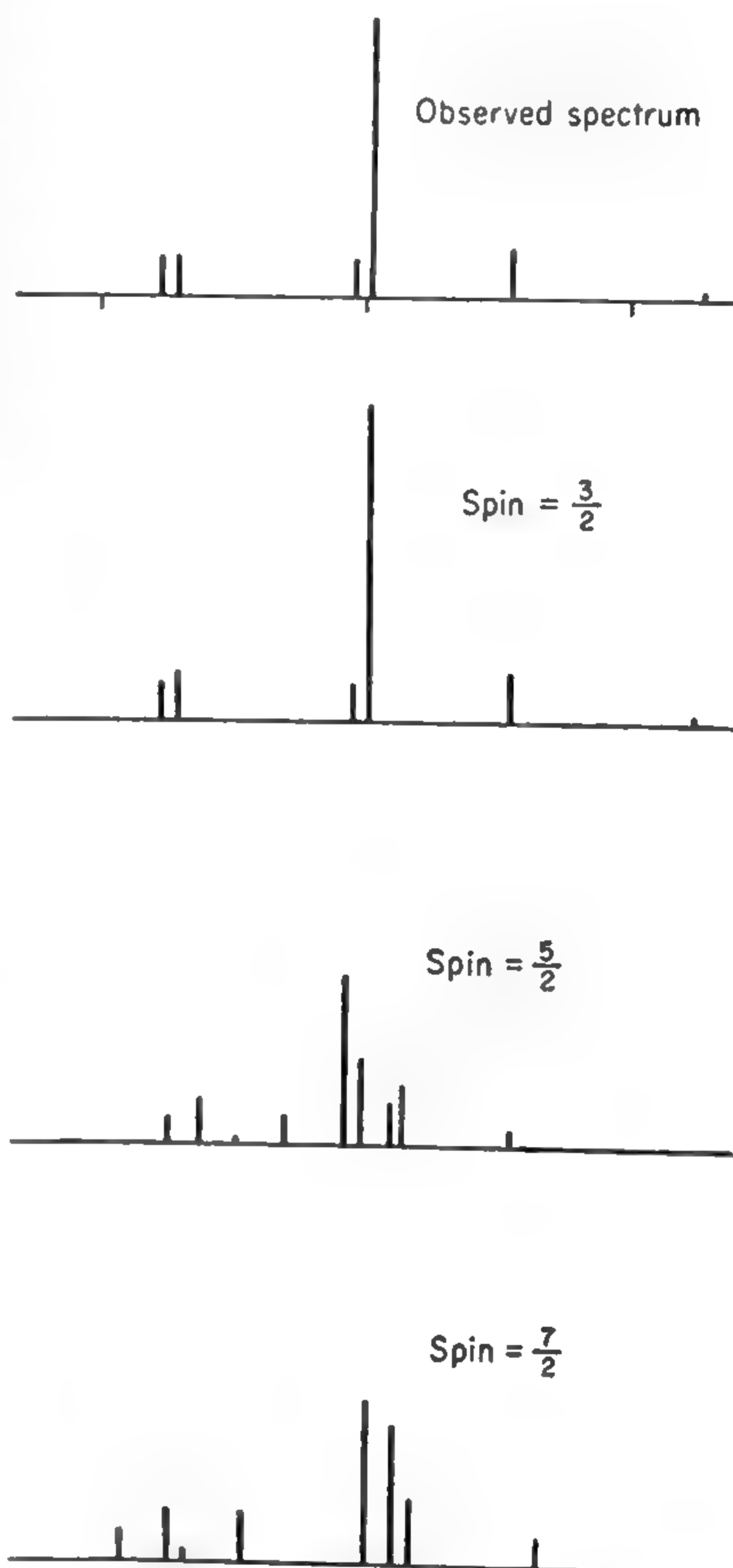


FIG. 6-1. Quadrupole hyperfine structure in the  $J = 2 \leftarrow 1$  transition of  $O^{16}C^{12}S^{33}$  due to  $S^{33}$ , showing the different patterns expected theoretically for various assumed values of the  $S^{33}$  spin. It is clear that the pattern for spin  $\frac{3}{2}$  agrees well with the observed spectrum, and that other values of spin do not agree. For this case  $eqQ = -29.2$  Mc.

observed hyperfine structure in  $\text{O}^{16}\text{C}^{12}\text{S}^{33}$  is compared with theoretically expected patterns assuming various values of the  $\text{S}^{33}$  spin.  $\text{OCS}$  is a linear molecule, and both  $\text{O}^{16}$  and  $\text{C}^{12}$  are known to have zero spins, and so produce no hyperfine structure. The quadrupole coupling constant assumed for  $\text{S}^{33}$  in  $\text{OCS}$  is chosen so that the computed hyperfine patterns will agree as closely as possible with the observed spectrum. It is evident that the observed structure agrees very well with the theory if the  $\text{S}^{33}$  spin is assumed to be  $\frac{3}{2}$ , whereas there is clear disagreement with the other calculated spectra. Thus a comparison of this type allows a determination of the  $\text{S}^{33}$  nuclear spin, its quadrupole coupling in  $\text{OCS}$ , and in addition the values of  $J$  involved in the transition, since both  $J$  and  $I$  determine the exact structure observed.

**6-3. Quadrupole Hyperfine Structure in Symmetric Tops.** For molecules which are not linear, the general theory of quadrupole coupling is unchanged, but the quantity  $q_J$  must be reevaluated. For the case of a nucleus on the axis of a symmetric top, this quantity is still rather simple in form. Because of the symmetry  $q_J$  may again be written, as in (6-2),

$$q_J = \frac{\partial^2 V}{\partial z_m^2} \left( \frac{3 \cos^2 \theta_{mJ} - 1}{2} \right)_{\text{av}}$$

where the direction  $z_m$  is as before along the molecular axis. For a symmetric top  $[(3 \cos^2 \theta_{mJ} - 1)/2]_{\text{av}}$  has a somewhat different form, however.

$$\begin{aligned} \left( \frac{3 \cos^2 \theta_{mJ} - 1}{2} \right)_{\text{av}} &= \int \psi_{J,K,M=J}^* \left( \frac{3 \cos^2 \theta_{mJ} - 1}{2} \right) \psi_{J,K,M=J} d\tau \\ &= \left[ \frac{3K^2}{J(J+1)} - 1 \right] \frac{J}{2J+3} \quad (6-7) \end{aligned}$$

where  $\psi_{J,K,M=J}$  is a symmetric-top wave function such as is given in Chap. 3. For  $J$  and  $K$  large, it can be seen that (6-7) gives the classically expected behavior, for then the cosine of the angle between  $J$  and the molecular axis ( $\cos \theta_{mJ}$ ) is easily shown to be  $K/J$  or  $K/\sqrt{J(J+1)}$  by use of the vector model.

The nuclear quadrupole energy for a nucleus on the axis of a symmetric top is, using (6-1), (6-2), and (6-7),

$$W_Q = \frac{eqQ \left[ 3 \frac{K^2}{J(J+1)} - 1 \right]}{2I(2I-1)(2J-1)(2J+3)} \left[ \frac{3}{4}C(C+1) - I(I+1)J(J+1) \right] \quad (6-8)$$

where  $q$ , or  $q_m$ , is the second derivative of the potential (excluding charges in a small sphere around the nucleus) along the direction of the molecular axis [143], [145]. This expression is identical with that for a linear



molecule except for a factor  $1 - 3K^2/J(J + 1)$ . The linear molecule is of course a special case of the symmetric top ( $K = 0$ ). Appendix I may be used for the quadrupole energy levels of a symmetric top if energy values are multiplied by the factor  $1 - 3K^2/J(J + 1)$ . Relative intensities of hyperfine components, which are also given by Appendix I, apply to this case.

It should be noted that, in deriving (6-8), the electric field was assumed to be symmetric about the molecular axis ( $\partial^2 V / \partial x_m^2 = \partial^2 V / \partial y_m^2$  on the axis). This will be true in all cases for a nucleus on the axis of a symmetric top, since to make the moments of inertia about  $x_m$  and  $y_m$  exactly equal, a symmetric arrangement of atoms is required. However, there may occur very rare cases of "accidentally" nearly symmetric tops for which this condition is not fulfilled, and the quadrupole levels must be described by the somewhat more complex theory developed in the latter part of this chapter for asymmetric molecules rather than by (6-8). If the nucleus is in a symmetric top, but not on the axis, then there is always present the complication of other like nuclei with quadrupole coupling, which will be treated later in this chapter.

The hyperfine structure of a symmetric rotor transition  $J + 1 \leftarrow J$  is usually more complex than that for a linear molecule because such a transition involves a number of different  $K$  values, each with its own hyperfine structure. An example is the structure of the  $J = 2 \leftarrow 1$  transition of  $\text{CH}_3\text{I}$ , shown in Fig. 6-2. Iodine has a spin of  $\frac{5}{2}$  and a rather large quadrupole coupling constant, whereas C and H have spins of 0 and  $\frac{1}{2}$ , respectively, and hence give no quadrupole effects.

**6-4. Second-order Quadrupole Effects.** The quadrupole hyperfine structure has so far been considered small by comparison with the frequency of the rotational transition. The quantity  $[(3 \cos^2 \theta_{mJ} - 1)/2]_{av}$  has been calculated, for example, in (6-3) and (6-7) with so-called first-order perturbation theory, or by using rotational wave functions which are assumed to be unchanged by the existence of quadrupole effects. If the quadrupole coupling is not small compared with the rotational frequencies, however, the molecular rotational wave functions will be modified and the energies for quadrupole effects given above will not be exactly correct.

A strong quadrupole interaction produces some exchange of angular momentum between the nucleus and the molecule; so the state of the rotating molecule can no longer be accurately specified by a fixed angular momentum  $J$ . Allowing for quadrupole interactions which are not small, the state of the molecule can only approximately be described by  $J$ , and the wave functions and quadrupole energy must be calculated from second-order perturbation theory. However, the total angular momentum  $F$  and its projection on a fixed axis  $M_F$  are quantized and cannot be changed by interactions within the molecule.

For a general symmetric top the energy given by second-order perturbation theory is of the form

$$W_Q = (IJKFM_F|H_Q|IJKFM_F) + \sum_{J'K'} \frac{|(IJKFM_F|H_Q|IJ'K'FM_F)|^2}{W_{JK} - W_{J'K'}} \quad (6-9)$$

where  $H_Q$  is the part of the Hamiltonian which represents the quadrupole energy. It is given by  $-\frac{1}{6}\mathbf{Q}:\nabla\mathbf{E}$ , as discussed in Chap. 5. The quantities

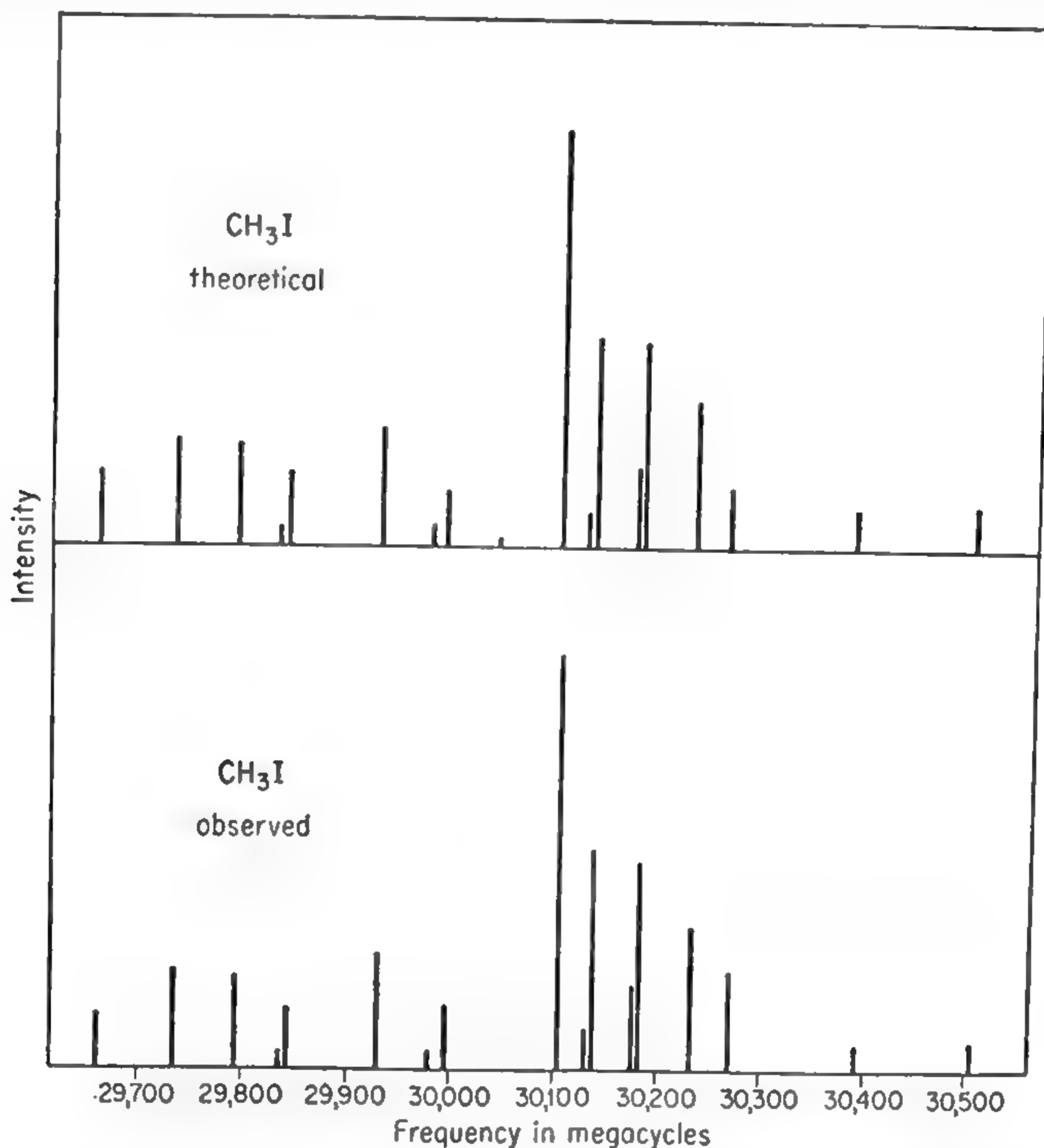


FIG. 6-2. Hyperfine structure in the  $J = 2 \leftarrow 1$  transition of the symmetric rotor  $\text{CH}_3\text{I}$  due to the nuclear quadrupole moment of  $\text{I}^{127}$ . The experimentally observed pattern may be seen to agree well with the theoretical pattern, which assumes a quadrupole coupling constant of  $-1934$  Mc and a spin of  $\frac{5}{2}$ . (From Gordy, Smith, and Simmons [205].)

$(IJKFM_F|H_Q|IJ'K'FM_F)$  are matrix elements of  $H_Q$  for the symmetric-rotor wave functions specified by the quantum numbers  $I, J, K, F, M_F$  and  $I, J', K', F, M_F$ . The quantum numbers  $I, F$ , and  $M_F$  are not summed over since they are unaffected by the perturbation, or in other words the matrix of  $H_Q$  is diagonal in  $I, F$ , and  $M_F$ . The first term of (6-9) is just the previously calculated first-order quadrupole energy (6-8) which gives quite accurately the entire quadrupole energy when  $W_{JK} - W_{J'K'}$  is much larger than  $eqQ$ . The only matrix elements in

the sum of (6-9) which are not identically zero are those for which  $K' = K$  and either  $J' = J \pm 1$  or  $J' = J \pm 2$ . They are [253]

$$\begin{aligned}
 \langle I, J, K, F, M_F | H_Q | I, J + 1, K, F, M_F \rangle &= \frac{3eqQK[F(F+1) - I(I+1) - J(J+2)]}{8I(2I-1)J(J+2)} \\
 &\times \left\{ \frac{\left[ \left( 1 - \frac{K^2}{(J+1)^2} \right) (I+J+F+2)(J+F-I+1) \times (I+F-J)(I+J-F+1) \right]}{(2J+1)(2J+3)} \right\}^{\frac{1}{2}} \\
 \langle I, J, K, F, M_F | H_Q | I, J + 2, K, F, M_F \rangle &= \frac{3eqQ}{16I(2I-1)(2J+3)} \\
 &\times \left\{ \left[ 1 - \frac{K^2}{(J+1)^2} \right] \left[ 1 - \frac{K^2}{(J+2)^2} \right] (I+J+F+3)(I+J+F+2) \right. \\
 &\times (I+J-F+2)(I+J-F+1)(J+F-I+2) \\
 &\times \left. \frac{(J+F-I+1)(I+F-J)(I+F-J-1)}{(2J+1)(2J+5)} \right\}^{\frac{1}{2}} \quad (6-10)
 \end{aligned}$$

From the matrix elements (6-10) and expression (6-9) the modifications in the quadrupole energy due to second-order perturbations may be taken into account. They are usually rather small, for they are less than first-order energies (6-8) by a factor usually somewhat smaller than  $eqQ/(W_{JK} - W_{J'K'}) \approx eqQ/\nu$ , where  $\nu$  is the frequency of the observed rotational transition. Usually  $eqQ$  is a few hundred megacycles, while  $\nu$  is a few ten thousands of megacycles. However, in some cases, such as a large molecule with the atoms I or Hg in it,  $eqQ/\nu$  may not be small; in fact it may possibly be so large that a still better approximation than that given by (6-9) will be needed in order to fit the experimentally measured hyperfine structure.

A linear molecule in the ground vibrational state is of course a special case of a symmetric top for which  $K$  equals zero. When  $K = 0$ , the matrix element given by (6-10) which connects  $J$  and  $J + 1$  is zero, and the matrix element connecting  $J$  and  $J + 2$  simplifies somewhat. If the linear molecule is excited in a degenerate vibrational mode so that there is an angular momentum  $|l|$  around the axis of the molecule, then as seen in Chap. 2, its rotational wave functions are similar to those for a symmetric top with  $|K|$  equal to  $|l|$ . Hence matrix elements (6-10) apply to a linear molecule excited to any vibrational mode if the value of  $l$  is substituted for  $K$ .

The molecule ICN is a case where  $eqQ/\nu$  is as large as is normally encountered. For  $I^{127}$ ,  $eqQ = -2420$  Mc, and the transition  $J = 4 \leftarrow 3$  occurs near 25,800 Mc. The  $N^{14}$  nucleus in ICN has a quadrupole coupling of  $-3.7$  Mc which is so small that, unless the spectrum is observed under very high resolution, the quadrupole effects due to N



may be neglected. The effect of second-order corrections on the observed spectrum for the ground vibrational state is indicated in Table 6-1, which gives the first-order and second-order energies due to the  $I^{127}$  quadrupole coupling. It should be noted that the transitions  $F = \frac{9}{2} \leftarrow \frac{7}{2}$  and  $F = \frac{9}{2} \leftarrow \frac{9}{2}$  should, according to the usually first-order theory of quadrupole effects, exactly coincide. Second-order effects split these two lines by 6.32 Mc. Actual measurements of the hyperfine structure of the  $J = 4 \leftarrow 3$  transition in ICN agree very well with the predicted combined first- and second-order effects.

TABLE 6-1. QUADRUPOLE SPLITTING OF THE  $J = 4 \leftarrow 3$  TRANSITION OF ICN IN THE GROUND VIBRATIONAL STATE

Without quadrupole effects, the transition would occur at 25,804 Mc. The frequency contributions to the various possible hyperfine transitions due to an I quadrupole coupling of -2420 Mc are listed.  $F'$  represents the initial value of  $F$  associated with a  $J$  of 3, and  $F$  is the final value.

Transition $F \leftarrow F'$	Quadrupole coupling contribution, Mc	
	First order	Second order
$\frac{13}{2} \leftarrow \frac{11}{2}$	18.33	0.55
$\frac{11}{2} \leftarrow \frac{11}{2}$	-410.65	0.10
$\frac{11}{2} \leftarrow \frac{9}{2}$	33.02	0.49
$\frac{9}{2} \leftarrow \frac{9}{2}$	- 18.84	4.52
$\frac{9}{2} \leftarrow \frac{7}{2}$	- 18.84	-1.80
$\frac{7}{2} \leftarrow \frac{7}{2}$	150.87	-0.83
$\frac{7}{2} \leftarrow \frac{5}{2}$	- 74.98	-0.49
$\frac{5}{2} \leftarrow \frac{5}{2}$	189.01	-0.83
$\frac{5}{2} \leftarrow \frac{3}{2}$	- 93.32	0.65
$\frac{3}{2} \leftarrow \frac{3}{2}$	165.95	-0.60
$\frac{3}{2} \leftarrow \frac{1}{2}$	- 51.84	0.37

Transitions of ICN molecules in the first excited bending mode are split by  $l$ -type doubling, and each of the two  $l$ -type doublets is further split by the I quadrupole effects. First- and second-order quadrupole effects for these doublets are listed in Table 6-2. In this case  $|l| = 1$ , and the value of the corresponding quantum number  $K$  for the angular momentum around the symmetry axis is set equal to 1 in calculating second-order effects from the expressions (6-10).

The second-order effects of quadrupole coupling on the hyperfine structure as given in Tables 6-1 and 6-2 are not large, even though the quadrupole coupling constant for  $I^{127}$  in ICN is a rather large one. If the quadrupole coupling constant had been ten times smaller, or about 240 Mc, the second-order effects on frequency would have been 100 times smaller, since they depend on  $(eqQ)^2$ , and would then be detectable only by very accurate microwave frequency measurements.

In addition to changing the frequencies of hyperfine components, second-order quadrupole effects may affect their intensities. The quadrupole coupling modifies the molecular rotational wave functions, adding to the wave function of rotational quantum number  $J$  a small component of the wave functions for  $J \pm 1$  (if  $K \neq 0$ ) and  $J \pm 2$ . Because of this modification of the wave function, the matrix elements for the transitions and hence the intensities are slightly changed. This change is usually too small to be of significance for the normal transitions unless extremely accurate intensity measurements are made. More noticeable and important, however, is that the selection rules are modified to allow the occurrence of new transitions. Thus since a small component of the wave function for  $J + 2$  is mixed with the wave function for  $J$ , a weak transi-

TABLE 6-2. QUADRUPOLE SPLITTING OF THE  $J = 4 \leftarrow 3$  TRANSITION OF ICN IN THE FIRST EXCITED BENDING MODE, FOR WHICH  $[l] = 1$

Notation is as in Table 6-1.  $l$ -type doubling is not included in this table but produces two sets of hyperfine components separated by the  $l$ -type doubling.

Transition $F \leftarrow F'$	Quadrupole coupling contribution, Mc	
	First order	Second order
$\frac{1}{2} \frac{3}{2} \leftarrow \frac{1}{2} \frac{1}{2}$	54.08	1.61
$\frac{1}{2} \frac{1}{2} \leftarrow \frac{1}{2} \frac{3}{2}$	22.18	-0.72
$\frac{3}{2} \frac{3}{2} \leftarrow \frac{1}{2} \frac{5}{2}$	-21.90	0.28
$\frac{1}{2} \frac{5}{2} \leftarrow \frac{3}{2} \frac{3}{2}$	-47.03	-0.20
$\frac{5}{2} \frac{3}{2} \leftarrow \frac{3}{2} \frac{5}{2}$	-34.40	-0.45

tion from this modified wave function to a  $J + 3$  state may occur. If the modified wave function is still identified (approximately) by the quantum number  $J$ , this effect would allow weak transitions corresponding to  $\Delta J = \pm 3$ . Similarly, when  $K$  is not equal to zero and the quadrupole coupling is large, weak transitions corresponding to  $\Delta J = \pm 2$  may be expected. These types of transitions have not yet been observed but could probably be found in the case of molecules with quadrupole couplings as large as is found in ICN. Their intensities may be calculated by evaluating the amounts of perturbation of the wave functions using the matrix elements given by (6-10).

**6-5. Asymmetric Tops.** In principle, evaluation of nuclear quadrupole effects in asymmetric rotors is straightforward. Expression (6-1) gives the energy, which is of the same form as for symmetric molecules, and  $q_J$ , the average second derivative of the potential along the direction of the angular momentum, is

$$q_J = \int \psi_{J K-1, K_1, M=J}^* \left( \frac{\partial^2 V}{\partial z_J^2} \right) \psi_{J K-1, K_1, M=J} d\tau \quad (6-11)$$

where  $\psi_{J_{K-1}K_1, M=J}$  is an asymmetric-rotor wave function. Evaluation of the integral in (6-11), however, is considerably more complex than evaluating the similar expression for symmetric rotors. We shall follow the method of Bragg [258].

For an evaluation of (6-11), we shall express  $\partial^2 V / \partial z_J^2$  in terms of the second derivatives of the potential along the principal axes of inertia  $x_m$ ,  $y_m$ , and  $z_m$  of the molecule and the direction cosines  $\alpha$  between this set of axes and  $z_J$  which is fixed in space.

$$\begin{aligned} \frac{\partial^2 V}{\partial z_J^2} = & \alpha_{z_J x_m}^2 \frac{\partial^2 V}{\partial x_m^2} + \alpha_{z_J y_m}^2 \left( \frac{\partial^2 V}{\partial y_m^2} \right) + \alpha_{z_J z_m}^2 \left( \frac{\partial^2 V}{\partial z_m^2} \right) \\ & + 2\alpha_{z_J x_m} \alpha_{z_J y_m} \left( \frac{\partial^2 V}{\partial x_m \partial y_m} \right) + 2\alpha_{z_J x_m} \alpha_{z_J z_m} \left( \frac{\partial^2 V}{\partial x_m \partial z_m} \right) \\ & + 2\alpha_{z_J y_m} \alpha_{z_J z_m} \left( \frac{\partial^2 V}{\partial y_m \partial z_m} \right) \end{aligned} \quad (6-12)$$

By an argument similar to that used to prove certain matrix elements of the dipole moment are zero (page 63), the integrals of the form

$$\int \psi^* \alpha_{z_J x_m} \alpha_{z_J y_m} \frac{\partial^2 V}{\partial x_m \partial y_m} \psi d\tau \quad (6-13)$$

may be shown to be zero. Because wave functions are either symmetric or antisymmetric with respect to a rotation around the principal axes,  $\psi^* \psi$  is unchanged as a result of a  $180^\circ$  rotation about the axis  $x_m$ . However,  $\alpha_{z_J y_m}$  is reversed in sign since the  $y_m$  direction has been reversed. Hence the integrand of (6-13) undergoes a reversal of sign due to this rotation and must be zero. Expression (6-11) becomes, therefore,

$$q = (\alpha_{z_J x_m}^2)_{av} \frac{\partial^2 V}{\partial x_m^2} + (\alpha_{z_J y_m}^2)_{av} \frac{\partial^2 V}{\partial y_m^2} + (\alpha_{z_J z_m}^2)_{av} \frac{\partial^2 V}{\partial z_m^2} \quad (6-14)$$

where

$$(\alpha_{z_J x_m}^2)_{av} = \int \psi_{J_{K-1}K_1, M=J}^* \alpha_{z_J x_m}^2 \psi_{J_{K-1}K_1, M=J} d\tau \quad (6-15)$$

Matrix elements of the direction cosines have already been discussed and the line strengths  $S_{J_{K-1}K_1, J'_{K'-1}K'_1}$  derived from their squares are tabulated in Appendix V. Matrix elements of the squares of direction cosines such as (6-15) may be obtained by squaring the direction cosine matrices. Some manipulation (*cf.* [258]) shows that  $(\alpha_{z_J x_m}^2)_{av}$  may hence be expressed in terms of the quantities tabulated in Appendix V as follows:

$$(\alpha_{z_J x_m}^2)_{av} = \frac{2J}{(2J+1)(2J+3)} \sum_{K'-1, K'_1} {}^x S_{J_{K-1}K_1, J'_{K'-1}K'_1} \quad (6-16)$$

where  $x$  or  $x_m$  may refer to the direction of any one of the three principal axes  $a$ ,  $b$ , or  $c$ . This gives



$$q_J = \frac{2J}{(2J+1)(2J+3)} \sum_{K'_{-1}K'_1} \frac{\partial^2 V}{\partial a^2} {}^a S_{J_{K_{-1}K_1}J_{K'_{-1}K'_1}} + \frac{\partial^2 V}{\partial b^2} {}^b S_{J_{K_{-1}K_1}J_{K'_{-1}K'_1}} + \frac{\partial^2 V}{\partial c^2} {}^c S_{J_{K_{-1}K_1}J_{K'_{-1}K'_1}} \quad (6-17)$$

where second derivatives of the potential along the three principal axes of inertia are indicated by  $\partial^2 V/\partial a^2$ ,  $\partial^2 V/\partial b^2$ , and  $\partial^2 V/\partial c^2$ . This potential as before (page 135) is due to all charges outside a small sphere around the nucleus. The quantities  $S$  in (6-17) are tabulated in Appendix V for values of the asymmetry parameter  $\kappa = -1.0, -0.5, 0, 0.5$ , and  $1.0$  only. Interpolation must be used for other values of  $\kappa$ .

Another form in which  $q_J$  may be expressed is [352]

$$q_J = \frac{1}{(J+1)(2J+3)} \frac{\partial^2 V}{\partial a^2} \left[ J(J+1) + E(\kappa) - (\kappa+1) \frac{\partial E(\kappa)}{\partial \kappa} \right] + \frac{2}{(J+1)(2J+3)} \frac{\partial^2 V}{\partial b^2} \frac{\partial E(\kappa)}{\partial \kappa} + \frac{1}{(J+1)(2J+3)} \frac{\partial^2 V}{\partial c^2} \left[ J(J+1) - E(\kappa) + (\kappa-1) \frac{\partial E(\kappa)}{\partial \kappa} \right] \quad (6-18)$$

where  $E(\kappa)$  is the energy parameter for an asymmetric rotor of asymmetry  $\kappa$  as defined in (4-10). In (6-18)  $E_{J_{K_{-1}K_1}}(\kappa)$  appropriate to the particular state for which  $q_J$  is being evaluated is of course used.  $E(\kappa)$  and  $\partial E(\kappa)/\partial \kappa$  may be obtained from Appendix IV. Although interpolation must still be used to evaluate  $E(\kappa)$  and  $\partial E(\kappa)/\partial \kappa$ , the tabulation in Appendix IV uses smaller steps of  $\kappa$  than does Appendix V, so that more accuracy may often be obtained from (6-18) than from (6-17).

Expression (6-18) is also very useful if  $q_J$  must be evaluated for states not tabulated in Appendices IV or V ( $J > 12$ ), since all the approximate methods discussed in Chap. 4 for evaluating  $E(\kappa)$  for large  $J$  are available. [See [352] for expression of (6-18) in terms of approximations for  $E(\kappa)$ .]

If better accuracy is needed than can be obtained by interpolation, the integral in (6-11) may be evaluated by expanding the wave function as a sum of symmetric-top functions as in (4-18). This leads to the expression [258]

$$q_J = \frac{q_m}{(J+1)(2J+3)} \sum_K a_{JK}^2 [3K^2 - J(J+1)] - 2a_{JK}a_{JK+2} [f'(J, K+1)]^{\frac{1}{2}} \eta \quad (6-19)$$

$$\text{where } f'(J, n) = \frac{1}{4}(J^2 - n^2)[(J+1)^2 - n^2] \quad (6-20)$$

$q_m = \partial^2 V/\partial z_m^2$  is the second derivative of the potential along the principal axis which most nearly represents a symmetry axis of the moment of inertia ellipsoid

$$\eta = \frac{\partial^2 V/\partial x_m^2 - \partial^2 V/\partial y_m^2}{q_m} \quad (6-21)$$

If the molecule is considered an oblate top,  $z_m$  is the  $c$  axis, and  $x_m$  and  $y_m$  must be taken as the  $a$  and  $b$  axes, respectively. If it is prolate,  $z_m$  is the  $a$  axis,  $x_m$  the  $b$  axis, and  $y_m$  the  $c$  axis.

Expression (6-19) can give  $q_J$  exactly, but only after evaluation of the  $a_{JK}$ 's, which is troublesome. For small values of the asymmetry parameter  $b$  [for definition of  $b$ , see (4-2) and (4-3)]  $q_J$  can be satisfactorily obtained for various values of  $K$  from the expressions below. Terms of order  $b^3$  or higher are omitted.\*

For  $K = 0$ :

$$q_J = \frac{q_m}{(J+1)(2J+3)} \{ -J(J+1) + (\frac{3}{2}b^2 - b\eta)f'(J,1) \} \quad (6-22a)$$

For  $K = 1$ :

$$q_J = \frac{q_m}{(J+1)(2J+3)} \left\{ 3 - J(J+1) \mp \frac{\eta}{2} J(J+1) + (\frac{3}{2}b^2 - b\eta) \frac{f'(J,2)}{4} \right. \\ \left. \pm \frac{3}{128} b^2 \eta J(J+1) f'(J,2) \right\} \quad (6-22b)$$

For  $K = 2$ :

$$q_J = \frac{q_m}{(J+1)(2J+3)} \left\{ 12 - J(J+1) + (\frac{3}{2}b^2 - b\eta) \right. \\ \left. \left[ \frac{f'(J,3)}{6} - \frac{f'(J,1)}{2} \mp \frac{f'(J,1)}{2} \right] \right\} \quad (6-22c)$$

For  $K = 3$ :

$$q_J = \frac{q_m}{(J+1)(2J+3)} \left\{ 27 - J(J+1) + (\frac{3}{2}b^2 - b\eta) \right. \\ \left. \left[ \frac{f'(J,4)}{8} - \frac{f'(J,2)}{4} \right] \mp \frac{3}{128} f'(J,2) J(J+1) b^2 \eta \right\} \quad (6-22d)$$

For  $K > 3$ :

$$q_J = \frac{q_m}{(J+1)(2J+3)} \left\{ 3K^2 - J(J+1) + (\frac{3}{2}b^2 - b\eta) \right. \\ \left. \left[ \frac{f'(J,K+1)}{2(K+1)} - \frac{f'(J,K-1)}{2(K-1)} \right] \right\} \quad (6-22e)$$

where  $f'(J,n) = \frac{1}{4}(J^2 - n^2)[(J+1)^2 - n^2]$

The upper signs apply to the upper-energy level of a  $K$ -type doublet for a prolate rotor or the lower doublet of an oblate rotor. The lower signs apply to the lower-energy level of a doublet for a prolate rotor, or the upper doublet of an oblate rotor. Since quadrupole effects are not

\* Expressions (6-22) were first given by G. Knight and B. T. Feld [379] but have been corrected by J. Kraitchman and A. Javan.

usually measured to high fractional accuracy, the approximate expressions (6-22) (neglecting terms in  $b^3$  and higher) are satisfactory in many cases, and when  $b$  is small they are more accurate than expressions (6-17) or (6-18) with interpolation.

There can be no asymmetry in  $\nabla E$  about the axis for a nucleus on the axis of a real symmetric top. Nuclei off the axis of a symmetric top always occur as three or more equivalent nuclei, for the sum of which the asymmetry of the field, or of  $\nabla E$ , cancels out. However, for a molecule which is accidentally very close to symmetric, an asymmetry of the electric field about the axis can give a sizable contribution to the quadrupole energy when  $K = 1$ . This shows up as the terms  $\pm q_m J \eta / 2J + 3$  in Eq. (6-22). In the case of  $\text{H}_2\text{C}=\text{CHCl}$ , for example, where the asymmetry  $b = -0.006$ , hyperfine structure of transitions between levels with  $K = 1$  can be fitted rather well by omitting all terms involving  $b$ , but these terms dependent on the asymmetry of the field  $\eta$  must be kept. When  $K \neq 1$ , an asymmetry of the field affects the quadrupole energy only if at the same time the molecule is asymmetric ( $b \neq 0$ ).

Hyperfine structure in an asymmetric rotor must be fitted by the two parameters  $\partial^2 V / \partial z_m^2$  and  $\partial^2 V / \partial x_m^2 - \partial^2 V / \partial y_m^2$ , or  $q_m$  and  $\eta$  instead of the one parameter  $q_m$  which is needed for symmetric tops. However, in many cases these two parameters can to a very good approximation be expressed in terms of a single property of the electric field,  $\partial^2 V / \partial z_b^2$ , the second derivative of the electrostatic potential along the direction of the chemical bond which binds the nucleus in question to the molecule. This is because the electrostatic fields are in many cases almost symmetric about the bond axis.

A clear example of this is the field at the Cl nucleus in the asymmetric varieties of methyl chloride. For  $\text{CH}_3\text{Cl}$ ,  $\nabla E$  at the chlorine nucleus is symmetric about the C—Cl axis because of the threefold-symmetry axis of the molecule. In  $\text{CH}_2\text{DCl}$ ,  $\nabla E$  must still be symmetrical about the C—Cl axis, but the molecule has become an asymmetric top, and no principal axis coincides with the C—Cl bond. In such case the various second derivatives of the potential along principal axes may be readily obtained.

$$\begin{aligned} \frac{\partial^2 V}{\partial z_m^2} &= \frac{\partial^2 V}{\partial z_b^2} \frac{3\alpha_{z_b z_m}^2 - 1}{2} \\ \frac{\partial^2 V}{\partial x_m^2} &= \frac{\partial^2 V}{\partial z_b^2} \frac{3\alpha_{z_b x_m}^2 - 1}{2} \\ \frac{\partial^2 V}{\partial y_m^2} &= \frac{\partial^2 V}{\partial z_b^2} \frac{3\alpha_{z_b y_m}^2 - 1}{2} \end{aligned} \quad (6-23a)$$

where  $\alpha_{z_b z_m}$ , etc., represent the cosines of angles between the various axes.

More generally, if the second derivatives of the potential with respect to one set of Cartesian coordinates  $x_1, x_2, x_3$  are known, those along any



other set of axes  $x'_1, x'_2, x'_3$  may be obtained from the relations

$$\frac{\partial^2 V}{\partial x'_1 \partial x'_j} = \sum_{kl} \alpha_{x'_1 x_k} \alpha_{x'_j x_l} \frac{\partial^2 V}{\partial x_k \partial x_l} \quad (6-23b)$$

Here  $\alpha_{x'_1 x_k}$  represents the cosine of the angle between the two axes  $x'_1$  and  $x_k$ .

Very frequently, the electric field at a nucleus is to good accuracy symmetric about a bond, as in the case of  $\text{CH}_2\text{DCl}$  above. In  $\text{CH}_2\text{Cl}_2$  it has been shown by Myers and Gwinn [732] that expressions (6-23) give the correct values for  $q_m$  and  $\eta$  to within the experimental accuracy of 1 per cent of  $\partial^2 V / \partial z_b^2$ . On the other hand, in cases where double bonds are involved, the fields may not be at all symmetric about the bond (see Chap. 9).  $\text{H}_2\text{C}=\text{CHCl}$  is a molecule in which apparently the double-bond character of the C—Cl bond is sufficient to make the field appreciably asymmetric.

The quadrupole energy so far discussed for asymmetric rotors has been of the first-order type. As in symmetric rotors, the quadrupole energy is sometimes large enough compared with the separation between rotational energy levels that second-order perturbations are important. Corresponding to Eq. (6-9), the quadrupole energy is then

$$W_Q = (I, J_{K-1, K_1}, F | H_Q | I, J_{K-1, K_1}, F) + \sum_{J'K'_{-1}K'_1} \frac{|(I, J_{K-1, K_1}, F | H_Q | I, J'_{K'-1, K'_1}, F)|^2}{W_{J_{K-1, K_1}} - W_{J'_{K'-1, K'_1}}} \quad (6-24)$$

where  $W_{J_{K-1, K_1}}$  is the rotational energy. The quantities in brackets are the matrix elements of the Hamilton for the quadrupole interaction  $H_Q$ , the first term being the first-order energy which has been discussed above. The sum is, of course, over all rotational states except the unperturbed state  $J_{K-1, K_1}$ .

It can be shown that all matrix elements involved in the sum of (6-24) are zero except those for which  $J' = J \pm 1$  or  $J' = J \pm 2$ . These matrix elements have been discussed by Bragg [258] but have not yet been evaluated in detail. In cases of near degeneracy where two asymmetric-top levels of appropriate symmetry lie close together, second-order quadrupole effects will, however, be of some importance.

**6-6. Hyperfine Structure from Two or More Nuclei in the Same Molecule.** A molecule may contain more than one nucleus which produces an observable hyperfine structure in its spectrum. This almost always occurs when more than one nucleus in the molecule has a spin greater than  $\frac{1}{2}$  and hence is coupled by its quadrupole moment to the rotational motion of the molecule. In such cases the quadrupole energies are no longer given by expressions like (6-8), since the interaction between one nucleus and the molecule will affect the interaction between the second nucleus and the molecule, and vice versa. We shall consider first

the case of two such nuclei, which is the one of most importance. The treatment follows that of Bardeen and Townes [252].

If nucleus 1 is coupled to the molecule much more strongly than nucleus 2, the system can be fairly well described by the vector model. In that case, the spin  $\mathbf{I}$  of nucleus 1 adds vectorially to the molecular angular momentum  $\mathbf{J}$  to form a resultant  $\mathbf{F}_1$ , which is quantized with the possible values  $J + I_1, J + I_1 - 1, \dots, |J - I_1|$ . The spin  $\mathbf{I}_2$  of the second, more weakly coupled nucleus then adds vectorially to  $\mathbf{F}_1$  to form the total angular momentum  $\mathbf{F}$  which may have the values  $F_1 + I_2, F_1 + I_2 - 1, \dots, |F_1 - I_2|$ . The two angular momenta  $\mathbf{I}_1$  and  $\mathbf{J}$  may be regarded as precessing around the vector  $\mathbf{F}_1$  with a precessional frequency approximately equal to the energy difference between  $F_1$  and  $F_1 + 1$  divided by  $h$ . Similarly the vectors  $\mathbf{I}_2$  and  $\mathbf{F}_1$  precess about the vector  $\mathbf{F}$ , which is fixed in space. If the first nucleus is coupled to the molecule much more strongly than the second nucleus, then  $\mathbf{I}_1$  precesses so much more rapidly than  $\mathbf{I}_2$  that  $\mathbf{F}_1$  and  $\mathbf{I}_2$  may be thought of as stationary during a complete cycle of the motion of  $\mathbf{I}_1$  and  $\mathbf{J}$ ; hence the interaction between  $\mathbf{I}_2$  and  $\mathbf{J}$  is averaged over this motion. If the interaction between  $\mathbf{I}_2$  and  $\mathbf{J}$  is proportional to the cosine of the angle between them, then the vector model allows a rather simple and accurate calculation of this interaction energy, as will be seen from the discussion of magnetic hyperfine structure in Chap. 8. However, if the interaction is proportional to the square of the cosine between  $\mathbf{I}_2$  and  $\mathbf{J}$  as is the quadrupole interaction, a calculation from more rigorous quantum mechanics must be used. In addition, if the coupling of nucleus 1 and nucleus 2 is not widely different, then averaging over the precession of nucleus 1 is no longer a good approximation, and the vector model must be abandoned for a more sophisticated treatment such as that below.

First consider wave functions which are formed by combining the vectors  $\mathbf{J}$  and  $\mathbf{I}_1$  to produce  $\mathbf{F}_1$ , and then combining  $\mathbf{F}_1$  and  $\mathbf{I}_2$  to produce  $\mathbf{F}$ , and let wave functions of this type be represented by  $\psi_1(F_1, F)$ . The Hamiltonian for the two nuclear interactions may be written

$$H = H_1(\mathbf{I}_1, \mathbf{J}) + H_2(\mathbf{I}_2, \mathbf{J}) \quad (6-25)$$

The energy due to  $H_1$  can be readily evaluated for wave functions of the type  $\psi_1$ . In the case of quadrupole interactions this energy is obtained simply by letting  $F_1$  take the place of  $F$  in expression (6-9). (Here second-order quadrupole interaction will be neglected, so that  $J$  is a good quantum number.) There will be a number of wave functions  $\psi_1(F_1, F)$  having the same  $F$  but different  $F_1$  and hence different energies associated with the interaction  $H_1$ . There may also be several wave functions of the same  $F_1$  and different  $F$ , which will have the same energy if  $H_2$  is negligibly small. This degeneracy is removed if  $H_2$  is appreciable, but

the energy associated with  $H_2$  is not immediately calculable, since the wave function  $\psi_1$  is not an eigenfunction of  $H_2$ .

Consider next wave functions formed by combining first the vectors  $\mathbf{I}_2$  and  $\mathbf{J}$  to make the vector which will be designated  $\mathbf{F}_2$ , then combining  $\mathbf{F}_2$  and  $\mathbf{I}_1$  to make the total angular momentum  $\mathbf{F}$ . These are eigenfunctions of  $H_2$  and may be designated  $\psi_2(F_2, F)$ . The number of different wave functions with the same  $F$  will be the same as before, and the two sets of wave functions are linearly related. Their relation may be written

$$\psi_1(F_1, F) = \sum_{F_2} c(F_1, F_2) \psi_2(F_2, F) \quad (6-26)$$

The matrix  $c(F_1, F_2)$  is unitary, and the phases of the wave functions may be chosen so that these coefficients are all real. Hence the reverse transformation is

$$\psi_2(F_2, F) = \sum_{F_1} c(F_1, F_2) \psi_1(F_1, F) \quad (6-27)$$

In case both interactions,  $H_1$  and  $H_2$ , are appreciable, the eigenfunctions are not given by either  $\psi_1(F_1, F)$  or  $\psi_2(F_2, F)$  but by appropriate linear combinations of either set. Let the correct wave function be given by the general expansion

$$\psi(F) = \sum_{F_1} a(F_1) \psi_1(F_1, F) \quad (6-28)$$

The Hamiltonian equation  $H\psi = W\psi$  becomes

$$\begin{aligned} \sum_{F_1} H_1(\mathbf{I}_1, \mathbf{J}) a(F_1) \psi_1(F_1, F) + \sum_{F_1} H_2(\mathbf{I}_2, \mathbf{J}) a(F_1) \sum_{F_2} c(F_1, F_2) \psi_2(F_2, F) \\ = W \sum_{F_1} a(F_1) \psi_1(F_1, F) \end{aligned} \quad (6-29)$$

in which use has been made of (6-25). Now  $\psi_1$  is an eigenfunction of  $H_1$  and  $\psi_2$  of  $H_2$ , or

$$\begin{aligned} H_1(\mathbf{I}_1, \mathbf{J}) \psi_1(F_1, F) &= W_1(F_1) \psi_1(F_1, F) \\ H_2(\mathbf{I}_2, \mathbf{J}) \psi_2(F_2, F) &= W_2(F_2) \psi_2(F_2, F) \end{aligned} \quad (6-30)$$

Using these relations and replacing  $\psi_2$  by (6-27), Eq. (6-29) becomes

$$\begin{aligned} \sum_{F_1} \{ [A(F_1, F_1) + W(F_1) - W] a(F_1) \\ + \sum_{F_1' \neq F_1} A(F_1, F_1') a(F_1') \} \psi_1(F_1, F) = 0 \end{aligned} \quad (6-31)$$

where

$$A(F_1, F_1') = \sum_{F_2} c(F_1, F_2) c(F_1', F_2) W_2(F_2) \quad (6-32)$$



Since all the  $\psi_1$ 's are orthogonal, (6-31) may be written as a group of homogeneous equations of the form

$$[A(F_1, F) + W(F_1) - W]a(F_1) + \sum_{F_1' \neq F_1} A(F_1, F_1')a(F_1') = 0 \quad (6-33)$$

for each value of  $F_1$  which, when added to  $I_2$ , gives the same value  $F$  for the total angular momentum. In order for these equations to have a solution, the determinant of their coefficients must be zero. A solution of this secular determinant gives the possible values of the energy  $W$ . If the interaction  $H_2$  is much smaller than  $H_1$  and there is no degeneracy in  $W_1$ , then the energy values are given to the first order in  $H_2$  by

$$W = W(F_1) + A(F_1, F_1)$$

or

$$W = W(F_1) + \sum_{F_2} [c(F_1, F_2)]^2 W_2(F_2) \quad (6-34)$$

This is the case when the eigenfunctions  $\psi_1(F_1, F)$  are essentially correct. Then the energy is given by the sum of the energy  $W(F_1)$  and the various possible energies  $W_2(F_2)$  weighted by the probability  $[c(F_1, F_2)]^2$  of finding  $\psi_2(F_2, F)$  in the transformation (6-26) of the wave function  $\psi_1(F_1, F)$ .

The quantities  $c(F_1, F_2)$  are given in terms of  $I_1$ ,  $I_2$ ,  $J$ ,  $F_1$ ,  $F_2$ , and  $F$  by Tables 6-3, 6-4, and 6-5. Table 6-3 gives these coefficients for an arbitrary  $I_1$ ,  $J$ ,  $F_1$ ,  $F_2$ , and  $F$  when  $I_2 = \frac{1}{2}$ , and Tables 6-4 and 6-5 give them when  $I_2 = 1$  and  $\frac{3}{2}$ , respectively.

TABLE 6-3. TRANSFORMATION COEFFICIENTS  
 $c(F_1, F_2)$  for  $I_1 = 1$ ,  $I_2 = \frac{1}{2}$ ,  $\Sigma = I + J + F + \frac{1}{2}$

$F_2$	$F_1 = F - \frac{1}{2}$	$F_1 = F + \frac{1}{2}$
$J - \frac{1}{2}$	$\left[ \frac{(\Sigma - 2F)(\Sigma - 2J)}{(2F + 1)(2J + 1)} \right]^{\frac{1}{2}}$	$\left[ \frac{(\Sigma + 1)(\Sigma - 2I)}{(2F + 1)(2J + 1)} \right]^{\frac{1}{2}}$
$J + \frac{1}{2}$	$-\left[ \frac{(\Sigma + 1)(\Sigma - 2I)}{(2F + 1)(2J + 1)} \right]^{\frac{1}{2}}$	$\left[ \frac{(\Sigma - 2F)(\Sigma - 2J)}{(2F + 1)(2J + 1)} \right]^{\frac{1}{2}}$

These coefficients are related as follows to certain  $W$  functions defined by Racah [113]:

$$c(F_1, F_2) = (-1)^{F+J-I_1-I_2} [(2F_1 + 1)(2F_2 + 1)]^{\frac{1}{2}} W(F_1 F J F_2; I_2 I_1)$$

The  $W$  functions ( $W$  is not to be confused with the energy) have now been tabulated for most values of the variables which are of interest [674] [854a]. Hence the coefficients  $c(F_1, F_2)$  for  $I_2 > \frac{3}{2}$  may be obtained from them.

*An Example of Two Nuclei with Hyperfine Structure.* Calculation of a specific case may be helpful. Let  $I_1 = \frac{3}{2}$ ,  $I_2 = 1$ , and  $J = 2$ .  $F_1$  may

TABLE 6-4. TRANSFORMATION COEFFICIENTS  $c(F_1, F_2)$  FOR  $I_1 = I_1, I_2 = 1, \Sigma = I + J + F + 1$   
(From Bardeen and Townes [252])

$F_2$	$F_1 = F - 1$	$F_1 = F$	$F_1 = F + 1$
$J - 1$	$\left( \frac{(\Sigma - 2F - 1)(\Sigma - 2F)(\Sigma - 2J - 1)(\Sigma - 2J)}{2J(2J + 1)2F(2F + 1)} \right)^{\frac{1}{2}}$	$\left( \frac{2(\Sigma - 2F - 1)(\Sigma - 2I - 1)\Sigma(\Sigma - 2J)}{2J(2J + 1)2F(2F + 2)} \right)^{\frac{1}{2}}$	$\left( \frac{(\Sigma - 2I - 1)(\Sigma - 2I)\Sigma(\Sigma + 1)}{2J(2J + 1)(2F + 1)(2F + 2)} \right)^{\frac{1}{2}}$
$J$	$\left( \frac{2(\Sigma - 2F)(\Sigma - 2I - 1)\Sigma(\Sigma - 2J - 1)}{2J(2J + 2)2F(2F + 1)} \right)^{\frac{1}{2}}$	$\frac{2F(F + 1) + 2J(J + 1) - 2I(I + 1)}{(2J(2J + 2)2F(2F + 2))^{\frac{1}{2}}}$	$-\left( \frac{2(\Sigma - 2F - 1)(\Sigma - 2I)(\Sigma - 2J)(\Sigma + 1)}{(2J(2J + 2)2F(2F + 1)(2F + 2))} \right)^{\frac{1}{2}}$
$J + 1$	$\left( \frac{(\Sigma - 2I - 1)(\Sigma - 2I)\Sigma(\Sigma + 1)}{(2J + 1)(2J + 2)2F(2F + 1)} \right)^{\frac{1}{2}}$	$-\left( \frac{2(\Sigma - 2J - 1)(\Sigma - 2F)(\Sigma - 2I)(\Sigma + 1)}{(2J + 1)(2J + 2)2F(2F + 2)} \right)^{\frac{1}{2}}$	$\left( \frac{(\Sigma - 2J - 1)(\Sigma - 2J)(\Sigma - 2F - 1)(\Sigma - 2F)}{(2J + 1)(2J + 2)(2F + 1)(2F + 2)} \right)^{\frac{1}{2}}$

TABLE 6-5. TRANSFORMATION COEFFICIENTS  $c(F_1, F_2)$  FOR  $I_1 = I, I_2 = \frac{3}{2}, \Sigma = I + J + F + \frac{3}{2}$   
(From Bardeen and Townes [252])

$F_2$	$F_1 = F - \frac{1}{2}$	$F_1 = F - \frac{1}{2}$
$J - \frac{3}{2}$	$\left( \frac{(\Sigma - 2F - 2)(\Sigma - 2F - 1)(\Sigma - 2F)(\Sigma - 2J - 2)(\Sigma - 2J - 1)(\Sigma - 2J)}{(2F - 1)2F(2F + 1)(2J - 1)2J(2J + 1)} \right)^{\frac{1}{2}}$	$\left( \frac{3(\Sigma - 1)(\Sigma - 2F - 2)(\Sigma - 2F - 1)(\Sigma - 2J - 1)(\Sigma - 2J)(\Sigma - 2I - 2)}{(2F - 1)(2F + 1)(2F + 2)(2J - 1)2J(2J + 1)} \right)^{\frac{1}{2}}$
$J - \frac{1}{2}$	$\left( \frac{3(\Sigma - 1)(\Sigma - 2F - 1)(\Sigma - 2F)(\Sigma - 2J - 2)(\Sigma - 2J - 1)(\Sigma - 2I - 2)}{(2F - 1)2F(2F + 1)(2J - 1)(2J + 1)(2J + 2)} \right)^{\frac{1}{2}}$	$\left[ \frac{2(2F - 1)(\Sigma - 2I - 1) + (\Sigma - 2F)(-3I + 3J + F - 1)(\Sigma - 2F - 1)(\Sigma - 2J - 1)}{(2F - 1)(2F + 1)(2F + 2)(2J - 1)(2J + 1)(2J + 2)} \right]^{\frac{1}{2}}$
$J + \frac{1}{2}$	$\left( \frac{3(\Sigma - 1)\Sigma(\Sigma - 2F)(\Sigma - 2J - 2)(\Sigma - 2I - 2)(\Sigma - 2I - 1)}{(2F - 1)2F(2F + 1)2J(2J + 1)(2J + 3)} \right)^{\frac{1}{2}}$	$-\left( \frac{3\Sigma(\Sigma + 1)(\Sigma - 2F)(\Sigma - 2J - 2)(\Sigma - 2I - 1)(\Sigma - 2I)}{(2F - 1)(2F + 1)(2F + 2)(2J + 1)(2J + 2)(2J + 3)} \right)^{\frac{1}{2}}$
$J + \frac{3}{2}$	$\left( \frac{3(\Sigma - 1)\Sigma(\Sigma - 2F - 2)(\Sigma - 2J)(\Sigma - 2I - 2)(\Sigma - 2I - 1)}{2F(2F + 1)(2F + 3)(2J - 1)2J(2J + 1)} \right)^{\frac{1}{2}}$	$\left( \frac{(\Sigma - 1)\Sigma(\Sigma + 1)(\Sigma - 2I - 2)(\Sigma - 2I - 1)(\Sigma - 2I)}{(2F + 1)(2F + 2)(2F + 3)(2J - 1)2J(2J + 1)} \right)^{\frac{1}{2}}$
$J - \frac{1}{2}$	$\left[ \frac{2F(-3I - J + 3F + \frac{1}{2}) + 3(\Sigma - 2F - 1)(\Sigma - 2I - 2)(\Sigma - 2I - 1)}{(2F(2F + 1)(2F + 3)(2J - 1)(2J + 1)(2J + 2))} \right]^{\frac{1}{2}}$	$-\left( \frac{3\Sigma(\Sigma + 1)(\Sigma - 2F - 2)(\Sigma - 2J)(\Sigma - 2I - 1)(\Sigma - 2I)}{(2F + 1)(2F + 2)(2F + 3)(2J - 1)(2J + 1)(2J + 2)} \right)^{\frac{1}{2}}$
$J + \frac{1}{2}$	$\left( \frac{2F(2F + 1)(2F + 3)(2J - 1)(2J + 1)(2J + 2)}{(2F(2F + 1)(2F + 3)(2J - 1)(2J + 1)(2J + 2))} \right)^{\frac{1}{2}}$	$\left( \frac{3(\Sigma + 1)(\Sigma - 2F - 1)(\Sigma - 2F)(\Sigma - 2J - 2)(\Sigma - 2I - 1)(\Sigma - 2I)}{(2F + 1)(2F + 2)(2F + 3)(2J - 1)(2J + 1)(2J + 2)} \right)^{\frac{1}{2}}$
$J + \frac{3}{2}$	$\left( \frac{3(\Sigma + 1)(\Sigma - 2F - 1)(\Sigma - 2F)(\Sigma - 2J - 2)(\Sigma - 2I - 1)(\Sigma - 2I)}{2F(2F + 1)(2F + 3)(2J + 1)(2J + 2)(2J + 3)} \right)^{\frac{1}{2}}$	$-\left( \frac{(\Sigma - 2F - 2)(\Sigma - 2F - 1)(\Sigma - 2F)(\Sigma - 2J - 2)(\Sigma - 2I - 1)(\Sigma - 2I)}{(2F + 1)(2F + 2)(2F + 3)(2J + 1)(2J + 2)(2J + 3)} \right)^{\frac{1}{2}}$

then have the values  $\frac{1}{2}$ ,  $\frac{3}{2}$ ,  $\frac{5}{2}$ , or  $\frac{7}{2}$ ,  $F_2$  the values 1, 2, or 3, and  $F$  may have values ranging from  $\frac{1}{2}$  to  $\frac{9}{2}$ . There is only one possible wave function  $\psi_1(F_1, F)$  or  $\psi_2(F_2, F)$  which gives  $F = \frac{9}{2}$ , namely,  $\psi_1(\frac{7}{2}, \frac{9}{2})$  or  $\psi_2(3, \frac{9}{2})$ , which two functions must hence be identical. Therefore for  $F = \frac{9}{2}$ , all  $c$ 's are zero except  $c(\frac{7}{2}, 3)$  which is unity, as may be found from Table 6-4 or Table 6-5. The secular determinant for  $F = \frac{9}{2}$  reduces to the single equation

$$W = W_1(\frac{7}{2}) + W_2(3)$$

There are two wave functions corresponding to  $F = \frac{7}{2}$ , linear combinations of  $\psi_1(\frac{7}{2}, \frac{7}{2})$  and  $\psi_1(\frac{5}{2}, \frac{7}{2})$ , or of  $\psi_2(3, \frac{7}{2})$  and  $\psi_2(2, \frac{7}{2})$ . The coefficients are, from Table 6-4 (or Table 6-5),

$$c(\frac{7}{2}, 3) = -\sqrt{\frac{1}{7}} \quad c(\frac{7}{2}, 2) = \sqrt{\frac{6}{7}} \quad c(\frac{5}{2}, 3) = \sqrt{\frac{6}{7}} \quad c(\frac{5}{2}, 2) = \sqrt{\frac{1}{7}}$$

The secular determinant becomes, therefore

$$\begin{vmatrix} [W_1(\frac{7}{2}) + \frac{1}{7}W_2(3) + \frac{6}{7}W_2(2) - W] & \frac{\sqrt{6}}{7}[W_2(2) - W_2(3)] \\ \frac{\sqrt{6}}{7}[W_2(2) - W_2(3)] & [W_1(\frac{5}{2}) + \frac{6}{7}W_2(3) + \frac{1}{7}W_2(2) - W] \end{vmatrix} = 0 \quad (6-35)$$

which gives two possible values of the energy  $E$  corresponding to the two different states with  $F = \frac{7}{2}$ . For  $H_2 \ll H_1$ , the first-order solutions derived from the diagonal terms are sufficiently accurate. They are

$$\begin{aligned} W &= W_1(\frac{7}{2}) + \frac{1}{7}W_2(3) + \frac{6}{7}W_2(2) \\ \text{and} \quad W &= W_1(\frac{5}{2}) + \frac{6}{7}W_2(3) + \frac{1}{7}W_2(2) \end{aligned} \quad (6-36)$$

If  $H_2$  is not very small, then the quadratic equation (6-35) must be solved.

The energies given by (6-36), which are correct when the coupling of nucleus 1 is much less than that of nucleus 2, are the energies for nucleus 1 coupled to the molecule and slightly perturbed by nucleus 2. If the coupling of nucleus 2 were much greater than that of nucleus 1, then the energies would be given primarily by coupling nucleus 2 to the molecule and these energies would be slightly perturbed by nucleus 1. For intermediate coupling cases, where neither of these approximations holds, description of the energies is much more complex. The energies of the various states have been computed for the case  $I_1 = \frac{3}{2}$ ,  $I_2 = 1$ ,  $J = 2$ , and their behavior is shown in Fig. 6-3. Assuming the couplings between the nuclei and the molecule are due to quadrupole moments, the energy levels are plotted as a function of the ratio of the quadrupole couplings of the two nuclei. This ratio,  $\alpha = (eqQ)_{I=1}/(eqQ)_{I=2}$ , is measured along the axis of abscissas, the function  $(1 + \alpha)/(1 + \alpha^2)^{\frac{1}{2}}$  being plotted linearly for positive  $\alpha$  and  $(1 - \alpha)/(1 + \alpha^2)^{\frac{1}{2}}$  linearly for negative  $\alpha$ . Energy is



measured along the ordinate axis,  $W/[( -eqQ)_{I=3/2}(1 + \alpha^2)^{1/2}]$  being plotted linearly. Such a plot produces smooth curves and allows  $\alpha$  a range from  $-\infty$  to  $+\infty$ . Values of  $1/\alpha$  rather than  $\alpha$  are marked off in the region where  $|\alpha| > 1$ .

Near the line where  $\alpha = 0$ , the first-order approximation holds with the levels being close to those expected for a nucleus of spin  $\frac{3}{2}$ . Near the lines where  $\alpha = \infty$ , or  $1/\alpha = 0$ , the first-order approximation again holds, the levels being close to those expected for a nucleus of spin 1. It may

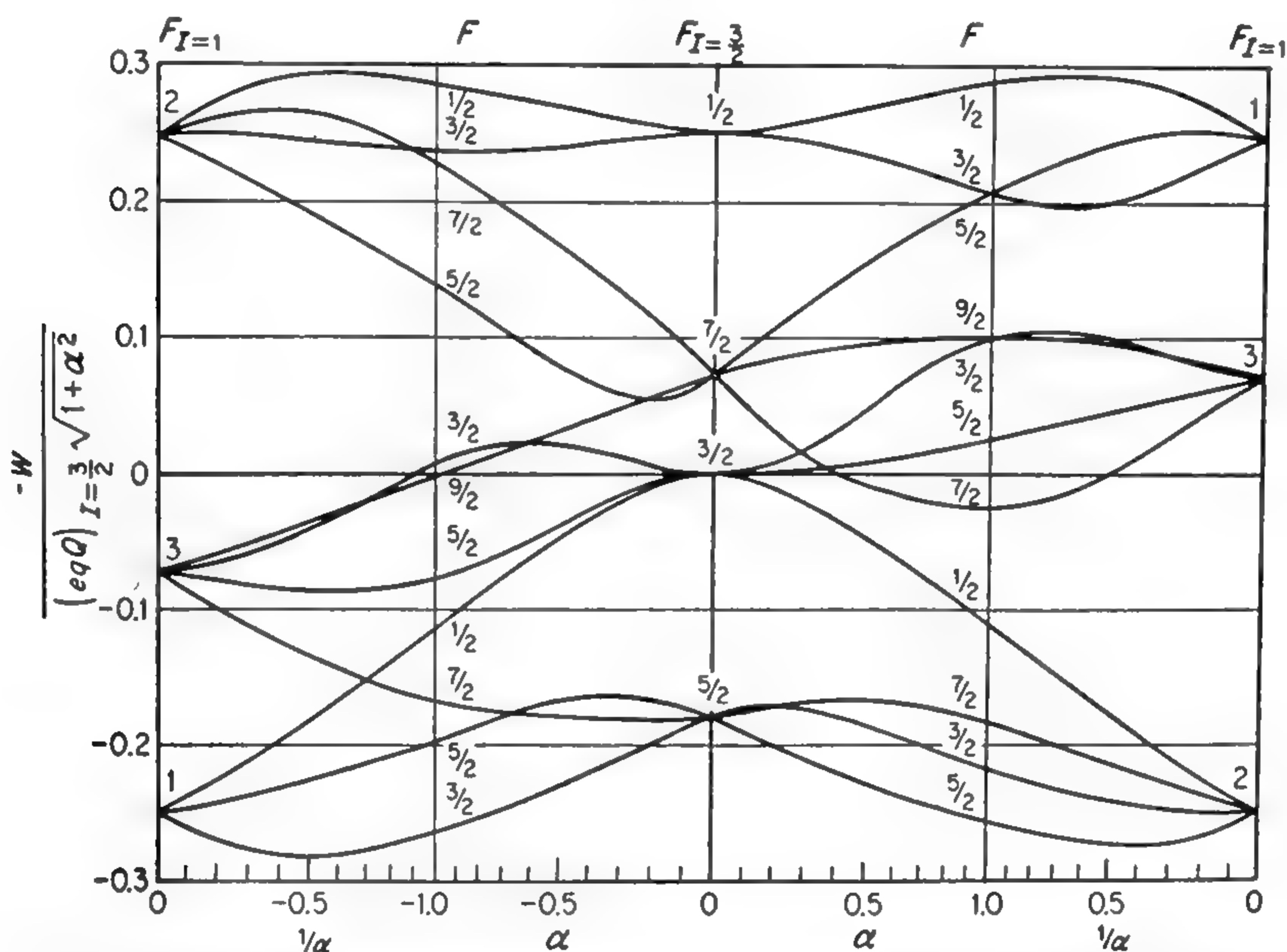


FIG. 6-3. Energies  $W$  resulting from quadrupole coupling of two nuclei of spin 1 and  $\frac{3}{2}$ , when  $J = 2$ . Parameter  $\alpha = (eqQ)_{I=1}/(eqQ)_{I=3/2}$ . (From Bardeen and Townes [252].)

be seen that the first-order approximation is fairly accurate for  $|\alpha| < 0.1$  or  $|1/\alpha| < 0.1$ , but that in intermediate ranges it can be very inaccurate, so that the secular equations must be solved in full. In these intermediate cases, the quantum numbers  $F_1$  and  $F_2$  do not have definite values for each state and the energy levels are designated in the figure only by the values of the total angular momentum  $F$ .

An example of a rotational spectrum with two quadrupole moments is given in Fig. 6-4. This is the  $J = 2 \leftarrow 1$  transition of the ground state of the linear molecule  $\text{Cl}^{35}\text{C}^{12}\text{N}^{14}$ . In this case Cl has a spin of  $\frac{3}{2}$  and a quadrupole coupling constant of  $-83.5$  Mc, whereas  $\text{N}^{14}$ , with a spin of 1, has a coupling constant  $-3.83$  Mc. Thus  $\alpha \approx 0.05$  and the first-order theory is rather accurate, although some small deviations from it are noticeable.

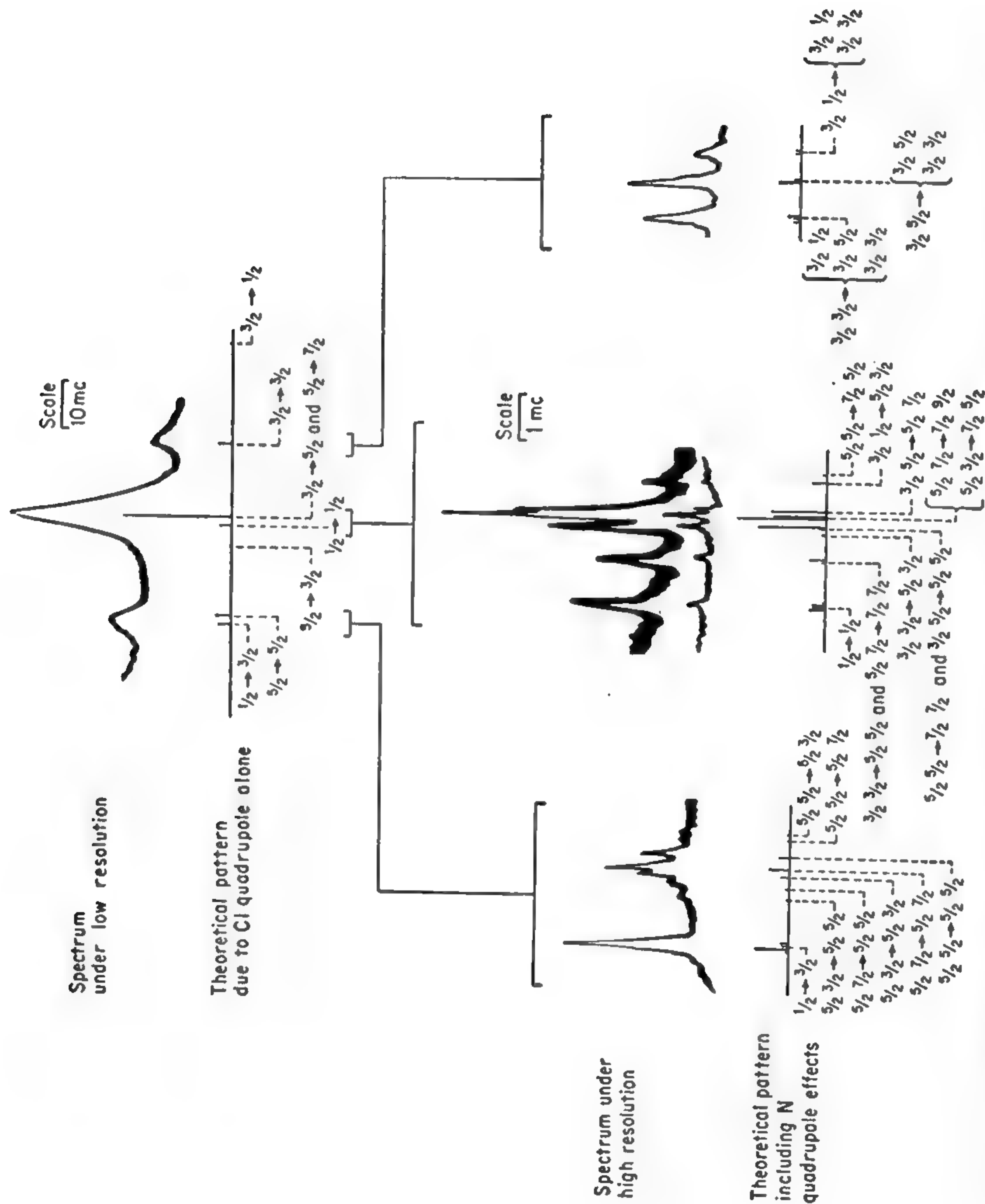


FIG. 6-4. Hyperfine structure of the  $J = 2 \leftarrow 1$  transition of  $\text{Cl}^{35}\text{CN}^{14}$  (ground vibrational state) with low and high dispersion and comparison with theoretical pattern. Spins for  $\text{Cl}^{35}$  and  $\text{N}^{14}$  are  $\frac{3}{2}$  and 1, respectively. (From Townes, Holden, and Merritt [329].)

It should be noted that the technique for calculating the energies for the case of two nuclei given above is not restricted to quadrupole coupling but may be used for any case in which the energies  $W_1$  and  $W_2$ , that is, the eigenvalues for the interaction between the individual nuclei and the molecule, can be obtained. The methods may thus also be used for magnetic coupling, which will be discussed in Chap. 8, or a combination of magnetic and quadrupole coupling.

*Intensities of Hyperfine Components.* In addition to energy levels, intensities are generally required. For the splitting of a line due to one nucleus alone, the fractional intensity in each hyperfine component may be formed from the fine- (or hyperfine-) structure intensity formulas (6-6), which are tabulated in Appendix I. If a second nucleus produces a hyperfine interaction, and its coupling is small compared with the coupling of the first nucleus, expressions (6-6) and the tables of Appendix I may again be applied to find intensities of all components of the still more finely split hyperfine structure. It is only necessary to replace  $L$  by  $F_1$ ,  $S$  by  $I_2$ , and  $J$  by  $F$  in using the tables. Appendix I does not list half-integral values of  $J$ , which will be needed when  $I_1$  is half integral and  $J$  is replaced by  $F_1$ . However, values of intensities for such cases can usually be obtained to sufficient accuracy by interpolation between the nearest integral values. If the couplings of the two nuclei are not widely different, then true intensities cannot be found so directly, but a fair approximation to the intensities may be obtained by interpolating between the two extreme cases when coupling of the first nucleus is large compared with coupling of the second nucleus, and when it is small. Intensities for these extreme cases may be readily obtained from Appendix I.

Exact intensities may, of course, be obtained in cases of intermediate coupling by making use of the energy values obtained by the method described above and solving equations of the type (6-33) for  $a(F_1)$ . The matrix elements between hyperfine states for a single nucleus may be found in Condon and Shortley [56]. They may be designated  $(I_1 J F_1 | \mu_J | I_1 J' F'_1)$  and their squares are proportional to the relative intensities given in Appendix I. A similar matrix element  $(I_2 F_1 F | \mu_{F_1} | I_2 F'_1 F')$  for the transition between the states specified by  $I_2$ ,  $F_1$ , and  $F$  can be obtained in the same way. For intermediate coupling cases, the relative intensity for a transition between states  $i$  and  $j$  would then be given by

$$\left| \sum_{F'_1} \sum_{F_1} a_i(F_1) a_j(F'_1) (I_1 J F_1 | \mu_J | I_1 J' F'_1) (I_2 F_1 F | \mu_{F_1} | I_2 F'_1 F') \right|^2$$

Careful attention must be paid to the phases (see [56], p. 277). This procedure would at best be tedious and in most cases could be replaced by the more rapid approximate method of the preceding paragraph.



*Hyperfine Structure Due to More Than Two Nuclei.* The case of three nuclei coupled by quadrupole effects to a molecule is uncommon except in symmetric tops involving three halogens such as  $\text{AsCl}_3$ ,  $\text{HClBr}_3$ , etc. The resulting hyperfine structure is so complex that so far only one example has been solved, the  $J = 1 \leftarrow 0$  transition of  $\text{HClBr}_3$  [620], [717]. Mizushima and Ito [620] give calculated patterns for the  $J = 1 \leftarrow 0$  transition with a nuclear spin of 1,  $\frac{3}{2}$ , 2, or  $\frac{5}{2}$ .

For more than two nuclei coupled to the same molecule the method discussed above does not apply. Bersohn [437] has given a satisfactory technique for dealing with these more complicated cases by the use of a formulation due to Racah [113]. The state of a molecular system of angular momentum  $J$  with three nuclei of spins  $I_1$ ,  $I_2$ , and  $I_3$  may be designated by the vectors  $\mathbf{I} = \mathbf{I}_1 + \mathbf{I}_2$ ,  $\mathbf{I}^0 = \mathbf{I} + \mathbf{I}_3$ , and  $\mathbf{F} = \mathbf{I}^0 + \mathbf{J}$ , or by the corresponding quantum numbers  $I$ ,  $I^0$ ,  $J$ , and  $F$ . Bersohn [437] obtains for the matrix elements of the quadrupole interactions  $H_Q$  for the three nuclei between states designated by the above quantum numbers, and when perturbations between different values of  $J$  are not important,

$$\begin{aligned}
 & (II^0JF|H_{Q_1} + H_{Q_2} + H_{Q_3}|I'I^0J'F) \\
 &= \frac{(J|eQ_1 \partial^2 V_1 / \partial z^2 |J)(-1)^{I_1+I_2-I_1-I-I'+J'-F}}{8[J(2J-1)I_1(2I_1-1)]^{\frac{1}{2}}} \times [(2I+1)(2I'+1)(2I^0+1) \\
 & \quad (2I^{0'}+1)(2I_1+1)(2I_1+2)(2I_1+3)(2J+1)(2J+2)(2J+3)]^{\frac{1}{2}} \\
 & \times W(I_1I_1II';2I_2)W(II'I^0I^0';2I_3)W(II'JJ';2F) \\
 & + \frac{(J|eQ_2 \partial^2 V_2 / \partial z^2 |J)(-1)^{I_1+I_2-I_2-I-I'+J'-F}}{8[J(2J-1)I_2(2I_2-1)]^{\frac{1}{2}}} \times [(2I+1)(2I'+1)(2I^0+1) \\
 & \quad (2I^{0'}+1)(2I_2+1)(2I_2+2)(2I+3)(2J+1)(2J+2)(2J+3)]^{\frac{1}{2}} \\
 & \times W(I_2I_2II';2I_1)W(II'I^0I^0';2I_3)W(II'JJ';2F) \\
 & + \frac{(J|eQ_3 \partial^2 V_3 / \partial z^2 |J)(-1)^{I-I_1+I^0-I^0'+J'-F}}{[J(2J-1)I_3(2I_3-1)]^{\frac{1}{2}}} \delta_{II'} \times [(2I^0+1)(2I^{0'}+1) \\
 & \quad (2I_3+1)(2I_3+2)(2I_3+3)(2J+1)(2J+2)(2J+3)]^{\frac{1}{2}} \\
 & \quad \times W(I_3I_3I^0I^0';2I)W(I^0I^0'JJ';2F) \quad (6-37)
 \end{aligned}$$

$\delta_{II'}$  is unity for  $I = I'$ , and is otherwise zero. The matrix elements in (6-37) of the form  $(J|eQ_1 \partial^2 V_1 / \partial z^2 |J')$  depend on matrix elements of the direction cosines as may be seen from (6-12). If the rotational state is not much perturbed so that  $J$  is a good quantum number, these take the form  $e(q_J Q)_1$ , where  $q_J$  is given by (6-17) or (6-18). The  $W$  functions of the particular form used in (6-37) may be found in tables by Biedenharn, Blatt, and Rose [674].

In order to solve a specific problem, secular equations must be set up by the use of matrix elements (6-37) and solved. These matrix elements may of course also be used for the case of two nuclei. However, techniques already discussed for handling this case are usually simpler to understand and to apply.

## CHAPTER 7

# MOLECULES WITH ELECTRONIC ANGULAR MOMENTUM

**7-1. Introduction.** Molecules so far discussed have been in  $^1\Sigma$  electronic states. That is, the sum of the orbital angular momenta of their electrons is zero, as is the sum of the electron spins. The  $^1\Sigma$  case is usually the only one which needs consideration since it is the lowest electronic energy level of the vast majority of molecules. However, there are a few gaseous molecules, approximately 0.1 per cent of the total, which do have electronic angular momentum in the ground state, and hence are normally in states other than  $^1\Sigma$ . These include  $O_2$  and the rare molecules with an odd number of electrons, such as NO,  $NO_2$ , and  $ClO_2$ . Molecules with an odd number of electrons cannot have zero electronic spin, and hence are never in  $^1\Sigma$  states. Furthermore, if microwave spectroscopy is done on gases at high temperature or excited in an electrical discharge, molecules will be found in excited or dissociated states which are not  $^1\Sigma$ . Many molecules dissociate under high excitation into smaller parts which have an odd number of electrons and hence possess electronic angular momentum. These dissociated parts are of considerable importance in chemical reactions and gaseous discharges, and are usually called free radicals since they are free, chemically active groups of atoms or radicals.

Since the electrons move much more rapidly than the nuclei of a molecule, to a good approximation the nuclei may be assumed stationary while electron motions in the molecule are being discussed (*cf.* Born-Oppenheimer approximation mentioned in Chap. 1). The electrons in a molecule may have both orbital and spin angular momentum, and the resulting electronic states can be described in a way quite analogous to the electronic states of atoms discussed in Chap. 5. There is a basic difference between the molecular and atomic cases, however, because the electric fields due to an atomic nucleus are spherically symmetric, while those due to the two or more nuclei in a molecule are by no means spherically symmetric. Since a molecular electron does not move in a spherically symmetric field, torques are exerted on it by the field, and its angular momentum cannot be constant as it is in an atom. The simplest molecular case is a diatomic or linear molecule, where the fields are symmetric about the molecular axis. Because of this symmetry, no torque about the axis is exerted on a molecular electron, and the com-



ponent of its angular momentum in the direction of the molecular axis is constant.

The diatomic molecule is somewhat similar to an atom subjected to a very large electric field along the direction of the molecular axis. This field produces a large Stark effect (see Chap. 10) which interferes with the orbital motion of the electrons. Although the orbital angular momentum is not constant and the quantum number  $L$  loses its significance, in many cases the projection  $M_L$  of  $\mathbf{L}$  on the axis is constant. For molecules, the symbol  $\Lambda$  is written for  $M_L$ , since  $L$  itself is not of significance, and  $\Lambda$  is the Greek substitute for  $L$ . The energy is dependent on the value of  $\Lambda$ , which is, of course, integral and may equal  $L$ ,  $L - 1$ , . . . ,  $-L$ . However, positive and negative values of  $\Lambda$  have the same energy (see Chap. 10), so that, unless  $\Lambda = 0$ , the levels are doubly degenerate. This degeneracy may be removed by the rotation-electron interaction discussed below called  $\Lambda$ -type doubling.

There is a close parallelism between the various angular momenta involved in molecules and those in atoms and the notation used in each case is outlined in Table 7-1. Molecules involve more types of angular momenta because of the possibility of end-over-end rotation of a molecule. In addition, for linear and symmetric-top molecules the projection of various angular momenta on the symmetry axis may be of interest as well as their projections on a direction fixed in space. Only the latter occur in discussions of atoms. It must be noted that not all the quantum numbers listed in Table 7-1 are normally used for any one case. For example, if the projection  $\Lambda$  of  $\mathbf{L}$  on the molecular axis is constant, then its projection  $M_L$  on a space-fixed axis is not constant, and usually not of interest.

In diatomic or linear molecules where spin-orbit effects are not enormously large, the projection  $\Lambda$  of  $\mathbf{L}$  on the molecular axis is constant and replaces  $L$  in importance. If the linear molecule is bent as in a bending vibrational mode, or if the molecule is not linear, then the electric fields are not symmetrical about the axis and  $\Lambda$  is no longer fixed or well defined. In nonlinear molecules, the orbital motion of electrons is almost completely "quenched" or suppressed, and a spin momentum is the only angular momentum in the molecule of distinctly electronic origin.

If the electronic orbital angular momentum  $\Lambda$  along the internuclear axis of a linear molecule is 0,  $\pm 1$ ,  $\pm 2$ ,  $\pm 3$ , . . . , the molecule is said to be in a  $\Sigma$ ,  $\Pi$ ,  $\Delta$ ,  $\Phi$ , . . . state, respectively, in analogy with the atomic  $S$ ,  $P$ ,  $D$ ,  $F$  states having  $L = 0$ , 1, 2, or 3. In this and several other respects, notation for molecular spectra can be regarded as the Greek translation of notation for atomic spectra. If the electronic spin is 0,  $\frac{1}{2}$ , 1, . . . , the state is said to be singlet, doublet, or triplet—again in analogy with the atomic case—and a corresponding superscript is applied to the left of the state designation. Thus  $^2\Pi$  indicates  $S = \frac{1}{2}$  and  $\Lambda = 1$ .



The component of the total angular momentum along the molecular axis may have the values  $\Lambda + S, \Lambda + S - 1, \dots, \Lambda - S$ , and is written as a right-hand subscript, for example,  ${}^2\Pi_{3/2}, {}^2\Pi_{1/2}$ . Its absolute value is called  $\Omega$ , that is,  $\Omega = |\Lambda + \Sigma|$ .

Van Vleck [657] has discussed the general problem of coupling angular-momentum vectors in molecules. He shows that, if the internal angular

TABLE 7-1. EXPLANATION OF NOTATION FOR ANGULAR MOMENTA INVOLVED IN MOLECULAR SPECTRA AND COMPARISON WITH NOTATION FOR ATOMIC SPECTRA

When the nuclear spin is zero or unimportant,  $J$  is used instead of  $F$ . When there is no electronic spin,  $J$  is identical with  $N$  and is used in its place. Similarly, when the electronic spin is zero, the projection of  $J$  on the molecular axis is equal to  $K$ , which is used instead of  $\Omega$ .

	Molecule	Atom
Nuclear spin angular momentum.....	<b>I</b>	<b>I</b>
Projection on space-fixed axis.....	$M_I$	$M_I$
Projection on molecular axis.....	$\Omega_I$	
Electron spin angular momentum.....	<b>S</b>	<b>S</b>
Projection on space-fixed axis.....	$M_S$	$M_S$
Projection on molecular axis.....	$\Sigma$	
Electronic orbital angular momentum.....	<b>L</b>	<b>L</b>
Projection on space-fixed axis.....	$M_L$	$M_L$
Projection on molecular axis.....	$\Lambda$	
Sum of spin and electronic orbital momentum ( $\mathbf{L} + \mathbf{S}$ ).....	$\mathbf{J}_e$	<b>J</b>
Orbital angular momentum due to nuclear motion (rotation of molecule).....	<b>O</b>	
Total orbital angular momentum including rotation of molecule...	<b>N</b>	<b>L</b>
Projection on molecular axis.....	$K$	
Total angular momentum excluding nuclear spin.....	<b>J</b>	<b>J</b>
Projection on space-fixed axis.....	$M_J$	$M_J$
Projection on molecular axis (absolute value).....	$\Omega$	
Total angular momentum including nuclear spin.....	<b>F</b>	<b>F</b>
Projection on space-fixed axis.....	$M_F$	$M_F$
Projection on molecular axis.....	$\Omega_F$	

momenta (all momenta except  $J$ , the total) are reversed in sign, they and the total angular-momentum vectors follow the same commutation rules as angular-momentum vectors in an atom. Hence for every problem of coupling angular-momentum vectors in a molecule there is a corresponding situation in atoms, and the matrix elements given by Condon and Shortley [56] for atoms can be applied in the molecular problem. Van Vleck's discussion is highly recommended to the advanced student, but it will not be needed below since no actual solution of intermediate coupling or other complex cases will be carried out.

**7-2. Hund's Coupling Cases.\*** The notation of the last section is not always appropriate because the molecular angular momenta may interact or couple together in a variety of ways. The coupling schemes or cases were first systematically treated by Hund, who described five ideal cases. Molecules do not fit such ideal descriptions exactly, but Hund's cases are very good approximations to the actual states of many linear molecules. (For nonlinear molecules Hund's considerations are not useful.) Which case applies most closely depends on the relative strength of the various couplings, or the relative energy of interaction between the vectors. In all known cases, coupling between the nuclear spin and other vectors by hyperfine interactions is much smaller than other couplings. Interactions whose relative magnitude needs to be considered occur between any two of the vectors  $L$ ,  $S$ ,  $N$ ,  $O$ , and  $A$ , where  $A$  is a vector along the molecular axis. Interactions between two of these vectors will be represented by a notation like  $SA$ , which indicates an interaction between the electronic spin and the molecular axis.

*Hund's Case (a).* In Hund's case (a) the strongest interactions are between the molecular axis and  $L$  and between the axis and  $S$ . That is,

$$\begin{aligned} LA &\gg LS \text{ or } LO \\ SA &\gg SN \end{aligned}$$

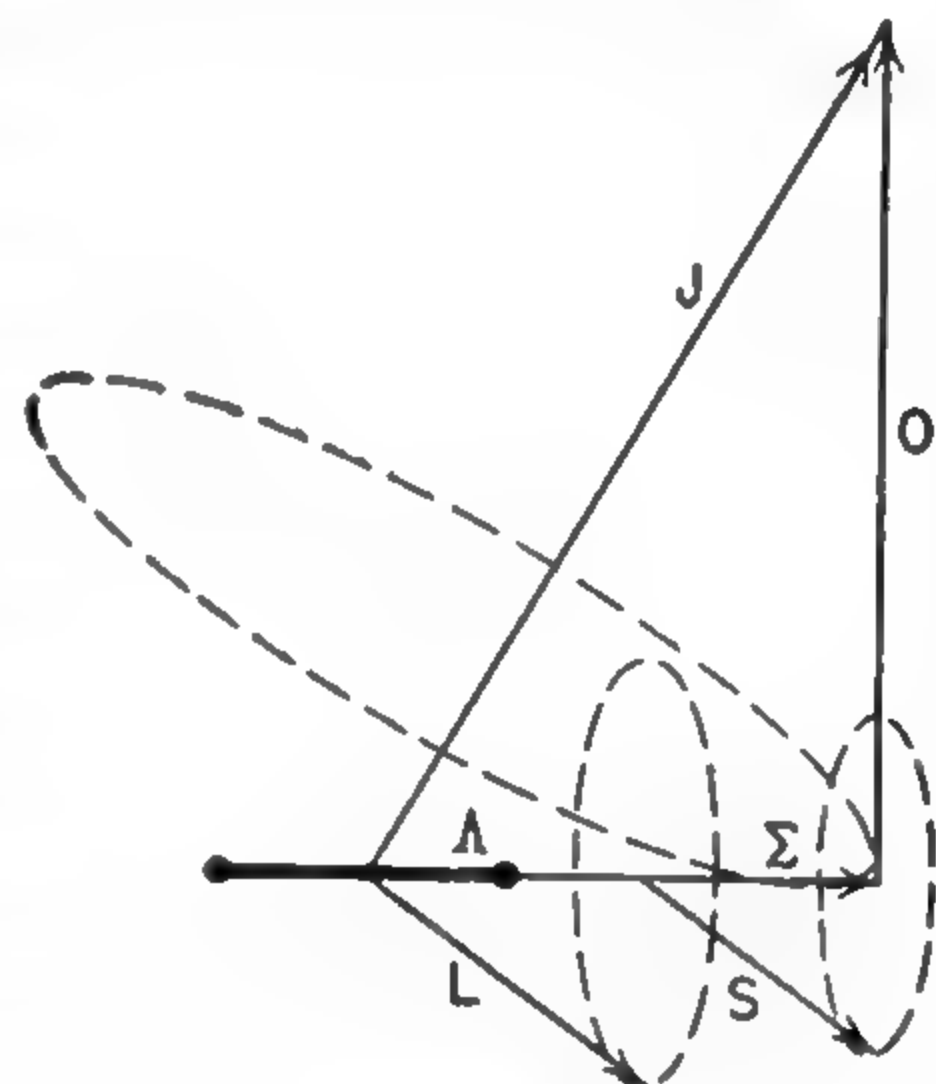


FIG. 7-1. Vector diagram of Hund's case (a).  $L$  and  $S$  precess rapidly around the molecular axis, which precesses more slowly around the total angular momentum  $J$ . Circles indicate these precessional motions.

The vector model of this case is shown in Fig. 7-1.  $L$  interacts strongly with the axial field of the molecule and hence precesses about the molecular axis, so that its projection  $\Lambda$  is constant. Similarly  $S$  precesses with constant projection  $\Sigma$ , so that the total angular momentum along the molecular axis is  $\Omega = |\Lambda + \Sigma|$ .  $\Lambda + \Sigma$  adds vectorially to the angular momentum  $O$  of the end-over-end molecular rotation to form the total angular momentum (excluding nuclear spin)  $J$ . The angular momenta  $\Omega$  and  $O$  hence precess around the vector  $J$  which is fixed in space.

The relations between  $J$  and  $\Omega$  in case (a) are just the same as those between  $J$  and the angular momentum  $K$  around the axis of a symmetric-top molecule. The quantity  $\Omega$  is integral if the molecule contains an even number of electrons, but it is half integral if the number of electrons is odd. This is because  $\Sigma$  takes on only the values  $S, S - 1, \dots, -S$ , and the sum of electron spins  $S$  is half integral if the number of electrons

\* For an extensive treatment of Hund's coupling cases see also Herzberg [471].

is odd. As in the case of a symmetric top, the total angular momentum  $J$  cannot be less than its projection  $\Omega$  on the axis so that  $J$  has values  $\Omega, \Omega + 1, \Omega + 2, \dots$

*Hund's Case (b).* In Hund's case (b) the electron spin is coupled more strongly to  $\mathbf{N} = \mathbf{L} + \mathbf{O}$  than to the molecular axis.  $\mathbf{L}$ , however, is still strongly coupled to the molecular axis.

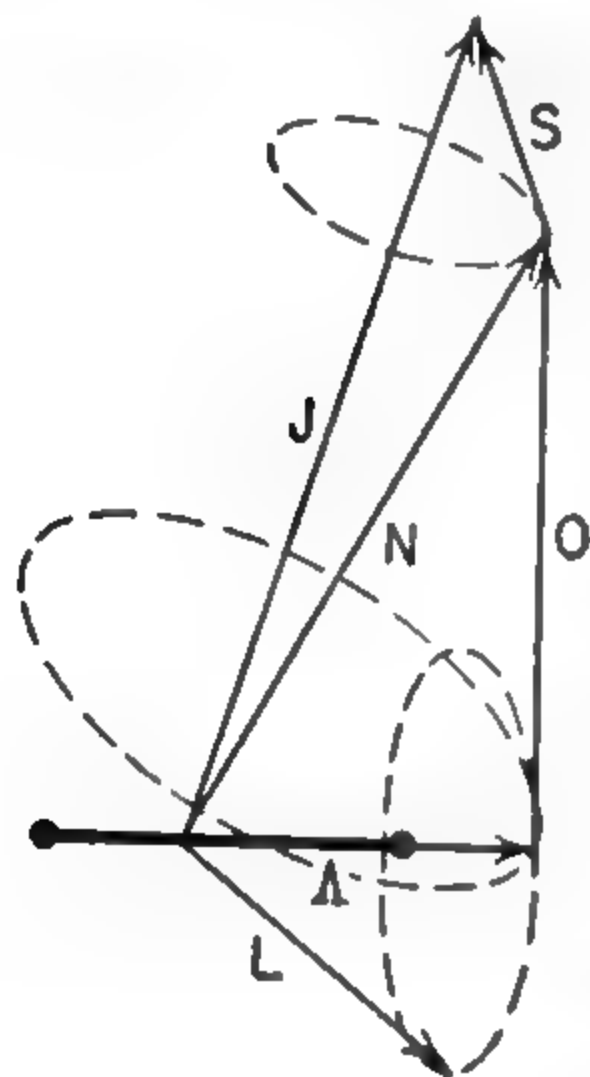


FIG. 7-2. Vector diagram for Hund's case (b). Precession of the molecular axis, represented by the largest ellipse, is slower than the precession of  $\mathbf{L}$  about the axis, but faster than the precessions of  $\mathbf{S}$  and  $\mathbf{N}$  about  $\mathbf{J}$ . When  $\Lambda = 0$ ,  $\mathbf{N}$  is identical with  $\mathbf{O}$  and is perpendicular to the molecular axis.

$$\mathbf{L}\mathbf{A} \gg \mathbf{L}\mathbf{S} \text{ or } \mathbf{L}\mathbf{O}$$

$$\mathbf{S}\mathbf{N} \gg \mathbf{S}\mathbf{A}$$

The appropriate vector diagram for this case is shown in Fig. 7-2.  $\mathbf{L}$  precesses rapidly around the molecular axis.  $\mathbf{L}$  adds to  $\mathbf{O}$  to form the total orbital angular momentum  $\mathbf{N}$ .  $\mathbf{N}$  and  $\mathbf{S}$  add to form  $\mathbf{J}$ , about which they precess.

The spin is usually coupled to the axis by spin-orbit coupling, *i.e.*, the spin is coupled to  $\mathbf{L}$  rather than to the axis itself. Hence for molecules with  $\Lambda = 0$ , coupling between the spin and molecular axis is small, and it is these molecules with  $\Lambda = 0$  which typically fall in Hund's case (b). When  $\Lambda = 0$ , the orbital angular momentum is entirely due to molecular rotation ( $\mathbf{N} \equiv \mathbf{O}$ ), and is perpendicular to the molecular axis.

There are molecules, however, with  $\Lambda$  not equal to zero which fall approximately in case (b). These are usually very light molecules such as hydrides which rotate rapidly and for large values of  $O$  produce a coupling between  $\mathbf{O}$  and  $\mathbf{S}$  which is greater than the spin-axis interaction. The  $\mathbf{S}\mathbf{A}$  interaction tends to be weak in these cases anyhow, because the nuclear charge  $Z$  is small (page 122), and spin-orbit coupling is small. The free radical  $\text{OH}$  is in a  ${}^2\Pi$  state and is a molecule of this type.

Hund's cases (a) and (b) are by far the most important. However, other cases are possible. More detailed discussion of the following three rare or nonexistent cases is given by Mulliken [22], [26], [100] and Weizel [29].

*Hund's Case (c).* For heavy nuclei, the atomic spin-orbit interaction becomes very large. Similarly in molecules involving heavy nuclei, the interaction  $\mathbf{L}\mathbf{S}$  may be larger than the interaction between  $\mathbf{L}$  and the molecular axis. This gives Hund's case (c), when

$$\mathbf{L}\mathbf{S} \gg \mathbf{L}\mathbf{A}$$

In this case  $\Lambda$  and  $S$  are not good quantum numbers, but  $\mathbf{L}$  and  $\mathbf{S}$  add vectorially to form a resultant  $\mathbf{J}_a$  which is then coupled to the inter-



nuclear axis with a projection  $\Omega$  on this axis.  $\Omega$  adds vectorially to the angular momentum  $O$  of end-over-end rotation to form the total angular momentum  $J$ . Figure 7-3 is a vector diagram for this case.

*Hund's Case (d).* If the coupling between  $L$  and the angular momentum  $O$  is much larger than that between  $L$  and the molecular axis, Hund's case (d) occurs.

$$LO \gg LA$$

A vector diagram of this case is shown in Fig. 7-4.

*Hund's Case (e).*  $L$  and  $S$  may conceivably be strongly coupled and their resultant coupled to  $O$  rather than to the internuclear axis. This would give Hund's case (e) which has not yet been observed.

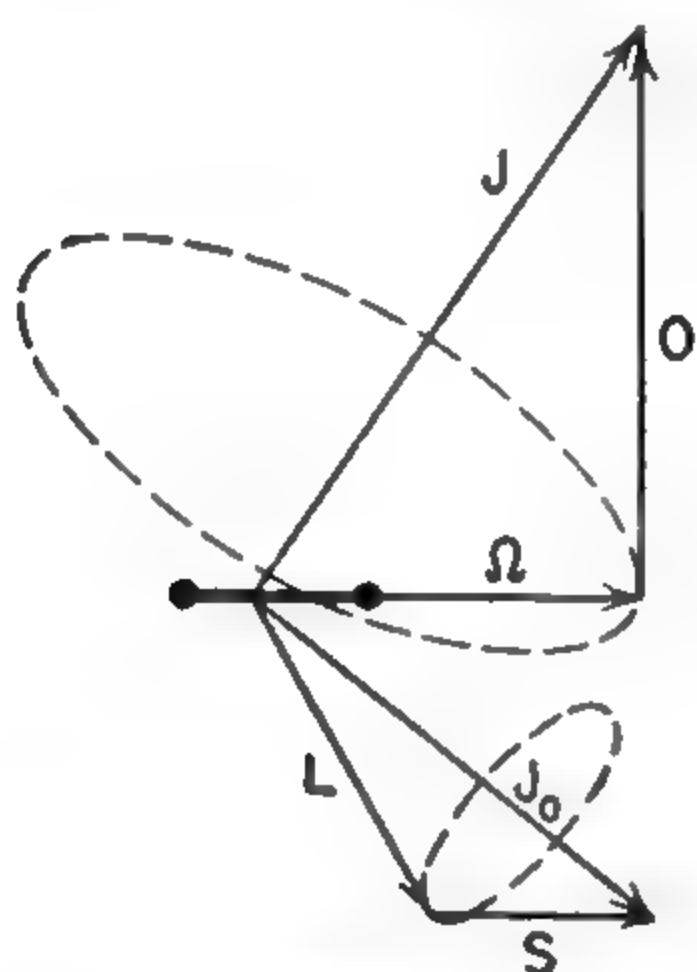


FIG. 7-3. Vector diagram for Hund's case (c). Precession of  $L$  and  $S$  about  $J_0$  is much faster than the precession (not shown) of  $J_0$  about the internuclear axis.

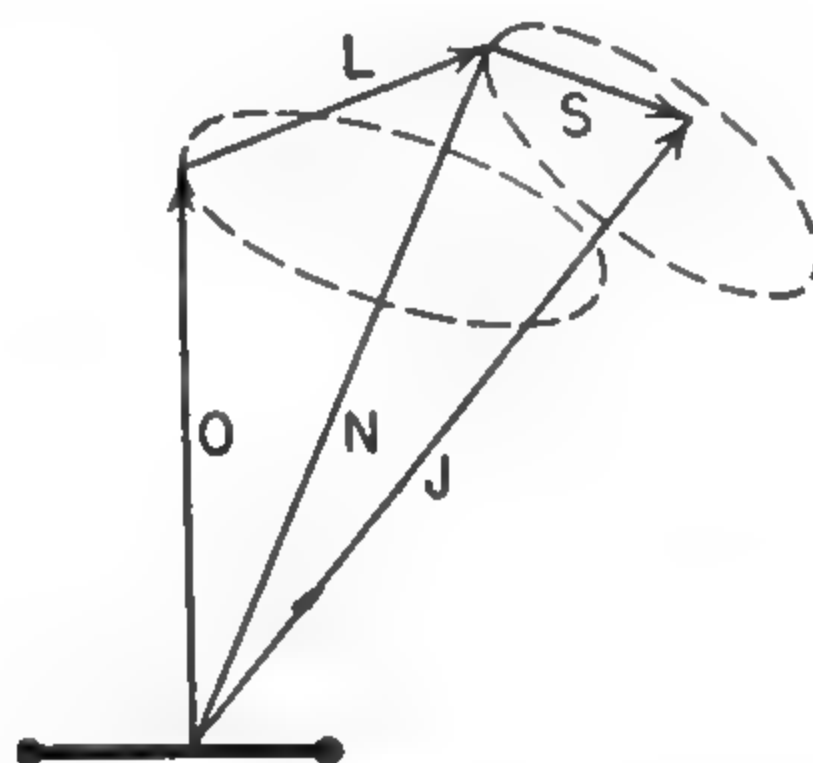


FIG. 7-4. Vector diagram for Hund's case (d).  $L$  is coupled to  $O$  rather than to the internuclear axis.  $S$  adds to the resultant  $N$  to form  $J$ .

Hund's coupling cases are idealizations to which many molecules approximately conform. However, noticeable deviations from these idealizations often occur and may be expected to be particularly evident if the spectra of these types of molecules are accurately measured by microwave spectroscopy. These deviations represent a partial uncoupling of two vectors by the effect of a third vector. In some cases, too, the deviations are very large, for a molecule may fall approximately into one coupling case for low rotational states, but into another case for high rotational states. For intermediate rotational states, such a molecule does not fall into any of Hund's coupling cases but is said to have intermediate coupling.

Some of the most interesting examples of uncoupling phenomena are those in which end-over-end rotation of the molecule uncouples the electronic momenta from the molecular axis, as it tends to do especially for high rotational states where the rotation is rapid. In extreme cases, rapid rotation may almost completely uncouple  $S$  from the molecular axis, producing a transition from Hund's case (a) for low rotational states

to case (b) for higher states. Molecular rotation also interacts with the electronic orbital angular momentum  $\Lambda$  and removes the degeneracy corresponding to the two different possible orientations of  $\Lambda$  or  $\Omega$  along the molecular axis which are degenerate when the molecule is not rotating. The effect is called  $\Lambda$ -type doubling, and may be regarded as an incipient uncoupling of  $\mathbf{L}$  from the molecular axis by the rotation which, in extreme cases, would lead to Hund's case (d).

Another phenomenon associated with uncoupling is the magnetic field produced by end-over-end molecular rotation. This rotation slightly uncouples  $\mathbf{L}$  from the molecular axis even in  $\Sigma$  states and orients  $\mathbf{L}$  with respect to the angular momentum of rotation. Thus  $\mathbf{L}$  uncoupling results in fields which interact with the electron spin moments or, when hyperfine structure can occur, with nuclear moments.

**7-3. Rotational Energies.** The rotational energies of molecules with electronic angular momentum will be treated first with the assumption of pure Hund's coupling cases, and then the additional energy terms due to uncoupling phenomena will be discussed.

*Case (a).* Because of the similarity of  $J$  and  $\Omega$  in Hund's case (a) to  $J$  and  $K$  for an ordinary symmetric top, the energy levels in this case must be of the same form as (3-5), letting  $B_v$  be in energy units rather than in cycles per second.

$$W = B_v[J(J + 1) - \Omega^2] + A\Omega^2 \quad (7-1)$$

In this case, however, the "rotational constant"  $A$  is extremely large, and  $A\Omega^2$  represents electronic energy. Since any transition involving electronic energy would not lie in the microwave range, and such energy is not usually called rotational energy, terms of this type are omitted, so that

$$W(J) = B_v[J(J + 1) - \Omega^2] \quad (7-2)$$

In addition, since changes in  $\Omega$  would almost always produce frequencies higher than the microwave range,  $B_v\Omega^2$  must be constant and may be neglected. Hence for the purposes of microwave spectroscopy the still simpler form

$$W(J) = B_vJ(J + 1) \quad (7-3)$$

may be used.

Rotational energy levels for case (a)  $^2\Pi$  and  $^3\Delta$  levels are shown in Fig. 7-5. Except for the nonexistence of values of  $J$  less than  $\Omega$  and for the added energy  $B_v\Omega^2$ , which is independent of  $J$ , the energy levels are much the same as those for a normal molecule in a  $^1\Sigma$  state. However, half-integral values of  $J$  may occur instead of only integral values, since  $J = \Omega, \Omega + 1, \Omega + 2, \dots$ . The levels also show an additional splitting, the  $\Lambda$ -doubling, which will be discussed more fully below.

*Case (b).* If the electron spin is neglected, then the rotational energy of a case (b) molecule is of the same simple form as (7-3), that is,

$$W_R = B_v N(N + 1)$$

or  $B_v J(J + 1)$ , since  $J \equiv N$  when spin is neglected.

The simplest type of case (b) molecules are in  $^2\Sigma$  states, having electron spin of  $\frac{1}{2}$ . The magnetic moment associated with this spin interacts

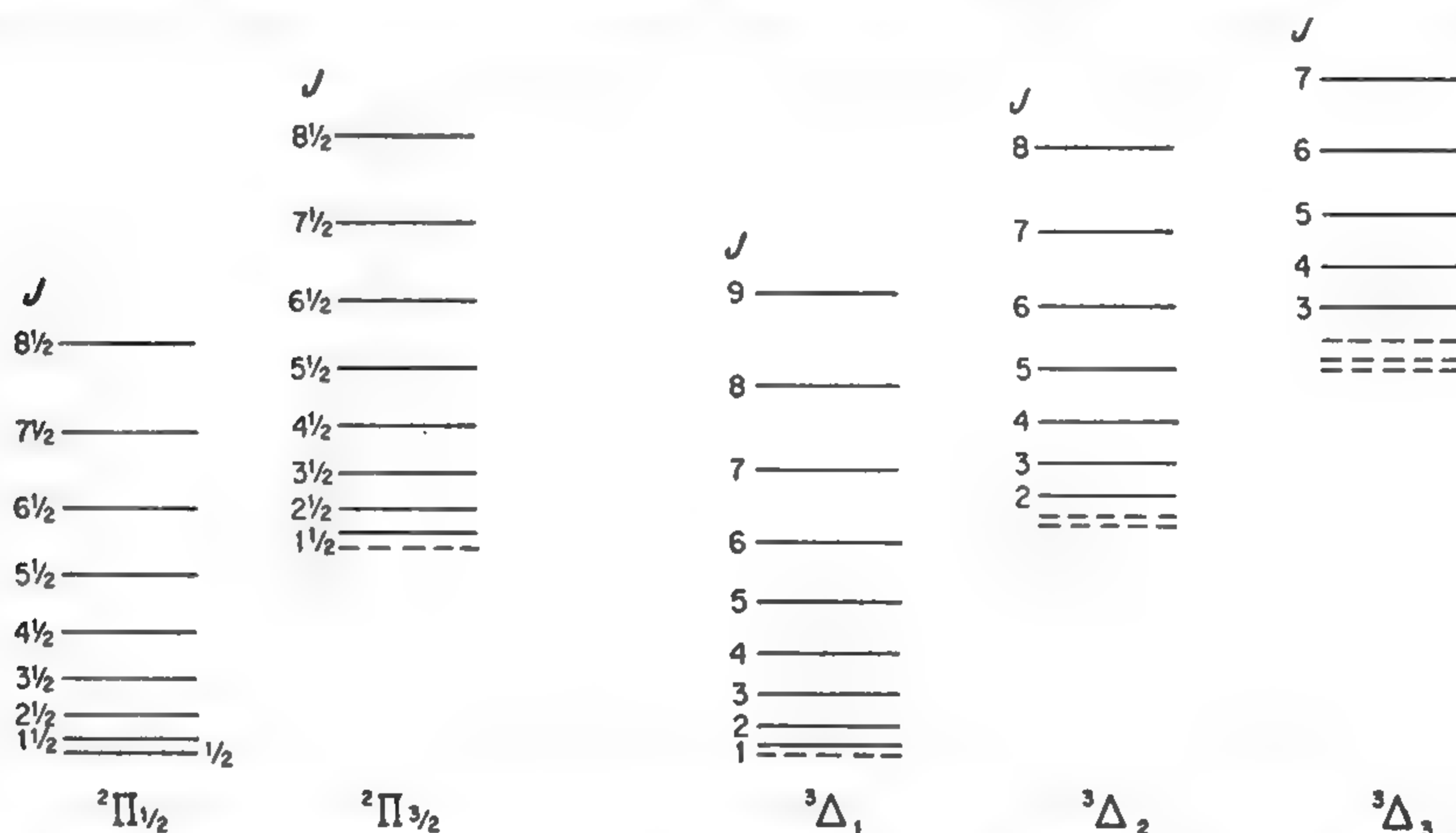


FIG. 7-5. The lower rotational energy levels of a case (a) molecule in  $^2\Pi$  or  $^3\Delta$  state.  $\Lambda$ -type doubling is too small to be shown on this scale. The dotted levels cannot occur, since  $J$  must be  $\geq \Omega$ .

with the magnetic fields produced by molecular rotation, thus giving an interaction energy proportional to the cosine of the angle between  $\mathbf{S}$  and  $\mathbf{N}$ , or of the form

$$W_M = \gamma \mathbf{S} \cdot \mathbf{N} \quad (7-4)$$

From the vector model,

$$\mathbf{S} \cdot \mathbf{N} = \frac{J(J + 1) - S(S + 1) - N(N + 1)}{2}$$

Hence for  $J = N + \frac{1}{2}$ ,  $W_M = (\gamma/2)N$ , and for  $J = N - \frac{1}{2}$ ,

$$W_M = -\frac{\gamma}{2}(N + 1)$$

Thus the total rotational energy including the electron spin interaction is [22]

$$\begin{aligned} W &= B_v N(N + 1) + \frac{\gamma}{2} N & \text{when } J &= N + \frac{1}{2} \\ W &= B_v N(N + 1) - \frac{\gamma}{2} (N + 1) & \text{when } J &= N - \frac{1}{2} \end{aligned} \quad (7-5)$$



These expressions neglect small centrifugal distortion terms of the form  $D_v N^2(N+1)^2$ , which occasionally may be needed.

The constant  $\gamma$  is a measure of the strength of the magnetic field produced by molecular rotation. This field can be regarded as partly due to the simple rotation of charges distributed in the molecule, but its largest part is due to  $L$  uncoupling [17].  $L$  uncoupling (also discussed in Chaps. 1 and 8) is a transfer of angular momentum from the end-over-end motion of the molecule to electronic orbital motion. Electrons are thus partly excited by the molecular rotation to a state with orbital angular momentum lying along  $N$  and hence have a magnetic field in this direction which interacts with the electron's magnetic moment. The ease of excitation, and therefore the size of  $\gamma$ , depends on how near the excited  $\Pi$  state lies to the ground  $\Sigma$  state. In any case the amount of excitation of electronic angular momentum is rather small, so that the electronic state may still be considered essentially a  $^2\Sigma$  state.

For case (b) molecules with  $S$  larger than  $\frac{1}{2}$ , i.e., in  $^3\Sigma$  or  $^4\Sigma$  states, other types of interactions occur. In a  $^3\Sigma$  state, there are two electrons with spins parallel, and the magnetic moments of these electrons interact. This "spin-spin interaction" varies as the  $\cos^2 \theta$ , where  $\theta$  is the angle between the direction of the two parallel spins and the line between the two electrons, which when averaged is equivalent to the angle between  $S$  and the molecular axis [15]. In addition, the magnetic moments of the electrons magnetically polarize the molecule. Their fields partly excite the electrons into  $\Pi$  orbits, and these excited states produce fields which react back on the electron moments. Hebb [73] showed that this energy of magnetic polarization varies also with the  $\cos^2 \theta$  and is not easily distinguishable from the spin-spin interaction. This type of interaction is also an  $L$  uncoupling due to  $S \cdot L$  type interaction, and is large if there is a low-lying  $\Pi$  state which can easily be excited. It does not occur when  $S = \frac{1}{2}$ , for the same reasons that no nuclear quadrupole interactions occur when the nuclear spin is  $\frac{1}{2}$ , since, like the quadrupole interaction, it depends on  $\cos^2 \theta$ . In fact, this type of effect is sometimes called a pseudo quadrupole interaction because of the formal similarity.

To a first approximation, energies for a  $^3\Sigma$  molecule are given by

$$\begin{aligned} W(J = N + 1) &= B_v N(N + 1) - \frac{2\lambda(N + 1)}{2N + 3} + \gamma(N + 1) \\ W(J = N) &= B_v N(N + 1) \\ W(J = N - 1) &= B_v N(N + 1) - \frac{2\lambda N}{2N - 1} - \gamma N \end{aligned} \tag{7-6}$$

where  $\gamma$  is a constant which is a measure of the magnetic interaction of the type described above for the  $^2\Sigma$  state and  $\lambda$  is a constant which measures the magnetic interaction of the spin-spin and polarization types.

The term involving  $\lambda$  represents "pseudo quadrupole" interactions, and except for the constants involved it may be obtained from the expression (5-45) for quadrupole energy in first-order perturbation theory.  $N$  takes the place of  $J$ ,  $S$  that of  $I$ , and  $J$  that of  $F$  in using (5-45). As might be expected, this energy is not strongly dependent on  $N$ , and for large  $N$  it has the same value for  $J = N + 1$  and  $J = N - 1$ , since these two states both have the same value of  $\cos^2 \theta$  in the classical limit of large  $N$ . The interaction involving  $\lambda$  is usually so big that the approximate formulas (7-6) are too inaccurate to be of much value in interpreting microwave spectra. This interaction perturbs the molecular rotational motion in much the same way as a large nuclear quadrupole coupling (*cf.* Chap. 6). A given energy state cannot have a precisely defined rotational angular momentum  $N$  but involves small admixtures of the states  $N + 2$  and  $N - 2$ . In the case of  $O_2$ , for which the ground state is  $^3\Sigma$ ,  $\lambda$  is approximately 60,000 Mc, while  $B$  is near 40,000 Mc, so that the pseudo quadrupole interaction represents a large perturbation of the rotational energy levels. The exact energies may be obtained by solving a secular equation, as was first done by Schlapp [85]. A more precise form of Schlapp's equations given by Miller and Townes [841] is

$$\begin{aligned}
 W(J = N - 1) &= B_v N(N + 1) - B_v(2N - 1) - \lambda - \frac{\gamma}{2} \\
 &\quad + \left[ \lambda^2 - 2\lambda \left( B_v - \frac{\gamma}{2} \right) + (2N - 1)^2 \left( B_v - \frac{\gamma}{2} \right)^2 \right]^{\frac{1}{2}} \\
 W(J = N) &= B_v N(N + 1) \\
 W(J = N + 1) &= B_v N(N + 1) + B_v(2N + 3) - \lambda - \frac{\gamma}{2} \\
 &\quad - \left[ \lambda^2 - 2\lambda \left( B_v - \frac{\gamma}{2} \right) + (2N + 3)^2 \left( B_v - \frac{\gamma}{2} \right)^2 \right]^{\frac{1}{2}}
 \end{aligned} \tag{7-7}$$

Constant terms  $2\lambda - \gamma$  have been subtracted from each of the expressions (7-7), since they do not contribute to the frequency of transitions. The fine-structure separations  $W(J = N) - W(J = N + 1)$  and

$$W(J = N) - W(J = N - 1)$$

are plotted in Fig. 7-6 for the  $O_2$  molecule.

The  $O_2$  molecule has no electric dipole moment, but since it is in a  $^3\Sigma$  state, there is a magnetic dipole moment which allows transitions between rotational levels and their fine-structure components. Since  $B_v$  for  $O_2$  is 43,100 Mc, and the rotational transitions obey the selection rule  $\Delta N = \pm 2$  [990], they occur at wavelengths too short for present microwave techniques. However, transitions between fine-structure components without a change in  $N$  occur at wavelengths near 5 mm and have been fairly

extensively studied. Matrix elements for these transitions are [56]

$$\begin{aligned} |\mu_{J=N+1 \leftarrow N}|^2 &= 4\mu_0^2 \frac{N(2N+3)}{(2N+1)(N+1)} \\ |\mu_{J=N-1 \leftarrow N}|^2 &= 4\mu_0^2 \frac{(N+1)(2N-1)}{(2N+1)N} \end{aligned} \quad (7-8)$$

Even though the Bohr magneton  $\mu_0$  which is involved is rather small ( $0.9 \times 10^{-20}$  emu as compared with  $10^{-18}$  esu for typical electric dipole

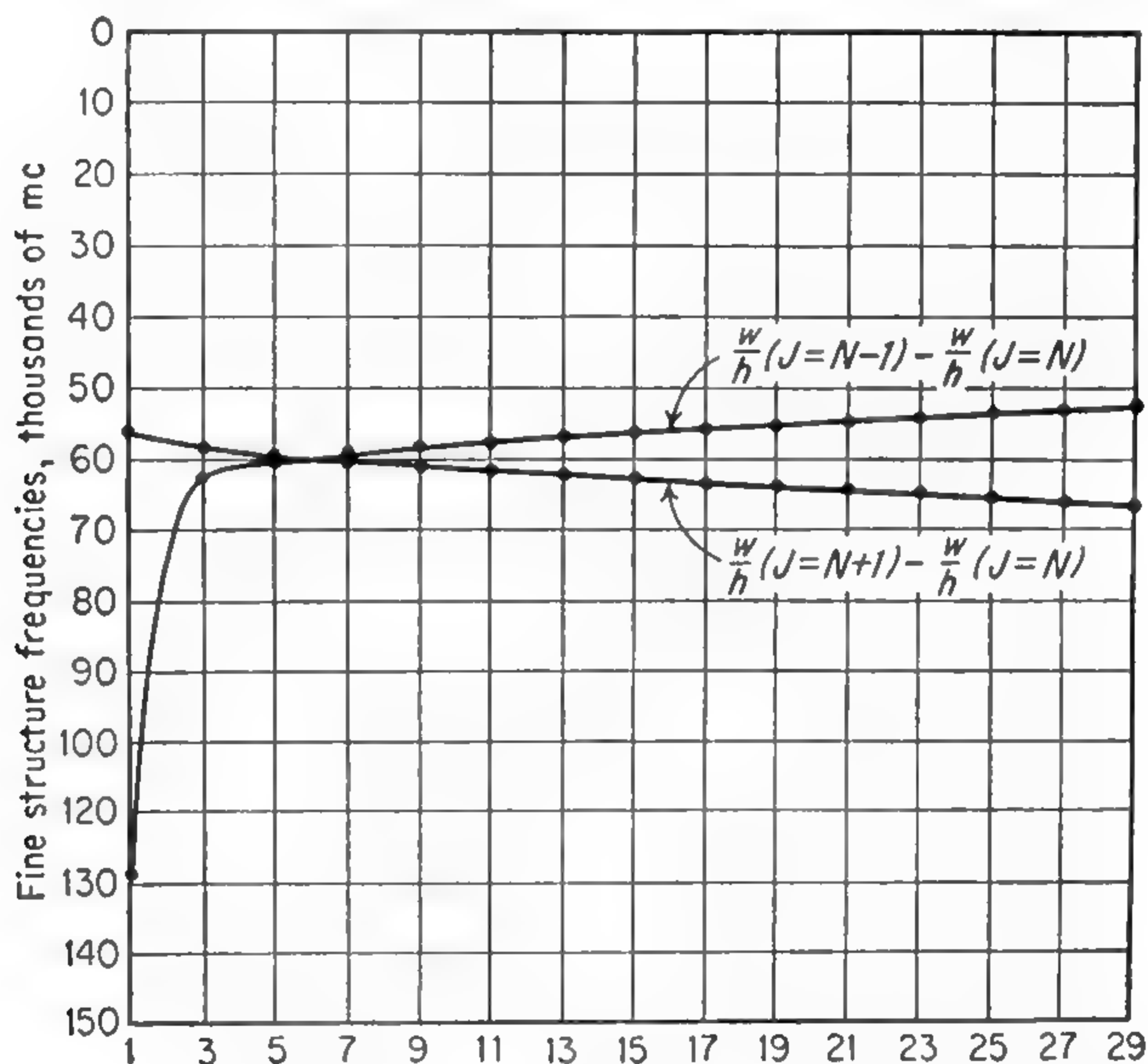


FIG. 7-6. Separation of spin triplets in  $^3\Sigma_g^-$  ground state of  $O_2$ . (From Artman [892b].)

moments), some of these transitions have intensities as large as  $10^{-5}$   $\text{cm}^{-1}$  because of the large fraction of  $O_2$  molecules in each state of low  $N$ .

Approximately 25 lines have been measured for  $O^{16}O^{16}$  ([441], [554], [576], and [963]) and fitted to expression (7-7). From this fit,  $B_0$  is found to be 43,101 Mc,  $\lambda = 59,501$  Mc, and  $\mu = 252.7$  Mc. However, it is necessary to replace  $B_v$  by

$$B_{ef} = B_0 - N(N+1)D_v \quad (7-9)$$

for an exact fit. Since  $N$  varies from 1 to about 25, and  $D_v = 4B^3/\omega_e^2$ ,  $N(N+1)D_v$  becomes as large as  $0.0025B_v$  in (7-9). In addition, centrifugal stretching of the molecule appears to vary  $\lambda$  a small amount for large  $N$ . The experimental measurements can be fitted with

$$\lambda = 59,501.6 + 0.0575N(N+1) \text{ Mc}$$

The spectrum of other isotopic species of  $O_2$  may be predicted from the determination of  $B_v$ ,  $\lambda$ , and  $\gamma$  for  $O^{16}O^{16}$ , since  $B_v$  and  $\gamma$  are inversely



proportional to the reduced mass, while  $\lambda$  is approximately independent of the isotopic mass. Frequencies for  $\text{O}^{16}\text{O}^{18}$  and  $\text{O}^{18}\text{O}^{18}$  have been found to agree rather well with such predictions [841].

Pseudo quadrupole interactions also occur in  $^4\Sigma$  states, another example of Hund's case (b). Since a quartet state has  $S = \frac{3}{2}$ ,  $J$  may have the values  $N + \frac{3}{2}$ ,  $N + \frac{1}{2}$ ,  $N - \frac{1}{2}$ , and  $N - \frac{3}{2}$ . A good approximation to the rotational energy levels of a  $^4\Sigma$  molecule has been given by Budó [78].

$$\begin{aligned}
 W(J = N - \tfrac{3}{2}) &= B_v N(N + 1) - B_v(2N - 1) \\
 &\quad + B_v[4(N - \tfrac{1}{2})^2 - 6\lambda(N + 1) + 9\lambda^2]^{\frac{1}{2}} - 3(\gamma/2)(N + 1) \\
 W(J = N - \tfrac{1}{2}) &= B_v N(N + 1) - B_v(2N - 1) \\
 &\quad + B_v[4(N - \tfrac{1}{2})^2 + 6\lambda(N - 2) + 9\lambda^2]^{\frac{1}{2}} - (\gamma/2)(N + 4) \\
 W(J = N + \tfrac{1}{2}) &= B_v N(N + 1) + B_v(2N + 3) \\
 &\quad - B_v[4(N + \tfrac{3}{2})^2 - 6\lambda(N + 3) + 9\lambda^2]^{\frac{1}{2}} + (\gamma/2)(N - 3) \\
 W(J = N + \tfrac{3}{2}) &= B_v N(N + 1) + B_v(2N + 3) \\
 &\quad - B_v[4(N + \tfrac{3}{2})^2 + 6\lambda N + 9\lambda^2]^{\frac{1}{2}} + 3(\gamma/2)N
 \end{aligned} \tag{7-10}$$

where  $\lambda$  and  $\gamma$  are coupling constants similar to those of expressions (7-6).

The general trend of fine-structure energy for  $^4\Sigma$  levels is shown in Fig. 7-7. For large  $N$ , the levels with  $J = N \pm \frac{3}{2}$  approach the same

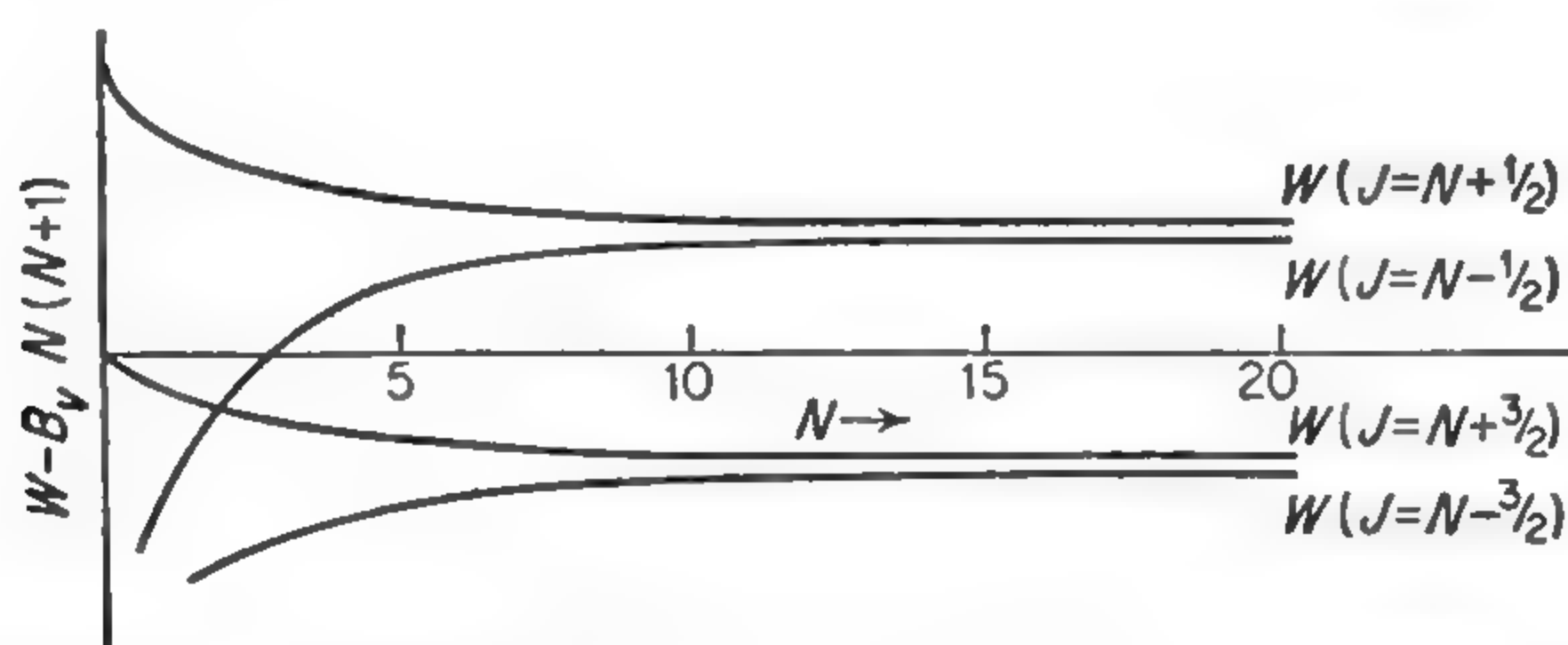


FIG. 7-7. Behavior of fine-structure energy for a  $^4\Sigma$  state. (From Budó [78].)

energy value except for the small terms dependent on  $\gamma$ . Similarly, the levels with  $J = N \pm \frac{1}{2}$  tend toward the same value.

*Case (c).* Rotational energies of molecules following case (c) are identical in form with those for case (a) and hence are given by (7-2) or (7-3).

*Case (d).* Rotational energies for case (d) molecules are given to a first approximation by

$$W(O) = B_v O(O + 1) \tag{7-11}$$

Each of the rotational levels is split into several components by the interaction **LO** and the smaller interaction **SK**.

**7-4. Spin Uncoupling.** A common case of intermediate coupling is a transition from case (a) to case (b). For low rotational states, **S** is coupled to  **$\Lambda$** , or to the molecular axis as in case (a). However, when

the rotational frequency becomes larger than the frequency of precession of  $\mathbf{S}$  about  $\mathbf{\Lambda}$ ,  $\mathbf{S}$  is uncoupled from the molecular axis and couples instead to the total orbital angular momentum  $N$  as in case (b). Energy levels in the intermediate conditions where  $\mathbf{S}$  is not simply coupled to  $\mathbf{\Lambda}$  or  $N$  must be obtained from solution of a secular equation. For a  $^2\Pi$  state with intermediate coupling, Hill and Van Vleck [10] obtain

$$\begin{aligned}
 W_1 &= B_v[(J + \tfrac{1}{2})^2 - \Lambda^2] - \left[ (J + \tfrac{1}{2})^2 \left( B_v - \frac{\gamma}{2} \right)^2 \right. \\
 &\quad \left. + \Lambda^2(A - \gamma) \left( \frac{A + \gamma}{4} - B \right) \right]^{\frac{1}{2}} - \frac{\gamma}{2} - D_v J^4 \\
 W_2 &= B_v[(J + \tfrac{1}{2})^2 - \Lambda^2] + \left[ (J + \tfrac{1}{2})^2 \left( B_v - \frac{\gamma}{2} \right)^2 \right. \\
 &\quad \left. + \Lambda^2(A - \gamma) \left( \frac{A + \gamma}{4} - B \right) \right]^{\frac{1}{2}} - \frac{\gamma}{2} - D_v(J + 1)^4
 \end{aligned} \tag{7-12}$$

where  $B_v$  is the usual rotational constant,  $A$  is the interaction constant between  $S$  and  $\Lambda$  (energy =  $A\mathbf{S} \cdot \mathbf{\Lambda}$ ), and  $\gamma$  is the same interaction constant between  $S$  and the molecular rotation given in Eqs. (7-4) or (7-5). The energy  $W_1$  applies to the state for which  $J = N + \frac{1}{2}$  when  $J$  is very large, and  $W_2$  to that for which  $J = N - \frac{1}{2}$ . The centrifugal distortion terms  $D_v J^4$  and  $D_v(J + 1)^4$  which are given are only approximately correct [77] but in most cases are so small that they are sufficiently accurate. Equations (7-12) are somewhat more complex than those usually given, because terms in  $\gamma$  have been included.  $\gamma$  is always much smaller than  $A$  and may for approximate results be omitted. For large  $J$ , where the transition to case (b) is complete, these equations reduce to the same form as (7-5). It is interesting to note that the molecular energies follow case (b) approximately not only when the rotational frequency  $2B_v J$  is much larger than the precessional frequency  $|A\Lambda|$  but also, rather unexpectedly, when  $(A + \gamma)/4$  is nearly equal to  $B_v$ .

For small spin uncoupling ( $2BJ \ll |A\Lambda|$ ), expressions (7-12) take the following form if terms independent of  $J$  are omitted.

$$\begin{aligned}
 W_1 &= B_v \left( 1 - \frac{B_v}{A\Lambda} \right) J(J + 1) - D_v J^4 \\
 W_2 &= B_v \left( 1 + \frac{B_v}{A\Lambda} \right) J(J + 1) - D_v(J + 1)^4
 \end{aligned} \tag{7-13}$$

Connections between energy levels in case (a), case (b), and intermediate coupling conditions are shown in Fig. 7-8. Since light molecules tend to have large rotational constants  $B$  and small fine-structure interaction constants  $A$ , they generally approach case (b) even for moderately low values of  $J$ . The free radical OH and other hydrides represent extremes

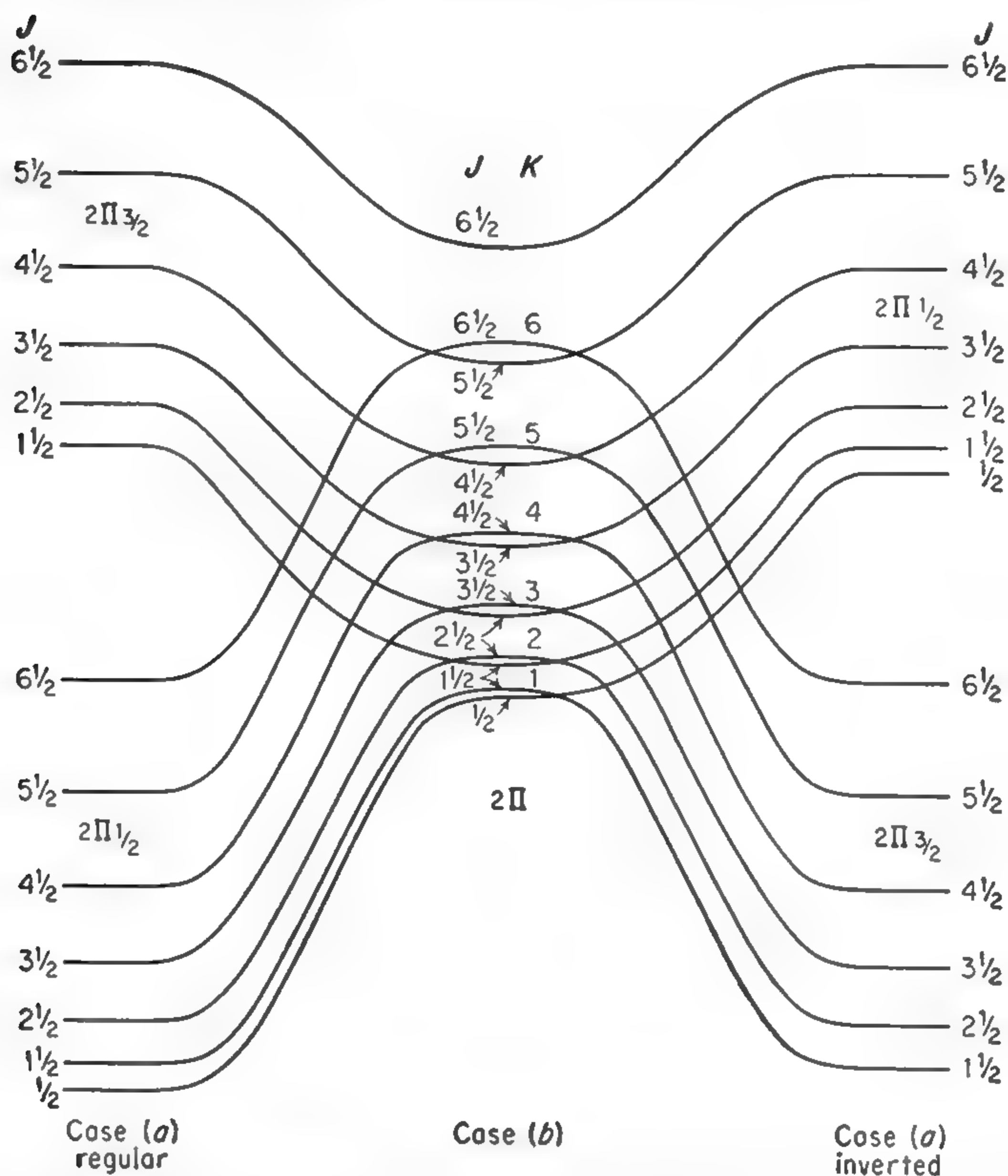


FIG. 7-8. Transition of  ${}^2\Pi$  states from case (a) to case (b). On the left is a regular case (a) with the constant  $A$  of the interaction  $A \mathbf{L} \cdot \mathbf{S}$  positive. On the right  $A$  is negative.

of this type. Heavier molecules tend to be close to case (a) for any rotational states of interest to microwave spectroscopy.

Similar formulas have been given for triplet states ( $S = 1$ ) [55], [69], [72]

$$\begin{aligned} W_1 &= B_v[J(J+1) - \sqrt{Z_1} - 2Z_2] - D_v(J - \tfrac{1}{2})^4 \\ W_2 &= B_v[J(J+1) + 4Z_2] - D_v(J + \tfrac{1}{2})^4 \\ W_3 &= B_v[J(J+1) + \sqrt{Z_1} - 2Z_2] - D_v(J + \tfrac{3}{2})^4 \end{aligned} \quad (7-14)$$

where  $Z_1 = \Lambda^2 A/B_v(A/B_v - 4) + \frac{4}{3} + 4J(J+1)$

$$Z_2 = \frac{1}{3Z_1} [\Lambda^2 A/B_v(A/B_v - 1) - \frac{4}{9} - 2J(J+1)]$$

The term dependent on  $\gamma$  has been omitted from these expressions. Here  $W_1$  is the energy of the state which for large  $J$  has  $J = N + 1$ ,  $W_2$  that for  $J = N$ , and  $W_3$  that for  $J = N - 1$ .



For small spin uncoupling ( $2B_v J \ll |A\Lambda|$ ), expressions (7-14) become (7-15) if energy terms independent of  $J$  are omitted.

$$\begin{aligned} W_1 &= B_v \left( 1 - \frac{2B_v}{A\Lambda} \right) J(J+1) - D_v \left( J - \frac{1}{2} \right)^4 \\ W_2 &= B_v J(J+1) - D_v \left( J + \frac{1}{2} \right)^4 \\ W_3 &= B_v \left( 1 + \frac{2B_v}{A\Lambda} \right) J(J+1) - D_v \left( J + \frac{3}{2} \right)^4 \end{aligned} \quad (7-15)$$

Formulas similar to (7-14) for quartet states ( $S = \frac{3}{2}$ ) are also available [68], [78], [83], [87].

**7-5.  $\Lambda$ -type Doubling.**  $\Lambda$ -type doubling is produced by an interaction between the rotational and electronic motions in a molecule. This may be regarded as an incipient uncoupling of  $L$  from the internuclear axis which, under extreme conditions, would lead to Hund's case ( $d$ ) where  $L$  is coupled to the molecular rotation. It is a doubling because this effect splits the two otherwise degenerate levels which are always present when  $\Lambda \neq 0$ . In general form and characteristics  $\Lambda$ -type doubling is entirely analogous to the  $l$ -type doubling described in Chap. 2, and in fact is the prototype of  $l$ -type doubling. As in the case of  $l$ -type doubling, the two perturbed states do not correspond simply to projections  $+\Lambda$  and  $-\Lambda$  of  $L$  on the internuclear axis, but are linear combinations of wave functions for positive and negative values of  $\Lambda$ .  $\Lambda$ -type doubling energies are in general smaller than rotational or fine-structure energies and hence have not been studied with high accuracy by the usual types of spectroscopy. However, they should be accurately measurable by microwave spectroscopy and may prove to be a particularly interesting feature of the microwave spectra of paramagnetic molecules.

The simplest cases of  $\Lambda$ -type doubling to discuss are singlet states, where the electron spin gives no complications since it is zero. In  $l$ -type doubling it may be remembered that the splitting was proportional to  $B(B/\omega_e)^l$ , where  $B/\omega_e$  is the ratio of rotational energy to vibrational energy. Similarly for  $\Lambda$ -type doubling, when the electronic motion rather than a vibration provides the angular momentum about the axis, the  $\Lambda$ -type splitting is proportional to  $B(B/\nu_e)^\Lambda$ , where  $\nu_e$  is the energy required to raise the electron from the ground state to some nearby excited state. Since the ratio  $B/\nu_e$  is generally small ( $\frac{1}{10000}$ ),  $\Lambda$ -type doubling for singlet states with  $\Lambda$  greater than 1 is almost always negligible, even for high-resolution microwave spectroscopy. When  $\Lambda = 1$ , the splitting of the two otherwise degenerate levels is given by

$$W = q_\Lambda J(J+1) \quad (7-16)$$

Theoretical evaluation of  $q_\Lambda$  is in general quite complicated. However, if an electron of orbital angular momentum is assumed to precess

so that the projection of  $l$  on the molecular axis is 1, and the only low-lying excited  $\Sigma$  and  $\Delta$  states correspond to the projection of this same  $l$  being 0 and 2, respectively, then  $q_\Lambda$  can be simply expressed [17], [27]. (This is the postulate of “pure precession.”)

$$q_\Lambda = 2B_v^2 \frac{l(l+1)}{h\nu_e[\Pi\Sigma]}$$

(7-17)

where  $h\nu_e(\Pi\Sigma)$  is the energy difference between the  $\Pi$  and  $\Sigma$  electronic levels. Expression (7-17) allows at least a rough estimate of  $q_\Lambda$  in more complex cases.

When the electron spin is not zero,  $\Lambda$ -type doubling may be modified, especially if Hund’s case (a) applies. However, when case (b) occurs,  $S$  does not affect the interaction between  $N$  and  $\Lambda$ , and (7-16) applies with the simple replacement of  $J$  by  $N$

$$W = q_\Lambda N(N+1)$$

(7-18)

A general summary of  $\Lambda$ -type doubling effects in pure cases (a) or (b) is given in Table 7-2. Rough magnitudes of the constants in Table 7-2

TABLE 7-2. SUMMARY OF  $\Lambda$ -TYPE DOUBLING EFFECTS  
(After Van Vleck [17])

State	Coupling case	$W$ (splitting of levels due to $\Lambda$ -type doubling effects)
$^1\Pi$		$q_\Lambda J(J+1)$
$^2\Pi$	Case (b)	$q_\Lambda N(N+1)$
$^2\Pi$	Case (a) $\Omega = \frac{1}{2}$	$a(J + \frac{1}{2})$
	$\Omega = \frac{3}{2}$	$b(J^2 - \frac{1}{4})(J + \frac{3}{2})$
$^3\Pi$	Case (b)	$q_\Lambda N(N+1)$
$^3\Pi$	Case (a) $\Omega = 0$	$f$
	$\Omega = 1$	$q_\Lambda J(J+1)$
	$\Omega = 2$	$\sim 0$
$^1\Delta$		$dJ(J^2 - 1)(J + 2)$

can be obtained from the pure-precession assumption as

$$q_\Lambda = \frac{4B_v^2}{h\nu_e} \qquad b = \frac{8B_v^3}{Ah\nu_e} \qquad d = \frac{48B_v^4}{(h\nu_e)^3}$$
$$a = \frac{4AB_v}{h\nu_e} \qquad f = \frac{2A^2}{h\nu_e}$$

where  $h\nu_e$  is the separation between the ground and first excited electronic energy level.

For intermediate cases of  ${}^2\Pi$  states the amount of  $\Lambda$ -type doubling has been given by Van Vleck [17].

$$W = \frac{q_{\Lambda}}{2}(J + \frac{1}{2}) \left[ \left(2 + \frac{A'}{B'}\right) \left(1 + \frac{2 - A/B}{X}\right) + \frac{4(J + \frac{3}{2})(J - \frac{1}{2})}{X} \right] \quad (7-19)$$

where  $X = \pm \left[ \frac{A}{B} \left( \frac{A}{B} - 4 \right) + 4(J + \frac{1}{2})^2 \right]^{\frac{1}{2}}$  and  $A'/B'$  is a quantity which is approximately equal to  $A/B$  for the  ${}^2\Pi$  state of the molecule in question, but which actually depends on matrix elements of  $A$  and  $B$  between this and other electronic states. When the interaction constant  $A$  is positive (regular fine structure), then a positive sign for  $X$  gives the state corresponding to  ${}^2\Pi_{\frac{1}{2}}$ , and a negative sign for  $X$  the state corresponding to  ${}^2\Pi_{\frac{3}{2}}$ . When  $A$  is negative (inverted fine structure), a negative  $X$  gives the  ${}^2\Pi_{\frac{1}{2}}$  state, and a positive  $X$  the  ${}^2\Pi_{\frac{3}{2}}$  state.

Matrix elements for transitions between  $\Lambda$ -type doublets are similar to those between  $l$ -type doublets, and hence for case (b) from (2-16) are

$$|\mu_{ij}|^2 = \frac{\mu^2 \Lambda^2}{(J + 1)(2J + 1)} \quad (7-20)$$

where  $\mu$  is the dipole moment along the molecular axis. For case (a),  $\Lambda$  in (7-20) is replaced by  $\Omega$ . Although many of the diatomic hydrides have rotational frequencies too high for ordinary microwave spectroscopy,  $\Lambda$ -type doubling in these hydrides should afford some microwave spectra. Microwave transitions between  $\Lambda$  doublets for several rotational states of the free radical OH have been observed and studied by Sanders, Schawlow, Dousmanis, and Townes [861], [971a].

Measurements on the ultraviolet spectrum of OH show that the rotational energy levels for this molecule can be fitted to an expression of the type [7-12] with  $\gamma \approx 0$ ,  $B_0 = 555,040$  Mc, and  $A = -7.547B_0$  for the ground vibrational state. Hence for relatively small values of  $J$ , the rotational frequency  $2JB_0$  becomes appreciable with respect to the fine-structure energy  $A$ , and intermediate coupling occurs. For higher  $J$ , the molecule corresponds to Hund's case (b).

The  $\Lambda$  doubling measured from ultraviolet spectra of OH can be fitted rather well to (7-19) with  $q_{\Lambda} = 1060$  Mc for the ground vibrational state and for values of  $N$  up to 15 as shown in Fig. 7-9. For higher values of  $N$ , the  $\Lambda$ -type doubling is somewhat better fitted by  $q_{\Lambda} = 925$  Mc. This decrease in  $q_{\Lambda}$  is presumably due to centrifugal effects. It may be noted from Fig. 7-9 that, except for small values of  $N$ , the  $\Lambda$  splitting is approximately proportional to  $N^2$ , as is indicated in Table 7-2 for a  ${}^2\Pi$  case (b).

Transitions between the  $\Lambda$ -type doublets of OH fall in the microwave



region for small and medium values of  $N$ , and have been observed [861], [971a] by microwave techniques for  $N = 2, 3, 4$ , and 5. The measured frequencies are fitted to expression (7-19) with an accuracy of about 40 Mc by the constants  $q_A = 1159$  and  $A'/B' = -6.073$ . It should be noted that  $A'/B'$  is different from  $A/B$ , which was given above as  $-7.547$ .

In obtaining  $q_A$  and  $A'/B'$ , small corrections to  $B$  and  $q_A$  in expression (7-19) have been made to allow for its variation with  $J$  due to centrifugal

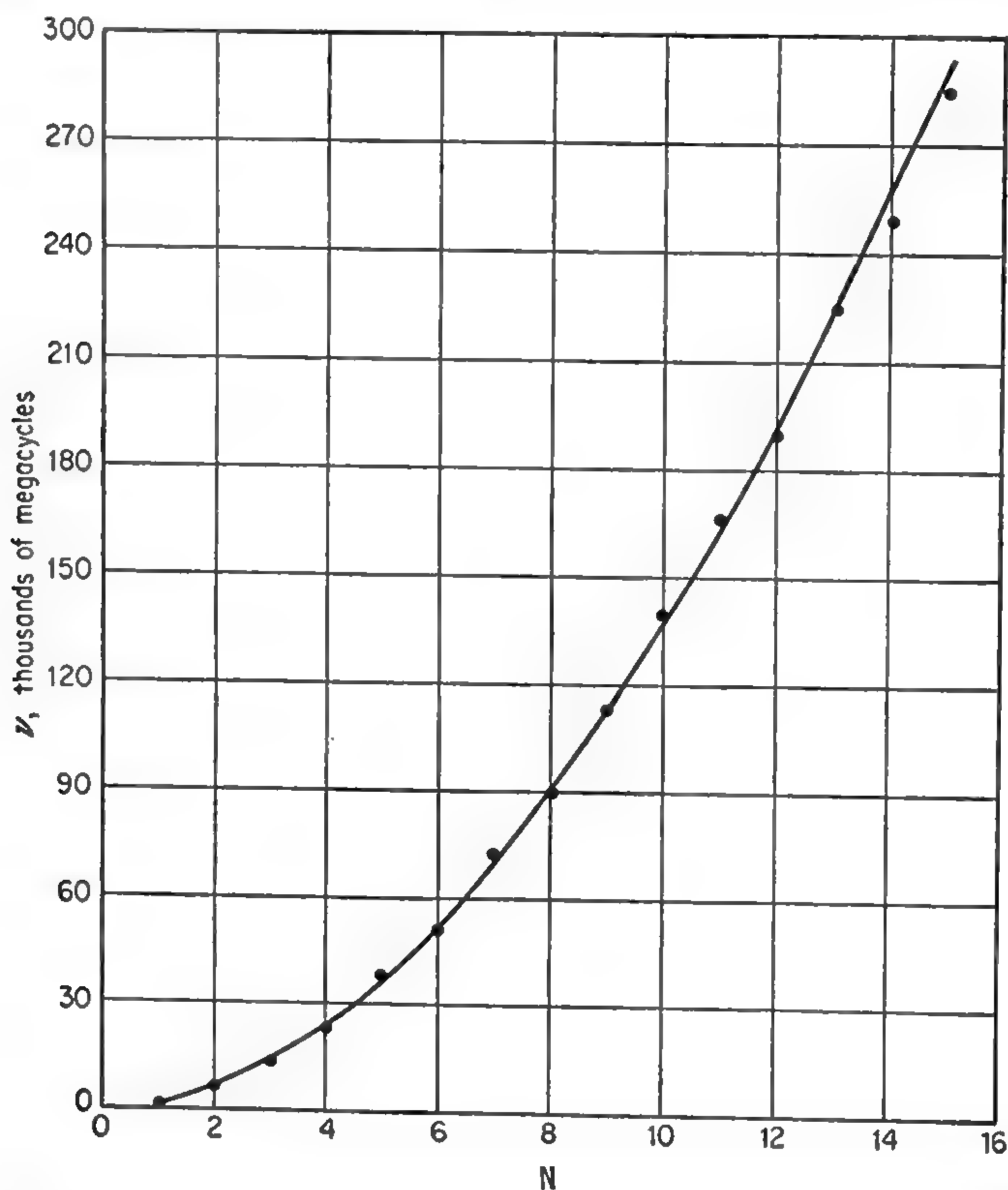


FIG. 7-9. Comparison of theory and experimental measurements of  $\Lambda$ -type doubling in OH. (Experimental measurements from Dieke and Crosswhite [266a].)

distortion. In addition, one may expect additional corrections to (7-19) of order  $B^3/\nu_e^2$ , or about  $\frac{1}{1000}$  as large as the measured splitting. These corrections are probably responsible for deviations noted between (7-19) and the experimental results for OH and for OD as given in Table 7-3.

A doubling in  $O^{18}H$  and OD can be fairly well predicted by noting that  $B$  and  $B'$  are inversely proportional to the reduced mass and  $q_A$  is proportional to  $B^2$ . A comparison between experimental measurements on four  $\Lambda$  doublets for OD with expression (7-19) is shown in Table 7-3.

Again in this case, variation in  $B$  and  $q_A$  due to centrifugal distortion has been allowed for, as indicated in the title of Table 7-3.

In NO,  $B$  is much smaller and  $A$  larger than for OH, so that  $A = 75B$ , and NO is a rather good case ( $a$ ) molecule. The  $\Lambda$ -type doubling of the  ${}^2\Pi_{1/2}$  state has been accurately measured from the  $\frac{3}{2} \leftarrow \frac{1}{2}$  rotational transition of NO [782*b*], [924], which gives the constant  $a$  of Table 7-2 a value of 355.2 Mc. From this value, the approximate magnitude of the constant  $b$  of Table 7-2 can be obtained, assuming the "pure-precession" relations of Table 7-2, as 0.13 Mc, and thus the  $\Lambda$ -type doubling of the  ${}^2\Pi_{1/2}$  state estimated. Experimental measurement [671] of the doubling of the  ${}^2\Pi_{1/2}$  state by microwave techniques gives the value  $b = 0.28$  Mc.

TABLE 7-3. COMPARISON BETWEEN THEORETICAL AND EXPERIMENTAL FREQUENCIES FOR  $\Lambda$ -TYPE DOUBLING IN  $O^{16}D$

Theoretical results come from expression (7-19) with  $A/B_0 = -14.147$ ,  
 $\frac{A'}{B_0'} = -11.461$ ,  $B = B' = B_0 - D_0N(N+1)$ ,  $q_A = 327.32 \left[ 1 - \frac{2D_0}{B_0} N(N+1) \right]$

(From Sanders, Dousmanis, and Townes [971*a*])

$N$	$J$	Measured frequency, Mc	Calculated frequency, Mc
$\Pi_{1/2}$ state			
3	$2\frac{1}{2}$	8,120.4	8,108.2
4	$3\frac{1}{2}$	9,587.9	9,582.1
5	$4\frac{1}{2}$	10,200.7	10,203.3
6	$5\frac{1}{2}$	9,922.8	9,931.4
$\Pi_{3/2}$ state			
5	$5\frac{1}{2}$	8,672.4	8,630.4
6	$6\frac{1}{2}$	12,918.0	12,882.8
7	$7\frac{1}{2}$	18,009.6	18,000.7
8	$8\frac{1}{2}$	23,907.1	23,949.5

Hyperfine structure appears prominently in the spectra of OH and NO. Such structure has been omitted in the discussion of rotational spectra of these molecules, and has been subtracted out of the experimental results to give the amount of  $\Lambda$  doubling. This hyperfine structure will be discussed in Chap. 8.

**7-6. Nonlinear Molecules.** Valence electrons in nonlinear molecules do not move in cylindrically symmetric fields, and hence no component of their orbital angular momentum is constant or "quantized." Rather, the electronic orbital momentum is part of the rotational momentum of the whole molecule. Any interaction between electron spin and orbit of the type  $AL \cdot S$  comes about only through some slight uncoupling of  $L$  from the rotation of the molecule, and hence occurs as second- or higher-order perturbation effects. Henderson and Van Vleck [283] have shown

that these have the form

$$W = A \frac{\left[ \alpha E + \beta \sum_K |a_{NK}|^2 K^2 + \gamma \right]}{N(N+1)} C + \frac{A^2}{2} \left[ \frac{\alpha' E + \beta' \sum_K |a_{NK}|^2 K^2}{N(N+1)} + \gamma' \right] \frac{\frac{3}{4}C(C+1) - S(S+1)N(N+1)}{(2N-1)(2N+3)} \quad (7-21)$$

where  $C = J(J+1) - S(S+1) - N(N+1)$

$E$  = energy of molecular rotation without electron spin effects

$a_{NK}$  = the coefficient in expression (4-17) which gives an expansion of any asymmetric-top wave function in terms of symmetric-top wave functions with quantum numbers  $K$ .

$\alpha, \beta, \gamma, \alpha', \beta'$  and  $\gamma'$  are all constants dependent on the structure of the molecule, and independent of angular-momentum quantum numbers.

It may be seen that the first term of (7-21) is a dipole-like interaction, and the second term a pseudo quadrupole interaction with the same dependence on angular-momentum quantum numbers as a genuine quadrupole interaction [cf. (5-45)]. In addition, the pseudo quadrupole term in (7-21) must be zero when  $S$  is less than 1, or for singlet and doublet states. For a symmetric-top molecule,  $|a_{NK}|^2$  is unity for one particular value of  $K$  and otherwise zero, and since

$$E = BN(N+1) + (A-B)K^2$$

(7-16) reduces to

$$W = \left[ \frac{aK^2}{N(N+1)} + b \right] C + \left[ \frac{a'K^2}{N(N+1)} + b' \right] \left[ \frac{\frac{3}{4}C(C+1) - S(S+1)N(N+1)}{(2N-1)(2N+3)} \right] \quad (7-22)$$

where  $a, b, a'$ , and  $b'$  are constants.

The only nonlinear molecules with unpaired electron spins which have so far been studied in the gaseous state are  $\text{NO}_2$  and  $\text{ClO}_2$ .  $\text{ClO}_2$  is somewhat asymmetric (asymmetry parameter  $\kappa \approx 0.85$ ) but its spectrum observed in the optical region [144] fits expression (7-22) satisfactorily [283]. Some spectral lines of  $\text{NO}_2$  have been observed in the microwave region, but their fine structure has not yet been well analyzed [497], [615].



## CHAPTER 8

# MAGNETIC HYPERFINE STRUCTURE IN MOLECULAR SPECTRA

**8-1. Introduction.** Although hyperfine structure due to nuclear magnetic dipole moments is not so prominent in molecular spectra as that involving nuclear electric quadrupole moments, it is by no means insignificant. In molecules with electronic angular momentum, magnetic hyperfine structure is comparable in size with magnetic hyperfine structure in atoms and is usually much larger than that due to quadrupole moments. It is only because this type of molecule is uncommon that magnetic hyperfine structure is not prominent in molecular spectra. For molecules in  $^1\Sigma$  states the average of each component of the electronic angular momentum is so small that it is usually considered zero. Even for these molecules, however, there are weak interactions involving nuclear magnetic moments. These include interaction between magnetic moments of two nuclei in the same molecule (spin-spin interactions), interaction between a nuclear magnetic moment and the rather small magnetic fields produced by molecular rotation ( $\mathbf{I} \cdot \mathbf{J}$  interactions), and magnetic polarization of a molecule by a nuclear magnetic moment (pseudo quadrupole interaction).

When a molecule has electronic angular momentum, hence is in some state other than  $^1\Sigma$ , the magnetic fields associated with this momentum interact strongly with the nuclear moments present in the molecule, giving a magnetic hyperfine structure comparable in size with that found in atoms ( $10^3$  Mc would be typical). The interaction is due either to electronic orbital angular momentum,  $\mathbf{L}$  or  $\Lambda$ , or to spin angular momentum,  $\mathbf{S}$  or  $\Sigma$ .

In the case of orbital angular momentum, the interaction energy is given by (5-49) if the spin is assumed to be zero, *i.e.*, if we let  $j = 1$ . Then (5-49) and (5-51) give the energy as

$$H_{II} = \frac{2\mu_0\mu_I}{Ir^3} \mathbf{I} \cdot \mathbf{l} \quad (8-1)$$

where  $\mu_0$  = the Bohr magneton

$\mu_I$  = nuclear magnetic moment

$\mathbf{I}$  = nuclear spin

$r$  = distance between the electron and the nucleus

$l$  = orbital angular momentum of an electron with respect to the nucleus in units of  $h/2\pi$  (the quantity  $h/2\pi$  will frequently be written  $\hbar$ )

To calculate the energy resulting from (8-1) in the first-order perturbation approximation, we need to average this expression (since in a molecule neither  $l$  nor  $r$  is constant) and to sum over all the electrons which contribute to the total orbital angular momentum  $\mathbf{L}$ . In the simplest cases, the nucleus may be assumed to lie on the molecular axis.  $\mathbf{L}$  has an average nonzero value only if the molecule is linear, so that the average value of  $\mathbf{L}$  is just  $\mathbf{k}\Lambda$ , where  $\mathbf{k}$  is a unit vector along the molecular axis and  $\Lambda$  is as usual the component of  $\mathbf{L}$  along this direction. Then if only one electron contributes to the orbital angular momentum  $\mathbf{L}$ ,

$$H_{IL} = \frac{2\mu_0\mu_I\Lambda}{I} \left( \frac{1}{r^3} \right)_{av} \mathbf{I} \cdot \mathbf{k} \quad (8-2a)$$

If more electrons are involved,

$$H_{IL} = \frac{2\mu_0\mu_I}{I} \sum_n \left( \frac{1}{r_n^3} \right)_{av} \Lambda_n \mathbf{I} \cdot \mathbf{k} \quad (8-2b)$$

where the sum is over each electron contributing to the hyperfine structure and  $\Lambda_n$  is the average projection of the orbital angular momentum of the  $n$ th electron on the axis.

Interaction between a nuclear magnetic moment and an electron spin moment is somewhat more complex. There is the classical interaction between two dipoles  $\mathbf{u}_1$  and  $\mathbf{u}_2$  of the form

$$W_{\mu_1\mu_2} = \frac{\mathbf{u}_1 \cdot \mathbf{u}_2}{r^3} - \frac{3(\mathbf{u}_1 \cdot \mathbf{r})(\mathbf{u}_2 \cdot \mathbf{r})}{r^5} \quad (8-3)$$

which for the nucleus  $\left( \mathbf{u}_1 = \frac{\mu_I}{I} \mathbf{I} \right)$  and electron spin  $(\mathbf{u}_2 = -2\mu_0\mathbf{S})$  becomes

$$(H_{IS})_1 = \frac{2\mu_0\mu_I}{I} \left[ \frac{\mathbf{I} \cdot \mathbf{S}}{r^3} - \frac{3(\mathbf{I} \cdot \mathbf{r})(\mathbf{S} \cdot \mathbf{r})}{r^5} \right] \quad (8-4)$$

In addition, there is an interaction of the type found between a nuclear magnetic moment and an  $S$  electron in atoms, which is not given simply by (8-4). It can be written approximately as in the atomic case from (5-49) and (5-54) as

$$(H_{IS})_2 = \frac{16\pi}{3} \frac{\mu_0\mu_I}{I} \psi^2(0) \mathbf{I} \cdot \mathbf{S} \quad (8-5)$$

Frosch and Foley [686] (cf. also [916a]) have discussed these magnetic interactions for a linear molecule, and obtain the sum of  $H_{IL}$ ,  $(H_{IS})_1$ , and

$(H_{IS})_2$  in the common Hund's cases (a) and (b) as

$$H^1 = a\Lambda\mathbf{I} \cdot \mathbf{k} + b\mathbf{I} \cdot \mathbf{S} + c(\mathbf{I} \cdot \mathbf{k})(\mathbf{S} \cdot \mathbf{k}) \quad (8-6)$$

where

$$a = \frac{2\mu_0\mu_I}{I} \left( \frac{1}{r^3} \right)_{av}$$

and to a good approximation

$$b = \frac{2\mu_0\mu_I}{I} \left[ \frac{8\pi}{3} \psi^2(0) - \frac{3 \cos^2 \theta - 1}{2r^3} \right]_{av}$$

$$c = \frac{3\mu_0\mu_I}{I} \left( \frac{3 \cos^2 \theta - 1}{r^3} \right)_{av}$$

Expression (8-6) applies accurately only when  $\Lambda$  is a "good" quantum number. Here  $\theta$  is the angle between the molecular axis and the radius  $r$  from the nucleus to the electron.  $\Lambda$  and  $S$  are assumed to be good quantum numbers, since second-order terms involving changes of  $\Lambda$  or  $S$  give extremely small contributions to the energy by comparison with the first-order terms of (8-6). Some of these second-order terms will be discussed below, however, in connection with magnetic effects in  $^1\Sigma$  molecules, where the first-order terms given by (8-6) are zero.

Expression (8-6) applies to each electron in the molecule. Of course, most of the electrons occupy orbits in pairs with oppositely directed spins so that the second and third parts of (8-6) cancel out, and the orbits are usually filled so that the orbital angular momentum  $\Lambda$  of most of the electrons cancel. Expression (8-6) need then only be applied to each of the "unpaired" electrons whose angular momentum is not cancelled. The quantity  $a$  refers only to electrons with orbital angular momentum. A spherical distribution of an electron around the nucleus would make  $\left( \frac{3 \cos^2 \theta - 1}{2} \right)_{av}$  equal to zero, so that in this case the electron spin would interact with the nuclear magnetic moment only through the term in  $b$  proportional to  $\psi^2(0)$ . The probability  $\psi^2(0)$  of the electron's being found at the nucleus is usually negligibly small for an electron in a  $p$  atomic orbit. For an  $S$ -type orbit, however, it is large enough so that  $\frac{8\pi}{3} \psi^2(0)$  is much larger than  $\left( \frac{3 \cos^2 \theta - 1}{2r^3} \right)_{av}$  for a  $p$  orbit and  $b \gg a$ . Hence, whenever there is an appreciable amount of  $S$  character to the wave function of an unpaired electron, the hyperfine interaction which is proportional to  $\psi^2(0)$  may be expected to dominate.

**8-2. Coupling Schemes for Magnetic Hyperfine Structure.** Evaluation of the energy resulting from the interaction (8-6) depends on the coupling scheme which is followed by the particular case of interest. In addition to the electron angular momentum which is coupled according to the usual Hund's coupling cases (cf. Chap. 7) to the molecular axis or to the momentum of end-over-end rotation of the molecule, we have also



the nuclear spin momentum. The nuclear spin may be coupled with varying strength to the several molecular vectors, providing additional coupling possibilities. The commonly expected coupling schemes are shown in Fig. 8-1. They are classified according to Hund's scheme, with a subscript  $\alpha$  indicating that the nuclear spin is most strongly coupled to the molecular axis [as is  $S$  in Hund's case (a)] and a subscript  $\beta$  indicating that the nuclear spin is not coupled to the molecular axis but to

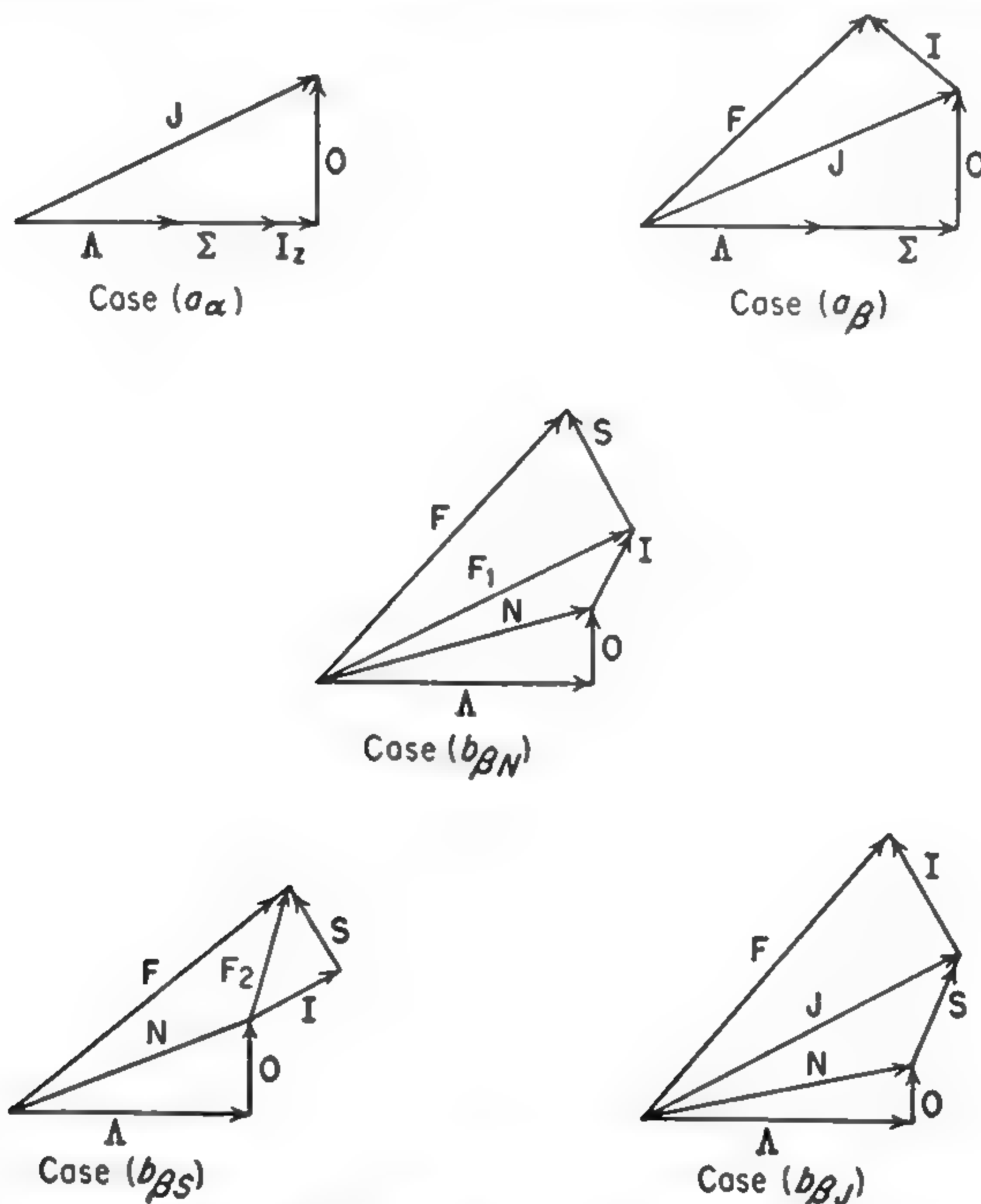


FIG. 8-1. Molecular coupling schemes including nuclear spin.

some other vector [as in case (b)]. For Hund's case (a), one may expect the nuclear spin to be coupled either to the molecular axis [case ( $a_\alpha$ )] or to  $J$  [case ( $a_\beta$ )]. However, for Hund's case (b), where the electron spin is not coupled to the molecular axis, it is very unlikely that the nuclear spin will be coupled to the molecular axis since the interaction of its small nuclear magnetic moment with the molecular fields should be considerably less than that between the electron moment and the molecular fields. Hence only case ( $b_\beta$ ) is expected to occur.

In case (a), (8-6) becomes (omitting the negligible perturbation of  $\Lambda$  by hyperfine interactions)

$$H^1 = [a\Lambda + (b + c)\Sigma]I \cdot k \quad (8-7)$$

since  $S \cdot k = \Sigma$ , and  $I \cdot S = (I \cdot k)(S \cdot k)$  when  $S$  precesses about the

molecular axis  $\mathbf{k}$ . The hyperfine energy for case ( $a_\alpha$ ) is the sum of a magnetic interaction given by (8-7) and a term dependent on the molecular moment of inertia. The entire effect of  $\Omega_I$ , or  $\mathbf{I} \cdot \mathbf{k}$ , the projection of  $I$  on the axis, is

$$W = [a\Lambda + (b + c)\Sigma]\Omega_I - hB[\Omega_I + 2(\Lambda + \Sigma)]\Omega_I \quad (8-8)$$

All parts of this expression are constant for a given electronic level except  $\Omega_I$ , which has one of the values  $I, I - 1, \dots, -I$ . The second term of (8-8) may be obtained from (7-2), which gives the rotational energy in case ( $a$ ) as  $W_J = hB[J(J + 1) - \Omega^2]$ . But in case ( $a_\alpha$ ),  $\Omega$  may include  $\Omega_I$ , which therefore affects the rotational energy. In case ( $a_\beta$ ), the vector model gives

$$\mathbf{I} \cdot \mathbf{k} = \frac{(\mathbf{I} \cdot \mathbf{J})(\mathbf{J} \cdot \mathbf{k})}{J(J + 1)}$$

or, since  $\mathbf{J} \cdot \mathbf{k} = \Lambda + \Sigma = \Omega$ ,

$$W = [a\Lambda + (b + c)\Sigma] \frac{\Omega}{J(J + 1)} \mathbf{I} \cdot \mathbf{J} \quad (8-9)$$

where

$$\mathbf{I} \cdot \mathbf{J} = \frac{F(F + 1) - J(J + 1) - I(I + 1)}{2}$$

In this case, the hyperfine structure decreases with increasing  $J$ , since  $\mathbf{I}$  becomes more and more nearly perpendicular to the molecular axis.

When neither the electronic nor nuclear spin is coupled to the molecular axis, one encounters the further complication of three possible coupling schemes:

1. Case ( $b_{\beta N}$ ):  $\mathbf{N}$  and  $\mathbf{I}$  are coupled to form  $\mathbf{F}_1$ , then  $\mathbf{F}_1$  and  $\mathbf{S}$  couple to form the total angular momentum  $\mathbf{F}$ .
2. Case ( $b_{\beta S}$ ):  $\mathbf{S}$  and  $\mathbf{I}$  are coupled to form  $\mathbf{F}_2$ , then  $\mathbf{F}_2$  and  $\mathbf{N}$  couple to give  $\mathbf{F}$ .
3. Case ( $b_{\beta J}$ ):  $\mathbf{N}$  and  $\mathbf{S}$  are coupled to form  $\mathbf{J}$ , then  $\mathbf{J}$  and  $\mathbf{I}$  couple to give  $\mathbf{F}$ .

It may be noted that a subscript has been added to the designation of the coupling scheme which indicates the vector to which  $\mathbf{I}$  is coupled. These three cases are illustrated in Fig. 8-1. Case ( $b_{\beta N}$ ) is not expected to occur commonly because the much larger magnetic moment associated with the electron spin should couple much more strongly to  $N$  than does the nuclear magnetic moment.

The energy resulting from the first two terms of the interaction (8-6) can be obtained from the vector model for each of the three above cases. However, the last term of (8-6) requires a more complicated procedure such as multiplication of the matrices for  $\mathbf{I} \cdot \mathbf{k}$  and  $\mathbf{S} \cdot \mathbf{k}$ . Frosch and Foley [686] have given all matrix elements necessary to evaluate the energy from (8-6) using the coupling schemes ( $b_{\beta S}$ ) and ( $b_{\beta J}$ ). For the

pure coupling case ( $b_{\beta J}$ ), which is expected to be more common than ( $b_{\beta S}$ ), the energies obtained are as follows:

When  $S = \frac{1}{2}$ :

$$\begin{aligned}
 W_{J=N+1} &= \left[ \frac{2a\Lambda^2}{(N+1)(2N+1)} + \frac{b}{2N+1} \right. \\
 &\quad \left. + \frac{c}{(2N+1)(2N+3)} \left( 1 + \frac{2\Lambda^2}{N+1} \right) \right] \mathbf{I} \cdot \mathbf{J} \\
 W_{J=N-1} &= \left[ \frac{2a\Lambda^2}{N(2N+1)} - \frac{b}{2N+1} \right. \\
 &\quad \left. + \frac{c}{(2N-1)(2N+1)} \left( 1 - \frac{2\Lambda^2}{N} \right) \right] \mathbf{I} \cdot \mathbf{J}
 \end{aligned} \tag{8-10}$$

where

$$\mathbf{I} \cdot \mathbf{J} = \frac{1}{2}[F(F+1) - J(J+1) - I(I+1)]$$

When  $S = 1$ :

$$\begin{aligned}
 W_{J=N+1} &= \left[ \frac{a\Lambda^2}{(N+1)^2} + \frac{b}{(N+1)} \right. \\
 &\quad \left. + \frac{c}{(N+1)(2N+3)} \left( 1 + \frac{2\Lambda^2}{N+1} \right) \right] \mathbf{I} \cdot \mathbf{J} \\
 W_{J=N} &= \left[ \frac{a\Lambda^2(N^2 + N - 1)}{N^2(N+1)^2} + \frac{b}{N(N+1)} \right. \\
 &\quad \left. + \frac{c}{N(N+1)} \left( 1 - \frac{2\Lambda^2}{N(N+1)} \right) \right] \mathbf{I} \cdot \mathbf{J} \\
 W_{J=N-1} &= \left[ \frac{a\Lambda^2}{N^2} - \frac{b}{N} + \frac{c}{N(2N-1)} \left( 1 - \frac{2\Lambda^2}{N} \right) \right] \mathbf{I} \cdot \mathbf{J}
 \end{aligned} \tag{8-11}$$

Because of the accuracy of microwave measurements, noticeable deviations from the pure coupling cases listed above are to be expected, and intermediate coupling cases must be considered. In addition, when large coupling constants occur,  $N$  may not be a "good" quantum number, and second-order effects involving excitation of other  $N$  states must be considered. Frosch and Foley [686] give most of the matrix elements needed for calculation of the energy in these cases.

**8-3. Examples of Magnetic Hyperfine Structure in Molecules with Electronic Angular Momentum.** The molecule NO is a rather good example of Hund's case ( $a$ ), its ground electronic state being  $^2\Pi$ . The nuclear magnetic moment of nitrogen and the molecular fields produce a hyperfine structure which follows case ( $a_\beta$ ). The  $^2\Pi_{\frac{1}{2}}$  state shows a hyperfine structure which is given by expression (8-9) with

$$a\Lambda + (b + c)\Sigma = 74.1 \text{ Mc}$$

[899], [686]. Hyperfine structure of the  $^2\Pi_{\frac{1}{2}}$  state involves some additional effects which are discussed in Sec. 8-6. The common isotope of



oxygen,  $O^{16}$ , has zero spin and hence produces no hyperfine structure in NO. The spectrum of the  ${}^2\Pi_3$  state of NO was actually measured in a strong magnetic field [435], [899] and will be discussed in more detail in Chap. 11 in connection with Zeeman effects.

The ground state of the oxygen molecule  $O_2$  is  ${}^3\Sigma$ , and hence a good Hund's case (b). The coupling between  $S$  and  $N$  is approximately 60,000 Mc, whereas the hyperfine coupling between  $S$  and  $I$  for  $O^{17}$  in  $O^{16}O^{17}$  is only a few hundred megacycles, so that  $O^{16}O^{17}$  represents a rather good case ( $b_{\beta J}$ ). For this molecule, having  $S = 1$  and  $\Lambda = 0$ , the energies given by (8-11) simplify to

$$\begin{aligned} W_{J=N+1} &= \frac{\mathbf{I} \cdot \mathbf{J}}{N+1} \left( b + \frac{c}{2N+3} \right) \\ W_{J=N} &= \frac{\mathbf{I} \cdot \mathbf{J}}{N(N+1)} (b + c) \\ W_{J=N-1} &= \frac{\mathbf{I} \cdot \mathbf{J}}{N} \left( -b + \frac{c}{2N-1} \right) \end{aligned} \quad (8-12)$$

where

$$\mathbf{I} \cdot \mathbf{J} = \frac{F(F+1) - I(I+1) - J(J+1)}{2}$$

The expressions (8-11) or (8-12) have been found to fit very satisfactorily the observed hyperfine splitting of the microwave spectrum of  $O^{16}O^{17}$  with the values  $I = \frac{5}{2}$ ,  $b = -102$  Mc, and  $c = 140$  Mc [841]. Effects of the quadrupole moment of  $O^{17}$  and second-order effects involving decoupling of  $S$  from  $N$  can be shown to be less than about 1 Mc, which was the accuracy of the measurements, and hence were neglected.

Magnetic hyperfine structure has also been observed in OH [861], [971a], where coupling intermediate between case (a) and case (b) occurs.

The way in which  $a$ ,  $b$ , and  $c$  depend on the electronic wave function of the molecule, and the information about NO and  $O_2$  which can be derived from them are discussed in Chap. 9.

**8-4. Nonlinear Molecules.** Electrons in molecules which are not linear have no constant component of orbital angular momentum, since the molecular electric fields interfere with each component of the electrons' orbital motion. Hence in first-order approximation the interaction (8-1) is zero because the average value of each component of  $L$  is zero. The electron spin, however, may still be nonzero in such a molecule and may give a sizable hyperfine structure through interactions of types (8-3) and (8-5). No detailed evaluation of the energies resulting from (8-3) and (8-5) has been made for nonlinear molecules. However, coupling of the case ( $b_{\beta J}$ ) type should be expected. For a given rotational state of angular momentum  $N$  due to end-over-end rotation, and given value of  $\mathbf{J} = \mathbf{N} + \mathbf{S}$ , the energy will have the form

$$W = 2C(\mathbf{I} \cdot \mathbf{J}) = C[F(F+1) - I(I+1) - J(J+1)] \quad (8-13)$$

Two examples of hyperfine structure in asymmetric molecules with electronic angular momentum have so far been observed,  $\text{NO}_2$  and  $\text{ClO}_2$ . Both these molecules have an odd number of electrons and a value  $S = \frac{1}{2}$ . Selection rules for the hyperfine structure ( $\Delta F = 0, \pm 1$ ) and relative intensities of the components are the same as with fine structure or other forms of hyperfine structure (see Chap. 5). Except for very small values of  $J$ , the dominantly strong hyperfine components are those for which  $\Delta F$  is the same as  $\Delta J$ . Assuming ( $b_{\beta J}$ ) coupling, the frequencies of the strong hyperfine components ( $\Delta F = \Delta J$ ) for a particular transition can be obtained from (8-13) as

$$\nu = \nu_0 + \frac{F - J}{h} [(C_2 - C_1)(F - J) + C_2(2J_2 + 1) - C_1(2J_1 + 1)] \quad (8-14)$$

where  $J_1$  and  $J_2$  = total angular momentum exclusive of nuclear spin in lower and upper states, respectively

$C_1$  and  $C_2$  = hyperfine constants in (8-13) for lower and upper states, respectively

$\nu_0$  = a constant given primarily by the frequency of the rotational transition without hyperfine structure

$F - J$  = difference between  $F$  and  $J$  in either upper or lower states, which may have the values  $I, I - 1, \dots, -I$

Expression (8-14) allows  $2I + 1$  hyperfine components for each rotational transition and fine-structure component, *i.e.*, for each transition for given values of  $N$  and  $J$  in initial and final states, since  $F - J$  can have  $2I + 1$  different values. This is provided  $I < J$ ; otherwise there are  $2J + 1$  components. The components may be approximately equally spaced if  $C_2 - C_1$  is small compared with

$$C_2(2J_2 + 1) - C_1(2J_1 + 1)$$

or may tend to converge when the two terms are comparable in magnitude. Figure 8-2 shows part of the spectrum of  $\text{ClO}_2$ , which can be seen to consist of two groups of four lines corresponding to the  $\frac{3}{2}$  spin of the two Cl isotopes ( $\text{O}^{16}$  has zero spin). One group of hyperfine components in this spectrum has approximately equal spacings, whereas spacings of the second group increase markedly from left to right.

It has been suggested [497], [615] that two nearby sets of three lines in the spectrum of  $\text{NO}_2$  are the  $J = 6_{06} \longleftrightarrow 5_{15}$  transition, one set with  $J = N + \frac{1}{2}$ , and the other with  $J = N - \frac{1}{2}$ . Certainly each set of three must correspond to the hyperfine lines due to  $\text{N}^{14}$  ( $I = 1$ ) of some rotational transition. However, the ratios of the separations between these



components has not yet been worked out in detail, and they do not seem to fit satisfactorily the approximate theoretical calculations which have been made. In addition, the Zeeman effect of these lines does not fit very well this assignment for the transitions [615].

**8-5. Spin-spin Interaction between Nuclei.** A nuclear magnetic moment may interact not only with an electron spin moment, but also with other nuclear magnetic moments which are present in a molecule. Expression (8-3) gives the interaction between two such dipole moments, from which the energy may be evaluated. This "spin-spin" interaction between nuclei is approximately 2000 times smaller than the hyperfine



FIG. 8-2. Two lines of the asymmetric rotor  $\text{ClO}_2$ , each split into four components by magnetic hyperfine structure. (From A. L. Schawlow and T. M. Sanders.)

interactions in paramagnetic molecules because the magnetic moments associated with nuclei are this much smaller than those due to electrons. A rough magnitude for these effects can be obtained from  $\mu_n^2/r^3$ , where  $\mu_n$  is a nuclear magneton and  $r$  is the distance between two nuclei in a molecule. For a typical value of  $r \approx 1.5 \text{ \AA}$ ,  $\mu_n^2/r^3$  is only about 3 kc, which is so small that this "spin-spin" interaction is only rarely detected.

Because of their small size, nuclear "spin-spin" interactions will be of importance only for  $^1\Sigma$  molecules, where the magnetic effect of electrons will also be very small. The vectors to be coupled are then the rotational angular momentum of the molecule  $J$ , and the spins of the two nuclei  $I_1$  and  $I_2$ . If the nucleus having spin  $I_1$  is more strongly coupled to  $J$  than is the other nucleus, then the coupling scheme for a  $^1\Sigma$  symmetric top is similar to case ( $b_{\beta J}$ ) discussed above, but with  $N$  replaced by  $J$ ,  $\Lambda$  by  $K$ ,  $S$  by  $I$ , and  $J$  replaced by  $F_1 = I_1 + J$ . This coupling scheme could occur when  $I_1$  is coupled by electric quadrupole effects to  $J$ , and would be the only pure coupling scheme of much interest for two nuclei. The energies are given for two nuclei in symmetric-top molecules by simplified forms of (8-10) and (8-11) or (8-12), or in more general form by Gunther-Mohr, Townes, and Van Vleck [931].



For  $I_1 = \frac{1}{2}$ :

$$\begin{aligned} W_{F_1=J+1} &= \frac{2J\mu_1\mu_2(3\cos^2\theta - 1)}{(2J+1)(2J+3)I_2r^3} \left[ \frac{3K^2}{J(J+1)} - 1 \right] \mathbf{I}_2 \cdot \mathbf{F}_1 \\ W_{F_1=J-1} &= \frac{-2(J+1)\mu_1\mu_2(3\cos^2\theta - 1)}{(2J-1)(2J+1)I_2r^3} \left[ \frac{3K^2}{J(J+1)} - 1 \right] \mathbf{I}_2 \cdot \mathbf{F}_1 \end{aligned} \quad (8-15a)$$

where  $r$  is the length of the vector between the two nuclei and  $\theta$  is the angle between this vector and the molecular axis.

For  $I_1 = 1$ :

$$\begin{aligned} W_{F_1=J+1} &= \frac{2J\mu_1\mu_2(3\cos^2\theta - 1)}{(J+1)(2J+3)I_2r^3} \left[ \frac{3K^2}{J(J+1)} - 1 \right] \mathbf{I}_2 \cdot \mathbf{F}_1 \\ W_{F_1=J} &= -\frac{2\mu_1\mu_2(3\cos^2\theta - 1)}{J(J+1)I_2r^3} \left[ \frac{3K^2}{J(J+1)} - 1 \right] \mathbf{I}_2 \cdot \mathbf{F}_1 \\ W_{F_1=J-1} &= -\frac{2(J+1)\mu_1\mu_2(3\cos^2\theta - 1)}{J(2J-1)I_2r^3} \left[ \frac{3K^2}{J(J+1)} - 1 \right] \mathbf{I}_2 \cdot \mathbf{F}_1 \end{aligned} \quad (8-15b)$$

A somewhat larger spin-spin effect, which occurs only when  $K = 1$ , will be discussed below in connection with the hyperfine structure of  $\text{NH}_3$ .

For intermediate coupling cases, the matrix elements given by Frosch and Foley [686] for the interaction of nuclear and electronic dipole moments may be used with a second nuclear moment replacing the electron spin  $S$ . The case of spin-spin interaction between two identical nuclei in a linear molecule, *i.e.*, two protons in  $\text{H}_2$  or two deuterons in  $\text{D}_2$ , has been discussed in some detail by Kellogg, Rabi, Ramsey, and Zacharias [91], [98]. However, such cases are not of great interest to microwave spectroscopy because linear molecules in which two identical nuclei are found would usually have no dipole moment.

**8-6. Effect of Hyperfine Structure on  $\Lambda$  Doubling—Hyperfine Doubling.** So far we have discussed only those types of hyperfine structure which would be identical for the two energy levels of a  $\Lambda$ -type doublet. However, for  $\Pi$  states certain additional hyperfine effects may occur which are different for the two  $\Lambda$ -doubled states.

Different hyperfine structure for two members of a  $\Lambda$  doublet arises only from electron spin–nuclear spin interactions. A general understanding of the phenomenon can be obtained from a consideration of the distribution of electron density in the two  $\Lambda$ -doubled states of a  $^2\Pi$  case (*b*) molecule. The part of the electron wave function depending on angle  $\phi$  of rotation about the symmetry axis has the form  $e^{i\phi} \pm e^{-i\phi}$  for the two  $\Lambda$ -doublet states of a  $\Pi$  electron. The probability distributions for the electron are then proportional to  $\cos^2\phi$  and  $\sin^2\phi$  for the two

states, giving large probabilities in the regions shown as shaded in Fig. 8-3. In Fig. 8-3*a*, corresponding to the lower  $\Lambda$ -doublet state with a  $\sin^2 \phi$  distribution, the field of the electron at the nucleus is parallel to  $I$  (the electron magnetic moment is antiparallel to its spin  $S$ ). In Fig. 8-3*b*, corresponding to the upper  $\Lambda$ -doublet state, the electron's field is directed oppositely to  $I$ . Hence the spin-spin interaction energy is quite different for the two cases. A reversal of  $I$  or  $S$  with respect to the

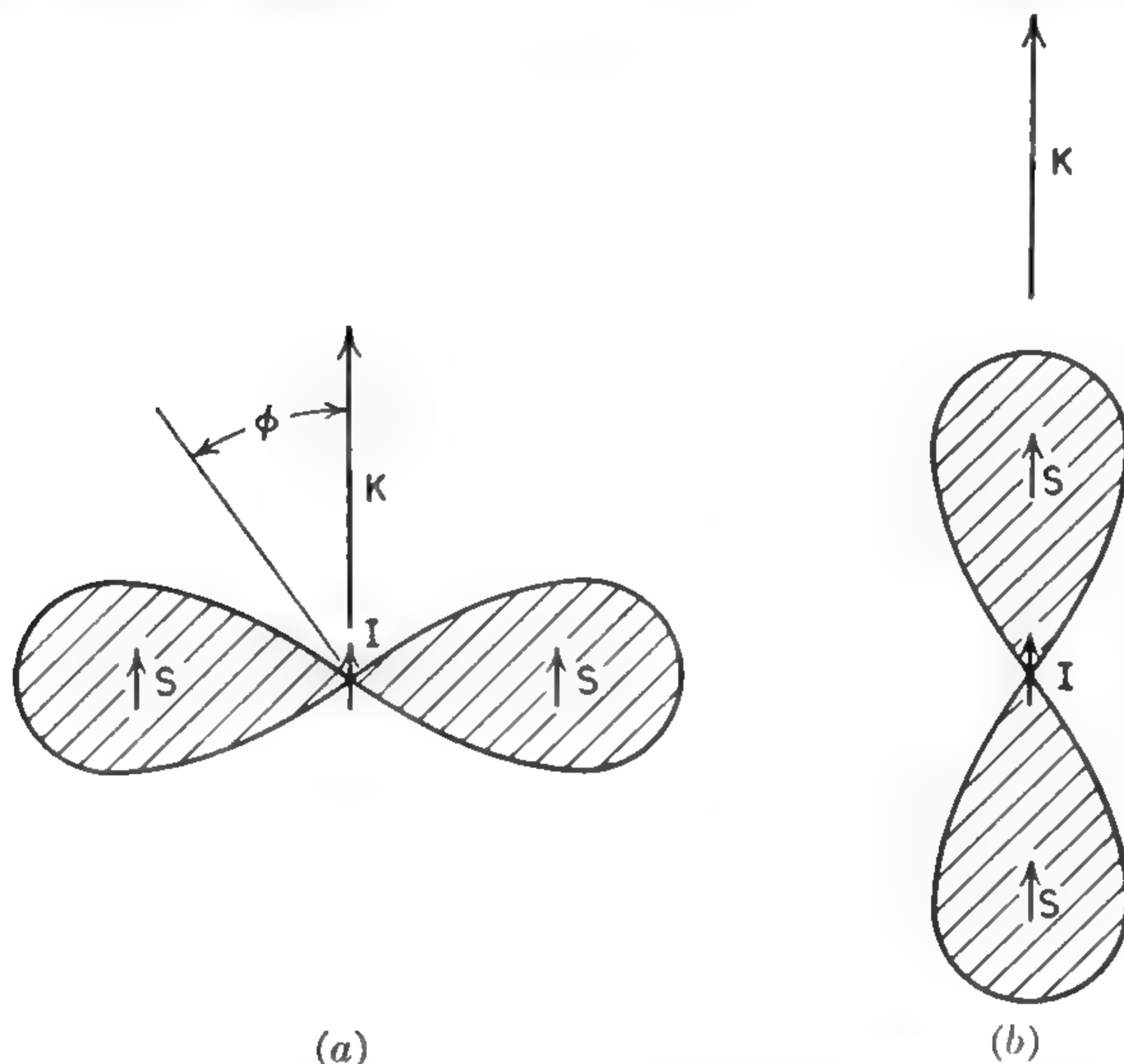


FIG. 8-3. Distribution of an unpaired electron in a  ${}^2\Pi$  case (b) molecule for the two  $\Lambda$ -doublet states. The molecular axis is perpendicular to the page. Interaction energy between magnetic moments associated with the electron spin  $S$  and the nuclear spin  $I$  is different for the two cases.  $K$  is the angular momentum due to rotation of the molecule.

rotational angular momentum  $K$  of course reverses the sign of the hyperfine interaction energy for both  $\Lambda$ -doublet levels.

More formal reasoning shows that these effects are possible because the matrix elements of hyperfine interactions may connect states with a difference in  $\Lambda$  of  $\pm 2$  (and hence with differences in  $\Omega$  [686]). The two  $\Lambda$ -doubled states actually involve equal mixtures of states with positive and negative values of  $\Lambda$ , in exact analogy with the  $l$ -doubled states discussed in Chap. 2 or the inversion states of Chap. 3. Hence in Hund's case (a) matrix elements connecting states with a difference in  $\Omega$  of  $\pm 1$  or  $\pm 2$  give first-order (diagonal) effects for a  ${}^2\Pi_1$  state but for no others. In case (b), first-order effects of such matrix elements are found for  ${}^2\Pi$  or  ${}^1\Pi$  states, but for no others.

The actual magnitude of the spin-spin interaction of the type described here, with case (a), case (b), or intermediate coupling, is given for a  ${}^2\Pi$

state by [971a]

$$\Delta W = \pm \frac{d(X + 2 - A/B)}{4XJ(J + 1)} (J + \frac{1}{2}) \mathbf{I} \cdot \mathbf{J} \quad (8-16)$$

where  $A$  = the fine-structure constant (energy =  $A \mathbf{S} \cdot \mathbf{\Lambda}$ )

$B$  = the rotational constant

$$X = \pm [(A/B)(A/B - 4) + 4(J + \frac{1}{2})^2]^{\frac{1}{2}}$$

$$d = 3\mu_0 \frac{\mu_I}{I} \left( \frac{\sin^2 \theta}{r^3} \right)_{av}$$

$r$  = distance from nucleus to electron

$\theta$  = angle between molecular axis and radius from nucleus to electron

The signs in (8-16) need explanation. When the constant  $A$  is positive (regular fine structure), then a positive sign for  $X$  is for the state which approaches  ${}^2\Pi_{\frac{1}{2}}$  in case (a), and a negative sign for  $X$  for the state which approaches  ${}^2\Pi_{\frac{3}{2}}$ . When  $A$  is negative (inverted fine structure), a negative  $X$  gives the  ${}^2\Pi_{\frac{1}{2}}$  state, and a positive  $X$  the  ${}^2\Pi_{\frac{3}{2}}$  state. The upper (positive) sign in front of  $d$  in (8-16) applies to the upper  $\Lambda$ -doublet level of the state for which  $J = N + \frac{1}{2}$  in the limiting case (b) or for both of the  ${}^2\Pi_{\frac{1}{2}}$  and  ${}^2\Pi_{\frac{3}{2}}$  states in case (a), and the lower sign to the lower state. The appropriate signs in front of  $d$  are the reverse in the state for which  $J = N - \frac{1}{2}$  in the limiting case (b).

In case (a),  $X = \pm A/B$ , and (8-16) gives

$$\Delta W = \pm \frac{d(J + \frac{1}{2})}{2J(J + 1)} \mathbf{I} \cdot \mathbf{J}$$

for the  ${}^2\Pi_{\frac{1}{2}}$  state and  $\Delta W = 0$  for the  ${}^2\Pi_{\frac{3}{2}}$  state. The upper sign in front of  $d$  applies to the upper  $\Lambda$ -doublet state. In case (b), (8-16) gives

$$\Delta W = - \frac{d(J - \frac{1}{2})}{4J(J + 1)} \mathbf{I} \cdot \mathbf{J} \quad \text{for } J = N + \frac{1}{2}$$

and

$$\Delta W = \pm \frac{d(J + \frac{3}{2})}{J(J + 1)} \mathbf{I} \cdot \mathbf{J} \quad \text{for } J = N - \frac{1}{2}$$

This type of hyperfine effect we shall call hyperfine doubling, since it can remove the degeneracy from or further split  $\Lambda$ -type doublets. For hyperfine doubling to occur, one of the interacting spins must lie off the axis of the molecule [ $\theta > 0$  in the definition of  $d$  under expression (8-16)]. This doubling can also occur in a symmetric-top molecule in a  ${}^1\Sigma$  state if there is interaction between a nuclear spin on the axis and one off the axis. An example is  $\text{NH}_3$ , which will be discussed more fully below. Here interaction between the N and H nuclear moments splits the otherwise degenerate levels  $K = \pm 1$ .

Hyperfine doubling has been found in OH [861], which is a case of



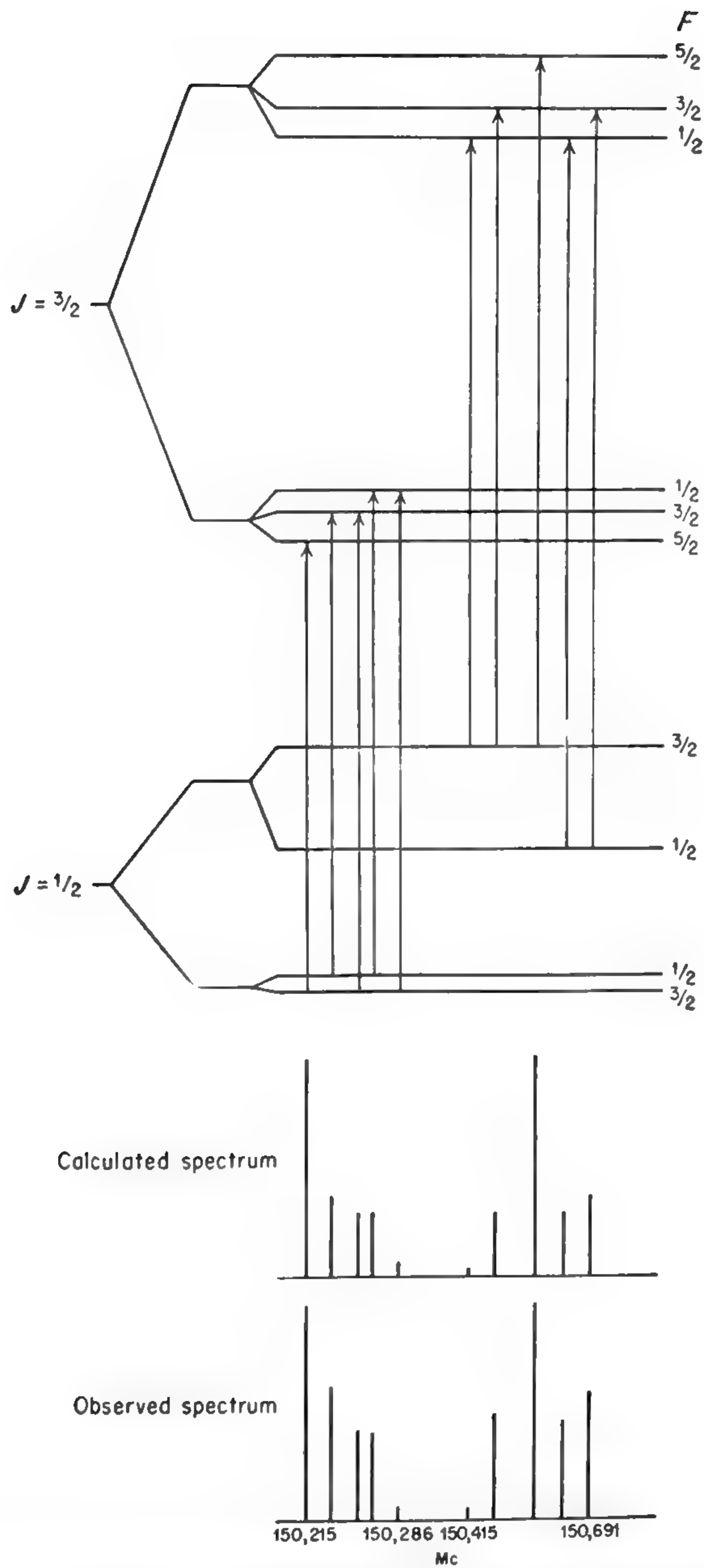


FIG. 8-4. Energy-level diagram and spectrum of the  $J = \frac{3}{2} \leftarrow \frac{1}{2}$  rotational transition of the  $^2\Pi_{1/2}$  state of  $\text{N}^{14}\text{O}^{16}$ . (After Gallagher, Bedard, and Johnson [924].)

intermediate coupling, and in the  ${}^2\Pi_{1/2}$  state of NO [782*b*], [924], which is rather close to case (a). For OH,  $d = 57$  Mc and for NO,  $d = 112.6$  Mc. In both OH and NO, the hyperfine doubling is superimposed on a hyperfine structure of the form (8-6) which is identical for the two  $\Lambda$  doublets. Structures of the two lowest rotational states of NO are illustrated in Fig. 8-4. Here the hyperfine doubling is somewhat larger than other hyperfine effects and consequently has interchanged the order of the hyperfine levels in the two  $\Lambda$ -type doublets of each rotational state.

**8-7. Electronic Angular Momentum in  ${}^1\Sigma$  Molecules and Its Contributions to Molecular Energy.** Although molecules in  ${}^1\Sigma$  states are often said to have no electronic angular momentum, there is in fact a small electronic angular momentum when a molecule of this type is rotating. For example, consider the motion of closed shells of electrons associated with a nucleus. These move with the nucleus during rotation of the molecule and hence possess angular momentum. Their rotation produces magnetic fields which can give magnetic hyperfine structure. A more interesting and complex case is a valence electron which is not definitely associated with one nucleus. Valence electrons may only partly rotate with the molecule, but still usually produce the dominating magnetic fields at the nuclei. Their behavior also produces complications in the purely mechanical rotational energy of the molecule.

In order to examine the behavior of electrons in a rotating molecule, we shall start with the energy or Hamiltonian for electrons in a molecule with fixed nuclei, which is of the form

$$\begin{aligned} H_e &= \frac{1}{2m} \sum_n [p_{nx}^2 + p_{ny}^2 + p_{nz}^2] + V \\ &= \frac{1}{2m} \sum_n \sum_g p_{ng}^2 + V \end{aligned} \quad (8-17)$$

where  $m$  is the electron mass,  $p_{ng}$  is the  $g$ th component of the momentum of the  $n$ th electron in Cartesian coordinates, and  $V$  is the potential energy of all the electrons. The energy of the electrons in the ground state may be found in principle by solving Schrödinger's equation with (8-17) as the Hamiltonian. Let this energy be  $W_{e0}$ .

If the molecule rotates, the Hamiltonian for the electrons is of the same form, but  $p_{ng}$  refers then to a Cartesian component of the generalized momentum of the  $n$ th electron referred to a set of axes fixed in the molecule and rotating with it. This momentum is not simply the mass times the velocity in the rotating coordinates, and must be found by the general method of differentiating the Lagrangian with respect to the velocity. The important point for our purposes, however, is that the Hamiltonian in rotating coordinates has the same form (8-17) as long as the coordinate system is Cartesian. The nuclei also acquire kinetic energy as a result of

rotation, which may be written

$$H_n = \frac{1}{2} \sum_{\sigma} \frac{O_{\sigma}^2}{A_{\sigma}} \quad (8-18)$$

where  $A_{\sigma}$  is the moment of inertia of the system of nuclei in the molecule about one of the principal axes, and  $O_{\sigma}$  is their angular momentum about this axis. We shall for simplicity assume that the nuclei are rigidly fixed in the molecule and disregard possible vibrational energies. The component  $J_{\sigma}$  of the total angular momentum about a principal axis of inertia is the sum of that due to the nucleus  $O_{\sigma}$  and the small angular momentum  $L_{\sigma}$  of the electrons, or

$$O_{\sigma} = (J_{\sigma} - L_{\sigma})\hbar \quad (8-19)$$

where  $J_{\sigma}$  and  $L_{\sigma}$  are in units of  $\hbar$ .

Combining (8-17), (8-18), and (8-19), the Hamiltonian for the rotating system becomes

$$H = \frac{1}{2} \sum_{\sigma} \frac{\hbar^2 J_{\sigma}^2}{A_{\sigma}} - \sum_{\sigma} \frac{\hbar^2 J_{\sigma} L_{\sigma}}{A_{\sigma}} + \frac{1}{2} \sum_{\sigma} \frac{\hbar^2 L_{\sigma}^2}{A_{\sigma}} + \frac{1}{2m} \sum_n \sum_{\sigma} p_{n\sigma}^2 + V \quad (8-20)$$

If the electrons are truly in a  $^1\Sigma$  state, there is no electronic angular momentum and  $L_{\sigma}$  is zero, so that the energy given by (8-20) is just the sum of the energy due to the last two terms, and that due to the first term. This first term gives the rotational energies  $W_R$  of a rigid rotor, but one without electrons since  $A_{\sigma}$  is the moment of inertia of the nuclei only. The total energy in this approximation is then just

$$W_0 = W_R + W_{e0} \quad (8-21)$$

It is only by allowing for perturbations of the ground  $^1\Sigma$  electron states by the term  $\sum_{\sigma} (\hbar^2 J_{\sigma} L_{\sigma} / A_{\sigma})$  that the energy associated with the contribution of the electrons to the moment of inertia of the molecule can be obtained. This perturbation introduces a small probability for electronic angular momentum states other than  $^1\Sigma$ ; hence it produces some electronic angular momentum which affects the rotational energy of the molecule. To a good approximation, the third term of (8-20),  $\frac{1}{2} \sum_{\sigma} (\hbar^2 L_{\sigma}^2 / A_{\sigma})$ , is a constant of the molecular rotation. Rotation will indeed produce perturbations of this term, but they are too small to be significant at present.

Since the perturbation  $\sum_{\sigma} (\hbar^2 J_{\sigma} L_{\sigma} / A_{\sigma})$  introduces electronic angular momentum, we must take into account the various other types of energy terms connected with electronic angular momentum in order to complete the Hamiltonian (8-20). One of these is the interaction between a



nuclear magnetic moment and the magnetic fields produced by an electronic angular momentum. Such interactions are similar in principle to the magnetic hyperfine structure due to orbital motion of an electron in an atom, and may be written as in (5-49) after letting  $\mathbf{j} = \mathbf{L}$ ,

$$a\mathbf{I} \cdot \mathbf{L}' = a \sum_{\sigma} I_{\sigma} L'_{\sigma} \quad (8-22)$$

where  $\mathbf{L}'$  is the electronic orbital angular momentum about the nucleus of spin  $\mathbf{I}$ , and  $a = (2\mu_I\mu_0/I)(1/r^3)_{av}$ . However, in a molecule,  $\mathbf{L}$  is not a constant of the motion, and hence both  $\mathbf{L}'$  and  $(1/r^3)_{av}$  must be averaged over the electronic wave function. It should be noted too that (8-22) contains  $\mathbf{L}'$ , the angular momentum about a particular nucleus, rather than  $\mathbf{L}$ , the angular momentum with respect to the center of mass of the molecule.  $\mathbf{L}'$  and  $\mathbf{L}$  are, of course, closely related.

Another common interaction associated with electronic angular momentum is the Zeeman effect due to an external applied field  $H$ . The interaction energy is given by

$$\mu_0\mathbf{H} \cdot \mathbf{L} = \mu_0 \sum_{\sigma} H_{\sigma} L_{\sigma} \quad (8-23)$$

where  $\mu_0$  is the Bohr magneton.

Although we shall not be concerned here with all possible types of magnetic interaction, still another interaction which we shall include is the direct interaction between the magnetic moment of the nucleus and the external field  $H$ . This is

$$-\mathbf{\mu}_I \cdot \mathbf{H} = - \sum_{\sigma} \mu_{\sigma} H_{\sigma} \quad (8-24)$$

where  $\mu_I$  is the nuclear magnetic moment. Adding the three terms (8-22), (8-23), and (8-24) and omitting the constant term  $\frac{1}{2} \sum_{\sigma} \hbar^2(L_{\sigma}^2/A_{\sigma})$

in (8-20), the Hamiltonian becomes

$$H = \frac{1}{2m} \sum_n \sum_{\sigma} p_{n\sigma}^2 + V + \frac{1}{2} \sum_{\sigma} \frac{\hbar^2 J_{\sigma}^2}{A_{\sigma}} + \sum_{\sigma} \left( \mu_0 H_{\sigma} - \frac{\hbar^2 J_{\sigma}}{A_{\sigma}} \right) L_{\sigma} + a\mathbf{I} \cdot \mathbf{L} - (\mathbf{\mu}_I \cdot \mathbf{H}) = H_0 + H' \quad (8-25)$$

Here  $H_0$  represents the first three terms which are the main parts of the Hamiltonian.  $H'$  consists of the remaining small perturbing terms.

It may be seen from (8-25) that the effect of a magnetic field on electrons is just equivalent to that of molecular rotation since they both enter (8-25) only in the factor  $\left( \mu_0 H_{\sigma} - \frac{\hbar^2 J_{\sigma}}{A_{\sigma}} \right)$ . Thus the effect of a mag-

netic field  $H_g$  is equivalent to a rotation  $\frac{-\hbar^2 J_g}{\mu_0 A_g}$ . Since  $\hbar J_g = \omega A_g$ , where  $\omega$  is the angular velocity, the rate of angular rotation which produces an effect on the molecular electrons precisely the same as that of the field  $H_g$  is  $\omega_g = \frac{eH_g}{2mc}$ . This is Larmor's theorem, and is responsible for the direct connection (I - 47) between  $L$  uncoupling and the molecular  $g$  factor due to electrons.

The first-order correction to the energy given by  $H_0$  is the average value of  $H'$  in the  $^1\Sigma$  state of the molecule. The parts of  $H'$  proportional to  $L$  have an average value of zero, so that the only term of  $H'$  which gives an energy in first order is  $-\mathbf{u}_l \cdot \mathbf{H}$ . The second-order correction to the energy is given as usual by

$$W' = \sum_n \frac{|(0|H'|n)|^2}{W_0 - W_n} \quad (8-26)$$

where  $W_0$  is the energy of the unperturbed state, and  $W_n$  the energy of the  $n$ th excited electronic state.  $(0|H'|n)$  is the matrix element of  $H'$  between the unperturbed and an excited electronic state.

To illustrate the nature of the various terms in (8-26), let us assume that only one excited state is of importance so the sum over  $n$  may be omitted. Second-order terms in  $\mathbf{u}_l \cdot \mathbf{H}$  will be assumed negligible, as they usually are.

$$\begin{aligned} W' = & \frac{|(0|a\mathbf{I} \cdot \mathbf{L}|n)|^2}{W_0 - W_n} + \sum_g \sum_{g'} \hbar^4 J_g J_{g'} \frac{(0|L_g|n)(n|L_{g'}|0)}{A_g A_{g'}(W_0 - W_n)} + \frac{|(0|\mu_0 \mathbf{H} \cdot \mathbf{L}|n)|^2}{W_0 - W_n} \\ & + \sum_{g'} \sum_g \mu_0 I_g H_{g'} \frac{(0|aL'_g|n)(n|L_{g'}|0) + (0|L_{g'}|n)(n|aL'_g|0)}{W_0 - W_n} \\ & - \sum_{g'} \sum_g \frac{\hbar^2 I_g J_{g'}}{A_{g'}} \frac{(0|aL'_g|n)(n|L_{g'}|0) + (0|L_{g'}|n)(n|aL'_g|0)}{W_0 - W_n} \\ & - 2 \sum_{g'} \sum_g \mu_0 \frac{\hbar^2 J_g H_{g'}}{A_g} \frac{(0|L_g|n)(n|L_{g'}|0)}{W_0 - W_n} \quad (8-27) \end{aligned}$$

Expression (8-27) appears rather formidable partly because it applies to the general asymmetric top and hence the sums over coordinate directions  $g$  and  $g'$  cannot be very much simplified. Its complexity is due also to the fact that each of the six terms of (8-27) corresponds to a different physical effect. These may be and usually are discussed separately.

The second term in (8-27) is the only one which does not involve magnetic effects. It is proportional to the square of the molecular angular momentum  $J$ , and represents the contribution of the electrons to the moment of inertia of the molecule or to the kinetic energy of rotation. Since  $W_0 - W_n$  is negative, this term is negative and corresponds to a

decrease in the energy of rotation. This is to be expected since the electrons should add to the moments of inertia  $A_0$  of the bare nuclei. It will be shown below that, at least for electrons closely bound to the nuclei, this term does in fact have the magnitude to be expected from the electronic contribution to the moment of inertia.

The first term in (8-27) is called the pseudo quadrupole effect [192] because it has the same form as a quadrupole interaction between  $\mathbf{I}$  and the molecular electric fields. In a simple  $^1\Sigma$  linear molecule, for example,  $\mathbf{L}$  may be thought of as precessing around the molecular axis, so that  $(\mathbf{I} \cdot \mathbf{L})^2$  becomes proportional to the square of the cosine of the angle between  $\mathbf{I}$  and the molecular axis, which is the same dependence on this angle shown by an electric quadrupole interaction. Hence experimentally the effect of this term cannot simply be distinguished from that of a nuclear quadrupole interaction. Fortunately, however, the pseudo quadrupole interaction is almost always negligibly small, since from (8-27) it is proportional to the square of a magnetic hyperfine interaction divided by the separation between electronic levels. It is hence not usually larger than a few cycles per second.

The pseudo quadrupole effect may be regarded as a magnetic polarization of the molecule by the nuclear magnetic moment, and then an interaction between the resulting molecular magnetic field and the nuclear moment. In principle the interaction discussed by Hebb (*cf.* page 182) in  $\rho$ -type tripling is identical with this nuclear effect, but it involves fine-structure rather than hyperfine-structure interactions and is consequently enormously greater.

The third term of (8-27) is an energy associated with the magnetic susceptibility or polarization of the molecule by an external field (*cf.* [38], p. 227) and is not of great interest here. It has no dependence on molecular rotation and corresponds to the interaction between the field  $\mathbf{H}$  and the molecular magnetic dipole induced by  $\mathbf{H}$ .

The fourth term of (8-27),

$$\sum_{\sigma'} \sum_{\sigma} \mu_0 I_{\sigma} H_{\sigma'} \frac{(0|aL'_{\sigma}|n)(n|L_{\sigma'}|0) + (0|L_{\sigma'}|n)(n|aL'_{\sigma}|0)}{W_0 - W_n}$$

also does not depend on the molecular rotation. It corresponds to a magnetic polarization of the molecule by an external field  $H$ , or creation of electronic angular momentum  $\mathbf{L}$  as a result of this field, and then an interaction between the nuclear magnetic moment and the magnetic field produced by the angular momentum  $\mathbf{L}$ . These effects are usually unimportant to microwave spectroscopy of gases, since they are normally smaller than the direct interaction  $\boldsymbol{\mu}_I \cdot \mathbf{H}$  between an external field  $H$  and a nuclear magnetic moment by a factor of  $10^4$ . However, for nuclear magnetic resonances in solids or liquids such effects are measurable and



are generally called "chemical effects," since they do not depend simply on the nucleus, but vary from one molecule to the next [569], [515].

The remaining two terms of (8-27),

$$- \sum_{g'} \sum_g \frac{\hbar^2 I_g J_{g'}}{A_{g'}} \frac{(0|aL'_g|n)(n|L_{g'}|0)(0|L_{g'}|n)(n|aL'_g|0)}{W_0 - W_n}$$

and  $-2 \sum_{g'} \sum_g \frac{\mu_0 \hbar^2 J_g H_{g'}}{A_{g'}} \frac{(0|L_g|n)(n|L_{g'}|0)}{W_0 - W_n}$ , are both dependent on the rotational angular momentum  $J$  of the molecule and are interesting terms from the point of view of microwave spectroscopy. They may be thought of as due to an excitation of electronic orbital angular momentum  $L$  by the rotation  $J$ . This electronic angular momentum produces an internal molecular magnetic field which interacts with the nuclear magnetic moment, and also a molecular magnetic moment which interacts with the external field  $H$ . The latter term, linearly proportional to  $H$  and to  $J$ , is a Zeeman effect which will be discussed at length in Chap. 11. The term linearly proportional to  $I$  and  $J$  is part of the common variety of magnetic hyperfine structure in  $^1\Sigma$  molecules which for simple linear molecules reduces to the form  $C_I \mathbf{I} \cdot \mathbf{J}$ , where  $C_I$  is a constant dependent on the molecule. This interaction is often called the " $I$  dot  $J$ " interaction and will be discussed at length below.

**8-8. Effect of Electronic Motion on Rotational Energy.** We shall digress from magnetic effects briefly to examine parts of the energy (8-26) of the type illustrated by the second term of (8-27), *i.e.*,

$$W'_2 = \sum_g \sum_{g'} \frac{\hbar^2 J_g J_{g'}}{A_g A_{g'}} \sum_n \frac{\hbar^2 (0|L_g|n)(n|L_{g'}|0)}{W_0 - W_n} \quad (8-28)$$

These terms give the effect of electrons on the rotational energy of the molecule, and illustrate some of the properties of the terms involved in magnetic hyperfine structure. For simplicity, consider a linear molecule and take the  $z$  direction along the molecular axis. Then  $L_z = 0$ , and the terms of (8-28) of the type

$$\sum_n \frac{\hbar^2}{W_0 - W_n} [(0|L_x|n)(n|L_y|0) + (0|L_y|n)(n|L_x|0)]$$

are also zero. The latter may be shown by a rotation of the molecule about the  $z$  axis by  $\pi/2$ . After the rotation,  $x$  becomes  $y$ , and  $y$  becomes  $(-x)$ . Since the directions  $x$  and  $y$  are equivalent, this term has changed sign but cannot have changed value, so that it must equal zero. The only nonzero terms of (8-28) are therefore

$$W'_2 = \hbar^2 \frac{J_x^2}{A_x^2} \sum_n \frac{\hbar^2 |(0|L_x|n)|^2}{W_0 - W_n} + \hbar^2 \frac{J_y^2}{A_y^2} \sum_n \frac{\hbar^2 |(0|L_y|n)|^2}{W_0 - W_n}$$

or, since the  $x$  and  $y$  directions are equivalent,

$$W'_2 = \hbar^2 \frac{J(J+1)}{A^2} \sum_n \frac{\hbar^2 |(0|L_x|n)|^2}{W_0 - W_n} \quad \text{or} \quad 4J(J+1)\hbar^2 B^2 \sum_n \frac{|(0|L_x|n)|^2}{W_0 - W_n} \quad (8-29)$$

where  $J(J+1) = J_x^2 + J_y^2$  is the square of the total angular momentum,  $A = A_x = A_y$ , and  $B = \hbar/8\pi^2 A$  is the rotation constant.

The "slippage" of electrons with respect to the nuclei as the molecule rotates may be seen from (8-29). If the electron distribution and the fields were completely spherical about the center of mass, then  $(0|L_x|n)$  would be zero. The fractional part of the valence electrons which is spherically distributed may be considered, as noted in Chap. 1, to slip with respect to the molecule and not contribute to the rotational energy.

The inner shells of electrons attached to a nucleus are not at all spherical with respect to the center of mass and may be more easily discussed with a coordinate system centered at this nucleus. Let  $\tau$  be the distance from the center of mass to the nucleus. Then

$$\hbar L_x = \hbar L'_x - \tau p_y \quad (8-30)$$

where  $L'_x$  is the electronic angular momentum (in units of  $\hbar$ ) of the spherical shell about the nucleus in question and  $p_y$  is the linear momentum in the  $y$  direction. But if we consider only a spherical closed shell of electrons in the spherical field of a nucleus,  $(0|L'_x|n) = 0$  for any  $n$ , so that, using (8-30), for closed shells

$$\sum_n \frac{\hbar^2}{W_0 - W_n} |(0|L_x|n)|^2 = \tau^2 \sum_n \frac{|(0|p_y|n)|^2}{W_0 - W_n} \quad (8-31)$$

This can be simplified by the general identity\* for any particle of mass  $m$

$$\sum_n \frac{|(0|p_y|n)|^2}{W_0 - W_n} = \frac{-m}{2} \quad (8-32)$$

\*This identity may be proved as follows:

$$p_y = m \frac{dy}{dt} = \frac{m}{i\hbar} (yH - Hy)$$

or

$$(0|p_y|n) = \frac{mi}{\hbar} (W_0 - W_n)(0|y|n)$$

(cf. [408], p. 139).

Hence

$$\sum_n \frac{(0|p_y|n)(n|p_y|0)}{W_0 - W_n} = \sum_n \frac{mi}{\hbar} \frac{(0|y|n)(n|p_y|0) - (0|p_y|n)(n|y|0)}{2} = \frac{-m}{2}$$

since  $yp_y - p_y y = i\hbar$ .

Hence (8-29) becomes for  $N$  electrons in spherical orbits around a nucleus which is a distance  $\tau$  from the center of mass

$$W'_2 = \frac{-\hbar^2 J(J+1) N m \tau^2}{2A^2} \quad (8-33)$$

This is a small decrease in the energy of rotation due to the presence of the electrons which should be added to the kinetic energy of the nuclei. Thus

$$W = W_0 + W'_2 = \frac{\hbar^2 J(J+1)}{2A} - \frac{\hbar^2 J(J+1)}{2A^2} N m \tau^2 \approx \frac{\hbar^2 J(J+1)}{2(A + N m \tau^2)} \quad (8-34)$$

Of course, (8-34) as written includes the effect of only those electrons "bound" to one particular nucleus, and all other closed electron shells should be similarly treated. This expression is sufficient to show, however, how the bound electrons add to the moment of inertia, and that, as stated in Chap. 1, the spherical closed electron shells in a molecule behave as if they follow the nuclei during molecular rotation, but remain fixed in orientation in space like the chairs on a rotating Ferris wheel.

For the valence shell of electrons, the sum in (8-29) cannot be so easily evaluated. One approximation which is often made involves the "pure-precession" hypothesis. In this case the electronic angular momentum  $L$  is assumed to have a fixed value and to precess around the molecular axis with a projection of zero on this axis for the ground state. The only low-lying electronic state for which  $(0|L_x|n)$  is not zero is the  $\Pi$  state corresponding to a unit projection of  $L$  on the molecular axis. In this case  $|(0|L_x|n)|^2 = L(L+1)/4$ , so that (8-29) may be written

$$W'_2 = -J(J+1)B^2 \left[ 8\pi^2 \sum_s N_s m \tau_s^2 + \frac{L(L+1)\hbar^2}{(W_\Pi - W_\Sigma)} \right] \quad (8-35)$$

where the sum is over all "bound" electrons in closed shells around nuclei of distance  $\tau_s$  from the center of gravity of the molecule, and  $J$  is the quantum number for the total angular momentum. The last term of (8-35) gives the contribution of valence electrons under the restrictive assumption of pure precession.  $W_\Pi - W_\Sigma$  is the excitation energy of the lowest electronic state.

In nonlinear polyatomic molecules the full form (8-28) must be used to obtain the effect of electrons on the rotational kinetic energy. However, for almost all purposes sufficient accuracy may be obtained by assuming the electrons associated with each nucleus to be located at the nucleus and using moments of inertia which include these electrons in calculating rotational energy. Only for the valence electrons does this involve some small error, and usually only by very accurate measurements on diatomic molecules can such small effects be detected. In more



complex molecules other inaccurately known effects tend to mask these errors.

**8-9. Magnetic Hyperfine Interaction ( $\mathbf{I} \cdot \mathbf{J}$ ) in  $^1\Sigma$  Molecules.** We shall examine now in more detail the term in (8-27) which is linearly proportional to  $I$  and  $J$ , and which represents a magnetic hyperfine interaction between a nucleus and electrons even in  $^1\Sigma$  molecules. It is

$$W'_5 = - \sum_n \sum_{g'} \sum_g \frac{\hbar^2 I_g J_{g'}}{A_{g'}} \frac{(0|aL'_g|n)(n|L_{g'}|0) + (0|L_{g'}|n)(n|aL'_g|0)}{W_0 - W_n} \quad (8-36)$$

where the summation over all excited states  $n$  has been included rather than over only one state as in (8-27).

Now an angular velocity about the center of mass of the molecule is equivalent to the same angular velocity about any nucleus in the molecule plus an appropriate instantaneous linear velocity  $v$ . The magnetic fields produced at the nucleus by rotation about the two different points should differ only by the effect of the velocity  $v$ . At the nucleus the average electric field is zero (because there is no average force on the nucleus at equilibrium), so that the velocity  $v$  in fact produces no magnetic field at the nucleus [magnetic field  $\approx (v/c) \times$  electric field]. Hence it may be expected that the angular momentum  $L_{g'}$  about the center of mass can be replaced in (8-36) by the angular momentum  $L'_g$  about the nucleus in question without changing the magnetic energy given by this expression.\* Furthermore, since the quantity  $a$  depends on  $1/r^3$ , but not on the angular position of the electron with respect to the nucleus, the part of the matrix element which depends on  $a$  may be factored out, that is,  $(0|aL'_g|n) = a_{0n}(0|L'_g|n)$ .  $a_{0n}$  may be taken as real so that  $a_{0n} = a_{n0}$ . Hence (8-36) becomes

$$W'_5 = -2 \sum_n \sum_{g'} \sum_g \frac{\hbar^2 I_g J_{g'}}{A_{g'}} a_{0n} \frac{(0|L'_g|n)(n|L_{g'}|0)}{W_0 - W_n} \quad (8-37)$$

The nature of expression (8-37) is perhaps most easily understood by applying it to the simple case of a diatomic molecule. It is evident that closed shells of electrons about the nucleus being considered do not contribute magnetic hyperfine structure, since for them  $(0|L_g|n)$  is zero. Closed shells of electrons around other nuclei can be treated in a way similar to that used in reducing (8-28) for a diatomic molecule, and their contribution to (8-37) can be shown to be

$$- \frac{\mu_I \hbar \mathbf{I} \cdot \mathbf{J}}{IA} \sum_s \frac{e}{cr_s} = -4\pi \frac{\mu_I}{I} B \mathbf{I} \cdot \mathbf{J} \sum_s \frac{e}{cr_s}$$

Here  $e$  is the electron charge in esu (negative sign) and  $r_s$  is the distance of the center of the  $s$ th electron distribution from the nucleus of spin  $I$

\* For a more detailed discussion, see [686], Secs. 7 and 8.

and  $g$  factor  $g_I$ . Valence electrons which are not spherically distributed about any nucleus cannot be so simply treated and their contributions must be left in essentially the form (8-37). The charges on nuclei contribute in the same way as those of electrons in closed shells about the nuclei, as may be seen by formally considering their changes to be due to closed shells of positively charged electrons tightly bound to the nucleus. Therefore for the diatomic or linear molecule, the combined effect of electrons from (8-37) and the nuclear charges gives

$$W'_5 + \text{effects of nuclear charges} = \mathbf{I} \cdot \mathbf{JB} \left[ 4h \sum_n \frac{a_{0n} | \langle 0 | L_x | n \rangle |^2}{W_n - W_0} - 4\pi \frac{\mu_I}{I} \sum_s \frac{q_s}{cr_s} \right] \quad (8-38)$$

where  $r_s$  is the distance between the nucleus for which (8-38) gives the magnetic hyperfine energy and any other nucleus in the molecule, and  $q_s$  is the net charge of the  $s$ th nucleus plus the electrons which are in closed shells about it. Assuming the pure precession approximation, (8-38) may be written

$$W'_5 + \text{nuclear effects} = \mathbf{I} \cdot \mathbf{JB} \left[ \frac{ha_{\Sigma n} L(L+1)}{W_{\Pi} - W_{\Sigma}} - 4\pi \frac{\mu_I}{I} \sum_s \frac{q_s}{cr_s} \right] \quad (8-39)$$

The general form of the magnetic hyperfine interaction of a nucleus in a linear  $^1\Sigma$  molecule (with no vibrational angular momentum) is, from (8-38)

$$W_{mag} = C_I \mathbf{I} \cdot \mathbf{J} \quad (8-40)$$

where the constant  $C_I$  is dependent on molecular parameters shown in (8-38). This type of interaction was first found in the hydrogen molecule by the use of molecular-beam techniques [91], and the constant  $C_I$  has now been evaluated for a number of molecules by both molecular beam and the usual microwave spectroscopic techniques. Table 8-1 shows the values of  $C_I$  for molecules so far measured, which vary from near 1 kc to somewhat greater than 100 kc. A few additional values of  $C_I$  have been reported for the alkali halides from measurements of line widths in molecular-beam magnetic resonance experiments. However, such measurements are subject to uncertainties in interpretation and hence these values have been omitted from Table 8-1. White [999] has shown that a number of interesting trends can be established from present measurements of  $C_I$ .

*Examples of  $\mathbf{I} \cdot \mathbf{J}$  Interaction.* Usually  $\mu_I$  for the nucleus is positive, and hence the first term of (8-38) due to the valence electrons is positive, while the second term due to nuclei and bound electrons is negative. In most cases  $C_I$  is positive.  $\text{O}^{17}$  and  $\text{Se}^{79}$  are the only nuclei with a negative  $\mu_I$  for which  $C_I$  has been measured. It may be seen from Table 8-1 that,

with the exception of hydrogen nuclei in  $\text{H}_2$ , these are precisely the only cases where  $C_I$  has been found to be negative. Hence except in the special cases of hydrogen the first term in (8-38), due to excitation of the valence electrons by rotation, always dominates.

TABLE 8-1. VALUES OF MAGNETIC HYPERFINE CONSTANTS  $C_I$  IN  $^1\Sigma$  MOLECULES  
(Magnetic hyperfine energy =  $C_I \mathbf{I} \cdot \mathbf{J}$ )

Molecule	Nucleus	$C_I$ , kc	$\frac{C_I}{g_I B(1/r^3)_{av}}$ , $10^{-33} \text{ cm}^3$	Reference
$\text{Li}^6\text{F}$	$\text{F}^{19}$	$37.3 \pm 0.3$	3.4	[753]
$\text{Li}^7\text{F}$	$\text{F}^{19}$	$32.9 \pm 0.1$	3.3	[999]
$\text{KF}$	$\text{F}^{19}$	$0 \pm 10$	$0 \pm 7$	[463]
$\text{Rb}^{85}\text{F}$	$\text{F}^{19}$	$11 \pm 3$	10	[476]
$\text{Rb}^{87}\text{F}$	$\text{F}^{19}$	$14 \pm 4$	13	[476]
$\text{CsF}$	$\text{F}^{19}$	$16 \pm 2$	14	[331]
$\text{Li}^7\text{F}$	$\text{Li}^7$	$2.2 \pm 0.6$	90	[999]
$\text{DI}$	$\text{I}^{127}$	140	11	[999]
$\text{ClF}$	$\text{Cl}^{35}$	$22 \pm 3$	54	[366] [999]
$\text{CS}$	$\text{S}^{33}$	$19 \pm 15$	54	[999]
$\text{Ti}^{205}\text{Cl}^{35}$	$\text{Cl}^{35}$	$1.4 \pm 0.1$	20	[676b]
$\text{Ti}^{206}\text{Cl}^{35}$	$\text{Ti}^{205}$	$73 \pm 2$	110	[676b]
$\text{H}_2$	$\text{H}$	$-113.904 \pm 0.030$	-40.8	[91] [716a] [807]
$\text{HD}$	$\text{H}$	$-87.00 \pm 0.85$	-41.4	[91a]
$\text{HD}$	$\text{D}$	$-12.6 \pm 0.3$	-39.0	[91a]
$\text{D}_2$	$\text{D}$	$-8.445 \pm 0.056$	-39.1	[91a] [716a] [807]
$\text{OCS}$	$\text{O}^{17}$	$-4.0 \pm 1.5$	28	[999]
$\text{OCS}$	$\text{S}^{33}$	$2 \pm 1$	23	[999]
$\text{OCSe}$	$\text{Se}^{79}$	$-3.2 \pm 1.0$	42	[999]
$\text{HCN}$	$\text{N}^{14}$	$10 \pm 4$	34	[999]
$\text{DCN}$	$\text{N}^{14}$	$8 \pm 3$	33	[999]
$\text{Cl}^{35}\text{CN}^{14}$	$\text{N}^{14}$	$2.5 \pm 0.8$	62	[999]
$\text{Cl}^{35}\text{CN}^{14}$	$\text{Cl}^{35}$	$3.0 \pm 1.0$	19	[999]
$\text{Cl}^{35}\text{CN}^{15}$	$\text{Cl}^{35}$	$3.5 \pm 0.6$	24	[999]
$\text{Cl}^{35}\text{CN}^{16}$ (in excited state $v_2 = 1$ )	$\text{Cl}^{35}$	$8 \pm 5$	52	[999]
$\text{NH}_3$	$\text{N}^{14}$	$6.1 \pm 0.2 +$ $(0.4 \pm 0.2) \frac{K^2}{J(J+1)}$	3.1	[999]
$\text{NH}_3$	$\text{H}$	See discussion in text		[999]

The proportionality of  $C_I$  to  $\mu_I/I$  or to the gyromagnetic ratio

$$g_I = \frac{\mu_I}{I\mu_n}$$

and the rotational constant  $B$  is illustrated by comparing its value for  $\text{H}_2$  and for  $\text{D}_2$ . The ratio of  $g_I B$  for the two cases is 13.0, whereas the



ratio of the value of  $C_I$  observed is 13.5. The small difference between these two values is due to the slightly different average internuclear distances for  $H_2$  and  $D_2$ .

Since the dominant contribution to  $C_I$  in all molecules except  $H_2$  comes from the valence electrons,

$$\frac{C_I}{g_I B} \text{ should be proportional to } \sum_n \frac{|(0|aL_x|n)|^2}{W_n - W_0}$$

To a rough approximation we may assume that only the first excited state is important in this summation and that  $a$  is proportional to the average value of  $1/r^3$  for a valence  $p$  electron of the atom. Hence

$$\frac{C_I}{g_I B(1/r^3)_{av}} \text{ should be proportional to } \frac{|(0|L_x|1)|^2}{W_1 - W_0}$$

It may be seen from Table 8-1 that this quantity is of the same order of magnitude for most molecules.

For a given atom it may be assumed that the matrix elements  $(0|aL_x|n)$  are approximately the same in a series of chemically similar molecules. The value of  $C_I$  for fluorine in LiF, RbF, and CsF represents such an example. The fact that  $\frac{C_I}{g_I B(1/r^3)_{av}}$  for F increases regularly in progressing from LiF to the larger molecules RbF and CsF is evidently due to decreasing separations  $W_n - W_0$  of the energy levels which can be expected for the larger molecules. Another similar series is provided by the values of  $\frac{C_I}{g_I B(1/r^3)_{av}}$  for Cl in  $CH_3Cl$ ,  $SiH_3Cl$ , and  $GeH_3Cl$  [999]. However, for these cases  $C_I$  is not yet very accurately known.

For  $O^{17}$  and  $S^{33}$  in the same molecule OCS, one would expect  $\frac{C_I}{g_I B(1/r^3)_{av}}$  to be essentially the same, since O and S are very similar chemically, and hence their electronic surroundings are very similar. Table 8-1 shows that this expectation is correct. On the other hand, Tl and Cl in the same molecule TlCl as well as Cl and N in ClCN have very different values of  $\frac{C_I}{g_I B(1/r^3)_{av}}$  since their electronic surroundings are quite dissimilar.

Certain types of molecular rotation may result in relatively little electronic angular momentum. Such is the case for the rotation of  $H_2$ , where the "slip effect" is quite important. Another case occurs in the bending mode of ClCN ( $\nu_2 = 1$ ). Here the bent ClCN molecule rotates very rapidly about the symmetry axis with a frequency roughly 100 times greater than the normal molecular rotational frequency. However, since the bending is slight, the rapid rotational motion does not excite much electronic angular momentum. This is shown by the fact that  $C_I$  in the

bending mode is not much greater than  $C_I$  for the ground vibrational state of ClCN.

*Relation between  $C_I$  and  $g_J$ .* Even though magnetic hyperfine-structure interactions are complex and involve excited electronic states, the discussion above shows that reasonable correlations with certain molecular properties can be observed. Furthermore, the coefficients  $C_I$  are connected with other measurable quantities. If one low-lying excited electron state dominates in the sum  $\sum_n \frac{|(0|L_x|n)|^2}{W_n - W_0}$ , then  $C_I$  may be expected to be closely related to the molecular magnetic moment produced by electron excitation. For, from (8-38), (11-15), and (11-19),

$$C_I = \frac{g_J \mu_n a_{0n}}{\mu_0} = 2g_J g_I (\mu_n)^2 \left( \frac{1}{r^3} \right)_{av} \quad (8-41)$$

Here  $g_J$  strictly includes only the contributions to  $g_J$  from the excited valence electrons. There should in addition be a connection between  $C_I$  and part of the rotational energy due to electrons as may be seen by comparing (8-29) or (8-35) with (8-39). OCS and OCSe are the only linear molecules in which both quantities  $C_I$  and  $g_J$  have already been measured so that a test of the relation (8-41) can be made. Assume that the electron which produces  $g_J$  spends half its time on the oxygen and half its time on the sulfur atom in OCS, so that  $(1/r^3)_{av}$  is just one-half that for an atomic electron in each case. Then (8-41) predicts from the measured value  $g_J = 0.025$  for OCS that  $C_I$  for  $O^{17}$  should be  $-2.3$  kc and that for  $S^{33}$   $C_I$  should be  $1.5$  kc. These values are very satisfactorily close to the measured values given in Table 8-1. Similarly, one may calculate the values of  $C_I$  for  $Se^{79}$  from relation (8-41) and the observed value of  $g_J$  for OCSe, which is  $g_J = 0.019$ . The result is  $C_I = -1.4$  kc, again in reasonable agreement with the observed value of  $C_I$  for  $Se^{79}$  found in Table 8-1.

**8-10. Magnetic Hyperfine Structure of Nonlinear Molecules in  $^1\Sigma$  States.** We now return to the general form (8-36) for any molecule. Since the hyperfine energy is a scalar and linearly proportional to the components of  $\mathbf{I}$  and of  $\mathbf{J}$ , it must be of the form

$$W_{mag} = \mathbf{I} \cdot \mathbf{Q} \cdot \mathbf{J} = \sum_{\sigma\sigma'} Q_{\sigma\sigma'} I_{\sigma} J_{\sigma'} \quad (8-42)$$

where  $\mathbf{Q}$  is a dyadic, or  $Q_{\sigma\sigma'}$  are components of a tensor which can be seen to be symmetric from inspection of (8-36). For a nucleus on the axis of a symmetric-top molecule, the principal axes of  $\mathbf{Q}$  must coincide with the principal axes of inertia, so that

$$W_{mag} = Q_{xx} I_x J_x + Q_{yy} I_y J_y + Q_{zz} I_z J_z \quad (8-43)$$

Since from the molecular symmetry,  $\alpha_{xx} = \alpha_{yy}$  ( $z$  is parallel to the molecular axis), (8-43) may be written

$$W_{mag} = \alpha_{xx} \mathbf{I} \cdot \mathbf{J} + (\alpha_{zz} - \alpha_{xx}) I_z J_z \quad (8-44)$$

Now  $J_z = K$ , and using the vector model  $I_z = \mathbf{I} \cdot \mathbf{J} [K/J(J+1)]$  so that for a nucleus on the axis of a symmetric top, the energy is of the form given by Henderson [283]

$$W_{mag} = \mathbf{I} \cdot \mathbf{J} \left[ a + (b - a) \frac{K^2}{J(J+1)} \right] \quad (8-45)$$

For the general asymmetric rotor, (8-42) does not simplify.

$\text{N}^{14}$  in  $\text{NH}_3$  affords a particularly good test of the dependence of magnetic interaction on  $J$  and  $K$ , since inversion lines for this molecule with many different values of  $J$  and  $K$  appear in the microwave region. Accurate measurement [930] of the  $\text{NH}_3$  hyperfine structure for values of  $J$  and  $K$  up to 6 shows that the relation (8-45) holds within the experimental error of about 5 per cent. The constants  $a$  and  $b$  are given in Table 8-1.

$\text{NH}_3$  also displays an interesting magnetic hyperfine structure associated with magnetic moments of the hydrogen nuclei. A rather complete treatment and examination of hyperfine effects in  $\text{NH}_3$  has been given by Gunther-Mohr *et al.* [930], [931]. Still more refined measurements and additional theoretical discussion are given by Gordon [925]. We shall discuss the various effects involving the hydrogen nuclei one at a time for the sake of simplicity.

Consider first the rotational states for which  $K \neq 1$  in order to avoid the complication of hyperfine doubling. Since the  $\text{N}^{14}$  spin  $I_N$  is coupled to  $J$  by a quadrupole interaction,  $I_N$  and  $J$  couple to form  $F_1$ , which then couples with the sum  $I_H$  of the three hydrogen spins to form the total angular momentum  $F$ . When  $K$  is a multiple of 3, the total spin  $I_H$  of the three hydrogens can only be  $\frac{3}{2}$  because of the exclusion principle (see Sec. 3-4). When  $K$  is not a multiple of 3,  $I_H$  can only be  $\frac{1}{2}$ .

There is an interaction between the hydrogen magnetic moments and the nitrogen moment which is given by expressions (8-15b). A somewhat larger interaction occurs between the moments of the hydrogen nuclei themselves, which can change in magnitude when  $I_H$  changes orientation with respect to  $J$  or  $F_1$ . This interaction has the form [925]

$$W = \frac{3}{4} \frac{g_I^2 \mu_n^2}{r^3} (I_z^2 - \frac{5}{4}) \quad (8-46)$$

where  $I_z$  is the component of  $I_H$  along the symmetry axis of the molecule and  $r$  is the distance between hydrogen nuclei. When  $K$  is not a multiple of 3,  $I_H = \frac{1}{2}$  and  $I_z^2 = \frac{1}{4}$  for all hyperfine states, so that (8-46) produces



no variation of energy. When  $K$  is a multiple of 3, however,  $I = \frac{3}{2}$  and (8-46) is given [925] by

$$\Delta W_{I_H=\frac{3}{2}} = \frac{3}{4} \frac{g_I^2 \mu_n^2}{r^3} \left[ \frac{3K^2}{J(J+1)} - 1 \right] \cdot \frac{4(\mathbf{I} \cdot \mathbf{F}_1)^2 + 2(\mathbf{I} \cdot \mathbf{F}_1) - 5F_1(F_1 + 1)}{2F_1(F_1 + 1)(2F_1 - 1)(2F_1 + 3)} \\ \cdot \frac{6(\mathbf{F}_1 \cdot \mathbf{J})^2 - 3(\mathbf{F}_1 \cdot \mathbf{J}) - 2F_1(F_1 + 1)J(J + 1)}{(2J - 1)(2J + 3)} \quad (8-47)$$

The coefficient  $\frac{3}{4} \frac{g_I^2 \mu_n^2}{r^3}$  in  $\Delta W$  corresponds to 20.7 kc for hydrogen in  $\text{NH}_3$ , and hence spin-spin interactions of this type can be detected only by microwave spectroscopy of the highest resolution.

Rotation of the  $\text{NH}_3$  molecule also creates a magnetic field which interacts with the moments of the hydrogen nuclei. Since the hydrogens are not on the molecular axis, the complete dyadic form (8-42) of this  $\mathbf{I} \cdot \mathbf{J}$  interaction must be considered. From symmetry, one can immediately identify the principal axes of the dyadic for an individual hydrogen nucleus. One is the symmetry axis of the molecule, which we shall call  $z$ ; a second is the perpendicular direction from the  $z$  axis through the nucleus, which we shall call  $x$ , and the  $y$  direction is of course perpendicular to each of these. Rotation of the molecule about the  $x$ ,  $y$ , or  $z$  axis each produces a different magnetic field at the nucleus and hence a different  $\mathbf{I} \cdot \mathbf{J}$  interaction energy. If, with respect to these principal axes, the dyadic  $\mathbf{Q}$  of Eq. (8-42) is taken to be  $\alpha \mathbf{i}\mathbf{i} + \beta \mathbf{j}\mathbf{j} + \gamma \mathbf{k}\mathbf{k}$ , the energy of the three hydrogens due to molecular rotation when  $K = 1$  is [931]

$$\Delta W_{\mathbf{I} \cdot \mathbf{J}} = \left[ \alpha + \beta + \frac{(\gamma - \alpha - \beta)K^2}{J(J+1)} \right] \mathbf{I}_H \cdot \mathbf{J} \quad (8-48)$$

Here  $\mathbf{I}_H \cdot \mathbf{J} = \frac{\mathbf{I}_H \cdot \mathbf{F}_1 \mathbf{F}_1 \cdot \mathbf{J}}{F_1(F_1 + 1)}$  can be evaluated by the vector model.

The hydrogen spin  $I$  can take on the usual orientations with respect to  $F_1$  which are allowed by quantum mechanics, giving a total angular momentum  $F = F_1 + I, F_1 + I - 1, \dots, |F_1 - I|$ . The usual selection rules  $\Delta F_1 = 0, \pm 1$  and  $\Delta F = 0, \pm 1$  and intensity relations such as (6-6) apply. The resulting spectrum is indicated in Fig. 8-5, and compared with experimental observations made in a high-resolution beam spectrometer [925]. It may be seen that the maximum splitting of the 3,3 inversion line due to energy of the type given by (8-48) is about 60 kc, and hence these effects are observable only with resolution higher than that of the usual microwave spectrometer.

When  $K = 1$ , hyperfine doubling can occur. A small doubling is due to spin-spin interaction between the N and H nuclei, of the type discussed in Sec. 8.6. Even though  $I_H = \frac{1}{2}$ , the interaction is just twice that given by (8-16), since three protons are involved rather than a single

one [931]. Additional doubling occurs because of the variation of the  $\mathbf{I}_H \cdot \mathbf{J}$  interaction with orientation. When  $K = 1$ , a distribution of hydrogen nuclear spin occurs which is similar to that of electron spin in Fig. 8-2. If  $\mathbf{I}_H$  is fixed in orientation with respect to  $\mathbf{J}$ , it may be seen from this figure and the inequivalence of magnetic effects in the  $x$  and  $y$  directions that the two otherwise degenerate  $K$  states do not have the same energy.

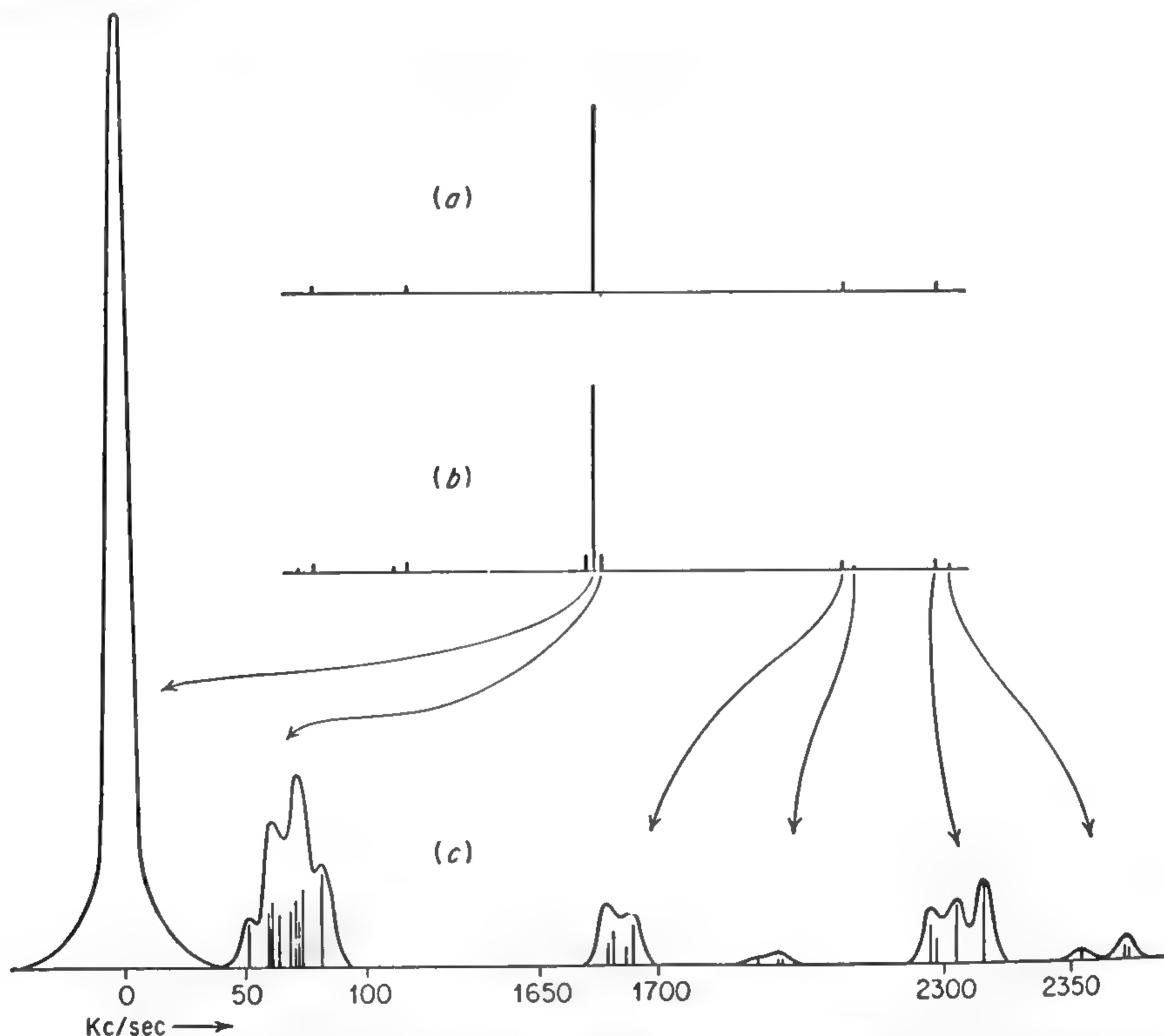


FIG. 8-5. Hyperfine structure of the  $\text{NH}_3$  3,3 inversion spectrum. (a) Structure due to  $\text{N}^{14}$  quadrupole coupling alone. (b) Grosser features of structure due to  $\text{N}^{14}$  quadrupole coupling plus magnetic coupling of the three hydrogens. (c) Spectrum observed in a beam spectrometer, showing finer features of the individual lines of (b). (After Gordon, Zeiger, and Townes [925].)

A diagram of the energy levels of  $\text{NH}_3$  for the 3,1 inversion transition and a particular value of  $F_1$  is given in Fig. 8-6. Without hyperfine doubling, the stronger transitions would involve no change in magnetic energy (*cf.* Fig. 8-6b). Inversion transitions occur between different members of the two  $K$ -type levels, and hence the hyperfine doubling adds to the transition frequency for  $F = \frac{7}{2}$ , and subtracts from it for  $F = \frac{5}{2}$ , giving an appreciable doubling. The dotted levels of Fig. 8-6c are forbidden for  $J = 3$  by the fact that hydrogen nuclei follow Fermi-Dirac

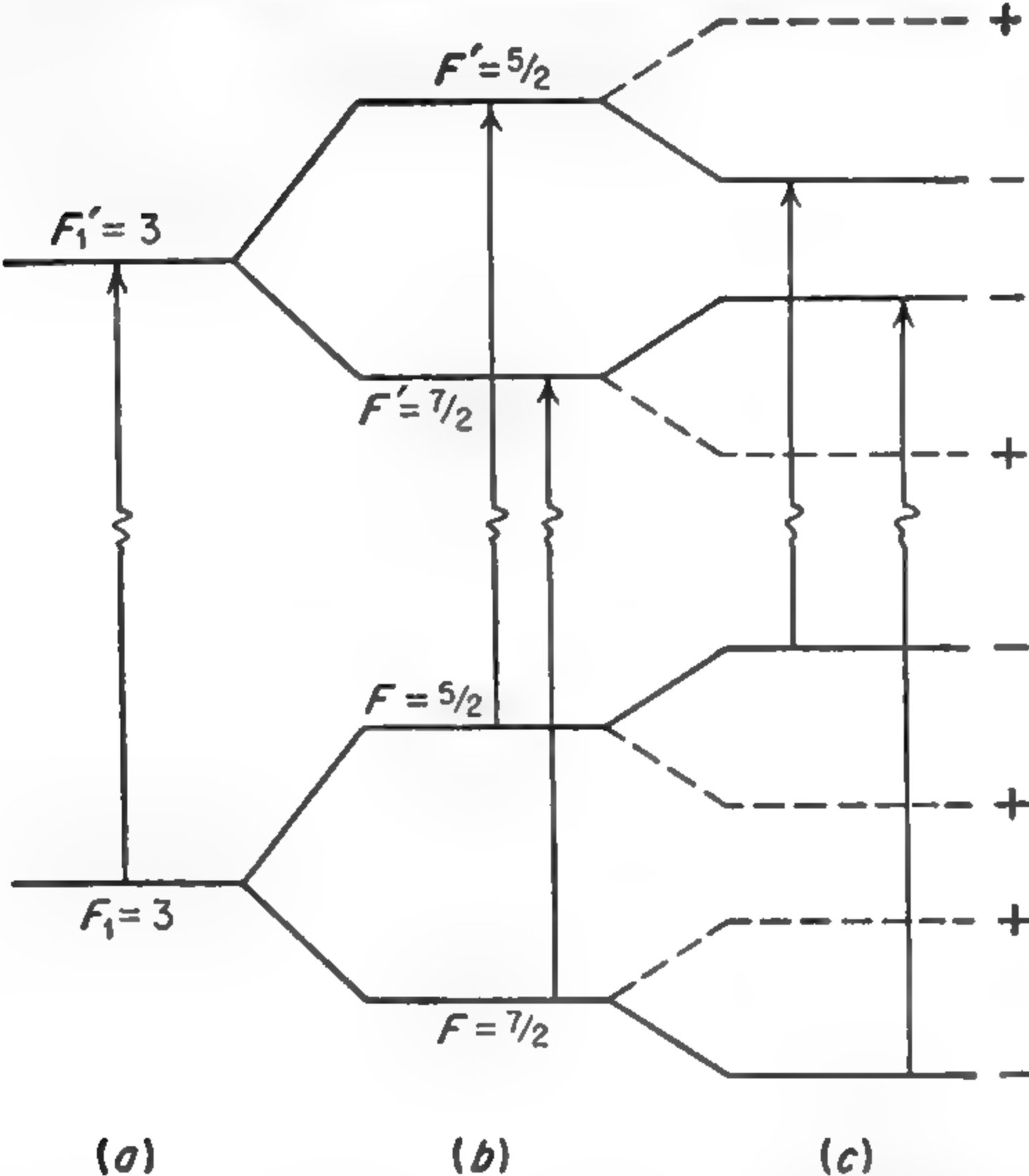


FIG. 8-6. Hyperfine structure of the 3,1 inversion transition of  $\text{NH}_3$ . Quantum numbers are  $J = 3$ ,  $K = 1$ ,  $F_1 = |\mathbf{J} + \mathbf{I}_\text{N}| = 3$ ,  $I_\text{H} = \frac{1}{2}$ . (a) represents energies due to inversion and  $\text{N}^{14}$  quadrupole coupling only. (b) includes part of magnetic interaction with hydrogen moments which is the same for the two degenerate  $K$  states. (c) includes hyperfine doubling effects due to hydrogen moments. Only the stronger hyperfine transitions are shown. Dotted levels are forbidden by the exclusion principle.

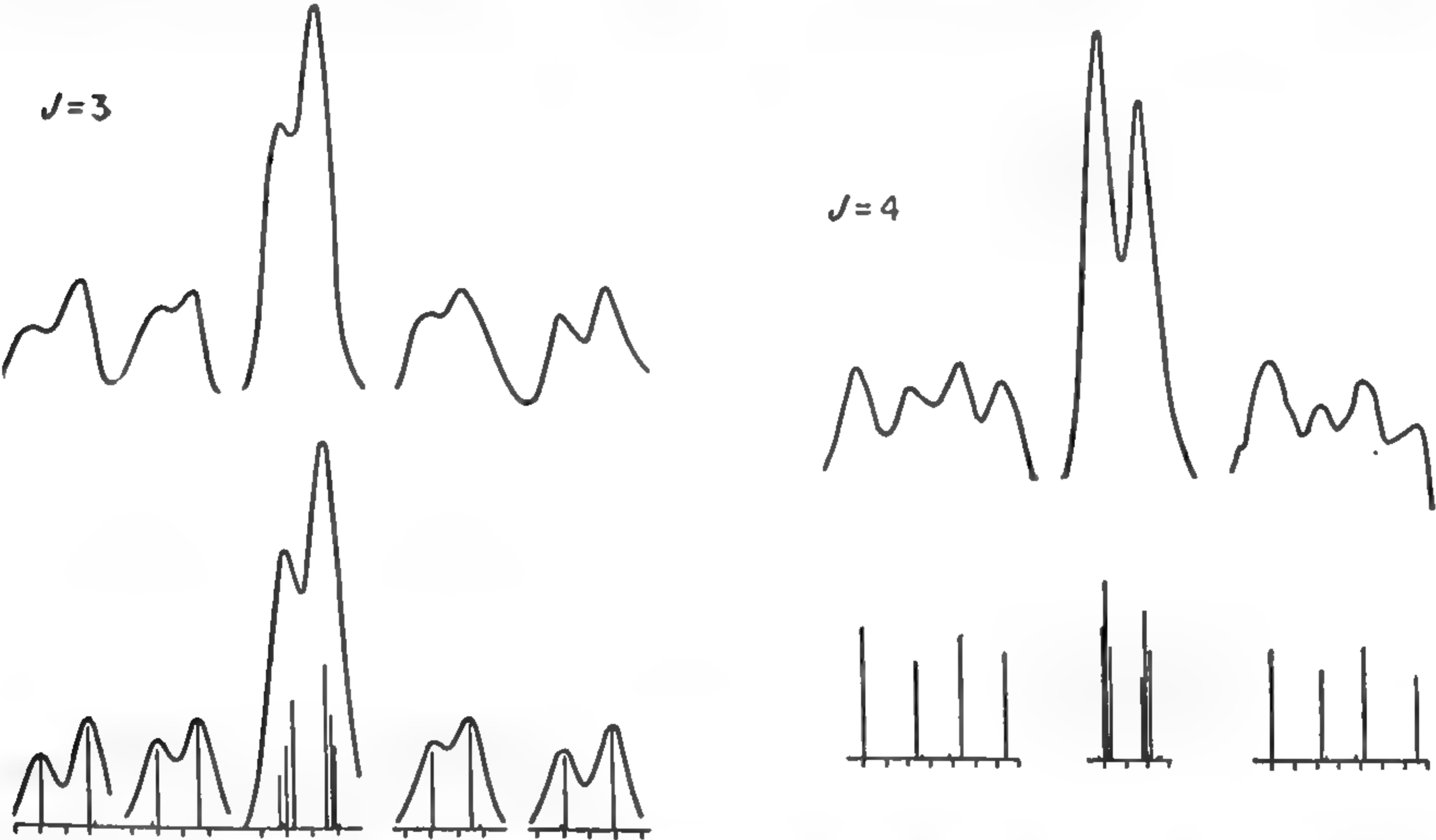


FIG. 8-7. Structure and hyperfine doubling of the  $\text{N}^{14}\text{H}_3$  inversion spectrum for  $J = 3$ ,  $K = 1$ , and  $J = 4$ ,  $K = 1$ . Upper curves show experimental observations, and lower part of figure the theoretical expectations. Frequency increases from left to right with 60-ke intervals indicated. (From Gunther-Mohr, White, Schawlow, Good, and Coles [930].)



statistics (see Sec. 3-4 for a detailed explanation). The levels indicated by a minus sign are antisymmetric with respect to interchange of two hydrogen nuclei; those labeled with a plus sign are symmetric with respect to such an interchange. For  $J = 4$ , or any even value of  $J$ , the symmetry of the levels is reversed, so that the dotted levels of Fig. 8-6c are allowed, and the solid ones forbidden (*cf.* page 71).

Hyperfine structure of the 3,1 and 4,1 inversion lines of  $\text{NH}_3$  is shown in Fig. 8-7, where the hyperfine doubling is quite prominent. The alternation in relative intensity of the doublets in changing from  $J = 3$  to  $J = 4$  is due to the alternation in the levels permitted by statistics which was noted above.

The magnitude of the energy shift of each level due to this type of hyperfine doubling is given [931] by

$$\Delta W = \pm (\beta - \alpha) \mathbf{I}_H \cdot \mathbf{J} = \pm (\beta - \alpha) \frac{(\mathbf{F}_1 \cdot \mathbf{I})(\mathbf{F}_1 \cdot \mathbf{J})}{F_1(F_1 + 1)} \quad (8-49)$$

When the magnetic interaction is the same for the  $x$  and  $y$  directions,  $\beta - \alpha = 0$ , and this doubling disappears.

In the particular case of  $\text{NH}_3$ ,  $\beta - \alpha = -14.4$  kc. From this value and the  $\mathbf{I}_H \cdot \mathbf{J}$  interaction of the type given by (8-48) for hydrogen in inversion lines for which  $K \neq 1$ , one can obtain the values  $\alpha = -1$  kc,  $\beta = -16$  kc, and  $\gamma = -19$  kc. As for  $C_1$  in  $\text{H}_2$ , the  $\mathbf{I} \cdot \mathbf{J}$  interaction constants here are negative, indicating a large amount of slippage of the valence electrons as the hydrogens rotate in  $\text{NH}_3$ .

## CHAPTER 9

# INTERPRETATION OF HYPERFINE COUPLING CONSTANTS IN TERMS OF MOLECULAR STRUCTURE AND NUCLEAR MOMENTS

Hyperfine structure in molecular spectra can be theoretically predicted with high accuracy if the rotational state of the molecule, the spin of the nucleus producing the hyperfine structure, and certain coupling coefficients between molecule and nucleus are known. The coupling coefficients are dependent on either the magnetic dipole or electric quadrupole moment of the nucleus and on various properties of the molecule. The purpose of this chapter is to examine in detail the dependence of these hyperfine coupling coefficients on molecular structure, and to show how they may be theoretically estimated or, when measured, how they may be interpreted to obtain information about molecular structure and nuclear moments. For most molecules hyperfine structure due to nuclear quadrupole moments is considerably more prominent than that due to magnetic moments. Hence we shall begin with a discussion of quadrupole coupling.

**9-1. Introductory Remarks on Quadrupole Coupling.** From measurement of hyperfine structure, the quadrupole coupling  $eqQ$  may be evaluated. The nuclear quadrupole moment  $Q$  is a property of the nucleus which depends on the state of the nucleus and may be considered fixed since nuclei will almost always be encountered in their ground state. The sign and magnitude of  $Q$  can be very roughly estimated for some nuclei ([326] and [513]), but present knowledge of nuclear structure allows only the crudest estimates of  $Q$  from nuclear theory. The quantity  $e$  is the proton charge, and  $q$ , or  $(\partial^2 V / \partial z^2)_{av}$ , is a molecular property, depending on the distribution of charges in the molecule. It cannot be exactly evaluated, but Townes and Dailey ([239] and [422]) have shown how it can be evaluated accurately enough in certain molecules to allow a useful determination of  $Q$  from the molecular coupling constant  $eqQ$ . In some cases  $Q$  may also be approximately determined from optical atomic spectra and with more accuracy from radio-frequency atomic-beam spectroscopy. Once  $Q$  for a given nucleus is known, it can provide a very convenient probe to test the electronic distribution in various molecules, since the quadrupole coupling allows a very direct measure-

ment of the second derivative of the potential at the nucleus due to molecular charges.

**9-2. Quadrupole Coupling in Atoms.** Before discussing in detail the relations between  $q$  and molecular structure and the evaluation of quadrupole coupling constants in molecules, we shall consider the simpler atomic case. Most of the electrons in atoms are arranged in groups of closed shells, corresponding to distributions of charge which are, on the average, spherical. These spherical shells produce zero average field at the nucleus and hence do not contribute to  $q$  (since from Chap. 5 charge density within the nucleus is neglected in obtaining  $q$ ). In addition to spherical shells, the atom may contain one or more valence electrons which are not in closed shells. If we choose an atom with only one such valence electron, then from (5-43)

$$q_J = e \int \psi_{JJ}^* \frac{3 \cos^2 \theta - 1}{r^3} \psi_{JJ} d\tau \quad (9-1)$$

If the electron is in a central field, then  $\psi$  may be separated into one factor depending on  $r$ , and another factor which is a spherical harmonic function of the angles. The angular part of the integral in (9-1) may be evaluated as  $-2l/(2l+3)$  so that

$$q_J = - \frac{2le}{2l+3} \left( \frac{1}{r^3} \right)_{av} \quad (9-2)$$

where  $l$  is the orbital angular momentum,  $e$  the electronic charge, and  $(1/r^3)_{av}$  is the average inverse third power of the distance between nucleus and electron. Expression (9-2) neglects the electron spin, which for a real atom must be taken into account. However, in the parallel case of a molecule, which is of prime interest in this chapter, spin can correctly be neglected.

For a hydrogenlike wave function,  $(1/r^3)_{av}$  is given by (5-13b). However, this quantity cannot usually be obtained with high accuracy because the radial wave functions for atoms are poorly known. Fortunately, other spectroscopically measurable quantities also depend on  $(1/r^3)_{av}$ , and from a measurement of these  $(1/r^3)_{av}$  may often be obtained. Thus, using the fine-structure doublet separation  $\Delta\nu$  and Eq. (5-13a)

$$q_J = q_{nll} = - \frac{2l-1}{l+1} q_{nlo} = - \frac{2le \Delta\nu}{Z_i R \alpha^2 a_0^3 (l + \frac{1}{2})(2l+3)} \quad (9-3)$$

where  $Z_i$  is the effective value of  $Z$  near the nucleus, which in heavy atoms is approximately the nuclear charge  $Z$  minus 4 for  $p$  electrons (*cf.* [895] for more precise values of  $Z_i$ ). The quantities  $q_{nll}$  and  $q_{nlo}$  are introduced here for later reference. They are defined after Eq. (9-6).

In case the nuclear gyromagnetic ratio  $g_I$  and the resulting magnetic hyperfine structure are known, the uncertainty of an effective  $Z$  may be



eliminated since the magnetic hyperfine structure depends directly on  $(1/r^3)_{av}$  [cf. 5-51)]. Then

$$q_J = \left( \frac{\partial^2 V}{\partial z^2} \right)_{atom} = - \frac{aeMJ(J+1)}{g_I \mu_0^2 m(l+1)(2l+3)} \tag{9-4}$$

where  $e, m$  = electronic charge and mass, respectively

$\mu_0$  = Bohr magneton

$M$  = proton mass

$J$  = total angular momentum of the electron ( $l$  plus spin)

$a$  = hyperfine structure parameter such that the energy of magnetic interaction between nucleus and electron is  $a(\mathbf{I} \cdot \mathbf{J})$ .

Values of  $Z_i$  and  $(1/r^3)_{av}$  for a valence  $p$  electron of a number of atoms have been derived by Barnes and Smith [895] from data on atomic spectra. These and other values of  $(1/r^3)_{av}$  obtained by interpolation are listed in Table 9-1. Table 9-1 neglects certain relativistic effects which are small for  $Z < 65$ , but which for the heaviest atoms may produce errors of 30 per cent in  $(1/r^3)_{av}$  or in  $q$  [70].

TABLE 9-1. VALUES OF  $(1/r^3)_{av}$  FOR VALENCE  $p$  ELECTRONS OF NEUTRAL ATOMS

Certain relativistic corrections are neglected. All values are in  $10^{24} \text{ cm}^{-3}$ . (After Barnes and Smith [895]. Value for  $N$  is from [916a].)

Li	0.26	Be	1.17	B	4.1	C	8.3	N	22.5	O	29	F	44
Na	1.65	Mg	5.2	Al	8.6	Si	15.6	P	24	S	34	Cl	48
K	3.0	Ca	7.6	Ga	24	Ge	39	As	51	Se	65	Br	92
Rb	5.7	Sr	13.5	In	39	Sn	76	Sb	88	Te	101	I	121
Cs	8.7	Ba	19.2	Tl	80	Pb	108	Bi	166				

Although expression (9-4) affords an exact way of obtaining  $q_J$  due to a single particle in a central field, in actual atomic cases it is in error by about 10 per cent. This is because the closed shells of electrons which have been assumed spherical are slightly polarized by the valence electron. As a result, electrons in the closed shell tend to move away from the position of the valence electron, producing a contribution to  $q_J$  at the nucleus which is of opposite sign to the part produced by the valence electron. Hence the closed shells may be regarded as shielding or screening the nucleus to some extent from fields of the valence electrons.

Accurate and detailed calculations of the magnitude of shielding are very difficult since they depend on radial wave functions of the electrons. However, Sternheimer, Foley, and others [539], [804], [979] have given approximate corrections for many atoms. For the ground states of atoms, the corrections to (9-3) or (9-4) correspond to approximately 10 per cent reduction in  $q_J$ . On the other hand, for an electron in an excited atomic state or for a charge as far away from the nucleus as an atomic radius, "antishielding" may occur, *i.e.*, "shielding" may actually increase

$q_J$  [923], [979]. The contribution of a charge one or two angstroms away to  $q$  at a nucleus may thus be increased by a factor of about 10 as a result primarily of polarization and distortion of the distribution of  $p$  electrons surrounding the nucleus.

Perturbation of the closed electron shells by a valence electron may affect magnetic hyperfine structure in atoms as well. This effect is, however, considerably smaller than the similar effect on quadrupole hyperfine structure [749].

In cases with two or more valence electrons in various atomic orbits, determination of their interaction with a nuclear quadrupole moment can be somewhat more complex. A few such cases, as well as corrections for relativistic effects, are discussed by Casimir [70].

**9-3. Quadrupole Coupling in Molecules—General Considerations.** For a nucleus in a molecule, contributions to  $q$  at the nucleus may come from the following sources:

1. Valence electrons of the nucleus or atom in question
2. Distortion of the closed shells of electrons around the nucleus
3. Charge distributions associated with adjacent atoms or ions, *i.e.*, charges essentially outside the radius of the atom

Contributions of type 3 might at first thought seem to be the only ones which differ from the atomic case. However, the wave functions or distribution of the valence electrons are very much affected by molecular bonds, and hence contributions of type 1 are much modified from the simpler atomic case.

In order to examine the contributions of valence electrons, we consider first an atom with one valence electron outside a closed shell. In the atom, this electron would be in some definite atomic state specified by the atomic wave function  $\psi_{nlm}$ . In the molecule, the wave function will be modified, perhaps radically changed, but it may be expressed as an expansion in terms of atomic wave functions:

$$\psi = \sum_{nlm} a_{nlm} \psi_{nlm} \quad (9-5)$$

In some cases the larger terms in this expansion are fairly well known from molecular structure. A single bond between two atoms involves only terms with  $m = 0$ . If the bond is a covalent bond, then usually a good first approximation to the expansion (9-5) is to assume that the electron is entirely in the lowest-energy atomic states of the two bonded atoms, since the molecular bond would have to supply a considerable amount of energy to give large values to the coefficients of more highly excited states. Each atom supplies one electron to the bond, so that, although any one electron has a probability of  $\frac{1}{2}$  of being found on a particular atom, there is on the average one electron in an orbit about



each atom which is much the same as before the atoms were bonded in a molecule.

The bonding energy is provided by an overlap of the wave functions of the two atoms which gives an exchange energy. This exchange energy is a typical quantum-mechanical effect which depends on electrostatic interactions, and which increases as the wave functions of the two atoms coincide or overlap more completely (*cf.* [133]). Overlap of two  $2p$  wave functions ( $n = 2, l = 1$ ) of two atoms is shown in Fig. 9-1*a*. This overlap can be very much increased by allowing in the expansion (9-5) a small

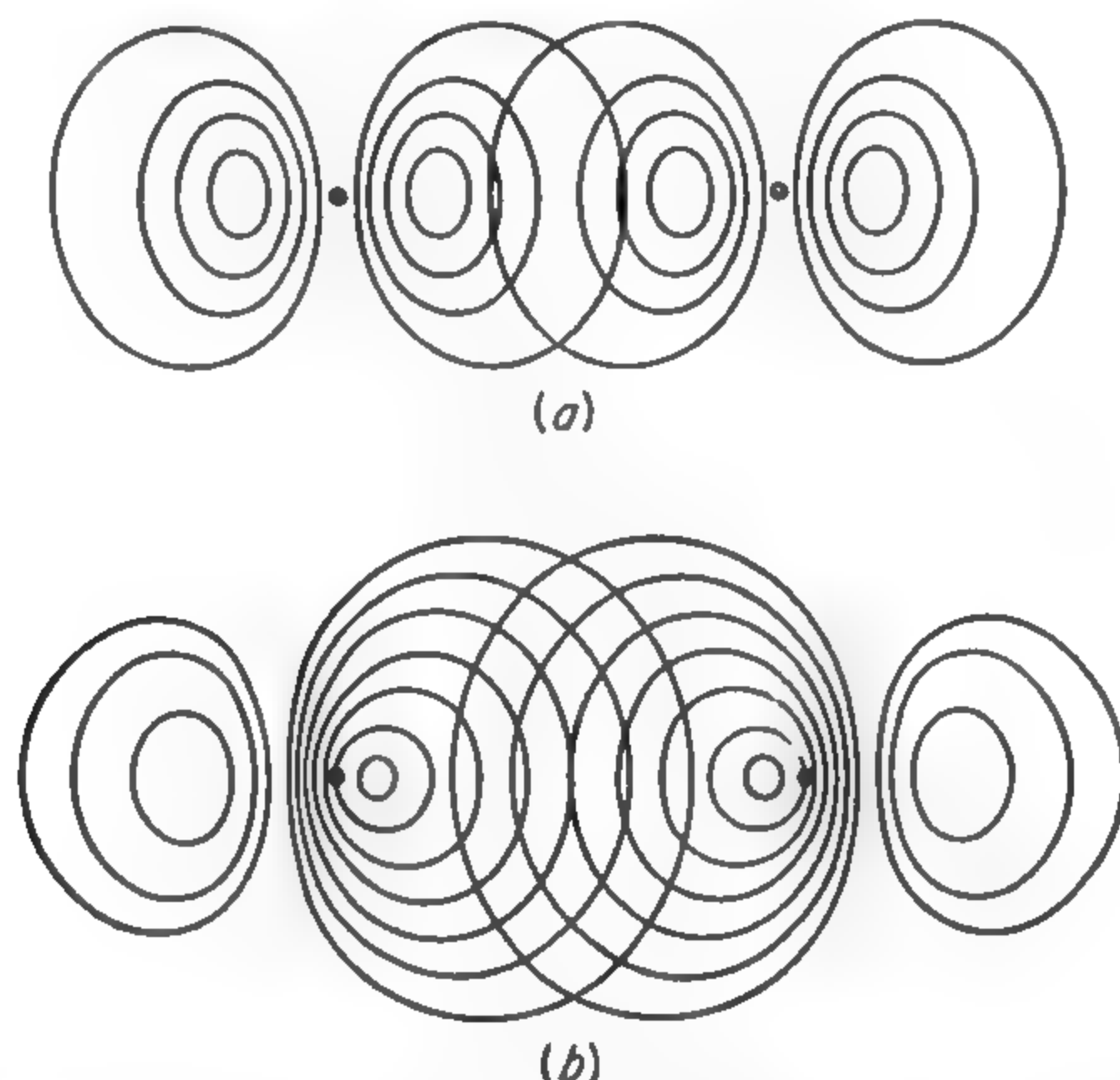


FIG. 9-1. Illustration of the increase of overlap or exchange integral with hybridization. (a) Overlap of two  $p$  wave functions; (b) overlap of two  $s$ - $p$  hybrid wave functions. The lines represent contours of equal electron density for the atomic wave functions.

amount of  $2s$  wave function, as shown in Fig. 9-1*b*. The  $s$  and  $p$  wave functions subtract on one side of an atom but add on the side of the bond, thus increasing the wave function in the region between the atoms substantially. The overlap and hence exchange energy of the bond increases until the bond has approximately 25 per cent  $s$  character ( $a_{200}^2 \approx \frac{1}{4}$ ). That the exchange energy is a maximum does not necessarily mean that this is the lowest-energy condition for the bonds, since energy may be required to promote the atom from its ground state to obtain the mixed or hybrid bond wave function. Mixture or hybridization of a  $p$  wave function with a  $d$  wave function will achieve the same type of increase in the exchange energy, but hybridization of a  $p$  wave function with another  $p$  or an  $f$  wave function does not give the same advantage, since the two functions have the same symmetry and they either add or subtract on both sides of the atom. A second approximation to the correct expansion (9-5) can hence be obtained by adding a judicious amount of  $p$  atomic wave function if the atomic ground state corresponds to an  $s$  function, or of the lowest available  $s$  or  $d$  wave function if the atomic ground state is a  $p$  state. The "judicious amount" may be judged from



a variety of helpful, though not too exact, methods (for a discussion see [913c]).

Of course, expression (9-5) must provide a probability of approximately  $\frac{1}{2}$  for the electron's being found in an approximately atomic orbit of the adjacent atom to which it forms a bond. This results in the presence of a large number of atomic wave functions of rather large  $n$  and  $l$ , each, however, with rather small coefficients  $a_{nlm}$  by comparison with the lowest atomic energy states of the particular atom on which our attention is centered.

The quantity  $q$  may be obtained from the wave functions since

$$q = \left( \frac{\partial^2 V}{\partial z^2} \right)_{av} = e \int \psi^* \left( \frac{3 \cos^2 \theta - 1}{r^3} \right) \psi d\tau$$

Using the expression (9-5),

$$q = \sum_{nlm} |a_{nlm}|^2 q_{nlm, nlm} + \sum_{nlm, n'l'm'} a_{nlm} a_{n'l'm'}^* q_{nlm, n'l'm'} \quad (9-6)$$

where

$$q_{nlm, n'l'm'} = e \int \psi_{nlm} \left( \frac{3 \cos^2 \theta - 1}{r^3} \right) \psi_{n'l'm'}^* d\tau$$

and the second sum is over all nonidentical  $nlm$  and  $n'l'm'$ , since all terms for which  $n = n'$ ,  $l = l'$ , and  $m = m'$  are collected in the first sum. Since  $\psi_{nlm}$  is an atomic wave function, its angular variation is given by a spherical harmonic as in (5-2), and  $q_{nlm, n'l'm'}$  is zero unless  $m = m'$  and either  $l = l' \neq 0$  or  $l = l' \pm 2$ . This conveniently eliminates a large number of terms from the second sum of (9-6).

The quantities  $q_{nlm, nlm}$  of (9-6), which may be shortened to  $q_{nlm}$ , are simply the values of  $q$  for each of the atomic states, and are multiplied by  $|a_{nlm}|^2$ , the fractional importance of the respective atomic states in the molecular wave function. For an  $s$  state ( $l = 0$ ),  $q_{n0m}$  is always zero, but for  $l \neq 0$ ,  $q_{nlm}$  decreases very rapidly as  $n$  or  $l$  increase, because for these states the electron spends less time close to the nucleus. The dominating term in the first sum of (9-6) will usually be the state of lowest allowed  $n$  because not only will energy considerations make the amplitude  $a_{nlm}$  of this wave function large but, in addition, the  $q_{nlm}$  for this state is considerably larger than for the higher-energy states. This will be demonstrated for the most common case, where  $m$ , the projection of  $l$  on the axis, is zero.

The value of  $q_{nl0}$  for an atomic wave function differs from  $q_l$  discussed above, which has  $m = l$ , by the factor  $-(l+1)/(2l-1)$ . For hydrogenlike wave functions, evaluation of  $(1/r^3)_{av}$  gives

$$q_{nl0} = \frac{2l(l+1)e}{(2l-1)(2l+3)} \left( \frac{1}{r^3} \right)_{av} = \frac{4Z^3}{n^3 a_0^3 (2l-1)(2l+1)(2l+3)} \quad (9-7)$$

Table 9-2 shows the relative magnitude of  $q_{nl0}$  for various states  $nl$  and compares the relative values computed for the hydrogenlike case from (9-7) with those obtained from the fine-structure splitting and Eq. (9-3). Because of dependence on  $n$  and screening which changes the effective value of  $Z$ ,  $q_{nl0}$  for the  $5p$  state of iodine is fourteen times larger than that for the  $6p$  state of cesium. Similarly the value for the  $6p$  state of Cs is considerably larger than that for any other state of Cs, the most marked differences occurring with a change of  $l$  and a consequent large change of screening. Although fine-structure measurements are less complete in F

TABLE 9-2. RELATIVE VALUES OF  $q_{nl0} = \partial^2 V / \partial z^2_{n,l,m=0}$  FOR VARIOUS ATOMIC STATES

The very large effect of screening is shown by comparison of the third and fourth columns.

Elec- tronic state	Atomic example for which fine structure is known	Values of $q_{nl0}$ from fine structure, esu	Relative values of $q_{nl0}$ assuming hydrogen wave functions and no screening [Eq. (9-7)]
			Relative to $5p$
$5p$	I	$-45 \times 10^{15}$	1.00
$5d$	Cs	$-0.31 \times 10^{15}$	0.14
$5f$	Cs		0.048
$6p$	Cs	$-3.4 \times 10^{15}$	0.58
$6d$	Cs	$-0.16 \times 10^{15}$	0.08
$6f$	Cs		0.028
$7p$	Cs	$-1.1 \times 10^{15}$	0.36
$7d$	Cs	$-0.09 \times 10^{15}$	0.05
			Relative to $2p$
$2p$	F	$-21 \times 10^{15}$	1.00
$3p$	Na	$-0.7 \times 10^{15}$	0.30
$4p$	Na	$-0.2 \times 10^{15}$	0.12

and Na, Table 9-2 shows that, even in these light nuclei where screening effects are less important,  $q$  decreases very rapidly with increasing  $n$  or  $l$ .

Although most of the terms in the second sum of (9-6) are zero, the nonzero parts with  $m = m'$  and  $l = l' \neq 0$  or  $l = l' \pm 2$  must be considered. The "cross-product integrals"  $q_{nlm,n'l'm'}$  cannot be evaluated accurately, but they decrease rapidly with increasing  $n$ ,  $l$ ,  $n'$ , or  $l'$ . In addition, they are usually not important because the coefficients  $a_{nlm}a_{n'l'm'}^*$  are small. If, for example, a  $p$ -type function is the largest component of the molecular wave function, cross-product terms involving its amplitude  $a_{n1m}$  might be expected to be largest. The only terms of this type involve mixing this  $p$  state with other  $p$  and  $f$  states. But the discussion

above of hybridization indicates that hybridization of a  $p$  function with either another  $p$  or  $f$  function should be small since it would not contribute very much to lowering the bond energy. The common types of hybridization, of a  $p$  function with either  $s$  or  $d$ , produce only zero cross terms involving  $a_{n1m}$  because then  $l \neq l' \pm 2$ . In some unusual cases, however, these cross terms could be an important part of  $q$ .

Contributions to  $q$  from neighboring atoms or ions (type 3) are much smaller than those of the valence electrons for many types of bonds. Assume, for example, that there is a neighboring ion with an average charge of one-half that of the electron and at a typical distance of 2.0 Å from the nucleus of interest. It produces a value of  $\partial^2 V / \partial z^2$ , or  $q$ , at the nucleus of only  $3 \times 10^{13}$  esu.

A neighboring ion also distorts the electron distribution about the nucleus, including that of the closed shells. This distorted distribution in turn gives a contribution to  $q$  (type 2), which is the "antishielding" effect mentioned above (page 227). Calculations and experimental evidence indicate that such distortions may increase the contribution of a neighboring ion to  $q$  by a factor of about 10 [923]. Hence the value of  $q$  produced by an ion of the type mentioned above would be increased to  $3 \times 10^{14}$  esu. However, this is less than 2 per cent of the value due to a valence  $p$  electron in I or F, as shown in Table 9-2. Hence quadrupole effects due to neighboring ions or to distortion of surrounding spherical shells of electrons can be neglected in many cases.

Thus the lowest-energy atomic  $p$  wave function for the valence electrons may in most cases be considered to be the sole source of  $q$ . Contributions of the valence  $p$  electrons can be very simply obtained as  $|a_{n1m}|^2 q_{n1m}$ , where  $|a_{n1m}|^2$  is the importance of the  $p$  wave function in an expansion of the type (9-5) and  $q_{n1m}$  is the value of  $q$  for an atomic state. However, there are cases for which the valence electrons produce only a very small contribution to  $q$ , and then some of the small and complicated terms discussed above must be taken into account. Some of these cases will be illustrated below.

**9-4. Procedure for Calculating  $q$  in a Molecule.** To evaluate  $q$  at a particular nucleus with the approximation discussed above, only the contributions of electrons in the valence shell need be considered, and these are taken to be of the form  $\Sigma |a_{nlm}|^2 q_{nlm}$ . The procedure will perhaps be made most clear by examples.

Consider first the value of  $\partial^2 V / \partial z^2$  at the In nucleus in the diatomic molecule InCl, where the  $z$  direction is chosen along the molecular axis. In has three valence electrons, the configuration of the ground state of the atom being  $5s^2 5p$ . Cl has seven valence electrons, with a ground atomic state  $3s^2 3p^5$ . A first approximation to the structure of the InCl molecule might be that the two atoms are essentially in their ground



atomic states and bound together by a covalent bond which uses the  $p$  atomic wave functions of each atom. This would be a so-called  $p_\sigma$  bond, the  $\sigma$  meaning simply that  $m = 0$ . The wave function then for the two electrons which form the bond may be written approximately

$$\psi = \frac{1}{\sqrt{2}} (\psi_{510})_{\text{In}} + \frac{1}{\sqrt{2}} (\psi_{310})_{\text{Cl}} \quad (9-8)$$

where the subscripts In and Cl indicate the atomic wave functions of In and Cl, respectively. If  $(\psi_{310})_{\text{Cl}}$  is expanded in terms of indium atomic wave functions, it will involve a large number of smaller terms of highly excited states, which contribute essentially nothing to  $q$  at the In nucleus. However, the first term of (9-8) contributes for each bonding electron an amount  $(1/\sqrt{2})^2 q_{510}$ , or for the two bonding electrons an amount  $q_{510}$ . There are in addition two valence  $s$  electrons which are not involved in the bonding, but since for an  $s$  electron  $q_{n00} = 0$ , they contribute nothing. Hence a first (and very rough) approximation to the molecular structure suggests that there is one excess  $p$  electron around the In nucleus with  $m = 0$ , and that  $q_{\text{In}} = q_{510}$ . The value of  $q_{510}$  may be calculated from the In atomic fine structure and expression (9-3), or more accurately from the magnetic hyperfine structure and expression (9-4). In each case it should be noted that these expressions give  $q_J = q_{n11}$ , which equals  $-\frac{1}{2}q_{n10}$ . In general the  $q$ 's for different values of  $m$  are related by

$$q_{nlm} = q_{nl0} \left[ 1 - \frac{3m^2}{l(l+1)} \right] \quad (9-9)$$

Similarly there is at the Cl nucleus a contribution  $q_{310}$  from the bonding electrons, but in addition an amount  $2q_{311}$  and  $2q_{3,1,-1}$  from the four nonbonding valence electrons. Now from (9-9)  $q_{311} = q_{3,1,-1} = -\frac{1}{2}q_{310}$ , so the total value of  $q_{\text{Cl}}$  is

$$q_{\text{Cl}} = q_{310} + 2q_{311} + 2q_{3,1,-1} = -q_{310} \quad (9-10)$$

While In might be expected to have an excess of one  $p$  electron oriented along the axis, Cl has a defect of one  $p$  electron, and hence the negative sign in (9-10).

It may be noted that any covalent single-bonded In or Cl atom should have roughly the same values of  $q$  given above. However, if these atoms are ionically bonded in a molecule, the situation is different. Consider, for example, NaCl, which we shall first approximate as a completely ionic molecule  $\text{Na}^+\text{Cl}^-$ . In this case the chlorine is surrounded by a closed spherical shell of electrons, the configuration of the ground state of  $\text{Cl}^-$  being  $3s^2 3p^6$ , and hence in the approximation used here  $q_{\text{Cl}} = 0$ . Similarly  $\text{Na}^+$  has a closed-shell configuration of electrons and  $q_{\text{Na}} = 0$ .

*Ionic Character and Hybridization.* This introduces the question whether InCl is indeed covalently bonded as assumed or is more nearly ionic like NaCl. Actually it must be intermediate between these two extremes, and it is customary to describe such an intermediate bond as a mixture of covalent and ionic bonds, or as “resonating” between the two different types. If, for example, the ionic bond has a fractional importance  $x$  in the actual InCl structure and the pure covalent bond an importance  $1 - x$ , then each contributes amounts to  $q$  given by the product of its fractional importance times the value of  $q$  for the pure type of bond. Hence

$$\begin{aligned} q_{\text{In}} &= (1 - x)q_{510} + (x)0 = (1 - x)q_{510} \\ q_{\text{Cl}} &= -(1 - x)q_{310} + (x)0 = -(1 - x)q_{310} \end{aligned} \quad (9-11)$$

A method of estimating the fractional importance,  $1 - x$ , of the covalent bond will be discussed below.

The quantity multiplying  $-q_{510}$  or  $-q_{310}$  in (9-11) is called the amount of unbalanced  $p$  electrons  $U_p$  oriented along the bond.\* Thus for In in InCl,  $U_p = -(1 - x)$  and for Cl,  $U_p = 1 - x$ . There may of course be a number of  $p$  valence electrons whose effects cancel, as in  $\bar{\text{Cl}}$ ,  $U_p = 0$ . For any type of bond, the net effect of the valence  $p$  electrons may be expressed as the number of unbalanced  $p$  electrons  $U_p$  oriented along the bond. The quadrupole coupling constant is  $-U_p$  times the coupling per  $p$  electron, or  $-U_p eq_{n10}Q$ .

Let us examine now the quadrupole coupling constants of  $\text{Cl}^{35}$  in a few typical molecules listed in Table 9-3. It is clear from the small coupling constant in NaCl that this molecule must be essentially ionic.  $\text{TlCl}$  must also be largely ionic, although not entirely so. The remaining molecules listed have bonds which are primarily covalent in nature. The value of  $eqQ$  for  $\text{FCl}$  is abnormally high because this molecule is partly ionic, but with the chlorine atom positive instead of negative since F is more electronegative (*i.e.*, tends more to attract electrons) than Cl. A  $\text{Cl}^+$  ion has two  $p$  electrons missing from its valence shell, and the additional missing electron must have come from a  $p_\sigma(m = 0)$  orbit if it is to migrate easily to the F atom. With two missing  $p_\sigma$  electrons,  $\text{Cl}^+$  should have a value of  $q = -2q_{310}^+$ . The plus is put on  $q_{310}$  to indicate that  $q_{310}$  for  $\text{Cl}^+$  may be slightly different from  $q_{310}$  for neutral Cl.

Most essentially covalently bonded Cl atoms have quadrupole coupling constants near  $-80$  Mc, which is considerably lower than the value  $-109.6$  Mc of  $eq_{310}Q$  for atomic Cl.  $\text{ICl}$  is such an example, where other

\*  $U_p$  might more logically be the quantity multiplying  $q_{510}$  rather than  $-q_{510}$  but the above definition has the sanction of usage.



molecular information would indicate that no large amount of ionic bonding is present, yet the coupling is appreciably less than that expected for essentially atomic Cl. Hybridization of the bonding orbital for Cl

TABLE 9-3. QUADRUPOLE COUPLING CONSTANTS OF  $\text{Cl}^{35}$  IN A FEW TYPICAL MOLECULES

<i>Molecule</i>	<i>eqQ</i>
Cl (atomic)	-109.6 ( $-eq_{310}Q$ )
FCI	-146
ICI	- 82.5
$\text{CH}_3\text{Cl}$	- 74.8
ClCN	- 83.3
TICI	- 15.8
NaCl	< 1

must be assumed for this and other similar cases. A decrease in  $eqQ$  is to be expected for hybridization of the  $3p_z$  orbit with some  $3s$  wave function. For, if the bonding electrons use a small amount of  $s$  wave function, then the pairs of nonbonding electrons must use a corresponding amount of  $3p_z$  wave function. By this process part of the  $p_z$  wave function becomes filled with two electrons rather than one, and the defect of electrons along the axis is reduced. Hybridization with a fraction  $y$  of  $s$  wave function gives for Cl a value  $U_p = 1 - y$ . If hybridization of the  $3p$  orbit with a  $3d$  wave function occurs, the value of the quadrupole coupling constant would have been increased rather than decreased, or  $U_p = 1 + y$ , where  $y$  is the fractional importance of the  $3d$  wave function. This situation is quite different from hybridization with a  $3s$  orbit, since the  $3d$  orbit is unoccupied, while the  $3s$  orbit contains two nonbonding electrons. In the case of In, where  $U_p$  is negative,  $s$ -hybridization increases the magnitude of the quadrupole coupling, giving  $U_p = -1 - y$  for an amount  $y$  of  $s$ -hybridization.

Probably the quadrupole coupling for an atom in a molecule is also affected by the overlap of its valence wave function with that of the atom to which it is bonded [422], [973]. Unfortunately the precise effect of overlap on the quadrupole coupling constant is very difficult to evaluate theoretically. However, there seems to be good experimental evidence that overlap effects probably do not contribute much to the quadrupole coupling constants [913c], and hence we shall neglect them in subsequent considerations.

Once the amount and type of hybridization and the amount of ionic character of a bond is determined, then  $q$  may be rather quickly calculated. Unfortunately, however, the amount of hybridization and the ionic character cannot be separately determined from a measurement of  $eqQ$  alone, since the quadrupole effect cannot directly distinguish between the two. The per cent ionic character of a bond between two atoms



$[x$  in (9-11)] can usually be approximately determined as a function of the electronegativity difference from the curve of Fig. 9-2. This curve has been obtained primarily from quadrupole coupling constants in diatomic molecules. After a small allowance for hybridization (described immediately below), these give values of the ionic character plotted in the figure.

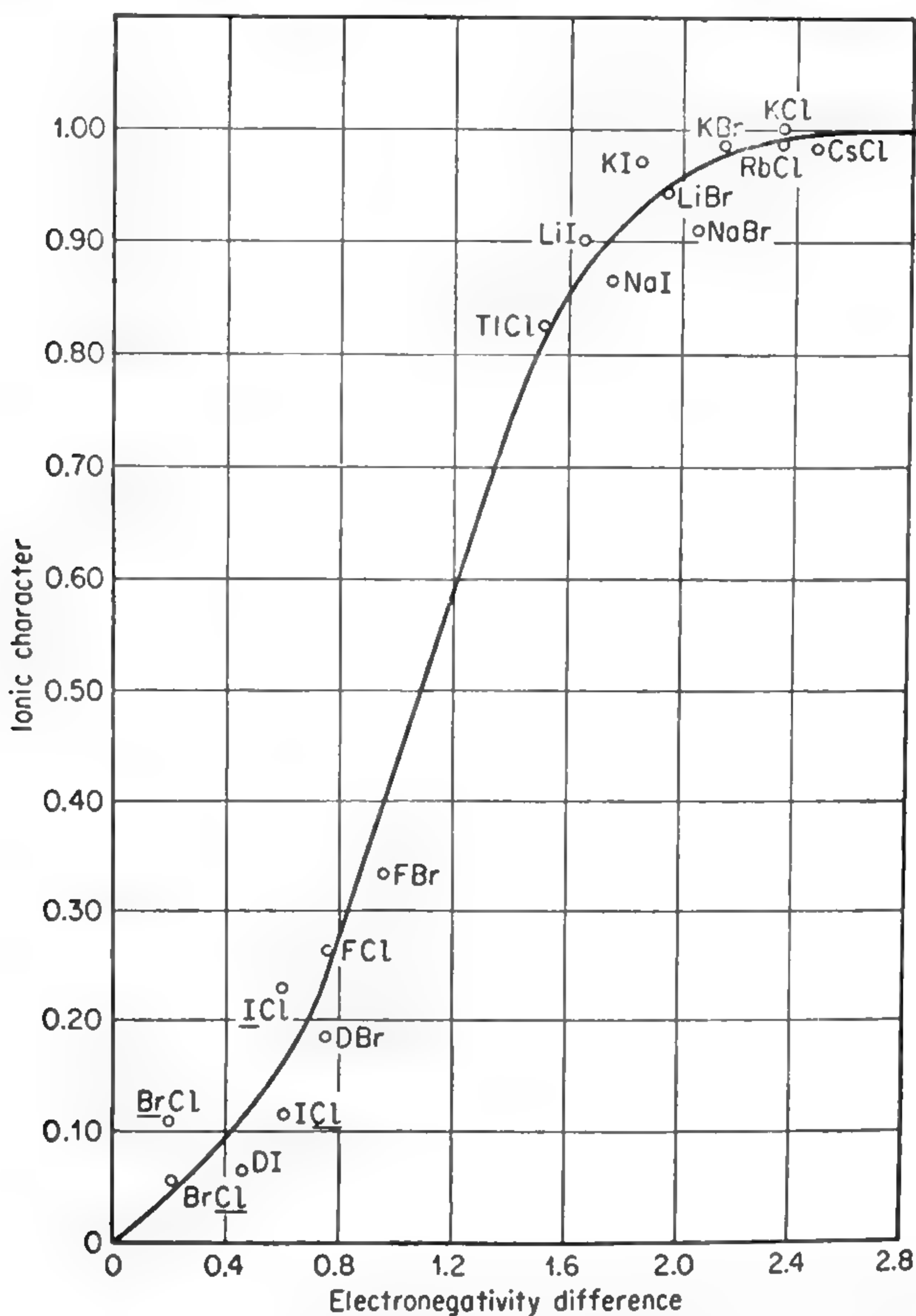


FIG. 9-2. Electronegativity difference. Ionic character of bonds vs. electronegativity difference between bonded atoms. (After Dailey and Townes [913c].)

Small deviations from the curve of Fig. 9-2 may occur for a variety of reasons, and hence no precise relation between ionic character and electronegativity difference can be established. The presence of three hydrogens near the carbon atom in  $\text{CH}_3\text{Cl}$  or  $\text{CH}_3\text{I}$ , for example, seems to decrease the effective electronegativity of C by several tenths of a unit. Internuclear distance and hybridization also affect the amount of ionic character. The normal electronegativities of various atoms are

listed in Table 9-4. Gordy [578] has suggested that ionic character is given by the linear relation: ionic character =  $\frac{1}{2}$  (electronegativity difference). This is a rough approximation to the solid curve of Fig. 9-2 but does not fit experimental observations quite so well [913c].

TABLE 9-4. ELECTRONEGATIVITIES AND COVALENT BOND RADII OF ATOMS

Values of electronegativities come from Huggins [814a] and Pauling [94] and are in arbitrary units. Differences in electronegativities may be considered approximately as electron volts. Atomic radii are those due to Pauling [94] and are given in angstrom units.

	H						
Electronegativity.....	2.2						
Single-bond radius.....	0.30						
	Li	Be	B	C	N	O	F
Electronegativity.....	1.0	1.5	2.0	2.6	3.0	3.5	3.9
Single-bond radius.....			0.88	0.771	0.70	0.66	0.72
Double-bond radius.....			0.76	0.665	0.60	0.55	0.62
Triple-bond radius.....			0.68	0.602	0.547	0.50	
	Na	Mg	Al	Si	P	S	Cl
Electronegativity.....	0.9	1.2	1.5	1.9	2.1	2.6	3.1
Single-bond radius.....				1.17	1.10	1.04	0.99
Double-bond radius.....				1.07	1.00	0.94	0.89
Triple-bond radius.....				1.00	0.93	0.87	
	K	Ca	Sc	Ge	As	Se	Br
Electronegativity.....	0.8	1.0	1.3	1.9	2.1	2.5	2.9
Single-bond radius.....				1.22	1.21	1.17	1.14
Double-bond radius.....				1.12	1.11	1.07	1.04
	Rb	Sr	Y	Sn	Sb	Te	I
Electronegativity.....	0.8	1.0	1.3	1.9	2.0	2.3	2.6
Single-bond radius.....				1.40	1.41	1.37	1.33
Double-bond radius.....				1.30	1.31	1.27	1.23
	Cs	Ba					
Electronegativity.....	0.7	0.9					

The amount of hybridization varies from bond to bond and no simple rules can give the hybridization exactly. In the case of Cl, Br, and I, a reasonable approximation is 15 per cent *s* hybridization for all cases where these atoms are more electronegative than the atom to which they are bonded by 0.25 units, and otherwise no hybridization [913c]. If an atom is singly bonded to two or more other atoms, the angle between the bonds often gives a fairly reliable estimate of the amount of hybridization (cf. [133]). If only *s* and *p* orbitals are involved in two or more equivalent

bonds, then the amount of  $s$  hybridization is

$$x = \frac{\cos \theta}{\cos \theta - 1} \quad (9-12)$$

where  $\theta$  is the angle between two of the bonds. For example, the bond angles for  $\text{AsCl}_3$  and  $\text{NH}_3$  are  $\theta = 98^\circ 25'$  and  $\theta = 106^\circ 47'$ , indicating  $s$  hybridizations of 13 and 18 per cent, respectively. However, expression (9-12) is not always an accurate indication of the hybridization; its use is especially misleading in some of the hydrides [903] which seem to involve more hybridization than is indicated by the bond angles. In the double or triple bonds of N, O, S, and probably those of other elements, the  $p_\sigma$  component of the bond appears to be hybridized by 10 to 25 per cent [903].

With the above rules for hybridization and ionic character, the quadrupole coupling constants of the halogens can be calculated in known molecules with an accuracy of a few per cent of  $eq_{n10}Q$ . For other atoms the approximations are not usually so accurate. For the alkalis, one can only say that the coupling should be rather small, since essentially no unbalanced  $p$  electrons are involved in bonding. For elements in the third to sixth columns of the periodic table, involving multiple bonds whose characteristics are not well known, the above approximations can usually give quadrupole coupling constants with an accuracy of about 25 per cent.

*Multiple Bonds.* In case there are many bonds to one atom in a molecule, as in the fifth-column elements mentioned above, the contributions to  $q$  of each bond and valence electron must be added. For example, a double bond, such as that for the end nitrogen in  $\bar{\text{N}} = \dot{\text{N}} = 0$ , involves a  $p_\sigma$  orbit ( $m = 0$ ) and a  $p_\pi$  orbit ( $m = \pm 1$ ), so that the value of  $q$  if no hybridization occurs is  $q = q_{210}^- + q_{211}^- + 2q_{211}^- = -\frac{1}{2}q_{210}^-$ . If the  $p_\sigma$  bond is assumed to be 45 per cent  $s$ -hybridized, two of the nonbonding electrons must correspondingly have 45 per cent  $p$  wave function. The resulting contributions to  $q$  are as follows:

Nonbonding electrons in $p_\pi$ orbit:	$2q_{211}^-$
Nonbonding electrons in $s$ plus 45% $p_\sigma$ orbit:	$0.90q_{210}^-$
Bonding electrons in $p_\pi$ orbit:	$q_{211}^-$
Bonding electrons in $p_\sigma$ plus 45% $s$ orbit:	$0.55q_{210}^-$

This gives a net of  $3q_{211}^- + 1.45q_{210}^- = -0.05q_{210}^-$ .

A minus superscript was attached to  $q_{210}$  above to indicate that  $q_{210}$  should be evaluated for a negative ion  $\bar{\text{N}}$  rather than for neutral N. Examination of the fine structure  $\Delta\nu$  for several states of ionization of various atoms indicates that each stage of ionization modifies  $q$  by a



factor  $1 + \epsilon$  which is approximately 1.25; positive ionization increases  $q$  by pulling all electrons closer to the nucleus, and negative ionization decreases  $q$ . We shall hence assume  $q_{210}^- = q_{210}/1.25$  and  $q_{210}^+ = 1.25q_{210}$ . More precise values of  $\epsilon$  can be found in Table 9-5. Thus for a structure like  $\bar{\text{N}}=\text{N}$  with no hybridization,  $q = -\frac{1}{2}(1/1.25)q_{210}$ , or  $U_p = 0.40$ . If an atom in the first two rows of the periodic table has four covalent bonds, then all valence orbits are equally occupied by electrons, and  $q = q_{210} + q_{211} + q_{2,1,-1} = 0$  ( $U_p = 0$ ). This is almost always the case

TABLE 9-5. VALUES OF  $\epsilon$  FOR A NUMBER OF ELEMENTS

The coupling constant produced by a  $p$  electron is modified by a factor approximately  $1 + \epsilon$  for each stage of ionization, being larger for positive ionization.

Be	0.90	B	0.50	C	0.45	N	0.30	O	0.25	F	0.20
Mg	0.70	Al	0.35	Si	0.30	P	0.20	S	0.20	Cl	0.15
Ca	0.60	Sc	0.30	Ge	0.25	As	0.15	Se	0.20	Br	0.15
Sr	0.60	Ga	0.20			Sb	0.15	Te	0.20	I	0.15

for C or Si, which are quadruply bonded. Nitrogen normally has three bonds and a quadrupole coupling constant near  $-4$  Mc. However, in  $\bar{\text{N}}=\text{N}^+=\text{O}$  and in  $\text{CH}_3-\text{N}\equiv\text{C}$ , the central nitrogens are quadruply bonded, and the observed coupling constants are very small as expected, being less than 0.3 Mc.

There are many cases of bonds which are partly single and partly double or triple, *i.e.*, of resonance between single and multiple bond structures. Fortunately single, double, and triple bonds for a particular pair of atoms have distinctly different lengths, so that the internuclear distances may be used to determine the relative importance of single or multiple bonds between two atoms. If  $R_1$  is the sum of the single-bond radii of two atoms, or the distance between them when there is a single bond,  $R_2$  the double-bond distance, and  $R_3$  the triple-bond distance, then the expected distance for an intermediate-type bond is (see [133] for a fuller discussion)

$$R = \frac{x_1 R_1 + 3x_2 R_2 + 6x_3 R_3}{x_1 + 3x_2 + 6x_3} \quad (9-13)$$

where  $x_1$  = fractional importance of the single-bond state

$x_2$  = fractional importance of the double-bond state

$x_3$  = fractional importance of the triple-bond state

Since  $x_1 + x_2 + x_3 = 1$ , if it is thought that only single and double bonds, or only double and triple bonds, are involved between two particular atoms, and if the internuclear distance  $R$  is known, then the fractional importance  $x$  of the two resonant bonding states can be determined. Standard atomic radii for single, double, and triple bonds for

various atoms are listed in Table 9-4. One cannot expect high precision in determination of the amount of double- or triple-bond character from (9-13), since observed bond distances in molecules often differ by as much as 0.01 or 0.02 Å from the values obtained by use of this expression and Table 9-4. In many of the heavier atoms the bond radii are still unknown.

A refinement in the calculation of internuclear distances is the Scho-

TABLE 9-6. THE NUMBER OF "UNBALANCED" *p* ELECTRONS, *U<sub>p</sub>*, FOR VARIOUS BOND STRUCTURES

The fraction of *s* or *d* hybridization is indicated by the symbols *s* or *d*, respectively. It is assumed that the hybridizing *s* or *d* wave functions have the same principal quantum number as the *p* function. *U<sub>p</sub>* is with respect to the axis of the bond or bonds unless otherwise stated. The quantity *ε* which appears here is given in Table 9-5.

Electron configuration of atom	Type of bond	Hybridization	<i>U<sub>p</sub></i>
<i>s</i> <sup>2</sup> <i>p</i> <sup>5</sup> (like Cl)	Single covalent	<i>s</i> and <i>d</i>	1 − <i>s</i> + <i>d</i>
<i>s</i> <sup>2</sup> <i>p</i> <sup>6</sup> (like Cl <sup>−</sup> )	Single ionic	—	0
<i>s</i> <sup>2</sup> <i>p</i> <sup>4</sup> (like Cl <sup>+</sup> )	Single ionic	—	2(1 + <i>ε</i> )
<i>s</i> <sup>2</sup> <i>p</i> <sup>4</sup> (like O)	Double covalent	$\begin{Bmatrix} p_{\sigma} \text{ } s \text{ and } d \\ p_{\pi} \text{ none} \end{Bmatrix}$	$\frac{1}{2} - s + d$
<i>s</i> <sup>2</sup> <i>p</i> <sup>3</sup> (like N)	Triple covalent	$\begin{Bmatrix} p_{\sigma} \text{ } s \text{ and } d \\ p_{\pi} \text{ none} \end{Bmatrix}$	− <i>s</i> + <i>d</i>
<i>s</i> <sup>2</sup> <i>p</i> <sup>4</sup> (like O)	Two single covalent, each of ionic character <i>i</i> , with O positive	<i>s</i>	$\left(\frac{1}{2} + \frac{i}{2} + 2s\right) (1 + 3i\epsilon)$ (along direction bisecting bond angle)
	With O negative	<i>s</i>	$(s - 1 - i)(1 + 2i\epsilon)$ (along direction perpendicular to plane of bonds)
			$\frac{(\frac{1}{2} - 2s)(1 - i)}{1 + 2i\epsilon}$ (along direction bisecting bond angle)
			$\frac{(s - i)(1 - i)}{1 + 2i\epsilon}$ (along direction perpendicular to plane of bonds)
<i>s</i> <sup>2</sup> <i>p</i> <sup>3</sup> (like N)	Three single bonds, each of ionic character <i>i</i> , with N positive	<i>s</i>	−3 <i>s</i> (1 + <i>i</i> )(1 + 3 <i>iε</i> )
	With N negative	<i>s</i>	$-\frac{3s(1 - i)}{(1 + 3i\epsilon)}$
<i>s</i> <sup>2</sup> <i>p</i> <sup>2</sup> (like C)	Four covalent bonds	Any <i>s</i> − <i>p</i> hybridization	0
<i>s</i> <sup>2</sup> <i>p</i> (like B)	Three bonds in a plane	<i>s</i>	1

maker-Stevenson rule [109], which states that ionic character of a bond shortens the bond by an amount

$$\Delta R = (-)0.09|x_1 - x_2| \quad (9-14)$$

where  $x_1 - x_2$  is the difference in electronegativity of the two bonded atoms. This shortening is particularly important for bonds to fluorine, but in most other cases it may be neglected, and in fact in some bonds which do not involve fluorine it does not seem to give correct results.

*Examples and Tables of Quadrupole Coupling Constants.* The number of unbalanced  $p$  electrons,  $U_p$ , for various important types of bonds is summarized in Table 9-6.  $U_p$  for structures which are intermediate between two or more varieties of bonds listed in this table may also be obtained from it by summing  $U_p$  times the fractional importance for each bond type.

The bond structure and expected values of  $U_p$  for a number of examples are indicated in Table 9-7. The percentage importance of the structures listed have been chosen from use of expressions (9-12) and (9-13) and consideration of molecular dipole moments and quadrupole couplings. The chosen combination of resonating structures gives values of quadrupole coupling (which may be obtained by multiplying the net unbalanced  $p$  electrons,  $U_p$ , by the negative of the quadrupole coupling per  $p$  electron given in Table 9-8) very close to those which are observed and at the same time is consistent with other known information about the molecules.

In rare cases the contribution to  $q$  of  $d$  or other orbitals may be taken into account in obtaining  $q$ . However, unless  $U_p$  is extremely small, contributions to  $q$  from  $p$ -type wave functions will be so much larger, as they are in all cases listed in Table 9-6, that the  $d$  orbital contribution may be considered to be zero.

Table 9-8 gives values for the quadrupole coupling constant of various isotopes produced by one  $p$  electron excess along the bond axis, *i.e.*, the value of  $eqQ$  when  $U_p$ , the "unbalance of  $p$  electrons," is unity. This might also be written  $eq_{n10}Q$ . These values are mostly obtained from observed coupling constants in a variety of molecules; however, some are obtained from measurements of atomic spectra. Table 9-8 also lists the best available values of  $q$  produced by one  $p$  electron excess along the bond axis, that is,  $q_{n10}$ . From  $eqQ$  and  $q$ , the nuclear quadrupole moments  $Q$  may be obtained, remembering that  $e$  is the charge of one proton. Best values of  $Q$  are given in Appendix VII.

**9-5. Quadrupole Coupling in Asymmetric Molecules.** The discussion so far has applied specifically to symmetric molecules, where one quadrupole coupling constant  $eqQ$  is sufficient to specify the energy of interaction between the nuclear quadrupole and the molecule. As mentioned in Chap. 6, for an asymmetric rotor two coupling constants are needed,



TABLE 9-7. STRUCTURES OF MOLECULES AND THEIR AMOUNTS  $U_p$  OF UNBALANCED  $p$  VALENCE ELECTRONS

Quadrupole coupling constants may be obtained by multiplying  $U_p$  by  $eq_{n10}Q$ , the quadrupole coupling per  $p_\sigma$  electron.

Nu- cleus	Mole- cule	Partial structures	Comments	$U_p$ for each structure	% impor- tance	Net $U_p$
Cl	FCl	F—Cl	No hybridization	1.00	75	1.37
		$\bar{F} \quad \overset{+}{Cl}$		2.50	25	
	ICl	I—Cl	15 % $s$ hybridization	0.85	85	0.72
		$\overset{+}{I} \quad \bar{Cl}$		0	15	
	TiCl	Ti—Cl	15 % $s$ hybridization	0.85	18	0.15
		$\overset{+}{Ti} \quad \bar{Cl}$		0	82	
	SiH <sub>3</sub> Cl	H <sub>3</sub> Si—Cl	15 % hybridization	0.85	30	0.38
		H <sub>3</sub> $\overset{+}{Si}\bar{Cl}$		0	40	
		H <sub>3</sub> $\bar{Si}=\overset{+}{Cl}$	$p_\sigma$ bond with 15 % $s$ hy- bridization	0.40	30	
	CHCl		$U_{pz}$ refers to $z$ axis along C—Cl bond. $y$ axis is in Cl—C—H plane and $x$ axis is perpendicular. 15 % $s$ hybridization	$U_{pz} = 0.85$ $U_{py} = -0.42$ $U_{px} = -0.42$	75	$U_{pz} = 0.66$ $U_{py} = -0.38$ $U_{px} = -0.28$
			$p_\pi$ bond assumed perpen- dicular to Cl—C—H plane	$U_{pz} = 0.55$ $U_{py} = -1.16$ $U_{px} = 0.72$	5	
				0	20	
S	OCS	$\bar{O}-C\equiv\overset{+}{S}$	No hybridization	$\bar{0}$	14	0.51
		$O=C=\bar{S}$		0.5	58	
		$\overset{+}{O}\equiv C-\bar{S}$	25 % $s$ hybridization of $p_\sigma$ bond	0.8	28	0.27
		or $\bar{O}-C\equiv\overset{+}{S}$		-0.31	14	
		$O=C=\bar{S}$		0.25	58	
N	N <sub>2</sub> O	$\overset{+}{O}\equiv C-\bar{S}$		0.60	28	
		$\overset{+}{H}$				
	NH <sub>3</sub>	$\bar{N}-H$	25 % hybridization	-0.40	100	-0.40
		$\bar{H}$				
		$\bar{N}=\overset{+}{N}=\bar{O}$				
		$N\equiv\overset{+}{N}-\bar{O}$				
As	AsH <sub>3</sub>	$\bar{N}=\overset{+}{N}=\bar{O}$	45 % hybridization of $p_\sigma$ bonds only	0.05	55	-0.17
		$N\equiv\overset{+}{N}-\bar{O}$	End nitrogen	-0.45	45	
		$\bar{N}=\overset{+}{N}=\bar{O}$	Central nitrogen	0	55	0
		$N\equiv\overset{+}{N}-\bar{O}$		$\bar{0}$	45	
	AsCl <sub>3</sub>		10 % hybridization	-0.30	50	-0.28

$eQ \frac{\partial^2 V}{\partial z_m^2}$  and  $eQ \left( \frac{\partial^2 V}{\partial x_m^2} - \frac{\partial^2 V}{\partial y_m^2} \right)$ , where  $x_m$ ,  $y_m$ , and  $z_m$  are directions of the principal axes of inertia. For a symmetric molecule, if  $z$  is the axis of symmetry,  $\frac{\partial^2 V}{\partial x_m^2} - \frac{\partial^2 V}{\partial y_m^2} = 0$ . Very often the electric field derivative

TABLE 9-8. QUADRUPOLE COUPLING CONSTANTS FOR VARIOUS NUCLEI DUE TO ONE VALENCE  $p$  ELECTRON

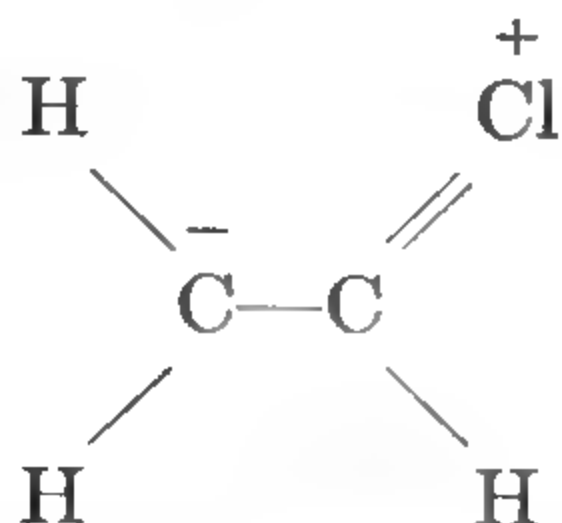
A range of values is given for  $N^{14}$ , which is poorly known.

	Quadrupole coupling constant for one valence $p$ electron with wave function oriented along bond ( $eq_{n10}Q$ ), in Mc	$\frac{\partial^2 V}{\partial z^2}$ for one valence $p$ electron with $m = 0$ ( $q_{n10}$ ), in $10^{16}$ esu
B <sup>10</sup>	— 10.9	1.6
B <sup>11</sup>	— 5.3	1.6
N <sup>14</sup>	— 10 to -24	8.6
O <sup>17</sup>	3.3	11
Al <sup>27</sup>	— 37.5	3.3
S <sup>33</sup>	55	13
S <sup>36</sup>	— 39	13
Cl <sup>35</sup>	109.7	20
Cl <sup>36</sup>	23.2	20
Cl <sup>37</sup>	86.4	20
Ga <sup>69</sup>	— 125	7.5
Ga <sup>71</sup>	— 78.8	7.5
Ge <sup>73</sup>	220	15
As <sup>75</sup>	600	20
Se <sup>79</sup>	—1400	25
Br <sup>79</sup>	— 769.8	34
Br <sup>81</sup>	— 643.1	34
In <sup>113</sup>	— 886.2	11
In <sup>115</sup>	— 899.1	11
Sb <sup>121</sup>	2000	34
Sb <sup>123</sup>	2500	34
I <sup>127</sup>	2292.8	45
I <sup>129</sup>	1688	45
Hg <sup>201</sup>	—1000	23

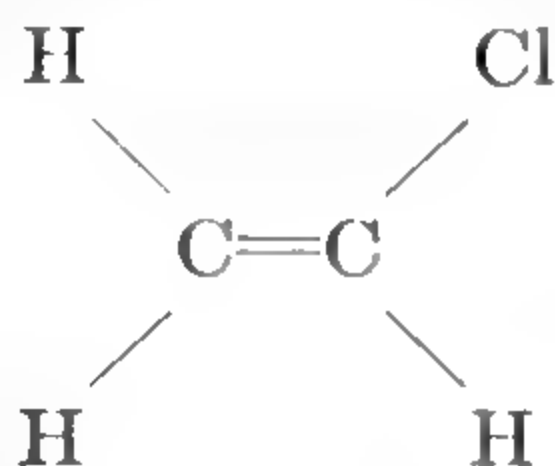
tensor  $\nabla E$  is symmetric about some molecular bond. For example,  $\nabla E$  at either Cl nucleus in  $CH_2Cl_2$  is approximately symmetric about the C—Cl bond, and choosing this direction as an axis,  $eqQ$  may be calculated as above. The quantities  $eQ \frac{\partial^2 V}{\partial z_m^2}$  and  $eQ \left( \frac{\partial^2 V}{\partial x_m^2} - \frac{\partial^2 V}{\partial y_m^2} \right)$  may be calculated from (6-23) by a rotation of coordinates to the principal axes of inertia.

There are some cases, however, for which the field is not symmetric

about the bond axis [370], [459], as for Cl in the structure



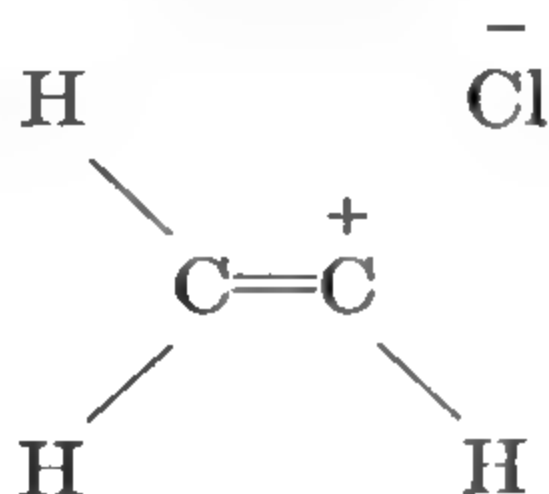
where a double bond occurs. Taking the double bond to be a non-hybridized  $p_\sigma$  bond along the C—Cl or  $z_b$  direction plus a  $p_\pi$  bond perpendicular to the Cl—C—H plane or in the  $x_b$  direction, we obtain an excess of one  $p$  electron in a  $p_\pi$  orbit in the  $y_b$  direction, *i.e.*, in the Cl—C—H plane. Hence  $\frac{\partial^2 V}{\partial y_b^2} = q_{310}(1 + \epsilon)$ ;  $\frac{\partial^2 V}{\partial x_b^2} = \frac{\partial^2 V}{\partial z_b^2} = -\frac{1}{2}q_{310}(1 + \epsilon)$ . If this double-bonded structure is of importance  $x$ , and the structure



is of importance  $1 - x$ , then the sum of their contributions gives values

$$\begin{aligned}
 \frac{\partial^2 V}{\partial z_b^2} &= \left[ -1 + \frac{x}{2}(1 - \epsilon) \right] q_{310} & \frac{\partial^2 V}{\partial x_b^2} &= \left[ \frac{1}{2} - x \left( 1 + \frac{\epsilon}{2} \right) \right] q_{310} \\
 \frac{\partial^2 V}{\partial y_b^2} &= \left[ \frac{1}{2} + x \left( \frac{1}{2} + \epsilon \right) \right] q_{310} & & \quad (9-15)
 \end{aligned}$$

Values of  $\frac{\partial^2 V}{\partial z_m^2}$  and  $\frac{\partial^2 V}{\partial x_m^2} - \frac{\partial^2 V}{\partial y_m^2}$  for the principal axes of inertia may then be obtained from (9-15) by a rotation of coordinates in accordance with (6-23b). In this case, the transformation to principal axes of inertia is somewhat more complicated than (6-23a) because of the lack of axial symmetry of the field about the bond axis. Table 9-7 gives values of  $U_p$  for  $x_b$ ,  $y_b$ , and  $z_b$  axes assuming 15 per cent  $s$  hybridization of the  $p_\sigma$  bond, and giving some importance to the structure



An interesting use of slight asymmetry occurs in the bending mode of molecules such as HCN, BrCN, and ICN [703], [754], [998a]. In the



ground state these molecules are linear and the electrostatic potential is axially symmetric. However, in the bending vibrational mode  $\nu_2 = 1$ , there is a slight asymmetry in the field due in part to the difference in direction between the principal axis of inertia and the C—N or I—C bonds, and in part to the fact that the dyadic  $\nabla\mathbf{E}$  is no longer symmetric about these bonds. Such effects afford a valuable measurement of the change in electronic structure of these molecules with bending.

**9-6. Interpretation of Magnetic Hyperfine Coupling Constants.** Magnetic hyperfine coupling constants are large and easily interpretable only for the rather rare molecules which have electronic angular momentum (cf. Chap. 8). For these molecules, however, magnetic hyperfine structure usually gives information about the electron distribution somewhat similar to that given by nuclear quadrupole effects.

It is primarily in diatomic or linear molecules that interpretation of magnetic coupling constants appears to be fruitful. For such cases, expressions (8-6) and (8-16) show that hyperfine effects depend primarily on four coupling constants:

$$\begin{aligned} a &= \frac{2\mu_0\mu_I}{I} \left( \frac{1}{r^3} \right)_{av} & b + \frac{c}{3} &= \frac{16\pi}{3} \frac{\mu_0\mu_I}{I} \psi^2(0) \\ c &= \frac{3\mu_0\mu_I}{I} \left( \frac{3 \cos^2 \theta - 1}{r^3} \right)_{av} & d &= \frac{3\mu_0\mu_I}{I} \left( \frac{\sin^2 \theta}{r^3} \right)_{av} \end{aligned} \quad (9-16)$$

The constant  $a$  contains  $(1/r^3)_{av}$ , which strictly is to be averaged over the electron or electrons which provide orbital angular momentum. The constants  $c$  and  $d$  involve similar averages, but over the electrons which provide spin angular momentum. Usually spin and orbital momentum involve precisely the same electrons, in which case the three constants  $a$ ,  $c$ , and  $d$  are related by  $c = 3(a - d)$ . Since the averages in the expressions (9-16) are to be taken only over those electrons which contribute angular momentum, these magnetic coupling constants are more

specific than the quadrupole coupling constant  $eqQ = eQ \left( \frac{3 \cos^2 \theta - 1}{r^3} \right)_{av}$ .

The latter average must be taken over all electrons in the molecule.

A sufficiently complete examination of the magnetic hyperfine structure will yield numerical values for the constants  $a$ ,  $b$ ,  $c$ , and  $d$  given by (9-16) and hence for the four quantities  $\left( \frac{3 \cos^2 \theta - 1}{r^3} \right)_{av}$ ,  $\left( \frac{1}{r^3} \right)_{av}$ ,  $\left( \frac{\sin^2 \theta}{r^3} \right)_{av}$ , and  $\psi^2(0)$ . The first may be evaluated or interpreted very much as the similar quantity  $q$  discussed above if it is remembered that only the electron or electrons which provide angular momentum are to be considered. The second quantity  $(1/r^3)_{av}$  has also already been discussed in connection with quadrupole effects but provides additional information, a direct measurement of  $(1/r^3)_{av}$ , which is not given by the quad-

rupole coupling constant. This average applies only to an electron with orbital angular momentum, hence not to an  $s$  orbit for which  $\left(\frac{3 \cos^2 \theta - 1}{r^3}\right)_{av}$  or  $\left(\frac{\sin^2 \theta}{r^3}\right)_{av}$  would also not apply. The fourth quantity,  $\psi^2(0)$ , is the square of the electron wave function at the nucleus, which is negligible except for an  $s$  orbit. This quantity therefore affords information which is never yielded by quadrupole effects, since they are never due to electrons in  $s$  orbits.

Since  $O_2$  is in a  $^3\Sigma$  state it has electronic spin momentum and provides an interesting example for examination of electron spin–nuclear spin interactions. The ordinary type of  $O_2$  has no hyperfine structure because of the zero spin of  $O^{16}$ . However,  $O^{16}O^{17}$  yields a rich hyperfine structure from which the constants  $b$  and  $c$  in (8-6) can be evaluated, and hence the quantities  $\psi^2(0)$  and  $\left(\frac{3 \cos^2 \theta - 1}{2r^3}\right)_{av}$  for the electrons with parallel spins [841], [842]. The value of  $\left(\frac{3 \cos^2 \theta - 1}{2r^3}\right)_{av}$  agrees within about 10 per cent with calculations using the expected structure of  $O_2$ . The value of  $\psi^2(0)$  corresponds to only 2.5 per cent  $s$  character for the electrons with parallel spins. Even this small amount of  $s$  character is not very well understood in terms of the molecular structure. In addition, it has a large effect on the observed hyperfine structure since magnetic hyperfine structure due to an  $s$  electron is usually enormously larger than that due to electrons in other types of orbits.

Other examples for which large magnetic hyperfine structure has been found are OH and NO, which are in  $^2\Pi$  ground states. The coupling coefficients of OH have not yet been interpreted, but those for NO allow a simple and rewarding discussion [916a]. NO is a rather good Hund's case ( $a$ ), so that the hyperfine energy is given by  $a\Lambda + (b + c)\Sigma$  from (8-9) plus doubling effects in the  $^2\Pi_{\frac{1}{2}}$  state from (8-16). Microwave measurements on the  $^2\Pi_{\frac{1}{2}}$  state [899] give  $a + (b + c)/2 = 74.1$  Mc, and those on the  $^2\Pi_{\frac{3}{2}}$  state [782b], [924] give  $a - (b + c)/2 = 92.2$  Mc and  $d = 112.6$  Mc. If one assumes that the electron which contributes orbital angular momentum is identical with that which contributes spin momentum, then  $c = -87.6$  Mc, and the following molecular constants may be derived.

$$\left(\frac{1}{r^3}\right)_{av} = 15 \times 10^{24} \text{ cm}^{-3} \quad (\sin^2 \theta)_{av} = 0.90 \quad \psi^2(0) = 0.85 \times 10^{24} \text{ cm}^{-3}$$

The first two quantities may be compared with the values

$$\left(\frac{1}{r^3}\right)_{av} = 23 \times 10^{24} \text{ cm}^{-3}$$

and  $(\sin^2 \theta)_{av} = 0.80$  for a  $p_\pi$  electron in an atomic orbit about the nitrogen. For an electron in an atomic orbit of the O atom,  $(1/r^3)_{av}$ , where  $r$  is the distance between the electron and N nucleus, is negligibly small. Hence the hyperfine coupling constants provide good evidence that the electron with angular momentum is approximately 15/23, or 65 per cent of the time in a  $p_\pi$  orbit about the N atom. The orbit is somewhat more confined to a plane through the N nucleus and perpendicular to the molecular axis than an atomic orbit would indicate, since  $(\sin^2 \theta)_{av}$  is greater than its value for an atomic orbit. The value of  $\psi^2(0)$  represents only about 2.5 per cent probability for the unpaired electron to be in a 2s atomic nitrogen state. As in the case of the O<sub>2</sub> molecule, only a small admixture of atomic s state is indicated, but this  $a$  makes an important contribution to the hyperfine structure.



## CHAPTER 10

### STARK EFFECTS IN MOLECULAR SPECTRA

**10-1. Introduction.** Stark effects are the changes in the spectrum of a system which may be observed when the system is subjected to an electric field. The rotational spectrum of a molecule which has an electric dipole may be expected to be modified when the molecule is in an electric field, since the field exerts torques on the molecular dipole moment and thereby can change its rotational motion. These types of effects can be understood in a qualitative way from classical mechanics, although any detailed explanation of them requires a quantum-mechanical approach.

Consider first a rotating linear molecule with angular momentum perpendicular to the electric field. The field tends to twist the dipole and give it a faster rotation when the dipole is oriented in the direction of the field, and a slower rate of rotation when it is pointed oppositely to the field. The dipole is hence oriented away from the field more often than with it, so that, on the average, the dipole is directed oppositely to the field (contrary to what would be expected if there were no rotation). The fractional difference between the time the dipole points in the two directions can be shown to be proportional to the ratio of the energy of the dipole in the field to the rotational energy

$$f \propto \frac{\mu E}{\frac{1}{2} I \omega^2} \quad (10-1)$$

where  $\mu$  is the dipole moment,  $E$  the electric field,  $I$  the moment of inertia, and  $\omega$  the angular velocity. The change in energy due to the field is then  $f\mu E$  or

$$\Delta W \propto \frac{(\mu E)^2}{h B J(J+1)} \quad (10-2)$$

where the rotational energy  $\frac{1}{2} I \omega^2$  has been written in terms of the rotational constant  $B$  and the rotational quantum number. There is also, of course, a change in the average rate of rotation of the molecule or its frequency.

If a linear molecule rotates with its angular momentum parallel or antiparallel to the electric field, then the rotating dipole is slightly twisted in the direction of the field, and the energy is decreased {an amount also proportional to  $(\mu E)^2/[h B J(J+1)]$ }. It will be seen below

that an average of the energy change over random orientations of a rotating molecule gives no net change in energy; the various positive and negative changes just cancel.

Symmetric-top molecules show a Stark effect of a rather different type, because their dipole moments may have components parallel to the angular momentum, and thus components which are fixed in direction rather than rotating. Thus for a symmetric top rotating about its symmetry axis, the dipole moment is in the direction of  $J$  and its energy in an electric field is  $-\mu E \cos \theta$ , where  $\theta$  is the angle between  $J$  and the field  $E$ . The projection of  $J$  on a fixed direction, such as that established by the direction of  $E$ , is always an integer  $M$ , the "magnetic" quantum number. Hence the energy might be expected to be

$$-\mu E \cos \theta = -\mu E \left( \frac{M}{J} \right)$$

In the more general case of the angular momentum  $J$  and a component of the angular momentum  $K$  along the symmetry axis, the component of  $\mu$  along the  $J$  direction is  $\mu(K/J)$ . Hence the energy might be expected to be

$$-\mu E \frac{K}{J} \cos \theta = -\frac{\mu E K M}{J^2}$$

Or, remembering that when the vector model is used  $J^2$  must always be replaced by  $J(J+1)$ ,

$$\Delta W = -\frac{\mu E M K}{J(J+1)} \quad (10-3)$$

This expression is correct but will be more rigorously derived below.

The change in energy, and hence in frequency of a symmetric-top molecule due to an electric field, is thus from (10-3) proportional to the first power of  $\mu E$ , whereas that for a linear molecule from (10-2) is proportional to the second power of  $\mu E$  and is much smaller because  $\mu E/[BJ(J+1)]$  is small (typically 0.01 to 0.001). These are often referred to as "first-order" and "second-order" Stark effects, respectively, names which might be attached to the power of  $\mu E$  which is involved, or to the order of perturbation approximation required to calculate these effects as will be seen below.

The first-order Stark effect characteristic of symmetric tops is more generally characteristic of a system with degenerate levels. It was shown in discussing nuclear moments (see page 132) that in the absence of an external field no system can have a dipole moment fixed in direction unless it is in a degenerate energy level. Symmetric tops can have a dipole moment of this type because of the degeneracy of the  $+K$  and  $-K$  levels, and this moment interacts with the electric field. Linear molecules have no degeneracy of this type, and a dipole moment must first

be produced by "polarization" of the molecule by a field. It is interesting to note that, in the symmetric-top ammonia, the two levels which are ordinarily degenerate are split by the inversion frequency, and a first-order Stark effect does not occur. Classically the  $\text{NH}_3$  dipole moment might be regarded as rapidly reversing in direction because of the inversion so that its average value in any direction is zero.

**10-2. Quantum-mechanical Calculation of Stark Energy for Static Fields.** The effect of an electric field on the molecular motion can be calculated quantum-mechanically by perturbation theory. The first-order perturbation is simply the average of the interaction energy over the quantum-mechanical state, or

$$\Delta W_1 = -\int \psi^* \mu E \cos \theta \psi dv \quad (10-4)$$

where  $\theta$  is the angle between the molecular dipole  $\mu$  and the field  $E$ . The expression (10-4) is just  $E$  times the  $z$  component of the dipole moment matrix element which is given in Table 4-4. For a symmetric-top wave function with rotational quantum numbers  $J, K, M$  this table gives

$$\Delta W_1 = -\mu E \phi_{JJ} \phi_{JKJK} (\phi_z)_{JMJM} = -\mu E \frac{MK}{J(J+1)} \quad (10-5)$$

which is identical with (10-3) and of course vanishes for a linear molecule when  $K = 0$ .

Transitions may occur with selection rules  $\Delta J = \pm 1$ ,  $\Delta K = 0$ , and  $\Delta M = 0$  or  $\pm 1$  (cf. Table 4-4). The observed frequencies are given for a transition  $J+1 \leftarrow J$  by  $W_{J+1} - W_J$ , so that, when  $\Delta M = 0$ ,

$$\nu = 2B(J+1) + \frac{2MK\mu E}{J(J+1)(J+2)h} \quad (10-5a)$$

and when  $\Delta M = \pm 1$ ,

$$\nu = 2B(J+1) + \frac{(2M \mp J)K\mu E}{J(J+1)(J+2)h} \quad (10-5b)$$

where  $M$  represents the "magnetic" quantum number for the initial or  $J$  state.

The next approximation, or second-order perturbation theory, takes into account the small changes in the molecular wave function due to the field, and the resulting energy may be written\*

$$\Delta W_2 = \sum_n \frac{|\mu_{nn'}|^2 E^2}{W_n - W_{n'}} \quad (10-6)$$

\* The Stark effects included in (10-6) are due only to the molecular dipole moments. There are other very much smaller terms due to the polarization of electron wave functions within the molecule. Such effects are usually negligible but will be discussed later in this chapter.



where  $W_n$  is the energy of the undisturbed state and  $W_{n'}$  is the energy of any other state unperturbed by the electric field.  $\mu_{nn'}$  is the  $z$  component of the dipole moment matrix element between the two states indicated by quantum numbers  $n$  and  $n'$ . The two states  $n$  and  $n'$  are sometimes said to "interact" through the perturbation  $\mu E \cos \theta$ . It may be noted that two interacting states always repel each other, that is, if  $W_n$  is greater than  $W_{n'}$ , (10-6) shows that the presence of the state  $n'$  increases the energy of the state  $n$  when there is a field. Similarly it decreases the energy of  $n'$  by the same amount so that the levels become further separated. The net change in energy of the state must be obtained by summing all such repulsions as indicated in (10-6). Again the matrix elements can be obtained from Table 4-4. For a symmetric top, the matrix element is zero for all combinations of states except  $J = J'$  or  $J = J' \pm 1$ , when  $M = M'$ , and  $K = K'$  (since  $\mu$  is always along the symmetry axis for a true symmetric top). The second-order energy  $\Delta W_2$  is hence affected only by the two neighboring states  $J' = J + 1$  and  $J' = J - 1$ , and the sum of their effects is

$$\Delta W_2 = \frac{\mu^2 E^2}{2Bh} \left\{ \frac{(J^2 - K^2)(J^2 - M^2)}{J^3(2J - 1)(2J + 1)} - \frac{[(J + 1)^2 - K^2][(J + 1)^2 - M^2]}{(J + 1)^3(2J + 1)(2J + 3)} \right\} \quad (10-7)$$

This second-order energy is usually so much smaller than the first-order given by (10-5), that it is rather unimportant unless  $K = 0$ , so that the first-order energy is zero. For a linear molecule, or for any symmetric molecule with  $K = 0$ ,  $\Delta W_2$  simplifies to

$$\Delta W_2 = \frac{\mu^2 E^2}{2hBJ(J + 1)} \frac{J(J + 1) - 3M^2}{(2J - 1)(2J + 3)} \quad (10-8)$$

However, in the special case where  $J = 0$ , (10-7) becomes

$$(\Delta W_2)_{J=0} = - \frac{\mu^2 E^2}{6hB} \quad (10-9)$$

The transition frequencies depend, of course, on the difference between Stark effects for the upper and lower levels of a transition. The resulting expression for the absorption of a linear molecule is given below by Eq. (10-25).

Second-order Stark energies are seen from (10-7) and (10-8) to be independent of the sign of  $M$ . Before Stark splitting there were  $2J + 1$  different degenerate levels for each value of  $J$  corresponding to the different values of  $M$ . First-order Stark effect, when present, removes this degeneracy completely. Second-order Stark effects depend on  $M^2$ , so that the levels are separated into pairs of degenerate levels ( $\pm M$ ) except for  $M = 0$ , which is nondegenerate.

Expression (10-8) shows that, for large  $J$ , for a molecule with angular momentum perpendicular to  $E$  ( $M = 0$ ), the change in energy is positive and proportional to  $\mu^2 E^2 / hBJ^2$  as found above in expression (10-2). Similarly for large  $J$  and  $M = J$ , the energy is negative and proportional to  $-\mu^2 E^2 / hBJ^2$ . For any particular value of  $J$ , other than  $J = 0$ , the average value of  $\Delta W_2$  from (10-8) is zero, since

$$3 \sum_{M=-J}^{M=J} M^2 = J(J+1)(2J+1) \quad (10-10)$$

so that the average value of  $3M^2$  is just  $J(J+1)$ .

Still higher-order perturbation terms may be included in the Stark energy. The fourth-order terms for the Stark energy of a linear molecule (third-order terms are zero) have been evaluated [20], [209], [375] but in most cases are very small. They are smaller than the second-order terms by somewhat less than the ratio of the second-order terms to the rotational frequency, or usually considerably less than 1 per cent. An exact expression for the energy  $W$  of a linear molecule in a strong electric field has also been written as the following continued fraction (W. E. Lamb, as quoted in [209]; cf. also [433]).

$$\begin{aligned} \frac{W}{hB} = M(M+1) \\ - \frac{(\mu E/hB)^2 A_{M,M}^2}{(M+1)(M+2) - \frac{W}{hB} - \frac{(\mu E/hB)^2 A_{M+1,M}^2}{(M+2)(M+3) - \frac{W}{hB} - \dots}} \end{aligned} \quad (10-11)$$

where  $B$ ,  $M$ ,  $\mu$ , and  $E$  have the meanings used above and

$$A_{xy}^2 = \frac{(x+1)^2 - y^2}{(2x+1)(2x+3)}$$

Each of the many solutions to (10-11) for a given  $M$  corresponds to a different value of  $J$ . This continued fraction is not very convenient to use, but it has been evaluated for a number of conditions with small  $J$  [209].

*Stark Effect for Two Nearby Levels.* An important and interesting special case of Stark effects occurs when two "interacting" levels lie rather close together—considerably closer than the energy separation between either one and any third level. This occurs typically for slightly asymmetric rotors, and also for  $l$ -type doubled levels of linear molecules in excited states. (It may be remembered that linear molecules excited to degenerate vibration levels are formally very much like slightly asymmetric rotors.) For two such close levels the energy due to the electric field cannot very well be considered a small perturbation; so an exact solution is necessary. Assume the unperturbed wave functions

for the two levels are  $\psi_1^0$  and  $\psi_2^0$ . The wave functions after application of the field  $E$  may be written

$$\psi_1 = a(E)\psi_1^0 + b(E)\psi_2^0 \quad \psi_2 = -b(E)\psi_1^0 + a(E)\psi_2^0 \quad (10-12)$$

and the matrix element due to the perturbing interaction  $-E\mu \cos \theta$  which connects the two states is

$$-E\mu_{12} = -E\mu \int \psi_1^0 \cos \theta \psi_2^0 \sin \theta d\theta d\phi \quad (10-13)$$

This quantity is  $-E$  times the dipole moment matrix element, which is proportional to the matrix element of the direction cosine.

This case is entirely parallel to the Fermi-resonance type of interaction between two neighboring states discussed in Chap. 2. The matrix element  $W_{12}$  of Chap. 2 corresponds to  $-E\mu_{12}$ , and the quantity  $\delta$  is the energy difference between the unperturbed states.

$$\delta = W_1^0 - W_2^0 \quad (10-14)$$

As in (2-22), the energy when a perturbing field is applied is given by

$$W = \frac{W_1^0 + W_2^0}{2} \pm \left[ \left( \frac{W_1^0 - W_2^0}{2} \right)^2 + E^2\mu_{12}^2 \right]^{\frac{1}{2}} \quad (10-15)$$

The values of  $a$  and  $b$  in (10-12) are, as in (2-24)

$$\begin{aligned} a &= \left[ \frac{\sqrt{\delta^2 + 4E^2\mu_{12}^2} + \delta}{2\sqrt{\delta^2 + 4E^2\mu_{12}^2}} \right]^{\frac{1}{2}} \\ b &= \left[ \frac{\sqrt{\delta^2 + 4E^2\mu_{12}^2} - \delta}{2\sqrt{\delta^2 + 4E^2\mu_{12}^2}} \right]^{\frac{1}{2}} \end{aligned} \quad (10-16)$$

Of first interest are the energies as given by (10-15). Let us assume  $W_1^0 > W_2^0$ . When the energy  $E\mu_{12}$  is less than  $(W_1^0 - W_2^0)/2$ , (10-15) may be expanded

$$W = W_1^0 + \frac{E^2\mu_{12}^2}{W_1^0 - W_2^0} + \dots \quad \text{or} \quad W = W_2^0 - \frac{E^2\mu_{12}^2}{W_1^0 - W_2^0} + \dots \quad (10-17)$$

This gives a Stark energy dependent on  $E^2$  as is typical of a second-order perturbation, but perhaps a very large second-order effect because  $W_1^0 - W_2^0$  may be rather small. When  $|E\mu_{12}|$  becomes larger than  $|W_1^0 - W_2^0|/2$ , (10-14) may be expanded

$$W = \frac{W_1^0 + W_2^0}{2} \pm E\mu_{12} + \dots \quad (10-18)$$

In this approximation the Stark effect appears linearly dependent on  $E$ , as in a first-order perturbation. This is just the approximation which holds for a symmetric top with doubly degenerate levels, since in this case  $W_1^0 - W_2^0 = 0$ . Thus (10-15) shows a smooth transition from a "second-order" to a "first-order" type of Stark effect.



Usually this intermediate type of Stark effect for a pair of almost degenerate levels occurs for a slightly asymmetric top. In this case pairs of the symmetric-top energy levels ( $K$ -degenerate levels) are split by an amount given by (4-9) due to the asymmetry. Even with fairly large asymmetries, certain pairs of levels may be nearly degenerate. For the slightly asymmetric rotor, the dipole matrix elements are fairly accurately given by those for symmetric tops (Table 4-4), so that for these slightly split levels,

$$\mu_{12} = \frac{\mu MK}{J(J+1)} \quad (10-19)$$

where  $K$  is the usual quantum number for the appropriate limiting symmetric top, and  $M$  is the projection of  $J$  in the direction of the field  $E$ . Linear molecules in excited bending vibrational states are very similar to slightly asymmetric molecules, and Stark effects on  $l$ -type doublets for these molecules are also described by (10-15) with matrix elements given by (10-19).

*Stark Effects in Asymmetric Rotors.* Stark effects in asymmetric rotors are usually "second-order," or proportional to  $E^2$ , since the energy levels are not degenerate, but not infrequently a pair of nearby levels give the type of Stark effect described above, and still other more special cases may occur. An extensive treatment has been given by Golden and Wilson [277]. For the usual case where near degeneracies do not occur, the Stark energy has the form (10-6), which involves the sum of a number of terms containing matrix elements between rotational states. The matrix elements take simple forms only when the rotor is approximately symmetric. However, the dipole matrix elements have been computed in connection with an evaluation of transition intensities, and certain sums  ${}^xS_{J\tau, J'\tau'}$  of these matrix elements have been tabulated [122].

For a dipole moment  $\mu_x$  lying along a principal axis of inertia of the molecule, it is seen from (4-22) that

$$\sum_M \sum_{M'} |\mu_{J\tau M, J'\tau' M'}|^2 = (2J+1) \frac{|\mu_{ij}|^2}{3} = \frac{\mu_x^2}{3} {}^xS_{J\tau, J'\tau'}(\kappa) \quad (10-20)$$

where  ${}^xS_{J\tau, J'\tau'}(\kappa)$ , or in other notation  ${}^xS_{J_k l J'_m n}(\kappa)$  is tabulated in Appendix V as a function of the asymmetry parameter  $\kappa$ . The sum over  $M$  and  $M'$  in (10-20) may be undone by using Table 4-4 to give

$$\begin{aligned} |\mu_{J, \tau, M; J-1, \tau', M}^{\circ}|^2 &= \mu_x^2 \frac{J^2 - M^2}{J(4J^2 - 1)} {}^xS_{J\tau, J-1\tau'} \\ |\mu_{J, \tau, M; J, \tau', M}|^2 &= \mu_x^2 \frac{M^2}{J(J+1)(2J+1)} {}^xS_{J\tau, J\tau'} \\ |\mu_{J, \tau, M; J+1, \tau', M}|^2 &= \mu_x^2 \frac{(J+1)^2 - M^2}{(J+1)(2J+1)(2J+3)} {}^xS_{J\tau, J+1\tau'} \end{aligned} \quad (10-21)$$

Here  $M'$  has been set equal to  $M$ , since otherwise the matrix element is zero, or since the angular momentum  $M$  in the direction of the field  $E$  cannot change.

As in the case of line intensities, each component of the dipole moment may be treated separately, so that the entire Stark energy in the case of no degeneracy may be written:

$$W_{J\tau M} = \sum_{x=a,b,c} \frac{\mu_x^2 E^2}{2J+1} \sum_{\tau'} \left[ \frac{J^2 - M^2}{J(2J-1)} \frac{{}^x S_{J\tau, J-1\tau'}}{W_{J\tau}^0 - W_{J-1\tau'}^0} + \frac{M^2}{J(J+1)} \frac{{}^x S_{J\tau, J\tau'}}{W_{J\tau}^0 - W_{J\tau'}^0} + \frac{(J+1)^2 - M^2}{(J+1)(2J+3)} \frac{{}^x S_{J\tau, J+1\tau'}}{W_{J\tau}^0 - W_{J+1\tau'}^0} \right] \quad (10-22)$$

where  $a$ ,  $b$ , and  $c$  indicate the directions of the three principal axes of inertia and  $W_{J\tau}^0$  represents the unperturbed energy of the rotational state designated by  $J\tau$ . The summation  $\Sigma'$  is over all states except  $J\tau$ . This energy has the general form

$$W_{J\tau M} = (A_{J\tau} + B_{J\tau} M^2) E^2 \quad (10-23)$$

Golden and Wilson [277] have tabulated quantities of the type  $A_{J\tau}$  and  $B_{J\tau}$  (differing, however, by certain factors) for all ranges of values of the rotational constants and for all levels with  $J = 0, 1$ , or  $2$ . Unless high accuracy is needed, the Stark effect may be calculated for levels with  $J$  as large as  $12$  by inserting values of  $S$  given in Appendix V into (10-22).

Golden and Wilson [277] also consider a number of special cases of degeneracy, where no matrix elements occur between the degenerate levels. These result in Stark effects proportional to  $E^2$  or some higher power of  $E$ .

**10-3. Relative Intensities of Stark Components and Identification of Transitions from Their Stark Patterns.** If  $M$  is the projection of  $J$  on the  $z$  axis or direction of a static electric field, then transitions produced by a microwave electric field in the  $z$  direction can occur only when

$$M' - M = \Delta M = 0$$

This may be understood classically from the fact that an electric field in the  $z$  direction can exert no torque about the  $z$  axis. If the microwave electric field is perpendicular to the static field, then  $\Delta M = \pm 1$ . From Table 4-4, dipole matrix elements may be obtained for each of these cases for symmetric tops. The dependence of these matrix elements on  $M$  is quite independent of the value of  $K$ . Since asymmetric-rotor wave functions are a combination of symmetric-rotor functions of the same  $J$  and  $M$ , but different  $K$ , the dependence of the matrix element on  $M$  is the same for asymmetric rotors as for symmetric ones. Hence the intensities of the various possible  $M$  transitions are proportional to the quantities in Table 10-1. This assumes that the Stark fields are small

enough to be treated as small perturbations. In special cases (*cf.* page 269) this assumption is not justified.

The experimental arrangement most often used for applying a “Stark” field will be discussed below. In this arrangement, and in others most likely to be used for microwave spectroscopy, the static and microwave electric fields have essentially the same direction. Hence  $\Delta M = 0$  tran-

TABLE 10-1. RELATIVE INTENSITIES OF STARK OR ZEEMAN COMPONENTS

$J'$  in each case is the larger of the two values of  $J$  involved in the transition and  $M'$  the larger (more positive)  $M$ .

	$\Delta J = +1$	$\Delta J = 0$	$\Delta J = -1$
Static and micro-wave fields parallel: $\Delta M = 0 \dots \dots$	$J'^2 - M'^2$	$M'^2$	$J'^2 - M'^2$
Static and micro-wave fields perpendicular: $\Delta M = +1 \dots \dots$ $\Delta M = -1 \dots \dots$	$(J' + M' - 1)(J' + M')$ $(J' - M')(J' - M' + 1)$	$(J + M')(J - M' + 1)$ $(J + M')(J - M' + 1)$	$(J' - M')(J' - M' + 1)$ $(J' + M')(J' + M' - 1)$

sitions are by far the strongest and are ordinarily the only ones observed. In this case, from (10-23) the change in frequencies of the Stark components is given by

$$\Delta \nu = \frac{1}{h} [A_{J',\tau'} - A_{J,\tau} + (B_{J',\tau'} - B_{J,\tau})M^2]E^2 \quad \text{or}$$
$$\Delta \nu = (A + BM^2)E^2 \quad (10-24)$$

For the particular case of a linear molecule, the coefficients involved in (10-24) may be evaluated from (10-8) giving

$$\nu = 2B(J + 1)$$
$$+ \frac{\mu^2 E^2}{(J + 1)Bh^2} \frac{3M^2(8J^2 + 16J + 5) - 4J(J + 1)^2(J + 2)}{J(J + 2)(2J - 1)(2J + 1)(2J + 3)(2J + 5)} \quad (10-25)$$

For the special case  $J = 0$ ,

$$\nu = 2B + \frac{4\mu^2 E^2}{15Bh^2}$$

If  $\Delta M = 0$ , the value of  $M$  must be no larger than the smallest  $J$  value involved in the transition. Hence a count of the number of components (different values of  $M^2$ ) gives quite directly the value of the lowest  $J$  involved in the transition. However, in case  $\Delta J = 0$ , the intensity decreases rapidly with  $M^2$ . The component  $M = 0$  is missing entirely, and other low values of  $M$  may be rather weak.



In case all Stark components are not visible, the relative spacings between components may be used to identify the largest value of  $M^2$  and hence the lowest value of  $J$  for the transition. The spacing between successive Stark components increases with  $M$  according to (10-24) so that it is usually easy to distinguish the components of higher  $M$  from those of lower  $M$ . Furthermore, accurate measurements of the relative spacing for a particular value of  $E$  will usually allow a definite assignment of  $M^2$  to each component.

Relative intensities of the Stark components usually allow an easy determination of the change in  $J$  involved. If  $\Delta J = 0$ , then from Table

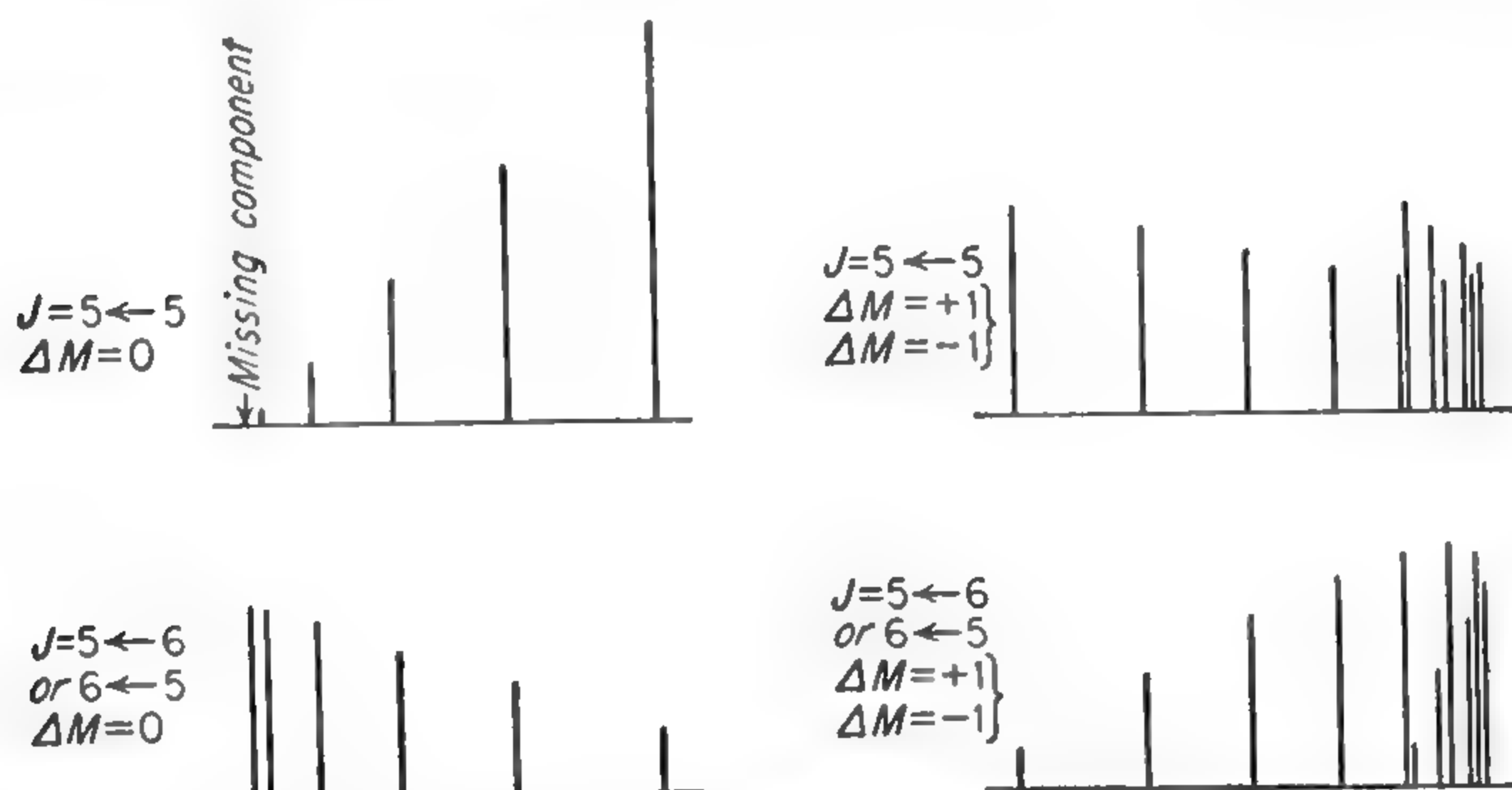


FIG. 10-1. Stark patterns for several types of transitions involving an energy level with  $J = 5$ . Relative spacings of components for  $\Delta M = 0$  depend only on  $J$  and  $M$ , while those for  $\Delta M = \pm 1$  depend to some extent on the particular energy levels involved.

10-1 the largest  $M$  values have the greatest intensity. If  $\Delta J = \pm 1$ , the intensity is proportional to  $J'^2 - M^2$  so that the smallest  $M$  values have the largest intensity. In this latter case, too, no component has zero intensity, since  $J'$  is at least greater by one than  $M$ .

Examination of Stark patterns, then, allows a rather direct determination of the lowest  $J$  value involved in the transition and of whether or not  $J$  changes. Plots of the relative spacings and intensities for several typical cases of Stark splitting are given in Fig. 10-1.

The absolute magnitude of the Stark effect, *i.e.*, the values of the constants  $A$  and  $B$  in (10-24), may also at times be very helpful in identifying transitions in asymmetric tops. If  $A$  or  $B$  is large, for example, one of the energy levels involved in the transition may be expected to have a close neighbor which makes the energy denominator  $W_{J,\tau}^0 - W_{J',\tau'}^0$  in (10-22) small. Often it is possible to evaluate  $W_{J,\tau}^0 - W_{J',\tau'}^0$  approximately from the size of  $A$  or  $B$ . In other cases the magnitudes of  $A$  and  $B$  or their ratio may be used to distinguish between two or more possible identifications of a transition.

**10-4. Stark Effect When Hyperfine Structure Is Present.** When hyperfine structure is present due to a nucleus of spin  $I$ , the total angular momentum of a molecule is given by the quantum number  $F = J + I, J + I - 1, \dots, |J - I|$  rather than by  $J$ . The projection of the angular momentum on some chosen direction is  $M_F = F, F - 1, \dots, -F$ . Thus the number of Stark components depends on  $F$  rather than  $J$ , and it may be expected that energies of the Stark components will be rather different from the case with no hyperfine structure discussed above. It is convenient to discuss Stark effects under three types of conditions: weak field, strong field, and intermediate field.

In the weak-field case, the electric field is so small that the Stark energy is considerably less than the interaction between the nucleus and the molecule, *i.e.*, the hyperfine energy. In this case the molecular wave functions and the hyperfine structure are only very slightly perturbed by the electric field. Expressed classically, the precession of the molecule due to the Stark field is so slow and gentle that the interaction between the nucleus and molecule is very little disturbed. The molecular state is satisfactorily specified by the quantum numbers  $I, J, F$ , and  $M_F$ .  $M_J$ , the projection of  $J$  on the electric field, is not a good quantum number, or not a constant of the molecular motion. Each hyperfine line is then split by the Stark effect into various components according to the values of  $M_F$ , and this splitting is small compared with the hyperfine splitting.

In the strong-field case, the Stark energy is much larger than the hyperfine energy. The molecule is precessed so violently by the electric field that the nuclear orientation cannot follow the motion.  $I$  and  $J$  are said to be decoupled, and the hyperfine structure is radically changed. The quantum number  $F$  is no longer good, since the vector sum of  $I$  and  $J$  is no longer fixed. Appropriate quantum numbers for describing the molecular state are  $I, J, M_I$ , and  $M_J$ , where  $M_I$  is the projection of  $I$  on the direction of the field. The Stark energies are the same as when no hyperfine structure is present, and the hyperfine structure gives a splitting of each Stark level which is much smaller than the separation between Stark levels. It is possible to have an electric field so large that the Stark energy is large compared with the separation between rotational levels, so that  $J$  is no longer a good quantum number. We shall discuss here only the cases in which the Stark energy is large compared with the hyperfine energy, but small compared with the rotational energy, since these are the common conditions.

Intermediate-field cases, or intermediate-coupling cases, occur when the Stark and hyperfine energies are comparable. In these cases neither  $M_J$  nor  $M_F$  and  $F$  are good quantum numbers. The wave functions are combinations of those appropriate for the weak- or the strong-field cases, and calculation of wave functions and energy levels is generally rather



complex. The Stark splitting is comparable with the hyperfine splitting, and relative intensities of the various components vary rapidly at times with the strength of the field. Wave functions, intensities, and energies can be evaluated for these cases but they involve solving secular equations which may be of high order if  $J$  and  $I$  are large. An example (although a rather specialized one) which has been worked out in some detail is the Stark effect in the ammonia inversion spectrum discussed by Jauch [212].

*Weak Electric Fields.* In the weak-field case the hyperfine structure is unperturbed, and the Stark splitting can be calculated by essentially the same methods used for the case of no hyperfine structure. Both first- and second-order (linear and quadratic) Stark effects occur. For a symmetric top the linear Stark effect may be calculated from the vector model. The Stark energy  $\Delta W$  is  $-\mu \cos \theta E$ , where  $\mu \cos \theta$  is the projection of the dipole moment on the field  $\mathbf{E}$ . Now  $\mu$  lies along the axis of the molecule or the angular momentum  $K$ , which precesses around the total rotational angular momentum  $J$ ,  $J$  precesses around  $\mathbf{F}$ , and  $\mathbf{F}$  precesses around the direction of the field  $\mathbf{E}$ . Averaged over time,

$$\cos \theta = \cos (\mathbf{KJ}) \cos (\mathbf{JF}) \cos (\mathbf{FE}) \quad (10-26)$$

where  $(\mathbf{KJ})$  represents the angle between the two vectors  $\mathbf{K}$  and  $\mathbf{J}$ . But  $\cos (\mathbf{KJ}) = K/J$ ;  $\cos (\mathbf{JF}) = (J^2 + F^2 - I^2)/2JF$ ;

$$\cos (\mathbf{FE}) = \frac{M_F}{F}$$

Hence

$$\Delta W = - \frac{\mu K M_F (J^2 + F^2 - I^2) E}{2J^2 F^2}$$

Remembering that the square of any vector  $J$  must be replaced by  $J(J+1)$  when vector model calculations are made,

$$\Delta W = - \frac{\mu K [J(J+1) + F(F+1) - I(I+1)] M_F E}{2J(J+1) F(F+1)} \quad (10-27)$$

It should be noted that (10-27) is proportional to  $K$ , so that no linear Stark effect occurs when  $K = 0$ . In addition, when  $F = 1 + J = M_F$ , (10-27) becomes  $\Delta W = -\mu E K / (J+1)$ , which is identical with what would be obtained if  $J = M_J$  and no hyperfine structure were present. For all other cases, however, the Stark effect is modified by the presence of hyperfine structure. A more detailed derivation of (10-27) is given by Low and Townes [391].

Second-order Stark effect may be calculated in general by expanding the wave function with hyperfine structure in terms of the rotational



wave functions which would occur if no hyperfine structure were present.

$$\psi(FMJ\tau I) = \sum_{M_J} C(FMJIM_J) U(J\tau M_J) \phi(IM_I) \quad (10-28)$$

where  $U(J\tau M_J)$  represents an asymmetric-top wave function with the indicated quantum numbers and  $\phi(IM_I)$  is a wave function for the nuclear spin whose exact nature need not concern us. Only those functions occur for which  $M_I + M_J = M$ . The coefficients  $C(FMJIM_J)$  are independent of the quantum number  $\tau$ , and are evaluated in Condon and Shortley ([56], pp. 76–77). For the general asymmetric top without degeneracy and without hyperfine structure, second-order Stark effects were shown in (10-23) to be of the form

$$\Delta W_{J\tau} = (A_{J\tau} + B_{J\tau} M_J^2) E^2 \quad (10-23)$$

Using the expansion (10-28), second-order Stark effects when hyperfine structure is present can be shown to be

$$\Delta W_{FJ\tau} = \sum_{M_J} |C(FMJIM_J)|^2 (A_{J\tau} + B_{J\tau} M_J^2) E^2 \quad (10-29)$$

which gives the net Stark effect as the sum of Stark effects for each value of  $M_J$  multiplied by the probability  $C^2$  of the molecule's being in the state  $M_J$ . This expression (10-29) is valid only if the hyperfine energy is small compared with the separation between rotational energy levels, which is the usual case. The sum of all probabilities  $\sum_{M_J} C(FMJIM_J)^2$  is unity, and from expressions given by Fano [269] the other sum

$$\sum_{M_J} |C(FMJIM_J)|^2 M_J^2$$

which is necessary can be obtained. Then (10-29) becomes

$$\begin{aligned} \Delta W_{F,J\tau} = & A_{J\tau} E^2 \\ & + B_{J\tau} \left\{ [3M^2 - F(F+1)] \frac{[3D(D-1) - 4F(F+1)J(J+1)]}{6F(F+1)(2F-1)(2F+3)} \right. \\ & \left. + \frac{J(J+1)}{3} \right\} E^2 \quad (10-30) \end{aligned}$$

where  $D = F(F+1) + J(J+1) - I(I+1)$ . Thus the weak-field Stark effect for an asymmetric rotor with hyperfine structure can be expressed in terms of the Stark-effect coefficients  $A$  and  $B$  for the case with no hyperfine structure. Expression (10-30) can be applied to a linear molecule (or symmetric top with  $K = 0$ ), for which it reduces to

an expression given by Fano [269]

$$\Delta W_J = - \frac{\mu^2 E^2}{Bh} \frac{[3M^2 - F(F+1)][3D(D-1) - 4F(F+1)J(J+1)]}{2J(J+1)(2J-1)(2J+3)2F(F+1)(2F-1)(2F+3)} \quad (10-31)$$

By using Eq. (10-22) to evaluate  $A_{Jr}$  and  $B_{Jr}$  in Eq. (10-30), the weak-field Stark effect when hyperfine structure is present may be expressed in terms of quantum numbers, rotational energies, and the line strengths tabulated in Appendix V (*cf.* [845]).

*Strong Electric Fields.* In the strong-field case the Stark energy is much larger than the hyperfine energy. The Stark splitting is identical with that obtained when no hyperfine structure is present as long as  $|M_J| \neq 1$ , and the hyperfine structure acts as a small perturbation. Hyperfine structure due to the nuclear magnetic dipole moment, for which the energy is of the form  $W = a\mathbf{I} \cdot \mathbf{J}$ , is given in this case by  $W(\mu) = aM_I M_J$ , where  $M_I$  takes on values  $I, I-1, \dots, -I$  for each possible value of  $M_J$ . Usually this magnetic hyperfine structure is very small, so that the strong-field case almost always applies. Hyperfine energy due to a nuclear quadrupole moment is given in the strong-field case (and where  $|M_J| \neq 1$ ) by

$$W(Q) = \frac{eqQ}{4I(2I-1)(2J-1)(2J+3)} \left[ \frac{3K^2}{J(J+1)} - 1 \right] \frac{[3M_I^2 - I(I+1)][3M_J^2 - J(J+1)]}{[3M_I^2 - I(I+1)][3M_J^2 - J(J+1)]} \quad (10-32)$$

In the strong-field case when  $|M_J| = 1$  and  $K = 0$ ,  $M_J$  is not necessarily a good quantum number because, regardless of how small the quadrupole coupling constant  $eqQ$  is, quadrupole effects may produce transitions between the degenerate levels  $M_J = 1$  and  $M_J = -1$ . Quadrupole effects do not produce transitions between other pairs of degenerate levels, but only those for which  $\Delta M_J = \pm 2$ . The total angular momentum along the direction of the field must be constant, so that  $M = M_J + M_I$  is a good quantum number, although  $M_J$  and  $M_I$  are not. When  $M = I + 1$  or  $M = I$ ,  $M_J$  can have values  $\pm 1$  only, so that then the state  $M_J = -1$  does not occur, and energies are given simply by (10-32). In other cases, a quadratic secular equation must be solved [269].

*Intermediate Electric Fields.* The "intermediate-field" case occurs when Stark and hyperfine energies are comparable in magnitude. Usually the energy levels must be determined for these cases from the solutions of second- or higher-order equations. If  $J$  or  $I$  is small, this is not too difficult since the most complex equation which needs solution is of order  $2J + 1$  or  $2I + 1$ , whichever is smaller. These equations are discussed by Fano [269] and Low and Townes [391]. The behavior of

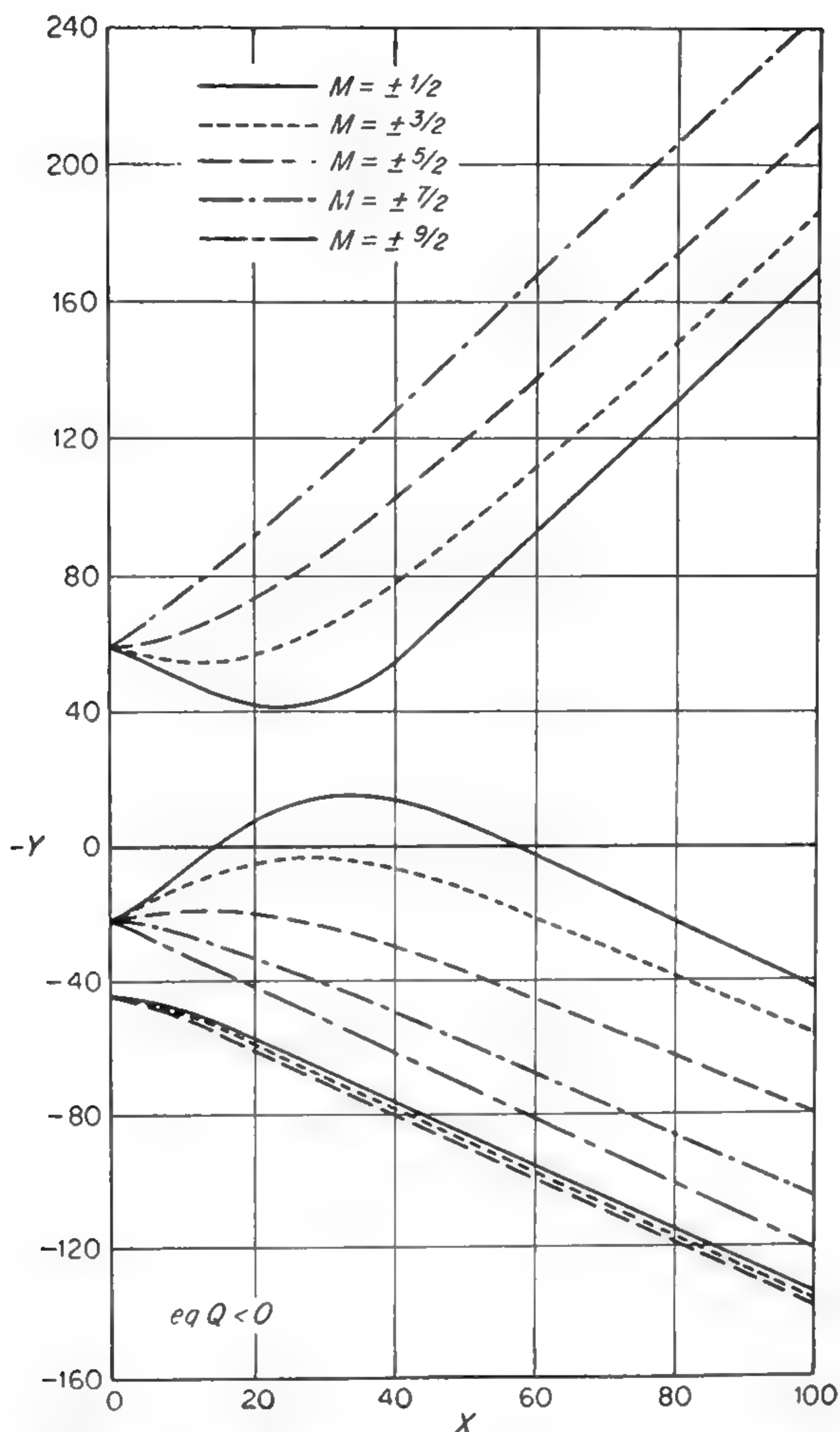


FIG. 10-2. Plot of energy due to Stark effect in a linear molecule for  $J = 1$  when a nucleus of spin  $I = \frac{7}{2}$  produces quadrupole hyperfine structure.

$$X = -\frac{21h^2}{2BeqQ} \mu^2 E^2$$

$$Y = \frac{420W}{eqQ}$$

where  $W$  is the sum of Stark and hyperfine energy. (After Fano [269].)

hyperfine energy levels with all values of electric-field strength and for the particular case of a symmetric molecule with  $K = 0$ ,  $J = 1$ , and  $I = \frac{7}{2}$  is shown in Fig. 10-2. It may be seen from this figure that a particular component may vary with field in completely different ways for high- and low-field conditions. The component with  $M = J + I$



always behaves simply because its secular equation is of first order, and Stark and hyperfine energies simply add without affecting each other. The plot of this level ( $M = \frac{9}{2}$ ) is hence a straight line on Fig. 10-2. Figure 10-3 shows a comparison between actual measured hyperfine structure and theoretically calculated curves for an intermediate-field case.

*Stark Effects in the Presence of Hyperfine Structure Due to Two Nuclei.* In case two nuclei produce hyperfine structure, the Stark effect shows

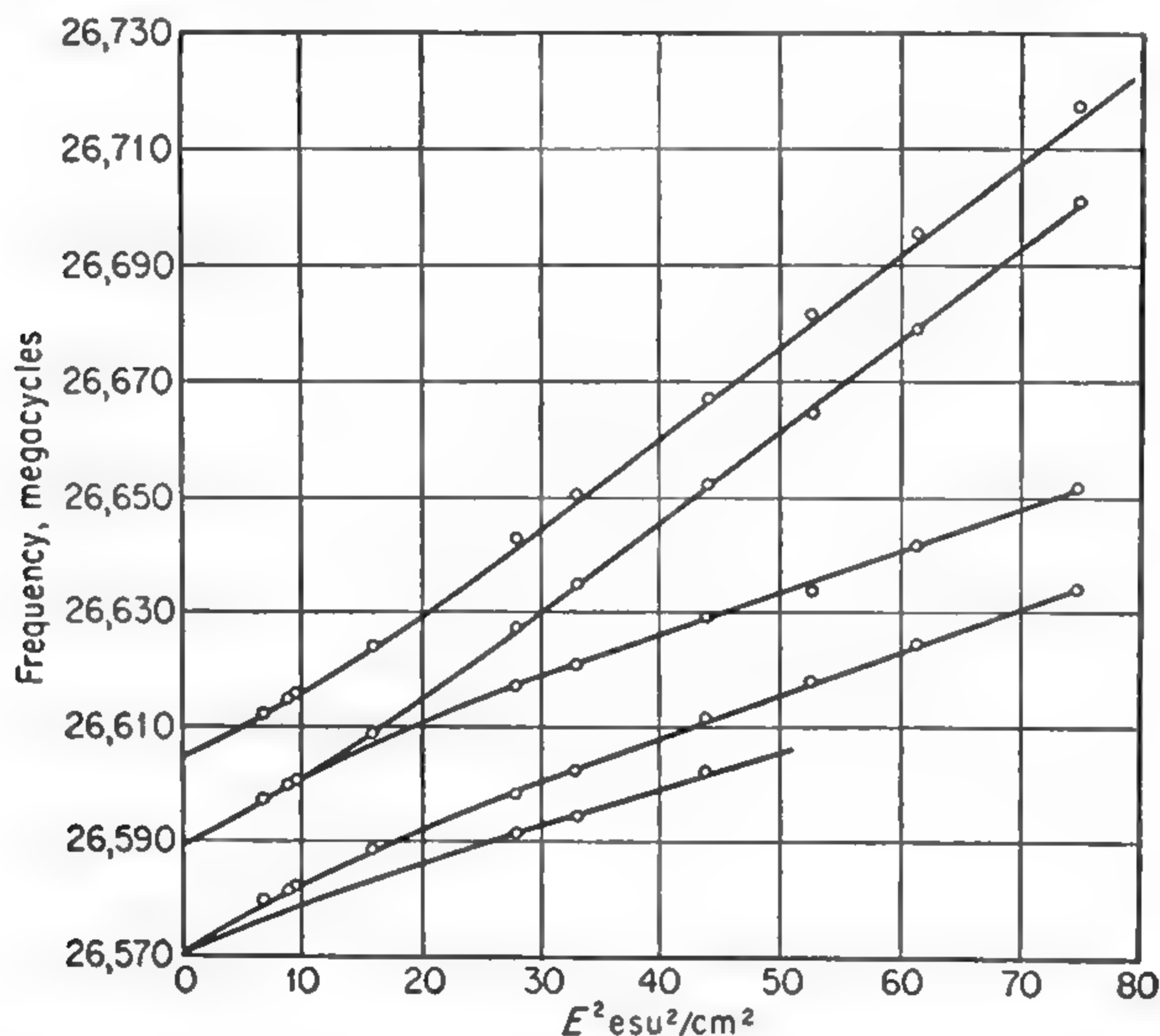


FIG. 10-3. Frequency of all components of  $\text{CH}_3\text{Cl}^{35}$   $J = 1 \leftarrow 0$  transition as a function of electric field strength. Curves are computed using  $\mu = 1.869$  debye. (From Shulman, Dailey, and Townes [528].)

still more complications. The strong-field case is rather simple, for the hyperfine energy is just the sum of that which would be due to each nucleus individually. For example, if two nuclei have quadrupole moments  $Q_1$  and  $Q_2$ , respectively, the hyperfine energy in the strong-field case is just  $W(Q_1) + W(Q_2)$ , where  $W(Q)$  is given by (10-32). In weak or intermediate fields the situation is more complex. The case of two nuclei, one of which has quadrupole and magnetic dipole hyperfine structure, and the other magnetic dipole structure only, has been discussed [307].

*Relative Intensities of Stark Components of Hyperfine Lines.* Relative intensities of Stark components when hyperfine structure is present is analogous under weak- or strong-field conditions to what is obtained without hyperfine effects. For a very small field, the relative intensities of the Stark components of one hyperfine transition are given by

when  $\Delta F = 0$  and  $\Delta M_F = 0$ :

$$I \propto M_F^2 \quad (10-33)$$

when  $\Delta F = \pm 1$  and  $\Delta M_F = 0$ :

$$I \propto F'^2 - M_F^2 \quad (10-34)$$

where  $F'$  represents the larger of the two  $F$  values involved in the transition. In the strong-field case, the relative intensities of each Stark component are the same as without hyperfine structure, or

when  $\Delta J = 0$  and  $\Delta M_J = 0$ :

$$I \propto M_J^2 \quad (10-35)$$

when  $\Delta J = \pm 1$  and  $\Delta M_J = 0$ :

$$I \propto J'^2 - M_J^2 \quad (10-36)$$

Each of these Stark components is broken up into hyperfine components corresponding to different  $M_I$  and which, for a given Stark component, all have the same intensity. For quadrupole hyperfine structure the components for  $\pm M_I$  have the same energy, so that the observed hyperfine lines are all of the same intensity except that for  $M_I = 0$ , which is half the intensity of the other lines. Intensities of components under intermediate-field conditions may be estimated by interpolation between the two extreme cases of weak and strong fields. They may be calculated exactly by solving equations of the type encountered in obtaining exact energies for intermediate-field cases [391].

**10-5. Determination of Molecular Dipole Moments.** In addition to aiding in identification of transitions, and providing a good means of modulating microwave lines for detection, the Stark effect affords a very accurate and convenient means of measuring molecular dipole moments since its size depends on the product of the dipole moment and the electric field strength. For such a measurement, a fairly uniform known electric field is needed.

By far the most convenient method of obtaining Stark effects is to insert a conducting plate in the waveguide as shown in Fig. 10-4. This conducting plate cuts the microwave electric field perpendicularly and hence does not distort the microwave field appreciably or interfere with its propagation. The plate or septum may be mounted on narrow grooved insulating strips of polystyrene, teflon, or any other dielectric which is not too lossy at microwave frequencies. An electrical lead is usually brought out through a small hole in the center of the narrow face of the waveguide so that d-c or low-frequency voltages may be applied between the septum and the outside shell of the waveguide.

The electric field in a "Stark waveguide" may be seen in Fig. 10-5

to deviate considerably from uniformity near the edges of the septum. In addition, it is parallel to the direction of the microwave electric field only in the center of the waveguide. The presence of dielectric material of finite width modifies this field only slightly. Equipotential surfaces for a particular waveguide with dielectric material have been given by Sharbaugh [519]. Happily, it is the central part of the waveguide

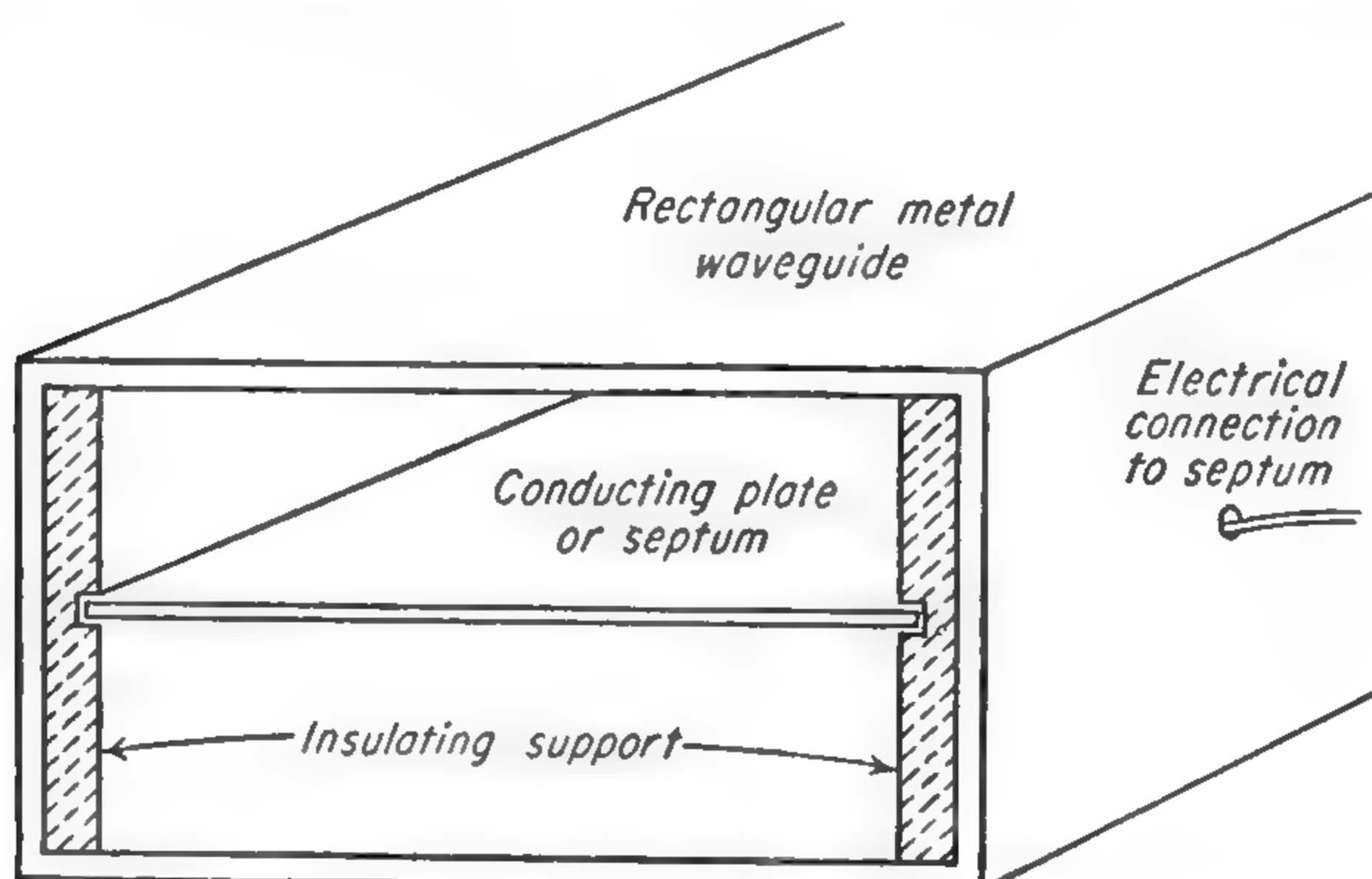


FIG. 10-4. Construction of waveguide for producing Stark effects. Central metal plate is parallel to broad face of waveguide and is insulated from it. Electrical connection to this plate is made by a lead through a small hole in the center of the narrow face of the waveguide.

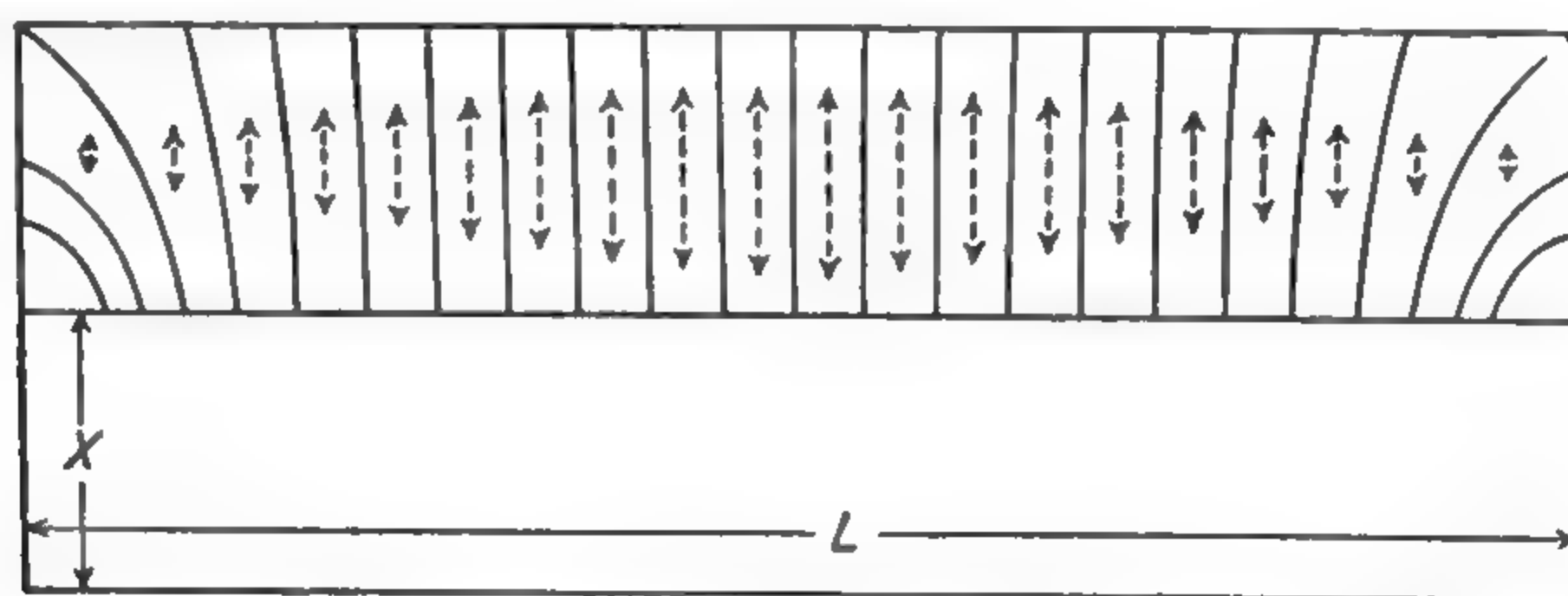


FIG. 10-5. Distribution of electric fields in "Stark waveguide." Dielectric supports of central septum are assumed to be of negligible thickness. D-c or low-frequency field direction is shown with solid lines, the density of lines being proportional to the intensity. The microwave electric field is everywhere in the same direction as indicated by the dotted lines whose length is proportional to the field intensity. Identical fields which are not shown exist in the lower half of the waveguide. (From Shulman, Dailey, and Townes [528].)

which is most important. The strength of the microwave electric field  $E$  is proportional to  $\sin \pi y/L$ , where  $L$  is the width of the guide and  $y$  the distance from one edge. The probability of a transition is proportional to  $E^2$  or  $\sin^2 \pi y/L$ , which has a maximum in the center of the guide and is zero on the edges. Hence if gas pressure in the waveguide is large enough to prevent molecules from moving around appreciably during a transition (mean free path much less than  $L$ ), most of the transi-



tions occur near the center of the guide. Since also in the center of the waveguide the Stark and microwave electric fields are closely parallel, transitions of type  $\Delta M = 0$  dominate. In fact, for the normal mode of microwave propagation ( $TE_{01}$ ), transitions of the type  $\Delta M = \pm 1$  are too weak to have been observed yet, although they must take place to some extent near the edges of the septum.

If the ratio of the guide width  $L$  to the spacing  $X$  between the septum and broad side of the waveguide is fairly large, then it can be assured that only transitions of the type  $\Delta M = 0$  occur and that molecular dipole moments can be calculated simply by assuming a uniform field equal to its value in the center of the waveguide. Shulman and Townes [530] have given approximate analytic expressions for the components of the Stark field and have calculated the effects of inhomogeneity in several waveguides. For a guide with the ratio  $L/X = 6$ , the measured dipole moment needs to be decreased by about 0.2 per cent because of field inhomogeneities, and for  $L/X = 5$ , the correction is approximately twice as large. Intensities of transitions  $\Delta M = \pm 1$  for such waveguides are only a few tenths of 1 per cent as strong as  $\Delta M = 0$  transitions. Although only small errors in the positions of the center of each Stark component are produced by the field inhomogeneities, the components are appreciably broadened. For a guide with  $L/X = 6$ , the breadth of a Stark component due to field inhomogeneities is roughly  $\frac{1}{25}$  of the Stark displacement. Hence as the change of frequency due to Stark effect is increased, each component broadens out and becomes weaker. Because of this, individual Stark components cannot usually be followed more than a few hundred megacycles.

If the electric field  $E$  is known and the transition positively identified, then the molecular dipole moment  $\mu$  may be determined by measuring the magnitude of the changes in frequency due to Stark effect. An appropriate one of the various formulas developed above for Stark energies is of course needed to connect the measured magnitude with the quantity  $\mu E$ . For symmetric molecules without hyperfine structure the case is particularly simple. When  $K \neq 0$ , (10-5a) may be used and the Stark effect is linearly proportional to  $E$  as long as the Stark displacement is not very large, so that second-order terms in  $E^2$  are unimportant. It is usually advantageous to choose the most widely split Stark component, since it is more isolated and easily measured. However, other components may often be used. The Stark displacement may be measured for several different field strengths. If this is plotted against  $E$ , a straight line should be obtained whose slope gives the coefficient of  $E$  in (10-5a), or  $2\mu KM/J(J+1)(J+2)h$ .  $E$  is measured of course in electrostatic units, or volts per centimeter divided by 299.8. If  $K = 0$ , then the Stark displacement is proportional to  $E^2$ . It is again usually convenient to measure the component with largest Stark displacement and

to plot this displacement against  $E^2$ . A straight line as shown in Fig. 10-6 should be obtained, whose slope is the coefficient of  $E^2$  in (10-25), and hence gives the value of  $\mu$ . In case hyperfine structure is present, similar measurements can be made, but interpretation of the Stark displacements from expressions (10-30), (10-32), or by calculation of intermediate-field energies is usually more complex. In addition, there are

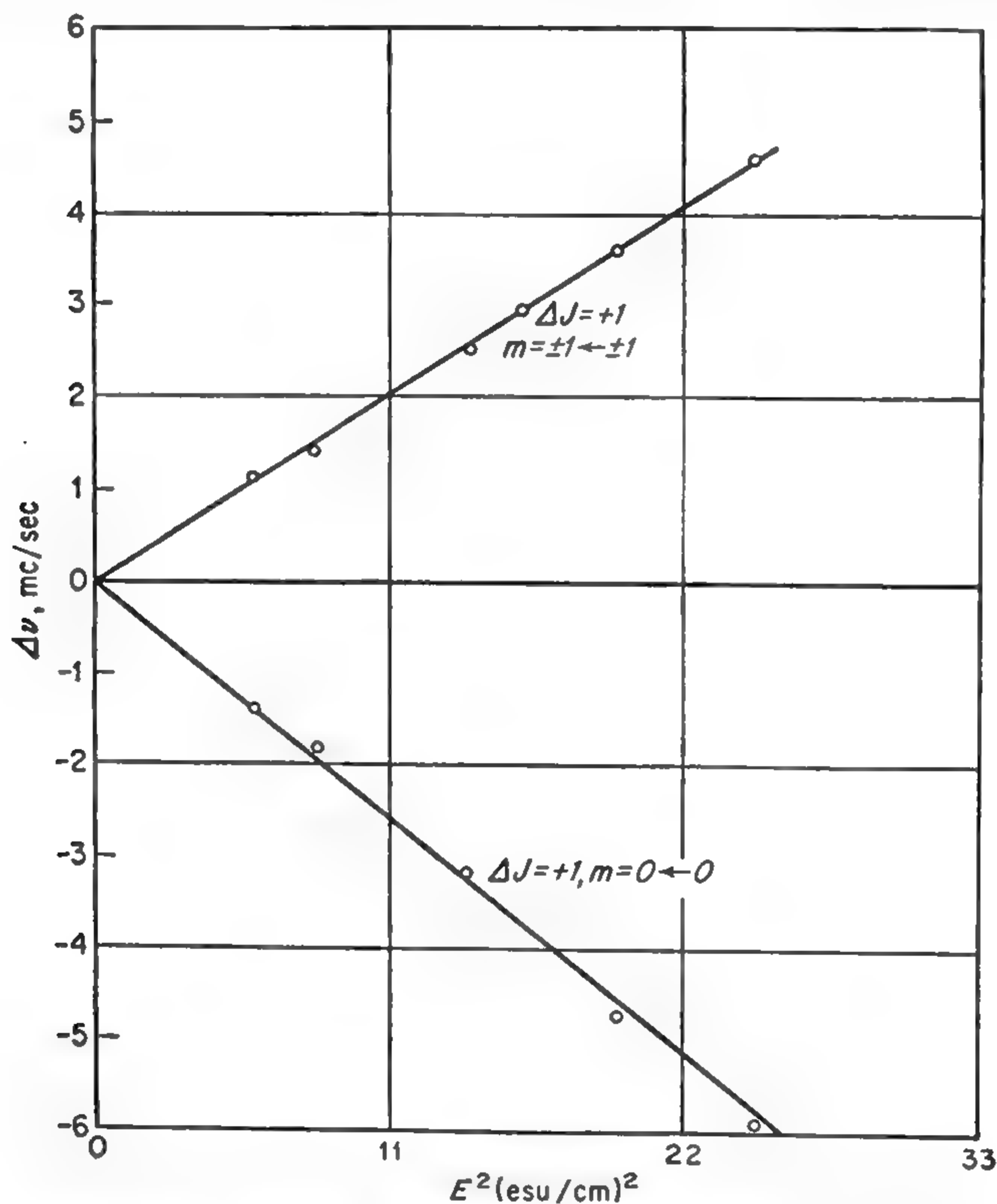


FIG. 10-6. Comparison between theory and experimental measurement of Stark effects in the  $J = 2 \leftarrow 1$  transition of the linear molecule OCS. (From Strandberg, Wentink, and Kyhl [419].)

often many Stark components whose relative intensities and spacings vary with field strength in the intermediate-field region, so that care must be taken to select and identify one particular component.

The dipole moment of the ground vibrational state of OCS has been measured rather accurately in a number of places and can conveniently be used to calibrate any Stark apparatus for measuring dipole moments. Thus if the electrode spacing  $X$  is unknown so that field strength  $E$  cannot be accurately determined from the potential applied to the Stark



waveguide, a measurement of the Stark effect in OCS and use of its known dipole moment will determine the proportionality constant between voltage or potential and the field strength. A weighted average of available values for the  $\text{O}^{16}\text{C}^{12}\text{S}^{32}$  dipole moment in the ground state is  $0.709 \pm 0.003 \times 10^{-18}$  esu, or 0.709 debye units.

Stark effects in asymmetric rotors may also be used to measure their dipole moments. In case the molecule has sufficient symmetry to establish the direction of the dipole moment as along one of the principal axes, calculation of the coefficient of  $\mu^2 E^2$  may be made from (10-22) and  $\mu$  fairly readily measured. If the direction of the dipole moment is not known, then Stark effects of several lines must be measured, and the several measured coefficients of  $E^2$  used to evaluate the various components of  $\mu$  along principal axes. This case is not common, but when it occurs, the direction of the dipole moment in the molecule may be established from the Stark measurements. Other techniques usually measure only the magnitude of the molecular dipole moment.

In addition to giving the direction of the dipole moment, determination of dipole moments by Stark effects has several other advantages. It can measure dipole moments as small as 0.1 debye with essentially the same accuracy as larger ones, or to about 0.2 per cent in waveguides of the type shown by Fig. 10-4. If a microwave spectrograph were designed with a very homogeneous field, dipole moments could undoubtedly be measured to an accuracy of 0.01 per cent or better. Another advantage of this type of dipole-moment determination over the classical technique of measuring dielectric constants is that dipole moments may be determined in rather impure gases, since a line of the particular molecule of interest may be singled out for measurement.

The dipole moment of molecules in a particular vibrational state may also be measured, rather than an average moment for all states as is done by other techniques. It has been found that the dipole moment of OCS in the first excited bending mode of vibration is 0.700 debye, or about 1.2 per cent less than the value 0.709 obtained for the ground state. This change in dipole moment depends not only on the bending or change in relative direction of the O—C and C—S bonds, but also on changes in the electronic wave functions involved in each bond due to the vibration. Since each different isotopic species of a molecule has a slightly different vibrational energy, it might be expected that the different isotopic molecules would have different dipole moments. However, a change in isotopic mass usually represents a smaller change in vibrational energy than a vibrational excitation. Hence this type of variation in dipole moment may be expected to be quite small, and not larger than a few tenths of 1 per cent except perhaps in the case of a hydrogen-deuterium substitution. In the case of  $\text{OCS}^{32}$  and  $\text{OCS}^{34}$ , for example, the difference in dipole moments seems to be less than 0.2 per cent.



**10-6. Forbidden Lines and Change of Intensity Due to Stark Effect.**

An electric field not only changes the rotational energies of a molecule but also modifies the molecular wave functions and thereby affects the dipole matrix elements and intensities of transitions. Let  $\psi_1$  be the wave function for one molecular energy level and  $\psi_2$  that for another when the electric field is zero. If  $\psi_1(E)$  and  $\psi_2(E)$  are the modified wave functions after an electric field is applied and if  $E$  is not too large they may be expanded in the form

$$\psi_1(E) = \psi_1 + \sum_n' C_{1n}\psi_n \quad (10-37)$$

where

$$C_{1n} = \frac{\mu_{1n}E}{W_1 - W_n}$$

$\mu_{1n}$  is the dipole matrix element between the unperturbed state designated by 1 and that designated by  $n$ .  $W_1$  and  $W_n$  are the energies of the two states. The summation  $\sum_n'$  is to be taken over all levels except level 1. If levels are degenerate so that  $W_1 = W_n$ , as in the case of the  $K$  degeneracy of a symmetric-top molecule, wave functions may be chosen to make  $\mu_{1n} = 0$  so that the expression (10-37) has no divergent terms.  $\psi_2(E)$  is similarly

$$\psi_2(E) = \psi_2 + \sum_n' C_{2n}\psi_n \quad (10-38)$$

The transition probability between states 1 and 2 depends on the dipole matrix element between them,

$$\mu_{12}(E) = \int \psi_1^*(E) \mu_z \psi_2(E) d\tau \quad (10-39)$$

as in (1-59). Using (10-37) and (10-38),

$$\mu_{12}(E) = \mu_{12} + \sum_n' E \left( \frac{\mu_{1n}\mu_{n2}}{W_1 - W_n} + \frac{\mu_{2n}\mu_{n1}}{W_2 - W_n} \right) \quad (10-40)$$

where  $\mu_{12}$  is the matrix element for zero field. Expression (10-40) is accurate only when the wave functions are not greatly changed by the electric field, *i.e.*, when  $\mu E / (W_1 - W_n) \ll 1$ .  $E$  must be taken as positive, and the relative phases of the matrix elements are such that

$$|\mu_{12}(E)| = |\mu_{12}| + \sum_n' |\mu_{1n}||\mu_{2n}|E \left( \frac{1}{W_1 - W_n} + \frac{1}{W_2 - W_n} \right) \quad (10-41)$$

Expression (10-41) allows an evaluation of the change in intensity of a transition, since from (1-49) intensity is proportional to  $|\mu|^2$ . It should be noticed that the fractional changes in intensity for the different Stark components of a transition are not usually the same, since the matrix elements  $\mu_{1n}$ , etc., depend on the magnetic quantum number  $M$ .

If  $|\mu_{12}|$  is not very small, (10-41) gives only a small fractional change in the dipole matrix element or in the intensity. Since intensities are generally not measured with an accuracy better than 5 per cent, a change in intensity of this type would usually be insignificant. Of course, Stark effects on energy levels are usually more obvious, since the transition frequencies are observed and measured to very high accuracy. When  $|\mu_{12}|$  happens to be zero, a transition is said to be "forbidden" (at least for zero field).

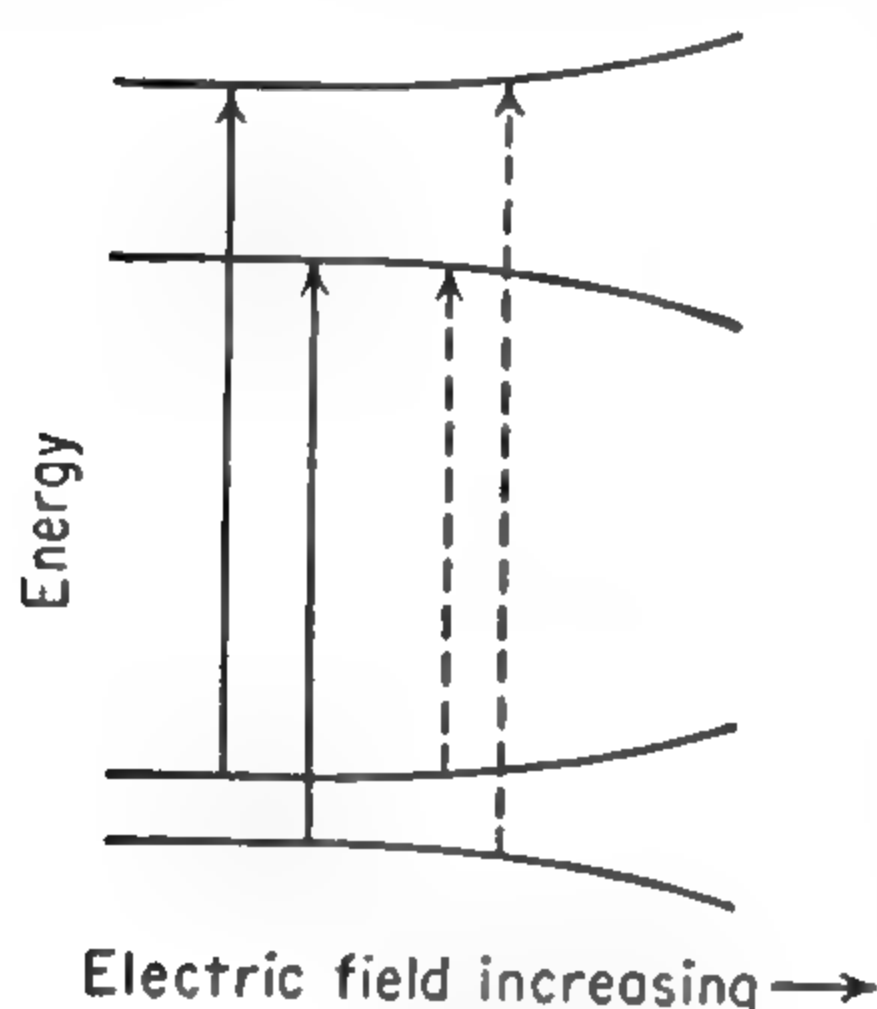


FIG. 10-7. Forbidden transitions between pairs of slightly split levels of a slightly asymmetric rotor. Solid lines represent permitted transitions; dotted lines forbidden transitions which occur when an electric field is applied.

In this case the electric field may perturb the wave function enough that (10-41) gives an appreciable value to  $|\mu_{12}(E)|$ , and the transition can be observed when the electric field is present. Since the transition probability is zero when no field is present, such a change in intensity and the appearance of new lines, even though they are relatively weak, can be easily noticed. The intensities of these forbidden lines are, from (10-41), proportional to  $E^2$ .

When two energy levels lie rather close together, large perturbations may occur so that the expansion (10-37) and consequently (10-41) are no longer valid. This is the type of case discussed above (page 252). A particularly common example is the slightly split levels of a slightly asymmetric rotor, or the  $l$ -doubled levels of a linear molecule in an excited degenerate vibrational mode. This case is illustrated in

Fig. 10-7. The perturbed wave functions are a mixture of the two unperturbed wave functions as in (10-12)

$$\begin{aligned}\psi &= a(E)\psi_1^0 + b(E)\psi_2^0 \\ \psi' &= -b'(E)\psi_1'^0 + a'(E)\psi_2'^0\end{aligned}\tag{10-42}$$

where the unprimed quantities refer to the lowest level of Fig. 10-7, and the primed quantities to the uppermost. The coefficients  $a$ ,  $b$ , or  $a'$  and  $b'$  are given by (10-16). The dipole matrix element  $\int \psi \mu_z \psi' d\tau$  is proportional to  $a'b - ab'$ , which is zero for zero electric field, has a maximum near fields for which  $\mu E \phi \approx W_{10} - W_{20}$ , and then approaches zero again for large electric fields. The intensity of these forbidden transitions depends markedly on the magnetic quantum number  $M$ . When  $M = 0$ , for example, the matrix element  $\phi$  between states 1 and 2 in slightly asymmetric rotors is zero, and forbidden transitions of the type  $\Delta M = 0$  do not occur.

**10-7. Polarization of Molecules by Electric Fields.** So far interactions between an electric field and a molecular dipole moment of fixed value

have been considered. In addition, the electric field can distort the distribution of electrons in the molecule or the relative positions of atoms, thus polarizing the molecule and changing its energy. These Stark effects are very much smaller than the type treated above but may not always be negligible. Stark energy due to these types of molecular polarization may be treated by second-order perturbation theory in much the same way as the larger effects discussed above. The result is [277]

$$\Delta W_p \equiv \frac{E^2}{2(2J+1)} \sum_{x=a,b,c} P_{xx} \sum_{r'} \left[ \frac{J^2 - M^2}{J(2J-1)} {}^xS_{Jr,J-1r'} + \frac{M^2}{J(J+1)} {}^xS_{Jr,Jr'} + \frac{(J+1)^2 - M^2}{(J+1)(2J+3)} {}^xS_{Jr,J+1r'} \right] \quad (10-43)$$

This equation is analogous to (10-22), and the symbols have the same meaning.  $P_{xx}$  is the component of the polarizability tensor along one of the principal axes of inertia  $x = a, b$ , or  $c$  of the molecule, or simply the polarizability along one of these directions. Again, analogously to (10-22) the polarizability  $P_{xx}$  is the sum

$$P_{xx} = 2 \sum_n \frac{\mu_{0n}^2}{W_0 - W_n} \quad (10-44)$$

where  $\mu_{0n}^2$  is the dipole matrix element between the ground state of the molecule and any excited electronic or vibrational state, and  $W_0 - W_n$  is their energy difference. The matrix-elements  $\mu_{0n}$  are not much larger than 1 debye or  $10^{-18}$  esu, and usually  $W_0 - W_n$  is a few hundred wave numbers for vibrational states, or a few thousand wave numbers for excited electronic states. Hence the energy  $\Delta W_p$  is in most cases less than 1/10,000 as large as second-order Stark effects of the type given by (10-22) because rotational energy levels tend to be about 1000 times closer than vibrational energy levels and thus give energy denominators which are smaller by this factor. In addition, the vibrational matrix elements  $\mu_{0n}$  are usually smaller than those for rotational transitions.

*Rotational Transitions in Nonpolar Molecules.* It may be possible, although very difficult, to induce rotational transitions in a nonpolar molecule by microwaves. If the molecule is nonpolar, it has zero electric dipole moment when unperturbed; but because of its polarization, a dipole moment may be induced by a large electric field and this induced dipole moment then used to produce rotational transitions [32].

As a simple typical case, consider a linear molecule such as  $\text{CO}_2$  which has zero dipole moment as a result of its symmetry. Its polarizability may be assumed to be  $P$  along the axis and zero perpendicular to the axis. The change in energy due to an electric field  $E$  is then

$$\Delta W = -\frac{1}{2}E^2P \cos^2 \theta \quad (10-45)$$



where  $\theta$  is the angle between the molecular axis and the direction of  $E$ . Expression (10-45) may be taken as a perturbation in the Hamiltonian for the molecule which can cause transitions between two states having wave functions  $\psi_1 e^{-iW_1 t/\hbar}$  and  $\psi_2 e^{-iW_2 t/\hbar}$  in accordance with the size of the integral

$$\frac{P}{2} \int E^2 \cos^2 \theta \psi_1^* e^{iW_1 t/\hbar} \psi_2 e^{-iW_2 t/\hbar} d\tau dt \quad (10-46)$$

Assume now that the field  $E$  is made of two parts, a static field  $E_s$  and a microwave field  $E_m e^{i\omega t}$  which will be assumed for simplicity to be parallel. Then

$$E^2 = E_s^2 + 2E_s E_m e^{i\omega t} + E_m^2 e^{2i\omega t} \quad (10-47)$$

If  $W_1$  and  $W_2$  are different, then the integration over time in (10-46) eliminates the constant term  $E_s^2$  in (10-47). The second term of (10-47) gives a nonzero contribution to (10-46) if  $\omega = (W_1 - W_2)/\hbar$  and if the matrix element

$$\mu_{12} = P E_s \int \psi_1^* \psi_2 \cos^2 \theta d\tau \quad (10-48)$$

is not zero. Now  $\psi_1$  and  $\psi_2$  are known from Chap. 1 to involve Legendre polynomials of the form  $P_J^M(\cos \theta)$ . It can be shown from them that  $\mu_{12}$  is zero unless the two states have values of  $J$  differing by 2, in which case

$$\mu_{J,J+2} = \frac{1}{2J+3} \left\{ \frac{[(J+2)^2 - M^2][(J+1)^2 - M^2]}{(2J+5)(2J+1)} \right\}^{\frac{1}{2}} P E_s \quad (10-49)$$

From the above, it can be seen that an absorption occurs at a frequency

$$\nu = \frac{W_{J+2} - W_J}{\hbar} = 2B(2J+3) \quad (10-50)$$

with an intensity that can be obtained by substituting  $\mu_{J,J+2}$  from (10-49) for the more usual dipole matrix element. The matrix element (10-49) is, however, very much smaller than a normal dipole matrix element of  $10^{-18}$  esu. The polarizability  $P$  of a linear molecule could be calculated from an expression of the type (10-44) if the electronic wave functions were sufficiently known. More simply,  $P$  is usually given to a rough approximation by the cube of the molecular length. If this length is taken as 3 Å, then  $E_s$  would have to be 300 esu, or about  $10^5$  volts/cm, in order for  $P E_s$  to be as large as  $10^{-2}$  debye or  $10^{-20}$  esu. Although it would be very useful to obtain rotational transitions of nonpolar molecules, these high field strengths which are necessary are not easily maintained in gases at low or moderate pressures.

The third term in (10-47) also produces transitions at frequencies given by

$$\nu = \frac{W_{J+2} - W_J}{\hbar} = 2B(2J+3) \quad (10-51)$$

The matrix element has the same form as (10-48), but with  $E_s$  replaced by  $E_m$ . Thus transitions in a nonpolar molecule can be produced simply by a microwave field of sufficiently high intensity. The required field strengths are again too high, however, for normal use.

**10-8. Stark Effects in Rapidly Varying Fields—Nonresonant Case.** Stark effects are usually considered for static or essentially static fields, as has been done above. However, with the techniques of microwave spectroscopy, a number of interesting effects may be observed in rapidly varying fields. The normal or static type of Stark effect occurs in a slowly varying electric field, but when the frequency of variation becomes comparable with or rapid compared with the width of an absorption line, new effects occur. Still other new effects appear when the frequency of variation becomes comparable with or greater than the frequency difference between two energy levels between which electric-dipole transitions can occur.

We shall consider first the behavior of a molecule in an electric field varying sinusoidally at a frequency  $\nu_0$  which is considerably less than any transition frequency of the molecule, but which may be greater than the half width  $\Delta\nu$  of an absorption line. The line width  $\Delta\nu$  is  $1/(2\pi\tau)$ , where  $\tau$  is the time between collisions. Hence  $1/\Delta\nu$  is a measure of the "relaxation time" of the molecules in a gas, or the time required for any transient phenomenon to disappear. Therefore, if the frequency  $\nu_0$  of the varying electric field is considerably less than the half width  $\Delta\nu$ , the field may be considered essentially static at any time and the Stark effect calculated accordingly. If the field varies at a frequency  $\nu_0 \ll \Delta\nu$  the frequency of an absorption line simply moves in synchronism with it. However, for  $\nu_0 > \Delta\nu$  the molecular state cannot adjust rapidly enough to follow the varying field, and the Stark effect has a different character. This general type of effect was examined theoretically by Blockinzew [39] who remarked that it was too small to be observed. After the advent of microwave spectroscopy, however, Townes and Merritt [243] were able to demonstrate a variety of such effects.

Figures 10-8 and 10-9 illustrate the above behavior. They represent absorption by the  $J = 2 \leftarrow 1$  transition of OCS. The gas was contained in an absorption cell made up of a short length in which there was zero electric field, and a larger length in which a field could be applied. Figure 10-8a shows a central absorption peak due to the portion of the gas which is not subjected to an electric field, a left-hand peak corresponding to absorption by molecules in a state  $M = 0$ , and a right-hand peak due to molecules in states  $M = \pm 1$ , both of which are displaced by a small amount due to an applied static field of approximately 650 volts/cm. In OCS, the change of frequency due to Stark effect is proportional to  $E^2$ , the square of the electric field, so that if the electric field varies slowly as  $E = E_0 \cos 2\pi\nu_0 t$  the absorption frequency should vary at a

frequency of  $2\nu_0$  between that of the undisplaced line and that corresponding to a static field  $E_0$ . Such behavior is indicated by Fig. 10-8b, which is the absorption by OCS in the same absorption cell as before, but with a field varying at 1 kc, with a peak value  $E_0$  essentially the same as the

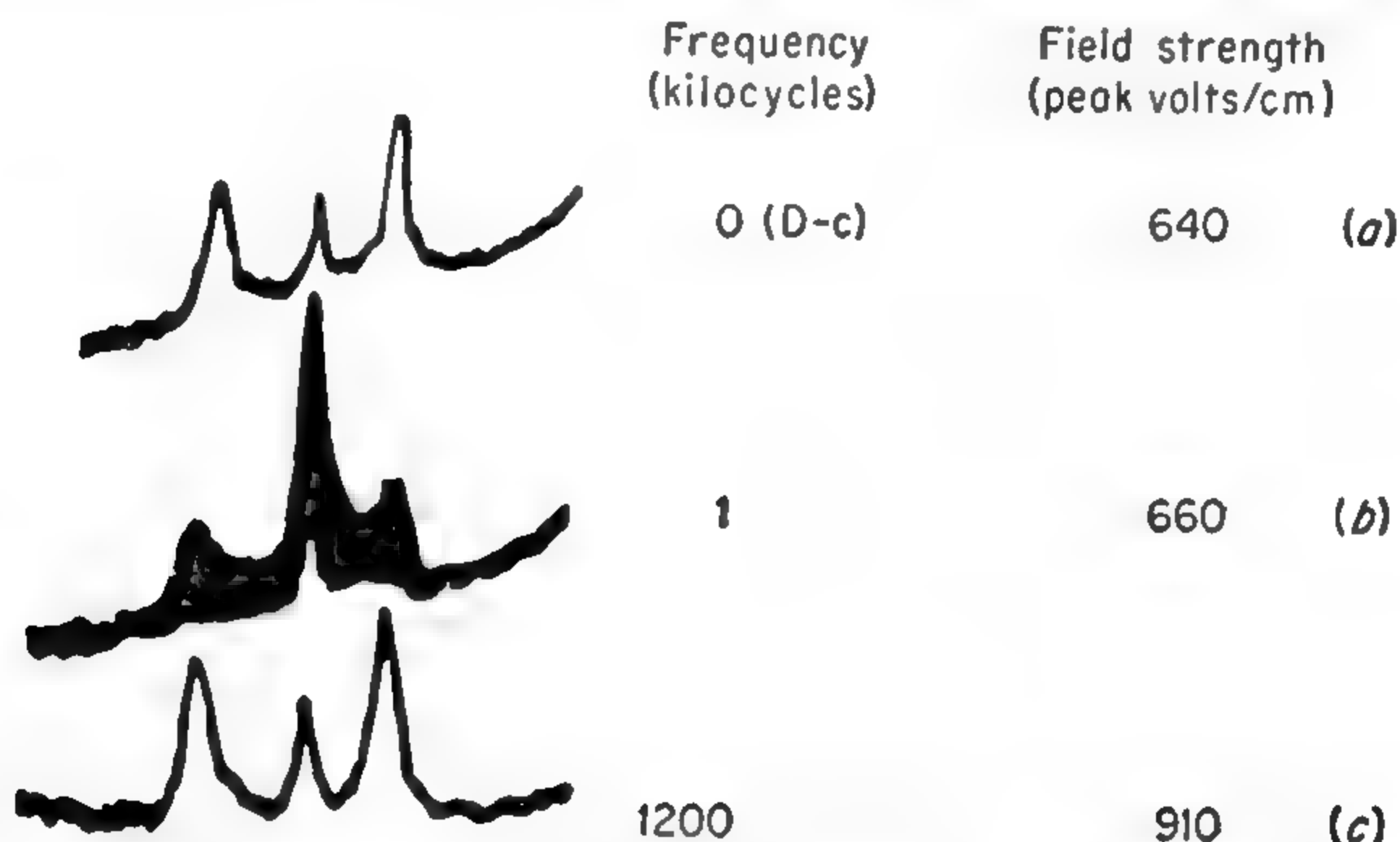


FIG. 10-8. Stark effect on OCS  $J = 2 \leftarrow 1$  transition with applied fields of various frequencies. (From Townes and Merritt [243].)

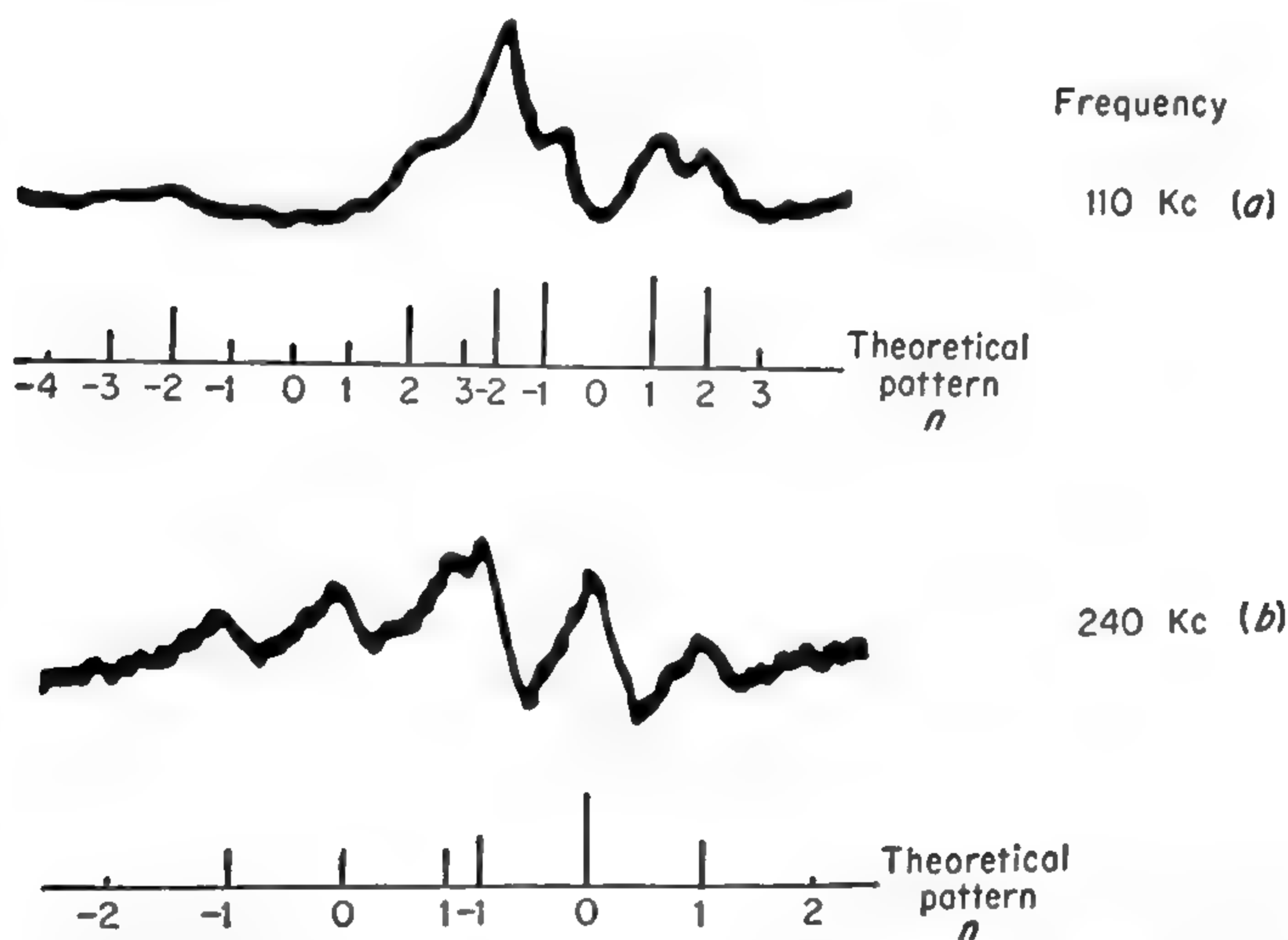


FIG. 10-9. Stark effect on OCS  $J = 2 \leftarrow 1$  transition showing additional lines produced by fields of intermediate frequencies. Peak field strengths of both fields are 640 volts/cm. (From Townes and Merritt [243].)

previous static field. The dark or fuzzy region in Fig. 10-8b corresponds to the various possible values of absorption which may occur as the field varies. In Fig. 10-8c, the field is varied in the same way at 1200 kc, a frequency much larger than the line half width of 100 kc, and also larger than the frequency shift due to Stark effect of a static field of the same magnitude. The Stark pattern for this high-frequency field is seen to



have the same appearance as for the static field of Fig. 10-8a. Figure 10-9 shows other more complex Stark patterns associated with modulation frequencies  $\nu_0$  of intermediate values.

In order to understand the behavior of a molecular system in a varying field, we start with the wave equation including the time.

$$[H_0 + H'(t)]\psi = -\frac{\hbar}{i} \frac{\partial \psi}{\partial t} \quad (10-52)$$

where  $H_0$  is the Hamiltonian operator without the varying electric field, and  $H'(t)$  represents the small time-dependent perturbation produced by the field. Its precise form for a field  $\mathbf{E}_0$  varying at a frequency  $\nu_0$  is

$$H'(t) = \mathbf{u} \cdot \mathbf{E}_0 \cos 2\pi\nu_0 t \quad (10-53)$$

To simplify the mathematics, let us assume that there are two nearby states which "interact" as the result of a dipole moment matrix element between them, and that no other states are sufficiently near in energy to be of importance in the Stark effect on these two. The unperturbed wave function for the lower state will be designated  $\psi_1$ , and that for the upper state  $\psi_2$ . The perturbed wave function for the lower state can then be written in the form

$$\psi'_1 = (a\psi_1 + b\psi_2) \exp \left[ \frac{i}{\hbar} \int_0^t f(t) dt \right] \quad (10-54)$$

In this expression  $a$  is approximately unity,  $-f(t)$  approximately the energy  $W_1$  of the lower state, and  $b$  is small as long as the perturbation is small. Substituting (10-54) into the wave equation (10-52), letting  $H_0\psi_1 = W_1\psi_1$ , where  $W_1$  is the energy for the unperturbed state, and  $H_0\psi_2 = W_2\psi_2$ ,

$$a[W_1 + f(t) + H'(t)]\psi_1 + \frac{\hbar}{i} \dot{a}\psi_1 + b[W_2 + f(t) + H'(t)]\psi_2 + \frac{\hbar}{i} \dot{b}\psi_2 = 0 \quad (10-55)$$

where  $\dot{a}$  and  $\dot{b}$  represent the time derivatives of  $a$  and  $b$ , respectively. If expression (10-55) is multiplied by  $\psi_1^*$  and integrated, then since  $\psi_1$  and  $\psi_2$  are orthogonal, one obtains

$$a[W_1 + H'_{11} + f(t)] + bH'_{12} + \frac{\hbar}{i} \dot{a} = 0 \quad (10-56)$$

where

$$H'_{11} = \int \psi_1^* H'(t) \psi_1 d\tau \quad \text{and} \quad H'_{12} = \int \psi_1^* H'(t) \psi_2 d\tau$$

similarly

$$b[W_2 + H'_{22} + f(t)] + aH'_{21} + \frac{\hbar}{i} \dot{b} = 0 \quad (10-57)$$

The solution of (10-56) and (10-57) may be obtained by successive approximations, assuming first that  $(\hbar/i)\dot{a}$  and  $(\hbar/i)\dot{b}$  are negligible. From (10-56), if  $b = 0$ ,

$$f^{(1)}(t) = -W_1 - H'_{11} \quad (10-58)$$

where  $f^{(1)}(t)$  is the first-order approximation as in the case of a static field. By putting  $f^{(1)}(t)$  from (10-58) into (10-57), one obtains

$$b = \frac{-H'_{21}}{W_2 + H'_{22} - W_1 - H'_{11}} \quad (10-59)$$

And, combining (10-59) with (10-56), the second-order approximation to  $f(t)$  may be obtained as

$$f^{(2)}(t) = -W_1 - H'_{11} + \frac{|H'_{12}|^2}{W_2 + H'_{22} - W_1 - H'_{11}} \quad (10-60)$$

In order to examine the significance of the above solution (10-60) to the observed spectrum, we shall assume that  $H'_{11} = H'_{22} = 0$ , so that only a second-order Stark effect is present. Expression (10-60) may then be written

$$f^{(2)}(t) = -W_1 - \Delta W_1 \cos^2 2\pi\nu_0 t \quad (10-61)$$

since  $H'_{12} = \mu_{12}E_0 \cos 2\pi\nu_0 t$ , where  $\mu_{12}$  is the dipole moment matrix element.  $\Delta W_1$  is the change in energy which would be produced by the Stark effect of a static field  $E_0$ . Substituting (10-61) into (10-54) the wave function is then

$$\psi'_1 = (a\psi_1 + b\psi_2) \exp \left[ -\frac{i}{\hbar} \left( W_1 t + \frac{\Delta W_1 t}{2} + \frac{\Delta W_1}{8\pi\nu_0} \sin 4\pi\nu_0 t \right) \right] \quad (10-62)$$

Consider now a transition induced by a microwave field of frequency  $\nu$  between  $\psi'_1$  and a different energy level designated by a wave function  $\psi_3$ . The intensity of the transition will depend on the absolute magnitude of the integral

$$\iint \psi_3^* \mu \cos \theta \psi'_1 d\tau e^{-2\pi i \nu t} dt \approx \quad (10-63)$$

$$\mu_{31} \int \exp \left( i \int_0^t \left\{ \frac{1}{\hbar} [W_1 - W_3 + (\Delta W_1 - \Delta W_3) \cos^2 2\pi\nu_0 x] - 2\pi\nu \right\} dx \right) dt$$

where  $\mu_{13}$  is the ordinary dipole moment matrix element between the two states. If the microwave frequency  $\nu$  is constant, then the intensity of absorption depends on the square of the amplitude of the various Fourier components of

$$\int \psi_3^* \mu \cos \theta \psi'_1 d\tau = \mu_{31} \exp \left\{ \frac{i}{\hbar} \left[ W_3 - W_1 + \frac{\Delta W_3 - \Delta W_1}{2} \right] t + \frac{i}{\hbar} (\Delta W_3 - \Delta W_1) \frac{\sin 4\pi\nu_0 t}{8\pi\nu_0} \right\} \quad (10-64)$$

$(W_1 - W_3)/h$  may be recognized as the frequency  $\nu_{13}$  of the transition before application of a perturbing field and  $(\Delta W_3 - \Delta W_1)/h$  as the change in frequency  $\Delta\nu_{13}$  due to the Stark effect of a static field  $E_0$ . Hence the right-hand side of (10-64) can be written

$$\mu_{13} \exp \left[ 2\pi i \left( \nu_{13} + \frac{\Delta\nu_{13}}{2} \right) t + i \frac{\Delta\nu_{13}}{4\nu_0} \sin 4\pi\nu_0 t \right] \quad (10-65a)$$

or

$$\mu_{13} \exp \left[ 2\pi i \int_0^t (\nu_{13} + \Delta\nu_{13} \cos^2 2\pi\nu_0 t) dt \right] \quad (10-65b)$$

The part of (10-65a) involving  $\sin 4\pi\nu_0 t$  can be expanded as a series of Bessel functions, giving

$$\int \psi_3'^* \mu \cos \theta \psi_1' d\tau = \mu_{13} e^{2\pi i \left( \nu_{13} + \frac{\Delta\nu_{13}}{2} \right) t} \sum_{n=-\infty}^{\infty} J_n \left( \frac{\Delta\nu_{13}}{2\nu_0} \right) e^{4\pi i n \nu_0 t} \quad (10-66)$$

The intensity of absorption of a particular frequency component of (10-65) is given by the square of its amplitude. Hence a transition of frequency  $\nu_{13} + \frac{\Delta\nu_{13}}{2} + 2n\nu_0$  will appear with intensity

$$\text{Int} \left( \nu_{13} + \frac{\Delta\nu_{13}}{2} + 2n\nu_0 \right) = I J_n^2 \left( \frac{\Delta\nu_{13}}{4\nu_0} \right) \quad (10-67)$$

where  $I$  is the intensity of the Stark component in a static field.

We can now discuss more completely the Stark effect with varying fields and compare expectations with observations shown in Figs. 10-8c and 10-9. The observed spectrum should be, according to (10-67), a series of lines differing in frequency by  $2n\nu_0$  and centered at  $\nu_{13} + \Delta\nu_{13}/2$ . These equally spaced lines might be called "sidebands" corresponding to modulation of the molecular wave function, and are demonstrated in Figs. 10-9a and 10-9b where relative intensities are seen to agree well with the values predicted from (10-67). If the modulation frequency  $\nu_0$  is much larger than the static Stark effect  $\nu_{13}$ , then all Bessel functions of (10-66) or (10-67) are quite small except  $J_0(\nu_{13}/4\nu_0)$ , which is approximately equal to unity. For such a case, all the intensity of the Stark component is concentrated in a single frequency  $\nu_{13} + \Delta\nu_{13}/2$ , displaced by an amount  $\Delta\nu_{13}/2$  which is just the average of the Stark displacement to be expected from a slowly varying field of the same magnitude  $E_0$ . The molecule may be said in this case simply to average the Stark effect, since it cannot respond to the rapid variation. Figure 10-8c shows an observed spectrum under this condition. It should be noted that the Stark displacement appears to be identical with that obtained with a static field but that the peak field required is 910 volts/cm, which is larger than the static field of 640 volts/cm by  $\sqrt{2}$ .

In case first-order Stark effects occur, the phenomena observed with



high-frequency modulation are very similar. However, in this case the average position of the Stark component is  $\nu_{13}$ . The molecular frequency is modulated with a frequency  $\nu_0$  instead of the  $2\nu_0$  which occurs with second-order Stark effect when the frequency depends on the square of the electric field. The observed frequencies are then  $\nu_{13} + n\nu_0$  and the intensities are

$$\text{Int}(\nu_{13} + n\nu_0) = IJ_n^2 \left( \frac{\nu_{13}}{\nu_0} \right) \quad (10-68)$$

It is useful to observe from (10-63) that the absorption intensity depends only on the difference between the frequency of the absorbed microwaves and  $\nu_{13} + \Delta\nu_{13} \cos^2 2\pi\nu_0 t$  which would be the frequency of the absorption line calculated on the basis of an essentially static field. Hence if the electric field is in fact constant and the microwave frequency  $\nu$  is modulated, a similar breakup of the spectrum into "sidebands" can be expected.

In order for the multiple components to appear as indicated by (10-67) or (10-68), the line widths must of course be smaller than the separation between components. If the line width is larger than the separation [ $2\nu_0$  or  $\nu_0$ ], then the intensity appears to be modulated, or the absorption line to move in frequency. When the line width is smaller than this modulation frequency, the line no longer appears to move, but to split up into its separate components. It is this effect which requires, as is discussed in Chap. 15, that the line width in a Stark modulation spectrometer be somewhat greater than the modulation frequency. A more detailed discussion of modulation effects of the above type, including modulation by a square wave instead of a sine wave, is given by Karplus [293].

It is appropriate now to examine the conditions under which  $\dot{a}$  and  $\dot{b}$  in Eqs. (10-56) and (10-57) can be properly omitted, as was done for the above solution, and the consequences of their inclusion. Using the value of  $b$  given by (10-59),

$$\frac{\hbar}{i} \dot{b} = \frac{\hbar\nu_0 H'_{21} \sin 2\pi\nu_0 t}{i(W_2 + H'_{22} - W_1 - H'_{11})} \quad (10-69)$$

Hence  $(\hbar/i)\dot{b}$  is comparable with the term  $aH'_{21}$  in (10-57) if

$$\frac{\hbar\nu_0}{W_2 + H'_{22} - W_1 - H'_{11}} \approx 1$$

or if the frequency of modulation  $\nu_0$  becomes comparable with the resonance frequency between the two levels 1 and 2. The quantity  $\dot{a}$  may be assumed to be zero, since any time variation of  $a$  may be taken as the part of the factor  $\exp[-i/\hbar \int f(t) dt]$  in (10-54). In order to solve (10-57) to terms of order  $H'$  without neglecting  $(\hbar/i)\dot{b}$ , we may neglect  $H'_{22}$ , use

$f_1(t) = -W_1$  and assume  $b$  has the general form

$$b = A \cos 2\pi\nu_0 t + B \sin 2\pi\nu_0 t \quad (10-70)$$

By substituting (10-70) into (10-57) and remembering that

$$H'_{12} = \mu_{12}E_0 \cos 2\pi\nu_0 t$$

the constants  $A$  and  $B$  can be determined. It will be seen below that the value of  $B$  is not important, so that after inserting the value of  $A$  into (10-70)

$$b = \frac{\mu_{12}E_0(W_1 - W_2)}{(W_1 - W_2)^2 - h^2\nu_0^2} \cos 2\pi\nu_0 t + B \sin 2\pi\nu_0 t \quad (10-71)$$

From (10-71) and (10-56) an approximate value of  $f(t)$  may be obtained which is good to terms in  $H'^2$ .

$$f_2(t) = -W_1 - \mu_{11}E_0 \cos 2\pi\nu_0 t - \frac{|\mu_{12}|^2 E_0^2 (W_1 - W_2) \cos^2 2\pi\nu_0 t}{(W_1 - W_2)^2 - h^2\nu_0^2} - \mu_{12}E_0 B \sin 2\pi\nu_0 t \cos 2\pi\nu_0 t \quad (10-72)$$

It has already been shown above that for small fields such that the Stark effect produces a frequency change much less than  $\nu_0$ , the observed frequencies depend only on the average value of  $f(t)$ . Hence the first and third terms of (10-72) are the important ones, and the varying field produces an effective change in the energy level of

$$\Delta W = \frac{|\mu_{12}|^2 E_0^2 (W_1 - W_2)}{2[(W_1 - W_2)^2 - h^2\nu_0^2]} \quad (10-73)$$

**10-9. Stark Effects in Rapidly Varying Fields—Resonant Modulation.** When  $h\nu_0 \ll |W_1 - W_2|$ , expression (10-73) reduces to the form

$$\frac{|\mu_{12}|^2 E_0^2}{2(W_1 - W_2)}$$

as was obtained previously for a rapidly oscillating field. As  $h\nu_0$  approaches  $|W_1 - W_2|$ , however, the Stark effect from (10-73) increases in size, becomes infinite at the resonant frequency  $\nu_0 = (1/h)|W_1 - W_2|$ , and then reverses in sign for  $h\nu_0 > |W_1 - W_2|$ . This general type of behavior, and the reversal of sign of the Stark effect, has been observed by Autler and Townes [892c]. However, the Stark effect never becomes infinite at the resonance frequency, since then the approximations used above which treated the field as a small perturbation are no longer good, and (10-73) is incorrect. Near the resonance frequency

$$\nu_0 \approx \frac{1}{h} |W_1 - W_2|,$$

the wave equation must be solved by a still different mathematical technique described below.

The change in apparent energy of a system due to an oscillating electric field  $E_0 \cos 2\pi\nu_0 t$  may be briefly summarized as follows:

*Case 1.*  $\nu_0 \ll \Delta\nu$  (half width of energy level or line)

Stark effect can be calculated at any instant as if field were static. Hence

$$\begin{aligned}\Delta W_1 &= \mu_{11}E_0 \cos 2\pi\nu_0 t + \sum_n \frac{|\mu_{1n}|^2}{W_1 - W_n} E_0^2 \cos^2 2\pi\nu_0 t \\ &= \Delta W_1^{(1)} \cos 2\pi\nu_0 t + \Delta W_1^{(2)} \cos^2 2\pi\nu_0 t\end{aligned}\quad (10-74)$$

*Case 2.*  $\nu_0 \gg \Delta\nu$  and  $\nu_0 \ll \frac{|W_1 - W_n|}{h}$  (transition frequency to any level connected by electric dipole matrix element)

A number of different component levels occur. If first-order Stark effect is present ( $\Delta W_1^{(1)} \neq 0$ ), the changes in "energy" of these components are

$$\Delta W_1 = \pm m\nu_0 \quad (10-75)$$

where  $m$  is an integer. Intensity of each component is proportional to  $[J_m(\Delta W_1^{(1)}/\nu_0)]^2$ . If  $\Delta W_1^{(1)} = 0$ , then only second-order Stark effects occur and the components are given by

$$\Delta W_1 = \pm 2m\nu_0 \quad (10-76)$$

with intensities proportional to  $[J_m(\Delta W_1^{(2)}/4\nu_0)]^2$ .

*Case 3.*  $\nu_0 \gg \Delta\nu$ ,  $\nu_0 \gg \frac{|\Delta W_1^{(1)}| + |\Delta W_1^{(2)}|}{h}$  and  $\nu_0 \neq \frac{W_1 - W_n}{h}$

$$\Delta W_1 = \sum_n \frac{|\mu_{1n}|^2 E_0^2 (W_1 - W_n)}{2[(W_1 - W_2)^2 - h^2\nu_0^2]} \quad (10-77)$$

*Case 4.*  $\nu_0 \approx \frac{W_1 - W_n}{h}$

This is the resonant case discussed below. The level splits into two separated by  $|\mu_{1n}E_0|/h$  if  $\nu_0 = (W_1 - W_n)/h$ .

If a molecule is initially in state 1, radiation of the resonant frequency will induce a transition to state 2, and then back to state 1, so that a regular oscillation between states 1 and 2 is produced. The result is that the wave function is modulated at the frequency of this regular oscillation, and the observed spectral lines split into two components.

Assume that the upper level is state 2 and the frequency of the Stark field

$$\nu_0 = \frac{W_2 - W_1 + \epsilon}{h} \quad (10-78)$$

where  $\epsilon/(W_2 - W_1) \ll 1$ , so that the above type of "resonant modula-



tion" can occur. Then it can be shown that an appropriate wave function for the system can be written to a good approximation [892c].

$$\begin{aligned} \psi = & \frac{\psi_2}{\sqrt{2}(\rho^2 + \beta^2)} e^{-i/\hbar(W_2 + \epsilon/2)t} [\rho(\rho - \beta e^{i\phi}) e^{i\gamma t/\hbar} + \beta(\beta + \rho e^{i\phi}) e^{-i\gamma t/\hbar}] \\ & + \frac{\psi_1}{\sqrt{2}(\rho^2 + \beta^2)} e^{-i/\hbar(W_1 - \epsilon/2)t} [-\beta(\rho - \beta e^{i\phi}) e^{i\gamma t/\hbar} + \rho(\beta + \rho e^{i\phi}) e^{-i\gamma t/\hbar}] \end{aligned} \quad (10-79)$$

where  $\beta$  is the amplitude of the electric field times the dipole moment matrix element  $\mu_{12}$  between the two states, or

$$\beta = \mu_{12} E_0 \quad \gamma = \frac{1}{2} \sqrt{|\beta|^2 + \epsilon^2} \quad \rho = \sqrt{|\beta|^2 + \epsilon^2} - \epsilon \quad (10-80)$$

and where  $\phi$  is an arbitrary phase angle whose value depends on the initial conditions at  $t = 0$ .

If a third state of energy  $W_3$  is considered which is connected by a dipole transition to state 1 but not to state 2, then it may be seen from (10-79) that transition frequencies

$$\nu = \frac{1}{h} (W_2 - W_3 + \epsilon/2 \pm \gamma) \quad (10-81)$$

may be expected. The ratio of intensities of these two is given by the ratio of the square of the amplitude of the two terms of (10-79) which multiply  $\psi_1$ . After averaging over the arbitrary phase angle  $\phi$ , this ratio is

$$R = \frac{\rho^2}{|\beta|^2} = \frac{|\beta|^2 - 2\epsilon \sqrt{|\beta|^2 + \epsilon^2} + 2\epsilon^2}{|\beta|^2} \quad (10-82)$$

Hence when  $\epsilon$  is small and positive [ $\nu_0 > (W_2 - W_1)/h$ ], the transition frequency given by the plus sign in (10-81) is the weaker; when  $\epsilon$  is small and negative [ $\nu_0 < (W_2 - W_1)/h$ ] this frequency is the stronger of the two. Precisely at resonance,  $R = 1$  from (10-82) and the frequency difference between the two components of equal intensity is, from (10-81),

$$\Delta\nu = \frac{2\gamma}{h} = |\mu_{12}| \frac{E_0}{h} \quad (10-83)$$

Just at resonance, (10-79) shows that the wave function can be considered as oscillating back and forth between  $\psi_1$  and  $\psi_2$  because a proper choice of  $\phi$  gives, from (10-79),

$$\psi = i\psi_1 e^{-iW_1 t/\hbar} \cos\left(\frac{\gamma t}{h} + \frac{\pi}{4}\right) + \psi_2 e^{-iW_2 t/\hbar} \sin\left(\frac{\gamma t}{h} + \frac{\pi}{4}\right) \quad (10-84)$$

Hence the frequency of oscillation between states is

$$\frac{\gamma}{h} = \frac{|\mu_{12}| E_0}{2h}$$

The type of splitting due to resonance modulation described above may be used to measure the separation between closely spaced levels [429]. Since the relative intensity of the two components is sensitively dependent on the deviation  $\epsilon$  from resonant frequency  $(W_2 - W_1)/h$ , the resonant frequency can be rather accurately measured by varying  $\nu_0$  until the two intensities are equal. This technique is particularly useful when no microwave transitions to level 1 are observed, and some transition frequency  $(W_2 - W_3)/h$  falls in the microwave region. Then if  $W_2$

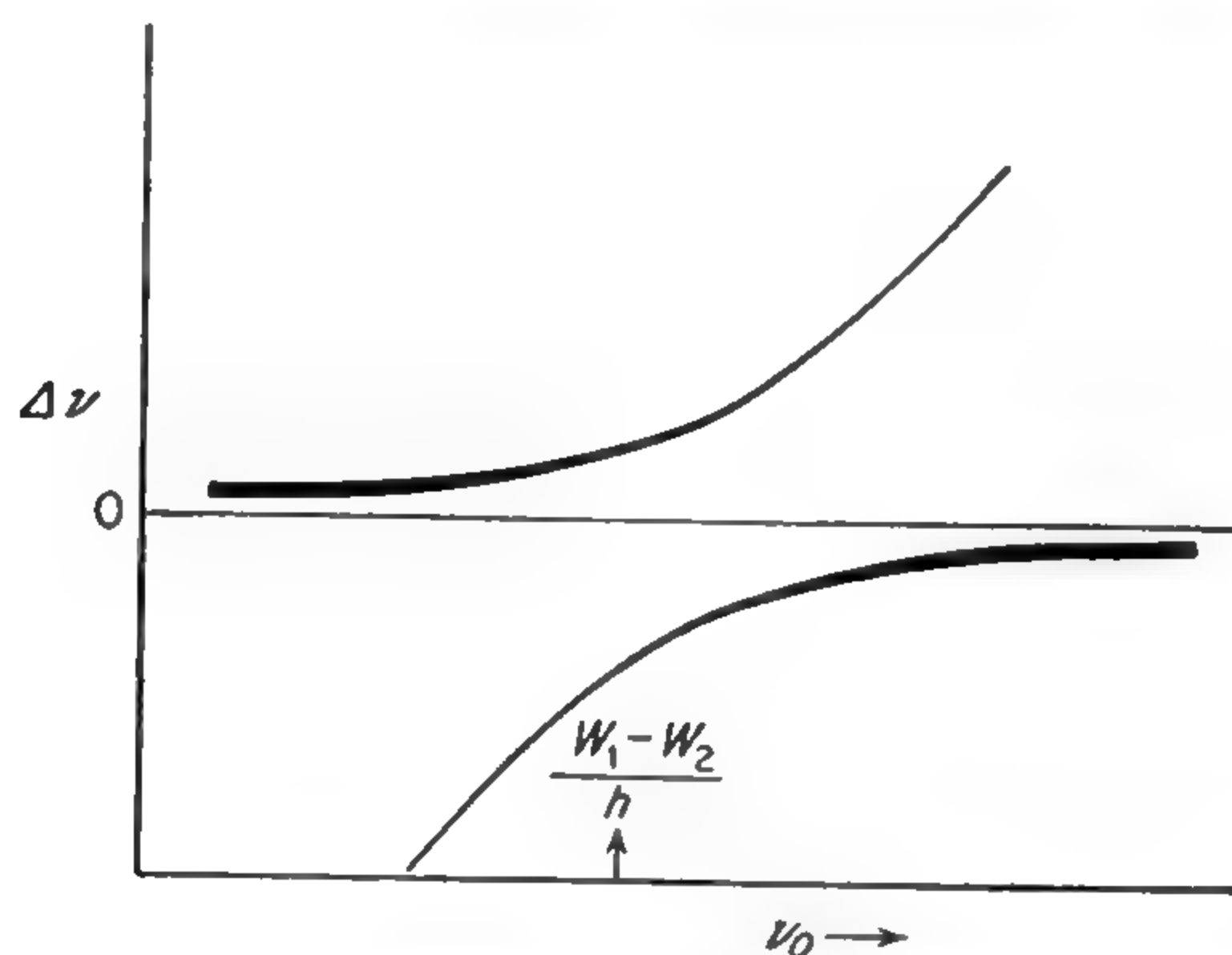


FIG. 10-10. Stark effect at frequencies  $\nu_0$  comparable to a resonance frequency  $\frac{W_1 - W_2}{h}$ . Width of lines correspond approximately to intensity of the Stark components. For low frequency, there is a single component. At resonance its frequency change  $\Delta\nu$  is large, and a second component with an opposite frequency change has equal intensity. For  $\nu_0 > \frac{W_1 - W_2}{h}$ , the second component dominates in intensity.

is not very different from  $W_1$ , the energy separation  $W_1 - W_2$  may be measured by resonant modulation.

For  $\epsilon$  large and positive,  $R$  from (10-82) becomes zero, and for  $\epsilon$  large and negative,  $R \rightarrow \infty$ , so that only one component has appreciable intensity in either case. This is in agreement with the nonresonant Stark effects discussed above and shows how the Stark effect can appear to change sign rather suddenly at resonance. In reality both components are always present, but on either side of resonance, different components predominate in intensity. This behavior is illustrated in Fig. 10-10.

Certain complications often occur in the use of resonant modulation. The above discussion assumes a simple nondegenerate transition so that  $|\mu_{12}|$  has a unique value. In many cases, each microwave line is in fact a superposition of transitions involving various magnetic quantum numbers  $M$ . For each value of  $M$  the matrix element  $\mu_{12}$  may be different, so that resonant modulation produces a number of pairs of components.

It should also be remembered that the wave function (10-79) is an

approximation. Terms in various powers of  $\beta/(W_1 - W_2)$  are neglected and these can be of importance for sufficiently large electric fields. A more complete solution has been obtained by Autler and Townes [892c]. They show that, for sufficiently strong electric fields, additional transition frequencies or "sidebands" occur at regular spacings equal to the modulation frequency  $\nu_0$ . In addition, splitting of lines similar to that observed at the resonant frequency occurs at frequencies of  $\frac{W_2 - W_1}{3h}$ ,

$$\frac{W_2 - W_1}{5h}, \frac{W_2 - W_1}{7h}, \dots$$



## CHAPTER 11

### ZEEMAN EFFECTS IN MOLECULAR SPECTRA

**11-1. Introduction.** Zeeman effects in molecular spectra bear about the same relation to Stark effects that magnetic hyperfine structure does to electric quadrupole hyperfine structure. That is, Stark effects are very much more prominent in the usual types of molecules, which are in  $^1\Sigma$  states; Zeeman effects are relegated to small second-order effects or to the small moments of the nuclei. However, in the unusual molecules which have electronic angular momentum and hence are not in  $^1\Sigma$  states, the Zeeman effect is quite large and comparable with Zeeman effects found in atomic spectra.

Perhaps the simplest cases to discuss and those giving the widest variety of effects are the cases of the rare molecules with electronic angular momenta; so they will be treated first. These molecules may also be classed as paramagnetic, since their paramagnetic response to a magnetic field occurs precisely because of the large Zeeman effect associated with electronic angular momentum. Each unit of angular momentum due to orbital motion of an electron produces one Bohr magneton, so that its magnetic moment is  $\mathbf{u}_L = -\mu_0\mathbf{L}$ , where  $\mu_0$  is the Bohr magneton (taken as a positive quantity) and  $\mathbf{L}$  is the orbital angular momentum in units of  $\hbar$ . Each unit of spin momentum produces slightly more than two Bohr magnetons, or  $\mathbf{u}_s = -2.00229\mu_0\mathbf{S}$ . The energy of interaction between these magnetic dipoles and an external field is simply

$$\Delta V = -(\mathbf{u}_L \cdot \mathbf{H} + \mathbf{u}_s \cdot \mathbf{H}) \quad (11-1)$$

**11-2. Zeeman Effect in Weak Fields for Molecules Having Electronic Angular Momentum.** The energy (11-1) can easily be evaluated by vector-model calculations when  $\mu_L H$  or  $\mu_s H$  are considerably smaller than certain other molecular energies (weak-field case) and when some pure-coupling case applies. Consider, for example, Hund's coupling case (*a*) for a diatomic (or linear) molecule.  $\mathbf{S}$  and  $\mathbf{L}$  precess about the molecular axis, which precesses about  $\mathbf{J}$  (cf. Chap. 7). When a magnetic field  $\mathbf{H}$  is applied,  $\mathbf{J}$  precesses about  $\mathbf{H}$  with a projection  $M$  on the direction of  $H$ , where  $M$  has one of the values  $J, J-1, \dots, -J$ . Now, using the vector model, the average value of  $\mathbf{u}_s \cdot \mathbf{H}$  is

$$\mu_s H [\cos (SH)]_{av} = \mu_s H [\cos (SA)]_{av} [\cos (AJ)]_{av} [\cos (JH)]_{av}$$

where  $\mathbf{A}$  represents the molecular axis and  $\cos(SA)$  the cosine of the angle between  $\mathbf{S}$  and the axis. Thus,

$$\mathbf{u}_s \cdot \mathbf{H} = \frac{(\mathbf{u}_s \cdot \mathbf{k})(\mathbf{k} \cdot \mathbf{J})(\mathbf{J} \cdot \mathbf{H})}{J(J+1)} \quad (11-2)$$

where  $\mathbf{k}$  is a unit vector along the molecular axis and  $J^2$  in the denominator has been replaced by  $J(J+1)$  according to the usual vector-model rule. Now  $\mathbf{u}_s \cdot \mathbf{k} \approx -2.002\mu_0$ ;  $\mathbf{S} \cdot \mathbf{k} = -2.002\mu_0\Sigma$ ;  $\mathbf{k} \cdot \mathbf{J} = \Omega$ , and

$$\mathbf{J} \cdot \mathbf{H} = MH$$

Hence

$$\mathbf{u}_s \cdot \mathbf{H} = \frac{-2.002\mu_0\Sigma\Omega MH}{J(J+1)} \quad (11-3)$$

A similar calculation can be made for  $\mathbf{u}_L \cdot \mathbf{H}$ , so that the energy from (11-1) in Hund's case (a) is

$$\Delta W = \mu_0 \frac{(\Lambda + 2.002\Sigma)\Omega MH}{J(J+1)} = \frac{(\Omega + 1.002\Sigma)\Omega M\mu_0 H}{J(J+1)} \quad (11-4)$$

Thus from (11-4) there are  $2J+1$  equally spaced Zeeman levels corresponding to the different possible values of  $M$ . The quantity  $\mu_0 H/h$ , which will occur frequently in this chapter, is conveniently expressed in megacycles, or  $\mu_0/h = 1.39967 \pm 0.00005$  Mc/oersted. Hence, if the numerical coefficient of  $\mu_0 H$  in (11-4) is approximately unity, a field of only 1 oersted (slightly larger than the earth's magnetic field) can produce Zeeman splittings as large as 1 Mc.

It is important to remember that  $\Lambda$  and  $\Sigma$  can be positive or negative in (11-4). Consider, for example, a  $^2\Pi$  state. For  $^2\Pi_{\frac{1}{2}}$ ,  $\Lambda + 2.002\Sigma \approx 2$  (or  $-2$ ), and Eq. (11-4) gives a large Zeeman effect, but for  $^2\Pi_{\frac{3}{2}}$ ,

$$\Lambda + 2.002\Sigma = 0.001$$

so that (11-4) gives only a very small Zeeman effect. The only other important cases which give small Zeeman effects according to (11-4) are  $^3\Delta_1$ , where  $\Lambda + 2.002\Sigma = 0.002$ , and  $^3\Pi_0$ , where  $\Omega = 0$ .

For Hund's coupling case (b), a vector-model calculation can also be made. It gives the weak-field Zeeman energy as

$$\Delta W = \frac{1}{2J(J+1)} \left\{ \frac{\Lambda^2[N(N+1) + S(S+1) - J(J+1)]}{N(N+1)} + 2.002[J(J+1) + S(S+1) - N(N+1)] \right\} M\mu_0 H \quad (11-5)$$

For linear molecules with electronic spin in  $\Sigma'$  states ( $\Lambda = 0$ ), or for nonlinear paramagnetic molecules where the electron orbital motion is

quenched ( $\Lambda$  is undefined), the Zeeman effect given by (11-5) becomes

$$\Delta W = \frac{1.001}{J(J+1)} [J(J+1) + S(S+1) - N(N+1)] M \mu_0 H \quad (11-6)$$

For the common case where  $S = \frac{1}{2}$ , (11-6) is simply

$$\begin{aligned} W_{J=N+\frac{1}{2}} &= \frac{1.001}{J} M \mu_0 H \\ W_{J=N-\frac{1}{2}} &= -\frac{1.001}{J+1} M \mu_0 H \end{aligned} \quad (11-7)$$

In cases intermediate between (a) and (b), calculation of the weak-field Zeeman effect is more complex. This is discussed more fully below (page 289).

**11-3. Characteristics of Zeeman Splitting of Spectral Lines.** Although the expressions given above for magnetic energy do not cover all cases, they are typical enough to give a general picture of Zeeman splitting of spectral lines in magnetic fields which are not too large. It is customary to write the magnetic energy in terms of a molecular  $g$  factor, which is a pure number defined by stating that the magnetic energy is given by

$$\Delta W = -\mathbf{\mu} \cdot \mathbf{H} = -\mu_0 g_J \mathbf{J} \cdot \mathbf{H} = -g_J M \mu_0 H \quad (11-8)$$

where  $\mu_0$  is the Bohr magneton (taken as a positive quantity). In molecules with electronic angular momentum,  $g_J$  is usually of the order of unity. However, for  $^1\Sigma$  molecules and for the magnetic moments of nuclei,  $g_J$  is about 1000 times smaller. In these cases it is customary to write instead of (11-8)

$$\Delta W = -g_J M \mu_n H \quad (11-9)$$

where  $\mu_n$  is the nuclear magneton, which is smaller than the Bohr magneton by the ratio of the electron-to-proton masses, or  $\frac{1}{1836}$ . Then  $g_J$  is again of the order of unity. It will usually be clear whether (11-8) or (11-9) is used to define  $g$ .

It is evident from some of the above expressions, *e.g.*, (11-4), (11-5), or (11-7), that  $g_J$  may depend not only on the molecule but also on its rotational angular momentum  $J$  and other quantum numbers. There are, however, common cases where  $g$  does not vary with  $J$  (for example, in the  $^1\Sigma$  molecule which will be discussed below), so that under some circumstances  $g$  may be considered a fixed constant of the molecule.

The energies given by (11-8) are proportional to the first power of  $M$  and of  $H$ , so that they correspond to "first-order" Stark effects seen in molecules with degenerate levels such as a symmetric top [*cf.* Eq. (10-5)]. However, Zeeman effects which are linear in the magnetic field do not require degeneracy as do "first-order" Stark effects. There are, in addition, second-order Zeeman effects proportional to  $H^2$ , but these are usu-



ally much smaller than those proportional to  $H$ , and hence have been omitted in the above formulas. A given energy level is, according to (11-8), split symmetrically about the zero field energy into  $2J + 1$  equally spaced energy levels.

The selection rules for transitions involving Zeeman effects are identical with those when Stark effects are present. Thus, when the exciting microwave field is parallel to  $H$ ,  $\Delta M = 0$ , and when it is perpendicular,  $\Delta M = \pm 1$ . Components of a line corresponding to  $\Delta M = 0$  are sometimes called  $\pi$  components and those for  $\Delta M = \pm 1$  are designated  $\sigma$  components. Relative intensities of these components for different values of  $J$  and  $M$  are similar to the Stark case and are given in Table 10-1.

A transition between upper and lower energy levels designated by  $J_1$  and  $J_2$ , respectively, which has a frequency  $\nu_0$  in zero field will be split into a number of components by Zeeman effect with the following frequencies:

For  $\Delta M = 0$  ( $\pi$  components),

$$\nu = \nu_0 + (g_{J_2} - g_{J_1})M\mu_0H/h \quad (11-10)$$

For  $\Delta M = M_2 - M_1 = \pm 1$  ( $\sigma$  components),

$$\nu = \nu_0 + [(g_{J_2} - g_{J_1})M_2 \pm g_{J_1}]\mu_0H/h \quad (11-11)$$

where  $M_2$  is the value of  $M$  in the lower state.

It may be seen that the average position of all the Zeeman components from either (11-10) or (11-11) is just  $\nu_0$ , the position of the undisturbed line. If intensities are allowed for, the "center of gravity" of all Zeeman components is also  $\nu_0$ , since Zeeman patterns of this type are always symmetrical about  $\nu_0$  [cf. Fig. 11-1]. However, when the smaller Zeeman effects dependent on  $H^2$  are allowed for, the "center of gravity" of a Zeeman split line need not be exactly equal to  $\nu_0$ .

If the  $g$  factor  $g_J$  is constant,  $\pi$  components show no Zeeman effect from (11-10), while  $\sigma$  components from (11-11) are all superimposed on two frequencies only,  $\nu_0 \pm g_J\mu_0H/h$ . In most cases  $g_J$  does not change very much from the lower to the upper states, so that  $\sigma$  components show larger Zeeman effects than do the  $\pi$  components. Thus for easiest observation of Zeeman effects in a rectangular waveguide,  $H$  should be either parallel to the length of the waveguide or parallel to its broadest faces, so that it is perpendicular to the electric field of the exciting microwave. If the  $g$  factor is not the same for the upper and lower molecular states, a more complex pattern is obtained, with  $2J + 1$   $\pi$  components or  $2(2J + 1)$   $\sigma$  components, where  $J$  is the smaller of  $J_1$  and  $J_2$ . General appearance of these spectra is shown in Fig. 11-1. This figure illustrates typical cases where  $g_{J_1} - g_{J_2} = 0$  and where  $g_{J_1} - g_{J_2}$  is not zero but is

smaller than  $g_{J_1}$ . When  $H$  is neither parallel nor perpendicular to the exciting microwave field, both  $\pi$  and  $\sigma$  components appear.

It is possible to excite transitions of the type  $\Delta M = M_2 - M_1 = +1$  without  $\Delta M = -1$ , or vice versa, by using circularly polarized microwaves. If the magnetic field is parallel to the direction of propagation of a circularly polarized microwave, then only one of the Zeeman  $\sigma$  components is excited, and it has all the intensity of the unsplit line. The

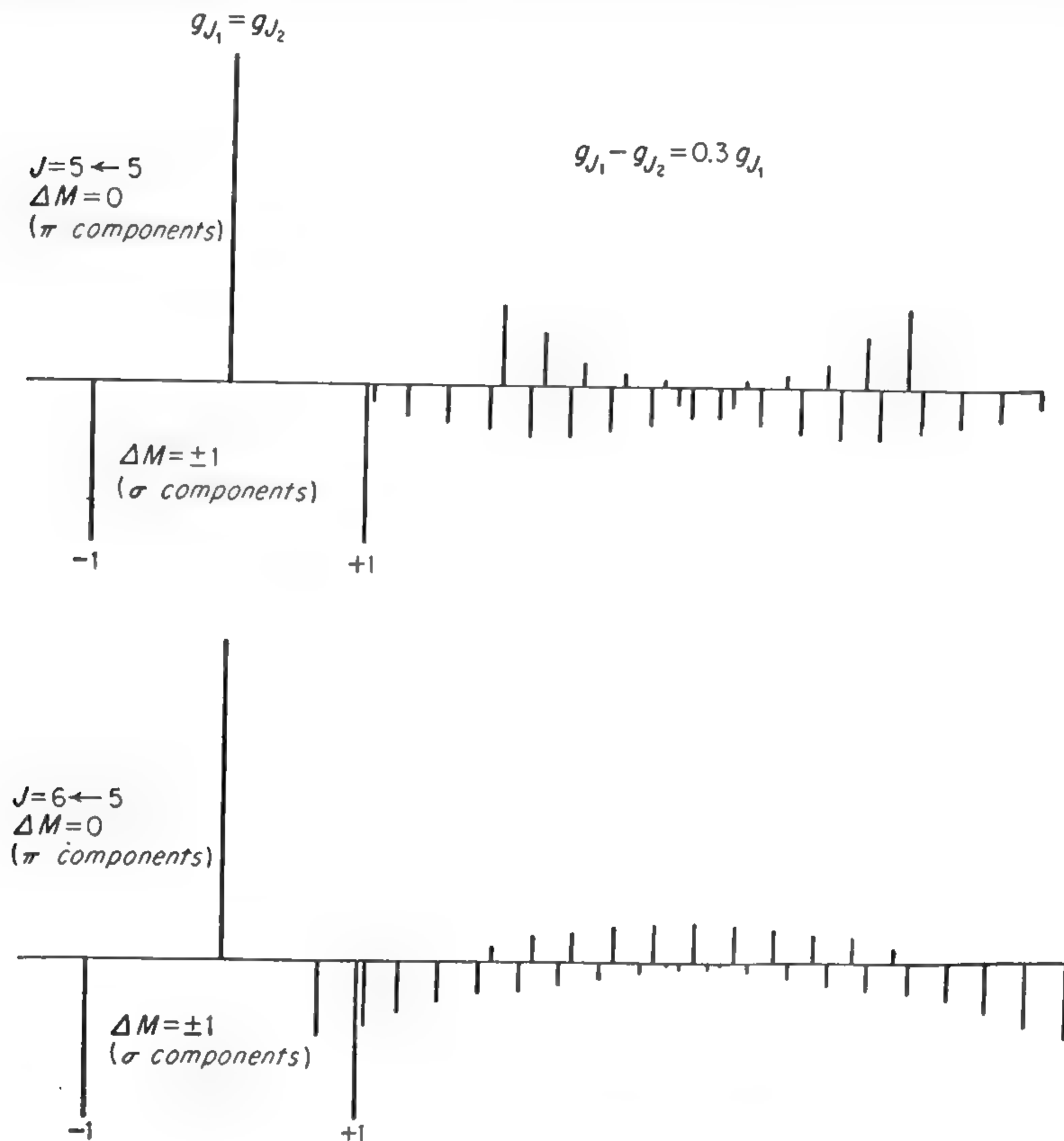


FIG. 11-1. Typical Zeeman patterns.

rotating electric component of the microwave field acts on the molecular dipole to give it some added rotational velocity in the same direction as the rotation of the field. This corresponds to  $\Delta M = +1$ , if the electric vector appears to rotate clockwise when viewed in the direction of the magnetic field, and  $\Delta M = -1$  if the rotation is counterclockwise.

The value of using circular polarization to study the Zeeman effect is that it allows a determination of the sign of the molecular magnetic moment, or of  $g_J$ . This may be seen from (11-11), where frequencies

for which the  $+$  sign applies correspond to  $\Delta M = +1$ , and those with the  $-$  sign to  $\Delta M = -1$ . Microwaves with circular polarization may be obtained in circular waveguide, or an approximately circularly polarized wave may be transmitted in a square waveguide. Even a small circular component of the microwave can give a noticeable difference in intensity of the two Zeeman  $\sigma$  components (*cf.* [705]).

**11-4. Intermediate Coupling and Intermediate Fields.** When a molecule follows no pure coupling scheme, or where the interaction between its magnetic moments and the external field becomes comparable with one of several other sources of molecular energy, the weak-field pure coupling case approximations used above may not be appropriate.

For example, the magnetic interaction  $\mathbf{\mu} \cdot \mathbf{H}$  may be large enough to somewhat disturb the end-over-end rotational motion of the molecule, or to partially uncouple the spin  $S$  from the molecular axis or from  $N$ . Hill [14], [47] has obtained a complete and closed expression for the energy of doublet states intermediate between Hund's cases (a) and (b) when a magnetic field is applied. However, this expression is so involved and difficult to evaluate that it is not given here.

The Zeeman effect in Hund's coupling case (a) is essentially the same as the Stark effect in a symmetric molecule as long as the magnetic field is not sufficiently strong to uncouple  $S$  from the molecular axis. Hence for fields large enough to disturb the molecular rotation but not to uncouple  $S$ , expressions (10-5) and (10-7) apply to case (a) with  $E$  replaced by  $H$ ,  $K$  by  $\Lambda + \Sigma$ , and  $\mu$  by  $\mu_0(\Lambda + 2.002\Sigma)$ .

There is one striking difference between the Zeeman and Stark effects, however, when  $\Lambda$  doubling or inversion doubling occurs. An electric field produces matrix elements only between different  $l$ -doubled,  $\Lambda$ -doubled, or inversion-doubled levels, so that the behavior of the Stark effect depends on the amount of doubling (*cf.* page 252). Although matrix elements for a magnetic field have the same form and value when the doubled states are degenerate, they differ in that they do not connect the two doubled states (*cf.* [14], p. 1510). Hence,  $\Lambda$ -type or  $K$ -type doubled energy is simply added to the Zeeman energy, whereas its effect on Stark energy is more complex.

The effect of large magnetic fields in Hund's coupling case (b) may be obtained for doublet states from the results of Hill [14] or for a  $^3\Sigma$  state from the recent work of Tinkham on  $O_2$  [990]. For moderate fields second-order perturbations due to the magnetic field may be obtained in a straightforward way from the matrix elements which they give. These second-order effects involve a perturbation both of the rotational levels and of the precession of  $S$  about  $K$ , so that the results tend to be somewhat complicated.

**11-5. Zeeman Effect with Hyperfine Structure.** When hyperfine structure is present, the Zeeman effect is modified both by the introduc-



tion of a new angular momentum  $I$ , the spin of the nucleus producing the hyperfine structure, and also by the interaction between the external field and the nuclear magnetic moment. Almost always the nuclear spin  $I$  will couple to the molecular angular momentum  $J$  to produce the total angular momentum  $F$ , since the coupling between  $I$  and the molecule is weak relative to the coupling between electronic vectors and the molecule. This corresponds to coupling case ( $a_\beta$ ) or ( $b_\beta$ ) of Chap. 8.

If the magnetic field is too weak to disturb the coupling between any molecular vectors except perhaps that between  $\mathbf{I}$  and  $\mathbf{J}$ , the molecule may be considered to have a magnetic moment  $\mu_0 g_J J$  oriented along  $\mathbf{J}$  and a moment  $\mu_n g_I I$  oriented along  $\mathbf{I}$ . The magnetic energy is

$$\Delta W = -\mu_n g_I \mathbf{I} \cdot \mathbf{H} - \mu_0 g_J \mathbf{J} \cdot \mathbf{H} \quad (11-12)$$

When  $\mathbf{H}$  is so small that it does not disturb the coupling between  $\mathbf{I}$  and  $\mathbf{J}$ , that is, when (11-12) is much smaller than the hyperfine energy, the energy (11-12) may be evaluated by the vector model. This is very similar to the case of first-order Stark effect with hyperfine structure [(10-26) and (10-27)]. The energy given by the vector model for weak fields is

$$\Delta W = \{ -\mu_n g_I [I(I+1) + F(F+1) - J(J+1)] \\ - \mu_0 g_J [J(J+1) + F(F+1) - I(I+1)] \} \frac{M_F H}{2F(F+1)} \quad (11-13)$$

where  $M_F$  is the projection of the total angular momentum  $\mathbf{F}$  on  $\mathbf{H}$ .

If the molecule is paramagnetic, then the first term of (11-13), which gives the interaction between  $\mathbf{H}$  and the nuclear moment, is usually at least 1000 times smaller than the second term and is negligible. However, in  $^1\Sigma$  molecules,  $\mu_0 g_J$  is of the same order of magnitude as  $\mu_n$ , and both terms of (11-13) are important.

When the Zeeman energy is not much smaller than the hyperfine energy, second-order perturbation theory must be used, or in larger fields a complete secular equation must be solved. The treatment is very similar to that for intermediate Stark effect in a symmetric top when  $K \neq 0$  (cf. page 261). The case has also been discussed by Coester [444]. In magnetic fields strong enough to decouple  $\mathbf{I}$  and  $\mathbf{J}$ , the Zeeman effect is just that found when no hyperfine structure is present. The hyperfine energy can be treated as a small perturbation, and is almost identical with that found in large Stark fields (cf. page 261). The only real difference is that the degeneracy between  $M_J = 1$  and  $M_J = -1$  is not present, so that the complications of transitions between these two levels produced by quadrupole effects do not occur.

**11-6. Zeeman Effects in Ordinary Molecules ( $^1\Sigma$  States).** Most molecules are in  $^1\Sigma$  states and hence have no electronic angular momentum. Their magnetic moments are proportional to the rotational angular

momentum and are approximately the same as magnetic moments of nuclei, or  $\frac{1}{1836}$  that of electrons. Hence, Zeeman effects in these molecules are quite small. Their moments would generally be neglected by comparison with electronic moments in paramagnetic molecules, but when the large electronic moments are not present, these small magnetic moments of  $^1\Sigma$  molecules give noticeable effects.

Consider just the Zeeman effect for a molecule in a  $^1\Sigma$  state with no hyperfine structure. The magnetic moment of the molecule comes partly from the rotation of the positively charged nuclei about the center of mass. This magnetic moment is usually canceled and reversed in sign by the electrons which provide a negative charge rotating with the nuclei. Closed electron shells about the nuclei can be simply thought of as moving with the nuclei, but the orientation of the shells remains fixed in space (slip effect, *cf.* page 213). The behavior of valence electrons is more complicated, since the amount of angular momentum these electrons acquire when the molecule rotates depends on details of their wave functions in the ground and excited states. It is expected that valence electrons will often have enough angular momentum to produce a magnetic moment larger than that due to the sum of the moments produced by the nuclei and bound electrons. Hence the observed sign of the magnetic moment of most molecules should be that produced by a negative charge rotating with the molecule.

The interaction between an external magnetic field and the electrons in a rotating molecule is given by terms similar to the last term in Eq. (8-27). That is,

$$\Delta W = -2 \sum_n \sum_{g'} \sum_g \mu_0 \hbar^2 \frac{J_g H_{g'}}{A_g} \frac{(0|L_g|n)(n|L_{g'}|0)}{W_0 - W_n} \quad (11-14)$$

For a linear molecule, (11-14) can be reduced, as was (8-36), to the form

$$\Delta W = -4\mu_0 B \hbar \mathbf{J} \cdot \mathbf{H} \sum_n \frac{|(0|L_x|n)|^2}{W_0 - W_n} \quad (11-15)$$

For  $N$  electrons in spherical orbits about a nucleus which is a distance  $\tau$  from the center of mass of the molecule, (11-15) may be further reduced to a form similar to (8-33)

$$\Delta W = \frac{\mu_0}{A} N m \tau^2 \mathbf{J} \cdot \mathbf{H} \quad (11-16)$$

where  $m$  is the electron mass. Remembering from Chap. 8 that the spherical electron shells move with the nuclei, but slip so that they remain fixed in orientation, one can obtain (11-16) from the following simple classical calculation. The molecular angular momentum is  $\hbar \mathbf{J}$ , and the fraction of this momentum carried by the  $N$  electrons is  $N m \tau^2 / A$ . Since the magnetic energy due to electron motion is  $\Delta W = -\mathbf{p}_L \cdot \mathbf{H} = \mu_0 \mathbf{L} \cdot \mathbf{H}$ , where now  $\mathbf{L} = (N m \tau^2 / A) \mathbf{J}$ , expression (11-16) is easily obtained.



So far the magnetic moment due to motion of the nuclear charges has been neglected. These charges must give a magnetic energy essentially the same as that to be expected from electrons closely bound to the nucleus in a spherical shell but, of course, of opposite sign. If the nuclear charge is  $+Ze$  and there are  $N$  electrons in closed shells around the nucleus, then the net charge due to the nucleus and electrons is  $(Z - N)e = N_s e$ . The net magnetic energy produced by nuclei and the spherical shells of electrons which may surround them is similar to (11-16), but with a modified charge.

$$\Delta W = - \sum_n \frac{\mu_0 N_s m \tau_s^2}{A} \mathbf{J} \cdot \mathbf{H} \quad (11-17)$$

where  $N_s$  is the net charge (nucleus and bound electrons) in units of the proton charge about the nucleus  $s$ , and  $\tau_s$  is its distance from the center of mass.

The magnetic energy due to valence electrons which are not spherically distributed about nuclei must be obtained from an expression like (11-15). Hence

$$\Delta W = -2\mu_0 B \left[ \sum_s \frac{N_s m \tau_s^2}{\hbar^2} + 2 \sum_n \frac{|(0|L_x|n)|^2}{W_0 - W_n} \right] \mathbf{J} \cdot \mathbf{H} \quad (11-18)$$

where  $B$  is the rotational constant  $h/8\pi^2 A$ , and  $L_x$  is the component of angular momentum of the valence electrons perpendicular to the molecular axis. It should be noted that (11-18) has the form

$$\Delta W = -\mu_n g_J \mathbf{J} \cdot \mathbf{H} = -\mu_n g_J M_J H \quad (11-19)$$

where  $g_J$  can be written  $g$  since it is independent of  $J$ .  $\mu_n$  is the nuclear magneton, which is less than  $\mu_0$  by  $m/M$ , the ratio of the electron mass to that of the proton. The Zeeman splitting for such a molecule is hence given by the simple spectra for  $g_{J_1} = g_{J_2}$  of Fig. 11-1.

If only one excited state of the valence electrons is important and pure precession is assumed, one can reduce (11-18) in analogy to (8-35) to

$$\Delta W = -2\mu_0 B h \left[ \sum_s \frac{N_s m \tau_s^2}{\hbar^2} - \frac{L(L+1)}{2(W_\Pi - W_\Sigma)} \right] M_J H \quad (11-20)$$

where  $W_\Pi - W_\Sigma$  is the excitation energy of the lowest excited electronic state, and  $L$  the precessing angular momentum of the valence electrons.

Except for the cases where hydrogens rotate, such as in  $H_2$  and  $NH_3$ , it seems likely that the second term of (11-18) or (11-20) dominates, and that hence molecular  $g$  factors are negative. That is, the magnetic moments of rotating molecules can be expected to have the sign given by rotating negative charges. This is true for OCS and OCSe, the only heavy molecules for which the sign of  $g$  has so far been measured.



The Zeeman effect for a general asymmetric rotor in a  $^1\Sigma$  state is similar in principle to that of a linear molecule but, of course, more complicated. The magnetic moment due to electrons is still given by (11-14), and the moment produced by the motion of the nuclei can be calculated by semiclassical methods which are simple enough in principle. However, actual expressions for the molecular magnetic moments are rather complicated. The molecular magnetic moment along one of the principal axes of inertia of the molecule can always be written [682]

$$\mu_x = \mathfrak{M}_{xx}\Omega_x + \mathfrak{M}_{xy}\Omega_y + \mathfrak{M}_{xz}\Omega_z = \mathfrak{M}_{xx}\hbar \frac{J_x}{I_x} + \mathfrak{M}_{xy}\hbar \frac{J_y}{I_y} + \mathfrak{M}_{xz}\hbar \frac{J_z}{I_z} \quad (11-21)$$

where the  $\mathfrak{M}$ 's are components of a symmetric dyadic or tensor whose values depend only on the molecule, and  $I_x$ ,  $I_y$ ,  $I_z$  are the principal moments of inertia. The  $\Omega$ 's are components of angular velocity about the principal axes of inertia. Expressions similar to (11-21) can be written for  $\mu_y$  and  $\mu_z$ . The principal axes of the dyadic  $\mathfrak{M}$  do not necessarily coincide with the principal axes of inertia. However, in molecules with symmetry it is often possible to simplify (11-21). For example, in  $\text{H}_2\text{O}$ , symmetry arguments show that the principal axes of inertia must coincide with those of the dyadic  $\mathfrak{M}$ , so that

$$\mu_x = \mathfrak{M}_{xx}\hbar \frac{J_x}{I_x} \quad \mu_y = \mathfrak{M}_{yy}\hbar \frac{J_y}{I_y} \quad \mu_z = \mathfrak{M}_{zz}\hbar \frac{J_z}{I_z}$$

The Zeeman energy is  $-\mathbf{u} \cdot \mathbf{H} = -[\mu \cos(\mu H)]_{av}H$ , where  $\cos(\mu H)$  is the cosine of the angle between the net magnetic moment  $\mathbf{u}$  and the field  $\mathbf{H}$ . Eshbach and Strandberg [682] have given matrix elements of  $\mu \cos(\mu H)$  for symmetric-top wave functions, and from these,

$$[\mu \cos(\mu H)]_{av}$$

for an asymmetric top may be found using expansions of the type (4-17). In the case of a symmetric top, the average value of  $\mu \cos(\mu H)$  is [592], [682]

$$\begin{aligned} [\mu \cos(\mu H)]_{av} &= (JKM|\mu_z|JKM) \\ &= \mu_n M \left[ g_{xx} + (g_{zz} - g_{xx}) \frac{K^2}{J(J+1)} \right] \end{aligned} \quad (11-22)$$

where  $\mu_n$  = the nuclear magneton

$$g_{xx} = g_{yy} = \hbar \mathfrak{M}_{xx} / I_x \mu_n$$

$$g_{zz} = \hbar \mathfrak{M}_{zz} / I_z \mu_n \quad (z \text{ is the symmetry axis})$$

$$M = \text{projection of } J \text{ on } H$$

It should be noted that the Zeeman energy can also be written, as mentioned above,  $\Delta W = -\mu_n g_J \mathbf{J} \cdot \mathbf{H}$ , where  $g_J = \frac{\mu_{av}}{\mu_n J}$  for the state  $M = J$ .

For a linear molecule where  $K = 0$ , (11-22) gives the form (11-19).

The symmetric tops for which molecular  $g$  factors have been measured are the second group of molecules in Table 11-1. In  $\text{NH}_3$  the general correctness of the form (11-22) has been checked experimentally for a variety of values of  $J$  and  $K$  [592], [682] and values  $g_{xx} = +0.560$ ,  $g_{zz} = +0.484$  obtained. The complication of hyperfine structure is present in  $\text{NH}_3$ , so that the Zeeman effect must be obtained from (11-13).

TABLE 11-1. MOLECULAR  $g$  FACTORS FOR MOLECULES IN  $^1\Sigma$  STATES

$g_J = \mu/J\mu_n$ , where  $\mu$  is the molecular magnetic dipole moment,  $\mu_n$  a nuclear magneton, and  $\hbar J$  the angular momentum.

Molecule	$g$ factors	Reference
$\text{H}_2$	$0.88291 \pm 0.00007$	[695a]
$\text{N}_2\text{O}$	$\pm 0.086 \pm 0.004$	[592]
$\text{OCS}$	$-0.025 \pm 0.002$	[682]
$\text{OCS}$	$-0.019 \pm 0.002$	[806a]
$\text{NH}_3$	$g_{zz} = 0.484 \pm 0.007$	[592] [682]
	$g_{xx} = g_{yy} = 0.560 \pm 0.007$	[682]
$\text{CH}_3\text{F}$	$g_{xx} = \pm 0.08$	[784]
$\text{CH}_3\text{CCH}$	$g_{zz} = \pm 0.30$	[784]
	$ g_{xx}  \ll  g_{zz} $	
$\text{H}_2\text{O}$	$g_{aa} = 0.585$	[592] [742]
	$g_{bb} = 0.742$	
	$g_{cc} = 0.666$	
$\text{H}_2\text{S}$	$g_J = \pm 0.24$ for $1_{01}$ and $1_{10}$ rotational states	[783]
$\text{O}_3$	$g_J = \pm 1.54 \pm 0.09$ for $1_{11}$ rotational state	[875]
	$g_J = 0.15 \pm 0.03$ for $2_{02}$ state	
$\text{SO}_2$	$g_J = \pm 0.084 \pm 0.010$ for $7_{26}$ and $8_{17}$ states	[592]
$\text{CH}_3\text{OH}$	$g_{zz} = \pm 0.078$	[592]
$\text{KClFeCl}_2$	$g_J = \pm 0.5$	[952a]
$\text{KBrFeBr}_2$	$g_J = \pm 0.25$	[952a]

Asymmetric rotors for which Zeeman effects have been studied are given in the last group of molecules of Table 11-1. The case of  $\text{H}_2\text{O}$  and  $\text{HDO}$  is particularly interesting since Zeeman effects on several lines have been measured, and since  $\text{H}_2\text{O}$  and  $\text{HDO}$  are similar electromagnetically. Schwarz [742] has related the  $g$  factors for these molecules and given the values listed in Table 11-1 for  $\text{H}_2\text{O}$ .  $g_{aa}$  indicates the  $g$  factor for the direction of smallest moment of inertia,  $I_a$ .  $\text{SO}_2$  is, of course, rather similar to  $\text{H}_2\text{O}$ , but so far the values of  $g_J$  for  $\text{SO}_2$  are known only for the  $8_{17} \leftarrow 7_{26}$  transition, for which the  $g$  factor is given in the table. The compounds  $\text{KClFeCl}_2$  and  $\text{KBrFeBr}_2$  have particularly large values of  $g_J$  for such heavy molecules. They appear to be cases where some excited electronic level lies rather close to the ground level and hence

makes large contributions to  $g_J$  of the type given by the second term of (11-18).

In  $\text{H}_2\text{O}$  the dyadic  $\mathfrak{M}$  has principal axes which coincide with the principal axes of inertia as pointed out above.  $\text{HDO}$  is electrically similar to  $\text{H}_2\text{O}$ , and hence if the center of gravity of  $\text{HDO}$  were in the same place as that for  $\text{H}_2\text{O}$ , the principal axes and elements of the dyadic  $\mathfrak{M}$  would be the same for the two molecules. However, in  $\text{HDO}$  the principal axes of inertia would no longer coincide with those for  $\mathfrak{M}$ . Actually the center of gravity of  $\text{HDO}$  is displaced from that of  $\text{H}_2\text{O}$ , which affects the dyadic  $\mathfrak{M}$  because these molecules involve rotating electric dipoles.

Consider as a simple example the case of a positive and negative charge  $Ne$  separated by a distance  $x_0$ . The  $g$  factor is given, from (11-17), by

$$g = \sum_s \frac{N_s M x_s^2}{A}$$

where  $x_s$  is the distance of each charge from the center of gravity,  $M$  is the proton mass, and  $A$  is the moment of inertia. If now the mass of one of the charges is changed so that the center of gravity is shifted by an amount  $\Delta x$  and  $A$  is changed to  $A'$ , the new  $g$  factor becomes

$$g' = \sum_s \frac{N_s M (x_s - \Delta x)^2}{A} = \sum_s \frac{N_s M x_s^2}{A} - \frac{2M \Delta x \sum_s N_s x_s}{A} + \frac{M (\Delta x)^2}{A} \sum_s N_s$$

Using the fact that  $\sum_s N_s e x_s$  is the electric dipole moment  $D_x$  and  $\sum_s N_s e$  is the total charge which is zero, we have then

$$g' = \frac{A}{A'} g - \frac{2M \Delta x D_x}{eA}$$

Here the symbol  $D$  is used for electric dipole moment rather than the usual  $\mu$  in order to avoid confusion with the magnetic moment  $\mu$ . More generally, one can show that, if the center of gravity of a molecule is shifted with respect to the principal axes of  $\mathfrak{M}$  by an amount  $x, y, z$ , components of the new dyadic  $\mathfrak{M}'$  may be obtained from those of the old dyadic  $\mathfrak{M}$  by the following relations [742]:

$$\begin{aligned} \mathfrak{M}'_{xx} &= \mathfrak{M}_{xx} - \frac{2M\mu_n}{e\hbar} (yD_y + zD_z) \\ \mathfrak{M}'_{yy} &= \mathfrak{M}_{yy} - \frac{2M\mu_n}{e\hbar} (xD_x + zD_z) \\ \mathfrak{M}'_{zz} &= \mathfrak{M}_{zz} - \frac{2M\mu_n}{e\hbar} (xD_x + yD_y) \end{aligned} \quad (11-23)$$

where  $D_x$ ,  $D_y$ , and  $D_z$  are components of the electric dipole moment



along the principal axes of  $M$ . Thus the dyadic  $\mathfrak{M}$ , and hence the molecular  $g$  factors for HDO or D<sub>2</sub>O, are derivable from those for H<sub>2</sub>O, assuming the geometry and dipole moment of this molecule are known.

It is interesting to note that Eqs. (11-23) afford a means of determining the sign of molecular dipole moments, in contrast to Stark effects which can only determine dipole moment magnitudes. Thus if an isotopic substitution shifts the center of gravity of a molecule sufficiently so that the change in  $M$  due to the molecular dipole moment can be observed, the sign of this change will allow a determination of the sign of the terms involving components of the dipole moment.

**11-7. Combined Zeeman-Stark Effects.** Both electric and magnetic fields have been applied to molecules a number of times by microwave spectroscopists. However, in such cases the electric field has been used only as a means of sensitive detection by Stark modulation, and no experimental study of combined Zeeman-Stark splittings has been attempted. Rather complete theoretical description of the combined Zeeman-Stark effect has been worked out, however [444]. This work includes treatment of molecules with hyperfine structure due to one nucleus with quadrupole moment and various types of intermediate- and strong-field conditions.

If the magnetic and electric fields are parallel, then weak-field Zeeman and Stark effects are simply additive, since the molecular wave functions are the same for either field (projection  $M$  of  $J$  on either field is a good quantum number). If the Stark effect varies linearly with the electric field (first-order Stark effect), then each different value of  $M$  produces a different Stark component, and the application of a parallel magnetic field cannot further split this component but may change its frequency. If the Stark effect is proportional to the square of the electric field (second-order Stark effect), then positive and negative values of  $M$  coincide in the same component and may be further split by the magnetic field.

If the magnetic and electric fields are not parallel, then  $M$  is no longer a good quantum number and the frequencies of the components of the lines depend in a more complex way on the strengths of the two fields. In addition, the relative intensities of the components depend on the two field strengths. The reader is referred to Coester's work [444] for details of the crossed electric- and magnetic-field case, and for some of the intermediate-field cases.

**11-8. Transitions between Zeeman Components.** Transitions between the Zeeman components of an energy level, corresponding to  $\Delta J = 0$ ,  $\Delta M = \pm 1$ , occur and give frequencies which increase more or less linearly with the magnetic field  $H$ . If a molecule has a magnetic moment as large as a Bohr magneton, then the Zeeman splittings can be so large that transitions between them fall in the microwave region. Since  $\mu_0/h$  is about 1.4 Mc/oersted, a magnetic field of 15,000 oersteds

would give a Zeeman splitting of 21,000 Mc if the molecular  $g$  factor is unity.

Beringer *et al.* have exploited transitions between Zeeman components in an interesting way to obtain microwave absorption spectra of several paramagnetic gases ([435], [443], [558]). The gas is contained in a cavity between the pole pieces of an electromagnet. The cavity is tuned to some convenient microwave frequency (*e.g.*, 24,000 Mc) and sensitive circuits are arranged to detect absorption of microwaves in the cavity. The magnetic field is then varied until some Zeeman component coincides with the cavity frequency, so that absorption due to the transition is

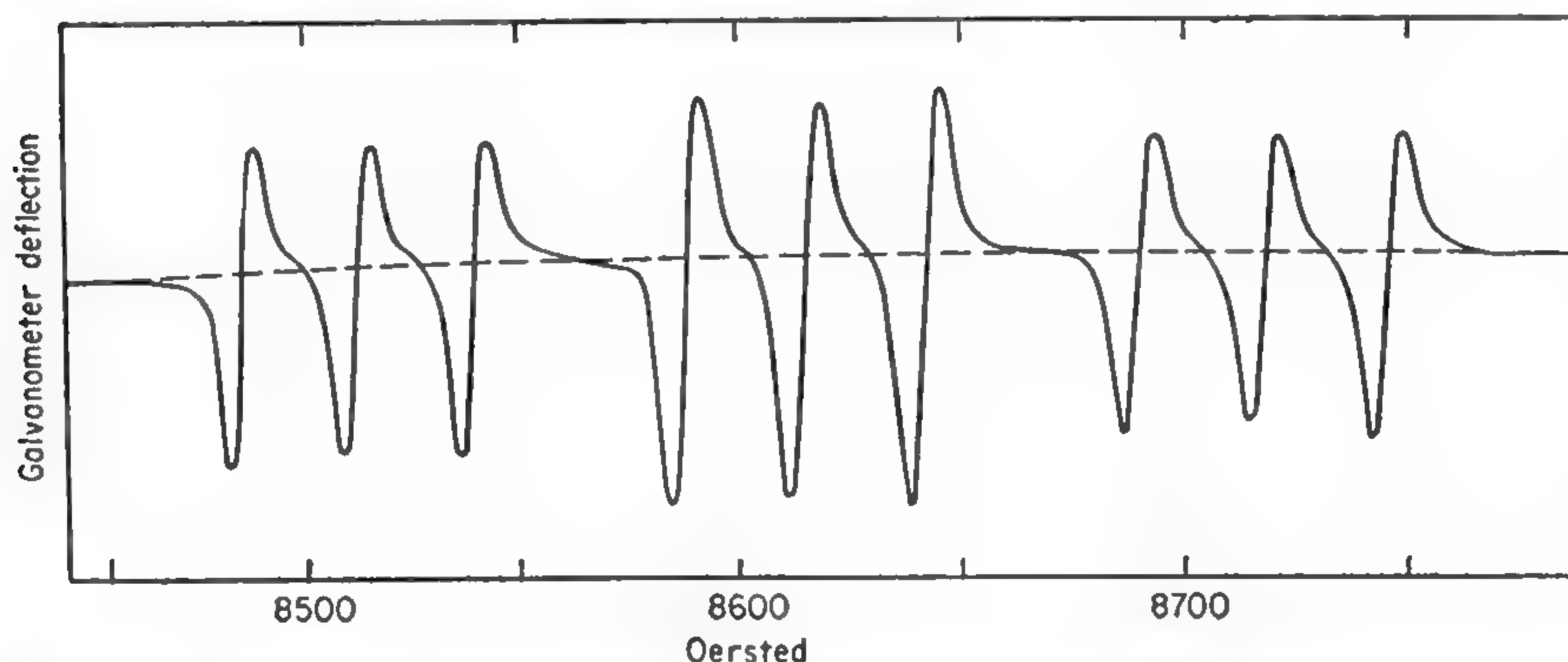


FIG. 11-2. Transitions between Zeeman components of  $\text{N}^{14}\text{O}^{16}$  at a pressure of 1.0 mm Hg. (From Beringer and Castle [435].)

detected. This technique gives a plot of absorption at a fixed frequency due to Zeeman transitions vs. magnetic field instead of the usual rotational transitions vs. frequency. A spectrum of this type for NO is shown in Fig. 11-2. The spectrometer used for Fig. 11-2 presented the derivative of the absorption, which is the reason for the unusual shapes of the lines seen in this figure.

The molecule NO is in a  $^2\Pi$  state, with the vectors coupled according to Hund's case (a). The transitions seen in Fig. 11-2 are between Zeeman components of the  $^2\Pi_{1/2}$  state with  $J = \frac{3}{2}$ , which is the state having the largest  $g$  factor. All other states have  $g$  factors which are small enough to make transitions between their Zeeman components occur at a very much lower frequency in the magnetic fields used. In the fields used, the molecule can be fairly accurately described as a case where the magnetic field is strong enough to uncouple the nuclear spin of  $\text{N}^{14}$  from the molecule ( $\text{O}^{16}$  has zero spin), but not sufficiently strong to uncouple  $\mathbf{S}$  and  $\mathbf{L}$ . A diagram of the resulting energy levels is shown in Fig. 11-3.

The hyperfine structure indicated in Fig. 11-3 is in fact very much smaller than the separation between the main levels shown as stage (b). The latter separations can be obtained from (11-4) and are approximately

9,400 Mc. The magnetic hyperfine structure is, according to (8-7),  $\Delta W_\mu = [a\Lambda + (b + c)\Sigma]\mathbf{I} \cdot \mathbf{k}$ . From the vector model,

$$\mathbf{I} \cdot \mathbf{k} = \frac{M_I M_J \Omega}{J(J + 1)} = \frac{2}{5} M_I M_J$$

so that  $\Delta W_\mu = A M_I M_J$ .  $A$  is found experimentally to be  $29.8 \pm 0.3$  Mc. The hyperfine energy due to quadrupole effects in this strong-field case

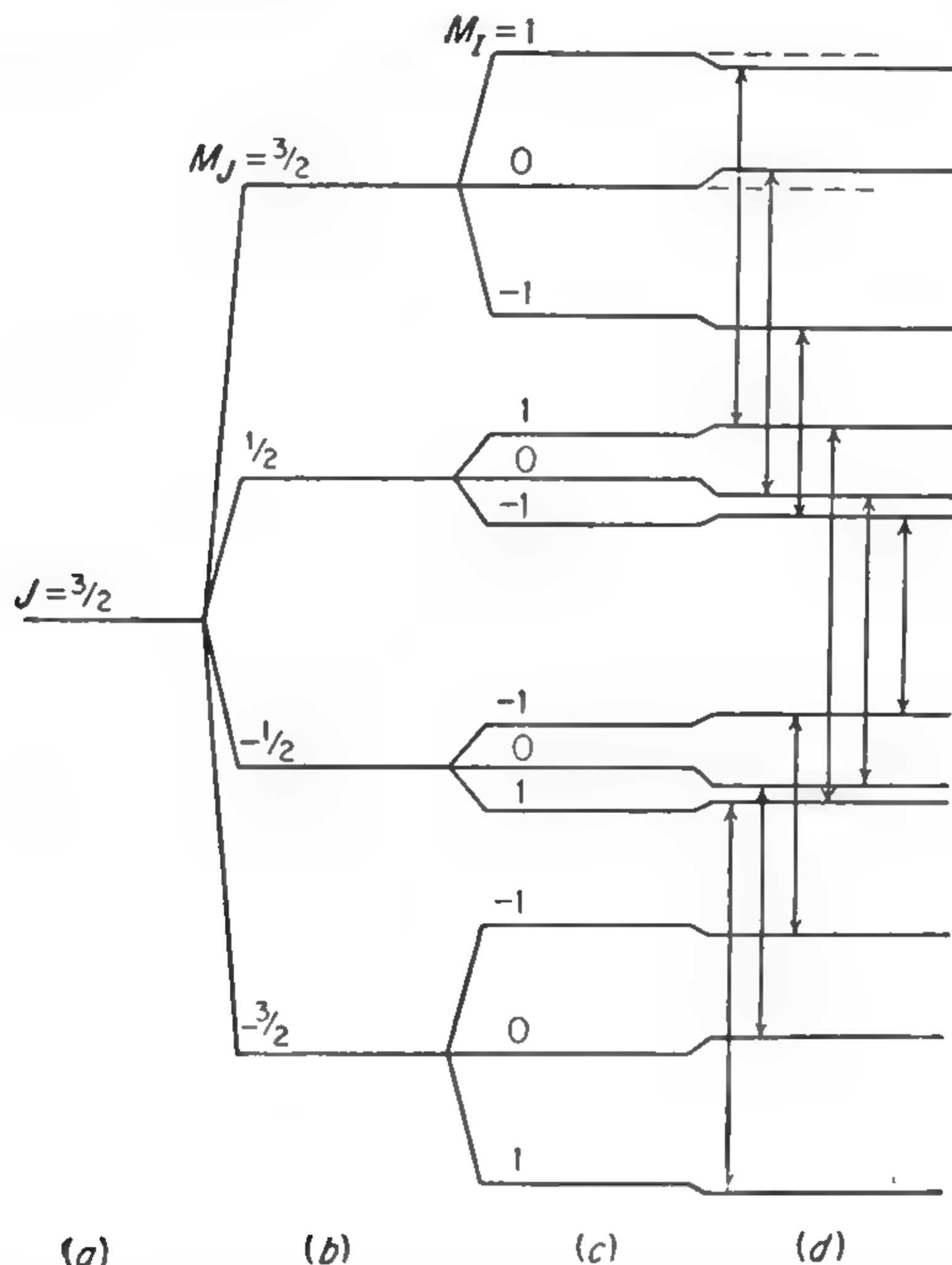


FIG. 11-3. Energy level diagram of the  $J = 3/2$  level of the  $^2\Pi_{1/2}$  state of  $\text{N}^{14}\text{O}^{16}$ . Stage (a) is in the absence of a magnetic field. Stage (b) shows the energy levels split by the presence of a magnetic field, but without hyperfine structure. Stage (c) shows the hyperfine structure due to the  $\text{N}^{14}$  nuclear magnetic moment. Stage (d) includes the energy due to the  $\text{N}^{14}$  electric quadrupole moment. (After Beringer and Castle [435].)

is given by (10-32), with a quadrupole coupling constant of  $-1.7 \pm 0.5$  Mc.

Each of the three groups of three lines shown in Fig. 11-2 corresponds to a particular  $M_J$  transition with hyperfine splitting. The above simple theory, where from (11-4)

$$\Delta W_H = \frac{2}{5}(\Lambda + 2.002\Sigma)M_J\mu_0H$$

would make the centers of the three groups coincide. Their separation is due to small second-order effects proportional to  $H^2$ . More detailed



discussion and more exact calculation of this spectrum have been given in several places ([468], [495], [686]).

Transitions between Zeeman levels in NO may occur because of interaction between the microwave field and either the molecular magnetic moment or its electric moment. The above discussion applies to either, except that transitions involving the electric moment involve  $\Lambda$ -type doubling. Allowed electric dipole transitions are similar to those allowed in a linear molecule where  $l$ -type doubling occurs, and these may be seen from expression (2-16) always to involve transitions between the two different states of the doublet. Hence the Zeeman transitions may be expected to be doublets separated by twice the  $\Lambda$ -type doubling if electric dipole transitions occur. Either magnetic or electric dipole transitions may be singled out by orienting the desired microwave field perpendicular to the fixed magnetic field and the other parallel to it. Beringer and Rawson were thus able to detect and measure the  $\Lambda$  doubling in NO as 1.7 Mc.

Transitions between Zeeman levels in  $O_2$  have also been examined [558], [990]. Although the Zeeman effect on the  $\rho$ -type triplets of the  $O_2$  spectrum is more complex than that for NO discussed above, and intermediate-field conditions occur, a fairly accurate theory for the observed transitions between Zeeman levels can be developed [74], [467], [990].

## CHAPTER 12

### THE AMMONIA SPECTRUM AND HINDERED MOTIONS

**12-1. Introduction.** Because of the intensity and richness of its spectrum, ammonia has played a major role in the development of microwave spectroscopy. It has provided a large number of easily observable lines on which to try both experimental techniques and theory.  $\text{NH}_3$  also provides the simplest and most thoroughly worked out example of a class of spectra which will continue to occupy and puzzle microwave spectroscopists for many years—spectra involving hindered motions.

The most important hindered motions all involve the quantum-mechanical tunneling effect. That is, they are motions which cannot occur in classical mechanics because of energy considerations, but are allowed by the wave nature of quantum mechanics. For example, in the ground vibrational state of  $\text{NH}_3$ , the molecule does not have enough energy to allow the nitrogen to be found in the plane of the hydrogens because of the large potential-energy hump at this position, as indicated in Fig. 12-1. Its actual penetration of the plane of the hydrogens and rapid vibration from one side of it to the other is called the tunnel effect because, if the nitrogen cannot climb the potential hill, it must “tunnel” in order to get through. In principle, the  $\text{NH}_3$  inversion is a vibrational motion. Although vibrations normally give frequencies in the infrared region, the  $\text{NH}_3$  inversion is so much slowed down by the hindering potential that its frequency lies in the microwave region. The qualitative change from ordinary vibrational levels where there is no hump in the potential to vibrational levels occurring in pairs when the hindering hump occurs is discussed in Chap. 3. When the vibrational energy is so great that the  $\text{NH}_3$  molecule has sufficient energy to invert classically, the vibrational levels no longer occur in close pairs but are similar to more normal equally spaced vibrational levels. However, they are still markedly influenced by the presence of the potential hump, and hence in this case of no “tunneling,” one may still speak of some hindering of the motion.

Another type of hindered motion is the rotation of one part of a molecule with respect to the remainder. Thus the hydrogen attached to oxygen in  $\text{CH}_3\text{OH}$  (Fig. 12-2) has three possible positions of equal energy but must tunnel through a potential hump between them as indicated in Fig. 12-3. Hence the rotation of this hydrogen around the C—O bond

is hindered. Similarly, the methyl group in  $\text{CH}_3\text{CF}_3$  (Fig. 12-4) has three positions of equal energy separated by potential humps. Usually hindered motions do involve two or more positions of equal energy. If these positions are only minima, which are not equal in energy, many of

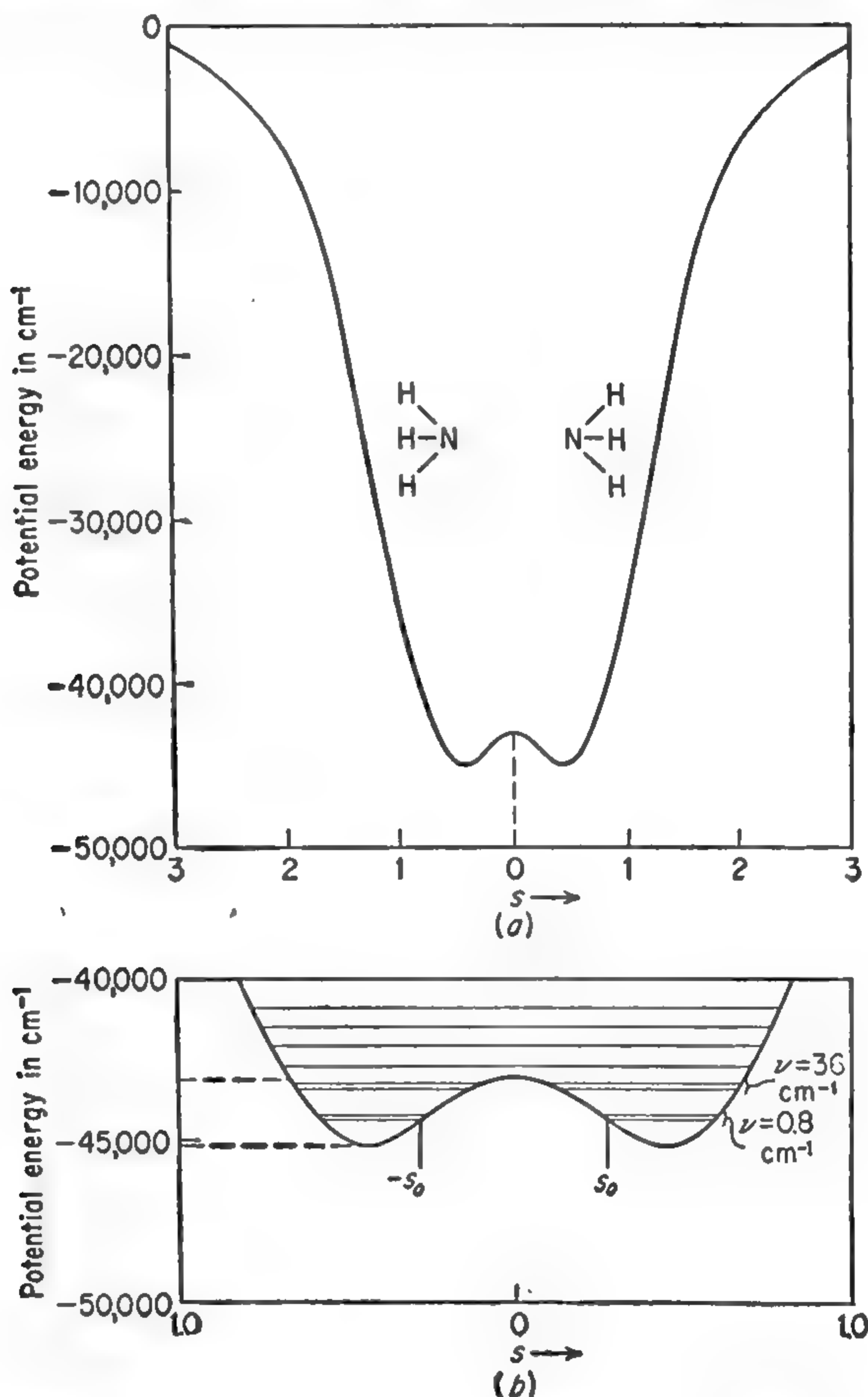


FIG. 12-1. Potential curve of  $\text{NH}_3$ . The variable  $s$  is a measure of the distance between the nitrogen and the plane of the hydrogens. (b) shows the lower part of the potential curve in more detail, and the energy levels.

the characteristic properties and interesting features of the hindered motions considered here do not occur.

When hindered motions have frequencies in or near the microwave region, the spectra are often quite difficult to interpret because the number of lines falling in the microwave region is greatly increased, and because there is no exact solution for the energy levels in these cases. In



addition, the frequencies of these motions are so strongly dependent on the potential humps or barriers that usually no helpful estimates of the frequency to be expected in a molecule can be made. However, hindered motions are of considerable importance to a knowledge of molecular structure and to chemistry. The difficulties they produce will be frequently encountered since hindered motions occur

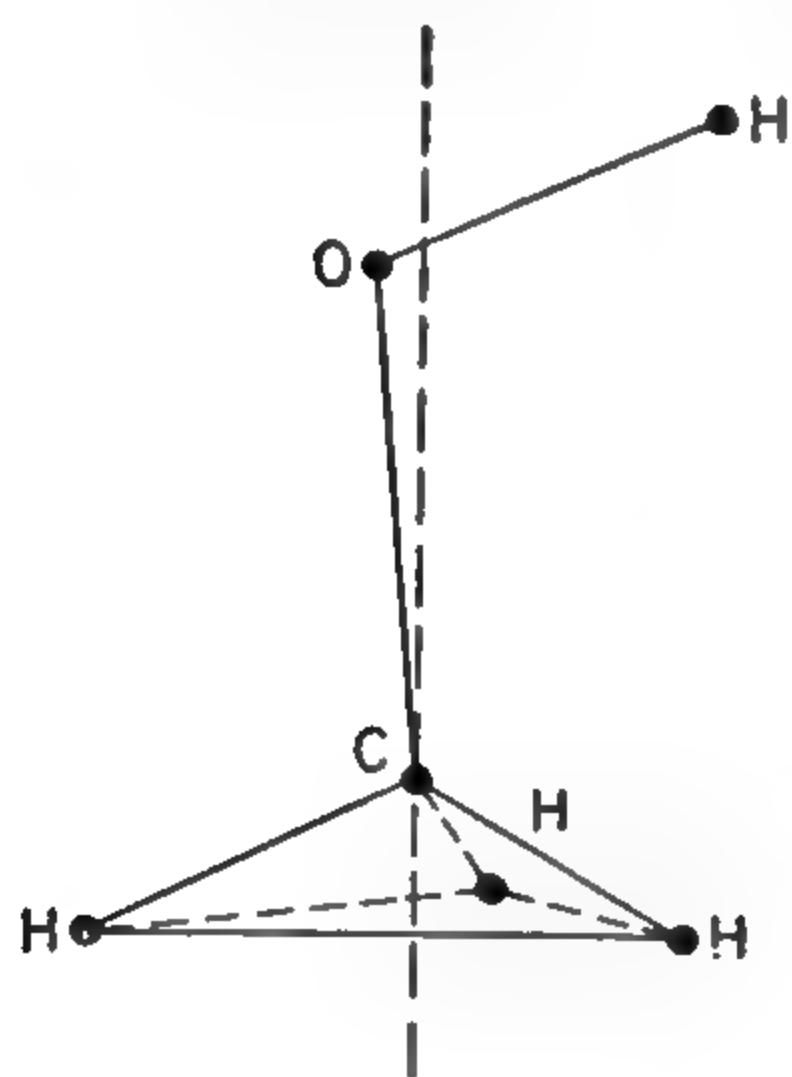


FIG. 12-2. Structure of methyl alcohol. The O—H bond may rotate about the axis with respect to the  $\text{CH}_3$  group, but this rotation is hindered by mutual interaction.

in a sizable fraction of the more complex gaseous molecules.

**12-2. Inversion Frequency of  $\text{NH}_3$ .** Consider now the vibration of  $\text{NH}_3$  in which the N moves perpendicular to the plane of the hydrogens, and which would lead to inversion if the N crossed this plane. As a function of the distance  $s$  of the nitrogen from the plane of the hydrogens, the potential is approximately as shown in Fig. 12-1. The molecule may vibrate at a fairly rapid rate in the potential minima with N on one side of the hydrogen plane, and after a large number of such vibrations, it may penetrate the potential barrier and begin oscillations on the other side. The rapid vibrations lie in the infrared region ( $950\text{ cm}^{-1}$ ), whereas the frequency of penetration back and forth is the inversion frequency which occurs for the ground state in the microwave range ( $0.8\text{ cm}^{-1}$ ).

The approximate energy of the ground vibrational state is indicated in Fig. 12-1, and equals the potential energy  $V(s)$  at  $s = \pm s_0$ , so that classically the nitrogen atom cannot be closer to the plane of the hydrogens than  $s_0$ .

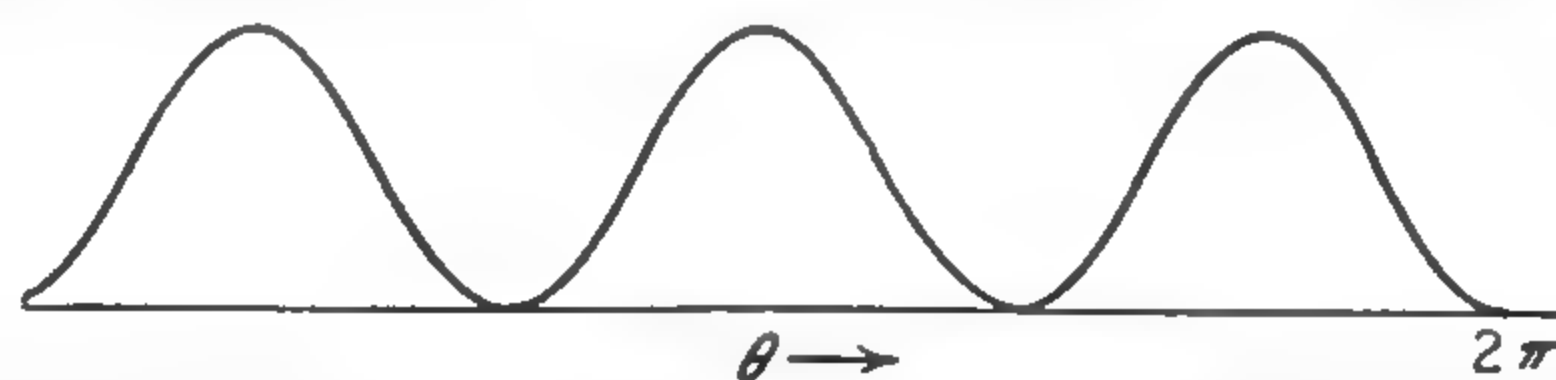


FIG. 12-3. Variation of the potential energy of  $\text{CH}_3\text{OH}$  with the relative rotation  $\theta$  of the O—H bond and  $\text{CH}_3$  group about the molecular axis. Probably the potential minima correspond to the hydrogen in O—H being a maximum distance from the nearest hydrogen of  $\text{CH}_3$ .

The inversion frequency has been calculated approximately by Denison and Uhlenbeck [33] as

$$\nu = \frac{\nu_0}{\pi A^2} \quad (12-1)$$

where  $A = \exp \left\{ \frac{2\pi}{h} \int_0^{s_0} [2\mu(V(s) - W)]^{\frac{1}{2}} ds \right\}$

$\nu_0$  = frequency of vibration in one of the potential minima

$\mu$  = reduced mass for the vibrational motion

$W$  = total vibrational energy

This expression was obtained by the Wentzel-Kramers-Brillouin (WKB) method which uses approximate wave functions in the various regions of the motion and matches them at the boundaries of these regions. The significance of (12-1) may perhaps better be made clear by the following approach.

Let the wave function corresponding to the lowest state of simple harmonic oscillation with the nitrogen on the left side of the hydrogens be  $u_L$  and that for the nitrogen on the right be  $u_R$ . The true molecular wave functions, having a definite energy, must be either symmetric or antisymmetric with respect to the inversion, so the wave functions for the two inversion levels of the lowest vibrational state must be the combinations

$$\psi_0 = (1/\sqrt{2})(u_L + u_R)$$

and 
$$\psi_1 = (1/\sqrt{2})(u_L - u_R),$$

as shown in Fig. 3-8. If now the N is definitely placed on the left side at a time  $t = 0$ , the appropriate wave function describing the system at that time (and not having one definite energy) is  $\psi = u_L = (1/\sqrt{2})(\psi_0 + \psi_1)$ . If, as noted in Chap. 3, the time variation of the wave function is included, it becomes

$$\psi = \frac{1}{\sqrt{2}} [\psi_0 + \psi_1 e^{2\pi i \nu t}] e^{2\pi i W_0 t/h} \quad (12-2)$$

where  $h\nu$  is the energy difference between the two inversion states and  $W_0$  is the energy of the lower state, which corresponds to  $\psi_0$ . After a time  $t = 1/2\nu$ , the wave function (12-2) becomes

$$\psi = \frac{1}{\sqrt{2}} [\psi_0 - \psi_1] e^{2\pi i W_0 t/h} = u_R e^{2\pi i W_0 t/h} \quad (12-3)$$

so that the nitrogen has moved over to the right side. Only a short time after the nitrogen has been initially placed on the left, the part of (12-2) in brackets may be written by expanding the exponential

$$\begin{aligned} \psi &= \left[ \frac{1}{\sqrt{2}} (\psi_0 + \psi_1) + \psi_1 \frac{2\pi i \nu t}{\sqrt{2}} + \dots \right] e^{2\pi i W_0 t/h} \\ &= u_L + \pi i \nu t (u_L - u_R) + \dots \end{aligned} \quad (12-4)$$

so that the amplitude of the wave function on the right has grown to  $\pi \nu t$ . This gives a measure of the rate of penetration of the potential

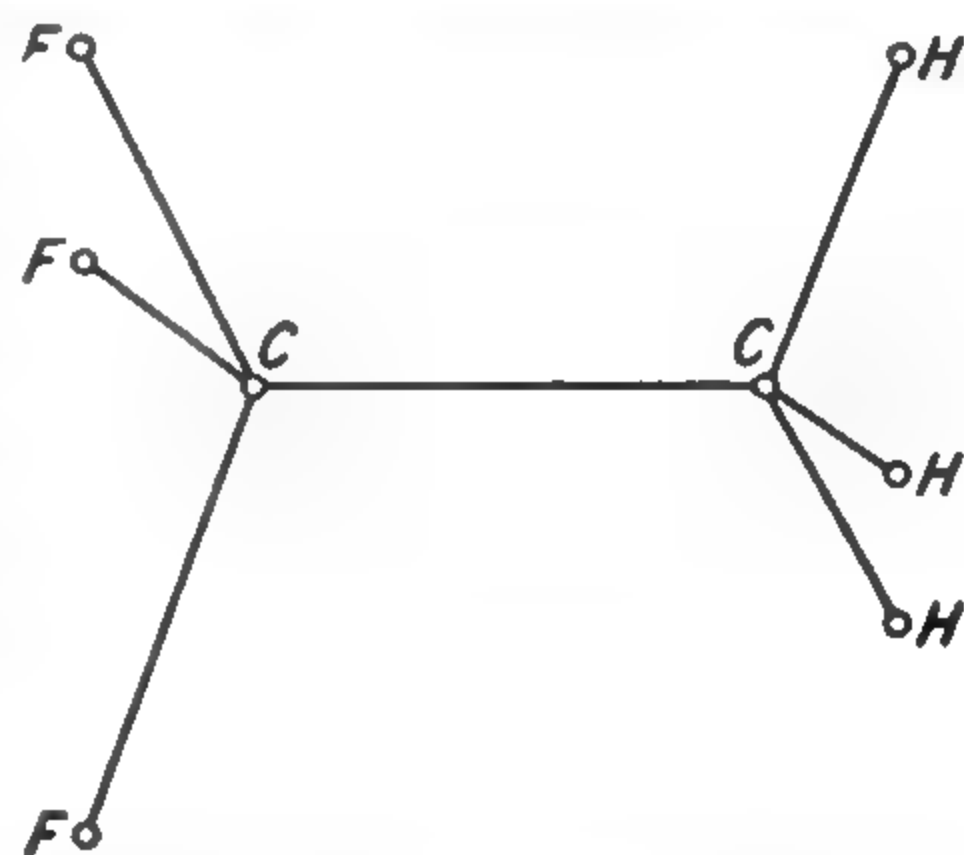


FIG. 12-4. Structure of  $\text{CH}_3\text{CF}_3$  where rotation of the  $\text{CH}_3$  group with respect to the  $\text{CF}_3$  group is hindered by mutual interaction.

barrier in terms of the frequency of inversion. This rate of penetration may also be calculated from the "tunnel effect."

Consider now the nitrogen striking the barrier at  $s = -s_0$  from the left. Its wave function will partly penetrate the barrier and extend over into the right-hand potential minimum. The amount of penetration can be roughly evaluated by examining Schrödinger's equation in the classically forbidden region.

$$\frac{d^2\psi}{ds^2} - \frac{2\mu}{\hbar^2} (V - W)\psi = 0 \quad (12-5)$$

An approximate solution to (12-4) is

$$\psi = \exp \left\{ -\frac{1}{\hbar} \int_{-s_0}^s [2\mu(V(s) - W)]^{\frac{1}{2}} ds \right\} \quad (12-6)$$

if  $V$  does not vary too rapidly with  $s$ . Since  $V - W$  is positive in the classically forbidden region, this corresponds to an exponentially decreasing function which has unity value at the boundary where the nitrogen strikes (the increasing exponential which is also a solution is omitted, since it would give the N the largest probability of being found on the right). The amplitude of the wave function which penetrates the boundary is then

$$\begin{aligned} \psi_{s=s_0} &= \exp \left\{ -\frac{1}{\hbar} \int_{-s_0}^{s_0} [2\mu(V - W)]^{\frac{1}{2}} ds \right\} \\ &= \exp \left\{ -\frac{2}{\hbar} \int_0^{s_0} [2\mu(V - W)]^{\frac{1}{2}} ds \right\} = \frac{1}{A^2} \end{aligned} \quad (12-7)$$

Now in a time  $t$  which is large enough for the nitrogen to oscillate on the left side many times, but small compared with the time required for inversion, the nitrogen will strike the left side of the potential barrier  $\nu_0 t$  times, where  $\nu_0$  is the vibrational frequency. Each time it may be considered to partially penetrate and transmit an amplitude  $1/A^2$  to the right side. The transmitted amplitudes add up to give a total amplitude after time  $t$  of  $\nu_0 t/A^2$ , so that the probability of penetration in time  $t$  is  $(\nu_0 t/A^2)^2$ . This is similar to, but differs slightly from, the usual expression for radioactive decay or other types of barrier penetration by tunneling ([305], p. 22), because the transmitted wave on the right-hand side of the barrier is trapped in an identical potential minimum and is added to by successive transmitted waves. Equating the amplitude  $\nu_0 t/A^2$  to the amplitude for  $u_R$  in (12-4), we have

$$\pi \nu t = \frac{\nu_0 t}{A^2} \quad \text{or} \quad \nu = \frac{\nu_0}{\pi A^2} \quad (12-8)$$

which is the result obtained by Dennison and Uhlenbeck.

In the ground state of  $\text{NH}_3$ ,  $\nu/\nu_0 \approx 1200$ , so that  $A^2 \approx 400$  or  $e^6$ .



Because  $A^2$  is large and varies exponentially with  $\mu^{\frac{1}{2}}$  or  $(V - W)^{\frac{1}{2}}$ , changes in either of these quantities can very drastically affect the inversion frequency  $\nu$ . For example, if the reduced mass  $\mu$  is increased by a factor of 2, such as would be roughly done by changing from  $\text{NH}_3$  to  $\text{ND}_3$ ,  $\nu$  decreases by  $e^{6(\sqrt{2}-1)}$  or a factor of 11. The inversion frequency is correspondingly sensitive to the potential, and most molecules have such high potentials and heavy masses that the inversion frequencies are less than 1 cycle/sec. Many molecules invert so slowly that they have not succeeded in inverting during the few billion years' life of our planet.

$\text{NH}_3$  in the first excited level of this vibrational mode has a much higher inversion frequency because of the increased value of  $W$ . Dennison and Uhlenbeck [33] were able to assume a simple shape for the potential barrier and obtain values for the inversion frequencies in the ground and excited states which agreed roughly with experimental observations.

The exact form of the potential barrier assumed is not critical, since  $A$  depends only on an integral of this energy, and not on details of shape. However, Manning [61] found a potential function which has the general shape to be expected for  $\text{NH}_3$ , and for which the wave equation could be more easily solved and accurate values for the energies obtained. Manning's potential function is

$$\frac{V}{hc} = 66,551 \operatorname{sech}^4 \frac{x}{2\rho} - 109,619 \operatorname{sech}^2 \frac{x}{2\rho} \quad (12-9)$$

where  $V/hc$  = potential in units of  $\text{cm}^{-1}$

$x$  = a coordinate which is dependent on the distance of the nitrogen from the plane of the hydrogens

$\rho = 6.98 \times 10^{-8}/\mu^{\frac{1}{2}}$  where  $\mu$  is the reduced mass in atomic mass units

This potential is zero for large  $s$  (or  $x$ ), is symmetric about  $s = 0$ , and has a peak at  $s = 0$ , where the potential is  $-43,068 \text{ cm}^{-1}$ . It has two minima where the potential is  $-45,140 \text{ cm}^{-1}$ . The constants in (12-9) are also chosen to give close to the correct equilibrium configuration for the molecule, the vibration frequency, and the correct inversion frequency for one level.

If the distance between hydrogens is assumed to stay constant during the motion so that they move together as a rigid triangle, then  $x$  is taken as equal to  $s$ , the distance between the nitrogen and the plane of this triangle. If  $m$  is the mass of the hydrogens and  $M$  that of nitrogen, then the reduced mass for this case is simply  $\mu = 3mM/(3m + M)$ . However, probably a better approximation to the motion is to assume the N—H distance remains constant, and only the H—N—H angles change with vibration [110]. In this case  $x$  is taken as the distance along an arc moved by the hydrogens from the median plane, *i.e.*, a plane through the nitrogen and perpendicular to the molecular axis. If the angle between

this plane and the N—H bond is taken as  $\alpha$ , the proper reduced mass can be shown to be  $\mu = 3m(M + 3m \sin^2 \alpha)/(3m + M)$ . This reduced mass varies only a small amount with  $\alpha$ , and its value may be assumed to be that at the equilibrium angle of  $\alpha_0 = 21^\circ 49'$ . Different reduced masses in Manning's potential will give different equilibrium heights for the  $\text{NH}_3$  pyramid. However, these heights do not deviate significantly from the observed value.

The values of inversion frequency for various isotopic species of ammonia calculated from Manning's potential are shown in Table 12-1

TABLE 12-1. INVERSION FREQUENCIES OF AMMONIA IN MEGACYCLES

The "first excited vibrational state" ( $\nu_2 = 1$ ) corresponds to approximately  $950 \text{ cm}^{-1}$  excitation of the vibration of the nitrogen against the plane of the hydrogens. The calculated values are given by Manning [61] and Newton and Thomas [306] except for the calculation of  $\text{N}^{14}\text{D}_3$  with the Manning potential, which was done by A. Javan and J. Lotspeich.

	Ground state			First excited vibrational state	
	$\text{N}^{14}\text{H}_3$	$\text{N}^{14}\text{D}_3$	$\text{N}^{15}\text{H}_3$	$\text{N}^{14}\text{H}_3$	$\text{N}^{14}\text{D}_3$
Observed value, Mc.....	23,786	1600	22,705	1,095,000	117,000
Calculated from Manning potential.....	25,000	1250	.....	780,000	83,000
Calculated from Newton-Thomas potential.....	23,800	.....	22,700	690,000	

and compared with experimental results. The potential constants have been chosen to fit some of the data, including the energy of the first vibrational level. The excited vibrational levels are fitted rather satisfactorily by this potential [61]. Although the inversion frequencies are given approximately correctly, it does not seem possible to obtain a really satisfactory fit of all the data with a potential of Manning's type. This will be seen again when fine structure of the inversion spectrum is discussed.

Newton and Thomas [306] used a potential of the form

$$\frac{V}{hc} = \left\{ \left[ \frac{(0.377)^2 - s^2}{0.536 + s^2} \right]^2 - 1 \right\} \times 3.17 \times 10^4 \text{ cm}^{-1} \quad (12-10)$$

where  $s$  is measured in angstrom units. Here the hydrogens are considered to move as a rigid triangle. Values for some of the inversion frequencies calculated by an approximate method [306] from this potential are given in Table 12-1. Form (12-10) for the potential appears to give results which are comparable in accuracy with those from the potential (12-9).

**12-3. Inversion of Other Symmetric Hydrides.** A very simple form of potential has been found by Costain and Sutherland [678] to give fairly accurate values for the inversion frequency of  $\text{NH}_3$ , and has been used to estimate the inversion frequencies of  $\text{PH}_3$  and  $\text{AsH}_3$ . This is a potential of the form

$$V = \frac{3}{2}k_r(\Delta r)^2 + \frac{3}{2}k_\delta(\Delta\delta)^2 \quad (12-11)$$

where  $\Delta r$  = change in the N—H bond length

$\Delta\delta$  = change in the H—N—H bond angle

The force constants  $k_r$  and  $k_\delta$ , as well as the ratio of  $\Delta r$  to  $\Delta\delta$ , can be obtained by a normal coordinate treatment of the observed vibrational frequencies of  $\text{NH}_3$ . Their evaluation gives

$$V = 3.89 \times 10^4(\Delta\delta)^2 \quad \text{cm}^{-1} \quad (12-12)$$

where  $\delta$  is measured in radians. This gives a potential hill of  $2077 \text{ cm}^{-1}$  between the two minima in good agreement with Manning's value of  $2072 \text{ cm}^{-1}$ . In fact, the entire potential curve given by (12-12) is very close to that given by (12-9).

A similar evaluation of the potential hill from vibrational constants and molecular geometry for  $\text{PH}_3$  and  $\text{AsH}_3$  gives the following results [678].

For  $\text{PH}_3$ :

$$V = 5.3 \times 10^4(\Delta\delta)^2 \text{ cm}^{-1} \quad (12-13)$$

Height of potential hill above minimum =  $6085 \text{ cm}^{-1}$

Inversion frequencies:

Ground state =  $0.14 \text{ Mc}$

First excited state =  $7.2 \text{ Mc}$

For  $\text{AsH}_3$ :

$$V = 4.56 \times 10^4(\Delta\delta)^2 \text{ cm}^{-1} \quad (12-14)$$

$\delta_0 = 0.585 \text{ radian}$

Height of potential hill above minimum =  $11,220 \text{ cm}^{-1}$

Inversion frequencies:

Ground state =  $1/2 \text{ cycle/year}$

First excited state =  $1 \text{ cycle/day}$

Thus the inversion splitting of  $\text{PH}_3$  is probably large enough to give a splitting in microwave measurements of the rotational spectrum, whereas  $\text{AsH}_3$  would take two years to go through a cycle of inversion and should hence have no observable splitting. These numbers illustrate the very rapid variation in frequency as the potential barrier height is changed.

**12-4. Fine Structure of the Ammonia Inversion Spectrum Rotation-Vibration Interactions.** Discussion of the inversion spectrum has so far



neglected the rotational motion of the molecule. There is, of course, an interaction between rotation and vibration which in most molecules shows up as a series of closely spaced lines in the rotational spectrum, each being due to different vibrational states. In an inversion spectrum, a type of vibration, there is similarly a series of lines at different inversion frequencies, each corresponding to a different rotational state.

A good qualitative view of the effect of rotation on the inversion spectrum of  $\text{NH}_3$  (or any other molecule) may be obtained from a classical discussion. The rotational frequencies of  $\text{NH}_3$  are considerably higher than the inversion frequencies of the ground state, so that no peculiar resonant interactions occur, but rather the centrifugal forces due to rotation simply change the effective potential in which the molecule vibrates. Consider first a rotation of the molecule about the symmetry axis. The resulting centrifugal force tends to distort the molecule by flattening it or increasing the  $\text{H—N—H}$  angle. Hence as a result of the centrifugal force the hydrogens can somewhat more readily move past the nitrogen and the inversion frequency is increased. The centrifugal force is proportional to the square of the angular momentum about this axis, or to  $K^2$ , so the inversion frequency can be expected to be increased roughly by an amount  $bK^2$ , where  $b$  is some positive constant. Now consider a rotation about an axis perpendicular to the molecular axis. In this case the centrifugal force tends to elongate the  $\text{NH}_3$  pyramid, or decrease the  $\text{H—N—H}$  angle. It is then more difficult for the hydrogens and nitrogen to move into the same plane, and the inversion frequency is decreased. Since the square of the angular momentum perpendicular to the symmetry axis is proportional to  $J(J + 1) - K^2$ , where  $J$  is the total angular momentum quantum number, this type of motion can be expected to decrease the inversion frequency roughly by an amount  $a[J(J + 1) - K^2]$ , where  $a$  is a positive constant. Thus the frequency should be of the form

$$\nu = \nu_0 - a[J(J + 1) - K^2] + bK^2 + \text{higher powers of } J \text{ and } K \quad (12-15)$$

A quantitative calculation of the effects of rotation can be made by considering in detail how the centrifugal forces act on the vibrational and inversion motion. They will affect the inversion frequency through the quantity  $A$  in expression (12-1). Allowing for rotation,  $A$  may be written [110]

$$A = \exp \left\{ \frac{2\pi}{h} \int_0^{s_0 + \delta s} [2\mu(V + \delta V - W - \delta W)]^{\frac{1}{2}} ds \right\} \quad (12-16)$$

where  $\delta V$  and  $\delta E$  represent the respective changes in the potential and vibrational energy as a result of rotation.  $\delta s$  is the change due to value of  $s$  where the kinetic energy is zero. The change in effective potential  $V$  due to centrifugal forces equals simply the change in kinetic energy of

rotation as the molecule vibrates, or

$$\delta V = \hbar^2[J(J+1) - K^2] \left( \frac{1}{2I_A} - \frac{1}{2I_A^0} \right) + \hbar^2 K^2 \left( \frac{1}{2I_C} - \frac{1}{2I_C^0} \right) \quad (12-17)$$

where  $I_A$  and  $I_C$  are the moments of inertia of the molecule as a function of the vibrational coordinate, while  $I_A^0$  and  $I_C^0$  are the values for the molecule in the equilibrium condition. The change  $\delta W$  contributes only a small amount to  $A$ , and  $\delta s$  is quite negligible; so both these quantities will be neglected here. If (12-16) is expanded, assuming  $\delta V$  is small, and the new value of  $A$  is inserted into (12-1), the change in inversion frequency  $\nu$  is

$$\delta \nu = - \frac{2\nu}{\hbar} \int_0^{s_0} \mu \delta V [2\mu(V - W)]^{-1/2} ds \quad (12-18)$$

Expression (12-18) must be numerically integrated, after inserting  $\delta V$  from (12-17) and allowing for the dependence of  $I_A$  and  $I_C$  on the parameter  $s$ . In addition, various possible paths for the motion of the hydrogens with respect to the nitrogen may be assumed. Sheng, Barker, and Dennison [110] choose a path intermediate between that obtained by considering the hydrogens as a rigid triangle and the path for the N—H

TABLE 12-2. VALUES OF THE FINE-STRUCTURE COEFFICIENTS FOR AMMONIA  
 $\nu = \nu_0 - a[J(J+1) - K^2] + bK^2 + \text{higher powers in } J \text{ and } K$

		Isotope				
		N <sup>14</sup> H <sub>3</sub>		N <sup>15</sup> H <sub>3</sub>	N <sup>14</sup> D <sub>3</sub>	
		Ground state	Excited state	Ground state	Ground state	Excited state
Experimental value, Mc	<i>a</i>	151.5	4860	141.9	7.16	
	<i>b</i>	59.9	1800	55.8	2.88	
Calculated value	<i>a</i>	102	4680	.....	3.61	267
Manning potential, Mc	<i>b</i>	55.5	1980	.....	2.60	187
Calculated value	<i>a</i>	180	.....	186		
Newton-Thomas potential, Mc	<i>b</i>	27	.....	6		

bond fixed in length during the inversion. The expression resulting from (12-18) is of the form (12-15) expected qualitatively. Calculated values of the coefficients  $a$  and  $b$  in (12-15) are compared in Table 12-2 with the experimentally determined constants.

Newton and Thomas [306] have calculated the fine structure of the inversion spectrum of N<sup>14</sup>H<sub>3</sub> and N<sup>15</sup>H<sub>3</sub> by introducing the centrifugal terms somewhat earlier in the calculation. These terms can be conveniently combined with their form of the potential (12-10) so that



rotational effects are included in the calculation of inversion frequencies *ab initio*. Their values for the fine-structure constants are also given in Table 12-2.

Although the agreement between theory and experiment in Tables 12-1 and 12-2 is reasonably good, it is clear that none of the potentials assumed is capable of giving the behavior of the inversion spectrum for all isotopes and vibrational states to an accuracy better than about 10 per cent. Hadley and Dennison [157] have tried some modifications in the potentials assumed here, but with no marked improvement in the results. It appears that probably a treatment which is not restricted to one dimension as are all those so far used will be necessary in order to obtain much improvement in the theoretical results. The relative success of a one-dimensional treatment comes from the fact that there is one normal mode of vibration which is primarily involved in its inversion. However, other normal modes of vibration are of some importance in affecting inversion.

About 65 lines of the  $\text{NH}_3$  inversion spectrum which have so far been measured are listed in Table 12-3 with their approximate intensities at room temperature. In computing relative intensities, it has been assumed that expression (13-62) is correct for the half widths of the lines. The extensive spectrum is often useful in calibrating wavemeters, checking the performance of spectrometers, and as standard frequency references in measuring accurately other spectra. Use of the  $\text{NH}_3$  spectrum in testing has the disadvantage, however, that  $\text{NH}_3$  tends to persist in the spectrometer absorption cell sometimes long after it is wanted.

The expression (12-15) is too much simplified to fit accurately all the lines of Table 12-3. A more complete expansion of the type indicated by (12-15), but including higher powers of  $J(J+1)$  and  $K^2$  can be made to fit the experimental frequencies reasonably well. A number of expansions of this general type have been given [141], [155], [172], [236], [317], [410]. One example [317] containing five terms in  $J$  and  $K$  is

$$\nu = 23,787 - 151.3J(J+1) + 211.0K^2 + 0.5503J^2(J+1)^2 - 1.531J(J+1)K^2 + 1.055K^4 \quad (12-19)$$

This fits the low  $J$  and  $K$  values best and gives deviations for some of the larger values of 25 to 50 Mc. The exponential dependence of (12-1) on the potential suggested to Costain that an exponential of various powers of  $J(J+1)$  and  $K^2$  might fit the frequencies [564]. His expansion

$$\nu = 23,785.88 \exp [-6.36996 \times 10^{-3}J(J+1) + 8.88986 \times 10^{-3}K^2 + 8.6922 \times 10^{-7}J^2(J+1)^2 - 1.7845 \times 10^{-6}J(J+1)K^2 + 5.3075 \times 10^{-7}K^4] \quad \text{Mc} \quad (12-20)$$

fits the lines in Table 12-3 with a mean deviation of 1.3 Mc and should hence predict other unmeasured lines with some accuracy.

There is a certain group of lines, those for which  $K = 3$ , which shows



TABLE 12-3. OBSERVED N<sup>14</sup>H<sub>3</sub> INVERSION LINES

Rotational state		Frequency, Mc	Intensity, cm <sup>-1</sup>
<i>J</i>	<i>K</i>		
9	5	16,798.3	8.7 × 10 <sup>-6</sup>
7	1	16,841.3	3.5 × 10 <sup>-6</sup>
7	2	17,291.6	1.0 × 10 <sup>-6</sup>
8	4	17,378.1	1.5 × 10 <sup>-6</sup>
7	3	18,017.6	4.3 × 10 <sup>-6</sup>
12	9	18,127.2	4.7 × 10 <sup>-6</sup>
11	8	18,162.6	4.8 × 10 <sup>-6</sup>
13	10	18,178.0	1.1 × 10 <sup>-6</sup>
10	7	18,285.6	9.4 × 10 <sup>-6</sup>
14	11	18,313.9	4.5 × 10 <sup>-7</sup>
6	1	18,391.6	4.2 × 10 <sup>-6</sup>
9	6	18,499.5	3.4 × 10 <sup>-6</sup>
15	12	18,535.1	3.6 × 10 <sup>-7</sup>
8	5	18,808.7	2.8 × 10 <sup>-6</sup>
16	13	18,842.9	6.6 × 10 <sup>-8</sup>
6	2	18,884.9	2.6 × 10 <sup>-6</sup>
7	4	19,218.52	4.0 × 10 <sup>-6</sup>
6	3	19,757.56	1.1 × 10 <sup>-4</sup>
5	1	19,838.4	1.8 × 10 <sup>-6</sup>
5	2	20,371.48	5.6 × 10 <sup>-6</sup>
8	6	20,719.20	1.0 × 10 <sup>-4</sup>
9	7	20,735.46	3.3 × 10 <sup>-6</sup>
7	5	20,804.80	7.4 × 10 <sup>-6</sup>
10	8	20,852.51	1.9 × 10 <sup>-6</sup>
6	4	20,994.62	9.9 × 10 <sup>-6</sup>
11	9	21,070.73	2.0 × 10 <sup>-6</sup>
4	1	21,134.37	4.0 × 10 <sup>-6</sup>
5	3	21,285.30	2.3 × 10 <sup>-4</sup>
12	10	21,391.55	5.2 × 10 <sup>-6</sup>
4	2	21,703.34	1.1 × 10 <sup>-4</sup>
13	11	21,818.1	6.0 × 10 <sup>-7</sup>
3	1	22,234.51	6.9 × 10 <sup>-6</sup>
14	12	22,355	2.2 × 10 <sup>-6</sup>
5	4	22,653.00	2.2 × 10 <sup>-4</sup>
4	3	22,688.24	4.4 × 10 <sup>-4</sup>
6	5	22,732.45	1.7 × 10 <sup>-4</sup>
3	2	22,834.10	2.0 × 10 <sup>-4</sup>
7	6	22,924.91	2.9 × 10 <sup>-4</sup>
15	13	23,004	4.8 × 10 <sup>-7</sup>
2	1	23,098.78	1.1 × 10 <sup>-4</sup>

TABLE 12-3. OBSERVED  $\text{N}^{14}\text{H}_3$  INVERSION LINES (*Continued*)

Rotational state		Frequency, Mc	Intensity, $\text{cm}^{-1}$
$J$	$K$		
8	7	23,232.20	$9.9 \times 10^{-6}$
9	8	23,657.46	$6.5 \times 10^{-6}$
1	1	23,694.48	$1.9 \times 10^{-4}$
2	2	23,722.61	$3.2 \times 10^{-4}$
16	14	23,777.4	$1.9 \times 10^{-7}$
3	3	23,870.11	$7.9 \times 10^{-4}$
4	4	24,139.39	$4.3 \times 10^{-4}$
10	9	24,205.25	$7.8 \times 10^{-6}$
5	5	24,532.94	$4.0 \times 10^{-4}$
17	15	24,680.1	$1.1 \times 10^{-7}$
11	10	24,881.90	$2.2 \times 10^{-6}$
6	6	25,056.04	$6.9 \times 10^{-4}$
12	11	25,695.23	$1.3 \times 10^{-6}$
7	7	25,715.14	$2.7 \times 10^{-4}$
8	8	26,518.91	$2.0 \times 10^{-4}$
13	12	26,655.00	$1.3 \times 10^{-6}$
9	9	27,478.00	$2.8 \times 10^{-4}$
14	13	27,772.52	$3.0 \times 10^{-6}$
10	10	28,604.73	$9.0 \times 10^{-6}$
15	14	29,061.14	$1.4 \times 10^{-6}$
11	11	29,914.66	$5.5 \times 10^{-6}$
12	12	31,424.97	$6.2 \times 10^{-6}$
13	13	33,156.95	$1.7 \times 10^{-6}$
14	14	35,134.44	$8.7 \times 10^{-6}$
15	15	37,385.18	$8.3 \times 10^{-6}$
16	16	39,941.54	$1.9 \times 10^{-6}$

peculiar and systematic deviations from expressions (12-19) or (12-20) [198], [236]. The magnitude of this deviation increases rapidly with  $J$  and is alternately positive or negative according to whether  $J$  is odd or even, as may be seen from Table 12-4. The deviations for high  $J$  values are very much greater than the average error in expression (12-20) of 1.3 Mc, and have consequently not been averaged into this error.

H. H. Nielsen and Dennison [223] have shown that the deviations of lines for which  $K = 3$  are due to still another rotation-vibration interaction of high order and hence small magnitude. It may be thought of as a splitting of the  $K$  degeneracy, *i.e.*, of the two levels corresponding to  $K = \pm 3$ . As explained in Chap. 3, the statistics and spin of the

hydrogen nuclei make only one of these levels possible in  $\text{NH}_3$ , so one displaced line is seen rather than two separated lines. From the discussion in Chap. 3, it may be remembered that the type of wave function that is allowed by the nuclear properties depends on the oddness or evenness of  $J$  and on the inversion level. Hence in the lowest inversion level for odd  $J$  the higher-frequency  $K$  doublet occurs, whereas for even  $J$  only the lower frequency doublet appears. In the upper inversion level the situation is reversed. A transition, therefore, gives one line shifted to higher frequency for even  $J$  by an amount equal to the  $K$  doubling, and shifted to a lower frequency for odd  $J$ .

Symmetry considerations can show quite generally that no  $K$ -type doubling or further splitting due to rotation-vibration interactions can

TABLE 12-4. DEVIATIONS OF AMMONIA LINES WITH  $K = 3$  FROM NORMAL INVERSION FREQUENCIES AS GIVEN BY FORMULA (12-20)  
Calculated shift for  $\text{NH}_3$  is according to expression (12-21).

$J$	$\text{NH}_3$		$\text{ND}_3$ Calculated shifts [223], Mc
	Calculated shift, Mc	Measured shift [564], Mc	
3	− 0.25	− 0.21	±0.03
4	1.76	1.76	±0.24
5	− 7.06	− 7.03	±0.95
6	21.18	21.18	±2.85
7	−52.9	−52.39	±7.14

occur for levels where  $K$  is not a multiple of 3 (*cf.* [66]). In addition, although levels with  $K = 6$  or 9 can, in principle, be split, the effect of vibration-rotation interaction in splitting these levels is very much smaller than their effect on the levels with  $K = 3$ . Even when  $K = 3$ , the disturbance of the levels by vibration-rotation interaction is a very small perturbation; Nielsen and Dennison [223] have shown that it is proportional to the fourth power of the ratio of rotational to vibrational energy: They obtain a value for the splitting of the two degenerate levels and hence for the shift in frequency of the observed lines

$$\Delta\nu = 3.50 \times 10^{-4} J(J+1)[J(J+1)-2][J(J+1)-6] \quad \text{Mc} \quad (12-21)$$

The constant in (12-21) can be evaluated to about 10 per cent accuracy from known rotational and vibrational constants of the  $\text{NH}_3$  molecule, but its precise value is picked to fit the data of Table 12-4 [564]. This table shows that expression (12-21) agrees quite well with the observed deviations of lines with  $K = 3$ .

In the case of  $\text{ND}_3$ , the nuclear spin of D is unity and both the  $K$  doublets are allowed. These have not yet been observed, but the calcu-



lated deviation of each member from normal frequency is given in Table 12-4.

**12-5. Asymmetric Forms of Ammonia.** In addition to the symmetric forms of ammonia  $\text{NH}_3$  and  $\text{ND}_3$ , the asymmetric rotors  $\text{NH}_2\text{D}$  and  $\text{NHD}_2$  occur and have inversion spectra. However, in these cases the inversion spectrum tends to be mixed up with rotational energies. Examination of the transitions allowed for  $\text{NH}_3$  in Fig. 3-9 shows that rotational transitions occur only at the same time as an inversion (or vibrational) transition. In addition, an inversion transition occurs only with a rotational transition, since upper and lower inversion levels have different rotational wave functions. In the case of  $\text{NH}_3$ , the molecular symmetry gives the two different rotational wave functions the same rotation energy. However, it can be shown to be always true that only transitions with a change of both rotational and inversion states occur, and in the cases of  $\text{NH}_2\text{D}$  and  $\text{NHD}_2$  the rotational transition contributes to the frequency of the observed lines because of their asymmetry [662].

If the energy difference due to the rotational transition  $J'_\tau \leftarrow J_\tau$  is small, then a pair of lines is observed of frequency  $\nu_i \pm \nu_{J_\tau J'_\tau}$ , where  $\nu_i$  is the inversion frequency and  $\nu_{J_\tau J'_\tau}$  the rotational frequency. If the inversion frequency is much smaller than that due to the rotational frequency, the observed spectrum has a pair of lines of frequencies  $\nu_{J_\tau J'_\tau} \pm \nu_i$ . In the extreme and very common case of an unobservably small inversion frequency, this last doublet becomes the single observed rotational frequency  $\nu_{J_\tau J'_\tau}$ . A number of lines of both the above types have been found in partially deuterated ammonia, and from these rotational constants and inversion frequencies have been obtained [662]. The rotational constants are consistent with the structural parameters of  $\text{NH}_3$  usually assumed [130] after some allowance is made for centrifugal distortion.

The inversion frequencies of the asymmetric forms of ammonia cannot be treated as easily as those for  $\text{NH}_3$  and  $\text{ND}_3$ . In the vibration which inverts the asymmetric forms, the N does not move strictly perpendicularly to the plane of the hydrogens. However, an approximate calculation of the inversion frequencies of these molecules, assuming the same motion and potential for the inversion as in the symmetric cases, gives surprisingly good agreement with the observed frequencies as shown in Table 12-5. The inversion frequencies for the ground states are in very close agreement, although the excited state frequencies show a sizable discrepancy.

It is also more difficult to calculate the fine structure, or rotation-vibration interaction, in the asymmetric ammonias because both the vibrational and the rotational motions are rather complex. Weiss and Strandberg [662] have obtained a reasonably good empirical approxima-

tion to the fine structure, however, by assuming it to be of the form

$$\nu = \nu_0 - a[J(J + 1) - (P_c^2)_{av}] + b(P_c^2)_{av} \quad (12-22)$$

where  $(P_c^2)_{av}$  is the average square of the angular momentum in units of  $h/2\pi$  parallel to the principal axis of largest moment of inertia. This axis differs by only about  $10^\circ$  from the "symmetry" axis perpendicular to the plane of the hydrogens.  $(P_c^2)_{av}$  is the analog of the quantity  $K^2$  in expression (12-15) for the symmetric ammonias. The more intense microwave transitions in  $\text{NH}_2\text{D}$  and  $\text{NHD}_2$  involve very little change in  $(P_c^2)_{av}$  and no change in  $J$ , again in analogy with the symmetric cases where  $\Delta K = 0$  and  $\Delta J = 0$ . Hence  $(P_c^2)_{av}$  and  $J$  can be assumed the

TABLE 12-5. CONSTANTS OF THE INVERSION SPECTRUM OF  $\text{NH}_2\text{D}$  AND  $\text{NHD}_2$   
(From Weiss and Strandberg [662])

	$\text{NH}_2\text{D}$		$\text{NHD}_2$	
	Observed	Calculated	Observed	Calculated
Inversion frequency of ground state, Mc.....	12,182	12,100	5,111	5,160
Fine-structure constant of $a$	23.6		8.1	
ground state, Mc $b$	76.7		26	
Inversion frequency of first excited state, Mc.....	592,000	465,000	295,000	204,000

same for upper and lower states of the transition. Empirical values for  $a$  and  $b$  of expression (12-22) for  $\text{NH}_2\text{D}$  and  $\text{NHD}_2$  are listed in Table 12-5.

The quantity  $(P_c^2)_{av}$  is just  $(\alpha_{zc}^2)_{av}J(J + 1)$ , where  $\alpha_{zc}$  is the cosine of the angle between the total angular momentum  $J$  and the molecular axis  $c$  of largest principal moment of inertia.  $(\alpha_{zc}^2)_{av}$  can be evaluated as in Chap. 6 [*cf.*, for example, expression (6-16)].

**12-6. Hindered Torsional Motions in Symmetric Rotors.** Another common type of hindered motion is the rotation of one part of a molecule with respect to the remainder, which, when hindering is large, becomes a torsional oscillation. An example is the relative rotation of  $\text{CH}_3$  and  $\text{CF}_3$  about the symmetry axis of the molecule  $\text{H}_3\text{C}-\text{CF}_3$ . Hindered torsional motion can also occur in an asymmetric rotor, as in  $\text{CH}_3\text{OH}$ , where the OH bond may rotate with respect to the  $\text{CH}_3$  group.

Consider first a symmetric top such as  $\text{H}_3\text{CCF}_3$  having an "internal" torsional motion of one end of the molecule with respect to the other end. In either one of the two extreme cases where the  $\text{CH}_3$  rotates perfectly freely about the molecular axis, or where it interacts strongly with the  $\text{CF}_3$  group so that it can scarcely rotate at all with respect to this group, the energy levels are relatively simple. We shall examine these two



extreme cases first before proceeding to the more complex intermediate case where tunneling effects are prominent.

If the two parts of the molecule are bound together tightly, the energy may be obtained in a straightforward way as the sum of the rotational energy of a symmetric top and various molecular vibrational energies. We shall consider only the torsional vibration. The reduced moment of inertia for the  $\text{CH}_3$  twisting with respect to  $\text{CF}_3$  is

$$I_r = \frac{I_1 I_2}{I_1 + I_2} \text{ or } \frac{I_1 I_2}{I}$$

where  $I_1$  is the moment of inertia for  $\text{CH}_3$  about the symmetry axis,  $I_2$  is that for  $\text{CF}_3$ , and  $I = I_1 + I_2$ . The potential energy has three minima corresponding to the three equivalent positions  $120^\circ$  apart of the  $\text{CH}_3$  with respect to  $\text{CF}_3$ , and there is a very high potential hump between each minimum—so high that tunneling from one minimum to another is negligibly small. In one of the minima, the potential energy can then be written  $V = \frac{1}{2}k\alpha^2$ , where  $\alpha = \chi_1 - \chi_2$  is the difference in the angular position  $\chi_1$  of  $\text{CH}_3$  about the symmetry axis and the angle  $\chi_2$  of  $\text{CF}_3$ . The force, or rather torque, constant is  $k$ . The frequency of torsional oscillation is then

$$\omega = \frac{1}{2\pi} \sqrt{\frac{kI}{I_1 I_2}}$$

and the energy of torsional and rotational motions is simply

$$W = hB[J(J + 1) - K^2] + hCK^2 + h\omega(v + \frac{1}{2}) \quad (12-23)$$

where  $B$  and  $C$  are the usual rotation constants ( $C = h/8\pi^2 I$ ) and  $v$  is the vibrational quantum number for the torsional motion. Each torsional vibrational level is triply degenerate since there are three equivalent positions in which the oscillation may occur.

In the other extreme case,  $\text{CH}_3$  and  $\text{CF}_3$  can rotate freely about the molecular axis. Let the angular momentum about the axis for  $\text{CH}_3$  be  $m_1\hbar$  and that of  $\text{CF}_3$  be  $m_2\hbar$  so that the total angular momentum about the symmetry axis is  $(m_1 + m_2)\hbar = K\hbar$ . The usual quantum-mechanical conditions require that  $m_1$ ,  $m_2$ , and  $K$  be integers. The energy of rotation is

$$W = hB[J(J + 1) - K^2] + \frac{(m_1\hbar)^2}{2I_1} + \frac{(m_2\hbar)^2}{2I_2}$$

or

$$W = hB[J(J + 1) - K^2] + hCK^2 + \frac{I\hbar^2}{2I_1 I_2} \left( m_1 - \frac{KI_1}{I} \right)^2 \quad (12-24)$$

The energies due to deviations from these ideal cases, or in the intermediate case when the barrier is of moderate height, remain to be calculated. Connections between the energy levels for the two extreme cases



are shown in Fig. 12-5. It may be seen from this figure that some of the degenerate levels of the extreme cases split in the intermediate case of moderate potential barrier heights. The amount of splitting must be obtained from a solution of the wave equation which, of course, gives (12-23) or (12-24) in the two extreme cases.

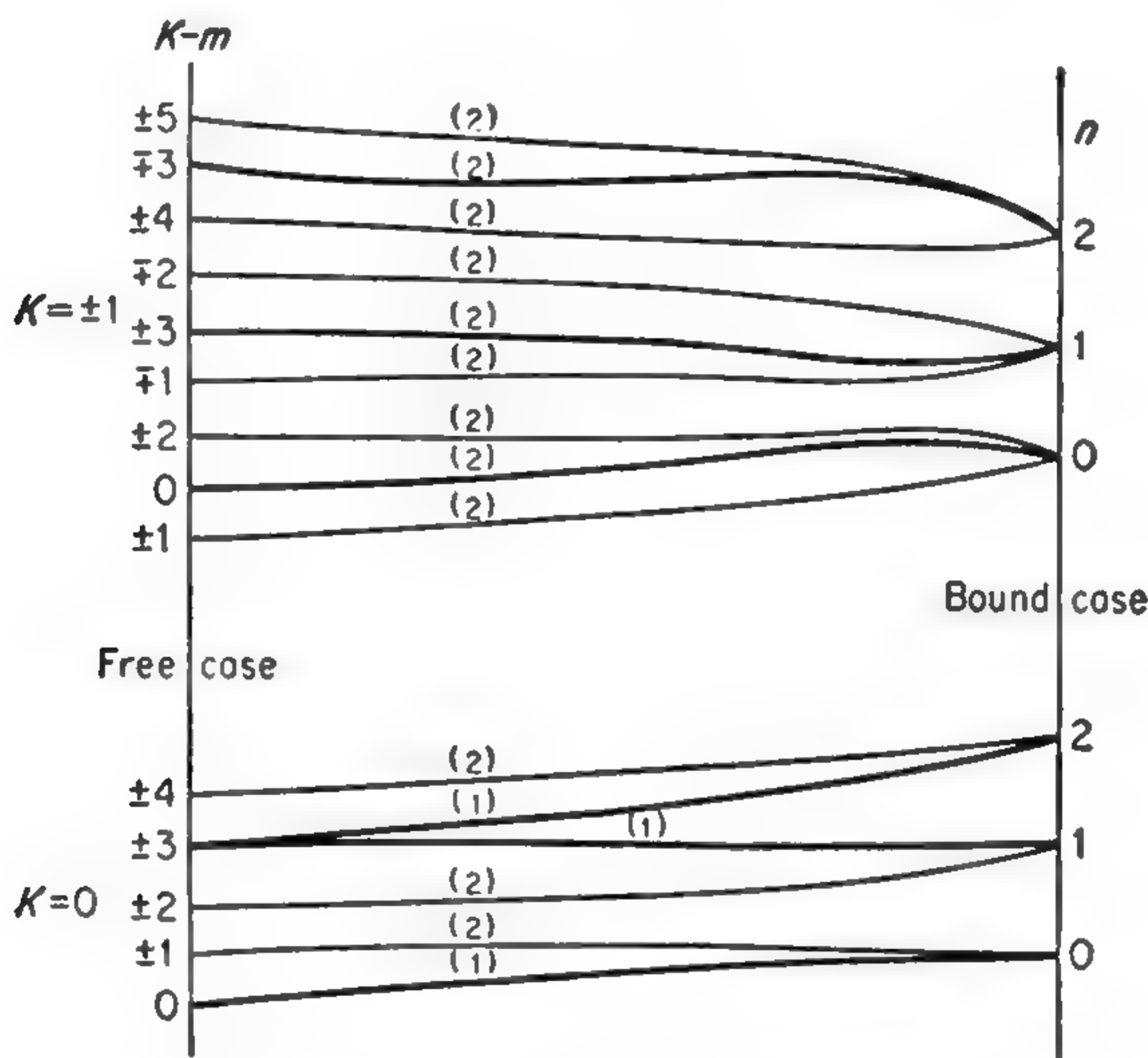


FIG. 12-5. Connections between energy levels with free internal rotation and those for torsional oscillation. Three potential minima are assumed, as in the molecule  $\text{CH}_3\text{CF}_3$ . Intermediate barrier heights, corresponding to neither very strong nor negligible interaction between the  $\text{CH}_3$  and  $\text{CF}_3$  groups, can be seen to split certain levels. Numbers (1) and (2) indicate the number of levels of the same energy. (After Koehler and Dennison [99].)

The kinetic energy due to rotation is

$$T = \frac{1}{2}I_x\omega_x^2 + \frac{1}{2}I_y\omega_y^2 + \frac{1}{2}I_1\dot{\chi}_1^2 + \frac{1}{2}I_2\dot{\chi}_2^2 \quad (12-25)$$

where  $I_x$  and  $I_y$  are the principal moments of inertia perpendicular to the axis and  $\omega_x$  and  $\omega_y$ , the angular velocities.  $I_1$  and  $I_2$  are the moments of inertia of the two parts of the molecule about which relative rotation occurs, and which is taken as the  $z$  direction with respect to the axis.  $\chi_1$  and  $\chi_2$  are angles specifying the rotation of these two parts about this axis. If new variables are defined so that

$$\chi = \frac{I_1\chi_1 + I_2\chi_2}{I} \quad \alpha = \chi_1 - \chi_2 \quad (12-26)$$

Then the energy is, from (12-25)

$$W = \frac{1}{2}I_x\omega_x^2 + \frac{1}{2}I_y\omega_y^2 + \frac{1}{2}I\dot{\chi}^2 + \frac{1}{2}\frac{I_1I_2}{I}\dot{\alpha}^2 + \frac{1}{2}V_0(1 - \cos 3\alpha) \quad (12-27a)$$

and the Hamiltonian is

$$H = \frac{1}{2} \frac{P_x^2}{I_x} + \frac{1}{2} \frac{P_y^2}{I_y} + \frac{1}{2} \frac{P_z^2}{I} + \frac{1}{2} \frac{I}{I_1 I_2} p_\alpha^2 + \frac{1}{2} V_0 (1 - \cos 3\alpha) \quad (12-27b)$$

where the symbols involved have been defined above. It may be observed that  $\chi$  gives the angle of torsion within the molecule, and that  $I\dot{\alpha} = I_1\dot{\chi}_1 + I_2\dot{\chi}_2$  is the total angular momentum about the symmetry axis.

Here the potential energy for torsional motion is assumed to be  $V = \frac{1}{2} V_0 (1 - \cos 3\alpha)$ , corresponding to three potential minima with intervening barriers of height  $V_0$ . The shape of the potential barrier will not, of course, be given perfectly by the  $\cos 3\alpha$  variation but more generally should be written as a Fourier series

$$V = \sum_p (a_p \cos 3p\alpha + b_p \sin 3p\alpha)$$

However, the energy levels of the molecule will not depend strongly on minor details of the potential. In addition, potential curves which have been calculated on the basis of simple assumptions about the origin of the hindering forces are in fact fitted extremely well by a  $\cos 3\alpha$  curve. There is some experimental evidence from the barrier in  $\text{CH}_3\text{NO}_2$ , to be discussed below, that the term proportional to  $\cos 6\alpha$  in this Fourier expansion is not more than a few per cent as large as that proportional to  $\cos 3\alpha$ .

*Properties of Quantum States with Hindered Torsional Motion.* It may be seen that the first three terms of (12-27) have just the same form as Eq. (3-2), which gives the energy of rotation for a rigid top. In this case,  $I_x = I_y$  so that the top is symmetric. Consequently the wave function describing the rotation and torsion of the molecule has the form [36], [99]

$$\psi = \frac{1}{2\pi} e^{iK\chi} e^{iM\phi} \Theta_{JKM}(\theta) \mathfrak{M}(\alpha) \quad (12-28)$$

where  $\theta$  and  $\phi$  are the usual Eulerian angles and  $e^{iK\chi} e^{iM\phi} \Theta(\theta)$  is identical with expression (3-12a), the wave function for a rigid symmetric top  $\mathfrak{M}$  satisfies the equation

$$\frac{I\hbar^2}{2I_1 I_2} \frac{d^2 \mathfrak{M}}{d\alpha^2} + \left[ W_\alpha - \frac{V_0}{2} (1 - \cos 3\alpha) \right] \mathfrak{M} = 0 \quad (12-29)$$

The energy is

$$W = W_R + W_\alpha = hB[J(J+1) - K^2] + hCK^2 + W_\alpha \quad (12-30)$$

where  $W_R$  is the rotational energy of the molecule considered as a rigid symmetric top and  $W_\alpha$  the torsional energy.  $B$  and  $C$  are the usual

rotational constants with

$$C = \frac{h}{8\pi^2(I_1 + I_2)}$$

Hence, the only new problem is to solve (12-29), a form which is equivalent to Mathieu's equation, and hence to obtain  $W_\alpha$ . Characteristics of the functions  $\mathfrak{M}(\alpha)$  have been discussed by Koehler and Dennison [99], whose treatment we shall follow.

Solutions of equation (12-29) are known from Floquet's theorem (see [65] and *Tables Relating to Mathieu Functions*, Columbia University Press, New York, 1951) to be of the type

$$\mathfrak{M}(\alpha) = e^{i\sigma\alpha}F(\alpha) \quad (12-31)$$

where  $F(\alpha)$  is periodic with period  $2\pi/3$ , that is,  $F(\alpha)$  may be expanded in the form

$$F(\alpha) = \sum_p a_p e^{3ip\alpha} \quad (12-32)$$

where  $p$  is any integer. The constant  $\sigma$  must be real in order to make the wave function finite everywhere. The other conditions imposed on the wave function by the physical situation it must describe are that it must be unchanged when either end of the molecule is rotated any number of complete rotations, that is, when

$$\chi_1 \rightarrow \chi_1 + 2\pi n_1 \quad \text{and} \quad \chi_2 \rightarrow \chi_2 + 2\pi n_2 \quad (12-33)$$

Making these substitutions into (12-27) and (12-31),

$$e^{iK\chi}e^{iM\phi}\Theta(\theta)e^{i\sigma\alpha}F(\alpha) = e^{iK\chi}e^{iM\phi}\Theta(\theta)e^{i\sigma\alpha}F(\alpha)e^{2\pi i\left[\frac{K(n_1I_1+n_2I_2)}{I}+\sigma(n_1-n_2)\right]}$$

so that

$$\frac{K(n_1I_1 + n_2I_2)}{I} + \sigma(n_1 - n_2) = p \quad (12-34)$$

where  $p$  is an integer.

Equation (12-34) can hold only if  $K$  is an integer (as would be expected since  $Kh$  is the total angular momentum around the symmetry axis) and if

$$\sigma = s - \frac{KI_1}{I} \quad (12-35a)$$

where  $s$  is any integer.

There are only three types of solutions, which may be obtained with values of  $s = 0, 1$ , or  $2$ ; that is, with

$$\sigma = -\frac{KI_1}{I}, 1 - \frac{KI_1}{I}, \text{ or } 2 - \frac{KI_1}{I} \quad (12-35b)$$

For, if  $\sigma = 3p + s - KI_1/I$ , where  $p$  is an integer, the exponent  $3p$  may be taken as part of  $F(\alpha)$  in (12-31), so that the solution is equivalent to



that with  $\sigma = s - KI_1/I$ . (These three types of solutions have in previous treatments often been designated by a quantum number  $\tau$ , with  $\tau = 1, 3$ , and  $2$ , corresponding to  $s = 0, 1$ , and  $2$ , respectively.) The solutions (12-31) are also periodic in  $K$  with a period  $3I/I_1$ , for if  $K = 3I/I_1$ ,  $\sigma = s - 3$ , which is equivalent to the solution with  $\sigma = s$ .

Actual solutions  $\mathfrak{M}(\alpha)$  must be obtained by using the expanded form (12-32) of  $F(\alpha)$ , substituting into the Eq. (12-29), and evaluating the coefficients  $a_p$  (or from tabulations). This also gives the various allowed values of the "internal" energy  $W_\alpha$  associated with the angle  $\alpha$ . There are an infinite number of allowed values of  $W_\alpha$ , but for reasonably high barriers the lower values are grouped in threes near the energies to be expected from the bound case with vibrational quantum numbers  $v = 0, 1, 2, 3, \dots$ . The calculated values of these energies for a particular case where

$$V_0 = 770 \text{ cm}^{-1} \quad \frac{Ih}{8\pi^2 I_1 I_2 c} = 24.8 \text{ cm}^{-1} \quad \frac{I_1}{I} = 0.21$$

are plotted in Fig. 12-6. The lower energy levels correspond essentially to vibrational levels which are slightly split into three levels. The higher levels (*e.g.*, with vibrational quantum number  $v = 2$  or  $3$ ) are still partly grouped by vibrational quantum numbers but are far enough above the hindering potential to correspond fairly closely to the levels of a free rotor which are plotted in the same figure for comparison. The internal energy of the free rotor is, from (12-24),

$$W_x = \frac{Ih^2}{2I_1 I_2} \left( m_1 - \frac{KI_1}{I} \right)^2$$

For a fixed value of  $m_1$  and varying  $K$ , this gives a parabola with a minimum energy at  $K = Im_1/I_1$ . The various parabolas in Fig. 12-6 correspond to different integral values of  $m_1$ .

Figure 12-6 also illustrates the rapid decrease in the frequency of tunneling as the energy sinks farther below the top of the potential barrier. Both sets of levels  $v = 1$  and  $v = 0$  are below the top of the barrier, and the spread in frequency in each set corresponds to the tunneling frequency. For  $v = 0$ , the tunneling frequency is very low, and it would be decreased further, of course, if the potential barrier were assumed to be higher.

The three different types of levels, with  $s = 0, 1$ , or  $2$ , are indicated by solid, short-dashed, or long-dashed curves, respectively, as are their counterparts in the free-rotor levels. The effect of a hindering potential is to separate groups of the free-rotor levels at the points where levels of like types cross in Fig. 12-6. Each type of level may be seen to be periodic in  $K$  with a period as shown above of  $3I/I_1$ , or approximately 14.

There are many molecules having hindered torsional motions with

more or fewer equilibrium positions than the three which apply to our present example. The ethylene molecule  $\text{H}_2\text{CCH}_2$  has only two equilibrium positions, while  $\text{F}_3\text{CSF}_5$  has twelve equilibrium positions of the  $\text{CF}_3$  group with respect to the four off-axis fluorines bonded in the  $\text{SF}_5$

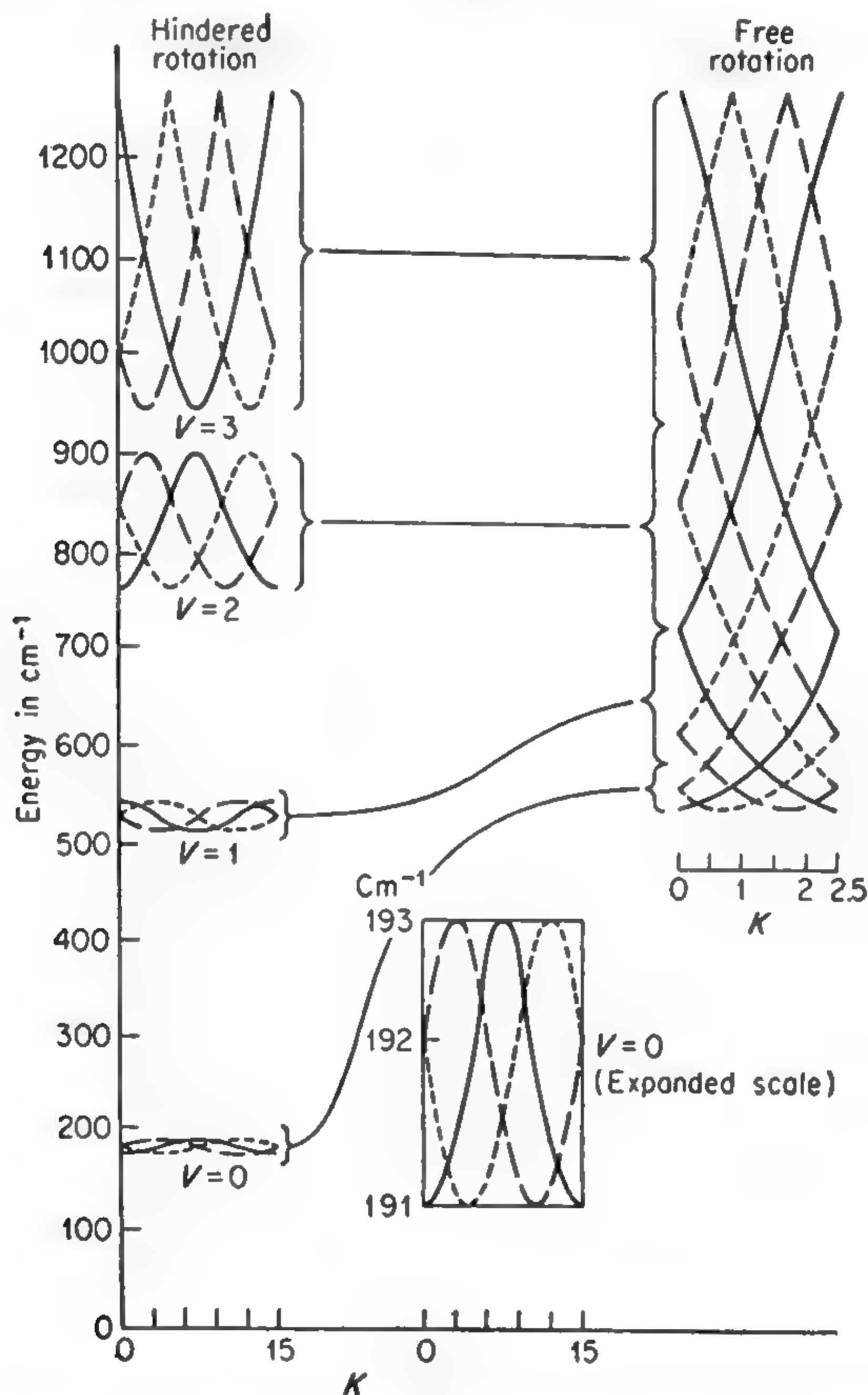


FIG. 12-6. Comparison of energy levels of torsional motion of a molecule of the type  $\text{H}_3\text{CCF}_3$  with free rotation and with a hindering potential. The hindering potential is assumed to have a height  $V_0 = 770 \text{ cm}^{-1}$ ,  $\frac{Ih}{8\pi^2 I_1 I_2 c} = 24.8 \text{ cm}^{-1}$ , and  $\frac{I_1}{I} = 0.21$ . (Adapted from Koehler and Dennison [99].)

group (Fig. 12-7). The general structure of the energy levels is similar to that of the case discussed above, but the number of levels is, of course, changed. If there are  $n$  equilibrium positions the potential may be written

$$V = \frac{V_0}{2} (1 - \cos n\alpha) \quad (12-36)$$

There are then  $n$  levels in each vibrational group, which repeat as  $K$  increases with a period of  $nI/I_1$ .

A truly symmetric rotor has a dipole moment only along the symmetry axis; hence a microwave field is not able to change the angular momentum around the symmetry axis of any part of the symmetric molecule with hindered rotation discussed here. It can only induce transitions in the total angular momentum  $J$ , so that the selection rules are  $\Delta J = 0, \pm 1, \Delta K = \Delta m_1 = \Delta v = 0$ . The frequencies observed are therefore just  $\nu = 2BJ$ , and one might suppose the above discussion of internal energies

which do not give spectra has been fruitless. This is not the case, however, because the same energy levels are good approximations to those of the slightly asymmetric rotor with hindered torsional motion, where dipole transitions between these levels do occur. In addition, the effects of the torsional motions on the rotational constant  $B$  are often seen.

**12-7. Heights of Hindering Barriers.** In the simplest case of strongly hindered torsion, where the levels are essentially those of a harmonic oscillator, their effect on  $B$  is expressible in terms of a rotation-vibration constant  $\alpha$  and the vibrational quantum number  $v$ , that is,

$$B = B_e - \alpha(v + \frac{1}{2})$$

One can be sure that the effect of torsional vibrational will be to push the two

interfering parts of the molecule farther apart on the average, which will almost always give a positive sign to  $\alpha$ . Very frequently also, the torsional motion is the lowest-frequency vibration in the molecule, so that one can identify the lines with  $v = 1, 2, \dots$  as the strongest set of excited vibrational lines in the rotational spectrum with a positive value of  $\alpha$ . A measurement of the relative intensities of the ground state rotational line and one or more of the excited states at a given temperature allows a determination of the torsional frequency  $\omega$ , since the intensities are proportional to the Boltzmann factor  $e^{-h\omega/kT}$ . A knowledge of the torsional frequency and the approximate moments of inertia involved in turn allows a determination of the barrier height, since approximately

$$\omega = \frac{1}{2\pi} \sqrt{\frac{kI}{I_1 I_2}} \quad (12-37)$$

where  $k$  is the torque constant at the position of the potential minimum.

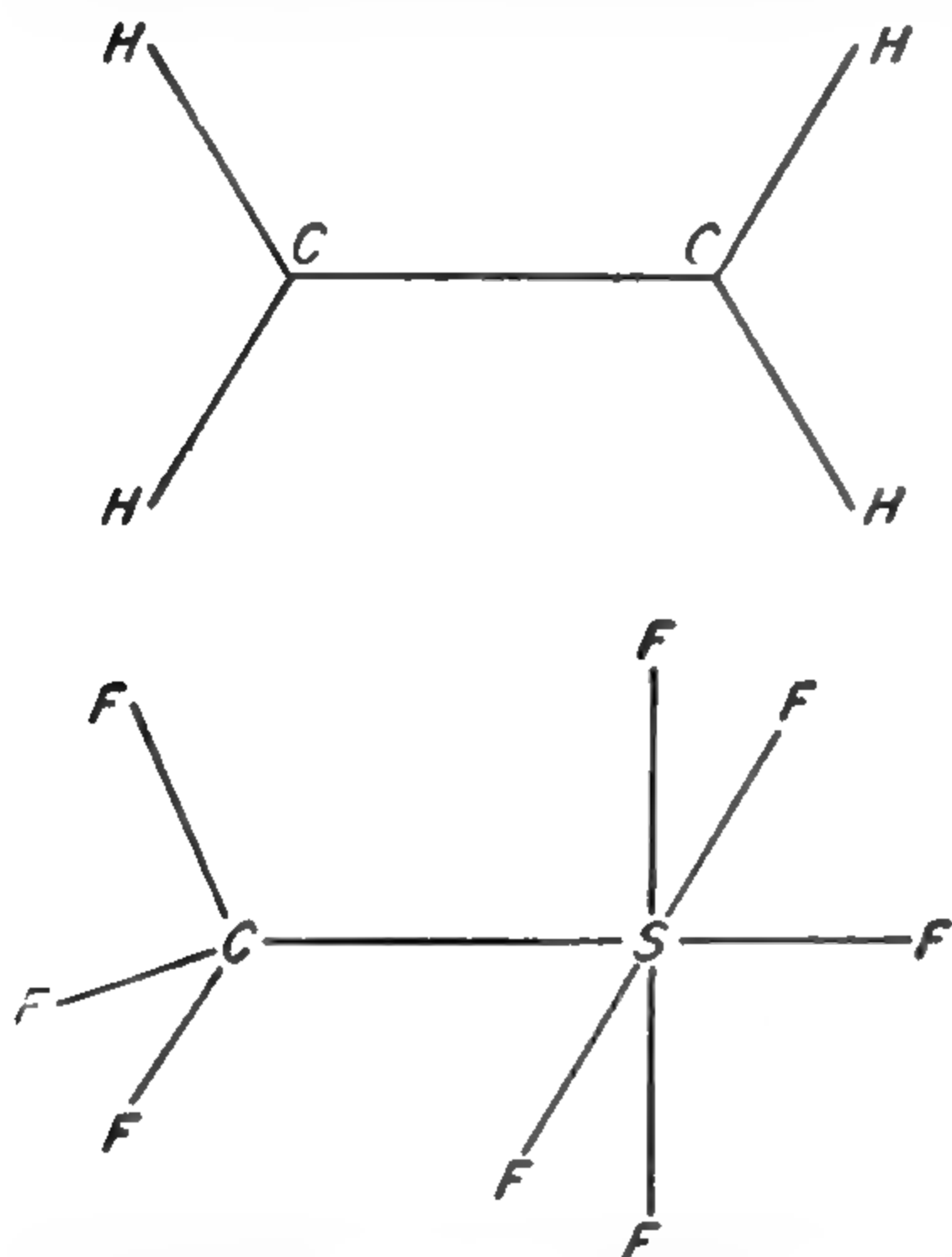


FIG. 12-7. Structure of ethylene with two potential minima and  $\text{CSF}_3$  with 12 minima.



If the potential has  $n$  minima, and is of the form (12-36), then

$$k = \left( \frac{d^2V}{d\alpha^2} \right)_{\alpha=0} = \frac{n^2 V_0}{2}$$

and from (12-37),

$$V_0 = \frac{8\pi^2\omega^2}{n^2} \frac{I_1 I_2}{I} \quad (12-38)$$

The barrier heights for a number of molecules determined by measurement of intensity ratios and use of (12-38) are listed in Table 12-6 with values of  $\alpha$  for the torsional vibration. Table 12-6 also lists some barrier

TABLE 12-6. BARRIER HEIGHT AND ROTATION-VIBRATION CONSTANT  $\alpha$  FOR HINDERED MOLECULAR VIBRATIONS

All barrier heights listed have been determined by microwave methods except for those in [130].

Molecule	Barrier height, cm <sup>-1</sup>	Rotation- vibrational constant $\alpha$ , Mc./sec.	Reference
CH <sub>3</sub> NO <sub>2</sub>	4.20	.....	[986]
CF <sub>3</sub> SF <sub>6</sub>	220	0.05	[713]
CH <sub>3</sub> CCl <sub>3</sub>	950	.....	[130]
CH <sub>3</sub> SiF <sub>3</sub>	410	4.2	[618] [641]
CH <sub>3</sub> OH	375	.....	[561] [817]
CH <sub>3</sub> SH	400	.....	[978a] [949a]
CH <sub>3</sub> SiH <sub>3</sub>	558	30	[604]
CH <sub>3</sub> SnH <sub>3</sub>	.....	10.8	[603]
CH <sub>3</sub> CF <sub>3</sub>	1200	.....	[618]
CH <sub>3</sub> CH <sub>3</sub>	960	.....	[130]
(CH <sub>3</sub> ) <sub>2</sub> O	1000	.....	[130]
CH <sub>3</sub> CHF <sub>2</sub>	1200	.....	[978]
CH <sub>3</sub> NH <sub>2</sub>	685	.....	[976]
H <sub>2</sub> O <sub>2</sub>	113	.....	[960]

heights which have been more precisely determined from spectroscopic observations, and some obtained by thermodynamic techniques. Usually the intensity ratios have not been determined more accurately than  $\pm 10$  per cent, so that there are sizable uncertainties in  $V_0$ . However, this method is one of the best available for barrier-height determinations, since the torsional frequencies do not often give detectable effects in either vibrational or Raman spectra (*cf.* [130], p. 496), and a determination from thermodynamic measurements, which has sometimes been used, is often tedious and inaccurate (*cf.* [130], p. 520).

Of course (12-38) assumes the particular form (12-36) for the potential. However, as pointed out above, calculations of potential shapes with

reasonable assumptions about the interactions give curves very close in shape to (12-36), so that actual potential curves are not likely to differ greatly from it. Expression (12-38) also assumes that the excited vibrational states whose relative intensities are measured lie sufficiently close to the bottom of the potential for a harmonic-oscillator approximation to apply. If this is not true, then the intensity ratios of successive excited states will not be constant, nor will  $\alpha$  be constant. In one or two cases so far measured, such deviations seem to have been observed.

The separation between the three levels in an individual vibrational state may be sufficient to produce slightly different values of the rotation-vibration constant  $\alpha$ . For example, Lide and Coles [604] report that in excited torsional vibrational states the  $J = 1 \leftarrow 0$  transition of  $\text{CH}_3\text{SiH}_3$  splits into two lines representing slightly different values of  $\alpha$ , and that the  $J = 1 \leftarrow 0$ ,  $K = 1$  transitions split into three components, corresponding to expectations from Fig. 12-6 (see also [948a]).

**12-8. Hindered Torsional Motions in Asymmetric Rotors.** Consider now the case where one of the two parts of the molecule with hindered torsional motion is not a symmetric rotor. Let the hindered motion involve rotation of the part which is a rigid symmetric rotor about its axis and with respect to a second part of the molecule which comprises a rigid asymmetric rotor. Also let the asymmetric rotor have a plane of symmetry which includes the axis of the symmetric rotor. Such a model is of course not completely general, but it includes a wide variety of interesting cases such as  $\text{CH}_3\text{OH}$ ,  $\text{CH}_3\text{NO}_2$ ,  $\text{CH}_3\text{NH}_2$ , and  $\text{CF}_3\text{CH}_2\text{Cl}$ . Our treatment will follow closely that of Hecht and Dennison [934a], which in turn relies heavily on a discussion by Burkhard and Dennison [561].

The kinetic energy due to rotation of such a molecule is

$$T = \frac{1}{2}I_x\omega_x^2 + \frac{1}{2}I_y\omega_y^2 + \frac{1}{2}I_1\dot{\chi}_1^2 + \frac{1}{2}I_2\dot{\chi}_2^2 - D\omega_y\dot{\chi}_1 \quad (12-39)$$

where, as in Eq. (12-25),  $I_x$  is the principal moment of inertia of the entire molecule about an axis perpendicular to the plane of symmetry and to the axis of hindered motion which is the  $z$  direction, and  $I_y$  is the moment of inertia about an axis perpendicular to  $x$  and  $z$ . The corresponding angular velocities are  $\omega_x$  and  $\omega_y$ .  $I_1$  and  $I_2$  are the moments of inertia of the two parts of the molecule about the axis or  $z$  direction,  $\chi_1$  is the angle specifying the rotation of the asymmetric part about the axis and  $\chi_2$  is the similar angle for the symmetric part. Since  $I_1$  is not necessarily a principal moment of inertia of the asymmetric rotor, the term  $-D\omega_y\dot{\chi}_1$  is needed in (12-39), where  $D$  is the product of inertia

$$D = \sum_i m_i y_i z_i \quad (12-40)$$

Here  $m_i$  is the mass of an atom of the asymmetric rotor and  $y_i$ ,  $z_i$  the coordinates of this mass with respect to the center of gravity of the entire

molecule. No products of inertia involving the  $x$  axis occur in (12-39), because the  $yz$  plane is taken to be the plane of symmetry of the molecule so that these products of inertia are zero.

Suitable rotations of axes and introduction of the variable  $\alpha = \chi_1 - \chi_2$  as in (12-26) transform [934a] the Hamiltonian derived from (12-39) to

$$\begin{aligned}
 H = & \left[ \frac{1}{4I_x} + \frac{I_y}{4(I_y^2 + D^2)} \right] (P_{x'}^2 + P_{y'}^2) \\
 & + \frac{1}{2} \left[ \frac{I_y + I}{I_y I - D^2} - \frac{I_y}{I_y^2 + D^2} \right] P_{z'}^2 \\
 & + \frac{(I_y I - D^2)}{2I_2(I_y I_1 - D^2)} p_\alpha^2 + V(\alpha) \\
 & + \frac{1}{4} \left( \frac{1}{I_x} - \frac{I_y}{I_y^2 + D^2} \right) \left[ (P_{x'}^2 - P_{y'}^2) \cos 2 \left( \frac{I_2}{I} \right)^* \alpha \right. \\
 & \quad \left. + (P_{x'} P_{y'} + P_{y'} P_{x'}) \sin 2 \left( \frac{I_2}{I} \right)^* \alpha \right] \\
 & + \frac{D}{2(I_y^2 + D^2)} \left[ (P_{y'} P_{x'} + P_{x'} P_{y'}) \cos \left( \frac{I_2}{I} \right)^* \alpha \right. \\
 & \quad \left. - (P_{x'} P_{x'} + P_{x'} P_{x'}) \sin \left( \frac{I_2}{I} \right)^* \alpha \right]
 \end{aligned} \tag{12-41}$$

where  $P_{x'}$ ,  $P_{y'}$ , and  $P_{z'}$  are components of the total angular momentum operator,  $p_\alpha$  is the momentum which is canonically conjugate to  $\alpha$  or  $\chi_1 - \chi_2$ ,  $I = I_1 + I_2$ , and  $\left( \frac{I_2}{I} \right)^* = \frac{I_2 \sqrt{I_y^2 + D^2}}{I_y I - D^2}$ . The potential  $V(\alpha)$  is assumed to have the form  $V(\alpha) = (V_0/2)(1 - \cos n\alpha)$ , where  $n$  is an integer.

The part of the Hamiltonian indicated by (I) is identical in form with (12-27b) for the completely symmetric hindered rotor and hence has solutions and energy values of the same type. In solutions of (12-41), however, the following quantities which occur in the symmetric-rotor cases will be replaced by their equivalents:

$$\frac{I}{I_1 I_2} \text{ is replaced by } \left( \frac{I}{I_1 I_2} \right)^* = \frac{I_y I - D^2}{I_2 (I_1 I_y - D^2)} \tag{12-42a}$$

$$\frac{I_2}{I} \text{ by } \left( \frac{I_2}{I} \right)^* = \frac{I_2 \sqrt{I_y^2 + D^2}}{I_y I - D^2} \tag{12-42b}$$

and

$$\frac{I_1}{I} \text{ by } \left( \frac{I_1}{I} \right)^* = 1 - \frac{I_2 \sqrt{I_y^2 + D^2}}{I_y I - D^2} \tag{12-42c}$$

Solutions of part (I) are

$$\psi_{JKMv_s} = \frac{1}{2\pi} e^{iKx'} e^{iM\phi'} \Theta_{JKM}(\theta') e^{i\sigma\alpha} F_{Kv_s}(\alpha) \tag{12-43}$$



where  $\chi'$ ,  $\phi'$ , and  $\theta'$  are Eulerian angles for the system corresponding to the transformed axes  $x'$ ,  $y'$ , and  $z'$ .  $F_{Kvs}(\alpha)$  is a function of the form (12-32) appropriate to a particular value of  $K$ , a particular torsional-vibrational quantum number  $v$ , and a particular value of  $s$ . The quantum number  $s$  is defined as  $\sigma + K(I_1/I)^*$  in analogy with (12-35a). In the common case when the potential has three minima,  $s = 0, 1$ , or  $2$  [cf. expression (12-35b)]. The energies are given by

$$H_{J_{Kvs}}^{J,Kvs} = hB[J(J+1) - K^2] + hCK^2 + W_{\alpha}^{Kvs} \quad (12-44)$$

$$\text{where } B = \frac{h}{16\pi^2} \left( \frac{1}{I_x} + \frac{I_y}{I_y^2 + D^2} \right)$$

$$C = \frac{h}{8\pi^2} \left( \frac{I_y + I}{I_y I - D^2} - \frac{I_y}{I_y^2 + D^2} \right)$$

$W_{\alpha}^{Kvs}$  = the torsional or internal energy for the particular state designated by the quantum numbers  $K$ ,  $v$ , and  $s$ .

The terms of the Hamiltonian (12-41) designated as (II) may be treated as perturbations of the solutions (12-43) for the symmetric case. Part (II) has no matrix elements diagonal in  $J$ ,  $K$ ,  $v$ ,  $s$ , and the off-diagonal elements are

$$H_{J_{Kvs}}^{J,K\pm 1,v,s'} = \frac{h^2 D(2K \pm 1) \sqrt{(J \mp K)(J \pm K + 1)}}{16\pi^2(I_y^2 + D^2)} \int_0^{2\pi} e^{i(s'-s\mp 1)\alpha} F_{Kvs}^*(\alpha) F_{K\pm 1,v,s'}(\alpha) d\alpha \quad (12-45)$$

$$H_{J_{Kvs}}^{J,K\pm 2,v,s'} = \frac{-h^2}{32\pi^2} \left( \frac{1}{I_x} - \frac{I_y}{I_y^2 + D^2} \right) \frac{\sqrt{(J \mp K)(J \mp K - 1)(J \pm K + 1)(J \pm K + 2)}}{\int_0^{2\pi} e^{i(s'-s\mp 2)\alpha} F_{Kvs}^*(\alpha) F_{K\pm 2,v,s'}(\alpha) d\alpha} \quad (12-46)$$

When the potential has three minima,  $F_{Kvs}(\alpha)$  from (12-32) is a sum of terms of the type  $a_p e^{3ip\alpha}$ , where  $p$  is an integer. Hence the integral in (12-45) is different from zero only when  $s' - s \mp 1 = 3p$ , and that in (12-46) is nonzero only when  $s' - s \mp 2 = 3p$ . Therefore, for  $K \rightarrow K \pm 1$ ,  $s' - s = \pm 1$  or  $\mp 2$ , and for  $K \rightarrow K \pm 2$ ,  $s' - s = \pm 2$  or  $\mp 1$  (cf. [561]). These rules may also be expressed as  $\Delta s = \Delta K \pm 3p$ , where  $p$  is an integer.

In principle, energies  $W$  of all levels can be found from the secular equation of the determinantal form

$$|H_{J_{Kvs}}^{J,K'v's'} - W\delta_{Kvs}^{K'n's'}| = 0 \quad (12-47)$$

where the matrix elements  $H_{J_{Kvs}}^{J,K'v's'}$  are given by (12-44), (12-45), and (12-46). The symbol  $\delta_{Kvs}^{K'n's'}$  equals unity when  $K' = K$ ,  $v' = v$ , and  $s' = s$ , but otherwise it is zero. For such a calculation, however, the

functions  $F_{Kvs}$  must be obtained and the integrals indicated in (12-45) and (12-46) carried out. This procedure is not practical except in individual cases, or when special conditions make simplifying approximations appropriate. However, before considering such approximations, we shall discuss the general nature of the solutions of the secular equation.

When the hindering potential has three minima

$$[V(\alpha) = \frac{1}{2}V_0(1 - \cos 3\alpha)]$$

the levels for which  $K = s \pm 3p \pm 1$ , where  $p$  is an integer, are always doubly degenerate. This degeneracy corresponds in the symmetric-rotor case to the degeneracy of the  $\pm K$  states but is not removed by

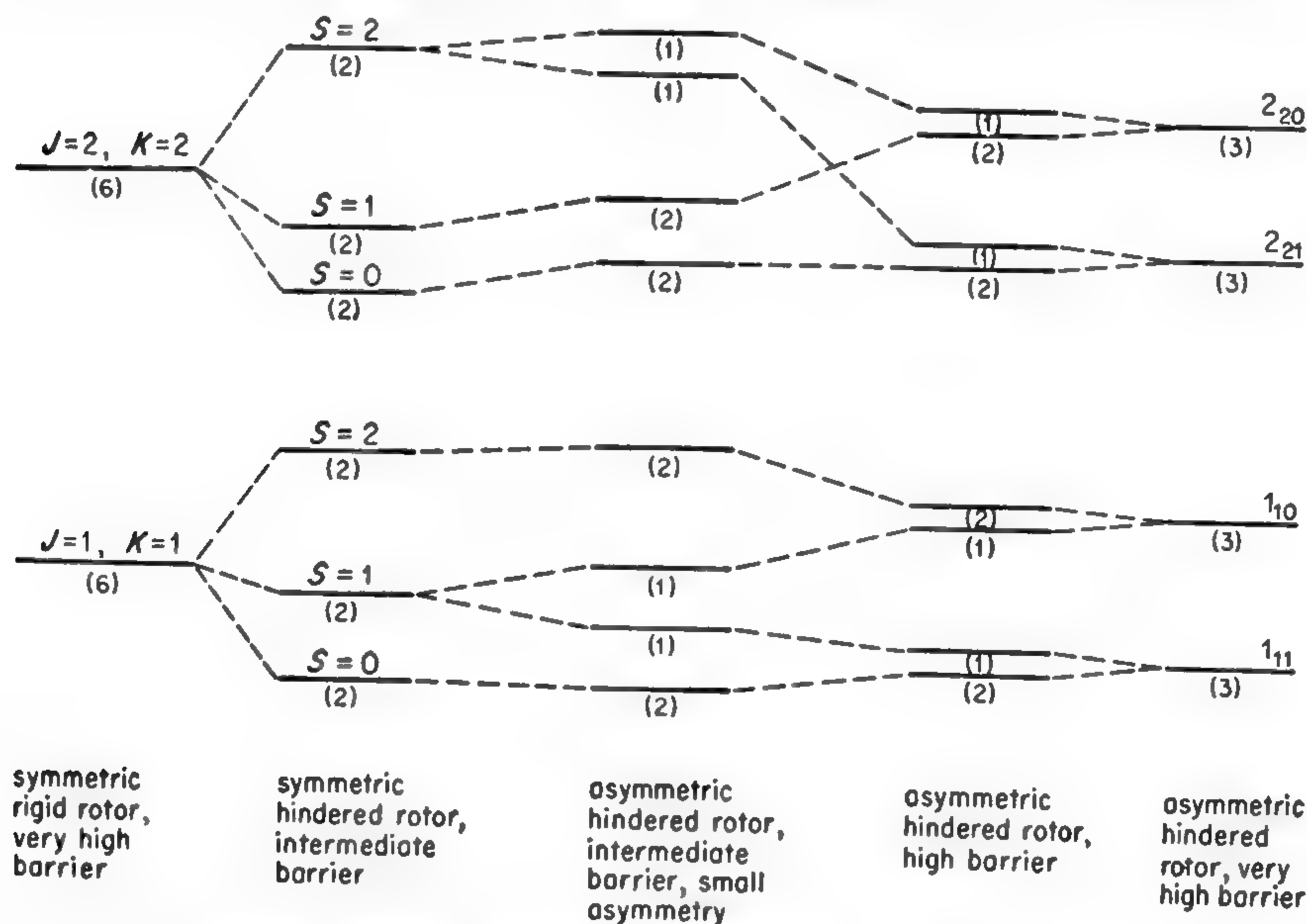


FIG. 12-8. Behavior of energy levels of a hindered rotor with three potential minima and with various asymmetries and barrier heights. Numbers in parentheses under energy levels represent the multiplicity of the level. (After Ivash and Dennison [817].)

asymmetry. However, for the states having  $K = s \pm 3p$ , asymmetry does remove the  $K$  degeneracy and splits the two levels by an amount which increases with asymmetry and decreases rapidly with increasing values of  $K$ . The general behavior of these levels for various barrier heights and asymmetries is illustrated in Fig. 12-8.

In the limit of a very high barrier, the molecule becomes a rigid asymmetric rotor. The energies  $W_{\alpha}^{Kvs}$  become simply the energies of torsional oscillation in a single potential minimum, and the integrals in the matrix elements (12-45) and (12-46) both equal unity.

Whether or not a barrier is "high" or "low" depends on the ratio of its height  $V_0$  to the kinetic energy associated with torsional momentum, or hence to the ratio

$$V' = \frac{V_0}{\frac{h^2}{2} \left( \frac{I}{I_1 I_2} \right)^*} \quad (12-48)$$

where

$$\left( \frac{I}{I_1 I_2} \right)^* = \frac{I_y I - D^2}{I_2 (I_1 I_y - D^2)}$$

For a barrier with  $V' > 200$ , the molecule may be treated as a rigid rotor for the lowest torsional-vibrational state. If  $V' \leq 100$  the lowest torsional-vibrational state will be appreciably split, and the rigid-rotor approximation is not accurate. When  $V' \approx 50$ , the lowest vibrational state is split by many megacycles and the third vibrational state lies near the top of the barrier. If  $V'$  is less than unity, the barrier is low enough for something like free rotation to exist in the lower torsional states.

*The High-barrier Case.* Good approximations for the energies when  $V' \geq 50$  have been worked out by Hecht and Dennison [934a]. They obtain for the torsional or internal energy

$$\begin{aligned} W_{\alpha}^{Kv0} &= W^v - \frac{2}{3} \Delta_v \cos \frac{2\pi K}{3} \left( \frac{I_1}{I} \right)^* \\ W_{\alpha}^{Kv1} &= W^v - \frac{2}{3} \Delta_v \cos \frac{2\pi}{3} \left[ K \left( \frac{I_1}{I} \right)^* - 1 \right] \\ W_{\alpha}^{Kv2} &= W^v - \frac{2}{3} \Delta_v \cos \frac{2\pi}{3} \left[ K \left( \frac{I_1}{I} \right)^* + 1 \right] \end{aligned} \quad (12-49)$$

where

$$\begin{aligned} W^v &= \frac{h^2}{2(I_1 I_2)^*} \left\{ 3 \sqrt{V'} \left( v + \frac{1}{2} \right) - \frac{9}{8} \left[ \left( v + \frac{1}{2} \right)^2 + \frac{1}{4} \right] \right. \\ &\quad \left. - \frac{27}{64} \frac{1}{\sqrt{V'}} \left[ \left( v + \frac{1}{2} \right)^3 + \frac{3}{4} \left( v + \frac{1}{2} \right) \right] + \dots \right\} \end{aligned} \quad (12-50)$$

and, for the ground vibrational state ( $v = 0$ ),  $\Delta_0$  is given to within a few per cent accuracy by

$$\Delta_0 = 7.05(V')^{\frac{1}{2}} \exp(-1.379 \sqrt{V'}) \quad (12-51)$$

A general expression for  $\Delta_v$  by use of the *WKB* approximation has also been obtained [934a]. The matrix elements (12-45) and (12-46) can be evaluated for the ground vibrational state of the high-barrier case from



the following values of the integrals which are involved:

$$\int_{\zeta}^{2\pi} F_{K0s}(\alpha) e^{i(s'-s\mp 2)\alpha} F_{K\pm 2,0,s'}(\alpha) d\alpha = 1 - \frac{2}{3\sqrt{V'}} \left[ 1 - \left( \frac{I_1}{I} \right)^* \right]^2 - \frac{4}{9V'} \left\{ \frac{9}{8} \left[ 1 - \left( \frac{I_1}{I} \right)^* \right]^2 - \frac{1}{2} \left[ 1 - \left( \frac{I_1}{I} \right)^* \right]^4 \right\} + \dots \quad (12-52a)$$

$$\int_0^{2\pi} F_{K0s}(\alpha) e^{i(s'-s\mp 1)\alpha} F_{K\pm 1,0,s'}(\alpha) d\alpha = 1 - \frac{1}{6\sqrt{V'}} \left[ 1 - \left( \frac{I_1}{I} \right)^* \right]^2 - \frac{1}{9V'} \left\{ \frac{9}{8} \left[ 1 - \left( \frac{I_1}{I} \right)^* \right]^2 - \frac{1}{8} \left[ 1 - \left( \frac{I_1}{I} \right)^* \right]^4 \right\} + \dots \quad (12-52b)$$

These integrals are approximately independent of the value of  $s$ . Hecht and Dennison [934a] have given explicit expressions for the energies in the high-barrier case for states with  $J = 1$  and  $J = 2$ .

*Barriers of Intermediate Height.* When the barrier is intermediate or low, that is, when  $V_0$  is not much greater than  $h^2 I_1 I_2 / 2I$ , the formulation and matrix elements discussed above may still be used. However, the approach of Burkhard and Dennison [561] may be advantageous in actual calculation of energy levels. They do not make the transformation of Eq. (12-39) required to eliminate the cross term  $D\omega_y \dot{\chi}_1$  but rather divide the Hamiltonian into two parts  $H_0$  and  $H'$ , where

$$H = H_0 + H' = \frac{(I_x + I_y)I_1 - D^2}{4I_x(I_y I_1 - D^2)} (P_x^2 + P_y^2) + \frac{1}{2(I_1 + I_2)} P_z^2 + \frac{I_1 + I_2}{2I_1 I_2} p_a^2 + V(\alpha) + H' \quad (12-53)$$

$H_0$  in this expression is identical in form with Eq. (12-27b) for the completely symmetric hindered rotor with the two equal moments of inertia replaced by  $I_B$ , where

$$I_B = \frac{2I_x(I_y I_1 - D^2)}{(I_x + I_y)I_1 - D^2} \quad (12-54)$$

Wave functions identical with Eq. (12-28) are therefore appropriate and matrix elements of  $H = H_0 + H'$  for these functions can be evaluated. They are

$$H_{JKvs}^{JKvs} = \frac{h^2}{8\pi^2 I_B} [J(J+1) - K^2] + \frac{h^2 K^2}{8\pi^2 (I_1 + I_2)} - \frac{h^2 D^2}{8\pi^2 I_1 (I_y I_1 - D^2)} \int_0^{2\pi} e^{-is\alpha} F_{Kvs}^{*(\alpha)} \frac{d^2}{d\alpha^2} (e^{is\alpha} F_{Kvs}^{(\alpha)}) d\alpha \quad (12-55)$$

$$H_{JKvs}^{JKvs} = - \frac{h^2 D^2}{8\pi^2 I_1 (I_y I_1 - D^2)} \int_0^{2\pi} e^{-is\alpha} F_{Kvs}^{*(\alpha)} \frac{d^2}{d\alpha^2} (e^{is\alpha} F_{Kvs}^{(\alpha)}) d\alpha \quad (12-56)$$

$$H_{J K v s}^{J, K \pm 1, v', s'} = \frac{\hbar^2 D \sqrt{(J \mp K)(J \pm K + 1)}}{8\pi^2(I_v I_1 - D^2)} \int_0^{2\pi} \left[ \pm \frac{e^{-i(s \pm 1)\alpha}}{i} F_{K v s}^{*(\alpha)} \frac{d}{d\alpha} \right. \\ \left. (e^{i s' \alpha} F_{K \pm 1, v' s'}) - \frac{e^{i(s' - s \mp 1)\alpha}}{2} F_{K v s}^{*(\alpha)} F_{K \pm 1, v' s'}^{(\alpha)} \right] d\alpha \quad (12-57)$$

$$H_{J K v s}^{J, K \pm 2, v', s'} = \hbar^2 \cdot \frac{(I_x I_1 - I_v I_1 + D^2)}{32\pi^2 I_x (I_v I_1 - D^2)} \sqrt{(J \mp K)(J \mp K - 1)} \\ \times \sqrt{(J \pm K + 1)(J \pm K + 2)} \int_0^{2\pi} e^{i(s' - s \mp 2)\alpha} F_{J K v s}^{*(\alpha)} F_{J, K \pm 2, v', s'} d\alpha \quad (12-58)$$

As for Eqs. (12-45) and (12-46), these matrix elements are nonzero only when  $\Delta S = \Delta K \pm 3p$ , where  $p$  is an integer. Energy levels may be determined from them by solution of a secular equation of the form (12-47).

The previous treatment, which eliminated the cross term  $D\omega_v \dot{\chi}_1$  and gave (12-41), is of advantage in avoiding matrix elements between states of different vibrational quantum number  $v$ . These are especially troublesome only in the high-barrier case, where their elimination affords considerable simplification.

*The Low-barrier Case.* When the barrier is very low, that is, when  $V_0 \leq \frac{\hbar^2}{2(I/I_1 I_2)^*}$ , the most appropriate starting point for approximations is free internal rotation. If  $V_0$  is assumed to equal zero, the part of the wave function for the internal motion, which is equivalent to (12-29), becomes

$$\frac{\hbar^2}{2} \left( \frac{I}{I_1 I_2} \right)^* \frac{d^2 \mathfrak{M}}{d\alpha^2} + W_\alpha \mathfrak{M} = 0$$

Hence

$$\mathfrak{M}(\alpha) = \frac{1}{\sqrt{2\pi}} e^{\pm i[m_1 - K(I_1/I)^*]\alpha} \quad (12-59)$$

and

$$W_\alpha^{m_1} = \frac{\hbar^2}{2} \left( \frac{I}{I_1 I_2} \right)^* \left[ m_1 - K \left( \frac{I_1}{I} \right)^* \right]^2 \quad (12-60)$$

To satisfy boundary conditions, as in (12-35a),  $m_1$  must be an integer.  $F_{K v s}(x)$  is just  $1/\sqrt{2\pi} e^{3ip\alpha}$ , where  $s + 3p = m_1$ . It may be seen from (12-24) that  $m_1$  is just the angular momentum in units of  $\hbar$  of the asymmetric part of the molecule about the  $z'$  axis. From the similarity of the two parts of the molecule,  $m_1 - K(I_1/I)^*$  in (12-59) and (12-60) might have been replaced by  $m_2 - K(I_2/I)^*$ , where  $m_2 \hbar$  is the angular momentum of the symmetric part and  $m_1 + m_2 = K$ . The quantum numbers  $v$  and  $s$  may be replaced by the number  $m_1$  or  $m_2$ . The matrix elements (12-45) and (12-46) then become

$$H_{JKm_1}^{J,K\pm 1,m_1\pm 1} = H_{JKm_2}^{J,K\pm 1,m_2} = \frac{h^2 D(2K \pm 1) \sqrt{(J \mp K)(J \pm K + 1)}}{16\pi^2(I_y^2 + D^2)} \quad (12-61)$$

$$H_{JKm_1}^{J,K\pm 2,m_1\pm 2} = H_{JKm_2}^{J,K\pm 2,m_2} = \frac{-h^2}{32\pi^2} \left( \frac{1}{I_z} - \frac{I_y}{I_y^2 + D^2} \right) \sqrt{(J \mp K)(J \mp K - 1)(J \pm K + 1)(J \pm K + 2)} \quad (12-62)$$

If the barrier is low, but not zero, then it may be considered a small perturbation. The largest effects of such a perturbation are to add a constant  $V_0/2$  to  $W_\alpha^m$ , and to split pairs of levels which are close together and for which  $m$  differs by  $n$ , where  $n$  is the number of potential minima. This splitting is due to the existence of off-diagonal matrix elements of

$$V(\alpha) = \frac{V_0}{2} (1 - \cos n\alpha)$$

which are

$$V_{JKm}^{J,K,m\pm n} = -\frac{V_0}{4} \quad (12-63)$$

Matrix elements such as (12-63) are most important when there is a near degeneracy of the two levels which they connect.

*Other Cases.* A number of other useful approximations can be obtained for various special cases. Wilson, Lin, and Lide [1,000a] have discussed the case of a hindered asymmetric rotor with the product of inertia  $D$  equal to zero. They use a similar but somewhat different approach from that adopted above and give useful approximations for cases of small asymmetry and of high and low barriers.

Burkhard [782a] has formulated the rather general case of two asymmetric parts of a molecule with a potential hindering their relative motion, and with the sole limitation that the center of mass of one of these parts must lie on the axis of hindered rotation. He has written out the wave equation for this case and the matrix elements needed for a solution. Burkhard has also written down the wave equation and matrix elements for the still more general case of hindered rotation of two asymmetric parts with the center of gravity of neither part on the axis of rotation [908a]. However, this case is too unwieldy to be very useful unless simplifying approximations apply.

**12-9. Selection Rules.** For hindered rotors, the usual selection rule  $\Delta J = 0, \pm 1$  for the total angular momentum applies, as well as

$$\Delta M = 0, \pm 1$$

for the projection of  $J$  on a space-fixed axis. One other general rule can be stated for transitions of a hindered rotor of which one part is a symmetric top. It was pointed out in discussion of the matrix elements (12-45) and (12-46) that if the potential has three minima these matrix



elements connect only states for which

$$\Delta K = \Delta s \pm 3p$$

where  $p$  is an integer. This rule breaks up the states into three types which may be divided as follows:

$$K = s \pm 3p \qquad K = s \pm 3p + 1 \qquad K = s \pm 3p - 1 \quad (12-64)$$

For a potential with  $n$  minima, the states may similarly be divided into  $n$  groups. There are also no electric dipole transitions between the different types of states specified by (12-64), so that one may write the selection rule  $\Delta K = \Delta s \pm 3p$ , or more generally

$$\Delta K = \Delta s \pm np \qquad (12-65)$$

where  $p$  is an integer and  $n$  is the number of potential minima. It should be noted that, if the rotor is asymmetric, it will involve a sum of symmetric-rotor states of various values of  $K$  so that  $K$  is not a well-defined quantity. However, from (12-64) a given state involves values of  $K - s$  which differ only by  $\pm 3p$ , so that the selection rule (12-65) is meaningful.

For the general asymmetric rotor, all transitions are allowed which satisfy (12-65) and for which  $\Delta J = 0$  or  $\pm 1$  and  $\Delta M = 0$  or  $\pm 1$ . However, unless the rotor is very asymmetric, the stronger transitions are given by the somewhat more restrictive selection rules of a symmetric rotor, which will now be discussed.

The electric dipole moment of a strictly symmetric rotor will always be parallel to the molecular axis. However, since we are also concerned with nearly symmetric tops, it will be assumed that the dipole moment may have a component perpendicular to the axis as well as one parallel to the axis. Selection rules are different for the two types of dipole moments, and intensities are in each case proportional to the square

TABLE 12-7. SELECTION RULES FOR SYMMETRIC OR NEARLY SYMMETRIC ROTORS WITH HINDERED ROTATION

The rules  $\Delta J = 0, \pm 1$  and  $\Delta M = 0, \pm 1$  apply to all transitions.  $m_1 \hbar$  is the angular momentum about the molecular axis of that part of the molecule which may have a dipole moment perpendicular to the axis.

	Very high barrier	Free rotation (zero barrier)	Intermediate barrier
Dipole moment parallel to molecular axis	$\begin{cases} \Delta K = 0 \\ \Delta s = 0 \\ \Delta v = 0 \end{cases}$	$\begin{matrix} \Delta K = 0 \\ \Delta m_1 = \Delta m_2 = 0 \end{matrix}$	$\begin{matrix} \Delta K = 0 \\ \Delta s = 0 \\ \Delta v = 0 \end{matrix}$
Dipole moment perpendicular to molecular axis	$\begin{cases} \Delta K = \pm 1 \\ \Delta v = 0, \pm 1 \end{cases}$	$\begin{matrix} \Delta K = \pm 1 \\ \Delta m_1 = \pm 1 \\ \Delta m_2 = 0 \end{matrix}$	$\begin{matrix} \Delta K = \pm 1 \\ \Delta K = \Delta s \pm np \\ \Delta v = \text{anything} \end{matrix}$

of the component of the dipole moment involved. The selection rules are given in Table 12-7. The very-high-barrier case with the dipole moment parallel to the axis corresponds to the normal rigid symmetric rotor. In the case of free rotation with a dipole perpendicular to the axis, the angular momentum about the axis  $m_1\hbar$  of only the asymmetric part of the molecule changes, since it alone would allow a perpendicular component of the dipole moment.

**12-10. Examples of Hindered Torsional Motion in Asymmetric Rotors.** The case of hindered torsional motion which has received by far the most complete and detailed analysis is  $\text{CH}_3\text{OH}$ . This is the molecule to which Koehler and Dennison [99] applied the symmetric-rotor approximation. However, little quantitative progress could be made until the advent of microwave spectroscopy allowed measurement of the  $\text{CH}_3\text{OH}$  spectrum under high resolution. Burkhard and Dennison [561] first worked out the  $\text{CH}_3\text{OH}$  hindered motion in detail, and quantitatively fitted the rather extensive microwave spectrum measured by Hughes, Good, and Coles [590] and by others. From this work the structure of  $\text{CH}_3\text{OH}$ , the components of the dipole moment perpendicular and parallel to the  $\text{CH}_3$  axis, and the barrier height listed in Table 12-6 was obtained. A similar but still more complete discussion of  $\text{CH}_3\text{OH}$  has been given by Ivash and Dennison [817].

The  $\text{CH}_3\text{OH}$  lines of primary interest here make up an intense series beginning near 25,000 Mc, extending to about 31,000 Mc, and then returning toward lower frequencies. Thirty members of the series have been found. Stark effects of these lines show that the series corresponds to  $\Delta J = 0$  transitions, that for the first line of the series  $J = 2$ , and that others involve successively higher values of  $J$ . The frequencies of the first dozen members of this series (for the common isotopic species of  $\text{CH}_3\text{OH}$ ) are fairly accurately given [561] by

$$\begin{aligned} \nu = & 24,948.13 - 2.9656J(J+1) + 0.11258J^2(J+1)^2 - 0.4094 \\ & \times 10^{-4}J^3(J+1)^3 - 0.3168 \times 10^{-6}J^4(J+1)^4 \quad \text{Mc} \quad (12-66) \end{aligned}$$

Burkhard and Dennison [561] showed that the only explanation of the origin of this series consistent with reasonable parameters for the  $\text{CH}_3\text{OH}$  molecule is a transition of the type  $\nu = 0, \Delta J = 0, K = 2 \leftarrow 1, s = 0 \leftarrow 2$ . The increase of rotational energy due to the transition  $K = 2 \leftarrow 1$  is approximately  $10 \text{ cm}^{-1}$ , which is almost canceled by the decrease in internal energy of about  $9 \text{ cm}^{-1}$  due to the transition  $s = 0 \leftarrow 2$ . The difference between these two quantities depends to some extent on  $J$ , which allows the series of lines for different values of  $J$ . The lowest value of  $J$  for such a series equals, of course, the maximum value of  $K$ , which is 2. This is in agreement with the results of Stark-effect measurements.

The value of  $V' = \frac{V_0}{h^2 I / 2 I_1 I_2}$  in  $\text{CH}_3\text{OH}$  is approximately 13, so that the barrier is of intermediate height, and neither the high-barrier nor low-barrier approximations discussed above are accurate. Burkhard and Dennison [561] have, however, worked out approximate expressions for the torsional energy.

An interesting example of a low barrier is afforded by  $\text{CH}_3\text{NO}_2$ , which has been studied by Tannenbaum, Johnson, Myers, and Gwinn [986].  $\text{CH}_3\text{NO}_2$  has a potential with 6 minima and a height of  $4.2 \text{ cm}^{-1}$ . The quantity  $h^2 I / 2 I_1 I_2$  is approximately  $5.8 \text{ cm}^{-1}$ , so that  $V' = 0.72$ , and the low-barrier approximation is appropriate. Table 12-8 gives observed components of the  $J = 2 \leftarrow 1$  transition of this molecule and calculated frequencies assuming either a zero barrier or a barrier of height  $V_0 = 4.20$

TABLE 12-8. STRUCTURE OF THE  $J = 2 \leftarrow 1$  TRANSITION OF  $\text{CH}_3\text{NO}_2$ , A MOLECULE WITH HINDERED TORSION AND A LOW BARRIER

Frequencies are calculated assuming  $B + C = 16,419.3 - 0.32m_2^2 \text{ Mc}$ ,  
 $B - C = 4,666.0 \text{ Mc}$ ,

$h/8\pi^2 I_1 = 13,277.5 \text{ Mc}$ , and  $h/8\pi^2 I_2 = 160,000 \text{ Mc}$ . (From Tannenbaum, Johnson, Myers, and Gwinn [986].)

$K$	$m_1$	$m_2$	Calculated frequencies, Mc		Measured frequencies, Mc
			$V_0 = 0$	$V_0 = 4.20 \text{ cm}^{-1}$	
0	0	0	30,010.7	30,011.5	30,035.6
$\pm 1$	$\pm 2$	$\mp 1$	32,033.4	32,034.1	32,034.1
$\pm 1$	0	$\pm 1$	33,642.5	33,643.5	33,643.5
0	$\mp 2$	$\pm 2$	32,959.8	32,959.8	32,959.2
$\pm 1$	$\mp 2$	$\pm 3$	33,174.4	33,474.6	33,476.5
$\mp 1$	$\pm 2$	$\mp 3$	33,174.4	31,676.2	31,677.3
$\pm 1$	$\pm 4$	$\mp 3$	32,491.6	32,191.4	32,189.7
$\mp 1$	$\mp 4$	$\pm 3$	32,491.6	33,989.8	33,988.5
0	$\mp 4$	$\pm 4$	32,856.6	32,856.6	32,859.5

$\text{cm}^{-1}$ . Since  $\text{NO}_2$  has no dipole moment perpendicular to the molecular axis, the torsional energy does not appear very directly in the transition frequencies, and hence the free-rotation approximation is fairly accurate. However, the potential does strongly affect the energy levels with  $m_2 = \pm 3 = \pm n/2$ . These levels are split by an interaction of the type indicated by (12-63).

In  $\text{CH}_3\text{NO}_2$ , the zero spin and Bose-Einstein statistics of  $\text{O}^{16}$  require that only levels with even  $m_1$  are permitted. For, if two oxygens in the  $\text{NO}_2$  group are interchanged, this is equivalent to a rotation about the axis of  $180^\circ$ , so that the wave function is changed by  $e^{im_1\pi}$ . Since the  $\text{O}^{16}$  spins are zero and only a symmetric-spin wave function can be formed,



the spatial part of the wave function must also be symmetric. This requires that  $e^{im_1\pi} = 1$ , or that  $m_1$  is an even integer.

The magnitude of  $V_0$  gives some interesting qualitative information about the nature of barriers in molecules with three potential minima. Consider the hypothetical molecule  $\text{CH}_3\text{NO}$ , which would have three potential minima, with a potential of the general form

$$V = \sum_p V_p \cos 3p\alpha \quad (12-67)$$

Presumably the height of the barrier would be approximately the same as found in most molecules of this geometry, that is,  $V_1$  equals a few hundred wave numbers. If a second oxygen  $180^\circ$  away from the first is added to the molecule to produce  $\text{CH}_3\text{NO}_2$ , the potential is

$$\begin{aligned} V &= \sum_p V_p [\cos 3p\alpha + \cos 3p(\alpha + \pi)] \\ &= \sum_p 2V_{2p} \cos 6p\alpha \end{aligned} \quad (12-68)$$

Since experimentally  $2V_2 = 4.2 \text{ cm}^{-1}$ , we have a good indication that  $V_2/V_1$  is only a few parts in 100; therefore, higher terms in a series such as (12-67) are probably not important. In view of this it is very surprising, however, that the 12-minima potential of  $\text{CF}_3\text{SF}_6$  is as large as is given in Table 12-6.

## CHAPTER 13

### SHAPES AND WIDTHS OF SPECTRAL LINES

A truly isolated, undisturbed, and stationary molecular system would have the attractive feature of definite and fixed energy levels, but various types of unavoidable disturbances do in fact vary the energy levels, giving a width to spectral lines and varying their average or center frequencies. The sources of spectral line broadening which need to be considered are:

1. Natural line breadth
2. Doppler effect
3. Pressure broadening, *i.e.*, disturbances due to interactions between molecules
4. Saturation broadening
5. Collisions between molecules and the walls of a containing vessel.

**13-1. Natural Line Breadth.** The natural line breadth may be interpreted classically as due to radiation damping, or quantum-mechanically as a disturbance of the molecule by zero-point vibration of electromagnetic fields which are always present in free space. For a transition of frequency  $\nu$  from an excited state to the ground state of the system, zero-point electromagnetic fields give an absorption line a half width at half maximum intensity of

$$\Delta\nu = \frac{32\pi^3\nu^3}{3hc^3} |\mu|^2 \quad \text{cycles/sec} \quad (13-1)$$

where  $\mu$  is the quantum-mechanical matrix element of the dipole moment—usually of the order of 1 debye unit, or  $10^{-18}$  esu. For radiation of 1 cm wavelength  $\Delta\nu$  is, from Eq. (13-1), approximately  $10^{-7}$  cycle/sec. For radio frequencies and ordinary temperatures, thermal radiation consists of stronger electromagnetic fields than the usual zero-point fields, since each mode of vibration of the field has a mean energy  $kT$  rather than  $\frac{1}{2}h\nu$ . This increases the value of  $\Delta\nu$  by a factor  $2kT/h\nu$ , or approximately 400 for room temperature, giving a “natural” width of  $4 \times 10^{-5}$  cycle/sec. This width is quite negligible in comparison with that caused by other types of broadening.

The natural line breadth is often regarded as an unchangeable effect of disturbance of the system by electromagnetic fields, which are uni-

formly present in all space. However, in the radio-frequency range the zero-point electromagnetic fields need not be uniform because cavities or circuits may be as small as one wavelength. Thus in a cavity with perfectly reflecting walls only certain resonant frequencies can occur, and a particular frequency necessary to cause a particular microwave transition may not occur. In this case no "spontaneous" emission of this frequency can occur, and the natural line breadth is zero. Similarly natural line breadths may be increased by the presence of resonant circuits which increase the local strength of zero-point electromagnetic vibrations.

Radiation broadening is of importance for microwave spectroscopy when transitions between levels of excited electronic states are observed. Then the line width is large because it is proportional to  $\nu_0^3$ , where  $\nu_0$  is now the frequency of the transition to the ground electronic state. For instance, the  $2p\ ^2P_{1/2}$  state of hydrogen, discussed in connection with the Lamb-Retherford experiment in Chap. 5, has a natural half width of 50 Mc.

**13-2. Doppler Effect.** The Doppler effect occurs when a molecule is moving parallel to the direction of propagation of the radiation being absorbed, and gives a frequency shift of  $\pm \nu(v/v_p)$ , where  $\nu$  is the resonant frequency without Doppler shift,  $v$  the molecular velocity, and  $v_p$  the velocity of phase propagation of the radiation. Although under some conditions  $v_p$  may be larger than  $c$  (e.g., for propagation in a waveguide near cutoff), usually  $v_p \approx c$ , and the fractional frequency shifts are simply  $v/c$ . The probability that a molecule in a gas at temperature  $T$  has a velocity  $v$  in a particular direction is proportional to  $e^{-mv^2/2kT}$ , where  $m$  is the molecular mass. Hence the line intensity as a function of change  $\epsilon$  from the resonance frequency is  $e^{-\frac{mc^2}{2kT}(\frac{\epsilon}{\nu})^2}$ . The line is consequently symmetric and has a half width at half maximum of

$$\Delta\nu = \frac{\nu}{c} \sqrt{\frac{2kT}{m} \ln 2} = \frac{\nu}{c} \sqrt{2kN_0 \ln 2} \sqrt{\frac{T}{M}} = 3.581 \times 10^{-7} \sqrt{\frac{T}{M}} \nu \quad (13-2)$$

where  $M$  is the molecular weight and  $N_0$  is Avogadro's number. For an ammonia molecule at room temperature,  $\Delta\nu/\nu = 1.5 \times 10^{-6}$ . Doppler effect can be decreased to some extent by use of heavier molecules and lower temperatures, but a decrease in line width of more than a factor of 2 can hardly be expected because at low temperatures molecules have not sufficient vapor pressure ( $\sim 10^{-2}$  mm Hg) to absorb radiation. A great decrease in Doppler width is obtained in some optical spectroscopy experiments by observing an atomic beam at right angles to its direction of motion [238]. This method is not so easy to apply or so popular in microwave spectroscopy, but it has been used in two different types of microwave spectrometers [709], [925], [982]. Newell and Dicke [622] have also developed a technique of selecting absorption only from



molecules in a certain narrow velocity range and thus decreasing the effect of Doppler broadening on the line width by a factor of 10 or more. Although these techniques sacrifice sensitivity to eliminate Doppler effect and obtain narrow lines, they should be useful for resolving very closely spaced lines in strong microwave spectra.

**13-3. Pressure Broadening.** The most important source of broadening in many microwave experiments is pressure broadening. It is also the most interesting because it provides information about how molecules behave in intermolecular collisions and hence about molecular force fields. This broadening arises from collisions between molecules.

The spectral distribution of a molecular oscillation of finite lifetime was first considered by Lorentz [2]. For an oscillator whose amplitude decreases exponentially with time ( $a = a_0 e^{-t/\tau}$ ), the radiation distribution corresponds to the well-known resonance-type curve with a half width in frequency of  $1/2\pi\tau$ . Exactly the same result is obtained for a group of oscillators, each of which oscillates with a constant amplitude but is abruptly stopped after time  $t$ , where the number oscillating for time  $t$  is given by  $n_t = n_0 e^{-t/\tau}$ . The theory assumes that after a collision, when the oscillation is stopped, it starts again with a phase having no relationship to the phase before collision; *i.e.*, "strong" collisions are assumed. When applied to the case of rotating molecules, this assumption is equivalent to assuming that the orientation of the molecules after collision is random.

A fairly complete qualitative description of pressure broadening in the microwave and radio-frequency region can be obtained with the simple assumption that collisions are very brief, but so strong that the behavior of the molecule after collision has no particular relationship to that before collision. We shall first explore the consequences of collisions of this type to obtain a general description of pressure broadening, and then return to examine in more detail what happens during a collision and the relation between pressure broadening and intermolecular forces.

Debye ([12], Chap. 5) considered the case of the fixed dipole with no rotation or translation energy. After each collision the dipole is assumed to be not completely random in orientation, but oriented with respect to the electric field present at the moment in accordance with the Boltzmann distribution  $\exp(-\mathbf{E} \cdot \mathbf{\mu}/kT)$ , where  $\mathbf{E}$  is the electric field strength existing at the time,  $\mathbf{\mu}$  is the dipole moment, and  $k$  and  $T$  are the Boltzmann constant and the absolute temperature, respectively. If the field has oscillated many times before the molecule makes another collision, the dipole has no special orientation with respect to the field at the time of this next collision. During the next collision, however, it is again oriented with respect to the field present, again absorbing a small quantity of energy from the field during this orientation process. Such a process is repeated many times and thus absorbs energy although there

is no characteristic resonance peak. Debye calculated the theoretical expression for this type of absorption (*cf.* Van Vleck and Weisskopf [136] for some discussion and generalization). In this case, the absorption per unit length is

$$\gamma = \frac{\omega}{c} \frac{4\pi N \mu^2}{3kT} \frac{\omega\tau}{1 + \omega^2\tau^2} \quad (13-3)$$

where  $\omega$  is the angular frequency ( $2\pi\nu$ ) of the incident radiation,  $\tau$  is the mean lifetime between collisions,  $N$  is the number of molecules per cubic centimeter,  $\mu$  is the dipole moment of a molecule,  $c$  is the velocity of light,  $k$  is the Boltzmann constant, and  $T$  is the absolute temperature.

*The Van Vleck-Weisskopf Line Shape.* The Debye and Lorentz theories have been synthesized by Van Vleck and Weisskopf ([136]; see also H. Fröhlich [154] for another derivation). Assuming that the molecule undergoes a violent collision the phase of its oscillation after such a collision will not be greatly dependent on its phase at the start of the collision. In this case there must be thermodynamic equilibrium between the molecule and the existing electric field immediately after each collision somewhat like the assumed equilibrium distribution in the orientation of the fixed dipole mentioned above. Using this assumption rather than Lorentz's assumption that the phase after a collision is arbitrary, an expression similar to Lorentz's formula may be obtained which is consistent with the Debye case.

Since the rotation of a molecule can always be resolved into two perpendicular vibrations, it is sufficient to consider a linear vibrator. To determine the absorption and the dielectric constant associated with a vibrating charge in a classical way, one needs only to solve the equation of motion of the oscillator in the field subject to the right boundary conditions. The equation is of the type

$$\ddot{x} + \omega_0^2 x = \frac{eE}{m} \cos \omega t \quad (13-4)$$

where  $\omega_0 = 2\pi$  times the natural molecular frequency

$\omega = 2\pi$  times the frequency of oscillation of the field  $E$

Before solving Eq. (13-4) we shall show how the absorption and dielectric constant may be obtained from the solution for  $x$ . The dielectric constant is defined as usual

$$K = \frac{D}{E} = 1 + 4\pi \frac{P}{E} \quad (13-5)$$

where  $P$  is the polarization per unit volume. After  $x$  has been averaged over all molecules, it will be of the form

$$\bar{x} = aE \cos \omega t + bE \sin \omega t \quad (13-6)$$

The real part of the polarization is  $P = naEe \cos \omega t$ , so that

$$K = 1 + 4\pi nae \quad (13-6a)$$

where  $n$  is the number of such oscillators per unit volume.

To obtain the fractional absorption of power per unit distance, consider a cube of unit volume with the radiation traveling through it perpendicular to one of the faces. The radiation absorbed during a time  $T$  will be

$$n \int_0^T e \dot{x} E \cos \omega t dt$$

The total radiation energy passing into the cube will be  $c(E^2/8\pi)T$ , where  $c$  is the velocity of light, so that the fractional absorption per unit distance or the absorption coefficient will be

$$\frac{neE \int_0^T \dot{x} \cos \omega t dt}{c(E^2/8\pi)T}$$

Remembering again the form of  $\bar{x}$  and integrating over a long period of time the absorption coefficient is seen to be

$$\gamma = \frac{4\pi neb\omega}{c} \quad (13-7)$$

We return to a solution of the equation of motion. For ease of solution we use a complex quantity  $e^{i\omega t}$  for  $\cos \omega t$  in the equation of motion so that  $x$  will be the real part of the solution, which is of the form

$$\frac{eEe^{i\omega t}}{m(\omega_0^2 - \omega^2)} + c_1e^{i\omega_0 t} + c_2e^{-i\omega_0 t} \quad (13-8)$$

where  $c_1$  and  $c_2$  depend on the initial values of  $x$  and  $\dot{x}$ . The average initial value of  $x$  and  $\dot{x}$  can be found from the energy

$$H = \frac{m}{2} (\dot{x})^2 + \frac{m}{2} (\omega_0 x)^2 - exE \cos \omega t \quad (13-9)$$

thus

$$\bar{x}_0 = \frac{\int x e^{-H/kT} dx d\dot{x}}{\int e^{-H/kT} dx d\dot{x}} = \frac{Ee \cos \omega t}{m\omega_0^2} \quad (13-10)$$

and similarly

$$\bar{\dot{x}}_0 = \dot{\bar{x}}_0 = 0 \quad (13-11)$$

For some time of interest  $t$  the constants  $c_1$  and  $c_2$  will be functions of  $t_1$ , the time of last collision of the molecule. We must average then over all values of  $t_1$ . The distribution of collisions in time can be written according to kinetic theory

$$n(t_1) = \frac{1}{\tau} e^{-(t-t_1)/\tau} dt \quad (13-12)$$



where  $\tau$  is the mean time between collisions, where  $n(t_1)$  is the probability that a molecule which made a collision at time  $t_1$  will make another at time  $t$ . Our expression for  $x$  must be averaged over this distribution. After performing the average one can find the in-phase and the quadrature terms of the real part of  $\bar{x}$  to be

$$a = \frac{e}{m(\omega_0^2 - \omega^2)} \left\{ 1 - \frac{\omega}{2\omega_0^2\tau^2} \left[ \frac{\omega_0 + \omega}{(1/\tau)^2 + (\omega_0 - \omega)^2} + \frac{\omega - \omega_0}{(1/\tau)^2 + (\omega_0 + \omega)^2} \right] \right\} \quad (13-13)$$

$$b = \frac{e\omega}{2m\omega_0^2\tau} \left\{ \frac{1}{(1/\tau)^2 + (\omega_0 - \omega)^2} + \frac{1}{(1/\tau)^2 + (\omega_0 + \omega)^2} \right\} \quad (13-14)$$

Correspondingly, from Eq. (13-6a) the dielectric constant is

$$K = 1 + \frac{ne^2}{\pi m(\nu_0^2 - \nu^2)} \left\{ 1 - \frac{\nu}{2\nu_0^2(2\pi\tau)^2} \left[ \frac{\nu_0 + \nu}{(1/2\pi\tau)^2 + (\nu_0 - \nu)^2} + \frac{\nu - \nu_0}{(1/2\pi\tau)^2 + (\nu_0 + \nu)^2} \right] \right\} \quad (13-15)$$

and the absorption coefficient from Eq. (13-7) is

$$\gamma = \frac{ne^2\nu^2}{mc\nu_0^2} \left[ \frac{1/2\pi\tau}{(\nu - \nu_0)^2 + (1/2\pi\tau)^2} + \frac{1/2\pi\tau}{(\nu + \nu_0)^2 + (1/2\pi\tau)^2} \right] \text{ cm}^{-1} \quad (13-16)$$

This is the complete expression for a classical oscillator. They must be modified to some extent, however, for the quantum-mechanical case. In such equations it is found that  $e^2/m$  in a classical expression corresponds to  $(8\pi^2/3h)|\mu_{ij}|^2\nu_0$  in the corresponding quantum-mechanical expression. This may be seen by comparing Eq. (19) on p. 38 with Eq. (19) on p. 180 of Heitler's *The Quantum Theory of Radiation* [936]. Here  $\mu_{ij}$  is the matrix element of the dipole moment, or may be called the dipole moment for the transition from state  $i$  to state  $j$ . These substitutions give the proper transition to the quantum-mechanical expression. It should be noted that  $|\mu_{ij}|^2$  is an average of the square of the matrix element for a transition from the lower state  $i$  to the upper state  $j$ . It is defined, as in Eq. (1-76), by

$$|\mu_{ij}|^2 = \sum_{M'} |\mu_x(JMJ'M')|^2 + |\mu_y(JMJ'M')|^2 + |\mu_z(JMJ'M')|^2$$

We have assumed so far that oscillators are absorbing energy only and not emitting energy. From the quantum-mechanical viewpoint there must be oscillators in the upper state of the transition as well as those in the lower state, and it can be shown that the electromagnetic field induces the oscillators in the upper state to emit with the same probability that the oscillators in the lower state absorb. Our net absorption is then

proportional to the difference in the number of oscillators in the upper and lower state, which is

$$\Delta n = (1 - e^{-h\nu_0/kT})n \quad (13-17)$$

where  $n$  is the number of molecules per unit volume in the lower state. In the radio-frequency region  $h\nu_0 \ll kT$ , so that this can be well approximated by

$$\Delta n = \frac{h\nu_0}{kT} n \quad (13-18)$$

In addition to these two states there may be many other molecular states which are occupied by molecules of our material. We may represent by  $f$  the fraction of the total which is in the lower of the two states of interest, so that  $n$  in the above equations may be replaced by  $Nf$ , where  $N$  is the total number of molecules per unit volume. Making this substitution we obtain the final expression

$$\gamma = \frac{8\pi^2 Nf}{3ckT} |\mu_{ij}|^2 \nu^2 \left[ \frac{1/2\pi\tau}{(\nu - \nu_0)^2 + (1/2\pi\tau)^2} + \frac{1/2\pi\tau}{(\nu + \nu_0)^2 + (1/2\pi\tau)^2} \right] \text{ cm}^{-1} \quad (13-19)$$

This can be shown to reduce to the Debye case when  $\nu_0$  is 0, for then  $\gamma$  becomes

$$\gamma = \frac{8\pi Nf\mu^2}{3ckT} \frac{\omega^2\tau}{1 + \omega^2\tau^2} \text{ cm}^{-1} \quad (13-20)$$

In that case also  $f = \frac{1}{2}$  and

$$\gamma = \frac{4\pi N\mu^2}{3ckT} \frac{\omega^2\tau}{1 + \omega^2\tau^2} \text{ cm}^{-1} \quad (13-21)$$

which is identical with expression (13-3) derived directly from the Debye theory.

At low pressures (*i.e.*, where  $1/2\pi\tau \ll \nu_0$ ), the first term in Eq. (13-19) is the predominant one. The intensity at the line center is then proportional to  $N$ , where  $N$  is the number of molecules per unit volume and  $\tau$  is the mean time between molecular collisions. But the time between collisions is inversely proportional to the pressure, so that  $N$  is independent of pressure. Thus the intensity at the peak of a microwave line is independent of pressure over a wider range of pressures. Moreover the line width is proportional to  $1/2\pi\tau$ , and therefore to the pressure.

The first term of Eq. (13-19) was given in Chap. 1 without proof as Eq. (1-49). It is the most commonly used expression because it does fit the observed microwave line intensities and widths well at low and medium pressures. Karplus and Schwinger [297] have given a quantum-mechanical derivation of the Van Vleck-Weisskopf formula for the shape

and intensity of a microwave spectral line. The assumptions are the same, *i.e.*, collisions so strong that the Boltzmann energy distribution is restored after each collision, and that the duration of a collision is short enough that the field does not change appreciably during the collision. It is not necessary that  $\Delta\nu$  be less than  $\nu$ , and the theory would appear to apply even at quite high pressures.

Van Vleck and Margenau [424] have also examined the Van Vleck-Weisskopf theory. They evaluated separately the work done between collisions and that done impulsively by sudden changes of position of the molecule in the electric field at collisions.

The dielectric constant  $K$  and absorption coefficient  $\gamma$  are both given for a particular line shape by (13-15) and (13-16). There are general relations between the dielectric constant and absorption coefficient for any system [8a], [135a], of which these equations are a special case. The general expressions are known as the Kramers-Kronig relations, and may be written

$$K(\omega) - 1 = \frac{2c}{\pi} \int_0^\infty \frac{\omega' \gamma(\omega') d\omega'}{\omega[\omega'^2 - \omega^2]}$$

$$\gamma(\omega) = \frac{-2\omega^2}{\pi c} \int_0^\infty \frac{[K(\omega') - 1] d\omega'}{\omega'^2 - \omega^2}$$

**13-4. Absolute or Integrated Line Intensity.** The Van Vleck-Weisskopf equation (13-19) in the region of  $\nu_0$  can be approximated

$$\gamma = \frac{8\pi^2 N f}{3ckT} |\mu_{ij}|^2 \nu^2 \frac{\Delta\nu}{(\nu - \nu_0)^2 + (\Delta\nu)^2} \quad (13-22)$$

if  $\Delta\nu \ll \nu_0$ . This is the form of a typical resonance absorption of half width  $\Delta\nu = 1/2\pi\tau$ . If one integrates over the absorption line, assuming  $\Delta\nu \ll \nu_0$ , the integral  $\int \gamma d\nu$  becomes

$$\frac{8\pi^3 N f}{3ckT} |\mu_{ij}|^2 \nu_0^2 \quad (13-23)$$

which is often called the absolute or integrated line intensity.

The approximation  $\Delta\nu \ll \nu_0$  is good in the infrared and optical regions, but not always good in the microwave region. In fact, sometimes  $\Delta\nu > \nu_0$  at high pressures. Absolute or integrated line intensity may be more appropriately defined as

$$\int_0^\infty \frac{\gamma}{\nu^2} d\nu$$

It may be noted that the first term of the expression in brackets in Eq. (13-19) corresponds to a resonant absorption at frequency  $\nu_0$ , and the second term to a resonant absorption at frequency  $-\nu_0$ . Integrating the sum of the two terms from 0 to  $\infty$  is equivalent to integrating either



one from  $-\infty$  to  $+\infty$ . Hence

$$\int_0^\infty \frac{\gamma}{\nu^2} d\nu = \frac{8\pi^2 Nf}{3ckT} |\mu_{ij}|^2 \int_{-\infty}^\infty \frac{1/2\pi\tau}{x^2 + (1/2\pi\tau)^2} dx = \frac{8\pi^3 Nf}{3ckT} |\mu_{ij}|^2 \quad (13-24)$$

This is independent of  $\tau$  and hence of the line width  $\Delta\nu$ . The invariance of the absolute intensity with perturbations such as collisions is connected with the principle of "spectroscopic stability." This principle is usually applied to a spectroscopic line split by Zeeman, Stark, or other effects into a fine structure. It states that the sum of intensities of all fine-structure components of a line is equal to the intensity of the unsplit line which would occur if the cause of fine structure were removed, or if the fine structure were not resolved.

**13-5. Comparison of the Van Vleck-Weisskopf Line Shape with Experiment.** The following general features of collision or pressure broadening have been demonstrated from microwave measurements and are predicted from the Van Vleck-Weisskopf theoretical shape [Eq. (13-19)].

1. The half width  $\Delta\nu$  is proportional to pressure over a wide range of low pressures.

2. The peak absorption intensity is independent of pressure over a wide range of low pressures.

3. The apparent resonant frequency  $\nu_0$  is constant over a wide range of low pressures.

4. At low pressure the line shape is fitted very accurately by a simple resonant expression.

5. At moderate pressures (1 atm) the absorption-line shape is very asymmetric and given qualitatively by Eq. (13-19).

6. At high frequencies ( $\nu \gg \nu_0$ ) the absorption is constant and has the value

$$\gamma_\infty = \frac{8\pi Nf}{3ckT\tau} |\mu_{ij}|^2 \quad (13-25)$$

The theoretical line shapes for several values of  $\Delta\nu$  are shown in Fig. 13-1. It should be noted that properties 1 to 4 are characteristic of impact theories in general, and only 5 and 6 distinguish the Van Vleck-Weisskopf formulation.

The observed shape of a line in the inversion spectrum of ammonia is compared at pressures near 1 mm Hg with a Lorentz resonance line shape in Fig. 13-2. The Van Vleck-Weisskopf line shape reduces to this Lorentz shape at these low pressures, since  $\Delta\nu \ll \nu_0$ .

At a pressure of 0.27 mm, the fit is good. When the pressure is raised to 0.83 mm, both the frequency and the intensity of the peak absorption remain unchanged, as predicted, and the line shape fits the theory, except on the low-frequency side where there is overlapping with the edge of a neighboring line [172]. Bleaney and Penrose [180] have shown that  $\Delta\nu/p$

is a constant from 0.5 mm up to 10 cm pressure while others have shown that this holds down to about  $10^{-3}$  mm Hg. Below this pressure other causes of broadening become important.

A more complete test of theoretical line shapes and discrimination between the Lorentz shape and its modification by Van Vleck and Weisskopf must be made at higher pressures. Only when the lines are so broad

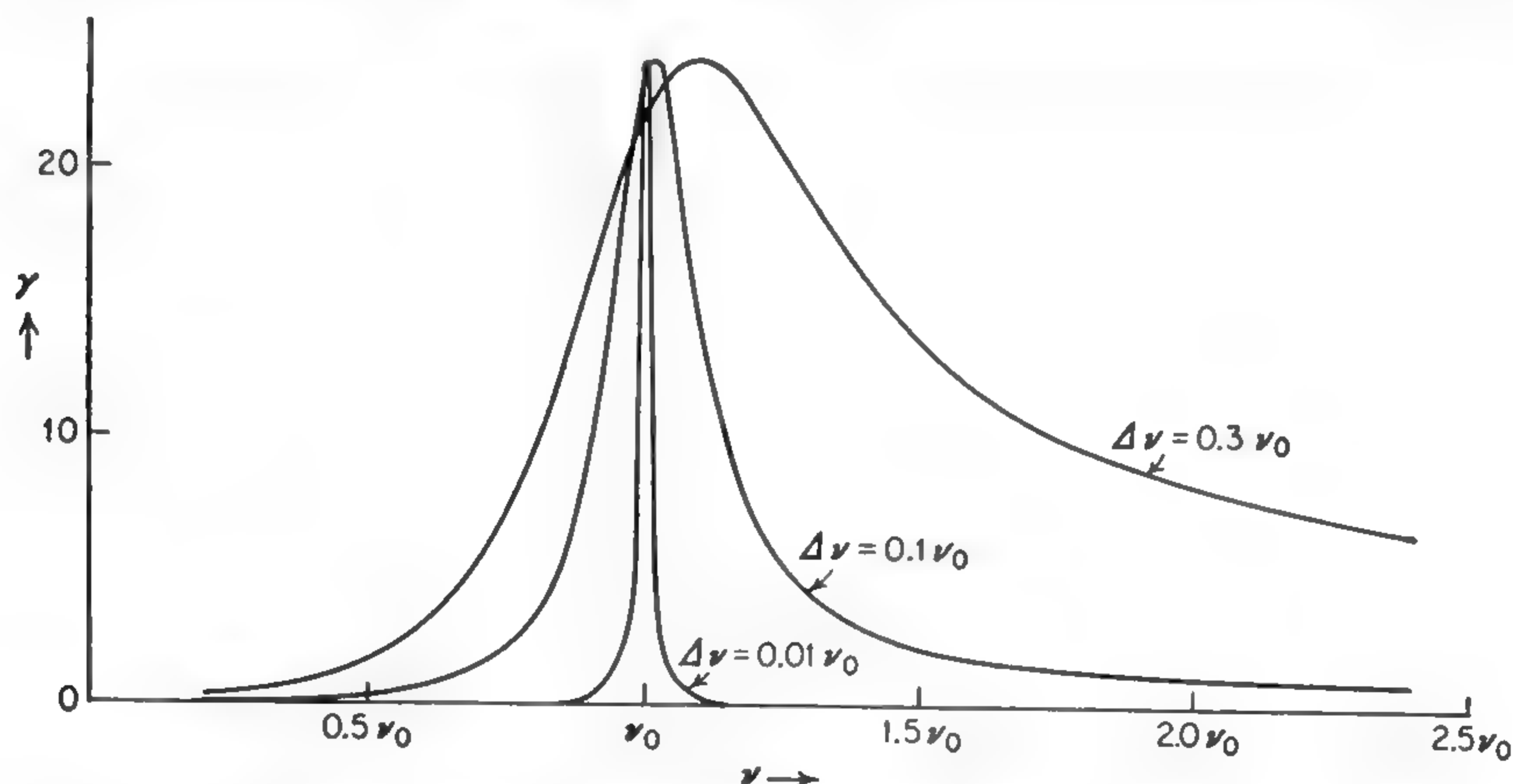


FIG. 13-1. Theoretical shape of pressure-broadened line. (After Van Vleck and Weisskopf [136].)

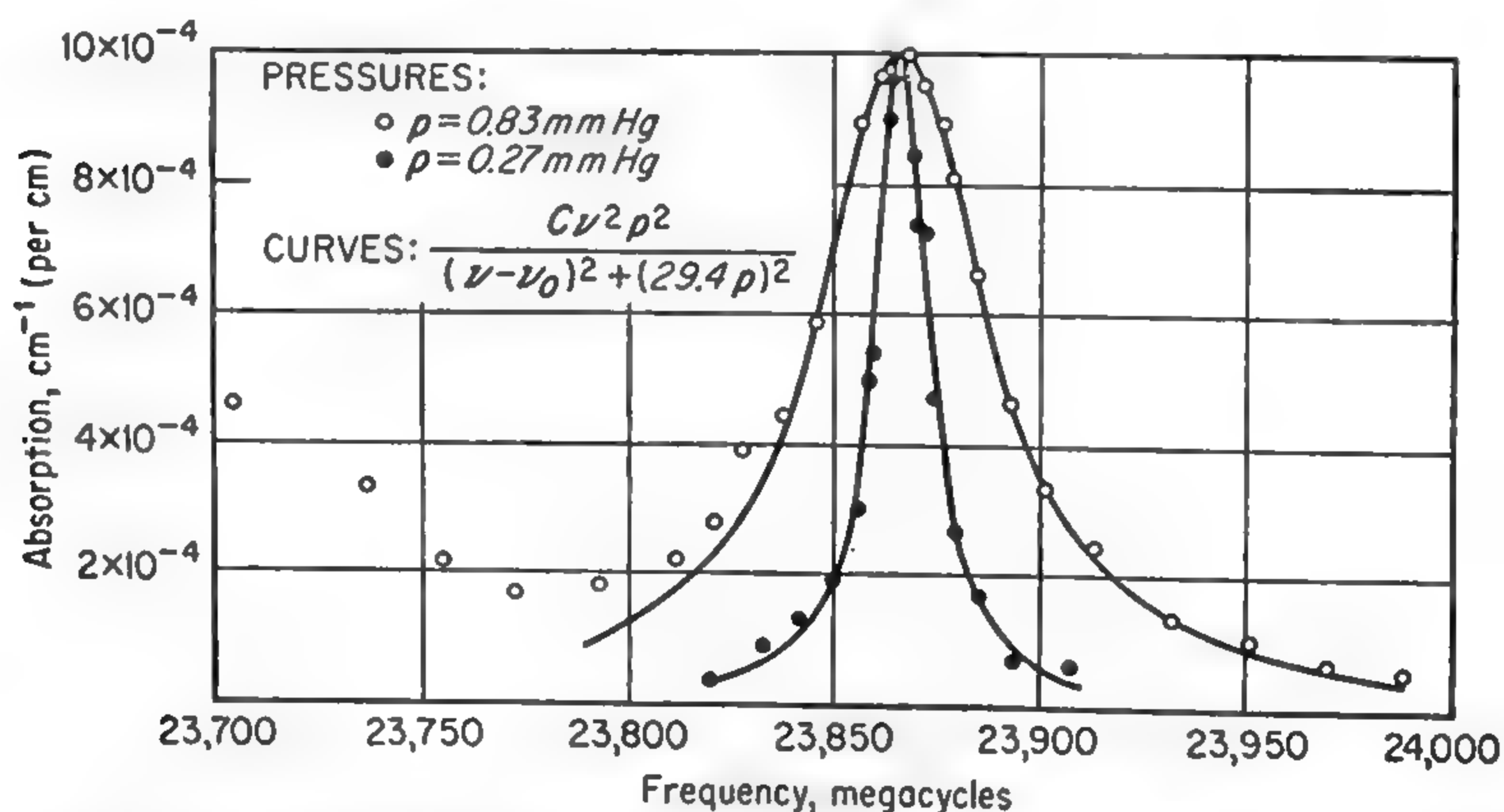


FIG. 13-2. Effect of pressure broadening on the  $\text{NH}_3$  3,3 absorption line. (From Townes [172].)

that  $\Delta\nu$  is comparable with  $\nu_0$  do the effects of the  $\nu^2$  factor and the “negative frequency resonance” term in (13-19) become apparent. The shape of a microwave line between 15,000 and 35,000 Mc for water vapor in air is compared in Fig. 13-3 with theoretical line shapes. Here  $\Delta\nu \approx \nu_0$ , and it is evident that the Van Vleck–Weisskopf line shape is

different from the Lorentz theory and more nearly correct. However, there is a deviation from the Van Vleck–Weisskopf line shape on the high-frequency side of the water line.

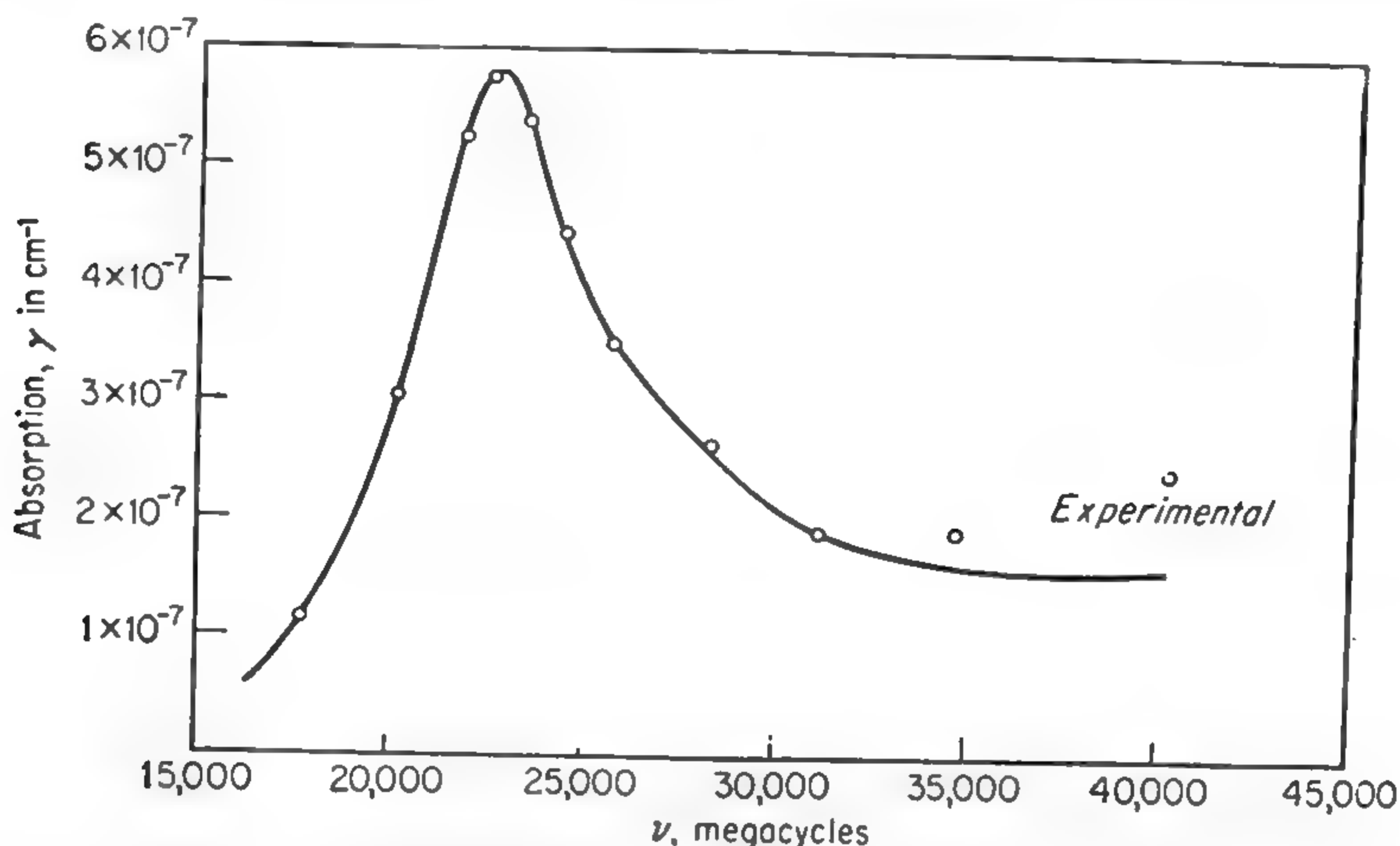


FIG. 13-3. Absorption by water vapor in air (10 g of  $\text{H}_2\text{O}$  per cubic meter). (From Becker and Autler [137].)

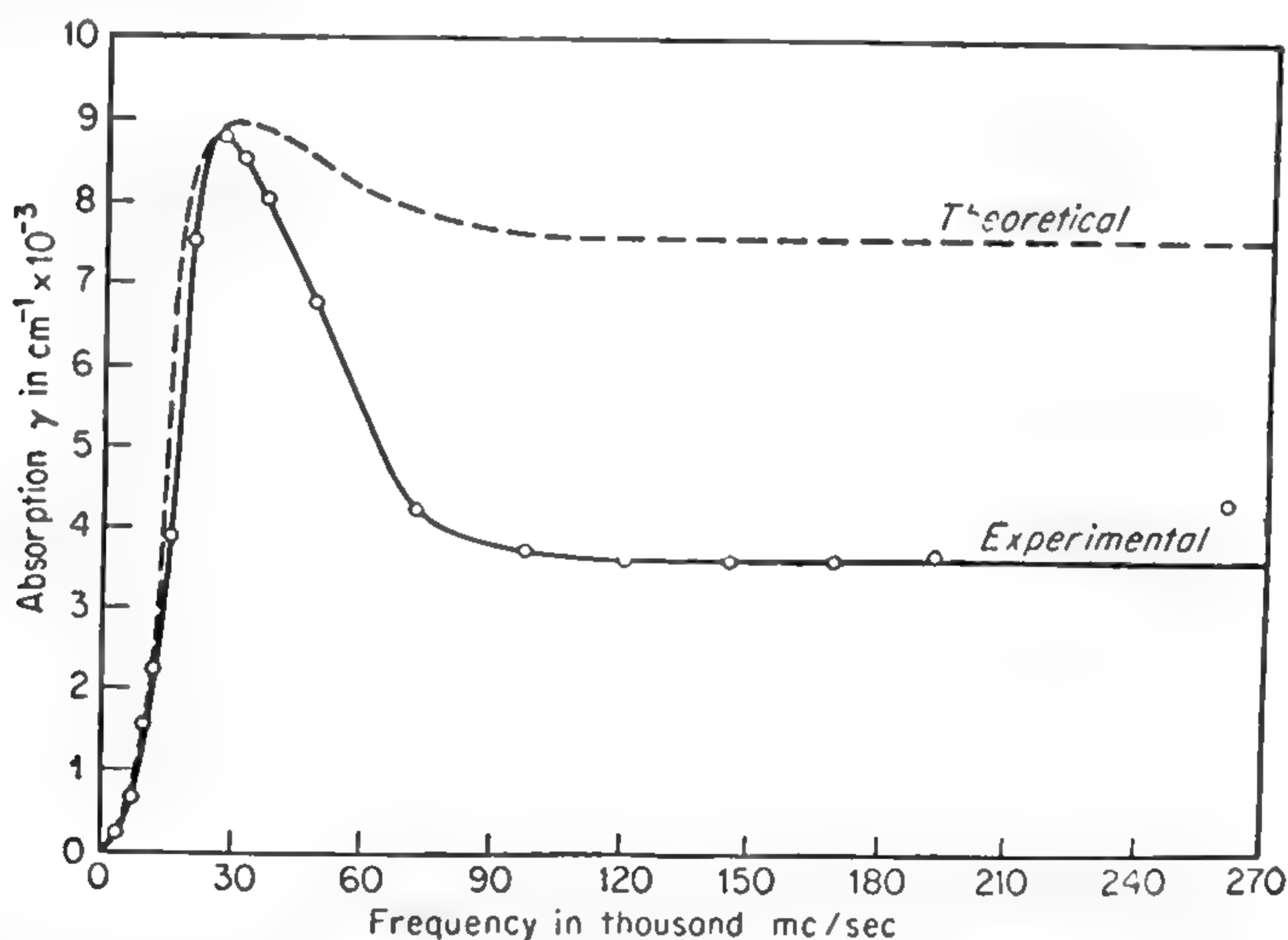


FIG. 13-4. Absorption in  $\text{NH}_3$  at 1 atm pressure. (From Bleaney and Loubser [439] and Nethercot, Klein, Loubser, and Townes [734].)

The microwave spectrum of ammonia at a pressure of 1 atm is shown in Fig. 13-4 [439], [734]. Since at this pressure the width of any one line is considerably greater than the over-all spacing of the individual lines, the spectrum should fit a Van Vleck–Weisskopf curve fairly well with a single value of  $\nu_0$  and of  $\Delta\nu = 1/2\pi\tau$ . Qualitatively the spectrum does



have the predicted shape. In particular the flat "tail," or region of constant absorption at high frequencies, is observed. However, a close comparison shows many deviations from the Van Vleck-Weisskopf line shape. If the line shape is fitted near the peak of the line, the theoretically expected absorption in the flat region should be considerably larger than the observed value. Birnbaum and Maryott [780] have shown that at pressures of 5 to 30 cm of Hg, the low-frequency tail of the ammonia absorption is about 40 per cent larger than that given by the Van Vleck-Weisskopf shape. Too large an observed intensity is, of course, necessary on the low-frequency side of the line to compensate for too small an intensity on the high-frequency side if the integrated intensity (13-24) is to remain constant. Furthermore, the magnitude of  $\Delta\nu$  used for the theoretical fit in Fig. 13-4 is only 14,000 Mc, whereas from measurements of line widths at lower pressures, and assuming  $\Delta\nu/p$  is constant, it would be expected to be 22,000 Mc. The fact that  $\Delta\nu/p$  is less at atmospheric pressure than at low pressure indicates that collisions of more than two molecules at a time have become important, a circumstance not allowed for by Van Vleck and Weisskopf.

Still another complication is that the best fits of the experimental absorption curves to the Van Vleck-Weisskopf shape require a decrease in  $\nu_0$  with pressures as high as 1 atm. At 2 atm pressure and higher,  $\nu_0$  must be taken as zero [255], [321], [338]. For  $\text{ND}_3$ , which has a lower inversion frequency than  $\text{NH}_3$ , the shift in  $\nu_0$  has been found [779] to occur at a proportionally lower pressure. This is in accord with the theory of Margenau [394] and Anderson [341]. They show that when the average energy of interaction between molecules is comparable with the inversion energy, the wave functions are sufficiently disturbed to shift the microwave absorption to lower frequencies. Such effects should occur for all gases of sufficient density, since the microwave absorption must approach that given by Debye (13-20) for the liquid state. The density at which such shifts occur can be expected to depend on the strength of the intermolecular interactions and to be approximately proportional to the frequency of the microwave transition.

**13-6. Pressure Broadening and Intermolecular Forces.** Even if a Lorentz-type theory were developed which fits the line shapes exactly, it would still not be completely satisfactory because the quantity  $\Delta\nu$  or  $\Delta\nu/p$  is taken as an empirical parameter. A more complete theory should evaluate  $\Delta\nu$  in terms of intermolecular forces or some known molecular properties. One might expect that the time between collisions,  $\tau$ , and hence  $\Delta\nu$  could be obtained from classical kinetic theory and measurements of collision diameters from viscosity or from van der Waals' equation of state. However, observed line widths are in most cases greater than those obtained by such methods, so that collision diameters for broadening of microwave lines are sometimes several times larger

than diameters calculated from kinetic theory (see table of values in [473]). This may be expected since kinetic-theory diameters are determined by the requirement that molecules come close enough for intermolecular forces to cause a transfer of most of the kinetic energy  $kT$ . Microwave lines on the other hand are disturbed by more distant collisions which transfer considerably less energy since  $h\nu \ll kT$ .

A complete treatment of pressure broadening and evaluation of  $\Delta\nu$  is so complex that a variety of different types of treatments and approximations have been developed to account for the wide range of phenomena encountered. Some approximations are suitable in the optical and infrared regions, others in the microwave region.

One is forced into making simplifying assumptions and approximations. However, no one approximate theory can be used for the wide range of phenomena encountered. Many of the earlier theories use approximations which are appropriate for optical and infrared frequencies, but not for the very different microwave frequencies. In addition some theories are nicely applicable to some types of intermolecular forces but must give way to other approximations for other types of forces.

All intermolecular forces are usually called van der Waals forces. This name includes a number of short-range interactions [93] which depend in various ways on the relative angles of orientation of the two interacting molecules and the distance  $r$  between them. The most important types are listed in Table 13-1. Note that each different type of force depends on the distance in a different way except types 4, 5, and 6 which are variations on the same basic type of interaction between a dipole and induced dipole. When the longer-range forces (dependent on lower inverse powers of  $r$ ) are present they are generally more important than the shorter-range forces in producing collisions simply because of the larger radius of effectiveness. For this reason it is often possible to attribute the major responsibility for pressure broadening to one or two types of interaction rather than all types which are known to be present. One of the reasons for studying pressure broadening is the information about the occurrence and relative importance of the various types of van der Waals forces which may be obtained.

**13-7. Comparison of Methods of Treating Pressure Broadening.** The pressure-broadening problem can be formulated in general terms without approximations. In arriving at useful numerical results, however, simplifying approximations must always be introduced. Jablonski [130a], [161] has pointed out that an entire volume of gas may be considered as one system with bands of energy levels between which transitions occur. Interactions between molecules are just part of the Hamiltonian of the complete system whose energy levels need to be determined. The mathematical difficulty of obtaining energy levels and transition intensities of the entire collection of molecules treated as one system is so great,



TABLE 13-1. TYPES OF VAN DER WAALS FORCES IMPORTANT TO PRESSURE BROADENING

Type of interaction	Variation of potential with $r$	Discussion
1. Dipole-dipole.....	$r^{-3}$	Interaction between two dipoles fixed in orientation, or "resonant," so that they may vary synchronously
2. Quadrupole-dipole.....	$r^{-4}$	Dipole and quadrupole fixed in orientation
3. Quadrupole-quadrupole....	$r^{-5}$	Interaction between two quadrupoles
4. Keesom alignment.....	$r^{-6}$	Two dipoles not fixed in orientation. One dipole induces an alignment of the other and hence a second-order dipole-dipole interaction
5. Dipole-induced dipole.....	$r^{-6}$	Molecular dipole which perturbs electronic wave function of second molecule thus inducing and interacting with a dipole moment. Same as type 4 but induced dipole due to perturbation of electron state
6. London dispersion.....	$r^{-6}$	Electrons in molecule or atom inducing electronic dipole moment. Same as type 4 but both dipoles due to electronic motions rather than being fixed molecular dipoles
7. Quadrupole-induced dipole.	$r^{-7}$	Dipole moment of first molecule induces dipole moment in second molecule which reacts back on quadrupole moment of first molecule
8. Exchange forces.....	Exponential or very high power of $1/r$	Strong, usually repulsive, forces due to direct interaction of electronic distributions in two molecules

however, that his approach has been used only in approximations which give essentially the same results obtained by the Kuhn-London statistical theory discussed below.

All other treatments of pressure broadening can be classified as collision or statistical theories. Collision theories assume that, during most of the time a molecule is sufficiently far from other molecules, it may be



considered free. Occasionally it comes close enough to one or more other molecules for the intermolecular fields to perturb its energy levels appreciably. After collision the molecule may be in the same state as before the encounter, with only a change in phase of its wave function, or a transition to another state may have been induced by the collision. Both types of collision contribute to pressure broadening. Collision theories usually assume that the radiation takes place only while the molecule is undisturbed by intermolecular interactions, the collisions being so brief and infrequent that they serve only to interrupt or change the phase of the normal process of radiation. Statistical theories, on the other hand, consider that molecules are always under the influence of intermolecular interactions, even though these may be weak, and that the frequency radiated depends on the amount of interaction occurring during radiation. The intensity emitted at a particular frequency  $\nu$  depends simply on the probability that a molecule is perturbed by other molecules just the correct amount to make its frequency  $\nu$ . Statistical theories hence always involve finding the probabilities of molecules being within a range  $R$  and  $R + \Delta R$  apart with various possible angles of orientation and hence of their levels being perturbed by various amounts. Collision theories, on the other hand, require calculation of the probability of various types of collisions, the changes in molecular states which occur during these collisions, and a Fourier analysis of the molecular radiation which has intermittent disturbances due to collisions.

Either the collision or statistical approach can give fairly complete and accurate theories if they are developed sufficiently far. However, collision theories usually neglect radiation during a collision and hence become poor approximations at pressures of a few atmospheres where molecules are always close together and collisions are frequent. Statistical theories cannot very well take into account the changes of interactions with time due to molecular motion and hence are good only when molecular velocities are so low that the rate of change of intermolecular interactions may be neglected. We shall see below that this limitation prevents the statistical approach from being very accurate in the microwave range, although it can be used as a guide and rough approximation.

Let us examine now the effect of collisions on microwave radiation, assuming that pressures are low enough so that only collisions between two molecules are important. Using classical language, assume the first molecule is oscillating or rotating so that it radiates a frequency of interest and that it collides with a second molecule. During the collision its oscillation is somewhat modified in frequency because of the interaction, but if the oscillation continues without loss in energy, the molecule emerges from the collision oscillating as before, but with a change in phase due to the changes in frequency during the collision. Such a collision is called adiabatic since no energy has been lost from the

oscillation of interest during collision. The radiated wave is as intense as before the collision, but new frequencies have been introduced because the change in phase due to the collision can be represented as a Fourier distribution of frequencies. Quantum-mechanically, this change of frequency during collision corresponds to a change in energy separation between the ground and excited states due to intermolecular interactions, and the change in phase is a change in relative phases of the ground and excited-state wave functions. The molecule could also appreciably change its energy of oscillation during collision, *i.e.*, make a transition from the excited to the ground state as a result of the collision or vice versa. Such a collision is diabatic.\* In this case the radiation emitted, if any, after collision will have no particular relation to that emitted before the disturbance.

In order for a change in phase as large as 1 radian to occur during an adiabatic collision,

$$2\pi\epsilon t \geq 1 \quad \text{or} \quad \epsilon \geq \frac{1}{2\pi t} \quad (13-26)$$

where  $\epsilon$  is an average change in frequency during the collision and  $t$  is the duration of the collision. A rough measure of  $\epsilon$  from the energy of the interaction  $W$  is

$$\epsilon = \frac{W}{h} \quad (13-27)$$

The time of collision is given approximately by

$$t = \frac{R}{v} \quad (13-28)$$

where  $R$  is the distance between molecules required to produce an appreciable interaction, and  $v$  is the thermal velocity of the molecule. Since  $R$  is a few angstroms and  $v$  near  $10^5$  cm/sec,  $t$  is approximately  $10^{-13}$  sec. Hence  $1/2\pi t$  is greater than any microwave frequency  $\nu$ , and from (13-26), (13-27), and (13-28),

$$W > h\nu \quad (13-29)$$

This shows that the energy of interaction required to give an appreciable change in phase during collision is greater than enough to cause a transition between the ground and excited states. Furthermore this energy fluctuates in a time short compared with the period of oscillation  $1/\nu$ , and hence the fluctuation has frequency components which can easily produce transitions. Another requirement for transitions to occur is that the kinetic energy of the molecules be sufficiently high to provide the

\* Adiabatic means without a transfer of energy. To describe the case where energy is transferred we use diabatic rather than the more usual but clumsy double negative nonadiabatic.



necessary energy, or

$$kT > h\nu \quad (13-30)$$

This condition is, of course, fulfilled for microwave frequencies. For these reasons, adiabatic collisions which have an appreciable effect in broadening a microwave line are rather rare; transitions occur in almost all significant collisions. That this is true can be shown from experimental measurements of saturation discussed below, as well as from comparison of observed line shapes with those predicted by various theories.

When energy levels are so far separated that transitions occur in the infrared or optical region, the situation is very different. There  $1/t$  is greater than the radiated frequency  $\nu'$ , and hence for a change of phase of approximately 1 radian

$$W < h\nu' \quad (13-31)$$

In addition the interactions fluctuate too slowly to excite frequencies as high as those of interest, and the kinetic energy is usually insufficient to cause these higher-frequency transitions ( $kT < h\nu'$ ). Thus, in contrast to the microwave region, adiabatic collisions are the common type of importance to pressure broadening of optical or infrared lines. It is for this reason that most of the early theories of pressure broadening, which were developed for the optical and infrared region, are not very good when applied to pressure broadening of microwave lines. Furthermore, such theories can be expected to be inadequate whenever fine structure is resolved which is so small that diabatic collisions producing transitions between the fine structure levels commonly occur.

Since statistical theories of pressure broadening have not been developed to take into account the variations of intermolecular interactions with time, they suffer the same difficulty as collision theories which allow only adiabatic collisions. In fact the two can be shown to be equivalent for slow collisions or for frequencies far removed from the line center [104], [472], [494]. However, these types of approximations are in some cases simpler than a theory of diabatic collisions, which should be more accurate for microwave lines, and hence are still of value.

The statistical method was introduced by Kuhn and London [50], [51] in a very simple form. Let the transition frequency be  $\nu_0$  and its change due to intermolecular interactions be of the form

$$\nu - \nu_0 = \frac{B}{r^n} \quad (13-32)$$

where  $B$  and  $n$  are constants and  $r$  is the distance between two molecules. If only two molecules are considered, the probability that the intermolecular distance will lie between  $r$  and  $r + dr$  is

$$dP = Ar^2 dr \quad (13-33)$$



where  $A$  is a constant. Then the fraction of the radiation intensity with frequency between  $\nu$  and  $\nu + d\nu$  is, from (13-32) and (13-33),

$$I = \frac{AB^{3/n}}{n(\nu - \nu_0)^{(n+3)/n}} \quad (13-34)$$

This simple form of the statistical theory gives an infinite relative intensity at  $\nu = \nu_0$  because there is an infinite probability of two molecules being separated by an infinite distance. Finite molecular densities must be taken into account to remove this divergence. In addition, expression (13-34) gives a shift of frequency only to one side of the resonance frequency  $\nu_0$ , and hence a very asymmetric line. Such asymmetric lines are observed in some optical spectra, but this type of asymmetry never occurs in the microwave region because of the prominence of diabatic collisions. However, the tail of a microwave line can be approximately fitted by an expression of the type (13-34). The tail is sometimes fitted to the tail of a resonance-shaped curve, and from this a half width of the resonance can be obtained.

Margenau has given a much more sophisticated statistical theory of the pressure broadening of the ammonia inversion spectrum [393] in case collisions between more than two molecules are negligible. The energy of interaction of the dipole moments of two symmetric tops is [82]

$$V(JKJ'K'\lambda) = \frac{\mu^2}{r^3} \frac{KK'}{J(J+1)J'(J'+1)} \epsilon_\lambda \quad (13-35)$$

where  $J, K$  and  $J', K'$  are the quantum numbers of the two molecules, each of which has a dipole moment  $\mu$ .  $\lambda$  is an index replacing the individual  $M$ 's of the molecules, which are not good quantum numbers during close approaches because the separate angular momenta about the intermolecular axis are not conserved.  $\epsilon_\lambda$  is a numerical factor for each  $\lambda$  state. The frequency of the line absorbed by one of the molecules ( $J, K$ ) is then

$$\nu = \nu_0 + \frac{B_{\lambda\lambda'}}{r^3} \quad (13-36)$$

where  $\nu_0$  is the unperturbed resonance frequency and

$$B_{\lambda\lambda'} = \frac{\mu^2}{h} \frac{KK'}{J(J+1)J'(J'+1)} (\epsilon_\lambda - \epsilon_{\lambda'}) \quad (13-37)$$

In passing from one inversion state to the other the dipole changes its orientation so that the system of two molecules changes from state  $\lambda$  to state  $\lambda'$ . By averaging over all possible types of collisions, or hence over all  $\lambda, \lambda', K',$  and  $J'$ , and using the same basic statistical approach discussed above, Margenau obtains

$$\frac{\Delta\nu}{p} = 33.9 \left[ \frac{K^2}{J(J+1)} \right]^{\frac{1}{2}} \text{ Mc/mm Hg at } 20^\circ\text{C} \quad (13-38)$$

where  $\Delta\nu$  is the half width of the line at half maximum intensity and  $p$  is the pressure in millimeters of mercury. This theory gives line widths of the right order of magnitude and varying in roughly the right way with  $K$  and  $J$ , as shown by the comparison with experimental line widths in Table 13-3 (page 362). However, a systematic deviation between the theoretical and experimental results can be seen in this table.

Collision theories for the optical and infrared region have been given by Lindholm [131] and Foley [153]. They consider the phase shifts produced during collisions, and assume that diabatic collisions are unimportant, so that their approximations are not good for pressure broadening of microwave lines, although they apply well in the higher-frequency infrared and optical regions. This type of theory considers the approach of a perturbing molecule during a collision to change the energies of both ground and excited states of the emitting molecule, the difference between their changes being  $W(t)$ . This changes the frequency of the emitting molecule by  $W(t)/h$ , and if the change in frequency persists for a time  $dt$ , there is a phase change of  $[2\pi W(t)/h] dt$  over what would have occurred for normal oscillation without a collision. The total phase shift due to the collision may be obtained by integrating over the duration of the collision as

$$P_1 = 2\pi \int_{-\infty}^{\infty} \frac{W(t) dt}{h} \quad (13-39)$$

The straight-line paths of the colliding molecules are assumed to be unaffected by the collision.

$P_1$  is a function of the impact parameter  $b$  (distance of closest approach), being large when  $b$  is small. If  $b$  is so small that the phase shift is very large, then the phase after collision has no very close connection with that before collision, and the collision can be considered strong, producing a complete and arbitrary interruption of the emitted wave train. Weisskopf, who originated this type of calculation [44], assumes that a phase shift larger than 1 radian is equivalent to a complete interruption of the radiation, and obtains an approximate collision diameter as the value of  $b$  for this particular phase shift, considering a collision to occur only for  $b$  less than this value.

The strong collisions, giving large phase shifts, produce a symmetrical line broadening of the Lorentz type with no shift in the central frequency. By taking into account the phase shifts produced by all types of collisions, including the weaker ones, and making a Fourier analysis of the resulting wave trains, Foley and Lindholm showed, however, that there is often an appreciable shift of the central line frequency due to phase shifts during collisions. Thus if  $W(t)/h$  corresponds to a decrease in frequency during a distant collision, the line will be both broadened and shifted slightly to lower frequencies by the distant or weak collisions.



These distant collisions are much less important than closer collisions if the potential drops off very rapidly with  $r$ , that is, when  $V = B/r^n$ , if  $n$  is large. The phase-shift approximation therefore gives an absorption line of the form

$$\gamma = \frac{A}{(\nu - \nu_0 \pm a \Delta\nu)^2 + (\Delta\nu)^2} \quad (13-40)$$

where the change in the center of the line  $a \Delta\nu$  is proportional to the line width and dependent on the force law as shown in Table 13-2. When  $n$  is 3, no frequency shift is observed because only "resonant" type interactions give  $n = 3$  (cf. Table 13-1), and they give a symmetrical splitting of energy levels. Although this type of frequency shift is often observed in infrared or optical spectra, no such frequency shifts have yet been found in the microwave region. They are in most cases certainly less than  $0.05 \Delta\nu$ . This is because adiabatic collisions are of little importance in broadening microwave lines. However, some collisions of this type occur, and they undoubtedly produce small frequency shifts which may be found with refined techniques.

TABLE 13-2. RATIO  $a$  OF SHIFT IN FREQUENCY TO LINE BREADTH  $\Delta\nu$  ON PHASE-SHIFT THEORY

Potential of interaction of two molecules is assumed to be of the form  $V = B/r^n$

$n$	3	4	5	6	7	$\infty$
$a$	0	0.866	0.500	0.363	0.289	0

**13-8. Impact Theory—Anderson's Treatment.** Anderson has given a more complete treatment of pressure broadening of the collision type which allows adequately for diabatic collisions, *i.e.*, those which induce transitions [342], [343]. Where the computations involved are not too complex, Anderson's theory may be very satisfactorily applied to pressure broadening in the microwave region. In some cases this approach, combined with experimental measurements, can be used to determine the magnitude of certain intermolecular interactions. However, there are always minor contributions to collision effects which involve computations that are prohibitively complex, and in many cases even the major sources of pressure broadening still involve such difficulties.

Anderson makes some assumptions usual to collision theories:

1. Colliding molecules follow definite classical paths. In very close collisions this is a poor assumption, but the errors introduced are unimportant since any path giving a close collision involves complete interruption of the radiation, and details of the path are unnecessary. Collisions near the limit of the effective collision radius are the ones which must be accurately treated, and the quantum-mechanical wave packet for each molecule may in almost all cases be considered sufficiently small compared with this distance to make the classical path a very good approximation.



2. The duration of a collision is small compared with the time between collisions. This is always true at sufficiently low pressures, and is true for most molecules if the pressure is below about 1 atm.

A line shape similar to that of Van Vleck and Weisskopf is obtained, but with the possibility of a shift in the central frequency,

$$\gamma = \frac{8\pi^2 N f}{3ckT} |\mu_{ij}|^2 \nu^2 \left[ \frac{\Delta\nu}{(\nu - \nu_0 - a\Delta\nu)^2 + (\Delta\nu)^2} + \frac{\Delta\nu}{(\nu + \nu_0 + a\Delta\nu)^2 + (\Delta\nu)^2} \right] \quad (13-41)$$

However, the frequency change  $a\Delta\nu$  is not so prominent as in the phase-shift theory or (13-40), and is usually negligible for microwave lines.

The number of collisions per second is given by  $Nv\sigma_2$ , where  $\sigma_2$  is an effective cross section,  $v$  the molecular velocity, and  $N$  the number of molecules per unit volume. Hence

$$\Delta\nu = \frac{Nv\sigma_2}{2\pi} \quad (13-42)$$

Similarly, the frequency shift is

$$a\Delta\nu = \frac{Nv}{2\pi} \sigma_1 \quad (13-43)$$

where  $\sigma_1$  is the effective cross section for frequency shifts. These cross sections may be written

$$\sigma = \int_0^\infty 2\pi b S(b) db \quad (13-44)$$

where  $b$  is the impact parameter, or distance of closest approach of the molecules, so that  $2\pi b db$  is proportional to the probability of a collision with impact parameter  $b$ , and  $S(b)$  is a weight factor which indicates whether or not a collision of this type is effective in disturbing the molecular radiation.  $S(b)$  is unity when  $b$  is small since every such collision is effective in broadening the spectrum and for larger  $b$  the most important parts of  $S$  are given by

$$S_2(b) = \frac{1}{2} \sum_{i,M} \left[ \frac{|(iM|P|l)|^2}{2J_i + 1} + \frac{|(fM|P|l)|^2}{2J_f + 1} \right] \quad (13-45)$$

where  $i, M$  represent all the quantum numbers of the initial state, and  $f, M$  those of the final state of the radiating transition.  $J_i$  and  $J_f$  are the angular momenta of initial and final states.  $l$  represents the quantum numbers of any state to which transitions are induced by the perturbing intermolecular interaction. The matrix elements  $(i, M|P|l)$  are

$$(a|P|b) = \frac{2\pi}{h} \int_{-\infty}^{\infty} [a|V_1(t)|b] \exp(2\pi i\nu_{ab}t) dt \quad (13-46)$$

where  $V_1(t)$  is the perturbing interaction, and  $\nu_{ab}$  is the frequency of a transition between states  $a$  and  $b$ . The sum over  $M$  divided by  $2J + 1$  involved in (13-45) is simply an average over the  $2J + 1$  different possible values of the magnetic quantum numbers  $M$ .

From (13-45),  $S_2(b)$  may be interpreted as the probability that the collision at a distance  $b$  produces a transition, averaged over the ground and excited states, and over the various possible orientations of the angular momentum. This is because  $|(iM|P|l)|^2$  is just the quantity which gives the transition probability (cf. [153]). It has been suggested [536] that a simplifying assumption might be applied to Anderson's theory by considering an effective collision to take place for any  $b$  small enough

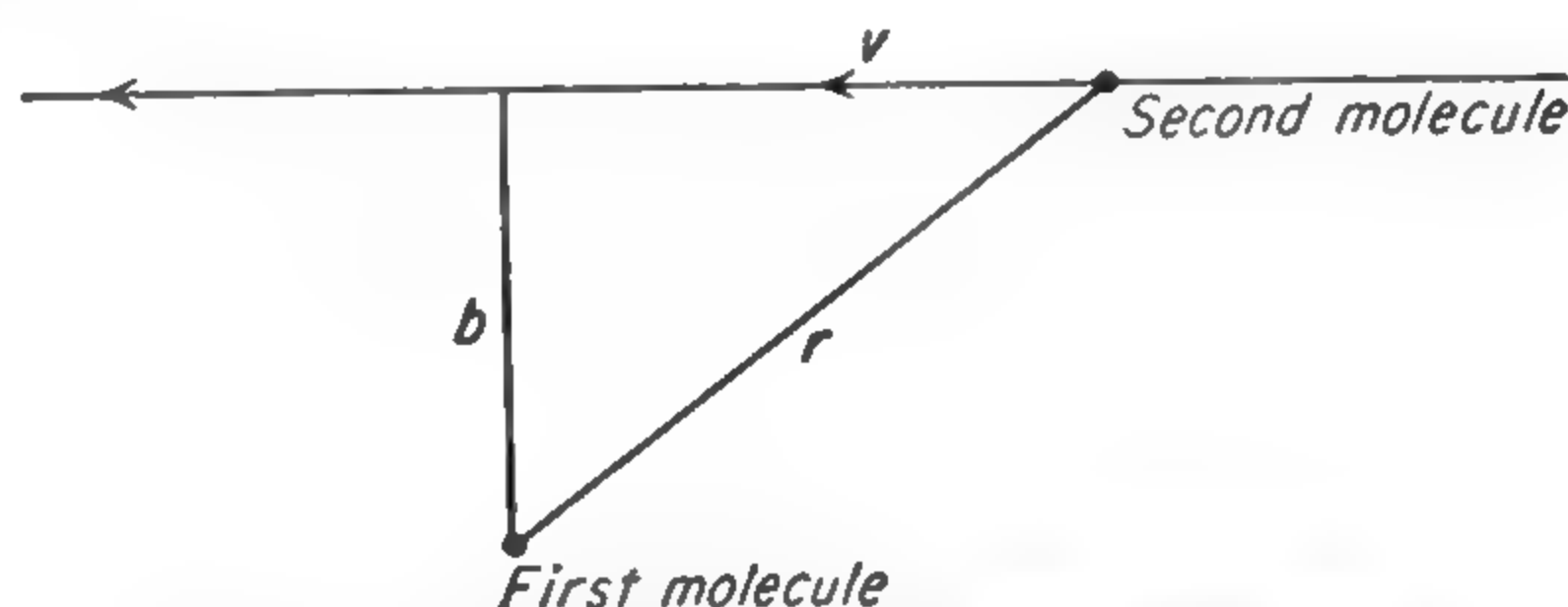


FIG. 13-5. Geometry of molecular collision.

to make this probability ( $S_2$ ) larger than  $\frac{1}{4}$ . This gives approximately the same result as an integration of (13-44) over all collision parameters. However, for force laws of the form  $1/r^n$  this approximation gives little simplification.

The expression for frequency shift similar to (13-45) is

$$S_1 = \sum_M \left[ \frac{(iM|P|iM)}{2J_i + 1} - \frac{(fM|P|fM)}{2J_f + 1} \right] \quad (13-47)$$

which is zero for most of the common interactions because the matrix elements in the sum are zero.

The relative positions of the two colliding molecules and the path over which the time integral in (13-46) is made is indicated by Fig. 13-5. The path of the second molecule with respect to the first is assumed to be a straight line since only the closer collisions which always interrupt the radiation will involve appreciable curvature of the path. Then

$$r(t)^2 = b^2 + v^2 t^2 \quad (13-48)$$

For an interaction energy which varies as  $1/r^n$  with the distance between molecules,  $[a|V_1(t)|b]$  is the form  $K/[r(t)]^n$ . Letting  $x = vt/b$  and  $k = (2\pi b/v)\nu_{ab}$ , (13-46) becomes

$$(a|P|b) = \frac{2\pi K}{hb^{n-1}v} \int_{-\infty}^{\infty} \frac{e^{ikx} dx}{(1 + x^2)^{n/2}} \quad (13-49)$$

When  $k \approx 0$ , the collision might be called "fast," and the  $P$  matrix element tends to be large if the interaction energy  $K/b^n$  is large. This value does not decrease much for values of  $k$  up to 1, but then falls off rapidly, being very small for  $k$  as large as 4 or 5.

The parameter  $k$  is roughly the ratio of the time  $b/v$  required for the collision to be completed to the time  $1/\omega$  required for the radiation to change phase. For a collision parameter  $b$  as large as 10 Å, and  $v$  a typical thermal velocity of  $10^5$  cm/sec,  $b/v \approx 10^{-12}$  sec. This is considerably smaller than  $1/\omega$  for 1 cm wavelength radiation, which is  $1/\omega = 3 \times 10^{-11}$ .

One may see from (13-49) two criteria for a transition to occur during collision: first the interaction energy must be large, and secondly the collision must be "fast," *i.e.*, the time variation of the interaction must involve frequencies as high as the transition frequency  $\nu_{ab}$ . For microwave transitions,  $k$  is almost always less than unity, so that diabatic collisions occur, and the exponential in (13-49) may be ignored. However, for optical frequencies the exponential could not be ignored, and the integral in (13-49) would take on a very different character.

Letting  $k = 0$ ,  $S_2$  is of the form

$$S_2 = \frac{A}{b^{2n-2}} \quad (13-50)$$

where  $b$  is the impact parameter and  $A$  is a quantity depending on various properties of the molecules and the quantum states involved. With some approximations which introduce errors of 10 per cent or less, the cross section and half width  $\Delta\nu$  may then be found from (13-42), (13-44), and (13-50) as

$$\sigma = \pi \left( \frac{n-1}{n-2} \right) A^{1/(n-1)} \quad \Delta\nu = \frac{Nv}{2} \left( \frac{n-1}{n-2} \right) A^{1/(n-1)} \quad (13-51)$$

The problem is then reduced to finding  $A$ , or evaluating the sum in (13-45). Since a particular molecule of interest may collide with molecules in a variety of states, each having a different effective cross section,  $\Delta\nu_a$  must be obtained for each different type of molecule with which collisions may occur, and weighed according to the fractional abundance  $f_a$  of each type. Then

$$\sigma = \sum_a f_a \sigma_a \quad \Delta\nu = \sum_a f_a \Delta\nu_a \quad (13-52)$$

In some cases the sum in (13-45) is very difficult to obtain, especially when both colliding molecules may make a variety of transitions. It has been worked out, however, for the important cases of dipole-dipole, dipole-induced dipole, and quadrupole-induced dipole interactions (types 1, 5, and 7 of Table 13-1).



The interaction energy of two dipole moments  $\mathbf{u}_1$  and  $\mathbf{u}_2$  separated by a distance  $r$  is

$$V_1 = \left[ \mathbf{u}_1 \cdot \mathbf{u}_2 - \frac{3(\mathbf{u}_1 \cdot \mathbf{r})(\mathbf{u}_2 \cdot \mathbf{r})}{r^2} \right] r^{-3} \quad (13-53)$$

For two interacting symmetric-top molecules, this energy is of the first order and proportional to  $1/r^3$ . This is because a symmetric-top molecule has a component of the dipole moment along the angular momentum  $J$ , which is fixed in orientation. For a linear molecule, no component of the dipole moment is fixed in direction, and the energy (13-53) averages to zero in the first order unless two interacting molecules happen to be rotating at essentially the same rate. Even two molecules like ammonia, which invert at microwave frequencies and thus reverse the direction of their dipole moments, give a first-order dipole-dipole interaction. Averaging over a long period of time would give no first-order interaction because unless the two ammonia molecules are in the same rotational state they invert at different frequencies and would change relative orientation with time. However, over the short duration of a collision, they may be considered to invert synchronously and remain with the same relative orientation. The matrix elements needed to evaluate these first-order interactions produced by dipole-dipole interactions [ $V_1$  given by (13-53)] turn out to be just those given by Table (4-4) for dipole radiation. After the time integration indicated by (13-46) is done, the matrix elements inserted and summed according to (13-45), one obtains [342], [343]

$$S_2(b) = \frac{8}{9} \frac{\mu_1^2 \mu_2^2}{b^4 v^2 (h/2\pi)^2} \frac{K_1^2 K_2^2}{J_1(J_1 + 1) J_2(J_2 + 1)} \quad (13-54)$$

where  $K_1, J_1, K_2, J_2$  are the usual angular-momentum quantum numbers for molecules 1 and 2, respectively, which are involved in the collision.  $v$  is the relative velocity of the two molecules.

Letting the molecule with index 1 be the one emitting microwave radiation of interest, and summing over all other colliding molecules, from (13-51), (13-52), and (13-54),

$$\Delta\nu = \frac{4\pi \sqrt{2} N |\mu_1 K_1|}{3h \sqrt{J_1(J_1 + 1)}} \sum_{\mu_2, J_2, K_2} \frac{|\mu_2 K_2|}{\sqrt{J_2(J_2 + 1)}} f_{J_2 K_2 \mu_2} \quad (13-55)$$

where  $f_{J_2 K_2 \mu_2}$  is the fraction of molecules having dipole moment  $\mu_2$  and quantum numbers  $K_2, J_2$  and  $N$  is the number of molecules per unit volume. The cross section  $\sigma$  may be easily obtained from  $\Delta\nu$  by (13-42) if some average velocity  $v$  is assumed. Sometimes an effective diameter  $b_e$  is calculated for collisions, which is given by

$$\sigma = \pi b_e^2 \quad (13-56)$$

Another case where the dipole moments of two molecules interact strongly, or in first-order perturbation approximation, is the case of "rotational resonance." Two molecules in rotational resonance may be considered classically to be rotating at the same rate so that the interaction between their dipole moments when averaged over time is not zero. Quantum-mechanically, rotational resonance requires two identical molecules with angular momenta differing by one unit ( $J_1 = J_2 \pm 1$ ). Using the interaction (13-53), this gives [342], [343], for collisions with  $J_2 = J_1 - 1$ ,

$$S_2(b) = \frac{8}{9} \frac{\mu_1^4}{b^4 v^2 (h/2\pi)^2} \frac{(J_1^2 - K_1^2)(J_1^2 - K_2^2)}{J_1^2(2J_1 + 1)(2J_1 - 1)} \quad (13-57)$$

$$\Delta\nu = \frac{4\pi\sqrt{2}}{3h} \frac{N\mu_1^2}{J_1} \left[ \frac{(J_1^2 - K_1^2)}{(2J_1)^2 - 1} \right]^{\frac{1}{2}} \sum_{K_2} (J_1^2 - K_2^2)^{\frac{1}{2}} f_{J_1-1, K_2} \quad (13-58)$$

When  $J_2 = J_1 + 1$ , the number  $J_1$  in (13-58) need only be replaced by  $J_1 + 1$ . The notation is the same as in Eqs. (13-54) and (13-55).

"Rotational-resonance" interactions can occur with either symmetric tops or linear molecules ( $K = 0$ ) and tend to be large when the dipole moments  $\mu_1$  and  $\mu_2$  are large and the fraction  $f$  of molecules in the proper state is not too small. However, for most rotational lines of molecules falling in the microwave region,  $f \approx h\nu/kT$ , or  $\frac{1}{200}$  [cf. (1-56)], and the rotational-resonance effects are usually small. The case of ammonia is somewhat unusual since its microwave lines show large effects due to rotational resonance. This is because the ammonia lines in the microwave region are due to inversion rather than rotational transitions, and the molecule is so light that for some rotational states  $f$  is as large as  $\frac{1}{18}$ . Other molecules do show a quasi resonance, because collisions are so short that the frequency cannot be established accurately. If a collision lasts  $10^{-12}$  sec, all levels within about  $10^{11}$  cycles are near enough to behave as resonant.

Other types of interactions which have been treated by Anderson's method involve a dipole moment induced by the distortion of the distribution of electrons on one molecule, which we shall label 1, by the molecular dipole moment of a second molecule labeled 2. The induced dipole moment on molecule 1 may interact back on the dipole moment of molecule 2, with an energy proportional to  $1/r^6$  (type 5 of Table 13-1). Because of certain symmetry relations, this type of interaction usually contributes a negligible amount to pressure broadening [342], [343], [428].

The induced dipole moment of molecule 1 of the last paragraph may also interact with the electric quadrupole moment of molecule 2 (type 7, Table 13-1). If molecule 2 is symmetric, the interaction energy is then

$$V_1 = - \frac{6\alpha_1\mu_2Q_2}{r^7} \cos^3 \theta \quad (13-59)$$



where  $\alpha_1$  = polarizability of molecule 1

$\mu_2, Q_2$  = dipole and quadrupole moments, respectively, of molecule 2

$r$  = radius between the two molecules

$\theta$  = angle between  $r$  and the axis of molecule 2

Anderson has obtained [428]

$$S_2 = \frac{3}{b^{12}} \left( \frac{15\pi^2 \alpha_1 \mu_2 Q_2}{64vh} \right)^2 \frac{K^2}{J(J+1)} \left\{ 1 + \frac{22}{5} \frac{K^2}{J(J+1)} + \frac{121}{21} \frac{K^4}{J^2(J+1)^2} \right. \\ \left. - \frac{K^2}{3J^2(J+1)^2} \left[ \frac{22}{5} + \frac{121}{7} \frac{K^2}{J(J+1)} \right] + \frac{121}{63} \frac{K^4}{J^4(J+1)^4} \right\} \quad (13-60)$$

which is of the form given by (13-50)

$$S_2 = \frac{A}{b^{12}}$$

so that from (13-51)

$$\sigma = 1.2\pi A^{\frac{1}{2}}$$

Leslie [602] has given a treatment of pressure broadening similar to that of Anderson but has eliminated the assumption of a classical path and used a Boltzmann distribution of velocities throughout rather than assuming an average molecular velocity. Although such a treatment is naturally more complicated because of elimination of these two simplifying assumptions, Leslie has obtained results similar to those discussed above.

**13-9. Comparison of Theories with Experiment.** After the above lengthy discussion of theoretical evaluation of line widths, the reader might expect extensive confirming comparisons between theory and experiment. Unfortunately, successful comparisons are rather limited, and many attempts to fit particular calculations to observations have been inconclusive. One of the reasons for this is that there are few cases in which only one of the wide variety of possible interactions predominates, and even the rough magnitudes of some of the molecular constants required by theory are unknown. In addition, there has been much conflicting experimental data. The one outstanding exception to these uncertainties is dipole-dipole broadening in  $\text{NH}_3$ , which is so far the only microwave case for which extensive quantitative agreement between theory and experiment seems to have been achieved.

The  $\text{NH}_3$   $J = 3, K = 3$  inversion line in pure  $\text{NH}_3$  at a pressure of 1 mm Hg and  $0^\circ\text{C}$  has a measured half width at half maximum of  $30 \pm 1$  Mc.\* The half width calculated from expression (13-54) is 31 Mc for the

\* This value is an average of the results of Bleaney and Penrose [179] and of Townes [172]. Both the directly measured line widths and those calculated from the measured intensities were averaged. A dipole moment of 1.468 debye units [562] was used. The reported widths were reduced to  $0^\circ\text{C}$  assuming the width is inversely proportional to temperature.



same conditions. Rotational-resonance terms (13-57) are zero for this line because  $J = K$ . The agreement between theory and experiment is well within the accuracy of the theoretical approximations and the experimental uncertainties.

The variation of the  $\text{NH}_3$  line-breadth parameter  $\Delta\nu$  with  $J$  and  $K$  is shown in Table 13-3 and compared with predictions of several types of theories. It may be seen that Anderson's approach, using broadening

TABLE 13-3. COMPARISON BETWEEN EXPERIMENTAL AND THEORETICAL LINE WIDTHS FOR AMMONIA SELF-BROADENING  
Experimental values apply to a temperature of 20°C.

Line		Line breadth, Mc/mm Hg					
$J$	$K$	Experi- mental, Bleaney and Penrose [179]	Anderson [342]	Anderson (neglecting rotational resonance) [342]	Bleaney and Penrose [257]	Margenau [393]	Mizu- shima [619]
2	1	16	16	13	16	14	12
3	1	14	14	9	13	10	9
3	2	19	20	18	20	20	16
3	3	27	27	27	27	29	23
4	4	27	28	28	28	30	24
5	1	11	11	6	10	6	6
5	2	16	15	11	15	12	11
5	3	20	20	17	20	19	16
5	5	28	29	29	28	31	24
6	3	19	17	14	19	15	13
6	4	22	21	19	22	21	17
6	6	28	29	29	28	31	24
7	5	25	22	21	23	23	18
7	6	23	26	25	26	27	22
8	7	25	26	26	26	28	22
10	9	25	27	27	27	29	23
11	9	17	25	25	25	27	21

of type (13-54) and allowing for rotational resonance (13-57), gives rather good agreement with experimental results. Omitting the rotational-resonance type of interaction (column 5 of Table 13-3) gives poor agreement when  $K < J$ . The values in Table 13-3 are measured by Bleaney and Penrose [257], and all the results of Anderson's theory have been multiplied by a constant factor to give exact agreement between this theory and the experimental value for the 3,3 line.

The closest fit to the experimental data is a formula given by Bleaney and Penrose (column 6, Table 13-3)

$$\Delta\nu = 30 \left[ \frac{K^2}{J(J+1)} \right]^{\frac{1}{2}} \quad (13-61)$$

where  $\Delta\nu$  is the half width in megacycles for a pressure of 1 mm Hg. The form of this expression is derived on the assumption that a collision occurs when two molecules approach closely enough for the interaction of their dipoles to reach some critical value  $W$ . However, since any effect of the perturbation depends on its duration, the criterion for a collision should be that the product of the interaction energy  $W$  and the duration of the collision reaches some critical value. With this modification, Bleaney and Penrose's approach becomes similar to the statistical theory and gives an expression of the form  $\Delta\nu \propto K/\sqrt{J(J+1)}$ . This is the type of variation found by Margenau from a statistical type of theory (column 7, Table 13-3). It does not fit so well as (13-61). Bleaney and Penrose's formula must be regarded essentially as empirical since their assumption in deriving it is quite artificial. Moreover, as may be seen from the discussion below, it gives the wrong temperature dependence of line width. Mizushima's calculation of line breadths (Table 13-3) is based on an adiabatic type of collision theory. The similarity between the results of Bleaney and Penrose, Mizushima, Margenau, and Anderson shows that approximate agreement with experiment can be obtained under a variety of assumptions. However, the line widths calculated by Anderson are clearly more accurate than those given by Margenau or Mizushima in the cases where rotational resonance is of importance.

Broadening of ammonia lines by foreign gases is treated in exactly the same manner as self-broadening if the perturbing molecule is a symmetric top with a reasonably large dipole moment (*e.g.*,  $\text{CH}_3\text{Cl}$  or  $\text{CHCl}_3$ ) and similarly good agreement is obtained ([536], Table 1). Line breadths and effective collision diameters for pressure broadening of  $\text{NH}_3$  by a number of gases are given in Table 13-4. These collision diameters are in many cases larger than the collision diameters given by kinetic theory, which are listed in Table 13-4 for comparison. This is because for pressure broadening the long-range and weak interactions can be important, whereas in processes of significance to kinetic theory the shorter-range stronger interactions are necessary. In the cases where the collision diameter for broadening is large, one can expect to obtain a relatively simple theory of the collision since the many short-range forces can be neglected. In the case of self-broadening in  $\text{NH}_3$ , for example, the collision diameter is more than three times as large as the kinetic theory diameter, or the cross section about ten times as large. The importance of long-range dipole-dipole forces in the case of  $\text{NH}_3$  self-broadening is the reason it can be treated so successfully with a theory that neglects other types of interactions.

Smith and Howard [536] have shown that the large effective collision diameters between  $\text{NH}_3$  and  $\text{N}_2$ ,  $\text{CO}_2$ ,  $\text{COS}$ , and  $\text{CS}_2$  are very probably due to interaction between the  $\text{NH}_3$  dipole moment and the molecular quadrupole moments of these molecules [536]. This type of interaction has not yet been treated accurately, but if broadening of the  $\text{NH}_3$

TABLE 13-4. COLLISION DIAMETERS AND LINE-WIDTH PARAMETERS FOR BROADENING OF THE  $\text{NH}_3$  3,3 LINE BY VARIOUS GASES\*

$\Delta\nu$  is the half width at half maximum intensity for a small amount of  $\text{NH}_3$  in 1 mm Hg pressure of the colliding molecule. Collision diameters computed from kinetic theory are included for comparison.

Colliding molecule	Dipole moment, debye units, or $10^{-18}$ esu	$\Delta\nu$ , Mc	Effective collision diameter $b_e$ , angstroms	Kinetic theory collision diameter $b$ , angstroms
$\text{NH}_3$	1.47	27	13.8	4.43
He	0	1.3	2.4	3.31
A	0	1.7	3.7	4.04
$\text{H}_2$	0	3.0	3.1	3.59
$\text{N}_2$	0	3.8	5.5	4.09
$\text{O}_2$	0	2.3	4.3	4.02
$\text{CO}_2$	0	6.8	7.6	4.46
$\text{COS}$	0.720	6.5	7.6	
$\text{CS}_2$	0	6.5	7.7	
$\text{HCN}$	2.96	13	10.0	
$\text{ClCN}$	2.80	16	11.9	
$\text{CH}_3\text{Cl}$	1.87	15	11.3	5.14
$\text{CH}_2\text{Cl}_2$	1.59	12	10.3	
$\text{CHCl}_3$	0.95	20	13.7	
$\text{CCl}_4$	0	5.5	7.2	
$\text{SO}_2$	1.7	12	10.4	

\* W. V. Smith and R. Howard [536]. Where other measurements have been published [658], [627] the results have been averaged with those of Smith and Howard. The numbers presumably all apply to room temperature.

3,3 line is due to the quadrupole moment  $Q$  of a foreign molecule, then approximately

$$|Q| = 5.3 \times 10^5 b_e^3 \left( \frac{M_1 + M_2}{M_1 M_2} \right)^{\frac{1}{2}} \quad (13-62a)$$

(cf. [536]). Here  $M_1$  and  $M_2$  are the molecular weights of the colliding molecules. The quadrupole moment of a symmetric molecule is defined as

$$Q = \int \rho (3z^2 - r^2) dv \quad (13-62b)$$

where  $\rho$  is the charge density at a point  $z, r$  in the molecule. Coordinates are measured from the center of mass and  $z$  is in the direction of the



molecular-symmetry axis. This definition is that commonly used in molecular theory but differs by a factor of the electron charge from that used for nuclear quadrupole moments.

Table 13-3 gives the molecular quadrupole moments for some molecules which have been measured by their effectiveness in broadening the ammonia 3,3 line [536], [586].

The values in the table are those measured directly for the normal rotating molecule. On the other hand, theoretical calculations [using (13-62)] of molecular quadrupole moments for a known or postulated molecular structure assume that the molecule is at rest. The effective quadrupole moment for a classically rotating linear molecule, averaged over the rotation, is one-half of that for the stationary molecule. This

TABLE 13-5. MOLECULAR QUADRUPOLE MOMENTS

$Q'$  is the effective quadrupole moment for rotating molecules. For a linear molecule,  $Q' = Q/2$ , where  $Q$  is defined by (13-62b).

Molecule	$b \times 10^8$ , cm, kinetic theory	$b \times 10^8$ , cm, from $\text{NH}_3$ 3,3 line broadening	Molecular $Q'$ , $10^{-26}$ esu
$\text{N}_2$	4.09	6.0	1.5
$\text{O}_2$	4.02	4.18	<0.55
NO	3.90	5.64	1.4
CO	3.96	5.97	1.6
$\text{CO}_2$	4.46	7.59	3.1
COS	....	7.56	2.9
$\text{CS}_2$	....	7.72	3.1
$\text{N}_2\text{O}$	4.35	9.1	4.4
HCN	....	10.0	7.7
ClCN	....	11.9	11.5
$\text{C}_2\text{H}_2$	....	8.79	5.3
$\text{C}_2\text{H}_4$	4.79	6.67	2.3
$\text{C}_2\text{H}_6$	4.86	5.64	<1.3

classical average is usually adequate in pressure-broadening studies, since the most abundant states of the perturbing molecules are usually those with high  $J$  values for which the classical approximation is good. Sometimes, particularly in molecular theory, the molecular quadrupole moment is defined as half the value given here.

Estimates of molecular quadrupole moments using what is known about molecular structures and bonding are consistent with the measured values [582].

For collisions between  $\text{NH}_3$  and  $\text{H}_2$ , He, or A, interactions of the quadrupole-induced dipole type discussed above [cf. (13-60)] may be of importance. The rather large dipole moment of  $\text{NH}_3$  may induce a dipole moment in a He or A atom, and this induced dipole moment

reacts back on the quadrupole moment of the  $\text{NH}_3$  molecule. It is perhaps surprising that such an interaction is more important than the reaction of the induced dipole back on the  $\text{NH}_3$  dipole. This is because the symmetry of the dipole-induced dipole interaction is such that it produces no inversion transitions and hence a small disturbance of the inversion spectrum [428]. The quadrupole-induced dipole interaction has such a symmetry that it can cause inversion transitions and is therefore of more importance. Unfortunately the quadrupole moment of  $\text{NH}_3$  is not accurately known. Estimates of this quadrupole moment and application of expressions (13-59) and (13-60) show that the collision diameters for broadening of the  $\text{NH}_3$  3,3 line by the gases  $\text{H}_2$ , He, A, and O are of approximately the magnitude to be expected from this type of interaction [428]. However, these collision diameters are not larger than the kinetic theory diameters (*cf.* Table 13-4), so other short-range interactions such as type 8 of Table 13-1 may also be of importance.

**13-10. Self-broadening of Linear Molecules.** Self-broadening of linear molecules in the infrared region has received considerable attention, and dipole-dipole interactions of the Keesom alignment type have been rather completely worked out for adiabatic collisions, which predominate in the infrared region. Rotational-resonance-type interactions are also of importance for the infrared spectra of these molecules and have been fairly completely treated [93], [153].

For microwave transitions adiabatic collision approximations are not very satisfactory. It might be thought that rotational resonance is unimportant because at room temperature the most abundant molecular states have high  $J$  values ( $J \approx 30$ ), whereas only molecules with low  $J$  values give microwave transitions. Hence an encounter between a molecule absorbing microwaves and another molecule differing by one unit in  $J$  is a rare event and contributes little to the line breadth. However, the short duration of collisions between molecules ( $10^{-12}$  sec) makes the requirements for rotational resonance much less stringent. That is, during a collision lasting  $\tau$  sec, the energy levels are uncertain by about  $h/2\pi\tau \approx 5 \text{ cm}^{-1}$ . Thus all levels within this distance are effectively in resonance with the transition being studied. For OCS, where  $B = 0.2 \text{ cm}^{-1}$ , the first five  $J$  levels are effective in rotational-resonance broadening of the lowest rotational level. The number of molecules with energies near enough to cause resonance broadening increases as  $J$  increases.

These qualitative expectations are confirmed by the measurements of Johnson and Slager [706] on OCS line widths. It is found that line widths increase with increasing  $J$ , which is to be expected as the number of molecules within the resonance interval is greater for those with higher values of  $J$ . The relative increase with  $J$  is greater at lower temperatures where the peak of the population distribution is shifted toward lower  $J$ .

By considering interactions between a given rotational state and all

other rotational states which may be considered resonant, Smith, Lackner, and Volkov [to be published] have calculated collision diameters for OCS and BrCN in good agreement with experimental observations. Thus for the  $J = 3 \leftarrow 2$  transition of BrCN, the theoretical collision diameter is 19.3 Å while the experimental value is 19.0 Å. Recent measurements on OCS by R. S. Anderson [to be published] give similarly good agreement.

No complete treatment of broadening of microwave lines by either dipole-quadrupole or Keesom alignment forces is available. However, Keesom alignment forces have been approximately treated by adiabatic theories [153], [303], [398], [499], [619].

Keesom alignment interactions are difficult to evaluate from Anderson's theory because of the particular matrix elements involved. While the mean of the diagonal elements of the square of the interaction matrix is desired, some idea of the magnitude of these effects may be obtained from the ordinary linear average of the energy which is more easily computed [93]. It is

$$(W_{dd})_{av} = \frac{2\mu^4}{3Br^6} \frac{J_1(J_1 + 1) + J_2(J_2 + 1)}{(J_1 + J_2)(J_1 + J_2 + 2)(J_1 - J_2 - 1)(J_1 - J_2 + 1)} \quad (13-63)$$

where  $\mu$  is the permanent dipole moment,  $B$  the rotational constant,  $J_1$  and  $J_2$  the rotational quantum numbers of the two colliding molecules, and  $r$  the distance between them. The most important collisions involve large quantum numbers  $J_2$  for the colliding molecules, or  $J_2 \gg J_1$ . For this case

$$(W_{dd})_{av} = \frac{\mu^4}{3r^6 E_{J_2}}$$

where  $E_{J_2}$  is the rotational energy of the colliding molecule, which may be approximated as  $kT$ , or

$$(W_{dd})_{av} = \frac{\mu^4}{3kTr^6} \quad (13-64)$$

An average value for the dipole-quadrupole interaction is [536]

$$(W_{dq})_{av} = \frac{1}{3} \frac{\mu Q_e}{r^4} \quad (13-65)$$

In many typical collisions the energies of interaction  $W_{dd}$  and  $W_{dq}$  are comparable in magnitude. However, for small dipole moments and distant collisions the longer-range dipole-quadrupole interactions may predominate. Thus for the collision diameter of OCS,  $b_e = 7.6$  Å and  $Q = 0.6 \times 10^{-16}$  cm<sup>2</sup>, the dipole moment  $\mu$  must be as large as 2 debyes for  $W_{dd}$  to equal  $W_{dq}$ . Since the dipole moment of OCS is only 0.7 debye,



the dipole-quadrupole interactions may be expected to dominate. For dipole moments as large as 2 or 3 debyes, the dipole-dipole Keesom alignment interactions usually are most important. While dipole moments are readily measurable, quadrupole moments have so far only been estimated roughly from the molecular structure [382] or deduced from ammonia pressure broadening. Smith and Howard [536] have estimated the quadrupole moments of several molecules in this way from their effectiveness in broadening the  $\text{NH}_3$  3,3 line and have used the resulting values to calculate dipole-quadrupole self-broadening in these gases. They obtained fair agreement with experiment.

**13-11. Oxygen Line Breadths.** The oxygen spectrum is unusual in that it arises from a molecule having a zero electric dipole moment. It might therefore be expected to have unusually narrow lines, and this is indeed the case. Because of its importance to atmospheric transmission, breadths of oxygen lines in pure oxygen and in air have been studied since the early days of microwave spectroscopy [139], [244], [301], [416], [576]. Half widths of the microwave oxygen lines are about 2 Mc per mm of Hg and are approximately independent of the rotational quantum numbers [667], [669], [770]. This, plus theoretical estimates of the magnitudes of various interactions, indicate that the width of these lines is mainly caused by the same short-range repulsive forces responsible for kinetic energy transfer [770]. Even though they decrease very rapidly with distance, they are probably large enough to cause rotational transitions (which involve little energy) at a distance  $1\frac{1}{2}$  times the kinetic theory radius, and so to cause the observed line widths.

**13-12. Temperature Dependence of Line Widths.** An elementary model of the collision process might be two colliding "hard" molecules of definite boundaries, so that the collision cross section is independent of the velocity of collision. Then since the number of molecules at a given pressure is inversely proportional to the temperature, and the velocity is proportional to the square root of the temperature,

$$\Delta\nu \propto nv\sigma \propto \frac{1}{\sqrt{T}}$$

In contrast to expectations from this model, experimentally the ammonia line width of fixed pressure is approximately proportional to  $1/T$  [536] so the collision cross section cannot be independent of velocity. Some such variation is to be expected from a more refined collision theory. A slow molecule spends more time near the radiator and so causes more disturbance than one which passes quickly.

The dependence of the collision cross section on velocity for an intermolecular potential proportional to  $1/r^n$  may be readily obtained. For such a potential, a measure of the disturbance is the matrix element  $(a|P|b)$  whose square is the probability of a collision-induced transition.

From (13-49),

$$(a|P|b) = \frac{\text{const}}{b^{n-1}v} \quad (13-66)$$

For a collision just strong enough to be effective in line broadening or to give a critical value of  $(a|P|b)$ , the collision parameter  $b$  is the effective collision diameter  $b_e$ . From (13-66)

$$b_e^{n-1} \propto \frac{1}{v}$$

Hence the line-breadth parameter is

$$\Delta\nu \propto nvb_e^2 \propto nv^{1-2/(n-1)}$$

Remembering that the average velocity is proportional to  $T^{1/2}$  and  $n$  to  $T^{-1}$ ,

$$\Delta\nu \propto T^{-(n+1)/2(n-1)} \quad (13-67)$$

For  $n = 3$  (the ammonia case),  $\Delta\nu \propto T^{-1}$ ; for  $n = 6$ ,  $\Delta\nu = T^{-0.7}$ . If  $T$  is increased by a factor of 2,  $\Delta\nu$  would change to 0.5 or 0.62, respectively, of its original value. Thus the temperature dependence of line width, when accurately measured, may give information about the force law between molecules. However, if it were to be so used, very precise line widths would be needed.

Furthermore, the measured collision diameter varies with temperature whenever resonance collisions between molecules are important because the distribution of molecules among the rotational or other quantum states changes with temperature. For the  $J = 2 \leftarrow 1$  transition of OCS the line-width parameter  $\Delta\nu$  varies as  $T^{-0.9}$  [921], so that, from Eq. (13-67), the collision diameter is approximately proportional to  $T^{-0.2}$ . About half of this temperature variation of collision diameter has been shown to be due to the change in first-order (resonant) dipole interactions [921].

**13-13. Effect of Temperature on Intensities.** Temperature enters into the peak intensity of a microwave line [Eq. (19)] through  $\Delta\nu$ ,  $kT$ ,  $N$ , and  $f$ , where  $f$  is the fraction of molecules in the lower state of the transition and  $N$  is the number of molecules per cubic centimeter. From the above discussion, at a given pressure  $\Delta\nu$  varies with temperature as  $T^{-1}$  for a very short-range force law, and as  $T^{-1}$  for the longer-range force laws. Assuming  $\Delta\nu \propto T^{-1}$ , Eq. (1-77) shows that for a diatomic or linear molecule the variation of intensity with  $T$  is

$$\gamma_{\max} \propto \frac{1}{T^2} \quad (13-68)$$

For a symmetric rotor, from (3-52),

$$\gamma_{\max} \propto \frac{1}{T^{3/2}}$$



In these expressions most of the variation with temperature is due to the change in the Boltzmann distribution which populates lower rotational states more fully at lower temperatures. That portion of the variation which is caused by changes in population of the vibrational state has not been taken into account. Although population of vibrational states is also affected by temperature, its variation can be neglected in the important case where the vibrational frequency is so high that almost all molecules are in the ground vibrational state.

For linear and symmetric rotor molecules in the ground vibrational state, intensity is always increased by operating at as low a temperature as possible, consistent with a reasonable vapor pressure. For microwave transitions between high-energy rotational levels of asymmetric tops, or those involving excited vibrational states, a decrease in temperature may decrease the intensity or leave it relatively unchanged.

**13-14. High Pressures.** Pressures may be called high from the point of view of line breadths when collisions involving more than two molecules become frequent enough to be important. In such cases the line width is no longer proportional to pressure, since the number of effective collisions undergone by one molecule is not simply proportional to the density of molecules. "High" pressure may occur as low as  $\frac{1}{2}$  atm for molecules with large collision diameters. For example, at 1 atm the average distance between molecules is approximately 30 Å, which is only twice the effective collision diameter for  $\text{NH}_3$ . "Low" pressure conditions may still apply at 1 atm to other gases such as  $\text{O}_2$  which have very small collision diameters. Collision theories which assume two-body impacts only and a long interval of time between impacts are, of course, not strictly applicable to high-pressure conditions. Statistical types of theories may be more appropriate since the radiating molecule is almost continually perturbed. However, as yet no quantitative theory of line broadening at high pressures is available.

The ammonia spectrum has been studied experimentally at pressures up to a few atmospheres by several observers [779], [257], [439], [321], [734]. It is found that the spectrum is fitted near the peak by a Van Vleck-Weisskopf shape but that  $\nu_0$  may be assumed to decrease with increasing pressure. For pressures equal to or greater than 2 atm  $\Delta\nu$  increases less than linearly with pressure and the best fit is obtained with  $\nu_0 = 0$ . This shift in  $\nu_0$  is proportional to the square of the pressure rather than its first power as might be expected from phase-shift theories. Diabatic collisions, of course, predict no shift at all. The observed shift in frequency has been explained qualitatively by Anderson [341] and by Margenau [393]. They point out that, with the small intermolecular distances which are common at high pressures, the perturbations are large enough to cause a change in molecular wave functions and hence in selection rules. In a strong field the molecule is characterized by either



of the wave functions  $\psi_{+K}$  or  $\psi_{-K}$  rather than by their weak-field combinations  $\psi = \psi_{+K} \pm \psi_{-K}$ . In other words, the inversion is eliminated and the nitrogen is held on one side of the hydrogens by the electric field. The only allowed transitions are changes in orientation or of one unit in magnetic quantum number. These transitions involve much smaller frequencies than inversion. At 1 atm pressure, where this effect begins to appear experimentally, the interaction between dipole moments is greater than the inversion splitting so that the strong-field approximation holds for about 50 per cent of the time. The importance of this effect and interpretation of the high-pressure line shape has, however, been questioned [504] on the basis of infrared measurements.

**13-15. Saturation Effects.** The well-known Lambert's law states that each layer of material of equal thickness absorbs an equal fraction of radiation which traverses it. From Lambert's law is derived the exponential decrease in intensity

$$I = I_0 e^{-\gamma x} \quad (13-69)$$

where  $\gamma$  is constant. In optical spectra departures from Lambert's law are usually associated with polychromatic radiation, individual components of which are absorbed at different rates. In the microwave region, however, Lambert's law breaks down even for monochromatic radiation because of saturation effects. The intensity of radiation can be made so large that absorbing molecules of a gas cannot get rid of the absorbed energy rapidly enough and  $\gamma$  becomes dependent on  $I$ .

Consider a molecular ground state in which there are  $n_0$  molecules per unit volume and an excited state containing  $n_1$  molecules per unit volume, with a microwave transition possible between the two states. From the derivation of Eq. (13-19), it can be seen that

$$\gamma = \frac{8\pi^2}{3ch} (n_0 - n_1) |\mu_{01}|^2 \frac{\nu(1/2\pi\tau)}{(\nu - \nu_0)^2 + (1/2\pi\tau)^2} \quad (13-70)$$

where the "negative frequency resonance" term of Eq. (13-19) has been omitted since it is quite unimportant under the low-pressure conditions which show saturation effects.

If essentially no microwave radiation is present, then collisions maintain an equilibrium between  $n_0$  and  $n_1$  such that

$$n_0 = n_1 e^{-h\nu/kT} \quad (13-71)$$

If  $1/t_{01}$  and  $1/t_{10}$  are the probabilities per second that a molecule is transferred from state 0 to state 1 or from state 1 to state 0, respectively, by collision, then for equilibrium with no radiation

$$\frac{n_0}{t_{01}} = \frac{n_1}{t_{10}} \quad (13-72)$$

If radiation of intensity  $I$  (in units of quanta per second per unit cross section of area) is absorbed with an absorption coefficient  $\gamma$ , then a new equilibrium condition must be set up

$$\frac{n_0}{t_{01}} + I\gamma = \frac{n_1}{t_{10}} \quad (13-73)$$

From Eqs. (13-71) and (13-72),  $1/t_{01} = (1 - h\nu/kT)/t_{10}$ , assuming  $h\nu/kT$  is small, so that Eq. (13-73) becomes

$$(n_0 - n_1) - n_0 \frac{h\nu}{kT} + I\gamma t_{10} = 0$$

or

$$n_0 - n_1 = n_0 \frac{h\nu}{kT} - I\gamma t \quad (13-74)$$

where  $t_{10}$  has been replaced by  $t$  since the subscripts will no longer be needed.

Combining Eqs. (13-74) and (13-70),

$$\gamma = \frac{8\pi^2}{3ch} \left( n_0 \frac{h\nu}{kT} - I\gamma t \right) |\mu_{01}|^2 \nu \frac{1/2\pi\tau}{(\nu - \nu_0)^2 + (1/2\pi\tau)^2} \quad (13-75)$$

or

$$\gamma = \gamma_0 \left( 1 - \frac{I\gamma kTt}{n_0 h\nu} \right) \quad (13-76)$$

where  $\gamma_0$  is the absorption coefficient when  $I$  is very small. When  $I$  is very large then  $\gamma \ll \gamma_0$  and the quantity in the parentheses in Eq. (13-76) approaches zero; so that for large radiation flux

$$\gamma \approx \frac{n_0 h\nu}{IkTt} \quad (13-77)$$

This equation written

$$\gamma I \approx \frac{n_0}{t} \frac{h\nu}{kT}$$

is simply equivalent to saying that the total number of quanta absorbed per unit time must equal the rate at which the energy of these quanta can be transformed into kinetic energy by collision.

Solving Eq. (13-75) for  $\gamma$  gives

$$\gamma = \frac{8\pi^2 n_0}{3ckT} |\mu_{01}|^2 \nu^2 \frac{1/2\pi\tau}{(\nu - \nu_0)^2 + (1/2\pi\tau)^2 + \frac{8\pi^2 t}{3ch} |\mu_{01}|^2 \nu I (1/2\pi\tau)} \quad (13-78)$$

Thus, as a result of saturation,  $\gamma$  is decreased at all frequencies. The most noticeable effects occur, of course, near the peak absorption  $\nu = \nu_0$ . The line shape is altered only in that the maximum intensity is decreased

by the factor

$$\frac{1}{1 + \frac{8\pi^2|\mu_{01}|^2\nu It}{3ch} 2\pi\tau}$$

and the half width increased by the factor

$$\sqrt{1 + \frac{8\pi^2|\mu_{01}|^2\nu It 2\pi\tau}{3ch}} \quad (13-79)$$

Essentially the same result is given by a more sophisticated quantum-mechanical treatment [297], [322].

At high pressures, saturation is generally unobservable. It becomes noticeable when

$$\frac{8\pi^2|\mu_{01}|^2\nu It 2\pi\tau}{3ch} \approx 1$$

Since both  $t$  and  $\tau$  are inversely proportional to the number of collisions per second, the radiation intensity  $I$  at which saturation occurs is proportional to the pressure squared. Experimentally, saturation is often noticed when the power flux is as high as one milliwatt per square centimeter and the pressure low enough to give line widths less than 1 Mc [172]. It is not uncommon for saturation effects to set a lower limit on the width of microwave lines. In order to obtain very narrow lines, the radiation intensity must be kept low.

In considering saturation, each Zeeman (or Stark) component of a line should be treated individually. Although individual components all have the same frequency, their matrix elements differ (*cf.* page 23) so that some components saturate more readily than others [295]. However, saturation effects may be described approximately by taking some average matrix element  $|\mu_{10}|^2$  for the entire transition.

Measurement of saturation effects allows determination of  $1/t$ , the rate at which molecules make transitions due to collisions. In ammonia, it has been shown that within the accuracy of measurement each collision which is effective in producing line broadening is also effective in producing a transition [172], [256], [294], [295]. This is the result to be expected from the earlier discussion of the predominance of diabatic collisions.

Saturation effects may also be used to obtain an estimate of the matrix element  $|\mu_{01}|^2$  in certain cases. The intensity of a line is influenced both by the dipole matrix elements  $|\mu_{01}|^2$  and by the number of molecules in the particular ground state from which transitions occur. Saturation effects may be seen from (13-78) or (13-79) not to depend on the number of molecules normally in the ground state, but they do depend on the matrix element. Thus the relative ease with which two different lines can be saturated affords some information about the relative sizes of their dipole matrix elements.



**13-16. Broadening by Collisions with Walls.** If a gas molecule strikes a wall of the cavity or waveguide in which it is contained, the process of absorption is interrupted.

A good approximate treatment of the broadening effects of wall collision can be obtained by assuming that the line shape due to wall collisions is the same as that produced by intermolecular collisions, *i.e.*

$$\gamma = \frac{\gamma_{\max}(\Delta\nu)^2}{(\nu - \nu_0)^2 + (\Delta\nu)^2} \quad (13-80)$$

Here the line-breadth parameter is given by  $\Delta\nu = 1/2\pi\tau$ , where  $\tau$  is the mean time between collisions.  $\tau$  may be evaluated from kinetic theory.\* The number of molecules hitting the surface of total area  $A$  in each second is

$$n = \frac{1}{4}N\bar{v}A \quad (13-81)$$

where  $N$  is the number of molecules per cubic centimeter of gas,  $\bar{v}$  is the average molecular velocity  $= 4(RT/2\pi M)^{1/2}$ ,  $R$  is the gas constant,  $T$  is the absolute temperature, and  $M$  is the molecular weight. Hence the number of collisions per second is

$$n = NA \left( \frac{RT}{2\pi M} \right)^{1/2} \quad (13-82)$$

But the total number of molecules in the absorption cell is  $NV$ , where  $V$  is the volume of the cell. Thus the average time between collisions for any molecule is

$$\tau = \frac{NV}{NA(RT/2\pi M)^{1/2}} = \frac{V}{A} \left( \frac{2\pi M}{RT} \right)^{1/2} \quad (13-83)$$

so that

$$\Delta\nu = \frac{A}{V} \left( \frac{RT}{8\pi^3 M} \right)^{1/2} \quad (13-84)$$

At 300°K,

$$\Delta\nu = 1.00 \times 10^4 \frac{A}{V} M^{-1/2} \quad (13-85)$$

As an example, for ammonia in a cell with a spacing of 4 mm between a Stark plate and the opposite face, and all other dimensions considerably larger,  $\Delta\nu = 12$  kc.

A more rigorous treatment of wall broadening has been given by Danos and Geschwind [788]. The line shape is shown to be close to the Lorentz shape and the line width is about 10 per cent greater than that given by the elementary treatment above.

If both Doppler and collision widths are appreciable, the total line-

\* See, for instance, M. Knudsen, *Kinetic Theory of Gases*, Methuen & Co., Ltd., London, and John Wiley & Sons, Inc., New York, 1950.

width parameter is given very nearly by\*

$$\Delta\nu \approx [(\Delta\nu_{\text{Doppler}})^2 + (\Delta\nu_{\text{collision}})^2]^{\frac{1}{2}} \quad (13-86)$$

Wall-collision broadening is ordinarily much less than pressure broadening. Where necessary for high-resolution spectroscopy it can always be reduced as much as desired by using a sufficiently large absorption cell.

**13-17. Microwave Absorption in Nonpolar Gases.** A nonpolar gas ordinarily does not absorb microwaves. However, if the gas molecules are sufficiently polarizable, some dipole moment may exist during collisions. At high pressures, the molecules are in collision for a large part of the time, so that an appreciable absorption occurs. Such a pressure-dependent absorption has been found in  $\text{CO}_2$  by Birnbaum, Maryott, and Wacker [905]. The observed absorption was approximately proportional to the square of the pressure and reached  $2.3 \times 10^{-5}$  at 3.3 cm wavelength for a pressure of 45 atm and a temperature of 25°C.

\* See numerical tabulation in M. Born, *Optik*, pp. 486, 431ff., Springer-Verlag OHG, Berlin, 1933.

## CHAPTER 14

# MICROWAVE CIRCUIT ELEMENTS AND TECHNIQUES

**14-1. Introduction. Electromagnetic Fields and Waves.** Although microwaves were produced by Hertz in the very earliest demonstration of electromagnetic waves, for many years waves of these short lengths were not much used. The interesting features of wavelengths comparable with the dimensions of laboratory apparatus (1 to 1000 mm) were recognized but could not easily be studied because of the lack of suitable generators.

With the development of klystron and magnetron oscillators and of waveguide techniques near the beginning of World War II, large-scale military applications of radar became possible. The attendant intensive development program saw the introduction or development of most of the microwave techniques currently used in spectroscopy. The status of the art at the end of the war is described most completely in the 28 volumes of the Massachusetts Institute of Technology Radiation Laboratory Series (McGraw-Hill Book Company, Inc., New York, 1947). A number of shorter treatments of microwave theory and practice on various levels have appeared since the war. Many of these are listed at the end of the present chapter.

Because the basic microwave techniques are described in detail elsewhere, they will be only outlined here except for those peculiar to microwave spectroscopy. References will for the most part be to books where fairly complete treatments are available rather than to original papers.

Devices with dimensions comparable with the radiation wavelength cannot usually be treated by the lumped circuit-element approximation used in ordinary electrical-circuit theory. On the other hand, microwave devices are seldom large enough in comparison with the wavelength for the approximations of geometrical optics to be employed. Both limiting cases do occasionally occur, but most microwave apparatus has to be discussed in terms of electromagnetic wave theory.

The behavior of the entire electromagnetic spectrum may be obtained from a study of Maxwell's equations combined with additions from quantum mechanics which are necessary to understand interactions between radiation and matter. In Gaussian units (for comparison with



mks units see, for instance, [537]), Maxwell's equations are

$$\nabla \times \mathbf{H} = \frac{4\pi\mathbf{i}}{c} + \frac{1}{c} \frac{\partial \mathbf{D}}{\partial t} \quad (14-1)$$

$$\nabla \times \mathbf{E} = - \frac{1}{c} \frac{\partial \mathbf{B}}{\partial t} \quad (14-2)$$

$$\nabla \cdot \mathbf{B} = 0 \quad (14-3)$$

$$\nabla \cdot \mathbf{D} = 4\pi\rho \quad (14-4)$$

where  $\mathbf{H}$  = magnetic field

$\mathbf{B}$  = magnetic induction

$\mathbf{E}$  = electric field

$\mathbf{D}$  = electric displacement

$\mathbf{i}$  = electric current

$\rho$  = electric charge density

$\nabla$  = the operator  $\mathbf{a}(\partial/\partial x) + \mathbf{b}(\partial/\partial y) + \mathbf{c}(\partial/\partial z)$

$\mathbf{a}$ ,  $\mathbf{b}$ , and  $\mathbf{c}$  are unit vectors along the  $x$ ,  $y$ , and  $z$  axes, respectively. To these equations must be added relationships which have to do with the properties of matter:

$$\mathbf{E} = \tau\mathbf{i} \quad (14-5)$$

$$\mathbf{B} = \mu\mathbf{H} \quad (14-6)$$

$$\mathbf{D} = \epsilon\mathbf{E} \quad (14-7)$$

where  $\tau$  = resistivity

$\mu$  = permeability and

$\epsilon$  = dielectric constant

From these seven equations the following important relations may be derived:

Energy density of an electric field =  $\epsilon\mathbf{E}^2/8\pi$

Energy density of a magnetic field =  $\mu\mathbf{H}^2/8\pi$

Energy flow from a volume bounded by a surface  $S = \frac{c}{4\pi} \int_S \frac{\mathbf{E} \times \mathbf{B}}{\mu} ds$

The quantity  $\frac{c\mathbf{E} \times \mathbf{B}}{4\pi\mu}$  is called Poynting's vector and usually can be regarded as the energy flux vector per unit surface, although it can be rigorously used only with integrations over a closed surface. For non-isotropic, ferromagnetic, or ferroelectric material, the relations (14-5), (14-6), and (14-7) are replaced by more complicated expressions. In addition, when one proceeds to a detailed study of interactions between microwaves and matter, a number of interesting cases appear in which  $\tau$ ,  $\mu$ , and  $\epsilon$  may no longer be usefully regarded as constants. However, in developing the general characteristics of microwave propagation, we shall accept  $\tau$ ,  $\mu$ , and  $\epsilon$  as constant properties of bulk matter.

If there are no free charges in a material ( $\rho = 0$ ), by taking the curl of Eq. (14-1) or Eq. (14-2) and using Eqs. (14-3), (14-4), (14-5), (14-6), and

(14-7), one obtains the wave equations

$$\nabla^2 \mathbf{E} = \frac{4\pi\mu}{c^2\tau} \frac{\partial \mathbf{E}}{\partial t} + \frac{\mu\epsilon}{c^2} \frac{\partial^2 \mathbf{E}}{\partial t^2} \quad (14-8)$$

$$\nabla^2 \mathbf{B} = \frac{4\pi\mu}{c^2\tau} \frac{\partial \mathbf{B}}{\partial t} + \frac{\mu\epsilon}{c^2} \frac{\partial^2 \mathbf{B}}{\partial t^2} \quad (14-9)$$

A solution of Eq. (14-8) for the electric field  $\mathbf{E}$  is a satisfactory solution of Maxwell's equations if it is paired with the proper solution of Eq. (14-9) for the magnetic field, if it satisfies Eq. (14-4), and if the appropriate boundary conditions are satisfied. The proper solution for  $\mathbf{B}$  may be obtained from  $\mathbf{E}$  by using Eq. (14-2).

Focusing attention on solutions of Eqs. (14-8) or (14-9) which involve a wave of definite frequency  $\nu = \omega/2\pi$  traveling along the  $z$  axis, we substitute the form  $E = E_0 e^{j(\omega t - \gamma z)}$  into Eq. (14-8), where  $j = \sqrt{-1}$ . The wave equation (14-8) is satisfied if

$$\gamma = \pm \sqrt{\frac{\mu\epsilon}{c^2} \omega^2 - \frac{4\pi\mu}{c^2\tau} j\omega} \quad (14-10)$$

This solution is given in the complex notation commonly employed in electrical theory. The actual physical quantities are the real parts of these expressions.

If the propagation constant  $\gamma$  is positive and real, the wave progresses in the positive  $z$  direction without damping or diminution. If  $\gamma$  is negative, the direction of propagation is in the negative  $z$  direction. If  $\gamma = j\alpha + \beta$  is complex, then  $E = E_0 e^{j(\omega t - \beta z) - \alpha z}$  represents an exponentially increasing or exponentially decreasing wave. To prevent violation of the principle of conservation of energy, the wave must usually decrease as it progresses, so that  $\alpha$  and  $\beta$  must have opposite signs. An exceptional case occurs inside the traveling-wave amplifier or oscillator tube where energy is supplied to the wave as it advances.

If the wave is in a good dielectric material (resistivity  $\tau$  very large), the propagation constant  $\gamma = \pm (\omega/c) \sqrt{\mu\epsilon}$  is real, giving an undamped wave in a medium with index of refraction  $\sqrt{\mu\epsilon}$ .

If the wave is propagated in a good conductor (resistivity  $\tau$  small), then usually  $4\pi/\tau \gg \epsilon\omega$ , and the first term under the radical of Eq. (14-10) can be neglected so that  $\gamma = \pm \sqrt{\frac{2\pi\mu\omega}{c^2\tau}} (1 - j)$ . Such a propagation constant corresponds to a very strongly damped wave since  $E$  decreases by  $1/e$  in a distance

$$\delta = \sqrt{\frac{c^2\tau}{2\pi\mu\omega}} \quad (14-11)$$

Because of the large damping, such a wave is usually appreciable only at the surface of a conductor, and  $\delta$  is called the skin depth since it gives

the amount of penetration of the wave into the material. For a good conductor and microwave frequencies  $\delta = 10^{-3}$  cm or less.

**14-2. Waveguides.** We shall now proceed to show by means of these relations that electromagnetic waves of suitable length are propagated in a hollow rectangular metal pipe or "waveguide." Figure 14-1 shows the coordinate system. In these coordinates the boundary conditions are

$$E_x = 0 \quad \text{at } y = 0 \text{ and at } y = b \quad (14-12)$$

$$E_y = 0 \quad \text{at } x = 0 \text{ and at } x = a \quad (14-13)$$

of the walls are perfect conductors.

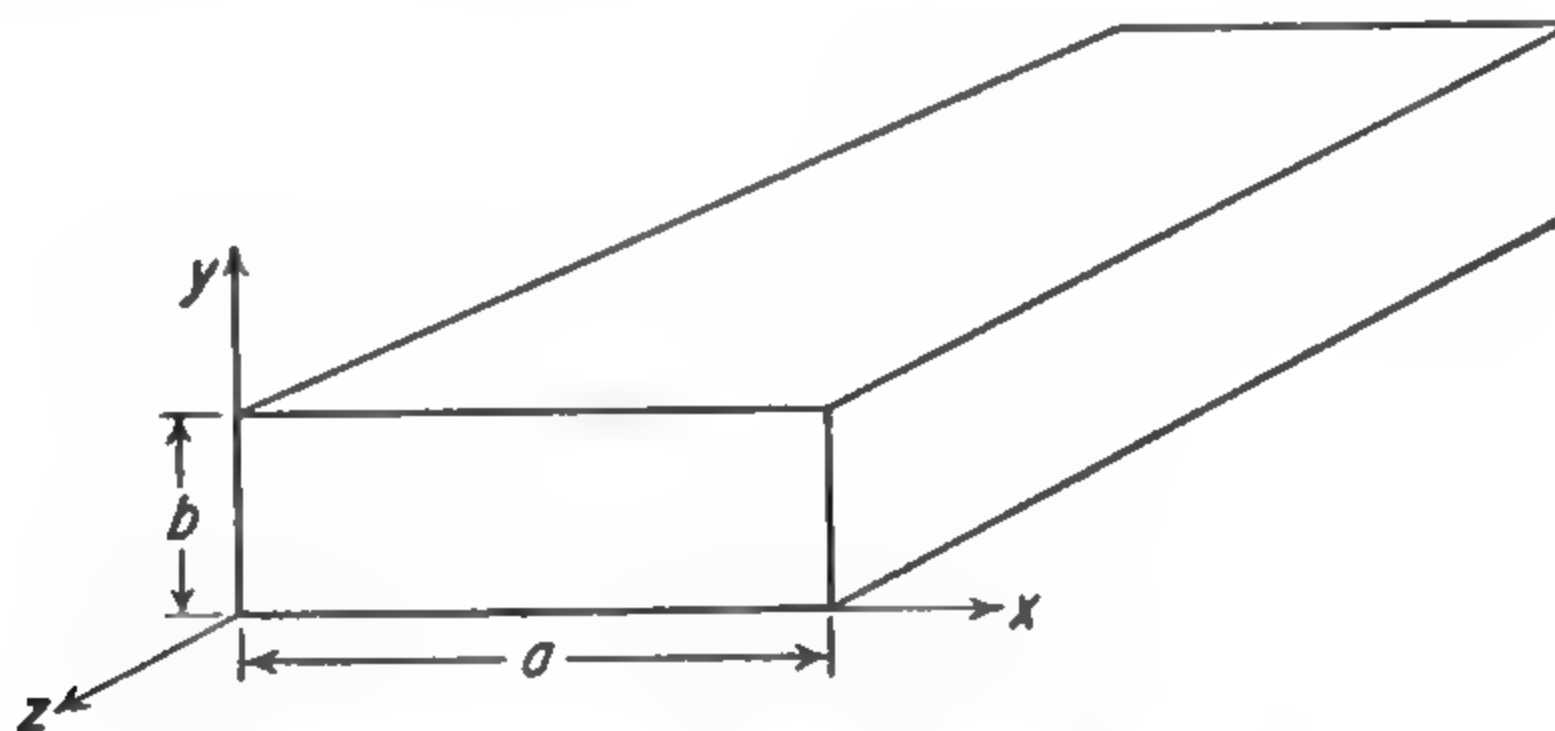


FIG. 14-1. Rectangular hollow metal pipe waveguide.

For a perfect dielectric (infinite resistivity) inside the waveguide  $\tau = \infty$  and the wave equation (14-8) becomes

$$\nabla^2 \mathbf{E} = \frac{\mu\epsilon}{c^2} \frac{\partial^2 \mathbf{E}}{\partial t^2} \quad (14-14)$$

Assume a solution of this wave equation, subject to the boundary conditions, of the form of a traveling wave with no longitudinal electric-field component.

$$\begin{aligned} E_x &= -E_0 \frac{k_y}{k_x} \cos k_x x \sin k_y y e^{+j(\omega t - \gamma z)} \\ E_y &= E_0 \sin k_x x \cos k_y y e^{+j(\omega t - \gamma z)} \\ E_z &= 0 \end{aligned} \quad (14-15)$$

These satisfy the wave equation provided that

$$k_x^2 + k_y^2 + \gamma^2 = \frac{\mu\epsilon\omega^2}{c^2} = \left(\frac{2\pi}{\lambda_0}\right)^2 \quad (14-16)$$

where  $\lambda_0$  is the wavelength in the free dielectric without walls.

From the boundary conditions at  $x = a$  and at  $y = b$

$$k_x = \frac{m\pi}{a} \quad k_y = \frac{n\pi}{b} \quad (14-17)$$



where  $m$  and  $n$  are integers. Then

$$\gamma = 2\pi \sqrt{\frac{1}{\lambda_0^2} - \left(\frac{m}{2a}\right)^2 - \left(\frac{n}{2b}\right)^2} \quad (14-18)$$

For waves whose  $\lambda_0$  is sufficiently small,  $\gamma$  is real and propagation occurs. Longer waves are not propagated through the guide, for  $\gamma$  is imaginary when  $\gamma_0$  is greater than a critical "cutoff" value designated  $\lambda_{0c}$ . The cutoff wavelength is given by

$$\frac{1}{\lambda_{0c}^2} = \frac{m^2}{(2a)^2} + \frac{n^2}{(2b)^2} \quad (14-19)$$

The length of the wave in the guide  $\lambda_g$  is related to the propagation constant by

$$\lambda_g = \frac{2\pi}{\gamma} = \frac{\lambda_0}{\sqrt{1 - (m\lambda_0/2a)^2 - (n\lambda_0/2b)^2}} = \frac{\lambda_0}{\sqrt{1 - (\lambda_0/\lambda_{0c})^2}} \quad (14-20)$$

$\lambda_g$  approaches infinity when  $\lambda_0$  approaches the cutoff wavelength. For shorter wavelengths,  $\lambda_g$  decreases and eventually approaches  $\lambda_0$  when both are much smaller than  $\lambda_{0c}$ .

It is interesting at this point to compare the behavior of low-frequency electromagnetic waves and of light in a hollow tube with that of microwaves. A low-frequency wave requires two insulated conductors for propagation. It cannot go down a single-conductor waveguide because its wavelength is beyond cutoff. Microwaves can be propagated down a waveguide, but the propagation is usually strongly affected by the boundary conditions required by the walls; *i.e.*, the microwaves are somewhat constrained in being made to "fit into" a waveguide. For optical wavelengths, however, the walls have relatively little effect since the fields vary rapidly with distance, and boundary conditions in a tube of ordinary dimensions are easily met. A tube of 1 cm dimension is almost equivalent to free space for light waves.

As mentioned above, Eq. (14-20) shows that, for  $\lambda_0$  just slightly smaller than the cutoff wavelength,  $\gamma$  is very small and hence the apparent wavelength measured along the  $z$  axis is very large. Since the phase velocity equals  $\omega/\gamma$ , the phase velocity may become very large and is always greater than  $c/\sqrt{\mu\epsilon}$ , the velocity of light in the free medium. Of course, the group velocity must obey the principles of relativity and cannot exceed  $c/\sqrt{\mu\epsilon}$ . The group velocity may be shown in the usual way to be  $v_g = (c/\sqrt{\mu\epsilon})(\lambda_0/\lambda_g)$ . The group velocity is always less than  $c/\sqrt{\mu\epsilon}$ , approaching this value when  $\lambda_0 \ll a$ , or for very short wavelengths.

The modes which have been discussed are those for which  $E_z = 0$ , that is, the electric field is purely transverse, and are designated  $TE_{mn}$  modes (transverse electric). Equation (14-15) gives the components of  $\mathbf{E}$ , and

the components of  $\mathbf{H}$  may be obtained from Eq. (14-15) and Eq. (14-2)

is

$$\begin{aligned} H_x &= -\frac{c\gamma}{\mu\omega} E_0 \sin k_x x \cos k_y y e^{j(\omega t - \gamma z)} \\ H_y &= -\frac{c\gamma k_y}{\mu\omega k_x} E_0 \cos k_x x \sin k_y y e^{j(\omega t - \gamma z)} \\ H_z &= \frac{cj(k_x^2 + k_y^2)}{\mu\omega k_x} E_0 \cos k_x x \cos k_y y e^{j(\omega t - \gamma z)} \end{aligned} \quad (14-21)$$

where  $k_x = m\pi/a$ ,  $k_y = n\pi/b$ ,  $k_x^2 + k_y^2 + \gamma^2 = \mu\epsilon\omega^2/c^2$ , and  $m$  and  $n$  are integers.

For any given rectangular waveguide having  $a > b$ , the lowest frequency, or longest  $\lambda_0$ , mode of the TE type which can be propagated is the one for which  $m = 1$ ,  $n = 0$ . It is known as the TE<sub>10</sub> mode, or the dominant mode, and is almost the only one used for microwave transmission and spectroscopy.

The complete set of field equations for the dominant mode may be written

$$\begin{aligned} E_x &= 0 & H_x &= -\frac{c\gamma}{\mu\omega} E_0 \sin k_x x e^{j(\omega t - \gamma z)} \\ E_y &= E_0 \sin k_x x e^{j(\omega t - \gamma z)} & H_y &= 0 \\ E_z &= 0 & H_z &= \frac{cj k_x}{\mu\omega} E_0 \cos k_x x e^{j(\omega t - \gamma z)} \end{aligned} \quad (14-22)$$

Except near cutoff,  $H_z$  is considerably smaller than  $H_x$ , and the wave may be visualized as an electric and a magnetic vector both approximately perpendicular to the direction of propagation and traveling down the waveguide in phase. Actually  $H_z$  is by no means negligible.

An instructive viewpoint is provided by realizing that the fields in the dominant mode given above are the same as those due to two plane waves reflected successively from the walls of the waveguide so that each zigzags its way down the guide in the  $z$  direction. The velocity with which power is propagated down the waveguide is slowed up an amount appropriate to the zigzag motion of the hypothetical plane waves.

Figure 14-2 shows the instantaneous electric field and wall currents in a rectangular waveguide carrying a TE<sub>10</sub> wave. Magnetic fields, which can also be obtained from the wave equations, are shown by broken lines. Wall currents are perpendicular at every point to the magnetic field.

Other modes satisfying the wave equation and boundary conditions exist, including some with a purely transverse magnetic field. The latter are designated TM waves, with the particular mode indicated by subscripts analogous to those used for TE modes. Their cutoff wavelength is also given by Eq. (14-20), but  $m$  and  $n$  must be greater than zero, so

that no TM mode has a cutoff wavelength as long as that of the dominant TE mode.

Circular-cylinder waveguides also can propagate microwaves in various modes governed by the boundary condition that the electric field at the wall must be perpendicular to the wall. Both TE and TM modes exist and are designated by those letters with added subscripts. The first subscript is the number of maxima of the field in a  $180^\circ$  angle measured

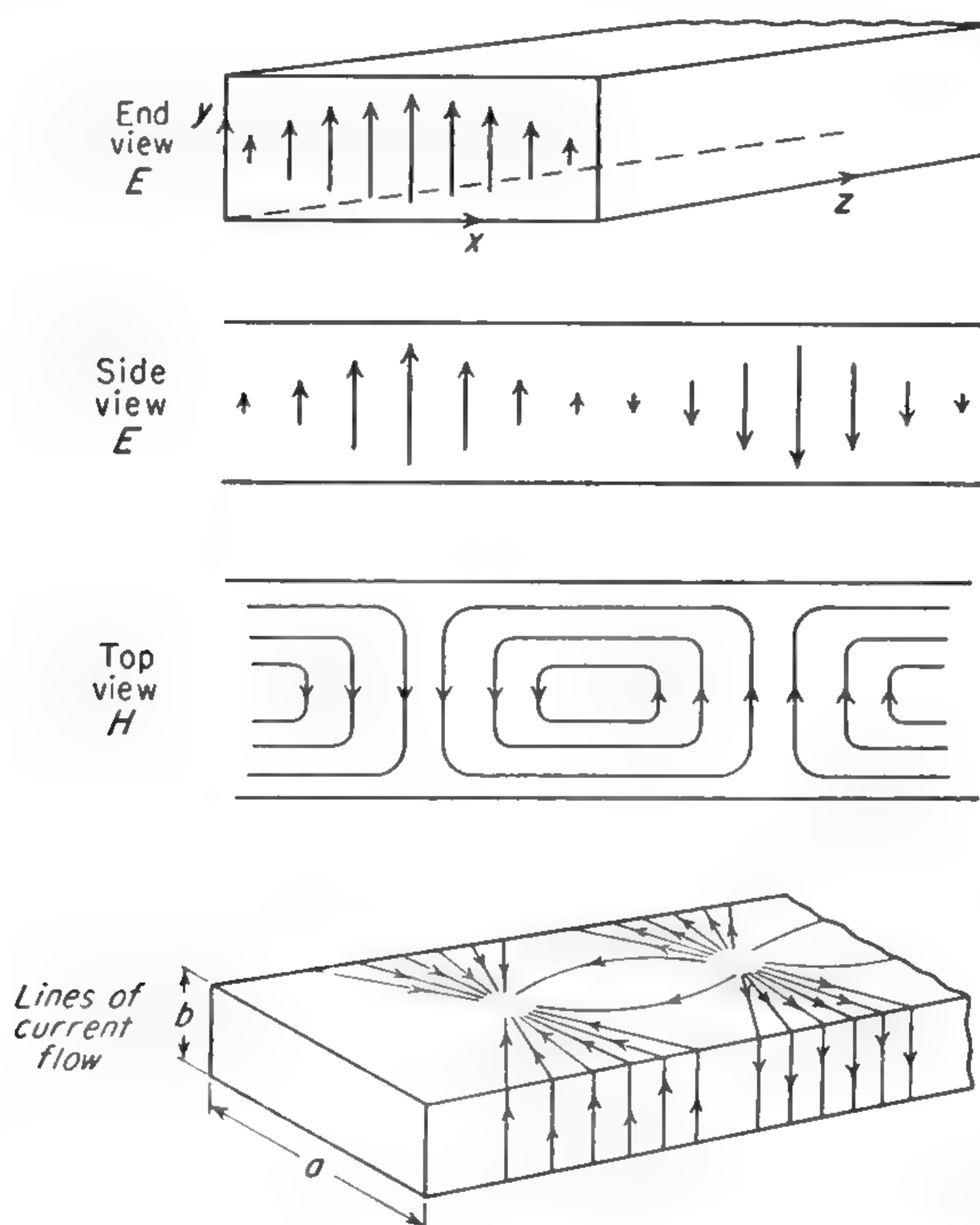


FIG. 14-2. Electric and magnetic fields and wall currents in a rectangular waveguide ( $TE_{1,0}$  mode). (After Pollard and Sturtevant [308].)

in a plane perpendicular to the axis of the cylinder. The second subscript is the number of maxima between the center and the wall of the waveguide. The fields of some of the circular modes are shown in Fig. 14-3, along with their cutoff wavelengths. As in the rectangular waveguide,  $\lambda_g$  is related to  $\lambda_0$  and  $\lambda_{0c}$  by Eq. (14-20), *i.e.*,

$$\lambda_g = \frac{\lambda_{0c}}{\sqrt{1 - (\lambda_0/\lambda_{0c})^2}}$$

While each of these modes has uses, most microwave spectrographs employ the  $TE_{01}$  mode in a rectangular guide. This mode has the advantage that, if the size of the pipe relative to the wavelength is properly chosen, no other mode can be propagated. In addition, no current flows



across the center of the broad face, so that a longitudinal slot may be cut there without disturbing the fields. Finally, the electric field is always perpendicular to the broad face, so that a metal plate parallel to that face may be put inside the guide without disturbing the fields.

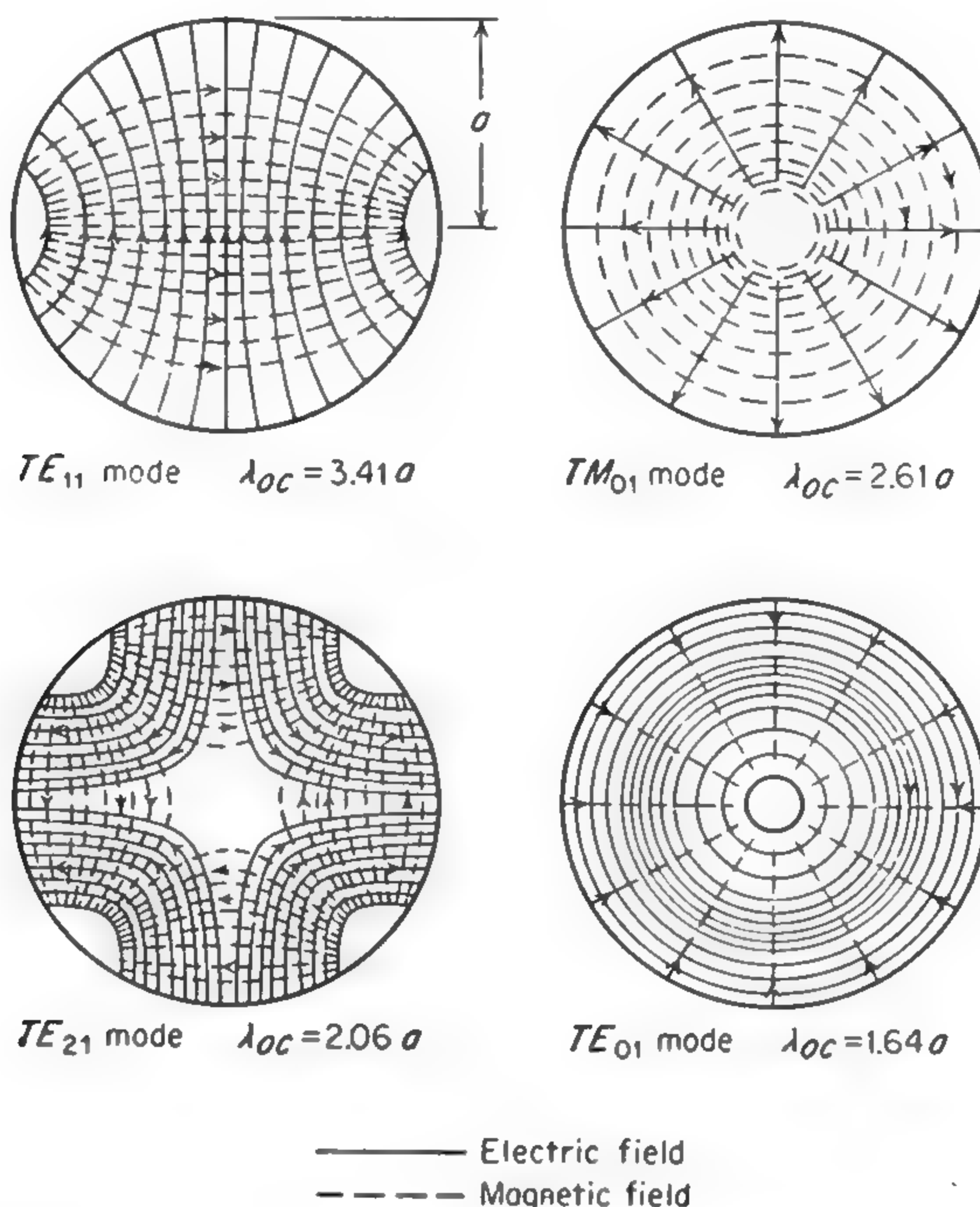


FIG. 14-3. Fields in circular waveguides.

**14-3. Attenuation.** Waveguide walls made of copper, brass, or silver approximate perfect conductors well enough that the field distributions discussed above are good approximations. However, since currents flow in the walls it is evident that some loss of power will accompany propagation of the wave. These losses give a small imaginary contribution to the propagation constant  $\gamma$  which may be fairly accurately determined by assuming that the fields in the waveguide are those appropriate to the perfectly conducting waveguide and computing the ohmic losses due to current flow.

The boundary conditions at the surface of a perfect conductor require that  $\mathbf{H}$  must be parallel to the surface. Considering any small area of a waveguide wall over which the oscillating magnetic field has essentially constant amplitude, the solution of Eq. (14-9) inside the conducting wall (analogous to the solution discussed for  $\mathbf{E}$  in conducting material) is

$$H_y = H_{0y} e^{j(\omega t - z/\delta) - z/\delta} \quad (14-23)$$

where  $\delta = \sqrt{c^2\tau/2\pi\mu\omega}$  is the skin depth. For copper  $\delta = 3.8 \times 10^{-5} \sqrt{\lambda}$  cm, where  $\delta$  and  $\lambda$  are in centimeters. Axes have been oriented so that the origin is at the surface,  $y$  is in the direction of  $\mathbf{H}$  over the small element of area having  $\mathbf{H}$  essentially constant, and the positive  $z$  axis extends perpendicularly into the wall.

From Eq. (14-1), since  $\partial\mathbf{D}/\partial t \approx 0$  in the conductor,

$$\mathbf{i} = \frac{c}{4\pi} \nabla \times \mathbf{H} \quad \text{or} \quad i_x = \frac{c}{4\pi\delta} (1 + j) H_{0y} e^{j(\omega t - z/\delta) - z/\delta} \quad (14-24)$$

The power loss due to ohmic resistance per unit volume is  $(i_R^2)_{av}\tau$  or  $\frac{1}{2}ii^*\tau$ , where  $i_R$  is the real part of Eq. (14-24). Integrating over  $z$  from 0 to  $\infty$ , the power loss per unit area is obtained as

$$\text{Power loss/area} = \int_0^\infty \frac{ii^*}{2} \tau dz = \frac{c^2\tau}{32\pi^2\delta} H_{0y}^2 = \frac{\mu\nu\delta}{8} H_{0y}^2 \quad (14-25)$$

where  $\nu$  is the frequency. The last expression for power loss has a simple interpretation. The total energy per unit area built up in the magnetic field inside the metal on every half cycle is approximately  $(\mu H_{0y}^2/8\pi)\delta$  since  $\mu H_{0y}^2/8\pi$  is the energy density at the metal surface and  $\delta$  is approximately the depth of penetration of the field. If all this energy associated with the magnetic field in the metal were dissipated in the metal on every half cycle, then the rate of power loss per unit area would be

$$2\nu \frac{\mu H_{0y}^2}{8\pi} \delta$$

which is approximately the same as Eq. (14-25). Thus the energy of the electromagnetic field penetrating the metal may be considered lost on every half cycle.

If the behavior of some field component of a microwave is described by  $E = E_0 e^{j(\omega t - \beta z) - \frac{\alpha}{2}z}$ , where  $\alpha$  and  $\beta$  are real, the constant  $\frac{\alpha}{2}$  is sometimes called the attenuation constant. Its unit is nepers per unit length. More commonly the quantity  $\alpha$  is called the attenuation constant, since the power or energy associated with the wave depends on the square of field strength, or as  $P = P_0 e^{-\alpha z}$ . The attenuation constant  $\alpha$  for power is given in units of inverse length, such as  $\text{cm}^{-1}$ . It can be calculated by computing the power flow through a waveguide and the power loss per unit length. Thus

$$\alpha = \frac{\int_{S_1} \frac{\mu\nu\delta}{8} H_{S_1}^2 dS_1}{\int_{S_2} \frac{c}{4\pi\mu} \mathbf{E} \times \mathbf{B} \cdot d\mathbf{S}_2} \quad (14-26)$$

where  $H_{s_1}$  is the component of  $\mathbf{H}$  at the surface of the waveguide,  $S_1$  is the surface of the waveguide walls of unit length,  $S_2$  is the cross-sectional surface of the waveguide (perpendicular to the direction of power flow).

Evaluation of  $\alpha$  for the  $\text{TE}_{10}$  mode gives, for a silver waveguide at wavelengths well below the cutoff wavelength

$$\alpha = \frac{3.384 \times 10^{-4}}{a^3} \left\{ \frac{(a/2b)(2a/\lambda_0)^{\frac{3}{2}} + (2a/\lambda_0)^{-\frac{1}{2}}}{[(2a/\lambda_0)^2 - 1]^{\frac{1}{2}}} \right\} \text{ cm}^{-1} \quad (14-27)$$

where  $a$  is the long dimension and  $b$  is the short dimension of the waveguide, both being measured in centimeters.  $\lambda_0$  is the free-space wavelength (in centimeters) of the radiation. To obtain the power loss in decibels per centimeter, the  $\alpha$  given by Eq. (14-27) should be multiplied by 4.343.

For metals other than silver, the attenuation is similar to that given by (14-27), but is proportional to the square root of the resistivity. For copper waveguide, the attenuation given by Eq. (14-27) is to be multiplied by 1.05; for gold the factor is 1.26 and for brass it is 2.08.

At the cutoff frequency, the attenuation given by this expression is infinite, and for slightly higher frequencies the attenuation falls rapidly. The large attenuation near the cutoff wavelength is to be expected from the equivalence of the wave to two plane waves zigzagging across the waveguide. Near cutoff the plane waves are reflected back and forth between the walls many times while moving down the waveguide one wavelength. There is consequently opportunity for considerable loss of power. The attenuation passes through a minimum at higher frequencies and then rises approximately proportionally to the frequency. For typical "K-band" copper waveguide, having inside dimensions 0.420 by 0.170 in., Eq. (14-25) gives for  $\lambda_0 = 1.25$  cm,  $\alpha = 1.1 \times 10^{-3} \text{ cm}^{-1}$ , or 0.48 db/meter. The actual measured attenuation is likely to be between 20 and 100 per cent greater because of surface imperfections ([312], pp. 117, 191). Similar expressions may be given for other modes and other types of waveguides, most of which give attenuation of the same order of magnitude, and with analogous frequency dependence. An exceptional case is the  $\text{TE}_{01}$  mode in a circular waveguide for which the attenuation decreases without limit as the frequency increases. If, in going to higher frequencies, the size of the waveguide is changed in proportion to the wavelength, the attenuation increases as  $a^{-1}$ , or  $\lambda_0^{-1}$ . If the size of guide is not changed, the attenuation increases for smaller wavelength only as  $\lambda_0^{-\frac{1}{2}}$ . A waveguide larger than that required to avoid cutoff is often used in the millimeter-wavelength region because of its lower attenuation. For wavelengths beyond cutoff ( $\lambda_0 > \lambda_{0c}$ ), the attenuation is given by  $\alpha = 54.6[1/\lambda_{0c}^2 - 1/\lambda_0^2]^{\frac{1}{2}}$  db/unit length and the impedance is reactive. Waveguides beyond cutoff are sometimes used as standards of attenuation.



**14-4. Reflections in Waveguides.** Reflection occurs whenever a wave in a guide encounters any irregularity. The irregularity may be a change in guide size, a bend or twist, or an obstacle. A treatment of reflection at irregularities is very complicated for the general waveguide case because the obstacle is likely to introduce higher modes into the reflected and transmitted waves. Very great simplifications are possible, however, when only one mode can be propagated at the wavelength considered. Then a reflected wave can be propagated only in the same mode as the incident wave, as in the case of a low-frequency transmission line. The analogy between a single-mode waveguide and a transmission line is very far-reaching and is quite useful because of the familiarity of transmission-line theory and behavior.

A transmission line for electrical impulses usually consists of two parallel conductors with current flowing along each conductor. Current also flows between the two conductors either because of current paths purposely introduced or because of the inevitable interconductor capacitance and leakage resistance. Let the series impedance of the line per unit length be  $T$ , and the shunt impedance per unit length be  $S$ . Then (*cf.* [117], Chap. 1) the instantaneous current at any point distant  $z$  along the line is given by

$$i = i_0 \exp j\omega t \pm \sqrt{T/S} z \quad (14-28)$$

where  $i_0 e^{j\omega t}$  represents the current at  $z = 0$ . The potential difference  $V$  between the conductors at any point is obtained by multiplying their shunt impedance per unit length by the current flowing through this impedance. The latter is  $-di/dz$  since the shunt current is that which is lost from the main line. Therefore

$$V = \mp \sqrt{TS} i \quad (14-29)$$

The characteristic impedance of the transmission line is defined as  $Z = V/i$ . If the wave travels toward positive  $z$  ( $i = i_0 e^{j\omega t - \sqrt{T/S}z}$ ),  $Z = \sqrt{TS}$ , and if the wave is traveling toward negative  $z$  the impedance appears to be  $Z = -\sqrt{TS}$ . Actually the impedance is usually taken as positive for both directions and  $V = Zi$  for the wave advancing in the  $z$  direction,  $V = -Zi$  for the reversed wave.

If the transmission line is not lossy, then  $T$  is usually purely inductive and may be written  $T = j\omega L$ , while  $S$  is purely capacitive and is  $S = 1/j\omega C$ . Hence  $Z = \sqrt{L/C}$  and

$$i = i_0 e^{j(\omega t \pm \gamma z)} \quad (14-30)$$

where  $\gamma = \sqrt{LC}$  is the propagation constant. Expressed in this form, it is clear that propagation of electromagnetic waves along a transmission line has much in common with the propagation of microwaves in a waveguide or in free space.

Instead of propagation on an infinitely long uniform transmission line, consider now the behavior of a current wave at a junction between two transmission lines of impedance  $Z_0$  and  $Z_1$  as indicated in Fig. 14-4. At the junction itself the current and voltage can be computed from the point of view of either transmission line, which must of course give equivalent results. Thus the current is either the algebraic sum of an incident current wave  $i_i$  and the reflected wave  $i_r$ , or equals the transmitted wave  $i_t$ . Hence when  $z = 0$ ,

$$i_i - i_r = i_t \quad (14-31)$$

and

$$i_i Z_0 + i_r Z_0 = i_t Z_1 \quad (14-32)$$



where the subscripts  $i$ ,  $r$ , and  $t$  denote, respectively, the incident, reflected, and transmitted currents. It is im-

FIG. 14-4. Currents at a junction of transmission lines of impedance  $Z_0$  and  $Z_1$ .

portant to remember that in Eq. (14-32) for a wave traveling to the right in Fig. 14-4,  $V = iZ$ , but for one traveling to the left,  $V = -iZ$ . Solving Eqs. (14-31) and (14-32) for  $i_t$  and  $i_r$  when  $z = 0$ ,

$$i_t = \frac{2Z_0}{Z_1 + Z_0} i_i \quad (14-33)$$

$$i_r = \frac{Z_1 - Z_0}{Z_1 + Z_0} i_i \quad (14-34)$$

At any point  $z$  to the left of the junction a new impedance may be defined as the ratio of voltage to current

$$\begin{aligned} Z = \frac{V}{i} &= \frac{i_i Z_0 + i_r Z_0}{i_i - i_r} = \frac{Z_0 \left( e^{-i\gamma z} + \frac{Z_1 - Z_0}{Z_1 + Z_0} e^{+i\gamma z} \right)}{e^{-i\gamma z} - \frac{Z_1 - Z_0}{Z_1 + Z_0} e^{+i\gamma z}} \\ &= Z_0 \left[ \frac{-\sinh j\gamma z + (Z_1/Z_0) \cosh j\gamma z}{\cosh j\gamma z - (Z_1/Z_0) \sinh j\gamma z} \right] \end{aligned} \quad (14-35)$$

It is to be noted that, for points to the left of  $z = 0$ ,  $z$  is a negative quantity. If  $Z_1 = Z_0$ , from Eq. (14-34) it is seen that there is no reflected wave. This condition is usually desirable because it gives a maximum power transfer and because it avoids standing waves on the transmission line.

If the transmission line to the right of  $z = 0$  consists simply of a short circuit ( $Z_1 = 0$ ) and  $\gamma$  is real, then from Eq. (14-35),  $Z = -Z_0 j \tan \gamma z$ , so that the impedance changes from zero to infinity when  $z$  varies from 0 to  $-\pi/2\gamma$ . Thus the short circuit at  $z = 0$  produces what appears to be an open-circuited line at  $z = -\pi/2\gamma$  (or  $-\lambda/4$ ), and the impedance varies periodically with  $z$  between the extremes of zero and infinity. If, however, there is some loss in the transmission line to the left of  $z = 0$ ,



$\gamma$  is partly imaginary ( $\gamma = j\alpha/2 + \beta$ ), and some distance from the junction  $z = 0$  the periodic impedance variation decreases in magnitude and  $Z$  approaches a constant value  $Z_0$ .

The impedance concept is particularly useful for transmission lines because Eq. (14-35) permits calculation of the effects of a discontinuity at any point on the line, provided that the propagation constant  $\gamma$  is known. That is, any discontinuity can be expressed as an equivalent impedance at that place, or by Eq. (14-35) at any other place on the line.

For microwave transmission in waveguides these impedance concepts and formulas are still useful. Since there is only one conductor and since different current densities flow over the various waveguide surfaces, both voltage and current are difficult to define. Although no unique definition of impedance can be made, it is customary to define the impedance as the ratio of electric to magnetic field strengths ( $E/H$ ) at some point in the guide. It is not strictly necessary to define the characteristic impedance.  $Z_0$  can be taken as an arbitrary constant, and other impedances, such as those due to obstacles in the guide, can be expressed in terms of  $Z_0$  because Eq. (14-35) involves only ratios  $Z/Z_0$  and  $Z_1/Z_0$ . Discontinuity in the guide propagation due to a sudden change of dielectric properties is easily interpreted as a sudden change in impedance, and the reflected-wave characteristics are given by Eq. (14-34).

However, if the waveguide suddenly changes dimensions, the reflected wave is not so easily obtained since it depends on the particular geometry at the discontinuity. Near the discontinuity the fields are complicated and can be represented as a combination of higher-order propagation modes with the fundamental modes. However, if the higher-order modes cannot be propagated, a wavelength or two from the discontinuity on the incident side one finds only an incident and a reflected wave in the dominant mode. As in a transmission line, these waves can be expressed in terms of an effective impedance at the position of the discontinuity which replaces the discontinuity for the calculation of the fields in the waveguide. Near the discontinuity higher modes are present and this approach cannot be used. It makes difficulty also if two discontinuities occur within a half wavelength or so, for then the higher-order waves from one discontinuity can reach the other before being completely attenuated. If several modes can be propagated, a different discontinuity impedance and propagation constant must be given for each mode; so the concept loses much of its usefulness. Moreover, a reflection can introduce a mode which was not present in the original wave.

In many cases it is desirable to minimize reflections at the junctions of transmission lines by making the terminating impedance for the first line equal to its characteristic impedance. This may be done at low frequencies by a simple transformer involving mutual inductance between two coils. A quarter wavelength of transmission line of characteristic



impedance  $Z'$  between the two lines of characteristic impedances  $Z_0$  and  $Z_1$  can also act as a matching transformer. Thus if the junction between  $Z'$  and  $Z_1$  is at  $z = 0$  and  $Z'$  extends one-quarter wavelength in the negative  $z$  direction the impedance of the combination is, from Eq. (14-35),  $Z = (Z')^2/Z_1$ . If it is desired to make  $Z$  equal  $Z_0$  so that the transmission lines may be joined with no reflections, then  $Z' = \sqrt{Z_1 Z_0}$ . Reflection can be eliminated by a number of other types of "transformers." Generally it is necessary to have two independent variables such as, in this case, the length and characteristic impedance of the auxiliary transmission line.

In many cases another approach based on simple ideas of wave interference and diffraction can be used to investigate microwave behavior at a discontinuity. For example, the quarter-wave transformer discussed above may be viewed as setting up two reflected waves. These waves are of equal magnitude because the ratios of characteristic impedance at the two reflecting discontinuities are equal. They are just opposite in phase and hence cancel because the path length for one is one-half wavelength (two quarter wavelengths) longer than for the other. The principle is the same as that used for making nonreflecting glass, where a quarter wavelength of surface material with index of refraction intermediate between air and glass produces two canceling reflections, or "matches impedances."

In many cases it is desirable to have a transformer produce little reflection over a wide range of frequencies. The quarter-wave transformer and many other impedance matching devices depend somewhat critically on the ratio of certain distance parameters to the wavelength and hence are not useful over a very wide frequency range. However, any change in waveguide dimensions or impedance which is so gradual that only a small fractional change occurs over one wavelength affords a good transformer from one impedance to another and shows approximately the same characteristics over a wide frequency range. A gradual change of impedance such as a long taper from one dimension of waveguide to another can easily be seen to produce very little reflection of power because for any reflecting point in the taper an essentially similar reflecting point can be found one-quarter wavelength farther down the taper and the reflected waves from these two will cancel.

Still another important method of reducing reflection is by means of attenuation. Equation (14-35) shows that the impedance approaches the characteristic impedance as  $z$  decreases if there is attenuation in the transmission line. This is because any reflected wave decreases as a result of the attenuation. A short section of highly attenuating waveguide will give the same effect. Such a section is customarily inserted between a klystron oscillator and a waveguide to minimize the effect of reflected waves in the guide on the operation of the klystron.

**14-5. Cavity Resonators.** A hollow space enclosed by metallic walls can support electromagnetic waves of some particular wavelengths in modes which fit the boundary conditions. Consider, for example, a section of rectangular waveguide which is closed at both ends by flat conducting plates (Fig. 14-5). The boundary conditions at the side walls are satisfied for any  $TE_{mn}$  waves provided only that their wavelength is short enough for propagation. If the length of the waveguide is  $l$  and the wavelength in the guide is  $\lambda_g$  for a particular  $TE_{mn}$  mode, the end



FIG. 14-5. Rectangular cavity resonator.

boundary conditions require that  $E_x$  and  $E_y$  vanish at  $z = 0$  and  $z = l$ . From Eq. (14-15) this will be satisfied if  $e^{j(\omega t - \gamma l)} = \pm e^{j\omega t}$ , or  $\gamma l = \pi p$ , where  $p$  is an integer. Since  $\gamma = 2\pi/\lambda_g$ ,

$$p = \frac{2l}{\lambda_g} \quad (14-36)$$

This relation is just what would be expected for a wave of length  $\lambda_g$  which is reflected with a  $180^\circ$  change of phase at the end of the guide so that a standing wave is produced. For nodes at  $z = 0$  and  $z = l$ , the guide must contain an integral number of half wavelengths.

From Eqs. (14-36) and (14-20), the values of  $\lambda_0$  for which the cavity is resonant may be obtained.

$$l = \frac{p\lambda_g}{2} = \frac{p\lambda_0}{2 \sqrt{1 - (m\lambda_0/2a)^2 - (n\lambda_0/2b)^2}} \quad (14-37)$$

so that

$$\left(\frac{m\lambda_0}{2a}\right)^2 + \left(\frac{n\lambda_0}{2b}\right)^2 + \left(\frac{p\lambda_0}{2l}\right)^2 = 1 \quad (14-38)$$

From this relation, the wavelength  $\lambda_0$  at which the cavity is resonant may be determined if its dimensions are known.

Rectangular cavities are not much used as resonators although a section of waveguide with partial reflections at each end behaves somewhat like a resonator.

Circular cylindrical cavities are more often used because they can easily be accurately machined and are suitable for wavelength measurements. As for a rectangular cavity, the resonance condition is that the length of the cavity be an integral multiple of  $\lambda_g/2$ . For either a TE or TM mode in a circular waveguide, the free-space resonant wavelength is given by

$$\lambda_0 = \frac{2}{\sqrt{(2x_{mn}/\pi D)^2 + (p/L)^2}}$$

- where  $D$  = the diameter and  $L$  the length of the cavity
- $m$  = the number of half-period variations of  $E_r$  with respect to  $\theta$   
(of  $H_r$  for TM modes)
- $n$  = the number of half-period variations of  $E_\theta$  with respect to  $r$   
(of  $H_\theta$  for TM modes)
- $p$  = the number of half-period variations of  $E_r$  with respect to  $z$   
(of  $H_r$  for TM modes)
- $x_{mn}$  = the  $n$ th root of  $J'_m(x) = 0$  for the TE modes or of  $J_m(x) = 0$  for the TM modes; the  $J$ 's are Bessel functions

Table 14-1 gives the values of some of the roots. For modes with  $p = 0$  the field does not vary in the  $z$  direction and so the resonant wavelength does not depend on the length of the cavity, but only on its diameter. This can occur only for TM modes. For wavemeter applications, the  $TE_{01p}$  mode is commonly used.

TABLE 14-1. ROOTS OF  $J_m(x)$  AND  $J'_m(x)$

TE mode	$x_{mn}$	TM mode	$x_{mn}$
11p	1.841	01p	2.405
21p	3.054	11p	3.832
01p	3.832	21p	5.136
31p	4.201	02p	5.520
41p	5.318	31p	6.380
12p	5.332	12p	7.016

A useful figure of merit for a resonator is the  $Q$ , defined as

$$Q = 2\pi \frac{\text{electromagnetic energy}}{\text{energy lost per cycle}} = -2\pi W \frac{\nu}{dW} \tag{14-39}$$

From this definition it follows that the energy in a freely oscillating resonator decays according to the equation

$$W = W_0 e^{-\omega t/Q} \tag{14-40}$$

where  $W$  is the energy remaining after time  $t$  and  $W_0$  is the initial energy at  $t = 0$ .  $Q$  is also a measure of the sharpness of resonance, for the width in frequency  $\Delta\nu$  of the resonance curve between points at which the response is one-half that at maximum is

$$\frac{\Delta\nu}{\nu_0} = \frac{1}{Q} \tag{14-41}$$

where  $\nu_0$  is the resonant frequency (cf. [121], p. 137).

$Q$  may be calculated from Eq. (14-39) by a procedure resembling that used to calculate attenuation (cf. [486], pp. 73-77). For instance, for a rectangular box with  $l = a$ , for the  $TE_{101}$  mode ( $E$  parallel to the  $b$



dimension)

$$Q = 0.71 \frac{\lambda_0}{\delta} \frac{b}{a + 2b} \quad (14-42)$$

where  $\delta$  is the skin depth and  $\lambda_0$  the wavelength. Since for copper  $\delta = 3.8 \times 10^{-5} \sqrt{\lambda_0}$  when  $\delta$  and  $\lambda_0$  are in centimeters, a cubic resonator in this mode at  $\lambda = 1$  cm would have a  $Q$  value of 6200. This  $Q$  is much higher than those obtainable with coils and condensers at frequencies where the latter are appropriate, but still higher  $Q$ 's can be obtained with other shapes or larger dimensions ([221], Chaps. 5 and 6). In general the  $Q$  is roughly proportional to the volume divided by the surface area because stored energy depends on the volume while losses occur only at the walls. An exceptional case is the  $TE_{01p}$  mode of a circular cylinder at high frequencies. For this mode the side-wall losses decrease continuously with increasing frequency, and it may be used to obtain very high  $Q$ 's.

**14-6. Coupling of Cavities to Waveguide.** In practice a cavity must be coupled to a microwave system. Then, in addition to the losses at the walls, there will be some energy delivered from the cavity to the system, so that the energy loss is greater, and the  $Q$  less, than for a completely enclosed cavity. As before,  $Q_E = 2\pi \times (\text{electromagnetic energy in the cavity})/(\text{energy lost per cycle})$ , where the denominator is the total energy lost and the subscript  $E$  denotes the "external"  $Q$  with a coupling connection. This may be expressed in terms of the "internal" unloaded  $Q_U$ , involving only wall losses, and the "radiation"  $Q_R$  involving only losses from the cavity to the external circuit, for

$$\frac{1}{Q_E} = \frac{1}{Q_U} + \frac{1}{Q_R} \quad (14-43)$$

The resonant frequency of the cavity may also be affected by the connection to the microwave circuit if the latter is reactive. However, the coupling is often not large enough to affect greatly either the  $Q$  or the resonant frequency ([221], Chap. 5), although in some applications these effects must be considered.

Coupling to a cavity is usually accomplished by one or two holes in the cavity wall. At lower frequencies (3000 Mc or less), coupling loops entering through a suitable hole provide a direct connection to a coaxial line. Usually the coupling is designed to excite preferentially some particular mode by making the electric or magnetic lines of force at the coupling region coincide with those of the desired mode. For instance, the  $TE_{01p}$  mode in a cylindrical cavity may be excited by two diametrically opposite holes in the end wall [178]. These holes coincide with holes in the narrow face of the waveguide approximately  $\lambda_g/2$  apart. The only field existing at the narrow edge of a waveguide carrying the dominant mode is a longitudinal magnetic field. Through the coupling holes

this field is transmitted to the cavity with opposite phases for the two holes, and so matches the  $TE_{01p}$  mode, but not other possible modes except the  $TE_{02p}$  mode. The latter may be avoided in a transmission-type resonator by taking the output from a coupling hole in the curved wall of the cylinder at a  $45^\circ$  angle to the input holes. Then an output is obtained only if the cavity is at or very near resonance for the desired mode.

The  $TE_{01p}$  mode has the advantage for wavemeter applications of a high  $Q$ , so that resonances are sharp. Moreover, there are no radial currents at the edges of the end plates, so that the latter need not make good contact with the walls. This is particularly useful in wavemeters where one end plate must be movable for tuning.

Another mode which is often used for wavemeters is the  $TE_{11p}$  mode. This is the lowest-frequency mode for a given cavity, and so the diameter of the cavity may be chosen to permit only this mode over an appreciable band of wavelengths (around 25 per cent—*cf.* Table 14-1). However, this mode is polarized in that it has a plane of symmetry containing the axis of the cylinder (*cf.* Fig. 14-3) and can be resolved into similar modes in any pair of perpendicular directions. If the cylinder is slightly elliptical, these modes have different propagation constants and so give slightly different resonant frequencies. A horseshoe-shaped strap across the coupling hole perpendicular to the electric vector in the waveguide produces a large effective eccentricity so that these resonances are far apart and cross coupling is prevented. Only the mode with polarization parallel to the electric vector in the waveguide is excited.

Good effective contact between the walls and the plunger is obtained by a quarter-wave "choke." That is, the plunger is one-half wavelength long, and in the back is cut a groove one-quarter wavelength deep. The wavelength involved here is the free-space wavelength since either in the groove or in the space between the plunger and the walls waves travel in the coaxial  $TE_{11}$  mode for which  $\lambda_g$  is very close to  $\lambda$ . The effect of the groove is to produce a high impedance at the edge of the plunger for waves flowing toward the back of the plunger and so to confine the radiation to the region in front of the plunger. Any radiation which does reach the region behind the plunger and might cause spurious resonances is further reduced by some suitable absorbing material such as "poly-iron" ([221], p. 723).

Resonant cavities may be used as either transmission or reaction wavemeters. For use as a transmission-type wavemeter, the cavity of Fig. 14-6 is modified to use two coupling holes, diametrically opposed on the curved wall  $\lambda_g/4$  from the base. Then the transmission is almost zero until near resonance it rises to a large value. A typical wavemeter might transmit 25 per cent of the incident power at resonance.

Alternatively, the wavemeter may be coupled to a hole in the side



of the waveguide. At the end of the waveguide is a crystal detector which matches the waveguide well enough to absorb most of the power reaching it. In the guide directly opposite the wavemeter is a post or "iris" diaphragm which is designed to cancel out as nearly as possible the reflections produced by the wavemeter when not in resonance. At resonance the wavemeter absorbs some power and reflects more, so that the power reaching the detector is reduced. Sometimes the detector is also coupled to the side of the waveguide before the wavemeter and detects a change in the reflected power. Depending on the relative phases of the wavemeter reflection and other reflections in the system, the crystal current may either increase or decrease at resonance. In either

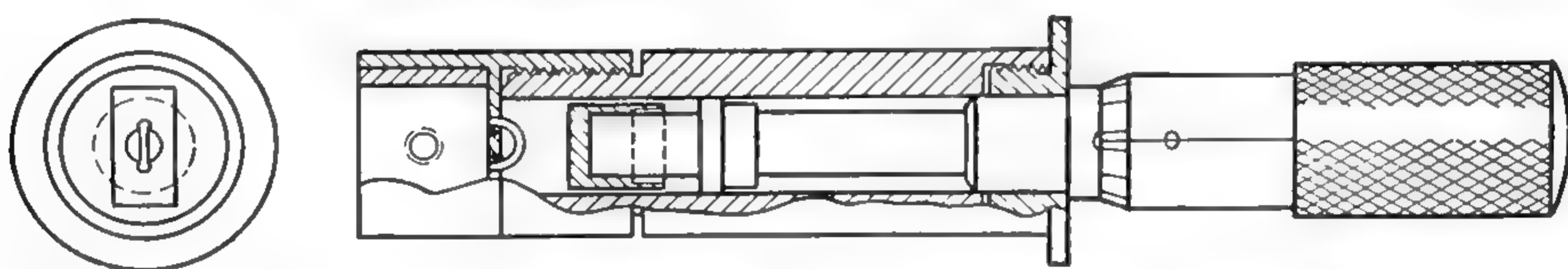


FIG. 14-6. A typical wavemeter for the 1.25-cm region (MIT Radiation Laboratory type TFK-2). Barrel diameter (inside) =  $0.3750 \pm 0.0002$  in. Coupling hole diameter = 0.111 in.

case the detector used with a reaction wavemeter may also be used to monitor the output of the microwave oscillator, for a signal is obtained as long as the wavemeter is not at resonance.

A loaded  $Q$  of the order of 3500 may be expected from a wavemeter in the 1-cm region, such as that shown in Fig. 14-6. As the plunger is moved by the micrometer screw two or three resonances separated by  $\lambda_g/2$  are reached, and from  $\lambda_g$  the wavelength  $\lambda$  is readily calculated. In practice, if many wavelength readings are to be made, a conversion table from  $\lambda_g$  to wavelength or frequency is worth the trouble required to make it.

**14-7. Directional Couplers.** It is often desirable to monitor the power delivered by a microwave generator to a waveguide system. For this purpose a directional coupler is very useful, for it permits a sampling of the power from the oscillator without any of the reflected waves from the system reaching the monitor detector.

The easiest type of directional coupler to understand is analogous to directional antennas. Two holes approximately  $\lambda_g/4$  apart are cut in the narrow edge of a waveguide which is to carry waves in the dominant mode. The holes match similar holes in the narrow edge of another waveguide (Fig. 14-7). Then a wave traveling from left to right in waveguide (1) will reach hole  $B$  one-quarter of a period later than hole  $A$ . A wave in the same direction starting at the same time and passing through hole  $A$  will reach hole  $B$  at the same time and the two will reinforce to produce a combined wave in waveguide (2) in the same direction.



On the other hand, a wave going through (1) to hole  $B$  and then back to  $A$  will arrive at  $A$  one-half wavelength behind a wave which passes directly through  $A$  and so be canceled by the wave from  $A$ . Thus a wave traveling from left to right in waveguide (1) will produce only a wave in the same direction in waveguide (2). A reflected wave traveling from right to left in (1) will produce only a wave traveling from right to left in (2), which will be absorbed by a suitable termination of the left end of (2). A wedge-shaped strip of lossy dielectric can be made to absorb this wave without serious reflection.

A detector at the right end of (2) then receives only waves from the oscillator, and none of the reflected power. It is thus suitable for monitoring the oscillator output power. A cavity wavemeter connected at

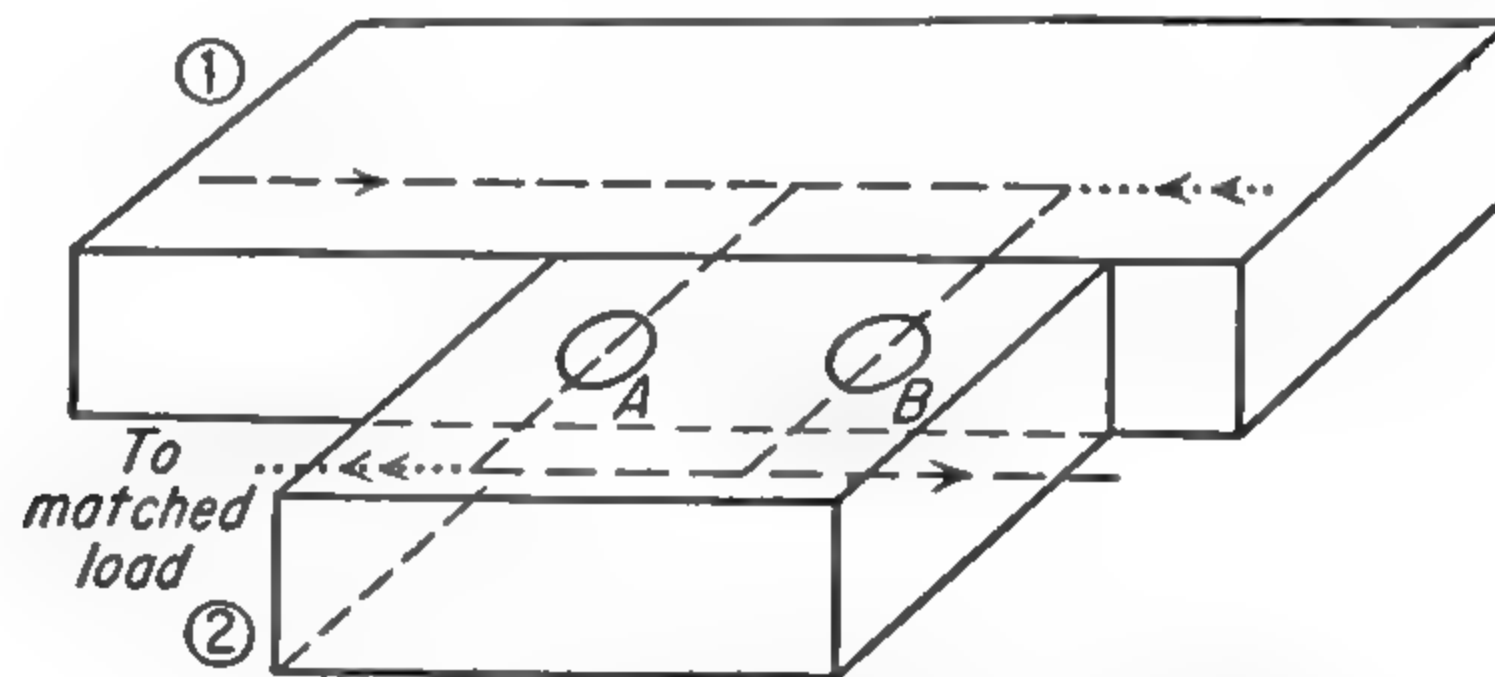


FIG. 14-7. Two-hole directional coupler.

this point is assured of a reliable power input regardless of reflections and in turn causes a minimum disturbance to the rest of the microwave circuit. For wavemeter connection a directional coupler which transmits from 1 to 10 per cent of the incident power into (2) is useful ("a 20-db" or "a 10-db" coupler).

Other types of directional couplers have been used which are merely variants of that described. For instance, the coupling holes may be in the broad face of the waveguide as long as they are far enough from the center line or wide enough to provide sufficient radiation. It should be mentioned that for either type the holes are usually large enough so that they cannot be treated exactly as points, and so their optimum spacing may not be exactly  $\lambda_g/4$ . In any case the spacing is not excessively critical so that the coupler is useful over a considerable wavelength band. However, better directivity (forward wave to back wave amplitude ratio) over a wide wavelength band can be obtained by using more than two coupling holes, with neighboring holes  $\lambda_g/4$  apart [222]. The diameters of the holes are chosen so that  $\alpha_r$ , the amplitude of the wave originating at the  $r$ th hole, is given by

$$\alpha_r = \alpha_0 \frac{n!}{r!(n-r)!} \quad (14-44)$$

where  $n + 1$  is the number of holes. That is, the amplitudes are pro-

portional to the binomial-expansion coefficients. Then the amplitude of the reflected wave is proportional to  $\cos^n (2\pi d/\lambda_0)$ , where  $d$  is the distance between successive holes. The reflected wave is zero for  $\lambda_0 = 4d$  regardless of the number of holes, but the larger  $n$  is, the more slowly the reflected wave increases when  $\lambda_0$  deviates from  $4d$ . Many other varieties of directional coupler have been used, and several are described in [221], Chap. 14.

Another waveguide device related to the directional coupler is the "magic T" shown in Fig. 14-8. Its operation may be understood from the fact that the plane bisecting arms  $C$  and  $D$  is a plane of symmetry.

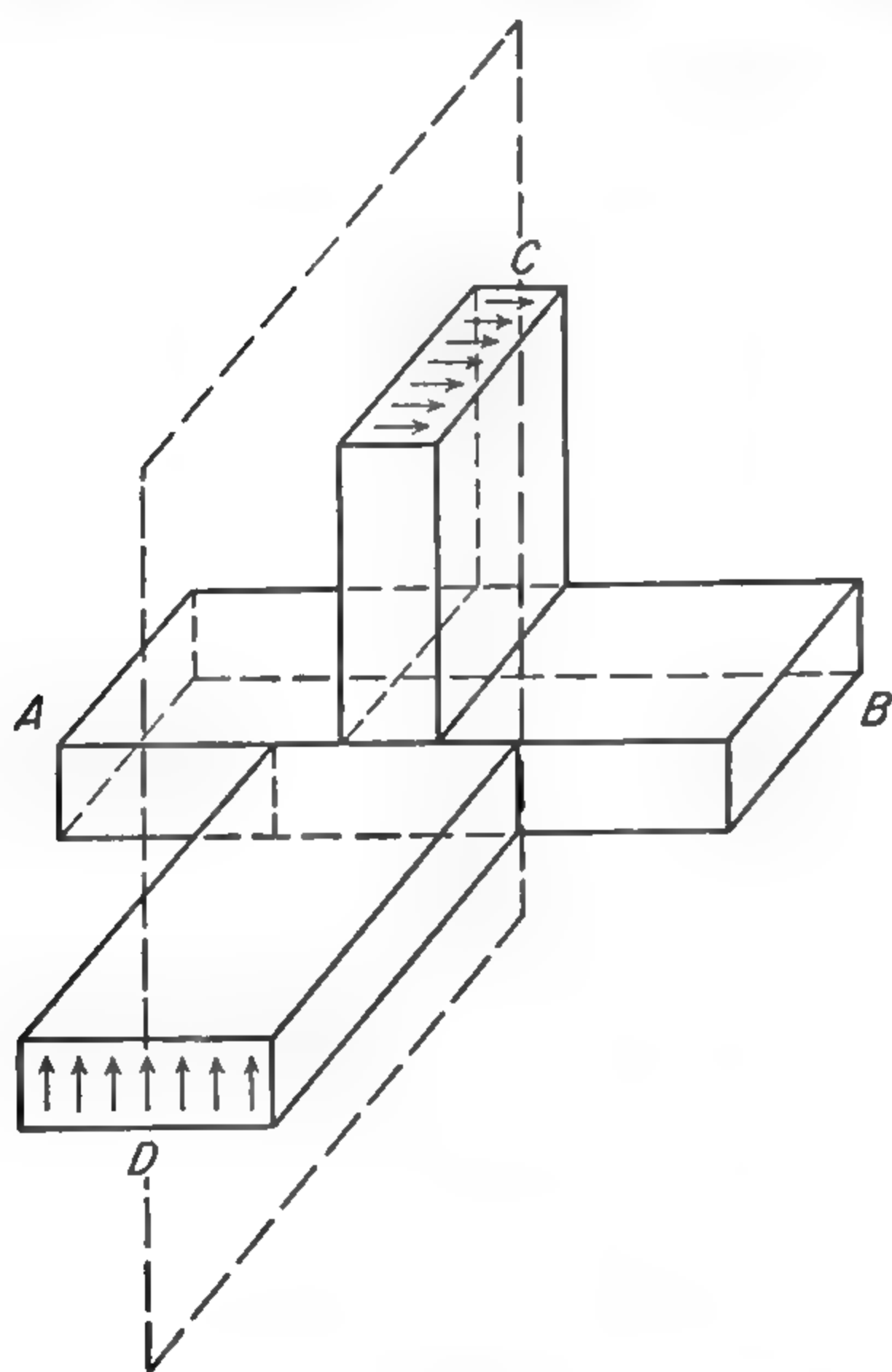


FIG. 14-8. Waveguide "magic T."

Thus a wave entering through branch  $D$  in the principal mode has its electric vector symmetric about that plane. However, a wave which can be propagated in  $C$  must have an electric vector which is antisymmetric with regard to the symmetry plane. Thus a wave entering from either  $C$  or  $D$  will excite waves in  $A$  and  $B$ , either symmetrically or antisymmetrically, but waves will not pass directly from  $C$  to  $D$ . Similarly waves from  $A$  or  $B$  can excite waves in  $C$  or  $D$ , but the amplitude in  $C$  will be proportional to the difference, and in  $D$  to the sum, of the amplitudes of the waves entering through  $C$  and  $D$ .

In a typical application as a directional coupler, the wave from the oscillator enters through  $A$ , and the waveguide system is connected to  $C$ .  $D$  has a power-monitoring crystal de-

detector or wavemeter, and  $B$  has a matched load such as a tapered lossy plastic strip designed to prevent reflections. Power is then transmitted to  $C$  and  $D$ , but reflected power from  $C$  cannot enter  $D$ . A monitor in  $D$  measures only the power delivered by the oscillator to the load, regardless of reflections.

Another important application of the magic T is to balanced systems analogous to bridge circuits in ordinary electrical measurements. Use is made of the fact that arm  $C$  gives a signal depending on the difference of the signals in  $A$  and  $B$ . It can then be used to show departures from balance in arms  $A$  and  $B$ .

To prevent reflections by the magic T itself, it is usually necessary to match it to the waveguides by "irises" or diaphragms in the waveguide



positioned so as to reflect a wave of phase opposite to, and amplitude equal to, the reflection from the magic T.

**14-8. Attenuators.** Most waveguide systems contain at least one attenuator. Sometimes an attenuator is used to reduce power input to the system, *e.g.*, to prevent power saturation in a spectroscopy absorption cell. Equally often, the attenuator is inserted principally to prevent reflections in the waveguide system from reaching the oscillator and affecting its operation.

It is always desirable, and sometimes very important, that standing waves be kept low to avoid variations in power at the detector as the frequency is varied. Attenuation in the system helps to reduce standing waves since reflected waves must pass an attenuator twice in each back-and-forth trip through the waveguide.

Most commonly attenuation is obtained by inserting a strip of lossy material such as bakelite coated with carbon (with surface resistance of a few hundred ohms per square) into the guide through a longitudinal slit in the center of the broad face. The strip is a few wavelengths long and is tapered to prevent reflections from the ends. Often it is pivoted at one end, and the attenuation is controlled by lowering the other end into the guide (see Fig. 14-9).

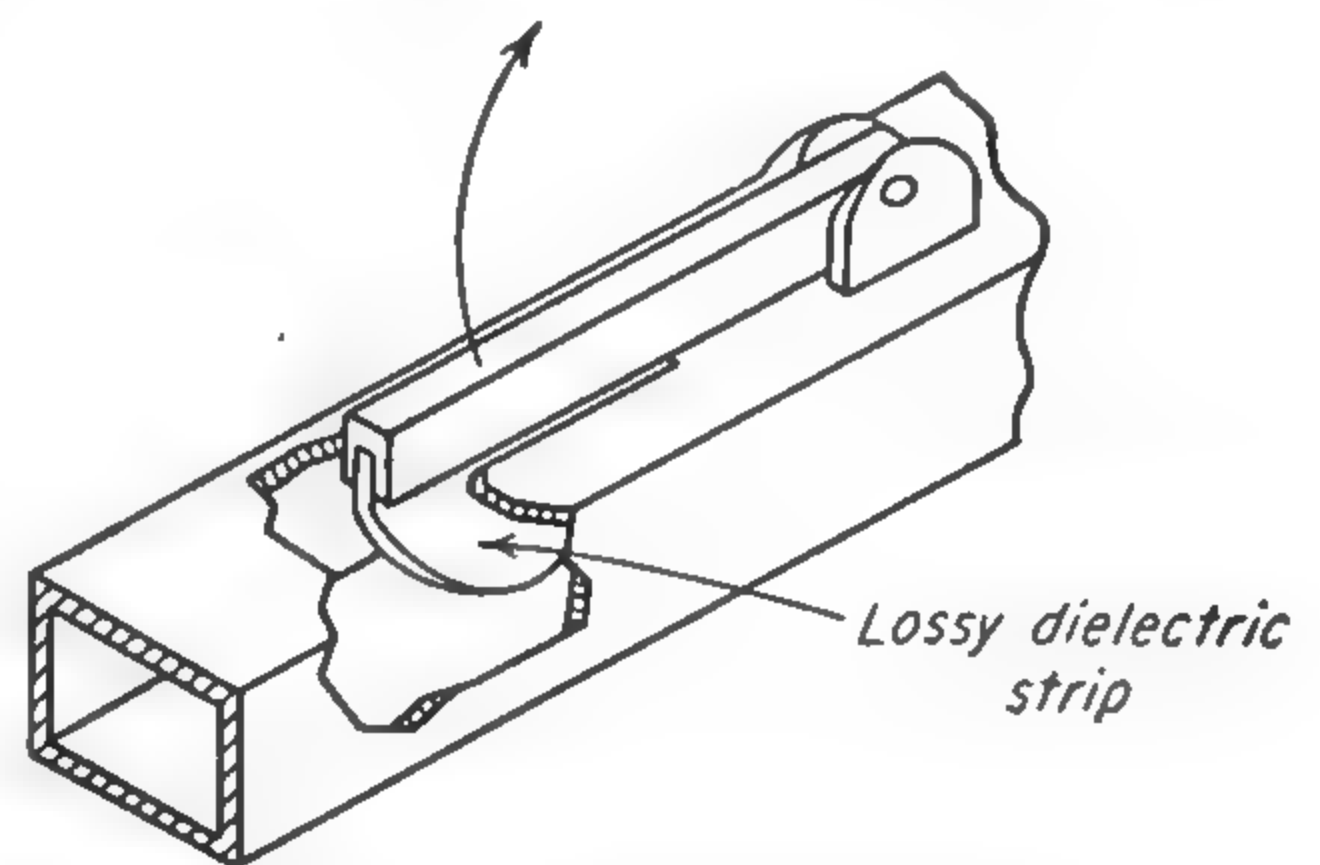


FIG. 14-9. Waveguide attenuator.

A fixed attenuator can be constructed in many ways. One of the simplest is to attach a strip of lossy dielectric to the narrow wall of the waveguide. In order that the attenuator will not itself introduce reflections its ends should be tapered. With carefully made attenuators of this type, it is possible to reduce the variation in transmitted power due to reflections to as low as about 1 per cent.

When the attenuation must be known absolutely, a short section of waveguide which is too small to propagate the wavelength produced by the oscillator may be used. The attenuation can then be calculated from the dimensions of the guide and the free-space wavelength (*cf.* page 385).

**14-9. Joints in Waveguide Systems.** Waveguide sections and devices are commonly joined by attaching suitable flanges and bolting them together. The flanges need only be large enough so that they can be conveniently bolted, but they must be soldered carefully flush with the ends of the waveguide. Especially if the guide is to transmit wavelengths short enough so that higher modes could be propagated, it is important to obtain good alignment of the two guides and locating pins may be provided for this purpose.



In a flat-flange joint, the longitudinal current components are carried by the capacitance between the flanges even if the contact between them is poor. However, there is a small voltage drop across the joint, and if the guide is to carry high power, as from a magnetron, arcing may occur at the joint, or there may be a small leakage of power. For these applications "choke" flanges are useful. A choke-flange joint is shown in Fig. 14-10. It differs from a flat-flange joint in that a groove  $\lambda/4$  deep is cut in one flange. The inner and outer walls of this groove act as conductors of a quarter-wave coaxial line, short-circuited at one end and

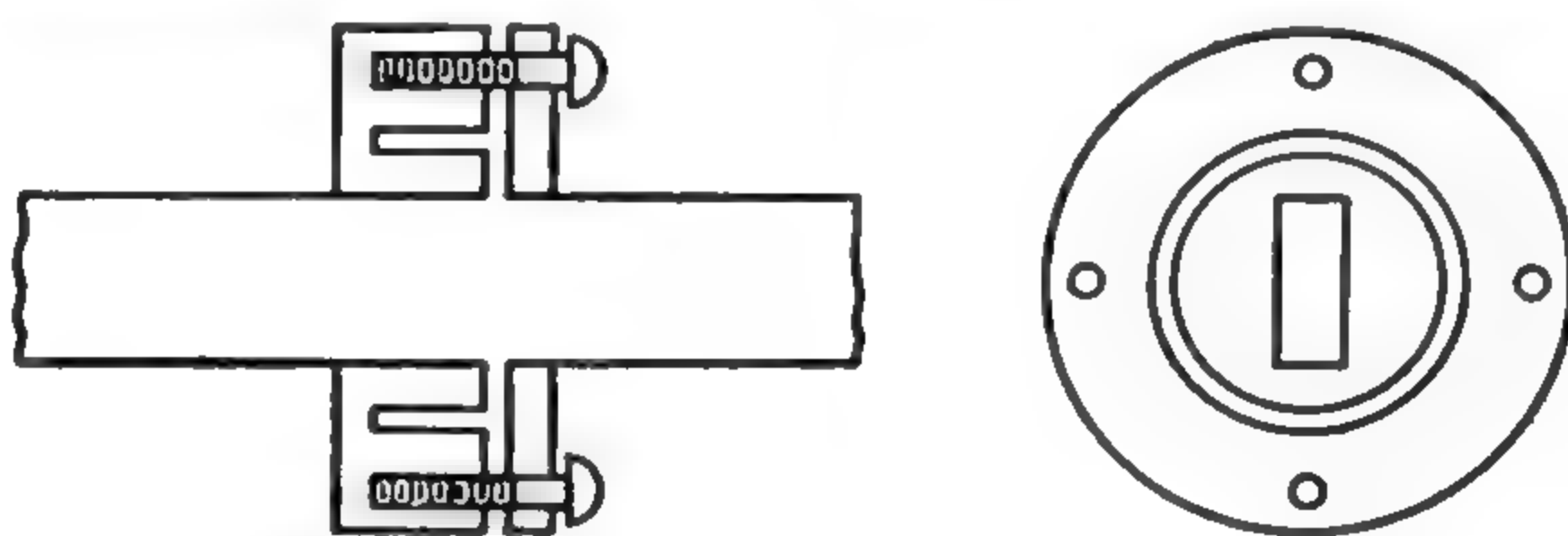


FIG. 14-10. Choke-flange waveguide joint.

thus having a very large impedance at the open end. This large impedance makes difficult a radial flow of power between the flanges. If, moreover, the distance from the groove to the waveguide is roughly another quarter wavelength, then the impedance at the waveguide wall is very small. This permits the wall currents to flow without large potential drops.

Since the dimensions of a choke flange depend on the wavelength, it is frequency-sensitive and so not well suited to equipment required to operate over large frequency ranges.

If leakage from flanges must be minimized, the completed joint may be wrapped in steel wool. If this is not done, waves radiated from the joint may be reflected from objects in the room and reenter the waveguide to cause a small change in the signal which varies as people move in the room. This precaution is usually needed only for spectrographs which do not employ modulation because they are sensitive to any change in microwave power at the detector, no matter how slowly the change occurs.

**14-10. Waveguide Windows.** It is often necessary to confine a gas to one section of a waveguide system. Windows for this purpose must be vacuumtight and yet reflect or absorb very little microwave power. A suitable window may be constructed of 0.001-in.-thick mica sheet sealed by a flat gasket stamped from rubber or polyethylene sheet a few mils thick and sandwiched between flat flanges. "Dental-dam" rubber obtained from dental supply houses is suitable for gaskets. A light coating of stopcock grease is used on the gasket.

For higher-temperature operation or for spectroscopy on certain reactive compounds, the rubber gaskets may be replaced by solder, lead, or

gold, and thin quartz windows have been used. A design for mica windows with lead gaskets has been described [637]. If the flanges are made sufficiently sturdy and the area of contact with the mica sufficiently small so that considerable pressure can be applied to the mica window, a good vacuum seal can be obtained without the use of a gasket. Mica windows may also be sealed permanently to metals. Such windows have been used in klystron tubes and might be applied to spectroscopy.

**14-11. Plungers.** Often, as in a cavity wavemeter or in a matching section, a waveguide must be terminated by a movable short-circuiting plunger. If the mode is such that currents flow across the gap between the plunger and the walls, care must be taken to provide a dependable low-impedance path for them. Sometimes, particularly at lower microwave frequencies, spring contacting fingers are sufficient. A good effective contact may be obtained by using the principle of the choke flange,

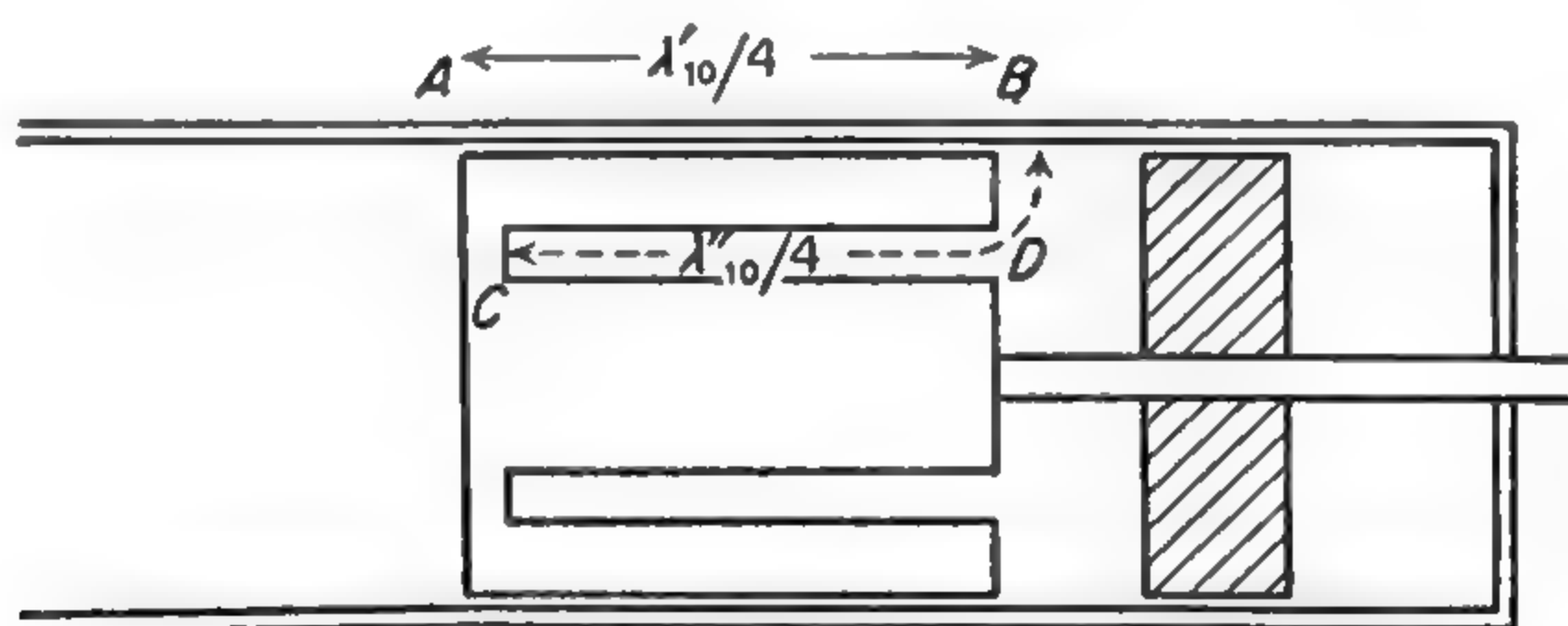


FIG. 14-11. Waveguide choke plunger.

as in Fig. 14-11, which shows a type of plunger often used in wavemeters. The inner and outer walls of the slot  $CD$  act as the conductors of a quarter-wave coaxial line short-circuited at  $C$ . Thus at  $D$  there is a high impedance which is transformed by the quarter-wave section  $BA$  to give a very low effective impedance at  $A$ . The lengths  $\lambda'_{10}$  and  $\lambda''_{10}$  are not free-space wavelengths and are not equal because the coaxial lines involved are not excited in the principal mode but in the  $TE_{10}$  mode for the appropriate coaxial waveguide ([312], Chap. 8). This type of device is of course designed for a particular wavelength but is fairly satisfactory over a wavelength range of 5 to 10 per cent.

**14-12. Other Types of Guided Waves.** It is possible to confine microwave radiation to a restricted region without requiring that region to be part of a hollow-tube waveguide. For instance, a horn radiator can be used to beam radiation toward a similarly directional receiving horn. A glass or quartz absorption cell between the horns could have the advantage of bringing no metal in contact with the sample, which would be helpful for corrosive materials.

If the radiation from the horns is polarized, thin metal plates can be placed in the path of the beam with their planes perpendicular to the electric vector without disturbing the fields. A low-frequency electric field can then be applied between the plates for Stark modulation.



When the horns are arranged to confine the radiation to the space between the plates, the plates constitute a parallel-plate waveguide. Alternatively the ordinary rectangular waveguide in the dominant mode may be imagined to have its width increased indefinitely. The electric field remains perpendicular to the broad faces and has a maximum value in the center, decreasing toward the now distant walls. If the extreme edges are then cut off at a point where the field is sufficiently small, the remaining portion behaves very much as the infinite-parallel-plate guide. The coupling horns serve to direct the waves from ordinary waveguides to the central region of the flat plate guide.

The use of parallel-plate waveguides for microwave spectroscopy has been suggested by Gordy [278] and investigated by Baird, Fristrom, and Sirvetz [430]. It has the advantage that small spacings can be used, and a large uniform d-c field can be applied between the plates. Moreover, the insulating spacers may be kept entirely outside the region occupied by the microwave energy so that their dielectric-loss properties are unimportant. For this reason, parallel-plate waveguides would appear to be

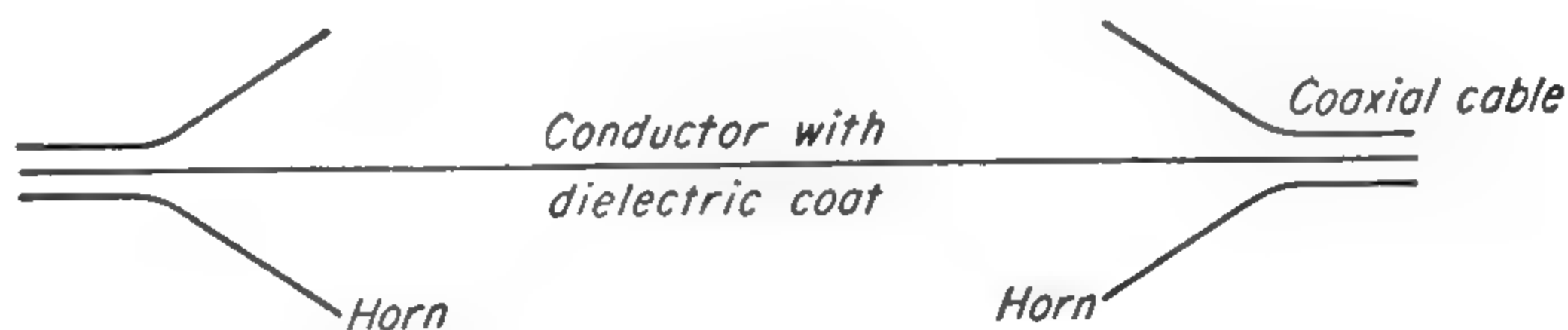


FIG. 14-12. Surface wave transmission line.

useful for operation at high temperatures where the insulators used to support Stark-effect electrodes inside ordinary waveguides give trouble. However, unless very large horns are used, the radiation tends to spread and produce rather bad frequency-sensitive reflections from obstacles outside the absorption cell.

Some of the advantages of the free-space waveguide cell, without the need for extremely large horns to provide high directivity, might be gained by using a single-conductor surface wave transmission line [575a]. This consists of a single wire with a thin coating of dielectric. The wave is launched and received by coaxial cables having their outer conductors flared to form horns (Fig. 14-12).

**14-13. Microwave Applications of Ferrites.** The name "ferrite" is applied to a group of materials which have high magnetic permeability and low electrical conductivity. Because of their low conductivity, microwaves can propagate through them without excessive loss. When a magnetic field is applied to a ferrite, the unpaired electron spins, which produce the high permeability, precess. A broad resonance of this precession is obtained at microwave frequencies in fields of a few thousand oersteds.

For fields lower than that needed to give resonance, a large Faraday



rotation of the plane of polarization is obtained. Figure 14-13 shows one way in which this rotation can be applied to provide variable attenuation.

The incoming wave is plane-polarized, and in a circular waveguide section the ferrite rotates the plane of polarization. If the plane of polarization is rotated  $45^\circ$  in one direction, the wave is transmitted by the output waveguide, but if it is rotated  $45^\circ$  in the opposite direction, the output waveguide cannot transmit it. Thus a control over the amplitude of the transmitted wave is obtained by varying the current in the solenoid and with it the degree of rotation.

If the magnetic field is adjusted to give  $45^\circ$  rotation for maximum transmission, then a reflected wave coming in the opposite direction is rotated a further  $45^\circ$  in the same sense. Thus the reflected wave emerges with its plane of polarization perpendicular to the short face of the input waveguide and so is not transmitted. The device therefore is a one-way

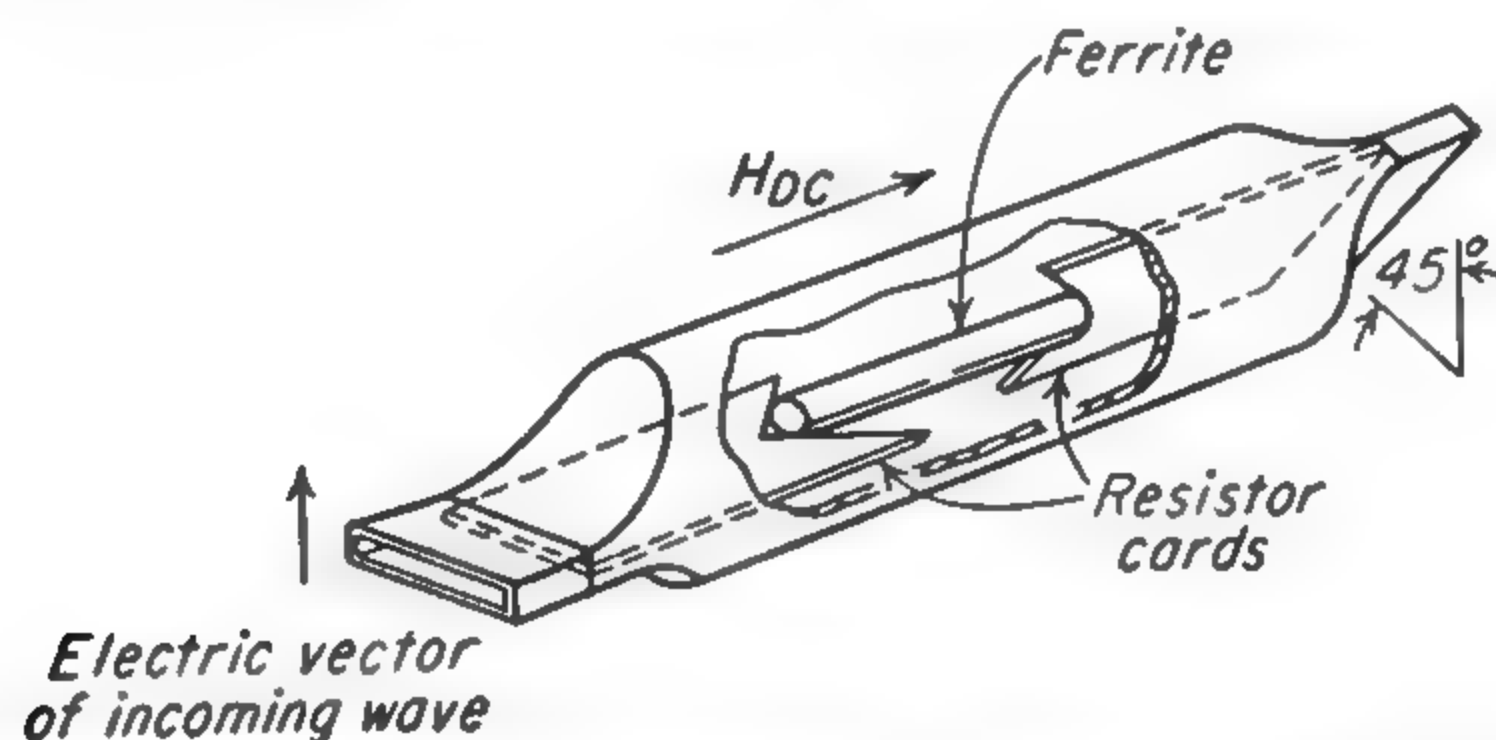


FIG. 14-13. A variable attenuator and one-way transmission device (isolator) using a ferrite. (After Rowen [860].)

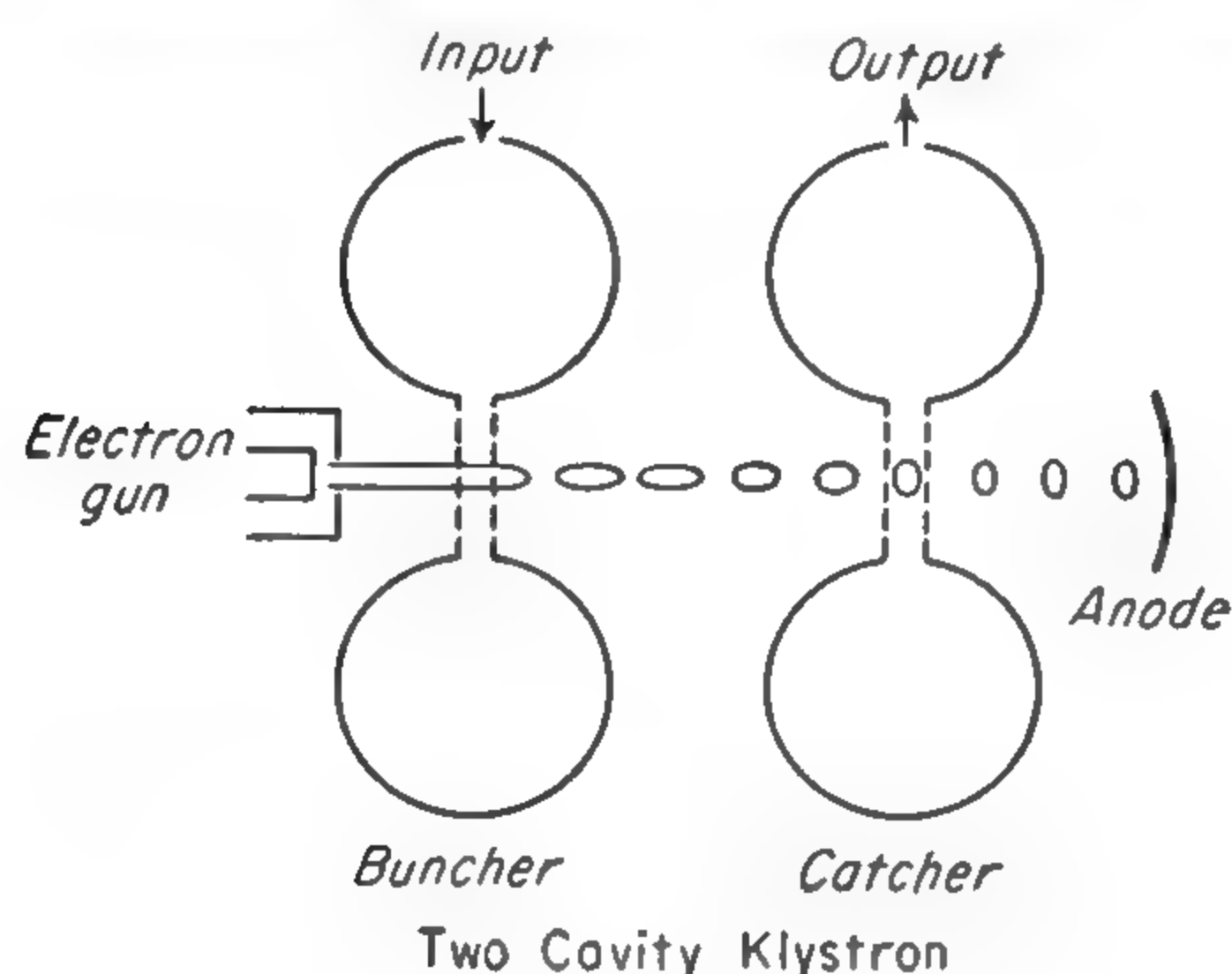
transmitter and can be used, for instance, to isolate a klystron from a long waveguide section in which reflections can occur.

Other useful devices employing ferrites can be constructed and some of them will undoubtedly find applications in microwave spectroscopy [696a], [860].

**14-14. Microwave Generators.** More than any other one thing work in the microwave region is characterized by the electronic sources used for microwave generation. Heat sources used in the infrared region hardly produce usable amounts of energy for wavelengths beyond  $\frac{1}{2}$  mm. The typical microwave sources provide milliwatts of power in a frequency band less than 1 Mc and sometimes less than  $\frac{1}{100}$  Mc. The temperature required of a hot body to produce a similar radiation would be approximately  $10^{14}^\circ\text{C}$ .

Electronic generators have the advantage over heat sources that their radiation is entirely confined to a small portion of the spectrum. Hence even a small amount of power from an electronic generator may represent a very high effective temperature and be easily detectable. Moreover, this nearly monochromatic radiation makes possible the study of absorption spectra by tuning the source rather than by making a selection from the radiation of a broad source, as by a prism or grating.

However, microwaves lie just in the region of the high-frequency limit for satisfactory operation of a normal electronic tube. This is because the electrons take a time which is an appreciable part of a cycle to pass between the electrodes. At microwave frequencies the field may actually alternate many times during the electron transit time unless the electrode spacing is extremely small. The time average of the field acting on the electron is then zero regardless of the field strength. Thus the grid in a



conventional triode cannot control at a microwave frequency the flow of the electrons through the tube. Triodes have been made to operate at 10,000 Mc by the use of extremely small grid-to-cathode spacing (less than the thickness of the oxide coating on most cathodes). However, with such close spacing interelectrode capacitance is a serious difficulty.

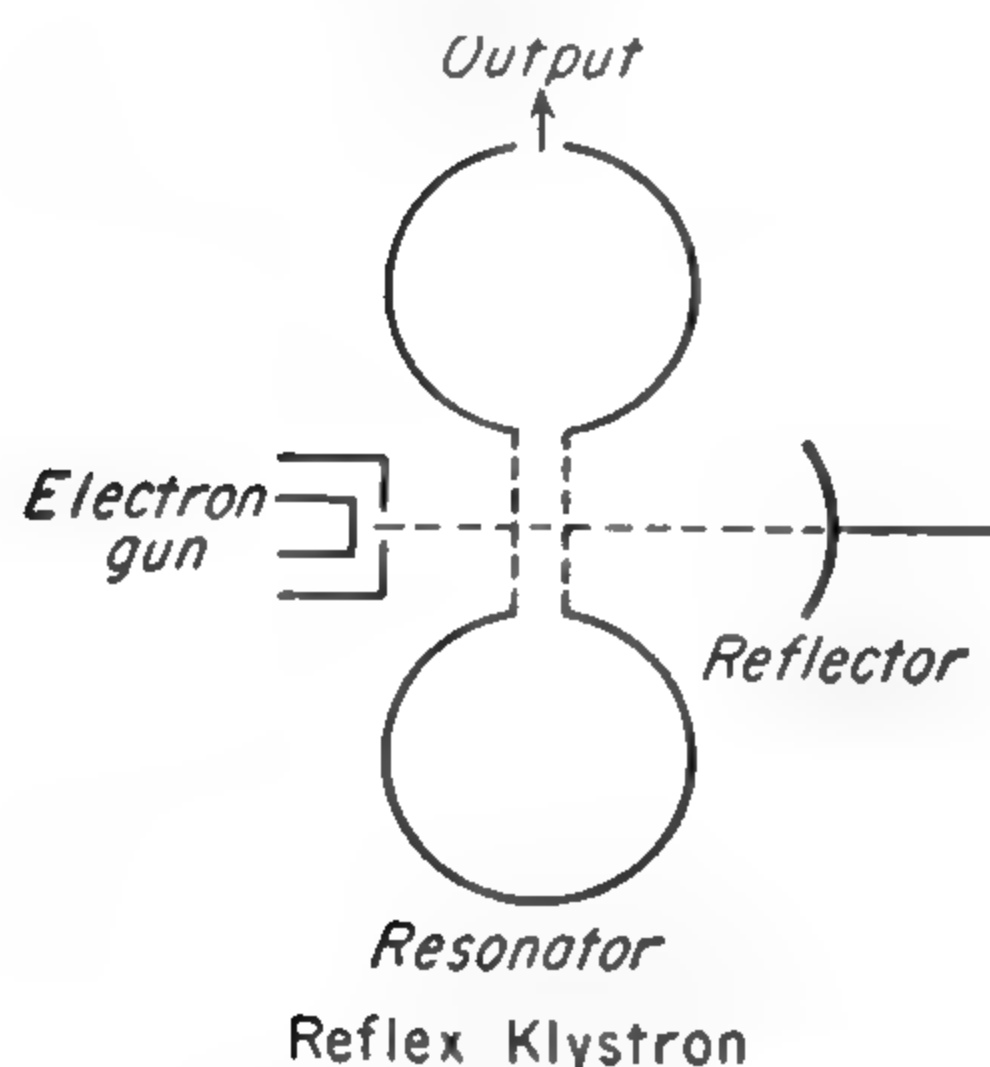


FIG. 14-14. Klystron oscillators.

of the radio-frequency cycle they traverse. After a distance of some millimeters the fast electrons have caught up with the slower ones ahead and maximum bunching occurs. It is at this point that the second resonator is placed, for farther along the beam the accelerated electrons have passed the slow ones and the electrons are again debunched. The two-cavity and reflex klystrons are illustrated in Fig. 14-14.

If some of the radio-frequency energy from the second resonator is fed back to the buncher resonator in the right phase, as by a coaxial transmission line of suitable length, the klystron becomes an oscillator. The frequency of oscillation is determined primarily by the size of the cavities, *i.e.*, by their resonant frequency. It can also be influenced slightly by changing the electron velocity, but if the frequency is changed too much

**14-15. Klystrons.** Most microwave generators allow for and make use of the electron transit time. The klystron [281] has two resonant cavities through which an electron beam passes. A radio-frequency field in the first cavity bunches the electrons into groups which pass through the second cavity and induce radio-frequency fields in it. More exactly, the first cavity accelerates some electrons slightly and decelerates others, depending on what portion



from the center of the cavity resonance by changing the electron velocity, oscillations are not maintained.

The second cavity may be eliminated and the klystron considerably simplified if the electron beam is reversed by a suitable reflector electrode, negatively charged. After reflection, the beam retraverses the cavity, delivering to it more energy than originally received from the cavity if the beam velocity and reflector distance are right.

"Reflex" klystrons of this type have been by far the most commonly used microwave oscillators for spectroscopy. They are available commercially for almost all frequencies from below 3000 Mc to about 60,000 Mc (Sperry Gyroscope Co., Great Neck, N.Y.; Raytheon Manufacturing Co., Waltham, Mass.; Varian Brothers, San Carlos, Calif.). Individual types of reflex klystrons require accelerating voltages in the range from 300 to 3000 volts. The reflector is operated at a negative voltage which is usually between zero and 300 volts. It is necessary to stabilize the power supplies, and this is especially true for the reflector voltage. Most general spectroscopic work requires a stability such that possible short period changes in voltage (such as ripple from the alternating current which has not been perfectly filtered after rectification) can cause a frequency change not greater than  $\frac{1}{50}$  Mc. This means that for the type 2K33 the accelerating voltage must be held within 0.1 volt and the reflector voltage within 0.01 volt. In addition, for this type of stability it is often helpful to operate the klystron cathode heater on direct current either from batteries or from a rectifier. Typical klystron power supplies suitable for general-purpose microwave spectroscopy use a series regulator tube controlled by reference to a voltage-regulator tube with a single stage of amplification ([221], Sec. 2-13, and [519]). An additional stage of d-c amplification in the control circuit may be needed for higher stability, particularly with 2K50 tubes.

The 2K33 family of tubes (Raytheon) has been most widely used because tubes are available for the entire wavelength region from 18,000 to 60,000 Mc with the same wiring connections and similar power requirements for all the members of the group. They have a variety of type numbers and each type covers a frequency range of only about 10 per cent. The tubes are reflex klystrons with a cavity partly inside and partly outside the vacuum. The cavity involves a bellows arrangement so that it can be compressed and thereby tuned. While the nominal range of the type 2K33 is 22,000 to 25,000 Mc, individual models sometimes may be found to oscillate anywhere in the range from 18,000 to 28,000 Mc. If a tube is not on hand for a particular desired frequency, it is possible to extend the range of another tube by loosening the locking screws which limit the range of the cavity adjustment (*cf.* [519]). Too large a change of this type may, however, damage the tube.

Another useful klystron type for the same region as the 2K33 is the



2K50. This is a smaller tube mechanically and somewhat more difficult to build. However, the completed tube is very convenient to use and requires only 300 volts on the accelerator and  $-150$  volts on the reflector. Tuning is accomplished by changing the size of cavity thermally. One of the cavity supports is made the anode of an auxiliary triode. When this triode plate current is increased, this support is heated by electron bombardment and expands enough to tune the klystron cavity. The tube may be tuned in 2 or 3 sec over about 2000 Mc by changing the tuner grid current. The tuner grid has a sensitivity of about 120 Mc/volt [225] so that its voltage must be accurately regulated. This is not very difficult in practice, because the voltage is low and little current is drawn. Batteries may be used if a suitable power supply is not available. Moreover the tuner response is slow enough that the effect of power-supply ripple is greatly reduced. The 2K50 reflector regulation requirements are similar to those for the 2K33 family. This tube is now being manufactured by Bendix Red Bank, Eatontown, N.J.

The Varian klystrons (*e.g.*, types X-12 and X-13) are available only for frequencies below 20,000 Mc. However, they give somewhat more power than the preceding types and are therefore especially useful for driving crystal harmonic generators.

If it is desired to sweep a 2K33 slowly through a frequency band wider than can be obtained by reflector voltage variation, a suitably geared motor can be attached to the screw which varies the cavity size. A friction clutch must be included in the drive to allow slippage at the end of the tuning range and thus avoid damage to the tube. In thermally tuned klystrons, a wide frequency sweep is obtained by deriving the tuner grid voltage from a motor-driven potentiometer, preferably of the 10-turn type (*e.g.*, Helipot potentiometer).

The sources of noise and extraneous modulation in the output of klystrons are varied, and their noise spectra are poorly known at frequencies near the oscillator frequency itself. However, the noise generated by a klystron oscillator is not usually so large as that produced by the crystal detector. Occasionally an individual tube will produce exceptionally large noise, particularly near the end of a mode. In addition, klystron noise is larger than that generated by a bolometer detector and is the factor limiting the ultimate sensitivity of spectrographs using thermal detectors.

In case klystron noise has a harmful effect on a microwave measurement, it can usually be decreased by one of a number of techniques. Beyond 50 or 100 Mc from the center frequency it is usually negligible, so that noise from a local oscillator can be eliminated by using a sufficiently high intermediate frequency. Local oscillator noise can also be avoided by the use of a balanced mixer. Noise at low frequencies (*i.e.*, close to the frequency of klystron oscillation) may be eliminated by

dividing the emitted microwave into two parts, one part transversing, for example, an absorption cell before detection and the other part being separately detected. If the two detected signals are compared, variations due to oscillator noise may be eliminated and distinguished from effects of absorption in the cell (see [172]). A microwave bridge also tends to balance out noise.

**14-16. Magnetrons.** Multicavity magnetrons have been made to produce wavelengths as short as 2.6 mm. However, they have not been much used for spectroscopy because of the difficulty in tuning them [262]. Moreover, magnetrons are often rather noisy, and their large power output is seldom necessary.

Magnetrons have been used for spectroscopy in the millimeter region and may find further application for that purpose (see Chap. 15).

**14-17. Traveling-wave and Backward-wave Tubes.** A more recent type of tube which is not yet commercially available for the regions of most interest for spectroscopy is the traveling-wave oscillator. Several varieties have been constructed experimentally and they have been operated at wavelengths as short as 6 mm [511], [617]. In these tubes an electron beam is surrounded by a structure through which a wave travels more slowly than the electrons. At low frequencies (hundreds of megacycles) the wave may be guided by a helix; at higher frequencies a corrugated waveguide has been used. With suitable wave and electron velocities and appropriate coupling between them, the electron beam imparts energy to the wave, thereby increasing its amplitude. An amplification of 18 db has been obtained over a 3 per cent bandwidth near 6 mm wavelength, and such a tube can be used as an oscillator.

The "backward-wave" tube [830] is related to the traveling-wave tube. It can be constructed to give good amplification or oscillation at millimeter wavelengths and is tunable over a wide range of frequencies. In this device the electron beam passes along a corrugated waveguide to a collecting anode. An electromagnetic wave sent in from near the collecting anode emerges near the cathode and hence the wave is backward from that of a traveling-wave tube. Along its path it interacts with the electron beam at regular intervals, determined by the waveguide corrugations. The beam is thereby bunched and on traveling toward the collector interacts further with the electromagnetic wave. This provides a feedback which can be positive if rates of progress of the waves and hence phases are correct. Since the feedback phase and therefore the frequency of maximum amplification is determined by the electron-beam velocity, the frequency can be controlled by varying electrode voltages. One model has oscillated at wavelengths from 6 to 7.5 mm and has been used as an amplifier with a gain of 20 db. The power output of the oscillator is of the order of 10 mw.

Table 14-2 summarizes the microwave generators which have been

TABLE 14-2. CHARACTERISTICS OF MICROWAVE SOURCES

Source	Wavelength range	Average power output	Comments
Hot body	All wavelengths	$kT \Delta\nu$ (into transmission line) as long as $h\nu < kT$ . For bandwidth $\Delta\nu = 10^6$ cycles/sec $kT \Delta\nu \leq 5 \times 10^{-14}$ watts	Of use only in exceptional cases for microwave work because of low power
Spark discharge*	$\infty$ –0.2 mm	$10^{-6}$ – $10^{-8}$ watt for bandwidth $\Delta\nu \approx 10^8$ cycles/sec	Low power and not monochromatic, but for short wavelengths one of the few available sources
Triode electronic tubes	$\infty$ – 3 cm	10–0.5 watts	Convenient for longer wavelengths
Klystrons	50 cm–5 mm	$100$ – $10^{-3}$ watts	Very convenient and tunable over about 10% range for high-frequency types
Klystrons plus crystal multipliers (harmonics)*	50 cm–0.6 mm	$10^{-2}$ – $10^{-9}$ watts	One of most convenient sources below 1 cm wavelength, and best source for spectroscopy below 4 mm
Magnetrons (fundamental)	50 cm–3 mm	100–1 watts	High power. Often pulsed with very high peak power. Usually tunable only over small range
Magnetron harmonics*	3 cm–1 mm	$10^{-1}$ – $10^{-9}$ watt	Good monochromatic source for wavelengths below 2.5 mm, but usually tunable only over small range
Traveling-wave and backward wave tubes	1 m–6 mm	$100$ – $10^{-3}$ watts	Expected performance similar to klystrons but not yet commercially available for short wavelengths. Tunable over wide range

\* Discussed more fully in Chap. 15.



used or suggested for microwave spectroscopy. The higher powers quoted are representative of performance at the lower frequency end of the range of each type. Tubes for higher frequencies are necessarily smaller and so have reduced power, dissipation, and usually lower efficiency.

**14-18. Detectors.** Crystal rectifiers are used almost exclusively for detectors of microwave power in spectroscopy, although thermal detectors have been applied in some special cases. The crystal detector [325] consists of a fine wire in contact with a block of semiconducting material (most often silicon but sometimes germanium). The contact resistance is greater in one direction than in the reverse, and the current-voltage characteristic is very nonlinear near the origin so that rectification occurs when an alternating voltage is applied. Because the contact is a fine point, contact capacitance is small and the rectifier can be used up to extremely high frequencies. Nevertheless, in the millimeter-wavelength range the stray capacitance shunting the contact becomes a limiting factor.

The sensitivity of a crystal is determined by its forward and backward low-current impedances. However, the usable sensitivity is limited by crystal noise. Both these factors vary greatly between individual crystals, but a typical good type 1N26 crystal matched to a waveguide gives an output current of about 1 ma/mw. The internal output impedance is near 200 ohms when 1 mw of power is received, and considerably higher for lower received powers. The impedances which govern the performance at microwave frequencies differ from those at low frequencies by the effects of shunt capacitance and series inductance, so that low-frequency measurements are only a rough guide to the performance of a crystal at microwave frequencies. The noise power generated in a crystal may be divided into two parts. The first is the thermal agitation, or "Johnson" noise,  $kT \Delta\nu$ , where  $k$  is Boltzmann's constant  $= 1.380 \times 10^{-23}$  joule per degree,  $T$  the absolute temperature, and  $\Delta\nu$  the output frequency bandwidth. The second part of the noise is not strongly temperature-dependent but is approximately proportional to the square of the crystal current and inversely proportional to the output frequency. Thus the noise power of a crystal is given by

$$P = \left( kT + \frac{CI^2}{\nu} \right) \Delta\nu \quad (14-45)$$

where  $C$  = a constant

$I$  = the d-c crystal current, amp

$\nu$  = output frequency

At room temperature (20°C),  $kT = 4.04 \times 10^{-21}$  watt/cycle/sec. For a reasonably good K-band crystal  $C$  is about  $10^{-7}$  ohms. Thus for an output frequency of 30 Mc, which is typical of superheterodyne detec-

tion, the second term of (14-45) is less than the first for normal crystal currents of 1 ma or less. For direct or "video" detection, however, lower output frequencies are used and the second term normally predominates. For  $\nu = 6000$  cycles/sec,  $I$  must be reduced to a few microamperes to keep excess noise due to the second term less than "thermal" noise. Such low crystal currents have distinct disadvantages.

Since the current-voltage characteristic of a crystal is represented fairly well by  $I = KV^2$ , where  $K$  is some constant, the output power is approximately proportional to the square of the input power, that is,  $P_{\text{out}} \propto I^2 \propto V^4 \propto P_{\text{in}}^2$ . Hence, for small variations  $\Delta P_{\text{in}}$  of the input power such as would be produced by gas absorption, the change in output signal is

$$\Delta P_{\text{out}} \propto P_{\text{in}} \Delta P_{\text{in}} \quad (14-46)$$

The conversion gain may be defined as  $\Delta P_{\text{out}}/\Delta P_{\text{in}}$ , which is a measure of the efficiency of the rectification process. It is usually considerably less than unity, and from (14-46) may be seen to decrease with decreasing power level. Hence usually the crystal current should be high enough to give good conversion and to make crystal noise predominate over amplifier noise. Since crystal noise power is proportional to the square of the current or input power from (14-45), and detected signal for a given fractional absorption is also proportional to the square of the power from (14-46), the precise value of crystal current does not affect the sensitivity or signal-to-noise ratio as long as the crystal current is large enough to make crystal noise predominate over other noise sources. Crystal currents as low as a few microamperes may hence still allow good sensitivity if exceptionally noise-free amplifiers are used. For very large crystal currents (greater than about 0.5 ma), the conversion gain no longer increases with current, which sets an upper limit to the desired crystal current.

The noise which is proportional to crystal current may be regarded as originating in a variable resistance of the rectifier. If, instead of a direct current through the rectifier, the microwaves are completely modulated with frequency  $\nu_0$  so that the rectified crystal current varies at frequency  $\nu_0$ , the noise of this type becomes  $\frac{CI^2}{\nu - \nu_0} \Delta\nu$  rather than  $\frac{CI^2}{\nu} \Delta\nu$  as given in Eq. (14-45). For this reason amplitude modulation of the source of microwave power at a high frequency does not obviate the large crystal-produced noise in a narrow band about the frequency of modulation  $\nu_0$ .

Figure 14-15 shows two typical crystal mounts for 1N26 crystals ([309], p. 171). The mount in Fig. 14-15a is tunable for optimum impedance match at a particular frequency, while the other is broadly resonant over



the *K*-band region. In the latter, especially, some adjustment may be obtained at the ends of the frequency band by moving the crystal slightly in or out of its holder.

Crystals are also used for harmonic generation, being well suited for these purposes because their nonlinear resistance characteristic persists to high frequencies, and for superheterodyne mixers. When superheterodyne detection is used, the beat oscillator should give adequate power (approximately 1 milliwatt) to the crystal to give good conversion

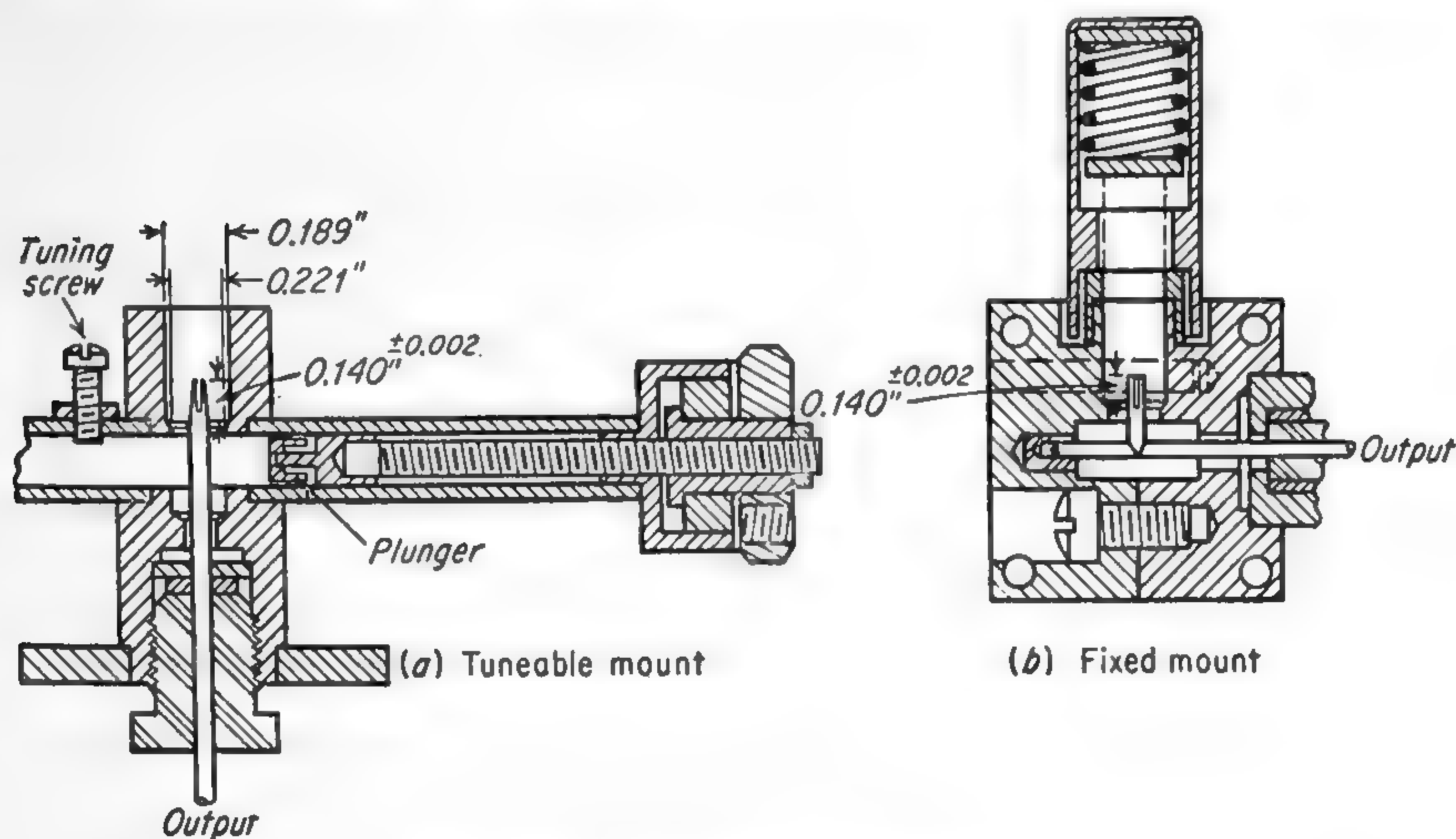


FIG. 14-15. Microwave crystal mounts.

gain [cf. (19-46)]. Its frequency should also differ from the signal frequency by an amount sufficiently large to prevent difficulty from crystal noise of the type indicated by the second term of (19-45) (cf. Sec. 15-7).

Welded contact germanium crystals have been used and are very sensitive and stable. However, they tend to have higher noise than good silicon crystals ([325], Chap. 13). When used as mixers, they may have a conversion gain greater than unity, giving an intermediate-frequency output power greater than the signal power, the local oscillator providing the difference. In the longer wavelength range, these crystals are very good for harmonic generation but unfortunately are no longer being manufactured.

Bolometers or barretters can also provide useful detection of microwaves if the power level is not too low. A bolometer consists of a small length of fine metal wire which is heated by the presence of a microwave signal, with a resulting change in resistance. The change in resistance can be detected as a voltage signal by passing a small current through the bolometer. Bolometers and their mounts are manufactured by the Sperry Gyroscope Company, Great Neck, N.Y., and by the Polytechnic Research and Development Co., Brooklyn, N.Y., with approximately



the following characteristics: resistance = 200 ohms; change of resistance = 8 ohms/milliwatt; maximum power before burnout = 15 milliwatts; time constant = 300  $\mu$ sec. Units are made for microwave frequencies near 3 cm and near 1 cm which give satisfactory reception over variations in wavelength of  $\pm 10$  per cent or more. If 5 ma of current is passed through the bolometer, the above change of resistance gives a voltage change of 0.04 volts/milliwatt of microwave power.

One of the most important advantages of a bolometer is that, in contrast with crystal detectors, it gives very low noise at low (audio) frequencies. Thus the bolometer noise is not much larger than thermal noise, which is about  $2 \times 10^{-9}$  volts for a 1 cycle/sec bandwidth and the bolometer described above. If an amplifier is used with a noise figure of 100, this means that microwave power changes of about  $5 \times 10^{-10}$  watts can be detected. Bolometers will not generally respond well to changes in microwave power more rapid than about 1000 cycles/sec (time constant  $\approx 10^{-4}$  sec), but for slower modulation frequencies they can be very convenient and sensitive. Additional discussion of their design and use can be found in reference [221].

#### References: Books on Microwaves

- Barlow, H. M., and A. L. Cullen, *Microwave Measurements*, Constable & Co., Ltd., London, 1950.
- Bronwell, Arthur B., and Robert E. Beam, *Theory and Application of Microwaves*, McGraw-Hill Book Company, Inc., New York, 1947.
- Lamont, H. R. L., *Wave Guides*, 3d ed., Methuen & Co., Ltd., London, and John Wiley & Sons, Inc., New York, 1950.
- MIT Radiation Laboratory Series, Vols. 1 to 28, members of the staff of the Massachusetts Institute of Technology Radiation Laboratory, McGraw-Hill Book Company, Inc., New York, 1947.
- Principles of Radar*, 3d ed., members of the staff of the Radar School, Massachusetts Institute of Technology, McGraw-Hill Book Company, Inc., New York, 1952.
- Moreno, T., *Microwave Transmission Design Data*, McGraw-Hill Book Company, Inc., New York, 1948.
- Pollard, Ernest C., and Julian M. Sturtevant, *Microwaves and Radar Electronics*, John Wiley & Sons, Inc., New York, and Chapman & Hall, Ltd., London, 1948.
- Reich, H. J., P. F. Ordung, H. L. Kraus, and J. G. Skalnack, *Microwave Theory and Techniques*, D. Van Nostrand Company, Inc., New York, 1953.
- Sarbacher, R. I., and W. A. Edson, *Hyper and Ultra-high Frequency Engineering*, John Wiley & Sons, Inc., New York, and Chapman & Hall, Ltd., London, 1943.
- Skilling, H. H., *Fundamentals of Electric Waves*, 2d ed., John Wiley & Sons, Inc., New York, and Chapman & Hall, Ltd., London, 1948.
- Slater, J. C., *Microwave Electronics*, D. Van Nostrand Company, Inc., New York, 1950.
- Slater, J. C., *Microwave Transmission*, McGraw-Hill Book Company, Inc., New York, 1942.
- Wind, M., and H. Rapaport, *Handbook of Microwave Measurements*, Polytechnic Institute of Brooklyn Microwave Research Institute, Brooklyn, 1954.

## CHAPTER 15

### MICROWAVE SPECTROGRAPHS

**15-1. General Principles and Ultimate Sensitivity.** Microwave absorption in gases is usually detected by passing microwave radiation from an oscillator through a long waveguide cell containing the gas, and measuring the amount of transmission as a function of the oscillator frequency. If the gas pressure is low enough so that the lines are not more than a megacycle or so wide, this is conveniently done by sweeping the oscillator frequency periodically and putting a voltage corresponding

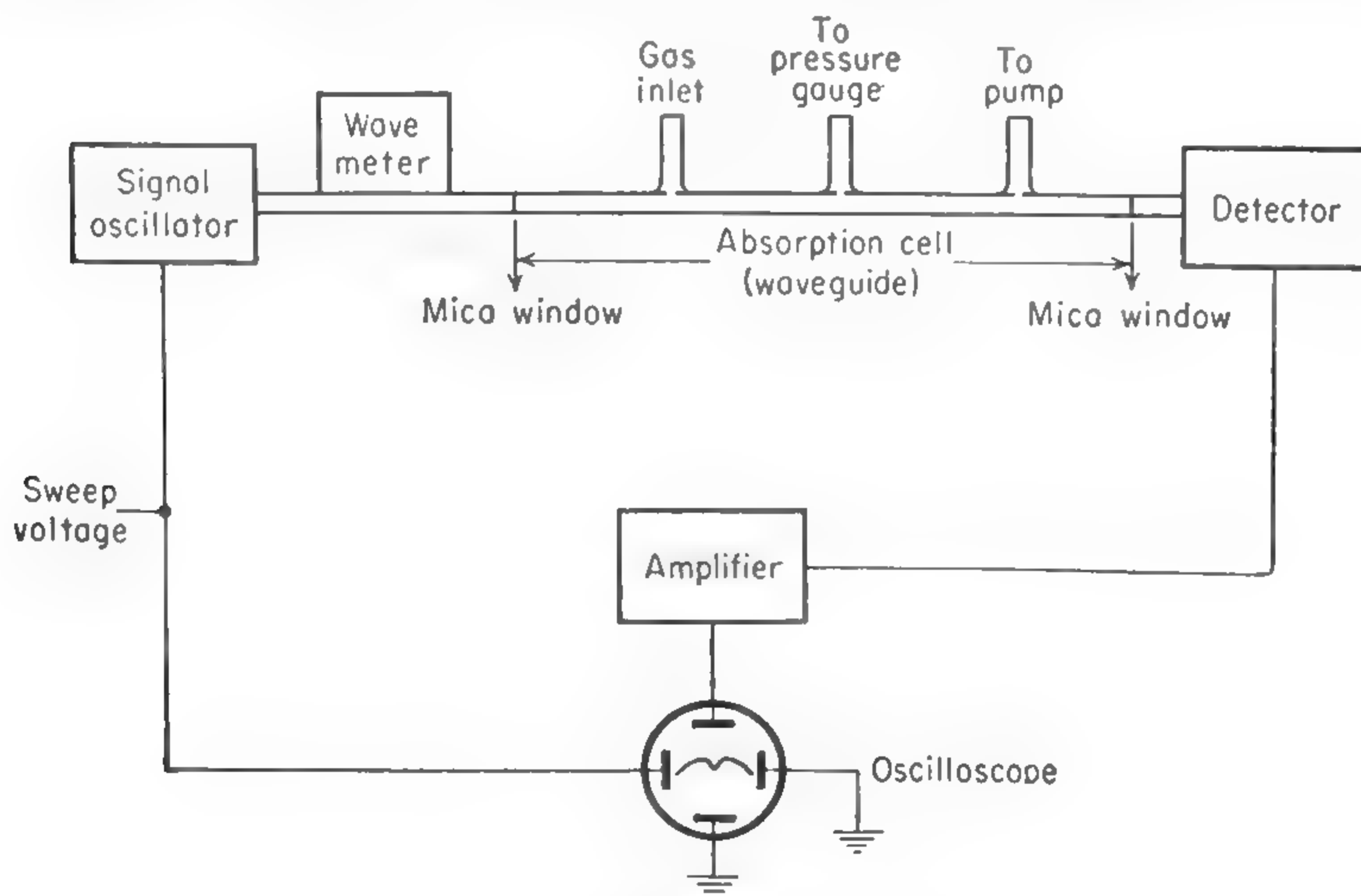


FIG. 15-1. A simple microwave spectrograph.

to this sweep on the horizontal axis of an oscilloscope, and a voltage corresponding to the transmitted power on the vertical axis. Such a system, shown in Fig. 15-1, thus plots the spectrum on the cathode-ray tube. The oscillator is swept over a region only 10 to 50 Mc wide, the center of its frequency being varied by hand to search for absorption lines or to move from one line to another. If, as is customary, the oscillator is a reflex klystron, a sweep of the order of 30 Mc is obtainable electrically by varying the repeller potential.

The type of spectrometer shown in Fig. 15-1 is simple and convenient

if the absorption lines are strong, *i.e.*, produce changes in power as large as 0.1 per cent. However, many lines give very weak absorption, so that, even with a cell length of several meters, changes in power due to gas absorption of 1 part in a million or less would have to be observed on the oscilloscope. Interfering variations in power can easily be produced by the variation in oscillator output as a function of frequency, or by variation in transmission due to reflections and standing waves in the waveguide. These difficulties generally limit a spectrometer of this type to detection of lines with absorption coefficients greater than  $10^{-6} \text{ cm}^{-1}$ , or producing a power change of 0.1 per cent in a 10-meter absorption cell. Another type of interfering fluctuation is "thermal noise." This is electromagnetic radiation in the waveguide and detector produced by thermal agitation of their electrons and is the only interfering variation of a fundamental nature. Other sources of variation can presumably be eliminated by sufficiently careful design and construction of a spectrometer, so that it is thermal noise which limits the ultimate sensitivity attainable. This limit on the minimum detectable absorption coefficient for a "perfect" spectrometer, *i.e.*, a spectrometer whose sensitivity is limited only by thermal noise, is discussed below.

If power  $P_0$  is introduced into a waveguide it will be attenuated by losses in the waveguide walls and also by possible gas absorption. These two sources of attenuation are designated by attenuation coefficients  $\alpha_0$  and  $\alpha_{\text{gas}}$ , respectively. The power after traversing a length  $L$  of the waveguide will therefore be

$$P = P_0 e^{-(\alpha_0 + \alpha_{\text{gas}})L} \quad (15-1)$$

If the gas is removed, the power is  $P = P_0 e^{-\alpha_0 L}$ , so that the change in power due to the gas is

$$\Delta P = P_0 e^{-\alpha_0 L} (1 - e^{-\alpha_{\text{gas}} L}) \approx \alpha_{\text{gas}} L P_0 e^{-\alpha_0 L} \quad (15-2)$$

where the exponential has been expanded because we shall be interested in very weak absorptions such that  $\alpha_{\text{gas}} L \ll 1$ .

To find the minimum detectable absorption, we need also to calculate the fluctuations in power caused by thermal agitation. Consider a long waveguide of length  $L$  which, for simplicity, supports only one mode of propagation for frequencies near  $\nu$ . The waveguide will be assumed to be lossless and to be shorted at both ends. This guide is in reality a cavity and its resonant modes are given by  $n = 2L/\lambda_g$ , where  $\lambda_g$  is the wavelength of radiation in the guide and  $n$  is an integer. Since  $\lambda_g$  is not very different from the wavelength  $\lambda$  in a vacuum (in most practical cases  $\lambda_g \approx 1.2\lambda$ ), we shall write  $n = 2L/\lambda$  and neglect the complications of modified wavelength and velocities in the waveguide. Then  $n = 2L\nu/c$ . As long as  $kT \gg h\nu$ , the classical equipartition law holds, and the average energy in each mode of oscillation is  $kT$ . Since the number of modes per



frequency interval is  $dn/d\nu = 2L/c$ , the energy per frequency interval is

$$\frac{dW}{d\nu} = \frac{2LkT}{c} \quad \text{or} \quad \Delta W = \frac{2LkT}{c} \Delta\nu \quad (15-3)$$

Each standing-wave mode can be resolved into two equal traveling waves moving in opposite directions. Each wave contains half the energy, so that the total energy per second moving down the guide in one direction is one-half the energy density per unit length times the velocity  $c$ , or

$$\frac{c \Delta W}{2L} = kT \Delta\nu \quad (15-4)$$

This is the thermal power in the frequency interval  $\Delta\nu$  which travels in either direction down the waveguide. It is independent of the length of the waveguide and so holds equally well for an infinite waveguide or for its practical equivalent, a finite lossy waveguide or one terminated by matching impedances. For instance, the thermal power flowing from a waveguide into a matched crystal detector is given by (15-4). In addition the crystal must radiate an equal amount of power into the waveguide if the entire system is in thermal equilibrium.

This thermal energy  $kT \Delta\nu$  produces a fluctuating signal at the crystal detector. It might, at first thought, appear that a signal due to gas absorption would be detectable as long as the change in power produced at the crystal was somewhat larger than the thermal power  $kT \Delta\nu$ . However, the thermal power is associated with a field strength in the waveguide which combines with the field strength due to the purposely transmitted microwave to produce apparent changes in power at the crystal considerably greater than  $kT \Delta\nu$ .

For convenience, let the transmitted microwave power from the signal oscillator be represented by a voltage defined so that  $V^2 = 2ZP$ , where  $P$  is the power and  $Z$  is the guide impedance.  $V$  is the voltage amplitude of the wave emitted by the oscillator. The similar voltage due to thermal radiation will then be  $(\Delta V)^2 = 4ZkT \Delta\nu$ , where an additional factor of 2 is required because there is a wave of thermal radiation in each direction along the guide which contributes to voltage fluctuations at the detector. The net power flow in the guide (assuming no gas absorption) is

$$\frac{(V \pm \Delta V)^2}{2Z} = P \pm 2 \sqrt{2kTP} \Delta\nu + 2kT \Delta\nu \quad (15-5)$$

Equation (15-5) shows that the thermal radiation produces changes of power of magnitude approximately  $\sqrt{PkT \Delta\nu}$ , which is considerably larger than the thermal power itself, since usually  $P \approx 10^{12}kT \Delta\nu$ . For a signal to be noticeable, the power change involved must be approximately as large as or larger than  $\sqrt{PkT \Delta\nu}$ . Then using the change in power due to gas absorption given by Eq. (15-2), the smallest detectable

absorption coefficient for a waveguide of length  $L$  is given when

$$\alpha_{\text{gas}} L P_0 e^{-\alpha_0 L} \approx 4 \sqrt{2 P_0 e^{-\alpha_0 L} k T \Delta \nu} \quad (15-6)$$

or

$$\alpha_{\text{gas}} = \frac{4}{L} \sqrt{\frac{2 k T \Delta \nu}{P_0 e^{-\alpha_0 L}}} \quad (15-7)$$

This expression is a minimum for a certain optimum waveguide length

$$L_{op} = \frac{2}{\alpha_0} \quad (15-8)$$

Then

$$\alpha_{\text{gas}}(\text{min}) = 2 e \alpha_0 \sqrt{\frac{2 k T \Delta \nu}{P_0}} \quad (15-9)$$

for the optimum waveguide length  $2/\alpha_0$ . The same result follows from a more rigorous treatment ([328]; cf. also [445], [278]).

Instead of absorption, it is possible to use dispersion, or variation in dielectric constant, to detect a gas resonance. The ultimate sensitivity attainable can be shown to be essentially the same as by detection of absorption [653].

The optimum guide length  $L = 2/\alpha_0$  is generally between 5 and 30 meters since  $\alpha_0 \approx 10^{-3} \text{ cm}^{-1}$ . If the power used in the waveguide is 1 mw, and the bandwidth of the detecting circuits is 30 cycles, the minimum detectable absorption coefficient would be  $\alpha_{\text{gas}}(\text{min}) \approx 10^{-10} \text{ cm}^{-1}$ . Actual spectrometers have not reached this ideal sensitivity, the best being approximately 30 times less sensitive for bandwidths of 30 cycles as assumed here.

The actual sensitivity of microwave spectrometers is usually limited by one of the following instead of by fundamental thermal fluctuations:

1. Random fluctuations of power due to
  - a. Noise in excess of thermal noise as a result of current flowing in the detecting crystal
  - b. "Oscillator noise," or variations in oscillator output
  - c. Noise in excess of thermal noise in the amplifying circuits
2. Changes in power which vary systematically with oscillator frequency as a result of
  - a. Variation of oscillator power as a function of frequency
  - b. Variation with frequency of transmission of the waveguide, absorption cell, and detecting crystal
3. "Conversion loss" in the crystal detector, *i.e.*, the loss in signal power when a microwave signal is converted into a lower-frequency signal by the detector.

The first and third difficulties are usually allowed for by introducing a noise figure  $N$ , which is the factor by which the ratio of noise to signal

power coming through the amplifying circuits has been changed by troubles of types 1 and 3. Thus for  $N = 1$ , a signal power of  $kT \Delta\nu$  would appear as large as noise, but for  $N = 20$ , the signal power would have to be 20 times larger to equal noise power. Hence (15-9) becomes for a nonideal system

$$\alpha_{\text{min}}(\text{min}) = 2e\alpha_0 \sqrt{\frac{2kT \Delta\nu N}{P}} \quad (15-10)$$

The noise figure  $N$  can easily vary with conditions and usually depends to some extent on the power  $P$  and the frequency. In typical good microwave spectrographs  $N$  is as large as  $10^3$ , as may be surmised from the discrepancy of a factor of 30 between  $\alpha_{\text{min}}(\text{min})$  observed and the ideal value. The fact that the crystal noise and hence the noise figure usually decreases with decreasing current means that optimum sensitivity is obtained with waveguides somewhat longer than that given by (15-8). However, from (15-7) the sensitivity varies only slowly with variations in lengths, which are near optimum, so that the precise value of the optimum length is not critical.

Usually the worst source of random noise is the detecting crystal, for which the noise at low frequencies is often much greater than thermal (cf. Chap. 14). Crystals vary by orders of magnitude; it is well worth while to select crystals for low noise. Oscillator-tube noise is usually less than crystal noise, but some klystrons have noisy frequency regions, particularly near the edge of a mode. Oscillator noise is also less serious than crystal noise because if necessary it can always be eliminated by bridge or compensating systems.

The most troublesome cause of systematic variation with frequency is usually reflections or standing waves in the absorption cell which vary the transmission from oscillator to crystal. As the signal oscillator frequency is varied, this produces a pattern of peaks and valleys in the power received by the crystal. If the waveguide cell is of length  $L$  and the offending reflections occur as usual near the two ends of the cell, the peaks and valleys repeat every time the oscillator frequency is varied by  $c/2L$ . If the cell is long, these reflection effects produce narrow peaks which closely resemble absorption lines. They may be reduced by introducing an attenuator between the two sources of reflections. The attenuator itself may, however, introduce new reflections. Carefully tapered attenuators can reduce power variations of this type to  $\frac{1}{10}$  per cent, but even so reflections make it difficult to detect a total gas absorption much less than this amount. Thus the simple microwave spectrograph of Fig. 15-1 is suitable only for the stronger absorption lines.

Electrical filters can help discriminate between absorption lines and noise or reflections. In a waveguide which is not too long, reflections give a slower variation of power with frequency than does a line, so that



a high-pass filter tends to suppress reflections with respect to the line. Since noise occurs with all frequencies, much of the noise can be eliminated by filtering out all frequencies higher than those essential to pass the absorption line. Often noise can be best eliminated by sweeping very slowly over a small region about the absorption line and rejecting all frequencies higher than about ten times the sweep frequency, which is all that is necessary to reproduce the line. If the sweep frequency is  $\nu_0$ , then this represents a bandwidth of  $10\nu_0$ , and if the noise power per frequency interval  $P/\Delta\nu$  is constant as in thermal noise,  $\nu_0$  should be made as small as possible to minimize the bandwidth  $\Delta\nu$ . On the other hand, if crystal noise dominates as is often the case, the noise power depends on  $\nu$ . From Eq. (14-45) the noise power per frequency interval is  $P/\Delta\nu = C/\nu$ , where  $C$  is a constant. The total noise power is the integral

$$P = \int_{\nu_1}^{\nu_2} \frac{CI^2}{\nu} d\nu = CI^2 \log \frac{\nu_2}{\nu_1}$$

The lower limit  $\nu_1$  of frequency passed should be not more than two or three times the sweep frequency  $\nu_0$ , and the highest frequency  $\nu_2$  not much lower than  $10\nu_0$ . Hence  $P = CI^2 \log (\nu_2/\nu_1) \sim CI^2 \log 5$ , and is independent of the sweep rate. This independence of noise power on sweep frequency (with appropriate filtering) holds only under conditions where crystal noise predominates. If any other sources of noise are important, a slow sweep rate is usually advantageous.

It might be thought that modulating the klystron power at a high frequency (*i.e.*, 100 kc) and amplification of the 100-kc signal on the crystal would allow discrimination against this crystal noise since crystal noise has a maximum at low frequency from (14-45). Unfortunately such a system gives no particular advantage, however, because the crystal noise acts as if it were produced by a variable resistance. Hence the maximum noise always occurs at the frequency of the current flowing through the crystal. Modulating the amplitude of the microwave power at 100 kc simply produces a maximum of the objectionable noise at 100 kc, and no improvement in signal-to-noise ratio (*cf.* Sec. 14-18).

**15-2. Source Modulation.** Considerable improvement in signal-to-noise ratio can be obtained by a small frequency modulation of the klystron oscillator at, say, a frequency of the order of 100 kc in addition to the slower sweep frequency [278], [286]. This modulation can be achieved easily by adding to the klystron slow sweep a 100-kc sine-wave or square-wave sweep voltage. If at a particular instant the klystron is just at the peak of an absorption line and a voltage pulse is applied to the repeller, the klystron moves off the line and the absorption disappears so that more power reaches the crystal. With a 100-kc modulation the line appears and disappears 100,000 times a second. If a line is

present, the 100-kc frequency modulation is converted into amplitude variations at the crystal, which may be amplified by a tuned amplifier. If the amplifier is tuned to 100 kc, only noise components near that frequency are amplified and these are much smaller than the low-frequency components. Note that this frequency modulation does not produce a large modulation of the crystal current, as would amplitude modulation of the klystron source.

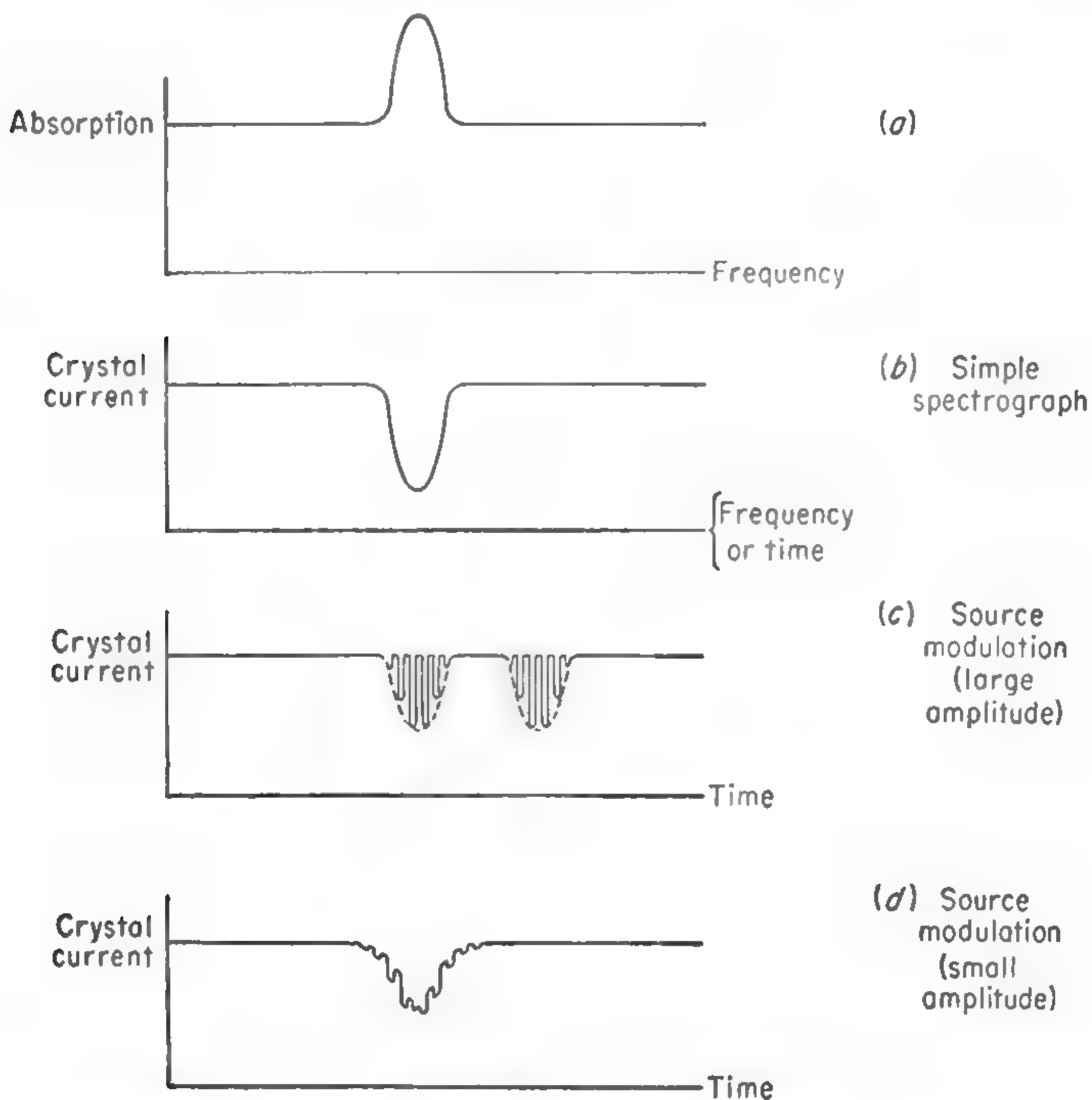


FIG. 15-2. Absorption and corresponding waveforms, one with a simple spectrograph and one using frequency modulation of the microwave source in addition to a slow frequency sweep.

Sharp variations in output power with frequency, as, for instance, those due to certain types of reflections, may also produce 100-kc components and such reflections have often been mistaken for lines. Transmitted power variations with frequency due to reflections are usually less rapid than those due to absorption lines and hence may often be distinguished from them. However, variations due to reflections are a serious limitation on the ultimate sensitivity of this type of spectrometer.

Figure 15-2 shows the crystal-current waveform for the simple spectrograph and for the frequency-modulated, or "double-modulated," spectrograph. In Fig. 15-2c, the modulation of the instantaneous klystron

frequency is assumed to be greater than the line width. The line first appears as one tip of the instantaneous frequency excursion strikes the absorption. However, the two appearances of the line are at opposite phases of the modulation frequency and if necessary they can be distinguished by a phase-sensitive detector.

If the modulation is small compared with the line width, the modulation-frequency component of the crystal current is proportional to the slope of the absorption curve. The line may be said to be differentiated, and the two modulation-frequency peaks occur at the points of largest slope, while the output at the peak absorption is zero. For a line with a Lorentz shape, as given by the first term of the Van Vleck-Weisskopf equation (13-19), these peaks occur at  $\Delta\nu/\sqrt{3}$  from the center of the absorption line, where  $\Delta\nu$  is the line-width parameter.

Square-wave modulation, which has been assumed, gives the most faithful reproduction of the line shape (or its derivative) [465]. However, sine-wave modulation may be used for simplicity [202], [248] with little loss of sensitivity, but with some distortion of the line shape.

**15-3. Stark Modulation.** If an electric field is applied to a polar molecule its absorption frequencies are shifted because of the Stark effect (Chap. 10). If at some instant the klystron frequency coincides with the peak of an absorption line, when the electric field is applied the absorption decreases. Thus high-frequency modulation can be obtained by subjecting the gas to a periodically interrupted electric field [210], [396]. In addition to the reduction in crystal and tube noise at the high modulation frequency, the method has the very great advantage of being almost completely insensitive to systematic power variations due to anything but spectral lines. Reflections and klystron power variations associated with the low-frequency sweep usually produce very small interfering signals at the high modulation frequency. This useful type of spectrometer was introduced by Hughes and Wilson [210].

Square-wave modulation is almost universally used with Stark spectrographs, with one tip of the square wave being at zero field. Then during this half of the cycle, the absorption pattern is that of the undisplaced line, while during the other half cycle the Stark spectrum occurs. With a phase-sensitive detector, the oscillograph pattern shows both the absorption line and the Stark pattern with the latter inverted. The Stark pattern may then be used to identify the transition or to measure the molecular dipole moment.

Figure 15-3 shows a cross section of a waveguide cell suitable for Stark modulation and a block diagram of the instrument. Stark spectrographs have been described by several authors [419], [396], [519]. The cell is usually a section of waveguide about 3 meters long, as the optimum length is reduced by the extra attenuation of the Stark plate and its supporting insulation. It may be constructed from ordinary waveguide, with the



addition of a central flat plate parallel to the broad faces of the guide and so perpendicular to the microwave electric field. The plate is supported by strips of good insulating material such as polystyrene or teflon in which guiding grooves are milled. Connection to the Stark electrode is made by a wire through a hermetic seal in the side wall, which may terminate in a screw threaded into the plate. An alternative support using mica strips rather than plastic is suitable for higher temperatures [637].

Most often the waveguide size chosen is that appropriate to the wavelength band being used, but larger sizes are sometimes desirable to reduce

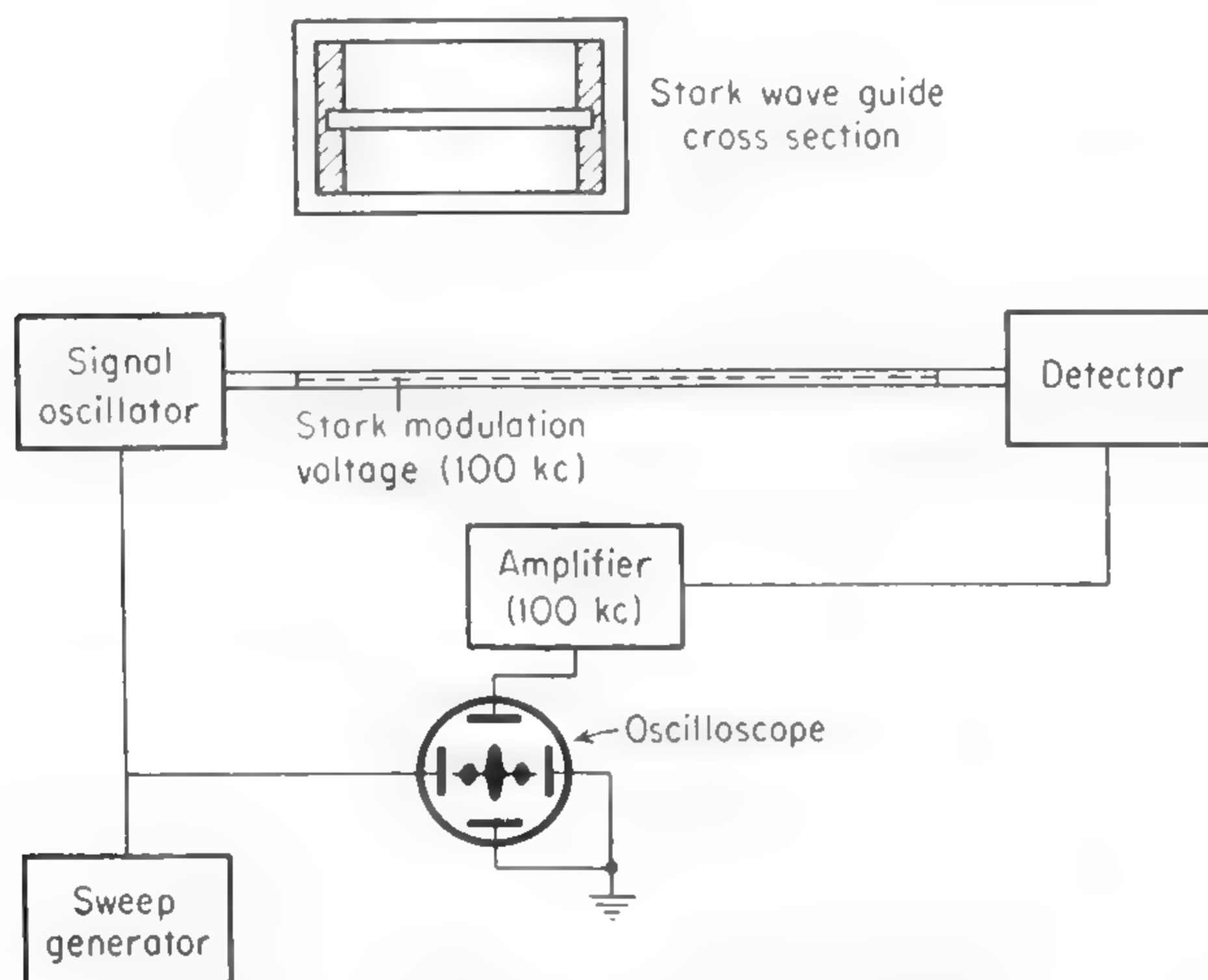


FIG. 15-3. Stark-modulation spectrograph.

the microwave energy density and so avoid saturation. However, larger sizes require larger applied voltages for a given Stark field, and this may be difficult to obtain. A large enough modulating field strength should be used so that all the Stark components are displaced more than the line width, if possible. Otherwise some of the Stark components (inverted by the phase-sensitive detector) will overlap the main line and subtract from it. A few volts per centimeter is usually sufficient for a line with a low  $J$  value having a first-order Stark effect. If only a second-order Stark effect occurs several hundred to several thousand volts per centimeter may be needed.

The requirements for the square-wave generator are made more severe by the capacitance between the central plate and the rest of the guide which may be as much as  $1000 \mu\text{f}$ . For this reason the square-wave generator must have a low output impedance and be capable of supplying large output currents. One such generator, constructed for the Columbia Radiation Laboratory by S. Geschwind, takes a sine wave from a

100-kc oscillator and clips it in several stages of pentode limiting amplifiers to produce a square voltage wave. The necessary low output impedance is obtained from a final cathode follower stage of two 829B or 3E29 tubes in parallel. Provision is made so that an adjustable direct voltage may be added to the square wave to ensure that one end of the square wave corresponds to zero voltage between the Stark plate and the waveguide. For lines which have only small second-order Stark effect, it is sometimes useful to adjust the d-c voltage so that the low-voltage half of the square wave is several hundred volts above zero. Since a second-order Stark effect is proportional to the square of the field, a given change in voltage produces a larger modulation at high field strengths, and so it may be useful to start from a nonzero field.

Another suitable type of square-wave generator [373], [585], [519] uses two sets of parallel output tubes. One set, connected to the high voltage, charges the capacitance of the Stark electrode while the other set discharges it on alternate half cycles. The two groups of output tubes are each triggered at the right time by a blocking oscillator controlled by a sine-wave input voltage of the same frequency as the desired square wave. If the square wave is to be very near zero on one half-cycle, an additional clamping diode is needed. Thus the plates of one group of triggered output tubes may be at a high positive voltage and the cathodes of the other group at about minus 40 volts. The diode clamping tubes are connected to ground so that the voltage cannot actually decrease to negative values, but is stopped sharply near zero. This type of circuit can provide a better and higher voltage square wave at high frequencies than the limiting amplifier, but the blocking oscillator must be readjusted if the frequency is changed.

**15-4. Modulation-frequency Signal Amplifiers.** The modulation-frequency amplifiers need to have sufficient gain and sufficiently low noise that crystal noise is the only limiting factor in the spectrograph's sensitivity. Since the signal is lowest in the first amplifier stage, that is the most critical one from the standpoint of noise. In fact, the signal voltage at the input may be as low as the crystal noise which, for a 30-cycle bandwidth and a few hundred microamperes of crystal current, is of the order of  $10^{-9}$  volt. A considerable increase in signal voltage can be obtained by using a series-resonant input circuit tuned to the modulation frequency, as shown in Fig. 15-4. The device may be considered as a matching network from the low crystal impedance (300 to 5000 ohms) to the high input impedance of the amplifier. Since the matching network output impedance is high, the cable connecting it to the amplifier must be short and of low capacitance. It is important that the matching network be well shielded. The circuit of Fig. 15-4 also includes a separate low-pass filter to permit measurement of the direct crystal current. If, to avoid saturation of the spectral line, it is neces-



sary to operate at low power levels so that the crystal noise and signal are both small, the resonant input circuit can be followed by a cascade amplifier using a low-noise tube such as the 12AY7 [460]. With this combination the amplifier noise is only slightly greater than the thermal noise of a resistor equal in value to the crystal impedance, *i.e.*, its noise figure is not much more than unity.

It is always easy to test whether or not the amplifier is sufficiently noise-free. If it is, then a decrease in crystal current should produce a decrease in noise voltage through the amplifier or on the oscilloscope which is approximately proportional to the change in current. If such a

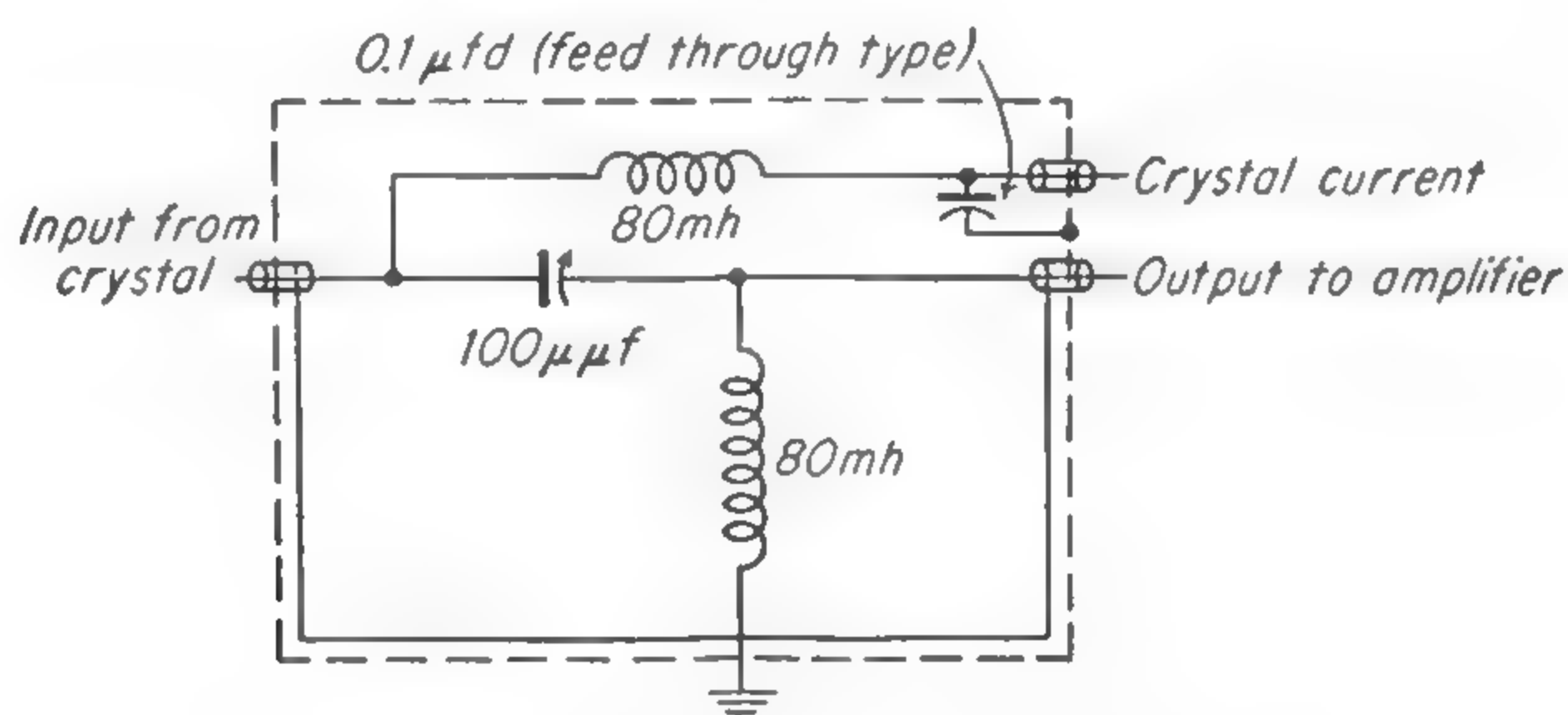


FIG. 15-4. Resonant input circuit for signal amplifier.

decrease occurs, the noise must originate either in the microwave oscillator or in the crystal, and for normal oscillators it will be crystal noise.

Various types of modulation-frequency amplifiers have been used. It is possible to use a commercial broad-band preamplifier followed by a tunable low-frequency radio receiver. Since the receiver does not need to be easily tunable and the preamplifier does not require a broad band, a specially constructed amplifier can be somewhat simpler. Many other amplifier combinations are possible, and some of them are described in the references [419], [396], [519], [460].

The bandwidth used in the receiver should, to reduce noise, be as low as possible. If it is too small, the line will not be faithfully reproduced unless the sweep rate is reduced. Moreover, a too narrow receiver band may lead to errors in frequency measurement [460]. The necessary ratio of bandwidth to sweep rate for good portrayal of a line cannot be specified uniquely, but is often of the order of 20. It is not difficult to have a sweep rate lower than 1 per second on a long-persistence oscilloscope. For use with a recorder on the receiver output, the klystron tuner may be driven slowly by a motor so as to cause the line to be traversed even more slowly. Bandwidths as low as 1 cycle/sec may then be usable. Since in this case the noise power is proportional to bandwidth, a narrow band and slow sweep are highly desirable for good sensitivity. Such a narrow effective bandwidth is most readily attained by means of a phase-sensitive detector (or "lock-in amplifier," as it is sometimes called).



Figure 15-5 is the circuit diagram of a simple type of phase-sensitive detector. The signal is applied to the control grid of a pentode amplifier. From the modulation generator a large voltage (10 to 100 volts depending on the tube used) is applied, through a phase shifter, to the suppressor grid. During one-half of the modulation cycle, the tube functions as a class A amplifier. During alternate half cycles, the lock-in voltage is sufficiently negative to cut off the plate current and with it the amplification.

In the absence of a signal, the plate current consists of a series of pulses once each cycle of the modulation frequency. If a signal of the same frequency and phase is present, the pulses are larger, while if it has opposite phase the pulses are smaller. The plate load resistance  $R$  and by-pass capacitor  $C$  produce an output voltage determined by the average

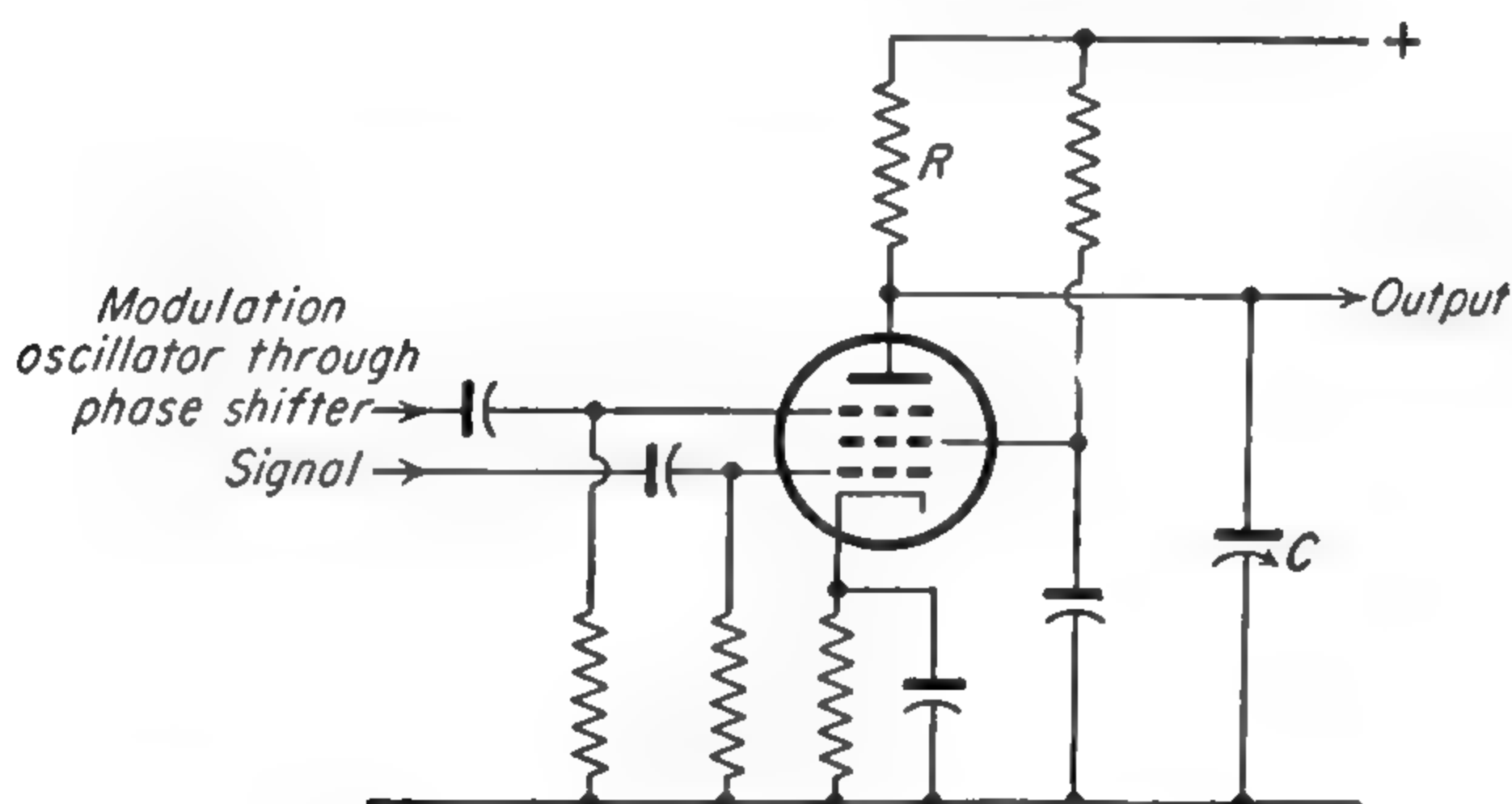


FIG. 15-5. A phase-sensitive detector.

size of these pulses averaged over a time determined by the time constant  $CR$ . Thus a signal of the modulation frequency will either increase or decrease this averaged output voltage, depending on its phase. A signal of any other frequency will have no fixed phase relative to the lock-in voltage and so will produce no effect on the average plate current or output voltage.

Interfering signals or noise at frequencies near the modulation frequency will produce fluctuations in output voltage if the time constant is not sufficiently large. The fluctuations might appear to be transient signals of the modulation frequency encountered during a sweep. It will be seen that the longer the time constant  $CR$ , the nearer an interfering signal must be in frequency to produce a signal, and so the narrower the effective bandwidth.

Figure 15-6 shows the signal waveforms at different places in a Stark spectrograph using a tuned amplifier and lock-in detector. Phases are indicated by "off" or "on" referring to the portions of the modulation cycle in which the Stark voltage, is, or is not, zero, respectively.

Both the line and its Stark components appear in the final output voltage. Since they occur at opposite phases, the Stark component is

inverted relative to the main line. The line shown in Fig. 15-6 is assumed to have only one Stark component, but commonly there are several.

To use a recording milliammeter with a lock-in detector of the type shown, the average plate current in the absence of a signal must be balanced out by an auxiliary supply. The balancing current may be obtained by means of a potentiometer from the plate supply.

For greater stability, the signal and balancing voltages may be obtained from matched amplifiers; *i.e.*, the balancing voltage may be supplied

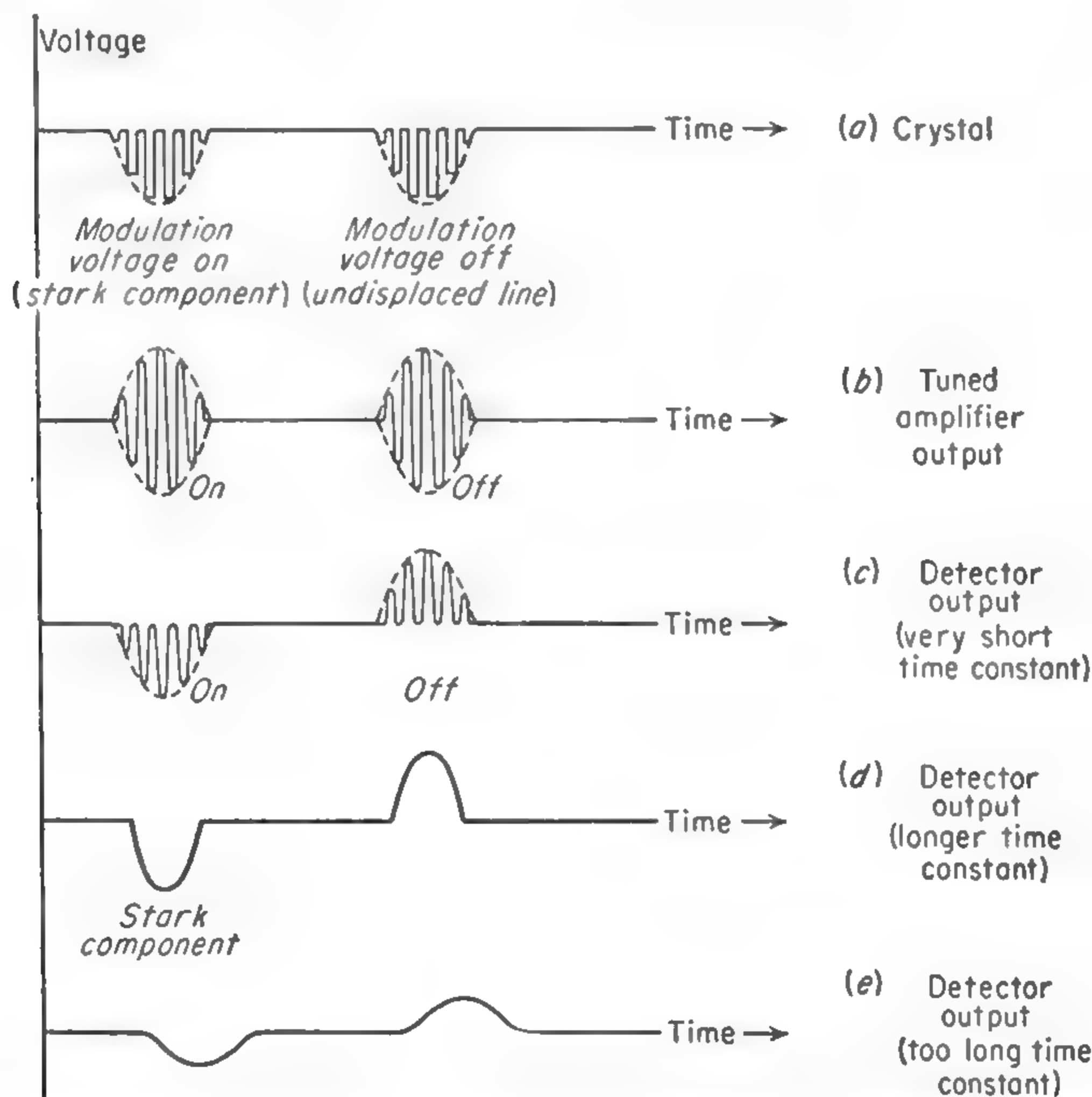


FIG. 15-6. Signal waveforms in a Stark-modulation spectrograph using a phase-sensitive detector.

by a second phase detector whose phase is such that its plate current charges in the opposite direction to the first one when a signal is received [396]. Inverse feedback may be applied to the amplifiers to improve the linearity and stability [737].

One of the primary advantages of a lock-in amplifier is that it provides an easy method for obtaining a very narrow bandwidth about any desired frequency. If a lock-in amplifier is used as part of an amplifying system, the effective bandwidth, *i.e.*, the band from which noise is received, is just the reciprocal of the time constant, or  $\Delta\nu_2 = 1/CR$ . (This assumes that  $\Delta\nu_2$  is the smallest bandwidth of the system, which is almost always the case.) If a lock-in is not used, the signal would

typically be passed through an amplifier of bandwidth  $\Delta\nu_1$ , then rectified by a conventional detector followed by a filter of time constant  $CR$  or bandwidth  $\Delta\nu_2$ . The effective bandwidth may then be considerably greater than  $\Delta\nu_2$ . This is because pairs of noise components throughout the whole amplifier bandwidth  $\Delta\nu_1$  are mixed in the detector to produce frequencies which lie within the band  $\Delta\nu_2$ . The effective bandwidth of this system is  $\sqrt{\Delta\nu_1 \Delta\nu_2}$ , so that the noise power may be considerably greater than that obtained with a lock-in amplifier.

If the detector time constant is too long relative to the time for a sweep, the output voltage cannot change fast enough to reproduce the line shape accurately. The line then appears to be broadened and reduced in height. Moreover, its peak is delayed and so comes at a point in the sweep corresponding to a different microwave frequency.

If a long time constant (*i.e.*, narrow bandwidth) must be used to reduce noise, the sweep rate must be proportionately lowered. The ultimate limit to the degree of improvement in signal-to-noise ratio which can be thus achieved is set by fluctuations in the klystron output frequency. Further improvement requires increased oscillator stability, which can be attained by use of an external stabilizing cavity resonator or by a controlling quartz-crystal oscillator with frequency multipliers.

**15-5. Zeeman Modulation Spectrographs.** For paramagnetic molecules such as NO, O<sub>2</sub>, NO<sub>2</sub>, ClO<sub>2</sub>, and free radicals, a magnetic modulation



FIG. 15-7. Zeeman modulation cell.

analogue of the Stark spectrograph can be constructed. The high-frequency magnetic field is most easily applied by a solenoid surrounding the waveguide.

Unless the modulation frequency is quite low, the guide must be slotted longitudinally to reduce eddy currents; such a slot can be put in the center of the broad face without disturbing the microwave fields. A glass tube surrounding the waveguide serves as a support for the coil and keeps the sample gas in the guide region (Fig. 15-7). At modulation frequencies less than 1000 cycles/sec, it is often possible to operate without the slot and then the glass envelope is no longer needed.

Since a square current wave through an inductance is hard to generate at high frequencies, sine-wave modulation may be used with a direct current added so that one extreme of the sine wave occurs at approximately zero field. The coil can then be part of a series-resonant circuit if large currents are desired.



**15-6. Choice of Modulation Frequency for Spectrographs.** Although crystal noise is reduced as the modulation frequency is raised [Eq. (14-45)], the apparent line width is increased (Chap. 10). The line breadth due to a square-wave modulation is somewhat greater than the modulation frequency, so that for the fine structures commonly encountered in microwave spectroscopy, modulation frequencies much greater than 100 kc have seldom been found desirable. Indeed, for particularly small line spacings even considerably lower frequencies may be desirable, even though the crystal noise is increased.

Whatever the modulation frequency, the amplifier should if possible have a low enough noise figure so that it contributes less noise than the crystal. As long as this is so, decreasing the microwave power level decreases the signal and the noise proportionately. Thus the signal-to-noise ratio is nearly independent of power. Very low microwave power levels (a few microwatts) are sometimes required in high resolution spectrographs to avoid saturation broadening, and then special precautions for amplifier input circuits may be needed. If such a low level must be used that most noise comes from the amplifier, the noise is independent of the signal. In that case, for any given microwave absorption, the signal is proportional to the power level, and so the sensitivity is also proportional to the power.

**15-7. Superheterodyne Detection.** At low microwave power levels, crystals are inefficient detectors, as their output voltage is approximately proportional to the square of the radio-frequency amplitude. It is then advantageous to use superheterodyne detection to produce a signal as large as possible relative to noise in the following amplifiers. Moreover, if the intermediate frequency is reasonably high (*e.g.*, 30 to 60 Mc) crystal noise within the intermediate-frequency amplifier bandwidth is reduced practically to the thermal noise.

Superheterodyne detection requires an auxiliary microwave oscillator which is kept at a constant frequency difference from the signal oscillator. This local oscillator may be made to follow the signal oscillator by a discriminator and automatic frequency-control system ([308], Sec. 8.3; [573]). Then as the signal oscillator is tuned, the frequency difference between it and the local oscillator is always such that the mixer output is at the desired intermediate frequency.

The need for an extra oscillator and automatic frequency control makes the superheterodyne more complicated than the simple detector. It is not usually possible to make the local oscillator follow automatically over more than a limited region. Moreover, the local oscillator may be an additional source of noise, although this noise can always be eliminated by the use of a balanced mixer [309].

**15-8. Bridge Spectrographs.** It has been seen that superheterodyne detection can be employed as an alternative to modulation for reducing

crystal noise. However, the carrier is enormously larger than the useful absorption signal. It persists at the output of the mixer and is amplified along with the signal. Thus saturation of the amplifier by the carrier is likely to occur before the signal has reached a suitable level. In addition, small fluctuations in power supplies or amplifier characteristics introduce noise into the carrier which is easily confused with the slow variation in the carrier level produced by gas absorption.

To reduce the carrier relative to the useful signal, a balanced bridge may be used. The bridge is shown schematically in Fig. 15-8. The microwave power is split by the first magic T into parts which travel

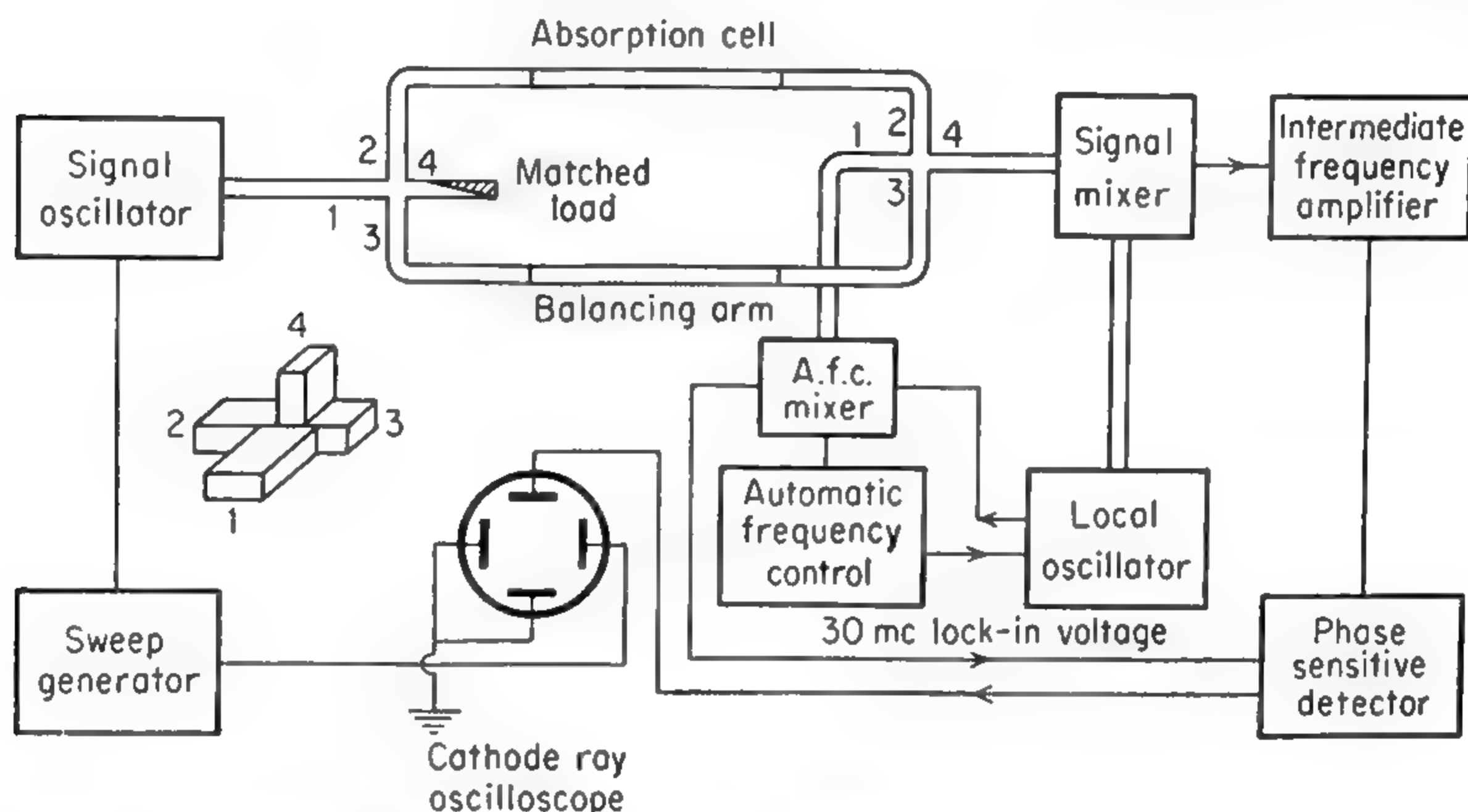


FIG. 15-8. Microwave bridge spectrograph. Many details, such as attenuators and phase shifters, have been omitted for simplicity.

through two waveguide arms. One arm is the absorption cell; the other is made as nearly identical to it as possible, although provision must be made for a final balance of phase and attenuation. A second T combines the waveguide outputs to give a voltage at the mixer which is the difference between those transmitted by the two arms. This difference signal is combined with the local oscillator in the signal mixer to produce the intermediate-frequency signal, which is then amplified by a fixed-tuned intermediate-frequency amplifier.

A second mixer combines the output of the second magic T's summation arm with the local oscillator to produce a second intermediate-frequency voltage. This signal is used as a lock-in reference voltage and also is applied to a discriminator to control the local oscillator's frequency. Finally, the output of the phase-sensitive detector is displayed on an oscilloscope or recorder.

It has been mentioned that the bridge permits the use of superheterodyne detection without overloading the intermediate-frequency amplifiers. It has the additional advantage that any signal-oscillator noise

appears equally in both bridge arms and so is balanced out. Moreover, with careful construction, reflections in the bridge arms tend to cancel although reflections outside the bridge proper do not cancel.

The bridge is more complicated to build and adjust than a modulation spectrograph. Its balance is usually good over only a small region because the two arms are never completely identical. Thus searching for unknown lines with a bridge spectrograph is very difficult. However, it is very effective in high-resolution studies of known lines, for which the absence of complications due to modulation and the ability to work with very small power levels to avoid saturation are important.

**15-9. High-resolution Spectrometers.** For some studies it is important to have as high resolving power as possible even at the expense of additional complications and reduced flexibility. At the same time it is desirable to sacrifice no more sensitivity than necessary. The principal sources of line breadth which need to be overcome or at least reduced are (*cf.* Chap. 13):

1. Collisions with other molecules (pressure broadening)
2. Collisions with the waveguide walls
3. Modulation broadening
4. Power saturation
5. Doppler broadening
6. Oscillator frequency fluctuations

Of these, items 1, 2, 4, and 5 are discussed in Chap. 13, while item 3 is described in Chap. 10.

Pressure breadth can be made as small as desired by using sufficiently low pressures. As long as the pressure width is predominant, reducing the pressure only narrows the line without decreasing the peak intensity [*cf.* Eq. (13-19)]. However, if the width is appreciably greater than that due to pressure, the peak of the observed line is proportional to the integrated intensity and so does decrease with further reduction of pressure. Thus in a high-resolution spectrograph the pressure is chosen just low enough so that it is no longer the limiting factor. Usually the Doppler width is the most difficult to reduce, so that the pressure is adjusted to give a width less than the expected Doppler width.

With such low pressures, collisions with the walls may actually be more frequent than collisions with other molecules, and so a suitably large waveguide or cavity must be chosen. Collisions with the walls are also made somewhat less frequent if molecular velocities are reduced by cooling.

As shown in Chap. 10, the use of modulation broadens the line. The width contributed by a square-wave modulation is somewhat greater than the modulation frequency because of the harmonics present in any square wave. However, the line is unable to follow modulation rates



greater than the pressure width, and so in practice a width of about two or three times the modulation frequency is produced. Thus for high-resolution spectroscopy the modulation frequency needs to be kept two or three times less than the pressure width, which in turn is a little less than the expected Doppler width. A few kilocycles is low enough for most gases unless special means are used to reduce the Doppler broadening. The use of low modulation frequencies implies relatively high crystal noise unless proportionately low microwave powers are used, since the noise power is approximately proportional to the square of the crystal current divided by the modulation frequency [Eq. (14-45)].

To avoid power saturation the energy density in the waveguide must be kept low. From Chap. 13, a power density of a few microwatts per square centimeter may produce a breadth comparable with Doppler width for some gases. With a given total power, the density is less when the waveguide is considerably larger than needed for propagation. However, a guide having a cross section more than a factor of 10 or so greater than ordinary *K*-band waveguide is likely to be inconveniently large and heavy. Thus even with oversize waveguide small total power is necessary to prevent saturation broadening. With small power, superheterodyne detection, preferably with a balanced waveguide bridge, is helpful in obtaining a good signal-to-noise ratio.

When narrow spectral lines are to be studied, the microwave oscillator frequency must be very stable. High-resolution spectroscopy usually involves measurement of frequencies to better than 1 part in a million, with correspondingly high requirements for oscillator stability. Not only must the oscillator power supplies be well regulated, but the tube must be protected against temperature variation and vibration. Air currents are the commonest source of rapid temperature fluctuations. Their effects can be greatly reduced by immersing the tube in an oil bath or by putting it in good thermal contact with a metal block, preferably of copper. With this thermal regulation and protection from vibration, a klystron can be made to stay within 1 Mc over a period of some minutes.

Better stability may be obtained by using an external cavity to control the frequency (see Chap. 17). A well-constructed cavity with temperature compensation can be used to hold frequency within 1 kc. It is also possible to stabilize a klystron by comparing its frequency with harmonics of a good crystal oscillator [*cf.* Chap. 17]. A crystal oscillator may be used to stabilize frequency even more directly by using special frequency-multiplier klystrons. They have been used at the National Bureau of Standards to give useful amounts of microwave power as harmonics of the crystal oscillator frequency [724].

**15-10. Some High-resolution Spectrometers.** A Stark modulation frequency of 6 kc has been used at Massachusetts Institute of Technology

for high-resolution spectroscopy [419], [546]. "X-band" waveguides (about 1 by  $1\frac{1}{2}$  in.) reduced collisions with walls and energy density in the waveguide ([710], but *cf.* also [788]). Both superheterodyne detection and direct crystal detection with a low-noise audio-frequency amplifier have been used with this spectrometer.

While the bridge spectrograph is more complex and less suited to searching than modulation spectrographs, its advantages for high-resolution spectroscopy with good sensitivity have been confirmed by the instrument at Columbia University [573], [688]. With this instrument, line widths not much greater than the Doppler breadth can be obtained for most molecules (*i.e.*, as narrow as 50 kc).

In its original form, the bridge operates without modulation. Its sensitivity is then limited by frequency-dependent reflections and vibration which make it difficult to maintain an accurate balance. Lines having an absorption  $\alpha$  as low as  $2 \times 10^{-8} \text{ cm}^{-1}$  have been detected. More recently the bridge has been modified by the addition of a very low frequency (about 1000 cycles) Stark modulation [930]. This has eliminated the effects of reflections and increased the usable sensitivity by about a factor of 10.

Any one gas molecule in a spectrograph has a definite velocity in the direction of propagation of the microwave signal. Its microwave absorption is displaced in frequency by the Doppler effect but not broadened. However, an actual gas contains molecules with all velocities so that the over-all absorption is a broadened average. This Doppler width can be reduced somewhat by cooling the gas since from (13-2) it is proportional to  $\sqrt{T}$ . The degree of improvement obtainable in this way is, however, limited by condensation of most molecular gases at a fairly high absolute temperature.

Any desired reduction in Doppler width can in principle be obtained by somehow selecting a group of molecules with only a small spread in velocity. There is necessarily a corresponding reduction in intensity of absorption because of the decreased number of effective molecules in the sample and the lower microwave power necessary to avoid saturation.

*Molecular Beams for Microwave Spectroscopy.* One method of accomplishing the above type of selection which has been applied in optical spectroscopy is the method of molecular-beam absorption [238]. The molecules are confined by collimating slits to a narrow beam through which the radiation passes transversely. Then there are no molecules having more than a very small component of velocity in the direction of propagation and so the line width is reduced in proportion to the degree of collimation. Doppler widths can rather easily be reduced by a factor of 10 this way [869a], [925], [982].

Johnson and Strandberg have constructed a microwave molecular-beam spectrograph [709]. A plane wave from a linear array antenna was passed



transversely through a molecular beam. After passing through the molecular beam, the wave was reflected back into the antenna. A magic 'T' separated the reflected wave from the incident power. Stark modulation of 660 cycles was provided by electrodes on opposite sides of the beam. A line width (total width at half maximum) for the ammonia 3,3 line of 40 kc was obtained, whereas the Doppler breadth was 70 kc. Considerably narrower lines were obtained by a later beam spectrometer [982]. However, the power needed to avoid saturation and the density of

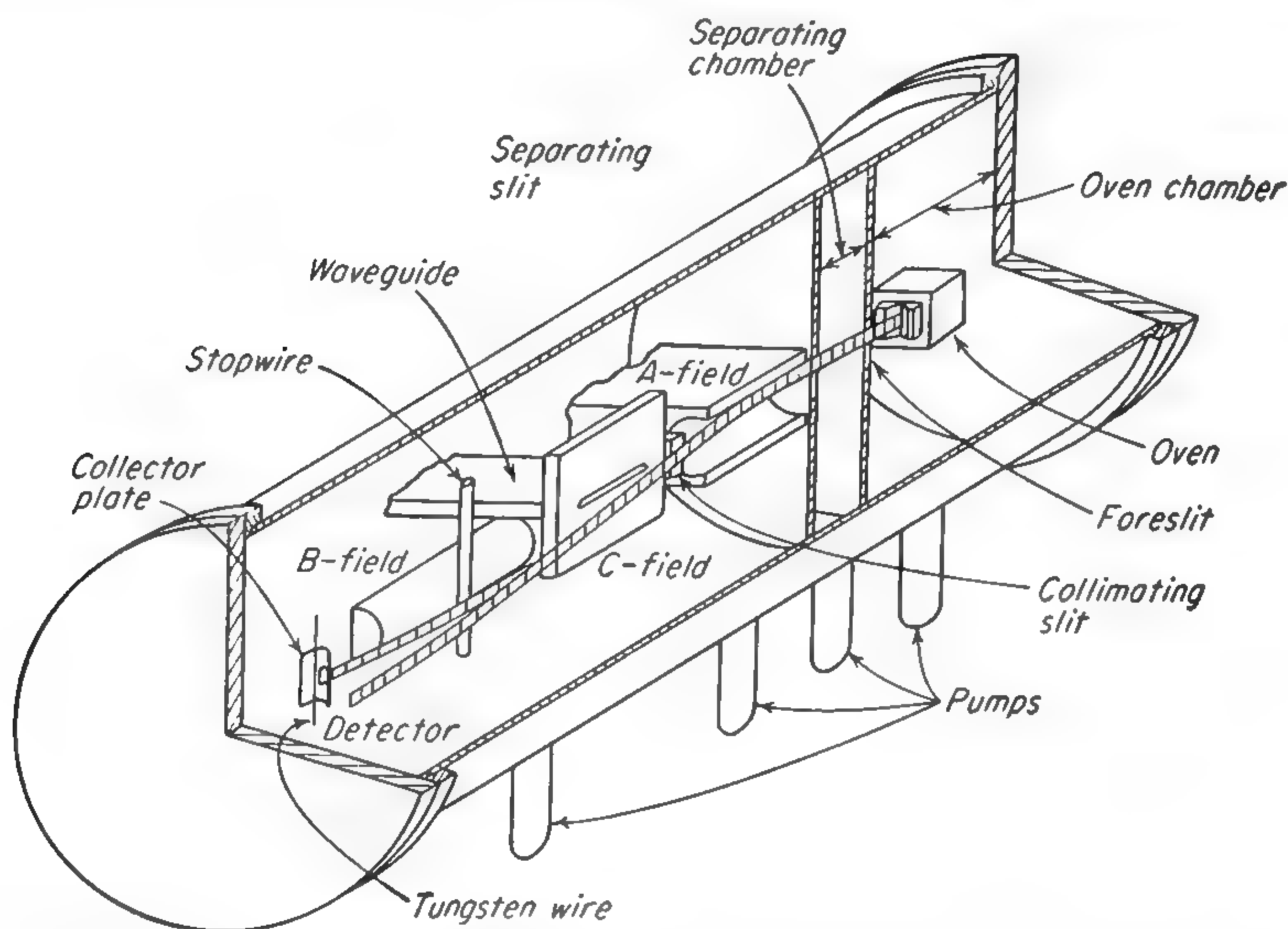


FIG. 15-9. Molecular-beam-resonance apparatus. (From Lee, Fabricand, Carlson, and Rabi [835].)

molecules obtainable in the beam are so low that only the strongest microwave lines could be observed.

Molecular beams can be, and most often are, used in spectroscopy in arrangements such that the resonance absorption of radiation is detected by its effect on the absorbing molecule rather than on the radiation. This type of technique has been extensively developed, particularly at frequencies somewhat lower than those in the microwave region, and has given a large amount of valuable information [163], [969a]. We shall not attempt any complete summary of this type of spectroscopy but shall rather try to indicate briefly the general principles involved and how this technique compares with more usual forms of microwave spectroscopy.

Figure 15-9 shows the arrangement of a typical molecular-beam deflection and resonance experiment. The molecules to be studied are evaporated in an oven and emerge through a narrow slit into a good vacuum. The beam is defined by one or more slits and then passes through two



deflecting fields marked *A* and *B* in the diagram. These are nonuniform electric (or magnetic) fields, the gradient of which acts on the electric (or magnetic) dipole moment to provide a force deflecting the molecule.

A molecule in an electric or magnetic field has a potential energy which is given by the Stark or Zeeman effects (*cf.* Chaps. 10 and 11) and which depends on the field strength and on the particular quantum state. Since the potential energy is dependent on the field strength, a varying or inhomogeneous static field exerts a force on the molecule and hence may deflect its path.

If the *A* and *B* fields are equal and oppositely directed their deflections can cancel each other, and the molecules can reach a detector placed in line with the beam's original direction. A stop wire in front of the detector excludes those molecules in states which are not appreciably deflected by the fields.

In the space between the two fields there is a region in which a uniform radio-frequency field and a steady field are applied. If the radio frequency is that corresponding to the energy difference between two molecular states, some of the molecules will make an induced transition in the *C*-field region. These molecules will have different quantum numbers and hence a different energy and accelerating force in the *B*-field region. Thus the molecules which have undergone a transition do not receive equal and opposite deflections in the *A* and *B* fields and so do not reach the detector. Alternatively, the fields can be arranged so that only the molecules which have undergone the transition reach the detector.

In either case, the resonance is indicated by a change in the number of molecules reaching the detector. For alkali metals and some others with low ionization potentials, the detector can be a hot tungsten wire, from which the incident atoms evaporate as ions [163]. A more complicated, but more generally applicable, detector introduced by Lew and Wessel [886a] uses a transverse electron beam to ionize the molecules. For each quantum absorbed, the path of a molecule in the beam is changed, so that one molecule more (or less, depending on the experimental arrangement) reaches the detector. This exchange of a quantum of radiation for a molecule becomes increasingly advantageous as the frequency is lowered, for the energy in the quantum is proportional to the frequency. At higher frequencies the advantage in sensitivity of this technique is not so marked, and the detection of quanta emitted or absorbed rather than deflected molecules becomes relatively more profitable.

The beams used in these resonance experiments are so narrow and unidirectional that the Doppler effect can be eliminated to a large extent. The chief limitation on resolving power is usually the transit time through the *C* field. This time is ordinarily about  $10^{-4}$  sec, and leads to a line

width of a few kilocycles. At microwave frequencies the line width will be much less than that given by ordinary Doppler effect only if the microwave field in the  $C$  region is approximately constant in amplitude and phase over a distance along the beam path which is greater than the wavelength in free space. This can be achieved by passing the beam parallel to the broad face of a very broad rectangular waveguide in the  $TE_{01}$  mode, or parallel to the axis of a waveguide near cutoff so that the wavelength in guide has been increased. The line width can also be reduced by using two radio-frequency fields separated by some distance [857], or by selecting the slowest molecules which therefore spend the longest time in the  $C$  region.

The resolving power of molecular-beam resonance experiments can be greater than that of most absorption microwave spectroscopy. However, the detected signals are often very weak so that the location and measurement of a spectrum is usually a slow process. The method is therefore particularly adapted to high-resolution work and might well be used to give detailed information about lines which have been located by absorption spectroscopy. In addition, in common with all methods employing beams, it does not require that the molecule studied be particularly stable, or that it have appreciable vapor pressure at ordinary temperatures.

A spectroscopic device which borrows from both molecular-beam deflection techniques and microwave absorption spectroscopy has been described by Gordon, Zeiger, and Townes [925]. This device can be used as a high-resolution spectrometer, or as a very stable microwave oscillator and frequency standard. The name "maser," an acronym for "microwave amplification by stimulated emission of radiation," has been given to this general type of device. A schematic indicating the general operation of the molecular beam maser is shown in Fig. 15-10.

A gas ( $NH_3$  in the illustration) issues from a number of small holes in a chamber at a pressure of about 1 mm Hg into a region where the vacuum is sufficiently low that a beam is formed. The beam enters a focusing region where inhomogeneous fields are arranged to deflect molecules in an upper state toward the axis and those in the lower state away from the axis. Thus a beam of molecules which are largely in an excited state is made to enter a cavity which is tuned to the resonant frequency  $W/h$ .  $W$  is of course the energy difference between the ground and excited states being considered. If a small amount of microwave power of frequency  $W/h$  is introduced into the cavity, it will react strongly enough with the molecules to make them give up their energy, which then increases the flow of power from the cavity into the output waveguide. The increased power occurs only if the microwave introduced is very near the resonant frequency, so that its occurrence indicates the presence of a molecular resonance. Therefore, as the frequency of the

microwave input power is varied, one may pass over one or more resonances and obtain a spectrum of the molecules.

The field in the focusing region comes from a potential of the approximate form [cf. [572a)]

$$V = V_0 + axy$$

where  $V_0$  and  $a$  are constants. The equipotentials are hyperbolas which, for the case of an electrostatic potential, are approximated by the inner

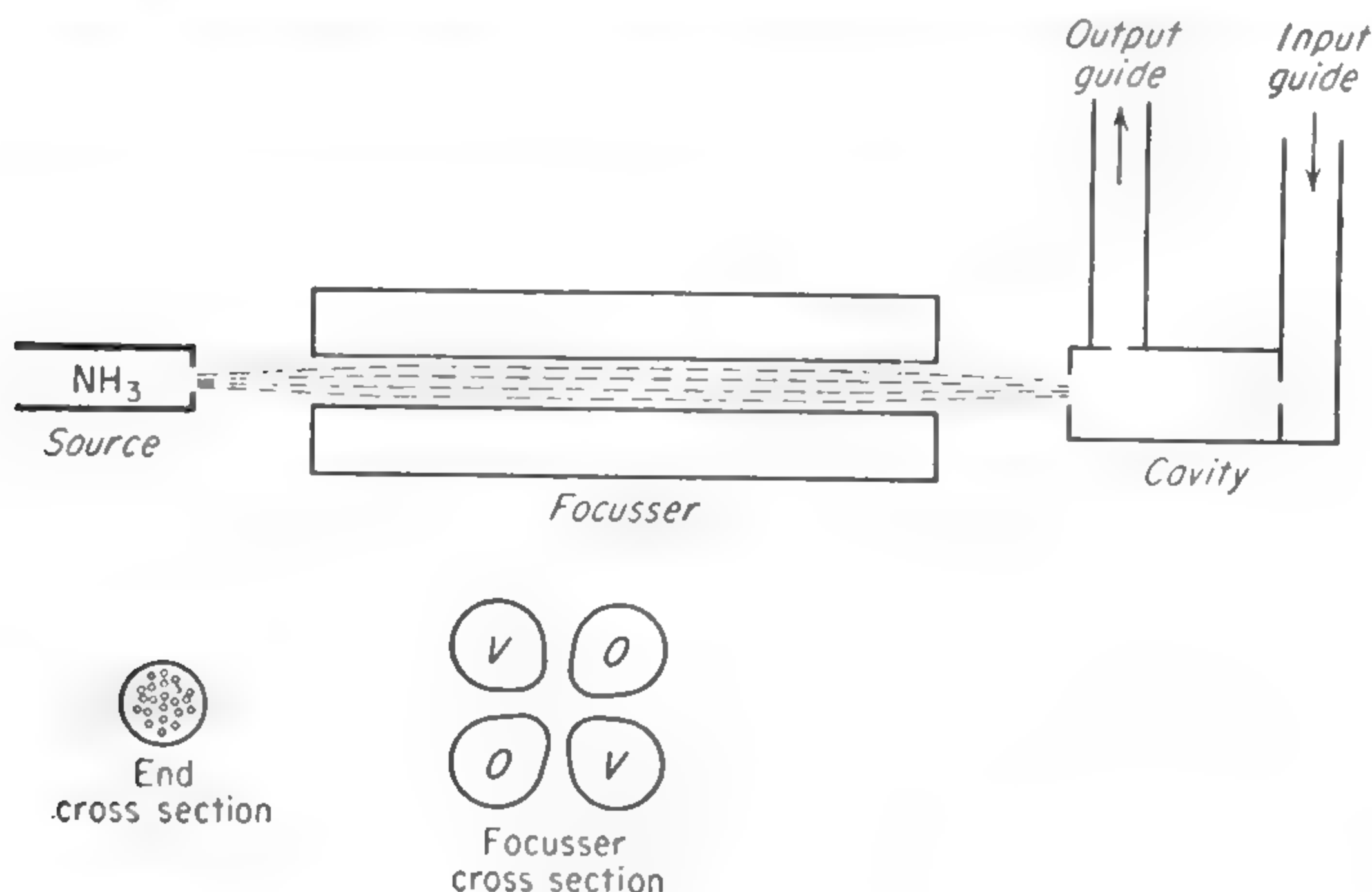


FIG. 15-10. Molecular-beam-emission spectrometer and oscillator (maser). (From Gordon, Zeiger, and Townes [925].)

surfaces of the four focusing electrodes. The  $x$  component of the electric field is  $-\frac{\partial V}{\partial x} = -ay$  and the  $y$  component is similarly equal to  $-ax$ . Hence the magnitude of the electric field is

$$|E| = |a| \sqrt{x^2 + y^2} = |a|r$$

where  $r$  is the distance from the axis. Therefore, if the Stark effect is such that the energy increases with increasing magnitude of  $E$  (as for the excited inversion level of  $\text{NH}_3$ ) the molecule is accelerated toward the axis with a force dependent only on  $r$  and not on its angular position with respect to the electrodes. If the molecule does not have too high a velocity perpendicular to the axis, it may be regarded as trapped in a potential well with a minimum on the axis. The molecule is brought back to its original displacement from the axis or focused after a distance of travel which depends on its axial velocity, the strength of the field  $E$ , the molecular dipole moment, and the quantum state involved. Molecules with a Stark energy which decreases with increasing field (as for the ground inversion level of  $\text{NH}_3$ ) are deflected away from the axis and hence would not in most cases enter the cavity. A number of other forms



of fields may be used for similarly directing molecules in selected states into a cavity.

This type of device allows high resolution because the molecules whose transitions are detected are traveling more or less in one direction along the axis of the apparatus and Doppler effect can therefore be reduced. If the cavity is of such a diameter that it is very near cutoff for the microwave frequency, the wavelength in the cavity is considerably greater than the free-space wavelength, and the Doppler effect is reduced.  $\text{NH}_3$  lines as narrow as 7 kc have been obtained by this method, which represents a reduction of the Doppler width by a factor of 10.

Such a spectrometer may be used to detect either emission or absorption of microwaves, depending on whether the upper or lower state of a transition is best focused into the cavity. If the upper state is focused, emission of microwave energy is detected, and the device acts as a microwave amplifier, since somewhat more energy may be emitted from the cavity than is introduced into it.

The intensity of the induced emission, and hence the amount of amplification, increases with an increasing number of molecules in the beam. If the beam gives a sufficiently large flow of molecules and the  $Q$  of the cavity is sufficiently high, the amplification may become infinite and radiation is emitted without any input microwave energy. Under such conditions the device is a very stable microwave oscillator with power being supplied from the molecular excitation, and with a frequency primarily determined by the molecular resonance.

The signal obtained by this device from the strongest ammonia lines is approximately  $10^{-9}$  watt, which is as much as a few thousand times noise in a well-designed spectrometer system. Its output power as an oscillator, which is the same  $10^{-9}$  watt, is not large, but it is large enough to serve as a frequency standard (see Sec. 17-7).

*Stark-wave Spectrograph.* Newell and Dicke [622] have found a method of selecting only those molecules in a gas within a small range of velocities in the direction of microwave propagation. A special electric field is used which is periodic in the direction of microwave propagation with the wavelength,  $\lambda/2$ , where  $\lambda$  is the microwave length. It is equivalent then to a forward and a backward Stark field traveling wave each with velocity  $\Omega\lambda/2$  where  $\Omega$  is the Stark wave frequency. The Stark modulation provides a regular variation in phase of the reflected wave so that those molecules moving with either Stark wave reflect energy coherently in the backward direction. Others produce reflections with random phases which are much weaker. Widths as low as 7 to 10 kc have been achieved in this way for the ammonia 3,3 line. The theoretically obtainable sensitivity of this device is less than that of other spectrometers by approximately the square of the ratio of line width to Doppler width, so that only rather strong microwave lines can be observed. However, in

some cases the higher resolution may be extremely valuable. Fig. 15-11 is a schematic of the apparatus.

**15-11. Cavity Spectrographs.** Microwave absorption can be detected by its effect on the resonance of a cavity. When an absorbing

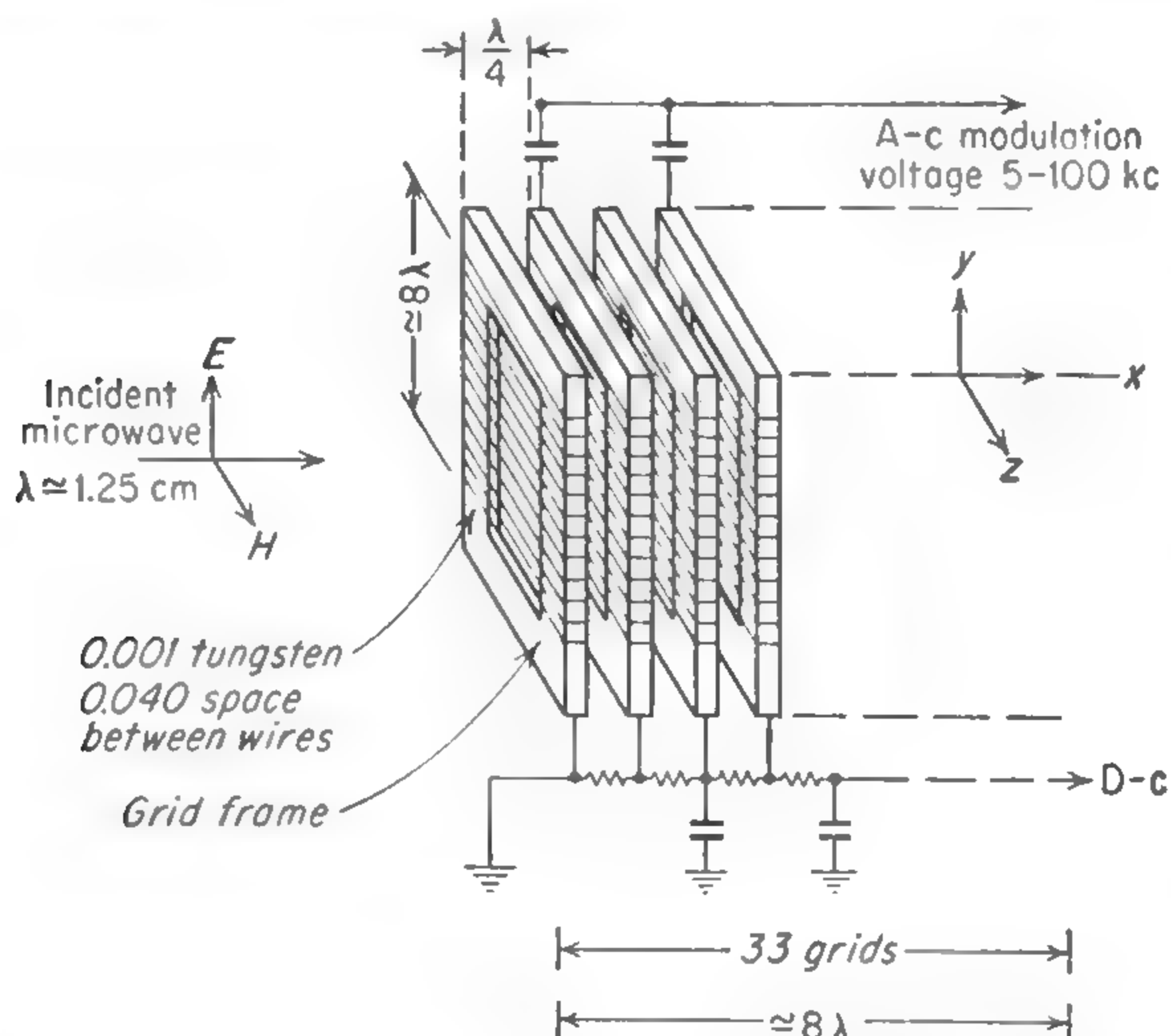


FIG. 15-11. Stark-wave spectrograph cell. (From Newell and Dicke [622].)

gas is present, the losses in the resonator are thereby increased, so that its quality factor  $Q$  is decreased. This change is shown either by a decrease in the relative amplitude of a wave transmitted through the cavity, or by a change in the wave reflected by the cavity into a waveguide coupled to it.

If the absorption line is narrower than the cavity resonance, it may be displayed by sweeping a microwave oscillator connected to the cavity through the resonance curve. Figure 15-12 shows the pattern observed with a detector and oscilloscope arranged to display either the transmitted or the reflected power. The absorption is obtained as the difference between the curves with and without the absorber. Very wide lines, as in gases at high pressures, can be studied by tuning the cavity to a number of frequencies in the line's width. At each point the change in  $Q$  is observed as a change in relative height or width of the cavity resonance when the gas is introduced, and from it the absorption is deduced [179]. Of course, if the effective absorption at a particular frequency can be removed by a suitable electric or magnetic field as in a Stark spectrograph,

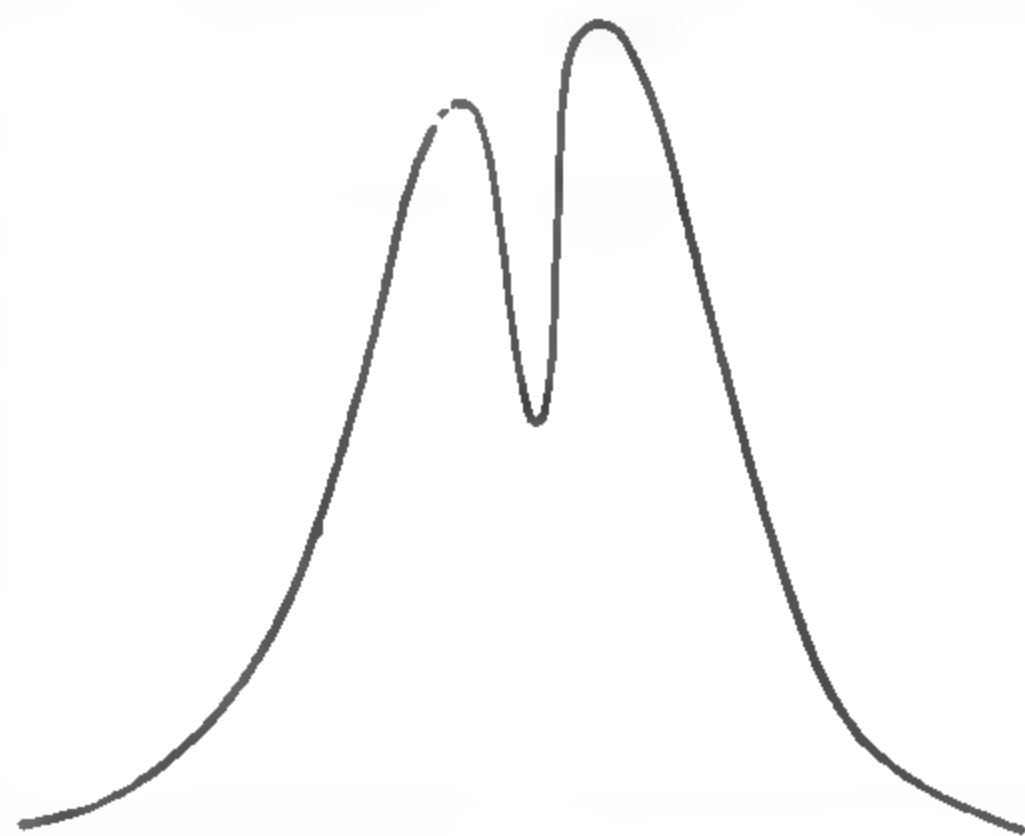


FIG. 15-12. Oscilloscope pattern with resonant cavity spectrograph and sharp absorbing line.

this can be used as an alternative to actual removal of the absorber from the cavity.

Whether used for narrow or broad lines, the cavity may be considered as a short section of waveguide in which microwave radiation is reflected back and forth many times before emerging. The effective number of reflections or the effective path in wavelengths is of the order of  $Q$ . The radiation finally emerges either from the input hole, in which case the cavity is used in reflection, or from another hole after transmission through the cavity. Although the external microwave circuits differ considerably in the two cases, there is little essential difference in the operation of the cavity. We shall consider further a reflection cavity coupled by a single hole.

As in Chap. 14, the quality factor  $Q$  of the resonator is defined as  $2\pi \times (\text{average energy stored})/(\text{energy lost per cycle}) = 1/\delta$ , where  $\delta$  is a loss factor.

When the cavity is coupled to a waveguide,  $\delta$  is increased an amount  $\delta_1$  by the energy loss through the coupling hole. The reflection factor  $\Gamma_0$  in the waveguide for an empty cavity, defined as the ratio of the complex amplitudes of the incident and reflected waves, and for frequencies  $\nu$  near the resonant frequency  $\nu_0$ , is [291]

$$\Gamma_0 = \frac{2\delta_1}{\delta_1 + \delta_0 + 2j[(\nu - \nu_0)/\nu_0]} - 1 \quad (15-11)$$

where  $\delta_0$  is the energy loss due to the cavity walls and  $j = (-1)^{1/2}$ . When a gas with complex dielectric constant  $\epsilon = \epsilon' - j\epsilon''$  is introduced (where usually  $\epsilon'' \ll \epsilon' \approx 1$ ), the resonant frequency is shifted to  $\nu_0/\epsilon^{1/2} \approx \nu_0/\epsilon'^{1/2}$  and  $\delta_0$  is increased to  $\delta_0 + \epsilon''$ , so that the reflection factor becomes

$$\Gamma_\theta = \frac{2\delta_1}{\delta_1 + \delta_0 + \epsilon'' + 2j[(\epsilon'^{1/2}\nu - \nu_0)/\nu_0]} - 1 \quad (15-12)$$

The fractional change in voltage amplitude of the reflected wave at resonance  $\nu = \nu_0$  or  $\nu = (\epsilon')^{1/2}\nu_0$  is then

$$\frac{\Delta V}{V_0} (\Gamma_0 - \Gamma_\theta)_{\text{res}} = \left[ \frac{2\delta_1}{(\delta_1 + \delta_0)^2} \right] \epsilon'' \quad (15-13)$$

For a given  $\delta_1$ ,  $\Delta V/V_0$  is maximum when  $\delta_1 = \delta_0$ . If

$$\begin{aligned} \delta_1 + \delta_0 &= \delta = \frac{1}{Q} \\ (\Delta V)_{\text{max}} &= Q\epsilon'' V_0 \end{aligned} \quad (15-14)$$

This voltage change may be expressed in terms of the free-space attenuation  $\alpha$  of the gas by using the relation

$$\alpha = \frac{2\pi}{\lambda} \frac{\epsilon''}{\epsilon'^{1/2}} \approx \frac{2\pi}{\lambda} \epsilon'' \quad (15-15)$$



where  $\lambda$  is the free-space wavelength. Then

$$(\Delta V)_{\min} = \frac{Q\lambda}{2\pi} V_{0\alpha} \quad (15-16)$$

The minimum detectable absorption is obtained by setting  $(\Delta V)_{\min}$  equal to the thermal rms noise voltage  $(4kTN \Delta\nu Z_0)^{1/2}$  so that

$$\alpha_{\min} = \left( \frac{4kTN \Delta\nu}{P_0} \right)^{1/2} \frac{2\pi}{Q\lambda} \quad (15-17)$$

where  $k$  = Boltzmann's constant

$T$  = absolute temperature

$N$  = noise figure, or factor by which the noise exceeds thermal noise

$\Delta f$  = frequency band width of the amplifiers

$P_0$  = power reflected from the cavity

For a cavity made of waveguide with attenuation  $\alpha_0$  per unit length, the factor  $2\pi/Q\lambda$  becomes approximately  $\alpha_0$ , so that (15-17) is closely equivalent to (15-10), and the limit of sensitivity for a cavity spectrometer is much the same as that for one using a waveguide ( $10^{-9}$  to  $10^{-8}$  in typical cases).

The factor  $Q\lambda/2\pi$  in Eq. (15-16) is the equivalent absorption-path length in free space. Since  $Q$  can be quite large, very long effective path lengths can be obtained in a small space. This property is particularly advantageous for experiments on Zeeman effects in ordinary molecules, where the necessary large magnetic fields can only be obtained over a small volume. However, spectrometers using small cavities tend to have much more difficulty with saturation than do those using waveguide absorption cells. Because of the smaller volume in which absorption takes place, field strengths are higher in the cavities and each molecule must absorb more energy.

For high sensitivity  $Q$  should be as large as possible. If the absorption line is to be displayed within the width of the cavity resonance, the usable value of  $Q$  is limited by the need for a resonance wide enough to include the entire line and perhaps its fine structure. Thus  $Q$  must be several times less than  $\nu/\Delta\nu$  where  $\nu$  is the frequency of the line, and  $\Delta\nu$  its half width at half maximum. It is convenient to use a tunable cavity large enough so that resonances can be obtained in several modes with different  $Q$ 's to suit individual lines.

As with the Stark modulation spectrograph, the bandwidth of the amplifiers following the crystal detector must be great enough to reproduce the line shape but small enough to give low noise. If the absorption line is swept out in a time  $1/t$ , then for accurate reproduction of the line shape the bandwidth in cycles per second must be as large as about  $20/t$ .

The microwave circuits used in cavity spectrographs resemble those

used for cavity wavemeters ([221], pp. 308–318). When the cavity is used by transmission an arrangement similar to that of Fig. 15-13 is needed, and the instrument then resembles the simple waveguide absorption spectrograph of Fig. 15-1. This type of instrument without the sweep and oscillograph can be used for studying the pressure-broadening of strong lines [179].

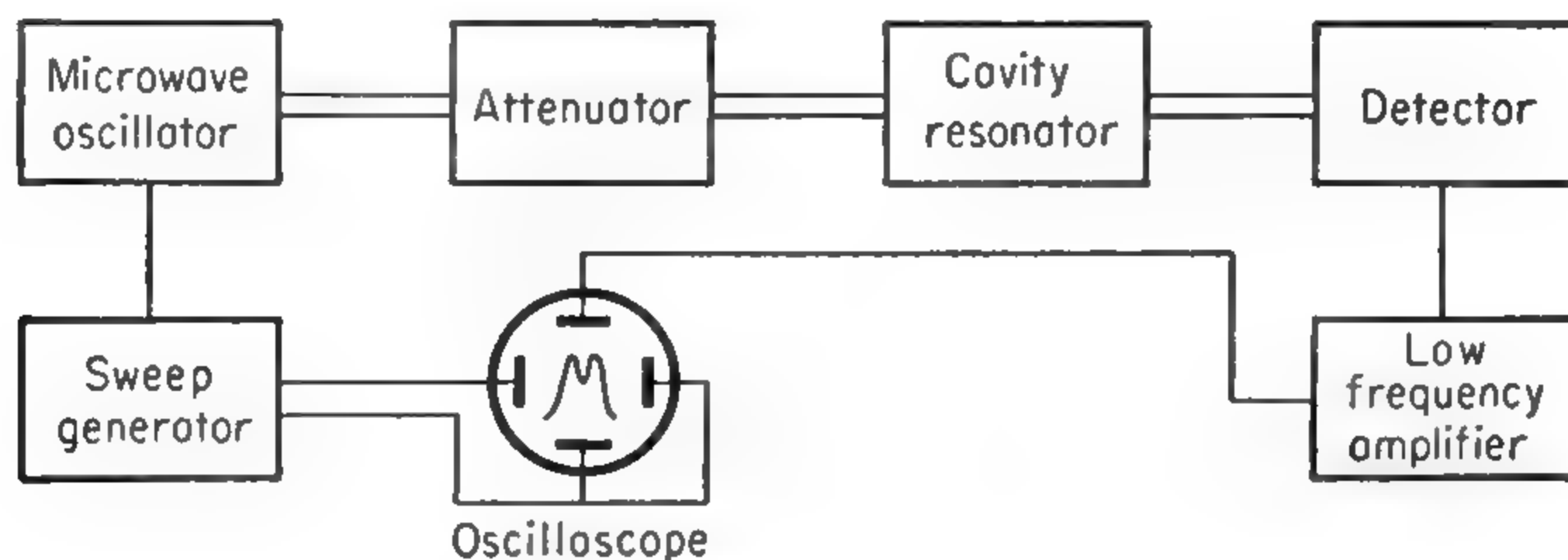


FIG. 15-13. Simple microwave cavity transmission spectrograph.

The simple cavity spectrograph is, like its waveguide prototype, limited in sensitivity by crystal noise. The same remedies of source modulation, field modulation, and superheterodyne detection are effective when they can be applied. Stark modulation is not so easily obtained as in a waveguide without disturbing the microwave fields, because the fields of the cavity modes usually employed are more complicated than those involved in waveguide transmission. For paramagnetic gases, weak-field Zeeman modulation by an external solenoid or short coils is satisfactory [642],

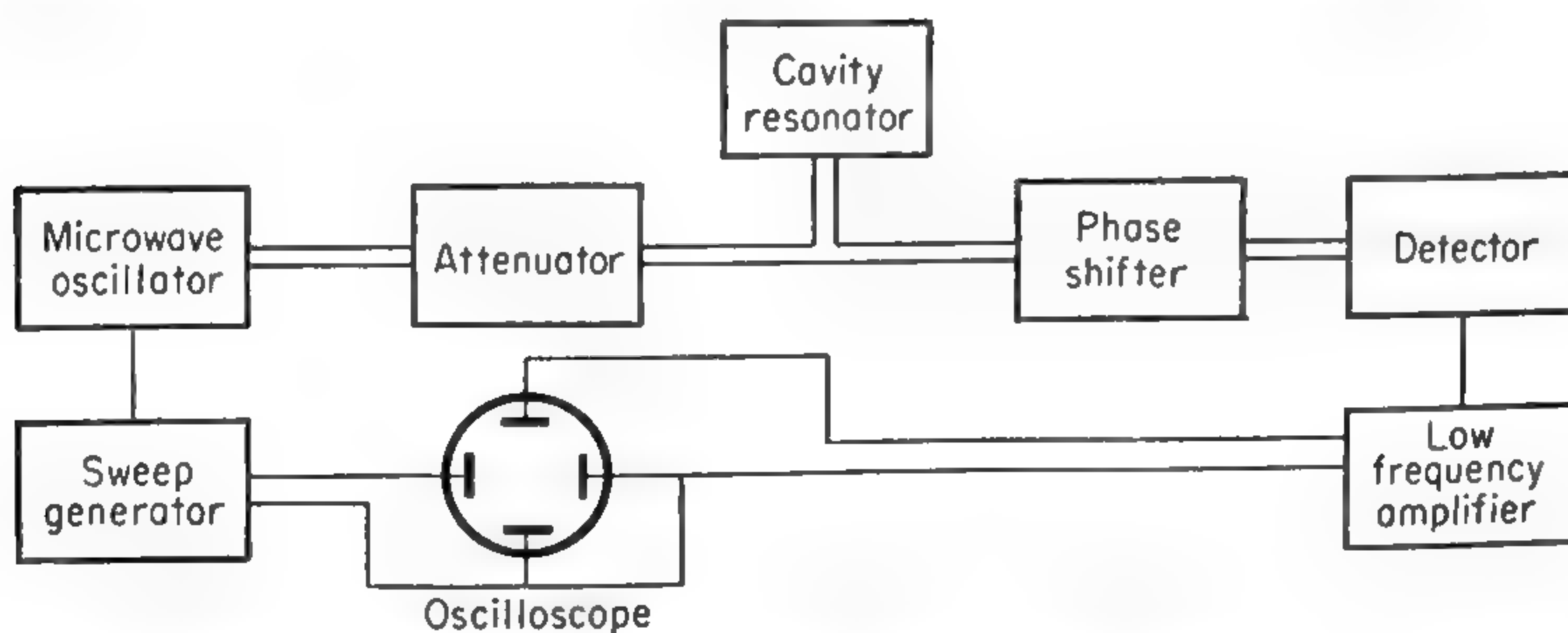


FIG. 15-14. Simple microwave cavity reflection spectrograph. The detector and resonator may be interchanged.

[643], [435], [558], although eddy currents in the walls usually limit the modulation to relatively low frequencies.

In reflection spectrographs the cavity may be placed on either the side or the end of a waveguide. When placed on the side as in Fig. 15-14, a resonance in the cavity changes an effective impedance in parallel with the guide and so affects the power reaching a detector at the end. Depending on the phase of the cavity reflection relative to the standing-

wave pattern in the guide, the detector power may increase or decrease at resonance; *i.e.*, the change in impedance of the cavity at resonance may either partially cancel reflections already existing in the waveguide or may add to them. At certain positions along the guide the resonance may have very small effect, but such difficulties may be avoided if necessary by the use of a phase-shifting adjustment between the cavity and the detector.

With only low modulation frequencies available and power limited by the need for avoiding saturation, superheterodyne detection is helpful in obtaining a good signal-to-noise ratio. It is then necessary that most of the carrier be balanced out before reaching the second detector, in

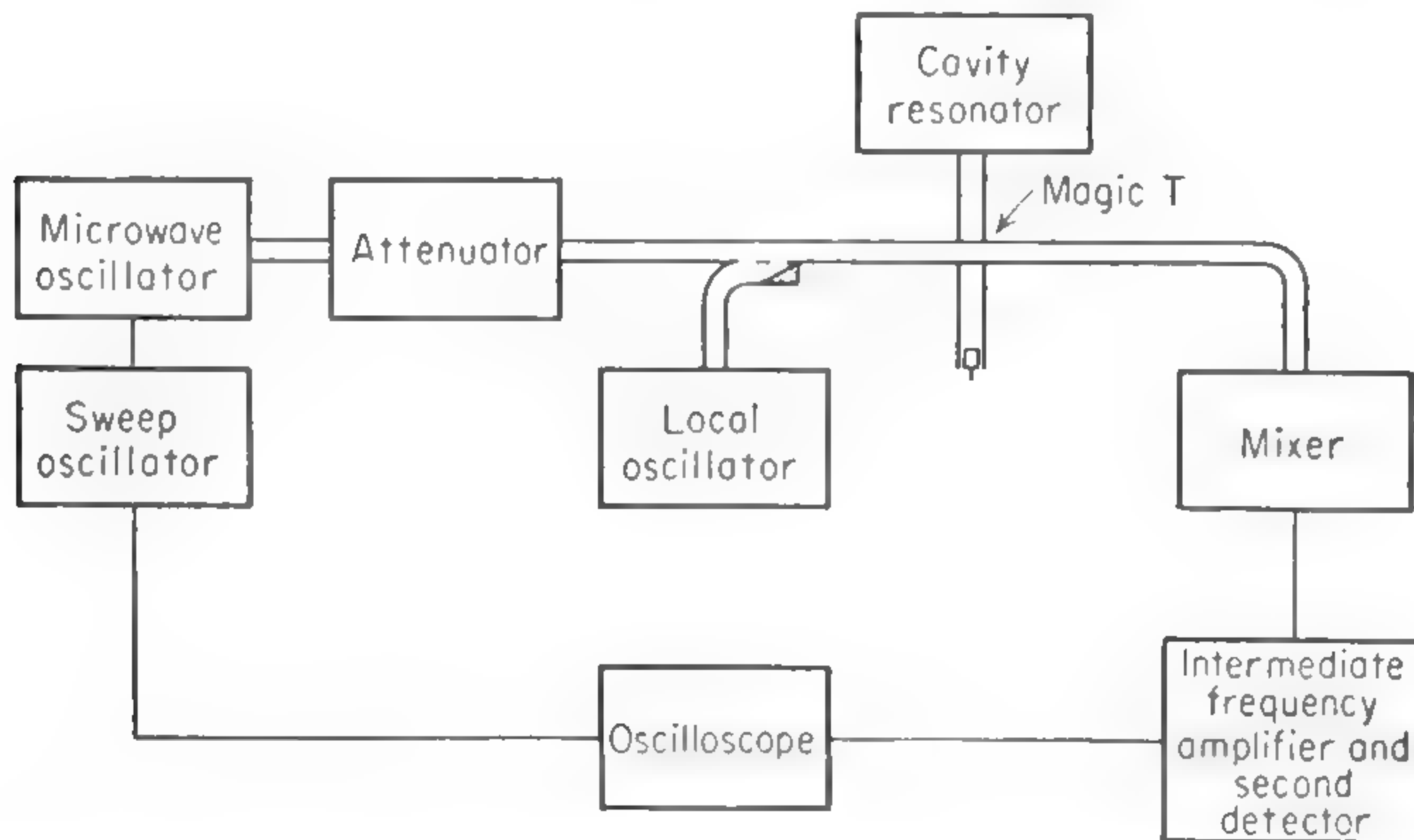


FIG. 15-15. Reflection cavity spectrograph with superheterodyne detection.

order that the intermediate-frequency amplifiers will not be overloaded. The balancing can be accomplished by a waveguide bridge. Partial balancing can be obtained with a magic T having a movable plunger in one arm and the cavity in another, as in Fig. 15-15 [291].

**15-12. Large Untuned Cavity.** Since the  $Q$  factor of a cavity is the ratio of energy stored to energy lost in the cavity walls, it is very large for a large cavity which has a high volume-to-area ratio. Nevertheless, such a cavity does not usually show a sharp resonance because many modes are excited simultaneously. Therefore its  $Q$  cannot be measured by the shape of the resonance curve.  $Q$  can be obtained, however, either from the decay time constant when the cavity is excited by a pulse, or by a measurement of the energy density in the cavity for a given exciting power.

Both methods involve sampling the energy in the cavity at a sufficient number of points to get a good average energy density. The sampling is carried out by a large number of detectors [137], such as strings of fine-wire bolometers [338] arranged at random in the cavity (Fig. 15-16). The thermal detectors need to have a sufficiently short time constant



that they will respond to changes in cavity energy density as the oscillator is tuned, or to modulation in oscillator power if that is used.

To ensure that many modes are excited and good average energy densities are measured, a metal-bladed fan, or "mixer," may be rotated in front of the input coupling horn. The incoming microwaves are reflected from the fan in varying directions as it rotates. Only when a large number of different modes are excited simultaneously is the response of the detectors proportional to  $Q$  [165].

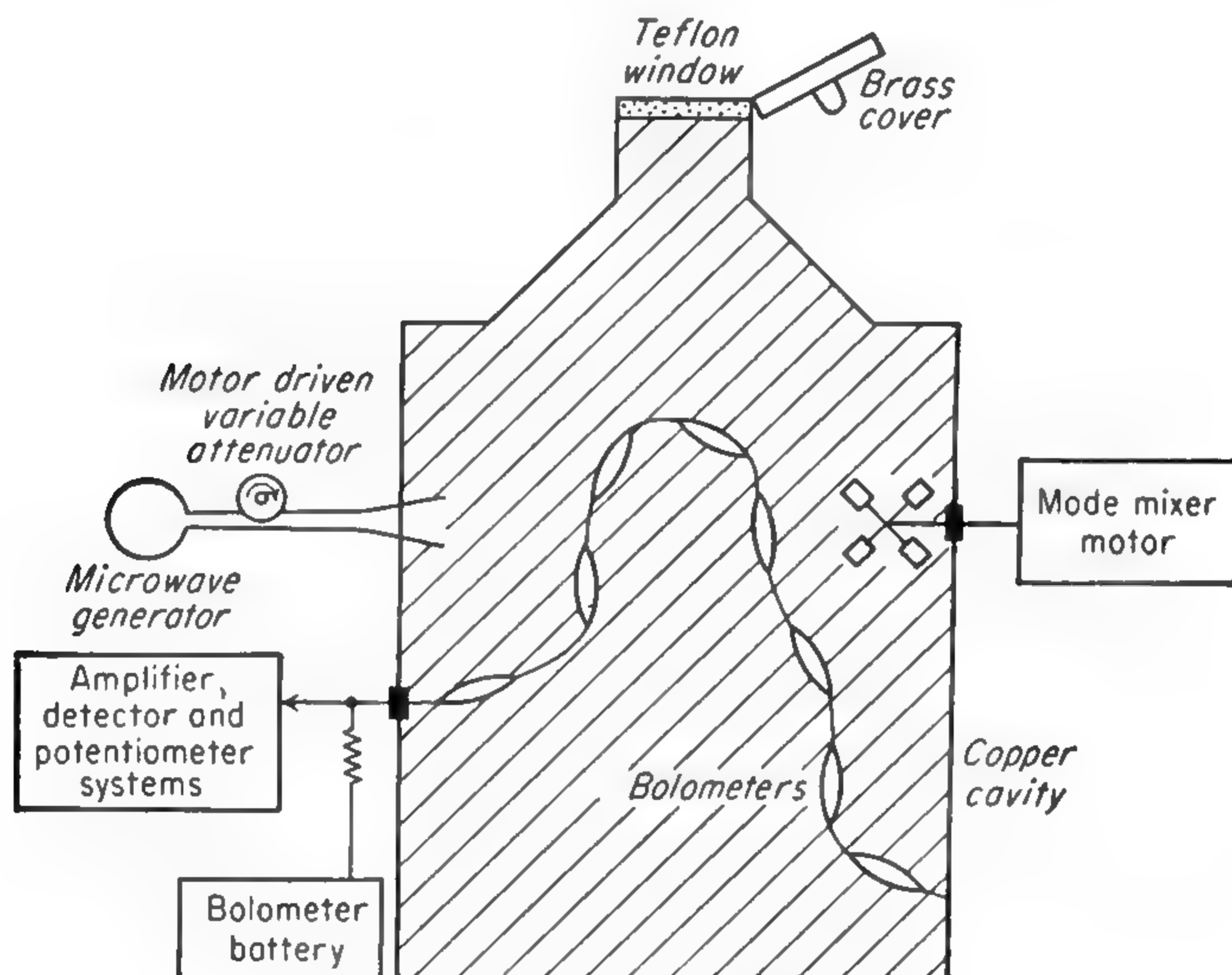


FIG. 15-16. Untuned cavity spectrograph.

This  $Q$  can be considered as being controlled by losses from three sources, to each of which we may attribute a separate  $Q$ .

1.  $Q_c$ : Losses in the walls and fittings of the cavity and through the coupling holes
2.  $Q_g$ : Losses in absorbing gas
3.  $Q_A$ : Losses through an aperture which can be opened in the cavity

Then the total  $Q$  is given by

$$\frac{1}{Q} = \frac{1}{Q_c} + \frac{1}{Q_g} + \frac{1}{Q_A} \quad (15-18)$$

$Q_g$  can be deduced by comparing expressions for the decay of a microwave pulse in the cavity viewed as a lossy cavity and as absorption of a microwave traveling through a lossy medium.

$$\left. \begin{aligned} W &= W_0 e^{-\omega t / Q_g} \\ &= W_0 e^{\alpha x} = W_0 e^{-\alpha c t} \end{aligned} \right\} \quad (15-19)$$

where  $c$  is the velocity of light,  $t$  is the time,  $\alpha$  is the absorption coefficient

in units of reciprocal length, and  $x$  is the path length in the vapor. Then

$$\frac{1}{Q_c} = \frac{\lambda\alpha}{2\pi} \quad (15-20)$$

which demonstrates that the absorption in the cavity is equivalent to that of a free-space path length of  $Q\lambda/2\pi$ .

The loss through the aperture is expressed by  $Q_A$  which, if its area is large enough to avoid diffraction effects but small in comparison with the wall area, is given by [165]

$$Q_A = \frac{8\pi V}{\lambda A} \quad (15-21)$$

where  $V$  is the volume of the box and  $A$  is the area of the hole. Thus

$$\frac{1}{Q} = \frac{1}{Q_c} + \frac{\lambda\alpha}{2\pi} + \frac{\lambda A}{8\pi V} \quad (15-22)$$

The response of the detectors is proportional to  $Q$ , with a constant of proportionality determined by the input power and the detector sensitivity. Let  $E_1$  be the detector output voltage with the cavity empty and the aperture closed,  $E_2$  be the output voltage with the aperture open, and  $E'_1$  and  $E'_2$  be the corresponding quantities after the absorbing sample has been admitted to the cavity. Then from the above equations

$$Q_c = \left( \frac{E_1 - E_2}{E_2} \right) \frac{8\pi V}{\lambda A} \quad (15-23)$$

and

$$\alpha = \frac{A}{4V} \left( \frac{E'_2}{E'_1 - E'_2} - \frac{E_2}{E_1 - E_2} \right) \quad (15-24)$$

If the absorption lines are not too broad,  $E_1$  and  $E_2$  can be measured without removing the sample by using a nearby frequency where the absorption is small.

The large cavity has not been much used because it is slow and cumbersome for general work. However, it is particularly suitable for measurements of absolute intensities and line widths.

**15-13. Spectrographs for Measurements of Zeeman Effect.** The type of spectrograph needed for Zeeman studies depends largely on the sensitivity of the particular molecule's frequencies to a magnetic field, *i.e.*, on the magnitude of the Zeeman effect. Paramagnetic molecules like  $O_2$ ,  $NO_2$ , and  $ClO_2$  which exhibit a large Zeeman effect can be conveniently studied in magnetic fields of only a few oersteds. Stark modulation [615] can be used for most paramagnetic molecules, with an additional small magnetic field provided by a long single-layer solenoid enclosing the waveguide. For these same molecules, Zeeman modulation is an alternative method of sensitive detection, while for  $O_2$  it is the only

method of modulation because the molecule has no electric dipole [441]. For high-field studies of paramagnetic molecules and for nonparamagnetic molecules which require large magnetic fields, a cavity is advantageous because of its small volume [435], [291].

For paramagnetic molecules, the cavity need not be tunable. Since the Zeeman effect is so large, individual Zeeman components can be brought to the desired frequency by varying the magnetic field [435], [558]. This gives a rather different view of the spectrum, however, than that obtained by varying the frequency of observation until an absorption line is found, and then applying a weak magnetic field to produce a small Zeeman splitting.

A moderately strong magnetic field can be obtained economically over the length of an ordinary waveguide absorption cell either by coiling the cell [371] or by using special pole pieces, long and narrow like the waveguide [683]. With a magnetic field transverse to the direction of propagation, it may still be either parallel or perpendicular to the microwave electric vector. In the former case,  $\pi$  components ( $\Delta M = 0$ ) are observed, while the second arrangement gives the  $\sigma$  components

$$(\Delta M = \pm 1)$$

A longitudinal field, as from a solenoid, is always perpendicular to the microwave electric vector if the principal mode is being used, and so gives  $\sigma$  components.

The signs of the nuclear and molecular magnetic moments cannot be determined as long as linearly polarized microwaves are used, because the Zeeman patterns are symmetrical; *i.e.*, the Zeeman pattern consists of pairs of lines equally displaced in frequency from the zero field position, and of equal intensity. In order to determine the sign, circularly polarized microwave fields in a square or circular guide may be used since circularly polarized radiation carries angular momentum [681], [683].  $\Delta M = +1$  transitions occur when the microwave electric vector rotates in a clockwise direction when viewed by a person looking in the direction of the longitudinal magnetic field. If the direction either of rotation or of the magnetic field is reversed,  $\Delta M = -1$  transitions occur.

The circular polarization can be obtained by a suitable length of waveguide having rhombic (or elliptical) cross section, connected to square waveguide by tapered sections. Such a rhombic waveguide can support modes in which the electric vector near the center is parallel to either the long or the short diagonal. These modes have different phase velocities and so different guide wavelengths,  $\lambda_g$ . If the length of the rhombic guide is chosen so that one wave lags  $90^\circ$  in phase behind the other, the emergent wave is circularly polarized. Adjustment can be made by squeezing the polarizing section and thus varying the phase difference between the two components of the wave.



If Stark effect is used to obtain high sensitivity in an absorption cell supporting a circularly polarized microwave, the usual flat septum must be avoided since it will disturb the microwave field distribution. The Stark electrode may be a wire or a rod of circular cross section along the axis of the waveguide. This arrangement gives a nonuniform Stark field, but the nonuniformity may be useful in smearing out the Stark components so that they do not interfere with observation of the Zeeman components. Further smearing can be obtained by use of a trapezoidal or similarly shaped Stark voltage rather than a square wave.

The hyperfine-structure transitions in atomic spectra of alkali metal vapors resemble paramagnetic molecules in their large Zeeman effect. In these cases interactions between the valence  $s$  electron and the nucleus are so large that the transitions between individual hyperfine components lie in the microwave range. Cesium [405] and sodium [642], [643] transitions have been observed by microwave absorption in resonant cavities. The alkali metal vapors were contained in glass or quartz liners within the cavity. External coils provided magnetic fields of a few oersteds for Zeeman modulation.

Roberts, Beers, and Hill [405] detected the dispersion on the edges of a line rather than the absorption at its center. The imaginary part of the permeability, which is maximum at the point of greatest change of absorption, slightly modifies the cavity's resonant frequency. This cavity controlled the frequency of an oscillator, and so varying the magnetic field caused a frequency modulation which was detected.

**15-14. Spectrometers for High and Low Temperatures.** Low temperatures are often used to increase the population of lower vibrational and rotational energy levels. The intensities of most microwave lines are thereby increased. Lines involving excited vibrational states can be distinguished because their intensities do not increase so much or may even decrease on cooling.

Few polar molecules have an appreciable vapor pressure at very low temperatures, so that it is seldom possible to observe their spectra at temperatures lower than those obtainable with dry ice. A rectangular trough of sheet copper, thermally insulated and supported in a wooden box, serves to hold either dry ice alone or a dry ice-acetone mixture. For the lowest temperatures such a trough can be used to contain liquid air, although the liquid air evaporates rapidly.

High-temperature spectroscopy is much more difficult, chiefly because the materials used to support a Stark electrode become poor insulators at high temperatures (*cf.* review in [728]). Waveguide windows tend to be lossy at high temperatures, and difficulties are experienced in sealing them to the waveguide.

For moderate temperatures (150 to 250°C), the designs used differ from ordinary Stark spectrographs only in details. The polystyrene

or teflon insulation of the Stark electrode can be replaced by mica fins crimped into slots on the electrode edges [637] or by grooved quartz strips [728]. Rather than rubber gaskets at the mica windows, lead gaskets [637] or copper gaskets [728] may be used. High temperatures are useful for outgassing the absorption cell and remaining traces of molecules previously introduced into the cell. If the instrument is used for

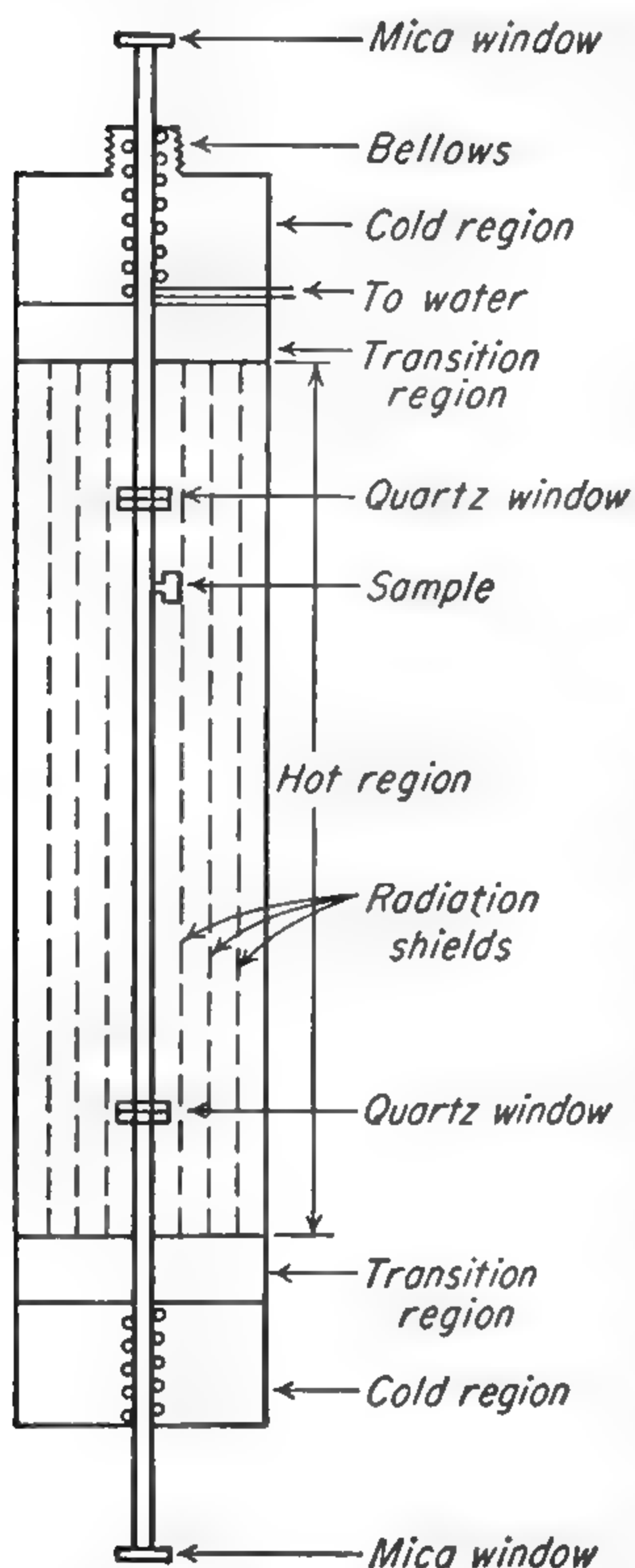


FIG. 15-17. Microwave spectrograph for high temperatures.

spectroscopy at high temperatures rather than just for outgassing, the sample may condense out at lower temperatures, and if so it must be introduced from a heated container through heated valves and connections.

For the high-temperature range (250 to 1000°C), which is necessary to obtain sufficient vapor pressure of many interesting diatomic molecules, more radical changes are needed to avoid the serious insulation difficulties and prevent rapid oxidation of metal surfaces. Several approaches have been used. One method reduces the amount of insulation required to position the Stark plate by supporting the entire waveguide vertically [980a]. The waveguide is contained inside an evacuated cylinder with radiation shields (Fig. 15-17). Since the container is evacuated, the waveguide seals need only have a reasonably slow leak rate for a pressure differential less than  $\frac{1}{10}$  mm Hg rather than for the entire pressure of the atmosphere. Quartz or ceramic windows with copper gaskets are used at the end of the hot waveguide. Outer mica windows at the points where the waveguide enters and leaves the vacuum jacket are at room temperature and so present no unusual difficulties.

The waveguide cell is made of nickel and gold-plated on the inside to resist corrosion by the gases being studied and to reduce the attenuation of the microwaves. Small ceramic spacers serve to center the Stark electrode. Modulation voltage is applied through a tantalum wire insulated by a lava bushing in the waveguide wall. Tantalum wire is used for heating the cell, and extra heaters near the ends assure that the windows are hotter than the rest of the system and so prevent condensation on the windows.

A molecular beam spectrograph has been designed to study substances which require high temperatures for their evaporation. Only the oven



need be at a high temperature, and Stark modulation electrodes can be outside the beam. Alternatively, mechanical modulation of the beam by a cooled shutter may be used [728]. The low modulation frequency attainable in this way necessitates a bolometer or superheterodyne detector for good signal-to-noise ratio. The method avoids the problems of windows and electrode insulation. Moreover, the beam can be used to reduce Doppler broadening, since the path of the radiation is transverse to the beam. However, the amount of absorption obtainable with a molecular beam is so small that only the strongest lines can give detectable signals.

A third type of high-temperature spectrograph uses a thin quartz liner for the waveguide [728]. The guide is split and the Stark voltage is applied between the two halves. Although this gives a nonuniform field so that Stark components are smeared, it should be adequate for detection of the lines. The guide assembly is inserted in a heated iron pipe and fed by horns from an external waveguide.

**15-15. Spectrographs for Intensity and Line-shape Measurements.** Line widths and relative intensities of nearby lines can be measured on a Stark modulation spectrograph if sufficient care is taken to minimize reflections in the waveguide system. When the microwave oscillator frequency is changed, any reflections present cause changes in the amount of power reaching the crystal. With Stark modulation, these changes do not usually cause spurious lines, but the apparent intensity of a real line changes with the power level at the crystal (cf. [968a]).

If standing waves are present in a section of waveguide because of reflections at its ends, it acts as a resonator. At those frequencies for which it is resonant, the energy density is large, and the attenuation caused by absorption lines is consequently large. Alternatively it may be said that the reflections produce a long effective path length because the radiation is reflected back and forth several times. When the input frequency is changed slightly, the section becomes antiresonant so that the energy density, and with it the attenuation produced by the line, becomes small.

Consider as an example a waveguide absorption cell of length  $L$  with small equal reflections occurring at its two ends with a fraction  $r$  of power reflected at either single reflection. The power transmitted through the cell may be written

$$P = \frac{P_0 e^{-\alpha L}}{[1 - r e^{-(\alpha + 4\pi i/\lambda_g)L}]^2} \quad (15-25)$$

where  $P_0$  is a constant proportional to, but not exactly equal to, input power;  $\alpha$  is the attenuation coefficient per unit length in the waveguide; and  $\lambda_g$  is the radiation wavelength in the waveguide. Expression (15-25) shows the variation in power transmitted through the guide to the



detector with variation in frequency (or hence  $\lambda_g$ ). The ratio of maximum to minimum power (or of detected crystal current,  $I$ , since power is approximately proportional to  $I$ ) is, from (15-25),

$$\frac{P_{\max}}{P_{\min}} = \frac{I_{\max}}{I_{\min}} = \left( \frac{1 + re^{-\alpha L}}{1 - re^{-\alpha L}} \right)^2 \quad (15-26)$$

Clearly from (15-26) attenuation tends to reduce the fractional variation in crystal current, since  $\frac{P_{\max}}{P_{\min}} \rightarrow 1$  when  $\alpha L$  becomes large.

In order to determine the effect on transmitted power of a small change in the absorption coefficient  $\alpha$  such as might be introduced by a gas absorption, (15-25) may be differentiated with respect to  $\alpha$ . This gives

$$\Delta P = -P_0 e^{-\alpha L} \frac{[1 + re^{-(\alpha + 4\pi j/\lambda_g)L}]}{[1 - re^{-(\alpha + 4\pi j/\lambda_g)L}]^3} \alpha_{\text{gas}} L \quad (15-27)$$

where  $\alpha_{\text{gas}}$  is the absorption coefficient of the gas. For a given value of gas absorption  $\alpha_{\text{gas}}$ , (15-27) shows the rapid change of absorbed power  $\Delta P$  with frequency or  $\lambda_g$ . The ratio of maximum to minimum values of  $\Delta P$  for a given  $\alpha$  is, from (15-27) and (15-26),

$$\frac{\Delta P_{\max}}{\Delta P_{\min}} = \left( \frac{1 + re^{-\alpha L}}{1 - re^{-\alpha L}} \right)^4 = \left( \frac{I_{\max}}{I_{\min}} \right)^2 \quad (15-28)$$

Hence the variations in apparent absorption coefficient due to reflections are considerably greater than the variations in crystal current. In some cases, approximate corrections for reflections might be possible by use of (15-27).

For low reflection, the Stark electrode must be tapered at each end. Individual sections of waveguide should have nearly identical cross sections and be carefully aligned where they meet. Windows should be thin, and of good dielectric material.

In addition to keeping reflections low, if intensities are to be measured accurately, the crystal current must not be large enough to cause non-linearity of the microwave-power-crystal-current relation. Usually a few hundred microamperes are permissible if the load resistance for the crystal is not too large. Finally, circuits which amplify the signal must be linear over the range of signals encountered (*cf.* [901]).

**15-16. Gas Handling for Microwave Spectrographs.** Most microwave spectrographs use gases at pressures of from  $10^{-3}$  to 1 mm mercury. For ordinary gases, the sample is kept in a glass bulb, with glass connections to the waveguide and vacuum pumps. Glass stopcocks, lubricated with some vacuum grease, regulate the flow of gas into the waveguide. If two stopcocks in series are used between the sample holder and the waveguide cell, gas may be admitted first into the space between the stopcocks. The sample tube is then shut off and the gas in the small

space between the stopcocks is allowed to expand into the waveguide. This arrangement is convenient because it admits only the small amounts of gas usually needed to fill the absorption cell. These small amounts of gas are often difficult to control by a single stopcock opening directly into the sample bulb. Pressure can be measured by any of the ordinary vacuum gauges (S. Dushman, *Scientific Foundations of High Vacuum Technique*, John Wiley & Sons, Inc., New York, 1950; R. T. Sanderson, *Vacuum Manipulation of Volatile Compounds*, John Wiley & Sons, Inc., New York, 1948).

Some gases react with the glass, stopcock grease, metal waveguide, mica windows, or plastic insulation and require careful choice of the materials in contact with the gas. Teflon (polymerized tetrafluoroethylene) is inert to most chemicals and can be used for insulating the Stark septum and leads. Polytrifluorochloroethylene (Kel-F) tubing is often useful in handling samples of fluoride compounds. Copper equipment is suitable for reactive fluorides and can be used for the entire gas-handling system.

Chlorinated and fluorinated greases are available for stopcocks. While they are generally more expensive and poorer lubricants than ordinary stopcock greases, they are much more resistant to chemical attack. A thin coating of such a grease can be used to protect windows. When highly reactive or unstable compounds are to be used in the absorption cell, the observable effect of decomposition is minimized by allowing a sample of gas to remain in the system for a few hours or even days in order that initial surface reaction may go to completion. The sample may be replenished occasionally or, if necessary, a continuous-flow method at low pressure may be used. For substances with sufficiently high vapor pressures, reaction and decomposition may be reduced by cooling the entire system [521], [447].

Some substances, such as ammonia and water, are strongly absorbed on the walls of the waveguide and are then evolved very slowly. It may take several weeks at room temperature before the ammonia or water lines disappear from a sensitive spectrometer. Heating the absorption cell to about 100°C usually outgases it sufficiently in a few hours. Differential absorption may also change the composition of a gas mixture, giving rise to serious errors in experiments on line broadening by foreign gases or in quantitative analysis.

**15-17. Spectrometers for Free Radicals.** Free radicals are usually extremely unstable or reactive and often exist as separate molecules for only a thousandth of a second or less (cf. E. W. R. Steacey, *Atomic and Free Radical Reactions*, Reinhold Publishing Corporation, New York, 1946; W. A. Waters, *Chemistry of Free Radicals*, Oxford University Press, Oxford, 1946; F. O. Rice and K. K. Rice, *The Aliphatic Free Radicals*, Johns Hopkins Press, Baltimore, 1935). Nevertheless some molecules

with odd numbers of electrons are stable (*e.g.*, NO, NO<sub>2</sub>, ClO<sub>2</sub>), and so radicals with intermediate stability and lifetimes should occur and give detectable microwave spectra. Lifetimes of these chemically active substances are often limited by the presence of other materials which combine with the radicals or catalyze their recombination.

Attempts to obtain microwave spectra of free radicals have been hampered by the paucity of knowledge about them and by the lack of suitable tests for the presence of radicals or for the elimination of interfering substances from the system (*cf.* review by J. Mays [728]). The microwave spectrum of the OH radical, arising from transitions between members of a  $\Lambda$  doublet, has been observed by Sanders, Schawlow, Dousmanis, and Townes [861], [971] using a system in which radicals

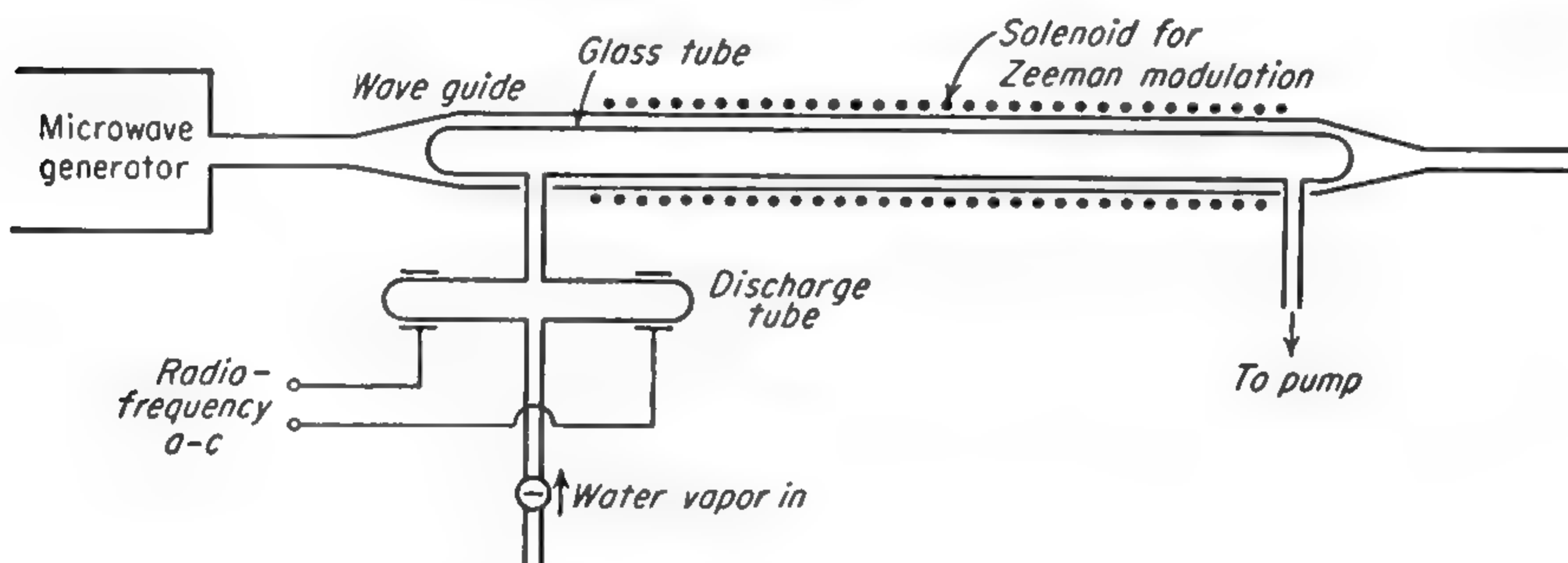


FIG. 15-18. Microwave spectrograph used to observe the spectrum of the free radical OH.

come in contact with no metal (Fig. 15-18). Radicals are produced by dissociation of water vapor in a radio-frequency discharge tube with external electrodes, and are then pumped through a straight tube of low-loss glass. This tube is the lining of a waveguide of circular cross section which is tapered at its ends to an ordinary rectangular waveguide. Zeeman modulation is applied by superimposed direct and 100-kc currents through a solenoid around the waveguide. The waveguide is slotted longitudinally to reduce eddy currents and allow the magnetic field to penetrate it. This method of modulation is particularly suitable for radicals which have large magnetic moments arising from an unpaired electron. Absorptions caused by substances other than radicals are not modulated and so are not observed.

**15-18. Microwave Radiometers.** A type of spectrograph introduced by Dicke [148] is especially suitable for microwave spectroscopy of astronomical sources. In radio astronomy neither the original source nor the absorber is under the control of the observer, so that neither can be modulated. Furthermore, the radiation from astronomical sources is usually spread over some range of frequencies rather than being essentially monochromatic as is a microwave oscillator. The instrument



designed by Dicke may be called a radiometer, since it detects the noise power radiated from an extended source and determines the apparent temperature of the source at microwave frequencies.

In the radiometer, which is shown in Fig. 15-19, a movable absorber is placed in the waveguide between the antenna and the detector. The absorber is moved in and out of the guide at a rate of 30 cycles/sec. When it is in the guide, the incoming signal is replaced by thermal radiation from the absorber at room temperature. Thus small variations between the effective temperature of the astronomical radiator and of the spectrograph show up as variations in the noise power received by the

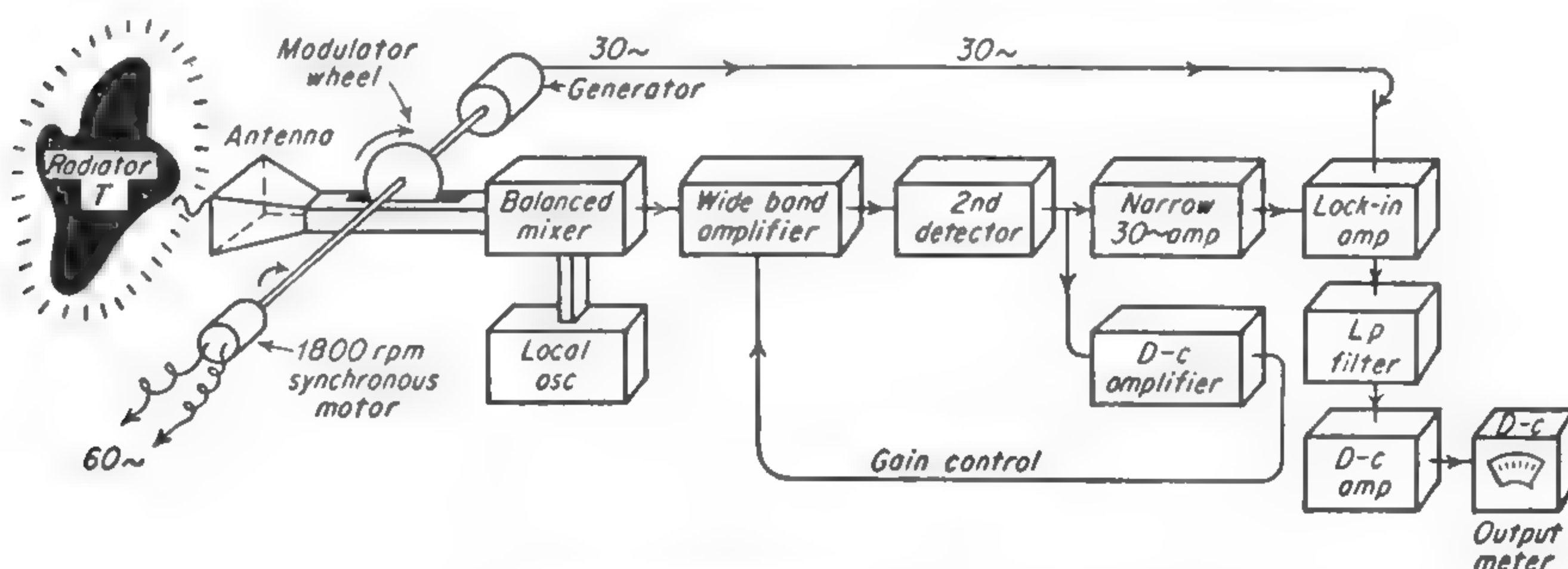


FIG. 15-19. Microwave radiometer. (From Dicke [148].)

detector during the two portions of the cycle. A relatively large intermediate-frequency bandwidth (8 Mc) is used so that all the thermal noise radiated by the source within a band of that size on either side of the oscillator frequency is available as signal to be amplified and detected.

The noise-power levels in the two positions (absorber in and absorber out of the guide) are compared sensitively by a lock-in detector which has a time constant large enough to average over a relatively long period. In this way fluctuations in the thermal noise power and in amplifier gain are minimized.

As in other spectrographs dealing with low signal powers, superheterodyne detection is used. A balanced mixer ensures that local oscillator power is not radiated into the waveguide where it might be reflected differently from the absorber than from the open waveguide.

With this instrument a change in source temperature somewhat less than  $1^\circ\text{C}$  is measurable, corresponding to a noise power of  $10^{-16}$  watt. It should be noted that the effective temperature measured with microwaves often differs from that of the optical region because of selective absorption or emission.

The change in temperature which can be detected by such a system is given [148] approximately by

$$\Delta T = NT \left( \frac{\Delta \nu_2}{\Delta \nu_1} \right)^{\frac{1}{2}}$$

where  $T$  is the temperature of the receiver (room temperature) and  $N$  is the receiver's noise figure (that is,  $NT$  is the apparent temperature of the receiver input circuit judged by the residual noise when no signal is present)  $\Delta\nu_1$  is the bandwidth of the receiver system before the second detector of Fig. 15-19, and  $\Delta\nu_2$  is the bandwidth of the low-pass filter following lock-in.

Microwave radiation from hydrogen atoms in interstellar space is spread over a frequency range of only a few tens of kilocycles. Hence for its detection a receiver bandwidth of a few tens of kilocycles is used, and the received frequency is shifted back and forth periodically at the lock-in frequency. This shifting of the frequency replaces the variable absorber of Fig. 15-19 and allows an accurate comparison between the amount of noise power radiated at the hydrogen resonance and that at other frequencies.

## CHAPTER 16

### MILLIMETER WAVES

**16-1. Introduction.** Conventional vacuum tubes and circuits do not operate well for wavelengths as short as the microwave region, because they use lumped circuit constants which require that the wavelength be considerably larger than the size of the tube or circuit element. Klystrons, magnetrons, and other microwave devices which do work successfully in the microwave region usually require only that the wavelength be comparable with the dimensions of the tube, and hence they are appropriate for microwaves as short as 1 cm. For wavelengths below about 4 mm, even these devices no longer work well because they cannot be satisfactorily scaled down to a sufficiently small size.

Short wavelengths are of course emitted by hot bodies, and this source of radiation is commonly used in infrared spectroscopy. However, the intensity of radiation in a given bandwidth or range of frequencies decreases at longer infrared wavelengths as  $1/\lambda^2$  and is so small beyond wavelengths of a few tenths of 1 mm that it can be used for spectroscopy only with great difficulty. For example, one square centimeter of a black body at 2500°K radiates only  $5 \times 10^{-8}$  watt within a 1 per cent range of frequencies centered at 1 mm wavelength. If one wishes a bandwidth or resolution of 1 Mc at this wavelength, the power is reduced to  $10^{-11}$  watt, which is too small to be useful at present—especially since heterodyne detection cannot be used without a more powerful local oscillator of the same frequency.

Thus neither electronic oscillators nor infrared sources provide much usable radiation in the wavelength range between a few tenths and a few millimeters. In approaching this range from either side, spectroscopy becomes increasingly difficult. However, techniques are not available which permit some rewarding spectroscopy for wavelengths as short as 1 mm, and these will be discussed. Spectroscopy in the longer millimeter region is not so difficult, but its techniques are sufficiently different from those in the centimeter range to warrant treatment in this chapter.

**16-2. Spark Oscillators for Millimeter Waves.** Since thermal sources give so little power in the millimeter and submillimeter region, stronger sources of broad-band radiation were sought many years before continuous-wave generators even approached the centimeter band. Spark



oscillators were used by Lebedew [1] to generate 0.6-mm waves in 1895, and by Nicholls and Tear in 1922 to reach a wavelength of 0.22 mm [3], [4].

A variant of the spark oscillator is the mass radiator, exploited first by Glagolewa-Arkadiewa [5], in which the sparks pass between many small metal particles. A pair of nearby particles with a spark passing between them acts as a dipole radiator of short wavelength. But since the particle separation is not fixed, a wide range of wavelengths is generated. Usually, the metal particles are immersed in an oil bath which flows or is carried past high-voltage electrodes [5], [13], [49], [92], [6], [128]. Wavelengths from 0.1 to 50 millimeters have been generated in this manner and used, with a diffraction grating, for low-resolution spectroscopy. One serious difficulty with this source, besides the continuous spectrum and low intensity, is the large voltage pulse as the spark breaks down the main gap. Even with careful shielding, this pulse tends to limit the usable amplifier sensitivity.

A variant of the mass radiator is obtained by dropping charged mercury droplets into a mercury pool of the opposite charge [503a]. Small powers in the 2- to 10-mm range have been produced by this method.

**16-3. Vacuum-tube Generators.** While vacuum-tube oscillators for the millimeter region are more difficult to construct than incoherent sources, their advantages are great. Since all the radiation is confined to a narrow band, the spectrometer need not have high resolving power and so can be relatively simple and efficient. In favorable cases, almost all the radiated energy lies in one narrow band.

One method of obtaining millimeter wave tubes is to scale down those types used at centimeter wavelengths. Klystrons, traveling-wave tubes, and backward-wave oscillators have been built to produce wavelengths near 4 mm, while pulsed magnetrons have reached 2.5 mm (*cf.* review in [510]). Of these, the rather new backward-wave oscillator appears most promising as a flexible high-frequency source for spectroscopy. The first three types of tubes are in practice inefficient and are necessarily small, so that neither conduction nor radiation is sufficient to dissipate heat for more than very low power operation. Furthermore circuit losses increase approximately as the square of the frequency. Magnetrons, by virtue of their pulsed operation, are able to operate with moderate efficiency and power output in the millimeter region. Figure 16-1 shows how the heat transfer limits possible power output. Since tubes are usually of the order of the wavelength  $\lambda$  in dimensions, the upper line on the graph of Fig. 16-1 is a natural upper limit to the amount of heat which can be dissipated by conduction. Actual tubes, as shown by the shaded area, come fairly close to this limit in the centimeter region. The power radiated by a hot body is very much less, especially when only those wavelengths in a small band are selected.

If the efficiency of vacuum-tube generators is not very small, they can produce powers enormously greater than hot bodies in the millimeter region. Efficiencies are usually somewhat greater for pulsed tubes than for continuous types; this accounts for some of the spread of the output powers shown for tubes of Fig. 16-1.

When tubes are made to work at shorter wavelengths by scaling down dimensions, the power output will be unaffected provided the current and losses are unchanged. But scaling down the tube reduces the cathode area in proportion to the square of the linear dimensions, so

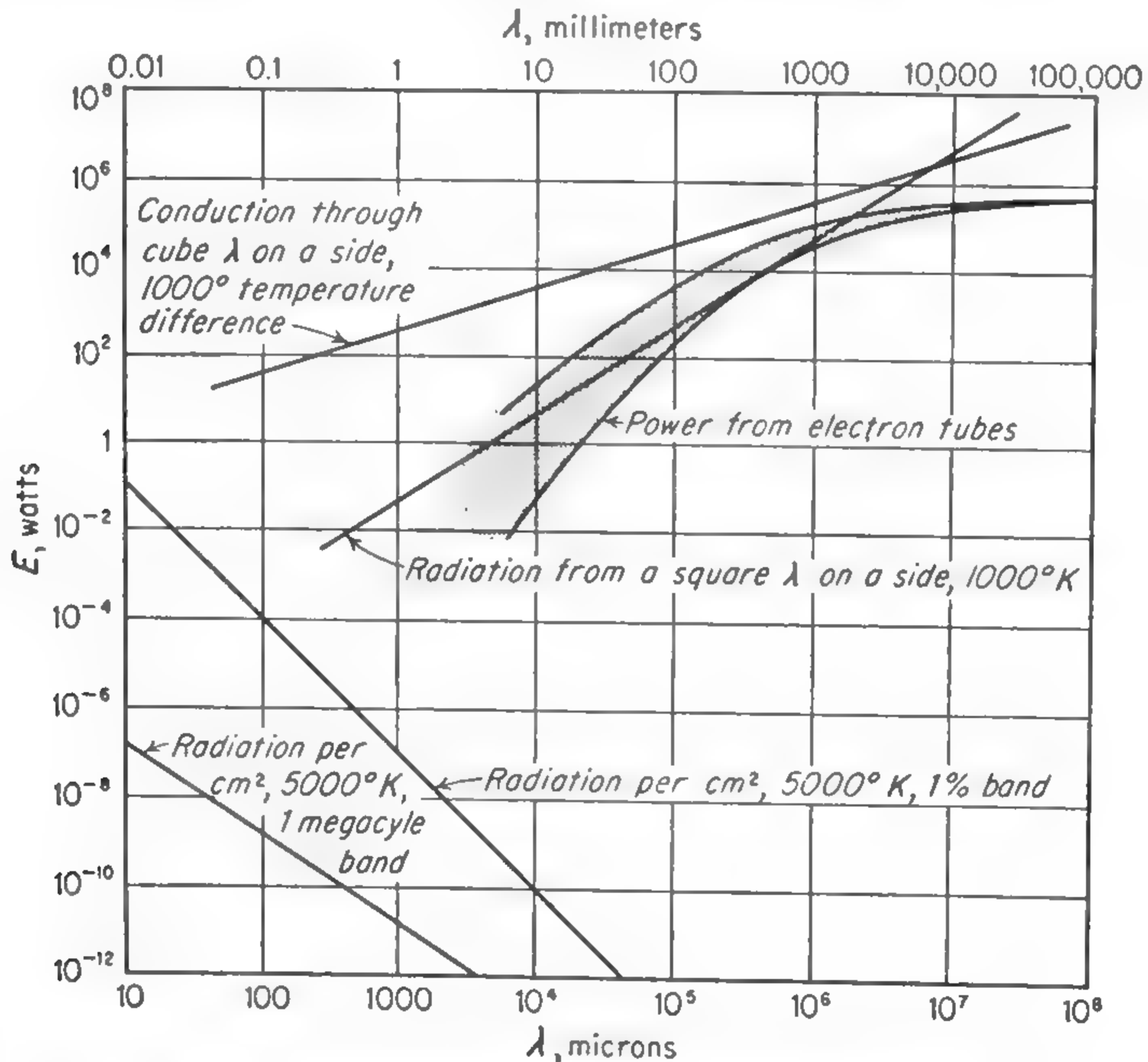


FIG. 16-1. Power limits of thermal sources, and thermal limitations on vacuum tubes. (From J. R. Pierce [510].)

that attainable beam current will fall unless means are found for greatly increasing emission-current density. Higher emission currents are accompanied by increased space-charge effects which modify the operation of the tube. Very high emission-current densities can be achieved for a short period, if the tube is allowed to rest before the next pulse. Thus a pulsed magnetron, with plate potential applied for about one out of every thousand microseconds and having intensive back bombardment of the cathode by some of the electrons, attains a much higher emission density than ordinary tubes. The high plate potential during the pulse tends to overcome the effects of space-charge concentration near the cathode.



Finally, fabrication tolerances become exceedingly critical when centimeter-wave klystrons are scaled to operate in the millimeter-wave range. For these reasons it is desirable to have tube types whose dimensions are all large in comparison with the wavelength. Klystrons, traveling-wave or backward-wave tubes, and magnetrons are an advance over conventional triodes for the microwave region in that they have sizes not very much less than the wavelength generated. Neither they nor any other type yet invented have critical dimensions which are greater than the output wavelength. Nevertheless, all these types have been successfully scaled down to operate in the millimeter region, and in spite of the difficulties, further progress may be expected.

Klystrons are commercially available to produce wavelengths as short as 5 mm (Raytheon Manufacturing Co., Waltham, Mass.) with a power output of a few milliwatts. Similar reflex klystrons for the longer millimeter wavelengths have been constructed in England (*cf.* review in [388]). However, millimeter-wave klystrons tend to be noisier and less stable than their centimeter-wave counterparts, and the power emitted sometimes varies rapidly over the range of tuning.

Traveling-wave generators of several types can be constructed for the millimeter region. One traveling-wave tube has been operated in the 6- to 8-mm region [617] as both an amplifier and an oscillator. Backward-wave oscillators have also been made in the 5-mm region with an output power of about 10 mw and with electronic tuning over a frequency range of about 30 per cent. However, no traveling-wave or backward-wave oscillators are as yet commercially available.

Pulsed magnetrons have been built to oscillate at wavelengths as short as 2.5 mm, but the shorter-wavelength tubes are not tunable (Bernstein, M. J., and others, Columbia Radiation Laboratory Progress Reports, 1947–1954). For the 6-mm region a few pulsed magnetrons have been built which are tunable over a band of 1 or 2 per cent. Because these magnetrons have simpler structures than, for example, klystrons and because of the advantages of pulsed operation discussed above, efficiencies of the order of 5 per cent are achieved. This efficiency permits fairly high output powers, and the millimeter-wave magnetrons have peak pulse outputs of around 25 kw.

**16-4. Harmonics from Vacuum Tubes.** Since several kinds of tubes are available which give power at a wavelength of about 1 cm, their overtones have been investigated as sources of millimeter waves. Magnetrons generate so much power that even relatively weak overtones are detectable. Klein, Loubser, Nethercot, and Townes [716] have detected harmonics as high as the tenth (1.25-mm wavelength) from *K*-band tubes and the third (1.1 mm) from a 3.3-mm tube. Peak powers of a few hundred microwatts were obtained at the shortest wavelengths. In the apparatus used, a side arm and phaser produced an adjustable load by



which the harmonic output could be maximized (Fig. 16-2). The filter which selected the high harmonics was a section of waveguide too small to permit the longer wavelengths to pass. The magnetron source was also used in conjunction with an echelette grating similar in principle to those used for infrared spectroscopy. This reflection grating was operated in free space and diffracted energy from the transmitter waveguide to the section containing the detector crystal. With this apparatus it was found that not all higher frequencies emitted by magnetrons are harmonics, *i.e.*, integral multiples of the fundamental frequency.

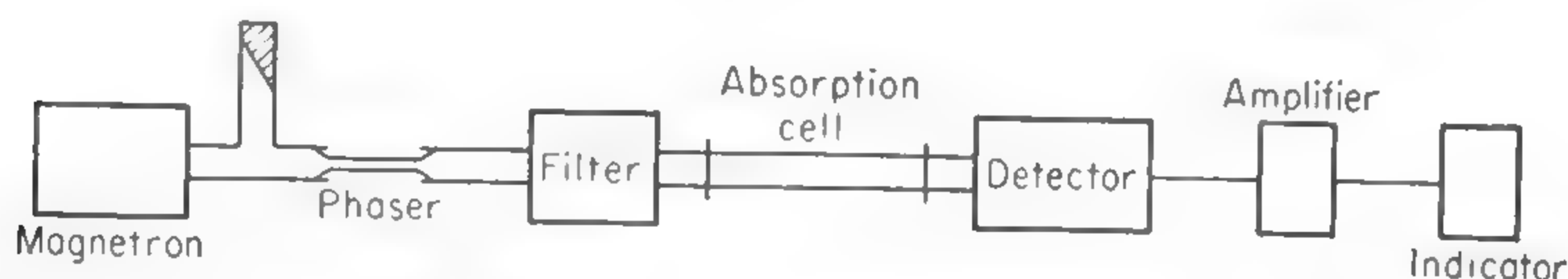


FIG. 16-2. Apparatus for isolating magnetron harmonics. (From Klein, Loubser, Nethercot, and Townes [716].)

These nonharmonic frequencies are, however, weaker than the true harmonics, so that they would not ordinarily lead to confusion. Individual tubes, even of the same type, vary considerably in their harmonic and overtone content. The use of magnetron harmonics for spectroscopy is limited by the difficulty of obtaining magnetrons which are tunable over a sufficient frequency range.

Klystrons for the 1-cm region give considerable amounts of power and are reasonably stable. Their output occasionally contains an appreciable power at some particular harmonic frequency, but the harmonic output is not sufficiently certain or controllable to be very useful.

Harmonics of microwave oscillators can also be produced by nonlinear circuit elements. Before discussing harmonic generation in a silicon crystal, which is the most convenient variety of nonlinear element, we shall consider detection of millimeter waves. Detection involves a similar, but somewhat simpler, application of silicon crystals.

**16-5. Detection of Millimeter Waves.** Techniques adapted from those used in both the infrared and the centimeter-wave region can be applied to detect millimeter waves. In the infrared region, thermal detectors predominate; for centimeter waves thermal detectors are sometimes used, but crystal detectors are usually best and are most widely used.

In the early work on mass radiators, various kinds of thermal detectors were employed. Cooley and Rohrbaugh [128] used a bismuth-antimony thermopile which had all junctions covered by a 2-mm-thick coating composed of equal parts lampblack and tellurium-plated cork dust. The mixture was equivalent to many absorbers whose size and separation were of the order of the wavelengths being received. The thermopile was used over a range of 0.2 to 2.2 mm and had a sensitivity such that,

after amplification, a flux of about  $3 \times 10^{-8}$  watt/cm<sup>2</sup> of exposed thermopile surface could be detected.

A more sensitive thermal detector is the Golay cell [195], [196]. The Golay detector contains an air space between two films, one of which is an absorber of radiation. The other film is a very light flexible mirror. When radiation falls on the absorber, it heats the film and hence the air in the cell which then expands and slightly deflects the mirror. Motion of the mirror affects the amount of light falling on a photocell, and the resultant photocurrent is proportional to the radiation intensity.

When the cell is used as a detector of millimeter waves, the end of the waveguide is pointed at the cell [716]. Some resonance effects are observed in this region because of the finite size of the cell aperture, so that it is helpful to optimize the cell response by adjusting its distance from the waveguide. The radiation is chopped at 10 cycles/sec by a rotating semicircular absorber passing into the waveguide through a slot. When used with a circuit having a time constant of 5 sec, one cell of this type had a sensitivity of about  $5 \times 10^{-11}$  watt. The same sensitivity can be expected for shorter wavelengths, and so the Golay cell may be useful for submillimeter waves.

In the longer millimeter range the packaged cartridge-type crystals designed for 1.25-cm (1N26) or 8-mm (1N53) wavelength are convenient as detectors or harmonic generators. One design of detector for cartridge-type crystals due to Beringer [139] introduces the signal from the waveguide into the crystal through a short coaxial line. Similar but simplified designs such as that shown in Fig. 16-3 have been extensively and successfully used for spectroscopic work in the millimeter range by Gordy and coworkers [413], [457], [694]. Such detectors, using commercial crystals, are most successful at wavelengths above 4 mm, but they have detected radiation from harmonic generators of similar design (see Fig. 16-3) at wavelengths as short as 2 mm. Their use at such short wavelengths is quite difficult because very careful selection of crystals is required and each crystal operates over only a narrow range of frequencies.

For most spectroscopic purposes, it is best to use components which are "broad-band" so that they operate satisfactorily over a wide range of frequencies without complicated and critical tuning. Detectors and other circuit components which are simple and broad-band are particularly desirable in the highest-frequency ranges. This is partly because at the shortest wavelengths any critical dimensions become so difficult to control that they are best avoided. Furthermore, present spectroscopy below a few millimeters is still in a rather primitive state and is limited enough by other difficulties that an additional restriction of detectors to a narrow frequency range is very objectionable.

Although detectors using pieces of silicon mounted individually in a

waveguide without a surrounding cartridge are somewhat time-consuming to construct and less rugged than the commercial 1N26 and 1N53 crystals, they give enormously better performance at the shortest wavelengths. Problems of matching the microwave power into the crystal are very much reduced and the detector is usable over a much broader frequency range. Detectors of this type, illustrated in Fig. 16-4, were

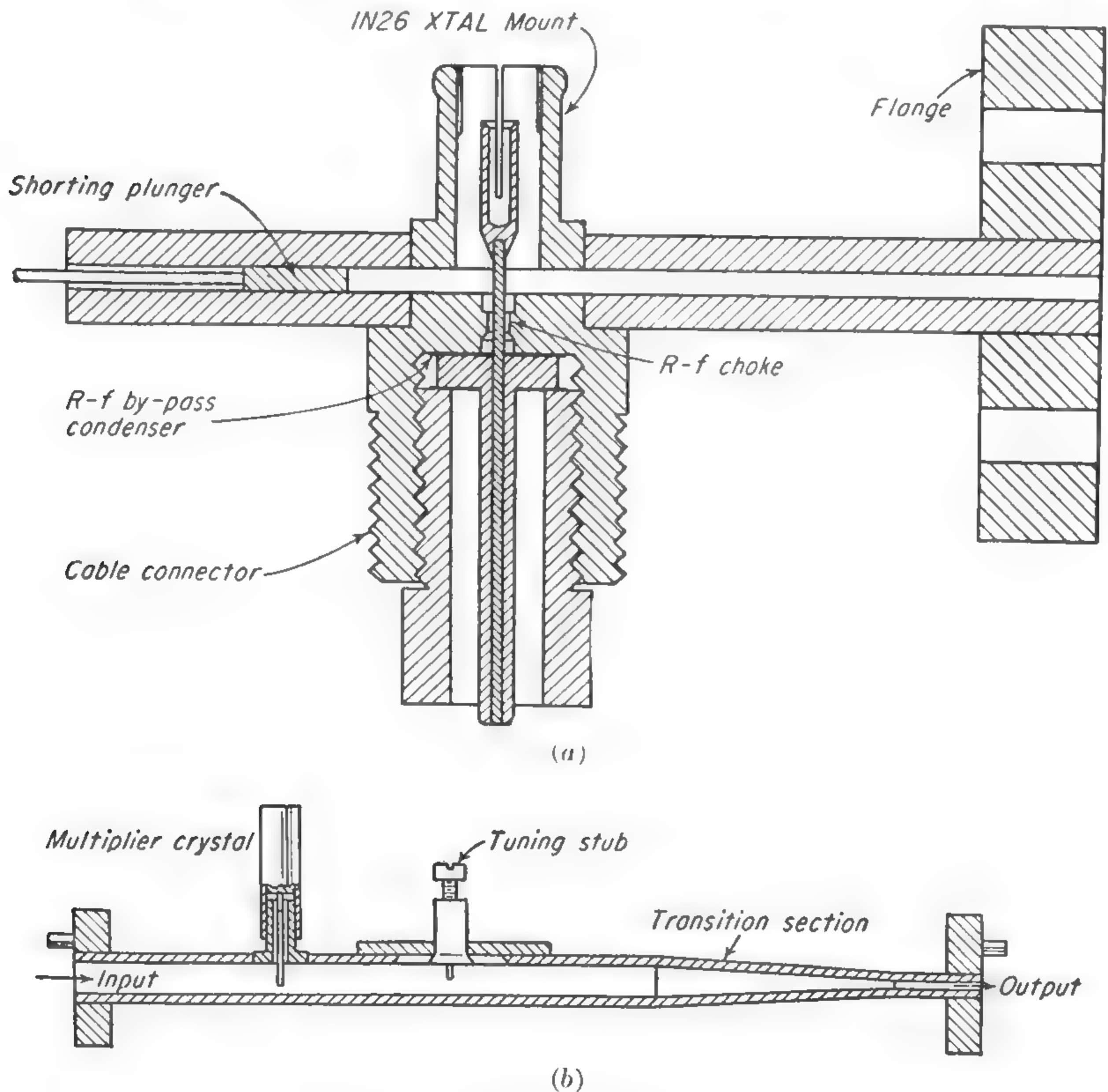


FIG. 16-3. Apparatus for generation and detection of millimeter waves using cartridge-type crystals. (a) Detector. (b) Simple harmonic generator. (From C. M. Johnson, reproduced in [694].)

shown by Klein, Loubser, Nethercot, and Townes [716] to be fairly sensitive over a wide range of frequencies and down to wavelengths at least as short as 1 mm. Near 1 mm, these detectors were only about one hundred times less sensitive than the best crystals at 1 cm wavelength. Johnson, Slager, and D. D. King [944] made a systematic comparison of several detectors and harmonic generators for the range 6 to 2 mm wavelength. They tested cartridge-type (1N26, 1N31, and 1N53) crystals, cartridge-type crystals with part of the walls of the cartridge cut away,



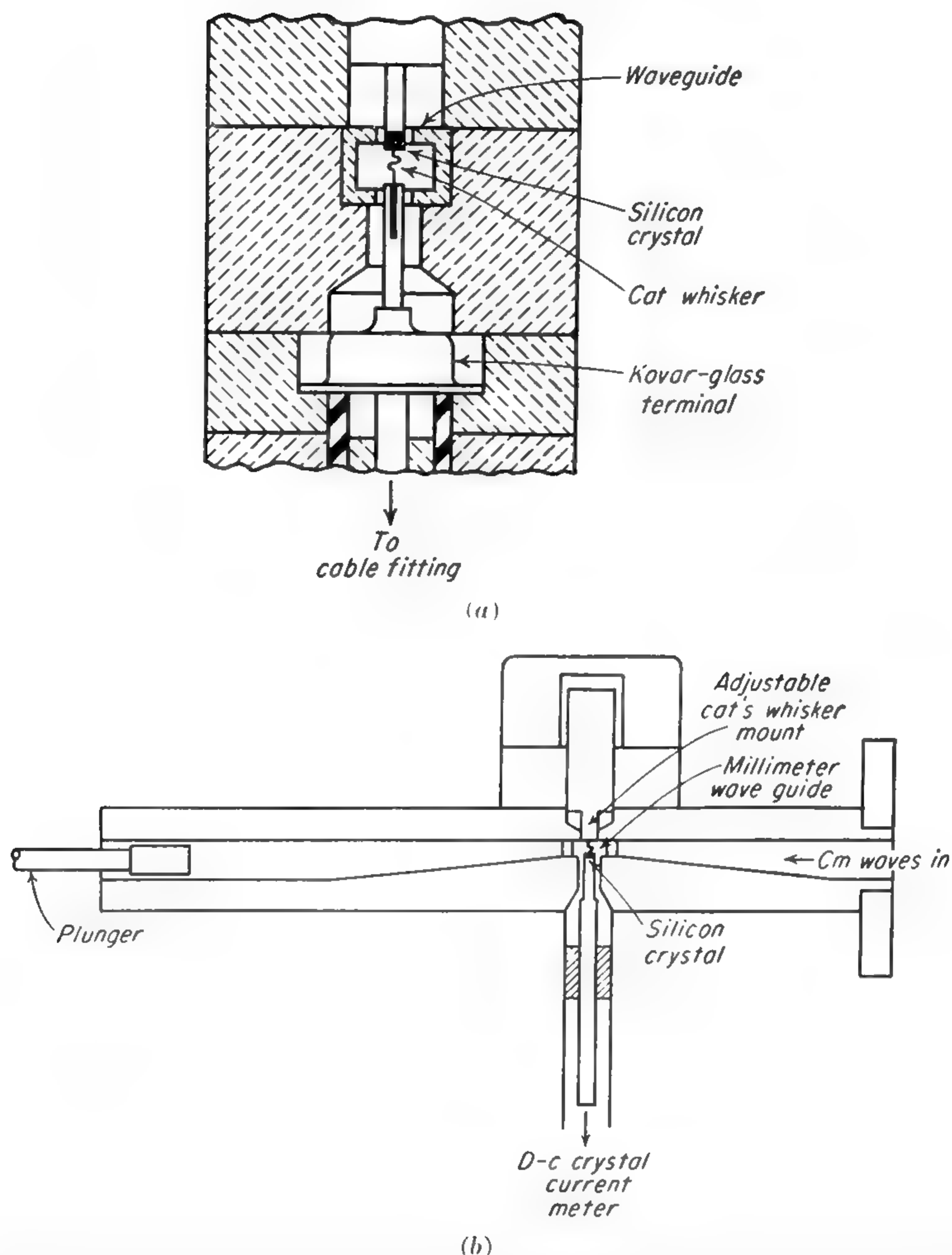


FIG. 16-4. Apparatus for generation and detection of millimeter waves using open-guide crystal mounts. (a) Detector. (From Klein, Loubser, Nethercot, and Townes [716].) (b) Harmonic generator. Waveguide for high harmonics crosses waveguide for fundamental at crystal, and is perpendicular to the page. (Design due to E. Richter [733].)

and “open-guide” mounts such as that of Fig. 16-4. They found that the last type were distinctly superior as detectors, especially at the highest frequencies.

**16-6. Semi-conducting Crystal Harmonic Generators.** Semiconducting crystal harmonic generators receive fundamental microwave power from an electronic oscillator (usually a klystron), and because of the nonlinear response of the semiconductor to the microwave field, they

produce harmonics of the fundamental. Good harmonic generators involve efficient matching of the fundamental microwave power into a crystal and appropriate nonlinear characteristics. They also require efficient radiation of the generated harmonics into a waveguide. Since they involve matching of the crystal to a waveguide at both the fundamental and harmonic frequencies they are somewhat more complex than are detectors. However, the principles involved in detectors and generators are very similar, and hence the designs used for the two functions in any one experiment usually involve the same types of crystal mounts as indicated by Figs. 16-3, 16-4, and 16-5. The generator design shown in Fig. 16-3 is quite convenient at the longer wavelengths but tends to be narrow-band and weak in output at the shortest wavelengths. The open-guide crystal mount such as that shown in Fig. 16-4 has strong advantages in being broad-band [733], and at the higher frequencies gives appreciably greater output [944] than the type shown in Fig. 16-3.

W. C. King and Gordy [823], [946] have recently made notable progress in pushing the limit of operation of crystal harmonic generators down to 1 mm or slightly below. The generators and detectors which they use are of the open-guide type and are illustrated in Fig. 16-5. The shortest wavelength which has so far been obtained by this type of harmonic generation is 0.77 mm [910] but it seems reasonable to expect that detectable amounts of power may eventually be obtained at wavelengths of a few tenths of 1 mm.

There is as yet very little definite or quantitative information about the best techniques for crystal harmonic generation of wavelengths near 1 millimeter. However, we shall attempt to summarize what information and suggestions are available.

For the shortest wavelengths it is quite important that the crystal be in an open and simple mount (see Figs. 16-4 and 16-5) with simple tuning adjustments. Several different mounts of this type have worked with some success [733], [944], [946], but details of an optimum design are not clear. It should be noted that each of these generators produces high harmonics in a variety of waveguide modes, so that transmission and matching problems cannot be treated so simply or successfully as in a waveguide with only one mode of propagation.

No study has yet been made of the best crystal material. King and Gordy [823], [946] have used pieces of silicon about 1 mm in diameter broken from the silicon slabs of 1N26 crystals. They indicate that small crystals are considerably better than large ones, but experimental evidence for this is not clear. 1N23 crystals contain cylinders of silicon of about 1 mm diameter which have also been successfully used. Best types of etching, polishing, or doping of the crystal surface are unknown. However, it is important to keep the crystals rather dry. High humidity will make at least some crystal contacts deteriorate rapidly.

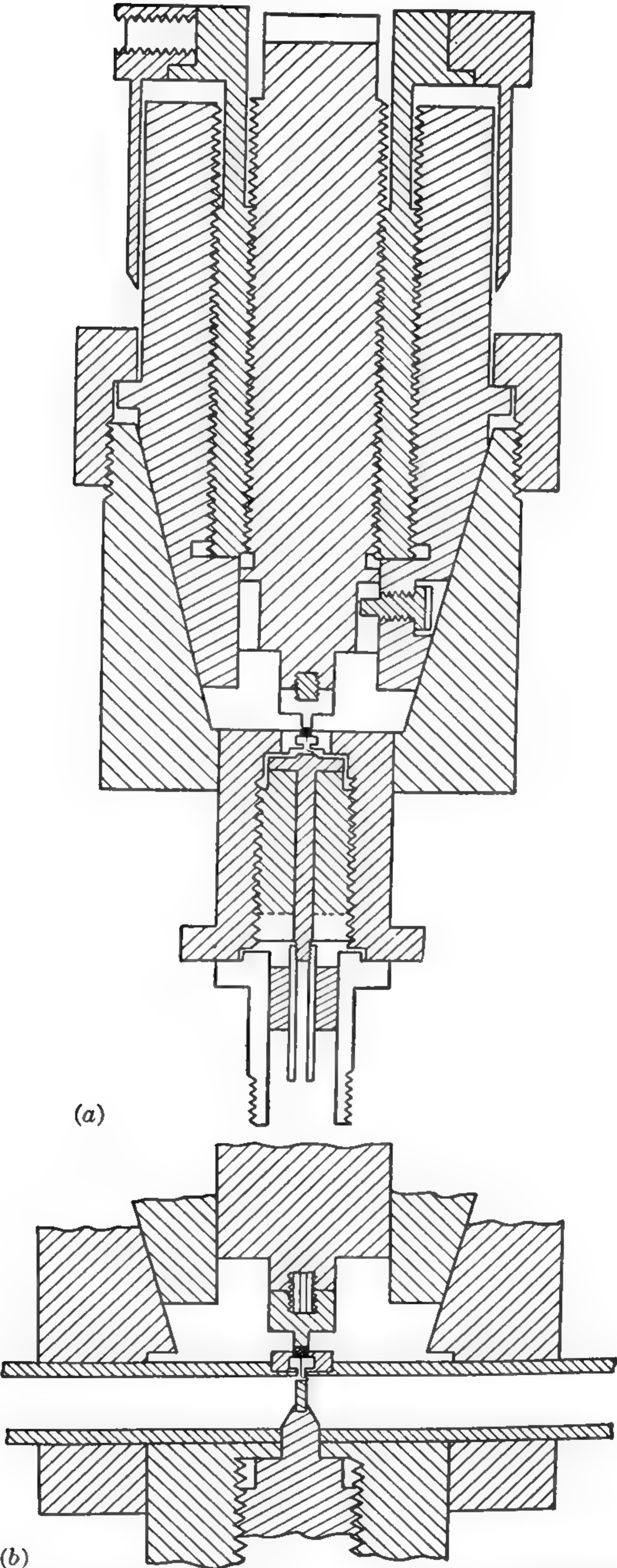


FIG. 16-5. Design of apparatus for generation and detection of millimeter waves using open-guide mount. In each case the waveguide for millimeter waves is perpendicular to the page. (a) Detector. (b) Harmonic generator. (From King and Gordy [946].)



Attention must be paid to obtaining a very small contact point on the crystal. A large contact surface provides a capacitance which shunts the desired nonlinear conduction characteristics of the contact and the impedance of the smallest contacts obtainable are still objectionably low at wavelengths near 1 mm. "Cat's whiskers," the fine tungsten wires which make contact, are usually about 2 mils (0.005 cm) in diameter. These may be sharply pointed by electrolytic etching [325]. Fine points may be blunted by pressure on the silicon surface, so that carefully controlled contact pressure is desirable, and repeated contacts may produce objectionable blunting. For accurate pressure control, a differential screw drive as shown in Fig. 16-5 is useful. Usually nearly optimum performance is obtained when the cat's whisker first contacts the silicon. Slightly increasing the pressure may worsen the performance, but there is often a somewhat higher pressure at which the contact properties pass through another optimum approximately as good as the first.

For high harmonics it is very important to drive the harmonic generator with a large amount of fundamental power. The harmonic output usually increases rapidly with increasing fundamental power until it reaches a "saturation" point where it stays approximately constant with further increases in fundamental power. At least for the first four harmonics of *K* band, each successive harmonic requires larger amounts of fundamental power to reach the saturation point.

Very probably the production of very high harmonics depends on having a microwave voltage at the crystal contact which is so large that the majority of the nonlinear crystal response is traversed by the varying voltage of the fundamental in a time comparable with the period of the harmonic. For the highest harmonics, fundamental power at least as large as 100 mw should be used. Crystal contacts can usually stand a few hundred milliwatts without damage due to "burn-out."

It might be expected that shorter wavelengths could be obtained by using fundamental microwave power of wavelength shorter than 1 cm. However, the higher-frequency klystrons emit appreciably less power than do those for *K* band, and the harmonic power at very short wavelengths which can be obtained from them is consequently no greater than that obtained from harmonics of the rather powerful 2K33 tubes.

Good harmonic generator and detector design should produce nearly 1 mw of power or 1 ma of detected current at the second harmonic of *K* band. Detected signals from harmonics up to the fifth or sixth will decrease by about a factor of 10 per harmonic. However, for harmonics above the seventh or eighth, the decrease in signal per harmonic is only a factor of 3 or 4 if the fundamental power is sufficiently large.

Harmonic generation and detection of wavelengths shorter than about 1.5 mm require at present a considerable amount of painstaking trial-and-error work in varying conditions and adjustments. The harmonic

obtained may be identified by the use of short sections of waveguide which are beyond cutoff for the lower harmonics and thus act as high-pass filters. King and Gordy [946] recommend that adjustments be made at a frequency for which the fundamental or one of the lower harmonics coincides with the rotational absorption line of a linear or symmetric molecule. This means that higher harmonics will coincide closely (but not exactly, because of centrifugal stretching) with higher rotational lines of the same molecule. As the frequency of the klystron providing fundamental power is then varied, absorption lines corresponding to successive harmonics appear—generally with decreasing amplitude

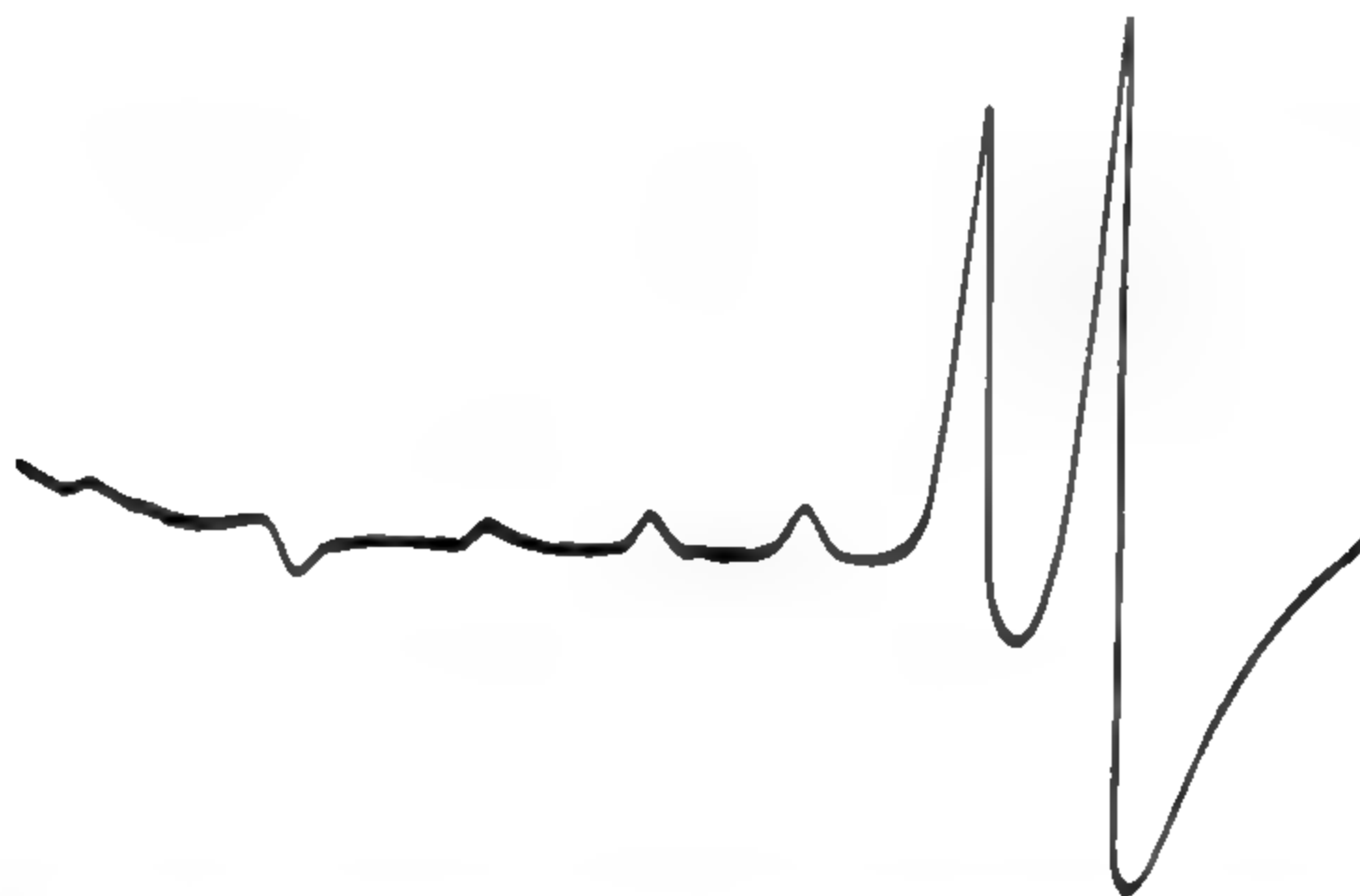


FIG. 16-6. The 8th, 10th, 12th, 16th, 18th and 20th (from right to left) rotational lines of OCS obtained with the 4th to 10th harmonics of 1.23 cm klystron. Frequency of fundamental increases from left to right. Harmonic frequencies range from 97,000 Mc to 243,000 Mc (3.08-mm to 1.23-mm wavelength). (*From King and Gordy [946].*)

as shown in Fig. 16-6. The number of harmonics present may then be judged by the number of absorption lines present, and a particular harmonic optimized by observing the magnitude of its absorption. For use of this technique, it is important to find a molecule with rotational lines very near the frequency which is desired, since harmonic power will not remain optimized when the klystron frequency is varied.

**16-7. Propagation of Millimeter Waves.** A conventional rectangular waveguide which propagates microwaves only in the dominant ( $TE_{10}$ ) mode is usable for millimeter waves, although attenuation increases with frequency [*cf.* Eq. (14-27)] and, at the shortest wavelengths, attenuation may be prohibitively large. Oversize waveguide (for example, *K*-band size) may be used if it is matched to the generator, or to a small guide used to filter out low frequencies, by a suitably gradual taper. However, such a guide will transmit any higher modes generated at discontinuities, and so special care must be taken to avoid irregularities. For instance, flanged joints must be carefully assembled to ensure accurate alignment of the waveguide sections. Many generators of millimeter waves emit the waves into a number of different modes in an

oversized waveguide. In such cases a complex of modes is already present, but careful elimination of irregularities at flanges is still important to reduce reflections and losses.

Attenuators used for millimeter waves resemble those for longer wavelengths, although they are reduced in dimensions. Carbon-coated tapered strips of mica inserted through an axial slot in the broad waveguide face are satisfactory.

Sometimes techniques based on those of optical spectroscopy may be used to advantage. For instance, reasonably small horns will produce a fairly narrow beam in free space or through an absorbing gas. This beam may also be reflected by a diffraction grating which permits rough wavelength measurements. For high efficiency, the grating can be of the echelette type, in which the rulings are shaped to throw as much of the diffracted radiation as possible into one order. One typical echelette grating, designed to operate around 1.6-mm wavelength, had eighty  $\frac{1}{8}$ -in. grooves milled into a flat metal surface. Focusing of the microwaves was effected by two spherical mirrors as shown in Fig. 16-7. An echelette grating is most efficient only for one particular

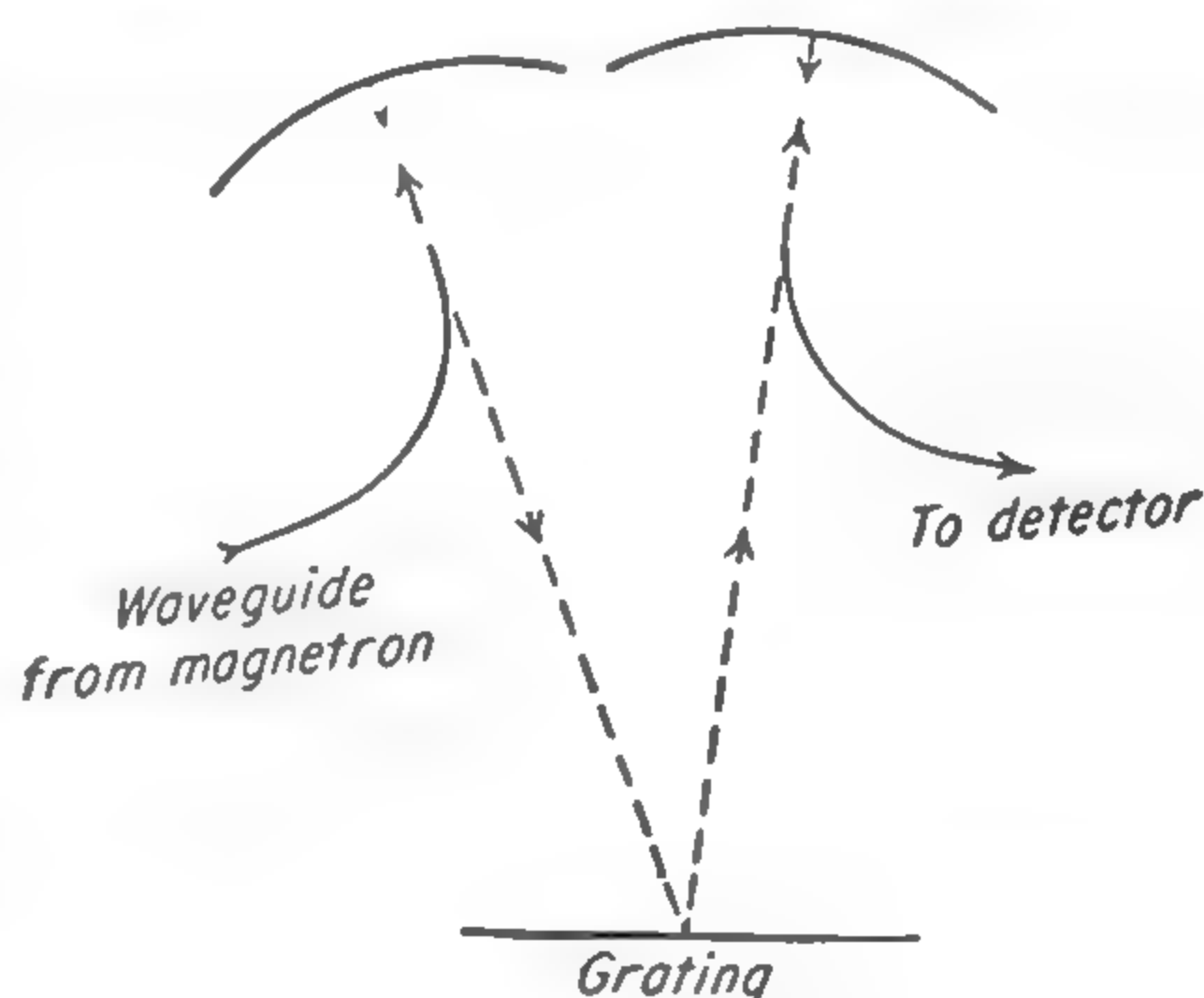


FIG. 16-7. Diffraction grating for measuring millimeter wavelengths. (From Klein, Loubser, Nethercot, and Townes [716].)

wavelength, although the maximum is fairly broad. A more elaborate design suitable for somewhat longer wavelengths has been constructed of semicircular rods which can be rotated to suit the wavelength [260].

**16-8. Frequency Measurement.** The methods employed for the measurement of frequency in the millimeter range are not essentially different from those used for longer microwaves (see Chap. 17). However, the relative importance and usefulness of the various techniques of frequency measurement are changed by the change in wavelength.

Cavity resonator wavemeters can be used for the longer millimeter waves. As the wavelength is shortened, construction tolerances become more critical. In addition,  $Q$  decreases for most modes as the wavelength decreases. Some improvement in  $Q$  may be obtained by using a larger cavity in a higher mode, such as one of the circular electric modes which have no currents across the gap between the end plunger and the wall. However, in this case mode ambiguity can occur, and so it is necessary to make sure that the resonances observed really correspond to the desired mode. One good way to do this is to use the wavemeter to check the frequency of a known spectral line. Another method of



checking the oscillator frequency roughly, and so of verifying the wavemeter mode, is to use a low- $Q$  wavemeter.

In the millimeter region broad-band interferometers based on similar optical types can serve this purpose. Among these are the Fabry-Perot [786], [770a] and Michelson types [214], [265], [385], [404]. These interferometers resemble their optical counterparts in most respects, although some of them use magic T's instead of partly reflecting mirrors as beam splitters. They can be refined to give moderately good accuracy but even in quite simple form can discriminate between successive harmonics of an oscillator, or between different wavemeter modes. A diffraction grating, either reflection or transmission, can also be used for rough frequency measurement.

If a harmonic generator is used, it is often more convenient to measure the fundamental wavelength by a wavemeter connected before the generator. The order of the harmonic can be identified by some rough frequency measurement as described above. Or the successive rotation lines of a simple molecule may be used to identify the frequency as indicated in the discussion on harmonic generation. A heterodyne method has also been used to discriminate between harmonics [457]. Two harmonic generators driven by separate klystrons are used, one of which is swept in frequency synchronously with an oscilloscope sweep. Beat frequencies between the klystron harmonics are passed through a tuned intermediate-frequency amplifier and applied to the oscilloscope. Different harmonics appear at different places on the oscilloscope screen and so may be identified. This is because the difference frequency between harmonic pairs is proportional to the harmonic number.

For precision frequency measurements, the unknown frequency may be compared with harmonics of a standard crystal oscillator (*cf.* Chap. 17). The comparison may be made at the klystron fundamental frequency where there is more than sufficient power to beat with the frequency standard.

**16-9. Absorption Spectrographs for the Millimeter Region.** In view of the difficulty in making satisfactory signal sources and detectors, it is fortunate that absorption lines in the millimeter region tend to be stronger than those at lower frequencies. This is partly because of the (frequency)<sup>2</sup> factor in Eq. (13-19), and partly because the higher-frequency transitions usually belong to states of higher rotational quantum number  $J$ , which are more populated at ordinary temperatures. For linear molecules, the intensity is proportional to  $J^3$  or  $\nu^3$ .

The line intensities are sometimes high enough so that straight absorption, without modulation, may be used, and absorption cells of a few feet or even a few inches may be sufficiently long. Stark modulation is more difficult to apply than at lower frequencies, because the Stark effect is proportional to  $1/J^3$ . Besides, Stark modulation cells often have

high attenuation at millimeter wavelengths. Frequency modulation of the source ("double modulation," see sec. 15-2) is a useful alternative in cases where Stark modulation cannot be applied.

Otherwise, millimeter-wave spectrographs generally resemble those for longer wavelengths and considerations similar to those of Chap. 15 are applicable.

## CHAPTER 17

# FREQUENCY MEASUREMENT AND CONTROL

Many of the lines observed in microwave spectroscopy are so narrow as to warrant extremely high precision in the measurement of their frequency. For instance, if a line is 100 kc wide, its center can be located to a tenth of its width, or 10 kc, without much difficulty, and in some cases the line center can be still more accurately determined. And if the line is near 25,000 Mc, 10 kc represents an accuracy of a part in 2.5 million. Precision of this order is rare in physical measurements and requires very good standards of frequency. In fact, refined techniques permit locating the line center to an accuracy at least as great as that of the very best earlier standards of frequency or time. Thus microwave spectral lines may themselves be used as frequency standards, making possible "atomic clocks."

The methods used for measuring microwave line frequencies and the converse problem of using the lines to control electronic oscillators or clocks will be discussed in this chapter.

**17-1. Wavemeters.** For rough frequency measurements, as when a new line is found, cavity wavemeters are extremely useful (*cf.* Chap. 14). For instance, a 1.25-cm-band wavemeter of the type shown in Fig. 14-6 has an unloaded  $Q$  of 8000 to 10,000, which is reduced to near 5000 by loading. With this instrument settings can be made on an oscillator frequency to about 1 Mc, or 1 part in 25,000. Even this accuracy, which requires very careful wavemeter construction, is much poorer than the narrowness of the spectral lines permits. Hence some better measuring device such as a quartz-crystal-controlled frequency standard is needed for accurate measurements.

A crystal-controlled frequency standard is usually designed to give a series of harmonic frequencies separated by perhaps 30 Mc. In this case a cavity wavemeter is needed to distinguish between the different harmonics, and its accuracy need only be as good as about 10 Mc. This accuracy (near 1 part in 3000) can be attained with ordinarily good machining tolerances and without compensation for temperature or atmospheric conditions. It is probably representative of the performance of the wavemeters used in most microwave spectroscopy.

When the wavemeter is used with a spectrograph, a circuit like that of



Fig. 17-1 is convenient. The wavemeter absorption pip is centered on the mode oscilloscope, which otherwise displays the variation of klystron output during its sweep. If previously a microwave line has been brought to the center of the spectrum oscilloscope by tuning the microwave oscillator, its frequency is thus measured by the wavemeter.

While the second oscilloscope is convenient because it permits viewing the klystron mode at the same time as the line, it can be eliminated. Then both the wavemeter and spectrograph signals are applied to the same oscilloscope. The pattern seen then is the sum of the sharp microwave resonance and the broader cavity resonance, which can be brought into coincidence with it. Probably the most satisfactory arrangement would be to use a double-beam oscilloscope if one is available.

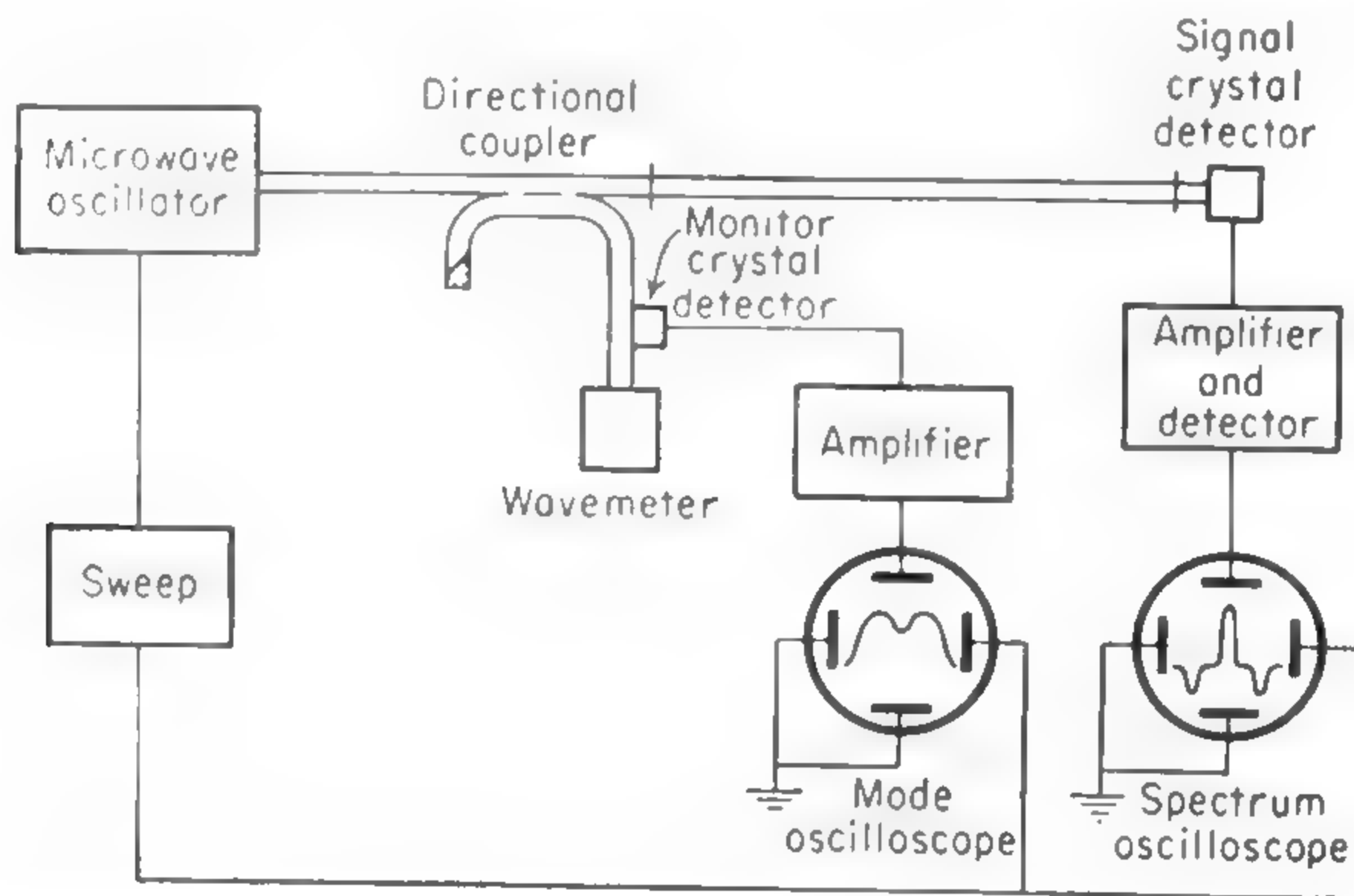


FIG. 17-1. Microwave spectrograph with absorption wavemeter.

To attain an accuracy appreciably greater than about 1 part in 3000 with a wavemeter alone, it must be constructed so that the plunger displacement can be measured to a thousandth of a millimeter or better. Compensation or correction for temperature changes is needed ([221], pp. 384-392; [288]). For a cavity constructed entirely of one material, the temperature coefficient of frequency is approximately the same as the coefficient of linear expansion, *i.e.*, about  $2 \times 10^{-5}$  per degree centigrade for brass.

The wavemeter of course directly measures wavelength, and conversion to frequency requires a knowledge of the dielectric constant or refractive index of air. This varies with temperature and humidity. The refractive index of air for the ranges encountered in the laboratory is given by the empirical equation [453], [675]

$$(N_{t,p} - 1)10^6 = \frac{103.49p_1}{T} + \frac{177.4p_2}{T} + \frac{96.0}{T} \left( 1 + \frac{5208}{T} \right) p_3 \quad (17-1)$$

where  $p_1$ ,  $p_2$ , and  $p_3$  are the respective partial pressures of dry air, carbon

dioxide, and water vapor in mm. Hg and  $T = 273 + t$  is the absolute temperature,  $t$  being the temperature in degrees centigrade. From this it follows that changes in temperature and humidity can shift the apparent frequency by as much as 0.02 per cent.

If the waveguide system to which the cavity is connected has standing waves, another error can be introduced. The standing waves correspond to a reactance such that the total circuit reactance will be a minimum at a frequency slightly different from the resonance frequency of the cavity alone. Errors of the order of 0.02 per cent may be produced in this way.

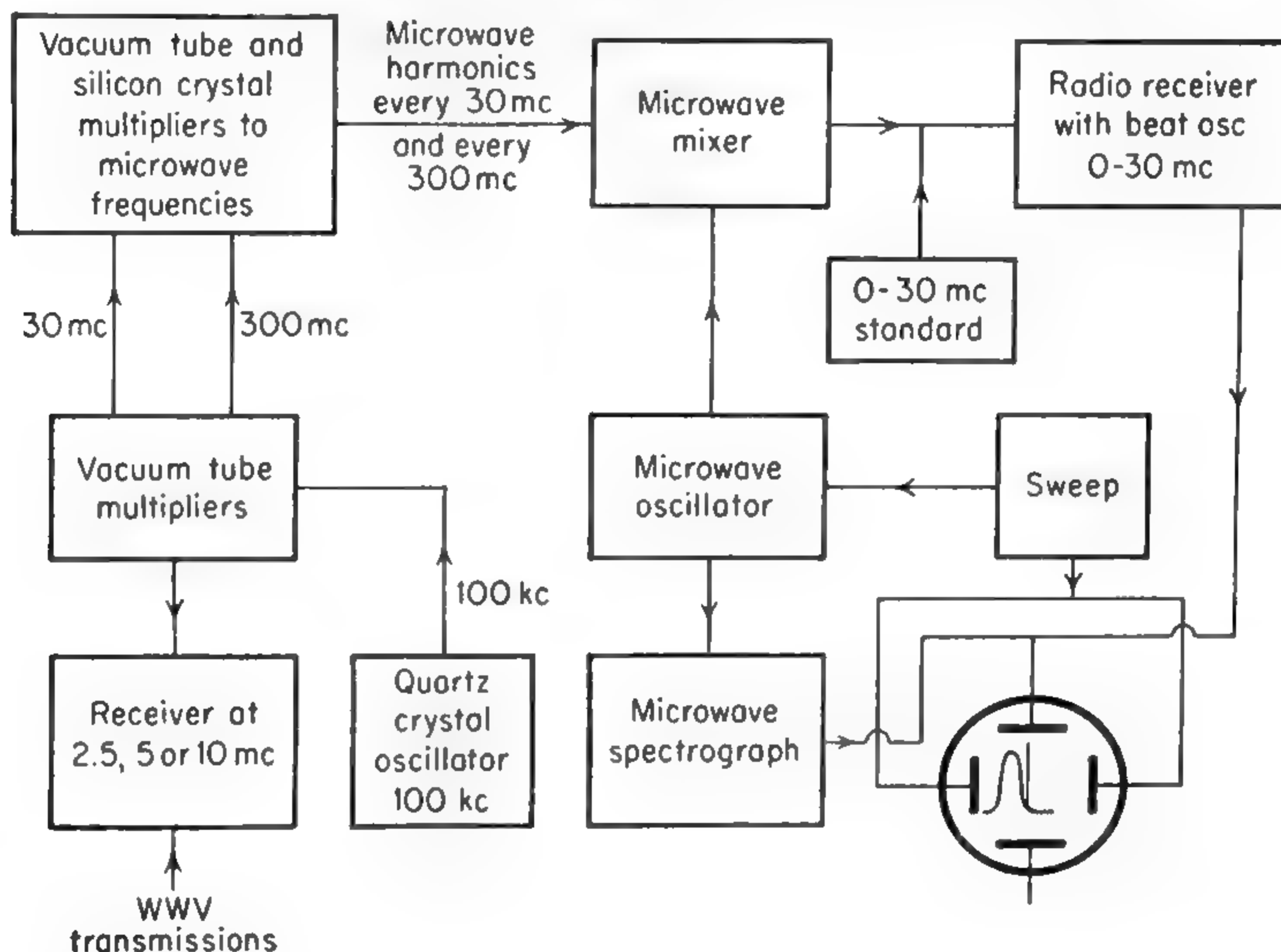


FIG. 17-2. Quartz-crystal-controlled microwave frequency standard.

While these sources of error can be reduced, even the best wavemeters are not good enough by themselves for really precise measurements of microwave spectral-line frequencies.

**17-2. Quartz-crystal-controlled Frequency Standards.** As noted above, for accurate measurements the spectral-line frequency is compared with harmonics of a high quality quartz-crystal-controlled oscillator. This in turn is standardized by comparison with the radio transmissions of a standard frequency like those of station WWV in Washington. Ultimately these transmitted frequencies are regulated by checking them against astronomical observations.

A commonly used type of frequency standard is shown schematically in Fig. 17-2. The multiplier chain produces harmonics in the microwave band whose frequencies are accurate multiples of 30 Mc. These are combined with the microwave oscillator output in a silicon or germanium crystal mixer to produce a beat frequency between 0 and 30 Mc. The

beat is observed at the output of the radio receiver only when it nearly coincides with the frequency to which the receiver is tuned. Therefore, as the klystron is swept over a range of a few megacycles to display an absorption line on the spectrograph, a sharp pulse appears as the difference frequency passes that to which the receiver is tuned. This pulse is displayed on the same oscilloscope or recorder as the line, and by tuning the receiver the pulse can be made to coincide with the line center. Then the receiver frequency is read from its calibrated dial or measured by a low-frequency (0 to 30 Mc) tunable standard. The latter need be of only moderate precision since it measures the difference between the 30-Mc harmonics and the line frequency. This difference is a small fraction of the whole frequency.

Beats are obtained whether the klystron frequency is above or below the harmonic or marker frequency. They may be distinguished by changing the receiver frequency a small amount in a known direction and noting the direction in which the frequency marker moves.

Occasionally a microwave line will lie so close to one of the 30-Mc harmonics that, when the klystron is adjusted into coincidence with the line, the beat frequency is below the receiver's tuning range. It is then necessary to use the beat with an adjacent harmonic, which will be just greater than 30 Mc.

In setting on a line, it must be noted that the line and the marker pulse or "pip" have very different waveforms and that they pass through separate and dissimilar amplifiers. They will each suffer a time delay during amplification, and the amounts of these delays will be unequal. Therefore if the true line frequency is to be determined accurately, a measurement should be made with the sweep going in the direction of increasing frequency, and again with the direction reversed (*cf.* [445]). The average of these two settings gives the true line frequency. The error may also be minimized by sweeping at a rate slow compared with the response time of the amplifying and "pip"-forming circuits.

The quartz crystal which controls an accurate frequency standard should be of a type such as the GT cut having a small temperature coefficient of frequency and furthermore should be operated at a fixed temperature if very high accuracy is desired. As the frequency generated by a crystal-controlled oscillator is affected slightly by the tube and other circuit elements, the circuit employed should be designed to minimize the effect of such variations. In the circuits commonly employed for frequency standards, the quartz crystal is placed in one arm of a bridge which controls the oscillator feedback [86*a*], [626*a*]. The same arm contains a small adjustable reactance which is used to adjust the frequency to coincide exactly with a primary standard such as station WWV. Because conditions for the reception of WWV are not always good, and the received signal sometimes exhibits fading or



frequency flutter [523], the oscillator ought to be stable enough that only occasional checking is required. To this end the oscillator should be protected from load variations, being coupled to output circuits through one, or possibly even several, successive cathode followers. This precaution is especially important if the crystal oscillator output is to be available for use as a general laboratory standard, so that different test circuits may be connected to it.

Recently spherically contoured polished quartz plates of very high stability have been developed. They can be used to control directly oscillators in the 5 to 10-Mc region, thereby eliminating several frequency-multiplier stages in the standard. Their  $Q$  is so high (several million) that fairly simple oscillator circuits, such as that in Fig. 17-3, may be used [760a], [882].

Frequency multipliers for use in the early stages of microwave standards are not essentially different from those used in radio transmitters (see, for instance, [121], pp. 458–462; [221], pp. 365–374). Harmonics are generated by a nonlinear amplifier, which has its output circuit tuned to the desired harmonic. Usually the harmonic generator is a class C amplifier with the grid biased to, or slightly beyond, cutoff, so that plate current flows only in bursts which are rich in harmonics. For best stability, no grid current should flow during any part of the cycle. Push-push amplifiers give only even harmonics, while a push-pull operation gives only odd harmonics. Some typical circuits are given in Fig. 17-4.

A higher order of multiplication is needed to produce microwave frequencies especially if one starts from an oscillator in the region of 100 kc. Therefore, care must be taken to avoid introducing undesired frequencies in the early stages, which will produce a rich spectrum in the microwave region, so that the desired harmonics are hard to identify. Harmonic generators, being highly nonlinear amplifiers, will mix undesired frequencies, such as 60 cycles from power supplies, to produce side frequencies, each of which has its own overtones. Excellent filtering is needed in the power supplies, which can best be achieved by the use of a series-tube regulated power supply. If successive multiplier stages are too tightly coupled, their tuning will be broadened sufficiently to permit them to pass undesired harmonics. Loosely coupled series-tuned link coupling between stages helps to select the desired frequency.

In some microwave-frequency standards conventional tubes are used up to a frequency of some hundreds of megacycles, and then followed by a silicon crystal harmonic generator. In one design, for example, the final vacuum-tube stage is a pair of 2C40's tripling from 270 to 810 Mc. Others use special multiplier klystrons up to 3000 Mc, or even higher, before the final crystal harmonic generator. Such klystrons give frequency multiplication by factors up to about 12 and yield much larger







power than can be obtained in the corresponding harmonic from a crystal harmonic generator. Somewhere in or just before the final stage, provision is made for mixing in frequencies such as 270, 30, or 10 Mc to give markers more closely spaced than the overtones of the last multiplier.

The crystal harmonic generator is similar in principle to those employed for generating millimeter waves (sec. 16-6). However, the lower input frequency usually requires coaxial cable connections rather than waveguide.

Some frequency standards generate a variable microwave frequency which is adjustable to the line frequency, rather than a series of fixed harmonics. To get an accurately known variable frequency, the output of a fixed crystal oscillator or one of its harmonics is combined with a low-frequency oscillator covering a small range. Then the sum frequency, which is selected by a filter, is known to the same absolute accuracy as the variable oscillator but to a much higher percentage accuracy ([221], p. 365).

There are many variations possible in the particular combination of circuits used to measure frequencies. However, those above appear at present to be the most convenient and widely used.

**17-3. Measurement of Frequency Differences.** Sometimes, as for hyperfine-structure measurements of microwave lines, only frequency differences are needed rather than accurate absolute frequencies. While these differences can be obtained readily by measuring the two components with an absolute frequency standard, the use of a standard can sometimes be avoided by measuring differences directly. This can be done by electronically frequency-modulating the klystron with an alternating repeller voltage whose frequency is adjustable over the range of separations to be measured. Then the klystron output contains the center frequency and sidebands separated from it by the modulation frequency. To make the measurement, the klystron is set on one component of the hyperfine structure and a sideband is simultaneously adjusted to coincide with the other component. The repeller modulation frequency is then the separation of the components, and since this is usually of the order of a few megacycles it can be easily measured with an accuracy comparable with the line width [145], [317]. This technique is useful only if the hyperfine structure is very simple so that there is no confusion between the several overlapping patterns which are produced. It is to be noted that the separation in megacycles of the line images is equal to the modulation frequency even for harmonics of the klystron frequency.

Another somewhat more complex, but more generally useful, system involves stabilizing a microwave oscillator on some fixed frequency near the lines to be measured. Its output is then mixed with the output of a low-frequency oscillator to provide frequency markers with separations

which are accurately known, even though the absolute frequencies are not known. Methods for stabilizing a microwave oscillator are discussed in the following section.

**17-4. Frequency Stabilization of Microwave Oscillators.** The frequency generated by a microwave oscillator can be stabilized by comparing it with an external standard. Since the standard can be relatively free from the thermal, electrical, and mechanical disturbances to which the klystron is sensitive, a considerable improvement in stability can be achieved. Among the standards which may be used as references for stabilization are resonant cavities, microwave spectral lines, and harmonics of quartz-crystal-controlled oscillators. These will be discussed separately.

Stabilization relative to another oscillator may be achieved by combining the outputs in a mixer and applying the difference frequency to the

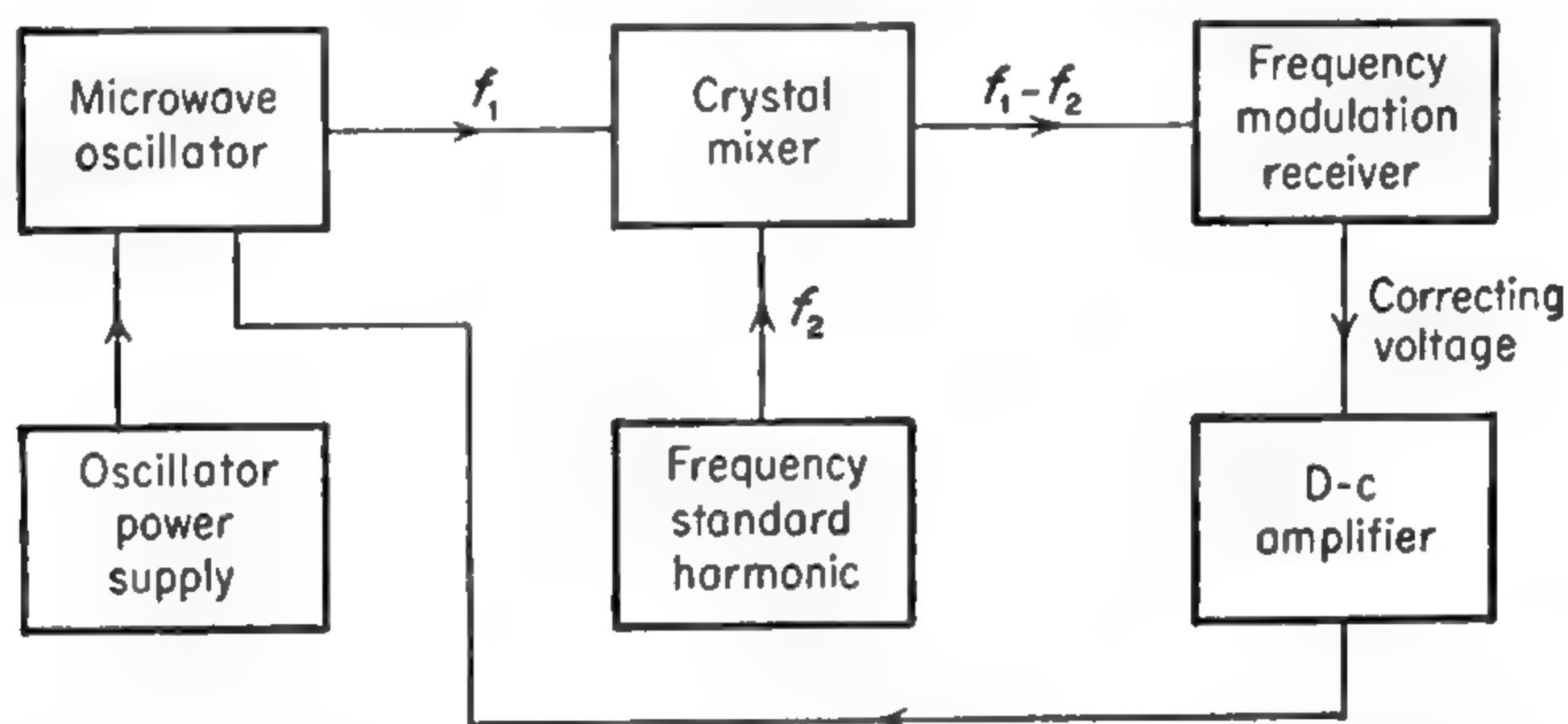


FIG. 17-5. Control of microwave oscillator by standard oscillator.

input of a conventional frequency-modulation receiver. From the receiver's discriminator a voltage is obtained which is zero when the microwave oscillators differ by just the frequency to which the receiver is tuned, and which changes sign on either side of the null point. Any discriminator output voltage can then be amplified by a d-c amplifier and applied to the klystron reflector or tuner electrode in such a direction as to counteract the frequency changes which produced it. (See Fig. 17-5.) The microwave oscillator can be made to follow the frequency-modulation receiver tuning over a range of some megacycles depending chiefly on the electronic tuning range of the tube and spurious competing signals picked up by the receiver. This type of stabilization is usually quite convenient for microwave spectroscopy, since a frequency standard is often readily available and can be used as the oscillator with respect to which the klystron is stabilized.

Sometimes the microwave oscillator is a reflex klystron in which the frequency-controlling electrode (the reflector) is operated at a high negative potential relative to ground. Then it may be convenient to couple it to the amplified discriminator signal through a magnetic control tube,

such as the 2B23 (General Electric) [567]. The signal from the d-c amplifier controls the current through a field coil, and this in turn varies the current through a resistor in series with the klystron reflector. The reflector voltage is thereby controlled without a direct connection between the high-voltage electrode and the d-c amplifier.

**17-5. Control of Frequency by a Resonant Cavity.** Since cavity resonators can be constructed with high  $Q$  and good stability, they can be used for controlling the frequency of a microwave oscillator. Some improvement in klystron stability can sometimes be made even by such a simple means as using a stabilizing voltage derived from a cavity wavemeter. If the oscillator is at a frequency which falls on one side of the sharp wavemeter response, a shift in frequency toward the wave-meter peak increases the detector crystal voltage, while a shift in the

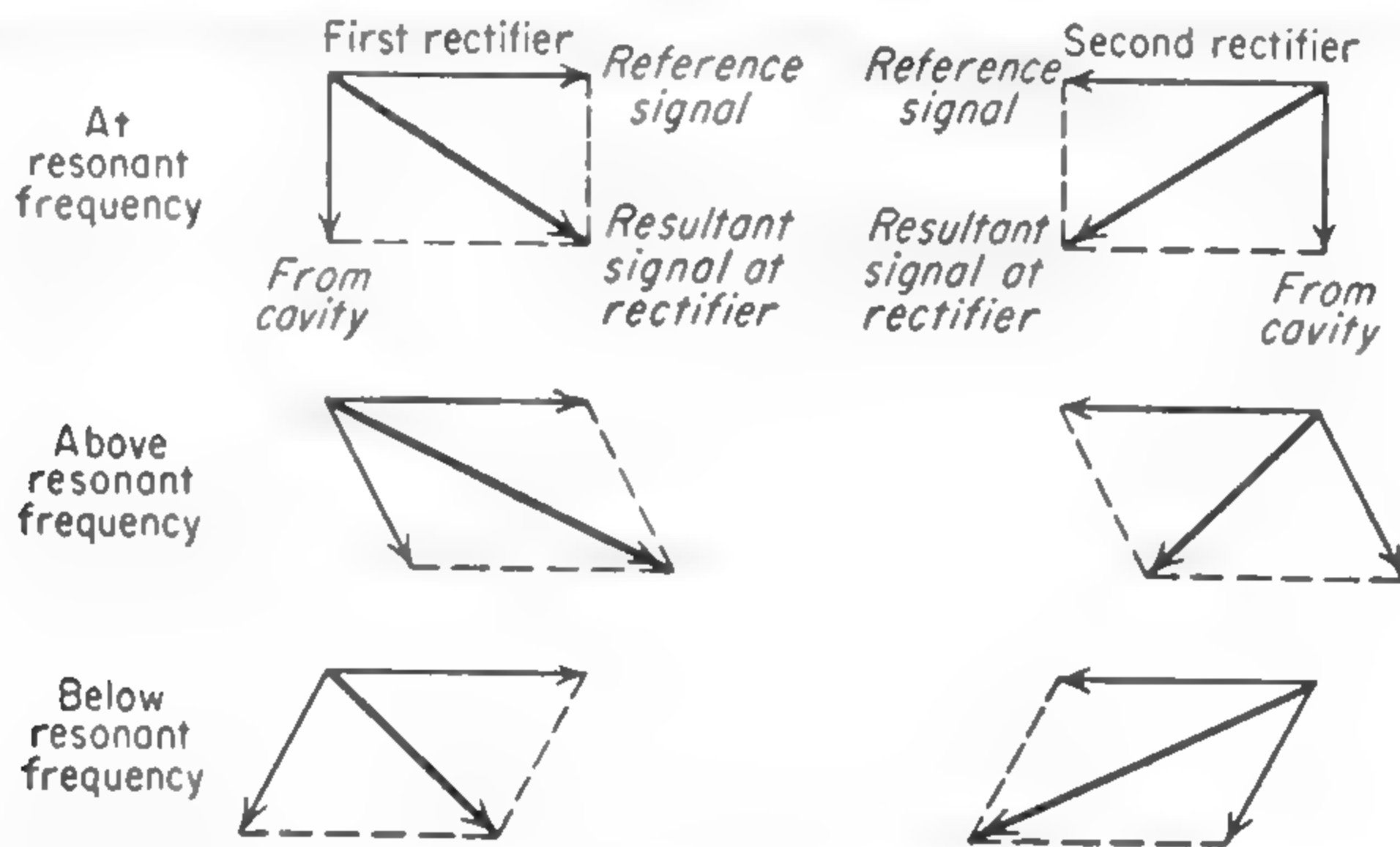


FIG. 17-6. Phase and amplitude relationships in microwave discriminator.

opposite direction decreases the voltage. After d-c amplification, this signal is applied to a controlling electrode of the oscillator. Such a method suffers from being sensitive to changes in oscillator amplitude, which can result from changes in loading. It is also sometimes a disadvantage that the frequency at which the oscillator is stabilized is not the cavity resonance center frequency.

The disadvantages of the simple method can be overcome by using a microwave discriminator analogous to those used with lumped circuit elements at lower frequencies. The discriminator uses two rectifiers in a circuit in which their outputs just balance each other at resonance. Changes in oscillator amplitude affect both outputs equally and so do not displace the balance frequency. On one side of resonance the first crystal rectifier produces a larger signal than does the second, and on the other side of resonance the situation is reversed.

This result may be obtained by combining the wave reflected from the cavity with waves which are, at resonance, respectively,  $90^\circ$  behind and  $90^\circ$  ahead of it in phase (Fig. 17-6). As the frequency changes on



either side of resonance, the phase of the reflected wave shifts rapidly in a direction dependent on the sense of the frequency change. The resultant amplitudes at the two crystals change accordingly, so that the difference between their rectified outputs indicates the magnitude and sign of any departure from resonance.

A microwave discriminator of this type is shown as part of a frequency-controlling circuit in Fig. 17-7 ([227]; [221], pp. 58–78). The cavity and a short circuit are at opposite ends of the coplanar arms (numbered 1 and 2 here) of a magic T ( $T_1$  in the diagram) but are positioned so that their effective distances from the median plane differ by  $\lambda_g/8$  near the cavity resonance frequency. Thus waves reflected from the cavity

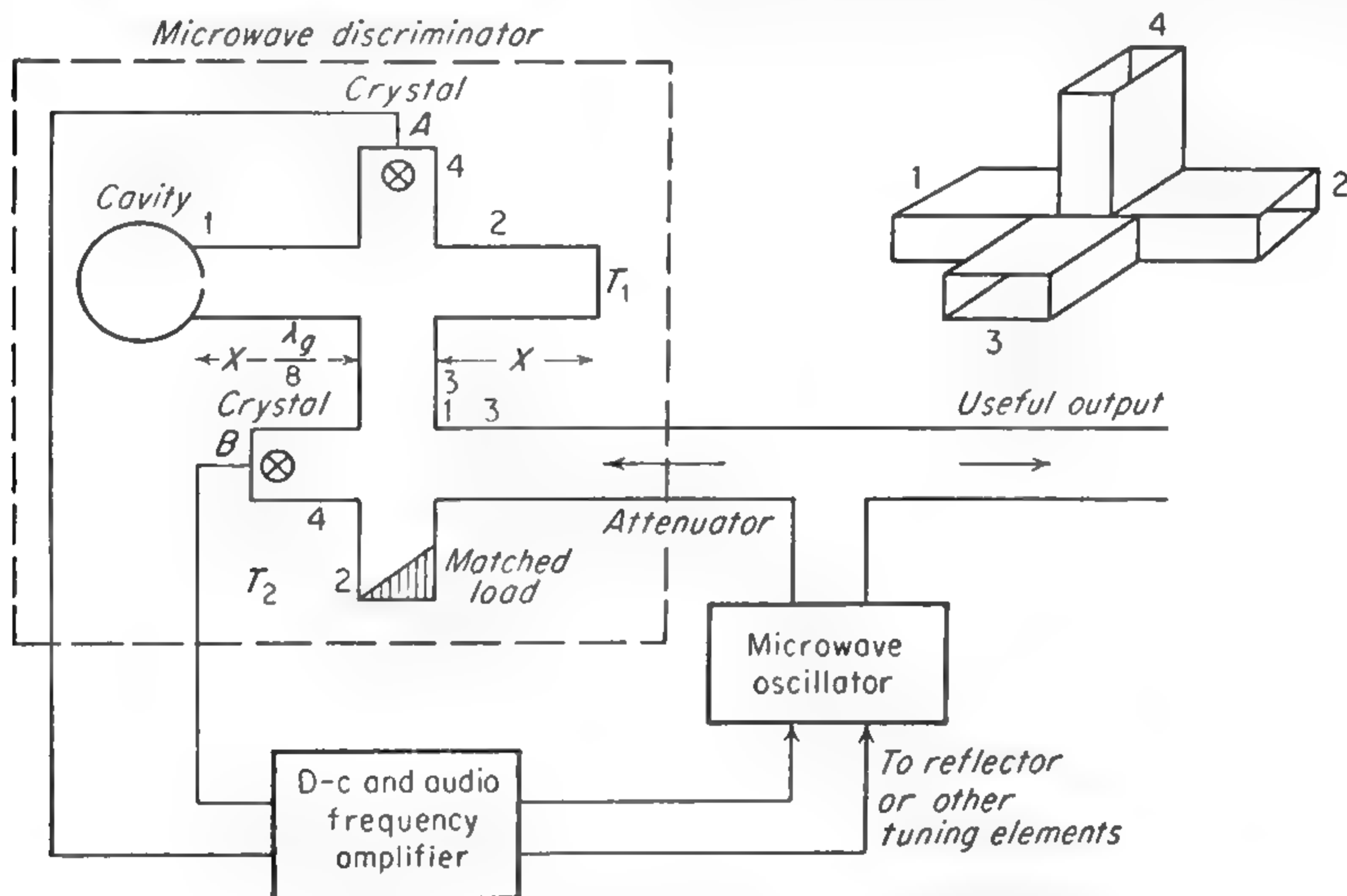


FIG. 17-7. D-c stabilizer—block diagram.

and the short differ by  $90^\circ$  in phase on reaching the median plane. Here the reflected waves combine to send a sum wave into arm 3 and a difference wave into arm 4, thus providing the two crystal detectors, A and B, respectively, with signals in which the cavity wave lags or leads the other wave by  $90^\circ$  in phase at resonance. On either side of resonance the cavity wave undergoes a rapid change of phase, producing the discriminator action described above. The second magic T ( $T_2$ ) directs only the reflected signal to crystal B, while sending the incoming klystron wave first to  $T_1$ . Crystal B actually receives only half as much power as crystal A, but this can be compensated by a balancing attenuator at the amplifier input.

For this circuit, the rate of change of discriminator voltage with frequency near resonance is

$$\frac{dV}{d\nu} = DP_0 \frac{Q_0}{\nu_0} \frac{4\alpha}{(1 + \alpha)^2} \quad (17-2)$$

where  $D$  = detector sensitivity in volts per unit power input

$P_0$  = microwave power applied to the discriminator

$Q_0$  = unloaded  $Q$  of the cavity resonator

$\nu_0$  = resonant frequency of the cavity

$\alpha = \delta_1/\delta_0$ , where  $\delta_0$  = decrement of the unloaded cavity and  $\delta_1$  = change in decrement when the cavity is coupled to a matched waveguide

For optimum sensitivity  $\alpha$  should be 1.

The d-c stabilizer is relatively simple and effective but it is limited by crystal noise, which is always largest at low frequencies. Moreover d-c amplifiers are seldom completely free from drift. Even so, d-c stabilizers have been used to hold two 9000-Mc oscillators within a few kilocycles over a period of hours.

The disadvantages of the d-c stabilizer are largely overcome by a circuit in which the signal amplification occurs at a high frequency ([227]; [221], pp. 58-78; [333]). The discriminator produces an intermediate-frequency voltage whose amplitude is proportional to the amount of the departure of the oscillator frequency from the cavity resonance and whose phase depends on the direction of departure. The phase-sensitive detector, similar to those described in Chap. 15, derives from this a d-c voltage whose magnitude and sign measure the departure of the oscillator from cavity resonance.

The error voltage derived from a microwave discriminator of either a d-c or an intermediate-frequency type can be applied to a servomechanism which tunes the microwave oscillator. Servomechanisms cannot respond as quickly as can an electronic system to rapid (audio-frequency) fluctuations in frequency, but are effective in counteracting slow drifts [228]. The electronic and servomechanical systems can be combined to control both the rapid changes in frequency and slow drifts [687].

**17-6. Stabilization of Microwave Oscillators by Absorption Lines.** Since a waveguide cell filled with a suitable gas shows a sharp absorption peak at the resonant frequency of the gas, it can be used in place of a resonant cavity to control the frequency of a microwave oscillator. Moreover the position of the line's center is nearly independent of temperature and pressure (Chap. 13), so that it can be made to serve as an absolute standard of frequency. An oscillator controlled by a spectral line can then be used to drive a clock through a chain of frequency dividers [492], [724].

If the microwave line is to be used as a primary frequency standard or "atomic clock" (a time standard dependent on a frequency of an approximately isolated nuclear, atomic, or molecular system), the associated circuits should hold the oscillator as accurately as possible to the center of the line. Since deviations from the center of a line are detected by the change in amplitude of a wave transmitted through a cell containing the gas, the minimum observable change in frequency is closely related

to the minimum observable absorption. For example, in Chap. 15 it is shown that the minimum detectable absorption, limited by thermal noise, is of the order of  $10^{-10} \text{ cm}^{-1}$  (for a 30-cycle noise bandwidth). Since the ammonia 3,3 line has a peak absorption roughly  $10^7$  times stronger than this, it ought to be possible to locate the line center to about  $(1/10^7)$  of its width. Since this width, as limited by Doppler effect at low pressures, is around 100 kc, *i.e.*, approximately  $1/(2 \times 10^5)$  of the line frequency, it seems reasonable that the ammonia line might ultimately be used to control microwave frequencies to about 1 part in  $5 \times 10^{13}$ , or even better with a narrower noise bandwidth. Although the method used in making this estimate is rather rough, the estimate of the ultimate stabilization limit agrees well with the more accurate treatment below (*cf.* also [653]). Actual atomic clocks constructed so far are limited by less fundamental difficulties to a much lower precision.

It has been shown previously that  $\Delta\gamma$ , the smallest detectable change in absorption coefficient, is [Eq. 15-9]

$$(\Delta\gamma)_{\min} = 2e(\alpha_0 + \gamma) \left( \frac{2kT \Delta f}{P_0} \right)^{\frac{1}{2}} \quad (17-3)$$

where  $\gamma$  = the absorption coefficient of the gas,  $\text{cm}^{-1}$

$\alpha_0$  = the loss coefficient of the waveguide,  $\text{cm}^{-1}$

$e$  = the base of natural logarithms

$k$  = Boltzmann's constant

$T$  = the absolute temperature

$P_0$  = the microwave power reaching the detector

$\Delta f$  = bandwidth of the detecting system

It is assumed that the optimum waveguide length,  $l = 2/(\alpha_0 + \gamma)$ , is used and that no sources of noise other than thermal are present.

The absorption coefficient of a narrow microwave line may be written approximately as [*cf.* Eq. (13-22)]

$$\gamma = \frac{\gamma_{\max}(\Delta\nu)^2}{(\nu - \nu_0)^2 + (\Delta\nu)^2} \quad (17-4)$$

where  $\gamma_{\max}$  = the absorption at the peak of the line

$\nu$  = the microwave frequency

$\Delta\nu$  = the half width of the line at the half maximum

$\nu_0$  = the frequency at the peak of the line

Some of the devices used at present for stabilizing on a spectral line set on the peak of the absorption. In that case a change  $\Delta\gamma$  in  $\gamma$  occurs if the frequency  $\nu$  differs from  $\nu_0$  by an amount  $\epsilon$  where

$$\epsilon = \Delta\nu \left( \frac{\Delta\gamma}{2\gamma_{\max}} \right)^{\frac{1}{2}} \quad (17-5)$$

Considerably better performance can be obtained by using the steep



slopes of the absorption lines, since then a small change in frequency corresponds to a greater change  $\Delta\gamma$ . For a distance from resonance  $\nu - \nu_0 = a \Delta\nu$ ,

$$\frac{\epsilon}{\nu} = \frac{\Delta\gamma(a^2 + 1)^2}{2a\gamma_{\max}} \frac{\Delta\nu}{\nu} \quad (17-6)$$

Using Eq. (17-3), the smallest detectable fractional change in frequency is

$$\frac{\epsilon}{\nu} = \frac{e(\alpha_0 + \gamma)(a^2 + 1)^2}{a\gamma_{\max}} \frac{\Delta\nu}{\nu} \left( \frac{2kT \Delta f}{P_0} \right)^{\frac{1}{2}} \quad (17-7)$$

For  $\gamma_{\max}$  considerably smaller than  $\alpha_0$ , the smallest value of  $\epsilon/\nu$ , or the steepest part of the resonance curve, is obtained when  $a = \pm (\frac{1}{3})^{\frac{1}{2}}$ , that is,  $\nu = \nu_0 \pm (\frac{1}{3})^{\frac{1}{2}} \Delta\nu$ . Best performance for larger values of  $\gamma_{\max}$  is obtained somewhat farther from the resonance frequency. For the other extreme

$\gamma \gg \alpha_0$ , optimum values of  $a$  are  $\pm 1$ , and  $\frac{(\alpha + \gamma)(a^2 + 1)^2}{a\gamma_{\max}} = 2$ . This

case may be assumed, since for strong absorbers such as  $\text{NH}_3$ , it is possible to have  $\gamma_{\max} > \alpha_0$ . Thus the minimum detectable frequency change given by Eq. (17-7) becomes

$$\frac{\epsilon}{\nu} = 2e \frac{\Delta\nu}{\nu} \left( \frac{2kT \Delta f}{P_0} \right)^{\frac{1}{2}} \quad (17-8)$$

The above expression would indicate that the error in frequency stabilization could be made arbitrarily small by making  $\Delta\nu$  or  $T$  small or  $\nu$  or  $P_0$  large. However,  $T$  cannot be reduced indefinitely without reducing the gas pressure to too low a value. Usually an upper limit to the power  $P_0$  is set by saturation effects. The line width  $\Delta\nu$  cannot be reduced below the limit set by Doppler effect except by methods which reduce the number of molecules available for absorption and so reduce  $\gamma$ . Thus the only method of obtaining arbitrarily small error is to decrease the bandwidth  $\Delta f$ .

If a particular absorption line is considered, an optimum power flux can be determined. As shown in Chap. 13, half width is obtained when saturation occurs which, when inserted in place of the  $\Delta\nu$  occurring in (17-8), gives

$$\frac{\epsilon}{\nu} = 2e \frac{\Delta\nu}{\nu} \left( 1 + \frac{8\pi^2 |\mu|^2 \nu I t}{3ch \Delta\nu} \right)^{\frac{1}{2}} \left( \frac{2kT \Delta f}{P_0} \right)^{\frac{1}{2}} \quad (17-9)$$

where  $\mu$  = the dipole moment matrix element of the transition

$c$  = the velocity of light

$h$  = Planck's constant

$$t \approx \frac{1}{2\pi \Delta\nu}$$

Since  $I$ , the number of quanta per second per unit cross-sectional area, is directly proportional to  $P_0$ , this expression approaches a limiting minimum value for large  $P_0$  and differs from the minimum value only by a factor of  $\sqrt{2}$  when saturation first becomes noticeable, *i.e.*, when

$$I \approx \frac{3ch(\Delta\nu)^2}{4\pi|\mu|^2\nu} \quad (17-10)$$

If the cross-sectional area of the waveguide is  $A$ , then  $P_0 = Ah\nu I$ , and for power  $P_0$  large enough to give saturation

$$\frac{\epsilon}{\nu} = \frac{8e|\mu|}{h} \left( \frac{\pi kT \Delta f}{3cA\nu^2} \right)^{\frac{1}{2}} \quad (17-11)$$

This expression very significantly does not contain the line width  $\Delta\nu$ . The advantage in sharpness of the line which is obtained by decreasing  $\Delta\nu$  is just counteracted by the loss in sensitivity due to power saturation of the absorption. Thus there is no strong reason for attempting to attain lines so narrow that their width is determined by Doppler effects. In practice a very wide line is not desirable because the maximum power available  $P_0$  and the power at which efficient detectors operate is usually near 1 mw. In addition nonfundamental variations of circuit response with frequency are very troublesome, and hence a sharp line is desirable to minimize their effects. However, Eq. (17-11) does show that, so far as the limitations of thermal noise are concerned, the line width is unimportant and can be adjusted to any convenient value. Since saturation of most spectral lines occurs with line widths of about 1 Mc and a power flux of a few milliwatts per square centimeter, pressures such that the line is somewhat narrower than 1 Mc would be a convenient choice. Of course the radiation density or the field strength is not uniform throughout the waveguide cross section or throughout the length of the guide because of attenuation. However, a reasonably accurate approximation for  $\epsilon/\nu$  is obtained by considering the "average" saturation condition at the end of the guide where the radiation is introduced.

If it is assumed that, to avoid higher modes of propagation, the waveguide cross-sectional dimensions are of the order of the waveguide  $\lambda$ , then  $A \approx (c/\nu)^2$ , and

$$\frac{\epsilon}{\nu} = \frac{8e|\mu|}{hc} \left( \frac{\pi kT \Delta f}{3c} \right)^{\frac{1}{2}} \quad (17-12)$$

For a numerical evaluation of (17-12), the specific case of the strongest ammonia line, the 3,3 line at 23,870 Mc is of interest. Taking  $T = 200^\circ\text{K}$  and  $\Delta f = 1$  cycle/sec, one obtains, since  $\mu = 1.4 \times 10^{-18}$  esu,

$$\frac{\epsilon}{\nu} = 1.5 \times 10^{-13} \quad (17-13)$$

for the accuracy limit imposed by thermal noise.

If the peak of the line is used in the same way for stabilization rather than the points of maximum slope the ultimate accuracy may be decreased by a factor of more than a thousand [724]. In this case, as when certain less efficient detectors are used, or noise is present which is greater than fundamental thermal noise, the attainable accuracy is no longer independent of the line-width parameter.

*Use of Dispersion.* The above discussion has considered using only the absorption of a molecular resonance in order to stabilize an atomic clock. The dispersion, or reactive part of the resonance, is equally usable. Figure 17-8 shows the behavior of the anomalous dispersion or variation in the dielectric constant near a resonant absorption. Near an absorption line the dielectric constant can be written [cf. Eq. (13-15)]

$$\begin{aligned} K &= K_0 + \frac{\lambda(\nu_0 - \nu)}{\Delta\nu} \frac{\gamma}{2\pi} \\ &= K_0 + \frac{\lambda(\nu_0 - \nu)\gamma_{\max}\Delta\nu}{(\nu - \nu_0)^2 + (\Delta\nu)^2} \end{aligned} \quad (17-14)$$

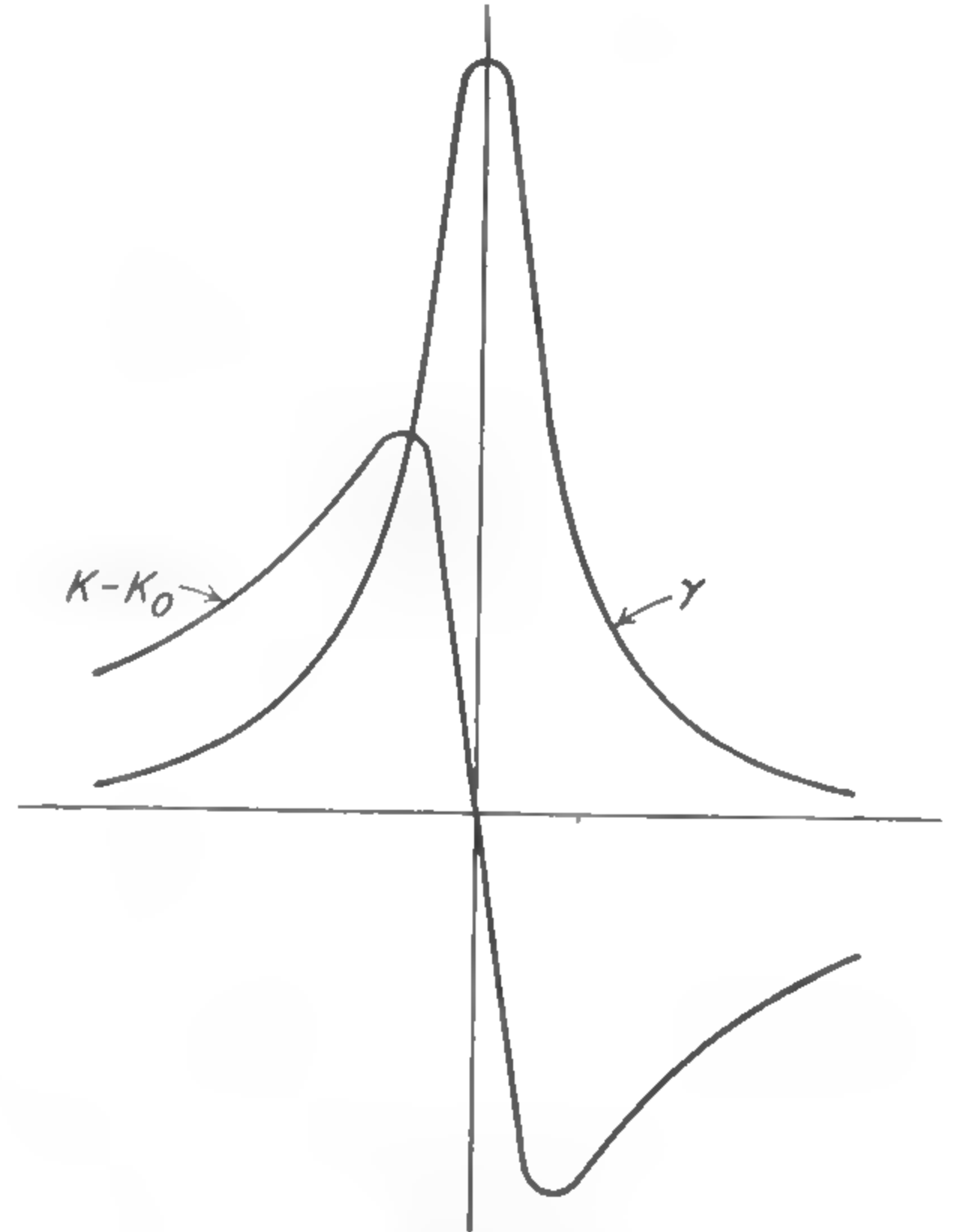


FIG. 17-8. Loss and dispersion near a spectral line.

where  $K_0$  is the dielectric constant some distance on either side of the line,  $\lambda$  is the wavelength, and other quantities are as defined for expression (17-4). For a gas at low pressure,  $K_0$  may be taken as 1 and  $K$  is not very different from 1, so that the index of refraction  $n$  is

$$n = K^{1/2} = 1 + \frac{\lambda(\nu_0 - \nu)\gamma}{4\pi\Delta\nu} \quad (17-15)$$

By methods shown in reference [653], one finds that the signal power derivable from this dispersion is a maximum for a length of waveguide  $l = 2/(\alpha + \gamma_{\max})$ , and has the value

$$\Delta P = P_0 \left( \frac{\gamma_{\max} e^{-1}}{\gamma_{\max} + \alpha} \frac{\epsilon}{\Delta\nu} \right)^2 \quad (17-16)$$

where  $P_0$  is the initial power introduced into the waveguide. If this power is equal to the thermal noise  $2kT\Delta f$ , then the fractional frequency error is

$$\frac{\epsilon}{\nu} = \frac{(\alpha + \gamma_{\max})e}{\gamma_{\max}} \frac{\Delta\nu}{\nu} \left( \frac{2kT\Delta f}{P_0} \right)^{1/2} \quad (17-17)$$



Thus use of dispersion gives not only essentially the same optimum length for the microwave path in gas, but also within a small factor the same fractional frequency error, as is shown by comparing (17-7) and (17-17).

**17-7. The Molecular-beam Maser.** One of the most promising atomic frequency standards is the molecular-beam oscillator shown in Fig. 15-10. This device can serve as a microwave amplifier or it can oscillate at a frequency determined primarily by the molecular resonance. It has the strong advantage of obtaining microwave oscillations directly from the molecules rather than requiring stabilization of an electronic oscillator on a molecular resonance.

Consider the amplification of noise by a *maser*—a cavity with wall and load losses given by  $1/Q$ , and containing a dielectric material with dielectric constant  $\epsilon = \epsilon' - i\epsilon'' = 1 + 4\pi\chi' + i(4\pi\chi'')$ . Here  $\chi'$  is the in-phase component of the polarizability per unit volume and  $\chi''$  is the component which is  $90^\circ$  out of phase with the polarizing electric field.  $\chi'$  and  $\chi''$  depend, of course, on the properties of the beam of molecules and, if amplification rather than power loss occurs,  $\chi''$  must be positive. The power which is generated at various frequencies in the cavity is given [925] by

$$P d\nu = \frac{(4\pi\chi''kT/Q)d\nu}{[(1/2Q) - 2\pi\chi'']^2 + [(\nu - \nu'_c)/\nu'_c]^2} \quad (17-18)$$

where  $\nu'_c$  is the resonance frequency of the cavity as modified by the presence of the molecules, or

$$\nu'_c = \nu_c(1 + 4\pi\chi')^{-1/2} \approx \nu_c(1 - 2\pi\chi') \quad (17-19)$$

since  $\chi' \ll 1$ . Here  $\nu_c$  is the resonance frequency when no molecules are present in the cavity. As in (15-12), the imaginary part of the dielectric constant or out-of-phase component of the polarization simply modifies the apparent loss factor  $1/Q$  of the cavity.

The maximum power generation occurs, from (17-18), when  $\nu_c = \nu'_c$ , and is large, corresponding to an oscillation, only if  $4\pi\chi'' \approx 1/Q$ . Near the center of the molecular resonance,  $\chi'$  may be written approximately as

$$\chi' = \frac{\chi''_0(\nu - \nu_0)}{\Delta\nu} \quad (17-20)$$

where  $\chi''_0$  is the value of  $\chi''$  at the resonance frequency  $\nu_0$  of the molecular line, and  $\Delta\nu$  is the half width of the line at half maximum intensity. Hence the oscillation occurs at

$$\nu = \nu'_c = \nu_0 + (\nu_c - \nu_0) \left(1 + \frac{2\pi\chi''_0\nu_c}{\Delta\nu}\right)^{-1} \approx \nu_0 + \frac{Q}{Q_L}(\nu_c - \nu_0) \quad (17-21)$$

Here  $\nu_c/2\Delta\nu$  has been set equal  $Q_L$ , which is an effective  $Q$  for the molec-

ular line, and the condition of oscillation  $4\pi\chi'' \approx 1/Q$  has been used, which makes  $2\pi\chi''\nu_c/\Delta\nu \gg 1$ .

Expression (17-21) shows that the oscillator frequency will be primarily determined by the molecular frequency  $\nu_0$ , but that if the cavity frequency  $\nu_c$  is not equal to  $\nu_0$ , the frequency will be "pulled" by approximately  $Q/Q_L(\nu_c - \nu_0)$ . For a typical case,  $Q/Q_L \approx \frac{1}{10000}$ , so that any variation  $\delta$  in cavity frequency will vary the oscillator frequency by about  $\delta/1000$ . Therefore, if the cavity frequency is constant to one part in  $10^8$ , the oscillator should be constant to about one part in  $10^{11}$ .

The total power, which is given by integrating over-all frequencies, should equal the power  $P_B$  delivered by the molecular beam. From this one can evaluate  $1/2Q - 2\pi\chi''$  which, although very small, is not exactly zero. Substituting the value of  $1/2Q - 2\pi\chi''$  into (17-18), it takes the form

$$P d\nu = \frac{4kT(\Delta\nu)^2 d\nu}{[4\pi kT(\Delta\nu)^2/P_B]^2 + [\nu - \nu_0 - (Q/Q_L)(\nu_c - \nu_0)]^2} \quad (17-22)$$

This expression for the spectrum of the oscillator is not strictly correct because, as in any oscillator, nonlinearities affect the frequency distribution. However, it gives an approximately correct value for the half width of the oscillator output, which is

$$\Delta\nu_{osc} = \frac{4\pi kT(\Delta\nu)^2}{P_B} \quad (17-23)$$

For a typical case,  $P_B \approx 10^{-10}$  watts and  $\Delta\nu \approx 2000$  cycles/sec, so that  $\Delta\nu_{osc} \approx 4 \times 10^{-3}$  cycles/sec. Experimental observations have shown that  $\Delta\nu_{osc} < 10^{-1}$  cycle/sec, and it seems probable that  $\Delta\nu_{osc}$  is actually near the theoretical value, which is  $2/10^{13}$  of the frequency  $\nu_0$ . This is by far the most monochromatic radiation which has yet been produced.

**17-8. Realization of Atomic Frequency and Time Standards.** No microwave frequency standard yet constructed approaches in accuracy the limits imposed by thermal noise. Difficulties involved in setting accurately and automatically on the center of a line to within a very small fraction of its width are great, even though in principle they can be overcome.

Almost all atomic frequency standards which have been based on a gas absorption line have used the ammonia 3,3 line. This line is very suitable because it is so strong ( $\gamma_{max} = 8 \times 10^{-4} \text{ cm}^{-1}$ ). Its only likely competitor is a line in the oxygen spectrum near 5-mm wavelength.

The oxygen molecule has a smaller dipole moment matrix element than ammonia since its electric dipole moment is zero and only the magnetic dipole moment exists to produce transitions. Thus the lines are not easily broadened or saturated. It has not been used because until recently oscillators giving sufficient power in the 5-mm region to use

these lines effectively were not available. Moreover, the oxygen lines exhibit a large Zeeman-effect broadening and so need to be shielded from fluctuating magnetic fields. Fortunately, the "first order" Zeeman effect is symmetrical and does not produce a displacement of the line center.

Even though one uses a single preferred line as a microwave standard, it can be used to control oscillators at other frequencies. These frequencies may be derived by using frequency multipliers and dividers, or by mixing in lower-frequency oscillators to generate sum or difference frequencies. The low-frequency oscillators need not be known to so great a percentage accuracy as the primary standard.

Several different methods have been employed to stabilize an oscillator relative to the ammonia line. They have succeeded in stabilizing to a

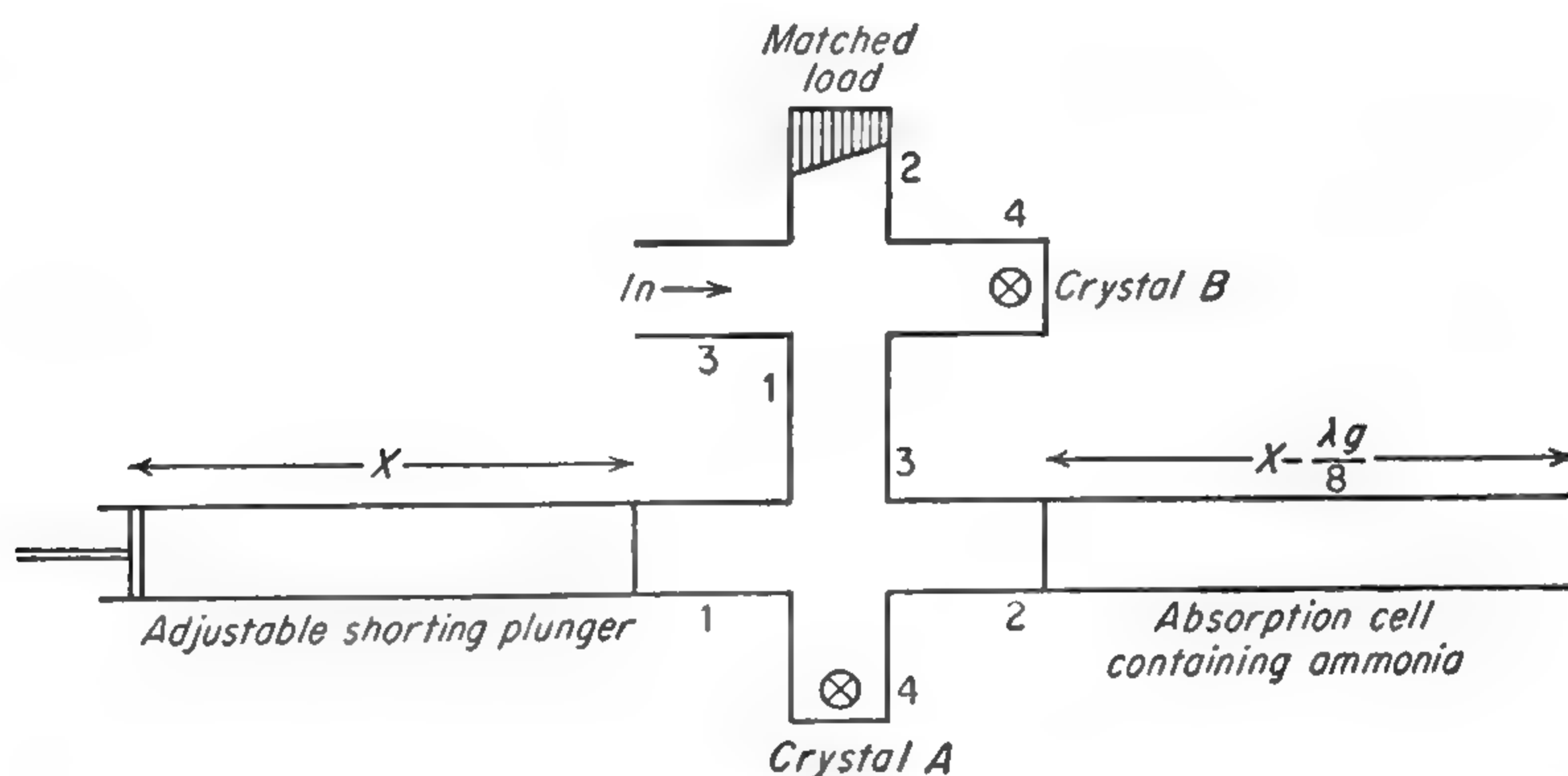


FIG. 17-9. Microwave discriminator using gas-absorption line in place of resonant cavity.

small fraction of the line's width. Nevertheless even the best is quite far from the theoretical limit [Eq. (13)].

The Pound microwave discriminator ([221], pp. 58–78) has been modified so that the reference cavity resonator is replaced by a short-circuited waveguide cell containing the gas under study [235], [310]. Figure 17-9 shows the modified discriminator. The discriminator output was applied through a d-c amplifier having a gain of 2000 to the frequency-controlling electrode of a 2K50 klystron oscillator. By this means drift was reduced by a factor of 1000 relative to that of an unstabilized tube.

Another method of locating the center of a spectral line is to sweep an oscillator across the line and detect the peak or the points of maximum slope by the ordinary methods of microwave spectroscopy [724], [287], [470], [600], [719], [329], [454]. For example, the microwave oscillator may be swept over a narrow range of frequencies (less than a line width) and the crystal detector current observed with a phase-sensitive detector. Output of the phase-sensitive detector passes through zero and reverses



at the peak of the line. A voltage derived from the detector is used to control the center frequency of this or another microwave oscillator which is compared with it. If the microwave oscillator is quite stable even when uncontrolled, relatively small and infrequent corrections will be needed. Then a more sensitive control system with a narrower band pass and a higher gain will be usable, resulting in a better final stability than if the oscillator is unstable. Quartz-crystal oscillators with harmonic generators can have excellent short-period stability and thus are advantageous [724].

These methods depend on the variation with frequency of the microwave amplitude at the detector. As noted in Chap. 15, reflections in the waveguide, and variations in klystron power, can cause changes of amplitude with frequency even without the presence of a line. These will limit the accuracy of any atomic clock, so that in practice it may be an advantage to have a narrow line even at some sacrifice of intensity. As with spectrographs, the effects of reflections and certain other disturbances can be minimized by using Stark modulation [329], [975], and some improvement in accuracy is possible by this means. Shimoda [975] has been able to stabilize an oscillator to an accuracy of about one part in  $10^9$  by the use of a combination of Stark, Zeeman, and source-frequency modulation.

Other natural frequency standards which promise accuracies comparable with microwave absorption are provided by molecular beams and by nuclear quadrupole resonances in solids. The molecular-beam lines are very sharp.  $Q$ 's of 30 million have already been obtained with a cesium atomic beam [724], and these may afford even better "atomic clocks" than do absorption lines in gases. Nuclear quadrupole resonances give  $Q$ 's comparable with the microwave lines. At ordinary temperatures the resonances are not intense and their frequency depends strongly on temperature, but in the liquid helium range they are much less sensitive to temperature changes and may afford accurate frequency standards.

The molecular-beam maser, discussed in sec. 17-7, appears to provide one of the simplest and most accurate frequency standards. Two such devices have been compared, using cavities which were not thermostated, and are shown to agree within one part in  $10^{10}$  over a time of about one-half hour. Presumably, thermostating of the cavities and reasonably careful design should allow this type of accuracy for an indefinite time. The oscillations of each such device were extremely monochromatic, as indicated in sec. 17-7, so that they could easily be compared over short periods of time to a few parts in  $10^{12}$ .

## CHAPTER 18

# THE USE OF MICROWAVE SPECTROSCOPY FOR CHEMICAL ANALYSIS

The well-known varieties of spectroscopy have been so widely and successfully used for chemical analysis that the reader has undoubtedly already wondered whether or not microwave spectroscopy can also be successfully applied in this way. Although microwave spectroscopy appears to be well suited for certain varieties of analytical work, actual applications of this type have so far been very limited. Several articles [361], [538], [589], [700] discussing analytic uses of microwaves have, however, appeared. It is the purpose of this chapter to examine the possible uses and limitations of microwave spectroscopy for gas analysis, and to give the reader basic information needed for such application.

**18-1. Microwave Spectroscopy for Analysis.** Spectroscopy in each of the major regions of the spectrum has its own characteristic techniques, and as a result of these and the nature of the spectra observed, it has particular advantages and disadvantages. The advantages of microwave spectroscopy of gases spring primarily from its high resolution, the use of very low pressure gases, and from the electronic techniques which are characteristic of spectroscopy in this region.

The high resolution and consequent accuracy of measurement mean that lines of two different substances—regardless of how small their difference—are generally well separated and easily differentiated. For example, the spectra of different isotopic species of the same molecule are almost always easily resolved and identified. Microwave spectra under high resolution are usually so highly specific that a measurement of one line will suffice to identify the molecule to which it belongs.

High resolution makes it possible in addition to isolate and identify the lines of a large number of substances in one gaseous mixture. Thus between 20,000 and 30,000 Mc there is room for about 40,000 microwave absorption lines (assuming a width of  $\frac{1}{4}$  Mc for each line). If each of 100 substances in a gas mixture has 20 lines in this region, there is less than one chance in  $10^6$  that more than one-third of the lines of some one of the substances will be overlapped by other lines. Thus, if the microwave lines are sufficiently intense, each of a very large number of substances can be identified in a gas mixture. The situation is very differ-



ent in the infrared region, where the rotation-vibration bands of one substance often give lines separated by less than the resolving power of infrared spectroscopy, so that the spectrum of each substance becomes a series of continuous bands, and interference between the spectra of two or more substances is often very troublesome.

The lines of even very small impurities in a gas mixture would usually not be masked by lines of the more abundant components. For some substances which have relatively strong lines, such as  $\text{H}_2\text{O}$  or  $\text{NH}_3$ , fractional abundances as small as 1 part in  $10^5$  or  $10^6$  can be detected by microwave spectroscopy. This is comparable with the minimum abundances which can be detected in the most favorable cases by other types of spectroscopy.

In addition to high resolution, another natural advantage of microwave spectroscopy is the rather small amount of gas required to detect absorption. Typically, a microwave absorption cell would have a volume of a few hundred cubic centimeters and be filled to a pressure of about  $10^{-2}$  mm Hg. This corresponds to only about  $10^{-7}$  mole of gas, or a few micrograms of material. If the gas has very strong lines, then an amount  $10^5$  times smaller than this, or about  $10^{-12}$  mole, is sufficient for detection. The small quantities of gas needed thus make analysis by microwave spectroscopy practical for microchemical work. In addition, microwave spectroscopy of a sample does not destroy it as might analysis by optical spectroscopy or by a mass spectrometer.

Although the electronic equipment needed for microwave spectroscopy may seem unfortunate to those who look for simplicity, the fact that microwave spectroscopy is based on electronic techniques offers certain advantages. The presence of absorption is indicated by an electrical voltage, which can hence be easily used to operate automatic controls or recording instruments. In addition, the electronic detecting circuits can be made to act very rapidly for rapid control or recording. Thus absorption by a strong line can be detected and translated into a voltage in times as short as 1 millisecond. It must be pointed out that, for the most sensitive detection of small amounts of material or of weak lines, a few seconds are required. Even this is very rapid, however, compared with many other types of analyses.

The natural limitations of analysis by microwave spectroscopy are mainly of two general types. First, one must usually deal with a dipolar gas. There are indeed certain types of characteristic microwave absorptions in liquids or solids, such as paramagnetic absorptions. However, these can be used only in rather limited and special ways for analysis, and analysis by microwave spectroscopy is practically restricted to gases. The substance to be analyzed need not have a vapor pressure more than about  $10^{-3}$  mm Hg at some obtainable temperature, such as a few hundred degrees centigrade, so that many substances ordinarily thought



of as liquids or solids can be used. However, restriction of analysis to gases does rule out direct study of a wide variety of interesting materials. The requirement that the molecule have a dipole moment eliminates a further number of molecules, *e.g.*, CO<sub>2</sub>, N<sub>2</sub>, benzene, and others, from detection and determination by microwave absorption.

A second variety of disadvantage inherent in analytic applications of microwaves springs, as do some of its strongest advantages, from the very high resolution and specificity of this technique. The microwave spectra of molecules depend on all the minute details of molecular structure; the slightest variation in structure may radically change a microwave spectrum.

This sensitivity of microwave spectra to very small changes within the molecule tends to prevent successful work with molecules having a large number of atoms. Thus a molecule with 25 atoms has approximately 70 modes of internal vibration, many of which may be excited at ordinary temperatures to split each rotational line into as many different frequencies. If each rotational line is so split into multiplets, each component is so weak that detection may be difficult, and it is hence doubtful that microwave spectroscopy will be very successful with molecules having more than about 25 atoms.

The great sensitivity of microwave spectra to details of molecular structure prevents the existence of any effect in the microwave range which is comparable with the characteristic vibrations of certain atomic groups or bonds which are prominent in infrared spectra. In some special cases hyperfine structure in microwave spectra can be used to identify atoms which are responsible for it in a way somewhat similar to the use of characteristic vibrational frequencies in the infrared region. However, this use of hyperfine structure has only limited application. The absence of spectra which are characteristic of certain groups within the molecule is a disadvantage only to those interested in studying new microwave spectra, and not to analysis of gases whose spectra are already known.

Microwave spectroscopy is characteristically done at very low pressures. There may be some occasions where pressures as high as a few centimeters of Hg or more might be used. One such case in which higher pressures could be useful is the case mentioned above where there are too many rotation-vibration lines. Higher pressure would amalgamate these lines and thus produce a stronger absorption. At these pressures, however, the resolution would be rather poor, so that probably not more than one or two different components of a gas mixture could be identified from the microwave spectrum.

**18-2. Qualitative Analysis.** Qualitative analysis by microwave spectroscopy is normally very much easier than quantitative measurement and hence will be discussed first. Identification of mixtures of gases for

which microwave spectra are known is in fact very simple and direct, once a sensitive microwave spectrometer is available.

Microwave spectra can be tabulated as a list of frequencies rather than as series of curves as are infrared spectra, since normally individual lines are resolved and measured. A table of known microwave lines of gases has been prepared by Kisliuk and Townes [714] under the auspices of the National Bureau of Standards. The latest edition of this table was published in 1952 and included approximately 1800 lines of 92 different substances which represented the microwave spectra known by 1950. This table probably will be revised and brought up to date from time to time by the National Bureau of Standards.

It has already been pointed out above that the high resolution and accuracy obtainable with microwave spectroscopy results in very little possibility of overlap or confusion of lines. This is illustrated by the fact that there are only about 10 cases among the 1800 lines listed by Kisliuk and Townes [714] where two lines of different substances are closer than 0.25 Mc, which is approximately the resolving power of an ordinary spectrometer. For each substance listed, it is possible to find lines which are more than 0.5 Mc away from any known lines of other substances. The measurement of a single line to an accuracy of about 0.1 Mc would hence suffice for positive identification of any one of this group of 92 substances.

As shown in Chap. 17, an accuracy in measurement of 0.1 Mc is easily achieved if a frequency standard based on a quartz-crystal oscillator is available. The considerably simpler type of frequency meter, a tunable resonant cavity, can measure frequencies to an accuracy of a few megacycles and hence would suffice in most cases to positively identify a substance by the presence of a single line. If identification were still in doubt, more than one line might be measured, or the Stark effect of the line might be examined. As discussed in Chap. 10, microwave transitions have characteristic Stark effects which differ in the number of Stark components, the spacing of these components, and their intensities. In the rare cases where frequency measurement does not suffice for identification of a line, the characteristic Stark effect of the line may be useful for identification.

A microwave spectrometer need not operate over all microwave frequencies, since most substances have a number of lines throughout the microwave region. A relatively limited frequency range can be chosen for a spectrometer which would allow analysis of a large fraction of gases suitable for microwave spectroscopy. Most microwave spectroscopy has been done in the *K*-band region (near 25,000 Mc) since this is the highest frequency for which components have been readily available. Suppose a spectrometer made for qualitative analysis operates in this region. The frequency range over which it must be operable to obtain absorption



lines for a given fraction of the substances listed in Appendix VI as having microwave spectra can be judged to some extent from Fig. 18-1. This figure gives the fraction of molecules with presently known microwave spectra which have at least one line within a frequency interval  $\pm \Delta f$  from 25,000 Mc. From Fig. 18-1, it may be seen that a spectrometer operating over a range 20,000 to 30,000 Mc would be able to detect lines of 90 per cent of the molecules whose microwave spectra are known. The molecules which could not be detected in this range are certain rather light linear and symmetric-top molecules for which spectra occur only at higher frequencies. There is nothing unusual about the region

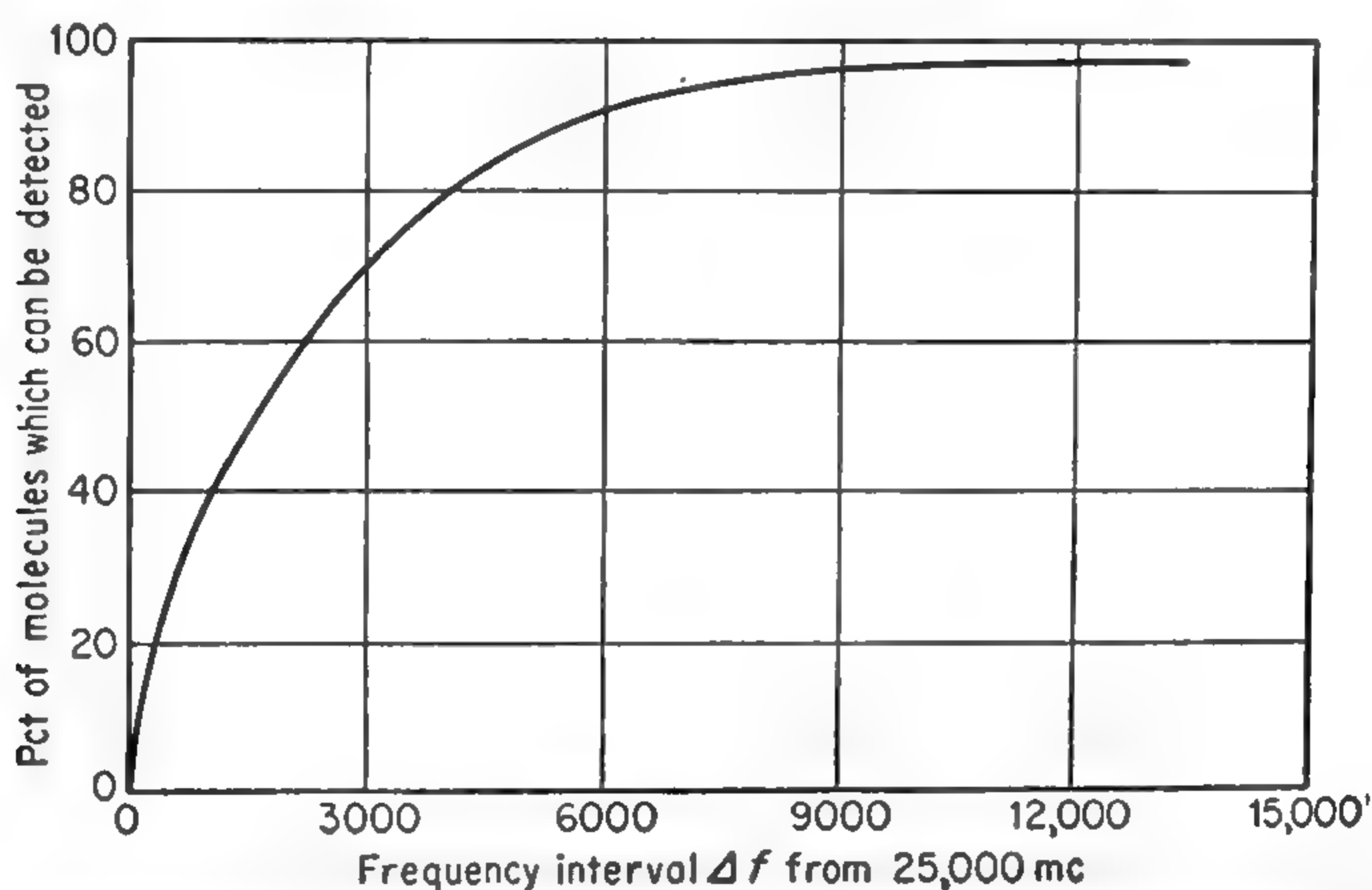


FIG. 18-1. Percentage of molecules with known microwave spectra having lines within a given frequency interval  $\Delta f$  from 25,000 Mc. Thus, within the range 23,000 to 27,000 Mc ( $\Delta f = 2000$ ), 57 per cent of the molecules with known microwave spectra have lines which may be used for spectroscopic identification.

near 25,000 Mc; so that a similar fraction of molecules can be expected to have spectra in almost an arbitrary spectral region of 10,000 Mc width in the microwave range.

If a spectrometer is required only to check the abundance of a number of possible known components of a gas mixture, then it can be adjusted at certain known frequencies to detect the required lines. This type of operation may be the most common one in analytic uses of microwave spectrometers. However, in some cases it may be useful to search over a wide range of frequencies in order to examine the composition of a completely unknown gas, or in order to find lines in a known gas for which the microwave spectrum has not yet been examined. In these cases consideration must be given to the time required for such a search.

A spectrometer sensitive enough to detect a line with an absorption coefficient as small as  $10^{-9} \text{ cm}^{-1}$  must have such a narrow bandwidth that it takes as long as about 2 sec to sweep over an individual line, or a



distance of 0.5 Mc. Hence a search for lines with this sensitivity over a 1000-Mc range requires approximately 1 hr, and searching times can be long enough to be inconvenient. If the sensitivity required is less, searching can be much faster. Thus search over 1000 Mc to detect an absorption as large as  $4 \times 10^{-9} \text{ cm}^{-1}$  would require in principle only about 5 min since sensitivity is proportional to the square root of the bandwidth [cf. (15-9)].

The fractional abundance of a given gas in a mixture required for detection of its microwave lines can be determined approximately from the intensity of its lines and the sensitivity of the spectrometer used. The intensity of a line due to a gas of fractional abundance  $x$  is given roughly by  $x$  times the intensity of the line for the pure gas (this relation

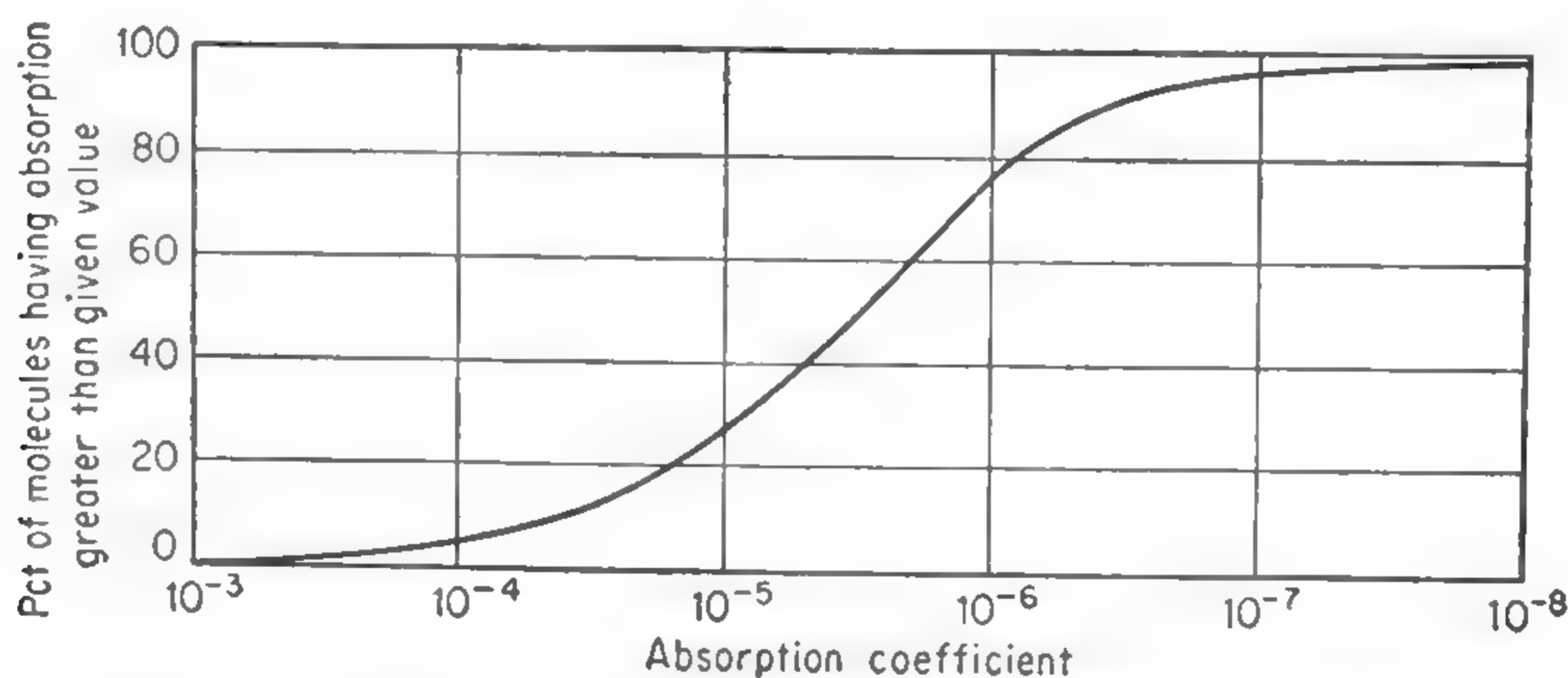


FIG. 18-2. Maximum intensities of known microwave spectra in the range 20,000 to 30,000 Mc. The curve gives the percentage of those molecules having spectra between 20,000 and 30,000 Mc for which at least one line in this region has an absorption coefficient greater than the values listed along the horizontal axis.

is not precise, as will be shown below in the discussion of quantitative analysis). Thus the intensity of the strongest line of  $\text{NH}_3$  is  $8 \times 10^{-4} \text{ cm}^{-1}$ , so that a spectrometer sensitive enough to detect an absorption coefficient of  $10^{-9} \text{ cm}^{-1}$  would be able to detect  $\text{NH}_3$  in a gas mixture with a fractional abundance as low as about  $10^{-6}$ . More commonly, stronger microwave lines of molecules have absorption coefficients near  $10^{-5}$  or  $10^{-6} \text{ cm}^{-1}$ , so that such a spectrometer could detect abundances as low as about  $10^{-4}$  or  $10^{-3}$ .

If a spectrometer operates in the frequency range 20,000 to 30,000 Mc, Fig. 18-2 indicates the sensitivity needed for detection of a certain fraction of the molecules which have microwave spectra (or for detection of a given fractional abundance of these molecules in a gas mixture). This figure shows the fraction of molecules listed in the tables of Kisliuk and Townes [714] which have a line with intensity greater than a given amount and falling in the frequency range 20,000 to 30,000 Mc. Since intensities of microwave lines increase with frequency approximately as  $\nu^2$  or  $\nu^3$  [cf. (1-49) and (1-78)], typical intensities in other frequency ranges

can be roughly obtained by multiplying those of Fig. 18-2 by the square of the frequency ratio.

It should be noted that microwave spectroscopy done so far has been somewhat concentrated on the simpler molecules. These tend to have fewer and stronger lines than the more complex molecules. Hence one may guess that, as work on additional molecules proceeds, a larger fraction of molecules will fall in a given range in Fig. 18-1, and line intensities will on the average be somewhat less than indicated in Fig. 18-2.

**18-3. Quantitative Analysis.** The most obvious type of quantitative analysis by microwave spectroscopy involves comparison of the strength of absorption lines due to an unknown mixture of gases with that in a known mixture. However, before discussing this technique, we shall examine other methods and some of the theory on which quantitative analysis by microwave methods depends.

It is possible, although not easy, to use microwave absorption lines for a quantitative determination of the abundance of a gas in an absolute way without using known samples for comparison. For this, the integrated intensity of the line must be measured. As shown in (13-23) the integrated intensity of a reasonably narrow line is

$$\int_0^\infty \gamma d\nu = \frac{8\pi^3 N f}{3ckT} |\mu_{ij}|^2 \nu^2 \quad (18-1)$$

where  $N$  = the number of molecules per cubic centimeter,  $T$  is the absolute temperature,  $\nu$  the frequency,  $f$  and  $|\mu_{ij}|^2$  are determinable from properties of the molecule involved, and  $c$  and  $k$  are known constants. Hence if the absorption coefficient  $\gamma$  could be accurately measured and the integrated intensity obtained, the density  $N$  of molecules of a given type could be found.

At the low pressures normally used in microwave spectroscopy, absorption lines are close to a Lorentz shape as given by (13-22), and the integrated intensity is

$$\int_0^\infty \gamma d\nu = \gamma_{\max} \Delta\nu = \frac{8\pi^3 N f}{3ckT} |\mu_{ij}|^2 \nu^2 \quad (18-2)$$

where  $\gamma_{\max}$  is the absorption coefficient at the peak intensity, and  $\Delta\nu$  the half width at half maximum. Hence a measurement of the peak absorption coefficient and the line width at half maximum absorption is sufficient to give the density of molecules  $N$  from (18-2).

The absolute value of the absorption coefficient  $\gamma_{\max}$  is rather difficult to measure, although it can with care be measured to an accuracy of about 5 per cent (*cf.* pages 445–446). It is usually sufficient and much easier, however, to measure  $\gamma_{\max}$  relative to some absorption line of a known  $\gamma_{\max}$  by comparing peak responses of a spectrometer to the two lines in question. The half width  $\Delta\nu$  may be measured to an accuracy

of about 5 per cent by setting frequency markers at points on the absorption line corresponding to half intensity. This method for obtaining the density of molecules is a rather cumbersome method, however, and is usually limited to an accuracy of about 5 per cent. Furthermore, the density  $N$  of molecules per cubic centimeter is usually not so much desired as the percentage abundance, which can be obtained from  $N$  only with an additional measurement of the pressure.

The simplest quantity to measure, and one which can be measured most accurately, is the maximum signal produced in a spectrometer by an absorption line, which is nearly proportional to  $\gamma_{\max}$  for most spectrometers. If a spectrometer is adjusted for a line at a particular frequency and all conditions are maintained constant, it will be found that the response or deflection of the spectrometer due to the line can be measured reproducibly to an accuracy of 1 per cent or better, assuming the signal due to the line is sufficiently large compared with noise.

Fortunately the deflection, which is proportional to  $\gamma_{\max}$ , is not only the easiest quantity to measure, but also it is rather directly related to the fractional abundance of the gas responsible for the absorption. From (18-2), the fractional abundance is proportional to  $(\gamma_{\max} \Delta\nu)/p$ , where  $p$  is the pressure. However,  $\gamma_{\max}$  is independent of pressure in the range of pressure normally used for spectroscopy (*cf.* Chap. 13), and  $\Delta\nu/p$  is also independent of pressure, since the line width is proportional to  $p$ . Thus it appears that  $\gamma_{\max}$  and hence the maximum spectrometer response is directly proportional to the fractional abundance of the gas responsible for the microwave absorption.

For some purposes,  $\gamma_{\max}$  can in fact be taken as proportional to fractional abundance, and the maximum spectrometer response affords a ready measurement of concentration of a component of a gas mixture. However, accurate measurements of fractional abundance require one to allow for the fact that the line-width parameter  $\Delta\nu$  is somewhat dependent on the composition of the gas and that the fractional abundance is strictly proportional not to  $\gamma_{\max}$  but to  $\gamma_{\max} \Delta\nu/p$ .

From (13-42), the number of collisions per second of a molecule of type 1 with molecules of type 2 in a gas mixture is

$$\frac{1}{\tau_{12}} = N_2 v_{12} \sigma_{12} \quad (18-3)$$

where  $N_2$  is the density of molecules of type 2,  $v_{12}$  an average relative velocity for the two molecular types, and  $\sigma_{12}$  the cross section between them. The number of collisions per second for molecules of type 1 in a mixture of two components only is therefore

$$\frac{1}{\tau_{11}} + \frac{1}{\tau_{12}} = N_1 v_{11} \sigma_{11} + N_2 v_{12} \sigma_{12} \quad (18-4)$$



and the half width of an absorption line is [cf. (13-19)]

$$\Delta\nu_1 = \frac{1}{2\pi} \left( \frac{1}{\tau_{11}} + \frac{1}{\tau_{12}} \right) = \frac{1}{2\pi} (Nx_1\nu_{11}\sigma_{11} + Nx_2\nu_{12}\sigma_{12}) \quad (18-5)$$

where  $x_1$  and  $x_2$  are the fractional abundance of each molecular species and  $N$  is the total molecular density. Expression (18-5) may also be written

$$\Delta\nu_1 = x_1 \Delta\nu_{11} + x_2 \Delta\nu_{12} \quad (18-6)$$

where  $\Delta\nu_{12}$  would be the half width of the absorption line of molecule 1 if it were in an almost pure sample of molecule 2. The fractional abundance of the first component of the gas is then proportional to

$$x_1 \propto \frac{\gamma_{\max} \Delta\nu_1}{p} = \gamma_{\max} \frac{N}{2\pi p} (x_1\nu_{11}\sigma_{11} + x_2\nu_{12}\sigma_{12}) \quad (18-7)$$

Since  $N/2\pi p$  is a universal constant at a given temperature, the last part of expression (18-7) depends only on the fractional abundances  $x_1$  and  $x_2$  and not on the pressure. It may also be written

$$x_1 \propto \gamma_{\max} \left( x_1 \frac{\Delta\nu_{11}}{p} + x_2 \frac{\Delta\nu_{12}}{p} \right) \quad (18-8)$$

where  $\Delta\nu_{11}/p$  and  $\Delta\nu_{12}/p$  are independent of pressure. For a mixture of more than two components, (18-8) can be easily generalized so that the fractional abundance of the  $i$ th component of a mixture of  $n$  different gases is proportional to

$$x_i \propto \gamma_{\max} \sum_{j=1}^n x_j \frac{\Delta\nu_{ij}}{p} \quad (18-9)$$

If component 2 were just as effective in broadening a microwave line as component 1, then  $\Delta\nu_{11}/p = \Delta\nu_{12}/p$  and (18-8) could be reduced to

$$x_1 \propto \gamma_{\max} \frac{\Delta\nu_{11}}{p} (x_1 + x_2) = \gamma_{\max} \frac{\Delta\nu_{11}}{p} \quad (18-10)$$

and the fractional abundance  $x_1$  would be strictly proportional to  $\gamma_{\max}$  regardless of the amount of dilution. If  $\Delta\nu_{11}/p \neq \Delta\nu_{12}/p$ , this strict proportionality is not true, as is shown in extreme cases by Fig. 18-3.

Usually for a mixture of more than two gases, the various values of line-width parameters  $\Delta\nu_{ij}/p$  will not be known, and one of the following procedures must be adopted:

1. Measure  $\gamma_{\max}$ ,  $\Delta\nu$ , and  $p$ .
2. Measure only  $\gamma_{\max}$  and accept the approximate results given by assuming  $\gamma_{\max}$  proportional to the fractional abundance.
3. Dilute the unknown mixture with a large amount of known gas for which the necessary information on line-width parameters  $\Delta\nu_{ij}/p$  is known.

4. Compare  $\gamma_{\max}$  for the unknown sample with values for known mixtures which are similar to it in composition.

The procedure indicated by item 3 above is useful when the absorption lines being examined are strong so that they can still be measured if a few per cent of the sample is mixed with a known gas (*e.g.*,  $N_2$ ). If most of the molecules in a sample are of one type (*e.g.*,  $N_2$ ), then the broadening produced by them is the only important source of broadening, and only one of the values of  $\Delta\nu_{ij}$  need be known to measure each component of the gas. This may be seen from Eq. (18-8) if  $x_2$  becomes very much larger than  $x_1$ , or more generally from Eq. (18-9).

The comparison method with use of standard mixtures indicated by item 4 above appears to be the simplest and most reliable technique if a large number of measurements are to be made on mixtures whose composition is approximately known. Such a measurement involves only a comparison of the peak response of a spectrograph to the absorption lines of two different samples of gas. Good accuracy depends only on having stable reproducible conditions in the spectrometer and an adequate

signal-to-noise ratio for the observed line. This type of measurement can fairly easily be made to an accuracy of a few per cent, and higher accuracy appears feasible if considerable care is taken.

In case a Stark spectrometer is used with Stark components and undisplaced absorption lines giving deflections in the opposite directions (*cf.* Chap. 15), the total deflection difference between the strongest Stark component and the undisplaced line may be used as a measure of intensity. This eliminates some uncertainties which might otherwise exist in the exact position of the base line where zero absorption occurs.

The comparison method has been tested by Southern, Morgan, Keilholtz, and Smith [650] for isotopic mixtures of  $NH_3$  and  $ClCN$ . For  $NH_3$ , the  $N^{15}/N^{14}$  ratio was determined to an accuracy of about 3 per cent with the  $N^{15}$  concentration in the range 0.38 to 4.5 per cent; and for  $ClCN$ , the ratio  $C^{13}/C^{12}$  was determined to an accuracy of 2 per cent with  $C^{13}$  abundances between 1.1 and 10 per cent. This work illustrates the usefulness of microwave spectroscopy for analyzing isotopic mixtures.

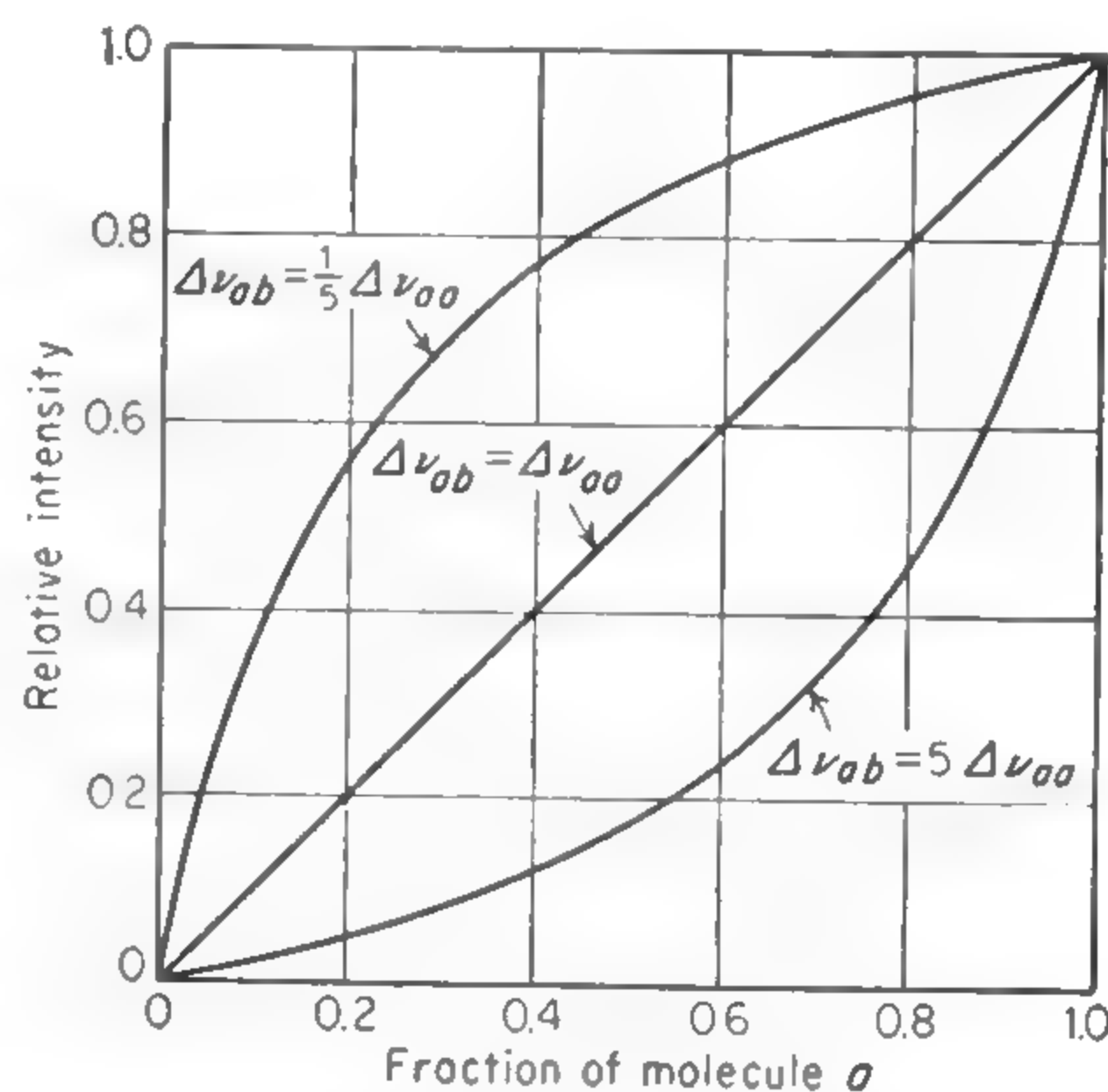


FIG. 18-3. Peak intensity of a line due to molecule *a* which is in a mixture of gases *a* and *b*. The peak intensity varies linearly with concentration only if the broadening effect of each molecule is the same. The curved lines indicate deviations from linearity which are as large as will ordinarily occur. (After Hughes [700].)

Unless very special spectrometers are built which allow absolute measurements of intensities, accurate quantitative work always requires some type of comparison method on absorption lines which are identical or very similar in frequency, width, and other characteristics. The inevitable presence of reflections in a waveguide absorption cell produces variations in the field strength with the absorption cell, and hence variations in the spectrometer's response as the frequency is varied. As shown in Chap. 15, if reflections produce a 10 per cent variation in power transmitted through the absorption cell as a function of frequency, they can produce a 20 per cent variation in the response of the spectrometer to a given absorption coefficient  $\gamma_{\max}$  [cf. Eq. (15-28)]. Nevertheless, if care is taken, the relative intensities of lines of different frequencies can be measured to an accuracy of about 5 per cent. For lines of the same frequency, reflections are of course constant and cause no errors in measurement of relative intensities.

Spectrometers using Stark modulation are the most convenient type of spectrometer for high sensitivity. However, they introduce additional uncertainties in the measurement of  $\gamma_{\max}$  unless comparison is made between two very similar lines.

A Stark modulation spectrometer detects lines by the periodic application of an electric field which shifts the frequency of the line because of the Stark effect (cf. sec. 15-3). In an electric field the line usually breaks up into a number of Stark components, with widely different amounts of frequency change for a given field strength. If a square wave of electric field is applied to the gas which is sufficiently large to shift all Stark components well away (more than the line width) from the absorption which occurs without an electric field, then the full intensity of the absorption line appears. For smaller fields, however, some of the Stark components may not be moved appreciably from the absorption line, and the apparent intensity as determined by the spectrometer response is correspondingly less. Partial splitting of the absorption line by Stark effect also distorts the line shape and gives errors in measurement of line width if width measurements are attempted. In addition, if the square-wave voltage is not nearly zero during half its cycle of variation, then the line is partly split at all times, and the line is broadened so that  $\gamma_{\max}$  is reduced. If a sine wave is used rather than a square wave, these difficulties are particularly acute, since the sine wave cannot usually have enough amplitude at maximum to move all Stark components far enough from the undisplaced line without at the same time broadening the undisplaced line because it is not sufficiently close to zero during the other half of the cycle. If a line is not completely split by Stark effect, then a variation in pressure, which produces a variation of line width, will also affect the apparent value of  $\gamma_{\max}$ . As the width increases the line is less completely split and  $\gamma_{\max}$  decreases. For the



above reasons, it is important in most cases to compare only similar lines under similar conditions if quantitative work with a Stark spectrometer is attempted.

**18-4. Special Equipment and Techniques for Spectroscopic Analysis.** Equipment for some types of analytic work with microwave spectroscopy need not be very special. Almost any sensitive spectrometer and moderately accurate frequency-measuring device should suffice for qualitative analysis and for rough quantitative work. Techniques and apparatus specifically for analytic work have not yet been well developed. However, certain considerations and problems of technique involved in analysis are well enough known to be discussed here.

A Stark modulation spectrometer probably provides the simplest means for obtaining good sensitivity, although it has some handicaps for quantitative work. If quantitative work is planned, care should be taken to ensure that the signal amplifiers are linear (*i.e.*, give an output strictly proportional to signal), that reflections are minimized, and that the modulation is produced by a well-formed and large square wave of electric field. Other precautions, which are common to other types of spectrometers, are to see that the rate of sweep over a line is sufficiently slow that its shape (and therefore height) is not distorted, and that the power is sufficiently low so that the absorption lines do not suffer from power saturation. Reflections in any spectrometer can usually be decreased by inserting well-tapered attenuators at either end of the absorption cell. In the Stark spectrometer, it is particularly important that the septum for producing the Stark field and its insulating supports inside the absorption cell be well tapered at the ends.

An absorption cell without a Stark septum is almost always freer of reflections than is a Stark cell. In addition, a simple spectrometer without Stark modulation has none of the complications of incomplete modulation of the line mentioned above. However, this type of spectrometer is usually suitable only for work with the most intense lines, because of the greater difficulty in obtaining good sensitivity.

In many cases a spectrometer may be used to observe the intensity of some particular line over a long period of time. In such circumstances, a cavity can conveniently be used for an absorption cell. Special care must be exercised, however, to see that power saturation of the absorption line does not occur when a cavity is used, since the power level in a cavity is likely to be higher than that in a waveguide cell.

There are many ways of measuring the magnitude of response of a spectrometer to an absorption line. Some have been tried and described [700], [901], but none seems to have particularly strong or unique advantages. The method chosen in an individual case should probably depend on details of the desired functions of the apparatus and on the available equipment.

Absorption of gases on surfaces can be a serious problem in the use of microwave spectroscopy for analysis. Since very small samples of gas are used, a relatively small amount of material absorbed by waveguide surfaces or outgassed from them can appreciably change the pressure and composition of a sample being analyzed. It is common experience, for example, that, if ammonia is let into an absorption cell, its lines may persist in a microwave spectrometer even after many days of pumping to evacuate the cell. Cells for Stark modulation are worse from the point of view of absorption than others, since they have the additional surfaces of septum and insulators. A cavity would minimize the ratio of surface to volume and thus decrease difficulties due to surface absorption. In the usual Stark cell absorption is a serious problem to analytic work, since certain components of the gas sample may be selectively absorbed, and foreign gas from previous samples may be released by the cell walls.

There are a number of ways of dealing with absorption.

1. Cell design should minimize absorption. It has been found, for example, that stainless steel absorbs gases far less than silver or copper, and stainless steel may be used for a cell. Teflon is also less absorbent than polystyrene and hence better suited for insulators of a Stark septum.

2. Several batches of gas may be let into the cell, or the gas may be flowed through the cell until no further exchange of gas with the walls occurs.

3. Chemical "getters" may be used to destroy gases on the walls which produce spurious lines. Thus  $\text{ClF}_3$  let into a waveguide will destroy water absorbed on the surfaces, and  $\text{BrCN}$  will help eliminate  $\text{NH}_3$ .

4. The cell may be heated up to outgas its walls or may be operated at an elevated temperature to minimize absorption. A temperature of  $100^\circ\text{C}$  seems to be fairly effective in outgassing, and  $200^\circ\text{C}$  would probably be adequate for most purposes.

A somewhat specialized technique to which microwave spectroscopy seems well adapted is the continuous monitoring of a mixture of gases. Gas may be flowed at very low pressure through the absorption cell of a spectrometer and the output of the spectrometer used to register or control the concentration of a given component. Changes in concentration would be very easily and sensitively detected, since the spectrometer itself would be under fixed adjustments and conditions. Furthermore, these changes could be quite rapidly recorded or controlled by the output of the spectrometer. In order to eliminate the effects on spectrometer output of possible fluctuations in klystron output powers, a bridge system can be used, with one arm of the bridge containing the absorption cell through which gas is being flowed, and the other arm involving only fixed components.



## APPENDIX I

### Intensities of Hyperfine Structure Components and Energies Due to Nuclear Quadrupole Interactions

Intensities of individual lines are given as a percentage of the intensity of the entire transition (sum of all hyperfine components). They are obtained from expressions (6-6). Values for angular momentum  $J$  between 0 and 10 and for the nuclear spin  $I$  equal to  $\frac{1}{2}$ , 1,  $\frac{3}{2}$ , 2,  $\frac{5}{2}$ , 3,  $\frac{7}{2}$ , 4,  $\frac{9}{2}$ , or  $\frac{11}{2}$  are included. The quantity  $F$  is the magnitude of  $\mathbf{I} + \mathbf{J}$ . These tables may also be used for relative intensities of atomic fine-structure transitions if  $I$ ,  $J$ , and  $F$  are replaced by  $S$ ,  $L$ , and  $J$ , respectively. The tabulation then corresponds to formulas (5-17) and (5-18). For  $J > 10$ , almost all the intensity of a transition is concentrated in components such that  $\Delta F = \Delta J$ , that is, with  $J + 1 \leftarrow J$  and  $F + 1 \leftarrow F$  or  $J \leftarrow J$  and  $F \leftarrow F$ . Approximate intensities of transitions for large  $J$  are as follows:

For transitions $J + 1 \leftarrow J$ ,	$F + 1 \leftarrow F$	Intensity is proportional to $F$
	$F \leftarrow F$	Intensity $\sim 1/2J^2$ of entire intensity
	$F - 1 \leftarrow F$	Intensity $\sim 1/10J^4$ of entire intensity
For $J \leftarrow J$ ,	$F \leftarrow F$	Intensity is proportional to $F$
	$F \pm 1 \leftarrow F$	Intensity $\sim 1/2J^2$ of entire intensity

The table also gives Casimir's function

$$f(I, J, F) = \frac{\frac{3}{4}C(C + 1) - I(I + 1)J(J + 1)}{2I(2I - 1)(2J - 1)(2J + 3)}$$

for rotational angular momentum  $J$  between 0 and 10, for the nuclear spin  $I = 1, \frac{3}{2}, 2, \frac{5}{2}, 3, \frac{7}{2}, 4, \frac{9}{2}$ , or  $\frac{11}{2}$  and all possible values of  $F$ . Here

$$C = F(F + 1) - I(I + 1) - J(J + 1)$$

The interaction energy due to a nuclear quadrupole moment coupled to a linear molecule is given by multiplying the appropriate value of  $f(I, J, F)$  in this table by  $-eqQ$ .

For a symmetric-top molecule the proper multiplying factor is  $eqQ \left[ \frac{3K^2}{J(J + 1)} - 1 \right]$  [cf. Eq. (6-4)]. When  $J > 10$ , the stronger hyperfine components of a transition (where  $\Delta F = \Delta J$ ) involve a change in quadrupole energy which is a very small fraction of the quadrupole coupling constant, being in almost all cases less than  $eqQ/4J^2$ . For the other, very much weaker, components, the change in energy is larger and can be approximated by

$$\Delta W_Q (\Delta F = \Delta J \pm 1) = \mp \frac{3[2(F - J) + 1]}{8I(2I - 1)} \left[ \frac{3K^2}{J(J + 1)} - 1 \right] eqQ$$

+ terms of order  $eqQ/2J$



$I = \frac{1}{2}$

<i>J</i>	<i>F</i>	<i>f(I,J,F)</i>	<i>J</i> + 1 ← <i>J</i>			<i>J</i> ← <i>J</i>	
			<i>F</i> + 1 ← <i>F</i>	<i>F</i> ← <i>F</i>	<i>F</i> − 1 ← <i>F</i>	<i>F</i> ← <i>F</i> + 1 or <i>F</i> + 1 ← <i>F</i>	<i>F</i> ← <i>F</i>
0	1/2	0	66.7	33.3			
1	3/2	0	60.0	6.66			55.6
	1/2	0	33.4			11.1	22.2
2	5/2	0	57.1	2.86			56.0
	3/2	0	40.0			4.00	36.0
3	7/2	0	55.6	1.59			55.1
	5/2	0	42.9			2.04	40.8
4	9/2	0	54.5	1.01			54.3
	7/2	0	44.4			1.23	43.2
5	11/2	0	53.8	0.699			53.7
	9/2	0	45.5			0.826	44.6
6	13/2	0	53.3	0.513			53.3
	11/2	0	46.2			0.592	45.6
7	15/2	0	52.9	0.392			52.9
	13/2	0	46.7			0.444	46.2
8	17/2	0	52.6	0.310			52.6
	15/2	0	47.1			0.346	46.7
9	19/2	0	52.4	0.251			52.4
	17/2	0	47.4			0.277	47.1
10	21/2	0	52.2	0.207			52.2
	19/2	0	47.6			0.227	47.4

$I = 1$

$J$	$F$	$f(I,J,F)$	$J + 1 \leftarrow J$			$J \leftarrow J$	
			$F + 1 \leftarrow F$	$F \leftarrow F$	$F - 1 \leftarrow F$	$F \leftarrow F + 1$ or $F + 1 \leftarrow F$	$F \leftarrow F$
0	1	0	55.5	33.3	11.1		
1	2	0.050000	46.6	8.33	0.556		41.7
	1	-0.250000	25.0	8.33		13.9	8.33
	0	0.500000	11.1			11.1	0
2	3	0.071429	42.9	3.70	0.106		41.5
	2	-0.250000	29.6	3.70		5.19	23.1
	1	0.250000	20.0			5.00	15.0
3	4	0.083333	40.7	2.08	0.033		40.2
	3	-0.250000	31.3	2.08		2.68	28.0
	2	0.200000	23.8			2.65	21.2
4	5	0.090909	39.4	1.33	0.013		39.1
	4	-0.250000	32.0	1.33		1.63	30.1
	3	0.178571	25.9			1.62	24.3
5	6	0.096154	38.5	0.926	0.006		38.3
	5	-0.250000	32.4	0.926		1.09	31.1
	4	0.166667	27.3			1.09	26.2
6	7	0.100000	37.8	0.680	0.003		37.7
	6	-0.250000	32.7	0.680		0.785	31.8
	5	0.159091	28.2			0.783	27.4
7	8	0.102941	37.3	0.521	0.002		37.2
	7	-0.250000	32.8	0.521		0.590	32.2
	6	0.153846	28.9			0.590	28.3
8	9	0.105263	36.8	0.412	0.001		36.8
	8	-0.250000	32.9	0.412		0.460	32.4
	7	0.150000	29.4			0.460	29.0
9	10	0.107143	36.5	0.333	0.001		36.5
	9	-0.250000	33.0	0.333		0.368	32.6
	8	0.147059	29.8			0.368	29.5
10	11	0.108696	36.2	0.275	0.001		36.2
	10	-0.250000	33.1	0.275		0.302	32.7
	9	0.144737	30.2			0.302	29.9

$I = \frac{3}{2}$

<i>J</i>	<i>F</i>	<i>f(I,J,F)</i>	<i>J</i> + 1 ← <i>J</i>			<i>J</i> ← <i>J</i>	
			<i>F</i> + 1 ← <i>F</i>	<i>F</i> ← <i>F</i>	<i>F</i> − 1 ← <i>F</i>	<i>F</i> ← <i>F</i> + 1 or <i>F</i> + 1 ← <i>F</i>	<i>F</i> ← <i>F</i>
0	3/2	0	50.0	33.3	16.7		
1	5/2	0.050000	40.0	9.0	1.00		35.0
	3/2	−0.200000	21.0	10.7	1.67	15.0	4.44
	1/2	0.250000	8.33	8.33		13.9	2.78
2	7/2	0.071429	35.7	4.08	0.204		34.3
	5/2	−0.178571	24.5	5.22	0.286	5.71	17.3
	3/2	0	16.0	4.00		7.00	8.00
	1/2	0.250000	10.0			5.00	5.00
3	9/2	0.083333	33.3	2.31	0.067		32.7
	7/2	−0.166667	25.5	3.02	0.085	2.98	21.8
	5/2	−0.050000	19.1	2.30		3.83	14.7
	3/2	0.200000	14.3			2.86	11.4
4	11/2	0.090909	31.8	1.49	0.028		31.5
	9/2	−0.159091	25.8	1.96	0.034	1.82	23.6
	7/2	−0.071429	20.7	1.48		2.38	18.1
	5/2	0.178571	16.7			1.79	14.9
5	13/2	0.096154	30.8	1.04	0.013		30.6
	11/2	−0.153846	25.9	1.37	0.016	1.22	24.4
	9/2	−0.083333	21.7	1.03		1.61	19.9
	7/2	0.166667	18.2			1.21	17.0
6	15/2	0.100000	30.0	0.762	0.007		29.9
	13/2	−0.150000	25.9	1.01	0.008	0.879	24.9
	11/2	−0.090909	22.3	0.761		1.16	21.0
	9/2	0.159091	19.2			0.874	18.4
7	17/2	0.102941	29.4	0.584	0.004		29.3
	15/2	−0.147059	25.9	0.775	0.005	0.662	25.1
	13/2	−0.096154	22.8	0.583		0.877	21.8
	11/2	0.153846	20.0			0.659	19.3
8	19/2	0.105263	28.9	0.462	0.003		28.9
	17/2	−0.144737	25.9	0.613	0.003	0.516	25.3
	15/2	−0.100000	23.1	0.461		0.685	22.3
	13/2	0.150000	20.6			0.515	20.1
9	21/2	0.107143	28.6	0.374	0.002		28.5
	19/2	−0.142857	25.8	0.497	0.002	0.414	25.4
	17/2	−0.102941	23.3	0.374		0.549	22.7
	15/2	−0.147059	21.1			0.413	20.6



$I = \frac{3}{2}$  (Continued)

$J$	$F$	$f(I,J,F)$	$J + 1 \leftarrow J$			$J \leftarrow J$	
			$F + 1 \leftarrow F$	$F \leftarrow F$	$F - 1 \leftarrow F$	$F \leftarrow F + 1$ or $F + 1 \leftarrow F$	$F \leftarrow F$
10	23/2	0.108696	28.3	0.309	0.001		28.2
	21/2	-0.141304	25.8	0.411	0.001	0.339	25.4
	19/2	-0.105263	23.5	0.309		0.450	23.0
	17/2	0.144737	21.4			0.338	21.1

$I = 2$

0	2	0	46.7	33.3	20.0		
1	3	0.050000	36.0	9.33	1.33		31.1
	2	-0.175000	18.7	11.7	3.00	15.6	2.78
	1	0.175000	7.00	9.00	4.00	15.0	5.00
2	4	0.071429	31.4	4.29	0.286		
	3	-0.142857	21.4	6.00	0.571	6.00	30.0
	2	-0.053571	13.7	5.71	0.571	8.00	14.0
	1	0.125000	8.00	4.00		7.00	5.00
	0	0.250000	4.00			4.00	1.00
3	5	0.083333	28.9	2.44	0.095		28.3
	4	-0.125000	22.0	3.54	0.179	3.14	18.1
	3	-0.091667	16.4	3.47	0.159	4.46	11.3
	2	0.050000	11.9	2.38		4.28	7.14
	1	0.200000	8.57			2.86	5.71
4	6	0.090909	27.3	1.58	0.040		27.0
	5	-0.113636	22.1	2.31	0.073	1.93	19.7
	4	-0.105519	17.6	2.29	0.061	2.80	14.5
	3	0.017857	14.0	1.56		2.75	11.0
	2	0.178571	11.0			1.85	9.26
5	7	0.096154	26.1	1.10	0.020		26.0
	6	-0.105769	22.0	1.62	0.035	1.30	20.4
	5	-0.112179	18.4	1.62	0.028	1.91	16.2
	4	0	15.3	1.09		1.89	13.2
	3	0.166667	12.7			1.27	11.5
6	8	0.100000	25.3	0.810	0.011		25.2
	7	-0.100000	21.9	1.20	0.019	0.934	20.8
	6	-0.115909	18.8	1.20	0.015	1.38	17.2
	5	-0.011364	16.1	0.806		1.37	14.6
	4	0.159091	13.8			0.923	12.9
7	9	0.102941	24.7	0.621	0.007		24.6
	8	-0.095588	21.7	0.924	0.011	0.704	20.9
	7	-0.118212	19.1	0.922	0.008	1.04	17.9
	6	-0.019231	16.7	0.619		1.04	15.6
	5	0.153846	14.7			0.698	14.0

$I = 2$  (Continued)

$J$	$F$	$f(I,J,F)$	$J + 1 \leftarrow J$			$J \leftarrow J$	
			$F + 1 \leftarrow F$	$F \leftarrow F$	$F - 1 \leftarrow F$	$F \leftarrow F + 1$ or $F + 1 \leftarrow F$	$F \leftarrow F$
8	10	0.105263	24.2	0.491	0.004		24.2
	9	-0.092105	21.6	0.732	0.007	0.549	21.0
	8	-0.119737	19.3	0.731	0.005	0.817	18.4
	7	-0.025000	17.2	0.490		0.815	16.3
	6	0.150000	15.3			0.546	14.7
9	11	0.107143	23.8	0.398	0.003		23.8
	10	-0.089286	21.5	0.594	0.005	0.440	21.0
	9	-0.120798	19.4	0.594	0.003	0.656	18.7
	8	-0.029412	17.5	0.398		0.655	16.8
	7	0.147059	15.8			0.439	15.4
10	12	0.108696	23.5	0.329	0.002		23.4
	11	-0.086957	21.4	0.492	0.003	0.361	21.0
	10	-0.121568	19.5	0.492	0.002	0.538	18.9
	9	-0.032895	17.8	0.329		0.538	17.2
	8	0.144737	16.2			0.360	15.8

$I = \frac{5}{2}$

0	5/2	0	44.4	33.3	22.2		
1	7/2	0.050000	33.3	9.52	1.59		28.6
	5/2	-0.160000	17.1	12.2	4.00	15.9	1.90
	3/2	0.140000	6.22	9.33	6.67	15.6	6.67
2	9/2	0.071429	28.6	4.41	0.353		27.2
	7/2	-0.121428	19.4	6.45	0.816	6.17	11.9
	5/2	-0.071429	12.2	6.61	1.14	8.57	3.43
	3/2	0.071429	6.86	5.42	1.06	8.00	0.148
	1/2	0.200000	2.96	3.70		5.19	1.48
3	11/2	0.083333	25.9	2.53	0.120		25.3
	9/2	-0.100000	19.7	3.85	0.265	3.25	15.7
	7/2	-0.100000	14.6	4.16	0.340	4.85	9.10
	5/2	-0.006667	10.4	3.63	0.265	5.10	4.90
	3/2	0.110000	7.14	2.38		4.29	2.59
	1/2	0.200000	4.76			2.65	2.12
4	13/2	0.090909	24.2	1.63	0.052		23.9
	11/2	-0.086364	19.6	2.53	0.110	1.99	17.2
	9/2	-0.107792	15.6	2.79	0.135	3.06	12.1
	7/2	-0.037662	12.3	2.46	0.096	3.33	8.57
	5/2	0.071429	9.52	1.59		2.91	6.35
	3/2	0.178571	7.41			1.85	5.56

$I = \frac{5}{2}$  (Continued)

<i>J</i>	<i>F</i>	<i>f(I,J,F)</i>	<i>J</i> + 1 ← <i>J</i>			<i>J</i> ← <i>J</i>	
			<i>F</i> + 1 ← <i>F</i>	<i>F</i> ← <i>F</i>	<i>F</i> − 1 ← <i>F</i>	<i>F</i> ← <i>F</i> + 1 or <i>F</i> + 1 ← <i>F</i>	<i>F</i> ← <i>F</i>
5	15/2	0.096154	23.1	1.13	0.026		22.9
	13/2	−0.076923	19.4	1.79	0.054	1.35	17.8
	11/2	−0.110256	16.1	1.98	0.064	2.11	13.8
	9/2	−0.053846	13.4	1.76	0.043	2.31	10.8
	7/2	0.050000	11.0	1.12		2.04	8.77
	5/2	0.166667	9.09			1.31	7.79
6	17/2	0.100000	22.2	0.840	0.014		22.1
	15/2	−0.070000	19.2	1.32	0.029	0.970	18.0
	13/2	−0.110909	16.4	1.48	0.034	1.53	14.7
	11/2	−0.063636	14.1	1.31	0.022	1.69	12.2
	9/2	0.036364	12.0	0.832		1.50	10.4
	7/2	0.159091	10.3			0.950	9.31
7	19/2	0.102941	21.6	0.645	0.009		21.5
	17/2	−0.064705	19.0	1.02	0.017	0.731	18.1
	15/2	−0.110859	16.6	1.14	0.020	1.15	15.3
	13/2	−0.070136	14.5	1.01	0.013	1.29	13.1
	11/2	0.026923	12.7	0.641		1.14	11.5
	9/2	0.153846	11.1			0.722	10.4
8	21/2	0.105263	21.1	0.511	0.005		21.0
	19/2	−0.062526	18.8	0.809	0.011	0.571	18.1
	17/2	−0.110526	16.7	0.906	0.012	0.903	15.7
	15/2	−0.074737	14.9	0.806	0.008	1.01	13.8
	13/2	0.020000	13.2	0.508		0.897	12.3
	11/2	0.150000	11.8			0.566	11.2
9	23/2	0.107143	20.6	0.414	0.004		20.6
	21/2	−0.057143	18.6	0.658	0.007	0.458	18.1
	19/2	−0.110084	16.8	0.737	0.008	0.726	16.0
	17/2	−0.078151	15.1	0.656	0.005	0.813	14.3
	15/2	0.014706	13.6	0.413		0.722	12.9
	13/2	0.147059	12.3			0.455	11.8
10	25/2	0.108696	20.3	0.343	0.003		20.3
	23/2	−0.054348	18.5	0.545	0.005	0.375	18.1
	21/2	−0.109610	16.8	0.611	0.005	0.596	16.2
	19/2	−0.080778	15.3	0.543	0.003	0.668	14.6
	17/2	0.010526	13.9	0.342		0.594	13.3
	15/2	0.144737	12.7			0.373	12.3



$$I = 3$$

$J$	$F$	$f(I, J, F)$	$J + 1 \leftarrow J$			$J \leftarrow J$	
			$F + 1 \leftarrow F$	$F \leftarrow F$	$F - 1 \leftarrow F$	$F \leftarrow F + 1$ or $F + 1 \leftarrow F$	$F \leftarrow F$
0	3	0	42.9	33.3	23.8		
1	4	0.050000	31.4	9.64	1.79		26.8
	3	-0.150000	16.1	12.5	4.76	16.1	1.39
	2	0.120000	5.71	9.52	8.57	15.9	7.94
2	5	0.071429	26.5	4.49	0.408		25.1
	4	-0.107142	18.0	6.73	1.02	6.29	10.5
	3	-0.078571	11.2	7.14	1.63	8.93	2.50
	2	0.042857	6.12	6.12	2.04	8.57	0.00
	1	0.171429	2.45	4.08	2.04	5.71	2.86
3	6	0.083333	23.8	2.58	0.142		23.2
	5	-0.083333	18.1	4.05	0.340	3.32	14.0
	4	-0.100000	13.3	4.59	0.510	5.10	7.65
	3	-0.033333	9.35	4.37	0.567	5.61	3.57
	2	0.063333	6.24	3.54	0.425	5.10	1.28
	1	0.150000	3.83	2.30		3.83	0.255
	0	0.200000	2.05			2.04	0
4	7	0.090909	22.1	1.67	0.062		21.8
	6	-0.068182	17.8	2.68	0.144	2.04	15.4
	5	-0.103246	14.1	3.11	0.208	3.24	10.5
	4	-0.061039	11.0	3.04	0.216	3.71	7.00
	3	0.019481	8.44	2.52	0.144	3.57	4.63
	2	0.107143	6.35	1.59		2.91	3.24
	1	0.178571	4.76			1.79	2.98
5	8	0.096154	20.9	1.17	0.031		20.7
	7	-0.057692	17.5	1.90	0.071	1.38	15.9
	6	-0.102564	14.6	2.23	0.100	2.23	12.1
	5	-0.074571	12.0	2.20	0.100	2.60	9.14
	4	-0.003846	9.80	1.84	0.062	2.55	7.03
	3	0.083333	7.95	1.14		2.11	5.68
	2	0.166667	6.49			1.30	5.19
6	9	0.100000	20.0	0.862	0.017		19.9
	8	-0.050000	17.2	1.41	0.039	0.994	16.1
	7	-0.100909	14.8	1.67	0.054	1.62	13.0
	6	-0.081818	12.6	1.65	0.052	1.91	10.5
	5	-0.018182	10.7	1.38	0.031	1.88	8.63
	4	0.068182	9.04	0.848		1.57	7.36
	3	0.159091	7.69			0.962	6.73

$I = 3$  (Continued)

$J$	$F$	$f(I,J,F)$	$J + 1 \leftarrow J$			$J \leftarrow J$	
			$F + 1 \leftarrow F$	$F \leftarrow F$	$F - 1 \leftarrow F$	$F \leftarrow F + 1$ or $F + 1 \leftarrow F$	$F \leftarrow F$
7	10	0.102941	19.3	0.662	0.011		19.3
	9	-0.044118	17.0	1.09	0.023	0.750	16.1
	8	-0.099095	14.9	1.29	0.032	1.23	13.5
	7	-0.086425	13.0	1.28	0.030	1.45	11.4
	6	-0.027828	11.3	1.07	0.018	1.44	9.73
	5	0.057692	9.82	0.655		1.20	8.54
	4	0.153846	8.57			0.735	7.84
8	11	0.105263	18.8	0.524	0.007		18.7
	10	-0.039474	16.8	0.863	0.015	0.586	16.1
	9	-0.097368	14.9	1.03	0.020	0.963	13.9
	8	-0.089474	13.2	1.02	0.018	1.14	12.0
	7	-0.034737	11.7	0.856	0.011	1.14	10.5
	6	0.050000	10.4	0.520		0.950	9.40
	5	0.150000	9.24			0.578	8.67
9	12	0.107143	18.4	0.425	0.004		18.3
	11	-0.035714	16.6	0.702	0.010	0.470	16.1
	10	-0.095798	14.9	0.837	0.013	0.775	14.1
	9	-0.091597	13.4	0.834	0.012	0.922	12.4
	8	-0.039916	12.1	0.697	0.007	0.919	11.1
	7	0.044118	10.9	0.423		0.768	10.0
	6	0.147059	9.77			0.465	9.31
10	13	0.108696	18.0	0.352	0.003		18.0
	12	-0.032609	16.4	0.582	0.007	0.385	16.0
	11	-0.094394	14.9	0.694	0.009	0.636	14.3
	10	-0.093135	13.6	0.693	0.008	0.759	12.8
	9	-0.043936	12.3	0.579	0.004	0.757	11.4
	8	0.039474	11.2	0.350		0.632	10.5
	7	0.144737	10.2			0.383	9.82

$I = \frac{7}{2}$

<i>J</i>	<i>F</i>	<i>f(I, J, F)</i>	<i>J</i> + 1 ← <i>J</i>			<i>J</i> ← <i>J</i>	
			<i>F</i> + 1 ← <i>F</i>	<i>F</i> ← <i>F</i>	<i>F</i> − 1 ← <i>F</i>	<i>F</i> ← <i>F</i> + 1 or <i>F</i> + 1 ← <i>F</i>	<i>F</i> ← <i>F</i>
0	7/2	0	41.7	33.3	25.0		
1	9/2	0.050000	30.0	9.72	1.94		25.5
	7/2	−0.142857	15.3	12.7	5.36	16.2	1.06
	5/2	0.107143	5.36	9.64	10.0	16.1	8.93
2	11/2	0.071429	25.0	4.55	0.455		23.6
	9/2	−0.096939	16.9	6.93	1.19	6.36	9.47
	7/2	−0.081633	10.5	7.48	2.04	9.17	1.90
	5/2	0.025510	5.61	6.53	2.86	8.93	0.071
	3/2	0.153061	2.14	4.29	3.57	6.00	4.00
3	13/2	0.083333	22.2	2.62	0.160		21.6
	11/2	−0.071429	16.8	4.20	0.406	3.37	12.8
	9/2	−0.097619	12.3	4.89	0.661	5.28	6.62
	7/2	−0.047619	8.60	4.84	0.850	5.95	2.72
	5/2	0.035714	5.61	4.21	0.893	5.61	0.638
	3/2	0.119048	3.27	3.17	0.694	4.46	0
	1/2	0.178571	1.49	2.08		2.68	0.893
4	15/2	0.090909	20.5	1.70	0.071		20.1
	13/2	−0.055195	16.5	2.78	0.175	2.07	14.0
	11/2	−0.097403	13.1	3.34	0.275	3.37	9.32
	9/2	−0.071892	10.1	3.43	0.337	3.98	5.90
	7/2	−0.009276	7.66	3.13	0.325	4.01	3.53
	5/2	0.065399	5.63	2.49	0.212	3.57	2.02
	3/2	0.132653	4.00	1.56		2.75	1.19
	1/2	0.178571	2.78			1.62	1.16
5	17/2	0.096154	19.2	1.19	0.036		19.1
	15/2	−0.043956	16.1	1.97	0.087	1.40	14.5
	13/2	−0.094322	13.4	2.40	0.134	2.32	10.8
	11/2	−0.082418	11.0	2.50	0.159	2.80	7.95
	9/2	−0.032051	8.90	2.32	0.146	2.89	5.82
	7/2	0.036630	7.14	1.86	0.087	2.65	4.33
	5/2	0.107143	5.68	1.14		2.11	3.44
	3/2	0.166667	4.55			1.27	3.27
6	19/2	0.100000	18.3	0.877	0.020		18.2
	17/2	−0.035174	15.8	1.47	0.048	1.01	14.6
	15/2	−0.090909	13.5	1.80	0.073	1.69	11.6
	13/2	−0.087662	11.5	1.89	0.085	2.06	9.25
	11/2	−0.045455	9.70	1.76	0.075	2.16	7.38
	9/2	0.018831	8.15	1.42	0.043	2.00	6.01
	7/2	0.090909	6.84	0.855		1.60	5.13
	5/2	0.159091	5.77			0.962	4.81



$I = \frac{7}{2}$  (Continued)

<i>J</i>	<i>F</i>	<i>f</i> ( <i>I</i> , <i>J</i> , <i>F</i> )	<i>J</i> + 1 ← <i>J</i>			<i>J</i> ← <i>J</i>	
			<i>F</i> + 1 ← <i>F</i>	<i>F</i> ← <i>F</i>	<i>F</i> − 1 ← <i>F</i>	<i>F</i> ← <i>F</i> + 1 or <i>F</i> + 1 ← <i>F</i>	<i>F</i> ← <i>F</i>
7	21/2	0.102941	17.6	0.674	0.012		17.6
	19/2	−0.029412	15.5	1.14	0.029	0.764	14.6
	17/2	−0.087750	13.6	1.40	0.043	1.28	12.1
	15/2	−0.090498	11.8	1.48	0.049	1.58	10.1
	13/2	−0.054137	10.2	1.38	0.042	1.66	8.46
	11/2	0.006787	8.87	1.11	0.023	1.55	7.21
	9/2	0.079670	7.67	0.663		1.24	6.35
	7/2	0.153846	6.67			0.741	5.93
8	23/2	0.105263	17.1	0.534	0.008		17.1
	21/2	−0.024436	15.3	0.903	0.018	0.600	14.6
	19/2	−0.084962	13.6	1.12	0.027	1.01	12.5
	17/2	−0.092105	12.0	1.18	0.030	1.24	10.7
	15/2	−0.060150	10.6	1.10	0.026	1.31	9.23
	13/2	−0.001880	9.39	0.889	0.014	1.23	8.08
	11/2	0.071429	8.29	0.528		0.985	7.25
	9/2	0.150000	7.35			0.585	6.77
9	25/2	0.107143	16.7	0.433	0.005		16.6
	23/2	−0.020408	15.0	0.734	0.012	0.479	14.5
	21/2	−0.082533	13.5	0.910	0.018	0.810	12.7
	19/2	−0.093037	12.2	0.965	0.020	1.00	11.1
	17/2	−0.064526	10.9	0.903	0.017	1.06	9.79
	15/2	−0.008403	9.79	0.727	0.009	0.993	8.73
	13/2	0.065126	8.78	0.430		0.798	7.94
	11/2	0.147059	7.89			0.472	7.42
10	27/2	0.018696	16.3	0.359	0.004		16.3
	25/2	−0.017081	14.9	0.609	0.008	0.392	14.4
	23/2	−0.080418	13.5	0.756	0.012	0.666	12.8
	21/2	−0.093576	12.3	0.802	0.013	0.826	11.4
	19/2	−0.067833	11.1	0.752	0.011	0.876	10.2
	17/2	−0.013485	10.1	0.604	0.006	0.820	9.24
	15/2	0.060150	9.17	0.357		0.659	8.48
	13/2	0.144737	8.33			0.389	7.94

$I = 4$

$J$	$F$	$f(I,J,F)$	$J + 1 \leftarrow J$			$J \leftarrow J$	
			$F + 1 \leftarrow F$	$F \leftarrow F$	$F - 1 \leftarrow F$	$F \leftarrow F + 1$ or $F + 1 \leftarrow F$	$F \leftarrow F$
0	4	0	40.7	33.3	25.9		
1	5	0.050000	28.9	9.78	2.07		24.4
	4	-0.137500	14.7	12.8	5.83	16.3	0.833
	3	0.098214	5.09	9.72	11.1	16.2	9.72
2	6	0.071429	23.8	4.59	0.494		22.5
	5	-0.089286	16.0	7.06	1.33	6.42	8.69
	4	-0.082908	9.90	7.71	2.38	9.33	1.50
	3	0.014031	5.24	6.79	3.53	9.17	0.216
	2	0.140306	1.94	4.41	4.76	6.17	4.94
3	7	0.083333	21.0	2.65	0.176		20.4
	6	-0.062500	15.9	4.30	0.463	3.40	11.8
	5	-0.094643	11.6	5.09	0.794	5.40	5.87
	4	-0.055952	8.02	5.16	1.10	6.19	2.14
	3	0.017857	5.16	4.63	1.32	5.95	0.309
	2	0.098214	2.91	3.64	1.39	4.85	0.110
	1	0.163690	1.21	2.31	1.23	2.98	1.79
4	8	0.090909	19.2	1.72	0.079		18.9
	7	-0.045455	15.5	2.86	0.202	2.10	13.0
	6	-0.091721	12.2	3.50	0.337	3.46	8.43
	5	-0.077110	9.43	3.70	0.449	4.17	5.09
	4	-0.026670	7.07	3.54	0.505	4.32	2.78
	3	0.038729	5.11	3.06	0.471	4.01	1.30
	2	0.102389	3.50	2.36	0.314	3.33	0.463
	1	0.151786	2.22	1.48		2.38	0.093
	0	0.178571	1.23			1.23	0
5	9	0.096154	17.9	1.20	0.040		17.8
	8	-0.033654	15.0	2.03	0.102	1.42	13.4
	7	-0.086767	12.5	2.53	0.167	2.39	9.82
	6	-0.085165	10.2	2.73	0.216	2.94	7.05
	5	-0.048077	8.22	2.66	0.233	3.14	4.94
	4	0.008013	6.53	2.36	0.204	3.03	3.41
	3	0.069368	5.10	1.85	0.121	2.65	2.38
	2	0.125000	3.93	1.12		2.04	1.80
	1	0.166667	3.03			1.21	1.82

$I = 4$  (Continued)

$J$	$F$	$f(I,J,F)$	$J + 1 \leftarrow J$			$J \leftarrow J$	
			$F + 1 \leftarrow F$	$F \leftarrow F$	$F - 1 \leftarrow F$	$F \leftarrow F + 1$ or $F + 1 \leftarrow F$	$F \leftarrow F$
6	10	0.100000	17.0	0.889	0.023		16.9
	9	-0.025000	14.7	1.52	0.057	1.03	13.5
	8	-0.081981	12.5	1.90	0.092	1.74	10.6
	7	-0.088474	10.6	2.07	0.116	2.17	8.29
	6	-0.060065	8.95	2.04	0.122	2.35	6.45
	5	-0.010389	7.47	1.83	0.013	2.31	5.04
	4	0.048864	6.20	1.44	0.057	2.05	4.04
	3	0.107955	5.13	0.855		1.60	3.43
	2	0.159091	4.27			0.950	3.32
7	11	0.102941	16.3	0.683	0.014		16.3
	10	-0.018382	14.3	1.17	0.034	0.774	13.5
	9	-0.077771	12.5	1.48	0.054	1.32	11.1
	8	-0.090417	10.9	1.62	0.068	1.67	9.11
	7	-0.067469	9.44	1.60	0.070	1.82	7.50
	6	-0.022503	8.13	1.44	0.057	1.80	6.23
	5	0.034947	6.99	1.13	0.031	1.61	5.28
	4	0.096154	6.00	0.667		1.26	4.67
	3	0.153846	5.19			0.741	4.44
8	12	0.105263	15.8	0.541	0.009		15.7
	11	-0.013158	14.1	0.932	0.022	0.605	13.4
	10	-0.074154	12.5	1.18	0.034	1.04	11.4
	9	-0.090132	11.1	1.30	0.042	1.32	9.66
	8	-0.072368	9.78	1.29	0.043	1.44	8.24
	7	-0.031015	8.61	1.16	0.034	1.43	7.09
	6	0.024906	7.57	0.911	0.018	1.28	6.21
	5	0.087500	6.66	0.533		1.01	5.60
	4	0.150000	5.88			0.588	5.29
9	13	0.107143	15.3	0.440	0.006		15.3
	12	-0.008929	13.8	9.759	0.015	0.486	13.3
	11	-0.071053	12.5	0.965	0.023	0.838	11.5
	10	-0.090036	11.2	1.06	0.028	1.06	10.0
	9	-0.075780	10.0	1.06	0.028	1.17	8.78
	8	-0.037290	8.97	0.953	0.022	1.16	7.73
	7	0.017332	8.01	0.747	0.011	1.05	6.91
	6	0.080882	7.17	0.434		0.819	6.31
	5	0.147059	6.43			0.477	5.96



$I = 4$  (Continued)

$J$	$F$	$f(I,J,F)$	$J + 1 \leftarrow J$			$J \leftarrow J$	
			$F + 1 \leftarrow F$	$F \leftarrow F$	$F - 1 \leftarrow F$	$F \leftarrow F + 1$ or $F + 1 \leftarrow F$	$F \leftarrow F$
10	14	0.108696	15.0	0.364	0.004		14.9
	13	-0.005435	13.6	0.630	0.010	0.399	13.2
	12	-0.068384	12.4	0.802	0.016	0.689	11.7
	11	-0.089715	11.3	0.885	0.019	0.877	10.3
	10	-0.078253	10.2	0.882	0.019	0.966	9.18
	9	-0.042089	9.24	0.795	0.015	0.962	8.22
	8	0.001142	8.37	0.622	0.007	0.866	7.45
	7	0.075658	7.58	0.361		0.678	6.87
	6	0.144737	6.88			0.393	6.49

$I = \frac{9}{2}$

0	9/2	0	40.0	33.3	26.7		
1	11/2	0.050000	28.0	9.82	2.18		23.6
	9/2	-0.133333	14.2	12.9	6.22	16.4	0.673
	7/2	0.091667	4.89	9.78	12.0	16.3	10.4
2	13/2	0.071429	22.9	4.62	0.527		21.5
	11/2	-0.083333	15.4	7.16	1.45	6.46	8.08
	9/2	-0.083333	9.45	7.88	2.67	9.45	1.21
	7/2	0.005952	4.95	6.97	4.08	9.33	0.381
	5/2	0.130952	1.79	4.49	5.71	6.29	5.71
3	15/2	0.083333	20.0	2.67	0.190		19.4
	13/2	-0.055556	15.1	4.38	0.513	3.43	11.1
	11/2	-0.091667	11.0	5.24	0.909	5.50	5.29
	9/2	-0.061111	7.58	5.39	1.32	6.36	1.73
	7/2	0.005556	4.81	4.91	1.70	6.19	0.136
	5/2	0.083333	2.65	3.92	2.00	5.10	0.326
	3/2	0.152777	1.05	2.44	2.22	3.14	2.57
4	17/2	0.090909	18.2	1.73	0.086		17.9
	15/2	-0.037879	14.6	2.92	0.226	2.12	12.1
	13/2	-0.086580	11.5	3.62	0.392	3.53	7.72
	11/2	-0.079545	8.88	3.91	0.551	4.31	4.48
	9/2	-0.037879	6.61	3.83	0.673	4.55	2.25
	7/2	0.020563	4.71	3.45	0.727	4.32	0.854
	5/2	0.081169	3.15	2.84	0.679	3.71	0.152
	3/2	0.132576	1.89	2.07	0.485	2.80	0.015
	1/2	0.166667	0.889	1.33		1.63	0.593

$I = \frac{9}{2}$  (Continued)

<i>J</i>	<i>F</i>	<i>f(I,J,F)</i>	<i>J</i> + 1 ← <i>J</i>			<i>J</i> ← <i>J</i>	
			<i>F</i> + 1 ← <i>F</i>	<i>F</i> ← <i>F</i>	<i>F</i> − 1 ← <i>F</i>	<i>F</i> ← <i>F</i> + 1 or <i>F</i> + 1 ← <i>F</i>	<i>F</i> ← <i>F</i>
5	19/2	0.096154	16.9	1.21	0.044		16.7
	17/2	−0.025641	14.2	2.08	0.115	1.44	12.5
	15/2	−0.080128	11.7	2.63	0.196	2.44	9.05
	13/2	−0.085470	9.57	2.89	0.269	3.06	6.34
	11/2	−0.057692	7.68	2.91	0.318	3.33	4.28
	9/2	−0.010684	6.05	2.71	0.326	3.31	2.76
	7/2	0.043803	4.66	2.33	0.280	3.03	1.70
	5/2	0.096154	3.50	1.79	0.168	2.55	1.02
	3/2	0.138889	2.55	1.09		1.89	0.655
	1/2	0.166667	1.82			1.09	0.727
6	21/2	0.100000	16.0	0.898	0.025		15.9
	19/2	−0.016667	13.8	1.55	0.065	1.04	12.6
	17/2	−0.074242	11.8	1.98	0.109	1.78	9.80
	15/2	−0.087121	9.95	2.21	0.147	2.26	7.54
	13/2	−0.068182	8.35	2.25	0.169	2.51	5.73
	11/2	−0.028788	6.94	2.12	0.168	2.54	4.32
	9/2	0.021212	5.71	1.85	0.137	2.38	3.26
	7/2	0.073485	4.65	1.43	0.075	2.05	2.53
	5/2	0.121212	3.77	0.848		1.57	2.12
	3/2	0.159091	3.08			0.923	2.15
7	23/2	0.102941	15.3	0.691	0.015		15.2
	21/2	−0.009804	13.4	1.20	0.039	0.783	12.5
	19/2	−0.069193	11.7	1.54	0.065	1.36	10.2
	17/2	−0.087104	10.2	1.73	0.087	1.74	8.32
	15/2	−0.074284	8.79	1.78	0.098	1.94	6.74
	13/2	−0.040347	7.55	1.69	0.095	1.98	5.47
	11/2	0.006222	6.45	1.48	0.075	1.88	4.48
	9/2	0.058069	5.49	1.14	0.039	1.64	3.77
	7/2	0.108974	4.67	0.667		1.26	3.34
	5/2	0.153846	4.00			0.735	3.27
8	25/2	0.105263	14.7	0.547	0.010		14.7
	23/2	−0.004386	13.1	0.956	0.025	0.612	12.4
	21/2	−0.064912	11.7	1.23	0.041	1.07	10.5
	19/2	−0.086404	10.3	1.39	0.054	1.37	8.85
	17/2	−0.078070	9.09	1.43	0.061	1.54	7.46
	15/2	−0.048246	7.99	1.37	0.058	1.59	6.32
	13/2	−0.004386	6.99	1.20	0.044	1.51	5.41
	11/2	0.046930	6.11	0.924	0.023	1.32	4.73
	9/2	0.100000	5.35	0.535		1.02	4.28
	7/2	0.150000	4.71			0.588	4.12

$I = \frac{9}{2}$  (Continued)

J	F	f(I,J,F)	J + 1 ← J			J ← J	
			F + 1 ← F	F ← F	F - 1 ← F	F ← F + 1 or F + 1 ← F	F ← F
9	27/2	0.107143	14.3	0.444	0.007		14.2
	25/2	0	12.9	0.778	0.017	0.491	12.3
	23/2	-0.061275	11.6	1.01	0.027	0.859	10.7
	21/2	-0.085434	10.4	1.14	0.036	1.11	9.22
	19/2	-0.080532	9.31	1.18	0.040	1.25	7.98
	17/2	-0.053922	8.31	1.13	0.037	1.29	6.95
	15/2	-0.012255	7.41	0.987	0.028	1.23	6.11
	13/2	0.038515	6.59	0.760	0.014	1.08	5.46
	11/2	0.093137	5.88	0.437		0.831	5.01
10	9/2	0.147059	5.26			0.478	4.78
	29/2	0.108696	13.9	0.368	0.005		13.9
	27/2	-0.003623	12.7	0.646	0.012	0.403	12.2
	25/2	-0.058162	11.5	0.839	0.019	0.707	10.8
	23/2	-0.084382	10.5	0.950	0.025	0.916	9.48
	21/2	-0.082189	9.47	0.984	0.027	1.04	8.37
	19/2	-0.058162	8.56	0.942	0.025	1.07	7.43
	17/2	-0.018307	7.73	0.826	0.019	1.03	6.65
	15/2	0.031941	6.98	0.635	0.009	0.898	6.03
	13/2	0.087719	6.30	0.364		0.690	5.58
	11/2	0.144737	5.71			0.396	5.32

$I = \frac{11}{2}$

0	11/2	0	38.9	33.3	27.8		
1	13/2	0.05000	26.7	9.87	2.35		22.4
	11/2	-0.12727	13.5	13.1	6.82	16.5	0.466
	9/2	-0.08273	4.60	9.85	13.3	16.4	11.4
2	15/2	0.07143	21.4	4.66	0.582		20.1
	13/2	-0.07468	14.4	7.29	1.65	6.52	7.20
	11/2	-0.83117	8.79	8.09	3.12	9.62	0.839
	9/2	-0.00455	4.55	7.18	4.94	9.55	0.701
	7/2	0.11818	1.60	4.59	7.14	6.42	6.91
3	17/2	0.08333	18.5	2.70	0.214		18.0
	15/2	-0.04545	14.0	4.48	0.595	3.47	9.96
	13/2	-0.08636	10.1	5.45	1.10	5.62	4.45
	11/2	-0.06667	6.92	5.68	1.68	6.59	1.20
	9/2	-0.01000	4.33	5.26	2.31	6.49	0.010
	7/2	0.06364	2.31	4.23	2.98	5.40	0.806
	5/2	0.13788	0.860	2.58	3.70	3.32	3.83



$I = \frac{11}{2}$  (Continued)

<i>J</i>	<i>F</i>	<i>f(I,J,F)</i>	<i>J</i> + 1 ← <i>J</i>			<i>J</i> ← <i>J</i>	
			<i>F</i> + 1 ← <i>F</i>	<i>F</i> ← <i>F</i>	<i>F</i> − 1 ← <i>F</i>	<i>F</i> ← <i>F</i> + 1 or <i>F</i> + 1 ← <i>F</i>	<i>F</i> ← <i>F</i>
4	19/2	0.09091	16.7	1.75	0.098		16.4
	17/2	−0.02686	13.4	3.00	0.267	2.14	10.9
	15/2	−0.07804	10.5	3.79	0.485	3.62	6.69
	13/2	−0.08070	8.06	4.18	0.725	4.50	3.62
	11/2	−0.05077	5.94	4.20	0.964	4.84	1.55
	9/2	−0.00207	4.16	3.92	1.18	4.71	0.378
	7/2	0.05372	2.69	3.37	1.35	4.17	0
	5/2	0.10702	1.52	2.59	1.45	3.24	0.389
	3/2	0.15041	0.613	1.58	1.52	1.93	1.78
5	21/2	0.09615	15.4	1.23	0.051		15.2
	19/2	−0.01399	12.9	2.14	0.138	1.46	11.2
	17/2	−0.06935	10.6	2.76	0.247	2.51	7.92
	15/2	−0.08322	8.64	3.12	0.363	3.21	5.33
	13/2	−0.06748	6.89	3.25	0.471	3.58	3.35
	11/2	−0.03263	5.37	3.17	0.556	3.67	1.91
	9/2	0.01224	4.05	2.92	0.604	3.51	0.921
	7/2	0.05944	2.94	2.53	0.599	3.14	0.321
	5/2	0.10268	2.00	2.02	0.524	2.60	0.039
	3/2	0.13706	1.22	1.45	0.356	1.91	0.027
	1/2	0.15909	0.589	0.926		1.09	0.421
6	23/2	0.10000	14.4	0.911	0.029		14.3
	21/2	−0.00455	12.4	1.60	0.079	1.05	11.2
	19/2	−0.06182	10.6	2.09	0.139	1.84	8.60
	17/2	−0.08223	8.94	2.40	0.201	2.39	6.44
	15/2	−0.07521	7.47	2.53	0.256	2.72	4.69
	13/2	−0.04917	6.15	2.52	0.295	2.85	3.32
	11/2	−0.01157	5.00	2.38	0.311	2.81	2.26
	9/2	0.03116	3.99	2.13	0.293	2.62	1.48
	7/2	0.07355	3.11	1.78	0.235	2.31	0.938
	5/2	0.11116	2.37	1.34	0.134	1.88	0.589
	3/2	0.14050	1.76	0.806		1.37	0.407
	1/2	0.15909	1.28			0.783	0.499
7	25/2	0.10294	13.7	0.701	0.018		13.7
	23/2	0.00267	12.0	1.24	0.048	0.794	11.1
	21/2	−0.05551	10.5	1.63	0.084	1.40	8.98
	19/2	−0.08013	9.10	1.89	0.120	1.84	7.16
	17/2	−0.07896	7.83	2.02	0.151	2.11	5.64
	15/2	−0.05903	6.69	2.03	0.172	2.25	4.39
	13/2	−0.02664	5.66	1.94	0.176	2.25	3.39
	11/2	0.01267	4.75	1.76	0.160	2.14	2.61
	9/2	0.05407	3.95	1.48	0.123	1.92	2.03
	7/2	0.09350	3.26	1.12	0.064	1.61	1.63
	5/2	0.12762	2.68	0.655		1.20	1.43
	3/2	0.15385	2.22			0.698	1.52

$I = \frac{11}{2}$  (Continued)

J	F	f(I,J,F)	J + 1 ← J			J ← J	
			F + 1 ← F	F ← F	F − 1 ← F	F ← F + 1 or F + 1 ← F	F ← F
8	27/2	0.10526	13.2	0.556	0.012		13.1
	25/2	0.00837	11.7	0.989	0.031	0.621	11.0
	23/2	−0.05024	10.4	1.31	0.054	1.10	9.21
	21/2	−0.07775	9.19	1.52	0.076	1.45	7.64
	19/2	−0.08077	8.07	1.63	0.095	1.69	6.31
	17/2	−0.06531	7.06	1.66	0.106	1.81	5.19
	15/2	−0.03684	6.14	1.59	0.107	1.82	4.27
	13/2	0.01297	5.32	1.45	0.095	1.75	3.53
	11/2	0.04019	4.58	1.23	0.070	1.58	2.96
	9/2	0.08072	3.94	0.927	0.035	1.34	2.56
	7/2	0.11818	3.39	0.533		1.01	2.34
	5/2	0.15000	2.94			0.578	2.36
9	29/2	0.10714	12.7	0.452	0.008		12.7
	27/2	0.01299	11.5	0.807	0.021	0.499	10.9
	25/2	−0.04580	10.3	1.07	0.036	0.890	9.33
	23/2	−0.07540	9.23	1.25	0.051	1.18	7.97
	21/2	−0.08155	8.24	1.35	0.063	1.37	6.80
	19/2	−0.06952	7.33	1.37	0.069	1.48	5.79
	17/2	−0.04412	6.50	1.32	0.069	1.50	4.95
	15/2	−0.00970	5.75	1.21	0.060	1.44	4.26
	13/2	0.02983	5.07	1.02	0.043	1.32	3.71
	11/2	0.07105	4.47	0.771	0.021	1.11	3.31
	9/2	0.11096	3.95	0.439		0.837	3.07
	7/2	0.14706	3.51			0.477	3.03
10	31/2	0.10870	12.3	0.374	0.006		12.3
	29/2	0.01680	11.2	0.670	0.015	0.410	10.8
	27/2	−0.04202	10.2	0.892	0.025	0.733	9.40
	25/2	−0.07320	9.24	1.04	0.035	0.974	8.21
	23/2	−0.08178	8.35	1.13	0.043	1.14	7.16
	21/2	−0.07245	7.53	1.15	0.047	1.23	6.25
	19/2	−0.04951	6.78	1.11	0.046	1.25	5.47
	17/2	−0.01690	6.08	1.02	0.040	1.21	4.83
	15/2	0.02182	5.46	0.864	0.028	1.10	4.31
	13/2	0.06348	4.89	0.649	0.013	0.935	3.92
	11/2	0.10526	4.40	0.366		0.702	3.66
	9/2	0.14474	3.97			0.397	3.57

# APPENDIX II

## Second-order Energies Due to Nuclear Quadrupole Interactions in Linear Molecules and Symmetric Tops

Entries in this table should be multiplied by  $\frac{(eqQ)^2}{B_0} \times 10^{-3}$  and added to the first-order energy of nuclear quadrupole interaction obtained from use of Appendix I [cf. Eq. (6-9)].  $B_0$  is the rotational constant. Values for  $I = \frac{3}{2}$ ,  $\frac{5}{2}$ , and  $\frac{7}{2}$  only are given since these spins are most commonly associated with large quadrupole coupling constants where second-order corrections are important. (This table was computed by N. M. McDermott.)

$$I = \frac{3}{2}$$

$J$	$F$	$K = 0$	$K = 1$	$K = 2$	$K = 3$
0	3/2	-10.417			
1	5/2	-6.000	-9.469		
	3/2	-2.250	-10.875		
	1/2	0	-11.719		
2	7/2	-4.100	-5.649	-7.289	
	5/2	-2.187	2.456	-3.887	
	3/2	10.417	5.208	-10.417	
	1/2	0	11.719	0	
3	9/2	-3.086	-3.852	-5.382	-5.376
	7/2	-1.929	0.217	3.472	-1.712
	5/2	6.000	3.447	-2.604	-7.324
	3/2	2.250	5.667	10.417	0
4	11/2	-2.465	-2.892	-3.909	-4.729
	9/2	-1.690	-0.594	1.857	3.155
	7/2	4.100	2.821	-0.461	-4.078
	5/2	2.187	3.566	6.492	7.324
5	13/2	-2.048	-2.308	-2.980	-3.738
	11/2	-1.494	-0.868	0.716	2.378
	9/2	3.086	2.372	0.444	-2.042
	7/2	1.929	2.611	4.278	5.790
6	15/2	-1.750	-1.920	-2.378	-2.970
	13/2	-1.333	-0.945	0.097	1.422
	11/2	2.465	2.029	0.818	-0.877
	9/2	1.690	2.075	3.080	4.263



$I = \frac{3}{2}$  (Continued)

<i>J</i>	<i>F</i>	<i>K</i> = 0	<i>K</i> = 1	<i>K</i> = 2	<i>K</i> = 3
7	17/2	−1.527	−1.644	−1.967	−2.417
	15/2	−1.202	−0.945	−0.233	0.756
	13/2	2.048	1.764	0.958	−0.223
	11/2	1.494	1.731	2.376	3.227
8	19/2	−1.353	−1.437	−1.673	−2.016
	17/2	−1.093	−0.915	−0.410	0.327
	15/2	1.750	1.554	0.993	0.147
	13/2	1.333	1.490	1.925	2.538
9	21/2	−1.215	−1.262	−1.440	−1.706
	19/2	−1.002	−0.873	−0.503	0.054
	17/2	1.527	1.386	0.981	0.357
	15/2	1.202	1.311	1.617	2.067
10	23/2	−1.102	−1.149	−1.285	−1.492
	21/2	−0.925	−0.828	−0.550	−0.122
	19/2	1.353	1.253	0.948	0.476
	17/2	1.093	1.172	1.396	1.733

$I = \frac{5}{2}$

0	5/2	−5.833			
1	7/2	−2.893	−6.417		
	5/2	−2.083	−3.639		
	3/2	−0.540	−8.235		
2	9/2	−1.804	−3.140	−4.844	
	7/2	−1.804	2.686	−0.826	
	5/2	4.948	0.066	−3.985	
	3/2	−0.197	5.699	−5.112	
	1/2	0	−0.833	−2.083	
3	11/2	−1.277	−1.911	−3.242	−3.557
	9/2	−1.477	0.301	3.140	−0.442
	7/2	2.000	0.786	−1.667	−1.797
	5/2	1.807	1.750	0.764	−3.593
	3/2	0.540	1.744	2.681	−2.788
	1/2	0	0.833	2.083	0
4	13/2	−0.975	−1.319	−2.160	−2.923
	11/2	−1.229	−0.404	1.453	2.495
	9/2	0.976	0.613	−0.280	−1.114
	7/2	1.508	1.201	0.330	−0.960
	5/2	0.886	1.200	1.735	1.266
	3/2	0.197	0.792	2.091	2.637

$I = \frac{5}{2}$  (Continued)

<i>J</i>	<i>F</i>	<i>K</i> = 0	<i>K</i> = 1	<i>K</i> = 2	<i>K</i> = 3
5	15/2	−0.783	−0.989	−1.529	−2.169
	13/2	−1.045	−0.607	0.503	1.671
	11/2	0.523	0.399	0.071	−0.341
	9/2	1.184	0.964	0.356	−0.482
	7/2	0.893	0.966	1.093	1.004
	5/2	0.276	0.623	1.486	2.327
6	17/2	−0.652	−0.784	−1.146	−1.626
	15/2	−0.905	−0.648	0.041	0.915
	13/2	0.290	0.247	0.126	−0.045
	11/2	0.947	0.802	0.396	−0.184
	9/2	0.828	0.832	0.820	0.723
	7/2	0.296	0.508	1.069	1.753
7	19/2	−0.557	−0.647	−0.898	−1.255
	17/2	−0.797	−0.634	−0.185	0.438
	15/2	0.158	0.145	0.106	0.046
	13/2	0.777	0.680	0.405	−0.002
	11/2	0.754	0.738	0.685	0.575
	9/2	0.293	0.431	0.807	1.315
8	21/2	−0.485	−0.549	−0.730	−0.998
	19/2	−0.711	−0.603	−0.296	0.151
	17/2	0.079	0.077	0.071	0.061
	15/2	0.652	0.585	0.393	0.102
	13/2	0.685	0.665	0.604	0.497
	11/2	0.282	0.376	0.637	1.012
9	23/2	−0.429	−0.476	−0.612	−0.815
	21/2	−0.642	−0.566	−0.348	−0.021
	19/2	0.029	0.031	0.039	0.050
	17/2	0.558	0.511	0.373	0.160
	15/2	0.625	0.606	0.548	0.452
	13/2	0.268	0.334	0.523	0.802
10	25/2	−0.384	−0.420	−0.523	−0.681
	23/2	−0.584	−0.529	−0.369	−0.125
	21/2	−0.004	0.000	0.013	0.033
	19/2	0.486	0.451	0.349	0.190
	17/2	0.573	0.556	0.505	0.421
	15/2	0.253	0.302	0.442	0.654

$I = \frac{7}{2}$

<i>J</i>	<i>F</i>	<i>K</i> = 0	<i>K</i> = 1	<i>K</i> = 2	<i>K</i> = 3
0	7/2	−4.464			
1	9/2	−2.020	−5.030		
	7/2	−1.804	−2.159		
	5/2	−0.656	−6.416		
2	11/2	−1.184	−2.369	−3.890	
	9/2	−1.455	2.462	−0.637	
	7/2	3.483	−0.530	−2.079	
	5/2	−0.409	2.095	−9.028	
	3/2	−0.084	−1.209	−2.882	
3	13/2	−0.802	−1.349	−2.514	−2.861
	11/2	−1.127	0.301	2.532	−0.595
	9/2	1.090	0.429	−0.852	−0.649
	7/2	1.272	0.937	−0.122	−2.062
	5/2	0.454	3.167	6.709	−2.720
	3/2	−0.039	0.642	2.346	−2.047
	1/2	0.000	−0.149	−0.478	−0.628
4	15/2	−0.592	−0.884	−1.601	−2.271
	13/2	−0.902	−0.281	1.101	1.803
	11/2	0.359	0.269	−0.016	−0.198
	9/2	0.913	0.633	−0.070	−0.845
	7/2	0.730	0.737	0.624	−0.016
	5/2	0.342	0.613	1.101	0.838
	3/2	0.084	0.370	2.320	0.973
	1/2	0.000	0.149	0.478	0.628
5	17/2	−0.463	−0.635	−1.088	−1.632
	15/2	−0.745	−0.432	0.354	1.157
	13/2	0.075	0.095	0.141	0.171
	11/2	0.611	0.454	0.087	−0.391
	9/2	0.664	0.589	0.363	−0.018
	7/2	0.450	0.520	0.658	0.644
	5/2	0.202	0.361	0.735	1.018
	3/2	0.039	0.196	0.587	1.074
6	19/2	−0.377	−0.486	−0.786	−1.187
	17/2	−0.630	−0.455	0.013	0.596
	15/2	−0.051	−0.014	0.085	0.207
	13/2	0.420	0.346	0.142	−0.137
	11/2	0.561	0.494	0.302	0.001
	9/2	0.454	0.462	0.468	0.418
	7/2	0.252	0.333	0.538	0.754
	5/2	0.067	0.181	0.483	0.854



$$I = \frac{7}{2} \text{ (Continued)}$$

$J$	$F$	$K = 0$	$K = 1$	$K = 2$	$K = 3$
7	21/2	-0.317	-0.391	-0.597	-0.891
	19/2	-0.544	-0.438	-0.144	0.258
	17/2	-0.111	-0.076	0.020	0.152
	15/2	0.297	0.257	0.145	-0.018
	13/2	0.471	0.421	0.278	0.061
	11/2	0.427	0.417	0.382	0.310
	9/2	0.266	0.309	0.422	0.558
	7/2	0.081	0.162	0.382	0.680
8	23/2	-0.272	-0.324	-0.472	-0.690
	21/2	-0.478	-0.409	-0.216	0.065
	19/2	-0.140	-0.112	-0.030	0.089
	17/2	0.215	0.193	0.129	0.033
	15/2	0.397	0.361	0.256	0.096
	13/2	0.393	0.379	0.335	0.260
	11/2	0.265	0.288	0.351	0.433
	9/2	0.088	0.145	0.306	0.537
9	25/2	-0.238	-0.276	-0.385	-0.550
	23/2	-0.426	-0.379	-0.246	-0.046
	21/2	-0.153	-0.130	-0.065	0.036
	19/2	0.159	0.146	0.108	0.050
	17/2	0.340	0.313	0.236	0.117
	15/2	0.360	0.346	0.303	0.234
	13/2	0.256	0.269	0.305	0.354
	11/2	0.090	0.132	0.252	0.430
10	27/2	-0.211	-0.239	-0.322	-0.449
	25/2	-0.383	-0.350	-0.255	-0.110
	23/2	-0.158	-0.140	-0.086	-0.004
	21/2	0.119	0.111	0.088	0.053
	19/2	0.294	0.275	0.217	0.127
	17/2	0.330	0.317	0.280	0.219
	15/2	0.246	0.254	0.274	0.303
	13/2	0.090	0.121	0.212	0.351

### APPENDIX III

## Coefficients for Energy Levels of a Slightly Asymmetric Top

Rotational energy is given by

$$w = K^2 + C_1 b + C_2 b^2 + C_3 b^3 + C_4 b^4 + C_5 b^5 + \dots$$

For a prolate top, energy =  $W = \frac{B+C}{2} J(J+1) + \left( A - \frac{B+C}{2} \right) w$

$$b = b_p = \frac{C-B}{2A-B-C}$$

For an oblate top, energy =  $W = \frac{A+B}{2} J(J+1) + \left( C - \frac{A+B}{2} \right) w$

$$b = b_o = \frac{A-B}{2C-B-A}$$

Where the first few constants  $K, C_1, C_2 \dots$  are identical for pairs of degenerate levels, they are usually listed for only the first of the two levels. ( $C_1, C_2$ , and  $C_3$  were computed by J. F. Lotspeich;  $C_4$  and  $C_5$  by J. Kraitchman and N. Solimene.)

Level designation		$K^2$	$C_1$	$C_2$	$C_3$	$C_4$	$C_5$
Pro-late top	Ob-late top						
0 <sub>0,0</sub>	0 <sub>0,0</sub>	0	0	0	0	0	0
1 <sub>1,0</sub>	1 <sub>0,1</sub>	1	-1	0	0	0	0
1 <sub>1,1</sub>	1 <sub>1,1</sub>	1	1	0	0	0	0
1 <sub>0,1</sub>	1 <sub>1,0</sub>	0	0	0	0	0	0
2 <sub>2,0</sub>	2 <sub>0,2</sub>	4	0	3	0	-2.25	0
2 <sub>2,1</sub>	2 <sub>1,2</sub>	4	0	0	0	0	0
2 <sub>1,1</sub>	2 <sub>1,1</sub>	1	-3	0	0	0	0
2 <sub>1,2</sub>	2 <sub>2,1</sub>	1	3	0	0	0	0
2 <sub>0,2</sub>	2 <sub>2,0</sub>	0	0	-3	0	2.25	0
3 <sub>3,0</sub>	3 <sub>0,3</sub>	9	0	1.875	-1.40625	0.615234	0.197754
3 <sub>3,1</sub>	3 <sub>1,3</sub>	9	0	1.875	1.40625	0.615234	-0.197754
3 <sub>2,1</sub>	3 <sub>1,2</sub>	4	0	15	0	-56.25	0
3 <sub>2,2</sub>	3 <sub>2,2</sub>	4	0	0	0	0	0
3 <sub>1,2</sub>	3 <sub>2,1</sub>	1	-6	-1.875	1.40625	-0.615234	-0.197754
3 <sub>1,3</sub>	3 <sub>3,1</sub>	1	6	-1.875	-1.40625	-0.615234	0.197754
3 <sub>0,3</sub>	3 <sub>3,0</sub>	0	0	-15	0	56.25	0

Level designation		K <sup>2</sup>	C <sub>1</sub>	C <sub>2</sub>	C <sub>3</sub>	C <sub>4</sub>	C <sub>5</sub>
Pro- late top	Ob- late top						
4 <sub>4,0</sub>	4 <sub>0,4</sub>	16	0	2.33333	0	1.73380	0
4 <sub>4,1</sub>	4 <sub>1,4</sub>					-0.453704	0
4 <sub>3,1</sub>	4 <sub>1,3</sub>	9	0	7.875	-9.84375	4.55273	13.6890
4 <sub>3,2</sub>	4 <sub>2,3</sub>	9	0	7.875	9.84375	4.55273	-13.6890
4 <sub>2,2</sub>	4 <sub>2,2</sub>	4	0	42.6667	0	-488.296	0
4 <sub>2,3</sub>	4 <sub>3,2</sub>	4	0	-2.33333	0	0.453704	0
4 <sub>1,3</sub>	4 <sub>3,1</sub>	1	-10	-7.875	9.84375	-4.55273	-13.6890
4 <sub>1,4</sub>	4 <sub>4,1</sub>	1	10	-7.875	-9.84375	-4.55273	13.6890
4 <sub>0,4</sub>	4 <sub>4,0</sub>	0	0	-45	0	486.563	0
5 <sub>5,0</sub>	5 <sub>0,5</sub>	25	0	2.8125	0	0.736084	-0.769043
5 <sub>5,1</sub>	5 <sub>1,5</sub>					0.736084	0.769043
5 <sub>4,1</sub>	5 <sub>1,4</sub>	16	0	9	0	12.9375	0
5 <sub>4,2</sub>	5 <sub>2,4</sub>					-6.75	0
5 <sub>3,2</sub>	5 <sub>2,3</sub>	9	0	18.1875	-39.375	22.8890	150.886
5 <sub>3,3</sub>	5 <sub>3,3</sub>	9	0	18.1875	39.375	22.8890	-150.886
5 <sub>2,3</sub>	5 <sub>3,2</sub>	4	0	96	0	-2592	0
5 <sub>2,4</sub>	5 <sub>4,2</sub>	4	0	-9	0	6.75	0
5 <sub>1,4</sub>	5 <sub>4,1</sub>	1	-15	-21	39.375	-23.625	-150.117
5 <sub>1,5</sub>	5 <sub>5,1</sub>	1	15	-21	-39.375	-23.625	150.117
5 <sub>0,5</sub>	5 <sub>5,0</sub>	0	0	-105	0	2579.06	0
6 <sub>6,0</sub>	6 <sub>0,6</sub>	36	0	3.3.	0	.847688	0
6 <sub>6,1</sub>	6 <sub>1,6</sub>					.847688	0
6 <sub>5,1</sub>	6 <sub>1,5</sub>	25	0	10.3125	0	3.02124	-8.45947
6 <sub>5,2</sub>	6 <sub>2,5</sub>					3.02124	8.45947
6 <sub>4,2</sub>	6 <sub>2,4</sub>	16	0	19.2	0	59.2695	0
6 <sub>4,3</sub>	6 <sub>3,4</sub>					-39.168	0
6 <sub>3,3</sub>	6 <sub>3,3</sub>	9	0	34.6875	-118.125	92.6038	950.999
6 <sub>3,4</sub>	6 <sub>4,3</sub>	9	0	34.6875	118.125	92.6038	-950.999
6 <sub>2,4</sub>	6 <sub>4,2</sub>	4	0	187.5	0	-10199.2	0
6 <sub>2,5</sub>	6 <sub>5,2</sub>	4	0	-22.5	0	38.3203	0
6 <sub>1,5</sub>	6 <sub>5,1</sub>	1	-21	-45	118.125	-95.625	-942.539
6 <sub>1,6</sub>	6 <sub>6,1</sub>	1	21	-45	-118.125	-95.625	942.539
6 <sub>0,6</sub>	6 <sub>6,0</sub>	0	0	-210	0	10139.06	0
7 <sub>7,0</sub>	7 <sub>0,7</sub>	49	0	3.79166	0	0.965032	0
7 <sub>7,1</sub>	7 <sub>1,7</sub>						
7 <sub>6,1</sub>	7 <sub>1,6</sub>	36	0	11.7	0	3.21019	0
7 <sub>6,2</sub>	7 <sub>2,6</sub>						
7 <sub>5,2</sub>	7 <sub>2,5</sub>	25	0	20.95834	0	7.77481	-50.7568
7 <sub>5,3</sub>	7 <sub>3,5</sub>					7.77481	50.7568
7 <sub>4,3</sub>	7 <sub>3,4</sub>	16	0	34.13334	0	210.599	0
7 <sub>4,4</sub>	7 <sub>4,4</sub>					-150.338	0
7 <sub>3,4</sub>	7 <sub>4,3</sub>	9	0	59.625	-295.313	308.985	4355.86



Level designation		$K^2$	$C_1$	$C_2$	$C_3$	$C_4$	$C_5$
Pro- late top	Ob- late top						
7 <sub>3,5</sub>	7 <sub>5,3</sub>	9	0	59.625	295.313	308.985	-4355.86
7 <sub>2,6</sub>	7 <sub>6,2</sub>	4	0	332.16667	0	-32686.4	0
7 <sub>2,6</sub>	7 <sub>6,2</sub>	4	0	-45.83333	0	147.128	0
7 <sub>1,6</sub>	7 <sub>6,1</sub>	1	-28	-84.375	295.313	-317.725	-4305.10
7 <sub>1,7</sub>	7 <sub>7,1</sub>	1	28	-84.375	-295.313	-317.725	4305.10
7 <sub>0,7</sub>	7 <sub>7,0</sub>	0	0	-378	0	32472.6	0
8 <sub>8,0</sub>	8 <sub>0,8</sub>	64	0	4.28572	0	1.08509	0
8 <sub>8,1</sub>	8 <sub>1,8</sub>						
8 <sub>7,1</sub>	8 <sub>1,7</sub>	49	0	13.125	0	3.48633	0
8 <sub>7,2</sub>	8 <sub>2,7</sub>						
8 <sub>6,2</sub>	8 <sub>2,6</sub>	36	0	23.01428	0	7.29259	0
8 <sub>6,3</sub>	8 <sub>3,6</sub>						
8 <sub>5,3</sub>	8 <sub>3,5</sub>	25	0	35.625	0	18.6035	-219.946
8 <sub>5,4</sub>	8 <sub>4,5</sub>					18.6035	219.946
8 <sub>4,4</sub>	8 <sub>4,4</sub>	16	0	55.2	0	624.552	0
8 <sub>4,5</sub>	8 <sub>5,4</sub>					-458.261	0
8 <sub>3,5</sub>	8 <sub>5,3</sub>	9	0	95.625	-649.688	882.510	16079.8
8 <sub>3,6</sub>	8 <sub>6,3</sub>	9	0	95.625	649.688	882.510	-16079.8
8 <sub>2,6</sub>	8 <sub>6,2</sub>	4	0	547.5	0	-90112.6	0
8 <sub>2,7</sub>	8 <sub>7,2</sub>	4	0	-82.5	0	449.883	0
8 <sub>1,7</sub>	8 <sub>7,1</sub>	1	-36	-144.375	649.688	-904.600	-15859.8
8 <sub>1,8</sub>	8 <sub>8,1</sub>	1	36	-144.375	-649.688	-904.600	15859.8
8 <sub>0,8</sub>	8 <sub>8,0</sub>	0	0	-630	0	89479.7	0
9 <sub>9,0</sub>	9 <sub>0,9</sub>	81	0	4.78125	0	1.20665	0
9 <sub>9,1</sub>	9 <sub>1,9</sub>						
9 <sub>8,1</sub>	9 <sub>1,8</sub>	64	0	14.5714	0	3.80084	0
9 <sub>8,2</sub>	9 <sub>2,8</sub>						
9 <sub>7,2</sub>	9 <sub>2,7</sub>	49	0	25.2187	0	7.36478	0
9 <sub>7,3</sub>	9 <sub>3,7</sub>						
9 <sub>6,3</sub>	9 <sub>3,6</sub>	36	0	37.9286	0	15.0663	0
9 <sub>6,4</sub>	9 <sub>4,6</sub>						
9 <sub>5,4</sub>	9 <sub>4,5</sub>	25	0	55.3125	0	43.0826	-769.812
9 <sub>5,5</sub>	9 <sub>5,5</sub>					43.0826	769.812
9 <sub>4,5</sub>	9 <sub>5,4</sub>	16	0	84	0	1617	0
9 <sub>4,6</sub>	9 <sub>6,4</sub>					-1198.31	0
9 <sub>3,6</sub>	9 <sub>6,3</sub>	9	0	145.688	-1299.38	2229.47	50660.4
9 <sub>3,7</sub>	9 <sub>7,3</sub>	9	0	145.688	1299.38	2229.47	-50660.4
9 <sub>2,7</sub>	9 <sub>7,2</sub>	4	0	853.5	0	-221323	0
9 <sub>2,8</sub>	9 <sub>8,2</sub>	4	0	-136.5	0	1179.45	0
9 <sub>1,8</sub>	9 <sub>8,1</sub>	1	-45	-231	1299.38	-2281.13	-49890.6
9 <sub>1,9</sub>	9 <sub>9,1</sub>	1	45	-231	-1299.38	-2281.13	49890.6
9 <sub>0,9</sub>	9 <sub>9,0</sub>	0	0	-990	0	219687	0

Level designation		$K^2$	$C_1$	$C_2$	$C_3$	$C_4$	$C_5$
Pro- late top	Ob- late top						
10 <sub>10,0</sub>	10 <sub>0,10</sub>	100	0	5.27778	0	1.32912	0
10 <sub>10,1</sub>	10 <sub>1,10</sub>						
10 <sub>9,1</sub>	10 <sub>1,9</sub>	81	0	16.0313	0	4.13529	0
10 <sub>9,2</sub>	10 <sub>2,9</sub>						
10 <sub>8,2</sub>	10 <sub>2,8</sub>	64	0	27.5079	0	7.66709	0
10 <sub>8,3</sub>	10 <sub>3,8</sub>						
10 <sub>7,3</sub>	10 <sub>3,7</sub>	49	0	40.6354	0	13.8541	0
10 <sub>7,4</sub>	10 <sub>4,7</sub>						
10 <sub>6,4</sub>	10 <sub>4,6</sub>	36	0	57.2143	0	30.3788	0
10 <sub>6,5</sub>	10 <sub>5,6</sub>						
10 <sub>5,5</sub>	10 <sub>5,5</sub>	25	0	81.1458	0	95.5982	-2309.44
10 <sub>5,6</sub>	10 <sub>6,5</sub>					95.5982	2309.44
10 <sub>4,6</sub>	10 <sub>6,4</sub>	16	0	122.333	0	3767.88	0
10 <sub>4,7</sub>	10 <sub>7,4</sub>					-2801.12	0
10 <sub>3,7</sub>	10 <sub>7,3</sub>	9	0	213.188	-2413.13	5107.54	141215
10 <sub>3,8</sub>	10 <sub>8,3</sub>	9	0	213.188	2413.13	5107.54	-141215
10 <sub>2,8</sub>	10 <sub>8,2</sub>	4	0	1272.67	0	-495992	0
10 <sub>2,9</sub>	10 <sub>9,2</sub>	4	0	-212.333	0	2761.81	0
10 <sub>1,9</sub>	10 <sub>9,1</sub>	1	-55	-351	2413.13	-5221.13	-138906
10 <sub>1,10</sub>	10 <sub>10,1</sub>	1	55	-351	-2413.13	-5221.13	138906
10 <sub>0,10</sub>	10 <sub>10,0</sub>	0	0	-1485	0	492185	0
11 <sub>11,0</sub>	11 <sub>0,11</sub>	121	0	5.775	0		
11 <sub>11,1</sub>	11 <sub>1,11</sub>						
11 <sub>10,1</sub>	11 <sub>1,10</sub>	100	0	17.5	0		
11 <sub>10,2</sub>	11 <sub>2,10</sub>						
11 <sub>9,2</sub>	11 <sub>2,9</sub>	81	0	29.85	0		
11 <sub>9,3</sub>	11 <sub>3,9</sub>						
11 <sub>8,3</sub>	11 <sub>3,8</sub>	64	0	43.5714	0		
11 <sub>8,4</sub>	11 <sub>4,8</sub>						
11 <sub>7,4</sub>	11 <sub>4,7</sub>	49	0	60	0		
11 <sub>7,5</sub>	11 <sub>5,7</sub>						
11 <sub>6,5</sub>	11 <sub>5,6</sub>	36	0	82.1786	0		
11 <sub>6,6</sub>	11 <sub>6,6</sub>						
11 <sub>5,6</sub>	11 <sub>6,5</sub>	25	0	114.375	0		
11 <sub>5,7</sub>	11 <sub>7,5</sub>						
11 <sub>4,7</sub>	11 <sub>7,4</sub>	16	0	171.750	0		
11 <sub>4,8</sub>	11 <sub>8,4</sub>						
11 <sub>3,8</sub>	11 <sub>8,3</sub>	9	0	301.875	-4222.97		
11 <sub>3,9</sub>	11 <sub>9,3</sub>	9	0	301.875	4222.97		
11 <sub>2,9</sub>	11 <sub>9,2</sub>	4	0	1830	0		
11 <sub>2,10</sub>	11 <sub>10,2</sub>	4	0	-315	0		
11 <sub>1,10</sub>	11 <sub>10,1</sub>	1	-66	-511.875	4222.97		
11 <sub>1,11</sub>	11 <sub>11,1</sub>	1	66	-511.875	-4222.97		
11 <sub>0,11</sub>	11 <sub>11,0</sub>	0	0	-2145	0		

Level designation		$K^2$	$C_1$	$C_2$	$C_3$	$C_4$	$C_5$
Pro- late top	Ob- late top						
12 <sub>12,0</sub>	12 <sub>0,12</sub>	144	0	6.27272	0		
12 <sub>12,1</sub>	12 <sub>1,12</sub>						
12 <sub>11,1</sub>	12 <sub>1,11</sub>	121	0	18.975	0		
12 <sub>11,2</sub>	12 <sub>2,11</sub>						
12 <sub>10,2</sub>	12 <sub>2,10</sub>	100	0	32.2273	0		
12 <sub>10,3</sub>	12 <sub>3,10</sub>						
12 <sub>9,3</sub>	12 <sub>3,9</sub>	81	0	46.650	0		
12 <sub>9,4</sub>	12 <sub>4,9</sub>						
12 <sub>8,4</sub>	12 <sub>4,8</sub>	64	0	63.2857	0		
12 <sub>8,5</sub>	12 <sub>5,8</sub>						
12 <sub>7,5</sub>	12 <sub>5,7</sub>	49	0	84	0		
12 <sub>7,6</sub>	12 <sub>6,7</sub>						
12 <sub>6,6</sub>	12 <sub>6,6</sub>	36	0	112.414	0		
12 <sub>6,7</sub>	12 <sub>7,6</sub>						
12 <sub>5,7</sub>	12 <sub>7,5</sub>	25	0	156.375	0		
12 <sub>5,8</sub>	12 <sub>8,5</sub>						
12 <sub>4,8</sub>	12 <sub>8,4</sub>	16	0	235.8	0		
12 <sub>4,9</sub>	12 <sub>9,4</sub>						
12 <sub>3,9</sub>	12 <sub>9,3</sub>	9	0	415.875	-7038.28		
12 <sub>3,10</sub>	12 <sub>10,3</sub>	9	0	415.875	7038.28		
12 <sub>2,10</sub>	12 <sub>10,2</sub>	4	0	2553	0		
12 <sub>2,11</sub>	12 <sub>11,2</sub>	4	0	-450	0		
12 <sub>1,11</sub>	12 <sub>11,1</sub>	1	-78	-721.875	7038.28		
12 <sub>1,12</sub>	12 <sub>12,1</sub>	1	78	-721.875	-7038.28		
12 <sub>0,12</sub>	12 <sub>12,0</sub>	0	0	-3003	0		



## APPENDIX IV

### Energy Levels of a Rigid Rotor

Energy (in cycles/sec)  $= W/h = \frac{1}{2}(A + C)J(J + 1) + \frac{1}{2}(A - C)E_r$ .

$E_r$  is tabulated as a function of the rotational level  $J_{K-1, K_1}$  (or  $J_r$ ) and of the asymmetry parameter  $\kappa = \frac{2B - A - C}{A - C}$ .

Values for positive  $\kappa$  only are tabulated, since those for negative  $\kappa$  can be obtained from the relation  $E_r(\kappa) = -E_{-r}(-\kappa)$ . For further explanation see Chap. 4.

This table was reproduced with the permission of the Ballistics Research Laboratories, Aberdeen, Md., from *Ballistics Research Laboratories Report* No. 878 (September, 1953), by T. E. Turner, B. L. Hicks, and G. Reitwiesner. It was prepared for reproduction by S. Poley with the aid of an IBM card-controlled typewriter at the Watson Scientific Computing Laboratory.

Tables of  $E_r$  for  $J$  up to 40 and values of  $\kappa = 0, 0.1, 0.2, 0.3, \dots, 1.0$  are given by G. Erlandsson, *Archiv för Fysik*, to be published.

$J_{K_1K_2}$ $J_r$ $K$	$0_0,0$ $0_0$	$1_1,0$ $1_1$	$1_1,1$ $1_0$	$1_0,1$ $1_{-1}$	$2_2,0$ $2_2$	$2_2,1$ $2_1$	$2_1,1$ $2_0$	$2_1,2$ $2_{-1}$	$2_0,2$ $2_{-2}$	$3_3,0$ $3_3$	$3_3,1$ $3_2$	$3_2,1$ $3_1$	$3_2,2$ $3_0$
.00	0	1.000000	0.000000	-1.000000	3.4641016	3.000000	0.000000	-3.000000	-3.4641016	7.8989794	7.7459666	1.8989794	0.000000
.01	0	1.010000	0.000000	-0.990000	3.4841593	3.010000	0.040000	-2.990000	-3.4441593	7.9245871	7.7659925	1.9735759	0.040000
.02	0	1.020000	0.000000	-0.980000	3.5043325	3.020000	0.080000	-2.980000	-3.4243325	7.9504020	7.7860699	2.0483734	0.080000
.03	0	1.030000	0.000000	-0.970000	3.5246211	3.030000	0.120000	-2.970000	-3.4046211	7.9764272	7.8061990	2.1233690	0.120000
.04	0	1.040000	0.000000	-0.960000	3.5450252	3.040000	0.160000	-2.960000	-3.3850252	8.0026659	7.8263797	2.1985597	0.160000
.05	0	1.050000	0.000000	-0.950000	3.5655446	3.050000	0.200000	-2.950000	-3.3655446	8.0291212	7.8466121	2.2739426	0.200000
.06	0	1.060000	0.000000	-0.940000	3.5861794	3.060000	0.240000	-2.940000	-3.3461794	8.0557964	7.8668961	2.3495148	0.240000
.07	0	1.070000	0.000000	-0.930000	3.6069294	3.070000	0.280000	-2.930000	-3.3269294	8.0826947	7.8872317	2.4252733	0.280000
.08	0	1.080000	0.000000	-0.920000	3.6277946	3.080000	0.320000	-2.920000	-3.3077946	8.1098195	7.9076189	2.5012155	0.320000
.09	0	1.090000	0.000000	-0.910000	3.6487749	3.090000	0.360000	-2.910000	-3.2887749	8.1371739	7.9280578	2.5773384	0.360000
.10	0	1.100000	0.000000	-0.900000	3.6698703	3.100000	0.400000	-2.900000	-3.2698703	8.1647615	7.9485482	2.6536394	0.400000
.11	0	1.110000	0.000000	-0.890000	3.6910805	3.110000	0.440000	-2.890000	-3.2510805	8.1925854	7.9690902	2.7301158	0.440000
.12	0	1.120000	0.000000	-0.880000	3.7124055	3.120000	0.480000	-2.880000	-3.2324055	8.2206493	7.9896838	2.8067648	0.480000
.13	0	1.130000	0.000000	-0.870000	3.7338451	3.130000	0.520000	-2.870000	-3.2138451	8.2489564	8.0103290	2.8835838	0.520000
.14	0	1.140000	0.000000	-0.860000	3.7553992	3.140000	0.560000	-2.860000	-3.1953992	8.2775102	8.0310257	2.9605703	0.560000
.15	0	1.150000	0.000000	-0.850000	3.7770677	3.150000	0.600000	-2.850000	-3.1770677	8.3063142	8.0517739	3.0377216	0.600000
.16	0	1.160000	0.000000	-0.840000	3.7988503	3.160000	0.640000	-2.840000	-3.1588503	8.3353720	8.0725737	3.1150352	0.640000
.17	0	1.170000	0.000000	-0.830000	3.8207470	3.170000	0.680000	-2.830000	-3.1407470	8.3646871	8.0934250	3.1925087	0.680000
.18	0	1.180000	0.000000	-0.820000	3.8427575	3.180000	0.720000	-2.820000	-3.1227575	8.3942630	8.1143278	3.2701396	0.720000
.19	0	1.190000	0.000000	-0.810000	3.8648816	3.190000	0.760000	-2.810000	-3.1048816	8.4241032	8.1352820	3.3479255	0.760000
.20	0	1.200000	0.000000	-0.800000	3.8871191	3.200000	0.800000	-2.800000	-3.0871191	8.4542114	8.1562877	3.4258639	0.800000
.21	0	1.210000	0.000000	-0.790000	3.9094698	3.210000	0.840000	-2.790000	-3.0694698	8.4845913	8.1773449	3.5039526	0.840000
.22	0	1.220000	0.000000	-0.780000	3.9319335	3.220000	0.880000	-2.780000	-3.0519335	8.5152463	8.1984534	3.5821893	0.880000
.23	0	1.230000	0.000000	-0.770000	3.9545099	3.230000	0.920000	-2.770000	-3.0345099	8.5461801	8.2196133	3.6605716	0.920000
.24	0	1.240000	0.000000	-0.760000	3.9771988	3.240000	0.960000	-2.760000	-3.0171988	8.5773964	8.2408246	3.7390973	0.960000
.25	0	1.250000	0.000000	-0.750000	4.0000000	3.250000	1.000000	-2.750000	-3.0000000	8.6088989	8.2620873	3.8177643	1.000000
.26	0	1.260000	0.000000	-0.740000	4.0229130	3.260000	1.040000	-2.740000	-2.9829130	8.6406911	8.2834013	3.8965703	1.040000
.27	0	1.270000	0.000000	-0.730000	4.0459378	3.270000	1.080000	-2.730000	-2.9659378	8.6727768	8.3047665	3.9755133	1.080000
.28	0	1.280000	0.000000	-0.720000	4.0690739	3.280000	1.120000	-2.720000	-2.9490739	8.7051596	8.3261831	4.0545910	1.120000
.29	0	1.290000	0.000000	-0.710000	4.0923211	3.290000	1.160000	-2.710000	-2.9323211	8.7378432	8.3476508	4.1338015	1.160000
.30	0	1.300000	0.000000	-0.700000	4.1156791	3.300000	1.200000	-2.700000	-2.9156791	8.7708313	8.3691698	4.2131427	1.200000
.31	0	1.310000	0.000000	-0.690000	4.1391476	3.310000	1.240000	-2.690000	-2.8991476	8.8041274	8.3907399	4.2926126	1.240000
.32	0	1.320000	0.000000	-0.680000	4.1627262	3.320000	1.280000	-2.680000	-2.8827262	8.8377352	8.4123612	4.3722092	1.280000
.33	0	1.330000	0.000000	-0.670000	4.1864146	3.330000	1.320000	-2.670000	-2.8664146	8.8716584	8.4340337	4.4519307	1.320000
.34	0	1.340000	0.000000	-0.660000	4.2102124	3.340000	1.360000	-2.660000	-2.8502124	8.9059006	8.4557571	4.5317750	1.360000
.35	0	1.350000	0.000000	-0.650000	4.2341194	3.350000	1.400000	-2.650000	-2.8341194	8.9404653	8.4775217	4.6117403	1.400000
.36	0	1.360000	0.000000	-0.640000	4.2581351	3.360000	1.440000	-2.640000	-2.8181351	8.9753562	8.4993572	4.6918248	1.440000
.37	0	1.370000	0.000000	-0.630000	4.2822591	3.370000	1.480000	-2.630000	-2.8022591	9.0105768	8.5212338	4.7720266	1.480000
.38	0	1.380000	0.000000	-0.620000	4.3064912	3.380000	1.520000	-2.620000	-2.7864912	9.0461307	8.5431613	4.8523440	1.520000
.39	0	1.390000	0.000000	-0.610000	4.3308308	3.390000	1.560000	-2.610000	-2.7708308	9.0820212	8.5651396	4.9327752	1.560000
.40	0	1.400000	0.000000	-0.600000	4.3552777	3.400000	1.600000	-2.600000	-2.7552777	9.1182520	8.5871689	5.0133185	1.600000
.41	0	1.410000	0.000000	-0.590000	4.3798314	3.410000	1.640000	-2.590000	-2.7398314	9.1548264	8.6092490	5.0939722	1.640000
.42	0	1.420000	0.000000	-0.580000	4.4044915	3.420000	1.680000	-2.580000	-2.7244915	9.1917477	8.6313798	5.1747345	1.680000
.43	0	1.430000	0.000000	-0.570000	4.4292576	3.430000	1.720000	-2.570000	-2.7092576	9.2290194	8.6535614	5.2556039	1.720000
.44	0	1.440000	0.000000	-0.560000	4.4541292	3.440000	1.760000	-2.560000	-2.6941292	9.2666448	8.6757937	5.3365788	1.760000
.45	0	1.450000	0.000000	-0.550000	4.4791060	3.450000	1.800000	-2.550000	-2.6791060	9.3046269	8.6980766	5.4176575	1.800000
.46	0	1.460000	0.000000	-0.540000	4.5041874	3.460000	1.840000	-2.540000	-2.6641874	9.3429692	8.7204102	5.4988386	1.840000
.47	0	1.470000	0.000000	-0.530000	4.5293732	3.470000	1.880000	-2.530000	-2.6493732	9.3816745	8.7427943	5.5801203	1.880000
.48	0	1.480000	0.000000	-0.520000	4.5546627	3.480000	1.920000	-2.520000	-2.6346627	9.4207461	8.7652290	5.6615014	1.920000
.49	0	1.490000	0.000000	-0.510000	4.5800555	3.490000	1.960000	-2.510000	-2.6200555	9.4601870	8.7877141	5.7429802	1.960000
.50	0	1.500000	0.000000	-0.500000	4.6055512	3.500000	2.000000	-2.500000	-2.6055512	9.5000000	8.8102496	5.8245553	2.000000

$J, K, K_1$ $J, \tau$ $K$	$0_0, 0$ $0_0$		$1_1, 0$ $1_1$	$1_{1,1}$ $1_0$	$1_{0,1}$ $1_{-1}$	$2_2, 0$ $2_2$	$2_2, 1$ $2_1$	$2_{1,1}$ $2_0$	$2_{1,2}$ $2_{-1}$	$2_{0,2}$ $2_{-2}$	$3_3, 0$ $3_3$	$3_{3,1}$ $3_2$	$3_{2,1}$ $3_1$	$3_{2,2}$ $3_0$
	$0_0$	$0_0$	$1_1$	$1_0$	$1_{-1}$	$2_2$	$2_1$	$2_0$	$2_{-1}$	$2_{-2}$	$3_3$	$3_2$	$3_1$	$3_0$
.50	0	0	1.500000	0.000000	-0.500000	4.6055512	3.500000	2.000000	-2.500000	-2.6055512	9.500000	8.8102496	5.8245553	2.000000
.51	0	0	1.510000	0.000000	-0.490000	4.6311494	3.510000	2.040000	-2.490000	-2.5911494	9.5401879	8.8328355	5.9062252	2.040000
.52	0	0	1.520000	0.000000	-0.480000	4.6568494	3.520000	2.080000	-2.480000	-2.5768494	9.5807536	8.8554718	5.9879887	2.080000
.53	0	0	1.530000	0.000000	-0.470000	4.6826509	3.530000	2.120000	-2.470000	-2.5626509	9.6216998	8.8781583	6.0698442	2.120000
.54	0	0	1.540000	0.000000	-0.460000	4.7085534	3.540000	2.160000	-2.460000	-2.5485534	9.6630291	8.9008950	6.1517904	2.160000
.55	0	0	1.550000	0.000000	-0.450000	4.7345563	3.550000	2.200000	-2.450000	-2.5345563	9.7047439	8.9236819	6.2338260	2.200000
.56	0	0	1.560000	0.000000	-0.440000	4.7606592	3.560000	2.240000	-2.440000	-2.5206592	9.7468468	8.9465190	6.3159496	2.240000
.57	0	0	1.570000	0.000000	-0.430000	4.7868616	3.570000	2.280000	-2.430000	-2.5068616	9.7893400	8.9694061	6.3981600	2.280000
.58	0	0	1.580000	0.000000	-0.420000	4.8131630	3.580000	2.320000	-2.420000	-2.4931630	9.8322258	8.9923431	6.4804559	2.320000
.59	0	0	1.590000	0.000000	-0.410000	4.8395628	3.590000	2.360000	-2.410000	-2.4795628	9.8755063	9.0153302	6.5628360	2.360000
.60	0	0	1.600000	0.000000	-0.400000	4.8660605	3.600000	2.400000	-2.400000	-2.4660605	9.9191835	9.0383671	6.6452990	2.400000
.61	0	0	1.610000	0.000000	-0.390000	4.8926557	3.610000	2.440000	-2.390000	-2.4526557	9.9633259	9.0614539	6.7278439	2.440000
.62	0	0	1.620000	0.000000	-0.380000	4.9193477	3.620000	2.480000	-2.380000	-2.4393477	10.0077359	9.0845904	6.8104694	2.480000
.63	0	0	1.630000	0.000000	-0.370000	4.9461361	3.630000	2.520000	-2.370000	-2.4261361	10.0526145	9.1077767	6.8931743	2.520000
.64	0	0	1.640000	0.000000	-0.360000	4.9730204	3.640000	2.560000	-2.3599999	-2.4130204	10.0978968	9.1310126	6.9759574	2.560000
.65	0	0	1.650000	0.000000	-0.350000	5.0000000	3.650000	2.600000	-2.350000	-2.4000000	10.1435844	9.1542981	7.0580178	2.600000
.66	0	0	1.660000	0.000000	-0.340000	5.0270743	3.660000	2.640000	-2.340000	-2.3870743	10.1896786	9.1776332	7.1417541	2.640000
.67	0	0	1.670000	0.000000	-0.330000	5.0542428	3.670000	2.680000	-2.330000	-2.3742428	10.2361806	9.2010177	7.2247654	2.680000
.68	0	0	1.680000	0.000000	-0.320000	5.0815050	3.680000	2.720000	-2.320000	-2.3615050	10.2830915	9.2244516	7.3078506	2.720000
.69	0	0	1.690000	0.000000	-0.310000	5.1088604	3.690000	2.760000	-2.310000	-2.3488604	10.3304123	9.2479349	7.3910085	2.760000
.70	0	0	1.700000	0.000000	-0.300000	5.1363083	3.700000	2.800000	-2.300000	-2.3363083	10.3781438	9.2714674	7.4742383	2.800000
.71	0	0	1.710000	0.000000	-0.290000	5.1638482	3.710000	2.840000	-2.290000	-2.3238482	10.4262868	9.2950492	7.5575387	2.840000
.72	0	0	1.720000	0.000000	-0.280000	5.1914797	3.720000	2.880000	-2.280000	-2.3114797	10.4748419	9.3186800	7.6409090	2.880000
.73	0	0	1.730000	0.000000	-0.270000	5.2192020	3.730000	2.920000	-2.270000	-2.2992020	10.5238094	9.3423600	7.7243480	2.920000
.74	0	0	1.740000	0.000000	-0.260000	5.2470147	3.740000	2.960000	-2.260000	-2.2870147	10.5731898	9.3660890	7.8078548	2.960000
.75	0	0	1.750000	0.000000	-0.250000	5.2749172	3.750000	3.000000	-2.250000	-2.2749172	10.6229833	9.3898669	7.8914284	3.000000
.76	0	0	1.760000	0.000000	-0.240000	5.3029089	3.760000	3.040000	-2.240000	-2.2629089	10.6731898	9.4136936	7.9750679	3.040000
.77	0	0	1.770000	0.000000	-0.230000	5.3309893	3.770000	3.080000	-2.230000	-2.2509893	10.7238094	9.4375692	8.0587724	3.080000
.78	0	0	1.780000	0.000000	-0.220000	5.3591578	3.780000	3.120000	-2.220000	-2.2391578	10.7748419	9.4614935	8.1425409	3.120000
.79	0	0	1.790000	0.000000	-0.210000	5.3874138	3.790000	3.160000	-2.210000	-2.2274138	10.8262868	9.4854664	8.2263727	3.160000
.80	0	0	1.800000	0.000000	-0.200000	5.4157568	3.800000	3.200000	-2.200000	-2.2157568	10.8781438	9.5094879	8.3102667	3.200000
.81	0	0	1.810000	0.000000	-0.190000	5.4441861	3.810000	3.240000	-2.190000	-2.2041861	10.9304123	9.5335579	8.3942222	3.240000
.82	0	0	1.820000	0.000000	-0.180000	5.4727013	3.820000	3.280000	-2.180000	-2.1927013	10.9830915	9.5576764	8.4782382	3.280000
.83	0	0	1.830000	0.000000	-0.170000	5.5013018	3.830000	3.320000	-2.170000	-2.1813018	11.0361806	9.5818432	8.5623140	3.320000
.84	0	0	1.840000	0.000000	-0.160000	5.5299870	3.840000	3.360000	-2.160000	-2.1699870	11.0896786	9.6060582	8.6464488	3.360000
.85	0	0	1.850000	0.000000	-0.150000	5.5587562	3.850000	3.400000	-2.150000	-2.1587562	11.1435844	9.6303215	8.7306416	3.400000
.86	0	0	1.860000	0.000000	-0.140000	5.5876090	3.860000	3.440000	-2.140000	-2.1476090	11.1978968	9.6546329	8.8148918	3.440000
.87	0	0	1.870000	0.000000	-0.130000	5.6165448	3.870000	3.480000	-2.130000	-2.1365448	11.2526145	9.6789923	8.8991986	3.480000
.88	0	0	1.880000	0.000000	-0.120000	5.6455630	3.880000	3.520000	-2.120000	-2.1255630	11.3077359	9.7033997	8.9835611	3.520000
.89	0	0	1.890000	0.000000	-0.110000	5.6746630	3.890000	3.560000	-2.110000	-2.1146630	11.3632595	9.7278550	9.0679787	3.560000
.90	0	0	1.900000	0.000000	-0.100000	5.7038442	3.900000	3.600000	-2.100000	-2.1038442	11.4191835	9.7523581	9.1524505	3.600000
.91	0	0	1.910000	0.000000	-0.090000	5.7331061	3.910000	3.640000	-2.090000	-2.0931061	11.4755063	9.7769089	9.2369759	3.640000
.92	0	0	1.920000	0.000000	-0.080000	5.7624482	3.920000	3.680000	-2.080000	-2.0824482	11.5322258	9.8015073	9.3215542	3.680000
.93	0	0	1.930000	0.000000	-0.070000	5.7918697	3.930000	3.720000	-2.070000	-2.0718697	11.5893400	9.8261534	9.4061846	3.720000
.94	0	0	1.940000	0.000000	-0.060000	5.8213703	3.940000	3.760000	-2.060000	-2.0613703	11.6468468	9.8508468	9.4908664	3.760000
.95	0	0	1.950000	0.000000	-0.050000	5.8509492	3.950000	3.800000	-2.050000	-2.0509492	11.7047439	9.8755877	9.5755990	3.800000
.96	0	0	1.960000	0.000000	-0.040000	5.8806060	3.960000	3.840000	-2.040000	-2.0406060	11.7630291	9.9003759	9.6603816	3.840000
.97	0	0	1.970000	0.000000	-0.030000	5.9103400	3.970000	3.880000	-2.030000	-2.0303400	11.8216998	9.9252113	9.7452137	3.880000
.98	0	0	1.980000	0.000000	-0.020000	5.9401507	3.980000	3.920000	-2.020000	-2.0201507	11.8807536	9.9500938	9.8300945	3.920000
.99	0	0	1.990000	0.000000	-0.010000	5.9700375	3.990000	3.960000	-2.010000	-2.0100375	11.9401879	9.9750234	9.9150235	3.960000
1.00	0	0	2.000000	0.000000	0.000000	6.0000000	4.000000	4.000000	-2.000000	-2.0000000	12.0000000	10.0000000	10.0000000	4.000000



$J_{K_1 K_2}$ $J_r$ $K$	$3_{1,2}$ $3_{-1}$		$3_{1,3}$ $3_{-2}$	$3_{0,3}$ $3_{-3}$	$4_{4,0}$ $4_4$	$4_{4,1}$ $4_3$	$4_{3,1}$ $4_2$	$4_{3,2}$ $4_1$	$4_{2,2}$ $4_0$	$4_{2,3}$ $4_{-1}$	$4_{1,3}$ $4_{-2}$	$4_{1,4}$ $4_{-3}$	$4_{0,4}$ $4_{-4}$
.00	-1.8989794	-1.8989794	-7.745666	-7.8989794	14.4222051	14.3808315	5.2915026	4.3808315	0.0000000	-4.3808315	-5.2915026	-14.3808315	-14.4222051
.01	-1.8245871	-1.8245871	-7.725925	-7.8735759	14.4530813	14.4095726	5.3918427	4.422125	0.1384601	-4.3095726	-5.1918427	-14.3522125	-14.3915415
.02	-1.7504020	-1.7504020	-7.7060699	-7.8483734	14.4841746	14.4384366	5.4928631	4.5231747	0.2769117	-4.2384366	-5.0928631	-14.3237147	-14.3610864
.03	-1.6764272	-1.6764272	-7.6861990	-7.8233690	14.5154893	14.4674245	5.5945632	4.5953374	0.4153464	-4.1674245	-4.9945632	-14.2953374	-14.3308358
.04	-1.6026659	-1.6026659	-7.6663797	-7.7985597	14.5470299	14.4965369	5.6969425	4.6670798	0.5537557	-4.0965369	-4.8969425	-14.2670798	-14.3007857
.05	-1.5291212	-1.5291212	-7.6466121	-7.7739426	14.5788012	14.5257749	5.8000000	4.7389409	0.6921310	-4.0257749	-4.8000000	-14.2389409	-14.2709322
.06	-1.4557964	-1.4557964	-7.6268961	-7.7495148	14.6108079	14.5551391	5.9037345	4.8109200	0.8304638	-3.9551391	-4.7037345	-14.2109200	-14.2421717
.07	-1.3826947	-1.3826947	-7.6072317	-7.7252733	14.6430549	14.5846304	6.0081446	4.8830163	0.9687455	-3.8846304	-4.6081446	-14.1830163	-14.2118005
.08	-1.3098195	-1.3098195	-7.5876189	-7.7012155	14.6755473	14.6142498	6.1132287	4.9552289	1.1069676	-3.8142498	-4.5132287	-14.1552289	-14.1825149
.09	-1.2371739	-1.2371739	-7.5680578	-7.6773384	14.7082904	14.6439980	6.2189848	5.0275570	1.2451212	-3.7439980	-4.4189848	-14.1275570	-14.1534117
.10	-1.1647615	-1.1647615	-7.5485482	-7.6536394	14.7412895	14.6738759	6.3254107	5.1000000	1.3831978	-3.6738759	-4.3254107	-14.1000000	-14.1244874
.11	-1.0925854	-1.0925854	-7.5290902	-7.6301158	14.7745501	14.7038844	6.4325041	5.1725568	1.5211886	-3.6038844	-4.2325041	-14.0725568	-14.0957387
.12	-1.0206493	-1.0206493	-7.5096838	-7.6067648	14.8080780	14.7340243	6.5402621	5.2452267	1.6590846	-3.5340243	-4.1402621	-14.0452267	-14.0671626
.13	-0.9489564	-0.9489564	-7.4903290	-7.5835838	14.8418788	14.7642964	6.6486820	5.3180091	1.7968769	-3.4642964	-4.0486820	-14.0180091	-14.0387558
.14	-0.8775102	-0.8775102	-7.4710257	-7.5605703	14.8759587	14.7947017	6.7577607	5.3909029	1.9345566	-3.3947017	-3.9577607	-13.9909029	-14.0105153
.15	-0.8063142	-0.8063142	-7.4517739	-7.5377216	14.9103238	14.8252410	6.8674947	5.4639075	2.0721145	-3.3252410	-3.8674947	-13.9639075	-13.9824383
.16	-0.7353720	-0.7353720	-7.4325737	-7.5150352	14.9449805	14.8559151	6.9778806	5.5370221	2.2095414	-3.2559151	-3.7778806	-13.9370221	-13.9545219
.17	-0.6646871	-0.6646871	-7.4134250	-7.4925087	14.9799352	14.8867250	7.0889145	5.6102458	2.3468280	-3.1867250	-3.6889145	-13.9102458	-13.9267633
.18	-0.5942630	-0.5942630	-7.3943278	-7.4701396	15.0151947	14.9176715	7.2005925	5.6835780	2.4839650	-3.1176715	-3.6005925	-13.8835780	-13.8991598
.19	-0.5241032	-0.5241032	-7.3752820	-7.4479255	15.0507660	14.9487554	7.3129104	5.7570178	2.6209426	-3.0487554	-3.5129104	-13.8570178	-13.8717086
.20	-0.4542114	-0.4542114	-7.3562877	-7.4258639	15.0866559	14.9799777	7.4258639	5.8305645	2.7577514	-2.9799777	-3.4258639	-13.8305645	-13.8444074
.21	-0.3845913	-0.3845913	-7.3373449	-7.4039526	15.1228720	15.0113391	7.5394485	5.9042173	2.8943815	-2.9113391	-3.3394485	-13.8042173	-13.8172535
.22	-0.3152463	-0.3152463	-7.3184534	-7.3821893	15.1594216	15.0428407	7.6536593	5.9779755	3.0308229	-2.8428407	-3.2536593	-13.7779755	-13.7902446
.23	-0.2461801	-0.2461801	-7.2996133	-7.3605716	15.1963125	15.0744831	7.7684915	6.0518382	3.1670656	-2.7744831	-3.1684915	-13.7518382	-13.7633781
.24	-0.1773964	-0.1773964	-7.2808246	-7.3390973	15.2335526	15.1062674	7.8839401	6.1258047	3.3030993	-2.7062674	-3.0839401	-13.7258047	-13.7366519
.25	-0.1088989	-0.1088989	-7.2620873	-7.3177643	15.2711500	15.1381944	8.0000000	6.1998743	3.4389136	-2.6381944	-3.0000000	-13.6998743	-13.7100637
.26	-0.0406911	-0.0406911	-7.2434013	-7.2965703	15.3091131	15.1702649	8.1166656	6.2740463	3.5744981	-2.5702649	-2.9166656	-13.6740463	-13.6836112
.27	0.0272231	0.0272231	-7.2247665	-7.2755133	15.3474505	15.2024798	8.2339316	6.3483198	3.7098419	-2.5024798	-2.8339316	-13.6483198	-13.6572924
.28	0.0948403	0.0948403	-7.2061831	-7.2545910	15.3861709	15.2348401	8.3517925	6.4226942	3.8449340	-2.4348401	-2.7517925	-13.6226942	-13.6311050
.29	0.1621567	0.1621567	-7.1876508	-7.2338015	15.4252835	15.2673465	8.4702423	6.4971687	3.9797636	-2.3673465	-2.6702423	-13.5971687	-13.6050471
.30	0.2291686	0.2291686	-7.1691698	-7.2131427	15.4647976	15.3000000	8.5892754	6.5717426	4.1143191	-2.3000000	-2.5892754	-13.5717426	-13.5791167
.31	0.2958725	0.2958725	-7.1507399	-7.1926126	15.5047226	15.3328013	8.7088858	6.6464152	4.2485892	-2.2328013	-2.5088858	-13.5464152	-13.5533119
.32	0.3622647	0.3622647	-7.1323612	-7.1722092	15.5450685	15.3657515	8.8290674	6.7211857	4.3825621	-2.1657515	-2.4290674	-13.5211857	-13.5276307
.33	0.4283415	0.4283415	-7.1140337	-7.1519307	15.5858452	15.3988513	8.9498141	6.7960534	4.5162260	-2.0988513	-2.3498141	-13.4960534	-13.5020713
.34	0.4940993	0.4940993	-7.0957571	-7.1317750	15.6270631	15.4321016	9.0711198	6.8710176	4.6495687	-2.0321016	-2.2711198	-13.4710176	-13.4766318
.35	0.5595346	0.5595346	-7.0775317	-7.1117403	15.6687328	15.4655034	9.1929781	6.9460776	4.7825778	-1.9655034	-2.1929781	-13.4460776	-13.4513107
.36	0.6246437	0.6246437	-7.0593572	-7.0918248	15.7108650	15.4990574	9.3153827	7.0212328	4.9152409	-1.8990574	-2.1153827	-13.4212328	-13.4261060
.37	0.6894231	0.6894231	-7.0412338	-7.0720266	15.7534710	15.5327645	9.4383272	7.0944823	5.0475452	-1.8327645	-2.0383272	-13.3964823	-13.4010162
.38	0.7538692	0.7538692	-7.0231613	-7.0523440	15.7965621	15.5666256	9.5618052	7.1718255	5.1794775	-1.7666256	-1.9618052	-13.3718255	-13.3760396
.39	0.8179787	0.8179787	-7.0051396	-7.0327752	15.8401499	15.6006415	9.6858102	7.2472617	5.3110247	-1.7006415	-1.8858102	-13.3472617	-13.3511747
.40	0.8817479	0.8817479	-6.9871689	-7.0133185	15.8842464	15.6348132	9.8103356	7.3227903	5.4421733	-1.6348132	-1.8103356	-13.3227903	-13.3264197
.41	0.9451735	0.9451735	-6.9692490	-6.9939722	15.9288638	15.6691414	9.9353748	7.3984105	5.5729056	-1.5691414	-1.7353748	-13.2984105	-13.3017734
.42	1.0082522	1.0082522	-6.9517398	-6.9747345	15.9740145	15.7036271	10.0609214	7.4741216	5.7032195	-1.5036271	-1.6609214	-13.2741216	-13.2772341
.43	1.0709805	1.0709805	-6.9335614	-6.9560339	16.0197114	15.7382710	10.1869686	7.5499230	5.8330889	-1.4382710	-1.5869686	-13.2499230	-13.2528003
.44	1.1333551	1.1333551	-6.9157937	-6.9365788	16.0659675	15.7730741	10.3133509	7.6258141	5.9625033	-1.3730741	-1.5135099	-13.2258141	-13.2284708
.45	1.1953730	1.1953730	-6.8980766	-6.9176575	16.1127960	15.8080371	10.4405386	7.7017941	6.0914480	-1.3080371	-1.4405386	-13.2017941	-13.2042441
.46	1.2570307	1.2570307	-6.8804102	-6.8988386	16.1602106	15.8431610	10.5680482	7.7786223	6.2199081	-1.2431610	-1.3680482	-13.1778623	-13.1801188
.47	1.3183254	1.3183254	-6.8627943	-6.8801203	16.2082251	15.8784465	10.6960320	7.8540182	6.3478885	-1.1784465	-1.2960320	-13.1540182	-13.1560937
.48	1.3792538	1.3792538	-6.8452290	-6.8615014	16.2568536	15.9138945	10.8244833	7.9302611	6.4753137	-1.1138945	-1.2244833	-13.1302611	-13.1321674
.49	1.4398129	1.4398129	-6.8277141	-6.8429802	16.3061104	15.9495058	10.9533957	8.0065903	6.6022282	-1.0495058	-1.1533957	-13.1065903	-13.1083387
.50	1.5000000	1.5000000	-6.8102496	-6.8245553	16.3560102	15.9852613	11.0827625	8.0830052	6.7285960	-0.9852813	-1.0827625	-13.0830052	-13.0846063

$J, K_1, K_2$	$3_{1,2}$		$3_{1,3}$	$3_{0,3}$	$4_{4,0}$	$4_{4,1}$	$4_{3,1}$	$4_{3,2}$	$4_{2,2}$	$4_{2,3}$	$4_{1,3}$	$4_{1,4}$	$4_{0,4}$
	$3_{-1}$	$3_{-2}$											
.50	1.5000000	-6.8102496	-6.8245553	-6.8245553	16.3560102	15.9852813	11.0827625	8.0830052	6.7285960	-0.9852813	-1.0827625	-13.0830052	-13.0846063
.51	1.5598120	-6.7928355	-6.8062252	-6.8062252	16.4065678	16.0212218	11.2157771	8.1595051	6.8544012	-0.9212218	-1.0125771	-13.0595051	-13.0609691
.52	1.6192463	-6.7754718	-6.7879887	-6.7879887	16.4571783	16.0733281	11.3483332	8.2360895	6.9796274	-0.8573281	-0.9428332	-13.0360895	-13.0374258
.53	1.6783001	-6.7581583	-6.7698442	-6.7698442	16.5077170	16.0936011	11.4735241	8.3127576	7.1042583	-0.7936011	-0.8735241	-13.0127576	-13.0139754
.54	1.7369708	-6.7408950	-6.7517904	-6.7517904	16.5623394	16.1300415	11.6046434	8.3895088	7.2282772	-0.7300415	-0.8046434	-12.9895088	-12.9906166
.55	1.7952560	-6.7236819	-6.7338260	-6.7338260	16.6156811	16.1666501	11.7361847	8.4663426	7.3516672	-0.666501	-0.7361847	-12.9663426	-12.9673484
.56	1.8531531	-6.7065190	-6.7159496	-6.7159496	16.6697581	16.2034278	11.8681416	8.5432583	7.4744116	-0.6034278	-0.6681416	-12.9432583	-12.9441698
.57	1.9106599	-6.6894061	-6.6981600	-6.6981600	16.7245864	16.2403754	12.0005079	8.6202553	7.5964931	-0.5403754	-0.6005079	-12.9202553	-12.9210796
.58	1.9677741	-6.6723431	-6.6804559	-6.6804559	16.7801821	16.2774936	12.1332771	8.6973330	7.7178946	-0.4774936	-0.5332771	-12.8973330	-12.8980768
.59	2.0244936	-6.6553302	-6.6628360	-6.6628360	16.8365616	16.3147833	12.2664432	8.7744907	7.8385988	-0.4147833	-0.4664432	-12.8744907	-12.8751605
.60	2.0808164	-6.6383671	-6.6452990	-6.6452990	16.8937412	16.3522452	12.4000000	8.8517279	7.9585883	-0.3522452	-0.4000000	-12.8517279	-12.8523296
.61	2.1367404	-6.6214539	-6.6278439	-6.6278439	16.9517374	16.3898800	12.5339412	8.9290440	8.0778457	-0.2898800	-0.3339412	-12.8290440	-12.8295832
.62	2.1922640	-6.6045904	-6.6104694	-6.6104694	17.0105666	16.4276887	12.6682609	9.0064384	8.1963536	-0.2276887	-0.2682609	-12.8064384	-12.8069203
.63	2.2473854	-6.5877767	-6.5931743	-6.5931743	17.0702455	16.4656719	12.8029531	9.0839105	8.3140944	-0.1656719	-0.2029531	-12.7839105	-12.7843400
.64	2.3021031	-6.5710126	-6.5759574	-6.5759574	17.1307904	16.5038304	12.9380119	9.1614597	8.4310509	-0.1038304	-0.1380119	-12.7614597	-12.7618414
.65	2.3564155	-6.5542981	-6.5588178	-6.5588178	17.1922180	16.5421649	13.0734313	9.2390854	8.5472056	-0.0421649	-0.0734313	-12.7390854	-12.7394236
.66	2.4103213	-6.5376332	-6.5417541	-6.5417541	17.2545444	16.5806763	13.2092057	9.3167871	8.6625413	0.0192336	-0.0092057	-12.7167871	-12.7170858
.67	2.4638193	-6.5210177	-6.5247654	-6.5247654	17.3177860	16.6193651	13.3453291	9.3945642	8.7770410	0.0805348	0.0546708	-12.6945642	-12.6948271
.68	2.5169084	-6.5044516	-6.5078506	-6.5078506	17.3819590	16.6582322	13.4817961	9.4724161	8.8906876	0.1417677	0.1182038	-12.6724161	-12.6726466
.69	2.5695876	-6.4879349	-6.4910085	-6.4910085	17.4470791	16.6972783	13.6186010	9.5503423	9.0034644	0.2027216	0.1813989	-12.6503423	-12.6505436
.70	2.6218561	-6.4714674	-6.4742383	-6.4742383	17.5131622	16.7365041	13.7557383	9.6283421	9.1153551	0.2634958	0.2442616	-12.6283421	-12.6285173
.71	2.6737131	-6.4550492	-6.4575387	-6.4575387	17.5802235	16.7759475	13.8932024	9.7064151	9.2263433	0.3240897	0.3067975	-12.6064151	-12.6065668
.72	2.7251580	-6.4386800	-6.4409090	-6.4409090	17.6482782	16.8154975	14.0309882	9.7845607	9.3364132	0.3845024	0.3690117	-12.5845607	-12.5846915
.73	2.7761905	-6.4223600	-6.4243480	-6.4243480	17.7173411	16.8552666	14.1690901	9.8627784	9.4455494	0.4447333	0.4309098	-12.5627784	-12.5628905
.74	2.8268101	-6.4060890	-6.4078548	-6.4078548	17.7874264	16.8952181	14.3075031	9.9410675	9.5537367	0.5047818	0.4924968	-12.5410675	-12.5411632
.75	2.8770166	-6.3898669	-6.3914284	-6.3914284	17.8585480	16.9353527	14.4462219	10.0194276	9.6609607	0.5646472	0.5537780	-12.5194276	-12.5195087
.76	2.9268101	-6.3736936	-6.3750679	-6.3750679	17.9307193	16.9756712	14.5852415	10.0978582	9.7672071	0.6243287	0.6147584	-12.4978582	-12.4979265
.77	2.9761905	-6.3575692	-6.3587724	-6.3587724	18.0039531	17.0161741	14.7245569	10.1763586	9.8724626	0.6838258	0.6754430	-12.4763586	-12.4764158
.78	3.0251580	-6.3414935	-6.3425409	-6.3425409	18.0782618	17.0568621	14.8641630	10.2549284	9.9767140	0.7431378	0.7358369	-12.4549284	-12.4549759
.79	3.0737131	-6.3254664	-6.3263727	-6.3263727	18.1536569	17.0977358	15.0040551	10.3333671	10.0799492	0.8022641	0.7959448	-12.4333671	-12.4336062
.80	3.1218561	-6.3094879	-6.3102667	-6.3102667	18.2301493	17.1387959	15.1442284	10.4122740	10.1821566	0.8612040	0.8557715	-12.4122740	-12.4123060
.81	3.1695876	-6.2935579	-6.2942222	-6.2942222	18.3077494	17.1800430	15.2846781	10.4910489	10.2833252	0.9199569	0.9153218	-12.3910489	-12.3910746
.82	3.2169084	-6.2776764	-6.2782382	-6.2782382	18.3864667	17.2214776	15.4253996	10.5698910	10.3834449	0.9785223	0.9746003	-12.3698910	-12.3699116
.83	3.2638193	-6.2618432	-6.2623140	-6.2623140	18.4663098	17.2631005	15.5663883	10.6487999	10.4825063	1.0368994	1.0336116	-12.3487999	-12.3488162
.84	3.3103213	-6.2460582	-6.2464488	-6.2464488	18.5472866	17.3049120	15.7076398	10.7277751	10.5805011	1.0950879	1.0923601	-12.3277751	-12.3277878
.85	3.3564155	-6.2303215	-6.2306416	-6.2306416	18.6294043	17.3469129	15.8491496	10.8068161	10.6774215	1.1530870	1.1508503	-12.3068161	-12.3068258
.86	3.4021031	-6.2146329	-6.2148918	-6.2148918	18.7126689	17.3891037	15.9909133	10.8859224	10.7732608	1.2108962	1.2090866	-12.2859224	-12.2859298
.87	3.4473854	-6.1989923	-6.1991986	-6.1991986	18.7970858	17.4314850	16.1329267	10.9650936	10.8680132	1.2685149	1.2670732	-12.2650936	-12.2650990
.88	3.4922640	-6.1833997	-6.1835611	-6.1835611	18.8826591	17.4740572	16.2751856	11.0483290	10.9616738	1.3259427	1.3248143	-12.2443290	-12.2443329
.89	3.5367404	-6.1678550	-6.1679787	-6.1679787	18.9693924	17.5168209	16.4176858	11.1236283	11.0542386	1.3831790	1.3823141	-12.2236283	-12.2236311
.90	3.5808164	-6.1523581	-6.1524505	-6.1524505	19.0572879	17.5597766	16.5604232	11.2029910	11.1457049	1.4402233	1.4395767	-12.2029910	-12.2029929
.91	3.6244936	-6.1369089	-6.1369759	-6.1369759	19.1463472	17.6029249	16.7033939	11.2824166	11.2360705	1.4970750	1.4966060	-12.1824166	-12.1824178
.92	3.6677741	-6.1215073	-6.1215542	-6.1215542	19.2365707	17.6462662	16.8465940	11.3619046	11.3253345	1.5537337	1.5534059	-12.1619046	-12.1619053
.93	3.7106599	-6.1061534	-6.1061846	-6.1061846	19.3279578	17.6898009	16.990195	11.4414545	11.4134970	1.6101990	1.6099804	-12.1414545	-12.1414549
.94	3.7531531	-6.0908468	-6.0908664	-6.0908664	19.4205070	17.7335297	17.1336666	11.5210659	11.5005590	1.6664702	1.6663333	-12.1210659	-12.1210661
.95	3.7952560	-6.0755877	-6.0755990	-6.0755990	19.5142159	17.7774528	17.275317	11.6007383	11.5865225	1.7225471	1.7224682	-12.1007383	-12.1007384
.96	3.8369708	-6.0603759	-6.0603816	-6.0603816	19.6090809	17.8215709	17.4216110	11.6804713	11.6713905	1.7784290	1.7783889	-12.0804713	-12.0804714
.97	3.8783001	-6.0452113	-6.0452137	-6.0452137	19.7050976	17.8658842	17.5659110	11.7602644	11.7551668	1.8341157	1.8340989	-12.0602644	-12.0602644
.98	3.9192463	-6.0300938	-6.0300945	-6.0300945	19.8022606	17.9103932	17.7103982	11.8401172	11.8378565	1.8896017	1.8896017	-12.0401172	-12.0401172
.99	3.9598120	-6.0150234	-6.0150235	-6.0150235	19.9005638	17.9550983	17.8550989	11.9200292	11.9194653	1.9449016	1.9449016	-12.0200292	-12.0200292
1.00	4.0000000	-6.0000000	-6.0000000	-6.0000000	20.0000000	18.0000000	18.0000000	12.0000000	12.0000000	2.0000000	2.0000000	-12.0000000	-12.0000000







$J, K_1, K_2$ $J, K$	$5_{5,0}$ $5_5$	$5_{4,1}$ $5_4$	$5_{4,2}$ $5_2$	$5_{3,2}$ $5_1$	$5_{3,3}$ $5_0$	$5_{2,3}$ $5_{-1}$	$5_{2,4}$ $5_{-2}$	$5_{1,4}$ $5_{-3}$	$5_{1,5}$ $5_{-4}$	$5_{0,5}$ $5_{-5}$	$6_{6,0}$ $6_6$
.50	25.2533452	17.9440500	15.8166538	13.0774679	6.2760123	5.9070198	-5.8166538	-5.8308132	-21.3509080	-21.3510698	36.196238
.51	25.3118653	18.1206188	15.9334482	13.2885399	6.3978594	6.0511432	-5.7334482	-5.7464052	-21.3216175	-21.3217620	36.262641
.52	25.3712134	18.2964204	16.0505483	13.4911720	6.5194837	6.1941419	-5.6505483	-5.6634854	-21.2924335	-21.2925624	36.329927
.53	25.4314179	18.4774437	16.1679226	13.6973300	6.6408803	6.3360259	-5.5679528	-5.5787480	-21.2633551	-21.2634697	36.398130
.54	25.4925086	18.6576772	16.2856602	13.9029787	6.7620444	6.4766057	-5.4856602	-5.4954874	-21.2343812	-21.2344829	36.467286
.55	25.5545163	18.8391086	16.4036691	14.1080819	6.8829713	6.6164324	-5.4036691	-5.4125982	-21.2055109	-21.2056010	36.537434
.56	25.6174729	19.0217252	16.5219778	14.3126021	7.0036562	6.7550975	-5.3219778	-5.3300750	-21.1767432	-21.1768228	36.608614
.57	25.6814119	19.2055141	16.6405849	14.5165007	7.1240941	6.8926371	-5.2405849	-5.2479126	-21.1480771	-21.1481473	36.680870
.58	25.7463678	19.3904616	16.7594890	14.7197382	7.2442803	7.0291118	-5.1594890	-5.1661060	-21.1195118	-21.1195734	36.754248
.59	25.8123765	19.5765538	16.8786884	14.9222736	7.3642099	7.1645465	-5.0786884	-5.0846501	-21.0910463	-21.0911003	36.828795
.60	25.8794753	19.7637763	16.9981816	15.1240649	7.4838781	7.2989505	-4.9981816	-5.0035402	-21.0626797	-21.0627268	36.904563
.61	25.9477029	19.9523147	17.1179671	15.3250687	7.6032798	7.4323374	-4.9179671	-4.9227716	-21.0344110	-21.0344521	36.981607
.62	26.0170992	20.1415539	17.2380433	15.5252404	7.7224103	7.5647212	-4.8380433	-4.8423397	-21.0062395	-21.0062752	37.059982
.63	26.0877057	20.3320787	17.3584085	15.7245342	7.8412647	7.6961163	-4.7584085	-4.7622400	-20.9761641	-20.9761950	37.139751
.64	26.1595652	20.5236736	17.4790613	15.9229029	7.9598379	7.8265371	-4.6790613	-4.6824681	-20.9501842	-20.9502108	37.220978
.65	26.2327217	20.7163231	17.6000000	16.1202982	8.0781252	7.9559984	-4.6000000	-4.6030200	-20.9222987	-20.9223216	37.303729
.66	26.3072209	20.9100113	17.7212229	16.3166703	8.1961215	8.0845152	-4.5212229	-4.5238913	-20.8945069	-20.8945265	37.388078
.67	26.3831097	21.1047221	17.8427285	16.5119683	8.3138219	8.2121025	-4.4427285	-4.4450781	-20.8668080	-20.8668247	37.474101
.68	26.4604363	21.3004396	17.9645152	16.7081490	8.4312216	8.3387756	-4.3645152	-4.3665764	-20.8392011	-20.8392152	37.561878
.69	26.5392502	21.4971474	18.0865812	16.8991323	8.5483155	8.4645498	-4.2865812	-4.2883825	-20.8116854	-20.8116973	37.651494
.70	26.6196019	21.6948293	18.2089250	17.0908906	8.6650986	8.5894407	-4.2089250	-4.2104925	-20.7842601	-20.7842701	37.743039
.71	26.7015435	21.8934690	18.3315448	17.2813594	8.7815662	8.7134637	-4.1315448	-4.1329030	-20.7569244	-20.7569328	37.836608
.72	26.7851276	22.0930501	18.4544391	17.4704826	8.8977132	8.8366344	-4.0544391	-4.0556102	-20.7296777	-20.7296846	37.932300
.73	26.8704080	22.2935563	18.5776061	17.6582027	9.0135346	8.9589683	-3.9776061	-3.9786108	-20.7025247	-20.7025247	38.030221
.74	26.9574393	22.4949712	18.7010441	17.8444620	9.1290256	9.0804810	-3.9010441	-3.9019014	-20.6754476	-20.6754523	38.130481
.75	27.0462767	22.6972787	18.8247516	18.0292020	9.2441812	9.2011880	-3.8247516	-3.8254787	-20.6484629	-20.6484667	38.233196
.76	27.1369758	22.9004623	18.9487268	18.2123637	9.3589964	9.3211047	-3.7487268	-3.7493396	-20.6215671	-20.6215671	38.338486
.77	27.2295926	23.1045061	19.0729679	18.3938882	9.4734665	9.4402466	-3.6734665	-3.6734808	-20.5947527	-20.5947527	38.446478
.78	27.3241830	23.3093939	19.1974734	18.5737164	9.5875864	9.5586289	-3.5974734	-3.5978994	-20.5680229	-20.5680229	38.557304
.79	27.4208028	23.5151098	19.3222414	18.7517895	9.7013513	9.6762670	-3.5222414	-3.5225924	-20.5413753	-20.5413768	38.671100
.80	27.5195076	23.7216380	19.4472704	18.9280493	9.8147563	9.7931758	-3.4472704	-3.4475569	-20.5148127	-20.5148139	38.788007
.81	27.6203519	23.9289629	19.5725585	19.1024382	9.9277965	9.9093704	-3.3725585	-3.3727901	-20.4883325	-20.4883334	38.908170
.82	27.7233894	24.1370689	19.6981041	19.2748998	10.0404672	10.0248856	-3.2981041	-3.2982893	-20.4619339	-20.4619346	39.031738
.83	27.8286726	24.3459407	19.8239055	19.4453790	10.1527634	10.1396760	-3.2239055	-3.2240517	-20.4356163	-20.4356168	39.158863
.84	27.9362523	24.5555631	19.9499610	19.6138224	10.2646805	10.2538162	-3.1499610	-3.1500748	-20.4093790	-20.4093794	39.289698
.85	28.0461772	24.7659211	20.0762688	19.7801787	10.3762136	10.3673006	-3.0762688	-3.0763560	-20.3832214	-20.3832217	39.424399
.86	28.1584940	24.9769998	20.2028272	19.9443989	10.4873580	10.4601432	-3.0028272	-3.0028929	-20.3571429	-20.3571430	39.563119
.87	28.2732464	25.1887848	20.3296345	20.1064365	10.5981089	10.5923580	-2.9296345	-2.9296830	-20.3311427	-20.3311426	39.706012
.88	28.3904755	25.4012615	20.4566890	20.2662484	10.7084618	10.7039588	-2.8566890	-2.8567239	-20.3052203	-20.3052204	39.853228
.89	28.5102189	25.6144158	20.5839890	20.4237945	10.8184120	10.8149592	-2.7839890	-2.7840135	-20.2793750	-20.2793751	40.004911
.90	28.6325106	25.8282337	20.7115327	20.5790387	10.9279548	10.9253726	-2.7115327	-2.7115493	-20.2536063	-20.2536064	40.161202
.91	28.7573807	26.0427015	20.8393185	20.7319485	11.0370857	11.0352120	-2.6393185	-2.6393293	-20.2279135	-20.2279136	40.322230
.92	28.8848553	26.2578057	20.9673446	20.8824959	11.1458002	11.1444904	-2.5673446	-2.5673513	-20.2022961	-20.2022961	40.483117
.93	29.0149559	26.4735329	21.0956093	21.0306573	11.2540939	11.2532205	-2.4956093	-2.4956132	-20.1767534	-20.1767534	40.648971
.94	29.1476994	26.6898700	21.2241109	21.1764135	11.3619622	11.3614148	-2.4241109	-2.4241130	-20.1512849	-20.1512849	40.814889
.95	29.2830981	26.9068043	21.3528477	21.3197506	11.4694009	11.4690856	-2.3528477	-2.3528487	-20.1258900	-20.1258900	41.015949
.96	29.4211592	27.1243232	21.4818180	21.4606592	11.5764056	11.5762449	-2.2818180	-2.2818184	-20.1005681	-20.1005681	41.202217
.97	29.5618851	27.3428142	21.6110201	21.5991351	11.6829720	11.6829045	-2.2110201	-2.2110202	-20.0753188	-20.0753188	41.391738
.98	29.7052731	27.5610652	21.7404522	21.7351791	11.7890959	11.7890760	-2.1404522	-2.1404522	-20.0501413	-20.0501413	41.590539
.99	29.8513155	27.7802643	21.8701127	21.8687971	11.8947733	11.8947708	-2.0701127	-2.0701127	-20.0250352	-20.0250352	41.792630
1.00	30.0000000	28.0000000	22.0000000	22.0000000	12.0000000	12.0000000	-2.0000000	-2.0000000	-20.0000000	-20.0000000	42.000000

$J_{K_1 K_2}$ $J_r$ $K$	$6_{6,1}$ $6_5$		$6_{5,1}$ $6_4$		$6_{5,2}$ $6_3$		$6_{4,2}$ $6_2$		$6_{4,1}$ $6_1$		$6_{3,3}$ $6_0$		$6_{3,4}$ $6_{-1}$		$6_{2,4}$ $6_{-2}$		$6_{2,5}$ $6_{-3}$		$6_{1,5}$ $6_{-4}$		$6_{1,6}$ $6_{-5}$		$6_{0,6}$ $6_{-6}$	
.00	33.565539	18.330302	18.228650	7.014366	5.663111	0.000000	-5.663111	-7.014366	-18.228650	-18.330302	-33.565539	-33.567821												
.01	33.609259	18.462197	18.354039	7.251477	5.845584	0.297136	-5.845584	-7.251477	-18.354039	-18.462197	-33.609259	-33.524155												
.02	33.653211	18.595039	18.480014	7.490377	6.026405	0.594232	-6.026405	-7.490377	-18.480014	-18.595039	-33.653211	-33.480727												
.03	33.697396	18.728847	18.605580	7.731060	6.208566	0.891250	-6.208566	-7.731060	-18.605580	-18.728847	-33.697396	-33.437531												
.04	33.741820	18.863644	18.733738	7.973520	6.391061	1.188148	-6.391061	-7.973520	-18.733738	-18.863644	-33.741820	-33.394566												
.05	33.786485	18.999452	18.861495	8.217745	6.573881	1.484888	-6.573881	-8.217745	-18.861495	-18.999452	-33.786485	-33.351827												
.06	33.831394	19.136292	18.989852	8.463726	6.757020	1.781430	-6.757020	-8.463726	-18.989852	-19.136292	-33.831394	-33.309310												
.07	33.876551	19.274188	19.118814	8.711449	6.940470	2.077733	-6.940470	-8.711449	-19.118814	-19.274188	-33.876551	-33.267012												
.08	33.921959	19.413163	19.248385	8.960902	7.124224	2.373758	-7.124224	-8.960902	-19.248385	-19.413163	-33.921959	-33.224930												
.09	33.967623	19.553243	19.378567	9.212068	7.308274	2.669464	-7.308274	-9.212068	-19.378567	-19.553243	-33.967623	-33.183061												
.10	34.013546	19.694451	19.509364	9.464931	7.492612	2.964811	-7.492612	-9.464931	-19.509364	-19.694451	-34.013546	-33.141401												
.11	34.059731	19.836815	19.640780	9.719474	7.677231	3.259758	-7.677231	-9.719474	-19.640780	-19.836815	-34.059731	-33.099948												
.12	34.106183	19.980360	19.772819	9.975676	7.862123	3.554264	-7.862123	-9.975676	-19.772819	-19.980360	-34.106183	-33.058698												
.13	34.152905	20.125113	19.905482	10.233517	8.047279	3.848288	-8.047279	-10.233517	-19.905482	-20.125113	-34.152905	-33.017649												
.14	34.199901	20.271102	20.038774	10.492974	8.232693	4.141790	-8.232693	-10.492974	-20.038774	-20.271102	-34.199901	-32.976797												
.15	34.247176	20.418355	20.172698	10.754026	8.418355	4.434727	-8.418355	-10.754026	-20.172698	-20.418355	-34.247176	-32.936140												
.16	34.294734	20.566902	20.307258	11.016647	8.604257	4.727057	-8.604257	-11.016647	-20.307258	-20.566902	-34.294734	-32.895675												
.17	34.342579	20.716772	20.442455	11.280812	8.790392	5.018739	-8.790392	-11.280812	-20.442455	-20.716772	-34.342579	-32.855400												
.18	34.390715	20.867994	20.578293	11.546494	8.976750	5.309730	-8.976750	-11.546494	-20.578293	-20.867994	-34.390715	-32.815312												
.19	34.439146	21.020601	20.714776	11.813666	9.163324	5.599987	-9.163324	-11.813666	-20.714776	-21.020601	-34.439146	-32.775408												
.20	34.487879	21.174624	20.851905	12.082300	9.350104	5.889468	-9.350104	-12.082300	-20.851905	-21.174624	-34.487879	-32.735269												
.21	34.536916	21.330094	20.989684	12.352365	9.537083	6.178130	-9.537083	-12.352365	-20.989684	-21.330094	-34.536916	-32.695764												
.22	34.586262	21.487044	21.128116	12.623832	9.724251	6.465929	-9.724251	-12.623832	-21.128116	-21.487044	-34.586262	-32.656433												
.23	34.635924	21.645508	21.267202	12.896669	9.911599	6.752821	-9.911599	-12.896669	-21.267202	-21.645508	-34.635924	-32.617274												
.24	34.685904	21.805519	21.408947	13.170846	10.099119	7.038764	-10.099119	-13.170846	-21.408947	-21.805519	-34.685904	-32.578286												
.25	34.736210	21.967110	21.547351	13.446327	10.286802	7.323712	-10.286802	-13.446327	-21.547351	-21.967110	-34.736210	-32.539466												
.26	34.786844	22.130317	21.688419	13.723082	10.474638	7.607623	-10.474638	-13.723082	-21.688419	-22.130317	-34.786844	-32.501047												
.27	34.837814	22.295175	21.830151	14.001075	10.662618	7.890452	-10.662618	-14.001075	-21.830151	-22.295175	-34.837814	-32.462536												
.28	34.889124	22.461717	21.972550	14.280272	10.850733	8.172155	-10.850733	-14.280272	-21.972550	-22.461717	-34.889124	-32.424188												
.29	34.940780	22.629980	22.115619	14.560637	11.038973	8.452688	-11.038973	-14.560637	-22.115619	-22.629980	-34.940780	-32.386003												
.30	34.992787	22.800000	22.259359	14.842135	11.227330	8.732007	-11.227330	-14.842135	-22.259359	-22.800000	-34.992787	-32.347979												
.31	35.045151	22.971810	22.403773	15.124729	11.415793	9.010068	-11.415793	-15.124729	-22.403773	-22.971810	-35.045151	-32.310113												
.32	35.097878	23.145448	22.548862	15.408382	11.604352	9.286828	-11.604352	-15.408382	-22.548862	-23.145448	-35.097878	-32.272403												
.33	35.150974	23.320949	22.694628	15.693058	11.792999	9.562244	-11.792999	-15.693058	-22.694628	-23.320949	-35.150974	-32.234733												
.34	35.204445	23.498348	22.841073	15.978717	11.981722	9.836272	-11.981722	-15.978717	-22.841073	-23.498348	-35.204445	-32.197447												
.35	35.258296	23.677680	22.989198	16.265321	12.170512	10.108870	-12.170512	-16.265321	-22.989198	-23.677680	-35.258296	-32.160196												
.36	35.312536	23.858979	23.136005	16.552831	12.359359	10.379996	-12.359359	-16.552831	-23.136005	-23.858979	-35.312536	-32.123095												
.37	35.367169	24.042281	23.284495	16.841208	12.548252	10.649609	-12.548252	-16.841208	-23.284495	-24.042281	-35.367169	-32.086142												
.38	35.422202	24.227618	23.433669	17.130411	12.737181	10.917668	-12.737181	-17.130411	-23.433669	-24.227618	-35.422202	-32.049335												
.39	35.477643	24.415025	23.583530	17.420400	12.926136	11.184134	-12.926136	-17.420400	-23.583530	-24.415025	-35.477643	-32.012672												
.40	35.533498	24.604532	23.734077	17.711134	13.115106	11.448969	-13.115106	-17.711134	-23.734077	-24.604532	-35.533498	-31.976153												
.41	35.589775	24.796171	23.885311	18.002571	13.304081	11.712134	-13.304081	-18.002571	-23.885311	-24.796171	-35.589775	-31.939775												
.42	35.646479	24.989973	24.037235	18.294668	13.493048	11.973593	-13.493048	-18.294668	-24.037235	-24.989973	-35.646479	-31.903536												
.43	35.703619	25.185966	24.189847	18.587382	13.681999	12.233312	-13.681999	-18.587382	-24.189847	-25.185966	-35.703619	-31.867436												
.44	35.761203	25.384178	24.343150	18.880669	13.870920	12.491257	-13.870920	-18.880669	-24.343150	-25.384178	-35.761203	-31.831473												
.45	35.819237	25.584636	24.497143	19.174485	14.059802	12.747395	-14.059802	-19.174485	-24.497143	-25.584636	-35.819237	-31.795645												
.46	35.877729	25.787364	24.651827	19.468785	14.248633	13.001697	-14.248633	-19.468785	-24.651827	-25.787364	-35.877729	-31.759952												
.47	35.936688	25.992386	24.807202	19.763522	14.437401	13.254134	-14.437401	-19.763522	-24.807202	-25.992386	-35.936688	-31.724390												
.48	35.996122	26.199723	24.963269	20.058648	14.626096	13.504680	-14.626096	-20.058648	-24.963269	-26.199723	-35.996122	-31.688960												
.49	36.056038	26.409394	25.120027	20.354116	14.814704	13.753309	-14.814704	-20.354116	-25.120027	-26.409394	-36.056038	-31.653660												
.50	36.116446	26.621416	25.277476	20.649876	15.003214	14.000000	-15.003214	-20.649876	-25.277476	-26.621416	-36.116446	-31.618489												



$J, K_1, K_2$	$6_{6,1}$		$6_{5,1}$		$6_{5,2}$		$6_{4,2}$		$6_{4,3}$		$6_{3,3}$		$6_{3,4}$		$6_{2,4}$		$6_{2,5}$		$6_{1,5}$		$6_{1,6}$		$6_{0,6}$	
	$J$	$K$	$6_5$		$6_3$		$6_2$		$6_1$		$6_0$		$6_{-1}$		$6_{-2}$		$6_{-3}$		$6_{-4}$		$6_{-5}$		$6_{-6}$	
.50	36.116436	26.621416	25.277476	20.649876	15.003214	14.000000	2.840997	2.772374	-12.619661	-12.621416	-31.618473	-31.618473	-31.618473	-31.618473	-31.618473	-31.618473	-31.618473	-31.618473	-31.618473	-31.618473	-31.618473	-31.618473	-31.618473	-31.618473
.51	36.177353	26.835806	25.435617	20.945878	15.191615	14.244731	2.997813	2.934924	-12.518969	-12.520538	-31.583431	-31.583431	-31.583431	-31.583431	-31.583431	-31.583431	-31.583431	-31.583431	-31.583431	-31.583431	-31.583431	-31.583431	-31.583431	-31.583431
.52	36.238769	27.052577	25.594449	21.242069	15.379894	14.487486	3.154065	3.09529	-12.418664	-12.420063	-31.548515	-31.548515	-31.548515	-31.548515	-31.548515	-31.548515	-31.548515	-31.548515	-31.548515	-31.548515	-31.548515	-31.548515	-31.548515	-31.548515
.53	36.300703	27.271740	25.753972	21.533396	15.568038	14.728247	3.309750	3.257206	-12.318742	-12.319988	-31.513733	-31.513733	-31.513733	-31.513733	-31.513733	-31.513733	-31.513733	-31.513733	-31.513733	-31.513733	-31.513733	-31.513733	-31.513733	-31.513733
.54	36.363163	27.493302	25.914185	21.834805	15.756036	14.967003	3.464868	3.416971	-12.219200	-12.220306	-31.479054	-31.479054	-31.479054	-31.479054	-31.479054	-31.479054	-31.479054	-31.479054	-31.479054	-31.479054	-31.479054	-31.479054	-31.479054	-31.479054
.55	36.426159	27.717272	26.075089	22.131238	15.943875	15.203742	3.619419	3.575842	-12.120035	-12.121015	-31.444515	-31.444515	-31.444515	-31.444515	-31.444515	-31.444515	-31.444515	-31.444515	-31.444515	-31.444515	-31.444515	-31.444515	-31.444515	-31.444515
.56	36.489700	27.943652	26.236680	22.427638	16.131542	15.438456	3.773401	3.733835	-12.021243	-12.022109	-31.410088	-31.410088	-31.410088	-31.410088	-31.410088	-31.410088	-31.410088	-31.410088	-31.410088	-31.410088	-31.410088	-31.410088	-31.410088	-31.410088
.57	36.553796	28.172445	26.398960	22.723943	16.319024	15.671139	3.926816	3.890967	-11.922821	-11.923585	-31.375781	-31.375781	-31.375781	-31.375781	-31.375781	-31.375781	-31.375781	-31.375781	-31.375781	-31.375781	-31.375781	-31.375781	-31.375781	-31.375781
.58	36.618457	28.403649	26.561927	23.020093	16.506309	15.901788	4.079661	4.047251	-11.824766	-11.825438	-31.341593	-31.341593	-31.341593	-31.341593	-31.341593	-31.341593	-31.341593	-31.341593	-31.341593	-31.341593	-31.341593	-31.341593	-31.341593	-31.341593
.59	36.683693	28.637262	26.725580	23.316021	16.693382	16.130402	4.231938	4.202705	-11.727075	-11.727664	-31.307519	-31.307519	-31.307519	-31.307519	-31.307519	-31.307519	-31.307519	-31.307519	-31.307519	-31.307519	-31.307519	-31.307519	-31.307519	-31.307519
.60	36.749514	28.873277	26.889918	23.611662	16.880231	16.356982	4.383646	4.357342	-11.629745	-11.630260	-31.273565	-31.273565	-31.273565	-31.273565	-31.273565	-31.273565	-31.273565	-31.273565	-31.273565	-31.273565	-31.273565	-31.273565	-31.273565	-31.273565
.61	36.815930	29.111686	27.054940	23.906945	17.066842	16.581534	4.534786	4.511177	-11.532773	-11.533221	-31.239727	-31.239727	-31.239727	-31.239727	-31.239727	-31.239727	-31.239727	-31.239727	-31.239727	-31.239727	-31.239727	-31.239727	-31.239727	-31.239727
.62	36.882952	29.352479	27.220645	24.201798	17.253202	16.804064	4.683358	4.664225	-11.436154	-11.436544	-31.206003	-31.206003	-31.206003	-31.206003	-31.206003	-31.206003	-31.206003	-31.206003	-31.206003	-31.206003	-31.206003	-31.206003	-31.206003	-31.206003
.63	36.950590	29.595643	27.387031	24.496145	17.439297	17.024582	4.835362	4.816497	-11.339887	-11.340225	-31.172393	-31.172393	-31.172393	-31.172393	-31.172393	-31.172393	-31.172393	-31.172393	-31.172393	-31.172393	-31.172393	-31.172393	-31.172393	-31.172393
.64	37.018856	29.841162	27.554096	24.789909	17.625113	17.243098	4.984798	4.968009	-11.243969	-11.244260	-31.138896	-31.138896	-31.138896	-31.138896	-31.138896	-31.138896	-31.138896	-31.138896	-31.138896	-31.138896	-31.138896	-31.138896	-31.138896	-31.138896
.65	37.087760	30.089019	27.721838	25.083006	17.810635	17.459626	5.133668	5.118772	-11.148396	-11.148646	-31.105508	-31.105508	-31.105508	-31.105508	-31.105508	-31.105508	-31.105508	-31.105508	-31.105508	-31.105508	-31.105508	-31.105508	-31.105508	-31.105508
.66	37.157315	30.339196	27.890257	25.375353	17.995850	17.674183	5.281972	5.268799	-11.053166	-11.053379	-31.072230	-31.072230	-31.072230	-31.072230	-31.072230	-31.072230	-31.072230	-31.072230	-31.072230	-31.072230	-31.072230	-31.072230	-31.072230	-31.072230
.67	37.227530	30.591669	28.059350	25.668588	18.180744	17.886787	5.429711	5.418102	-10.958274	-10.958457	-31.039062	-31.039062	-31.039062	-31.039062	-31.039062	-31.039062	-31.039062	-31.039062	-31.039062	-31.039062	-31.039062	-31.039062	-31.039062	-31.039062
.68	37.298419	30.846416	28.229115	25.957430	18.365301	18.097458	5.576886	5.566694	-10.863720	-10.863875	-30.996002	-30.996002	-30.996002	-30.996002	-30.996002	-30.996002	-30.996002	-30.996002	-30.996002	-30.996002	-30.996002	-30.996002	-30.996002	-30.996002
.69	37.369992	31.103411	28.399550	26.246970	18.549507	18.306218	5.723498	5.714585	-10.769499	-10.769630	-30.973049	-30.973049	-30.973049	-30.973049	-30.973049	-30.973049	-30.973049	-30.973049	-30.973049	-30.973049	-30.973049	-30.973049	-30.973049	-30.973049
.70	37.442262	31.362628	28.570653	26.535377	18.733347	18.513091	5.869549	5.861786	-10.675610	-10.675719	-30.940203	-30.940203	-30.940203	-30.940203	-30.940203	-30.940203	-30.940203	-30.940203	-30.940203	-30.940203	-30.940203	-30.940203	-30.940203	-30.940203
.71	37.515241	31.624037	28.742421	26.822544	18.916806	18.718102	6.015039	6.008309	-10.582048	-10.582140	-30.907462	-30.907462	-30.907462	-30.907462	-30.907462	-30.907462	-30.907462	-30.907462	-30.907462	-30.907462	-30.907462	-30.907462	-30.907462	-30.907462
.72	37.588941	31.887608	28.914853	27.108360	19.099870	18.921279	6.159971	6.154164	-10.488812	-10.488886	-30.874825	-30.874825	-30.874825	-30.874825	-30.874825	-30.874825	-30.874825	-30.874825	-30.874825	-30.874825	-30.874825	-30.874825	-30.874825	-30.874825
.73	37.663376	32.153311	29.087945	27.392709	19.282522	19.122650	6.304345	6.299360	-10.395898	-10.395961	-30.842291	-30.842291	-30.842291	-30.842291	-30.842291	-30.842291	-30.842291	-30.842291	-30.842291	-30.842291	-30.842291	-30.842291	-30.842291	-30.842291
.74	37.738556	32.421112	29.261696	27.675471	19.464748	19.322244	6.448164	6.443908	-10.303305	-10.303356	-30.809860	-30.809860	-30.809860	-30.809860	-30.809860	-30.809860	-30.809860	-30.809860	-30.809860	-30.809860	-30.809860	-30.809860	-30.809860	-30.809860
.75																								



$J_{K_1K_2}$ $J_r$ $K$	$T_{7,0}$ $T_7$	$T_{7,1}$ $T_6$	$T_{6,1}$ $T_5$	$T_{6,2}$ $T_4$	$T_{5,2}$ $T_3$	$T_{5,3}$ $T_2$	$T_{4,3}$ $T_1$	$T_{4,4}$ $T_0$	$T_{3,4}$ $T_{-1}$	$T_{3,5}$ $T_{-2}$	$T_{2,5}$ $T_{-3}$	$T_{2,6}$ $T_{-4}$
.00	46.151161	46.150665	28.027676	28.000000	13.416079	12.888603	3.539564	0.000000	-3.539564	-12.888603	-13.416079	-28.000000
.01	46.202045	46.201501	28.178025	28.148142	13.676825	13.118324	3.920105	0.264486	-3.160624	-12.659730	-13.157583	-27.852629
.02	46.253206	46.252609	28.329312	28.297063	13.939860	13.348888	4.302184	0.528956	-2.783346	-12.431708	-12.901296	-27.706020
.03	46.304646	46.303991	28.481557	28.446774	14.205225	13.580292	4.685739	0.793392	-2.407792	-12.204541	-12.647180	-27.560166
.04	46.356370	46.355653	28.634779	28.597281	14.472956	13.812531	5.070705	1.057776	-2.034021	-11.978233	-12.395193	-27.415057
.05	46.408383	46.407598	28.788999	28.748594	14.743092	14.045600	5.457018	1.327091	-1.662091	-11.752785	-12.145295	-27.270686
.06	46.460691	46.459831	28.944237	28.900723	15.015671	14.279493	5.844613	1.586321	-1.292060	-11.528201	-11.897446	-27.127045
.07	46.513297	46.512356	29.100515	29.053675	15.290728	14.514205	6.233424	1.850448	-0.923983	-11.304484	-11.651607	-26.984124
.08	46.566207	46.565178	29.257857	29.207460	15.568298	14.749730	6.623386	2.114556	-0.557916	-11.081634	-11.407738	-26.841917
.09	46.619426	46.618301	29.416285	29.362088	15.848414	14.986063	7.014432	2.378326	-0.193911	-10.859654	-11.165798	-26.700414
.10	46.672959	46.671731	29.575824	29.517566	16.131110	15.223196	7.406495	2.642043	0.167980	-10.638546	-10.925750	-26.559609
.11	46.726813	46.725471	29.736500	29.673905	16.416415	15.461123	7.799509	2.905588	0.527710	-10.418311	-10.687555	-26.419494
.12	46.780993	46.779528	29.898338	29.831114	16.704358	15.699837	8.193406	3.168946	0.885230	-10.198949	-10.451175	-26.280061
.13	46.835504	46.833906	30.061367	29.989201	16.994365	15.939330	8.588118	3.432100	1.240495	-9.980463	-10.216572	-26.141301
.14	46.890354	46.888610	30.225614	30.148177	17.288263	16.179595	8.983577	3.695031	1.593462	-9.762851	-9.983710	-26.003209
.15	46.945548	46.943646	30.391108	30.308051	17.584272	16.420624	9.379714	3.957724	1.944091	-9.546115	-9.752553	-25.865776
.16	47.001092	46.999019	30.557881	30.468833	17.883014	16.662408	9.776461	4.220162	2.292345	-9.330254	-9.523066	-25.728996
.17	47.056995	47.054736	30.725983	30.630531	18.184506	16.904940	10.173748	4.482329	2.638186	-9.115269	-9.295213	-25.592860
.18	47.113262	47.110801	30.895398	30.793155	18.488763	17.148209	10.571507	4.744206	2.981584	-8.901159	-9.068960	-25.457362
.19	47.169901	47.167221	31.066190	30.956715	18.795797	17.392207	10.969665	5.005779	3.322507	-8.687923	-8.844275	-25.322494
.20	47.226920	47.224003	31.238404	31.121220	19.105618	17.636924	11.368154	5.267030	3.660930	-8.475561	-8.621125	-25.188251
.21	47.284326	47.281151	31.412066	31.286681	19.418231	17.882350	11.766902	5.527943	3.996828	-8.264071	-8.399478	-25.054624
.22	47.342128	47.338673	31.587216	31.453105	19.733640	18.128475	12.165837	5.788502	4.330181	-8.053452	-8.179303	-24.921608
.23	47.400333	47.396576	31.763893	31.620504	20.051846	18.375288	12.564887	6.048690	4.660971	-7.843703	-7.960571	-24.789195
.24	47.458951	47.454865	31.942137	31.788687	20.372845	18.622779	12.963979	6.308492	4.989182	-7.634822	-7.743250	-24.657379
.25	47.517991	47.513549	32.121991	31.958263	20.696630	18.870937	13.363039	6.567890	5.314805	-7.426807	-7.527314	-24.526153
.26	47.577462	47.572634	32.303500	32.128641	21.023193	19.119749	13.761994	6.826870	5.637829	-7.219656	-7.312733	-24.395512
.27	47.637374	47.632127	32.486709	32.300032	21.352520	19.368204	14.160767	7.085416	5.958251	-7.013367	-7.099482	-24.265448
.28	47.697736	47.692037	32.671665	32.472444	21.684594	19.619289	14.559283	7.345111	6.276069	-6.807938	-6.887532	-24.135955
.29	47.758561	47.752371	32.858417	32.645888	22.019397	19.869993	14.957465	7.601140	6.591283	-6.603365	-6.676860	-24.007028
.30	47.819858	47.813136	33.047017	32.820372	22.356906	20.121302	15.355235	7.858288	6.903897	-6.399647	-6.467440	-23.878660
.31	47.881640	47.874342	33.237517	32.995906	22.697094	20.373204	15.752515	8.114939	7.213919	-6.196780	-6.259247	-23.750846
.32	47.943918	47.935996	33.429971	33.172500	23.039932	20.625683	16.149223	8.371078	7.521358	-5.994761	-6.052259	-23.623578
.33	48.006705	47.998108	33.624436	33.350161	23.385388	20.878728	16.545280	8.626691	7.826228	-5.793587	-5.846452	-23.496853
.34	48.070014	48.060685	33.820968	33.528901	23.733427	21.132323	16.940603	8.881762	8.128544	-5.593254	-5.641805	-23.370663
.35	48.133859	48.123738	34.019628	33.708726	24.084008	21.386453	17.335110	9.136276	8.428323	-5.393760	-5.438295	-23.245003
.36	48.198254	48.187276	34.220477	33.889648	24.437093	21.641105	17.728716	9.390219	8.725586	-5.195100	-5.235903	-23.119868
.37	48.263215	48.251308	34.423579	34.071674	24.792635	21.898262	18.121336	9.643578	9.020356	-4.997271	-5.034608	-22.995252
.38	48.328757	48.315844	34.628998	34.254813	25.150589	22.151908	18.512883	9.896336	9.312658	-4.800269	-4.834390	-22.871149
.39	48.394897	48.380894	34.836801	34.439073	25.510904	22.408029	18.903271	10.148481	9.602518	-4.604089	-4.635231	-22.747555
.40	48.461652	48.446470	35.047057	34.624465	25.873529	22.664607	19.292410	10.400000	9.889964	-4.408729	-4.437113	-22.624465
.41	48.529041	48.512582	35.259834	34.810994	26.238409	22.921626	19.680212	10.650877	10.175028	-4.214182	-4.240016	-22.501872
.42	48.597083	48.579240	35.475205	34.998671	26.605486	23.179068	20.066587	10.901100	10.457741	-4.020446	-4.043925	-22.379772
.43	48.665798	48.646458	35.693242	35.187502	26.974703	23.436916	20.451442	11.150657	10.738137	-3.827516	-3.848823	-22.258160
.44	48.735207	48.714245	35.914018	35.377497	27.345998	23.695152	20.834687	11.399533	11.016249	-3.635388	-3.654692	-22.137030
.45	48.805334	48.782615	36.137609	35.568661	27.719307	23.953757	21.216230	11.647717	11.292113	-3.444056	-3.461519	-22.016379
.46	48.876201	48.851580	36.364090	35.761004	28.094564	24.212714	21.595977	11.895196	11.565766	-3.253516	-3.269287	-21.896201
.47	48.947835	48.921152	36.593537	35.954532	28.471703	24.472002	21.973837	12.141958	11.837244	-3.063764	-3.077982	-21.776491
.48	49.020261	48.991346	36.826028	36.149253	28.850654	24.731602	22.349717	12.387992	12.106586	-2.874794	-2.887589	-21.657246
.49	49.093508	49.062174	37.061640	36.345173	29.231345	24.991494	22.723524	12.633285	12.373830	-2.686602	-2.698096	-21.538459
.50	49.167606	49.133651	37.300448	36.542300	29.613703	25.251658	23.095167	12.877827	12.639013	-2.499183	-2.509487	-21.420127

$J_{K_1 K_2}$ $J_r$	$J_{7,0}$ $J_7$	$J_{7,1}$ $J_6$	$J_{6,1}$ $J_5$	$J_{6,2}$ $J_4$	$J_{5,2}$ $J_3$	$J_{5,3}$ $J_2$	$J_{4,3}$ $J_1$	$J_{4,4}$ $J_0$	$J_{3,4}$ $J_{-1}$	$J_{3,5}$ $J_{-2}$	$J_{2,5}$ $J_{-3}$	$J_{2,6}$ $J_{-4}$
$K$												
.50	49.167606	49.133651	37.300448	36.542300	29.633703	25.251658	23.095167	12.87827	12.639013	-2.499183	-2.509487	-21.420127
.51	49.242586	49.205791	37.542530	36.740639	29.977654	25.512073	23.464554	13.121606	12.902176	-2.312531	-2.31751	-21.302245
.52	49.318483	49.278609	37.787962	36.940196	30.383118	25.772717	23.831597	13.364612	13.163357	-2.126643	-2.134875	-21.184609
.53	49.395330	49.352120	38.036817	37.14079	30.770019	26.033509	24.196207	13.60835	13.422595	-1.941513	-1.948847	-21.067815
.54	49.473168	49.426340	38.289168	37.342993	31.158273	26.294607	24.558298	13.848265	13.679929	-1.757135	-1.763654	-20.951258
.55	49.552035	49.501285	38.545089	37.546242	31.547798	26.555807	24.917786	14.088891	13.935397	-1.573504	-1.579286	-20.835133
.56	49.631976	49.576973	38.804644	37.750733	31.938507	26.817146	25.274590	14.328705	14.189038	-1.390616	-1.395731	-20.719438
.57	49.713036	49.653419	39.067903	37.956470	32.330113	27.078602	25.628631	14.567697	14.440689	-1.208466	-1.212978	-20.604168
.58	49.795264	49.730642	39.334927	38.163458	32.723125	27.340149	25.979335	14.808659	14.690989	-1.031018	-1.031018	-20.489318
.59	49.878713	49.808660	39.605777	38.371701	33.116849	27.601762	26.328130	15.043183	14.939374	-0.846355	-0.849839	-20.374885
.60	49.963439	49.887492	39.880507	38.581204	33.511388	27.863418	26.673451	15.279660	15.186081	-0.666384	-0.669432	-20.260864
.61	50.049502	49.967156	40.159168	38.791970	33.906643	28.125089	27.015736	15.515283	15.431145	-0.487130	-0.489788	-20.147253
.62	50.136967	50.047674	40.441806	39.004002	34.302510	28.386749	27.354928	15.750045	15.674602	-0.308587	-0.310597	-20.034047
.63	50.225902	50.129064	40.728463	39.211704	34.698860	28.648373	27.690976	15.983939	15.916486	-0.130749	-0.132751	-19.921243
.64	50.316383	50.211349	41.019172	39.431878	35.095644	28.909931	28.023835	16.216958	16.156831	0.046387	0.044660	-19.808836
.65	50.408488	50.294550	41.313965	39.647728	35.492683	29.171396	28.353466	16.449096	16.395670	0.222830	0.221345	-19.696824
.66	50.502305	50.378688	41.612863	39.864854	35.889877	29.432739	28.679836	16.680347	16.633034	0.398582	0.397311	-19.585202
.67	50.597925	50.463787	41.915884	40.083260	36.287098	29.693932	29.002920	16.910707	16.868956	0.573650	0.572566	-19.473367
.68	50.695448	50.549871	42.223038	40.302946	36.684213	29.954944	29.322697	17.140170	17.103465	0.748039	0.747119	-19.363116
.69	50.794980	50.636962	42.534328	40.523913	37.081081	30.215745	29.639157	17.368731	17.336591	0.921754	0.920977	-19.252645
.70	50.896639	50.725087	42.849751	40.746163	37.477554	30.476303	29.952293	17.596387	17.568364	1.094800	1.094147	-19.142551
.71	51.000549	50.814271	43.169297	40.963696	37.873476	30.736588	30.262107	17.823134	17.798810	1.267183	1.266637	-19.032830
.72	51.106844	50.904539	43.492950	41.194512	38.265683	30.996565	30.568607	18.048968	18.027956	1.438454	1.438454	-18.923480
.73	51.215670	50.995918	43.820686	41.420610	38.663000	31.256204	30.871810	18.273886	18.255830	1.609978	1.609004	-18.814496
.74	51.327182	51.089437	44.152476	41.647991	39.056241	31.515469	31.171737	18.497685	18.482455	1.780095	1.780095	-18.705877
.75	51.441551	51.182123	44.488283	41.876652	39.448211	31.774327	31.468417	18.720965	18.707857	1.950182	1.949932	-18.597618
.76	51.558958	51.277005	44.828065	42.106594	39.838700	32.027242	31.761683	18.943122	18.932059	2.119324	2.119123	-18.489716
.77	51.679599	51.373112	45.171776	42.33814	40.227488	32.290679	32.052177	19.164355	19.155083	2.287834	2.287673	-18.382169
.78	51.803684	51.470476	45.519362	42.570310	40.614338	32.548102	32.339343	19.384663	19.376952	2.455589	2.455589	-18.274974
.79	51.931441	51.569127	45.870766	42.804080	40.999000	32.804973	32.623434	19.604046	19.597685	2.622976	2.622876	-18.168127
.80	52.063111	51.669096	46.225926	43.039122	41.381210	33.061255	32.904503	19.822503	19.817304	2.789618	2.789540	-18.061625
.81	52.198953	51.770417	46.584774	43.275432	41.760685	33.316909	33.162612	20.040034	20.035828	2.955587	2.955587	-17.955466
.82	52.339244	51.873123	46.947242	43.513006	42.137122	33.571897	33.457823	20.256641	20.253275	3.121023	3.121023	-17.849647
.83	52.484277	51.977247	47.313256	43.751842	42.510225	33.826178	33.730203	20.472323	20.469663	3.285986	3.285982	-17.744166
.84	52.634361	52.082824	47.682741	43.991936	42.879647	34.079714	33.993621	20.687082	20.685009	3.450081	3.450081	-17.639018
.85	52.789822	52.189889	48.055617	44.233282	43.245050	34.332462	34.266751	20.900919	20.899329	3.613732	3.613732	-17.534202
.86	52.951000	52.298478	48.431806	44.475877	43.606075	34.584361	34.531065	21.113833	21.112639	3.776769	3.776769	-17.429715
.87	53.118247	52.408627	48.811225	44.719715	43.962352	34.835430	34.792840	21.325838	21.324953	3.939223	3.939214	-17.325554
.88	53.291925	52.520373	49.193793	44.964792	44.313504	35.085566	35.052153	21.536924	21.536286	4.101097	4.101091	-17.221717
.89	53.472401	52.633755	49.579424	45.211101	44.659147	35.3334746	35.309080	21.747099	21.746652	4.262396	4.262392	-17.116200
.90	53.660044	52.748809	49.968037	45.458637	44.990896	35.582927	35.563701	21.956365	21.956062	4.423124	4.423122	-17.015002
.91	53.855219	52.865575	50.359547	45.707393	45.323372	35.830065	35.810094	22.164726	22.164529	4.581287	4.581286	-16.91210
.92	54.058280	52.984091	50.753870	45.957365	45.659206	36.076115	36.063336	22.372187	22.372064	4.742888	4.742883	-16.809532
.93	54.269565	53.104397	51.150924	46.208543	45.979049	36.321033	36.313506	22.578750	22.578679	4.901933	4.901932	-16.707294
.94	54.489385	53.226532	51.550627	46.460923	46.291576	36.564775	36.560680	22.784421	22.784383	-5.060424	5.060424	-16.605345
.95	54.718019	53.350536	51.952896	46.714496	46.596495	36.807296	36.804935	22.989205	22.989187	5.218367	5.218367	-16.503702
.96	54.955706	53.476450	52.357653	46.969256	46.893557	37.048549	37.047346	23.193107	23.193100	5.375765	5.375765	-16.402163
.97	55.202638	53.604313	52.764818	47.225194	47.182558	37.288492	37.287966	23.396131	23.396129	5.532624	5.532624	-16.301326
.98	55.458953	53.734165	53.174314	47.482302	47.463349	37.527077	37.526928	23.598284	23.598284	5.686946	5.686946	-16.200587
.99	55.724734	53.866048	53.586066	47.740574	47.735840	37.764262	37.764243	23.799572	23.799572	5.844737	5.844737	-16.100146
1.00	56.000000	54.000000	54.000000	48.000000	48.000000	38.000000	38.000000	24.000000	24.000000	6.000000	6.000000	-16.000000







$J_{K-1}K_1$ $J_r$	$J_{1,6}$ $7_{-II}$	$7_{1,7}$ $7_{-6}$	$7_{0,7}$ $7_{-7}$	$8_{0,0}$ $8_8$	$8_{8,1}$ $8_7$	$7_{1,1}$ $8_6$	$8_{7,2}$ $8_5$	$8_{6,2}$ $8_4$	$8_{6,3}$ $8_3$	$8_{5,3}$ $8_2$	$8_{5,4}$ $8_1$	$8_{4,4}$ $8_0$
.50	-21.420324	-43.886126	-43.686128	64.155586	64.139632	50.066598	49.678953	40.185479	37.096694	33.210921	24.301577	23.642820
.51	-21.302417	-43.845332	-43.645333	64.237767	64.222440	50.333599	49.915120	40.646455	37.430948	33.718496	24.643683	24.035765
.52	-21.184959	-43.804683	-43.604684	64.322913	64.306075	50.602389	50.151109	41.111127	37.766088	34.224388	24.985004	24.425105
.53	-21.067945	-43.764177	-43.564177	64.409059	64.390560	50.875102	50.392942	41.579406	38.102085	34.728427	25.325511	24.810885
.54	-20.951371	-43.723812	-43.523813	64.496243	64.475917	51.151877	50.634637	42.051193	38.438908	35.230439	25.665175	25.193153
.55	-20.835231	-43.683588	-43.483588	64.584505	64.562170	51.432859	50.878214	42.526386	38.776525	35.730250	26.003965	25.571961
.56	-20.719222	-43.643503	-43.443503	64.673889	64.649341	51.718192	51.123692	43.004875	39.114904	36.227679	26.341855	25.947363
.57	-20.604240	-43.603555	-43.603555	64.764440	64.737458	52.008026	51.371091	43.486546	39.454012	36.722549	26.678814	26.319417
.58	-20.489379	-43.563744	-43.563744	64.856208	64.826546	52.302512	51.620429	43.971280	39.793812	37.214678	27.014816	26.688183
.59	-20.374937	-43.524068	-43.524068	64.949247	64.916631	52.601805	51.871724	44.458949	40.134269	37.703883	27.349832	27.053725
.60	-20.260909	-43.484525	-43.484525	65.043612	65.007743	52.906057	52.124995	44.949424	40.475346	38.189983	27.681837	27.416105
.61	-20.147291	-43.445115	-43.445115	65.139366	65.099910	53.215424	52.380258	45.442569	40.817003	38.672796	28.016803	27.775390
.62	-20.034079	-43.405837	-43.405837	65.236574	65.193163	53.530059	52.637531	45.938240	41.159200	39.152143	28.346706	28.131645
.63	-19.921270	-43.366688	-43.366688	65.335307	65.287533	53.850116	52.896831	46.436292	41.501897	39.627846	28.679519	28.484937
.64	-19.808859	-43.327668	-43.327668	65.435643	65.383054	54.175742	53.158172	46.936570	41.845049	40.099732	29.009219	28.835334
.65	-19.696843	-43.288776	-43.288776	65.537664	65.479759	54.507084	53.421571	47.438914	42.188613	40.567632	29.337781	29.182904
.66	-19.585218	-43.250011	-43.250011	65.641461	65.577684	54.844282	53.687043	47.941159	42.532544	41.031382	29.665183	29.527713
.67	-19.473980	-43.211371	-43.211371	65.747133	65.676865	55.187469	53.954601	48.449131	42.876793	41.490828	29.991402	29.869828
.68	-19.363127	-43.172855	-43.172855	65.854784	65.777341	55.536771	54.224259	48.956649	43.221312	41.945823	30.316416	30.209314
.69	-19.252654	-43.134462	-43.134462	65.964533	65.879152	55.892305	54.496030	49.465523	43.566051	42.396229	30.640206	30.546238
.70	-19.142558	-43.096192	-43.096192	66.076506	65.982339	56.254177	54.769925	49.975554	43.910958	42.841920	30.962750	30.880663
.71	-19.032836	-43.058042	-43.058042	66.190841	66.086945	56.622795	55.045957	50.486533	44.259978	43.282784	31.284030	31.212652
.72	-18.923484	-43.020012	-43.020012	66.307691	66.193014	56.992297	55.324136	50.998238	44.601057	43.718721	31.604027	31.542266
.73	-18.814500	-42.982102	-42.982102	66.427221	66.300593	57.378692	55.604472	51.510435	44.946137	44.149645	31.922724	31.869565
.74	-18.705879	-42.944309	-42.944309	66.549614	66.409730	57.766720	55.886973	52.022877	45.291160	44.575488	32.240105	32.194607
.75	-18.597620	-42.906633	-42.906633	66.675071	66.520475	58.161414	56.171649	52.535298	45.636063	44.996198	32.556154	32.517449
.76	-18.489718	-42.869072	-42.869072	66.803813	66.632880	58.562795	56.458505	53.047415	45.980786	45.411737	32.870857	32.838145
.77	-18.382170	-42.831627	-42.831627	66.936083	66.746993	58.970865	56.747549	53.558926	46.325261	45.822088	33.184200	33.156749
.78	-18.274975	-42.794295	-42.794295	67.072148	66.862886	59.385610	57.038785	54.069504	46.669424	46.227250	33.496170	33.473311
.79	-18.168127	-42.757076	-42.757076	67.212303	66.980601	59.806999	57.332219	54.578798	47.013204	46.627238	33.806757	33.787880
.80	-18.061626	-42.719970	-42.719970	67.356875	67.100203	60.234983	57.627855	55.086428	47.356532	47.022087	34.115949	34.100504
.81	-17.955467	-42.682974	-42.682974	67.506220	67.221754	60.669498	57.925694	55.591985	47.699333	47.411845	34.423737	34.411228
.82	-17.849648	-42.646088	-42.646088	67.660735	67.345319	61.110466	58.225739	56.095025	48.041533	47.796579	34.730113	34.720094
.83	-17.744166	-42.609312	-42.609312	67.820850	67.470964	61.557793	58.527990	56.595065	48.383054	48.176369	35.035069	35.027144
.84	-17.639018	-42.572644	-42.572644	67.987043	67.598757	62.011372	58.832447	57.091586	48.723817	48.551308	35.338600	35.332418
.85	-17.534202	-42.536083	-42.536083	68.159832	67.728770	62.471884	59.139110	57.584024	49.063741	48.921503	35.640699	35.635952
.86	-17.429715	-42.499629	-42.499629	68.339782	67.861076	62.936798	59.447976	58.071772	49.402740	49.287071	35.941362	35.937783
.87	-17.325554	-42.463281	-42.463281	68.527506	67.995750	63.408176	59.759041	58.554179	49.740730	49.648139	36.240587	36.237943
.88	-17.221717	-42.427037	-42.427037	68.723660	68.132869	63.885671	60.072303	59.030550	50.077621	50.004843	36.538371	36.536463
.89	-17.118200	-42.390898	-42.390898	68.928946	68.272514	64.368527	60.387755	59.500147	50.413324	50.357326	36.834713	36.833375
.90	-17.015002	-42.354861	-42.354861	69.144102	68.414766	64.856787	60.705392	59.962198	50.747747	50.705736	37.129614	37.128706
.91	-16.912120	-42.318927	-42.318927	69.369895	68.559710	65.350285	61.025208	60.415904	51.080794	51.050225	37.423073	37.422491
.92	-16.809552	-42.283095	-42.283095	69.600112	68.707430	65.848856	61.347194	60.860449	51.412370	51.390948	37.715093	37.714726
.93	-16.707294	-42.247363	-42.247363	69.856536	68.858016	66.352332	61.671342	61.295019	51.742378	51.728064	38.005678	38.005464
.94	-16.605345	-42.211732	-42.211732	70.118935	69.011556	66.860544	61.997642	61.718821	52.070717	52.061729	38.294830	38.294715
.95	-16.503702	-42.176199	-42.176199	70.395032	69.168140	67.373325	62.326084	62.131106	52.397287	52.392103	38.582554	38.582500
.96	-16.402363	-42.140766	-42.140766	70.685481	69.327862	67.890507	62.656657	62.531197	52.721986	52.719341	38.868857	38.868835
.97	-16.301326	-42.105429	-42.105429	70.990840	69.490815	68.411926	62.989348	62.918514	53.044710	53.043599	39.153746	39.153739
.98	-16.200587	-42.070190	-42.070190	71.311545	69.657092	68.937420	63.324145	63.292600	53.365357	53.365029	39.437226	39.437225
.99	-16.100146	-42.035047	-42.035047	71.647887	69.826788	69.466829	63.661033	63.653146	53.683822	53.683781	39.719308	39.719308
1.00	-16.000000	-42.000000	-42.000000	72.000000	70.000000	70.000000	64.000000	64.000000	54.000000	54.000000	40.000000	40.000000

$J_{K_1K_2}$ $J_r$	$K$	$J_{K_1K_2}$											
		8 <sub>4,5</sub> 8-1	8 <sub>1,5</sub> 8-2	8 <sub>1,4</sub> 8-3	8 <sub>2,4</sub> 8-4	8 <sub>2,7</sub> 8-5	8 <sub>1,7</sub> 8-6	8 <sub>1,8</sub> 8-7	8 <sub>0,8</sub> 8-8	9 <sub>9,0</sub> 9-9	9 <sub>9,1</sub> 9-8	9 <sub>8,1</sub> 9-7	9 <sub>8,2</sub> 9-6
.00	.00	-6.841208	-8.668876	-21.898573	-22.072159	-39.752915	-39.759911	-60.735550	-60.735655	77.320583	77.320562	53.504332	53.502655
.01	.01	-6.539629	-8.240594	-21.628224	-21.789455	-39.584076	-39.590458	-60.677939	-60.678033	77.385572	77.385548	53.695492	53.693628
.02	.02	-6.198779	-7.815889	-21.359185	-21.500643	-39.416137	-39.421956	-60.620627	-60.620711	77.450905	77.450878	53.887718	53.885648
.03	.03	-5.858681	-7.394769	-21.091451	-21.230272	-39.249088	-39.254390	-60.563609	-60.563684	77.516588	77.516557	54.081026	54.078729
.04	.04	-5.519355	-6.977239	-20.825016	-20.955367	-39.082916	-39.087744	-60.506881	-60.506948	77.582625	77.582591	54.275436	54.272889
.05	.05	-5.180823	-6.563296	-20.559872	-20.679071	-38.917610	-38.922003	-60.450439	-60.450499	77.649023	77.648984	54.470966	54.468142
.06	.06	-4.843107	-6.152936	-20.296012	-20.406350	-38.753158	-38.757153	-60.394279	-60.394333	77.715767	77.715743	54.667634	54.664505
.07	.07	-4.506225	-5.746148	-20.033429	-20.135493	-38.589549	-38.593179	-60.338397	-60.338445	77.782923	77.782874	54.855461	54.851997
.08	.08	-4.170199	-5.342916	-19.772116	-19.866457	-38.426772	-38.430068	-60.282789	-60.282832	77.850437	77.850382	55.044466	55.040634
.09	.09	-3.835047	-4.943221	-19.512065	-19.599203	-38.264816	-38.267807	-60.227451	-60.227490	77.918336	77.918274	55.264672	55.260434
.10	.10	-3.500789	-4.547038	-19.253268	-19.333693	-38.103671	-38.106383	-60.172380	-60.172415	77.986626	77.986556	55.466100	55.461415
.11	.11	-3.167442	-4.154342	-18.995716	-19.069389	-37.943326	-37.945783	-60.117572	-60.117603	78.055234	78.055234	55.663596	55.663596
.12	.12	-2.835025	-3.765099	-18.739403	-18.807756	-37.783771	-37.785995	-60.063023	-60.063051	78.124316	78.124316	55.872712	55.866997
.13	.13	-2.503555	-3.379276	-18.484318	-18.547258	-37.624996	-37.627007	-60.008731	-60.008755	78.193906	78.193907	56.077943	56.071636
.14	.14	-2.173049	-2.996835	-18.230454	-18.288363	-37.466991	-37.468808	-59.954691	-59.954712	78.263827	78.263716	56.294491	56.277533
.15	.15	-1.843522	-2.617735	-17.977802	-18.031039	-37.309745	-37.311387	-59.900900	-59.900919	78.334174	78.334050	56.492381	56.484710
.16	.16	-1.514992	-2.241932	-17.726354	-17.775253	-37.153251	-37.154732	-59.847355	-59.847372	78.404954	78.404815	56.701641	56.693187
.17	.17	-1.187474	-1.869382	-17.476099	-17.520976	-36.997498	-36.998833	-59.794052	-59.794067	78.476176	78.476020	56.912298	56.902985
.18	.18	-0.860981	-1.500035	-17.227030	-17.268179	-36.842477	-36.843679	-59.740990	-59.741003	78.547847	78.547673	57.124381	57.114127
.19	.19	-0.535529	-1.133844	-16.979136	-17.016833	-36.688180	-36.689261	-59.688164	-59.688176	78.619976	78.619781	57.337921	57.326635
.20	.20	-0.211131	-0.770755	-16.732410	-16.766913	-36.534597	-36.535568	-59.635572	-59.635582	78.692571	78.692354	57.552947	57.540531
.21	.21	0.112199	-0.410718	-16.486841	-16.518391	-36.381719	-36.382592	-59.583211	-59.583220	78.765642	78.765399	57.769494	57.755839
.22	.22	0.434449	-0.053678	-16.242420	-16.271242	-36.229539	-36.230322	-59.531077	-59.531085	78.839198	78.838926	57.987594	57.972583
.23	.23	0.755608	0.300417	-15.999138	-16.025442	-36.078048	-36.078749	-59.479169	-59.479176	78.913247	78.912944	58.207282	58.190788
.24	.24	1.075664	0.651625	-15.756986	-15.780968	-35.927237	-35.927864	-59.427483	-59.427489	78.987801	78.987463	58.428596	58.410478
.25	.25	1.394605	1.000000	-15.515954	-15.537795	-35.777098	-35.777659	-59.376017	-59.376022	79.062869	79.062492	58.651574	58.631680
.26	.26	1.712421	1.345597	-15.276032	-15.295903	-35.627624	-35.628125	-59.324772	-59.324772	79.138463	79.138041	58.876256	58.854418
.27	.27	2.029103	1.688472	-15.037211	-15.055271	-35.478807	-35.479254	-59.273733	-59.273737	79.214592	79.214121	59.102683	59.078721
.28	.28	2.344640	2.028681	-14.799482	-14.815876	-35.330640	-35.331037	-59.222910	-59.222914	79.291268	79.290743	59.330899	59.304615
.29	.29	2.659025	2.366278	-14.562835	-14.577701	-35.183113	-35.183467	-59.172297	-59.172300	79.368503	79.367918	59.560949	59.532129
.30	.30	2.972249	2.701318	-14.327261	-14.340724	-35.036222	-35.036536	-59.121890	-59.121893	79.446309	79.445657	59.792883	59.761290
.31	.31	3.284304	3.033856	-14.092750	-14.104928	-34.889957	-34.890236	-59.071688	-59.071691	79.524699	79.523973	60.026748	59.992128
.32	.32	3.595183	3.363944	-13.859292	-13.870294	-34.744312	-34.744559	-59.021689	-59.021691	79.603686	79.602877	60.262599	60.224673
.33	.33	3.904880	3.691636	-13.626878	-13.636806	-34.599280	-34.599499	-58.971889	-58.971891	79.683284	79.682382	60.500490	60.458954
.34	.34	4.213389	4.016983	-13.395500	-13.404445	-34.454854	-34.455047	-58.922288	-58.922289	79.763507	79.762502	60.740478	60.695004
.35	.35	4.520704	4.340037	-13.165146	-13.173196	-34.311028	-34.311198	-58.872881	-58.872883	79.844369	79.843251	60.982626	60.932852
.36	.36	4.826820	4.660847	-12.935809	-12.943042	-34.167794	-34.167944	-58.823668	-58.823670	79.925887	79.924641	61.226995	61.172533
.37	.37	5.131733	4.979461	-12.707479	-12.713969	-34.025146	-34.025278	-58.774647	-58.774648	80.008076	80.006689	61.473655	61.414077
.38	.38	5.435439	5.295928	-12.480146	-12.485961	-33.883079	-33.883194	-58.725814	-58.725815	80.090954	80.089409	61.722674	61.657519
.39	.39	5.737934	5.610295	-12.253801	-12.259003	-33.741585	-33.741686	-58.677168	-58.677169	80.174537	80.172818	61.974129	61.902893
.40	.40	6.039215	5.922606	-12.028435	-12.033081	-33.600658	-33.600746	-58.628708	-58.628708	80.258844	80.256930	62.228097	62.150233
.41	.41	6.339281	6.232907	-11.804040	-11.808183	-33.460292	-33.460370	-58.580430	-58.580431	80.343894	80.341765	62.484661	62.399575
.42	.42	6.638128	6.541239	-11.580605	-11.584293	-33.320482	-33.320549	-58.532334	-58.532334	80.429708	80.427338	62.743909	62.650953
.43	.43	6.935756	6.847645	-11.358123	-11.361400	-33.181280	-33.181280	-58.484417	-58.484417	80.516307	80.513669	63.005932	62.904406
.44	.44	7.232164	7.152166	-11.136584	-11.139490	-33.042504	-33.042555	-58.436677	-58.436677	80.603712	80.600776	63.270829	63.159969
.45	.45	7.527351	7.454840	-10.915980	-10.918552	-32.904325	-32.904369	-58.389112	-58.389113	80.691948	80.688679	63.538703	63.417679
.46	.46	7.821316	7.755706	-10.698574	-10.698574	-32.766779	-32.766717	-58.341722	-58.341722	80.781037	80.777399	63.809661	63.677576
.47	.47	8.114061	8.054801	-10.477539	-10.479543	-32.629559	-32.629592	-58.294503	-58.294503	80.871007	80.866958	64.083819	63.939698
.48	.48	8.405586	8.352160	-10.259685	-10.261449	-32.492962	-32.492990	-58.247454	-58.247454	80.961885	80.957377	64.361300	64.204033
.49	.49	8.695893	8.647819	-10.042732	-10.044280	-32.356880	-32.356904	-58.200574	-58.200574	81.053698	81.048680	64.642230	64.470771
.50	.50	8.984982	8.941810	-9.826670	-9.828026	-32.221309	-32.221330	-58.153860	-58.153860	81.146477	81.140891	64.926747	64.739802



$J_{K-1}K_1$ $J_T$ $K$	$8_{4,5}$ $8_{-1}$	$8_{3,5}$ $8_{-2}$	$8_{1,6}$ $8_{-3}$	$8_{2,6}$ $8_{-4}$	$8_{2,7}$ $8_{-5}$	$8_{1,7}$ $8_{-6}$	$1_{,8}$ $8_{-7}$	$0_{,8}$ $8_{-8}$	$9_{9,0}$ $9_9$	$9_{9,1}$ $9_8$	$9_{8,1}$ $9_7$	$9_{8,2}$ $9_6$
.50	8.984982	8.941810	-9.826670	-9.828026	-32.221309	-32.221330	-58.153860	-58.153860	81.146477	81.140891	64.926747	64.739802
.51	9.272856	9.234166	-9.611491	-9.612676	-32.086245	-32.086263	-58.107311	-58.107311	81.240255	81.234035	65.214995	65.011217
.52	9.559517	9.524918	-9.397188	-9.398220	-31.951681	-31.951696	-58.060926	-58.060926	81.335065	81.328138	65.507124	65.285055
.53	9.844968	9.814096	-9.183751	-9.184649	-31.817614	-31.817626	-58.014702	-58.014702	81.423943	81.416328	65.803296	65.561359
.54	10.129211	10.101730	-8.971172	-8.971951	-31.684037	-31.684048	-57.968639	-57.968639	81.527927	81.519334	66.103680	65.840169
.55	10.412251	10.387847	-8.759445	-8.760118	-31.550947	-31.550956	-57.922734	-57.922734	81.626059	81.616485	66.408454	66.121526
.56	10.694092	10.672474	-8.548560	-8.549140	-31.418338	-31.418346	-57.876987	-57.876987	81.725381	81.714713	66.717808	66.405473
.57	10.974736	10.955637	-8.338510	-8.339009	-31.286206	-31.286213	-57.831395	-57.831395	81.825941	81.814050	67.031940	66.692052
.58	11.254188	11.237361	-8.129288	-8.129715	-31.154547	-31.154552	-57.785957	-57.785957	81.927787	81.914530	67.351057	66.981304
.59	11.532454	11.517671	-7.920885	-7.921250	-31.023356	-31.023360	-57.740671	-57.740671	82.030972	82.016189	67.675378	67.273271
.60	11.809538	11.796590	-7.713295	-7.713605	-30.892627	-30.892631	-57.695537	-57.695537	82.135554	82.119063	68.005133	67.567995
.61	12.085445	12.074140	-7.506509	-7.506772	-30.762358	-30.762361	-57.650553	-57.650553	82.241594	82.223193	68.340560	67.865518
.62	12.360180	12.350343	-7.300520	-7.300743	-30.632544	-30.632547	-57.605717	-57.605717	82.349158	82.328619	68.681909	68.165881
.63	12.633749	12.625219	-7.095322	-7.095509	-30.503180	-30.503182	-57.561028	-57.561028	82.458318	82.435384	69.029436	68.469126
.64	12.906159	12.898789	-6.890907	-6.891063	-30.374263	-30.374265	-57.516485	-57.516485	82.569150	82.543532	69.383410	68.775294
.65	13.177415	13.171072	-6.687267	-6.687397	-30.245788	-30.245789	-57.472086	-57.472086	82.681738	82.653110	69.744104	69.084424
.66	13.447523	13.442087	-6.484396	-6.484504	-30.117751	-30.117752	-57.427830	-57.427830	82.796173	82.764169	70.111801	69.396558
.67	13.716490	13.711851	-6.282287	-6.282377	-29.990148	-29.990149	-57.383715	-57.383715	82.912554	82.876758	70.486787	69.711734
.68	13.984322	13.980382	-6.080934	-6.081007	-29.862976	-29.862977	-57.339741	-57.339741	83.030990	82.990933	70.869351	70.029991
.69	14.251026	14.247696	-5.880329	-5.880388	-29.736230	-29.736231	-57.295907	-57.295907	83.151599	83.106750	71.259785	70.351367
.70	14.516610	14.513810	-5.680465	-5.680513	-29.609907	-29.609908	-57.252210	-57.252210	83.274510	83.224269	71.658378	70.675898
.71	14.781079	14.778738	-5.481337	-5.481376	-29.484003	-29.484004	-57.208650	-57.208650	83.399866	83.343553	72.065414	71.003622
.72	15.044442	15.042497	-5.282938	-5.282969	-29.358515	-29.358515	-57.165226	-57.165226	83.527825	83.464667	72.481172	71.334571
.73	15.306706	15.305099	-5.085261	-5.085285	-29.233437	-29.233438	-57.121936	-57.121936	83.658561	83.587680	72.905919	71.668781
.74	15.567877	15.566559	-4.888300	-4.888319	-29.108768	-29.108769	-57.078779	-57.078779	83.792266	83.712666	73.339906	72.006284
.75	15.827964	15.826891	-4.692049	-4.692064	-28.984504	-28.984504	-57.035754	-57.035754	83.929155	83.839699	73.783368	72.347109
.76	16.086974	16.086107	-4.496502	-4.496513	-28.860640	-28.860640	-56.992860	-56.992860	84.069467	83.968860	74.236516	72.691288
.77	16.344914	16.344220	-4.301652	-4.301661	-28.737175	-28.737175	-56.950096	-56.950096	84.213467	84.100233	74.699535	73.038847
.78	16.601792	16.601242	-4.107495	-4.107502	-28.614103	-28.614103	-56.907461	-56.907461	84.361454	84.233907	75.172583	73.389814
.79	16.857616	16.857185	-3.914023	-3.914028	-28.491422	-28.491422	-56.864953	-56.864953	84.513762	84.369973	75.655783	73.744211
.80	17.112394	17.112059	-3.721232	-3.721236	-28.369129	-28.369129	-56.822572	-56.822572	84.670766	84.508530	76.149223	74.102063
.81	17.366133	17.365876	-3.529115	-3.529118	-28.247221	-28.247221	-56.780316	-56.780316	84.832690	84.649679	76.652955	74.463388
.82	17.618840	17.618647	-3.337667	-3.337669	-28.125693	-28.125693	-56.738185	-56.738185	85.000611	84.793528	77.166993	74.828207
.83	17.870525	17.870381	-3.146882	-3.146884	-28.004544	-28.004544	-56.696177	-56.696177	85.174466	84.940188	77.691310	75.196535
.84	18.121194	18.121089	-2.956756	-2.956757	-27.883770	-27.883770	-56.654291	-56.654291	85.355063	85.089778	78.225840	75.568387
.85	18.370855	18.370780	-2.767281	-2.767282	-27.763367	-27.763367	-56.612528	-56.612528	85.543088	85.242420	78.770482	75.943775
.86	18.619517	18.619464	-2.578854	-2.578854	-27.643334	-27.643334	-56.570884	-56.570884	85.739313	85.398244	79.325095	76.322709
.87	18.867186	18.867150	-2.390268	-2.390268	-27.523666	-27.523666	-56.529360	-56.529360	85.944608	85.557385	79.809508	76.705196
.88	19.113870	19.113846	-2.202719	-2.202719	-27.404361	-27.404361	-56.487954	-56.487954	86.159947	85.719982	80.463516	77.091242
.89	19.359578	19.359562	-2.015802	-2.015802	-27.285417	-27.285417	-56.446666	-56.446666	86.386414	85.886183	81.046889	77.480849
.90	19.604315	19.604306	-1.829511	-1.829511	-27.166829	-27.166829	-56.405495	-56.405495	86.625206	86.056141	81.639373	77.874017
.91	19.848091	19.848086	-1.643842	-1.643842	-27.048596	-27.048596	-56.364439	-56.364439	86.877636	86.230014	82.240693	78.270746
.92	20.090913	20.090910	-1.458789	-1.458789	-26.930715	-26.930715	-56.323498	-56.323498	87.145111	86.407967	82.850560	78.671030
.93	20.332788	20.332786	-1.274348	-1.274348	-26.813182	-26.813182	-56.282671	-56.282671	87.429125	86.590171	83.468672	79.074863
.94	20.573723	20.573722	-1.090514	-1.090514	-26.695996	-26.695996	-56.241958	-56.241958	87.731213	86.776801	84.094718	79.482235
.95	20.813725	20.813725	-0.907283	-0.907283	-26.579153	-26.579153	-56.201356	-56.201356	88.052907	86.968019	84.728184	79.893136
.96	21.052802	21.052802	-0.724649	-0.724649	-26.462651	-26.462651	-56.160865	-56.160865	88.395673	87.164071	85.369353	80.307551
.97	21.290961	21.290961	-0.542608	-0.542608	-26.346487	-26.346487	-56.120485	-56.120485	88.760831	87.365087	86.017308	80.725464
.98	21.528209	21.528209	-0.361156	-0.361156	-26.230659	-26.230659	-56.080215	-56.080215	89.149473	87.571283	86.671938	81.146857
.99	21.764553	21.764553	-0.180288	-0.180288	-26.115164	-26.115164	-56.040053	-56.040053	89.562388	87.782854	87.332935	81.571710
1.00	22.000000	22.000000	0.000000	0.000000	-26.000000	-26.000000	-56.000000	-56.000000	90.000000	88.000000	88.000000	82.000000



$J, K_1, K_2$	97,2 95	97,3 94	96,3 93	96,4 92	95,4 91	95,5 90	94,5 9-1	94,6 9-2	93,6 9-3	93,7 9-4	92,7 9-5	92,8 9-6
.00	32.876883	32.825762	16.009233	15.279589	4.316093	0.000000	-4.316098	-15.279589	-16.009233	-32.825762	-32.876883	-53.502655
.01	33.191018	33.135175	16.470100	15.689918	4.940251	0.453211	-3.694871	-14.870834	-15.552621	-32.518021	-32.564788	-53.312712
.02	33.507237	33.446278	16.935304	16.101805	5.567182	0.906378	-3.076717	-14.463667	-15.100184	-32.211935	-32.254688	-53.123786
.03	33.825587	33.759087	17.404922	16.512333	6.196740	1.359457	-2.461775	-14.058102	-14.651838	-31.907488	-31.946544	-52.935861
.04	34.146117	34.073620	17.879031	16.930185	6.828770	1.812404	-1.850186	-13.654151	-14.207498	-31.604662	-31.640315	-52.748923
.05	34.468876	34.389892	18.357701	17.346642	7.463118	2.265174	-1.242082	-13.251825	-13.767080	-31.303441	-31.335962	-52.562958
.06	34.793917	34.707922	18.841002	17.764584	8.099625	2.717723	-0.637593	-12.851137	-13.330499	-31.003806	-31.033450	-52.377953
.07	35.121295	35.027725	19.328998	18.183991	8.738131	3.170008	-0.036843	-12.452095	-12.897671	-30.705743	-30.732742	-52.193894
.08	35.451067	35.349318	19.821749	18.604842	9.378475	3.621985	0.560049	-12.054708	-12.468510	-30.409233	-30.433804	-52.010768
.09	35.783293	35.672717	20.319309	19.027112	10.020495	4.073611	1.152971	-11.658984	-12.042934	-30.114260	-30.136604	-51.828562
.10	36.118033	35.997938	20.821727	19.450779	10.664026	4.524843	1.741817	-11.264929	-11.620860	-29.820807	-29.841109	-51.647264
.11	36.455353	36.324998	21.329045	19.875817	11.308903	4.975636	2.326487	-10.872551	-11.202207	-29.528858	-29.547289	-51.466862
.12	36.795318	36.653910	21.841299	20.302200	11.954960	5.425950	2.906889	-10.481854	-10.786894	-29.238396	-29.255114	-51.287343
.13	37.137999	36.984692	22.358517	20.729903	12.602029	5.875741	3.482937	-10.092842	-10.374842	-28.949405	-28.964556	-51.108696
.14	37.483468	37.317358	22.880720	21.158896	13.249941	6.324967	4.054554	-9.705520	-9.965974	-28.661869	-28.675587	-50.930909
.15	37.831801	37.651923	23.407920	21.589150	13.898527	6.773587	4.621672	-9.319889	-9.560216	-28.375771	-28.388181	-50.753972
.16	38.183074	37.988400	23.940122	22.020636	14.547616	7.221560	5.184230	-8.935951	-9.157493	-28.091096	-28.102312	-50.577872
.17	38.537370	38.326804	24.477322	22.453323	15.197035	7.668843	5.742177	-8.553708	-8.757734	-27.807828	-27.817955	-50.402600
.18	38.894774	38.667148	25.019507	22.887178	15.846612	8.115398	6.295468	-8.173161	-8.360869	-27.525951	-27.535086	-50.228144
.19	39.255371	39.009445	25.566654	23.322168	16.496172	8.561184	6.844069	-7.794308	-7.966830	-27.245449	-27.253682	-50.054495
.20	39.619253	39.353707	26.118732	23.758260	17.145540	9.006161	7.387955	-7.417149	-7.575551	-26.966309	-26.973719	-49.881642
.21	39.986514	39.699947	26.675700	24.195418	17.794538	9.450291	7.927109	-7.041682	-7.186968	-26.695177	-26.695177	-49.709575
.22	40.357251	40.048175	27.237508	24.633605	18.442989	9.893536	8.461522	-6.667904	-6.801020	-26.412048	-26.418034	-49.538284
.23	40.731564	40.398402	27.804098	25.072786	19.090714	10.335857	8.991195	-6.295813	-6.477647	-26.136899	-26.142270	-49.367761
.24	41.109556	40.750638	28.375400	25.512922	19.737531	10.777217	9.516136	-5.925405	-6.036790	-25.863050	-25.867864	-49.197995
.25	41.491334	41.104893	28.951339	25.953974	20.383259	11.217580	10.036361	-5.556676	-5.658394	-25.590488	-25.594797	-49.028977
.26	41.877006	41.461174	29.531829	26.395902	21.027714	11.656910	10.551895	-5.189621	-5.282404	-25.319198	-25.323051	-48.860699
.27	42.266886	41.819491	30.116774	26.838665	21.670712	12.095172	11.062769	-4.824234	-4.908769	-25.049166	-25.052607	-48.693151
.28	42.660489	42.179848	30.706074	27.282221	22.312068	12.532332	11.569020	-4.460511	-4.537438	-24.780379	-24.783448	-48.526326
.29	43.058530	42.542253	31.299617	27.726529	22.951596	12.968356	12.070694	-4.098444	-4.168362	-24.512822	-24.515555	-48.360214
.30	43.460931	42.906710	31.897287	28.171543	23.589108	13.403211	12.567840	-3.738027	-3.801495	-24.246482	-24.248913	-48.194807
.31	43.867812	43.273223	32.498958	28.617220	24.224417	13.836865	13.060515	-3.379252	-3.436791	-23.981346	-23.983505	-48.030096
.32	44.279296	43.641797	33.104499	29.063515	24.857336	14.269287	13.548778	-3.022113	-3.074208	-23.717400	-23.719316	-47.866075
.33	44.695507	44.012431	33.713771	29.510381	25.487677	14.700446	14.032696	-2.666600	-2.713703	-23.454632	-23.456328	-47.702735
.34	45.116570	44.385129	34.326631	29.957771	26.115254	15.130314	14.512336	-2.312706	-2.355236	-23.193028	-23.194528	-47.540069
.35	45.542609	44.759888	34.942929	30.405638	26.739881	15.558861	14.987771	-1.960422	-1.998768	-22.932576	-22.933901	-47.378068
.36	45.973747	45.136709	35.562509	30.853932	27.361372	15.986061	15.459075	-1.609739	-1.644262	-22.673265	-22.674433	-47.216725
.37	46.410108	45.515588	36.185209	31.302604	27.979548	16.411885	15.926326	-1.260647	-1.291681	-22.415080	-22.416108	-47.056034
.38	46.851812	45.896521	36.810866	31.751605	28.594227	16.836310	16.389603	-0.913137	-0.940992	-22.158011	-22.158914	-46.895987
.39	47.298977	46.279503	37.439306	32.200882	29.205235	17.259309	16.848986	-0.567199	-0.592160	-21.902046	-21.902838	-46.736576
.40	47.751716	46.664528	38.070357	32.650386	29.812400	17.680860	17.304557	-0.222823	-0.245154	-21.647172	-21.647866	-46.577796
.41	48.210140	47.051587	38.703837	33.100062	30.415555	18.100939	17.756398	0.120001	0.100057	-21.393379	-21.393985	-46.419638
.42	48.674352	47.440671	39.339563	33.549859	31.014540	18.519525	18.204590	0.461285	0.443503	-21.140654	-21.141183	-46.262098
.43	49.144450	47.831768	39.977345	33.999722	31.609201	18.936598	18.649216	0.801038	0.785214	-20.888988	-20.889447	-46.105167
.44	49.620524	48.224868	40.616992	34.449598	32.199390	19.352137	19.090358	1.139273	1.125217	-20.638368	-20.638767	-45.948840
.45	50.102656	48.619954	41.258304	34.899431	32.784971	19.766124	19.528096	1.475999	1.463539	-20.388783	-20.389129	-45.793110
.46	50.590918	49.017012	41.901081	35.349165	33.365815	20.178542	20.962510	1.811229	1.800204	-20.140224	-20.140523	-45.637972
.47	51.085372	49.416023	42.545114	35.798746	33.941802	20.589374	20.393680	2.144973	2.135239	-19.892938	-19.892938	-45.483418
.48	51.586070	49.816970	43.190193	36.248117	34.512824	20.998605	20.821681	2.477242	2.468666	-19.646140	-19.646362	-45.329443
.49	52.093048	50.219829	43.836100	36.697221	35.078786	21.406221	21.246591	2.808049	2.800510	-19.400594	-19.400784	-45.176042
.50	52.606335	50.624580	44.482612	37.146000	35.639603	21.812208	21.668482	3.137404	3.130793	-19.156032	-19.156195	-45.023208

$\sqrt{K_1 K_2}$ $\sqrt{r}$ $K$	$9_{7,7}$ $9_5$	$9_{7,3}$ $9_4$	$9_{6,3}$ $9_3$	$9_{6,1}$ $9_2$	$9_{5,4}$ $9_1$	$9_{5,5}$ $9_0$	$9_{4,1}$ $9_{-1}$	$9_{3,6}$ $9_{-2}$	$9_{3,7}$ $9_{-4}$	$9_{2,7}$ $9_{-5}$	$9_{2,8}$ $9_{-6}$
	$9_5$	$9_4$	$9_3$	$9_2$	$9_1$	$9_0$	$9_{-1}$	$9_{-2}$	$9_{-4}$	$9_{-5}$	$9_{-6}$
.50	52.606335	50.624580	44.482612	37.146000	35.639603	21.812208	21.668482	3.137404	-19.156032	-19.156195	-45.023208
.51	53.125941	51.031196	45.129501	37.594397	36.1195203	22.216555	22.037428	3.465320	-18.912444	-18.912583	-44.870935
.52	53.651865	51.439652	45.776534	38.042354	36.745528	22.619249	22.503499	3.791809	-18.669821	-18.669940	-44.719218
.53	54.184092	51.849918	46.423469	38.489813	37.290531	23.020282	22.916763	4.116879	-18.428153	-18.428253	-44.568052
.54	54.722589	52.261963	47.070060	38.936715	37.830182	23.419643	23.327286	4.440546	-18.187430	-18.187515	-44.417431
.55	55.267310	52.675756	47.716051	39.383003	38.364461	23.817326	23.735133	4.762820	-17.947644	-17.947715	-44.267350
.56	55.818193	53.091260	48.361181	39.828616	38.893364	24.213322	24.140366	5.083712	-17.708784	-17.708844	-44.117803
.57	56.375162	53.508439	49.005182	40.273498	39.416898	24.607627	24.543044	5.403235	-17.470893	-17.470893	-43.968785
.58	56.938123	53.927253	49.647776	40.717588	39.935083	25.000234	24.943226	5.721399	-17.233811	-17.233853	-43.820292
.59	57.506969	54.347660	50.288679	41.160829	40.447954	25.391141	25.340967	6.038217	-16.997679	-16.997714	-43.672318
.60	58.081579	54.769615	50.927597	41.603162	40.955553	25.780343	25.736320	6.353701	-16.762439	-16.762468	-43.524859
.61	58.661813	55.193073	51.564230	42.044529	41.457936	26.167838	26.129338	6.667861	-16.528083	-16.528107	-43.377909
.62	59.247522	55.617983	52.198270	42.484873	41.955169	26.553426	26.520069	6.980709	-16.294622	-16.294622	-43.231463
.63	59.838540	56.044295	52.829402	42.924135	42.447325	26.937705	26.908562	7.292256	-16.061988	-16.062004	-43.085518
.64	60.434688	56.471952	53.457303	43.362260	42.934488	27.320077	27.294861	7.602514	-15.830233	-15.830246	-42.940068
.65	61.035774	56.900897	54.081645	43.799190	43.416746	27.700741	27.679010	7.911494	-15.599329	-15.599340	-42.795109
.66	61.641592	57.331070	54.702096	44.234871	43.894197	28.079701	28.061051	8.219207	-15.369268	-15.369277	-42.650637
.67	62.251925	57.762408	55.318321	44.66247	44.366943	28.456958	28.441023	8.525665	-15.140043	-15.140050	-42.506647
.68	62.866540	58.194843	55.929982	45.102265	44.835088	28.832517	28.818965	8.830877	-14.911645	-14.911651	-42.363134
.69	63.485193	58.628306	56.536744	45.533872	45.298742	29.206382	29.194913	9.134855	-14.684068	-14.684072	-42.220095
.70	64.107624	59.062725	57.138273	45.964015	45.758019	29.578556	29.568902	9.437370	-14.457304	-14.457307	-42.077525
.71	64.733562	59.498021	57.732423	46.392644	46.213030	29.949046	29.940966	9.739153	-14.231346	-14.231348	-41.935420
.72	65.362719	59.934115	58.324334	46.819710	46.663892	30.317858	30.311135	10.039338	-14.006186	-14.006189	-41.793775
.73	65.994789	60.370923	58.908243	47.245165	47.110719	30.684998	30.679441	10.338641	-13.781818	-13.781819	-41.652588
.74	66.629451	60.800357	59.485680	47.668961	47.553624	31.050474	31.045911	10.636608	-13.558234	-13.558236	-41.511854
.75	67.266361	61.246326	60.056375	48.091054	47.992723	31.414292	31.410575	10.933404	-13.335429	-13.335430	-41.371569
.76	67.905155	61.684732	60.620081	48.511401	48.428125	31.776462	31.773457	11.229039	-13.113395	-13.113395	-41.231729
.77	68.545443	62.123476	61.176582	48.929960	48.859941	32.136991	32.134584	11.523523	-12.892125	-12.892125	-41.092331
.78	69.186806	62.562453	61.725687	49.346690	49.288277	32.495889	32.493978	11.816865	-12.671613	-12.671613	-40.953370
.79	69.828792	63.001552	62.267244	49.761555	49.713237	32.853164	32.851664	12.109076	-12.451652	-12.451653	-40.814843
.80	70.470911	63.440661	62.801133	50.174519	50.134922	33.208828	33.207662	12.400164	-12.232837	-12.232837	-40.676747
.81	71.112630	63.879658	63.327276	50.585547	50.553428	33.562888	33.561995	12.690140	-12.014561	-12.014561	-40.539077
.82	71.753366	64.318420	63.845631	50.994609	50.968848	33.915356	33.914681	12.979013	-11.797018	-11.797018	-40.401830
.83	72.392478	64.756817	64.356199	51.401675	51.381273	34.266242	34.265739	13.266705	-11.580201	-11.580201	-40.265004
.84	73.029261	65.194713	64.859019	51.806719	51.790786	34.615557	34.615189	13.553486	-11.364105	-11.364105	-40.128593
.85	73.662937	65.631967	65.354170	52.209715	52.197468	34.963312	34.963048	13.839104	-11.148723	-11.148723	-39.992595
.86	74.292643	66.068432	65.841767	52.610642	52.601397	35.309517	35.309331	14.123655	-10.934051	-10.934051	-39.857007
.87	74.917426	66.503955	66.321959	53.009481	53.002643	35.654183	35.654057	14.407147	-10.720082	-10.720082	-39.721825
.88	75.536232	66.938379	66.794929	53.406213	53.401277	35.997323	35.997239	14.689590	-10.506810	-10.506810	-39.587046
.89	76.147901	67.371537	67.260885	53.800825	53.797360	36.338947	36.338893	14.970992	-10.294231	-10.294231	-39.452667
.90	76.751164	67.803260	67.720061	54.193305	54.190952	36.679066	36.679033	15.251361	-10.082337	-10.082337	-39.318684
.91	77.344645	68.233371	68.172711	54.583643	54.582108	37.017693	37.017673	15.530705	-9.871125	-9.871125	-39.185095
.92	77.928870	68.661687	68.619104	54.971832	54.970880	37.354837	37.354826	15.809032	-9.660589	-9.660589	-39.051896
.93	78.496292	69.088020	69.059524	55.357869	55.357314	37.690511	37.690506	16.086351	-9.450723	-9.450723	-38.919084
.94	79.051320	69.512178	69.494262	55.741750	55.741453	38.024727	38.024724	16.362670	-9.241522	-9.241522	-38.786657
.95	79.590371	69.933960	69.923615	56.123478	56.123335	38.357494	38.357493	16.637996	-9.032980	-9.032980	-38.654611
.96	80.111935	70.353164	70.347882	56.503054	56.502997	38.688825	38.688824	16.912337	-8.825094	-8.825094	-38.522943
.97	80.614651	70.769582	70.767361	56.880486	56.880468	39.018730	39.018730	17.185700	-8.617858	-8.617858	-38.391651
.98	81.097388	71.183004	71.182348	57.255780	57.255776	39.347220	39.347220	17.458094	-8.411267	-8.411267	-38.260732
.99	81.559321	71.593133	71.593133	57.628947	57.628947	39.674306	39.674306	17.729524	-8.205316	-8.205316	-38.130182
1.00	82.000000	72.000000	72.000000	58.000000	58.000000	40.000000	40.000000	18.000000	-8.000000	-8.000000	-38.000000



$J_{K_1 K_2}$	$J_{K_1 K_2}$	$9_{1,1}$	$9_{1,1}$	$9_{0,9}$	$10_{10,0}$	$10_{10,1}$	$10_{9,1}$	$10_{9,2}$	$10_{8,2}$	$10_{8,3}$	$10_{7,3}$	$10_{7,4}$	$10_{6,4}$
$J_{K_1 K_2}$	$J_{K_1 K_2}$	$9_{1,1}$	$9_{1,1}$	$9_{0,9}$	$10_{10,0}$	$10_{10,1}$	$10_{9,1}$	$10_{9,2}$	$10_{8,2}$	$10_{8,3}$	$10_{7,3}$	$10_{7,4}$	$10_{6,4}$
$K$	$K$	$9_{1,1}$	$9_{1,1}$	$9_{0,9}$	$10_{10,0}$	$10_{10,1}$	$10_{9,1}$	$10_{9,2}$	$10_{8,2}$	$10_{8,3}$	$10_{7,3}$	$10_{7,4}$	$10_{6,4}$
.00	.00	-53.504332	-77.320562	-77.320583	95.905729	95.905725	69.253465	69.253079	45.744324	45.730373	25.689636	25.435926	10.273643
.01	.01	-53.314221	-77.255914	-77.255933	95.977790	95.977785	69.465166	69.465181	46.091014	46.075548	26.180856	25.904954	10.959151
.02	.02	-53.125141	-77.191600	-77.191617	96.050230	96.050224	69.678928	69.678438	46.439808	46.422676	26.676121	26.376336	11.650686
.03	.03	-52.937078	-77.127614	-77.127629	96.123055	96.123048	69.893420	69.892868	46.798748	46.779782	27.175539	26.850074	12.348184
.04	.04	-52.750015	-77.063953	-77.063966	96.196271	96.196264	70.109111	70.108490	47.143873	47.122893	27.679224	27.326172	13.051569
.05	.05	-52.563937	-77.000610	-77.000622	96.269885	96.269877	70.326021	70.325322	47.499229	47.476036	28.187291	27.804630	13.760750
.06	.06	-52.378830	-76.937582	-76.937592	96.343903	96.343893	70.544168	70.543384	47.856860	47.831238	28.699858	28.285447	14.475625
.07	.07	-52.194679	-76.874865	-76.874874	96.418331	96.418320	70.763574	70.762693	48.216813	48.188526	29.217048	28.768622	15.196079
.08	.08	-52.011470	-76.812453	-76.812461	96.493176	96.493164	70.984260	70.983272	48.579137	48.547928	29.738984	29.254151	15.921984
.09	.09	-51.829190	-76.750343	-76.750350	96.568445	96.568431	71.206248	71.205140	48.943883	48.909472	30.265791	29.742030	16.653203
.10	.10	-51.647825	-76.688530	-76.688536	96.644145	96.644128	71.429560	71.428318	49.311103	49.273186	30.797600	30.232251	17.389586
.11	.11	-51.467362	-76.627011	-76.627016	96.720282	96.720264	71.654219	71.652829	49.680854	49.639099	31.334538	30.724809	18.130973
.12	.12	-51.287789	-76.565781	-76.565785	96.796866	96.796845	71.880250	71.878693	50.053194	50.007240	31.876738	31.219693	18.877194
.13	.13	-51.109094	-76.504836	-76.504840	96.873902	96.873878	72.107676	72.105935	50.428182	50.377637	32.424329	31.716892	19.628070
.14	.14	-50.931263	-76.444174	-76.444177	96.951400	96.951373	72.336524	72.334577	50.805881	50.750319	32.977444	32.216394	20.383414
.15	.15	-50.754286	-76.383789	-76.383792	97.029366	97.029336	72.566820	72.564644	51.186358	51.125317	33.536213	32.718185	21.143031
.16	.16	-50.578151	-76.323679	-76.323682	97.107811	97.107776	72.798590	72.796159	51.569682	51.502658	34.100764	33.222249	21.906719
.17	.17	-50.402848	-76.263840	-76.263843	97.186741	97.186702	73.031864	73.029149	51.955923	51.882374	34.671225	33.728568	22.674267
.18	.18	-50.228364	-76.204271	-76.204271	97.266167	97.266122	73.266669	73.263640	52.345159	52.264493	35.247719	34.237123	23.445462
.19	.19	-50.054689	-76.144961	-76.144963	97.346096	97.346046	73.503037	73.499658	52.737467	52.649045	35.830366	34.747891	24.220081
.20	.20	-49.881814	-76.085915	-76.085915	97.426540	97.426482	73.740999	73.737230	53.132931	53.036059	36.419280	35.260851	24.997899
.21	.21	-49.709727	-76.027124	-76.027125	97.507507	97.507441	73.980586	73.976385	53.531636	53.425565	37.014571	35.775976	25.778684
.22	.22	-49.538418	-75.968589	-75.968590	97.589007	97.588933	74.221832	74.217153	53.933674	53.817593	37.616338	36.293240	26.562201
.23	.23	-49.367879	-75.910304	-75.910306	97.671051	97.670968	74.464773	74.459561	54.339139	54.212172	38.224677	36.812614	27.348210
.24	.24	-49.198099	-75.852268	-75.852269	97.753650	97.753555	74.709444	74.703642	54.748132	54.609331	38.839671	37.334066	28.136468
.25	.25	-49.029069	-75.794477	-75.794478	97.836814	97.836707	74.955883	74.949426	55.160755	55.009098	39.461395	37.857564	28.926727
.26	.26	-48.860779	-75.736928	-75.736929	97.920556	97.920435	75.204130	75.196947	55.577119	55.411503	40.089911	38.383072	29.718737
.27	.27	-48.693222	-75.679618	-75.679619	98.004886	98.004750	75.454224	75.446236	55.997338	55.816573	40.725271	38.910555	30.512242
.28	.28	-48.526387	-75.622545	-75.622545	98.089818	98.089664	75.706209	75.697329	56.421530	56.224336	41.367511	39.439971	31.306985
.29	.29	-48.360267	-75.565705	-75.565706	98.175364	98.175190	75.960129	75.950260	56.849823	56.634820	42.016656	39.971281	32.102704
.30	.30	-48.194853	-75.509096	-75.509097	98.261337	98.261341	76.216030	76.205066	57.282346	57.048051	42.672715	40.504442	32.899135
.31	.31	-48.030137	-75.452716	-75.452716	98.348352	98.348130	76.473960	76.461784	57.719236	57.464055	43.335681	41.039407	33.696010
.32	.32	-47.866111	-75.396561	-75.396561	98.435821	98.435571	76.733970	76.720451	58.160636	57.882857	44.005532	41.576129	34.493056
.33	.33	-47.702766	-75.340629	-75.340629	98.523961	98.523678	76.996112	76.981107	58.606696	58.304482	44.682230	42.114560	35.289993
.34	.34	-47.540095	-75.284917	-75.284918	98.612786	98.612467	77.260443	77.243792	59.057571	58.728953	45.365719	42.654647	36.086557
.35	.35	-47.378091	-75.229424	-75.229424	98.702312	98.701952	77.527020	77.508548	59.513422	59.156293	46.055928	43.196336	36.882451
.36	.36	-47.216745	-75.174147	-75.174147	98.792556	98.792150	77.795904	77.775417	59.974416	59.586524	46.752769	43.739573	37.677393
.37	.37	-47.056051	-75.119082	-75.119082	98.883077	98.883077	78.067159	78.044443	60.440730	60.019666	47.456137	44.284299	38.471093
.38	.38	-46.896001	-75.064229	-75.064229	98.975267	98.974750	78.340853	78.315671	60.912541	60.455738	48.165911	44.830454	39.263259
.39	.39	-46.736589	-75.009584	-75.009584	99.067771	99.067188	78.617055	78.589147	61.390036	60.894758	48.881952	45.377976	40.053593
.40	.40	-46.577807	-74.955146	-74.955146	99.161067	99.160409	78.895842	78.864919	61.873407	61.336743	49.604109	45.926801	40.841795
.41	.41	-46.419649	-74.900912	-74.900912	99.255174	99.254432	79.177291	79.143035	62.362850	61.781706	50.332214	46.476863	41.627564
.42	.42	-46.262106	-74.846880	-74.846880	99.350115	99.349278	79.461485	79.423545	62.858565	62.229661	51.066084	47.028094	42.410594
.43	.43	-46.105174	-74.793047	-74.793047	99.445911	99.444968	79.748513	79.706500	63.360757	62.680620	51.805523	47.580424	43.190578
.44	.44	-45.948846	-74.739413	-74.739413	99.542586	99.541522	80.038468	79.991954	63.869633	63.134592	52.550322	48.133779	43.967209
.45	.45	-45.793115	-74.685974	-74.685974	99.640165	99.638965	80.331447	80.279960	64.385403	63.591584	53.300257	48.688087	44.740180
.46	.46	-45.637976	-74.632729	-74.632729	99.738673	99.737320	80.627556	80.570574	64.908276	64.051602	54.055095	49.243271	45.509183
.47	.47	-45.483422	-74.579676	-74.579676	99.836611	99.836611	80.926904	80.863852	65.438461	64.514649	54.814590	49.799253	46.273913
.48	.48	-45.329446	-74.526813	-74.526813	99.938587	99.938587	81.229609	81.159853	65.976166	64.980725	55.578484	50.355953	47.034069
.49	.49	-45.176044	-74.474137	-74.474137	100.040051	100.040051	81.535798	81.458636	66.521593	65.449829	56.346510	50.913288	47.789354
.50	.50	-45.023210	-74.421647	-74.421647	100.142561	100.142561	81.845601	81.760262	67.074940	65.921956	57.118390	51.471176	48.539478



$J_{K_1K_2}$		$9_{1,0}$ $9_{-7}$	$9_{1,9}$ $9_{-8}$	$9_{0,9}$ $9_{-9}$	$10_{10,0}$ $10_{10}$	$10_{10,1}$ $10_9$	$10_{9,1}$ $10_8$	$10_{9,2}$ $10_7$	$10_{8,2}$ $10_6$	$10_{8,3}$ $10_5$	$10_{7,3}$ $10_4$	$10_{7,4}$ $10_3$	$10_{6,4}$ $10_2$
$J$	$K$												
.50		-45.023210	-74.421647	-74.421647	100.142561	100.140369	81.835601	81.760262	67.074940	65.921956	57.118390	51.471176	48.539478
.51		-44.870937	-74.369341	-74.369341	100.246151	100.243677	82.159162	82.064794	67.616197	66.397099	57.891834	52.029530	49.284159
.52		-44.719220	-74.317218	-74.317218	100.350856	100.348063	82.476632	82.372295	68.206142	66.875249	58.672545	52.586263	50.023126
.53		-44.568053	-74.265275	-74.265275	100.456712	100.453560	82.799170	82.682831	68.734344	67.356392	59.454214	53.147287	50.756117
.54		-44.417432	-74.213511	-74.213511	100.563761	100.560201	83.123951	82.996468	69.371155	67.840512	60.238522	53.706511	51.482889
.55		-44.267350	-74.161924	-74.161924	100.672042	100.668022	83.454156	83.313273	69.966713	68.327590	61.025140	54.265841	52.203211
.56		-44.117803	-74.110512	-74.110512	100.781602	100.777060	83.783984	83.633317	70.571134	68.817603	61.813729	54.825186	52.916872
.57		-43.968786	-74.059273	-74.059273	100.892487	100.887354	84.128643	83.956669	71.184516	69.310525	62.603936	55.384449	53.623682
.58		-43.820293	-74.008207	-74.008207	101.004749	100.998945	84.473358	84.283401	71.606930	69.806326	63.395401	55.943534	54.323470
.59		-43.672319	-73.957310	-73.957310	101.118440	101.111876	84.823368	84.613586	72.438426	70.304972	64.187746	56.502343	55.016091
.60		-43.524859	-73.906583	-73.906583	101.233620	101.226194	85.178932	84.947298	73.079023	70.806425	64.980584	57.060777	55.701423
.61		-43.377909	-73.856022	-73.856022	101.350350	101.341945	85.540321	85.284610	73.728716	71.310644	65.773513	57.618736	56.379369
.62		-43.231463	-73.805627	-73.805627	101.468697	101.459180	85.907830	85.625599	74.387466	71.817582	66.566115	58.176120	57.049860
.63		-43.085518	-73.755396	-73.755396	101.588733	101.577952	86.281770	85.970342	75.055208	72.327168	67.357958	58.732825	57.712653
.64		-42.940068	-73.705327	-73.705327	101.710536	101.698317	86.662473	86.318915	75.731842	72.839409	68.148593	59.288751	58.368329
.65		-42.795109	-73.655420	-73.655420	101.834189	101.820333	87.050294	86.671397	76.417240	73.354182	68.937554	59.843793	59.016299
.66		-42.650637	-73.605672	-73.605672	101.959766	101.944063	87.445606	87.027864	77.111241	73.871444	69.724358	60.397850	59.656795
.67		-42.506647	-73.556082	-73.556082	102.087424	102.069574	87.843809	87.388397	77.813655	74.391123	70.508503	60.950816	60.289876
.68		-42.363134	-73.506649	-73.506649	102.217212	102.196933	88.260319	87.753073	78.524259	74.913145	71.289471	61.502589	60.915621
.69		-42.220095	-73.457371	-73.457371	102.349270	102.326216	88.680579	88.121970	79.242602	75.437428	72.066726	62.053065	61.534131
.70		-42.077525	-73.408247	-73.408247	102.483727	102.457499	89.110046	88.495167	79.969002	75.963884	72.839716	62.602141	62.145527
.71		-41.935420	-73.359275	-73.359275	102.620728	102.590866	89.549201	88.872741	80.703551	76.492420	73.607875	63.149715	62.749943
.72		-41.793775	-73.310455	-73.310455	102.760430	102.726403	89.998537	89.254770	81.443108	77.022937	74.370625	63.695687	63.347531
.73		-41.652588	-73.261784	-73.261784	102.903010	102.864204	90.458562	89.641329	82.190306	77.555328	75.127377	64.239954	63.938453
.74		-41.511854	-73.213263	-73.213263	103.048662	103.004366	90.929790	90.032493	82.943751	78.089480	75.877542	64.782419	64.522882
.75		-41.371569	-73.164888	-73.164888	103.197606	103.146994	91.412739	90.428336	83.703015	78.625271	76.620529	65.322985	65.100999
.76		-41.231729	-73.116660	-73.116660	103.350084	103.292193	91.907920	90.826929	84.467642	79.162574	77.355755	65.861555	65.672988
.77		-41.092331	-73.068576	-73.068576	103.506373	103.440096	92.415837	91.234342	85.237143	79.701251	78.082652	66.398036	66.239039
.78		-40.953370	-73.020636	-73.020636	103.666782	103.590814	92.936969	91.644644	86.010991	80.241158	78.800676	66.932338	66.799342
.79		-40.814843	-72.972838	-72.972838	103.831662	103.744483	93.471770	92.059898	86.788619	80.782141	79.509314	67.464373	67.354089
.80		-40.676747	-72.925182	-72.925182	104.001413	103.901244	94.020650	92.480168	87.569415	81.324036	80.208097	67.994055	67.903469
.81		-40.539077	-72.877665	-72.877665	104.176490	104.061249	94.583973	92.905513	88.352714	81.866671	80.896607	68.521303	68.447665
.82		-40.401830	-72.830287	-72.830287	104.357415	104.246555	95.162044	93.359899	89.137789	82.409863	81.574487	69.046039	68.986861
.83		-40.265004	-72.783047	-72.783047	104.544789	104.391633	95.755101	93.771648	89.923840	82.953416	82.241448	69.568188	69.521232
.84		-40.128593	-72.735944	-72.735944	104.739303	104.562362	96.363307	94.212538	90.709985	83.497127	82.897280	70.087680	70.050948
.85		-39.992595	-72.688976	-72.688976	104.941757	104.737034	96.986746	94.658706	91.495239	84.040778	83.541855	70.604449	70.576170
.86		-39.857007	-72.642142	-72.642142	105.153077	104.915852	97.625418	95.110190	92.278500	84.584139	84.175127	71.118434	71.097055
.87		-39.721825	-72.595442	-72.595442	105.374336	105.099031	98.279241	95.567027	93.058526	85.126969	84.797138	71.629578	71.613747
.88		-39.587046	-72.548874	-72.548874	105.606781	105.286799	98.948049	96.029247	93.833913	85.669012	85.408013	72.137831	72.126387
.89		-39.452667	-72.502437	-72.502437	105.851850	105.479397	99.631600	96.496877	94.603071	86.209999	86.007957	72.643145	72.635102
.90		-39.318684	-72.456130	-72.456130	106.111206	105.677082	100.329578	96.969936	95.364197	86.749646	86.597249	73.145480	73.140013
.91		-39.185095	-72.409953	-72.409953	106.386750	105.880124	101.041605	97.448442	96.115260	87.287656	87.176233	73.644801	73.641232
.92		-39.051896	-72.363903	-72.363903	106.680637	106.088805	101.767246	97.932405	96.853983	87.823717	87.745308	74.141077	74.138861
.93		-38.919084	-72.317980	-72.317980	106.995269	106.303425	102.506023	98.421829	97.577851	88.357502	88.304921	74.634285	74.632994
.94		-38.786657	-72.272184	-72.272184	107.333269	106.524297	103.257421	98.916714	98.284137	88.888671	88.855554	75.124406	75.123713
.95		-38.654611	-72.226513	-72.226513	107.697413	106.751747	104.020900	99.417054	98.969973	89.416868	89.397717	75.611428	75.611096
.96		-38.522943	-72.180965	-72.180965	108.090513	106.986117	104.795907	99.922838	99.632460	89.941725	89.931936	76.095208	76.095208
.97		-38.391651	-72.135541	-72.135541	108.515259	107.227758	105.581879	100.434050	100.268833	90.462862	90.458742	76.576151	76.576109
.98		-38.260732	-72.090240	-72.090240	108.974009	107.477036	106.378253	100.950666	100.876665	90.979889	90.978672	77.053856	77.053856
.99		-38.130182	-72.045059	-72.045059	109.468570	107.74323	107.184474	101.472660	101.454090	91.492403	91.492252	77.528467	77.528466
1.00		-38.000000	-72.000000	-72.000000	110.000000	108.000000	108.000000	102.000000	102.000000	92.000000	92.000000	78.000000	78.000000

$J_{K_1K_2}$	$10_{6,5}$ $10_1$	$10_{5,5}$ $10_0$	$10_{5,6}$ $10_{-1}$	$10_{4,6}$ $10_{-2}$	$10_{4,7}$ $10_{-3}$	$10_{3,7}$ $10_{-4}$	$10_{3,8}$ $10_{-5}$	$10_{2,8}$ $10_{-6}$	$10_{2,9}$ $10_{-7}$	$10_{1,9}$ $10_{-8}$	$10_{1,10}$ $10_{-9}$	$10_{0,10}$ $10_{-10}$
$K$												
.00	8.052907	0.000000	-8.052907	-10.273643	-25.435926	-25.689636	-45.730373	-45.744324	-69.253079	-69.253465	-95.905725	-95.905729
.01	8.608031	0.798341	-7.498971	-9.594212	-24.969248	-25.202356	-45.387125	-45.399700	-69.042116	-69.042458	-95.834039	-95.834043
.02	9.164289	1.596439	-6.946274	-8.920896	-24.504915	-24.718911	-45.045777	-45.057104	-68.832274	-68.832578	-95.762724	-95.762724
.03	9.721626	2.394050	-6.394870	-8.253717	-24.042919	-24.239204	-44.706307	-44.716501	-68.623538	-68.623806	-95.691766	-95.691769
.04	10.279986	3.190930	-5.844806	-7.592688	-23.583253	-23.763139	-44.368688	-44.377855	-68.415890	-68.416127	-95.621168	-95.621171
.05	10.839312	3.986836	-5.296133	-6.937806	-23.125910	-23.290623	-44.032896	-44.041134	-68.209315	-68.209525	-95.550923	-95.550925
.06	11.399546	4.781524	-4.748898	-6.289058	-22.670879	-22.821567	-43.698907	-43.706304	-68.003799	-68.003984	-95.481027	-95.481027
.07	11.960630	5.574752	-4.203147	-5.646418	-22.218151	-22.355886	-43.366699	-43.373334	-67.799489	-67.799489	-95.411469	-95.411471
.08	12.522503	6.366277	-3.658925	-5.009851	-21.767715	-21.893497	-43.036247	-43.042194	-67.595880	-67.596024	-95.342251	-95.342252
.09	13.085104	7.155857	-3.116275	-4.379309	-21.319559	-21.434321	-42.707529	-42.712855	-67.393448	-67.393575	-95.273367	-95.273367
.10	13.648373	7.943250	-2.575238	-3.754737	-20.873671	-20.978282	-42.380522	-42.385287	-67.192017	-67.192128	-95.204809	-95.204810
.11	14.212246	8.728218	-2.033587	-3.136069	-20.430037	-20.525306	-42.055205	-42.059464	-66.991572	-66.991670	-95.136575	-95.136576
.12	14.776660	9.510522	-1.498169	-2.523232	-19.988645	-20.075324	-41.731555	-41.735359	-66.792186	-66.792186	-95.068662	-95.068662
.13	15.341552	10.289924	-0.962212	-1.916144	-19.549480	-19.628267	-41.409552	-41.412946	-66.593587	-66.593663	-95.001063	-95.001064
.14	15.906858	11.066190	-0.428022	-1.314721	-19.112528	-19.184070	-41.089173	-41.092199	-66.396022	-66.396088	-94.933775	-94.933776
.15	16.472511	11.839089	0.104365	-0.718867	-18.677773	-18.742672	-40.770400	-40.773094	-66.199392	-66.199450	-94.866795	-94.866795
.16	17.038448	12.608392	0.634918	-0.128487	-18.245199	-18.304013	-40.453211	-40.455607	-66.003683	-66.003734	-94.800117	-94.800117
.17	17.604600	13.373875	1.163606	0.456521	-17.814791	-17.868034	-40.137586	-40.139715	-65.808886	-65.808930	-94.733738	-94.733738
.18	18.170904	14.135317	1.690397	1.036262	-17.386532	-17.434682	-39.823507	-39.825396	-65.614986	-65.615025	-94.667654	-94.667654
.19	18.737290	14.892506	2.215265	1.610845	-16.960406	-17.003902	-39.510953	-39.512628	-65.421975	-65.422008	-94.601862	-94.601862
.20	19.303692	15.645232	2.738181	2.180377	-16.536396	-16.575644	-39.199906	-39.201389	-65.229839	-65.229868	-94.536357	-94.536357
.21	19.870044	16.393296	3.259121	2.744969	-16.114483	-16.149860	-38.890347	-38.891659	-65.038568	-65.038593	-94.471136	-94.471137
.22	20.436276	17.136503	3.778062	3.304732	-15.694652	-15.726501	-38.582259	-38.583418	-64.848173	-64.848173	-94.406196	-94.406197
.23	21.002322	17.874670	4.294981	3.859777	-15.276884	-15.305524	-38.275622	-38.276645	-64.658578	-64.658597	-94.341534	-94.341534
.24	21.568113	18.607623	4.809857	4.410216	-14.861161	-14.886885	-37.970421	-37.971322	-64.469838	-64.469854	-94.277144	-94.277145
.25	22.133581	19.335198	5.322672	4.956158	-14.447466	-14.470541	-37.666637	-37.667430	-64.281921	-64.281935	-94.213026	-94.213026
.26	22.698660	20.057242	5.833408	5.497712	-14.035780	-14.056453	-37.364253	-37.364950	-64.094830	-64.094830	-94.149174	-94.149175
.27	23.263280	20.773616	6.342049	6.034985	-13.626086	-13.644583	-37.063253	-37.063865	-63.908518	-63.908528	-94.085587	-94.085587
.28	23.827375	21.484192	6.848581	6.568083	-13.218364	-13.234892	-36.763621	-36.764157	-63.723012	-63.723021	-94.022261	-94.022261
.29	24.390876	22.188858	7.352990	7.097109	-12.812596	-12.827345	-36.465340	-36.465809	-63.538291	-63.538298	-93.959192	-93.959192
.30	24.953718	22.887515	7.855265	7.622164	-12.408765	-12.421908	-36.168395	-36.168805	-63.354345	-63.354352	-93.896378	-93.896378
.31	25.515833	23.580077	8.353396	8.143346	-12.006853	-12.018547	-35.872770	-35.873128	-63.171166	-63.171171	-93.833816	-93.833816
.32	26.077155	24.266477	8.853374	8.660751	-11.606839	-11.617230	-35.578451	-35.578762	-62.988749	-62.988749	-93.771504	-93.771504
.33	26.637619	24.946659	9.349191	9.174473	-11.208708	-11.217926	-35.285421	-35.285692	-62.807072	-62.807076	-93.709437	-93.709437
.34	27.197159	25.620584	9.842842	9.684602	-10.812439	-10.820604	-34.993667	-34.993902	-62.626140	-62.626143	-93.647614	-93.647614
.35	27.755710	26.288230	10.334321	10.191224	-10.418016	-10.425236	-34.703174	-34.703378	-62.445940	-62.445943	-93.586031	-93.586031
.36	28.313209	26.949587	10.823625	10.694426	-10.025420	-10.031795	-34.413929	-34.414105	-62.266464	-62.266467	-93.524687	-93.524687
.37	28.869594	27.604661	11.310751	11.194287	-9.634633	-9.640251	-34.125916	-34.126068	-62.087704	-62.087707	-93.463578	-93.463578
.38	29.424801	28.253471	11.795699	11.690887	-9.245637	-9.250580	-33.839123	-33.839254	-61.909653	-61.909655	-93.402702	-93.402702
.39	29.978770	28.896052	12.278468	12.184303	-8.858416	-8.862757	-33.553535	-33.553648	-61.732302	-61.732303	-93.342056	-93.342056
.40	30.531441	29.532448	12.759059	12.674605	-8.472950	-8.476755	-33.269141	-33.269238	-61.555643	-61.555645	-93.281638	-93.281638
.41	31.082754	30.162718	13.237474	13.161866	-8.089223	-8.092551	-32.985927	-32.986010	-61.379671	-61.379672	-93.221445	-93.221445
.42	31.632652	30.786930	13.713716	13.646152	-7.707217	-7.710123	-32.703880	-32.703951	-61.204376	-61.204377	-93.161475	-93.161475
.43	32.181078	31.405163	14.187790	14.127528	-7.326915	-7.329447	-32.422988	-32.423048	-61.029752	-61.029753	-93.101726	-93.101726
.44	32.727977	32.017504	14.659700	14.606056	-6.948300	-6.950502	-32.143239	-32.143290	-60.855792	-60.855792	-93.042195	-93.042195
.45	33.273295	32.624050	15.129452	15.081795	-6.571356	-6.573266	-31.864620	-31.864663	-60.682488	-60.682489	-92.982881	-92.982881
.46	33.816979	33.224903	15.597054	15.554803	-6.196066	-6.197719	-31.587120	-31.587156	-60.509835	-60.509836	-92.923780	-92.923780
.47	34.358978	33.820171	16.062511	16.025135	-5.822413	-5.823840	-31.310726	-31.310757	-60.337825	-60.337826	-92.864890	-92.864890
.48	34.899243	34.409968	16.525833	16.492842	-5.450381	-5.451610	-31.035429	-31.035455	-60.166452	-60.166453	-92.806210	-92.806210
.49	35.437726	34.994411	16.987029	16.957976	-5.079953	-5.081009	-30.761216	-30.761238	-59.995710	-59.995710	-92.747738	-92.747738
.50	35.974381	35.573619	17.446108	17.420584	-4.711115	-4.712020	-30.488076	-30.488094	-59.825591	-59.825591	-92.689470	-92.689470



$J_{K_1 K_2}$	$10_{\square, 5}$		$10_{5, 5}$		$10_{4, 6}$		$10_{3, 7}$		$10_{3, 8}$		$10_{2, 8}$		$10_{2, 9}$		$10_{1, 9}$		$10_{1, 10}$		$10_{0, 10}$					
	$10_{\square, 5}$	$10_5$	$10_{5, 5}$	$10_{4, 6}$	$10_{3, 7}$	$10_{3, 8}$	$10_{2, 8}$	$10_{2, 9}$	$10_{1, 9}$	$10_{1, 10}$	$10_{0, 10}$	$10_{-10}$	$10_{-9}$	$10_{-8}$	$10_{-7}$	$10_{-6}$	$10_{-5}$	$10_{-4}$	$10_{-3}$	$10_{-2}$	$10_{-1}$	$10_0$	$10_5$	$10_{\square, 5}$
$\kappa$																								
.50	35.974381	35.573619	17.446108	17.420584	-4.711115	-4.712020	-30.488076	-59.825591	-59.825591	-30.488076	-30.488076	-92.689470	-92.689470	-59.825591	-59.825591	-30.488076	-30.488076	-92.689470	-92.689470	-92.689470	-92.689470	-92.689470	-92.689470	-92.689470
.51	36.509163	36.147716	17.903080	17.880712	-4.343650	-4.344623	-30.215998	-59.656090	-59.656090	-30.215998	-30.215998	-92.631406	-92.631406	-59.656090	-59.656090	-30.215998	-30.215998	-92.631406	-92.631406	-92.631406	-92.631406	-92.631406	-92.631406	-92.631406
.52	37.042031	36.716825	18.357957	18.338405	-3.978802	-3.978802	-29.944973	-59.487200	-59.487200	-29.944973	-29.944973	-92.573543	-92.573543	-59.487200	-59.487200	-29.944973	-29.944973	-92.573543	-92.573543	-92.573543	-92.573543	-92.573543	-92.573543	-92.573543
.53	37.572943	37.281070	18.810749	18.793704	-3.614538	-3.614538	-29.674988	-59.318916	-59.318916	-29.674988	-29.674988	-92.515880	-92.515880	-59.318916	-59.318916	-29.674988	-29.674988	-92.515880	-92.515880	-92.515880	-92.515880	-92.515880	-92.515880	-92.515880
.54	38.101860	37.640574	19.261469	19.246651	-3.251342	-3.251342	-29.406035	-59.151231	-59.151231	-29.406035	-29.406035	-92.458413	-92.458413	-59.151231	-59.151231	-29.406035	-29.406035	-92.458413	-92.458413	-92.458413	-92.458413	-92.458413	-92.458413	-92.458413
.55	38.628746	38.395460	19.710128	19.697284	-2.890218	-2.890218	-28.871180	-58.984140	-58.984140	-28.871180	-28.871180	-92.401142	-92.401142	-58.984140	-58.984140	-28.871180	-28.871180	-92.401142	-92.401142	-92.401142	-92.401142	-92.401142	-92.401142	-92.401142
.56	39.153565	38.945851	20.156740	20.145640	-2.530591	-2.530591	-28.605259	-58.817637	-58.817637	-28.605259	-28.605259	-92.344064	-92.344064	-58.817637	-58.817637	-28.605259	-28.605259	-92.344064	-92.344064	-92.344064	-92.344064	-92.344064	-92.344064	-92.344064
.57	39.676285	39.491866	20.601318	20.591755	-2.172447	-2.172447	-28.340329	-58.651716	-58.651716	-28.340329	-28.340329	-92.287178	-92.287178	-58.651716	-58.651716	-28.340329	-28.340329	-92.287178	-92.287178	-92.287178	-92.287178	-92.287178	-92.287178	-92.287178
.58	40.196874	40.033621	21.043875	21.035664	-1.815773	-1.815773	-28.076384	-58.486372	-58.486372	-28.076384	-28.076384	-92.230481	-92.230481	-58.486372	-58.486372	-28.076384	-28.076384	-92.230481	-92.230481	-92.230481	-92.230481	-92.230481	-92.230481	-92.230481
.59	40.715304	40.571233	21.484424	21.477399	-1.460553	-1.460553	-27.813408	-58.321599	-58.321599	-27.813408	-27.813408	-92.173973	-92.173973	-58.321599	-58.321599	-27.813408	-27.813408	-92.173973	-92.173973	-92.173973	-92.173973	-92.173973	-92.173973	-92.173973
.60	41.231547	41.104812	21.922981	21.916991	-1.106775	-1.106775	-27.551395	-58.157391	-58.157391	-27.551395	-27.551395	-92.117650	-92.117650	-58.157391	-58.157391	-27.551395	-27.551395	-92.117650	-92.117650	-92.117650	-92.117650	-92.117650	-92.117650	-92.117650
.61	41.745579	41.634467	22.359558	22.354471	-0.754557	-0.754557	-27.290334	-57.993745	-57.993745	-27.290334	-27.290334	-92.061512	-92.061512	-57.993745	-57.993745	-27.290334	-27.290334	-92.061512	-92.061512	-92.061512	-92.061512	-92.061512	-92.061512	-92.061512
.62	42.257376	42.160302	22.794172	22.789868	-0.403486	-0.403486	-27.030221	-57.830653	-57.830653	-27.030221	-27.030221	-92.005557	-92.005557	-57.830653	-57.830653	-27.030221	-27.030221	-92.005557	-92.005557	-92.005557	-92.005557	-92.005557	-92.005557	-92.005557
.63	42.766919	42.682421	23.226836	23.223211	-0.053948	-0.053948	-26.771044	-57.668111	-57.668111	-26.771044	-26.771044	-91.949783	-91.949783	-57.668111	-57.668111	-26.771044	-26.771044	-91.949783	-91.949783	-91.949783	-91.949783	-91.949783	-91.949783	-91.949783
.64	43.274188	43.200919	23.657565	23.654525	0.294201	0.294201	-26.512795	-57.506115	-57.506115	-26.512795	-26.512795	-91.894188	-91.894188	-57.506115	-57.506115	-26.512795	-26.512795	-91.894188	-91.894188	-91.894188	-91.894188	-91.894188	-91.894188	-91.894188
.65	43.779165	43.715891	24.086375	24.083837	0.640918	0.640918	-26.255465	-57.344658	-57.344658	-26.255465	-26.255465	-91.838771	-91.838771	-57.344658	-57.344658	-26.255465	-26.255465	-91.838771	-91.838771	-91.838771	-91.838771	-91.838771	-91.838771	-91.838771
.66	44.281838	44.227428	24.513280	24.511172	0.986343	0.986343	-25.999045	-57.183737	-57.183737	-25.999045	-25.999045	-91.783530	-91.783530	-57.183737	-57.183737	-25.999045	-25.999045	-91.783530	-91.783530	-91.783530	-91.783530	-91.783530	-91.783530	-91.783530
.67	44.782192	44.735614	24.930296	24.936554	1.330456	1.330456	-25.743529	-57.023346	-57.023346	-25.743529	-25.743529	-91.728463	-91.728463	-57.023346	-57.023346	-25.743529	-25.743529	-91.728463	-91.728463	-91.728463	-91.728463	-91.728463	-91.728463	-91.728463
.68	45.280216	45.240534	25.361437	25.360006	1.673184	1.673184	-25.488907	-56.863480	-56.863480	-25.488907	-25.488907	-91.673570	-91.673570	-56.863480	-56.863480	-25.488907	-25.488907	-91.673570	-91.673570	-91.673570	-91.673570	-91.673570	-91.673570	-91.673570
.69	45.775902	45.742264	25.782719	25.781550	2.014564	2.014564	-25.235171	-56.704135	-56.704135	-25.235171	-25.235171	-91.618848	-91.618848	-56.704135	-56.704135	-25.235171	-25.235171	-91.618848	-91.618848	-91.618848	-91.618848	-91.618848	-91.618848	-91.618848
.70	46.269242	46.240881	26.202158	26.201209	2.354679	2.354679	-24.982314	-56.545306	-56.545306	-24.982314	-24.982314	-91.564295	-91.564295	-56.545306	-56.545306	-24.982314	-24.982314	-91.564295	-91.564295	-91.564295	-91.564295	-91.564295	-91.564295	-91.564295
.71	46.760230	46.736455	26.619768	26.619003	2.693456	2.693456	-24.730327	-56.386989	-56.386989	-24.730327	-24.730327	-91.509911	-91.509911	-56.386989	-56.386989	-24.730327	-24.730327	-91.509911	-91.509911	-91.509911	-91.509911	-91.509911	-91.509911	-91.509911
.72	47.248864	47.229054	27.035565	27.034952	3.030972	3.030972	-24.479204	-56.229179	-56.229179	-24.479204	-24.479204	-91.455694	-91.455694	-56.229179	-56.229179	-24.479204	-24.479204	-91.455694	-91.455694	-91.455694	-91.455694	-91.455694	-91.455694	-91.455694
.73	47.735140	47.718742	27.449563	27.449077	3.367197	3.367197	-24.228937	-56.071871	-56.071871	-24.228937	-24.228937	-91.401643	-91.401643	-56.071871	-56.071871	-24.228937	-24.228937	-91.401643	-91.401643	-91.401643	-91.401643	-91.401643	-91.401643	-91.401643
.74	48.219059	48.205579	27.861779	27.861396	3.702155	3.702155	-23.979517	-55.915062	-55.915062	-23.979517	-23.979517	-91.347755	-91.347755	-55.915062	-55.915062	-23.979517	-23.979517	-91.347755	-91.347755	-91.347755	-91.347755	-91.347755	-91.347755	-91.347755
.75	48.700622	48.689624	28.272227	28.271927	4.035853	4.035853	-23.730938	-55.758747	-55.758747	-23.730938	-23.730938	-91.294030	-91.294030	-55.758747	-55.758747	-23.730938	-23.730938	-91.294030	-91.294030	-91.294030	-91.294030	-91.294030	-91.294030	-91.294030
.76	49.179831	49.170931	28.680921	28.680690	4.368317	4.368317	-23.483194	-55.602921	-55.602921	-23.483194	-23.483194	-91.240467	-91.240467	-55.602921	-55.602921	-23.483194	-23.483194	-91.240467	-91.240467	-91.240467	-91.240467	-91.240467	-91.240467	-91.240467
.77	49.656689	49.649551	29.087877	29.087700	4.699541	4.699541	-23.236275	-55.447582	-55.447582	-23.236275	-23.236275	-91.187063	-91.187063	-55.447582	-55.447582	-23.236275	-23.236275	-91.187063	-91.187063	-91.187063	-91.187063	-91.187063	-91.187063	-91.187063
.78	50.131204	50.125532	29.493110	29.492976	5.029544	5.029544	-22.990176	-55.292723	-55.292723	-22.990176	-22.990176	-91.133817	-91.133817	-55.292723	-55.292723	-22.990176	-22.990176	-91.133817	-91.133817	-91.133817	-91.133817	-91.133817	-91.133817	-91.133817
.79	50.603380	50.598921	29.896634	29.896533	5.358337	5.358337	-22.744890	-55.138342	-55.138342	-22.744890	-22.744890	-91.080729	-91.080729	-55.138342	-55.138342	-22.744890	-22.744890	-91.080729	-91.080729	-91.080729	-91.080729	-91.080729	-91.080729	-91.080729
.80	51.073226	51.069760	30.298463	30.298389	5.685927	5.685927	-22.500410	-54.984435	-54.984435	-22.500410	-22.500410	-91.027797	-91.027797	-54.984435	-54.984435	-22.500410	-22.500410	-91.027797	-91.027797	-91.027797	-91.027797	-91.027797	-91.027797	-91.027797
.81	51.540751	51.538091	30.698612	30.698558	6.012325	6.012325	-22.256728	-54.830997	-54.830997	-22.256728	-22.256728	-90.975019	-90.975019	-54.830997	-54.830997	-22.256728	-22.256728	-90.975019	-90.975019	-90.975019	-90.975019	-90.975019	-90.975019	-90.975019
.82	52.005964	52.003952	31.097095	31.097056	6.337541	6.337541	-22.013840	-54.678024	-54.678024	-22.013840	-22.013840	-90.922394	-90.922394	-54.678024	-54.678024	-22.013840	-22.013840	-90.922394	-90.922394	-90.922394	-90.922394	-90.922394	-90.922394	-90.922394
.83	52.468878	52.467378	31.493925	31.4																				



$J_K, K_1$	$J_r$	$11_{11,0}$	$11_{11,1}$	$11_{10,1}$	$11_{10,2}$	$11_{9,2}$	$11_{9,3}$	$11_{8,3}$	$11_{8,4}$	$11_{7,4}$	$11_{7,5}$	$11_{6,5}$	$11_{6,6}$
$K$		$11_{11}$	$11_{10}$	$11_9$	$11_8$	$11_7$	$11_6$	$11_5$	$11_4$	$11_3$	$11_2$	$11_1$	$11_0$
.00		116.491011	116.491010	87.004844	87.004758	60.636950	60.633351	37.578159	37.498959	18.528459	17.590939	5.073416	0.000000
.01		116.570147	116.570146	87.238086	87.237987	61.017653	61.013604	38.108034	38.020543	19.246058	18.234087	6.002491	0.694530
.02		116.649698	116.649696	87.472591	87.472479	61.400564	61.396015	38.641635	38.545066	19.970846	18.879736	6.936016	1.388969
.03		116.729670	116.729669	87.708380	87.708251	61.785724	61.780614	39.179057	39.072555	20.702957	19.527845	7.873687	2.083227
.04		116.810070	116.810069	87.945471	87.945325	62.173169	62.167435	39.720394	39.603034	21.442519	20.178371	8.815195	2.777213
.05		116.890905	116.890904	88.183887	88.183720	62.562941	62.556511	40.265749	40.136530	22.189651	20.831268	9.760223	3.470836
.06		116.972182	116.972180	88.423649	88.423458	62.955082	62.947876	40.815229	40.673064	22.944459	21.486486	10.708453	4.164007
.07		117.053908	117.053905	88.664777	88.664561	63.349635	63.341565	41.368942	41.212661	23.707040	22.143976	11.659557	4.856636
.08		117.136089	117.136086	88.907296	88.907049	63.746645	63.737614	41.927007	41.755343	24.477475	22.803682	12.613209	5.548635
.09		117.218734	117.218731	89.151228	89.150948	64.146159	64.136059	42.489543	42.301130	25.255832	23.465549	13.569075	6.239915
.10		117.301850	117.301846	89.396597	89.396279	64.548224	64.536936	43.056677	42.850043	26.042164	24.129518	14.526822	6.930390
.11		117.385445	117.385441	89.643428	89.643066	64.952891	64.940284	43.628540	43.402100	26.836503	24.795529	15.486109	7.619972
.12		117.469528	117.469523	89.891746	89.891335	65.360213	65.346141	44.205272	43.957320	27.638868	25.463517	16.446598	8.308576
.13		117.554105	117.554100	90.141576	90.141111	65.770242	65.754546	44.787014	44.515718	28.449255	26.133416	17.407946	8.996118
.14		117.639187	117.639181	90.392947	90.392419	66.183037	66.165538	45.373915	45.077309	29.267642	26.805159	18.368808	9.682515
.15		117.724782	117.724775	90.645885	90.645287	66.598655	66.579159	45.966132	45.642106	30.093987	27.478674	19.331836	10.367684
.16		117.810899	117.810891	90.900419	90.899742	67.017158	66.995449	46.563824	46.210121	30.928224	28.153888	20.293682	11.051545
.17		117.897548	117.897538	91.156579	91.155813	67.436610	67.414450	47.167158	46.781364	31.770271	28.830727	21.254996	11.734020
.18		117.984738	117.984727	91.414395	91.413528	67.863077	67.836206	47.776307	47.355842	32.620020	29.509113	22.215424	12.415029
.19		118.072479	118.072466	91.673898	91.672919	68.290630	68.260759	48.391448	47.933561	33.477347	30.188966	23.174614	13.094497
.20		118.160781	118.160766	91.935122	91.934015	68.721341	68.688154	49.012763	48.514525	34.342103	30.870204	24.132211	13.772351
.21		118.249656	118.249638	92.198099	92.196848	69.155287	69.118435	49.640440	49.098736	35.214122	31.552745	25.087857	14.448516
.22		118.339113	118.339093	92.462865	92.461452	69.592547	69.551648	50.274672	49.688194	36.092216	32.236502	26.041198	15.122924
.23		118.429165	118.429142	92.729455	92.727861	70.033206	69.987838	50.915652	50.276894	36.979182	32.921387	26.991875	15.795503
.24		118.519822	118.519797	92.997907	92.996108	70.477352	70.427052	51.563581	50.870831	37.871795	33.607313	27.939533	16.466189
.25		118.611098	118.611069	93.268259	93.266231	70.925076	70.869338	52.218658	51.467997	38.770117	34.294187	28.883816	17.134917
.26		118.703005	118.702971	93.540552	93.538266	71.376476	71.314742	52.881085	52.068382	39.675990	34.981916	29.824370	17.801622
.27		118.795554	118.795515	93.814827	93.812251	71.831653	71.763312	53.551064	52.671971	40.587046	35.670408	30.760845	18.466247
.28		118.888761	118.888716	94.091128	94.088226	72.290716	72.215098	54.228794	53.278748	41.503698	36.359565	31.692895	19.128731
.29		118.982638	118.982587	94.369500	94.366231	72.753777	72.670148	54.914472	53.888693	42.425649	37.049292	32.620176	19.789020
.30		119.077142	119.077142	94.649989	94.646309	73.220954	73.128511	55.608293	54.501783	43.352590	37.739488	33.542354	20.447060
.31		119.172462	119.172395	94.926433	94.928502	73.692374	73.590236	56.310442	55.117993	44.284200	38.430056	34.459102	21.102800
.32		119.268439	119.268363	95.217515	95.212855	74.168168	74.055373	57.021098	55.737292	45.220147	39.120894	35.370100	21.756190
.33		119.365148	119.365060	95.504657	95.499415	74.648476	74.523972	57.740430	56.359649	46.160089	39.811900	36.275043	22.407186
.34		119.462604	119.462504	95.794124	95.788230	75.133445	74.996081	58.468594	56.985027	47.103677	40.502972	37.173636	23.055743
.35		119.560825	119.560711	96.085974	96.079347	75.623229	75.471752	59.205733	57.613387	48.050551	41.194007	38.065599	23.701820
.36		119.659829	119.659699	96.380267	96.372819	76.117992	75.951032	59.951973	58.244685	49.000343	41.884900	38.950671	24.345378
.37		119.759635	119.759486	96.677067	96.668697	76.617907	76.433971	60.707422	58.878875	49.952678	42.575547	39.828607	24.986381
.38		119.860261	119.860091	96.976440	96.967037	77.123156	76.920617	61.472168	59.515905	50.907172	43.265844	40.699182	25.624795
.39		119.961729	119.961534	97.278455	97.267893	77.633930	77.411019	62.246275	60.155721	51.863434	43.955685	41.562194	26.260589
.40		120.064059	120.063836	97.583186	97.571325	78.150433	77.905223	63.029785	60.798265	52.821064	44.644965	42.417463	26.893734
.41		120.167273	120.167019	97.890709	97.877391	78.672877	78.402276	63.822712	61.443474	53.779655	45.333578	43.264832	27.524204
.42		120.271394	120.271104	98.201106	98.186155	79.201487	78.905223	64.625046	62.091283	54.738792	46.021420	44.104172	28.151975
.43		120.376446	120.376114	98.514461	98.497679	79.736497	79.411109	65.436747	62.741621	55.698053	46.708386	44.935378	28.777025
.44		120.482455	120.482075	98.830864	98.812030	80.278157	79.920976	66.257745	63.394414	56.657005	47.394371	45.758372	29.399335
.45		120.589445	120.589012	99.150411	99.129276	80.826724	80.434866	67.087943	64.049583	57.615210	48.079272	46.573101	30.018889
.46		120.697446	120.696951	99.473201	99.449489	81.382470	80.952818	67.927212	64.707045	58.572221	48.762986	47.379541	30.635672
.47		120.806485	120.805919	99.799342	99.772740	81.945677	81.474870	68.775394	65.366715	59.527581	49.445411	48.177689	31.249671
.48		120.916594	120.915946	100.128947	100.099106	82.516641	82.001058	69.632302	66.028501	60.480829	50.126447	48.967570	31.860876
.49		121.027803	121.027063	100.462134	100.428664	83.095665	82.531414	70.497719	66.692309	61.431492	50.805992	49.749233	32.469280
.50		121.140146	121.139299	100.799033	100.761495	83.683066	83.065969	71.371402	67.358039	62.379095	51.483950	50.522746	33.074876

$J_{K_1 K_2}$ $J_r$ $K$	$11_{11,0}$ $11_{11}$	$11_{11,1}$ $11_{10}$	$11_{10,1}$ $11_9$	$11_{10,2}$ $11_8$	$11_{9,2}$ $11_7$	$11_{9,3}$ $11_6$	$11_{8,3}$ $11_5$	$11_{8,4}$ $11_4$	$11_{7,4}$ $11_3$	$11_{7,5}$ $11_2$	$11_{6,5}$ $11_1$	$11_{6,6}$ $11_0$
.50	121.140146	121.139299	100.799033	100.761495	83.683066	83.065969	71.371402	67.358039	62.379095	51.483950	50.522746	33.074876
.51	121.253658	121.252690	101.197778	101.097632	84.279166	83.604751	72.253078	68.025587	63.323154	52.160324	51.288199	33.677661
.52	121.367378	121.367270	101.485516	101.437311	84.884299	84.147784	73.142448	68.694847	64.263180	52.834720	52.045700	34.277631
.53	121.484143	121.483075	101.833401	101.780470	85.498801	84.695090	74.039190	69.365706	65.198664	53.507343	52.795376	34.874787
.54	121.601515	121.600144	102.186599	102.127251	86.123013	85.246686	74.942956	70.038049	66.129173	54.178005	53.537365	35.469130
.55	121.720179	121.718517	102.544287	102.477748	86.757278	85.802587	75.853373	70.711756	67.054156	54.846616	54.271820	36.060663
.56	121.840140	121.838237	102.906656	102.832058	87.401935	86.362800	76.770050	71.386703	67.973145	55.513091	54.998904	36.649391
.57	121.961529	121.959549	103.273912	103.190281	88.057320	86.927332	77.692570	72.062761	68.865660	56.177346	55.718787	37.235319
.58	122.084399	122.081899	103.646273	103.552520	88.723756	87.496182	78.620499	72.739793	69.791231	56.839301	56.431649	37.818456
.59	122.208804	122.205937	104.023979	103.918882	89.401555	88.069346	79.553377	73.417678	70.689401	57.498878	57.137670	38.398810
.60	122.334806	122.331516	104.407283	104.289475	90.091010	88.646813	80.990729	74.096261	71.579733	58.156003	57.837037	38.976392
.61	122.462468	122.458692	104.796464	104.664410	90.792388	89.228568	81.432056	74.775404	72.461812	58.810605	58.529936	39.551211
.62	122.591859	122.587522	105.191818	105.043803	91.505932	89.814588	82.376337	75.454959	73.335250	59.462614	59.216554	40.123282
.63	122.723054	122.718069	105.593669	105.427772	92.231847	90.404844	83.324532	76.134775	74.199692	60.111967	59.897077	40.692617
.64	122.856131	122.850399	106.002337	105.816436	92.970301	90.999303	84.274575	76.814698	75.054818	60.758602	60.571687	41.259231
.65	122.991177	122.984582	106.418286	106.209919	93.721418	91.597920	85.226376	77.494570	75.900349	61.402463	61.240564	41.823139
.66	123.128285	123.120690	106.841838	106.608346	94.485276	92.200646	86.179319	78.174230	76.736048	62.043494	61.903882	42.384356
.67	123.267556	123.258804	107.273466	107.011847	95.261898	92.807423	87.137631	78.853515	77.561726	62.681645	62.561811	42.942900
.68	123.409099	123.399006	107.713646	107.420550	96.051254	93.418185	88.06032	79.532259	78.377241	63.316871	63.214516	43.498787
.69	123.553036	123.541385	108.162897	107.834589	96.853256	94.032856	89.038423	80.210293	79.182504	63.949128	63.862155	44.052035
.70	123.699497	123.686037	108.621774	108.254097	97.667757	94.651354	90.99197	80.887447	79.977471	64.578377	64.504880	44.602663
.71	123.848627	123.833062	109.090877	108.679211	98.494549	95.273584	90.937511	81.563550	80.762151	65.204584	65.142836	45.150690
.72	124.000586	123.982569	109.570850	109.110067	99.333365	95.899441	91.822765	82.238426	81.536600	65.827717	65.776161	45.696134
.73	124.155550	124.134671	110.062378	109.546804	100.183876	96.524811	92.8223904	82.911903	82.300917	66.447749	66.404989	46.239016
.74	124.313715	124.289494	110.566191	109.989560	101.045695	97.161568	93.760115	83.583805	83.055244	67.064655	67.029440	46.779353
.75	124.475302	124.447169	111.083062	110.438473	101.918375	97.797574	94.690483	84.253957	83.799761	67.678415	67.649635	47.317167
.76	124.640555	124.607837	111.613798	110.893681	102.601411	98.436679	95.614061	84.922185	84.534681	68.289013	68.265685	47.852478
.77	124.809752	124.771650	112.159242	111.355322	103.694240	99.078718	96.529878	85.588316	85.260243	68.96435	68.877694	48.385305
.78	124.983205	124.938770	112.720255	111.823530	104.596243	99.723513	97.436947	86.252177	85.976712	69.500671	69.485760	48.915669
.79	125.161273	125.109374	113.297714	112.298441	105.506737	100.370972	98.334276	86.913600	86.684369	70.11714	70.089976	49.443590
.80	125.344363	125.283647	113.892493	112.780184	106.424979	101.020586	99.220880	87.572419	87.383511	70.699561	70.690426	49.969088
.81	125.532942	125.461794	114.505444	113.268887	107.350156	101.672429	100.095801	88.228469	88.074439	71.294212	71.287192	50.492183
.82	125.727553	125.644030	115.137381	113.764675	108.291381	102.324159	100.958128	88.891592	88.757462	71.880349	71.880349	51.012896
.83	125.928826	125.830590	115.789057	114.267665	109.217677	102.931513	101.607015	89.531635	89.432887	72.473932	72.469965	51.531245
.84	126.137496	126.021726	116.461136	114.777972	110.157969	103.636209	102.641708	90.178450	90.101019	73.059014	73.056106	52.047252
.85	126.354427	126.217710	117.154177	115.295704	111.101059	104.295944	103.461567	90.821895	90.762151	73.640923	73.638833	52.560935
.86	126.580639	126.418834	117.868608	115.820960	112.045605	104.954390	104.266085	91.461836	91.416580	74.218200	74.218200	53.072314
.87	126.817340	126.625413	118.604709	116.353836	112.990084	105.613199	105.054908	92.098147	92.064575	74.794260	74.794260	53.581408
.88	127.065970	126.837785	119.362600	116.894415	113.932763	106.271994	105.827847	92.730708	92.706399	75.367730	75.367062	54.088236
.89	127.328247	127.056315	120.142232	117.442775	114.871643	106.930372	106.584884	93.359411	93.342301	75.937077	75.936648	54.592818
.90	127.606222	127.281395	120.943390	117.998982	115.804408	107.587903	107.326172	93.984158	93.972513	76.503326	76.503062	55.095170
.91	127.902338	127.513445	121.765699	118.563096	116.728369	108.244126	108.052027	94.604858	94.597249	77.066495	77.066341	55.595312
.92	128.219494	127.752914	122.608635	119.135162	117.640397	108.898551	108.762916	95.221435	95.216705	77.626606	77.626521	56.093262
.93	128.561096	128.000284	123.471547	119.715217	118.536880	109.550656	109.459436	95.833820	95.831061	78.183679	78.183635	56.589037
.94	128.931069	128.256067	124.353677	120.303286	119.413698	110.199886	110.142296	96.441960	96.440478	78.737735	78.737716	57.082655
.95	129.333829	128.520807	125.254184	120.893985	120.266266	110.845656	110.812286	97.05808	97.045098	79.288799	79.288791	57.574133
.96	129.774142	128.795079	126.172167	121.503514	121.089661	111.487347	111.470262	97.645335	97.645046	79.836891	79.836888	58.063487
.97	130.256863	129.079490	127.106690	122.115667	121.878894	112.124314	112.117115	98.240519	98.240428	80.382034	80.382033	58.550735
.98	130.786521	129.374672	128.056800	122.735821	122.629317	112.755880	112.753752	98.831354	98.831336	80.924252	80.924252	59.035892
.99	131.366799	129.681282	129.021547	123.363946	123.337148	113.381348	113.381083	99.417842	99.417841	81.463566	81.463566	59.518975
1.00	132.000000	130.000000	130.000000	124.000000	124.000000	114.000000	114.000000	100.000000	100.000000	82.000000	82.000000	60.000000







$J_{K_1 K_2}$	$11_5, 6$		$11_4, 7$		$11_4, 8$		$11_3, 8$		$11_3, 9$		$11_2, 9$		$11_2, 10$		$11_1, 10$		$11_1, 11$		$11_0, 11$		$12_{12}, 0$	
	$11_5$	$11_6$	$11_4$	$11_7$	$11_4$	$11_8$	$11_3$	$11_5$	$11_3$	$11_6$	$11_2$	$11_7$	$11_2$	$11_8$	$11_1$	$11_9$	$11_1$	$11_{10}$	$11_{11}$	$12_{12}$	$12_{12}$	
.50	32.992217	32.992217	11.086171	11.086171	-14.566110	-14.566224	-43.822032	-43.822032	-43.822032	-43.822032	-76.628301	-76.628301	-76.628301	-76.628301	-112.957319	-112.957319	-112.957319	-112.957319	-112.957319	-112.957319	144.138478	144.138478
.51	33.605046	33.605046	11.593827	11.593827	-14.559373	-14.559469	-43.521386	-43.521386	-43.521386	-43.521386	-76.441557	-76.441557	-76.441557	-76.441557	-112.893495	-112.893495	-112.893495	-112.893495	-112.893495	-112.893495	144.261968	144.261968
.52	34.214011	34.214011	12.099108	12.099108	-13.754309	-13.754388	-43.221881	-43.221881	-43.221881	-43.221881	-76.255481	-76.255481	-76.255481	-76.255481	-112.829892	-112.829892	-112.829892	-112.829892	-112.829892	-112.829892	144.386762	144.386762
.53	34.819201	34.819201	12.602043	12.602043	-13.350899	-13.350964	-42.923504	-42.923504	-42.923504	-42.923504	-76.070065	-76.070065	-76.070065	-76.070065	-112.766506	-112.766506	-112.766506	-112.766506	-112.766506	-112.766506	144.512901	144.512901
.54	35.420703	35.420703	13.104745	13.104745	-12.949127	-12.949161	-42.626246	-42.626246	-42.626246	-42.626246	-75.885304	-75.885304	-75.885304	-75.885304	-112.703336	-112.703336	-112.703336	-112.703336	-112.703336	-112.703336	144.640429	144.640429
.55	36.018599	36.018599	13.600993	13.600993	-12.548977	-12.549022	-42.330094	-42.330094	-42.330094	-42.330094	-75.701190	-75.701190	-75.701190	-75.701190	-112.640380	-112.640380	-112.640380	-112.640380	-112.640380	-112.640380	144.769394	144.769394
.56	36.612966	36.612966	14.097063	14.097063	-12.150473	-12.150470	-42.035039	-42.035039	-42.035039	-42.035039	-75.517718	-75.517718	-75.517718	-75.517718	-112.577635	-112.577635	-112.577635	-112.577635	-112.577635	-112.577635	144.899844	144.899844
.57	37.203881	37.203881	14.590899	14.590899	-11.753479	-11.753509	-41.741068	-41.741068	-41.741068	-41.741068	-75.334882	-75.334882	-75.334882	-75.334882	-112.515101	-112.515101	-112.515101	-112.515101	-112.515101	-112.515101	145.031831	145.031831
.58	37.791413	37.791413	15.082525	15.082525	-11.358100	-11.358124	-41.448173	-41.448173	-41.448173	-41.448173	-75.152675	-75.152675	-75.152675	-75.152675	-112.452773	-112.452773	-112.452773	-112.452773	-112.452773	-112.452773	145.165412	145.165412
.59	38.375629	38.375629	15.572831	15.572831	-10.964279	-10.964299	-41.156342	-41.156342	-41.156342	-41.156342	-74.971092	-74.971092	-74.971092	-74.971092	-112.390652	-112.390652	-112.390652	-112.390652	-112.390652	-112.390652	145.300645	145.300645
.60	38.956595	38.956595	16.059250	16.059250	-10.572002	-10.572018	-40.865566	-40.865566	-40.865566	-40.865566	-74.790126	-74.790126	-74.790126	-74.790126	-112.328734	-112.328734	-112.328734	-112.328734	-112.328734	-112.328734	145.437594	145.437594
.61	39.534370	39.534370	16.544396	16.544396	-10.181255	-10.181267	-40.575835	-40.575835	-40.575835	-40.575835	-74.609771	-74.609771	-74.609771	-74.609771	-112.267018	-112.267018	-112.267018	-112.267018	-112.267018	-112.267018	145.576325	145.576325
.62	40.109013	40.109013	17.027429	17.027429	-9.792022	-9.792032	-40.287138	-40.287138	-40.287138	-40.287138	-74.430023	-74.430023	-74.430023	-74.430023	-112.205501	-112.205501	-112.205501	-112.205501	-112.205501	-112.205501	145.716910	145.716910
.63	40.680579	40.680579	17.508371	17.508371	-9.404290	-9.404297	-39.999467	-39.999467	-39.999467	-39.999467	-74.250875	-74.250875	-74.250875	-74.250875	-112.144183	-112.144183	-112.144183	-112.144183	-112.144183	-112.144183	145.859428	145.859428
.64	41.249121	41.249121	17.987244	17.987244	-9.018043	-9.018049	-39.712811	-39.712811	-39.712811	-39.712811	-74.072322	-74.072322	-74.072322	-74.072322	-112.083061	-112.083061	-112.083061	-112.083061	-112.083061	-112.083061	146.003959	146.003959
.65	41.814687	41.814687	18.464069	18.464069	-8.633269	-8.633274	-39.427161	-39.427161	-39.427161	-39.427161	-73.894359	-73.894359	-73.894359	-73.894359	-112.022134	-112.022134	-112.022134	-112.022134	-112.022134	-112.022134	146.150594	146.150594
.66	42.377327	42.377327	18.939077	18.939077	-8.249954	-8.249957	-39.142508	-39.142508	-39.142508	-39.142508	-73.716979	-73.716979	-73.716979	-73.716979	-111.961399	-111.961399	-111.961399	-111.961399	-111.961399	-111.961399	146.299429	146.299429
.67	42.937084	42.937084	19.411659	19.411659	-7.868083	-7.868086	-38.858844	-38.858844	-38.858844	-38.858844	-73.540178	-73.540178	-73.540178	-73.540178	-111.900855	-111.900855	-111.900855	-111.900855	-111.900855	-111.900855	146.450568	146.450568
.68	43.494002	43.494002	19.882597	19.882597	-7.487645	-7.487647	-38.576158	-38.576158	-38.576158	-38.576158	-73.363951	-73.363951	-73.363951	-73.363951	-111.840501	-111.840501	-111.840501	-111.840501	-111.840501	-111.840501	146.604124	146.604124
.69	44.048122	44.048122	20.351301	20.351301	-7.108625	-7.108627	-38.294443	-38.294443	-38.294443	-38.294443	-73.188292	-73.188292	-73.188292	-73.188292	-111.780334	-111.780334	-111.780334	-111.780334	-111.780334	-111.780334	146.760220	146.760220
.70	44.599484	44.599484	20.818272	20.818272	-6.731013	-6.731013	-38.013689	-38.013689	-38.013689	-38.013689	-73.013197	-73.013197	-73.013197	-73.013197	-111.720352	-111.720352	-111.720352	-111.720352	-111.720352	-111.720352	146.918991	146.918991
.71	45.148123	45.148123	21.283213	21.283213	-6.354791	-6.354792	-37.733888	-37.733888	-37.733888	-37.733888	-72.838660	-72.838660	-72.838660	-72.838660	-111.660556	-111.660556	-111.660556	-111.660556	-111.660556	-111.660556	147.080584	147.080584
.72	45.694077	45.694077	21.746246	21.746246	-5.979952	-5.979953	-37.455032	-37.455032	-37.455032	-37.455032	-72.664676	-72.664676	-72.664676	-72.664676	-111.600941	-111.600941	-111.600941	-111.600941	-111.600941	-111.600941	147.245160	147.245160
.73	46.237380	46.237380	22.207388	22.207388	-5.606482	-5.606482	-37.177112	-37.177112	-37.177112	-37.177112	-72.491242	-72.491242	-72.491242	-72.491242	-111.541508	-111.541508	-111.541508	-111.541508	-111.541508	-111.541508	147.412900	147.412900
.74	46.778063	46.778063	22.666657	22.666657	-5.234368	-5.234368	-36.900121	-36.900121	-36.900121	-36.900121	-72.318351	-72.318351	-72.318351	-72.318351	-111.482254	-111.482254	-111.482254	-111.482254	-111.482254	-111.482254	147.584002	147.584002
.75	47.316159	47.316159	23.124047	23.124047	-4.863599	-4.863599	-36.624050	-36.624050	-36.624050	-36.624050	-72.145999	-72.145999	-72.145999	-72.145999	-111.423178	-111.423178	-111.423178	-111.423178	-111.423178	-111.423178	147.758687	147.758687
.76	47.851698	47.851698	23.579624	23.579624	-4.494163	-4.494163	-36.348891	-36.348891	-36.348891	-36.348891	-71.974182	-71.974182	-71.974182	-71.974182	-111.364279	-111.364279	-111.364279	-111.364279	-111.364279	-111.364279	147.937202	147.937202
.77	48.384708	48.384708	24.033376	24.033376	-4.126043	-4.126043	-36.074636	-36.074636	-36.074636	-36.074636	-71.802895	-71.802895	-71.802895	-71.802895	-111.305554	-111.305554	-111.305554	-111.305554	-111.305554	-111.305554	148.119826	148.119826
.78	48.915217	48.915217	24.485316	24.485316	-3.759244	-3.759244	-35.801278	-35.801278	-35.801278	-35.801278	-71.632134	-71.632134	-71.632134	-71.632134	-111.247003	-111.247003	-111.247003	-111.247003	-111.247003	-111.247003	148.306875	148.306875
.79	49.443252	49.443252	24.935467	24.935467	-3.393738	-3.393738	-35.528810	-35.528810	-35.528810	-35.528810	-71.461894	-71.461894	-71.461894	-71.461894	-111.188624	-111.188624	-111.188624	-111.188624	-111.188624	-111.188624	148.498707	148.498707
.80	49.968838	49.968838	25.383818	25.383818	-3.029521	-3.029521	-35.257223	-35.257223	-35.257223	-35.257223	-71.292170	-71.292170	-71.292170	-71.292170	-111.130415	-111.130415	-111.130415	-111.130415	-111.130415	-111.130415	148.695733	148.695733
.81	50.492002	50.492002	25.830447	25.830447	-2.666581	-2.666581	-34.986510	-34.986510	-34.986510	-34.986510	-71.122959	-71.122959	-71.122959	-71.122959	-111.072376	-111.072376	-111.072376	-111.072376	-111.072376	-111.072376	148.898425	148.898425
.82	51.012766	51.012766	26.275312	26.275312	-2.304907	-2.304907	-34.716665	-34.716665	-34.716665	-34.716665	-70.954256	-70.954256	-70.954256	-70.954256	-111.014504	-111.014504	-111.014504	-111.014504	-111.014504	-111.014504	149.107333	149.107333
.83	51.531154	51.531154	26.718441	26.718441	-1.944489	-1.944489	-34.447679	-34.447679	-34.447679	-34.447679	-70.786058	-70.786058	-70.786058	-70.786058	-110.956798	-110.956798	-110.956798	-110.956798	-110.956798	-110.956798	149.323096	149.323096
.84	52.047189	52.047189	27.159853	27.159853	-1.585316	-1.585316	-34.179546	-34.179546	-34.179546	-34.179546	-70.618359	-70.618359	-70.618359	-70.618359	-110.899258	-110.899258	-110.899258	-110.899258	-110.899258	-110.899258	149.546470	149.546470
.85	52.560893	52.560893	27.599562	27.599562	-1.227379	-1.227379	-33.912259	-33.912259	-33.912259	-33.912259	-70.451156	-70.451156	-70.451156	-70.451156</								

$J_{K-1}K_1$ $J_T$ $K$	$12_{12,1}$ $12_{11}$	$12_{11,1}$ $12_{10}$	$12_{11,2}$ $12_9$	$12_{10,2}$ $12_8$	$12_{10,3}$ $12_7$	$12_{11,3}$ $12_6$	$12_{9,4}$ $12_5$	$12_{8,4}$ $12_4$	$12_{8,5}$ $12_3$	$12_{7,5}$ $12_2$	$12_{7,6}$ $12_1$	$12_{6,6}$ $12_0$
	$12_{12,1}$ $12_{11}$	$12_{11,1}$ $12_{10}$	$12_{11,2}$ $12_9$	$12_{10,2}$ $12_8$	$12_{10,3}$ $12_7$	$12_{11,3}$ $12_6$	$12_{9,4}$ $12_5$	$12_{8,4}$ $12_4$	$12_{8,5}$ $12_3$	$12_{7,5}$ $12_2$	$12_{7,6}$ $12_1$	$12_{6,6}$ $12_0$
.00	139.076386	106.757543	106.757524	77.540834	77.539946	51.562056	51.539141	29.209203	28.869165	11.839818	9.188833	0.000000
.01	139.162600	107.011923	107.011901	77.956153	77.955139	52.136039	52.110339	29.961313	29.587693	12.838631	10.009771	1.141872
.02	139.249265	107.267670	107.267645	78.373825	78.372669	52.7113673	52.684876	30.720012	30.309919	13.846763	10.832409	2.283284
.03	139.336387	107.524807	107.524778	78.791890	78.792572	53.295035	53.262796	31.485495	31.035839	14.864079	11.656640	3.423775
.04	139.423974	107.783355	107.783321	79.216385	79.214885	53.880205	53.844141	32.257965	31.765445	15.890416	12.482356	4.562884
.05	139.512033	108.043335	108.043296	79.641352	79.639647	54.469264	54.428956	33.037630	32.498725	16.925584	13.309443	5.700153
.06	139.600572	108.304772	108.304726	80.066833	80.066894	55.062299	55.017284	33.824701	33.235664	17.969165	14.137790	6.835124
.07	139.689598	108.567688	108.567635	80.498870	80.496668	55.659401	55.609169	34.619395	33.976244	19.021515	14.967280	7.967342
.08	139.779119	108.832107	108.832047	80.921508	80.929009	56.260664	56.204656	35.421931	34.720444	20.081765	15.797795	9.096355
.09	139.869144	109.098056	109.097986	81.366793	81.363959	56.866189	56.803789	36.232530	35.468239	21.149824	16.629217	10.221714
.10	139.959679	109.365558	109.365479	81.804772	81.801560	57.476078	57.406610	37.051414	36.219601	22.225377	17.461425	11.342973
.11	140.050735	109.634641	109.634550	82.245495	82.241857	58.090442	58.013166	37.878804	36.974498	23.308090	18.294297	12.459694
.12	140.142320	109.905332	109.905227	82.689010	82.684893	58.709396	58.623497	38.714920	37.732893	24.397609	19.127710	13.571443
.13	140.234444	110.177658	110.177537	83.135373	83.130715	59.333059	59.237649	39.559978	38.494746	25.493564	19.961539	14.677798
.14	140.327114	110.451649	110.451509	83.584635	83.579371	59.961559	59.855663	40.414186	39.260014	26.595569	20.795661	15.778342
.15	140.420341	110.727333	110.727173	84.036855	84.030908	60.595029	60.477582	41.277746	40.028649	27.703222	21.629948	16.872673
.16	140.514135	111.004741	111.004553	84.492089	84.485375	61.233608	61.103447	42.150850	40.800600	28.816110	22.464275	17.960400
.17	140.608506	111.283905	111.283695	84.950400	84.942824	61.877445	61.733299	43.036777	41.575809	29.933808	23.298515	19.041149
.18	140.703465	111.564857	111.564616	85.411850	85.403307	62.526693	62.367177	43.926392	42.354217	31.055881	24.132541	20.114560
.19	140.799022	111.847631	111.847354	85.876504	85.866875	63.181515	63.005120	44.829141	43.135760	32.181884	24.966226	21.180296
.20	140.895188	112.132260	112.131944	86.344430	86.333585	63.842083	63.647164	45.742054	43.920369	33.311363	25.799443	22.238038
.21	140.991975	112.418782	112.418419	86.815701	86.803491	64.508575	64.293347	46.665234	44.707971	34.443858	26.632067	23.287491
.22	141.089395	112.707231	112.706816	87.290389	87.276651	65.181180	64.943702	47.598764	45.498489	35.578899	27.463970	24.328387
.23	141.187460	112.997647	112.997172	87.768573	87.753122	65.860096	65.598261	48.542699	46.291842	36.716011	28.295028	25.360481
.24	141.286183	113.290069	113.289526	88.250332	88.232965	66.545530	66.257056	49.497064	47.087944	37.854715	29.125117	26.383559
.25	141.385576	113.584538	113.583917	88.735752	88.716240	67.237699	66.920115	50.461857	47.886706	38.994522	29.954113	27.397436
.26	141.485654	113.881095	113.880387	89.224921	89.203011	67.936829	67.587465	51.437043	48.688034	40.134940	30.781894	28.401456
.27	141.586429	114.179786	114.178976	89.717931	89.693339	68.643158	68.259129	52.422553	49.491829	41.275470	31.608340	29.396996
.28	141.687918	114.480654	114.479730	90.214880	90.187291	69.356932	68.935128	53.418287	50.297990	42.415610	32.433331	30.382463
.29	141.790133	114.783746	114.782692	90.715869	90.684934	70.078407	69.615481	54.424110	51.106410	43.554653	33.256750	31.358295
.30	141.893092	115.089113	115.087910	91.221007	91.186333	70.807849	70.300203	55.439854	51.916979	44.692684	34.078482	32.324462
.31	141.996809	115.396804	115.395433	91.730405	91.691560	71.545532	70.989306	56.465318	52.729584	45.828590	34.898415	33.280961
.32	142.101303	115.706873	115.705309	92.244183	92.200683	72.291740	71.682798	57.500266	53.544105	46.962048	35.716436	34.227822
.33	142.206588	116.017591	116.017375	92.762466	92.713775	73.046763	72.380684	58.544433	54.360423	48.092539	36.532439	35.165097
.34	142.312685	116.334363	116.332332	93.285385	93.230909	73.810896	73.082965	59.597521	55.178411	49.219536	37.346317	36.092868
.35	142.419610	116.651901	116.649587	93.813082	93.752157	74.584442	73.789637	60.659203	55.997941	50.342516	38.157967	37.011236
.36	142.527384	116.972050	116.969414	94.345702	94.277596	75.367703	74.500692	61.729126	56.818880	51.460956	38.967290	37.920328
.37	142.636027	117.294874	117.291873	94.883403	94.807302	76.160985	75.216119	62.806907	57.641094	52.574333	39.774189	38.820284
.38	142.745558	117.620442	117.617025	95.426351	95.341351	76.964593	75.935899	63.892143	58.464444	53.682132	40.578571	39.711266
.39	142.856000	117.948824	117.944934	95.974720	95.879821	77.778824	76.660010	64.984403	59.288788	54.783843	41.380345	40.593446
.40	142.967375	118.280093	118.275666	96.528697	96.422791	78.603972	77.388425	66.083237	60.113983	55.878965	42.179426	41.467010
.41	143.079708	118.614328	118.609291	97.088480	96.970340	79.440319	78.121111	67.188174	60.939881	56.967011	42.975729	42.3







$J_{K_1K_2}$ $J_r$ $K$	12 <sub>6,7</sub> 12 <sub>-1</sub>	12 <sub>5,7</sub> 12 <sub>-2</sub>	12 <sub>5,8</sub> 12 <sub>-3</sub>	12 <sub>4,9</sub> 12 <sub>-5</sub>	12 <sub>3,9</sub> 12 <sub>-6</sub>	12 <sub>3,10</sub> 12 <sub>-7</sub>	12 <sub>2,10</sub> 12 <sub>-8</sub>	12 <sub>2,11</sub> 12 <sub>-9</sub>	12 <sub>1,11</sub> 12 <sub>-10</sub>	12 <sub>1,12</sub> 12 <sub>-11</sub>	12 <sub>0,12</sub> 12 <sub>-12</sub>
	$K$	$K$	$K$	$K$	$K$	$K$	$K$	$K$	$K$	$K$	$K$
.00	-9.188833	-11.839818	-28.869165	-51.539141	-51.562056	-77.539946	-77.540834	-106.757524	-106.757543	-139.076386	-139.076386
.01	-8.369700	-10.850429	-28.154340	-50.971238	-50.991654	-77.127054	-77.127833	-106.504493	-106.504510	-138.990616	-138.990616
.02	-7.552474	-9.870542	-27.443216	-50.406589	-50.424761	-76.716430	-76.717111	-106.252790	-106.252804	-138.905283	-138.905283
.03	-6.737254	-8.900205	-26.735792	-49.845152	-49.861312	-76.308041	-76.308636	-106.002393	-106.002405	-138.820382	-138.820382
.04	-5.924137	-7.939440	-26.032061	-49.286884	-49.301241	-75.901852	-75.902371	-105.753284	-105.753294	-138.735905	-138.735905
.05	-5.113216	-6.988241	-25.332017	-48.731744	-48.744488	-75.497832	-75.498285	-105.505445	-105.505453	-138.651846	-138.651846
.06	-4.304582	-6.046579	-24.635650	-48.179692	-48.190993	-75.095950	-75.096345	-105.258864	-105.258864	-138.568201	-138.568201
.07	-3.498322	-5.114397	-23.942947	-47.630687	-47.640699	-74.696176	-74.696520	-105.013501	-105.013507	-138.484961	-138.484961
.08	-2.694521	-4.191619	-23.253896	-47.084690	-47.093550	-74.298479	-74.298778	-104.769362	-104.769367	-138.402123	-138.402123
.09	-1.893259	-3.278148	-22.568481	-46.541662	-46.549495	-73.902830	-73.903090	-104.526421	-104.526426	-138.319681	-138.319681
.10	-1.094615	-2.373866	-21.886685	-46.001563	-46.008481	-73.509201	-73.509426	-104.284663	-104.284667	-138.237628	-138.237628
.11	-0.298663	-1.478640	-21.208488	-45.464356	-45.470459	-73.117564	-73.117759	-104.044071	-104.044075	-138.155960	-138.155960
.12	0.494526	-0.592323	-20.533870	-44.930003	-44.935381	-72.727891	-72.728061	-103.804630	-103.804633	-138.074672	-138.074672
.13	1.284885	0.285244	-19.862811	-44.398467	-44.403201	-72.340157	-72.340303	-103.566323	-103.566326	-137.993758	-137.993758
.14	2.072349	1.154236	-19.195286	-43.869712	-43.873875	-71.954334	-71.954461	-103.329137	-103.329139	-137.913214	-137.913214
.15	2.856858	2.014831	-18.531271	-43.343702	-43.347358	-71.570398	-71.570507	-103.093055	-103.093057	-137.833034	-137.833034
.16	3.638355	2.867214	-17.870743	-42.820403	-42.823610	-71.188417	-71.188417	-102.858064	-102.858065	-137.753214	-137.753214
.17	4.416787	3.711579	-17.213673	-42.299779	-42.302588	-70.808086	-70.808167	-102.624149	-102.624150	-137.673750	-137.673750
.18	5.192103	4.548119	-16.560037	-41.781796	-41.784254	-70.429661	-70.429731	-102.391297	-102.391298	-137.594636	-137.594636
.19	5.964256	5.377032	-15.909805	-41.266421	-41.268569	-70.053027	-70.053087	-102.159493	-102.159494	-137.515868	-137.515868
.20	6.733204	6.198515	-15.262950	-40.753621	-40.755496	-69.678159	-69.678211	-101.928726	-101.928726	-137.437442	-137.437442
.21	7.498907	7.012765	-14.619442	-40.243365	-40.244999	-69.305037	-69.305080	-101.698981	-101.698981	-137.359354	-137.359354
.22	8.261329	7.819977	-13.979252	-39.735619	-39.737041	-68.933636	-68.933674	-101.470246	-101.470246	-137.281599	-137.281599
.23	9.020437	8.620343	-13.342351	-39.230354	-39.231590	-68.563938	-68.563970	-101.242509	-101.242509	-137.204173	-137.204173
.24	9.776201	9.414053	-12.708708	-38.727538	-38.728611	-68.195919	-68.195946	-101.015757	-101.015757	-137.127073	-137.127073
.25	10.528596	10.201291	-12.078292	-38.227142	-38.228072	-67.829560	-67.829583	-100.789978	-100.789978	-137.050294	-137.050294
.26	11.277598	10.982237	-11.451072	-37.729136	-37.729940	-67.464841	-67.464860	-100.565161	-100.565161	-136.973833	-136.973833
.27	12.023187	11.757066	-10.827018	-37.233492	-37.234186	-67.101741	-67.101758	-100.341294	-100.341295	-136.897685	-136.897685
.28	12.765347	12.525949	-10.206099	-36.740180	-36.740779	-66.740241	-66.740256	-100.118367	-100.118367	-136.821848	-136.821848
.29	13.504062	13.289049	-9.588283	-36.249173	-36.249689	-66.380323	-66.380335	-99.896367	-99.896367	-136.746316	-136.746316
.30	14.239322	14.046524	-8.973540	-35.760444	-35.760887	-66.021968	-66.021978	-99.675284	-99.675284	-136.671088	-136.671088
.31	14.971119	14.798526	-8.361837	-35.273966	-35.274346	-65.665157	-65.665165	-99.455108	-99.455108	-136.596159	-136.596159
.32	15.699447	15.545203	-7.753144	-34.789712	-34.790037	-65.309873	-65.309880	-99.235828	-99.235828	-136.521526	-136.521526
.33	16.424302	16.286692	-7.147431	-34.307656	-34.307935	-64.956097	-64.956103	-99.017433	-99.017433	-136.447185	-136.447185
.34	17.145684	17.023130	-6.544665	-33.827774	-33.828012	-64.603814	-64.603819	-98.799915	-98.799915	-136.373134	-136.373134
.35	17.863593	17.754645	-5.944817	-33.350040	-33.350243	-64.253005	-64.253009	-98.583262	-98.583262	-136.299369	-136.299369
.36	18.578035	18.481359	-5.347856	-32.874430	-32.874602	-63.903655	-63.903658	-98.367466	-98.367466	-136.225817	-136.225817
.37	19.289014	19.203389	-4.758236	-32.400920	-32.401066	-63.555746	-63.555749	-98.152517	-98.152517	-136.152684	-136.152684
.38	19.996538	19.920847	-4.166348	-31.929486	-31.929609	-63.209264	-63.209267	-97.938406	-97.938406	-136.079758	-136.079758
.39	20.700618	20.633840	-3.573991	-31.460105	-31.460209	-62.864193	-62.864194	-97.725123	-97.725123	-136.007106	-136.007106
.40	21.401263	21.342469	-2.988277	-30.992754	-30.992842	-62.520516	-62.520518	-97.512659	-97.512659	-135.934724	-135.934724
.41	22.098488	22.046831	-2.405301	-30.527412	-30.527485	-62.178219	-62.178221	-97.301006	-97.301006	-135.862611	-135.862611
.42	22.792308	22.747019	-1.825035	-30.064055	-30.064116	-61.837288	-61.837289	-97.090156	-97.090156	-135.790762	-135.790762
.43	23.482737	23.443119	-1.247449	-29.602663	-29.602714	-61.497707	-61.497708	-96.880099	-96.880099	-135.719175	-135.719175
.44	24.169793	24.135215	-0.672515	-29.143214	-29.143257	-61.159462	-61.159463	-96.670827	-96.670827	-135.647848	-135.647848
.45	24.853496	24.823387	-0.100206	-28.685688	-28.685724	-60.822540	-60.822540	-96.462333	-96.462333	-135.576778	-135.576778
.46	25.533864	25.507711	0.469504	-28.230064	-28.230094	-60.486926	-60.486926	-96.254607	-96.254607	-135.505962	-135.505962
.47	26.210919	26.188259	1.036446	-27.776347	-27.776377	-60.152607	-60.152607	-96.047643	-96.047643	-135.435397	-135.435397
.48	26.884682	26.865099	1.601245	-27.324444	-27.324464	-59.819569	-59.819570	-95.841432	-95.841432	-135.365081	-135.365081
.49	27.555175	27.538297	2.163326	-26.874408	-26.874424	-59.487800	-59.487800	-95.635966	-95.635966	-135.295011	-135.295011
.50	28.222421	28.207915	2.722917	-26.426196	-26.426210	-59.157287	-59.157287	-95.431239	-95.431239	-135.225186	-135.225186







## APPENDIX V

### Transition Strengths for Rotational Transitions

Intensity of a transition between rotational levels  $J_{kl}$  and  $J'_{mn}$  is proportional to

$$(\mu_x)^2 {}^xS_{J_{kl}J'_{mn}}(\kappa) = (2J + 1)|(\mu_x)_{J_{kl}J'_{mn}}|^2$$

Here  $\mu_x$  is the dipole moment along one of the principal axes of inertia ( $x = a, b$ , or  $c$ ), and  $S$  is the quantity tabulated here as a function of initial and final state and of the asymmetry parameter  $\kappa$ . The axis along which a dipole moment is required to produce a given transition is indicated by a superscript to the left of the subbranch designation. Thus  ${}^cQ_{10}$  indicates a  $Q$  branch ( $\Delta J = 0$ ) with a change in  $K_{-1}$  of 1, a change in  $K_1$  of 0, and that a dipole moment  $\mu_c$  along the  $c$  axis is required for the transition. For further discussion see Chap. 4. (Tables in this appendix are taken from Cross, Hainer, and King [122].)

SYMMETRIC-ROTOR SUBBRANCHES—*a* AND *c* PROLATE-AND-OBULATE SUBBRANCHES

Subbranch		$\kappa$				Subbranch	
${}^cQ_{1,0}$ $J + K_{-1} + K_1$ even	${}^cQ_{-1,0}$ $J + K_{-1} + K_1$ odd	$\mp 1$	$\mp 0.5$	0	$\pm 0.5$	${}^aQ_{0,1}$ $J + K_{-1} + K_1$ even	${}^aQ_{0,-1}$ $J + K_{-1} + K_1$ odd
1 <sub>0,1</sub>	1 <sub>1,1</sub>	15000	15000	15000	15000	1 <sub>1,0</sub>	1 <sub>1,1</sub>
2 <sub>0,2</sub>	2 <sub>1,2</sub>	25000	28223	31100	32845	2 <sub>2,0</sub>	2 <sub>2,1</sub>
3 <sub>0,3</sub>	3 <sub>1,3</sub>	35000	45104	50431	52155	3 <sub>3,0</sub>	3 <sub>3,1</sub>
4 <sub>0,4</sub>	4 <sub>1,4</sub>	45000	64494	70244	71708	4 <sub>4,0</sub>	4 <sub>4,1</sub>
5 <sub>0,5</sub>	5 <sub>1,5</sub>	55000	84696	90073	91399	5 <sub>5,0</sub>	5 <sub>5,1</sub>
6 <sub>0,6</sub>	6 <sub>1,6</sub>	65000	104928	109923	111174	6 <sub>6,0</sub>	6 <sub>6,1</sub>
7 <sub>0,7</sub>	7 <sub>1,7</sub>	75000	125065	129799	131004	7 <sub>7,0</sub>	7 <sub>7,1</sub>
8 <sub>0,8</sub>	8 <sub>1,8</sub>	85000	145135	149698	150871	8 <sub>8,0</sub>	8 <sub>8,1</sub>
9 <sub>0,9</sub>	9 <sub>1,9</sub>	95000	165170	169614	170764	9 <sub>9,0</sub>	9 <sub>9,1</sub>
10 <sub>0,10</sub>	10 <sub>1,10</sub>	105000	185187	189544	190677	10 <sub>10,0</sub>	10 <sub>10,1</sub>
11 <sub>0,11</sub>	11 <sub>1,11</sub>	115000	205194	209484	210603	11 <sub>11,0</sub>	11 <sub>11,1</sub>
12 <sub>0,12</sub>	12 <sub>1,12</sub>	125000	225195	229434	230542	12 <sub>12,0</sub>	12 <sub>12,1</sub>
2 <sub>1,1</sub>	2 <sub>2,1</sub>	8333	8333	8333	8333	2 <sub>1,1</sub>	2 <sub>1,2</sub>
3 <sub>1,2</sub>	3 <sub>2,2</sub>	14583	16278	18811	21875	3 <sub>2,1</sub>	3 <sub>2,2</sub>
4 <sub>1,3</sub>	4 <sub>2,3</sub>	20250	26168	34242	39363	4 <sub>3,1</sub>	4 <sub>3,2</sub>
5 <sub>1,4</sub>	5 <sub>2,4</sub>	25667	39338	52949	57742	5 <sub>4,1</sub>	5 <sub>4,2</sub>
6 <sub>1,5</sub>	6 <sub>2,5</sub>	30952	56179	72319	76548	6 <sub>5,1</sub>	6 <sub>5,2</sub>
7 <sub>1,6</sub>	7 <sub>2,6</sub>	36161	75597	91744	95646	7 <sub>6,1</sub>	7 <sub>6,2</sub>
8 <sub>1,7</sub>	8 <sub>2,7</sub>	41319	95950	111231	114943	8 <sub>7,1</sub>	8 <sub>7,2</sub>
9 <sub>1,8</sub>	9 <sub>2,8</sub>	46444	116333	130792	134381	9 <sub>8,1</sub>	9 <sub>8,2</sub>
10 <sub>1,9</sub>	10 <sub>2,9</sub>	51545	136551	150418	153921	10 <sub>9,1</sub>	10 <sub>9,2</sub>
11 <sub>1,10</sub>	11 <sub>2,10</sub>	56629	156642	170100	173540	11 <sub>10,1</sub>	11 <sub>10,2</sub>
12 <sub>1,11</sub>	12 <sub>2,11</sub>	61699	176660	189825	193216	12 <sub>11,1</sub>	12 <sub>11,2</sub>

3 <sub>2,1</sub>	3 <sub>3,1</sub>	8750	7403	6406	5944	5833	3 <sub>1,2</sub>	3 <sub>1,3</sub>
4 <sub>2,2</sub>	4 <sub>3,2</sub>	15750	13221	13196	15598	18000	4 <sub>2,2</sub>	4 <sub>2,3</sub>
5 <sub>2,3</sub>	5 <sub>3,3</sub>	22000	19105	23397	30662	33000	5 <sub>3,2</sub>	5 <sub>3,3</sub>
6 <sub>2,4</sub>	6 <sub>3,4</sub>	27857	26374	38620	47709	49524	6 <sub>4,2</sub>	6 <sub>4,3</sub>
7 <sub>2,5</sub>	7 <sub>3,5</sub>	33482	36237	57062	65399	66964	7 <sub>5,2</sub>	7 <sub>5,3</sub>
8 <sub>2,6</sub>	8 <sub>3,6</sub>	38958	49682	76155	83565	85000	8 <sub>6,2</sub>	8 <sub>6,3</sub>
9 <sub>2,7</sub>	9 <sub>3,7</sub>	44333	66864	95251	103089	103444	9 <sub>7,2</sub>	9 <sub>7,3</sub>
10 <sub>2,8</sub>	10 <sub>3,8</sub>	49636	86630	114393	120880	122183	10 <sub>8,2</sub>	10 <sub>8,3</sub>
11 <sub>2,9</sub>	11 <sub>3,9</sub>	54886	107332	133621	139873	141136	11 <sub>9,2</sub>	11 <sub>9,3</sub>
12 <sub>2,10</sub>	12 <sub>3,10</sub>	60096	128002	152940	159022	160256	12 <sub>10,2</sub>	12 <sub>10,3</sub>
4 <sub>3,1</sub>	4 <sub>4,1</sub>	9000	7587	6026	4847	4500	4 <sub>1,3</sub>	4 <sub>1,4</sub>
5 <sub>3,2</sub>	5 <sub>4,2</sub>	16500	13464	11058	11750	14667	5 <sub>2,3</sub>	5 <sub>2,4</sub>
6 <sub>3,3</sub>	6 <sub>4,3</sub>	23214	18339	17488	23981	27857	6 <sub>3,3</sub>	6 <sub>3,4</sub>
7 <sub>3,4</sub>	7 <sub>4,4</sub>	29464	22914	27745	39794	42857	7 <sub>4,3</sub>	7 <sub>4,4</sub>
8 <sub>3,5</sub>	8 <sub>4,5</sub>	35417	28185	43063	56506	59028	8 <sub>5,3</sub>	8 <sub>5,4</sub>
9 <sub>3,6</sub>	9 <sub>4,6</sub>	41167	35293	61523	73754	76000	9 <sub>6,3</sub>	9 <sub>6,4</sub>
10 <sub>3,7</sub>	10 <sub>4,7</sub>	46773	45350	80547	91464	93546	10 <sub>7,3</sub>	10 <sub>7,4</sub>
11 <sub>3,8</sub>	11 <sub>4,8</sub>	52273	59213	99473	109542	111515	11 <sub>8,3</sub>	11 <sub>8,4</sub>
12 <sub>3,9</sub>	12 <sub>4,9</sub>	57692	76888	118383	127913	129808	12 <sub>9,3</sub>	12 <sub>9,4</sub>
5 <sub>4,1</sub>	5 <sub>5,1</sub>	9167	7777	6127	4374	3667	5 <sub>1,4</sub>	5 <sub>1,5</sub>
6 <sub>4,2</sub>	6 <sub>5,2</sub>	17024	14084	10758	9464	12381	6 <sub>2,4</sub>	6 <sub>2,5</sub>
7 <sub>4,3</sub>	7 <sub>5,3</sub>	24107	19340	15156	18769	24107	7 <sub>3,4</sub>	7 <sub>3,5</sub>
8 <sub>4,4</sub>	8 <sub>5,4</sub>	30694	23768	21441	33034	37778	8 <sub>4,4</sub>	8 <sub>4,5</sub>
9 <sub>4,5</sub>	9 <sub>5,5</sub>	36944	27638	31860	49002	52778	9 <sub>5,4</sub>	9 <sub>5,5</sub>
10 <sub>4,6</sub>	10 <sub>5,6</sub>	42955	31542	47402	65474	68727	10 <sub>6,4</sub>	10 <sub>6,5</sub>
11 <sub>4,7</sub>	11 <sub>5,7</sub>	48788	36457	66028	82425	85379	11 <sub>7,4</sub>	11 <sub>7,5</sub>
12 <sub>4,8</sub>	12 <sub>5,8</sub>	54487	43527	85120	99805	102564	12 <sub>8,4</sub>	12 <sub>8,5</sub>



SYMMETRIC-ROTOR SUBBRANCHES—*a* AND *c* PROLATE-AND-OBULATE SUBBRANCHES

Subbranch		$\kappa$					Subbranch	
${}^cQ_{1,0}$ $J + K_{-1} + K_1$ even	${}^cQ_{1,0}$ $J + K_{-1} + K_1$ odd	$\mp 1$	$\mp 0.5$	0	$\pm 0.5$	$\pm 1$	${}^aQ_{0,1}$ $J + K_{-1} + K_1$ even	${}^aQ_{0,-1}$ $J + K_{-1} + K_1$ odd
6 <sub>5,1</sub>	6 <sub>5,1</sub>	9286	7913	6271	4244	3095	6 <sub>1,5</sub>	6 <sub>1,5</sub>
7 <sub>5,2</sub>	7 <sub>5,2</sub>	17411	14552	11116	8220	10714	7 <sub>2,5</sub>	7 <sub>2,5</sub>
8 <sub>5,3</sub>	8 <sub>5,3</sub>	24792	20246	14956	14996	21250	8 <sub>3,5</sub>	8 <sub>3,5</sub>
9 <sub>5,4</sub>	9 <sub>5,4</sub>	31667	25157	18940	27035	33778	9 <sub>4,5</sub>	9 <sub>4,5</sub>
10 <sub>5,5</sub>	10 <sub>5,5</sub>	38182	29364	25162	42308	47727	10 <sub>5,5</sub>	10 <sub>5,5</sub>
11 <sub>5,6</sub>	11 <sub>5,6</sub>	44432	32945	35783	58220	62727	11 <sub>6,5</sub>	11 <sub>6,5</sub>
12 <sub>5,7</sub>	12 <sub>5,7</sub>	50481	36135	51610	74526	78526	12 <sub>7,5</sub>	12 <sub>7,5</sub>
7 <sub>6,1</sub>	7 <sub>7,1</sub>	9375	8011	6383	4273	2679	7 <sub>1,6</sub>	7 <sub>1,7</sub>
8 <sub>6,2</sub>	8 <sub>7,2</sub>	17708	14899	11514	7682	9444	8 <sub>2,6</sub>	8 <sub>2,7</sub>
9 <sub>6,3</sub>	9 <sub>7,3</sub>	25333	20931	15562	12549	19000	9 <sub>3,6</sub>	9 <sub>3,7</sub>
10 <sub>6,4</sub>	10 <sub>7,4</sub>	32455	26254	18837	21925	30545	10 <sub>4,6</sub>	10 <sub>4,7</sub>
11 <sub>6,5</sub>	11 <sub>7,5</sub>	39205	30943	22510	36052	43561	11 <sub>5,6</sub>	11 <sub>5,7</sub>
12 <sub>6,6</sub>	12 <sub>7,6</sub>	45673	35027	28709	51607	57692	12 <sub>6,6</sub>	12 <sub>6,7</sub>
8 <sub>7,1</sub>	8 <sub>8,1</sub>	9444	8087	6468	4346	2361	8 <sub>1,7</sub>	8 <sub>1,8</sub>
9 <sub>7,2</sub>	9 <sub>8,2</sub>	17944	15167	11832	7594	8444	9 <sub>2,7</sub>	9 <sub>2,8</sub>
10 <sub>7,3</sub>	10 <sub>8,3</sub>	25773	21462	16215	11172	17182	10 <sub>3,7</sub>	10 <sub>3,8</sub>
11 <sub>7,4</sub>	11 <sub>8,4</sub>	33106	27105	19675	18011	27879	11 <sub>4,7</sub>	11 <sub>4,8</sub>
12 <sub>7,5</sub>	12 <sub>8,5</sub>	40064	32174	22501	30163	40064	12 <sub>5,7</sub>	12 <sub>5,8</sub>
9 <sub>8,1</sub>	9 <sub>9,1</sub>	9500	8146	6535	4418	2111	9 <sub>1,8</sub>	9 <sub>1,9</sub>
10 <sub>8,2</sub>	10 <sub>9,2</sub>	18136	15380	12081	7731	7636	10 <sub>2,8</sub>	10 <sub>2,9</sub>
11 <sub>8,3</sub>	11 <sub>9,3</sub>	26136	21887	16748	10598	15682	11 <sub>3,8</sub>	11 <sub>3,9</sub>
12 <sub>8,4</sub>	12 <sub>9,4</sub>	33654	27788	20570	15383	25641	12 <sub>4,8</sub>	12 <sub>4,9</sub>

10 <sub>9,1</sub> 11 <sub>9,2</sub> 12 <sub>9,1</sub>	10 <sub>10,1</sub> 11 <sub>10,2</sub> 12 <sub>10,3</sub>	9545 18295 26442	8194 15554 22237	6588 12280 17176	4479 7933 10563	1909 6970 14423	10 <sub>1,9</sub> 11 <sub>2,9</sub> 12 <sub>3,9</sub>	10 <sub>1,10</sub> 11 <sub>2,10</sub> 12 <sub>3,10</sub>
11 <sub>10,1</sub> 12 <sub>10,2</sub>	11 <sub>11,1</sub> 12 <sub>11,2</sub>	9583 18429	8234 15699	6631 12443	4530 8126	1742 6410	11 <sub>1,10</sub> 12 <sub>2,10</sub>	11 <sub>1,11</sub> 12 <sub>2,11</sub>
12 <sub>11,1</sub>	12 <sub>12,1</sub>	9615	8268	6667	4571	1603	12 <sub>1,11</sub>	12 <sub>1,12</sub>

${}^cR_{1,0}$ $J + K_{-1} + K_1$ even	${}^cP_{-1,0}$ $J + K_{-1} + K_1$ even	$\mp 1$	$\mp 0.5$	0	$\pm 0.5$	$\pm 1$	${}^aR_{0,1}$ $J + K_{-1} + K_1$ even	${}^aP_{0,-1}$ $J + K_{-1} + K_1$ even
0 <sub>0,0</sub> 1 <sub>1,0</sub> 2 <sub>2,0</sub> 3 <sub>3,0</sub> 4 <sub>4,0</sub> 5 <sub>5,0</sub> 6 <sub>6,0</sub> 7 <sub>7,0</sub> 8 <sub>8,0</sub> 9 <sub>9,0</sub> 10 <sub>10,0</sub> 11 <sub>11,0</sub>	1 <sub>1,0</sub> 2 <sub>2,0</sub> 3 <sub>3,0</sub> 4 <sub>4,0</sub> 5 <sub>5,0</sub> 6 <sub>6,0</sub> 7 <sub>7,0</sub> 8 <sub>8,0</sub> 9 <sub>9,0</sub> 10 <sub>10,0</sub> 11 <sub>11,0</sub> 12 <sub>12,0</sub>	10000 15000 25000 35000 45000 55000 65000 75000 85000 95000 105000 115000	10000 16934 25893 35773 45745 55730 65721 75714 85708 95704 105701 115698	10000 18660 27201 36728 46619 56582 66562 76549 86539 96531 106525 116519	10000 19707 29029 38312 47897 57727 67660 77628 87610 97597 107588 117580	10000 20000 30000 40000 50000 60000 70000 80000 90000 100000 110000 120000	0 <sub>0,0</sub> 1 <sub>0,1</sub> 2 <sub>0,2</sub> 3 <sub>0,3</sub> 4 <sub>0,4</sub> 5 <sub>0,5</sub> 6 <sub>0,6</sub> 7 <sub>0,7</sub> 8 <sub>0,8</sub> 9 <sub>0,9</sub> 10 <sub>0,10</sub> 11 <sub>0,11</sub> 12 <sub>0,12</sub>	1 <sub>0,1</sub> 2 <sub>0,2</sub> 3 <sub>0,3</sub> 4 <sub>0,4</sub> 5 <sub>0,5</sub> 6 <sub>0,6</sub> 7 <sub>0,7</sub> 8 <sub>0,8</sub> 9 <sub>0,9</sub> 10 <sub>0,10</sub> 11 <sub>0,11</sub> 12 <sub>0,12</sub>

SYMMETRIC-ROTOR SUBBRANCHES—*a* AND *c* PROLATE-AND-OBULATE SUBBRANCHES

Subbranch		$\kappa$					Subbranch	
${}^cR_{1,0}$ $J + K_{-1} + K_1$ even	${}^cP_{-1,0}$ $J + K_{-1} + K_1$ even	$\mp 1$	$\mp 0.5$	0	$\pm 0.5$	$\pm 1$	${}^aR_{0,1}$ $J + K_{-1} + K_1$ even	${}^aP_{0,-1}$ $J + K_{-1} + K_1$ even
1 <sub>0,1</sub>	2 <sub>1,1</sub>	15000	15000	15000	15000	15000	1 <sub>1,0</sub>	2 <sub>1,1</sub>
2 <sub>1,1</sub>	3 <sub>2,1</sub>	16667	22500	25581	26509	26667	2 <sub>1,1</sub>	3 <sub>1,2</sub>
3 <sub>2,1</sub>	4 <sub>3,1</sub>	26250	29261	33801	36902	37500	3 <sub>1,2</sub>	4 <sub>1,3</sub>
4 <sub>3,1</sub>	5 <sub>4,1</sub>	36000	38400	41758	46530	48000	4 <sub>1,3</sub>	5 <sub>1,4</sub>
5 <sub>4,1</sub>	6 <sub>5,1</sub>	45833	48106	50867	55604	58333	5 <sub>1,4</sub>	6 <sub>1,5</sub>
6 <sub>5,1</sub>	7 <sub>6,1</sub>	55714	57930	60533	64605	68571	6 <sub>1,5</sub>	7 <sub>1,6</sub>
7 <sub>6,1</sub>	8 <sub>7,1</sub>	65625	67805	70356	73938	78750	7 <sub>1,6</sub>	8 <sub>1,7</sub>
8 <sub>7,1</sub>	9 <sub>8,1</sub>	75556	77710	80235	83593	88889	8 <sub>1,7</sub>	9 <sub>1,8</sub>
9 <sub>8,1</sub>	10 <sub>9,1</sub>	85500	87636	90142	93412	99000	9 <sub>1,8</sub>	10 <sub>1,9</sub>
10 <sub>9,1</sub>	11 <sub>10,1</sub>	95455	97576	100068	103301	109091	10 <sub>1,9</sub>	11 <sub>1,10</sub>
11 <sub>10,1</sub>	12 <sub>11,1</sub>	105416	107526	110008	113219	119166	11 <sub>1,10</sub>	12 <sub>1,11</sub>
2 <sub>0,2</sub>	3 <sub>1,2</sub>	20000	18636	17345	16724	16667	2 <sub>2,0</sub>	3 <sub>2,1</sub>
3 <sub>1,2</sub>	4 <sub>2,2</sub>	18750	29055	30992	30230	30000	3 <sub>2,1</sub>	4 <sub>2,2</sub>
4 <sub>2,2</sub>	5 <sub>3,2</sub>	28000	34387	41441	42462	42000	4 <sub>2,2</sub>	5 <sub>2,3</sub>
5 <sub>3,2</sub>	6 <sub>4,2</sub>	37500	41961	49227	53738	53333	5 <sub>2,3</sub>	6 <sub>2,4</sub>
6 <sub>4,2</sub>	7 <sub>5,2</sub>	47143	51182	56697	64087	64286	6 <sub>2,4</sub>	7 <sub>2,5</sub>
7 <sub>5,2</sub>	8 <sub>6,2</sub>	56875	60756	65450	73564	75000	7 <sub>2,5</sub>	8 <sub>2,6</sub>
8 <sub>6,2</sub>	9 <sub>7,2</sub>	66667	70451	74899	82413	85556	8 <sub>2,6</sub>	9 <sub>2,7</sub>
9 <sub>7,2</sub>	10 <sub>8,2</sub>	76500	80218	84567	91174	96000	9 <sub>2,7</sub>	10 <sub>2,8</sub>
10 <sub>8,2</sub>	11 <sub>9,2</sub>	86364	90031	94328	100297	106364	10 <sub>2,8</sub>	11 <sub>2,9</sub>
11 <sub>9,2</sub>	12 <sub>10,2</sub>	96250	99880	104134	109796	116666	11 <sub>2,9</sub>	12 <sub>2,10</sub>
3 <sub>0,3</sub>	4 <sub>1,3</sub>	25000	20331	18001	17567	17500	3 <sub>3,0</sub>	4 <sub>3,1</sub>
4 <sub>1,3</sub>		21000	34848	33475	32109	32000	4 <sub>3,1</sub>	5 <sub>3,2</sub>



5 <sub>2,3</sub>	6 <sub>3,3</sub>	30000	41218	47032	45219	45000	5 <sub>3,2</sub>	6 <sub>3,3</sub>
6 <sub>2,3</sub>	7 <sub>4,3</sub>	39286	46575	57381	57683	57143	6 <sub>3,3</sub>	7 <sub>3,4</sub>
7 <sub>4,3</sub>	8 <sub>5,3</sub>	48750	54876	64788	69691	68750	7 <sub>3,4</sub>	8 <sub>3,5</sub>
8 <sub>5,3</sub>	9 <sub>6,3</sub>	58333	64092	71834	80981	80000	8 <sub>3,5</sub>	9 <sub>3,6</sub>
9 <sub>6,3</sub>	10 <sub>7,3</sub>	68000	73557	80274	91312	91000	9 <sub>3,6</sub>	10 <sub>3,7</sub>
10 <sub>7,3</sub>	11 <sub>8,3</sub>	77727	83147	89526	100665	101818	10 <sub>3,7</sub>	11 <sub>3,8</sub>
11 <sub>8,3</sub>	12 <sub>9,3</sub>	87500	92819	90948	109320	112500	11 <sub>3,8</sub>	12 <sub>3,9</sub>
4 <sub>0,4</sub>	5 <sub>1,4</sub>	30000	20650	18478	18082	18000	4 <sub>4,0</sub>	5 <sub>4,1</sub>
5 <sub>1,4</sub>	6 <sub>2,4</sub>	23333	38686	34370	33475	33333	5 <sub>4,1</sub>	6 <sub>4,2</sub>
6 <sub>2,4</sub>	7 <sub>3,4</sub>	32143	48639	49439	47326	47143	6 <sub>4,2</sub>	7 <sub>4,3</sub>
7 <sub>3,4</sub>	8 <sub>4,4</sub>	41250	52676	63082	60238	60000	7 <sub>4,3</sub>	8 <sub>4,4</sub>
8 <sub>4,4</sub>	9 <sub>5,4</sub>	50556	59229	73357	72645	72222	8 <sub>4,4</sub>	9 <sub>4,5</sub>
9 <sub>5,4</sub>	10 <sub>6,4</sub>	60000	67888	80428	84877	84000	9 <sub>4,5</sub>	10 <sub>4,6</sub>
10 <sub>6,4</sub>	11 <sub>7,4</sub>	69546	77064	87093	96881	95455	10 <sub>4,6</sub>	11 <sub>4,7</sub>
11 <sub>7,4</sub>	12 <sub>8,4</sub>	79167	86444	95254	108226	106666	11 <sub>4,7</sub>	12 <sub>4,8</sub>
5 <sub>0,5</sub>	6 <sub>1,5</sub>	35000	20660	18847	18422	18333	5 <sub>5,0</sub>	6 <sub>5,1</sub>
6 <sub>1,5</sub>	7 <sub>2,5</sub>	25714	40254	35224	34447	34286	6 <sub>5,1</sub>	7 <sub>5,2</sub>
7 <sub>2,5</sub>	8 <sub>3,5</sub>	34375	54914	50352	48971	48750	7 <sub>5,2</sub>	8 <sub>5,3</sub>
8 <sub>3,5</sub>	9 <sub>4,5</sub>	43333	60334	65354	62490	62222	8 <sub>5,3</sub>	9 <sub>5,4</sub>
9 <sub>4,5</sub>	10 <sub>5,5</sub>	52500	64543	79136	75309	75000	9 <sub>5,4</sub>	10 <sub>5,5</sub>
10 <sub>5,5</sub>	11 <sub>6,5</sub>	61818	72156	89354	87664	87273	10 <sub>5,5</sub>	11 <sub>5,6</sub>
11 <sub>6,5</sub>	12 <sub>7,5</sub>	71250	80944	96120	99820	99167	11 <sub>5,6</sub>	12 <sub>5,7</sub>
6 <sub>0,6</sub>	7 <sub>1,6</sub>	40000	20793	19108	18664	18571	6 <sub>6,0</sub>	7 <sub>6,1</sub>
7 <sub>1,6</sub>	8 <sub>2,6</sub>	28125	40367	35988	35171	35000	7 <sub>6,1</sub>	8 <sub>6,2</sub>
8 <sub>2,6</sub>	9 <sub>3,6</sub>	36667	58807	51410	50241	50000	8 <sub>6,2</sub>	9 <sub>6,3</sub>
9 <sub>3,6</sub>	10 <sub>4,6</sub>	45500	68406	66193	64301	64000	9 <sub>6,3</sub>	10 <sub>6,4</sub>
10 <sub>4,6</sub>	11 <sub>5,6</sub>	54546	71334	81252	77627	77273	10 <sub>6,4</sub>	11 <sub>6,5</sub>
11 <sub>5,6</sub>	12 <sub>6,6</sub>	63750	77023	95192	90399	90000	11 <sub>6,5</sub>	12 <sub>6,6</sub>

SYMMETRIC-ROTOR SUBBRANCHES—*a* AND *c* PROLATE-AND-OBULATE SUBBRANCHES

Subbranch		$\kappa$					Subbranch	
${}^cR_{1,0}$ $J + K_{-1} + K_1$ even	${}^cP_{-1,0}$ $J + K_{-1} + K_1$ even	$\mp 1$	$\mp 0.5$	0	$\pm 0.5$	$\pm 1$	${}^aR_{0,1}$ $J + K_{-1} + K_1$ even	${}^aP_{0,-1}$ $J + K_{-1} + K_1$ even
7 <sub>0,7</sub>	8 <sub>1,7</sub>	45000	20990	19300	18844	18750	7 <sub>7,0</sub>	8 <sub>7,1</sub>
8 <sub>1,7</sub>	9 <sub>2,7</sub>	30556	40255	36587	35733	35556	8 <sub>7,1</sub>	9 <sub>7,2</sub>
9 <sub>2,7</sub>	10 <sub>1,7</sub>	39000	60147	52457	51252	51000	9 <sub>7,2</sub>	10 <sub>7,3</sub>
10 <sub>3,7</sub>	11 <sub>4,7</sub>	47727	75043	67350	65775	65455	10 <sub>7,3</sub>	11 <sub>7,4</sub>
11 <sub>4,7</sub>	12 <sub>5,7</sub>	56667	79651	81971	79549	79167	11 <sub>7,4</sub>	12 <sub>7,5</sub>
8 <sub>0,8</sub>	9 <sub>1,8</sub>	50000	21170	19449	18985	18889	8 <sub>8,0</sub>	9 <sub>8,1</sub>
9 <sub>1,8</sub>	10 <sub>2,8</sub>	33000	40430	37059	36182	36000	9 <sub>8,1</sub>	10 <sub>8,2</sub>
10 <sub>2,8</sub>	11 <sub>3,8</sub>	41364	59963	53330	52078	51818	10 <sub>8,2</sub>	11 <sub>8,3</sub>
11 <sub>3,8</sub>	12 <sub>4,8</sub>	50000	78946	68596	66999	66667	11 <sub>8,3</sub>	12 <sub>8,4</sub>
9 <sub>0,9</sub>	10 <sub>1,9</sub>	55000	21315	19566	19097	19000	9 <sub>9,0</sub>	10 <sub>9,1</sub>
10 <sub>1,9</sub>	11 <sub>2,9</sub>	35454	40779	37443	36548	36364	10 <sub>9,1</sub>	11 <sub>9,2</sub>
11 <sub>2,9</sub>	12 <sub>3,9</sub>	43750	59640	54051	52766	52500	11 <sub>9,2</sub>	12 <sub>9,3</sub>
10 <sub>0,10</sub>	11 <sub>1,10</sub>	60000	21432	19662	19189	19091	10 <sub>10,0</sub>	11 <sub>10,1</sub>
11 <sub>1,10</sub>	12 <sub>2,10</sub>	37917	41138	37761	36854	36667	11 <sub>10,1</sub>	12 <sub>10,2</sub>
11 <sub>0,11</sub>	12 <sub>1,11</sub>	65000	21527	19742	19265	19167	11 <sub>11,0</sub>	12 <sub>11,1</sub>

${}^cR_{1,0}$ $J + K_{-1} + K_1$ odd	${}^cP_{-1,0}$ $J + K_{-1} + K_1$ odd	$\mp 1$	$\mp 0.5$	0	$\pm 0.5$	$\pm 1$	${}^aR_{0,1}$ $J + K_{-1} + K_1$ odd	${}^aP_{0,-1}$ $J + K_{-1} + K_1$ odd
1 <sub>1,1</sub>	2 <sub>2,1</sub>	15000	15000	15000	15000	15000	1 <sub>1,1</sub>	2 <sub>1,2</sub>
2 <sub>2,1</sub>	3 <sub>3,1</sub>	25000	25710	26243	26564	26667	2 <sub>1,2</sub>	3 <sub>1,3</sub>

3 <sub>1,1</sub>	4 <sub>1,1</sub>	35000	35758	36540	37210	37500	3 <sub>1,3</sub>	4 <sub>1,4</sub>
4 <sub>1,1</sub>	5 <sub>1,1</sub>	45000	45743	46583	47478	48000	4 <sub>1,4</sub>	5 <sub>1,5</sub>
5 <sub>1,1</sub>	6 <sub>1,1</sub>	55000	55730	56576	57578	58333	5 <sub>1,5</sub>	6 <sub>1,6</sub>
6 <sub>1,1</sub>	7 <sub>1,1</sub>	65000	65721	66561	67607	68571	6 <sub>1,6</sub>	7 <sub>1,7</sub>
7 <sub>1,1</sub>	8 <sub>1,1</sub>	75000	75714	76550	77609	78750	7 <sub>1,7</sub>	8 <sub>1,8</sub>
8 <sub>1,1</sub>	9 <sub>1,1</sub>	85000	85708	86539	87603	88889	8 <sub>1,8</sub>	9 <sub>1,9</sub>
9 <sub>1,1</sub>	10 <sub>1,1</sub>	95000	95704	96531	97595	99000	9 <sub>1,9</sub>	10 <sub>1,10</sub>
10 <sub>1,1</sub>	11 <sub>1,1</sub>	105000	105701	106525	107587	109091	10 <sub>1,10</sub>	11 <sub>1,11</sub>
11 <sub>1,1</sub>	12 <sub>1,1</sub>	115000	115698	116519	117580	119166	11 <sub>1,11</sub>	12 <sub>1,12</sub>
2 <sub>1,2</sub>	3 <sub>2,2</sub>	16667	16667	16667	16667	16667	2 <sub>2,1</sub>	3 <sub>2,2</sub>
3 <sub>2,2</sub>	4 <sub>2,2</sub>	26250	28258	29391	29882	30000	3 <sub>2,2</sub>	4 <sub>2,3</sub>
4 <sub>2,2</sub>	5 <sub>2,2</sub>	36000	38290	40354	41637	42000	4 <sub>2,3</sub>	5 <sub>2,4</sub>
5 <sub>2,2</sub>	6 <sub>2,2</sub>	45833	48094	50537	52600	53333	5 <sub>2,4</sub>	6 <sub>2,5</sub>
6 <sub>2,2</sub>	7 <sub>2,2</sub>	55714	57929	60461	63088	64286	6 <sub>2,5</sub>	7 <sub>2,6</sub>
7 <sub>2,2</sub>	8 <sub>2,2</sub>	65625	67805	70340	73291	75000	7 <sub>2,6</sub>	8 <sub>2,7</sub>
8 <sub>2,2</sub>	9 <sub>2,2</sub>	75556	77710	80231	83338	85556	8 <sub>2,7</sub>	9 <sub>2,8</sub>
9 <sub>2,2</sub>	10 <sub>2,2</sub>	85500	87636	90142	93314	96000	9 <sub>2,8</sub>	10 <sub>2,9</sub>
10 <sub>2,2</sub>	11 <sub>10,2</sub>	95455	97576	100068	103262	106364	10 <sub>2,9</sub>	11 <sub>12,10</sub>
11 <sub>10,2</sub>	12 <sub>11,2</sub>	105416	107526	110008	113205	116666	11 <sub>12,10</sub>	12 <sub>12,11</sub>
3 <sub>1,3</sub>	4 <sub>2,3</sub>	18750	18207	17796	17564	17500	3 <sub>3,1</sub>	4 <sub>3,2</sub>
4 <sub>2,3</sub>	5 <sub>3,3</sub>	28000	31148	32063	32074	32000	4 <sub>3,2</sub>	5 <sub>3,3</sub>
5 <sub>3,3</sub>	6 <sub>4,3</sub>	37500	41486	44187	45001	45000	5 <sub>3,3</sub>	6 <sub>3,4</sub>
6 <sub>4,3</sub>	7 <sub>5,3</sub>	47143	51127	54949	56948	57143	6 <sub>3,4</sub>	7 <sub>3,5</sub>
7 <sub>5,3</sub>	8 <sub>6,3</sub>	56875	60749	64999	68208	68750	7 <sub>3,5</sub>	8 <sub>3,6</sub>
8 <sub>6,3</sub>	9 <sub>7,3</sub>	66667	70450	74791	78959	80000	8 <sub>3,6</sub>	9 <sub>3,7</sub>
9 <sub>7,3</sub>	10 <sub>8,3</sub>	76500	80217	84543	89339	91000	9 <sub>3,7</sub>	10 <sub>3,8</sub>
10 <sub>8,3</sub>	11 <sub>9,3</sub>	86364	90031	94320	99469	101818	10 <sub>3,8</sub>	11 <sub>3,9</sub>
11 <sub>9,3</sub>	12 <sub>10,3</sub>	96250	99880	104133	109453	112500	11 <sub>3,9</sub>	12 <sub>3,10</sub>



SYMMETRIC-ROTOR SUBBRANCHES—*a* AND *c* PROLATE-AND-OBULATE SUBBRANCHES

Subbranch		$\kappa$					Subbranch	
${}^cR_{1,0}$ $J + K_{-1} + K_1$ odd	${}^cP_{-1,0}$ $J + K_{-1} + K_1$ odd	$\mp 1$	$\mp 0.5$	0	$\pm 0.5$	$\pm 1$	${}^aR_{0,1}$ $J + K_{-1} + K_1$ odd	${}^aP_{0,-1}$ $J + K_{-1} + K_1$ odd
4 <sub>1,4</sub>	5 <sub>2,4</sub>	21000	19363	18449	18082	18000	4 <sub>4,1</sub>	5 <sub>4,2</sub>
5 <sub>2,4</sub>	6 <sub>3,4</sub>	30000	33887	33934	33473	33333	5 <sub>4,2</sub>	6 <sub>4,3</sub>
6 <sub>3,4</sub>	7 <sub>4,4</sub>	39286	45000	47370	47311	47143	6 <sub>4,3</sub>	7 <sub>4,4</sub>
7 <sub>4,4</sub>	8 <sub>5,4</sub>	48750	54655	59178	60145	60000	7 <sub>4,4</sub>	8 <sub>4,5</sub>
8 <sub>5,4</sub>	9 <sub>6,4</sub>	58333	64063	69788	72255	72222	8 <sub>4,5</sub>	9 <sub>4,6</sub>
9 <sub>6,4</sub>	10 <sub>7,4</sub>	68000	73554	79716	83787	84000	9 <sub>4,6</sub>	10 <sub>4,7</sub>
10 <sub>7,4</sub>	11 <sub>8,4</sub>	77727	83147	89384	94830	95455	10 <sub>4,7</sub>	11 <sub>4,8</sub>
11 <sub>8,4</sub>	12 <sub>9,4</sub>	87500	92819	99012	105459	106666	11 <sub>4,8</sub>	12 <sub>4,9</sub>
5 <sub>1,5</sub>	6 <sub>2,5</sub>	23333	20137	18843	18422	18333	5 <sub>5,1</sub>	6 <sub>5,2</sub>
6 <sub>2,5</sub>	7 <sub>3,5</sub>	32143	36189	35151	34447	34286	6 <sub>5,2</sub>	7 <sub>5,3</sub>
7 <sub>3,5</sub>	8 <sub>4,5</sub>	41250	48511	49684	48970	48750	7 <sub>5,3</sub>	8 <sub>5,4</sub>
8 <sub>4,5</sub>	9 <sub>5,5</sub>	50556	58512	62686	62483	62222	8 <sub>5,4</sub>	9 <sub>5,5</sub>
9 <sub>5,5</sub>	10 <sub>6,5</sub>	60000	67785	74286	75273	75000	9 <sub>5,5</sub>	10 <sub>5,6</sub>
10 <sub>6,5</sub>	11 <sub>7,5</sub>	69546	77050	84774	87504	87273	10 <sub>5,6</sub>	11 <sub>5,7</sub>
11 <sub>7,5</sub>	12 <sub>8,5</sub>	79167	86442	94594	99259	99167	11 <sub>5,7</sub>	12 <sub>5,8</sub>
6 <sub>1,6</sub>	7 <sub>2,6</sub>	25714	20629	19107	18664	18571	6 <sub>6,1</sub>	7 <sub>6,2</sub>
7 <sub>2,6</sub>	8 <sub>3,6</sub>	34375	37948	35978	35171	35000	7 <sub>6,2</sub>	8 <sub>6,3</sub>
8 <sub>3,6</sub>	9 <sub>4,6</sub>	43333	51721	51284	50241	50000	8 <sub>6,3</sub>	9 <sub>6,4</sub>
9 <sub>4,6</sub>	10 <sub>5,6</sub>	52500	62496	65297	64301	64000	9 <sub>6,4</sub>	10 <sub>6,5</sub>
10 <sub>5,6</sub>	11 <sub>6,6</sub>	61818	71831	78026	77624	77273	10 <sub>6,5</sub>	11 <sub>6,6</sub>
11 <sub>6,6</sub>	12 <sub>7,6</sub>	71250	80896	89476	90385	90000	11 <sub>6,6</sub>	12 <sub>6,7</sub>

7 <sub>1,7</sub>	8 <sub>2,7</sub>	28125	20944	19300	18844	18750	7 <sub>7,1</sub>	8 <sub>7,2</sub>
8 <sub>2,7</sub>	9 <sub>3,7</sub>	36667	39200	36585	35733	35556	8 <sub>7,2</sub>	9 <sub>7,3</sub>
9 <sub>3,7</sub>	10 <sub>4,7</sub>	45500	54420	52436	51252	51000	9 <sub>7,3</sub>	10 <sub>7,4</sub>
10 <sub>4,7</sub>	11 <sub>5,7</sub>	54546	66365	67167	65775	65455	10 <sub>7,4</sub>	11 <sub>7,5</sub>
11 <sub>5,7</sub>	12 <sub>6,7</sub>	63750	76087	80851	79549	79167	11 <sub>7,5</sub>	12 <sub>7,6</sub>
8 <sub>1,8</sub>	9 <sub>2,8</sub>	30556	21157	19449	18985	18889	8 <sub>8,1</sub>	9 <sub>8,2</sub>
9 <sub>2,8</sub>	10 <sub>3,8</sub>	39000	40063	37061	36182	36000	9 <sub>8,2</sub>	10 <sub>8,3</sub>
10 <sub>3,8</sub>	11 <sub>4,8</sub>	47727	56523	53327	52078	51818	10 <sub>8,3</sub>	11 <sub>8,4</sub>
11 <sub>4,8</sub>	12 <sub>5,8</sub>	56667	69870	68563	66999	66667	11 <sub>8,4</sub>	12 <sub>8,5</sub>
9 <sub>1,9</sub>	10 <sub>2,9</sub>	33000	21311	19566	19097	19000	9 <sub>9,1</sub>	10 <sub>9,2</sub>
10 <sub>2,9</sub>	11 <sub>3,9</sub>	41364	40664	37443	36548	36364	10 <sub>9,2</sub>	11 <sub>9,3</sub>
11 <sub>3,9</sub>	12 <sub>4,9</sub>	50000	58070	54050	52766	52500	11 <sub>9,3</sub>	12 <sub>9,4</sub>
10 <sub>1,10</sub>	11 <sub>2,10</sub>	35454	21431	19662	19189	19091	10 <sub>10,1</sub>	11 <sub>10,2</sub>
11 <sub>2,10</sub>	12 <sub>3,10</sub>	43750	41102	37761	36854	36667	11 <sub>10,2</sub>	12 <sub>10,3</sub>
11 <sub>1,11</sub>	12 <sub>2,11</sub>	37917	21526	19742	19265	19167	11 <sub>11,1</sub>	12 <sub>11,2</sub>

SYMMETRIC-ROTOR SUBBRANCHES—*a* AND *c* PROLATE-OR-OBLATE SUBBRANCHES

Subbranch		$\kappa$					Subbranch	
${}^cQ_{-1,2}$ $J + K_{-1} + K_1$ even	${}^cQ_{1,-2}$ $J + K_{-1} + K_1$ odd	$\mp 1$	$\mp 0.5$	0	$\pm 0.5$	$\pm 1$	${}^aQ_{2,-1}$ $J + K_{-1} + K_1$ even	${}^aQ_{-2,1}$ $J + K_{-1} + K_1$ odd
2 <sub>2,0</sub>	2 <sub>1,2</sub>	8333	5110	2233	488		2 <sub>0,2</sub>	2 <sub>2,1</sub>
3 <sub>2,1</sub>	3 <sub>1,3</sub>	14583	5722	1328	165		3 <sub>1,2</sub>	3 <sub>3,1</sub>
4 <sub>2,2</sub>	4 <sub>1,4</sub>	20250	4363	650	78		4 <sub>2,2</sub>	4 <sub>4,1</sub>
5 <sub>2,3</sub>	5 <sub>1,5</sub>	25667	2859	374	54		5 <sub>3,2</sub>	5 <sub>5,1</sub>
6 <sub>2,4</sub>	6 <sub>1,6</sub>	30952	1843	266	43		6 <sub>4,2</sub>	6 <sub>6,1</sub>
7 <sub>2,5</sub>	7 <sub>1,7</sub>	36161	1262	218	35		7 <sub>5,2</sub>	7 <sub>7,1</sub>
8 <sub>2,6</sub>	8 <sub>1,8</sub>	41319	945	183	30		8 <sub>6,2</sub>	8 <sub>8,1</sub>
9 <sub>2,7</sub>	9 <sub>1,9</sub>	46444	770	160	26		9 <sub>7,2</sub>	9 <sub>9,1</sub>
10 <sub>2,8</sub>	10 <sub>1,10</sub>	51545	664	141	23		10 <sub>8,2</sub>	10 <sub>10,1</sub>
11 <sub>2,9</sub>	11 <sub>1,11</sub>	56629	590	125	21		11 <sub>9,2</sub>	11 <sub>11,1</sub>
12 <sub>2,10</sub>	12 <sub>1,12</sub>	61699	533	115	19		12 <sub>10,2</sub>	12 <sub>12,1</sub>
3 <sub>3,0</sub>	3 <sub>2,2</sub>	8750	7055	4522	1458		3 <sub>0,3</sub>	3 <sub>2,3</sub>
4 <sub>3,1</sub>	4 <sub>2,3</sub>	15750	11214	4568	638		4 <sub>1,3</sub>	4 <sub>3,3</sub>
5 <sub>3,2</sub>	5 <sub>2,4</sub>	22000	12576	2754	274		5 <sub>2,3</sub>	5 <sub>4,3</sub>
6 <sub>3,3</sub>	6 <sub>2,5</sub>	27587	11283	1492	171		6 <sub>3,3</sub>	6 <sub>5,3</sub>
7 <sub>3,4</sub>	7 <sub>2,6</sub>	33482	8559	925	132		7 <sub>4,3</sub>	7 <sub>6,3</sub>
8 <sub>3,5</sub>	8 <sub>2,7</sub>	38958	5932	685	108		8 <sub>5,3</sub>	8 <sub>7,3</sub>
9 <sub>3,6</sub>	9 <sub>2,8</sub>	44333	4077	567	92		9 <sub>6,3</sub>	9 <sub>8,3</sub>
10 <sub>3,7</sub>	10 <sub>2,9</sub>	49636	2945	490	80		10 <sub>7,3</sub>	10 <sub>9,3</sub>
11 <sub>3,8</sub>	11 <sub>2,10</sub>	54886	2294	433	71		11 <sub>8,3</sub>	11 <sub>10,3</sub>
12 <sub>3,9</sub>	12 <sub>2,11</sub>	60096	1917	387	64		12 <sub>9,3</sub>	12 <sub>11,3</sub>
4 <sub>4,0</sub>	4 <sub>3,3</sub>	9000	7558	5617	2547		4 <sub>0,4</sub>	4 <sub>3,3</sub>
5 <sub>4,1</sub>	5 <sub>3,3</sub>	16500	13242	7983	1599		5 <sub>1,4</sub>	5 <sub>3,3</sub>



6 <sub>4,2</sub>	6 <sub>3,4</sub>	23214	17320	6820	681	6 <sub>2,4</sub>	6 <sub>4,3</sub>
7 <sub>4,3</sub>	7 <sub>3,5</sub>	29464	19464	4223	374	7 <sub>3,4</sub>	7 <sub>5,3</sub>
8 <sub>4,4</sub>	8 <sub>3,6</sub>	35417	19178	2433	273	8 <sub>4,4</sub>	8 <sub>6,3</sub>
9 <sub>4,5</sub>	9 <sub>3,7</sub>	41167	16526	1579	222	9 <sub>5,4</sub>	9 <sub>7,3</sub>
10 <sub>4,6</sub>	10 <sub>3,8</sub>	46773	12665	1205	188	10 <sub>6,4</sub>	10 <sub>8,3</sub>
11 <sub>4,7</sub>	11 <sub>3,9</sub>	52273	9080	1014	163	11 <sub>7,4</sub>	11 <sub>9,3</sub>
12 <sub>4,8</sub>	12 <sub>3,10</sub>	57692	6485	888	144	12 <sub>8,4</sub>	12 <sub>10,3</sub>
5 <sub>5,0</sub>	5 <sub>4,2</sub>	9167	7775	6052	3368	5 <sub>0,5</sub>	5 <sub>2,4</sub>
6 <sub>5,1</sub>	6 <sub>4,3</sub>	17024	14062	9982	3054	6 <sub>1,5</sub>	6 <sub>3,4</sub>
7 <sub>5,2</sub>	7 <sub>4,4</sub>	24107	19225	11103	1459	7 <sub>2,5</sub>	7 <sub>4,4</sub>
8 <sub>5,3</sub>	8 <sub>4,5</sub>	30694	23287	9000	720	8 <sub>3,5</sub>	8 <sub>5,4</sub>
9 <sub>5,4</sub>	9 <sub>4,6</sub>	36944	26001	5708	481	9 <sub>4,5</sub>	9 <sub>6,4</sub>
10 <sub>5,5</sub>	10 <sub>4,7</sub>	42955	26852	3433	382	10 <sub>5,5</sub>	10 <sub>7,4</sub>
11 <sub>5,6</sub>	11 <sub>4,8</sub>	48788	25327	2306	321	11 <sub>6,5</sub>	11 <sub>8,4</sub>
12 <sub>5,7</sub>	12 <sub>4,9</sub>	54487	21546	1796	277	12 <sub>7,5</sub>	12 <sub>9,4</sub>
6 <sub>6,0</sub>	6 <sub>5,2</sub>	9286	7912	6257	3863	6 <sub>0,6</sub>	6 <sub>2,5</sub>
7 <sub>6,1</sub>	7 <sub>5,3</sub>	17411	14550	10952	4657	7 <sub>1,6</sub>	7 <sub>3,5</sub>
8 <sub>6,2</sub>	8 <sub>5,4</sub>	24792	20233	13841	2772	8 <sub>2,6</sub>	8 <sub>4,5</sub>
9 <sub>6,3</sub>	9 <sub>5,5</sub>	31667	25098	14023	1322	9 <sub>3,6</sub>	9 <sub>5,5</sub>
10 <sub>6,4</sub>	10 <sub>5,6</sub>	38182	29140	11121	785	10 <sub>4,6</sub>	10 <sub>6,5</sub>
11 <sub>6,5</sub>	11 <sub>5,7</sub>	44432	32202	7197	595	11 <sub>5,6</sub>	11 <sub>7,5</sub>
12 <sub>6,6</sub>	12 <sub>5,8</sub>	50481	33921	4472	494	12 <sub>6,6</sub>	12 <sub>8,5</sub>
7 <sub>7,0</sub>	7 <sub>6,2</sub>	9375	8011	6381	4141	7 <sub>0,7</sub>	7 <sub>2,6</sub>
8 <sub>7,1</sub>	8 <sub>6,3</sub>	17708	14899	11480	5982	8 <sub>1,7</sub>	8 <sub>3,6</sub>
9 <sub>7,2</sub>	9 <sub>6,4</sub>	25333	20930	15306	4603	9 <sub>2,7</sub>	9 <sub>4,6</sub>
10 <sub>7,3</sub>	10 <sub>6,5</sub>	32455	26247	17406	2348	10 <sub>3,7</sub>	10 <sub>5,6</sub>
11 <sub>7,4</sub>	11 <sub>6,6</sub>	39205	30913	16805	1258	11 <sub>4,7</sub>	11 <sub>6,6</sub>
12 <sub>7,5</sub>	12 <sub>6,7</sub>	45673	34922	13192	878	12 <sub>5,7</sub>	12 <sub>7,6</sub>

SYMMETRIC-ROTOR SUBBRANCHES—*a* AND *c* PROLATE-OR-OBLATE SUBBRANCHES

Subbranch		$\kappa$					Subbranch	
${}^cQ_{-1,2} + K_1$ even	${}^cQ_{1,-2} + K_1$ odd	$\mp 1$	$\mp 0.5$	0	$\pm 0.5$	$\pm 1$	${}^aQ_{2,-1} + K_1$ even	${}^aQ_{-2,1} + K_1$ odd
8 <sub>8,0</sub>	8 <sub>7,2</sub>	9444	8087	6468	4302		8 <sub>0,8</sub>	8 <sub>2,7</sub>
9 <sub>8,1</sub>	9 <sub>7,3</sub>	17944	15167	11825	6888		9 <sub>1,8</sub>	9 <sub>3,7</sub>
10 <sub>8,2</sub>	10 <sub>7,4</sub>	25773	21462	16158	6602		10 <sub>2,8</sub>	10 <sub>4,7</sub>
11 <sub>8,3</sub>	11 <sub>7,5</sub>	33106	27105	19325	3955		11 <sub>3,8</sub>	11 <sub>5,7</sub>
12 <sub>8,4</sub>	12 <sub>7,6</sub>	40064	32170	20771	2027		12 <sub>4,8</sub>	12 <sub>6,7</sub>
9 <sub>9,0</sub>	9 <sub>8,2</sub>	9500	8146	6535	4403		9 <sub>0,9</sub>	9 <sub>2,8</sub>
10 <sub>9,1</sub>	10 <sub>8,3</sub>	18136	15380	12079	7464		10 <sub>1,9</sub>	10 <sub>3,8</sub>
11 <sub>9,2</sub>	11 <sub>8,4</sub>	26136	21887	16736	8319		11 <sub>2,9</sub>	11 <sub>4,8</sub>
12 <sub>9,3</sub>	12 <sub>8,5</sub>	33654	27788	20487	6108		12 <sub>3,9</sub>	12 <sub>5,8</sub>
10 <sub>10,0</sub>	10 <sub>9,2</sub>	9545	8194	6588	4474		10 <sub>0,10</sub>	10 <sub>2,9</sub>
11 <sub>10,1</sub>	11 <sub>9,3</sub>	18295	15554	12279	7835		11 <sub>1,10</sub>	11 <sub>3,9</sub>
12 <sub>10,2</sub>	12 <sub>9,4</sub>	26442	22237	17173	9567		12 <sub>2,10</sub>	12 <sub>4,9</sub>
11 <sub>11,0</sub>	11 <sub>10,2</sub>	9583	8234	6631	4528		11 <sub>0,11</sub>	11 <sub>2,10</sub>
12 <sub>11,1</sub>	12 <sub>10,3</sub>	18429	15699	12443	8090		12 <sub>1,11</sub>	12 <sub>3,10</sub>
12 <sub>12,0</sub>	12 <sub>11,2</sub>	9615	8268	6667	4571		12 <sub>0,12</sub>	12 <sub>2,11</sub>

${}^cR_{-1,2} + K_1$ even	${}^cP_{1,-2} + K_1$ even	$\mp 1$	$\mp 0.5$	0	$\pm 0.5$	$\pm 1$	${}^aR_{2,-1} + K_1$ even	${}^aP_{-2,1} + K_1$ even
1 <sub>1,0</sub>	2 <sub>0,2</sub>	5000	3066	1340	293		1 <sub>0,1</sub>	2 <sub>2,0</sub>
2 <sub>1,1</sub>	3 <sub>0,3</sub>	10000	4167	1086	157		2 <sub>1,1</sub>	3 <sub>3,0</sub>

3 <sub>1,2</sub>	4 <sub>0,4</sub>	15000	3944	800	123	3 <sub>2,1</sub>	4 <sub>4,0</sub>
4 <sub>1,3</sub>	5 <sub>0,5</sub>	20000	3386	696	117	4 <sub>3,1</sub>	5 <sub>5,0</sub>
5 <sub>1,4</sub>	6 <sub>0,6</sub>	25000	2976	667	114	5 <sub>4,1</sub>	6 <sub>6,0</sub>
6 <sub>1,5</sub>	7 <sub>0,7</sub>	30000	2770	656	112	6 <sub>5,1</sub>	7 <sub>7,0</sub>
7 <sub>1,6</sub>	8 <sub>0,8</sub>	35000	2686	649	111	7 <sub>6,1</sub>	8 <sub>8,0</sub>
8 <sub>1,7</sub>	9 <sub>0,9</sub>	40000	2652	644	110	8 <sub>7,1</sub>	9 <sub>9,0</sub>
9 <sub>1,8</sub>	10 <sub>0,10</sub>	45000	2634	640	109	9 <sub>8,1</sub>	10 <sub>10,0</sub>
10 <sub>1,9</sub>	11 <sub>0,11</sub>	50000	2621	637	109	10 <sub>9,1</sub>	11 <sub>11,0</sub>
11 <sub>1,10</sub>	12 <sub>0,12</sub>	55000	2610	634	108	11 <sub>10,1</sub>	12 <sub>12,0</sub>
2 <sub>2,0</sub>	3 <sub>1,2</sub>	1667	2062	1905	776	2 <sub>0,2</sub>	3 <sub>2,1</sub>
3 <sub>2,1</sub>	4 <sub>1,3</sub>	3750	5114	2884	480	3 <sub>1,2</sub>	4 <sub>3,1</sub>
4 <sub>2,2</sub>	5 <sub>1,4</sub>	6000	7788	2336	310	4 <sub>2,2</sub>	5 <sub>4,1</sub>
5 <sub>2,3</sub>	6 <sub>1,5</sub>	8333	8748	1768	268	5 <sub>3,2</sub>	6 <sub>5,1</sub>
6 <sub>2,4</sub>	7 <sub>1,6</sub>	10714	8172	1529	254	6 <sub>4,2</sub>	7 <sub>6,1</sub>
7 <sub>2,5</sub>	8 <sub>1,7</sub>	13125	7135	1445	246	7 <sub>5,2</sub>	8 <sub>7,1</sub>
8 <sub>2,6</sub>	9 <sub>1,8</sub>	15556	6332	1406	240	8 <sub>6,2</sub>	9 <sub>8,1</sub>
9 <sub>2,7</sub>	10 <sub>1,9</sub>	18000	5885	1380	235	9 <sub>7,2</sub>	10 <sub>9,1</sub>
10 <sub>2,8</sub>	11 <sub>1,10</sub>	20455	5673	1360	232	10 <sub>8,2</sub>	11 <sub>10,1</sub>
11 <sub>2,9</sub>	12 <sub>1,11</sub>	22917	5570	1344	229	11 <sub>9,2</sub>	12 <sub>11,1</sub>
3 <sub>3,0</sub>	4 <sub>2,2</sub>	1250	1176	1316	1061	3 <sub>0,3</sub>	4 <sub>2,2</sub>
4 <sub>3,1</sub>	5 <sub>2,3</sub>	3000	3166	3516	1032	4 <sub>1,3</sub>	5 <sub>3,2</sub>
5 <sub>3,2</sub>	6 <sub>2,4</sub>	5000	6089	4448	613	5 <sub>2,3</sub>	6 <sub>4,2</sub>
6 <sub>3,3</sub>	7 <sub>2,5</sub>	7143	9630	3653	469	6 <sub>3,3</sub>	7 <sub>5,2</sub>
7 <sub>3,4</sub>	8 <sub>2,6</sub>	9375	12493	2828	426	7 <sub>4,3</sub>	8 <sub>6,2</sub>
8 <sub>3,5</sub>	9 <sub>2,7</sub>	11667	13383	2447	404	8 <sub>5,3</sub>	9 <sub>7,2</sub>
9 <sub>3,6</sub>	10 <sub>2,8</sub>	14000	12500	2301	389	9 <sub>6,3</sub>	10 <sub>8,2</sub>
10 <sub>3,7</sub>	11 <sub>2,9</sub>	16364	11048	2226	378	10 <sub>7,2</sub>	11 <sub>9,2</sub>
11 <sub>3,8</sub>	12 <sub>2,10</sub>	18750	9884	2174	370	11 <sub>8,3</sub>	12 <sub>10,2</sub>



SYMMETRIC-ROTOR SUBBRANCHES—*a* AND *c* PROLATE-OR-OBLATE SUBBRANCHES

Subbranch		$\kappa$					Subbranch	
${}^cR_{-1,2}$ $J + K_{-1} + K_1$ even	${}^cP_{1,-2}$ $J + K_{-1} + K_1$ even	$\mp 1$	$\mp 0.5$	0	$\pm 0.5$	$\pm 1$	${}^aR_{2,-1}$ $J + K_{-1} + K_1$ even	${}^aP_{-2,1}$ $J + K_{-1} + K_1$ even
4 <sub>4,0</sub>	5 <sub>3,2</sub>	1000	882	849	963		4 <sub>0,4</sub>	5 <sub>2,3</sub>
5 <sub>4,1</sub>	6 <sub>3,3</sub>	2500	2272	2651	1677		5 <sub>1,4</sub>	6 <sub>3,3</sub>
6 <sub>4,2</sub>	7 <sub>3,4</sub>	4286	4145	5108	1110		6 <sub>2,4</sub>	7 <sub>4,3</sub>
7 <sub>4,3</sub>	8 <sub>3,5</sub>	6250	6720	6025	747		7 <sub>3,4</sub>	8 <sub>5,3</sub>
8 <sub>4,4</sub>	9 <sub>3,6</sub>	8333	10196	5011	636		8 <sub>4,4</sub>	9 <sub>6,3</sub>
9 <sub>4,5</sub>	10 <sub>3,7</sub>	10500	14160	3947	590		9 <sub>5,4</sub>	10 <sub>7,3</sub>
10 <sub>4,6</sub>	11 <sub>3,8</sub>	12727	17215	3427	561		10 <sub>6,4</sub>	11 <sub>8,3</sub>
11 <sub>4,7</sub>	12 <sub>3,9</sub>	15000	18047	3214	540		11 <sub>7,4</sub>	12 <sub>9,3</sub>
5 <sub>5,0</sub>	6 <sub>4,2</sub>	833	730	638	723		5 <sub>0,6</sub>	6 <sub>2,4</sub>
6 <sub>5,1</sub>	7 <sub>4,3</sub>	2143	1898	1863	2013		6 <sub>1,6</sub>	7 <sub>3,4</sub>
7 <sub>5,2</sub>	8 <sub>4,4</sub>	3750	3384	4016	1833		7 <sub>2,6</sub>	8 <sub>4,4</sub>
8 <sub>5,3</sub>	9 <sub>4,5</sub>	5556	5182	6701	1165		8 <sub>3,6</sub>	9 <sub>5,4</sub>
9 <sub>5,4</sub>	10 <sub>4,6</sub>	7500	7437	7610	901		9 <sub>4,6</sub>	10 <sub>6,4</sub>
10 <sub>5,5</sub>	11 <sub>4,7</sub>	9545	10443	6398	809		10 <sub>5,6</sub>	11 <sub>7,4</sub>
11 <sub>5,6</sub>	12 <sub>4,8</sub>	11667	14380	5109	758		11 <sub>6,6</sub>	12 <sub>8,4</sub>
6 <sub>6,0</sub>	7 <sub>5,2</sub>	714	625	533	530		6 <sub>0,6</sub>	7 <sub>2,6</sub>
7 <sub>6,1</sub>	8 <sub>5,3</sub>	1875	1652	1470	1860		7 <sub>1,6</sub>	8 <sub>3,6</sub>
8 <sub>6,2</sub>	9 <sub>5,4</sub>	3333	2968	2958	2593		8 <sub>2,6</sub>	9 <sub>4,6</sub>
9 <sub>6,3</sub>	10 <sub>5,5</sub>	5000	4516	5406	1801		9 <sub>3,6</sub>	10 <sub>5,6</sub>
10 <sub>6,4</sub>	11 <sub>5,6</sub>	6818	6288	8298	1256		10 <sub>4,6</sub>	11 <sub>6,6</sub>
11 <sub>6,5</sub>	12 <sub>5,7</sub>	8750	8348	9203	1069		11 <sub>5,6</sub>	12 <sub>7,6</sub>

7 <sub>7,0</sub>	8 <sub>1,2</sub>	625	546	463	411	7 <sub>0,7</sub>	8 <sub>2,6</sub>
8 <sub>7,1</sub>	9 <sub>6,3</sub>	1667	1465	1267	1486	8 <sub>1,7</sub>	9 <sub>3,11</sub>
9 <sub>7,2</sub>	10 <sub>6,4</sub>	3000	2656	2402	2962	9 <sub>2,7</sub>	10 <sub>4,6</sub>
10 <sub>7,3</sub>	11 <sub>6,5</sub>	4545	4065	4106	2664	10 <sub>3,7</sub>	11 <sub>5,11</sub>
11 <sub>7,4</sub>	12 <sub>6,6</sub>	6250	5659	6816	1772	11 <sub>4,7</sub>	12 <sub>5,6</sub>
8 <sub>8,0</sub>	9 <sub>7,2</sub>	556	485	411	341	8 <sub>0,8</sub>	9 <sub>2,7</sub>
9 <sub>8,1</sub>	10 <sub>7,3</sub>	1500	1316	1129	1154	9 <sub>1,8</sub>	10 <sub>3,7</sub>
10 <sub>8,2</sub>	11 <sub>7,4</sub>	2727	2407	2110	2759	10 <sub>2,8</sub>	11 <sub>4,7</sub>
11 <sub>8,3</sub>	12 <sub>7,5</sub>	4167	3705	3398	3519	11 <sub>3,8</sub>	12 <sub>5,7</sub>
9 <sub>9,0</sub>	10 <sub>8,2</sub>	500	436	369	298	9 <sub>0,9</sub>	10 <sub>2,8</sub>
10 <sub>9,1</sub>	11 <sub>8,3</sub>	1364	1195	1021	932	10 <sub>1,9</sub>	11 <sub>3,8</sub>
11 <sub>9,2</sub>	12 <sub>8,4</sub>	2500	2201	1910	2276	11 <sub>2,9</sub>	12 <sub>4,8</sub>
10 <sub>10,0</sub>	11 <sub>9,2</sub>	455	397	335	268	10 <sub>0,10</sub>	11 <sub>2,9</sub>
11 <sub>10,1</sub>	12 <sub>9,3</sub>	1250	1094	933	797	11 <sub>1,10</sub>	12 <sub>3,9</sub>
11 <sub>11,0</sub>	12 <sub>10,2</sub>	417	363	307	244	11 <sub>0,11</sub>	12 <sub>2,10</sub>

SYMMETRIC-ROTOR SUBBRANCHES—*a* AND *c* PROLATE-OR-OBLATE SUBBRANCHES

Subbranch		$\kappa$				Subbranch		
${}^cR_{-1,2}$ $J + K_{-1} + K_1$ odd	${}^cP_{1,-2}$ $J + K_{-1} + K_1$ odd	$\mp 1$	$\mp 0.5$	0	$\pm 0.5$	$\pm 1$	${}^aR_{2,-1}$ $J + K_{-1} + K_1$ odd	${}^aP_{-2,1}$ $J + K_{-1} + K_1$ odd
2 <sub>2,1</sub>	3 <sub>1,3</sub>	1667	956	423	103		2 <sub>1,2</sub>	3 <sub>3,1</sub>
3 <sub>2,2</sub>	4 <sub>1,4</sub>	3750	1742	609	118		3 <sub>2,2</sub>	4 <sub>4,1</sub>
4 <sub>2,3</sub>	5 <sub>1,5</sub>	6000	2228	657	116		4 <sub>3,2</sub>	5 <sub>5,1</sub>
5 <sub>2,4</sub>	6 <sub>1,6</sub>	8333	2480	661	114		5 <sub>4,2</sub>	6 <sub>6,1</sub>
6 <sub>2,5</sub>	7 <sub>1,7</sub>	10714	2590	655	112		6 <sub>5,2</sub>	7 <sub>7,1</sub>
7 <sub>2,6</sub>	8 <sub>1,8</sub>	13125	2627	649	111		7 <sub>6,2</sub>	8 <sub>8,1</sub>
8 <sub>2,7</sub>	9 <sub>1,9</sub>	15556	2633	644	110		8 <sub>7,2</sub>	9 <sub>9,1</sub>
9 <sub>2,8</sub>	10 <sub>1,10</sub>	18000	2627	640	109		9 <sub>8,2</sub>	10 <sub>10,1</sub>
10 <sub>2,9</sub>	11 <sub>1,11</sub>	20455	2619	637	109		10 <sub>9,2</sub>	11 <sub>11,1</sub>
11 <sub>2,10</sub>	12 <sub>1,12</sub>	22917	2610	634	108		11 <sub>10,2</sub>	12 <sub>12,1</sub>
3 <sub>3,1</sub>	4 <sub>2,3</sub>	1250	1025	643	213		3 <sub>1,3</sub>	4 <sub>3,2</sub>
4 <sub>3,2</sub>	5 <sub>2,4</sub>	3000	2317	1159	269		4 <sub>2,3</sub>	5 <sub>4,2</sub>
5 <sub>3,3</sub>	6 <sub>2,5</sub>	5000	3522	1389	265		5 <sub>3,3</sub>	6 <sub>5,2</sub>
6 <sub>3,4</sub>	7 <sub>2,6</sub>	7143	4450	1442	254		6 <sub>4,3</sub>	7 <sub>6,2</sub>
7 <sub>3,5</sub>	8 <sub>2,7</sub>	9375	5049	1429	246		7 <sub>5,3</sub>	8 <sub>7,2</sub>
8 <sub>3,6</sub>	9 <sub>2,8</sub>	11667	5372	1403	240		8 <sub>6,3</sub>	9 <sub>8,2</sub>
9 <sub>3,7</sub>	10 <sub>2,9</sub>	14000	5507	1379	235		9 <sub>7,3</sub>	10 <sub>9,2</sub>
10 <sub>3,8</sub>	11 <sub>2,10</sub>	16364	5539	1360	232		10 <sub>8,3</sub>	11 <sub>10,2</sub>
11 <sub>3,9</sub>	12 <sub>2,11</sub>	18750	5523	1344	229		11 <sub>9,3</sub>	12 <sub>11,2</sub>
4 <sub>4,1</sub>	5 <sub>3,3</sub>	1000	869	664	300		4 <sub>1,4</sub>	5 <sub>3,3</sub>
5 <sub>4,2</sub>	6 <sub>3,4</sub>	2500	2168	1455	440		5 <sub>2,4</sub>	6 <sub>4,3</sub>
6 <sub>4,3</sub>	7 <sub>3,5</sub>	4286	3662	2018	447		6 <sub>3,4</sub>	7 <sub>5,3</sub>
7 <sub>4,4</sub>	8 <sub>3,6</sub>	6250	5157	2266	424		7 <sub>4,4</sub>	8 <sub>6,3</sub>



8 <sub>4,5</sub> 9 <sub>4,6</sub> 10 <sub>4,7</sub> 11 <sub>4,8</sub>	9 <sub>3,7</sub> 10 <sub>3,8</sub> 11 <sub>3,9</sub> 12 <sub>3,10</sub>	8333 10500 12727 15000	6471 7475 8130 8481	2309 2272 2220 2173	404 389 378 370	8 <sub>5,4</sub> 9 <sub>5,4</sub> 10 <sub>7,4</sub> 11 <sub>8,4</sub>	9 <sub>7,3</sub> 10 <sub>8,3</sub> 11 <sub>9,3</sub> 12 <sub>10,3</sub>
5 <sub>5,1</sub> 6 <sub>5,2</sub> 7 <sub>5,3</sub> 8 <sub>5,4</sub> 9 <sub>5,5</sub> 10 <sub>5,6</sub> 11 <sub>5,7</sub>	6 <sub>4,3</sub> 7 <sub>4,4</sub> 8 <sub>4,5</sub> 9 <sub>4,6</sub> 10 <sub>4,7</sub> 11 <sub>4,8</sub> 12 <sub>4,9</sub>	833 2143 3750 5556 7500 9545 11667	729 1889 3329 4947 6629 8239 9627	601 1489 2360 2953 3209 3235 3171	346 603 656 626 589 561 540	5 <sub>1,5</sub> 6 <sub>2,5</sub> 7 <sub>3,5</sub> 8 <sub>4,5</sub> 9 <sub>5,5</sub> 10 <sub>6,5</sub> 11 <sub>7,5</sub>	6 <sub>2,4</sub> 7 <sub>4,4</sub> 8 <sub>5,4</sub> 9 <sub>6,4</sub> 10 <sub>7,4</sub> 11 <sub>8,4</sub> 12 <sub>9,4</sub>
6 <sub>6,1</sub> 7 <sub>6,2</sub> 8 <sub>6,3</sub> 9 <sub>6,4</sub> 10 <sub>6,5</sub> 11 <sub>6,6</sub>	7 <sub>5,3</sub> 8 <sub>5,4</sub> 9 <sub>5,5</sub> 10 <sub>5,6</sub> 11 <sub>5,7</sub> 12 <sub>5,8</sub>	714 1875 3333 5000 6818 8750	625 1651 2962 4489 6181 7975	527 1386 2400 3326 3940 4195	357 726 873 858 804 758	6 <sub>1,6</sub> 7 <sub>2,6</sub> 8 <sub>3,6</sub> 9 <sub>4,6</sub> 10 <sub>5,6</sub> 11 <sub>6,6</sub> 12 <sub>7,6</sub>	7 <sub>3,5</sub> 8 <sub>4,5</sub> 9 <sub>5,5</sub> 10 <sub>6,5</sub> 11 <sub>7,5</sub> 12 <sub>8,5</sub>
7 <sub>7,1</sub> 8 <sub>7,2</sub> 9 <sub>7,3</sub> 10 <sub>7,4</sub> 11 <sub>7,5</sub>	8 <sub>6,3</sub> 9 <sub>6,4</sub> 10 <sub>6,5</sub> 11 <sub>6,6</sub> 12 <sub>6,7</sub>	625 1667 3000 4545 6250	546 1465 2656 4062 5646	462 1251 2267 3368 4336	341 793 1069 1110 1050	7 <sub>1,7</sub> 8 <sub>2,7</sub> 9 <sub>3,7</sub> 10 <sub>4,7</sub> 11 <sub>5,7</sub>	8 <sub>3,6</sub> 9 <sub>4,6</sub> 10 <sub>5,6</sub> 11 <sub>6,6</sub> 12 <sub>7,6</sub>
8 <sub>8,1</sub> 9 <sub>8,2</sub> 10 <sub>8,3</sub> 11 <sub>8,4</sub>	9 <sub>7,3</sub> 10 <sub>7,4</sub> 11 <sub>7,5</sub> 12 <sub>7,6</sub>	556 1500 2727 4167	485 1316 2407 3704	411 1126 2082 3209	317 808 1216 1361	8 <sub>1,8</sub> 9 <sub>2,8</sub> 10 <sub>3,8</sub> 11 <sub>4,8</sub>	9 <sub>3,7</sub> 10 <sub>4,7</sub> 11 <sub>5,7</sub> 12 <sub>6,7</sub>

SYMMETRIC-ROTOR SUBBRANCHES—*a* AND *c* PROLATE-OR-OBLATE SUBBRANCHES

Subbranch		$\kappa$					Subbranch	
${}^cR_{-1,2}$ $J + K_{-1} + K_1$ odd	${}^cP_{1,-2}$ $J + K_{-1} + K_1$ odd	$\mp 1$	$\mp 0.5$	0	$\pm 0.5$	$\pm 1$	${}^aR_{2,-1}$ $J + K_{-1} + K_1$ odd	${}^aP_{-2,1}$ $J + K_{-1} + K_1$ odd
$9_{9,1}$	$10_{8,3}$	500	436	369	290		$9_{1,9}$	$10_{3,8}$
$10_{9,2}$	$11_{8,4}$	1364	1195	1021	786		$10_{2,9}$	$11_{4,8}$
$11_{9,3}$	$12_{8,5}$	2500	2201	1904	1296		$11_{3,9}$	$12_{5,8}$
$10_{10,1}$	$11_{9,3}$	455	397	335	265		$10_{1,10}$	$11_{3,9}$
$11_{10,2}$	$12_{9,4}$	1250	1094	931	741		$11_{2,10}$	$12_{4,9}$
$11_{11,1}$	$12_{10,3}$	417	363	307	243		$11_{1,11}$	$12_{3,10}$

SYMMETRIC-ROTOR SUBBRANCHES—*b* PROLATE-AND-OBLATE SUBBRANCHES

Subbranch		$\kappa$				Subbranch	
${}^bQ_{-1,1}$ $J + K_{-1} + K_1$ even	${}^bQ_{1,-1}$ $J + K_{-1} + K_1$ even	$\mp 1$	$\mp 0.5$	0	$\pm 0.5$	$\pm 1$	${}^bQ_{-1,1}$ $J + K_{-1} + K_1$ even
$1_{1,0}$	$1_{0,1}$	15000	15000	15000	15000	15000	$1_{1,0}$
$2_{1,1}$	$2_{0,2}$	25000	21289	16667	12044	8333	$2_{2,0}$
$3_{1,2}$	$3_{0,3}$	35000	23196	14583	10583	8750	$3_{3,0}$
$4_{1,3}$	$4_{0,4}$	45000	22157	13527	10617	9000	$4_{4,0}$
$5_{1,4}$	$5_{0,5}$	55000	20634	13413	10753	9167	$5_{5,0}$
$6_{1,5}$	$6_{0,6}$	65000	19779	13484	10861	9286	$6_{6,0}$
$7_{1,6}$	$7_{0,7}$	75000	19511	13559	10943	9375	$7_{7,0}$

8 <sub>1,7</sub>	8 <sub>0,8</sub>	85000	19487	13620	11008	9444	8 <sub>7,1</sub>	8 <sub>8,0</sub>
9 <sub>1,8</sub>	9 <sub>0,9</sub>	95000	19524	13669	11060	9500	9 <sub>8,1</sub>	9 <sub>9,0</sub>
10 <sub>1,9</sub>	10 <sub>0,10</sub>	105000	19565	13710	11103	9545	10 <sub>9,1</sub>	10 <sub>10,0</sub>
11 <sub>1,10</sub>	11 <sub>0,11</sub>	115000	19604	13744	11139	9583	11 <sub>10,1</sub>	11 <sub>11,0</sub>
12 <sub>1,11</sub>	12 <sub>0,12</sub>	125000	19633	13774	11170	9615	12 <sub>11,1</sub>	12 <sub>12,0</sub>
2 <sub>2,0</sub>	2 <sub>1,1</sub>	8333	12044	16667	21289	25000	2 <sub>0,2</sub>	2 <sub>1,1</sub>
3 <sub>2,1</sub>	3 <sub>1,2</sub>	14583	24417	28872	24417	14583	3 <sub>1,2</sub>	3 <sub>2,1</sub>
4 <sub>2,2</sub>	4 <sub>1,3</sub>	20250	36119	31154	20622	15750	4 <sub>2,2</sub>	4 <sub>3,1</sub>
5 <sub>2,3</sub>	5 <sub>1,4</sub>	25667	43650	28164	20038	16500	5 <sub>3,2</sub>	5 <sub>4,1</sub>
6 <sub>2,4</sub>	6 <sub>1,5</sub>	30952	45529	26402	20356	17024	6 <sub>4,2</sub>	6 <sub>5,1</sub>
7 <sub>2,5</sub>	7 <sub>1,6</sub>	36161	43602	26163	20670	17411	7 <sub>5,2</sub>	7 <sub>6,1</sub>
8 <sub>2,6</sub>	8 <sub>1,7</sub>	41319	41002	26300	20926	17708	8 <sub>6,2</sub>	8 <sub>7,1</sub>
9 <sub>2,7</sub>	9 <sub>1,8</sub>	46444	39408	26465	21134	17944	9 <sub>7,2</sub>	9 <sub>8,1</sub>
10 <sub>2,8</sub>	10 <sub>1,9</sub>	51545	38815	26611	21307	18136	10 <sub>8,2</sub>	10 <sub>9,1</sub>
11 <sub>2,9</sub>	11 <sub>1,10</sub>	56629	38701	26737	21452	18295	11 <sub>9,2</sub>	11 <sub>10,1</sub>
12 <sub>2,10</sub>	12 <sub>1,11</sub>	61699	38736	26846	21576	18429	12 <sub>10,2</sub>	12 <sub>11,1</sub>
3 <sub>3,0</sub>	3 <sub>2,1</sub>	8750	10583	14583	23196	35000	3 <sub>0,3</sub>	3 <sub>1,2</sub>
4 <sub>3,1</sub>	4 <sub>2,2</sub>	15750	20622	31154	36119	20250	4 <sub>1,3</sub>	4 <sub>2,2</sub>
5 <sub>3,2</sub>	5 <sub>2,3</sub>	22000	32340	44017	32340	22000	5 <sub>2,3</sub>	5 <sub>3,2</sub>
6 <sub>3,3</sub>	6 <sub>2,4</sub>	27857	45986	45920	29422	23214	6 <sub>3,3</sub>	6 <sub>4,2</sub>
7 <sub>3,4</sub>	7 <sub>2,5</sub>	33482	58783	41862	29481	24107	7 <sub>4,3</sub>	7 <sub>5,2</sub>
8 <sub>3,5</sub>	8 <sub>2,6</sub>	38958	66715	39333	29932	24792	8 <sub>5,3</sub>	8 <sub>6,2</sub>
9 <sub>3,6</sub>	9 <sub>2,7</sub>	44333	68174	38859	30348	25333	9 <sub>6,3</sub>	9 <sub>7,2</sub>
10 <sub>3,7</sub>	10 <sub>2,8</sub>	49636	65282	38980	30705	25773	10 <sub>7,3</sub>	10 <sub>8,2</sub>
11 <sub>3,8</sub>	11 <sub>2,9</sub>	54886	61636	39182	31011	26136	11 <sub>8,3</sub>	11 <sub>9,2</sub>
12 <sub>3,9</sub>	12 <sub>2,10</sub>	60096	59285	39377	31275	26442	12 <sub>9,3</sub>	12 <sub>10,2</sub>



SYMMETRIC-ROTOR SUBBRANCHES—*b* PROLATE-AND-OBLATE SUBBRANCHES

Subbranch		$\kappa$					Subbranch	
${}^bQ_{-1,1}$ $J + K_{-1} + K_1$ even	${}^bQ_{1,-1}$ $J + K_{-1} + K_1$ even	$\mp 1$	$\mp 0.5$	0	$\pm 0.5$	$\pm 1$	${}^bQ_{1,-1}$ $J + K_{-1} + K_1$ even	${}^bQ_{-1,1}$ $J + K_{-1} + K_1$ even
4 <sub>4,0</sub>	4 <sub>3,1</sub>	9000	10617	13527	22157	45000	4 <sub>0,4</sub>	4 <sub>1,3</sub>
5 <sub>4,1</sub>	5 <sub>3,2</sub>	16500	20038	28164	43650	25667	5 <sub>1,4</sub>	5 <sub>2,3</sub>
6 <sub>4,2</sub>	6 <sub>3,3</sub>	23214	29422	45920	45986	27857	6 <sub>2,4</sub>	6 <sub>3,3</sub>
7 <sub>4,3</sub>	7 <sub>3,4</sub>	29464	39987	59402	39987	29464	7 <sub>3,4</sub>	7 <sub>4,3</sub>
8 <sub>4,4</sub>	8 <sub>3,5</sub>	35417	52950	60829	38601	30694	8 <sub>4,4</sub>	8 <sub>5,3</sub>
9 <sub>4,5</sub>	9 <sub>3,6</sub>	41167	67954	55712	38960	31667	9 <sub>5,4</sub>	9 <sub>6,3</sub>
10 <sub>4,6</sub>	10 <sub>3,7</sub>	46773	81732	52398	39466	32455	10 <sub>6,4</sub>	10 <sub>7,3</sub>
11 <sub>4,7</sub>	11 <sub>3,8</sub>	52273	89952	51626	39938	33106	11 <sub>7,4</sub>	11 <sub>8,3</sub>
12 <sub>4,8</sub>	12 <sub>3,9</sub>	57692	90961	51673	40360	33654	12 <sub>8,4</sub>	12 <sub>9,3</sub>
5 <sub>5,0</sub>	5 <sub>4,1</sub>	9167	10753	13413	20634	55000	5 <sub>0,5</sub>	5 <sub>1,4</sub>
6 <sub>5,1</sub>	6 <sub>4,2</sub>	17024	20356	26402	45529	30952	6 <sub>1,5</sub>	6 <sub>2,4</sub>
7 <sub>5,2</sub>	7 <sub>4,3</sub>	24107	29481	41862	58783	33482	7 <sub>2,5</sub>	7 <sub>3,4</sub>
8 <sub>5,3</sub>	8 <sub>4,4</sub>	30694	38601	60829	52950	35417	8 <sub>3,5</sub>	8 <sub>4,4</sub>
9 <sub>5,4</sub>	9 <sub>4,5</sub>	36944	48332	74852	48332	36944	9 <sub>4,5</sub>	9 <sub>5,4</sub>
10 <sub>5,5</sub>	10 <sub>4,6</sub>	42955	59745	75829	47998	38182	10 <sub>5,5</sub>	10 <sub>6,4</sub>
11 <sub>5,6</sub>	11 <sub>4,7</sub>	48788	73909	69690	48463	39205	11 <sub>6,5</sub>	11 <sub>7,4</sub>
12 <sub>5,7</sub>	12 <sub>4,8</sub>	54487	90148	65598	48989	40064	12 <sub>7,5</sub>	12 <sub>8,4</sub>
6 <sub>6,0</sub>	6 <sub>5,1</sub>	9280	10861	13484	19779	65000	6 <sub>0,6</sub>	6 <sub>1,5</sub>
7 <sub>6,1</sub>	7 <sub>5,2</sub>	17411	20670	26163	43602	36161	7 <sub>1,6</sub>	7 <sub>2,5</sub>
8 <sub>6,2</sub>	8 <sub>5,3</sub>	24792	29932	39333	66715	38958	8 <sub>2,6</sub>	8 <sub>3,5</sub>
9 <sub>6,3</sub>	9 <sub>5,4</sub>	31667	38960	55712	67954	41167	9 <sub>3,6</sub>	9 <sub>4,5</sub>
10 <sub>6,4</sub>	10 <sub>5,5</sub>	38182	47998	75829	59745	42955	10 <sub>4,6</sub>	10 <sub>5,5</sub>

11 <sub>6,5</sub> 12 <sub>7,5</sub>	11 <sub>6,6</sub> 12 <sub>7,6</sub>	44432 45673	57343 57486	90410 90893	57343 67590	44432 50481	11 <sub>6,6</sub> 12 <sub>7,6</sub>	11 <sub>6,5</sub> 12 <sub>7,5</sub>
7 <sub>1,6</sub> 8 <sub>2,6</sub> 9 <sub>3,6</sub> 10 <sub>4,6</sub> 11 <sub>5,6</sub> 12 <sub>6,6</sub>	7 <sub>0,7</sub> 8 <sub>1,7</sub> 9 <sub>2,7</sub> 10 <sub>3,7</sub> 11 <sub>4,7</sub> 12 <sub>5,7</sub>	75000 41319 44333 46773 48788 50481	19511 41002 68174 81732 73909 67590	13559 26300 38859 52398 69690 90893	10943 20926 30348 39466 48463 57486	9375 17708 25333 32455 39205 45673	7 <sub>6,1</sub> 8 <sub>6,2</sub> 9 <sub>6,3</sub> 10 <sub>6,4</sub> 11 <sub>6,5</sub> 12 <sub>6,6</sub>	7 <sub>7,0</sub> 8 <sub>7,1</sub> 9 <sub>7,2</sub> 10 <sub>7,3</sub> 11 <sub>7,4</sub> 12 <sub>7,5</sub>
8 <sub>1,7</sub> 9 <sub>2,7</sub> 10 <sub>3,7</sub> 11 <sub>4,7</sub> 12 <sub>5,7</sub>	8 <sub>0,8</sub> 9 <sub>1,8</sub> 10 <sub>2,8</sub> 11 <sub>3,8</sub> 12 <sub>4,8</sub>	85000 46444 49636 52273 54487	19487 39408 65282 89952 90148	13620 26465 38980 51626 65598	11008 21134 30705 39938 48989	9444 17944 25773 33106 40064	8 <sub>7,1</sub> 9 <sub>7,2</sub> 10 <sub>7,3</sub> 11 <sub>7,4</sub> 12 <sub>7,5</sub>	8 <sub>8,0</sub> 9 <sub>8,1</sub> 10 <sub>8,2</sub> 11 <sub>8,3</sub> 12 <sub>8,4</sub>
9 <sub>1,8</sub> 10 <sub>2,8</sub> 11 <sub>3,8</sub> 12 <sub>4,8</sub>	9 <sub>0,9</sub> 10 <sub>1,9</sub> 11 <sub>2,9</sub> 12 <sub>3,9</sub>	95000 51545 54886 57692	19524 38815 61636 90961	13669 26611 39182 51673	11060 21307 31011 40360	9500 18136 26136 33654	9 <sub>8,1</sub> 10 <sub>8,2</sub> 11 <sub>8,3</sub> 12 <sub>8,4</sub>	9 <sub>9,0</sub> 10 <sub>9,1</sub> 11 <sub>9,2</sub> 12 <sub>9,3</sub>
10 <sub>1,9</sub> 11 <sub>2,9</sub> 12 <sub>3,9</sub>	10 <sub>0,10</sub> 11 <sub>1,10</sub> 12 <sub>2,10</sub>	105000 56629 60096	19565 38701 59285	13710 26737 39377	11103 21452 31275	9545 18295 26442	10 <sub>9,1</sub> 11 <sub>9,2</sub> 12 <sub>9,3</sub>	10 <sub>10,0</sub> 11 <sub>10,1</sub> 12 <sub>10,2</sub>
11 <sub>1,10</sub> 12 <sub>2,10</sub>	11 <sub>0,11</sub> 12 <sub>1,11</sub>	115000 61699	19604 38736	13744 26846	11139 21576	9583 18429	11 <sub>10,1</sub> 12 <sub>10,2</sub>	11 <sub>11,0</sub> 12 <sub>11,1</sub>
12 <sub>1,11</sub>	12 <sub>0,11</sub>	125000	19633	13774	11170	9615	12 <sub>11,1</sub>	12 <sub>12,0</sub>

SYMMETRIC-ROTOR SUBBRANCHES—b PROLATE-AND-OBLATE SUBBRANCHES

Subbranch		$\kappa$					Subbranch	
${}^bQ_{-1,1}$ $J + K_{-1} + K_1$ odd	${}^bQ_{1,-1}$ $J + K_{-1} + K_1$ odd	$\mp 1$	$\mp 0.5$	0	$\pm 0.5$	$\pm 1$	${}^bQ_{1,-1}$ $J + K_{-1} + K_1$ odd	${}^bQ_{-1,1}$ $J + K_{-1} + K_1$ odd
2 <sub>2,1</sub>	2 <sub>1,2</sub>	8333	8333	8333	8333	8333	2 <sub>2,1</sub>	2 <sub>2,1</sub>
3 <sub>2,2</sub>	3 <sub>1,3</sub>	14583	10173	11667	13160	14583	3 <sub>2,2</sub>	3 <sub>3,1</sub>
4 <sub>2,3</sub>	4 <sub>1,4</sub>	20250	10584	12886	16126	8750	4 <sub>2,3</sub>	4 <sub>4,1</sub>
5 <sub>2,4</sub>	5 <sub>1,5</sub>	25667	10751	13300	17823	9000	5 <sub>2,4</sub>	5 <sub>5,1</sub>
6 <sub>2,5</sub>	6 <sub>1,6</sub>	30952	10860	13464	18716	9167	6 <sub>2,5</sub>	6 <sub>6,1</sub>
7 <sub>2,6</sub>	7 <sub>1,7</sub>	36161	10943	13555	19158	9286	7 <sub>2,6</sub>	7 <sub>7,1</sub>
8 <sub>2,7</sub>	8 <sub>1,8</sub>	41319	11008	13619	19374	9375	8 <sub>2,7</sub>	8 <sub>8,1</sub>
9 <sub>2,8</sub>	9 <sub>1,9</sub>	46444	11060	13669	19487	9444	9 <sub>2,8</sub>	9 <sub>9,1</sub>
10 <sub>2,9</sub>	10 <sub>1,10</sub>	51545	11103	13710	19553	9500	10 <sub>2,9</sub>	10 <sub>10,1</sub>
11 <sub>2,10</sub>	11 <sub>1,11</sub>	56629	11139	13744	19598	9545	11 <sub>2,10</sub>	11 <sub>11,1</sub>
12 <sub>2,11</sub>	12 <sub>1,12</sub>	61699	11170	13774	19632	9583	12 <sub>2,11</sub>	12 <sub>12,1</sub>
3 <sub>2,1</sub>	3 <sub>2,2</sub>	8750	13160	11667	10173	14583	3 <sub>2,2</sub>	3 <sub>2,2</sub>
4 <sub>2,3</sub>	4 <sub>2,3</sub>	15750	18280	19208	18280	15750	4 <sub>2,3</sub>	4 <sub>3,2</sub>
5 <sub>2,3</sub>	5 <sub>2,4</sub>	22000	19781	23333	24936	16500	5 <sub>2,4</sub>	5 <sub>4,2</sub>
6 <sub>2,4</sub>	6 <sub>2,5</sub>	27857	20331	25173	30089	17024	6 <sub>2,5</sub>	6 <sub>5,2</sub>
7 <sub>2,5</sub>	7 <sub>2,6</sub>	33482	20668	25914	33722	17411	7 <sub>2,6</sub>	7 <sub>6,2</sub>
8 <sub>2,6</sub>	8 <sub>2,7</sub>	38958	20926	26251	36030	17708	8 <sub>2,7</sub>	8 <sub>7,2</sub>
9 <sub>2,7</sub>	9 <sub>2,8</sub>	44333	21134	26455	37360	17944	9 <sub>2,8</sub>	9 <sub>8,2</sub>
10 <sub>2,8</sub>	10 <sub>2,9</sub>	49636	21307	26609	38072	18136	10 <sub>2,9</sub>	10 <sub>9,2</sub>
11 <sub>2,9</sub>	11 <sub>2,10</sub>	54886	21452	26737	38443	18295	11 <sub>2,10</sub>	11 <sub>10,2</sub>
12 <sub>2,10</sub>	12 <sub>2,11</sub>	60096	21576	26846	38646	18429	12 <sub>2,11</sub>	12 <sub>11,2</sub>
4 <sub>2,1</sub>	4 <sub>2,2</sub>	9000	16126	12886	10584	20250	4 <sub>2,2</sub>	4 <sub>2,2</sub>
5 <sub>2,2</sub>	5 <sub>2,3</sub>	16500	24936	23333	19781	22000	5 <sub>2,3</sub>	5 <sub>3,3</sub>



6 <sub>4,3</sub>	6 <sub>3,4</sub>	23214	28237	30910	28237	30910	28237	23214	6 <sub>4,3</sub>
7 <sub>4,4</sub>	7 <sub>3,5</sub>	29464	35974	35396	35974	35396	29347	24107	7 <sub>5,3</sub>
8 <sub>4,5</sub>	8 <sub>3,6</sub>	35417	42717	37550	42717	37550	29917	24792	8 <sub>6,3</sub>
9 <sub>4,6</sub>	9 <sub>3,7</sub>	41167	48149	38467	48149	38467	30347	25333	9 <sub>7,3</sub>
10 <sub>4,7</sub>	10 <sub>3,8</sub>	46773	52121	38896	52121	38896	30705	25773	10 <sub>8,3</sub>
11 <sub>4,8</sub>	11 <sub>3,9</sub>	52273	54738	39163	54738	39163	31011	26136	11 <sub>9,3</sub>
12 <sub>4,9</sub>	12 <sub>3,10</sub>	57692	56299	39373	56299	39373	31275	26442	12 <sub>10,3</sub>
5 <sub>5,1</sub>	5 <sub>4,2</sub>	9167	10751	13300	10751	13300	17823	25667	5 <sub>2,4</sub>
6 <sub>5,2</sub>	6 <sub>4,3</sub>	17024	20331	25173	20331	25173	30089	27857	6 <sub>3,4</sub>
7 <sub>5,3</sub>	7 <sub>4,4</sub>	24107	29347	35396	29347	35396	35974	29464	7 <sub>4,4</sub>
8 <sub>5,4</sub>	8 <sub>4,5</sub>	30694	38050	43064	38050	43064	38050	30694	8 <sub>5,4</sub>
9 <sub>5,5</sub>	9 <sub>4,6</sub>	36944	46432	47757	46432	47757	38893	31667	9 <sub>6,4</sub>
10 <sub>5,6</sub>	10 <sub>4,7</sub>	42955	54266	50083	54266	50083	39458	32455	10 <sub>7,4</sub>
11 <sub>5,7</sub>	11 <sub>4,8</sub>	48788	61181	51087	61181	51087	39937	33106	11 <sub>8,4</sub>
12 <sub>5,8</sub>	12 <sub>4,9</sub>	54487	66823	51551	66823	51551	40360	33654	12 <sub>9,4</sub>
6 <sub>6,1</sub>	6 <sub>5,2</sub>	9286	10860	13464	10860	13464	18716	30952	6 <sub>2,5</sub>
7 <sub>6,2</sub>	7 <sub>5,3</sub>	17411	20668	25914	20668	25914	33722	33482	7 <sub>3,5</sub>
8 <sub>6,3</sub>	8 <sub>5,4</sub>	24792	29917	37550	29917	37550	42717	35417	8 <sub>4,5</sub>
9 <sub>6,4</sub>	9 <sub>5,5</sub>	31667	38893	47757	38893	47757	46432	36944	9 <sub>5,5</sub>
10 <sub>6,5</sub>	10 <sub>5,6</sub>	38182	47745	55515	47745	55515	47745	38182	10 <sub>6,5</sub>
11 <sub>6,6</sub>	11 <sub>5,7</sub>	44432	56495	60341	56495	60341	48430	39205	11 <sub>7,5</sub>
12 <sub>6,7</sub>	12 <sub>5,8</sub>	50481	65013	62764	65013	62764	48985	40064	12 <sub>8,5</sub>
7 <sub>7,1</sub>	7 <sub>6,2</sub>	9375	10943	13555	10943	13555	19158	36161	7 <sub>2,6</sub>
8 <sub>7,2</sub>	8 <sub>6,3</sub>	17708	20926	26251	20926	26251	36030	38958	8 <sub>3,6</sub>
9 <sub>7,3</sub>	9 <sub>6,4</sub>	25333	30347	38467	30347	38467	48149	41167	9 <sub>4,6</sub>
10 <sub>7,4</sub>	10 <sub>6,5</sub>	32455	39458	50083	39458	50083	54266	42955	10 <sub>5,6</sub>
11 <sub>7,5</sub>	11 <sub>6,6</sub>	39205	48430	60341	48430	60341	56495	44432	11 <sub>6,6</sub>
12 <sub>7,6</sub>	12 <sub>6,7</sub>	45673	57370	68182	57370	68182	57370	45673	12 <sub>7,6</sub>

SYMMETRIC-ROTOR SUBBRANCHES—*b* PROLATE-AND-OBULATE SUBBRANCHES

Subbranch		$\kappa$					Subbranch	
${}^bQ_{-1,1}$ $J + K_{-1} + K_1$ odd	${}^bQ_{1,-1}$ $J + K_{-1} + K_1$ odd	$\mp 1$	$\mp 0.5$	0	$\pm 0.5$	$\pm 1$	${}^bQ_{1,-1}$ $J + K_{-1} + K_1$ odd	${}^bQ_{-1,1}$ $J + K_{-1} + K_1$ odd
$8_{8,1}$	$8_{7,2}$	9444	11008	13619	19374	41319	$8_{1,8}$	$8_{2,7}$
$9_{8,2}$	$9_{7,3}$	17944	21134	26455	37360	44333	$9_{2,8}$	$9_{3,7}$
$10_{8,3}$	$10_{7,4}$	25773	30705	38896	52121	46773	$10_{3,8}$	$10_{4,7}$
$11_{8,4}$	$11_{7,5}$	33106	39937	51087	61181	48788	$11_{4,8}$	$11_{5,7}$
$12_{8,5}$	$12_{7,6}$	40064	48985	62764	65013	50481	$12_{5,8}$	$12_{6,7}$
$9_{9,1}$	$9_{8,2}$	9500	11060	13669	19487	46444	$9_{1,9}$	$9_{2,8}$
$10_{9,2}$	$10_{8,3}$	18136	21307	26609	38072	49636	$10_{2,9}$	$10_{3,8}$
$11_{9,3}$	$11_{8,4}$	26136	31011	39163	54738	52273	$11_{3,9}$	$11_{4,8}$
$12_{9,4}$	$12_{8,5}$	33654	40360	51551	66823	54487	$12_{4,9}$	$12_{5,8}$
$10_{10,1}$	$10_{9,2}$	9545	11103	13710	19553	51545	$10_{1,10}$	$10_{2,9}$
$11_{10,2}$	$11_{9,3}$	18295	21452	26737	38443	54886	$11_{2,10}$	$11_{3,9}$
$12_{10,3}$	$12_{9,4}$	26442	31275	39373	56299	57692	$12_{3,10}$	$12_{4,9}$
$11_{11,1}$	$11_{10,2}$	9583	11139	13744	19598	56629	$11_{1,11}$	$11_{2,10}$
$12_{11,2}$	$12_{10,3}$	18429	21576	26846	38646	60096	$12_{2,11}$	$12_{3,10}$
$12_{12,1}$	$12_{11,2}$	9615	11170	13774	19632	61699	$12_{1,12}$	$12_{2,11}$
${}^bR_{1,1}$ $J + K_{-1} + K_1$ even	${}^bP_{-1,-1}$ $J + K_{-1} + K_1$ odd	$\mp 1$	$\mp 0.5$	0	$\pm 0.5$	$\pm 1$	${}^bR_{1,1}$ $J + K_{-1} + K_1$ even	${}^bP_{-1,-1}$ $J + K_{-1} + K_1$ odd
$0_{0,0}$	$1_{1,1}$	10000	10000	10000	10000	10000	$0_{0,0}$	$1_{1,1}$
$1_{1,0}$	$2_{2,1}$	15000	15000	15000	15000	15000	$1_{0,1}$	$2_{1,2}$

2 <sub>2,0</sub>	3 <sub>3,1</sub>	25000	24086	22847	21383	20000	2 <sub>0,2</sub>	3 <sub>1,3</sub>
3 <sub>3,0</sub>	4 <sub>4,1</sub>	35000	34083	32533	29584	25000	3 <sub>0,3</sub>	4 <sub>1,4</sub>
4 <sub>4,0</sub>	5 <sub>5,1</sub>	45000	44117	42585	39100	30000	4 <sub>0,4</sub>	5 <sub>1,5</sub>
5 <sub>5,0</sub>	6 <sub>6,1</sub>	55000	54140	52653	49126	35000	5 <sub>0,5</sub>	6 <sub>1,6</sub>
6 <sub>6,0</sub>	7 <sub>7,1</sub>	65000	64155	62702	59250	40000	6 <sub>0,6</sub>	7 <sub>1,7</sub>
7 <sub>7,0</sub>	8 <sub>8,1</sub>	75000	74165	72737	69364	45000	7 <sub>0,7</sub>	8 <sub>1,8</sub>
8 <sub>8,0</sub>	9 <sub>9,1</sub>	85000	84173	82763	79453	50000	8 <sub>0,8</sub>	9 <sub>1,9</sub>
9 <sub>9,0</sub>	10 <sub>10,1</sub>	95000	94179	92782	89522	55000	9 <sub>0,9</sub>	10 <sub>1,10</sub>
10 <sub>10,0</sub>	11 <sub>11,1</sub>	105000	104184	102798	99576	60000	10 <sub>0,10</sub>	11 <sub>1,11</sub>
11 <sub>11,0</sub>	12 <sub>12,1</sub>	115000	114188	112810	109620	65000	11 <sub>0,11</sub>	12 <sub>1,12</sub>
1 <sub>0,1</sub>	2 <sub>1,2</sub>	15000	15000	15000	15000	15000	1 <sub>1,0</sub>	2 <sub>2,1</sub>
2 <sub>1,1</sub>	3 <sub>2,2</sub>	16667	16667	16667	16667	16667	2 <sub>1,1</sub>	3 <sub>2,2</sub>
3 <sub>2,1</sub>	4 <sub>3,2</sub>	26250	23549	21079	19563	18750	3 <sub>1,2</sub>	4 <sub>2,3</sub>
4 <sub>3,1</sub>	5 <sub>4,2</sub>	36000	33165	28748	23919	21000	4 <sub>1,3</sub>	5 <sub>2,4</sub>
5 <sub>4,1</sub>	6 <sub>5,2</sub>	45833	43122	38409	30161	23333	5 <sub>1,4</sub>	6 <sub>2,5</sub>
6 <sub>5,1</sub>	7 <sub>6,2</sub>	55714	53091	48508	38383	25714	6 <sub>1,5</sub>	7 <sub>2,6</sub>
7 <sub>6,1</sub>	8 <sub>7,2</sub>	65625	63059	58609	48001	28125	7 <sub>1,6</sub>	8 <sub>2,7</sub>
8 <sub>7,1</sub>	9 <sub>8,2</sub>	75556	73030	68678	58192	30556	8 <sub>1,7</sub>	9 <sub>2,8</sub>
9 <sub>8,1</sub>	10 <sub>9,2</sub>	85500	83002	78720	68479	33000	9 <sub>1,8</sub>	10 <sub>2,9</sub>
10 <sub>9,1</sub>	11 <sub>10,2</sub>	95455	92979	88749	78723	35454	10 <sub>1,9</sub>	11 <sub>2,10</sub>
11 <sub>10,1</sub>	12 <sub>11,2</sub>	105416	102958	98767	88911	37917	11 <sub>1,10</sub>	12 <sub>2,11</sub>
2 <sub>0,2</sub>	3 <sub>1,3</sub>	20000	21383	22847	24086	25000	2 <sub>2,0</sub>	3 <sub>3,1</sub>
3 <sub>1,2</sub>	4 <sub>2,3</sub>	18750	19563	21079	23549	26250	3 <sub>2,1</sub>	4 <sub>3,2</sub>
4 <sub>2,2</sub>	5 <sub>3,3</sub>	28000	23609	22028	23609	28000	4 <sub>2,2</sub>	5 <sub>3,3</sub>
5 <sub>3,2</sub>	6 <sub>4,3</sub>	37500	32338	26305	24633	30000	5 <sub>2,3</sub>	6 <sub>3,4</sub>
6 <sub>4,2</sub>	7 <sub>5,3</sub>	47143	42259	34093	27060	32143	6 <sub>2,4</sub>	7 <sub>3,5</sub>
7 <sub>5,2</sub>	8 <sub>6,3</sub>	56875	52226	43935	31293	34375	7 <sub>2,5</sub>	8 <sub>3,6</sub>
8 <sub>6,2</sub>	9 <sub>7,3</sub>	66667	62172	54199	37664	36667	8 <sub>2,6</sub>	9 <sub>3,7</sub>
9 <sub>7,2</sub>	10 <sub>8,3</sub>	76500	72110	64411	46127	39000	9 <sub>2,7</sub>	10 <sub>3,8</sub>
10 <sub>8,2</sub>	11 <sub>9,3</sub>	86364	82050	74550	56030	41364	10 <sub>2,8</sub>	11 <sub>3,9</sub>
11 <sub>9,2</sub>	12 <sub>10,3</sub>	96250	91993	84638	66512	43750	11 <sub>2,9</sub>	12 <sub>3,10</sub>



SYMMETRIC-ROTOR SUBBRANCHES—*b* PROLATE-AND-OBULATE SUBBRANCHES

Subbranch		$\kappa$					Subbranch	
${}^bR_{1,1}$ $J + K_{-1} + K_1$ even	${}^bP_{-1,-1}$ $J + K_{-1} + K_1$ odd	$\mp 1$	$\mp 0.5$	0	$\pm 0.5$	$\pm 1$	${}^bR_{1,1}$ $J + K_{-1} + K_1$ even	${}^bP_{-1,-1}$ $J + K_{-1} + K_1$ odd
3 <sub>0,3</sub>	4 <sub>1,4</sub>	25000	29584	32533	34083	35000	3 <sub>3,0</sub>	4 <sub>4,1</sub>
4 <sub>1,3</sub>	5 <sub>2,4</sub>	21000	23919	28748	33165	36000	4 <sub>3,1</sub>	5 <sub>4,2</sub>
5 <sub>2,3</sub>	6 <sub>3,4</sub>	30000	24633	26305	32338	37500	5 <sub>3,2</sub>	6 <sub>4,3</sub>
6 <sub>3,3</sub>	7 <sub>4,4</sub>	39286	31500	26801	31500	39286	6 <sub>3,3</sub>	7 <sub>4,4</sub>
7 <sub>4,3</sub>	8 <sub>5,4</sub>	48750	41277	31054	31018	41250	7 <sub>3,4</sub>	8 <sub>4,5</sub>
8 <sub>5,3</sub>	9 <sub>6,4</sub>	58333	51336	39046	31553	43333	8 <sub>3,5</sub>	9 <sub>4,6</sub>
9 <sub>6,3</sub>	10 <sub>7,4</sub>	68000	61325	49147	33704	45500	9 <sub>3,6</sub>	10 <sub>4,7</sub>
10 <sub>7,3</sub>	11 <sub>8,4</sub>	77727	71271	59638	37919	47727	10 <sub>3,7</sub>	11 <sub>4,8</sub>
11 <sub>8,3</sub>	12 <sub>9,4</sub>	87500	81200	70013	44472	50000	11 <sub>3,8</sub>	12 <sub>4,9</sub>
4 <sub>0,4</sub>	5 <sub>1,5</sub>	30000	39100	42585	44117	45000	4 <sub>4,0</sub>	5 <sub>5,1</sub>
5 <sub>1,4</sub>	6 <sub>2,5</sub>	23333	30161	38409	43122	45833	5 <sub>4,1</sub>	6 <sub>5,2</sub>
6 <sub>2,4</sub>	7 <sub>3,5</sub>	32143	27060	34093	42259	47143	6 <sub>4,2</sub>	7 <sub>5,3</sub>
7 <sub>3,4</sub>	8 <sub>4,5</sub>	41250	31018	31054	41277	48750	7 <sub>4,3</sub>	8 <sub>5,4</sub>
8 <sub>4,4</sub>	9 <sub>5,5</sub>	50556	40057	31211	40057	50556	8 <sub>4,4</sub>	9 <sub>5,5</sub>
9 <sub>5,4</sub>	10 <sub>6,5</sub>	60000	50269	35484	38709	52500	9 <sub>4,5</sub>	10 <sub>5,6</sub>
10 <sub>6,4</sub>	11 <sub>7,5</sub>	69546	60393	43709	37729	54546	10 <sub>4,6</sub>	11 <sub>5,7</sub>
11 <sub>7,4</sub>	12 <sub>8,5</sub>	79167	70407	54102	37878	56667	11 <sub>4,7</sub>	12 <sub>5,8</sub>
5 <sub>0,5</sub>	6 <sub>1,6</sub>	35000	49126	52653	54140	55000	5 <sub>5,0</sub>	6 <sub>6,1</sub>
6 <sub>1,5</sub>	7 <sub>2,6</sub>	25714	38383	48508	53091	55714	6 <sub>5,1</sub>	7 <sub>6,2</sub>
7 <sub>2,5</sub>	8 <sub>3,6</sub>	34375	31293	43935	52226	56875	7 <sub>5,2</sub>	8 <sub>6,3</sub>
8 <sub>3,5</sub>	9 <sub>4,6</sub>	43333	31553	39046	51336	58333	8 <sub>5,3</sub>	9 <sub>6,4</sub>
9 <sub>4,5</sub>	10 <sub>5,6</sub>	52500	38709	35484	50269	60000	9 <sub>5,4</sub>	10 <sub>6,5</sub>

10 <sub>6,5</sub>	11 <sub>6,6</sub>	61818	48913	35365	48913	61818	10 <sub>6,5</sub>	11 <sub>6,6</sub>
11 <sub>6,5</sub>	12 <sub>6,6</sub>	71250	59273	39679	47228	63750	11 <sub>6,5</sub>	12 <sub>6,7</sub>
6 <sub>6,6</sub>	7 <sub>1,7</sub>	40000	59250	62702	64155	65000	6 <sub>6,6</sub>	7 <sub>7,1</sub>
7 <sub>1,6</sub>	8 <sub>2,7</sub>	28125	48001	58609	63059	65625	7 <sub>6,1</sub>	8 <sub>7,2</sub>
8 <sub>2,6</sub>	9 <sub>3,7</sub>	36667	37664	54199	62172	66667	8 <sub>6,2</sub>	9 <sub>7,3</sub>
9 <sub>3,6</sub>	10 <sub>4,7</sub>	45500	33704	49147	61325	68000	9 <sub>6,3</sub>	10 <sub>7,4</sub>
10 <sub>4,6</sub>	11 <sub>5,7</sub>	54546	37729	43709	60393	69546	10 <sub>6,4</sub>	11 <sub>7,5</sub>
11 <sub>5,6</sub>	12 <sub>6,7</sub>	63750	47228	39679	59273	71250	11 <sub>6,5</sub>	12 <sub>7,6</sub>
7 <sub>0,7</sub>	8 <sub>1,8</sub>	45000	69364	72737	74165	75000	7 <sub>7,0</sub>	8 <sub>8,1</sub>
8 <sub>1,7</sub>	9 <sub>2,8</sub>	30556	58192	68678	73030	75556	8 <sub>7,1</sub>	9 <sub>8,2</sub>
9 <sub>2,7</sub>	10 <sub>3,8</sub>	39000	46127	64411	72110	76500	9 <sub>7,2</sub>	10 <sub>8,3</sub>
10 <sub>3,7</sub>	11 <sub>4,8</sub>	47727	37919	59638	71271	77727	10 <sub>7,3</sub>	11 <sub>8,4</sub>
11 <sub>4,7</sub>	12 <sub>5,8</sub>	56667	37878	54102	70407	79167	11 <sub>7,4</sub>	12 <sub>8,5</sub>
8 <sub>0,8</sub>	9 <sub>1,9</sub>	50000	79453	82763	84173	85000	8 <sub>8,0</sub>	9 <sub>9,1</sub>
9 <sub>1,8</sub>	10 <sub>2,9</sub>	33000	68479	78720	83002	85500	9 <sub>8,1</sub>	10 <sub>9,2</sub>
10 <sub>2,8</sub>	11 <sub>3,9</sub>	41364	56030	74550	82050	86364	10 <sub>8,2</sub>	11 <sub>9,3</sub>
11 <sub>3,8</sub>	12 <sub>4,9</sub>	50000	44472	70013	81200	87500	11 <sub>8,3</sub>	12 <sub>9,4</sub>
9 <sub>0,9</sub>	10 <sub>1,10</sub>	55000	89522	92782	94179	95000	9 <sub>9,0</sub>	10 <sub>10,1</sub>
10 <sub>1,9</sub>	11 <sub>2,10</sub>	35454	78723	88749	92979	95455	10 <sub>9,1</sub>	11 <sub>10,2</sub>
11 <sub>2,9</sub>	12 <sub>3,10</sub>	43750	66512	84638	91993	96250	11 <sub>9,2</sub>	12 <sub>10,3</sub>
10 <sub>0,10</sub>	11 <sub>1,11</sub>	60000	99576	102798	104184	105000	10 <sub>10,0</sub>	11 <sub>11,1</sub>
11 <sub>1,10</sub>	12 <sub>2,11</sub>	37917	88911	98767	102958	105416	11 <sub>10,1</sub>	12 <sub>11,2</sub>
11 <sub>0,11</sub>	12 <sub>1,12</sub>	65000	109620	112810	114188	115000	11 <sub>11,0</sub>	12 <sub>12,1</sub>

SYMMETRIC-ROTOR SUBBRANCHES—*b* PROLATE-AND-OBULATE SUBBRANCHES

Subbranch		$\kappa$					Subbranch	
${}^bR_{-1,1}$ $J + K_{-1} + K_1$ odd	${}^bP_{1,-1}$ $J + K_{-1} + K_1$ even	$\mp 1$	$\mp 0.5$	0	$\pm 0.5$	$\pm 1$	${}^bR_{1,-1}$ $J + K_{-1} + K_1$ odd	${}^bP_{-1,1}$ $J + K_{-1} + K_1$ even
1 <sub>1,1</sub>	2 <sub>0,2</sub>	5000	7226	10000	12774	15000	1 <sub>1,1</sub>	2 <sub>2,0</sub>
2 <sub>1,2</sub>	3 <sub>0,3</sub>	10000	16667	21498	23874	25000	2 <sub>2,1</sub>	3 <sub>3,0</sub>
3 <sub>1,3</sub>	4 <sub>0,4</sub>	15000	27406	32266	34065	35000	3 <sub>3,1</sub>	4 <sub>4,0</sub>
4 <sub>1,4</sub>	5 <sub>0,5</sub>	20000	38266	42535	44115	45000	4 <sub>4,1</sub>	5 <sub>5,0</sub>
5 <sub>1,5</sub>	6 <sub>0,6</sub>	25000	48829	52643	54140	55000	5 <sub>5,1</sub>	6 <sub>6,0</sub>
6 <sub>1,6</sub>	7 <sub>0,7</sub>	30000	59146	62700	64155	65000	6 <sub>6,1</sub>	7 <sub>7,0</sub>
7 <sub>1,7</sub>	8 <sub>0,8</sub>	35000	69327	72736	74165	75000	7 <sub>7,1</sub>	8 <sub>8,0</sub>
8 <sub>1,8</sub>	9 <sub>0,9</sub>	40000	79440	82762	84173	85000	8 <sub>8,1</sub>	9 <sub>9,0</sub>
9 <sub>1,9</sub>	10 <sub>0,10</sub>	45000	89517	92782	94179	95000	9 <sub>9,1</sub>	10 <sub>10,0</sub>
10 <sub>1,10</sub>	11 <sub>0,11</sub>	50000	99574	102798	104184	105000	10 <sub>10,1</sub>	11 <sub>11,0</sub>
11 <sub>1,11</sub>	12 <sub>0,12</sub>	55000	109619	112810	114188	115000	11 <sub>11,1</sub>	12 <sub>12,0</sub>
2 <sub>2,1</sub>	3 <sub>1,2</sub>	1667	2792	5168	10000	16667	2 <sub>1,2</sub>	3 <sub>2,1</sub>
3 <sub>2,2</sub>	4 <sub>1,3</sub>	3750	7602	15000	22398	26250	3 <sub>2,2</sub>	4 <sub>3,1</sub>
4 <sub>2,3</sub>	5 <sub>1,4</sub>	6000	14796	26797	33039	36000	4 <sub>3,2</sub>	5 <sub>4,1</sub>
5 <sub>2,4</sub>	6 <sub>1,5</sub>	8333	24389	37946	43109	45833	5 <sub>4,2</sub>	6 <sub>5,1</sub>
6 <sub>2,5</sub>	7 <sub>1,6</sub>	10714	35443	48405	53090	55714	6 <sub>5,2</sub>	7 <sub>6,1</sub>
7 <sub>2,6</sub>	8 <sub>1,7</sub>	13125	46736	58587	63059	65625	7 <sub>6,2</sub>	8 <sub>7,1</sub>
8 <sub>2,7</sub>	9 <sub>1,8</sub>	15556	57689	68672	73029	75556	8 <sub>7,2</sub>	9 <sub>8,1</sub>
9 <sub>2,8</sub>	10 <sub>1,9</sub>	18000	68283	78719	83002	85500	9 <sub>8,2</sub>	10 <sub>9,1</sub>
10 <sub>2,9</sub>	11 <sub>1,10</sub>	20455	78648	88749	92979	95455	10 <sub>9,2</sub>	11 <sub>10,1</sub>
11 <sub>2,10</sub>	12 <sub>1,11</sub>	22917	88882	98767	102958	105416	11 <sub>10,2</sub>	12 <sub>11,1</sub>
3 <sub>3,1</sub>	4 <sub>2,2</sub>	1250	1537	2692	6941	18750	3 <sub>1,3</sub>	4 <sub>2,2</sub>
4 <sub>3,2</sub>	5 <sub>2,3</sub>	3000	4022	8877	19900	28000	4 <sub>2,3</sub>	5 <sub>3,2</sub>



5 <sub>3,3</sub>	6 <sub>2,4</sub>	5000	7698	19335	31792	37500	5 <sub>3,3</sub>	6 <sub>4,2</sub>
6 <sub>3,4</sub>	7 <sub>2,5</sub>	7143	13138	31685	42193	47143	6 <sub>4,3</sub>	7 <sub>5,2</sub>
7 <sub>3,5</sub>	8 <sub>2,6</sub>	9375	20912	43306	52219	56875	7 <sub>5,3</sub>	8 <sub>6,2</sub>
8 <sub>3,6</sub>	9 <sub>2,7</sub>	11667	31041	54046	62172	66667	8 <sub>6,3</sub>	9 <sub>7,2</sub>
9 <sub>3,7</sub>	10 <sub>2,8</sub>	14000	42620	64375	72111	76500	9 <sub>7,3</sub>	10 <sub>8,2</sub>
10 <sub>3,8</sub>	11 <sub>2,9</sub>	16364	54434	74542	82050	86364	10 <sub>8,3</sub>	11 <sub>9,2</sub>
11 <sub>3,9</sub>	12 <sub>2,10</sub>	18750	65840	84638	91993	96250	11 <sub>9,3</sub>	12 <sub>10,2</sub>
4 <sub>4,1</sub>	5 <sub>3,2</sub>	1000	1162	1666	4522	21000	4 <sub>1,4</sub>	5 <sub>2,3</sub>
5 <sub>4,2</sub>	6 <sub>3,3</sub>	2500	2920	5238	16127	30000	5 <sub>2,4</sub>	6 <sub>3,3</sub>
6 <sub>4,3</sub>	7 <sub>3,4</sub>	4286	5148	12183	29700	39286	6 <sub>3,4</sub>	7 <sub>4,3</sub>
7 <sub>4,4</sub>	8 <sub>3,5</sub>	6250	8062	23299	41022	48750	7 <sub>4,4</sub>	8 <sub>6,3</sub>
8 <sub>4,5</sub>	9 <sub>3,6</sub>	8333	12161	36249	51302	58333	8 <sub>6,4</sub>	9 <sub>6,3</sub>
9 <sub>4,6</sub>	10 <sub>3,7</sub>	10500	18094	48371	61321	68000	9 <sub>6,4</sub>	10 <sub>7,3</sub>
10 <sub>4,7</sub>	11 <sub>3,8</sub>	12727	26418	59438	71271	77727	10 <sub>7,4</sub>	11 <sub>8,3</sub>
11 <sub>4,8</sub>	12 <sub>3,9</sub>	15000	37104	69962	81200	87500	11 <sub>8,4</sub>	12 <sub>9,3</sub>
5 <sub>5,1</sub>	6 <sub>4,2</sub>	833	966	1253	2984	23333	5 <sub>1,6</sub>	6 <sub>2,4</sub>
6 <sub>5,2</sub>	7 <sub>4,3</sub>	2143	2475	3549	11918	32143	6 <sub>2,6</sub>	7 <sub>3,4</sub>
7 <sub>5,3</sub>	8 <sub>4,4</sub>	3750	4309	7685	26263	41250	7 <sub>3,6</sub>	8 <sub>4,4</sub>
8 <sub>5,4</sub>	9 <sub>4,5</sub>	5556	6389	15266	39231	50556	8 <sub>4,6</sub>	9 <sub>5,4</sub>
9 <sub>5,5</sub>	10 <sub>4,6</sub>	7500	8819	27015	50150	60000	9 <sub>5,6</sub>	10 <sub>6,4</sub>
10 <sub>5,6</sub>	11 <sub>4,7</sub>	9545	11954	40562	60377	69546	10 <sub>6,6</sub>	11 <sub>7,4</sub>
11 <sub>5,7</sub>	12 <sub>4,8</sub>	11667	16365	53190	70405	79167	11 <sub>7,6</sub>	12 <sub>8,4</sub>
6 <sub>6,1</sub>	7 <sub>5,2</sub>	714	829	1052	2102	25714	6 <sub>1,6</sub>	7 <sub>2,6</sub>
7 <sub>6,2</sub>	8 <sub>5,3</sub>	1875	2170	2825	8386	34375	7 <sub>2,6</sub>	8 <sub>3,6</sub>
8 <sub>6,3</sub>	9 <sub>5,4</sub>	3333	3839	5485	21522	43333	8 <sub>3,6</sub>	9 <sub>4,6</sub>
9 <sub>6,4</sub>	10 <sub>5,5</sub>	5000	5717	10057	36378	52500	9 <sub>4,6</sub>	10 <sub>6,6</sub>
10 <sub>6,5</sub>	11 <sub>5,6</sub>	6818	7736	18198	48537	61818	10 <sub>6,6</sub>	11 <sub>6,6</sub>
11 <sub>6,6</sub>	12 <sub>5,7</sub>	8750	9912	30549	59217	71250	11 <sub>6,6</sub>	12 <sub>7,6</sub>

SYMMETRIC-ROTOR SUBBRANCHES—*b* PROLATE-AND-OBULATE SUBBRANCHES

Subbranch		$\kappa$					Subbranch	
${}^bR_{-1,1}$ $J + K_{-1} + K_1$ odd	${}^bP_{1,-1}$ $J + K_{-1} + K_1$ even	$\mp 1$	$\mp 0.5$	0	$\pm 0.5$	$\pm 1$	${}^bR_{1,-1}$ $J + K_{-1} + K_1$ odd	${}^bP_{-1,1}$ $J + K_{-1} + K_1$ even
7 <sub>1,1</sub>	8 <sub>6,2</sub>	625	726	918	1615	28125	7 <sub>1,7</sub>	8 <sub>2,6</sub>
8 <sub>7,2</sub>	9 <sub>6,3</sub>	1667	1932	2461	5953	36667	8 <sub>2,7</sub>	9 <sub>3,6</sub>
9 <sub>7,3</sub>	10 <sub>6,4</sub>	3000	3467	4517	16387	45500	9 <sub>3,7</sub>	10 <sub>4,6</sub>
10 <sub>7,4</sub>	11 <sub>6,5</sub>	4545	5226	7432	32088	54546	10 <sub>4,7</sub>	11 <sub>5,6</sub>
11 <sub>7,5</sub>	12 <sub>6,6</sub>	6250	7134	12369	46152	63750	11 <sub>5,7</sub>	12 <sub>6,6</sub>
8 <sub>8,1</sub>	9 <sub>7,2</sub>	556	645	816	1342	30556	8 <sub>1,8</sub>	9 <sub>2,7</sub>
9 <sub>8,2</sub>	10 <sub>7,3</sub>	1500	1741	2210	4454	39000	9 <sub>2,8</sub>	10 <sub>3,7</sub>
10 <sub>8,3</sub>	11 <sub>7,4</sub>	2727	3158	4030	12003	47727	10 <sub>3,8</sub>	11 <sub>4,7</sub>
11 <sub>8,4</sub>	12 <sub>7,5</sub>	4167	4808	6264	26503	56667	11 <sub>4,8</sub>	12 <sub>5,7</sub>
9 <sub>9,1</sub>	10 <sub>8,2</sub>	500	581	734	1176	33000	9 <sub>1,9</sub>	10 <sub>2,8</sub>
10 <sub>9,2</sub>	11 <sub>8,3</sub>	1364	1583	2009	3581	41364	10 <sub>2,9</sub>	11 <sub>3,8</sub>
11 <sub>9,3</sub>	12 <sub>8,4</sub>	2500	2898	3688	8874	50000	11 <sub>3,9</sub>	12 <sub>4,8</sub>
10 <sub>10,1</sub>	11 <sub>9,2</sub>	455	528	667	1059	35454	10 <sub>1,10</sub>	11 <sub>2,9</sub>
11 <sub>10,2</sub>	12 <sub>9,3</sub>	1250	1452	1841	3076	43750	11 <sub>2,10</sub>	12 <sub>3,9</sub>
11 <sub>11,1</sub>	12 <sub>10,2</sub>	417	484	611	967	37917	11 <sub>1,11</sub>	12 <sub>2,10</sub>

SYMMETRIC-ROTOR SUBBRANCHES—*b* PROLATE-OR-OBULATE SUBBRANCHES

Subbranch		$\kappa$						Subbranch	
${}^bR_{-1,3}$ $J + K_{-1} + K_1$ even	${}^bP_{1,-3}$ $J + K_{-1} + K_1$ odd	$\mp 1$	$\mp 0.5$	0	$\pm 0.5$	$\pm 1$	${}^bR_{3,-1}$ $J + K_{-1} + K_1$ even	${}^bP_{-3,1}$ $J + K_{-1} + K_1$ odd	
		1667	1097	486	101				
		3750	1452	297	32				
$2_{2,0}$	$3_{1,3}$						$2_{0,2}$	$3_{3,1}$	
$3_{2,1}$	$4_{1,4}$						$3_{1,2}$	$4_{4,1}$	

4 <sub>2,2</sub>	5 <sub>1,5</sub>	6000	1159	140	14	4 <sub>2,2</sub>	5 <sub>6,1</sub>
5 <sub>2,2</sub>	6 <sub>1,6</sub>	8333	758	77	9	5 <sub>3,2</sub>	6 <sub>6,1</sub>
6 <sub>2,4</sub>	7 <sub>1,7</sub>	10714	481	54	7	6 <sub>4,2</sub>	7 <sub>7,1</sub>
7 <sub>2,5</sub>	8 <sub>1,8</sub>	13125	323	42	6	7 <sub>5,2</sub>	8 <sub>8,1</sub>
8 <sub>2,6</sub>	9 <sub>1,9</sub>	15556	238	35	5	8 <sub>6,2</sub>	9 <sub>9,1</sub>
9 <sub>2,7</sub>	10 <sub>1,10</sub>	18000	191	30	4	9 <sub>7,2</sub>	10 <sub>10,1</sub>
10 <sub>2,8</sub>	11 <sub>1,11</sub>	20455	163	27	4	10 <sub>8,2</sub>	11 <sub>11,1</sub>
11 <sub>2,9</sub>	12 <sub>1,12</sub>	22917	144	24	3	11 <sub>9,2</sub>	12 <sub>12,1</sub>
3 <sub>3,0</sub>	4 <sub>2,3</sub>	1250	1323	1091	416	3 <sub>0,3</sub>	4 <sub>3,2</sub>
4 <sub>3,1</sub>	5 <sub>2,4</sub>	3000	2753	1252	163	4 <sub>1,3</sub>	5 <sub>4,2</sub>
5 <sub>3,2</sub>	6 <sub>2,5</sub>	5000	3538	737	62	5 <sub>2,3</sub>	6 <sub>5,2</sub>
6 <sub>3,3</sub>	7 <sub>2,6</sub>	7143	3362	375	35	6 <sub>3,3</sub>	7 <sub>6,2</sub>
7 <sub>3,4</sub>	8 <sub>2,7</sub>	9375	2573	219	26	7 <sub>4,3</sub>	8 <sub>7,2</sub>
8 <sub>3,5</sub>	9 <sub>2,8</sub>	11667	1754	155	20	8 <sub>5,3</sub>	9 <sub>8,2</sub>
9 <sub>3,6</sub>	10 <sub>2,9</sub>	14000	1174	124	17	9 <sub>6,3</sub>	10 <sub>9,2</sub>
10 <sub>3,7</sub>	11 <sub>2,10</sub>	16364	826	104	14	10 <sub>7,3</sub>	11 <sub>10,2</sub>
11 <sub>3,8</sub>	12 <sub>2,11</sub>	18750	628	90	12	11 <sub>8,3</sub>	12 <sub>11,2</sub>
4 <sub>4,0</sub>	5 <sub>3,3</sub>	1000	1144	1259	855	4 <sub>0,4</sub>	5 <sub>3,3</sub>
5 <sub>4,1</sub>	6 <sub>3,4</sub>	2500	2771	2305	514	5 <sub>1,4</sub>	6 <sub>4,3</sub>
6 <sub>4,2</sub>	7 <sub>3,5</sub>	4286	4433	2107	189	6 <sub>2,4</sub>	7 <sub>5,3</sub>
7 <sub>4,3</sub>	8 <sub>3,6</sub>	6250	5663	1258	92	7 <sub>3,4</sub>	8 <sub>6,3</sub>
8 <sub>4,4</sub>	9 <sub>3,7</sub>	8333	6007	676	62	8 <sub>4,4</sub>	9 <sub>7,3</sub>
9 <sub>4,5</sub>	10 <sub>3,8</sub>	10500	5335	411	47	9 <sub>5,4</sub>	10 <sub>8,3</sub>
10 <sub>4,6</sub>	11 <sub>3,9</sub>	12727	4082	298	38	10 <sub>6,4</sub>	11 <sub>9,3</sub>
11 <sub>4,7</sub>	12 <sub>3,10</sub>	15000	2866	241	32	11 <sub>7,4</sub>	12 <sub>10,3</sub>



SYMMETRIC-ROTOR SUBBRANCHES—*b* PROLATE-OR-OBLATE SUBBRANCHES

Subbranch		$\kappa$					Subbranch	
${}^bR_{-1,3}$ $J + K_{-1} + K_1$ even	${}^bP_{1,-3}$ $J + K_{-1} + K_1$ odd	$\mp 1$	$\mp 0.5$	0	$\pm 0.5$	$\pm 1$	${}^bR_{3,-1}$ $J + K_{-1} + K_1$ even	${}^bP_{-3,1}$ $J + K_{-1} + K_1$ odd
5 <sub>5,0</sub>	6 <sub>4,3</sub>	833	965	1174	1186		5 <sub>0,5</sub>	6 <sub>3,4</sub>
6 <sub>5,1</sub>	7 <sub>4,4</sub>	2143	2461	2707	1158		6 <sub>1,5</sub>	7 <sub>4,4</sub>
7 <sub>5,2</sub>	8 <sub>4,5</sub>	3750	4229	3560	488		7 <sub>2,5</sub>	8 <sub>5,4</sub>
8 <sub>5,3</sub>	9 <sub>4,6</sub>	5556	6040	3008	209		8 <sub>3,5</sub>	9 <sub>6,4</sub>
9 <sub>5,4</sub>	10 <sub>4,7</sub>	7500	7603	1831	125		9 <sub>4,5</sub>	10 <sub>7,4</sub>
10 <sub>5,5</sub>	11 <sub>4,8</sub>	9545	8531	1026	92		10 <sub>5,5</sub>	11 <sub>8,4</sub>
11 <sub>5,6</sub>	12 <sub>4,9</sub>	11667	8452	644	73		11 <sub>6,5</sub>	12 <sub>9,4</sub>
6 <sub>6,0</sub>	7 <sub>5,3</sub>	714	829	1039	1321		6 <sub>0,6</sub>	7 <sub>3,5</sub>
7 <sub>6,1</sub>	8 <sub>5,4</sub>	1875	2169	2640	1942		7 <sub>1,6</sub>	8 <sub>4,5</sub>
8 <sub>6,2</sub>	9 <sub>5,5</sub>	3333	3830	4213	1086		8 <sub>2,6</sub>	9 <sub>5,5</sub>
9 <sub>6,3</sub>	10 <sub>5,6</sub>	5000	5676	4833	447		9 <sub>3,6</sub>	10 <sub>6,5</sub>
10 <sub>6,4</sub>	11 <sub>5,7</sub>	6818	7575	3937	234		10 <sub>4,6</sub>	11 <sub>7,5</sub>
11 <sub>6,5</sub>	12 <sub>5,8</sub>	8750	9349	2441	161		11 <sub>5,6</sub>	12 <sub>8,5</sub>
7 <sub>7,0</sub>	8 <sub>6,3</sub>	625	726	916	1313		7 <sub>0,7</sub>	8 <sub>3,6</sub>
8 <sub>7,1</sub>	9 <sub>6,4</sub>	1667	1932	2426	2561		8 <sub>1,7</sub>	9 <sub>4,6</sub>
9 <sub>7,2</sub>	10 <sub>6,5</sub>	3000	3466	4214	2032		9 <sub>2,7</sub>	10 <sub>5,6</sub>
10 <sub>7,3</sub>	11 <sub>6,6</sub>	4545	5221	5738	917		10 <sub>3,7</sub>	11 <sub>6,6</sub>
11 <sub>7,4</sub>	12 <sub>6,7</sub>	6250	7114	6113	427		11 <sub>4,7</sub>	12 <sub>7,6</sub>
8 <sub>8,0</sub>	9 <sub>7,3</sub>	556	645	816	1238		8 <sub>0,8</sub>	9 <sub>3,7</sub>
9 <sub>8,1</sub>	10 <sub>7,4</sub>	1500	1741	2204	2870		9 <sub>1,8</sub>	10 <sub>4,7</sub>
10 <sub>8,2</sub>	11 <sub>7,5</sub>	2727	3158	3967	3126		10 <sub>2,8</sub>	11 <sub>5,7</sub>
11 <sub>8,3</sub>	12 <sub>7,6</sub>	4167	4807	5836	1752		11 <sub>3,8</sub>	12 <sub>6,7</sub>

9 <sub>0,0</sub>	10 <sub>0,0</sub>	10 <sub>0,1</sub>	10 <sub>0,2</sub>	500	581	734	1143	9 <sub>0,9</sub>	10 <sub>0,8</sub>
10 <sub>0,1</sub>	11 <sub>0,0</sub>	11 <sub>0,1</sub>	11 <sub>0,2</sub>	1364	1583	2008	2924	10 <sub>0,9</sub>	11 <sub>0,8</sub>
11 <sub>0,2</sub>	10 <sub>1,0</sub>	11 <sub>1,0</sub>	12 <sub>0,5</sub>	2500	2898	3676	4014	11 <sub>0,9</sub>	12 <sub>0,8</sub>
10 <sub>1,0</sub>	11 <sub>1,0</sub>	11 <sub>1,1</sub>	11 <sub>1,2</sub>	455	528	667	1049	10 <sub>1,10</sub>	11 <sub>1,9</sub>
11 <sub>1,0</sub>	12 <sub>1,0</sub>	12 <sub>1,1</sub>	12 <sub>1,2</sub>	1250	1452	1841	2831	11 <sub>1,10</sub>	12 <sub>1,9</sub>
11 <sub>1,1</sub>	12 <sub>1,0</sub>	12 <sub>1,1</sub>	12 <sub>1,2</sub>	417	484	611	964	11 <sub>1,11</sub>	12 <sub>1,10</sub>

FORBIDDEN SUBBRANCHES—*a* AND *c* SUBBRANCHES

Subbranch		$\kappa$				Subbranch	
$J + K_{-1} + K_1$ even	$J + K_{-1} + K_1$ odd	$\pm 1$	$\mp 0.5$	0	$\pm 0.5$	$J + K_{-1} + K_1$ odd	$J + K_{-1} + K_1$ even
3 <sub>0,1</sub>	3 <sub>0,2</sub>	3 <sub>0,3</sub>	4 <sub>0,4</sub>	5 <sub>0,5</sub>	6 <sub>0,6</sub>	7 <sub>0,7</sub>	8 <sub>0,8</sub>
4 <sub>0,2</sub>	4 <sub>0,3</sub>	5 <sub>0,4</sub>	6 <sub>0,5</sub>	7 <sub>0,6</sub>	8 <sub>0,7</sub>	9 <sub>0,8</sub>	10 <sub>0,9</sub>
5 <sub>0,3</sub>	5 <sub>0,4</sub>	6 <sub>0,5</sub>	7 <sub>0,6</sub>	8 <sub>0,7</sub>	9 <sub>0,8</sub>	10 <sub>0,9</sub>	11 <sub>0,10</sub>
6 <sub>0,4</sub>	6 <sub>0,5</sub>	7 <sub>0,6</sub>	8 <sub>0,7</sub>	9 <sub>0,8</sub>	10 <sub>0,9</sub>	11 <sub>0,10</sub>	12 <sub>0,11</sub>
7 <sub>0,5</sub>	7 <sub>0,6</sub>	8 <sub>0,7</sub>	9 <sub>0,8</sub>	10 <sub>0,9</sub>	11 <sub>0,10</sub>	12 <sub>0,11</sub>	12 <sub>0,12</sub>
8 <sub>0,6</sub>	8 <sub>0,7</sub>	9 <sub>0,8</sub>	10 <sub>0,9</sub>	11 <sub>0,10</sub>	12 <sub>0,11</sub>	12 <sub>0,12</sub>	12 <sub>0,13</sub>
9 <sub>0,7</sub>	9 <sub>0,8</sub>	10 <sub>0,9</sub>	11 <sub>0,10</sub>	12 <sub>0,11</sub>	12 <sub>0,12</sub>	12 <sub>0,13</sub>	12 <sub>0,14</sub>
10 <sub>0,8</sub>	10 <sub>0,9</sub>	11 <sub>0,10</sub>	12 <sub>0,11</sub>	12 <sub>0,12</sub>	12 <sub>0,13</sub>	12 <sub>0,14</sub>	12 <sub>0,15</sub>
11 <sub>0,9</sub>	11 <sub>0,10</sub>	12 <sub>0,11</sub>	12 <sub>0,12</sub>	12 <sub>0,13</sub>	12 <sub>0,14</sub>	12 <sub>0,15</sub>	12 <sub>0,16</sub>
12 <sub>0,10</sub>	12 <sub>0,11</sub>	12 <sub>0,12</sub>	12 <sub>0,13</sub>	12 <sub>0,14</sub>	12 <sub>0,15</sub>	12 <sub>0,16</sub>	12 <sub>0,17</sub>

FORBIDDEN SUBBRANCHES—*a* AND *c* SUBBRANCHES

Subbranch		$\kappa$					Subbranch	
${}^cQ_{-3,2}$ $J + K_{-1} + K_1$ even	${}^cQ_{3,-2}$ $J + K_{-1} + K_1$ odd	$\mp 1$	$\mp 0.5$	0	$\pm 0.5$	$\pm 1$	${}^aQ_{2,-1}$ $J + K_{-1} + K_1$ odd	${}^aQ_{-2,1}$ $J + K_{-1} + K_1$ even
4 <sub>4,1</sub> 5 <sub>4,2</sub> 6 <sub>4,3</sub> 7 <sub>4,4</sub> 8 <sub>4,5</sub> 9 <sub>4,6</sub> 10 <sub>4,7</sub> 11 <sub>4,8</sub> 12 <sub>4,9</sub>	4 <sub>1,3</sub> 5 <sub>1,4</sub> 6 <sub>1,5</sub> 7 <sub>1,6</sub> 8 <sub>1,7</sub> 9 <sub>1,8</sub> 10 <sub>1,9</sub> 11 <sub>1,10</sub> 12 <sub>1,11</sub>		31 174 527 1057 1557 1855 1940 1888 1770	164 504 708 716 642 559 489 432 387	153 193 163 131 108 92 80 71 64		4 <sub>1,4</sub> 5 <sub>2,4</sub> 6 <sub>3,4</sub> 7 <sub>4,4</sub> 8 <sub>5,4</sub> 9 <sub>6,4</sub> 10 <sub>7,4</sub> 11 <sub>8,4</sub> 12 <sub>9,4</sub>	4 <sub>3,1</sub> 5 <sub>4,1</sub> 6 <sub>5,1</sub> 7 <sub>6,1</sub> 8 <sub>7,1</sub> 9 <sub>8,1</sub> 10 <sub>9,1</sub> 11 <sub>10,1</sub> 12 <sub>11,1</sub>
5 <sub>5,1</sub> 6 <sub>5,2</sub> 7 <sub>5,3</sub> 8 <sub>5,4</sub> 9 <sub>5,5</sub> 10 <sub>5,6</sub> 11 <sub>5,7</sub> 12 <sub>5,8</sub>	5 <sub>2,3</sub> 6 <sub>2,4</sub> 7 <sub>2,5</sub> 8 <sub>2,6</sub> 9 <sub>2,7</sub> 10 <sub>2,8</sub> 11 <sub>2,9</sub> 12 <sub>2,10</sub>		9 52 187 515 1123 1924 2650 3098	79 413 919 1216 1236 1128 999 885	191 342 325 268 222 188 163 144		5 <sub>1,5</sub> 6 <sub>2,5</sub> 7 <sub>3,5</sub> 8 <sub>4,5</sub> 9 <sub>5,5</sub> 10 <sub>6,5</sub> 11 <sub>7,5</sub> 12 <sub>8,5</sub>	5 <sub>3,2</sub> 6 <sub>4,2</sub> 7 <sub>5,2</sub> 8 <sub>6,2</sub> 9 <sub>7,2</sub> 10 <sub>8,2</sub> 11 <sub>9,2</sub> 12 <sub>10,2</sub>
6 <sub>6,1</sub> 7 <sub>6,2</sub> 8 <sub>6,3</sub> 9 <sub>6,4</sub> 10 <sub>6,5</sub>	6 <sub>3,3</sub> 7 <sub>3,4</sub> 8 <sub>3,5</sub> 9 <sub>3,6</sub> 10 <sub>3,7</sub>		4 22 68 184 445	33 212 714 1385 1777	168 457 524 456 379		6 <sub>1,6</sub> 7 <sub>2,6</sub> 8 <sub>3,6</sub> 9 <sub>4,6</sub> 10 <sub>5,6</sub>	6 <sub>3,3</sub> 7 <sub>4,3</sub> 8 <sub>5,3</sub> 9 <sub>6,3</sub> 10 <sub>7,3</sub>



11 <sub>3,3</sub> 12 <sub>3,3</sub>	11 <sub>3,3</sub> 12 <sub>3,3</sub>	320 277	1816 1681	971 1829	11 <sub>3,3</sub> 12 <sub>3,3</sub>
7 <sub>3,4</sub> 8 <sub>4,4</sub> 9 <sub>5,4</sub> 10 <sub>6,4</sub> 11 <sub>7,4</sub> 12 <sub>8,4</sub>	7 <sub>1,7</sub> 8 <sub>2,7</sub> 9 <sub>3,7</sub> 10 <sub>4,7</sub> 11 <sub>5,7</sub> 12 <sub>6,7</sub>	114 480 714 686 584 493	17 98 385 1053 1885 2375	3 13 36 84 183 384	7 <sub>4,3</sub> 8 <sub>4,4</sub> 9 <sub>4,5</sub> 10 <sub>4,6</sub> 11 <sub>4,7</sub> 12 <sub>4,8</sub>
8 <sub>3,5</sub> 9 <sub>4,5</sub> 10 <sub>5,5</sub> 11 <sub>6,5</sub> 12 <sub>7,5</sub>	8 <sub>1,8</sub> 9 <sub>2,8</sub> 10 <sub>3,8</sub> 11 <sub>4,8</sub> 12 <sub>5,8</sub>	69 403 830 931 832	10 52 190 588 1419	2 8 23 52 102	8 <sub>5,3</sub> 9 <sub>5,4</sub> 10 <sub>5,5</sub> 11 <sub>5,6</sub> 12 <sub>5,7</sub>
9 <sub>3,6</sub> 10 <sub>4,6</sub> 11 <sub>5,6</sub> 12 <sub>6,6</sub>	9 <sub>1,9</sub> 10 <sub>2,9</sub> 11 <sub>3,9</sub> 12 <sub>4,9</sub>	41 282 817 1141	7 34 106 304	1 6 17 36	9 <sub>6,3</sub> 10 <sub>6,4</sub> 11 <sub>6,5</sub> 12 <sub>6,6</sub>
10 <sub>3,7</sub> 11 <sub>4,7</sub> 12 <sub>5,7</sub>	10 <sub>1,10</sub> 11 <sub>2,10</sub> 12 <sub>3,10</sub>	25 180 677	5 24 70	1 5 12	10 <sub>7,3</sub> 11 <sub>7,4</sub> 12 <sub>7,5</sub>
11 <sub>3,8</sub> 12 <sub>4,8</sub>	11 <sub>1,11</sub> 12 <sub>2,11</sub>	17 112	4 19	1 4	11 <sub>8,3</sub> 12 <sub>8,4</sub>
12 <sub>3,9</sub>	12 <sub>1,12</sub>	13	3	0	12 <sub>9,3</sub>

FORBIDDEN SUBBRANCHES—*a* AND *c* SUBBRANCHES

Subbranch		$\kappa$					Subbranch	
${}^cQ_{-3,-4}$ $J + K_{-1} + K_1$ even	${}^cQ_{3,-4}$ $J + K_{-1} + K_1$ odd	$\mp 1$	$\mp 0.5$	0	$\pm 0.5$	$\pm 1$	${}^aQ_{4,-3}$ $J + K_{-1} + K_1$ even	${}^aQ_{-4,3}$ $J + K_{-1} + K_1$ odd
4 <sub>4,0</sub>	4 <sub>1,4</sub>		8	10	2		4 <sub>0,4</sub>	4 <sub>4,1</sub>
5 <sub>4,1</sub>	5 <sub>1,5</sub>		24	14	1		5 <sub>1,4</sub>	5 <sub>5,1</sub>
6 <sub>4,2</sub>	6 <sub>1,6</sub>		42	9	0		6 <sub>2,4</sub>	6 <sub>6,1</sub>
7 <sub>4,3</sub>	7 <sub>1,7</sub>		51	2	0		7 <sub>3,4</sub>	7 <sub>7,1</sub>
8 <sub>4,4</sub>	8 <sub>1,8</sub>		48	1	0		8 <sub>4,4</sub>	8 <sub>8,1</sub>
9 <sub>4,5</sub>	9 <sub>1,9</sub>		35	1	0		9 <sub>5,4</sub>	9 <sub>9,1</sub>
10 <sub>4,6</sub>	10 <sub>1,10</sub>		22	0	0		10 <sub>6,4</sub>	10 <sub>10,1</sub>
11 <sub>4,7</sub>	11 <sub>1,11</sub>		12	0	0		11 <sub>7,4</sub>	11 <sub>11,1</sub>
12 <sub>4,8</sub>	12 <sub>1,12</sub>		7	0	0		12 <sub>8,4</sub>	12 <sub>12,1</sub>
5 <sub>5,0</sub>	5 <sub>2,4</sub>		7	17	7		5 <sub>0,5</sub>	5 <sub>4,2</sub>
6 <sub>5,1</sub>	6 <sub>2,5</sub>		27	39	4		6 <sub>1,5</sub>	6 <sub>6,2</sub>
7 <sub>5,2</sub>	7 <sub>2,6</sub>		62	44	1		7 <sub>2,5</sub>	7 <sub>6,2</sub>
8 <sub>5,3</sub>	8 <sub>2,7</sub>		106	28	0		8 <sub>3,5</sub>	8 <sub>7,2</sub>
9 <sub>5,4</sub>	9 <sub>2,8</sub>		142	13	0		9 <sub>4,5</sub>	9 <sub>8,2</sub>
10 <sub>5,5</sub>	10 <sub>2,9</sub>		154	5	0		10 <sub>5,5</sub>	10 <sub>9,2</sub>
11 <sub>5,6</sub>	11 <sub>2,10</sub>		137	3	0		11 <sub>6,5</sub>	11 <sub>10,2</sub>
12 <sub>5,7</sub>	12 <sub>2,11</sub>		102	1	0		12 <sub>7,5</sub>	12 <sub>11,2</sub>
6 <sub>6,0</sub>	6 <sub>3,4</sub>		4	16	14		6 <sub>0,6</sub>	6 <sub>4,3</sub>
7 <sub>6,1</sub>	7 <sub>3,5</sub>		19	53	15		7 <sub>1,6</sub>	7 <sub>5,3</sub>
8 <sub>6,2</sub>	8 <sub>3,6</sub>		50	88	5		8 <sub>2,6</sub>	8 <sub>6,3</sub>
9 <sub>6,3</sub>	9 <sub>3,7</sub>		102	88	2		9 <sub>3,6</sub>	9 <sub>7,3</sub>

10 <sub>6,4</sub>	10 <sub>3,8</sub>	170	56	1	10 <sub>4,6</sub>	10 <sub>8,3</sub>
11 <sub>6,5</sub>	11 <sub>3,9</sub>	240	27	0	11 <sub>5,6</sub>	11 <sub>9,3</sub>
12 <sub>6,6</sub>	12 <sub>3,10</sub>	289	12	0	12 <sub>6,6</sub>	12 <sub>10,3</sub>
7 <sub>7,0</sub>	7 <sub>4,4</sub>	3	13	19	7 <sub>0,7</sub>	7 <sub>4,4</sub>
8 <sub>7,1</sub>	8 <sub>4,5</sub>	12	51	30	8 <sub>1,7</sub>	8 <sub>5,4</sub>
9 <sub>7,2</sub>	9 <sub>4,6</sub>	34	108	17	9 <sub>2,7</sub>	9 <sub>6,4</sub>
10 <sub>7,3</sub>	10 <sub>4,7</sub>	74	152	5	10 <sub>3,7</sub>	10 <sub>7,4</sub>
11 <sub>7,4</sub>	11 <sub>4,8</sub>	137	144	2	11 <sub>4,7</sub>	11 <sub>8,4</sub>
12 <sub>7,5</sub>	12 <sub>4,9</sub>	223	93	1	12 <sub>5,7</sub>	12 <sub>9,4</sub>
8 <sub>8,0</sub>	8 <sub>5,4</sub>	2	10	20	8 <sub>0,8</sub>	8 <sub>4,5</sub>
9 <sub>8,1</sub>	9 <sub>5,5</sub>	8	41	46	9 <sub>1,8</sub>	9 <sub>5,5</sub>
10 <sub>8,2</sub>	10 <sub>5,6</sub>	23	102	39	10 <sub>2,8</sub>	10 <sub>6,5</sub>
11 <sub>8,3</sub>	11 <sub>5,7</sub>	51	179	15	11 <sub>3,8</sub>	11 <sub>7,5</sub>
12 <sub>8,4</sub>	12 <sub>5,8</sub>	97	129	5	12 <sub>4,8</sub>	12 <sub>8,5</sub>
9 <sub>9,0</sub>	9 <sub>6,4</sub>	1	7	19	9 <sub>0,9</sub>	9 <sub>4,6</sub>
10 <sub>9,1</sub>	10 <sub>6,5</sub>	6	32	56	10 <sub>1,9</sub>	10 <sub>5,6</sub>
11 <sub>9,2</sub>	11 <sub>6,6</sub>	17	84	67	11 <sub>2,9</sub>	11 <sub>6,6</sub>
12 <sub>9,3</sub>	12 <sub>6,7</sub>	36	169	37	12 <sub>3,9</sub>	12 <sub>7,6</sub>
10 <sub>10,0</sub>	10 <sub>7,4</sub>	1	5	17	10 <sub>0,10</sub>	10 <sub>4,7</sub>
11 <sub>10,1</sub>	11 <sub>7,5</sub>	5	24	59	11 <sub>1,10</sub>	11 <sub>5,7</sub>
12 <sub>10,2</sub>	12 <sub>7,6</sub>	12	66	93	12 <sub>2,10</sub>	12 <sub>6,7</sub>
11 <sub>11,0</sub>	11 <sub>8,4</sub>	1	4	14	11 <sub>0,11</sub>	11 <sub>4,8</sub>
12 <sub>11,1</sub>	12 <sub>8,5</sub>	4	19	57	12 <sub>1,11</sub>	12 <sub>5,8</sub>
12 <sub>12,0</sub>	12 <sub>9,4</sub>	0	3	12	12 <sub>0,12</sub>	12 <sub>4,9</sub>



FORBIDDEN SUBBRANCHES—*a* AND *c* SUBBRANCHES

Subbranch		$\kappa$					Subbranch	
$J + K_{-1} + K_1$ even	${}^cP_{-3,2}$ $J + K_{-1} + K_1$ even	$\mp 1$	$\mp 0.5$	0	$\pm 0.5$	$\pm 1$	${}^aR_{-2,3}$ $J + K_{-1} + K_1$ even	${}^aP_{2,-3}$ $J + K_{-1} + K_1$ even
2 <sub>0,2</sub>	3 <sub>3,0</sub>		75	215	138		2 <sub>2,0</sub>	3 <sub>0,3</sub>
3 <sub>0,3</sub>	4 <sub>3,1</sub>		294	313	51		3 <sub>3,0</sub>	4 <sub>1,3</sub>
4 <sub>0,4</sub>	5 <sub>3,2</sub>		528	176	17		4 <sub>4,0</sub>	5 <sub>2,3</sub>
5 <sub>0,5</sub>	6 <sub>3,3</sub>		558	79	9		5 <sub>5,0</sub>	6 <sub>3,3</sub>
6 <sub>0,6</sub>	7 <sub>3,4</sub>		418	41	5		6 <sub>6,0</sub>	7 <sub>4,3</sub>
7 <sub>0,7</sub>	8 <sub>3,5</sub>		263	26	4		7 <sub>7,0</sub>	8 <sub>5,3</sub>
8 <sub>0,8</sub>	9 <sub>3,6</sub>		159	19	3		8 <sub>8,0</sub>	9 <sub>6,3</sub>
9 <sub>0,9</sub>	10 <sub>3,7</sub>		102	14	2		9 <sub>9,0</sub>	10 <sub>7,3</sub>
10 <sub>0,10</sub>	11 <sub>3,8</sub>		70	11	2		10 <sub>10,0</sub>	11 <sub>8,3</sub>
11 <sub>0,11</sub>	12 <sub>3,9</sub>		53	9	1		11 <sub>11,0</sub>	12 <sub>9,3</sub>
3 <sub>1,3</sub>	4 <sub>4,0</sub>		24	146	272		3 <sub>2,1</sub>	4 <sub>0,4</sub>
4 <sub>1,3</sub>	5 <sub>4,1</sub>		122	538	212		4 <sub>3,1</sub>	5 <sub>1,4</sub>
5 <sub>1,4</sub>	6 <sub>4,2</sub>		377	665	76		5 <sub>4,1</sub>	6 <sub>2,4</sub>
6 <sub>1,5</sub>	7 <sub>4,3</sub>		803	409	34		6 <sub>5,1</sub>	7 <sub>3,4</sub>
7 <sub>1,6</sub>	8 <sub>4,4</sub>		1171	206	21		7 <sub>6,1</sub>	8 <sub>4,4</sub>
8 <sub>1,7</sub>	9 <sub>4,5</sub>		1200	115	15		8 <sub>7,1</sub>	9 <sub>5,4</sub>
9 <sub>1,8</sub>	10 <sub>4,6</sub>		938	76	11		9 <sub>8,1</sub>	10 <sub>6,4</sub>
10 <sub>1,9</sub>	11 <sub>4,7</sub>		631	57	9		10 <sub>9,1</sub>	11 <sub>7,4</sub>
11 <sub>1,10</sub>	12 <sub>4,8</sub>		409	45	7		11 <sub>10,1</sub>	12 <sub>8,4</sub>
4 <sub>2,3</sub>	5 <sub>5,0</sub>		11	70	262		4 <sub>2,2</sub>	5 <sub>0,5</sub>
5 <sub>2,3</sub>	6 <sub>5,1</sub>		46	359	464		5 <sub>3,2</sub>	6 <sub>1,5</sub>
6 <sub>2,4</sub>	7 <sub>5,2</sub>		142	894	220		6 <sub>4,2</sub>	7 <sub>2,5</sub>

7 <sub>2,5</sub>	8 <sub>5,3</sub>	364	1038	92	7 <sub>5,2</sub>	8 <sub>3,5</sub>
8 <sub>2,6</sub>	9 <sub>5,4</sub>	793	675	52	8 <sub>6,2</sub>	9 <sub>4,5</sub>
9 <sub>2,7</sub>	10 <sub>5,5</sub>	1395	365	36	9 <sub>7,2</sub>	10 <sub>5,5</sub>
10 <sub>2,8</sub>	11 <sub>5,6</sub>	1869	215	27	10 <sub>8,2</sub>	11 <sub>5,5</sub>
11 <sub>2,9</sub>	12 <sub>5,7</sub>	1887	148	21	11 <sub>9,2</sub>	12 <sub>7,5</sub>
5 <sub>2,2</sub>	6 <sub>6,0</sub>	7	39	184	5 <sub>2,3</sub>	6 <sub>0,6</sub>
6 <sub>2,3</sub>	7 <sub>6,1</sub>	27	187	624	6 <sub>3,3</sub>	7 <sub>1,6</sub>
7 <sub>2,4</sub>	8 <sub>6,2</sub>	69	610	487	7 <sub>4,3</sub>	8 <sub>2,6</sub>
8 <sub>2,5</sub>	9 <sub>6,3</sub>	157	1272	210	8 <sub>5,3</sub>	9 <sub>3,6</sub>
9 <sub>2,6</sub>	10 <sub>6,4</sub>	336	1426	108	9 <sub>6,3</sub>	10 <sub>4,6</sub>
10 <sub>2,7</sub>	11 <sub>6,5</sub>	684	963	71	10 <sub>7,3</sub>	11 <sub>5,6</sub>
11 <sub>2,8</sub>	12 <sub>6,6</sub>	1276	548	53	11 <sub>8,3</sub>	12 <sub>6,6</sub>
6 <sub>4,2</sub>	7 <sub>7,0</sub>	5	27	119	6 <sub>2,4</sub>	7 <sub>0,7</sub>
7 <sub>4,3</sub>	8 <sub>7,1</sub>	19	110	574	7 <sub>3,4</sub>	8 <sub>1,7</sub>
8 <sub>4,4</sub>	9 <sub>7,2</sub>	46	338	816	8 <sub>4,4</sub>	9 <sub>2,7</sub>
9 <sub>4,5</sub>	10 <sub>7,3</sub>	94	887	435	9 <sub>5,4</sub>	10 <sub>3,7</sub>
10 <sub>4,6</sub>	11 <sub>7,4</sub>	176	1662	205	10 <sub>6,4</sub>	11 <sub>4,7</sub>
11 <sub>4,7</sub>	12 <sub>7,5</sub>	321	1825	126	11 <sub>7,4</sub>	12 <sub>5,7</sub>
7 <sub>5,2</sub>	8 <sub>8,0</sub>	4	21	81	7 <sub>2,5</sub>	8 <sub>0,8</sub>
8 <sub>5,3</sub>	9 <sub>8,1</sub>	15	78	424	8 <sub>3,5</sub>	9 <sub>1,8</sub>
9 <sub>5,4</sub>	10 <sub>8,2</sub>	36	206	995	9 <sub>4,5</sub>	10 <sub>2,8</sub>
10 <sub>5,5</sub>	11 <sub>8,3</sub>	69	514	790	10 <sub>5,5</sub>	11 <sub>3,8</sub>
11 <sub>5,6</sub>	12 <sub>8,4</sub>	121	1183	381	11 <sub>6,5</sub>	12 <sub>4,8</sub>
8 <sub>6,2</sub>	9 <sub>9,0</sub>	4	18	60	8 <sub>2,6</sub>	9 <sub>0,9</sub>
9 <sub>6,3</sub>	10 <sub>9,1</sub>	13	62	292	9 <sub>3,6</sub>	10 <sub>1,9</sub>
10 <sub>6,4</sub>	11 <sub>9,2</sub>	29	149	910	10 <sub>4,6</sub>	11 <sub>2,9</sub>
11 <sub>6,5</sub>	12 <sub>9,3</sub>	55	324	1182	11 <sub>5,6</sub>	12 <sub>3,9</sub>

FORBIDDEN SUBBRANCHES—*a* AND *c* SUBBRANCHES

Subbranch		$\kappa$					Subbranch	
${}^cR_{3,-2}$ $J + K_{-1} + K_1$ even	${}^cP_{-3,2}$ $J + K_{-1} + K_1$ even	$\mp 1$	$\mp 0.5$	0	$\pm 0.5$	$\pm 1$	${}^aR_{-2,3}$ $J + K_{-1} + K_1$ even	${}^aP_{2,-3}$ $J + K_{-1} + K_1$ even
$9_{7,2}$ $10_{7,3}$ $11_{7,4}$	$10_{10,0}$ $11_{10,1}$ $12_{10,2}$		3 11 24	15 52 121	48 207 694		$9_{2,7}$ $10_{3,7}$ $11_{4,7}$	$10_{0,10}$ $11_{1,10}$ $12_{2,10}$
$10_{8,2}$ $11_{8,3}$	$11_{11,0}$ $12_{11,1}$		3 9	13 45	41 158		$10_{2,8}$ $11_{3,8}$	$11_{0,11}$ $12_{1,11}$
$11_{9,2}$	$12_{12,0}$		2	12	36		$11_{2,9}$	$12_{0,12}$

${}^cR_{3,-2}$ $J + K_{-1} + K_1$ odd	${}^cP_{-3,2}$ $J + K_{-1} + K_1$ odd	$\mp 1$	$\mp 0.5$	0	$\pm 0.5$	$\pm 1$	${}^aR_{-2,3}$ $J + K_{-1} + K_1$ odd	${}^aP_{2,-3}$ $J + K_{-1} + K_1$ odd
$3_{1,3}$ $4_{1,4}$ $5_{1,5}$ $6_{1,6}$ $7_{1,7}$ $8_{1,8}$ $9_{1,9}$ $10_{1,10}$ $11_{1,11}$	$4_{4,1}$ $5_{4,2}$ $6_{4,3}$ $7_{4,4}$ $8_{4,5}$ $9_{4,6}$ $10_{4,7}$ $11_{4,8}$ $12_{4,9}$		10 31 56 73 80 77 68 58 49	21 38 39 32 24 18 14 11 9	13 12 8 5 4 3 2 2 1		$3_{3,1}$ $4_{4,1}$ $5_{5,1}$ $6_{6,1}$ $7_{7,1}$ $8_{8,1}$ $9_{9,1}$ $10_{10,1}$ $11_{11,1}$	$4_{1,4}$ $5_{2,4}$ $6_{3,4}$ $7_{4,4}$ $8_{5,4}$ $9_{6,4}$ $10_{7,4}$ $11_{8,4}$ $12_{9,4}$



4 <sub>2,3</sub>	5 <sub>5,1</sub>	9	31	32	4 <sub>3,2</sub>	5 <sub>1,5</sub>
5 <sub>2,4</sub>	6 <sub>5,2</sub>	33	79	39	5 <sub>4,2</sub>	6 <sub>2,5</sub>
6 <sub>2,5</sub>	7 <sub>5,3</sub>	73	108	30	6 <sub>5,2</sub>	7 <sub>3,5</sub>
7 <sub>2,6</sub>	8 <sub>5,4</sub>	124	108	21	7 <sub>6,2</sub>	8 <sub>4,5</sub>
8 <sub>2,7</sub>	9 <sub>5,5</sub>	172	91	15	8 <sub>7,2</sub>	9 <sub>5,5</sub>
9 <sub>2,8</sub>	10 <sub>5,6</sub>	205	72	11	9 <sub>8,2</sub>	10 <sub>5,5</sub>
10 <sub>2,9</sub>	11 <sub>5,7</sub>	216	56	9	10 <sub>9,2</sub>	11 <sub>7,5</sub>
11 <sub>2,10</sub>	12 <sub>5,8</sub>	209	45	7	11 <sub>10,2</sub>	12 <sub>8,5</sub>
5 <sub>3,3</sub>	6 <sub>6,1</sub>	7	30	46	5 <sub>3,3</sub>	6 <sub>1,6</sub>
6 <sub>3,4</sub>	7 <sub>6,2</sub>	25	92	76	6 <sub>4,3</sub>	7 <sub>2,6</sub>
7 <sub>3,5</sub>	8 <sub>6,3</sub>	60	163	67	7 <sub>5,3</sub>	8 <sub>3,6</sub>
8 <sub>3,6</sub>	9 <sub>6,4</sub>	115	202	50	8 <sub>6,3</sub>	9 <sub>4,6</sub>
9 <sub>3,7</sub>	10 <sub>6,5</sub>	187	199	36	9 <sub>7,3</sub>	10 <sub>5,6</sub>
10 <sub>3,8</sub>	11 <sub>6,6</sub>	267	171	27	10 <sub>8,3</sub>	11 <sub>6,6</sub>
11 <sub>3,9</sub>	12 <sub>6,7</sub>	337	139	21	11 <sub>9,3</sub>	12 <sub>7,6</sub>
6 <sub>4,3</sub>	7 <sub>7,1</sub>	5	25	53	6 <sub>3,4</sub>	7 <sub>1,7</sub>
7 <sub>4,4</sub>	8 <sub>7,2</sub>	19	86	110	7 <sub>4,4</sub>	8 <sub>2,7</sub>
8 <sub>4,5</sub>	9 <sub>7,3</sub>	46	177	118	8 <sub>5,4</sub>	9 <sub>3,7</sub>
9 <sub>4,6</sub>	10 <sub>7,4</sub>	89	268	94	9 <sub>6,4</sub>	10 <sub>4,7</sub>
10 <sub>4,7</sub>	11 <sub>7,5</sub>	154	316	70	10 <sub>7,4</sub>	11 <sub>6,7</sub>
11 <sub>4,8</sub>	12 <sub>7,6</sub>	241	309	53	11 <sub>8,4</sub>	12 <sub>6,7</sub>
7 <sub>5,3</sub>	8 <sub>8,1</sub>	4	21	53	7 <sub>3,5</sub>	8 <sub>1,8</sub>
8 <sub>5,4</sub>	9 <sub>8,2</sub>	15	73	134	8 <sub>4,5</sub>	9 <sub>2,8</sub>
9 <sub>5,5</sub>	10 <sub>8,3</sub>	35	163	173	9 <sub>5,5</sub>	10 <sub>3,8</sub>
10 <sub>5,6</sub>	11 <sub>8,4</sub>	69	281	155	10 <sub>6,5</sub>	11 <sub>4,8</sub>
11 <sub>5,7</sub>	12 <sub>8,5</sub>	119	390	120	11 <sub>7,5</sub>	12 <sub>5,8</sub>

FORBIDDEN SUBBRANCHES—*a* AND *c* SUBBRANCHES

Subbranch		$\kappa$					Subbranch	
${}^cR_{3,-2}$ $J + K_{-1} + K_1$ odd	${}^cP_{-3,2}$ $J + K_{-1} + K_1$ odd	$\mp 1$	$\mp 0.5$	0	$\pm 0.5$	$\pm 1$	${}^aR_{-2,3}$ $J + K_{-1} + K_1$ odd	${}^aP_{2,-3}$ $J + K_{-1} + K_1$ odd
$8_{6,3}$	$9_{9,1}$		4	18	49		$8_{3,6}$	$9_{1,9}$
$9_{6,4}$	$10_{9,2}$		13	61	143		$9_{4,6}$	$10_{2,9}$
$10_{6,5}$	$11_{9,3}$		29	140	219		$10_{5,6}$	$11_{3,9}$
$11_{6,6}$	$12_{9,4}$		54	258	224		$11_{6,6}$	$12_{4,9}$
			.					
$9_{7,3}$	$10_{10,1}$		3	15	44		$9_{3,7}$	$10_{1,10}$
$10_{7,4}$	$11_{10,2}$		11	52	140		$10_{4,7}$	$11_{2,10}$
$11_{7,5}$	$12_{10,3}$		24	119	249		$11_{5,7}$	$12_{3,10}$
$10_{8,3}$	$11_{11,1}$		3	13	40		$10_{3,8}$	$11_{1,11}$
$11_{8,4}$	$12_{11,2}$		9	45	131		$11_{4,8}$	$12_{2,11}$
$11_{9,3}$	$12_{12,1}$		2	12	36		$11_{3,9}$	$12_{1,12}$

${}^cR_{-3,4}$ $J + K_{-1} + K_1$ even	${}^cP_{3,-4}$ $J + K_{-1} + K_1$ even	$\mp 1$	$\mp 0.5$	0	$\pm 0.5$	$\pm 1$	${}^aR_{4,-3}$ $J + K_{-1} + K_1$ even	${}^aP_{-4,3}$ $J + K_{-1} + K_1$ even
$3_{3,0}$	$4_{0,4}$		28	18	2		$3_{0,3}$	$4_{4,0}$
$4_{3,1}$	$5_{0,5}$		78	17	0		$4_{1,3}$	$5_{5,0}$
$5_{3,2}$	$6_{0,6}$		107	8	0		$5_{2,3}$	$6_{6,0}$
$6_{3,3}$	$7_{0,7}$		96	3	0		$6_{3,3}$	$7_{7,0}$

7 <sub>2,4</sub>	8 <sub>0,3</sub>	65	2	0	7 <sub>4,3</sub>	8 <sub>8,0</sub>
8 <sub>2,5</sub>	9 <sub>0,9</sub>	39	1	0	8 <sub>5,3</sub>	9 <sub>9,0</sub>
9 <sub>2,6</sub>	10 <sub>0,10</sub>	23	1	0	9 <sub>6,3</sub>	10 <sub>10,0</sub>
10 <sub>2,7</sub>	11 <sub>0,11</sub>	14	1	0	10 <sub>7,3</sub>	11 <sub>11,0</sub>
11 <sub>2,8</sub>	12 <sub>0,12</sub>	9	0	0	11 <sub>8,3</sub>	12 <sub>12,0</sub>
4 <sub>4,0</sub>	5 <sub>1,4</sub>	11	31	7	4 <sub>0,4</sub>	5 <sub>4,1</sub>
5 <sub>4,1</sub>	6 <sub>1,5</sub>	58	62	3	5 <sub>1,4</sub>	6 <sub>5,1</sub>
6 <sub>4,2</sub>	7 <sub>1,6</sub>	152	51	1	6 <sub>2,4</sub>	7 <sub>6,1</sub>
7 <sub>4,3</sub>	8 <sub>1,7</sub>	252	25	0	7 <sub>3,4</sub>	8 <sub>7,1</sub>
8 <sub>4,4</sub>	9 <sub>1,8</sub>	290	11	0	8 <sub>4,4</sub>	9 <sub>8,1</sub>
9 <sub>4,5</sub>	10 <sub>1,9</sub>	250	6	0	9 <sub>5,4</sub>	10 <sub>9,1</sub>
10 <sub>4,6</sub>	11 <sub>1,10</sub>	175	4	0	10 <sub>6,4</sub>	11 <sub>10,1</sub>
11 <sub>4,7</sub>	12 <sub>1,11</sub>	109	3	0	11 <sub>7,4</sub>	12 <sub>11,1</sub>
5 <sub>5,0</sub>	6 <sub>2,4</sub>	3	21	15	5 <sub>0,5</sub>	6 <sub>4,2</sub>
6 <sub>5,1</sub>	7 <sub>2,5</sub>	17	83	12	6 <sub>1,5</sub>	7 <sub>5,2</sub>
7 <sub>5,2</sub>	8 <sub>2,6</sub>	65	124	4	7 <sub>2,5</sub>	8 <sub>6,2</sub>
8 <sub>5,3</sub>	9 <sub>2,7</sub>	173	96	1	8 <sub>3,5</sub>	9 <sub>7,2</sub>
9 <sub>5,4</sub>	10 <sub>2,8</sub>	335	50	1	9 <sub>4,5</sub>	10 <sub>8,2</sub>
10 <sub>5,5</sub>	11 <sub>2,9</sub>	477	23	0	10 <sub>5,5</sub>	11 <sub>9,2</sub>
11 <sub>5,6</sub>	12 <sub>2,10</sub>	517	13	0	11 <sub>6,5</sub>	12 <sub>10,2</sub>
6 <sub>6,0</sub>	7 <sub>3,4</sub>	1	9	21	6 <sub>0,6</sub>	7 <sub>4,3</sub>
7 <sub>6,1</sub>	8 <sub>3,5</sub>	5	59	28	7 <sub>1,6</sub>	8 <sub>5,3</sub>
8 <sub>6,2</sub>	9 <sub>3,6</sub>	20	151	12	8 <sub>2,6</sub>	9 <sub>6,3</sub>
9 <sub>6,3</sub>	10 <sub>3,7</sub>	60	198	4	9 <sub>3,6</sub>	10 <sub>7,3</sub>
10 <sub>6,4</sub>	11 <sub>3,8</sub>	155	151	2	10 <sub>4,6</sub>	11 <sub>8,3</sub>
11 <sub>6,5</sub>	12 <sub>3,9</sub>	329	81	1	11 <sub>5,6</sub>	12 <sub>9,3</sub>



FORBIDDEN SUBBRANCHES—*a* AND *c* SUBBRANCHES

Subbranch		$\kappa$					Subbranch	
${}^cR_{-3,4}$ $J + K_{-1} + K_1$ even	${}^cP_{3,-4}$ $J + K_{-1} + K_1$ even	$\mp 1$	$\mp 0.5$	0	$\pm 0.5$	$\pm 1$	${}^aR_{4,-3}$ $J + K_{-1} + K_1$ even	${}^aP_{-4,3}$ $J + K_{-1} + K_1$ even
7 <sub>7,0</sub>	8 <sub>4,4</sub>		0	4	20		7 <sub>0,7</sub>	8 <sub>4,4</sub>
8 <sub>7,1</sub>	9 <sub>4,5</sub>		2	26	46		8 <sub>1,7</sub>	9 <sub>5,4</sub>
9 <sub>7,2</sub>	10 <sub>4,6</sub>		8	107	31		9 <sub>2,7</sub>	10 <sub>6,4</sub>
10 <sub>7,3</sub>	11 <sub>4,7</sub>		22	230	11		10 <sub>3,7</sub>	11 <sub>7,4</sub>
11 <sub>7,4</sub>	12 <sub>4,8</sub>		55	282	4		11 <sub>4,7</sub>	12 <sub>8,4</sub>
8 <sub>8,0</sub>	9 <sub>5,4</sub>		0	2	15		8 <sub>0,8</sub>	9 <sub>4,5</sub>
9 <sub>8,1</sub>	10 <sub>5,5</sub>		1	12	56		9 <sub>1,8</sub>	10 <sub>5,5</sub>
10 <sub>8,2</sub>	11 <sub>5,6</sub>		4	54	59		10 <sub>2,8</sub>	11 <sub>6,5</sub>
11 <sub>8,3</sub>	12 <sub>5,7</sub>		11	165	27		11 <sub>3,8</sub>	12 <sub>7,5</sub>
9 <sub>9,0</sub>	10 <sub>6,4</sub>		0	1	10		9 <sub>0,9</sub>	10 <sub>4,6</sub>
10 <sub>9,1</sub>	11 <sub>6,5</sub>		1	6	53		10 <sub>1,9</sub>	11 <sub>5,6</sub>
11 <sub>9,2</sub>	12 <sub>6,6</sub>		3	25	87		11 <sub>2,9</sub>	12 <sub>6,6</sub>
10 <sub>10,0</sub>	11 <sub>7,4</sub>		0	1	5		10 <sub>0,10</sub>	11 <sub>4,7</sub>
11 <sub>10,1</sub>	12 <sub>7,5</sub>		1	4	41		11 <sub>1,10</sub>	12 <sub>5,7</sub>
11 <sub>11,0</sub>	12 <sub>8,4</sub>		0	0	3		11 <sub>0,11</sub>	12 <sub>4,8</sub>

Subbranch		$\mp 1$	$\mp 0.5$	0	$\pm 0.5$	$\pm 1$	${}^aR_{4,-3}$ $J + K_{-1} + K_1$ odd	${}^aP_{-4,3}$ $J + K_{-1} + K_1$ odd
${}^cR_{-3,4}$ $J + K_{-1} + K_1$ odd	${}^cP_{3,-4}$ $J + K_{-1} + K_1$ odd							
4 <sub>4,1</sub>	5 <sub>1,5</sub>		2	1	0		4 <sub>1,4</sub>	5 <sub>5,1</sub>
5 <sub>4,2</sub>	6 <sub>1,6</sub>		5	2	0		5 <sub>2,4</sub>	6 <sub>6,1</sub>

6 <sub>4,3</sub>	7 <sub>1,7</sub>	8	2	0	6 <sub>3,4</sub>	7 <sub>7,1</sub>
7 <sub>4,4</sub>	8 <sub>1,8</sub>	11	1	0	7 <sub>4,4</sub>	8 <sub>8,1</sub>
8 <sub>4,5</sub>	9 <sub>1,9</sub>	12	1	0	8 <sub>5,4</sub>	9 <sub>9,1</sub>
9 <sub>4,6</sub>	10 <sub>1,10</sub>	11	1	0	9 <sub>4,4</sub>	10 <sub>10,1</sub>
10 <sub>4,7</sub>	11 <sub>1,11</sub>	9	1	0	10 <sub>7,4</sub>	11 <sub>11,1</sub>
11 <sub>4,8</sub>	12 <sub>1,12</sub>	8	0	0	11 <sub>3,4</sub>	12 <sub>12,1</sub>
5 <sub>5,1</sub>	6 <sub>2,6</sub>	1	2	0	5 <sub>1,5</sub>	6 <sub>5,2</sub>
6 <sub>5,2</sub>	7 <sub>2,7</sub>	6	5	0	6 <sub>2,6</sub>	7 <sub>6,2</sub>
7 <sub>5,3</sub>	8 <sub>2,8</sub>	14	6	0	7 <sub>3,5</sub>	8 <sub>7,2</sub>
8 <sub>5,4</sub>	9 <sub>2,9</sub>	23	6	0	8 <sub>4,5</sub>	9 <sub>8,2</sub>
9 <sub>5,5</sub>	10 <sub>2,10</sub>	32	4	0	9 <sub>5,5</sub>	10 <sub>9,2</sub>
10 <sub>5,6</sub>	11 <sub>2,11</sub>	36	3	0	10 <sub>6,5</sub>	11 <sub>10,2</sub>
11 <sub>5,7</sub>	12 <sub>2,12</sub>	37	3	0	11 <sub>7,6</sub>	12 <sub>11,2</sub>
6 <sub>6,1</sub>	7 <sub>3,6</sub>	1	2	1	6 <sub>1,6</sub>	7 <sub>5,3</sub>
7 <sub>6,2</sub>	8 <sub>3,7</sub>	4	8	1	7 <sub>2,6</sub>	8 <sub>6,3</sub>
8 <sub>6,3</sub>	9 <sub>3,8</sub>	11	13	1	8 <sub>3,6</sub>	9 <sub>7,3</sub>
9 <sub>6,4</sub>	10 <sub>3,9</sub>	23	14	1	9 <sub>4,6</sub>	10 <sub>8,3</sub>
10 <sub>6,5</sub>	11 <sub>3,10</sub>	39	13	0	10 <sub>5,6</sub>	11 <sub>9,3</sub>
11 <sub>6,6</sub>	12 <sub>3,11</sub>	56	10	0	11 <sub>6,6</sub>	12 <sub>10,3</sub>
7 <sub>7,1</sub>	8 <sub>4,8</sub>	0	2	2	7 <sub>1,7</sub>	8 <sub>5,4</sub>
8 <sub>7,2</sub>	9 <sub>4,9</sub>	2	8	3	8 <sub>2,7</sub>	9 <sub>6,4</sub>
9 <sub>7,3</sub>	10 <sub>4,10</sub>	7	17	2	9 <sub>3,7</sub>	10 <sub>7,4</sub>
10 <sub>7,4</sub>	11 <sub>4,11</sub>	16	24	1	10 <sub>4,7</sub>	11 <sub>8,4</sub>
11 <sub>7,5</sub>	12 <sub>4,12</sub>	32	25	1	11 <sub>5,7</sub>	12 <sub>9,4</sub>
8 <sub>8,1</sub>	9 <sub>5,9</sub>	0	1	2	8 <sub>1,8</sub>	9 <sub>5,5</sub>
9 <sub>8,2</sub>	10 <sub>5,10</sub>	1	6	4	9 <sub>2,8</sub>	10 <sub>6,5</sub>
10 <sub>8,3</sub>	11 <sub>5,11</sub>	4	17	4	10 <sub>3,9</sub>	11 <sub>7,5</sub>
11 <sub>8,4</sub>	12 <sub>5,12</sub>	10	29	3	11 <sub>4,8</sub>	12 <sub>8,5</sub>

FORBIDDEN SUBBRANCHES—*a* AND *c* SUBBRANCHES

Subbranch		$\kappa$				Subbranch	
$J + K_{-1} + K_1$ odd	${}^cP_{3,-4}$ $J + K_{-1} + K_1$ odd	$\mp 1$	$\mp 0.5$	0	$\pm 0.5$	$\pm 1$	${}^aR_{4,-3}$ $J + K_{-1} + K_1$ odd
$9_{9,1}$ $10_{9,2}$ $11_{9,3}$	$10_{6,5}$		0	1	2		$10_{5,6}$
	$11_{6,6}$		1	5	5		$11_{6,6}$
	$12_{6,7}$		3	14	7		$12_{7,6}$
$10_{10,1}$ $11_{10,2}$	$11_{7,5}$		0	1	2		$11_{5,7}$
	$12_{7,6}$		1	3	6		$12_{6,7}$
$11_{11,1}$	$12_{8,5}$		0	0	2		$12_{5,8}$

FORBIDDEN SUBBRANCHES—*b* SUBBRANCHES

Subbranch		$\kappa$				Subbranch	
$J + K_{-1} + K_1$ even	${}^bQ_{3,-3}$ $J + K_{-1} + K_1$ even	$\mp 1$	$\mp 0.5$	0	$\pm 0.5$	$\pm 1$	${}^bQ_{-3,3}$ $J + K_{-1} + K_1$ even
$3_{3,0}$ $4_{3,1}$ $5_{3,2}$ $6_{3,3}$ $7_{3,4}$ $8_{3,5}$	$3_{0,3}$		138	297	138		$3_{3,0}$
	$4_{0,4}$		445	319	41		$4_{4,0}$
	$5_{0,5}$		674	158	13		$5_{5,0}$
	$6_{0,6}$		640	67	6		$6_{6,0}$
	$7_{0,7}$		450	33	4		$7_{7,0}$
	$8_{0,8}$		273	21	3		$8_{8,0}$



9 <sub>3,6</sub> 10 <sub>3,7</sub> 11 <sub>3,8</sub> 12 <sub>3,9</sub>	9 <sub>0,9</sub> 10 <sub>0,10</sub> 11 <sub>0,11</sub> 12 <sub>0,12</sub>	162 101 69 52	15 11 9 7	2 1 1 1	9 <sub>6,3</sub> 10 <sub>7,3</sub> 11 <sub>8,3</sub> 12 <sub>9,3</sub>	9 <sub>9,0</sub> 10 <sub>10,0</sub> 11 <sub>11,0</sub> 12 <sub>12,0</sub>
4 <sub>4,0</sub> 5 <sub>4,1</sub> 6 <sub>4,2</sub> 7 <sub>4,3</sub> 8 <sub>4,4</sub> 9 <sub>4,5</sub> 10 <sub>4,6</sub> 11 <sub>4,7</sub> 12 <sub>4,8</sub>	4 <sub>1,3</sub> 5 <sub>1,4</sub> 6 <sub>1,5</sub> 7 <sub>1,6</sub> 8 <sub>1,7</sub> 9 <sub>1,8</sub> 10 <sub>1,9</sub> 11 <sub>1,10</sub> 12 <sub>1,11</sub>	41 230 684 1287 1640 1513 1105 713 449	319 846 793 422 197 105 67 49 38	445 230 70 29 17 11 8 6 5	4 <sub>3,1</sub> 5 <sub>4,1</sub> 6 <sub>5,1</sub> 7 <sub>6,1</sub> 8 <sub>7,1</sub> 9 <sub>8,1</sub> 10 <sub>9,1</sub> 11 <sub>10,1</sub> 12 <sub>11,1</sub>	4 <sub>3,1</sub> 5 <sub>4,1</sub> 6 <sub>5,1</sub> 7 <sub>6,1</sub> 8 <sub>7,1</sub> 9 <sub>8,1</sub> 10 <sub>9,1</sub> 11 <sub>10,1</sub> 12 <sub>11,1</sub>
5 <sub>5,0</sub> 6 <sub>5,1</sub> 7 <sub>5,2</sub> 8 <sub>5,3</sub> 9 <sub>5,4</sub> 10 <sub>5,5</sub> 11 <sub>5,6</sub> 12 <sub>5,7</sub>	5 <sub>2,3</sub> 6 <sub>2,4</sub> 7 <sub>2,5</sub> 8 <sub>2,6</sub> 9 <sub>2,7</sub> 10 <sub>2,8</sub> 11 <sub>2,9</sub> 12 <sub>2,10</sub>	13 70 248 681 1444 2306 2749 2519	158 793 1513 1360 763 380 212 141	674 684 248 91 48 31 22 16	5 <sub>3,2</sub> 6 <sub>4,2</sub> 7 <sub>5,2</sub> 8 <sub>6,2</sub> 9 <sub>7,2</sub> 10 <sub>8,2</sub> 11 <sub>9,2</sub> 12 <sub>10,2</sub>	5 <sub>3,2</sub> 6 <sub>4,2</sub> 7 <sub>5,2</sub> 8 <sub>6,2</sub> 9 <sub>7,2</sub> 10 <sub>8,2</sub> 11 <sub>9,2</sub> 12 <sub>10,2</sub>
6 <sub>6,0</sub> 7 <sub>6,1</sub> 8 <sub>6,2</sub> 9 <sub>6,3</sub> 10 <sub>6,4</sub> 11 <sub>6,5</sub> 12 <sub>6,6</sub>	6 <sub>3,3</sub> 7 <sub>3,4</sub> 8 <sub>3,5</sub> 9 <sub>3,6</sub> 10 <sub>3,7</sub> 11 <sub>3,8</sub> 12 <sub>3,9</sub>	6 29 91 245 592 1278 2337	67 422 1360 2252 1993 1165 609	640 1287 681 245 112 69 48	6 <sub>3,3</sub> 7 <sub>4,3</sub> 8 <sub>5,3</sub> 9 <sub>6,3</sub> 10 <sub>7,3</sub> 11 <sub>8,3</sub> 12 <sub>9,3</sub>	6 <sub>3,3</sub> 7 <sub>4,3</sub> 8 <sub>5,3</sub> 9 <sub>6,3</sub> 10 <sub>7,3</sub> 11 <sub>8,3</sub> 12 <sub>9,3</sub>

FORBIDDEN SUBBRANCHES—b SUBBRANCHES

Subbranch		$\kappa$					Subbranch	
${}^bQ_{-3,3}$ $J + K_{-1} + K_1$ even	${}^bQ_{3,-3}$ $J + K_{-1} + K_1$ even	$\mp 1$	$\mp 0.5$	0	$\pm 0.5$	$\pm 1$	${}^bQ_{3,-3}$ $J + K_{-1} + K_1$ even	${}^bQ_{-3,3}$ $J + K_{-1} + K_1$ even
7 <sub>7,0</sub>	7 <sub>0,7</sub>		4	33	450		7 <sub>0,7</sub>	7 <sub>3,4</sub>
8 <sub>7,1</sub>	8 <sub>1,7</sub>		17	197	1640		8 <sub>1,7</sub>	8 <sub>4,4</sub>
9 <sub>7,2</sub>	9 <sub>2,7</sub>		48	763	1444		9 <sub>2,7</sub>	9 <sub>6,4</sub>
10 <sub>7,3</sub>	10 <sub>3,7</sub>		112	1993	592		10 <sub>3,7</sub>	10 <sub>6,4</sub>
11 <sub>7,4</sub>	11 <sub>4,7</sub>		244	3040	244		11 <sub>4,7</sub>	11 <sub>7,4</sub>
12 <sub>7,5</sub>	12 <sub>5,7</sub>		512	2675	136		12 <sub>5,7</sub>	12 <sub>8,4</sub>
8 <sub>8,0</sub>	8 <sub>0,8</sub>		3	21	273		8 <sub>0,8</sub>	8 <sub>3,5</sub>
9 <sub>8,1</sub>	9 <sub>1,8</sub>		11	105	1513		9 <sub>1,8</sub>	9 <sub>4,5</sub>
10 <sub>8,2</sub>	10 <sub>2,8</sub>		31	380	2306		10 <sub>2,8</sub>	10 <sub>5,5</sub>
11 <sub>8,3</sub>	11 <sub>3,8</sub>		69	1165	1278		11 <sub>3,8</sub>	11 <sub>6,5</sub>
12 <sub>8,4</sub>	12 <sub>4,8</sub>		136	2675	512		12 <sub>4,8</sub>	12 <sub>7,5</sub>
9 <sub>9,0</sub>	9 <sub>0,9</sub>		2	15	162		9 <sub>0,9</sub>	9 <sub>3,6</sub>
10 <sub>9,1</sub>	10 <sub>1,9</sub>		8	67	1105		10 <sub>1,9</sub>	10 <sub>4,6</sub>
11 <sub>9,2</sub>	11 <sub>2,9</sub>		22	212	2749		11 <sub>2,9</sub>	11 <sub>5,6</sub>
12 <sub>9,3</sub>	12 <sub>3,9</sub>		48	609	2337		12 <sub>3,9</sub>	12 <sub>6,6</sub>
10 <sub>10,0</sub>	10 <sub>0,10</sub>		1	11	101		10 <sub>0,10</sub>	10 <sub>3,7</sub>
11 <sub>10,1</sub>	11 <sub>1,10</sub>		6	49	713		11 <sub>1,10</sub>	11 <sub>4,7</sub>
12 <sub>10,2</sub>	12 <sub>2,10</sub>		16	141	2519		12 <sub>2,10</sub>	12 <sub>5,7</sub>
11 <sub>11,0</sub>	11 <sub>0,11</sub>		1	9	69		11 <sub>0,11</sub>	11 <sub>3,8</sub>
12 <sub>11,1</sub>	12 <sub>1,11</sub>			38	449		12 <sub>1,11</sub>	12 <sub>4,8</sub>
12 <sub>12,0</sub>	12 <sub>0,12</sub>		1	7	52		12 <sub>0,12</sub>	12 <sub>3,9</sub>

${}^bQ_{-3,3}$ $J + K_{-1} + K_1$ odd	${}^bQ_{3,-3}$ $J + K_{-1} + K_1$ odd	$\pm 1$	$\pm 0.5$	0	$\mp 0.5$	$\mp 1$	${}^bQ_{3,-3}$ $J + K_{-1} + K_1$ odd	${}^bQ_{-3,3}$ $J + K_{-1} + K_1$ odd
4 <sub>4,1</sub> 5 <sub>5,1</sub> 6 <sub>6,1</sub> 7 <sub>7,1</sub> 8 <sub>8,1</sub> 9 <sub>9,1</sub> 10 <sub>10,1</sub> 11 <sub>11,1</sub> 12 <sub>12,1</sub>	4 <sub>1,4</sub> 5 <sub>2,4</sub> 6 <sub>3,4</sub> 7 <sub>4,4</sub> 8 <sub>5,4</sub> 9 <sub>6,4</sub> 10 <sub>7,4</sub> 11 <sub>8,4</sub> 12 <sub>9,4</sub>		10 9 6 4 3 2 1 1 1	20 33 33 26 19 14 11 9 7	10 34 58 76 82 77 68 58 48		4 <sub>1,4</sub> 5 <sub>1,5</sub> 6 <sub>1,6</sub> 7 <sub>1,7</sub> 8 <sub>1,8</sub> 9 <sub>1,9</sub> 10 <sub>1,10</sub> 11 <sub>1,11</sub> 12 <sub>1,12</sub>	4 <sub>4,1</sub> 5 <sub>5,1</sub> 6 <sub>6,1</sub> 7 <sub>7,1</sub> 8 <sub>8,1</sub> 9 <sub>9,1</sub> 10 <sub>10,1</sub> 11 <sub>11,1</sub> 12 <sub>12,1</sub>
5 <sub>5,1</sub> 6 <sub>6,2</sub> 7 <sub>6,3</sub> 8 <sub>5,4</sub> 9 <sub>5,5</sub> 10 <sub>5,6</sub> 11 <sub>5,7</sub> 12 <sub>5,8</sub>	5 <sub>1,5</sub> 6 <sub>2,5</sub> 7 <sub>3,5</sub> 8 <sub>4,5</sub> 9 <sub>5,5</sub> 10 <sub>6,5</sub> 11 <sub>7,5</sub> 12 <sub>8,5</sub>		34 36 25 16 11 8 6 5	33 83 108 102 83 63 48 38	9 36 84 144 199 233 241 228		5 <sub>2,4</sub> 6 <sub>2,5</sub> 7 <sub>2,6</sub> 8 <sub>2,7</sub> 9 <sub>2,8</sub> 10 <sub>2,9</sub> 11 <sub>2,10</sub> 12 <sub>2,11</sub>	5 <sub>4,2</sub> 6 <sub>5,2</sub> 7 <sub>6,2</sub> 8 <sub>7,2</sub> 9 <sub>8,2</sub> 10 <sub>9,2</sub> 11 <sub>10,2</sub> 12 <sub>11,2</sub>
6 <sub>6,1</sub> 7 <sub>6,2</sub> 8 <sub>6,3</sub> 9 <sub>6,4</sub> 10 <sub>6,5</sub> 11 <sub>6,6</sub> 12 <sub>6,7</sub>	6 <sub>1,6</sub> 7 <sub>2,6</sub> 8 <sub>3,6</sub> 9 <sub>4,6</sub> 10 <sub>5,6</sub> 11 <sub>6,6</sub> 12 <sub>7,6</sub>		58 84 67 45 31 22 16	33 108 187 221 206 169 132	6 25 67 136 228 328 410		6 <sub>3,4</sub> 7 <sub>3,5</sub> 8 <sub>3,6</sub> 9 <sub>3,7</sub> 10 <sub>3,8</sub> 11 <sub>3,9</sub> 12 <sub>3,10</sub>	6 <sub>4,3</sub> 7 <sub>5,3</sub> 8 <sub>6,3</sub> 9 <sub>7,3</sub> 10 <sub>8,3</sub> 11 <sub>9,3</sub> 12 <sub>10,3</sub>



FORBIDDEN SUBBRANCHES—*b* SUBBRANCHES

Subbranch		$\kappa$					Subbranch	
${}^bQ_{-3,3}$ $J + K_{-1} + K_1$ odd	$J + K_{-1} + K_1$ odd	$\mp 1$	$\mp 0.5$	0	$\pm 0.5$	$\pm 1$	${}^bQ_{3,-3}$ $J + K_{-1} + K_1$ odd	${}^bQ_{-3,3}$ $J + K_{-1} + K_1$ odd
$7_{7,1}$	$7_{4,4}$		4	26			$7_{1,7}$	$7_{4,4}$
$8_{7,2}$	$8_{4,5}$		16	102			$8_{2,7}$	$8_{6,4}$
$9_{7,3}$	$9_{4,6}$		45	221			$9_{3,7}$	$9_{6,4}$
$10_{7,4}$	$10_{4,7}$		98	327			$10_{4,7}$	$10_{7,4}$
$11_{7,5}$	$11_{4,8}$		183	367			$11_{5,7}$	$11_{8,4}$
$12_{7,6}$	$12_{4,9}$		299	340			$12_{6,7}$	$12_{9,4}$
$8_{8,1}$	$8_{5,4}$		3	19			$8_{1,8}$	$8_{4,5}$
$9_{8,2}$	$9_{5,5}$		11	83			$9_{2,8}$	$9_{6,5}$
$10_{8,3}$	$10_{5,6}$		31	206			$10_{3,8}$	$10_{6,5}$
$11_{8,4}$	$11_{5,7}$		68	367			$11_{4,8}$	$11_{7,5}$
$12_{8,5}$	$12_{5,8}$		129	498			$12_{5,8}$	$12_{8,5}$
$9_{9,1}$	$9_{6,4}$		2	14			$9_{1,9}$	$9_{4,6}$
$10_{9,2}$	$10_{6,5}$		8	63			$10_{2,9}$	$10_{6,6}$
$11_{9,3}$	$11_{6,6}$		22	169			$11_{3,9}$	$11_{6,6}$
$12_{9,4}$	$12_{6,7}$		48	340			$12_{4,9}$	$12_{7,6}$
$10_{10,1}$	$10_{7,4}$		1	11			$10_{1,10}$	$10_{4,7}$
$11_{10,2}$	$11_{7,5}$		6	48			$11_{2,10}$	$11_{6,7}$
$12_{10,3}$	$12_{7,6}$		16	132			$12_{3,10}$	$12_{6,7}$
$11_{11,1}$	$11_{8,4}$		1	9			$11_{1,11}$	$11_{4,8}$
$12_{11,2}$	$12_{8,5}$		5	38			$12_{2,11}$	$12_{6,8}$
$12_{12,1}$	$12_{9,4}$		1	7			$12_{1,12}$	$12_{4,9}$

${}^bR_{-1,1} + K_1 \text{ odd}$	${}^bP_{1,-1} + K_1 \text{ even}$	$\mp 1$	$\mp 0.5$	0	$\pm 0.5$	$\pm 1$	${}^bR_{1,-1} + K_1 \text{ odd}$	${}^bP_{-1,1} + K_1 \text{ even}$
$3_{1,1}$ $4_{2,2}$ $5_{3,3}$ $6_{4,4}$ $7_{5,5}$ $8_{6,6}$ $9_{7,7}$ $10_{8,8}$ $11_{9,9}$	$4_{0,4}$ $5_{0,5}$ $6_{0,6}$ $7_{0,7}$ $8_{0,8}$ $9_{0,9}$ $10_{0,10}$ $11_{0,11}$ $12_{0,12}$		38 111 175 206 209 195 177 158 142	41 62 59 50 42 35 30 27 24			$3_{1,1}$ $4_{2,2}$ $5_{3,3}$ $6_{4,4}$ $7_{5,5}$ $8_{6,6}$ $9_{7,7}$ $10_{8,8}$ $11_{9,9}$	$4_{4,0}$ $5_{5,0}$ $6_{6,0}$ $7_{7,0}$ $8_{8,0}$ $9_{9,0}$ $10_{10,0}$ $11_{11,0}$ $12_{12,0}$
$4_{4,1}$ $5_{4,2}$ $6_{4,3}$ $7_{4,4}$ $8_{4,5}$ $9_{4,6}$ $10_{4,7}$ $11_{4,8}$	$5_{1,4}$ $6_{1,5}$ $7_{1,6}$ $8_{1,7}$ $9_{1,8}$ $10_{1,9}$ $11_{1,10}$ $12_{1,11}$		14 77 209 370 493 549 550 519	63 149 182 170 146 122 104 90			$4_{1,4}$ $5_{2,4}$ $6_{3,4}$ $7_{4,4}$ $8_{5,4}$ $9_{6,4}$ $10_{7,4}$ $11_{8,4}$	$5_{4,1}$ $6_{5,1}$ $7_{6,1}$ $8_{7,1}$ $9_{8,1}$ $10_{9,1}$ $11_{10,1}$ $12_{11,1}$
$5_{5,1}$ $6_{5,2}$ $7_{5,3}$ $8_{5,4}$ $9_{5,5}$ $10_{5,6}$ $11_{5,7}$	$6_{2,4}$ $7_{2,5}$ $8_{2,6}$ $9_{2,7}$ $10_{2,8}$ $11_{2,9}$ $12_{2,10}$		3 23 87 234 466 715 896	43 175 305 347 324 279 237			$5_{1,5}$ $6_{2,5}$ $7_{3,5}$ $8_{4,5}$ $9_{5,5}$ $10_{6,5}$ $11_{7,5}$	$6_{4,2}$ $7_{5,2}$ $8_{6,2}$ $9_{7,2}$ $10_{8,2}$ $11_{9,2}$ $12_{10,2}$

FORBIDDEN SUBBRANCHES—*b* SUBBRANCHES

Subbranch		$\kappa$					Subbranch	
${}^bR_{-3,3}$ $J + K_{-1} + K_1$ odd	${}^bP_{3,-3}$ $J + K_{-1} + K_1$ even	$\mp 1$	$\mp 0.5$	0	$\pm 0.5$	$\pm 1$	${}^bR_{3,-3}$ $J + K_{-1} + K_1$ odd	${}^bP_{-3,3}$ $J + K_{-1} + K_1$ even
6 <sub>6,1</sub>	7 <sub>3,4</sub>		1	19	87		6 <sub>1,6</sub>	7 <sub>4,3</sub>
7 <sub>6,2</sub>	8 <sub>3,5</sub>		7	118	162		7 <sub>2,6</sub>	8 <sub>5,3</sub>
8 <sub>6,3</sub>	9 <sub>3,6</sub>		26	321	153		8 <sub>3,6</sub>	9 <sub>6,3</sub>
9 <sub>6,4</sub>	10 <sub>3,7</sub>		80	495	119		9 <sub>4,6</sub>	10 <sub>7,3</sub>
10 <sub>6,5</sub>	11 <sub>3,8</sub>		208	547	91		10 <sub>5,6</sub>	11 <sub>8,3</sub>
11 <sub>6,6</sub>	12 <sub>3,9</sub>		446	511	73		11 <sub>6,6</sub>	12 <sub>9,3</sub>
7 <sub>7,1</sub>	8 <sub>4,4</sub>		1	7	82		7 <sub>1,7</sub>	8 <sub>4,4</sub>
8 <sub>7,2</sub>	9 <sub>4,6</sub>		3	55	218		8 <sub>2,7</sub>	9 <sub>6,4</sub>
9 <sub>7,3</sub>	10 <sub>4,6</sub>		11	218	247		9 <sub>3,7</sub>	10 <sub>6,4</sub>
10 <sub>7,4</sub>	11 <sub>4,7</sub>		29	492	205		10 <sub>4,7</sub>	11 <sub>7,4</sub>
11 <sub>7,5</sub>	12 <sub>4,8</sub>		73	711	158		11 <sub>6,7</sub>	12 <sub>8,4</sub>
8 <sub>8,1</sub>	9 <sub>5,4</sub>		0	4	62		8 <sub>1,8</sub>	9 <sub>4,5</sub>
9 <sub>8,2</sub>	10 <sub>5,5</sub>		2	24	241		9 <sub>2,8</sub>	10 <sub>6,5</sub>
10 <sub>8,3</sub>	11 <sub>5,6</sub>		6	108	346		10 <sub>3,8</sub>	11 <sub>6,5</sub>
11 <sub>8,4</sub>	12 <sub>5,7</sub>		14	336	319		11 <sub>4,8</sub>	12 <sub>7,5</sub>
9 <sub>9,1</sub>	10 <sub>6,4</sub>		0	2	38		9 <sub>1,9</sub>	10 <sub>4,6</sub>
10 <sub>9,2</sub>	11 <sub>6,5</sub>		1	12	219		10 <sub>2,9</sub>	11 <sub>6,6</sub>
11 <sub>9,3</sub>	12 <sub>6,6</sub>		4	50	420		11 <sub>3,9</sub>	12 <sub>6,6</sub>
10 <sub>10,1</sub>	11 <sub>7,4</sub>		0	1	22		10 <sub>1,10</sub>	11 <sub>4,7</sub>
11 <sub>10,2</sub>	12 <sub>7,6</sub>		1	7	165		11 <sub>2,10</sub>	12 <sub>6,7</sub>
11 <sub>11,1</sub>	12 <sub>8,4</sub>		0	1	12		11 <sub>1,11</sub>	12 <sub>4,8</sub>



FORBIDDEN SUBBRANCHES—*b* SUBBRANCHES

Subbranch		$\kappa$					Subbranch	
${}^bR_{-3,5} + K_{-1} + K_1$ even	${}^bP_{3,-5} + K_{-1} + K_1$ odd	$\mp 1$	$\mp 0.5$	0	$\pm 0.5$	$\pm 1$	${}^bR_{5,-3} + K_{-1} + K_1$ even	${}^bP_{-5,3} + K_{-1} + K_1$ odd
4 <sub>4,0</sub>	5 <sub>1,5</sub>		2	2	0		4 <sub>0,4</sub>	5 <sub>5,1</sub>
5 <sub>4,1</sub>	6 <sub>1,6</sub>		6	3	0		5 <sub>1,4</sub>	6 <sub>6,1</sub>
6 <sub>4,2</sub>	7 <sub>1,7</sub>		11	2	0		6 <sub>2,4</sub>	7 <sub>7,1</sub>
7 <sub>4,3</sub>	8 <sub>1,8</sub>		13	1	0		7 <sub>3,4</sub>	8 <sub>8,1</sub>
8 <sub>4,4</sub>	9 <sub>1,9</sub>		12	0	0		8 <sub>4,4</sub>	9 <sub>9,1</sub>
9 <sub>4,5</sub>	10 <sub>1,10</sub>		9	0	0		9 <sub>5,4</sub>	10 <sub>10,1</sub>
10 <sub>4,6</sub>	11 <sub>1,11</sub>		5	0	0		10 <sub>6,4</sub>	11 <sub>11,1</sub>
11 <sub>4,7</sub>	12 <sub>1,12</sub>		3	0	0		11 <sub>7,4</sub>	12 <sub>12,1</sub>
5 <sub>5,0</sub>	6 <sub>2,5</sub>		2	4	2		5 <sub>0,5</sub>	6 <sub>5,2</sub>
6 <sub>5,1</sub>	7 <sub>2,6</sub>		8	9	1		6 <sub>1,5</sub>	7 <sub>6,2</sub>
7 <sub>5,2</sub>	7 <sub>2,7</sub>		18	10	0		7 <sub>2,5</sub>	8 <sub>7,2</sub>
8 <sub>5,3</sub>	9 <sub>2,8</sub>		30	6	0		8 <sub>3,5</sub>	9 <sub>8,2</sub>
9 <sub>5,4</sub>	10 <sub>2,9</sub>		40	3	0		9 <sub>4,5</sub>	10 <sub>9,2</sub>
10 <sub>5,5</sub>	11 <sub>2,10</sub>		43	1	0		10 <sub>5,5</sub>	11 <sub>10,2</sub>
11 <sub>5,6</sub>	12 <sub>2,11</sub>		37	1	0		11 <sub>6,5</sub>	12 <sub>11,2</sub>
6 <sub>6,0</sub>	7 <sub>3,5</sub>		1	5	4		6 <sub>0,6</sub>	7 <sub>5,3</sub>
7 <sub>6,1</sub>	8 <sub>3,6</sub>		5	15	4		7 <sub>1,6</sub>	8 <sub>6,3</sub>

FORBIDDEN SUBBRANCHES—b SUBBRANCHES

Subbranch		$\kappa$					Subbranch	
${}^bR_{5,-3}$ $J + K_{-1} + K_1$ even	${}^bP_{3,-5}$ $J + K_{-1} + K_1$ odd	$\mp 1$	$\mp 0.5$	0	$\pm 0.5$	$\pm 1$	${}^bR_{5,-3}$ $J + K_{-1} + K_1$ even	${}^bP_{-5,3}$ $J + K_{-1} + K_1$ odd
8 <sub>6,3</sub>	9 <sub>3,7</sub>		15	24	1		8 <sub>2,6</sub>	9 <sub>7,3</sub>
9 <sub>6,3</sub>	10 <sub>3,8</sub>		31	23	0		9 <sub>3,6</sub>	10 <sub>8,3</sub>
10 <sub>6,4</sub>	11 <sub>3,9</sub>		52	14	0		10 <sub>4,6</sub>	11 <sub>9,3</sub>
11 <sub>6,5</sub>	12 <sub>3,10</sub>		73	6	0		11 <sub>5,6</sub>	12 <sub>10,3</sub>
7 <sub>7,0</sub>	8 <sub>4,5</sub>		1	4	6		7 <sub>0,7</sub>	8 <sub>5,4</sub>
8 <sub>7,1</sub>	9 <sub>4,6</sub>		3	16	9		8 <sub>1,7</sub>	9 <sub>6,4</sub>
9 <sub>7,2</sub>	10 <sub>4,7</sub>		9	33	4		9 <sub>2,7</sub>	10 <sub>7,4</sub>
10 <sub>7,3</sub>	11 <sub>4,8</sub>		22	44	1		10 <sub>3,7</sub>	11 <sub>8,4</sub>
11 <sub>7,4</sub>	12 <sub>4,9</sub>		42	39	0		11 <sub>4,7</sub>	12 <sub>9,4</sub>
8 <sub>8,0</sub>	9 <sub>5,5</sub>		0	3	7		8 <sub>0,8</sub>	9 <sub>5,5</sub>
9 <sub>8,1</sub>	10 <sub>5,6</sub>		2	13	15		9 <sub>1,8</sub>	10 <sub>6,5</sub>
10 <sub>8,2</sub>	11 <sub>5,7</sub>		6	33	11		10 <sub>2,8</sub>	11 <sub>7,5</sub>
11 <sub>8,3</sub>	12 <sub>5,8</sub>		14	57	4		11 <sub>3,8</sub>	12 <sub>8,5</sub>
9 <sub>9,0</sub>	10 <sub>6,5</sub>		0	2	8		9 <sub>0,9</sub>	10 <sub>5,6</sub>
10 <sub>9,1</sub>	11 <sub>6,6</sub>		1	9	21		10 <sub>1,9</sub>	11 <sub>6,6</sub>
11 <sub>9,2</sub>	12 <sub>6,7</sub>		4	28	22		11 <sub>2,9</sub>	12 <sub>7,6</sub>
10 <sub>10,0</sub>	11 <sub>7,5</sub>		0	1	7		10 <sub>0,10</sub>	11 <sub>5,7</sub>
11 <sub>10,1</sub>	12 <sub>7,6</sub>		1	7	24		11 <sub>1,10</sub>	12 <sub>6,7</sub>
11 <sub>11,0</sub>	12 <sub>8,6</sub>		0	1	6		11 <sub>0,11</sub>	12 <sub>5,8</sub>

## APPENDIX VI

### Molecular Constants Involved in Microwave Spectra

In accordance with accepted practice, molecules are listed alphabetically according to their empirical formulas by the following procedures:

1. Symbols for the elements in the empirical formula for a molecule are in alphabetical order except that within a molecular formula:

- a. C for carbon precedes all other symbols. This groups all organic compounds together.
- b. In organic compounds, H precedes all other symbols except C.
- c. D (for deuterium) is regarded for purposes of listing as H<sup>2</sup>.

2. All molecules with formulas of the form X<sub>n</sub>Y precede those of the form X<sub>n+1</sub>YZ, etc.

To aid in identification, in some cases the usual chemical formula or the name of a compound is given in parentheses. The more abundant isotopic species of molecules are usually listed before those which are less abundant.

The table lists molecular constants which determine or are determined by microwave spectra. These include rotational constants *A*, *B*, and *C* (cf. pages 5 and 83), centrifugal stretching constants *D*, (cf. pages 9 and 25) or *D<sub>J</sub>* and *D<sub>JK</sub>* (page 78), rotation-vibration constants *α* (pages 9 and 25), and *l*-type doubling constants (pages 33 and 79). Vibrational frequencies *ω*<sub>1</sub>, *ω*<sub>2</sub>, etc., usually obtained from infrared spectra, are listed in the better known or more important cases since they affect the relative intensities of excited state lines. Quadrupole coupling constants *eqQ* (page 150) or  $eQ \frac{\partial^2 V}{\partial a^2}$ ,  $eQ \frac{\partial^2 V}{\partial b^2}$ , and  $eQ \frac{\partial^2 V}{\partial c^2}$  (pages 159 to 162), are listed for each nucleus in the molecule. The molecular dipole moment *μ*, or its components *μ<sub>a</sub>*, *μ<sub>b</sub>*, and *μ<sub>c</sub>* along principal axes, is also given. In the column labeled "Remarks," a number of less frequently measured molecular constants may be found for cases where they are known. These include magnetic hyperfine constants (pages 216 and 220), molecular *g* factors (pages 292 to 296), line-width parameters *Δν* (page 343), and others.

References are usually given adjacent to each molecular constant. In the case of dipole moments which are listed by Wesson [336*a*] and which have not been measured by microwave techniques, no reference is given. Similarly references are omitted for vibrational frequencies which are given in one of Herzberg's volumes on molecular spectra ([130] or [471]) and which have not been measured by microwave techniques.

Most of this table has been compiled by Mr. G. C. Dousmanis.



Chemical symbol	Rotational constants <i>A, B, and C, Mc</i>	Vibrational fre- quencies $\omega$ in wave numbers ( $\text{cm}^{-1}$ ); <i>d</i> indicates a degenerate vibration	Rotation-vibration constants, <i>Mc</i> ( $\alpha, D$ , or $q$ )	Quadrupole coupling constant $eqQ$ , <i>Mc</i>	Dipole moment $\mu$ in $10^{-18}$ esu (Debye)	Reference for structure	Remarks
$\text{AsCl}_3^{16}$ .....	$B_0 = 2147.2$ [481]	$\omega_1 = 410$ $\omega_2 = 193$ $\omega_3 = 370d$ $\omega_4 = 159d$	$\alpha_2 = 4.2$ [481]	$\text{As}^{76} = -173$ [597]	1.97	[481]	
$\text{AsCl}_2^{13}\text{C}^{17}$ .....	.....	.....	.....	.....	.....	.....	5 lines measured [481]
$\text{AsCl}^{10}\text{Cl}_2^{17}$ .....	.....	.....	.....	.....	.....	.....	2 lines measured [481]
$\text{AsCl}_2^{17}$ .....	$B_0 = 2044.7$ [481]	.....	.....	.....	.....	.....	
$\text{AsF}_3$ .....	$B_0 = 5878.971$ [26], [824]	$\omega_1 = 707$ $\omega_2 = 341$ $\omega_3 = 644d$ $\omega_4 = 274d$	$\alpha_2 = -5$ [824] $\alpha_4 = -0.16$ [824] $D_{JK} = 0.009$ [824]	$\text{As}^{76} = -236.23$ [266], [824]	2.52 [528]	[266],[824]	Magnetic h.f.s. interaction $-I \cdot J \left[ -0.012 - \frac{0.012K^2}{J(J+1)} \right]$ <i>Mc</i> [824]
$\text{AsH}_3\text{D}$ .....	.....	.....	.....	$\text{As}^{75} = -184$ [606]	0.22 [606]	[735],[736], [806]	
$\text{AsD}_3$ .....	$B_0 = 57,476.15$ [943]	.....	.....	$\text{As}^{76} = -165.5$ [943]	.....	[447]	
$\text{B}_2^{11}\text{Br}^{79}\text{H}_6$ ( $\text{B}_2\text{H}_6\text{Br}_2$ bromodiborane)	$B_0 = 3369.65$ [447] $C_0 = 3141.48$ [447]	.....	.....	$\text{Br}^{79} = 293$ [447]	.....	.....	
$\text{BuB}^{10}\text{Br}^{79}\text{H}_6$ ( $\text{B}^{10}$ nearest $\text{Br}^{79}$ )	$B_0 = 3398.62$ [447] $C_0 = 3176.05$ [447]	.....	.....	$\text{Br}^{79} = 293$ [447]	.....	.....	
$\text{B}^{10}\text{Bu}^{11}\text{Br}^{79}\text{H}_6$ ( $\text{B}^{10}$ nearest $\text{Br}^{79}$ )	$B_0 = 3523.72$ [447] $C_0 = 3278.42$ [447]	.....	.....	$\text{Br}^{79} = 293$ [447]	.....	.....	
$\text{B}_2^{11}\text{Br}^{81}\text{H}_6$ .....	$B_0 = 3350.75$ [447] $C_0 = 3124.95$ [447]	.....	.....	$\text{Br}^{81} = 244$ [447]	.....	.....	
$\text{BuB}^{10}\text{Br}^{81}\text{H}_6$ ( $\text{B}^{10}$ nearest $\text{Br}^{81}$ )	$B_0 = 3379.95$ [447] $C_0 = 3159.85$ [447]	.....	.....	$\text{Br}^{81} = 244$ [447]	.....	.....	
$\text{B}^{10}\text{Bu}^{11}\text{Br}^{81}\text{H}_6$ ( $\text{B}^{10}$ nearest $\text{Br}^{81}$ )	$B_0 + C_0 = 6766.4$ [447]	.....	.....	$\text{Br}^{81} = 244$ [447]	.....	.....	
$\text{B}_5^{11}\text{H}_9$ (pentaborane)...	$B_0 = 7002.9$ [697],[939] $C_0 = 48.9 \times 10^2$ [939]	.....	.....	.....	2.13 [919]	[697],[939]	Lines for other asymmetric species measured
$\text{B}^{10}\text{B}_4^{11}\text{H}_9$ ( $\text{B}^{10}$ at apex)	$B_0 = 7089.8$ [697]	.....	.....	.....	.....	.....	
$\text{B}_4^{11}\text{D}_5$ .....	$B_0 = 5211.35$ [939] $C_0 = 37 \times 10^2$ [939]	.....	.....	.....	2.16 [939]	.....	

Br <sup>79</sup> Cl <sup>35</sup> .....	B <sub>e</sub> = 4570.92 [535]	~430	α = 23.22 [535]	Br <sup>79</sup> = 876.8 [535] Cl <sup>35</sup> = -103.6 [535]	0.57 [535]	[535]	Rotation-vibration constant γ <sub>v</sub> = 0.0031 Mc [938]
Br <sup>81</sup> Cl <sup>35</sup> .....	B <sub>e</sub> = 4536.14 [535]	~430	α = 22.95 [535]	Br <sup>81</sup> = 732.9 [535]			
Br <sup>79</sup> Cl <sup>37</sup> .....	B <sub>e</sub> = 4499.84 [535]	~420	α = 21.94 [535]	Cl <sup>37</sup> = -103.6 [535] Br <sup>79</sup> = 876.8 [535]			
Br <sup>81</sup> Cl <sup>37</sup> .....	B <sub>e</sub> = 4365.01 [535]	~420	α = 21.67 [535]	Cl <sup>37</sup> = -81.1 [535] Br <sup>81</sup> = 732.9 [535]			
Br <sup>79</sup> Cs (CsBr).....	B <sub>e</sub> = 1081.34 [938]	171 [772c]	α = 3.718 [938] D = 0.0027 [938] α = 3.631 [938] α = 156.3 [534] α = 155.8 [534] D <sub>J</sub> K = 0.0008 [641] D <sub>J</sub> K = 0.0008 [641]	.....	.....	[938]	
Br <sup>81</sup> Cs.....	B <sub>e</sub> = 1064.59 [938]						
Br <sup>79</sup> F.....	B <sub>e</sub> = 10,706.9 [534]	671	α = 156.3 [534]	Br <sup>79</sup> = 1089.0 [534] Br <sup>81</sup> = 909.2 [534]	1.29 [534]	[534]	
Br <sup>81</sup> F.....	B <sub>e</sub> = 10,655.7 [534]		α = 155.8 [534]	Br <sup>79</sup> = 440 [641] Br <sup>81</sup> = 370 [641]		[525],[641]	
Br <sup>79</sup> F <sub>3</sub> Si <sup>28</sup> (SiF <sub>3</sub> Br).....	B <sub>0</sub> = 1549.9 [641] B <sub>0</sub> = 1534.1 [641]		D <sub>J</sub> K = 0.0008 [641] D <sub>J</sub> K = 0.0008 [641]	Br <sup>79</sup> = 380 [521] Br <sup>81</sup> = 321 [521]		[521],[727]	
Br <sup>79</sup> Ge <sup>70</sup> H <sub>2</sub> (GeH <sub>3</sub> Br).....	B <sub>0</sub> = 2438.57 [521] B <sub>0</sub> = 2410.17 [521]			Br <sup>79</sup> = 380 [521] Br <sup>81</sup> = 321 [521]			
Br <sup>81</sup> Ge <sup>70</sup> H <sub>2</sub> .....	B <sub>0</sub> = 2406.42 [521] B <sub>0</sub> = 2378.01 [521]			Br <sup>79</sup> = 380 [521] Br <sup>81</sup> = 321 [521]			
Br <sup>79</sup> Ge <sup>72</sup> H <sub>2</sub> .....	B <sub>0</sub> = 2375.88 [521] B <sub>0</sub> = 2347.46 [521]			Br <sup>79</sup> = 380 [521] Br <sup>81</sup> = 321 [521]			
Br <sup>81</sup> Ge <sup>72</sup> H <sub>2</sub> .....	B <sub>0</sub> = 2378.01 [521] B <sub>0</sub> = 2375.88 [521]			Br <sup>79</sup> = 380 [521] Br <sup>81</sup> = 321 [521]			
Br <sup>79</sup> Ge <sup>74</sup> H <sub>2</sub> .....	B <sub>0</sub> = 2347.46 [521] B <sub>0</sub> = 2346.84 [521]			Br <sup>79</sup> = 380 [521] Br <sup>81</sup> = 321 [521]			
Br <sup>81</sup> Ge <sup>74</sup> H <sub>2</sub> .....	B <sub>0</sub> = 2346.84 [521] B <sub>0</sub> = 2318.37 [521]			Br <sup>79</sup> = 380 [521] Br <sup>81</sup> = 321 [521]			
Br <sup>79</sup> Ge <sup>76</sup> H <sub>2</sub> .....	B <sub>0</sub> = 2318.37 [521] B <sub>0</sub> = 4321.77 [409]			Br <sup>79</sup> = 336 [409]	1.31 [521]	[409],[521], [727]	
Br <sup>79</sup> H <sub>3</sub> Si <sup>28</sup> (SiH <sub>3</sub> Br).....	B <sub>0</sub> = 4321.77 [409]						
Br <sup>81</sup> H <sub>3</sub> Si <sup>28</sup> .....	B <sub>0</sub> = 4292.62 [409] B <sub>0</sub> = 4232.96 [409]			Br <sup>81</sup> = 278 [409] Br <sup>79</sup> = 336 [409]			
Br <sup>79</sup> H <sub>3</sub> Si <sup>29</sup> .....	B <sub>0</sub> = 4203.70 [409] B <sub>0</sub> = 4149.39 [409]			Br <sup>81</sup> = 278 [409] Br <sup>79</sup> = 336 [409]			
Br <sup>81</sup> H <sub>3</sub> Si <sup>30</sup> .....	B <sub>0</sub> = 4120.09 [409] Y <sub>01</sub> (≈B <sub>e</sub> ) = 2434.947 [799]	231	α <sub>e</sub> = 12.136 [799]	Br <sup>81</sup> = 278 [409] Br <sup>79</sup> = 10.244 [799] K <sup>39</sup> = -5.003 [799]	10.41 [799]	[799]	γ <sub>v</sub> = 0.023 Mc [799]; variation of eqQ with vibrational state [799] γ <sub>v</sub> = 0.022 Mc [938]
Br <sup>79</sup> K <sup>39</sup> (KBr).....							
Br <sup>81</sup> K <sup>39</sup> .....	Y <sub>01</sub> (≈B <sub>e</sub> ) = 2415.075 [799]		α <sub>e</sub> = 11.987 [799]	Br <sup>81</sup> = 8.555 [799] K <sup>39</sup> = -5.002 [799]			
Br <sup>79</sup> Li <sup>7</sup> (LiBr).....	Y <sub>01</sub> (≈B <sub>e</sub> ) = 16,650.57 [938]	~480 [938]	α <sub>e</sub> = 169.09 [938]	Br <sup>79</sup> = 37.2 [938]	6.2 [938]	[938]	
Br <sup>81</sup> Li <sup>6</sup> .....	Y <sub>01</sub> (≈B <sub>e</sub> ) = 19,161.51 [938]						

Chemical symbol	Rotational constants $A$ , $B$ , and $C$ , Mc	Vibrational frequencies $\omega$ in wave numbers ( $\text{cm}^{-1}$ ); $d$ indicates a degenerate vibration	Rotation-vibration constants, Mc ( $\alpha$ , $D$ , or $q$ )	Quadrupole coupling constant $eqQ$ , Mc	Dipole moment $\mu$ in $10^{-18}$ esu (Debye)	Reference for structure	Remarks
$\text{Br}^{81}\text{Li}^7$ .....	$Y_{01}(\approx B_e) = 16,650.00$ [938]	.....	$\alpha_n = 168.58$ [938]	$\text{Br}^{81} = 30.7$ [938]	.....	.....	$\gamma_e = 0.65$ Mc [938]
$\text{Br}^{79}\text{N}^{14}$ ( $\text{NaBr}$ ).....	$Y_{01}(\approx B_e) = 45,444.51$ [938]	315	$\alpha_n = 28.55$ [938] $D = 0.007$ [938] $\alpha_e = 28.06$ [938]	$\text{Br}^{79} = 58$ [938]	.....	[938]	$\gamma_e = 0.08$ Mc [938]
$\text{Br}^{81}\text{Na}$ .....	$Y_{01}(\approx B_e) = 4509.34$ [938]	.....	.....	.....	.....	[938]	$\gamma_e = 0.008$
$\text{Br}^{79}\text{Rb}^{85}$ ( $\text{RbBr}$ ).....	$B_e = 1424.83$ [938]	181 [938]	$\alpha_e = 5.575$ [938] $D = 0.0004$ [938] $\alpha_e = 5.474$ [938] $\alpha_e = 5.461$ [938]	.....	.....	.....	.....
$\text{Br}^{79}\text{Rb}^{87}$ .....	$B_e = 1409.06$ [938]	.....	.....	.....	.....	.....	.....
$\text{Br}^{81}\text{Rb}^{85}$ .....	$B_e = 1406.59$ [938]	.....	.....	.....	.....	.....	.....
$\text{Br}^{79}\text{P}$ .....	$B_0 = 996.4$ [551]	.....	.....	.....	.....	.....	.....
$\text{Br}^{81}\text{P}$ .....	$B_0 = 974.4$ [551]	.....	.....	.....	.....	.....	.....
$\text{CBr}^{79}\text{F}_3$ ( $\text{CF}_3\text{Br}$ ).....	$B_0 = 2098.06$ [520], [743]	.....	$D_{Jn} = 0.0013$ [743]	$\text{Br}^{79} = 119$ [520], [743]	.....	[520], [743]	$B_0$ may be incorrect [947] $B_0$ may be incorrect [947]
$\text{CBr}^{81}\text{F}_3$ .....	$B_0 = 2078.50$ [520], [743]	.....	$D_{JK} = 0.0012$ [743]	$\text{Br}^{81} = 517$ [520], [743]	.....	.....	.....
$\text{CuBr}^{79}\text{N}^{14}$ ( $\text{BrCN}$ ).....	$B_0 = 4120.198$ [329], [320], [754]	$\omega_1 = 580$ $\omega_2 = 368d$ $\omega_3 = 2187$	$\alpha_1 = 15.51$ [329], [754] $\alpha_2 = -11.564$ [329], [754] $D_J = 0.0009$ [531] $q_t = 3.918$ [329], [754]	$\text{Br}^{79} = 686.1$ [329], [320], [754] $\text{N}^{14} = -3.83$ [329]	2.94	[329], [320]	$eqQ$ for $\text{Br}^{79}$ in vibrational state (010) = 082.8 [320], [744]; $\alpha_1$ from vibrational state (0220) = -11.528 [744]; Fermi resonance energy $W_{12} = 61.5 \text{ cm}^{-1}$ [744]; $\Delta\nu = 27.1 \text{ Mc/mm Hg}$ [922]; $\Delta\nu \propto T^{-1.6}$ [922]
$\text{CuBr}^{79}\text{N}^{14}$ .....	$B_0 = 4073.373$ [320], [754]	.....	.....	.....	.....	.....	.....
$\text{CuBr}^{81}\text{N}^{14}$ .....	$B_0 = 4086.788$ [329], [320], [754]	.....	$\alpha_1 = 15.48$ [329], [754] $D_J = 0.0008$ [531] $q_t = 3.874$ [329], [754]	$\text{Br}^{81} = 572.27$ [329], [320], [754]	.....	.....	$eqQ$ for $\text{Br}^{81}$ in vibrational state (010) = 570.4 [320], [754]; $\alpha_1$ from vibrational state (0220) = -11.462 [754]; Fermi resonance energy $W_{12} = 60.5 \text{ cm}^{-1}$ [754]
$\text{CuBr}^{81}\text{N}^{14}$ .....	$B_0 = 4049.608$ [320], [754]	.....	.....	.....	.....	.....	.....



$C^{12}Br^{79}N^{15}$ .....	$B_0 = 3944.846$ [754]	.....	.....	$C^{135} = -78.05$ [358]	[358]	
$C^{12}Br^{81}N^{15}$ .....	$B_0 = 3921.787$ [754]	.....	.....	$C^{137} = -61.44$ [358]		
$CCl^{35}F_2$ ( $CF_2Cl$ ).....	$B_0 = 3335.56$ [358]	.....	.....	$C^{135} = -83.33$ [329],	[329],[320]	$\Delta \nu = 50$ Mc/mm Hg
$CCl^{37}F_2$ .....	$B_0 = 3251.51$ [358]	.....	.....	[320],[575]		
$C^{12}Cl^{35}N^{14}$ ( $ClCN$ )....	$B_0 = 5970.821$ [329],	$\alpha_2 = -16.39$ [329]	$\omega_1 = 729$	$N^{14} = -3.63$ [329]	2.80 [528]	
	[320]	$q_1 = 7.500$ [329]	$\omega_2 = 397d$			
			$\omega_3 = 2201$			
$CuCl^{63}N^{14}$ .....	$B_0 = 5939.795$ [329],	.....	.....			
	[320]	.....	.....			
$C^{12}Cl^{35}N^{14}$ .....	$B_0 = 5907.31$ [421]	.....	.....	$C^{135} = 42.2$ [421]		
$C^{12}Cl^{37}N^{14}$ .....	$B_0 = 5847.252$ [329],	.....	.....	$C^{137} = -65.3$ [329],[320]		
	[320]	.....	.....			
$C^{12}Cl^{37}N^{14}$ .....	$B_0 = 5814.710$ [329],	.....	.....			
	[320]	.....	.....			
$CCl_2^{32}O$ ( $COCl_2$ , phosgene)	$A_0 = 7918.75$ [859b] $B_0 = 3474.99$ [859b] $C_0 = 2412.25$ [859b]	.....	.....	$e \frac{\partial^2 V}{\partial a^2} Q_{Cl^{35}} = -37.20$ [859b] $e \frac{\partial^2 V}{\partial c^2} Q_{Cl^{35}} = 27.07$ [859b] $e \frac{\partial^2 V}{\partial c^2} Q_{Cl^{37}} = 24.20$ [859b]	[859b]	
$CCl^{35}Cl^{37}O$ .....	$A_0 = 7867.76$ [859b] $B_0 = 3379.94$ [859b] $C_0 = 2361.48$ [859b]	.....	.....			
$CF_3I$ .....	$B_0 = 1523.23$ [524],	$D_{JK} = 0.0006$ [524]	.....	$I_{E7} = -2143.8$ [524],	[524]	
	[897]	.....	.....	[897]		
$CHBr^{79}$ .....	$B_0 = 1247.61$ [551],	.....	.....		[764]	
	[764]	.....	.....			
$CDBr^{79}$ .....	$B_0 = 1239.45$ [764]	.....	.....			
$CHBr^{81}$ .....	$B_0 = 1217.30$ [551],	.....	.....			
	[764]	.....	.....			
$CDBr^{81}$ .....	$B_0 = 1209.51$ [764]	.....	.....			
$CHClF_2$ .....	.....	.....	$\omega_1 = 3030$	.....	.....	
$CHCl_3$ .....	$B_0 = 3301.94$ [414],	.....	$\omega_2 = 672$	.....	.....	
	[545],[690]	.....	$\omega_3 = 363$	.....	.....	
		.....	$\omega_4 = 1217d$	.....	.....	
		.....	$\omega_5 = 760d$	.....	.....	
		.....	$\omega_6 = 261d$	.....	.....	
				.....	.....	18 lines measured [714]

Chemical symbol	Rotational constants <i>A</i> , <i>B</i> , and <i>C</i> , Mc	Vibrational fre- quencies $\omega$ in wave numbers (cm <sup>-1</sup> ); <i>d</i> indicates a degenerate vibration	Rotation-vibration constants, Mc ( $\alpha$ , <i>D</i> , or <i>q</i> )	Quadrupole coupling constant <i>eqQ</i> , Mc	Dipole moment $\mu$ in 10 <sup>-18</sup> esu (Debye)	Reference for structure	Remarks
CDCl <sub>3</sub> <sup>35</sup>	<i>B</i> <sub>0</sub> = 3250.17 [414], [545],[690]						
CHCl <sub>3</sub> <sup>37</sup>	<i>B</i> <sub>0</sub> = 3129.51 [690]						
C <sup>13</sup> HF <sub>3</sub>	<i>B</i> <sub>0</sub> = 10,348.74 [367], [690]				1.64 [690]	[367],[690]	$\Delta v = 18$ Mc/mm Hg [367]
C <sup>13</sup> HF <sub>3</sub>	<i>B</i> <sub>0</sub> = 10,422.00 [690]						
C <sup>13</sup> DF <sub>3</sub>	<i>B</i> <sub>0</sub> = 9921.35 [690]						
C <sup>13</sup> HN (HCN)	<i>B</i> <sub>0</sub> = 44,315.97 [532], [733]	$\omega_1 = 2041.2$ $\omega_2 = 711.7d$ $\omega_3 = 3368.6$	<i>D</i> <i>J</i> = 0.1 [532] <i>q</i> <sub>1</sub> = 224.471 - 0.002614 <i>J</i> ( <i>J</i> + 1) [529],[761],[911],[997]	<i>N</i> <sub>14</sub> = -4.58 [532]	3.00 [803]		Dipole moment in vibrational state (010) = 2.96 [529]
C <sup>13</sup> HN	<i>B</i> <sub>0</sub> = 43,170.1 [532], [733]						
C <sup>13</sup> DN	<i>B</i> <sub>0</sub> = 33,207.5 [532], [733]		<i>q</i> <sub>1</sub> = 188.37 - 0.0022 <i>J</i> ( <i>J</i> + 1) [761]	<i>D</i> = 0.15 [998]		[532],[733]	$\Delta v = 25$ Mc/mm Hg [413]
C <sup>13</sup> DN	<i>B</i> <sub>0</sub> = 35,587.57 [532]						
CHN <sup>14</sup> O (HCNO)	<i>A</i> <sub>0</sub> = 9194 × 10 <sup>2</sup> [479] <i>B</i> <sub>0</sub> = 10992 [479] <i>C</i> <sub>0</sub> = 10991 [479] <i>B</i> <sub>0</sub> = 10199 [479] <i>C</i> <sub>0</sub> = 10197 [479] <i>B</i> <sub>0</sub> = 10663 [479] <i>C</i> <sub>0</sub> = 10662 [479] <i>B</i> <sub>0</sub> = 5903.0 [434] <i>C</i> <sub>0</sub> = 5828.0 [434]			<i>N</i> <sub>14</sub> = 2.00 [446]		[479]	
CDN <sup>14</sup> O							
CHN <sup>13</sup> O							
C <sup>13</sup> HNNS <sup>32</sup> (HNCS)				<i>N</i> <sub>14</sub> = 1.20 [646]	1.72 [434]	[434],[794]	<i>B</i> <sub>0</sub> and <i>C</i> <sub>0</sub> are for rotational state with <i>K</i> = 1; for <i>K</i> = 0, $\frac{1}{2}(B_0 + C_0) = 5864.5$ [434] $\frac{1}{2}(B_0 + C_0)$ is for <i>K</i> = 1
C <sup>13</sup> HNNS <sup>32</sup>	$\frac{1}{2}(B_0 + C_0) = 5847.8$ [434]						
C <sup>13</sup> DNNS <sup>32</sup>	<i>B</i> <sub>0</sub> = 5529.5 [794] <i>C</i> <sub>0</sub> = 5418.7 [794]					[794]	<i>B</i> <sub>0</sub> and <i>C</i> <sub>0</sub> are for <i>K</i> = 1; for <i>K</i> = 0, $\frac{1}{2}(B_0 + C_0) = 5472.9$ [794]
C <sup>13</sup> DNNS <sup>32</sup>	$\frac{1}{2}(B_0 + C_0) = 5459.8$ [434]						$\frac{1}{2}(B_0 + C_0)$ for <i>K</i> = 1

$C^{12}HNS^{34}$ .....	$\frac{1}{2}(B_0 + C_0) = 5793.5$ [794]	.....	.....	$S^M = -27.5$ [794]	.....	.....	$\frac{1}{2}(B_0 + C_0)$ is for $K = 0$
$C^{12}HNS^{34}$ .....	$B_0 = 5763.6$ [794] $C_0 = 5691.7$ [794]	.....	.....	.....	.....	.....	$B_0$ and $C_0$ are for $K = 1$ ; for $K = 0$ , $\frac{1}{2}(B_0 + C_0) = 5726.7$ [794] 16 lines measured [334],[403]
$CH_2Br$ .....	.....	.....	.....	.....	1.5	.....	.....
$CH_2Cl^{35}$ .....	$A_0 = 32,001.8$ [732]	.....	.....	$e \frac{\partial^2 V}{\partial a^2} Q_{Cl^{35}} = -41.8$ [732]	1.62 [732]	[732]	.....
	$B_0 = 3320.4$ [732]	.....	.....	$e \frac{\partial^2 V}{\partial b^2} Q_{Cl^{35}} = 2.6$ [732]	.....	.....	.....
	$C_0 = 3065.2$ [732]	.....	.....	$e \frac{\partial^2 V}{\partial c^2} Q_{Cl^{35}} = 39.2$ [732]	.....	.....	.....
$CDHCl^{35}$ .....	$A_0 = 27,198$ [732] $B_0 = 3305$ [732] $C_0 = 3027$ [732]	.....	.....	.....	.....	.....	.....
$CD_2Cl^{35}$ .....	$A_0 = 23,676$ [732] $B_0 = 3284$ [732] $C_0 = 2993$ [732]	.....	.....	.....	.....	.....	.....
$CH_3Cl^{35}Cl^{37}$ .....	$A_0 = 31,878.2$ [732] $B_0 = 3231.5$ [732] $C_0 = 2988.2$ [732] $A_0 = 27,090$ [732] $B_0 = 3217$ [732] $C_0 = 2951$ [732]	.....	.....	.....	.....	.....	.....
$CDHCl^{35}Cl^{37}$ .....	$A_0 = 23,582$ [732] $B_0 = 3197$ [732] $C_0 = 2920$ [732]	.....	.....	.....	.....	.....	.....
$CD_2Cl^{35}Cl^{37}$ .....	$A_0 = 31,754$ [732] $B_0 = 3143$ [732] $C_0 = 2912$ [732]	.....	.....	.....	.....	.....	.....
$CH_2Cl^{37}$ .....	$A_0 = 49,138.4$ [722] $B_0 = 10,603.89$ [722] $C_0 = 9249.20$ [722]	.....	.....	.....	1.96 [712]	[722]	.....
$CH_2F_2$ .....	$A_0 = 282,106$ [353], [601] $B_0 = 38,834$ [353], [601] $C_0 = 34,004$ [353], [601]	$\omega_1 = 2780$ $\omega_2 = 1743.6$ $\omega_3 = 1503$ $\omega_4 = 2874$ $\omega_5 = 1280$ $\omega_6 = 1167$	.....	.....	2.31 [601]	[601]	$\Delta\nu = 10$ Mc/mm Hg [601] cen- trifugal distortion effects [601]



Chemical symbol	Rotational constants $A, B,$ and $C, \text{ Mc}$	Vibrational frequencies $\omega$ in wave numbers ( $\text{cm}^{-1}$ ); $d$ indicates a degenerate vibration	Rotation-vibration constants, $\text{Mc}$ ( $\alpha, D,$ or $q$ )	Quadrupole coupling constant $eqQ, \text{ Mc}$	Dipole moment $\mu$ in $10^{-18}$ esu (Debye)	Reference for structure	Remarks
$\text{CH}_3\text{O}_2 (\text{HCOOH})$ .....	$A_0 \approx 80 \times 10^3$ [134] $B_0 = 12,055.9$ [634], [796b],[991] $C_0 = 10,415.3$ [634], [796b],[991] $B_0 = 11,762.4$ [991] $C_0 = 9970.3$ [991] $B_0 = 8657.2$ [461]	.....	.....	.....	1.7	[991]	The rotational constants given in [796b] are incorrect. (Private communication from G. Erlundson.)
$\text{CHDO}_2 (\text{HCOOD})$ .....		.....					
$\text{CH}_3\text{BuO} (\text{BH}_3\text{CO})$ .....		.....	$D_J = 0.177$ [417] $D_{JK} = 0.36$ [461] $D_{JK} = 0.24$ [461] $\alpha_a = -22.6$ [417],[546] $\alpha_b = -5.7$ [417],[546] $D_{JK} = 0.39$ [461] $D_{JK} = 0.29$ [461]	$B_{11} = 1.55$ [461]	1.80 [417],[546], [461]	[461]	
$\text{CD}_3\text{BuO}$ .....	$B_0 = 7336.5\text{b}$ [461]	.....					
$\text{CH}_3\text{B}^{10}\text{O}$ .....	$B_0 = 8980.1$ [417], [546],[461]	.....					
$\text{CD}_3\text{B}^{10}\text{O}$ .....	$B_0 = 7530.34$ [461]	.....					
$\text{C}^{12}\text{H}_5\text{Br}^{79}$ .....	$B_0 = 9568.19$ [240], [411],[531]	$\omega_1 = 2972$ $\omega_2 = 1305.1$ $\omega_3 = 611$ $\omega_4 = 3055.9d$ $\omega_5 = 1445.3d$ $\omega_6 = 952.0d$	$\alpha_3 = 72.77$ [950a] $D_J = 0.010$ [531],[989] $D_{JK} = 0.12\text{b}$ [531],[989]	$B_{17^9} = 577.15$ [280], [411],[950a]	1.797 [52b]	[280],[533], [319],[729]	
$\text{C}^{13}\text{H}_5\text{Br}^{79}$ .....	$B_0 = 9119.51$ [533]						
$\text{C}^{12}\text{HD}_2\text{Br}^{79}$ .....	$B_0 - C_0 = 158.85$ [721]	$\omega_1 = 2151$ $\omega_2 = 987$ $\omega_3 = 577$ $\omega_4 = 2293d$ $\omega_5 = 1053d$ $\omega_6 = 717d$	$D_{JK} = 0.03\text{b}$ [746]	$B_{17^9} = 574.\text{b}$ [746]			
$\text{C}^{13}\text{D}_3\text{Br}^{79}$ .....	$B_0 = 7714.57$ [746]						
$\text{C}^{13}\text{H}_5\text{Br}^{81}$ .....	$B_0 = 9531.84$ [280], [411],[531]	.....	$\alpha_3 = 77.3\text{b}$ [950a]				
$\text{C}^{13}\text{H}_5\text{Br}^{81}$ .....	$B_0 = 9082.86$ [533]						
$\text{C}^{13}\text{HD}_2\text{Br}^{81}$ .....	$B_0 - C_0 = 157.22$ [729]						

C <sup>12</sup> D <sub>2</sub> Br <sup>81</sup> .....	B <sub>0</sub> = 7681.23 [746]	.....	D <sub>JK</sub> = 0.039 [746]	Br <sup>81</sup> = 479.8 [746]	.....	[928]
CH <sub>3</sub> Br <sup>79</sup> Hg <sup>199</sup> (CH <sub>3</sub> HgBr)	B <sub>0</sub> = 1142.86 [928]	.....	D <sub>JK</sub> = 0.008 [928]	Br <sup>79</sup> = 3 [928]	.....	
CH <sub>3</sub> Br <sup>79</sup> Hg <sup>199</sup> .....	B <sub>0</sub> = 1142.10 [928]	.....	D <sub>JK</sub> = 0.008 [928]			
CH <sub>3</sub> Br <sup>79</sup> Hg <sup>200</sup> .....	B <sub>0</sub> = 1141.36 [928]	.....	D <sub>JK</sub> = 0.008 [928]			
CH <sub>3</sub> Br <sup>79</sup> Hg <sup>201</sup> .....	B <sub>0</sub> = 1139.88 [928]	.....	D <sub>JK</sub> = 0.008 [928]			
CH <sub>3</sub> Br <sup>81</sup> Hg <sup>199</sup> .....	B <sub>0</sub> = 1125.26 [928]	.....	D <sub>JK</sub> = 0.008 [928]	Br <sup>81</sup> = 290 [928]		
CH <sub>3</sub> Br <sup>81</sup> Hg <sup>199</sup> .....	B <sub>0</sub> = 1124.51 [928]	.....	D <sub>JK</sub> = 0.008 [928]			
CH <sub>3</sub> Br <sup>81</sup> Hg <sup>200</sup> .....	B <sub>0</sub> = 1123.76 [928]	.....	D <sub>JK</sub> = 0.008 [928]			
CH <sub>3</sub> Br <sup>81</sup> Hg <sup>201</sup> .....	B <sub>0</sub> = 1122.27 [928]	.....	D <sub>JK</sub> = 0.008 [928]			
C <sup>12</sup> H <sub>5</sub> Cl <sup>35</sup> .....	A <sub>0</sub> ≈ 150 × 10 <sup>3</sup> [318], [412]	ω <sub>1</sub> = 2966.2 ω <sub>2</sub> = 1354.9 ω <sub>3</sub> = 732.1 ω <sub>4</sub> = 3041.8d ω <sub>5</sub> = 1454.6d ω <sub>6</sub> = 1015.0d	α <sub>3</sub> = 115.21 [950a] α <sub>6</sub> = 49.01 [950a] D <sub>J</sub> = 0.0180 [531],[913] D <sub>JK</sub> = 0.198 [531],[989]	Cl <sup>35</sup> = -74.740 [280], [378],[575],[746],[999]	1.869 [528]	[280],[318], [362],[412], [496],[531], [729]
C <sup>12</sup> H <sub>5</sub> Cl <sup>35</sup> .....	B <sub>0</sub> = 12,796.2 [362]					Δν = 21 Mc/mm Hg [802]
C <sup>12</sup> HD <sub>2</sub> Cl <sup>35</sup> .....	B <sub>0</sub> = 11,681.5 [496], [729]					
	C <sub>0</sub> = 11,372.6 [496], [729]					
C <sup>12</sup> D <sub>2</sub> Cl <sup>35</sup> .....	B <sub>0</sub> = 10,841.88 [412], [746]	ω <sub>1</sub> = 2161 ω <sub>2</sub> = 1029 ω <sub>3</sub> = 695 ω <sub>4</sub> = 2286d ω <sub>5</sub> = 1058d ω <sub>6</sub> = 776d	.....	Cl <sup>35</sup> = -74.41 [746]		
C <sup>12</sup> H <sub>5</sub> Cl <sup>37</sup> .....	.....	.....	.....			
C <sup>12</sup> H <sub>5</sub> Cl <sup>37</sup> .....	B <sub>0</sub> = 13,088.137 [280], [531],[999]	.....	α <sub>3</sub> = 112.30 [950a] α <sub>6</sub> = 48.19 [950a] D <sub>J</sub> = 0.027 [531] D <sub>JK</sub> = 0.184 [531]	Cl <sup>36</sup> = -15.8 [691],[594] Cl <sup>37</sup> = -58.921 [280], [378],[746],[950a],[999]	.....	D <sub>J</sub> probably more nearly 0.018 Mc than 0.027 [783b]
C <sup>12</sup> H <sub>5</sub> Cl <sup>37</sup> .....	B <sub>0</sub> = 12,590.0 [362]					
C <sup>12</sup> HD <sub>2</sub> Cl <sup>37</sup> .....	B <sub>0</sub> + C <sub>0</sub> = 24,674 [496]					
C <sup>12</sup> D <sub>2</sub> Cl <sup>37</sup> .....	B <sub>0</sub> = 10,658.43 [412], [746]	.....	.....	Cl <sup>37</sup> = -58.58 [746]		
CH <sub>3</sub> Cl <sup>35</sup> Hg <sup>199</sup> .....	B <sub>0</sub> = 2077.44 [928]	.....	D <sub>JK</sub> = 0.022 [928]	Cl <sup>35</sup> = -42 [928]	.....	[928]
CH <sub>3</sub> Cl <sup>35</sup> Hg <sup>199</sup> .....	B <sub>0</sub> = 2077.13 [928]					
CH <sub>3</sub> Cl <sup>35</sup> Hg <sup>200</sup> .....	B <sub>0</sub> = 2076.82 [928]					

Chemical symbol	Rotational constants <i>A</i> , <i>B</i> , and <i>C</i> , Mc	Vibrational fre- quencies $\omega$ in wave numbers ( $\text{cm}^{-1}$ ); <i>d</i> indicates a degenerate vibration	Rotation-vibration constants, Mc ( $\alpha$ , <i>D</i> , or <i>q</i> )	Quadrupole coupling constant <i>eqQ</i> , Mc	Dipole moment $\mu$ in $10^{-18}$ esu (Debye)	Reference for structure	Remarks
$\text{CH}_3\text{Cl}^{35}\text{Hg}^{202}$ .....	$B_0 = 2076.20$ [928]						
$\text{CH}_3\text{Cl}^{35}\text{Hg}^{204}$ .....	$B_0 = 2075.59$ [928]						
$\text{CH}_3\text{Cl}^{37}\text{Hg}^{198}$ .....	$B_0 = 2006.14$ [928]			$C^{37} = -33$ [928]			
$\text{CH}_3\text{Cl}^{37}\text{Hg}^{199}$ .....	$B_0 = 2005.79$ [928]						
$\text{CH}_3\text{Cl}^{37}\text{Hg}^{200}$ .....	$B_0 = 2005.45$ [928]						
$\text{CH}_3\text{Cl}^{37}\text{Hg}^{202}$ .....	$B_0 = 2004.76$ [928]						
$\text{CH}_3\text{Cl}^{37}\text{Hg}^{204}$ .....	$B_0 = 2004.09$ [928]						
$\text{CH}_3\text{Cl}_3^{35}\text{Si}$ ( $\text{CH}_3\text{SiCl}_3$ )	$B_0 = 1769.84$ [847]						
$\text{CH}_3\text{Cl}_3^{37}\text{Si}$ .....	$B_0 = 1699.79$ [847]						
$\text{C}^{13}\text{H}_5\text{F}$ .....	$A_0 \approx 154 \times 10^3$ [318] $B_0 = 25,536.12$ [367], [457],[595],[946]	$\omega_1 = 2964.5$ $\omega_2 = 1475.3$ $\omega_3 = 1048.2$ $\omega_4 = 2982.2d$ $\omega_5 = 1471.1d$ $\omega_6 = 1195.5d$	$D_J = 0.059$ [595],[946],[989] $D_{JK} = 0.445$ [457],[595],[946], [989]		1.79 [367],[803]	[847] [280],[318], [367],[457]	$\Delta\nu = 20$ Mc/mm Hg [367]
$\text{C}^{12}\text{H}_2\text{DF}$ .....	$B_0 = 24,043$ [974] $C_0 = 22,939$ [974] $\frac{1}{2}(B_0 + C_0) = 21,844.96$ [974]						
$\text{C}^{12}\text{HD}_2\text{F}$ .....	$B_0 = 24,862.37$ [367] $B_0 = 20,449.83$ [746]						
$\text{C}^{13}\text{H}_2\text{F}$ .....							
$\text{CH}_3\text{F}_2\text{Si}^{32}$ ( $\text{CH}_3\text{SiF}_3$ )...	$B_0 = 3715.63$ [525], [641]	$\omega$ (torsional) = 140 [618],[641]	$D_J = 0.033$ [595] $D_{JK} = 0.228$ [457],[595] .....			[525],[641]	Potential barrier height = 410 $\text{cm}^{-1}$ [618],[641]; rotation- vibration structure for torsional vibrations [641]
$\text{CH}_3\text{HgI}$ .....	$B_0 = 788$ [462]	$\omega_1 = 2969.8$ $\omega_2 = 1251.5$ $\omega_3 = 532.8$ $\omega_4 = 3060.3d$ $\omega_5 = 1440.3d$ $\omega_6 = 880.1d$	$D_J = 0.0063$ [531],[989] $D_{JK} = 0.099$ [531],[989]				
$\text{C}^{12}\text{H}_2\text{I}^{127}$ .....	$A_0 \approx 150 \times 10^3$ [280] $B_0 = 7501.31$ [280], [531],[989]			$I^{127} = -1934$ [280]	1.65 [528]	[280],[318], [412],[729]	





Chemical symbol	Rotational constants <i>A</i> , <i>B</i> , and <i>C</i> , Mc	Vibrational fre- quencies $\omega$ in wave numbers ( $\text{cm}^{-1}$ ); <i>d</i> indicates a degenerate vibration	Rotation-vibration constants, Mc ( $\alpha$ , <i>D</i> , or <i>q</i> )	Quadrupole coupling constant <i>eqQ</i> , Mc	Dipole moment $\mu$ in $10^{-18}$ esu (Debye)	Reference for structure	Remarks
$\text{CH}_3\text{Si}^{28}(\text{CH}_3\text{SiH}_3)\dots$	$B_0 = 10,999.0$ [604]				0.73 [604]		Potential barrier height = 558 $\text{cm}^{-1}$ [604],[948a] Analysis of rotation interaction with hindered motion [948a].
$\text{CH}_3\text{Si}^{28}\text{D}_3\dots$	$B_0 = 9622.8$ [604]						
$\text{CH}_3\text{Si}^{29}\dots$	$B_0 = 10,885.5$ [604]						
$\text{CH}_3\text{Si}^{29}\text{D}_3\dots$	$B_0 = 8572$ [604]						
$\text{CH}_3\text{Si}^{30}\dots$	$B_0 = 10,806.5$ [604]						
$\text{CH}_3\text{Si}^{30}\text{D}_3\dots$	$B_0 = 9525$ [604]						
$\text{CH}_3\text{Sn}^{116}(\text{CH}_3\text{SnH}_3)\dots$	$B_0 = 6910.5$ [603]				0.68 [603]	[603]	
$\text{CH}_3\text{Sn}^{117}\dots$	$B_0 = 6905.3$ [603]						
$\text{CH}_3\text{Sn}^{118}\dots$	$B_0 = 6900.2$ [603]						
$\text{CH}_3\text{Sn}^{119}\dots$	$B_0 = 6895.1$ [603]						
$\text{CH}_3\text{Sn}^{120}\dots$	$B_0 = 6890.2$ [603]						
$\text{C}^{13}\text{N}$ (ICN) $\dots$	$B_0 = 3225.527$ [320], [329]	$\omega_1 = 470$ $\omega_2 = 321d$ $\omega_3 = 1158$	$\alpha_1 = 9.33$ [329] $\alpha_2 = -9.52$ [329] $D_J = 0.0009$ [531] $q_1 = 2.69$ [329]	$I_{127} = -2420$ [329] $N_{14} = 3.80$ [329]	8.71	[320],[329]	$\Delta v = 20$ Mc/mm Hg [329]; anomalous in $I_{137}$ h.f.s. [703]
$\text{CuIN}\dots$	$B_0 = 3177.035$ [320]						
$\text{C}^{12}\text{O}^{16}\dots$	$B_0 = 57,897.5$ [457]	2170.21	$\alpha = 524.1$ [457] $D_0 = 0.189$ [457],[773a] $\alpha = 488.3$ [457] $D_0 = 0.174$ [457]		0.10	[457]	
$\text{C}^{12}\text{O}^{18}\dots$	$B_0 = 55,344.1$ [457]	2074.81					
$\text{COF}_2\dots$	$\frac{A_0 - C_0}{2} = 2961.2$ [649]						Asymmetry parameter $\kappa = 0.9796$ [649] Dipole moment in vibrational state (01 <sup>0</sup> ) = 0.700 [530]; $\Delta v =$ 6.1 Mc/mm Hg [329],[706]; Fermi resonance energy $W_{12} =$ 43.2 $\text{cm}^{-1}$ [752]; molecular <i>g</i> factor = -0.025 [682]; varia- tion of line width with <i>J</i> and <i>T</i> [706],[921]
$\text{C}^{12}\text{O}^{16}\text{S}^{32}$ (OCS) $\dots$	$B_0 = 6081.490$ [189], [755],[823]	$\omega_1 = 859$ $\omega_2 = 527d$ $\omega_3 = 2079$	$\alpha_1 = 20.56$ [329],[755] $\alpha_2 = -10.56$ [329],[755] $\alpha_3 = 36.36$ [968] $D_J = 0.001310$ [595],[946] $q_1 = 6.144$ [329],[755]		0.709 [146],[530]	[329]	

C <sup>12</sup> O <sup>16</sup> S <sup>32</sup> .....	$B_0 = 6061.88$ [329], [755]	.....	$\alpha_1 = 17.94$ [714] $\alpha_2 = -10.10$ [329] $q_1 = 6.45$ [329] $\alpha_2 = -9.4$ [314] $q_1 = 6.7$ [314]	.....	0.709 [530]	.....
C <sup>14</sup> O <sup>16</sup> S <sup>32</sup> .....	$B_0 = 6043.25$ [314]	.....	.....	O <sup>17</sup> = -1.32 [688]		
C <sup>12</sup> O <sup>17</sup> S <sup>32</sup> .....	$B_0 = 5883.67$ [392]	.....	.....	.....		
C <sup>12</sup> O <sup>16</sup> S <sup>34</sup> .....	$B_0 = 5704.83$ [329]	.....	$\alpha_1 = 16.19$ [714] $\alpha_2 = -10.16$ [714] $q_1 = 5.62$ [714]	.....		
C <sup>12</sup> O <sup>16</sup> S <sup>36</sup> .....	$B_0 = 6004.905$ [127], [755], [999]	.....	.....	S <sup>33</sup> = -29.130 [327], [681], [999]	0.709 [530]	
C <sup>12</sup> O <sup>16</sup> S <sup>34</sup> .....	$B_0 = 5932.81$ [189], [755]	.....	$\alpha_1 = 17.68$ [714] $\alpha_2 = -10.37$ [329] $q_1 = 6.07$ [329]	.....		
C <sup>12</sup> O <sup>16</sup> S <sup>36</sup> .....	$B_0 = 58$ [2] [356]	.....	.....	S <sup>33</sup> = 21.90 [356], [908]		
C <sup>12</sup> O <sup>16</sup> S <sup>38</sup> .....	$B_0 = 5799.17$ [392]	.....	.....	.....		
C <sup>12</sup> O <sup>16</sup> S <sup>34</sup> .....	$B_0 = 5911.730$ [327]	.....	$\alpha_1 = 13.27$ [418] $\alpha_2 = -6.92$ [418] $D_J = 0.0008$ [418] $q_1 = 3.15$ [418]	.....	0.754 [418]	[418]
C <sup>12</sup> O <sup>16</sup> Se <sup>80</sup> (OCSe).....	$B_0 = 4017.68$ [418]	.....	.....	.....		Dipole moment in vibrational states (010) = 0.730 [418], (100) = 0.728 [418]; molecular $q$ factor = -0.019 [806a] Frequency ratios for Se isotopes [456]
C <sup>12</sup> O <sup>16</sup> Se <sup>80</sup> .....	$B_0 = 3980.05$ [418]	.....	.....	.....		
C <sup>12</sup> O <sup>16</sup> Se <sup>74</sup> .....	$B_0 = 4095.79$ [418]	.....	$\alpha_2 = -7.00$ [418] $q_1 = 3.24$ [418]	Se <sup>76</sup> = 946 Mc [392]		
C <sup>12</sup> O <sup>16</sup> Se <sup>76</sup> .....	.....	.....	$\alpha_1 = 13.48$ [418] $\alpha_2 = -6.98$ [418] $q_1 = 1.21$ [418]	.....		
C <sup>12</sup> O <sup>16</sup> Se <sup>78</sup> .....	$B_0 = 4068.47$ [418]	.....	$\alpha_1 = 13.40$ [418] $\alpha_2 = -6.96$ [418] $D_J = 0.0008$ [418] $q_1 = 3.19$ [418]	.....		
C <sup>12</sup> O <sup>16</sup> Se <sup>77</sup> .....	$B_0 = 4055.30$ [418]	.....	.....	.....		
C <sup>12</sup> O <sup>16</sup> Se <sup>79</sup> .....	$B_0 = 4012.46$ [418]	.....	.....	.....		
C <sup>12</sup> O <sup>16</sup> Se <sup>79</sup> .....	$B_0 = 4005.11$ [418]	.....	.....	Se <sup>79</sup> = 752.09 [806a]		
C <sup>12</sup> O <sup>16</sup> Se <sup>79</sup> .....	.....	.....	$\alpha_1 = 13.12$ [418] $\alpha_2 = -6.86$ [418] $D_J = 0.0008$ [418] $q_1 = 3.12$ [418]	.....		
C <sup>12</sup> O <sup>16</sup> Se <sup>82</sup> .....	$B_0 = 3994.01$ [418]	.....	.....	.....		



Chemical symbol	Rotational constants <i>A</i> , <i>B</i> , and <i>C</i> , Mc	Vibrational fre- quencies $\omega$ in wave numbers ( $\text{cm}^{-1}$ ); <i>d</i> indicates a degenerate vibration	Rotation-vibration constants, Mc ( $\alpha$ , <i>D</i> , or <i>q</i> )	Quadrupole coupling constant <i>eqQ</i> , Mc	Dipole moment $\mu$ in $10^{-18}$ esu (Debye)	Reference for structure	Remarks
$\text{C}^{13}\text{S}^{32}$ .....	<i>B</i> <sub>0</sub> = 24,584.35 [777]	1285.1	$\alpha_e = 177.54$ [777] <i>D</i> <sub>e</sub> = 0.040 [777]	.....	2.0 [777]	[777]	
$\text{C}^{13}\text{S}^{32}$ .....	<i>B</i> <sub>0</sub> = 23,205.26 [777]	.....	.....	<i>S</i> <sup>33</sup> = 12.84 [777]	.....	.....	Magnetic h.f.s. = 0.021·J [777]
$\text{C}^{12}\text{S}^{32}$ .....	<i>B</i> <sub>0</sub> = 24,381.01 [777]	.....	.....	.....	.....	.....	Potential barrier height = 220 $\text{cm}^{-1}$ [713]; rotation-vibration effects for torsional vibration [713]
$\text{C}^{12}\text{S}^{34}$ .....	<i>B</i> <sub>0</sub> = 24,190.20 [777]	.....	.....	.....	.....	.....	Data on several isotopes question- able [432]
$\text{CSF}_6$ ( $\text{CF}_5\text{SF}_6$ ).....	<i>B</i> <sub>0</sub> = 1097.6 [713]	$\omega$ (torsional) = 94 [713]	.....	.....	.....	[713]	
$\text{CSSe}$ ( $\text{SCSe}$ ).....	<i>B</i> <sub>0</sub> ≈ 2010 [432]	.....	.....	.....	.....	.....	
$\text{CSTe}^{120}$ ( $\text{SCTe}$ ).....	<i>B</i> <sub>0</sub> = 1559.9303 [932]	.....	$\alpha_2 = -3.2446$ [932] <i>q</i> <sub>1</sub> = 0.6599 [932] $\alpha_2 = -3.2870$ [932] <i>q</i> <sub>1</sub> = 0.6786 [932] $\alpha_2 = -3.2818$ [932] <i>q</i> <sub>1</sub> = 0.6776 [932] $\alpha_2 = -3.2764$ [932] <i>q</i> <sub>1</sub> = 0.6752 [932] $\alpha_2 = -3.2712$ [932] <i>q</i> <sub>1</sub> = 0.6728 [932] $\alpha_2 = -3.2657$ [932] <i>q</i> <sub>1</sub> = 0.6706 [932] $\alpha_2 = -3.2551$ [932] <i>q</i> <sub>1</sub> = 0.6649 [932] <i>D</i> <sub>J</sub> = 0.0004 [743] <i>D</i> <sub>JK</sub> = 0.0058 [743] <i>D</i> <sub>J</sub> = 0.0004 [743] <i>D</i> <sub>JK</sub> = 0.0056 [743]	.....	0.172 [932]	[932]	
$\text{CSTe}^{122}$ .....	<i>B</i> <sub>0</sub> = 1584.1224 [932]	.....	.....	.....	.....	.....	
$\text{CSTe}^{124}$ .....	<i>B</i> <sub>0</sub> = 1580.9211 [932]	.....	.....	.....	.....	.....	
$\text{CSTe}^{124}$ .....	<i>B</i> <sub>0</sub> = 1577.7898 [932]	.....	.....	.....	.....	.....	
$\text{CSTe}^{125}$ .....	<i>B</i> <sub>0</sub> = 1574.6921 [932]	.....	.....	.....	.....	.....	
$\text{CSTe}^{126}$ .....	<i>B</i> <sub>0</sub> = 1571.6524 [932]	.....	.....	.....	.....	.....	
$\text{CSTe}^{127}$ .....	<i>B</i> <sub>0</sub> = 1565.7021 [932]	.....	.....	.....	.....	.....	
$\text{C}_2\text{F}_2\text{N}^{14}$ ( $\text{CF}_2\text{CN}$ ).....	<i>B</i> <sub>0</sub> = 2945.54 [743]	.....	.....	<i>N</i> <sup>14</sup> = -4.70 [743]	.....	[743]	
$\text{C}_2\text{F}_2\text{N}^{15}$ .....	<i>B</i> <sub>0</sub> = 2855.86 [743]	.....	.....	.....	.....	.....	
$\text{C}_2\text{HCl}^{35}$ ( $\text{HCCCl}$ ).....	<i>B</i> <sub>0</sub> = 5684.2 [425]	.....	.....	$\text{Cl}^{35} = -79.7$ [425] $\text{Cl}^{35} = -79.6$ <i>D</i> = 0.18 [998]	.....	.....	
$\text{C}_2\text{DCl}^{35}$ .....	<i>B</i> <sub>0</sub> = 5187.0 [425]	.....	.....	.....	0.44 [425]	[425]	

$C_2H_3Cl^m$ .....	$B_0 = 5572.3$ [425]	.....	.....	.....	$Cl^m = -62.7$ [425]				
$C_2DCl^m$ .....	$B_0 = 5084.2$ [425]	.....	.....	.....	$Cl^m = -63.1$ [425]				
$C_2H_3Cl^mF$ ( $CH_2CFCl$ )	$A_0 = 10,681.8$ [440] $B_0 = 5102.2$ [440] $C_0 = 3448.4$ [440]	.....	.....	.....	$e \frac{\partial^2 V}{\partial a^3} Q_{Cl^{12}} = -73.3$ [440] $e \frac{\partial^2 V}{\partial b^3} Q_{Cl^{12}} = 39.8$ [440]				
$C_2H_3Cl^mF$ .....	$A_0 = 10,681.3$ [440] $B_0 = 4955.0$ [440] $C_0 = 3380.5$ [440]	.....	.....	.....	.....	1.37 [406]	[406]		
$C_2H_3F_2$ ( $CH_2CF_2$ ).....	$A_0 = 11,001$ [406] $B_0 = 10,427$ [406] $C_0 = 5345.1$ [406]	.....	.....	.....	.....	1.41 [708]	[708],[769a]		Dipole moments measured in excited states [708]; rotation-vibration constants [708]
$C_2H_3O$ ( $H_2C_2O$ , ketene)	$A_0 \approx 280 \times 10^3$ [431], [708] $B_0 = 10,193.28$ [431], [708] $C_0 = 9915.87$ [431], [708]	$\omega_7 = 670$ [708] $\omega_8 = 570$ [708] $\omega_9 = 490$ [708]	$D_{JK} = 0.477$ [708] $D_J = 0.003 \pm 0.002$ [708]	.....	.....	.....	.....		
$C_2HDO$ (dmuterated ketene)	$A_0 \approx 195 \times 10^3$ [708] $B_0 = 9647.05$ [708] $C_0 = 9174.63$ [708]	.....	.....	.....	.....	1.42 [708]			
$C_2D_2O$ .....	$B_0 = 9120.80$ [431], [708] $C_0 = 8552.66$ [411], [708]	.....	$D_{JK} = 0.35$ [708]	.....	.....	1.44 [708]			
$C_2H_3Br^m$ (vinyl bromide)	$B_0 = 4162.2$ [447] $C_0 = 3862.9$ [447]	.....	.....	.....	$Br^{12} = 479$ [447]				
$C_2H_3Br^{s1}$ .....	$B_0 = 4138.0$ [447] $C_0 = 3841.9$ [447]	.....	.....	.....	$Br^{s1} = 399$ [447]				
$C_2H_3Cl^{12}$ (vinyl chloride)	$A_0 = 56121$ [370] $B_0 = 6030.5$ [370] $C_0 = 5445.2$ [370]	.....	.....	.....	$e \frac{\partial^2 V}{\partial a^3} Q_{Cl^{12}} = -57$ [370] $e \frac{\partial^2 V}{\partial b^3} Q_{Cl^{12}} = 26$ [370]	1.44			
$C_2H_3Cl^m$ .....	$A_0 = 56281$ [370] $B_0 = 5903.7$ [370] $C_0 = 5341.3$ [370]	.....	.....	.....	.....				
$C_2H_3F_3$ ( $CF_3CH_2$ , methyl fluoroform)	$B_0 = 5185$ [268],[528]	$\omega$ (torsional) = 234 [618]	.....	.....	.....	2.32 [528],[690]	.....		Potential barrier height = 1216 $cm^{-1}$ [363],[618]





$C_2H_5NS^{22}$ (CH <sub>3</sub> NCs, methyl isothiocyanate)	$(B_0 + C_0)/2 = 2527.1$ [345] $A_0 = 78.2 \times 10^3$ $(B_0 + C_0)/2 = 2462.6$ [345]	.....	.....	.....	3.18	[345]	
$C_2H_5NS^{24}$ (CH <sub>3</sub> NCs)...	$(B_0 + C_0)/2 = 2837$ [345]	.....	.....	.....	3.16	[345]	
$C_2H_5NS$ (CH <sub>3</sub> SCN, methyl thiocyanate)	$A_0 = 9491.95$ [978] $B_0 = 8962.65$ [978] $C_0 = 5170.43$ [978] $A_0 = 25.484$ [316], [264],[360],[566] $B_0 = 22.121$ [316], [264],[360],[566] $C_0 = 14.098$ [316], [264],[360],[566]	.....	.....	.....	.....	[978]	Height of potential barrier = 1250 cm <sup>-1</sup> [978]
$C_2^{13}H_4O$ (ethylene oxide)	$A_0 = 25.291.2$ [566] $B_0 = 21.597.4$ [566] $C_0 = 13.825.2$ [566] $A_0 = 20.399$ [360], [566] $B_0 = 15.457$ [360], [566] $C_0 = 11.544$ [360], [566]	.....	.....	.....	1.88 [566]	[316],[360], [566]	
$C_2^{13}C^{18}H_4O$ .....	$A_0 = 25.291.2$ [566] $B_0 = 21.597.4$ [566] $C_0 = 13.825.2$ [566] $A_0 = 20.399$ [360], [566] $B_0 = 15.457$ [360], [566] $C_0 = 11.544$ [360], [566]	.....	.....	.....	.....		
$C_2^{13}D_4O$ .....	$A_0 = 25.291.2$ [566] $B_0 = 21.597.4$ [566] $C_0 = 13.825.2$ [566] $A_0 = 20.399$ [360], [566] $B_0 = 15.457$ [360], [566] $C_0 = 11.544$ [360], [566]	.....	.....	.....	.....		
$C_2H_4S^{22}$ (ethylene sulfide)	$A_0 = 21.974$ [566] $B_0 = 10.824.9$ [566] $C_0 = 8026.3$ [566] $A_0 = 15.471$ [566] $B_0 = 9197.6$ [566] $C_0 = 6819.0$ [566] $A_0 = 21.974$ [566] $B_0 = 10.551.0$ [566] $C_0 = 7874.7$ [566]	.....	.....	.....	1.84 [566]	[566]	
$C_2D_4S^{22}$ .....	$A_0 = 21.974$ [566] $B_0 = 10.824.9$ [566] $C_0 = 8026.3$ [566] $A_0 = 15.471$ [566] $B_0 = 9197.6$ [566] $C_0 = 6819.0$ [566] $A_0 = 21.974$ [566] $B_0 = 10.551.0$ [566] $C_0 = 7874.7$ [566]	.....	.....	.....	.....		
$C_2H_4S^{24}$ .....	$A_0 = 21.974$ [566] $B_0 = 10.824.9$ [566] $C_0 = 8026.3$ [566] $A_0 = 15.471$ [566] $B_0 = 9197.6$ [566] $C_0 = 6819.0$ [566] $A_0 = 21.974$ [566] $B_0 = 10.551.0$ [566] $C_0 = 7874.7$ [566]	.....	.....	.....	.....		
$C_2H_5Cl^{22}$ (ethyl chloride)	$B_0 = 5493.76$ [995] $C_0 = 4962.24$ [995]	$\omega$ (torsional) = 215 [995]	.....	$e \frac{\partial^2 V}{\partial a^2} Q_{Cl} = -48.44$ [995] $e \frac{\partial^2 V}{\partial b^2} Q_{Cl} = 13.9$ [995]	.....	[995]	Potential barrier height = 1050 cm <sup>-1</sup> [995]

Chemical symbol	Rotational constants <i>A</i> , <i>B</i> , and <i>C</i> , Mc	Vibrational fre- quencies $\omega$ in wave- numbers ( $\text{cm}^{-1}$ ); <i>d</i> indicating degenerate vibration	Rotation-vibration constants, Mc ( $\alpha$ , <i>D</i> , or <i>q</i> )	Quadrupole coupling constant $eqQ$ , Mc	Dipole moment $\mu$ in $10^{-18}$ esu (Debye)	Reference for structure	Remarks
$\text{C}_2\text{H}_5\text{Cl}^{137}$	$B_0 = 5397.29$ [995] $C_0 = 4812.22$ [995]	.....	.....	$e \frac{\partial^2 V}{\partial \alpha^2} Q_{\text{Cl}} = -36.9$ [995] $e \frac{\partial^2 V}{\partial \delta^2} Q_{\text{Cl}} = 10.1$ [995] .....	.....	[995]	
$\text{C}_2\text{H}_5\text{N}$ (ethylenimine)	$A_0 = 22,734.1$ [877], [889], [820] $B_0 = 21,192.3$ [877], [889], [820] $C_0 = 13,383.3$ [877], [889], [820] ..... $B_0 = 2877.95$ [557]	.....	.....	.....	$\mu_a = 1.89$ [820] $\mu_b = 1.67$ [820] $\mu_c = 0.89$ [820] .....	[877]	Discrepancy between <i>A</i> , <i>B</i> , and <i>C</i> given by [877], [889], and [820]
$\text{C}_2\text{H}_5\text{O}$ (ethyl alcohol) $\text{C}_2\text{HF}_3$ ( $\text{CF}_3\text{CCH}$ )	..... $B_0 = 2877.95$ [557]	.....	$\alpha_{10} = -6.51$ [557] $D_J = 0.0002$ [557] $D_{JK} = 0.0063$ [557] $q_{10} = 3.62$ [557] $D_J = 0.0002$ [557] $D_{JK} = 0.0062$ [557] .....	.....	1.7 .....	[557]	9 lines measured [344]
$\text{CF}_3\text{CCD}$	$B_0 = 2096.07$ [537]	.....	.....	$N^{14} = -4.2$ [548]	3.6	[548]	
$\text{C}_3\text{H}_5\text{N}^{14}$ ( $\text{HCCCN}$ , cyanoacetylene) $\text{HC}^{13}\text{C}^{12}\text{C}^{13}\text{N}^{14}$ ..... $\text{HC}^{12}\text{C}^{13}\text{C}^{12}\text{N}^{14}$ ..... $\text{HC}^{12}\text{C}^{12}\text{C}^{13}\text{N}^{14}$ ..... $\text{DC}^{12}\text{C}^{12}\text{C}^{13}\text{N}^{14}$ ..... $\text{DC}^{12}\text{C}^{12}\text{C}^{12}\text{N}^{14}$ ..... $\text{DC}^{12}\text{C}^{13}\text{C}^{12}\text{N}^{14}$ ..... $\text{DC}^{12}\text{C}^{12}\text{C}^{12}\text{N}^{14}$ ..... $\text{HC}^{12}\text{C}^{12}\text{C}^{12}\text{N}^{15}$ ..... $\text{DC}^{12}\text{C}^{12}\text{C}^{12}\text{N}^{15}$ ..... $\text{C}_3\text{H}_5\text{O}_2$ (vinylene carbonate) $\text{C}_3\text{H}_5\text{Br}^{79}$ ( $\text{H}_3\text{CCCBBr}$ , methyl bromoacetylene)	$B_0 = 4408.47$ [548] $B_0 = 4029.84$ [548] $B_0 = 4530.23$ [548] $B_0 = 4221.60$ [548] $B_0 = 4107.21$ [548] $B_0 = 4207.50$ [548] $B_0 = 4202.54$ [548] $B_0 = 4416.91$ [548] $B_0 = 4100.41$ [548] $A_0 = 9346.79$ [977] $B_0 = 4188.46$ [977] $C_0 = 2891.54$ [977] $B_0 = 1561.11$ [744]	.....	.....	.....	$\mu_a = 4.51$ [977] $\mu_b = \mu_c = 0$ .....	[977]	
		.....	$D_{JK} = 0.0114$ [744]	$B^{79} = 547$ [744]	.....	[744]	

C <sub>2</sub> H <sub>3</sub> Br <sup>11</sup> .....	B <sub>0</sub> = 1550.42 [744] B <sub>0</sub> = 1259.02 [744]	..... .....	D <sub>JK</sub> = 0.0111 [744] D <sub>JK</sub> = 0.0072 [744]	Br <sup>11</sup> = 539 [744] I <sup>17</sup> = -2230 [744]	..... [744]
C <sub>2</sub> H <sub>3</sub> I (H <sub>3</sub> CCCI, methyl iodoacetylene)	A <sub>0</sub> = 49,076.2 [1000] B <sub>0</sub> = 4971.33 [1000] C <sub>0</sub> = 4514.05 [1000]	.....	.....	$e \frac{\partial^2 V}{\partial a^2} Q_N = -3.0$ [1000]	[1000] μ = 3.89 [1000] μ <sub>a</sub> = 3.68 [1000] μ <sub>b</sub> = 1.25 [1000]
C <sub>2</sub> H <sub>3</sub> N (vinyl cyanide)	B <sub>0</sub> = 8545.84 [544], [595]	ω <sub>10</sub> = 336 [544]	α <sub>10</sub> = -23.92 [544] D <sub>J</sub> = 0.0031 [544],[595] D <sub>JK</sub> = 0.16 [544],[595] q <sub>10</sub> = 16.7 [544] D <sub>JK</sub> = 0.1 [544] D <sub>JK</sub> = 0.1 [544] D <sub>JK</sub> = 0.1 [544] D <sub>JK</sub> = 0.1 [544] D <sub>J</sub> ≈ 0.003 [988a] D <sub>JK</sub> = 0.13 [988a] D <sub>J</sub> ≈ 0.002 [988a] D <sub>JK</sub> = 0.13 [988a] D <sub>J</sub> ≈ 0.001 [988a] D <sub>JK</sub> = 0.12 [988a] D <sub>J</sub> ≈ 0.004 [988a] D <sub>JK</sub> = 0.11 [988a] D <sub>J</sub> ≈ 0.002 [974] D <sub>JK</sub> = 0.102 [974] D <sub>JK</sub> = 0.09 [544]	.....	[544],[988a]
C <sub>2</sub> H <sub>3</sub> H <sub>4</sub> (CH <sub>3</sub> CCH, methyl acetylene)	B <sub>0</sub> = 8542.28 [544] B <sub>0</sub> = 8313.23 [544] B <sub>0</sub> = 8290.24 [544] B <sub>0</sub> = 7788.14 [544] B <sub>0</sub> = 8155.67 [974] C <sub>0</sub> = 8025.46 [974] B <sub>0</sub> = 7765.73 [974] C <sub>0</sub> = 7630.99 [974] B <sub>0</sub> = 7440.77 [974] C <sub>0</sub> = 7331.96 [974] B <sub>0</sub> = 7095.09 [974] C <sub>0</sub> = 6982.56 [974] B <sub>0</sub> = 7355.75 [974]	..... ..... ..... ..... ..... ..... ..... ..... ..... ..... ..... ..... ..... .....	..... ..... ..... ..... ..... ..... ..... ..... ..... ..... ..... ..... ..... .....	.....	Molecular ρ factor parallel to axis = 0.31 [784]; perpendicular to axis = 0 [784]
C <sup>12</sup> H <sub>3</sub> C <sup>13</sup> C <sup>12</sup> H.....	B <sub>0</sub> = 8542.28 [544]	.....	.....	.....	.....
C <sup>13</sup> H <sub>3</sub> C <sup>12</sup> C <sup>12</sup> H.....	B <sub>0</sub> = 8313.23 [544]	.....	.....	.....	.....
C <sup>12</sup> H <sub>3</sub> C <sup>12</sup> C <sup>13</sup> H.....	B <sub>0</sub> = 8290.24 [544]	.....	.....	.....	.....
C <sup>12</sup> H <sub>3</sub> C <sup>12</sup> C <sup>12</sup> D.....	B <sub>0</sub> = 7788.14 [544]	.....	.....	.....	.....
C <sup>12</sup> H <sub>3</sub> DC <sup>12</sup> C <sup>12</sup> H.....	B <sub>0</sub> = 8155.67 [974] C <sub>0</sub> = 8025.46 [974] B <sub>0</sub> = 7765.73 [974] C <sub>0</sub> = 7630.99 [974] B <sub>0</sub> = 7440.77 [974] C <sub>0</sub> = 7331.96 [974] B <sub>0</sub> = 7095.09 [974] C <sub>0</sub> = 6982.56 [974] B <sub>0</sub> = 7355.75 [974]	..... ..... ..... ..... ..... ..... ..... ..... ..... ..... ..... ..... ..... .....	..... ..... ..... ..... ..... ..... ..... ..... ..... ..... ..... ..... ..... .....	.....	.....
C <sup>12</sup> HD <sub>2</sub> C <sup>12</sup> C <sup>12</sup> H.....	B <sub>0</sub> = 8542.28 [544]	.....	.....	.....	.....
C <sup>12</sup> H <sub>2</sub> DC <sup>12</sup> C <sup>12</sup> D.....	B <sub>0</sub> = 8313.23 [544]	.....	.....	.....	.....
C <sup>12</sup> HD <sub>2</sub> C <sup>12</sup> C <sup>12</sup> D.....	B <sub>0</sub> = 8290.24 [544]	.....	.....	.....	.....
C <sup>12</sup> D <sub>3</sub> C <sup>12</sup> C <sup>12</sup> H.....	B <sub>0</sub> = 7788.14 [544]	.....	.....	.....	.....
C <sup>12</sup> D <sub>3</sub> C <sup>12</sup> C <sup>12</sup> D.....	B <sub>0</sub> = 8155.67 [974] C <sub>0</sub> = 8025.46 [974] B <sub>0</sub> = 7765.73 [974] C <sub>0</sub> = 7630.99 [974] B <sub>0</sub> = 7440.77 [974] C <sub>0</sub> = 7331.96 [974] B <sub>0</sub> = 7095.09 [974] C <sub>0</sub> = 6982.56 [974] B <sub>0</sub> = 7355.75 [974]	..... ..... ..... ..... ..... ..... ..... ..... ..... ..... ..... ..... ..... .....	..... ..... ..... ..... ..... ..... ..... ..... ..... ..... ..... ..... ..... .....	.....	.....
C <sup>12</sup> H <sub>5</sub> Cl <sup>15</sup> (cyclopropyl chloride)	A <sub>0</sub> = 17,695.1 [787] B <sub>0</sub> = 3905.4 [787] C <sub>0</sub> = 3622.4 [787]	.....	.....	$e \frac{\partial^2 V}{\partial a^2} Q_{Cl^{15}} = -55.8$ [(787) and private comm.] $e \frac{\partial^2 V}{\partial b^2} Q_{Cl^{15}} = 24.4$ [(787) and private comm.]	.....
C <sub>2</sub> H <sub>5</sub> Cl <sup>17</sup> .....	A <sub>0</sub> = 17,930 [787] B <sub>0</sub> = 3810.0 [787] C <sub>0</sub> = 3405.5 [787]	.....	.....	.....	.....



Chemical symbol	Rotational constants <i>A</i> , <i>B</i> , and <i>C</i> , Mc	Vibrational fre- quencies $\omega$ in wave numbers (cm <sup>-1</sup> ); <i>d</i> indicates a degenerate vibration	Rotation-vibration constants, Mc ( $\alpha$ , <i>D</i> , or <i>q</i> )	Quadrupole coupling constant <i>eqQ</i> , Mc	Dipole moment $\mu$ in 10 <sup>-18</sup> esu (Debye)	Reference for structure	Remarks
C <sub>2</sub> H <sub>6</sub> O [(CH <sub>3</sub> ) <sub>2</sub> CO, acetone]	.....	.....	.....	.....	2.8	.....	Approx. 20 lines measured [344], [762]
C <sub>3</sub> H <sub>6</sub> O <sub>3</sub> (trioxane)...	<i>B</i> <sub>0</sub> = 5273.6 [553]	.....	.....	.....	2.0 [553]	[553]	
C <sub>7</sub> H <sub>12</sub> O <sub>3</sub> .....	<i>B</i> <sub>0</sub> = 5225.0 [553]	.....	.....	.....	.....	[847], [848]	
C <sub>2</sub> H <sub>6</sub> C <sup>13</sup> Si [(CH <sub>3</sub> ) <sub>3</sub> SiCl]	<i>B</i> <sub>0</sub> = 2197.44 [847], [848]	.....	.....	.....	.....		
C <sub>2</sub> H <sub>6</sub> Cl <sup>37</sup> Si.....	<i>B</i> <sub>0</sub> = 2147.88 [847], [848]	.....	.....	.....	.....		
C <sub>2</sub> H <sub>6</sub> FSi[(CH <sub>3</sub> ) <sub>2</sub> SiF]...	<i>B</i> <sub>0</sub> = 3411.0 [931 <i>a</i> ]	.....	.....	.....	[931 <i>a</i> ]		
C <sub>2</sub> N <sub>2</sub> P [P(CN) <sub>2</sub> ].....	<i>B</i> <sub>0</sub> = 2326 [712 <i>a</i> ]	.....	.....	.....	.....	[712 <i>b</i> ]	
C <sub>2</sub> H <sub>4</sub> (vinylacetylene)...	<i>A</i> <sub>0</sub> = 4262 × 10 [731] <i>B</i> <sub>0</sub> = 4744.85 [731] <i>C</i> <sub>0</sub> = 4329.73 [731] <i>A</i> <sub>0</sub> = 9447.04 [648] <i>B</i> <sub>0</sub> = 9246.76 [648] <i>C</i> <sub>0</sub> = 4670.84 [648]	.....	.....	.....	0.601 [648]	[648]	
C <sub>4</sub> H <sub>4</sub> O (furan).....	.....	.....	.....	.....	.....		16 lines measured and identified [763]
C <sub>4</sub> H <sub>4</sub> N (pyrrol).....	.....	.....	.....	.....	.....	[763]	
C <sub>4</sub> H <sub>9</sub> Br <sup>79</sup> [(CH <sub>3</sub> ) <sub>2</sub> CBr, tertiary butyl bromide]	<i>B</i> <sub>0</sub> = 2044 [550]	.....	.....	.....	2.21	[550]	
C <sub>4</sub> H <sub>9</sub> Br <sup>81</sup> .....	<i>B</i> <sub>0</sub> = 2028 [550]	.....	.....	.....	.....		
C <sub>4</sub> H <sub>9</sub> Cl <sup>35</sup> [(CH <sub>3</sub> ) <sub>2</sub> CCl, tertiary butyl chloride]	<i>B</i> <sub>0</sub> = 3016 [550]	.....	.....	.....	2.15	[550]	
C <sub>4</sub> H <sub>9</sub> Cl <sup>37</sup> .....	<i>B</i> <sub>0</sub> = 2954 [550]	.....	.....	.....	.....		
C <sub>4</sub> H <sub>9</sub> I [(CH <sub>3</sub> ) <sub>2</sub> CI, tertiary butyl <i>i</i> , <i>i</i> -dide]	<i>B</i> <sub>0</sub> = 1562 [550]	.....	.....	.....	2.1 [550]	[550]	
C <sub>4</sub> H <sub>10</sub> O [(C <sub>2</sub> H <sub>5</sub> ) <sub>2</sub> O, diethyl ether]	.....	.....	.....	.....	.....		28 lines measured [714]
C <sub>2</sub> H <sub>4</sub> (CH <sub>3</sub> C≡C-C≡CH)	<i>B</i> <sub>0</sub> = 2035.73 [934]	.....	<i>D</i> <sub>J</sub> ≤ 0.0002 [934] <i>D</i> <sub>JK</sub> = 0.020 [934]	.....	.....	[934]	



Chemical symbol	Rotational constants <i>A</i> , <i>B</i> , and <i>C</i> , Mc	Vibrational fre- quencies $\omega$ in wave numbers (cm <sup>-1</sup> ); <i>d</i> indicates a degenerate vibration	Rotation-vibration constants, Mc ( $\alpha$ , <i>D</i> , or <i>q</i> )	Quadrupole coupling constant <i>eqQ</i> , Mc	Dipole moment $\mu$ in 10 <sup>-18</sup> esu (Debye)	Reference for structure	Remarks
Cl <sup>37</sup> F <sub>3</sub> .....	<i>A</i> <sub>0</sub> = 13,653.2 [867] <i>B</i> <sub>0</sub> = 4611.9 [867] <i>C</i> <sub>0</sub> = 3442.8 [867]	.....	.....	$e \frac{\partial^2 V}{\partial a^2} Q_{Cl^{37}} = -65$ [867]	.....		
Cl <sup>35</sup> F <sub>3</sub> Ge <sup>70</sup> (GeF <sub>3</sub> Cl)....	<i>B</i> <sub>0</sub> = 2158.52 [555]	.....	<i>D<sub>J</sub></i> = 0.0006 [555] <i> D<sub>JK</sub> </i> < 0.001 [555]	$e \frac{\partial^2 V}{\partial b^2} Q_{Cl^{37}} = -51$ [8W7] .....	.....	[555]	
Cl <sup>37</sup> F <sub>3</sub> Ge <sup>70</sup> .....	<i>B</i> <sub>0</sub> = 2108.13 [555]	.....					
Cl <sup>35</sup> F <sub>3</sub> Ge <sup>72</sup> .....	<i>B</i> <sub>0</sub> = 2167.53 [555]	.....					
Cl <sup>37</sup> F <sub>3</sub> Ge <sup>72</sup> .....	<i>B</i> <sub>0</sub> = 2107.04 [555]	.....					
Cl <sup>35</sup> F <sub>3</sub> Ge <sup>74</sup> .....	<i>B</i> <sub>0</sub> = 2166.60 [555]	.....					
Cl <sup>37</sup> F <sub>3</sub> Ge <sup>74</sup> .....	<i>B</i> <sub>0</sub> = 2105.98 [555]	.....					
Cl <sup>35</sup> F <sub>3</sub> Si (SiF <sub>3</sub> Cl).....	<i>B</i> <sub>0</sub> = 2477.7 [525], [641] <i>B</i> <sub>0</sub> = 2413.0 [525], [641] <i>B</i> <sub>0</sub> = 4401.71 [423]	.....	<i>D<sub>JK</sub></i> = 0.0018 [525],[641]	Cl <sup>35</sup> = -43 [525],[641] Cl <sup>37</sup> = -34 [525],[641]	.....	[641]	
Cl <sup>35</sup> Ge <sup>70</sup> H <sub>3</sub> (GeH <sub>3</sub> Cl)...	<i>B</i> <sub>0</sub> = 4333.91 [423] <i>B</i> <sub>0</sub> = 4177.90 [423].....	.....		Cl <sup>35</sup> = -46 [423] Ge <sup>72</sup> = -95 [423],[614]	2.148 [727]	[413],[727]	
Cl <sup>37</sup> Ge <sup>70</sup> H <sub>3</sub> .....	<i>B</i> <sub>0</sub> = 4146.5 [423]	.....		Cl <sup>37</sup> = -86 [423]			
Cl <sup>35</sup> H <sub>3</sub> Si <sup>28</sup> (SiH <sub>3</sub> Cl)....	<i>B</i> <sub>0</sub> = 6673.81 [315], [423],[727],[772] <i>B</i> <sub>0</sub> = 6512.40 [315], [423],[727],[772] <i>B</i> <sub>0</sub> = 5917.7 [772] <i>B</i> <sub>0</sub> = 5772.8 [772] <i>B</i> <sub>0</sub> = 5850.6 [772] <i>B</i> <sub>0</sub> = 6485.8 [423], [727],[772] <i>B</i> <sub>0</sub> = 5787.0 [772] <i>B</i> <sub>0</sub> = 3422.300 [337], [330]	.....		Cl <sup>35</sup> = -40.0 [315],[772] Cl <sup>37</sup> = -30.8 [315] Cl <sup>35</sup> = -39.4 [772]	1.303 [423]	[315],[423], [727],[772]	
Cl <sup>35</sup> D <sub>3</sub> Si <sup>28</sup> .....		.....					
Cl <sup>37</sup> D <sub>3</sub> Si <sup>28</sup> .....		.....					
Cl <sup>35</sup> D <sub>3</sub> Si <sup>28</sup> .....		.....					
Cl <sup>35</sup> H <sub>3</sub> Si <sup>28</sup> .....		.....					
Cl <sup>35</sup> D <sub>3</sub> Si <sup>28</sup> .....		.....					
Cl <sup>35</sup> I (ICl).....		184.18	$\alpha$ = 11.06 [330]	Cl <sup>35</sup> = -82.5 [330] I <sup>127</sup> = -2930.0 [330]	0.65 [330]	[330]	$\Delta^2 = 5.5$ Mc/mm Hg for <i>J</i> = 3 → 4 [330] = 3.15 Mc/mm Hg for <i>J</i> = 0 → 1 [337]



$\text{Cl}^{37}\text{I}$ $\text{Cl}^{35}\text{K}^{37}(\text{KCl})$	$B_0 = 3277.365$ [330] $Y_{01}(\approx B_e) = 3856.370$ [750],[835]	..... 305 [772c]	$\alpha = 15.05$ [330] $\alpha = 23.680$ [750],[835]	$ \text{Cl}^{35}  < 0.04$ [835] $K^{30} = -5.656$ [835]	10.48 [835],[988]	[835],[938]	Quadrupole coupling constants and dipole moments in several vibrational states [835]; rotation-vibration constants $\gamma_e = 0.050$ [835] Rotation-vibration constant $\gamma_e = 0.047$ [835] Quadrupole coupling constant in excited vibrational state [835]; rotation-vibration constant $\gamma_e = 0.048$ [835]
$\text{Cl}^{37}\text{K}^{39}$	$Y_{01}(\approx B_e) = 3746.583$ [835]	.....	$\alpha = 22.676$ [835]	.....	.....	.....	.....
$\text{Cl}^{35}\text{K}^{41}$	$Y_{01}(\approx B_e) = 3767.394$ [835]	.....	$\alpha = 22.865$ [835]	$K^{41} = -6.899$ [835]	.....	.....	.....
$\text{Cl}^{35}\text{Na}$ ( $\text{NaCl}$ )	$Y_{01}(\approx B_e) = 6536.86$ [751],[938]	380	$\alpha = 48.1$ [751]	$\text{Na}^{23} = -5.40$ [722d]	8.5 [988]	[751],[938]	.....
$\text{Cl}^{35}\text{NO}$ ( $\text{NOCl}$ )	$A_0 = 85.290$ [632] $B_0 = 5738.3$ [632] $C_0 = 5376.4$ [632]	.....	.....	$e \frac{\partial^2 V}{\partial a^2} Q_{\text{Cl}^{35}} = 30$ [632] $e \frac{\partial^2 V}{\partial b^2} Q_{\text{Cl}^{35}} = 19.6$ [632]	1.83 [632] parallel to $a$ axis = 1.28 [632]	[436]	.....
$\text{Cl}^{37}\text{NO}$	$A_0 = 85.560$ [632] $B_0 = 5600.7$ [632] $C_0 = 5259.2$ [632]	.....	.....	$e \frac{\partial^2 V}{\partial a^2} Q_{\text{Cl}^{37}} = 23$ $e \frac{\partial^2 V}{\partial b^2} Q_{\text{Cl}^{37}} = 14$	.....	.....	.....
$\text{Cl}^{85}\text{Rb}^{85}$ ( $\text{RbCl}$ )	$B_e = 2627.414$ [993], [938]	270 [772c]	$\alpha_e = 13.601$ [993],[938]	$\text{Cl}^{35} = 0.774$ [993] $\text{Rb}^{85} = -52.675$ [993]	.....	[938],[993]	$\gamma_e = 0.021$ Mc [993] Magnetic h.f.s. for $\text{Rb}^{85} = (0.3 \pm 0.3)\text{I}\cdot\text{J}$ Mc [993] $\gamma_e = 0.021$ Mc [993] $\Delta\nu = 60$ Mc/mm Hg [665]
$\text{Cl}^{85}\text{Rb}^{87}$ $\text{Cl}^{35}\text{Re}^{85}\text{O}_3$ ( $\text{ReO}_2\text{Cl}$ )	$B_e = 2609.779$ [993] $B_0 = 2094.23$ [665]	.....	$\alpha_e = 13.464$ [993]	$\text{Rb}^{87} = -25.485$ [993] $\text{Cl}^{35} = -34$ [818],[943a] $\text{Re}^{185} = 270$ [818],[943a]	.....	.....	.....
$\text{Cl}^{37}\text{Re}^{185}\text{O}_3$ $\text{Cl}^{35}\text{Re}^{187}\text{O}_3$ $\text{Cl}^{37}\text{Re}^{187}\text{O}_3$ $\text{Cl}^{35}\text{Ti}^{303}$ ( $\text{TiCl}$ )	$B_0 = 2025.02$ [665] $B_0 = 2093.59$ [665] $B_0 = 2024.36$ [665] $B_e = 2743.94$ [561a], [958a]	..... ..... ..... 287.47	..... ..... ..... $\alpha_e = 11.96$ [958a]	$\text{Re}^{187} = 253$ [818],[943a] $\text{Cl}^{35} = -15.795$ [561a]	4.444 [561a]	[561a]	Magnetic h.f.s. for $\text{Ti}$ , $0.073\text{I}\cdot\text{J}$ ; for $\text{Cl}^{35}$ , $0.0012\text{I}\cdot\text{J}$ ; [561a]
$\text{Cl}^{35}\text{Ti}^{303}$ $\text{Cl}^{74}\text{Ge}^{70}\text{H}$ ( $\text{GeCl}_2\text{H}$ )	$B_e = 2617.5$ [958a] $B_0 = 2172.75$ [881]	..... .....	..... $ D_J  < 0.002$ [881] $ D_{JK}  < 0.004$ [881]	$\text{Cl}^{37} = -12.446$ [561a]	.....	[881]	Spectra for excited vibrational states [881]
$\text{Cl}^{74}\text{Ge}^{72}\text{H}$ $\text{Cl}^{74}\text{Ge}^{74}\text{H}$	$B_0 = 2169.26$ [881] $B_0 = 2165.84$ [881]	..... .....	.....	.....	.....	.....	.....

Chemical symbol	Rotational constants <i>A</i> , <i>B</i> , and <i>C</i> , Mc	Vibrational fre- quencies $\omega$ in wave numbers ( $\text{cm}^{-1}$ ); <i>d</i> indicates a degenerate vibration	Rotation-vibration constants, Mc ( $\omega$ , <i>D</i> , or <i>q</i> <i>l</i> )	Quadrupole coupling constant <i>eqQ</i> , Mc	Dipole moment $\mu$ in $10^{-18}$ esu (Debye)	Reference for structure	Remarks
$\text{Cl}_2^{37}\text{Ge}^{70}\text{H}$ .....	<i>B</i> <sub>0</sub> = 2063.74 [881]						
$\text{Cl}_2^{37}\text{Ge}^{72}\text{H}$ .....	<i>B</i> <sub>0</sub> = 2060.43 [881]						
$\text{Cl}_2^{37}\text{Ge}^{74}\text{H}$ .....	<i>B</i> <sub>0</sub> = 2057.20 [881]						
$\text{Cl}_2^{34}\text{SiH}$ ( $\text{SiCl}_3\text{H}$ ).....	<i>B</i> <sub>0</sub> = 2472.49 [847]					[730 <i>a</i> ],[847]	
$\text{Cl}_2^{37}\text{SiH}$ .....	<i>B</i> <sub>0</sub> = 2346.07 [847]					[765]	
$\text{Cl}_2^{34}\text{OP}$ ( $\text{POCl}_3$ ).....	<i>B</i> <sub>0</sub> = 2015.20 [765]					[765]	
$\text{Cl}_2^{37}\text{OP}$ .....	<i>B</i> <sub>0</sub> = 1932.38 [765]					[481]	
$\text{Cl}_2^{36}\text{P}$ ( $\text{PCl}_3$ ).....	<i>B</i> <sub>0</sub> = 2617.1 [481]	$\omega_1 = 510$ $\omega_2 = 257$ $\omega_3 = 480d$ $\omega_4 = 190d$	$\alpha_2 = 1.9$ [481] $\alpha_4 = -1.9$ [481]		0.80		Lines of $\text{PCl}_2^{35}\text{Cl}^{37}$ and $\text{PCl}_2^{37}\text{Cl}_2^{35}$ measured [481]
$\text{Cl}_2^{37}\text{P}$ .....	<i>B</i> <sub>0</sub> = 2487.5 [481]						
$\text{Cl}_2^{34}\text{PS}_{32}$ ( $\text{PSCl}_3$ ).....	<i>B</i> <sub>0</sub> = 1402.65 [765]					[765]	
$\text{Cl}_2^{37}\text{PS}_{32}$ .....	<i>B</i> <sub>0</sub> = 1355.72 [765]						
$\text{Cl}_2^{34}\text{PS}_{34}$ .....	<i>B</i> <sub>0</sub> = 1370.13 [765]						
$\text{Cl}_2^{34}\text{Sb}_{32}$ ( $\text{SbCl}_3$ ).....	<i>B</i> <sub>0</sub> = 1753.9 [597]	$\omega_1 = 360$ $\omega_2 = 165$ $\omega_3 = 320d$ $\omega_4 = 134d$			3.93	[597],[947]	Ratio quadrupole coupling con- stants [597]
$\text{Cl}_2^{34}\text{Sb}_{32}$ .....	<i>B</i> <sub>0</sub> = 1750.7 [597]						
$\text{CaF}$ .....	<i>B</i> <sub>e</sub> = 5527.27 [938]	385 [772 <i>c</i> ]	$\alpha = 33.13$ [938]		7.874 [160],[423 <i>a</i> ], [938]	[938]	$\gamma_e = 0.009$ [938]
$\text{CaI}$ .....	<i>B</i> <sub>e</sub> = 708.36 [938]	120 [772 <i>c</i> ]	$\alpha = 2.044$ [938]		12.1 [938]	[938]	$\gamma_e = 0.0015$ Mc [938]
$\text{FH}_3\text{Si}_{32}$ ( $\text{SiH}_3\text{F}$ ).....	<i>B</i> <sub>0</sub> = 14327.9 [522]				1.268 [522]	[522],[888]	
$\text{FD}_2\text{Si}_{32}$ .....	<i>B</i> <sub>0</sub> = 12,253.114 [771], [888]					[888]	
$\text{FH}_3\text{Si}_{32}$ .....	<i>B</i> <sub>0</sub> = 14,196.7 [522]						
$\text{FD}_2\text{Si}_{32}$ .....	<i>B</i> <sub>0</sub> = 12,175.580 [771], [888]						
$\text{FH}_3\text{Si}_{32}$ .....	<i>B</i> <sub>0</sub> = 14,072.6 [522]						
$\text{FD}_2\text{Si}_{32}$ .....	<i>B</i> <sub>0</sub> = 12,101.949 [771], [888]						





Chemical symbol	Rotational constants <i>A</i> , <i>B</i> , and <i>C</i> , Mc	Vibrational fre- quencies $\omega$ in wave numbers ( $\text{cm}^{-1}$ ); <i>d</i> indicates a degenerate vibration	Rotation-vibration constants, Mc ( $\alpha$ , <i>D</i> , or <i>q</i> <i>l</i> )	Quadrupole coupling constant <i>eqQ</i> , Mc	Dipole moment $\mu$ in $10^{-18}$ esu (Debye)	Reference for structure	Remarks
$\text{F}_3\text{O}^{18}\text{P}$ .....	<i>B</i> <sub>0</sub> = 4395.27 [765], [696]						
$\text{F}_2\text{P}$ ( $\text{PF}_3$ ).....	<i>B</i> <sub>0</sub> = 7810.90 [367], [712 <i>a</i> ]	$\omega_1$ = 890 $\omega_2$ = 531 $\omega_3$ = 840 <i>d</i> $\omega_4$ = 486 <i>d</i>	$\alpha_1$ = 38 [712 <i>a</i> ] $\alpha_2$ = 10.8 [712 <i>a</i> ] $\alpha_3$ = -13.8 [712 <i>a</i> ] $\alpha_4$ = -3.5 [712 <i>a</i> ] <i>q</i> <sub>4</sub> = 33.8 [712 <i>a</i> ] <i>D</i> <sub><i>J</i></sub> $\approx$ 0.0003 [765] <i>D</i> <sub><i>JK</i></sub> = 0.0018 [765]	.....	1.025 [528],[803]	[307],[712 <i>a</i> ]	$\Delta\nu$ = 16 Mc/mm Hg [367]
$\text{F}_2\text{PS}^{32}$ ( $\text{PSF}_3$ ) .....	<i>B</i> <sub>0</sub> = 2657.63 [765], [696]	.....		.....	0.033 [696]	[765],[696]	
$\text{F}_2\text{PS}^{\text{III}}$ .....	<i>B</i> <sub>0</sub> = 2614.73 [765], [696]						
$\text{F}_2\text{PS}^{34}$ .....	<i>B</i> <sub>0</sub> = 2579.77 [765], [696]						
$\text{H}^3\text{Br}^{79}$ ( $\text{DBr}$ ).....	<i>B</i> <sub>0</sub> = 127,358.2 [927]	.....	$\alpha_e$ = 1257 [821 <i>a</i> ] <i>D</i> <sub><i>e</i></sub> = 2.8 [821 <i>a</i> ]	<i>Br</i> <sup>79</sup> = 533 [927]	0.79	[927]	
$\text{DBr}^{81}$ .....	<i>B</i> <sub>0</sub> = 127,280.0 [927]	.....	$\alpha_e$ = 1258 [821 <i>a</i> ] <i>D</i> <sub><i>e</i></sub> = 2.8 [821 <i>a</i> ]	<i>Br</i> <sup>81</sup> = 455 [927]			HBr constants known from I.R. measurements [471] HI molecular constants known from I.R. measurements [471]; magnetic h.f.s. for <i>I</i> = 0.141·J Mc [782 <i>b</i> ]
$\text{HI}$ ( $\text{DI}$ ).....	<i>B</i> <sub>0</sub> = 97,537.2 [827 <i>a</i> ], [782 <i>b</i> ]	.....	.....	<i>I</i> <sup>127</sup> = -1823 [827 <i>m</i> ], [782 <i>b</i> ]	0.30	.....	
$\text{HN}_2^{14}$ .....	<i>A</i> <sub>0</sub> = 609,850 [427], [633] <i>B</i> <sub>0</sub> + <i>C</i> <sub>0</sub> = 23,815.7 [427],[633] <i>B</i> <sub>0</sub> + <i>C</i> <sub>0</sub> = 22,316.1 [427] <i>B</i> <sub>0</sub> + <i>C</i> <sub>0</sub> = 23,048.2 [427] <i>B</i> <sub>0</sub> + <i>C</i> <sub>0</sub> = 23,096.7 [427] <i>B</i> <sub>0</sub> + <i>C</i> <sub>0</sub> = 23,814 [427]	.....	.....	<i>N</i> <sup>14</sup> (end nitrogen) = -4.67 [740]	0.847 [427]	[427]	
$\text{DN}_2^{14}$ .....							
$\text{HN}^{14}\text{N}^{14}\text{N}^{14}$ .....							
$\text{HN}^{14}\text{N}^{14}\text{N}^{14}$ .....							
$\text{HN}^{14}\text{N}^{14}\text{N}^{14}$ .....							







D <sub>2</sub> P.....	B <sub>0</sub> = 9,470.41 [909]	.....	D <sub>J</sub> = 0.71 [909]		0.116 [606]	[606]	
H <sub>2</sub> DSb <sup>121</sup> .....	.....	.....	.....	Sb <sup>121</sup> = 455 [606]			
H <sub>2</sub> DSb <sup>123</sup> .....	.....	.....	.....	Sb <sup>123</sup> = 57 [606]			
IK <sup>35</sup> (KI).....	B <sub>0</sub> = 1825.01 [938]	300 [772c]	α = 8.034 [938] D = 0.0010 [938]	I <sup>127</sup> = -60 [938]	11.05 [938]	[938]	γ <sub>0</sub> = 0.0122 Mc [938]
IK <sup>41</sup> .....	B <sub>0</sub> = 1756.90 [938]		α = 122.6 [93]	I <sup>127</sup> = -198.2 [938]	6.15 [938]	[93]	γ <sub>0</sub> = 0.455 [93]
ILi <sup>7</sup> (LiI).....	Y <sub>01</sub> (≈B <sub>0</sub> ) = 13,286.39 [938]	450	α = 152.6 [938]				
ILi <sup>9</sup> .....	Y <sub>01</sub> (≈B <sub>0</sub> ) = 15,381.45 [938]						
INa (NaI).....	B <sub>0</sub> = 3531.76 [938]	216	α = 19.44 [938]	I <sup>111</sup> = -259.9 [938]		[938]	γ <sub>0</sub> = 0.047 [938]
IRb <sup>85</sup> (RbI).....	B <sub>0</sub> = 984.31 [938]	147 [138]	α = 3.281 [938] D = 0.00023 [938]			[938]	γ <sub>0</sub> = 0.0030 [938]
IRb <sup>87</sup> .....	B <sub>0</sub> = 970.7 [938]		α = 3.214 [938]				
NO.....	B <sub>0</sub> = 51,084.5 [782b], [924]	1904	α <sub>0</sub> = 534 [782b], [924]	N <sup>14</sup> = -1.9 [435], [782b], [899], [962]	0.1		Λ-doubling [671], [872b], [924], magnetic h.f.s. for N <sup>14</sup> [435], [899], [872b], [924]
NO <sub>2</sub> .....	.....				0.2		J = 6-6 ←→ 5-4 transition [497], [615]; magnetic h.f.s. not completely understood [340], [615]
NO <sub>2</sub> (nitryl fluoride).....	A <sub>0</sub> = 13203 [748] B <sub>0</sub> = 11447 [748] C <sub>0</sub> = 6120 [748]			$e \frac{\partial^2 V}{\partial d^2} Q_{N^{14}} = 0.7$ [748] $e \frac{\partial^2 V}{\partial b^2} Q_{N^{14}} = 1.5$ [748]	0.47 [748]	[748]	
N <sub>2</sub> <sup>14</sup> O <sup>18</sup> .....	B <sub>0</sub> = 12,116.66 [184], [357], [595]	ω <sub>1</sub> = 1285.0 ω <sub>2</sub> = 588.8d ω <sub>3</sub> = 2223.5	α <sub>1</sub> = 52 [915] α <sub>2</sub> = -13 [915] α <sub>3</sub> = 104 [915] D <sub>J</sub> = 0.0057 [95], [755] q <sub>1</sub> = 26 [915] α <sub>1</sub> = 46 [915] α <sub>2</sub> = -11 [915] α <sub>3</sub> = 101 [915]	N <sup>14</sup> (end atom) = -0.8 [357], [755] N <sup>14</sup> (central atom) = -0.3 [184]	0.16 [357], [528]	[184], [357], [915]	Δν = 4.2 Mc/mm Hg [357]  ρ <sub>J</sub>   = 0.086 [592]
N <sup>14</sup> N <sup>14</sup> O <sup>18</sup> .....	B <sub>0</sub> = 12,137.30 [114], [357]						
N <sup>14</sup> N <sup>15</sup> O <sup>18</sup> .....	B <sub>0</sub> = 12,560.78 [357]						
N <sup>15</sup> N <sup>15</sup> O <sup>18</sup> .....	B <sub>0</sub> = 12,137.39 [357]						
N <sup>14</sup> N <sup>14</sup> O <sup>18</sup> .....	B <sub>0</sub> = 11,859.11 [714]						
N <sup>14</sup> N <sup>15</sup> O <sup>18</sup> .....	B <sub>0</sub> = 11,855.82 [714]						
N <sup>14</sup> N <sup>16</sup> O <sup>18</sup> .....	B <sub>0</sub> = 11,449.66 [714]						
N <sup>15</sup> N <sup>16</sup> O <sup>18</sup> .....	B <sub>0</sub> = 11,448.04 [714]						

Chemical symbol	Rotational constants <i>A</i> , <i>B</i> , and <i>C</i> , Mc	Vibrational fre- quencies $\omega$ in wave numbers (cm <sup>-1</sup> ); <i>d</i> indicates a degenerate vibration	Rotation-vibration constants, Mc ( $\alpha$ , <i>D</i> , or <i>q</i> )	Quadrupole coupling constant <i>eqQ</i> , Mc	Dipole moment $\mu$ in 10 <sup>-18</sup> esu (Debye)	Reference for structure	Remarks
O <sub>2</sub> <sup>16</sup> .....	<i>B</i> <sub>0</sub> = 43,102 [667],[963]	1580.36	.....	.....	.....	[842]	<i>p</i> -type triplet frequencies see p. 184; [139],[441],[669], $\Delta\nu$ = 1.9 Mc/mm Hg [667],[892b], [937]; temperature dependence of $\Delta\nu$ [937]; Zeeman effect [937], [990] Magnetic h.f.s. for O <sup>17</sup> = -1011·S + 140 <i>I</i> ·S, [841] Lines compared with theory [841] Lines and alternating intensities [816] Centrifugal distortion [647],[948] [ <i>g</i> <sub>J</sub> ] = 0.084 [592]
O <sup>18</sup> O <sup>17</sup> .....	.....	.....	.....	.....	.....	.....	.....
O <sup>16</sup> O <sup>18</sup> .....	.....	.....	.....	.....	.....	.....	.....
O <sup>18</sup> O <sup>18</sup> .....	.....	.....	.....	.....	.....	.....	.....
O <sub>2</sub> S <sup>32</sup> (SO <sub>2</sub> ).....	<i>A</i> <sub>0</sub> = 60,778.79 [187], [565],[647],[948] <i>B</i> <sub>0</sub> = 10,318.10 [187], [565],[647],[948] <i>C</i> <sub>0</sub> = 8799.96 [187], [565],[647],[948]	$\omega_1$ = 1151.2 $\omega_2$ = 519 $\omega_3$ = 1361	.....	.....	1.59 [565]	[187],[565], [647],[948]	.....
O <sub>2</sub> S <sup>34</sup> .....	.....	.....	.....	$e \frac{\partial^2 V}{\partial a^2} = -1.7$ [903] $e \frac{\partial^2 V}{\partial b^2} = 25.71$ [903]	.....	.....	.....
O <sub>3</sub> .....	<i>A</i> <sub>0</sub> = 106,530.0 [875] <i>B</i> <sub>0</sub> = 13,349.1 [875] <i>C</i> <sub>0</sub> = 11,834.3 [875]	$\omega_1$ = 1043.4 $\omega_2$ = 710 $\omega_3$ = 1740	.....	.....	0.53 [699],[875]	[699],[875]	Effective molecular <i>g</i> factors for <i>J</i> <sub>11</sub> and 2 <i>o</i> <sub>3</sub> rotational states [875]

## APPENDIX VII

### Properties of the Stable Nuclei (Abundance, Mass, and Moments)

Relative abundances of isotopes are taken from the table of Hollander, Perlman, and Seaborg [813]. Masses are principally those listed by E. Segre [*Experimental Nuclear Physics*, Vol. I, John Wiley & Sons, Inc., (1953)] supplemented by more recent work. For isotopes with masses which have not been accurately measured, calculated values are given based on the semiempirical formula of Green and Engler [A. E. S. Green and N. Engler, *Phys. Rev.*, **91**, 40 (1953)]. These are given only to three decimal places. The basic compilations of nuclear moment data used are those of Poss [H. L. Poss, Brookhaven National Laboratories report (Oct. 1, 1949)], Mack [J. E. Mack, *Rev. Mod. Phys.* **22**, 64 (1952)] and Walchli [H. E. Walchli, Oak Ridge National Laboratory report *ORNL*—1469, (Apr. 1, 1953)] with the addition of some recent results not included in the above tables.

The nuclear magnetic moment values have not been corrected for the effects of atomic or molecular diamagnetism. These diamagnetic effects increase with increasing  $Z$  from about 0.01 per cent to somewhat more than 1 per cent (see Walchli, *ibid.*). Quadrupole moments have been corrected for screening by inner electron shells [539], [749], [979].



Atomic number	Element	Mass number	Atomic mass in atomic mass units	Abundance, per cent	Spin	Magnetic moment, nuclear magnetons	Quadrupole moment $\times 10^{24}$ cm <sup>2</sup>	Ratio of quadrupole moments
1	H	1	1.008142	99.9851	$\frac{1}{2}$	+2.792670		
		2	2.014735	0.0149	1	+0.857392	+0.002738	
2	He	3	3.016977	$1.3 \times 10^{-4}$	$\frac{1}{2}$	-2.12741		
		4	4.003873	99.9999	0			
3	Li	6	6.017021	7.52	1	+0.82193		$Q_6/Q_7 = 1.9 \times 10^{-3}$
		7	7.018223	92.48	$\frac{3}{2}$	+3.25598		
4	Be	9	9.015043	100	$\frac{3}{2}$	-1.1772	$\pm 0.02$	
5	B	10	10.016114	18.98-18.45	3	+1.8004	+0.086	$Q_{10}/Q_{11} = 2.084$
		11	11.012789	81.02-81.55	$\frac{3}{2}$	+2.68798	+0.042	
6	C	12	12.003804	98.892	0			
		13	13.007473	1.108	$\frac{1}{2}$	+0.7021		
7	N	14	14.007515	99.635	1	+0.4036	+0.02	
		15	15.004863	0.365	$\frac{1}{2}$	-0.2830		
8	O	16	16.000000	99.758	0			
		17	17.004533	0.0373	$\frac{5}{2}$	-1.89295	-0.005	
		18	18.004874	0.2039	0			
9	F	19	19.004456	100	$\frac{1}{2}$	+2.62728		
10	Ne	20	19.998860	90.92	0			
		21	21.000589	0.257	$\frac{3}{2}$			
		22	21.998270	8.82	0			
11	Na	23	22.997139	100	$\frac{3}{2}$	+2.2161	+0.10	
12	Mg	24	23.992696	78.60				
		25	24.993815	10.11	$\frac{5}{2}$	-0.8547		
		26	25.990871	11.29				
13	Al	27	26.990140	100	$\frac{5}{2}$	+3.63853	+0.150	
14	Si	28	27.985837	92.27	0			
		29	28.985719	4.68	$\frac{1}{2}$	(-)0.5547		
		30	29.983313	3.05	0			
15	P	31	30.983622	100	$\frac{1}{2}$	+1.1305		
16	S	32	31.982236	95.02	0			
		33	32.98197	0.75	$\frac{3}{2}$	+0.6427	-0.067	
		34	33.97860	4.22				
17	Cl	35	34.97993	75.4	$\frac{3}{2}$	+0.82086	-0.085	$Q_{16}/Q_{17} = 1.2688$
		37	36.97754	24.6	$\frac{5}{2}$	+0.68330	-0.067	
18	A	36	35.97892	0.337				
		38	37.97479	0.063				
		40	39.97502	99.600				
19	K	39	38.97593	93.08	$\frac{3}{2}$	+0.39094		$Q_{19}/Q_{21} = 1.220$
		40	39.97658	0.0119	4	-1.2964		
		41	40.97476	6.91	$\frac{3}{2}$	+0.21506		
20	Ca	40	39.97534	96.97	0			
		42	41.97202	0.64				
		43	42.97237	0.145	$\frac{7}{2}$	-1.3160		
		44	43.96920	2.06				
		46	45.968	0.0033				
		48	47.96763	0.185				
21	Sc	45	44.97000	100	$\frac{7}{2}$	+4.7491		
22	Ti	46	45.96697	7.95				
		47	46.96668	7.75	$\frac{5}{2}$	-0.78710		
		48	47.96317	73.45				
		49	48.96358	5.51	$\frac{7}{2}$	-1.1022		
		50	49.96077	5.34				
23	V	50	49.96210	0.24	6	+3.3413		
		51	50.96052	99.76	$\frac{7}{2}$	+5.138	+0.3	
24	Cr	50	49.96210	4.31				
		52	51.95707	83.76				
		53	52.95772	9.55		-0.47354		
		54	53.9563	2.38				

Atomic number	Element	Mass number	Atomic mass in atomic mass units	Abundance, per cent	Spin	Magnetic moment, nuclear magnetons	Quadrupole moment $\times 10^{24}$ cm <sup>2</sup>	Ratio of quadrupole moments			
25	Mn	55	54.95581	100	$\frac{5}{2}$	+3.4611	+0.4	$Q_{55}/Q_{56} = 1.0806$			
26	Fe	54	53.95704	5.84	$\frac{7}{2}$	+4.6389	+0.5				
		56	55.95272	91.68							
		57	56.95359	2.17							
		58	57.9520	0.31							
27	Co	59	58.95182	100							
28	Ni	58	57.95345	67.76	$\frac{3}{2}$	+2.2213	-0.16				
		60	59.94901	26.16							
		61	60.94907	1.25							
		62	61.94681	3.66							
		64	63.94755	1.16							
29	Cu	63	62.94926	69.1	$\frac{3}{2}$	+2.3790	-0.14				
		65	64.94835	30.9							
30	Zn	64	63.94955	48.89				$\frac{5}{2}$	+0.8735	$Q_{69}/Q_{71} = 1.5867$	
		66	65.94722	27.81							
		67	66.94815	4.11							
		68	67.94686	18.56							
		70	69.94779	0.62							
31	Ga	69	68.94778	60.2	$\frac{3}{2}$	+2.0108	+0.24				
		71	70.94752	39.8							
32	Ge	70	69.94637	20.55				0	+2.5549		+0.15
		72	71.94462	27.37							
		73	72.94669	7.67							
		74	73.94466	36.74							
		76	75.94559	7.67							
33	As	75	74.94570	100	$\frac{3}{2}$	+1.43491	+0.3				
34	Se	74	73.94620	0.87							
		76	75.94357	9.02							
		77	76.94459	7.58							
		78	77.94232	23.52							
		80	79.94205	49.82	$\frac{3}{2}$	+2.0990	+0.33				
35	Br	79	78.94365	50.52							
		81	80.94232	49.48							
36	Kr	78	77.94513	0.354				0	+2.2626	+0.28	
		80	79.94194	2.27							
		82	81.93967	11.56							
		83	82.94059	11.55							
		84	83.93836	56.90							
		85	85.93828	17.37	$\frac{5}{2}$	-0.966	+0.16				
37	Rb	85	84.93920	72.15							
		87	86.93709	27.85							
38	Sr	84	83.94011	0.56				$\frac{5}{2}$	+1.3482	+2.8	
		86	85.93684	9.86							
		87	86.93677	7.02							
		88	87.93408	82.56							
39	Y	89	88.93421	100							
40	Zr	90	89.93311	51.46	$\frac{3}{2}$	+2.7414	+1.4				
		91	90.934	11.23							
		92	91.933	17.11							
		94	93.934	17.40							
		96	95.936	2.80							
41	Nb	93	92.93540	100	$\frac{5}{2}$	+1.3	$Q_{87}/Q_{88} = 2.07$				
42	Mo	92	91.935	15.86							
		94	93.93522	9.12							
		95	94.936	15.70							
		96	95.93558	16.50							
		97	96.93693	9.45	$\frac{5}{2}$	-0.9290					
		98	97.937	23.75							
		100	99.93829	9.62							

Atomic number	Element	Mass number	Atomic mass in atomic mass units	Abundance, per cent	Spin	Magnetic moment, nuclear magnetons	Quadrupole moment $\times 10^{24}$ cm <sup>2</sup>	Ratio of quadrupole moments			
44	Ru	96	95.941	5.68	$\frac{5}{2}$						
		98	97.9363	2.22							
		99	98.938	12.81							
		100	99.9378	12.70	$\frac{5}{2}$						
		101	100.937	16.98							
		102	101.936	31.34							
		104	103.937	18.27	$\frac{1}{2}$						
45	Rh	103	102.937	100		(-)0.11					
	46	Pd	102	101.939		0.8	$\frac{5}{2}$	-0.6			
104			103.93690	9.3							
105			104.938	22.6							
106			105.936	27.2							
108			107.93690	26.8							
110			109.94098	13.5							
107			106.937	51.35	$\frac{1}{2}$	-0.11303					
109	108.937	48.65	-0.12994								
48	Cd	106	105.943	1.215	$\frac{1}{2}$						
		108	107.940	0.875							
		110	109.93911	12.39							
		111	110.941	12.75							
		112	111.93999	24.07	$\frac{1}{2}$		-0.59216				
		113	112.94206	12.26			-0.61947				
		114	113.94013	28.86							
49	In	116	115.94212	7.58	$\frac{9}{2}$	+5.4962	+1.18				
		113	112.942	4.23		+5.5074	+1.20				
		115	114.94207	95.77		$Q_{115}/Q_{113} = 1.0146$					
50	Sn	112	111.944	0.95	$\frac{1}{2}$		-0.91320				
		114	113.94109	0.65							
		115	114.94154	0.34							
		116	115.93806	14.24							
		117	116.94171	7.57	$\frac{1}{2}$			-0.9949			
		118	117.938	24.01				-1.0409			
		119	118.940	8.58							
51	Sb	120	119.93904	32.97	$\frac{5}{2}$		+3.3416	-1.3			
		122	121.94260	4.71							
		124	123.945	5.98							
		121	120.942	57.25					$\frac{5}{2}$	+2.5334	-1.8
		123	122.944	42.75							
		52	Te	120		119.940				0.089	$\frac{1}{2}$
				122		121.9391			2.46		
123	122.9422			0.87							
124	123.9393			4.61							
125	124.9427			6.99	$\frac{1}{2}$	-0.8825					
126	125.9417			18.71							
128	127.9438			31.79							
53	I	130	129.9475	34.49	$\frac{5}{2}$	+2.7938	-0.61				
		127	126.946	100							
		54	Xe	124				123.944	0.096	$\frac{1}{2}$	-0.77244
				126				125.943	0.090		
				128				127.944	1.919		
				129				128.94533	26.44		
				130				129.945	4.08	$\frac{3}{2}$	
131	130.947			21.18							
132	131.94618			26.89							
55	Cs	134	133.94804	10.44	$\frac{7}{2}$	+2.5642	-0.03				
		136	135.95046	8.87							
		133	132.948	100							



Atomic number	Element	Mass number	Atomic mass in atomic mass units	Abundance, per cent	Spin	Magnetic moment, nuclear magnetons	Quadrupole moment $\times 10^{24} \text{ cm}^2$	Ratio of quadrupole moments
56	Ba	130	129.943	0.101				
		132	131.942	0.097				
		134	133.944	2.42				
		135	134.945	6.59	$\frac{3}{2}$	+0.830		
		136	135.946	7.81				
		137	136.948	11.32	$\frac{3}{2}$	+0.927		
		138	137.9498	71.66				
57	La	138	137.947	0.089	5	+3.68	+3	$Q_{138}/Q_{139} = 3.0$
		139	138.949	99.911	$\frac{7}{2}$	+2.7615	+0.9	
58	Ce	136	135.946	0.193				
		138	137.947	0.250				
		140	139.9488	88.48				
		142	141.9528	11.07				
59	Pr	141	140.9509	100	$\frac{5}{2}$	+3.8	-0.054	
60	Nd	142	141.959	27.13				
		143	142.956	12.20	$\frac{7}{2}$	-1.0		
		144	143.9562	23.87				
		145	144.959	8.30	$\frac{7}{2}$	-0.62		
		146	145.959	17.18				
		148	147.9642	5.72				
		150	149.9676	5.60				
		152	151.9677	26.63				
62	Sm	144	143.9567	3.16				
		147	146.961	15.07	$\frac{5}{2}$	-0.68		
		148	147.9616	11.27				
		149	148.963	13.84	$\frac{5}{2}$	-0.55		
		150	149.9632	7.47				
		152	151.9677	26.63				
		154	153.9712	22.53				
63	Eu	151	150.963	47.77	$\frac{5}{2}$	+3.4	+1.2	
		153	152.965	52.23	$\frac{5}{2}$	+1.5	+2.6	
64	Gd	152	151.970	0.20				
		154	153.9694	2.15				
		155	154.970	14.73				
		156	155.9715	20.47				
		157	156.973	15.68				
		158	157.9736	24.87				
		160	159.9785	21.90				
		159	158.972	100	$\frac{3}{2}$			
		156	155.972	0.0524				
66	Dy	158	159.975	0.0902				
		160	159.9752	2.294				
		161	160.977	18.88	$\frac{7}{2}$			
		162	161.9779	25.53				
		163	162.980	24.97	$\frac{7}{2}$			
		164	163.9814	28.18				
		165	164.9822	100	$\frac{7}{2}$			
		162	161.980	0.136				
68	Er	164	163.9827	1.56				
		166	165.982	33.41				
		167	166.983	22.94	$\frac{7}{2}$		+10	
		168	167.9849	27.07				
		170	169.9907	14.88				
		169	168.985	100	$\frac{1}{2}$			
		168	167.983	0.140				
		170	169.985	3.03				
69	Tm	171	170.987	14.31	$\frac{1}{2}$	+0.45		
		172	171.988	21.82				
		173	172.989	16.13	$\frac{5}{2}$	-0.66	+4.0	
		174	173.991	31.84				
		176	175.995	12.73				
		170	169.985	3.03				
		171	170.987	14.31	$\frac{1}{2}$	+0.45		
		172	171.988	21.82				
70	Yb	173	172.989	16.13	$\frac{5}{2}$	-0.66	+4.0	
		174	173.991	31.84				
		176	175.995	12.73				
		170	169.985	3.03				

Atomic number	Element	Mass number	Atomic mass in atomic mass units	Abundance, per cent	Spin	Magnetic moment, nuclear magnetons	Quadrupole moment $\times 10^{24}$ cm <sup>2</sup>	Ratio of quadrupole moments	
71	Lu	175	174.993	97.40	$\frac{7}{2}$	+2.9	+6.5	$Q_{186}/Q_{187} = 1.06$	
		176	175.995	2.60	7	+4.2	+8		
72	Hf	174	173.992	0.18	$(\frac{1}{2}, \frac{3}{2})$				
		176	175.9957	5.15					
		177	176.998	18.39	$(\frac{1}{2}, \frac{3}{2})$				
		178	177.9988	27.08					
		179	179.002	13.78	$(\frac{1}{2}, \frac{3}{2})$				
		180	180.0031	35.44					
73	Ta	181	180.999	100	$\frac{7}{2}$	+2.1	+7		
74	W	180	180.001	0.135	$\frac{1}{2}$	+0.087			
		182	182.0041	26.4					
		183	183.0066	14.4					
		184	184.0074	30.6					
		186	186.010	28.4					
75	Re	185	185.009	37.07	$\frac{5}{2}$	+3.1438	+2.9		
		187	187.012	62.93	$\frac{5}{2}$	+3.1760	+2.7		
76	Os	184	184.010	0.018	$\frac{3}{2}$	+0.65066	+2.0		
		186	186.012	1.59					
		187	187.014	1.64					
		188	188.0157	13.3					
		189	189.017	16.1					
		190	190.0174	26.4					
		192	192.0225	41.0					
77	Ir	191	191.020	38.5	$\frac{3}{2}$	0.17	+1.5		
		193	193.024	61.5	$\frac{3}{2}$	+0.17	+1.5		
78	Pt	190	190.018	0.012	$\frac{1}{2}$	+0.6036			
		192	192.021	0.78					
		194	194.0241	32.8					
		195	195.0265	33.7					
		196	196.0267	25.4					
		198	198.0327	7.23					
79	Au	197	197.030	100	$\frac{3}{2}$	+0.14	+0.5		
80	Hg	196	196.029	0.146	$\frac{1}{2}$	+0.49930			
		198	198.032	10.02					
		199	199.034	16.84	$\frac{3}{2}$	-0.607			
		200	200.036	23.13					
		201	201.038	13.22	$\frac{1}{2}$	+0.58367			
		202	202.040	29.80					
		204	204.045	6.85					
81	Tl	203	203.03499	29.50	$\frac{1}{2}$	+1.5960	-0.4		
		205	205.03792	70.50	$\frac{1}{2}$	+1.6116			
82	Pb	204	204.0363	1.48	$\frac{1}{2}$	+0.58367			
		206	206.0388	23.6					
		207	207.0405	22.6					
		208	208.0416	52.3					
83	Bi	209	209.0446	100	$\frac{9}{2}$	+4.388			
90	Th	232	232.11034	100	$(\frac{5}{2})$				
92	U	234	234.11379	0.0058					
		235	235.11704	0.715					
		238	238.12493	99.28					

## BIBLIOGRAPHY

The bibliography has been arranged by year and within each year alphabetically according to the name of the first author. A brief statement of the contents of each reference will be found in the right hand column of the bibliography except when a book is listed, in which case the title is expected to serve as a statement of contents.

In addition to references concerning microwave spectroscopy directly, there are others listed because they contain closely related material, or because they are referred to in the text. References which are not directly connected with microwave spectroscopy are identified by numbers in italics.

### Prior to 1929

- |  |                          |
|--|--------------------------|
| 1. Lebedew, P., <i>Wied. Ann.</i> , <b>56</b> , 1 (1895).  | Mm-wave spark generator  |
| 2. Lorentz, H. A., <i>Proc. Amst. Akad. Sci.</i> , <b>8</b> , 591 (1906).                                    | Th. pressure broadening  |
| 3. Nicholls, E. F., and J. D. Tear, <i>Phys. Rev.</i> , <b>21</b> , 587 (1923).                              | Mm waves                 |
| 4. Nicholls, E. F., and J. D. Tear, <i>Proc. Natl. Acad. Sci. U.S.</i> , <b>9</b> , 221 (1923).              | Mm waves                 |
| 5. Glagolewa-Arkadiewa, A., <i>Nature</i> , <b>113</b> , 640 (1924).   | Mm-wave spark generator  |
| 6. Lewitzky, M., <i>Phys. Zeits.</i> , <b>25</b> , 107 (1924); <b>27</b> , 177 (1926).                       | Mm-wave spark generator  |
| 7. Thomas, L. H., <i>Nature</i> , <b>117</b> , 514 (1926).   | Thomas precession        |
| 8. Born, M., and J. R. Oppenheimer, <i>Ann. Physik</i> , <b>4-84</b> , 457 (1927).                           | Separation of motions    |
| 8a. Kramers, H. A., <i>Atti del Congr. intern. dei fisici, Como</i> , <b>2</b> , 545 (1927).                 | Kramers-Kronig relations |
| 9. Grotrian, W., <i>Graphische Darstellung der Spektren von Atomen</i> , Springer-Verlag-OHG, Berlin (1928). |                          |
| 10. Hill, E. L., and J. H. Van Vleck, <i>Phys. Rev.</i> , <b>32</b> , 250 (1928).                            | $\Lambda$ -doubling      |
| 11. Mulholland, H. P., <i>Proc. Cambridge Phil. Soc.</i> , <b>24</b> , 280 (1928).                           | Partition function       |

### 1929

- |   |                         |
|---|-------------------------|
| 12. Debye, P., <i>Polar Molecules</i> , Chemical Catalog Company, Inc., New York. |                         |
| 13. Glagolewa-Arkadiewa, A., <i>Z. Physik</i> , <b>55</b> , 234.                  | Mm-wave spark generator |
| 14. Hill, E. L., <i>Phys. Rev.</i> , <b>34</b> , 1507.                            | Th. mol. Zeeman effect  |
| 15. Kramers, H. A., <i>Z. Physik</i> , <b>53</b> , 422.                           | $\rho$ tripling         |
| 16. Morse, P. M., <i>Phys. Rev.</i> , <b>34</b> , 57.                             | Mol. potential          |
| 17. Van Vleck, J. H., <i>Phys. Rev.</i> , <b>33</b> , 467.                        | $\Lambda$ doubling      |
| 18. Wang, S. C., <i>Phys. Rev.</i> , <b>34</b> , 243.                             | Asymmetric rotator      |

### 1930

- |  |                        |
|--|------------------------|
| 19. Breit, G., <i>Phys. Rev.</i> , <b>35</b> , 1447.                   | Atomic h.f.s.          |
| 19a. Breit, G., and I. I. Rabi, <i>Phys. Rev.</i> , <b>38</b> , 2082L. | Zeeman effect in atoms |



20. Brouwer, F., Dissertation, Amsterdam. Stark effect diatomic molecules
21. Kronig, R. de L., *Band Spectra and Molecular Structure*, Cambridge University Press, New York.
22. Mulliken, R. S., *Revs. Mod. Phys.*, **2**, 60. Review mol. spectra
23. Pauling, L., and S. A. Goudsmit, *The Structure of Line Spectra*, McGraw-Hill Book Company, Inc., New York.

## 1931

24. Casimir, H. B. G., *Rotation of a Rigid Body in Quantum Mechanics*, J. B. Wolter's, The Hague.
25. Dennison, D. M., *Revs. Mod. Phys.*, **3**, 280. Review mol. spectra
26. Mulliken, R. S., *Revs. Mod. Phys.*, **3**, 89. Review mol. spectra
27. Mulliken, R. S., and A. Christy, *Phys. Rev.*, **38**, 87.  $\Lambda$  doubling
28. Racah, G., *Z. Physik*, **71**, 431. Atomic h.f.s.
29. Weizel, W., *Bandenspektren*, Akad. Verlagsges., Leipzig.

## 1932

30. Bacher, R., and S. A. Goudsmit, *Atomic Energy States*, McGraw-Hill Book Company, Inc., New York.
31. Betz, O., *Ann. Physik*, **15**, 321. Exp. H fine structure
32. Condon, E. U., *Phys. Rev.*, **41**, 759. Induced dipole transitions
33. Dennison, D. M., and G. E. Uhlenbeck, *Phys. Rev.*, **41**, 313. Th.  $\text{NH}_3$
34. Dunham, J. L., *Phys. Rev.*, **41**, 721. Rotation-vibration interaction
36. Nielsen, H. H., *Phys. Rev.*, **40**, 445. Th. hindered rotation
37. Ray, B. S., *Z. Physik*, **78**, 74. Asymmetric rotator
38. Van Vleck, J. H., *Theory of Electric and Magnetic Susceptibilities*, Clarendon Press, Oxford.

## 1933

39. Blockinzew, D., *Phys. Zeit. U.S.S.R.*, **4**, 501. High-frequency modulation
40. Fermi, E., and E. Segre, *Z. Physik*, **82**, 729; *Reale Accad. D'Italia—Scienze Fизiche, Mat. E. Naturali Memorie*, **4**, 131. Atomic h.f.s.
41. Goudsmit, S. A., *Phys. Rev.*, **43**, 636. Atomic h.f.s.
42. Kronig, R. de L., *Physica*, **1**, 617. Masses from mol. spectra
43. Placzek G., and E. Teller, *Z. Physik*, **81**, 209. Mol. symmetries and statistical weights
44. Weisskopf, V. F., *Phys. Zeits.*, **34**, 1. Th. pressure broadening
- 44a. Wright, N., and H. M. Randall, *Phys. Rev.*, **44**, 391.  $\text{NH}_3$  I.R. spectrum

## 1934

45. Cleeton, C. E., and N. H. Williams, *Phys. Rev.*, **45**, 234.  $\text{NH}_3$  microwave spectrum
46. Cosens, C. R., *Proc. Phys. Soc. London*, **46**, 818. Lock-in amplifier
47. Crawford, F. H., *Revs. Mod. Phys.*, **6**, 90. Survey mol. Zeeman effect
- 47a. Dieke, G. H., and G. B. Kistiakowsky, *Phys. Rev.*, **45**, 4. Asymmetric rotor
48. Gordon, A. R., *J. Chem. Phys.*, **2**, 65. Partition function
49. Glagolewa-Arkadiewa, A., *Compt. rend. U.S.S.R.*, **3**, 415. Mm-wave spark generator

50. Kuhn, H., and F. London, *Phil. Mag.*, **18**, 983.  
 51. Kuhn, H., *Phil. Mag.*, **18**, 987.  
 52. Pekeris, C. L., *Phys. Rev.*, **45**, 98.  
 53. White, H. E., *Introduction to Atomic Spectra*, McGraw-Hill Book Company, Inc., New York.

Th. pressure broadening  
 Th. pressure broadening  
 Rotation-vibration  
 diatomic molecule

## 1935

54. Bartunek, P. F., and E. F. Barker, *Phys. Rev.*, **48**, 516.  
 55. Budó, A., *Z. Physik*, **96**, 219.  
 56. Condon, E. U., and G. H. Shortley, *The Theory of Atomic Spectra*, The Macmillan Company, New York.  
 57. Crawford, F. H., and T. Jorgensen, Jr., *Phys. Rev.*, **47**, 358.  
 58. Crawford, F. H., and T. Jorgensen, Jr., *Phys. Rev.*, **47**, 932.  
 59. Cross, P. C., *Phys. Rev.*, **47**, 7.  
 60. Haase, T., *Ann. Physik*, **23**, 675.  
 61. Manning, M. F., *J. Chem. Phys.*, **3**, 136.  
 62. Pauling, L., and E. B. Wilson, Jr., *Introduction to Quantum Mechanics*, McGraw-Hill Book Company, Inc., New York.  
 63. Page, L., *Introduction to Theoretical Physics*, D. Van Nostrand Company, Inc., New York.  
 64. Wilson, E. B., Jr., *J. Chem. Phys.*, **3**, 276.  
 65. Whittaker, E. T., and G. N. Watson, *Modern Analysis*, Cambridge University Press, New York.  
 66. Wilson, E. B., Jr., *J. Chem. Phys.*, **3**, 818.

OCS I.R. spectrum

Fine-structure  $^3\Pi$   
 molecules

Rotation-vibration in  
 LiH

Rotation-vibration in  
 LiH

I.R. spectrum  $H_2S$   
 Exp. H fine structure  
 Theory  $NH_3$

Statistical weights

Symmetry and  
 statistical weights

## 1936

67. Bethe, H. A., and R. F. Bacher, *Revs. Mod. Phys.*, **8**, 82.  
 68. Brandt, W. H., *Phys. Rev.*, **50**, 778.  
 69. Budó, A., *Z. Physik*, **98**, 437.  
 70. Casimir, H. B. G., *On the Interaction between Atomic Nuclei and Electrons*, Teyler's Tweede Genootschap, E. F. Bohn, Haarlem.  
 71. Crawford, F. H., and T. Jorgensen, Jr., *Phys. Rev.*, **49**, 745.  
 72. Gilbert, C., *Phys. Rev.*, **49**, 619.  
 73. Hebb, M. H., *Phys. Rev.*, **49**, 610.  
 74. Schmid, R., A. Budó, and J. Zemlén, *Z. Physik*, **103**, 250.  
 75. Van Vleck, J. H., *J. Chem. Phys.*, **4**, 327.  
 76. Wilson, E. B., Jr., and J. B. Howard, *J. Chem. Phys.*, **4**, 260.

Review nuclei also  
 atomic h.f.s.  
 Electronic quartet  
 states  
 $^3\Pi$  states

Rotation-vibration  
 LiH

Fine-structure triplet  
 molecules

$\rho$ -type tripling  
 Zeeman effect  $O_2$

Isotope shift molecular  
 spectra

General formulation  
 rotation-vibration

## 1937

77. Almy, G. M., and R. B. Horsfall, *Phys. Rev.*, **51**, 491.  
 78. Budó, A., *Z. Physik*, **105**, 73.  
 79. Candler, A. C., *Atomic Spectra and the Vector Model*, Cambridge University Press, New York.

$^2\Pi$  states  
 Mol. quartet states

80. Houston, W. V., *Phys. Rev.*, **51**, 446. H fine structure  
 81. Kemble, E. C., *The Fundamental Principles of Quantum Mechanics*, McGraw-Hill Book Company, Inc., New York.  
 82. Margenau, H., and D. T. Warren, *Phys. Rev.*, **51**, 748. Theory mol. interaction  
 83. Nevin, T. E., *Nature*, **140**, 1101. Mol. quartet states  
 84. Randall, H. M., D. M. Dennison, N. Ginsburg, and L. R. Weber, *Phys. Rev.*, **52**, 160. H<sub>2</sub>O I.R. spectrum  
 85. Schlapp, R., *Phys. Rev.*, **51**, 342.  $\rho$ -type tripling

## 1938

86. Kennard, E. H., *Kinetic Theory of Gases*, McGraw-Hill Book Company, Inc., New York.  
 86a. Meacham, L. A., *Proc. IRE*, **26**, 1278. Stabilized crystal oscillator  
 87. Nevin, T. E., *Phil. Trans. Roy. Soc. London*, **237**, 471. Mol. quartet states  
 88. Pasternack, S., *Phys. Rev.*, **54**, 1113. H fine structure  
 89. Williams, R. C., *Phys. Rev.*, **54**, 558. H fine structure  
 90. Wilson, E. B., Jr., *J. Chem. Phys.*, **6**, 740. Symmetry and statistical weights

## 1939

91. Kellogg, J. M. B., I. I. Rabi, N. F. Ramsey, and J. R. Zacharias, *Phys. Rev.*, **56**, 728. H<sub>2</sub> R.F. spectrum  
 91a. Kellogg, J. M. B., N. F. Ramsey, Jr., I. I. Rabi, and J. R. Zacharias, *Phys. Rev.*, **57**, 677. HD and D<sub>2</sub> R.F. spectrum  
 92. Kalugina, A., *J. Exp. Theor. Phys. U.S.S.R.*, **9**, 362. Mm-wave spark generator  
 93. Margenau, H., *Revs. Mod. Phys.*, **11**, 1. Review mol. interactions  
 94. Pauling, L., *Nature of the Chemical Bond*, Cornell University Press, Ithaca, N.Y.  
 94a. Slawsky, Z. I., and D. M. Dennison, *J. Chem. Phys.*, **7**, 509. Theory centrifugal distortion  
 95. Wu, T. Y., *Vibrational Spectra and Structure of Polyatomic Molecules*, National University of Peking, Kun-ming, China.

## 1940

96. Dennison, D. M., *Revs. Mod. Phys.*, **12**, 175. Review mol. spectra  
 97. Drinkwater, J. W., O. Richardson, and W. E. Williams, *Proc. Roy. Soc. London A*, **174**, 164. H fine structure  
 98. Kellogg, J. M. B., I. I. Rabi, N. F. Ramsey, and J. R. Zacharias, *Phys. Rev.*, **57**, 677. H<sub>2</sub> R.F. spectrum  
 99. Koehler, J. S., and D. M. Dennison, *Phys. Rev.*, **57**, 1006. Th. CH<sub>3</sub>OH  
 100. Mulliken, R. S., *Phys. Rev.*, **57**, 500. Hund's case (c)  
 101. Nordsieck, A., *Phys. Rev.*, **60**, 310.  $q$  for H<sub>2</sub>  
 102. Ramsey, N. F., *Phys. Rev.*, **58**, 226. H<sub>2</sub> R.F. spectrum  
 103. Sandeman, I., *Proc. Roy. Soc. Edinburgh*, **60**, 210. Rotation-vibration diatomic molecules  
 104. Spitzer, L., Jr., *Phys. Rev.*, **58**, 348. Th. pressure broadening  
 105. Wills, A. P., *Vector Analysis*, Prentice-Hall, Inc., New York.

## 1941

106. Hulburt, H. M., and J. O. Hirschfelder, *J. Chem. Phys.*, **8**, 61. Molecular potential  
 107. Michaels, W. C., and N. L. Curtis, *Rev. Sci. Instr.*, **12**, 444. Lock-in amplifier



108. Nielsen, H. H., *Phys. Rev.*, **60**, 794. Rotation-vibration  
polyatomic molecules
109. Schomaker, V., and D. P. Stevenson, *J. ACS*, **63**, 37. Bond lengths
110. Sheng, H. Y., E. F. Barker, and D. M. Dennison, *Phys. Rev.*, **60**, 786. Th. and exp.  $\text{NH}_3$
- 110a. Shrader, J. H., and E. C. Pollard, *Phys. Rev.*, **59**, 277. Cl masses
111. Torrey, H. C., *Phys. Rev.*, **59**, 293. Theory intensities R.F.  
spectra

## 1942

112. Pitzer, K. S., and W. D. Gwinn, *J. Chem. Phys.*, **10**, 428. Internal rotation
113. Racah, G., *Phys. Rev.*, **62**, 438. Theory complex spectra
114. Shaffer, W. H., *J. Chem. Phys.*, **10**, 1. Rotation-vibration  
 $\text{XY}_2\text{Z}$  molecules
115. Silver, S., *J. Chem. Phys.*, **10**, 565. Rotation-vibration  
 $\text{XY}_2\text{Z}$  molecules
116. Silver, S., and E. S. Ebers, *J. Chem. Phys.*, **10**, 559. Rotation-vibration  
 $\text{XYZ}$  molecules
117. Slater, J. C., *Microwave Transmission*, McGraw-Hill Book Company, Inc., New York.

## 1943

118. King, G. W., R. M. Hainer, and P. C. Cross, *J. Chem. Phys.*, **11**, 27. Energy levels  
asymmetric rotor
119. Nielsen, H. H., *J. Chem. Phys.*, **11**, 160. Rotation-vibration  
linear  $\text{XYZ}$  molecules
120. Nielsen, H. H., and W. H. Shaffer, *J. Chem. Phys.*, **11**, 140. *Errata: Phys. Rev.*, **75**, 1961 (1949). *l*-type doubling
121. Terman, F. E., *Radio Engineers' Handbook*, McGraw-Hill Book Company, Inc., New York.

## 1944

122. Cross, P. C., R. M. Hainer, and G. W. King, *J. Chem. Phys.*, **12**, 210. Intensities asymmetric  
rotor
123. Eyring, H., J. Walter, and G. E. Kimball, *Quantum Chemistry*, John Wiley & Sons, Inc., New York
124. Herzberg, G., *Atomic Spectra and Atomic Structure*, 2d ed., Dover Publications, New York.
125. Nielsen, H. H., *J. Opt. Soc. Amer.*, **34**, 521. Rotation-vibration  
interactions
126. Nielsen, H. H., *Phys. Rev.*, **66**, 282. Th. linear molecules
127. Shaffer, W. H., and R. P. Schuman, *J. Chem. Phys.*, **12**, 504. Rotation-vibration  
 $\text{XYZ}$  molecules

## 1945

128. Cooley, J. P., and J. H. Rohrbaugh, *Phys. Rev.*, **67**, 296. Spark radiator
129. Feld, B. T., and W. E. Lamb, Jr., *Phys. Rev.*, **76**, 15. Quadrupole h.f.s. in  
molecules
130. Herzberg, G., *Infrared and Raman Spectra*, D. Van Nostrand Company, Inc., New York.
- 130a. Jablónski, A., *Phys. Rev.*, **68**, 78. *Errata: Phys. Rev.*, **69**, 31 (1946). Th. pressure broadening
131. Lindholm, E., *Ark. Mat. Astron. Fysik*, **32**, 17. Th. pressure broadening
132. Nielsen, H. H., *Phys. Rev.*, **68**, 181. Rotation-vibration  
polyatomic molecules
133. Pauling, L., *Nature of the Chemical Bond*, Cornell University Press, Ithaca, N.Y.

134. Shaffer, W. H., and R. C. Herman, *J. Chem. Phys.*, **13**, 83. Rotation-vibration  
X<sub>2</sub>XZ<sub>2</sub> molecules
- 134a. Southworth, G. C., *J. Franklin Inst.*, **239**, 285. Microwaves from the  
sun
135. Van Vleck, J. H., *Report 664 from MIT Radiation Laboratory* (Div. 14, N.D.R.C.). Atmospheric absorption  
microwaves
- 135a. Van Vleck, J. H., *Report 735 from MIT Radiation Laboratory*. Kramers-Kronig  
relations
136. Van Vleck, J. H., and V. F. Weisskopf, *Revs. Mod. Phys.*, **17**, 227. Th. pressure broadening

## 1946

137. Becker, G. E., and S. H. Autler, *Phys. Rev.*, **70**, 300. H<sub>2</sub>O pressure  
broadening
139. Beringer, R., *Phys. Rev.*, **70**, 53. O<sub>2</sub> high pressure  
Review
140. Bleaney, B., *Physica*, **12**, 595. NH<sub>3</sub>
141. Bleaney, B., and R. P. Penrose, *Nature*, **157**, 339. NH<sub>3</sub>
142. Bleaney, B., and R. P. Penrose, *Phys. Rev.*, **70**, 775L. NH<sub>3</sub> quadrupole  
structure
143. Coles, D. K., and W. E. Good, *Phys. Rev.*, **70**, 979L. ClO<sub>2</sub> electronic  
spectrum
144. Coon, J., *J. Chem. Phys.*, **14**, 665. NH<sub>3</sub> quadrupole  
structure
145. Dailey, B. P., R. L. Kyhl, M. W. P. Strandberg, J. H. Van Vleck, and E. B. Wilson, Jr., *Phys. Rev.*, **70**, 984L. OCS, Stark effect
146. Dakin, T. W., W. E. Good, and D. K. Coles, *Phys. Rev.*, **70**, 560L. Microwave radiometer
148. Dicke, R. H., *Rev. Sci. Instr.*, **17**, 268. Microwaves from sun
149. Dicke, R. H., and R. Beringer, *Astrophys. J.*, **103**, 375. Atmospheric absorption
150. Dicke, R. H., R. Beringer, R. L. Kyhl, and A. B. Vane, *Phys. Rev.*, **70**, 340. Review magnetrons
151. Fisk, J. B., H. D. Hagstrum, and P. L. Hartman, *Bell System Tech. J.*, **25**, 167. Waveguide windows
152. Fiske, M. D., *Rev. Sci. Instr.*, **17**, 478. Th. pressure broadening
153. Foley, H. M., *Phys. Rev.*, **69**, 616. Th. pressure broadening
154. Fröhlich, H., *Nature*, **157**, 478. NH<sub>3</sub>
155. Good, W. E., *Phys. Rev.*, **70**, 109A; 213; *Phys. Rev.*, **69**, 539L. Vibration anharmonic  
oscillator
156. Haar, D. ter, *Phys. Rev.*, **70**, 222. Th. NH<sub>3</sub> inversion
157. Hadley, L. N., and D. M. Dennison, *Phys. Rev.*, **70**, 780. Absorption at medium  
pressures
158. Hershberger, W. D., *J. Appl. Phys.*, **17**, 495. Thermal, acoustic  
effects microwave  
absorption
159. Hershberger, W. D., E. T. Bush, and G. W. Leck, *RCA Rev.*, **7**, 422. Electric field technique  
molecular beam
160. Hughes, H. K., *Phys. Rev.*, **70**, 570. *Errata: Phys. Rev.*, **70**, 909. Th. pressure broadening
161. Jablónski, A., *Phys. Rev.*, **69**, 31. Th. pressure broadening
162. Jablónski, A., *Physica's Grav.*, **7**, 541. Review mol. beams
163. Kellogg, J. M. B., and S. Millman, *Revs. Mod. Phys.*, **18**, 323. H<sub>2</sub>O atmospheric  
absorption
164. Kyhl, R. L., R. H. Dicke, and R. Beringer, *Phys. Rev.*, **69**, 694A. Th. large cavity
165. Lamb, W. E., Jr., *Phys. Rev.*, **70**, 308. 6 mm atm. absorption
166. Lamont, H. R. L., and A. G. D. Watson, *Nature*, **158**, 943.

167. Malter, L., R. L. Jepsen, and L. R. Bloom, *RCA Rev.*, **7**, 622. Mica windows
168. Nielsen, H. H., *Phys. Rev.*, **70**, 184. Rotation-vibration symmetric top
169. Pound, R. V., *Rev. Sci. Instr.*, **17**, 490. Stabilized microwave oscillator
170. Roberts, A., Y. Beers, and A. G. Hill, *Phys. Rev.*, **70**, 112A. Atomic Cs h.f.s.
171. Sproull, R. L., and E. G. Linder, *Proc. IRE*, **34**, 305. Resonant cavities
172. Townes, C. H., *Phys. Rev.*, **70**, 109A, 665.  $\text{NH}_3$
173. Townes, C. H., and F. R. Merritt, *Phys. Rev.*, **70**, 558L.  $\text{H}_2\text{O}$ , HDO
174. Walter, J. E., and W. D. Hersberger, *J. Appl. Phys.*, **17**, 814. Absorption at medium pressures
175. Wilson, I. G., C. W. Schramm, and J. P. Kinzer, *Bell System Tech. J.*, **25**, 408. Resonant cavities
- 1947
176. Beard, C. I., and B. P. Dailey, *J. Chem. Phys.*, **15**, 762L. HNCS, DNCS
177. Bethe, H. A., *Phys. Rev.*, **72**, 339. H fine-structure theory
178. Bleaney, B., J. H. N. Loubser, and R. P. Penrose, *Proc. Phys. Soc.*, **59**, 185. Cavity resonators
179. Bleaney, B., and R. P. Penrose, *Proc. Roy. Soc.*, **189**, 358.  $\text{NH}_3$
180. Bleaney, B., and R. P. Penrose, *Proc. Phys. Soc.*, **59**, 418.  $\text{NH}_3$  pressure broadening
181. Bracewell, R. N., *Proc. IRE*, **35**, 830. Cavity resonators
182. Carter, R. L., and W. V. Smith, *Phys. Rev.*, **72**, 1265L. Frequency markers
183. Coles, D. K., *Proc. Nat. Electronics Conf.*, **1947**, 180. Review
184. Coles, D. K., E. S. Elyash, and J. G. Gorman, *Phys. Rev.*, **72**, 973L.  $\text{N}_2\text{O}$
185. Coles, D. K., and W. E. Good, *Phys. Rev.*, **72**, 157A. Stark, Zeeman effects
186. Dailey, B. P., *Phys. Rev.*, **72**, 84L.  $\text{CH}_3\text{OH}$
187. Dailey, B. P., S. Golden, and E. Bright Wilson, Jr., *Phys. Rev.*, **72**, 871L.  $\text{SO}_2$
188. Dailey, B. P., and E. Bright Wilson, Jr., *Phys. Rev.*, **72**, 522A.  $\text{SO}_2$ ,  $\text{CH}_3\text{NO}_2$ ,  $\text{CH}_3\text{OH}$
189. Dakin, T. W., W. E. Good, and D. K. Coles, *Phys. Rev.*, **71**, 640L. OCS
190. Feld, B. T., *Phys. Rev.*, **72**, 1116L. Th. quad. interactions
191. Foley, H. M., *Phys. Rev.*, **71**, 747. Th. quad. interactions
192. Foley, H. M., *Phys. Rev.*, **72**, 504. Magnetic effects  $^1\Sigma$  mols
194. Ginsburg, V. L., *Bull. Acad. Sci. U.S.S.R., Ser. Phys.*, **11**, 165. Survey mm waves
195. Golay, M. J. E., *Rev. Sci. Instr.*, **18**, 357. Pneumatic detector
196. Golay, M. J. E., *Rev. Sci. Instr.*, **18**, 347. Th. pneumatic detector
197. Good, W. E., and D. K. Coles, *Phys. Rev.*, **71**, 383L.  $\text{N}^{14}\text{H}_3$
198. Good, W. E., and D. K. Coles, *Phys. Rev.*, **72**, 157A.  $\text{N}^{15}\text{H}_3$
199. Gordy, W., *J. Chem. Phys.*, **15**, 305.  $\text{N}^{14}\text{H}_3$
200. Gordy, W., *J. Chem. Phys.*, **15**, 81.  $\text{N}^{15}\text{H}_3$
201. Gordy, W., and M. Kessler, *Phys. Rev.*, **71**, 640L. Bond lengths
202. Gordy, W., and M. Kessler, *Phys. Rev.*, **72**, 644L. Bond lengths
203. Gordy, W., J. W. Simmons, and A. G. Smith, *Phys. Rev.*, **72**, 344L.  $\text{NH}_3$  h.f.s.
- Double modulation spectrograph
- $\text{CH}_3\text{Cl}$ ,  $\text{CH}_3\text{Br}$



204. Gordy, W., A. G. Smith, and J. W. Simmons, *Phys. Rev.*, **71**, 917L. CH<sub>3</sub>I
205. Gordy, W., A. G. Smith, and J. W. Simmons, *Phys. Rev.*, **72**, 249L. CH<sub>3</sub>I
206. Gordy, W., W. V. Smith, A. G. Smith, and H. Ring, *Phys. Rev.*, **72**, 259. BrCN, ICN
207. Hershberger, W. D., and J. Turkevich, *Phys. Rev.*, **71**, 554L. CH<sub>3</sub>OH, CH<sub>3</sub>NH<sub>2</sub>
208. Hillger, R. E., M. W. P. Strandberg, T. Wentink, and R. Kyhl, *Phys. Rev.*, **72**, 157A. OCS
209. Hughes, H. K., *Phys. Rev.*, **72**, 614. CsF molecular beam
210. Hughes, R. H., and E. B. Wilson, Jr., *Phys. Rev.*, **71**, 562L. Stark spectrograph
211. Hunt, L. E., *Proc. IRE*, **35**, 979. Frequency measurement
212. Jauch, J. M., *Phys. Rev.*, **72**, 715; 535A. NH<sub>3</sub> theory h.f.s. and Stark effect
213. Jen, C. K., *Phys. Rev.*, **72**, 986L. Zeeman; NH<sub>3</sub>
214. Kahan, T., *J. Phys. Radium*, **8**, 192. Microwave interferometer
215. King, G. W., *J. Chem. Phys.*, **15**, 820. Asymmetric rotor correspondence principle
216. King, G. W., and R. M. Hainer, *Phys. Rev.*, **71**, 135. HDO
217. King, G. W., R. M. Hainer, and P. C. Cross, *Phys. Rev.*, **71**, 433; **70**, 108A (1946). Predicted absorption H<sub>2</sub>O, etc.
218. Kinzer, J. P., and I. G. Wilson, *Bell System Tech. J.*, **410**. Cavity resonators
219. Lamb, W. E., Jr., and R. C. Retherford, *Phys. Rev.*, **72**, 241. H fine structure
220. Miller, P. H., *Proc. IRE*, **35**, 252. Crystal detector noise
221. Montgomery, C. G., *Technique of Microwave Measurements*, MIT Radiation Laboratory Series, Vol. 11, McGraw-Hill Book Company, Inc., New York.
222. Mumford, W. W., *Proc. IRE*, **35**, 160. Directional couplers
223. Nielsen, H. H., and D. M. Dennison, *Phys. Rev.*, **72**, 86L; 1101. NH<sub>3</sub> anomalies
224. Nierenberg, W. A., and N. F. Ramsey, *Phys. Rev.*, **72**, 1075. NaCl, NaBr, NaI mol. beams
225. Pierce, J. R., and W. G. Shepherd, *Bell System Tech. J.*, **26**, 460. Reflex klystrons
226. Pond, T. A., and W. F. Cannon, *Phys. Rev.*, **72**, 1121L. NH<sub>3</sub> saturation
227. Pound, R. V., *Proc. IRE*, **35**, 1405. Stabilization of oscillators
228. Rideout, V. C., *Proc. IRE*, **35**, 767. Stabilization of oscillators
229. Ring, H., H. Edwards, M. Kessler, and W. Gordy, *Phys. Rev.*, **72**, 1262. CH<sub>3</sub>CN, CH<sub>3</sub>NC
230. Roberts, A., *Nucleonics*, **1**, 10. Review nuclear effects
231. Saxton, J. A., *Rept. Phys. Soc., London; Rept. Met. Soc.*, **1947**, 215. Water-vapor absorption
232. Sherbin, L. E., *Electronics*, **20**, 122. Waveguide data
233. Smith, W. V., *Phys. Rev.*, **71**, 126L. Spin from intensities
234. Smith, W. V., and R. L. Carter, *Phys. Rev.*, **72**, 638L. NH<sub>3</sub> saturation
235. Smith, W. V., J. L. Garcia de Quevedo, R. L. Carter, and W. S. Bennett, *J. Appl. Phys.*, **18**, 1112. Frequency stabilization
236. Strandberg, M. W. P., R. Kyhl, T. Wentink, and R. E. Hillger, *Phys. Rev.*, **71**, 326L. *Errata: Phys. Rev.*, **71**, 639L. NH<sub>3</sub>

237. Talpey, R. G., and H. Goldberg, *Proc. IRE*, **35**, 965. Frequency standard
238. Tolansky, S., *High Resolution Spectroscopy*, Methuen & Co., Ltd., London.
239. Townes, C. H., *Phys. Rev.*, **71**, 909L. Quadrupole moments,  $q$
240. Townes, C. H., A. N. Holden, J. Bardeen, and F. R. Merritt, *Phys. Rev.*, **71**, 644L. *Errata*: 829L. Br, Cl, N moments
241. Townes, C. H., A. N. Holden, and F. R. Merritt, *Phys. Rev.*, **71**, 64L, 479A. Linear molecules
242. Townes, C. H., A. N. Holden, and F. R. Merritt, *Phys. Rev.*, **72**, 513, 740A. Linear molecules, mass ratios,  $l$  doubling
243. Townes, C. H., and F. R. Merritt, *Phys. Rev.*, **72**, 1266L; *Phys. Rev.*, **73**, 1249A. High-frequency Stark effect
244. Van Vleck, J. H., *Phys. Rev.*, **71**, 413.  $O_2$
245. Van Vleck, J. H., *Phys. Rev.*, **71**, 425.  $H_2O$
246. Van Vleck, J. H., *Phys. Rev.*, **71**, 468A. Symmetric-top quad. coupling
247. Watts, R. J., and D. Williams, *Phys. Rev.*, **71**, 639L; *Phys. Rev.*, **72**, 157A; 263.  $NH_3$  quad.
248. Watts, R. J., and D. Williams, *Phys. Rev.*, **72**, 1122L. Double-modulation spectrograph
249. Watts, R. J., and D. Williams, *Phys. Rev.*, **72**, 980L. Stark spectrograph
250. Weidner, R. T., *Phys. Rev.*, **72**, 1268L. ICl
251. Williams, D., *Phys. Rev.*, **72**, 974L.  $NH_3$

## 1948

252. Bardeen, J., and C. H. Townes, *Phys. Rev.*, **73**, 97. Th. h.f.s. in molecules
253. Bardeen, J., and C. H. Townes, *Phys. Rev.*, **73**, 647. Second-order
- Errata: Phys. Rev.*, **73**, 1204. quadrupole h.f.s.
254. Bleaney, B., *Repts. Progr. Phys.*, **11**, 178 (1946-1947). Review
255. Bleaney, B., and J. H. N. Loubser, *Nature*, **161**, 522L.  $NH_3$  pressure broadening
256. Bleaney, B., and R. P. Penrose, *Proc. Phys. Soc. London*, **60**, 83. Power saturation
257. Bleaney, B., and R. P. Penrose, *Proc. Phys. Soc. London*, **60**, 540.  $NH_3$  pressure broadening
258. Bragg, J. K., *Phys. Rev.*, **74**, 533. Th. quad. h.f.s.
259. Carter, R. L., and W. V. Smith, *Phys. Rev.*, **73**, 1053; **74**, 123A. asymmetric molecules
260. Coates, R. J., *Rev. Sci. Instr.*, **19**, 586. Power saturation
261. Coles, Donald K., *Phys. Rev.*, **74**, 1194L. Grating for mm waves
262. Collins, G. B., *Microwave Magnetrons*, MIT Radiation Laboratory Series, Vol. 6, McGraw-Hill Book Company, Inc., New York.  $CH_3OH$
263. Crain, C. M., *Phys. Rev.*, **74**, 691. Dielectric constants of gases
264. Cunningham, G. L., W. I. LeVan, and W. D. Gwinn, *Phys. Rev.*, **74**, 1537L. Ethylene oxide
265. Culshaw, W., *Proc. Phys. Soc.*, **61**, 562. Microwave Michelson interferometer
266. Dailey, B. P., K. Rusinow, R. G. Shulman, and C. H. Townes, *Phys. Rev.*, **74**, 1243A.  $AsF_3$
267. Dumond, J. W. M., and E. R. Cohen, *Revs. Mod. Phys.*, **20**, 82. Survey physical constants
268. Edgell, W. F., and A. Roberts, *J. Chem. Phys.*, **16**, 1002L.  $CF_3CH_3$
269. Fano, U., *J. Research Natl. Bur. Standards*, **40**, 215. Th. Stark effect with h.f.s.
270. Foley, H. M., *Phys. Rev.*, **73**, 259L. Th. pressure broadening

271. LeBot, Jean, *J. Phys. Radium* **9**, 1D; Freymann, M., and R. Freymann, 29D; M. Freymann, R. Freymann, and Jean LeBot, 45D. Review
272. Gilliam, O. R., H. D. Edwards, and W. Gordy, *Phys. Rev.*, **73**, 635L. H.f.s. in  $\text{CH}_3\text{I}$ ,  $\text{ICN}$
273. Ginsburg, N., *Phys. Rev.*, **74**, 1052. I.R. spectrum  $\text{H}_2\text{O}$ ,  $\text{D}_2\text{O}$
274. Golden, S., *J. Chem. Phys.*, **16**, 78. Th. rotational energy asymmetric rotor
275. Golden, S., *J. Chem. Phys.*, **16**, 250. *Errata*: **17**, 586L. Th. rotational energy asymmetric rotor
276. Golden, S., T. Wentink, R. Hillger, and M. W. P. Strandberg, *Phys. Rev.*, **73**, 92. Stark effect  $\text{H}_2\text{O}$
277. Golden, S., and E. Bright Wilson, Jr., *J. Chem. Phys.*, **16**, 669. Th. Stark effect asymmetric rotor
278. Gordy, W., *Revs. Mod. Phys.*, **20**, 668. Review
279. Gordy, W., H. Ring, and A. B. Burg, *Phys. Rev.*, **74**, 1191L. *Errata*: **75**, 208L. Nuclear moments  $\text{B}^{10}$ ,  $\text{B}^{11}$
280. Gordy, W., James W. Simmons, and A. G. Smith, *Phys. Rev.*, **74**, 243; 1246A.  $\text{CH}_3\text{Cl}$ ,  $\text{CH}_3\text{Br}$ ,  $\text{CH}_3\text{I}$
281. Hamilton, D. R., J. K. Knipp, and J. B. H. Kuper, *Klystrons and Microwave Triodes*, MIT Radiation Laboratory Series, Vol. 7, McGraw-Hill Book Company, Inc., New York.
282. Henderson, R. S., *Phys. Rev.*, **74**, 107L. *Errata*: **74**, 626L.  $\text{NH}_3$  h.f.s.
283. Henderson, R. S., and J. H. Van Vleck, *Phys. Rev.*, **74**, 106L. Fine-structure polyatomic molecules
284. Herman, H., and R. J. Coates, *N.R.L. Rept.* R-3223. Mm-wave components
285. Herman, R. C., and W. H. Shaffer, *J. Chem. Phys.*, **16**, 453. Rotation-vibration polyatomic molecules
286. Hershberger, W. D., *J. Appl. Phys.*, **19**, 411; *Phys. Rev.*, **73**, 1249A. Sensitivity Stark spectrometer
287. Hershberger, W. D., and L. E. Norton, *RCA Rev.*, **9**, 38. Frequency stabilization on microwave lines
288. Husten, B. F., and H. Lyons, *Trans. AIEE*, Part 1, **67**, 321. Microwave frequency measurement
289. Jablónski, A., *Phys. Rev.*, **73**, 258L. Th. pressure broadening
290. Jauch, J. M., *Phys. Rev.*, **74**, 1262A. Th.  $\text{NH}_3$  h.f.s.
291. Jen, C. K., *Phys. Rev.*, **73**, 1248A; **74**, 1246A; **74**, 1396. Zeeman effect  $\text{NH}_3$ ,  $\text{CH}_3\text{Cl}$ ,  $\text{SO}_2$
292. Jen, C. K., *J. Appl. Phys.*, **19**, 649. Dielectric constant gases
293. Karplus, R., *Phys. Rev.*, **73**, 1027. High-frequency modulation
294. Karplus, R., *Phys. Rev.*, **73**, 1120L. Power saturation  $\text{NH}_3$
295. Karplus, R., *Phys. Rev.*, **74**, 223. Power saturation
296. Karplus, R., *J. Chem. Phys.*, **16**, 1170. Th. molecular rotational energy
297. Karplus, R., and J. Schwinger, *Phys. Rev.*, **73**, 1020. Th. power saturation
298. Kessler, M., and Gordy, W., *Phys. Rev.*, **74**, 354A. Microwave spectrometer
299. Klinger, H. H., *Funk und Ton*, **2**, 135. Review mm waves
300. Klinger, H. H., *Funk und Ton*, **2**, 183. Review microwaves
301. Lamont, H. R. L., *Phys. Rev.*, **74**, 353L. Atmospheric absorption 6 mm
302. Lamont, H. R. L., *Proc. Phys. Soc. London*, **61**, 562. Atmospheric absorption 6 mm
303. Mizushima, M., *Phys. Rev.*, **74**, 705L. Th.  $\text{NH}_3$  pressure broadening



304. Montgomery, C. G., R. H. Dicke, and E. M. Purcell, *Principles of Microwave Circuits*, MIT Radiation Laboratory Series, Vol. 8, McGraw-Hill Book Company, Inc., New York.
305. Mott, N. F., and I. N. Sneddon, *Wave Mechanics and Its Applications*, Oxford University Press, London.
306. Newton, R. R., and L. H. Thomas, *J. Chem. Phys.*, **16**, 310. Th.  $\text{NH}_3$  inversion
307. Nierenberg, W. A., I. I. Rabi, and M. Slotnick, *Phys. Rev.*, **73**, 1430; **74**, 1246A. Stark effect with h.f.s.
308. Pollard, E. C., and J. M. Sturtevant, *Microwaves and Radar Electronics*, John Wiley & Sons, Inc., New York.
309. Pound, R. V., *Microwave Mixers*, MIT Radiation Laboratory Series, Vol. 16, McGraw-Hill Book Company, Inc., New York.
310. de Quevedo, J. L., and W. V. Smith, *J. Appl. Phys.*, **19**, 831. Frequency stabilization on microwave lines
311. Raev, A., *Annuaire Univ. Sofia, Fac. Sci., Livre 1*, **45**, 303. Review
312. Ragan, G. L., *Microwave Transmission Circuits*, MIT Radiation Laboratory Series, Vol. 9, McGraw-Hill Book Company, Inc., New York.
313. Richards, P. I., and H. S. Snyder, *Phys. Rev.*, **73**, 269L. Th. power saturation
314. Roberts, A., *Phys. Rev.*, **73**, 1405L.  $\text{C}^{14}$  in OCS
315. Sharbaugh, A. H., *Phys. Rev.*, **74**, 1870L.  $\text{SiH}_3\text{Cl}$
316. Shulman, R. G., B. P. Dailey, and C. H. Townes, *Phys. Rev.*, **74**, 846L. Ethylene oxide
317. Simmons, J. W., and W. Gordy, *Phys. Rev.*, **73**, 713; **74**, 123A.  $\text{NH}_3$  h.f.s.
318. Skinner, H. A., *J. Chem. Phys.*, **16**, 553L. Structure methyl halides
319. Smith, A. G., H. Ring, W. V. Smith, and W. Gordy, *Phys. Rev.*, **73**, 633. H.f.s. ICN,  $\text{N}_2\text{O}$
320. Smith, A. G., H. Ring, W. V. Smith, and W. Gordy, *Phys. Rev.*, **74**, 370, 123A. ClCN, BrCN, ICN
321. Smith, D. F., *Phys. Rev.*, **74**, 506L.  $\text{NH}_3$  pressure broadening
322. Snyder, H. S., and P. I. Richards, *Phys. Rev.*, **73**, 1178. Th. power saturation
323. Strandberg, M. W. P., *Phys. Rev.*, **74**, 1245A.  $\text{D}_2\text{O}$
324. Strandberg, M. W. P., T. Wentink, R. E. Hillger, G. H. Wannier, and M. L. Deutsch, *Phys. Rev.*, **73**, 188L. Stark effect HDO
325. Torrey, H. C., and C. A. Whitmer, *Crystal Rectifiers*, MIT Radiation Laboratory Series, Vol. 15, McGraw-Hill Book Company, Inc., New York.
326. Townes, C. H., H. M. Foley, and W. Low, *Phys. Rev.*, **76**, 1415L. Th. nuclear quad. moments
327. Townes, C. H., and S. Geschwind, *Phys. Rev.*, **74**, 626L.  $\text{S}^{33}$  in OCS
328. Townes, C. H., and S. Geschwind, *J. Appl. Phys.*, **19**, 795L. Th. sensitivity of spectrometer
329. Townes, C. H., A. N. Holden, and F. R. Merritt, *Phys. Rev.*, **74**, 1113. OCS, ClCN, BrCN, ICN
330. Townes, C. H., F. R. Merritt, and B. D. Wright, *Phys. Rev.*, **73**, 1334; 1249A. ICl

331. Trischka, J. W., *Phys. Rev.*, **74**, 718. H.f.s. CsF  
 332. Trischka, J. W., *Phys. Rev.*, **76**, 1365. CsF mol. beam  
 333. Tuller, W. G., W. C. Galloway, and F. P. Zaffarano, *Proc. IRE*, **36**, 794. Frequency stabilization  
 334. Turner, T. E., Thesis, McGill University. CH<sub>2</sub>Cl<sub>2</sub>, CH<sub>2</sub>Br<sub>2</sub>  
 335. Unterberger, R. R., and Smith, W. V., *Rev. Sci. Instr.*, **19**, 580. Microwave frequency standard  
 336. Watts, R. J., W. J. Pietenpol, J. D. Rogers, and D. Williams, *Phys. Rev.*, **74**, 1246A. Power saturation  
 336a. Wesson, L. G., *Tables of Electric Dipole Moments*, Technology Press, Cambridge, Mass.  
 337. Weidner, R. T., *Phys. Rev.*, **73**, 254L. ICl  
 338. Weingarten, I. R., Thesis, Columbia University. NH<sub>3</sub> high pressure  
 339. Wick, G. C., *Phys. Rev.*, **73**, 51. Mol. magnetic effects  
 340. Witmer, E. E., *Phys. Rev.*, **74**, 1247A; **74**, 1250A. Th. asymmetric rotor
- 1949**
341. Anderson, P. W., *Phys. Rev.*, **75**, 1450L. Th. NH<sub>3</sub> pressure broadening  
 342. Anderson, P. W., *Phys. Rev.*, **76**, 647, 471A. Th. pressure broadening  
 343. Anderson, P. W., Thesis, Harvard. Th. pressure broadening  
 344. Bak, B., E. S. Knudsen, and E. Madsen, *Phys. Rev.*, **75**, 1622L. C<sub>6</sub>H<sub>5</sub>Br, C<sub>2</sub>H<sub>5</sub>OH  
 345. Beard, C. I., and B. P. Dailey, *J. ACS*, **71**, 929. (CH<sub>3</sub>)<sub>2</sub>CO, CH<sub>3</sub>NO<sub>2</sub>  
 346. Benedict, W. S., *Phys. Rev.*, **75**, 1317A. CH<sub>3</sub>NCS, CH<sub>3</sub>SCN  
 347. Beringer, R., and J. G. Castle, Jr., *Phys. Rev.*, **75**, 1963L. Centrifugal distortion  
 348. Beringer, R., and J. G. Castle, Jr., *Phys. Rev.*, **76**, 868L. Zeeman effect O<sub>2</sub>  
 349. Bianco, D., G. Matlack, and A. Roberts, *Phys. Rev.*, **76**, 473A. Zeeman effect NO  
 350. Birks, J. B., *J. Brit. Inst. Radio Engrs.*, **9**, 10. OCS, CH<sub>3</sub>Cl  
 351. Bitter, F., *Phys. Rev.*, **76**, 833. Review microwave physics  
 352. Bragg, J. K., and S. Golden, *Phys. Rev.*, **75**, 735. Resonant modulation  
 353. Bragg, J. K., and A. H. Sharbaugh, *Phys. Rev.*, **75**, 1774L. Th. h.f.s. asymmetric rotor  
 354. Burgess, J. S., *Phys. Rev.*, **76**, 1267L. CH<sub>2</sub>O  
 355. Carrara, N., P. Lombardini, R. Cine, and L. Sacconi, *Nuovo Cimento*, **6**, 552. I.R. spectrum  
 356. Cohen, V. W., W. S. Koski, and T. Wentink, Jr., *Phys. Rev.*, **76**, 703L. deuteroammonia  
 357. Coles, D. K., and R. H. Hughes, *Phys. Rev.*, **76**, 178A. NH<sub>3</sub> inversion  
 358. Coles, D. K., and R. H. Hughes, *Phys. Rev.*, **76**, 858L. S<sup>35</sup> in OCS  
 359. Crawford, M. F., and A. L. Schawlow, *Phys. Rev.*, **76**, 1310. N<sub>2</sub>O  
 360. Cunningham, G. L., A. W. Boyd, W. D. Gwinn, and W. I. LeVan, *J. Chem. Phys.*, **17**, 211L. CF<sub>3</sub>Cl  
 361. Dailey, B. P., *Anal. Chem.*, **21**, 540. Atomic h.f.s.  
 362. Dailey, B. P., J. M. Mays, and C. H. Townes, *Phys. Rev.*, **76**, 136L, 472A. Ethylene oxide  
 363. Dailey, B. P., H. Minden, and R. G. Shulman, *Phys. Rev.*, **75**, 1319(A). Chemical analysis by microwave spectroscopy  
 364. Davis, L., B. T. Feld, C. W. Zabel, and J. R. Zacharias, *Phys. Rev.*, **76**, 1076. CH<sub>3</sub>Cl, SiH<sub>3</sub>Cl, GeH<sub>3</sub>Cl  
 CH<sub>3</sub>CF<sub>3</sub>  
 H.f.s. atomic Cl

365. Edwards, H. D., O. R. Gilliam, and W. Gordy, *Phys. Rev.*, **76**, 196A.
366. Gilbert, D. A., A. Roberts, and P. A. Griswold, *Phys. Rev.*, **76**, 1723L; *Phys. Rev.*, **77**, 742A (1950).
367. Gilliam, O. R., H. D. Edwards, and W. Gordy, *Phys. Rev.*, **75**, 1014; *Phys. Rev.*, **76**, 195A.
368. Golay, M. J. E., *Rev. Sci. Instr.*, **20**, 816.
369. Golden, S., and J. K. Bragg, *J. Chem. Phys.*, **17**, 439.
370. Goldstein, J. H., and J. K. Bragg, *Phys. Rev.*, **75**, 1453L.
371. Gordy, W., O. R. Gilliam, and R. Livingston, *Phys. Rev.*, **75**, 443.
372. Hainer, R. M., P. C. Cross, and G. W. King, *J. Chem. Phys.*, **17**, 826.
373. Hedrick, L. C., *Rev. Sci. Instr.*, **20**, 781.
374. Hicks, B. L., E. Ossofsky, and R. N. Jones, *Ballistics Res. Lab., Tech. Note* 130.
375. Hughes, H. K., *Phys. Rev.*, **76**, 1675.
376. Jen, C. K., *Phys. Rev.*, **76**, 1494; **75**, 1319A.
377. Jen, C. K., *Phys. Rev.*, **76**, 471A.
378. Karplus, R., and A. H. Sharbaugh, *Phys. Rev.*, **75**, 889L. *Errata*: 1449L.
379. Knight, G., and B. T. Feld, *MIT Research Lab., Rept.* 123; *Phys. Rev.*, **74**, 354A (1948).
380. Kusch, P., *Phys. Rev.*, **75**, 887.
381. Lamb, W. E., Jr., and M. Skinner, *Phys. Rev.*, **75**, 1325.
382. Lassettre, E. N., and L. B. Dean, Jr., *J. Chem. Phys.*, **17**, 317.
383. Lawrance, R. B., *Research Lab. Electronics, MIT, Prog. Rept.*, Jan. 15 (1949).
384. Lenard, A., *Tables for Calculation of Stark and Zeeman effects*, Department of Physics, State University of Iowa.
385. Lengyel, B. A., *Proc. IRE*, **37**, 1242.
386. Lengyel, B. A., and A. J. Simmons, *N.R.L. Rept.*, 3562.
387. Lew, H., *Phys. Rev.*, **76**, 1086.
388. Lines, A. W., *T.R.E. J.*, July, 1949, p. 1.
389. Livingston, R., O. R. Gilliam, and W. Gordy, *Phys. Rev.*, **76**, 149L.
390. Loubser, J. H. N., and C. H. Townes, *Phys. Rev.*, **76**, 178A.
391. Low, W., and C. H. Townes, *Phys. Rev.*, **76**, 1295; **75**, 1319A.
392. Low, W., and C. H. Townes, *Phys. Rev.*, **75**, 529L; 1318A.
393. Margenau, H., *Phys. Rev.*, **76**, 121; 585A.
394. Margenau, H., *Phys. Rev.*, **76**, 1423.
395. Matossi, F., *Phys. Rev.*, **76**, 1845.
396. McAfee, K. B., Jr., R. H. Hughes, and E. B. Wilson, Jr., *Rev. Sci. Instr.*, **20**, 821.
397. Millman, G. H., and R. C. Raymond, *J. Appl. Phys.*, **20**, 413L.

CH<sub>3</sub>OH, CH<sub>3</sub>NH<sub>2</sub>

FCl

CH<sub>3</sub>F, CHF<sub>3</sub>, PF<sub>3</sub>

I.R. detector

Th. asymmetric rotor

H.f.s. vinyl chloride

Magnetic moment I<sup>127</sup>,  
I<sup>129</sup>

Th. asymmetric rotor

Square-wave generator

Free radicals

Stark effect strong fields

Paschen-Back effect;

NH<sub>3</sub>, N<sub>2</sub>OMagnetic effects H<sub>2</sub>O,  
HDOStark effect CH<sub>3</sub>ClTh. h.f.s. asymmetric  
rotorMol. h.f.s. Li<sup>6</sup>Fine-structure He<sup>+</sup>

Mol. quad. moments

H.f.s. in H

Tables Stark and  
Zeeman effectsMicrowave  
interferometerMicrowave  
interferometer

H.f.s. atomic Al

Survey mm waves

I<sup>129</sup> in CH<sub>3</sub>I1.5 to 2-mm magnetron  
harmonicsTh. Stark effect  
symmetric rotorO<sup>17</sup> and S<sup>36</sup> in OCSTh. NH<sub>3</sub> pressure  
broadeningTh. NH<sub>3</sub> pressure  
broadeningI.R. pressure  
broadening

Stark spectrometer

Absorption at high  
pressure



398. Mizushima, M., *J. Phys. Soc. Japan*, **4**, 191 (1949). Th.  $\text{NH}_3$
400. Moore, C. E., Atomic Energy Levels, *Natl. Bur. Standards Circ.* 467.
401. Mulliken, R. S., C. A. Rieke, D. Orloff, and H. Orloff, *J. Chem. Phys.*, **17**, 510L. Overlap integrals
402. Nielsen, H. H., *Phys. Rev.*, **75**, 1961L. Th. *l*-type doubling
403. Pietenpol, W. J., and J. D. Rogers, *Phys. Rev.*, **76**, 690L.  $\text{CH}_2\text{Br}_2$
404. Pippard, A. B., *J. Sci. Instr.*, **26**, 296. Microwave interferometer
405. Roberts, A., Y. Beers, and A. G. Hill, *MIT Research Lab. Electronics, Tech. Rept.* 120. H.f.s. atomic Cs
406. Roberts, A., and W. F. Edgell, *J. Chem. Phys.*, **17**, 742L; *Phys. Rev.*, **76**, 178A.  $\text{CF}_2\text{CH}_2$
407. Robinson, D. Z., *J. Chem. Phys.*, **17**, 1022. Th. HCl structure
408. Schiff, L. I., *Quantum Mechanics*, McGraw-Hill Book Company, Inc., New York.
409. Sharbaugh, A. H., J. K. Bragg, T. C. Madison, and V. G. Thomas, *Phys. Rev.*, **76**, 1419L.  $\text{SiH}_3\text{Br}$
410. Sharbaugh, A. H., T. C. Madison, and J. K. Bragg, *Phys. Rev.*, **76**, 1529L.  $\text{NH}_3$  inversion
411. Sharbaugh, A. H., and J. Mattern, *Phys. Rev.*, **75**, 1102L.  $\text{CH}_3\text{Br}$
412. Simmons, J. W., *Phys. Rev.*, **76**, 686L.  $\text{CD}_3\text{Cl}$ ,  $\text{CD}_3\text{I}$
413. Smith, A. G., W. Gordy, J. W. Simmons, and W. V. Smith, *Phys. Rev.*, **75**, 260. Techniques 3 to 5 mm
414. Smith, W. V., and R. R. Unterberger, *J. Chem. Phys.*, **17**, 1348L.  $\text{CHCl}_3$
415. Strandberg, M. W. P., *J. Chem. Phys.*, **17**, 901. HDO
416. Strandberg, M. W. P., C. Y. Meng, and J. G. Ingersoll, *Phys. Rev.*, **75**, 1524.  $\text{O}_2$
417. Strandberg, M. W. P., C. S. Pearsall, and M. T. Weiss, *J. Chem. Phys.*, **17**, 429L.  $\text{H}_3\text{B}^{10}\text{CO}$
418. Strandberg, M. W. P., T. Wentink, Jr., and A. G. Hill, *Phys. Rev.*, **75**, 827; *Phys. Rev.*, **73**, 1249A. OCSe
419. Strandberg, M. W. P., T. Wentink, Jr., and R. L. Kyhl, *Phys. Rev.*, **75**, 270. OCS
420. Stutt, C. A., *MIT Research Lab. Electronics, Tech. Rept.* 105. Lock-in amplifier
421. Townes, C. H., and L. C. Aamodt, *Phys. Rev.*, **76**, 691L.  $\text{Cl}^{36}$  in  $\text{ClCN}$
422. Townes, C. H., and B. P. Dailey, *J. Chem. Phys.*, **17**, 782; *Phys. Rev.*, **74**, 1245A. Th. quad. coupling
423. Townes, C. H., J. M. Mays, and B. P. Dailey, *Phys. Rev.*, **76**, 700L, 137A. Nuclear moments
- 423a. Trischka, J. W., *Phys. Rev.*, **76**, 1365. Ge, Si
424. Van Vleck, J. H., and H. Margenau, *Phys. Rev.*, **76**, 1211, 585A. CsF, mol. beam
425. Westenberg, A. A., J. H. Goldstein, and E. B. Wilson, Jr., *J. Chem. Phys.*, **17**, 1319; *Phys. Rev.*, **76**, 472A. Th. pressure broadening
- HCCCl

## 1950

426. Allen, P. W., and L. E. Sutton, *Acta Cryst.*, **3**, Part 1, 46. Table mol. structure from electron diffraction
427. Amble, E., and B. P. Dailey, *J. Chem. Phys.*, **18**, 1422L.  $\text{HN}_3$
428. Anderson, P. W., *Phys. Rev.*, **80**, 511.  $\text{NH}_3$  pressure broadening quad.-induced dipole

429. Autler, S. H., and C. H. Townes, *Phys. Rev.*, **78**, 340A. Resonant modulation
430. Baird, D. H., R. M. Fristrom, and M. H. Sirvetz, *Rev. Sci. Instr.*, **21**, 881L. Stark cells
431. Bak, B., E. S. Knudsen, E. Madsen, and J. Rastrup-Andersen, *Phys. Rev.*, **79**, 190L. CH<sub>2</sub>CO
432. Bak, B., R. Sloan, and D. Williams, *Phys. Rev.*, **80**, 101L. SCSe
433. Barriol, J., *J. phys. radium*, **11**, 52. Stark effect th.
434. Beard, C. I., and B. P. Dailey, *J. Chem. Phys.*, **18**, 1437; *Phys. Rev.*, **75**, 1318A. *Errata*: **19**, 975L (1951). HNCS
435. Beringer, R., and J. G. Castle, Jr., *Phys. Rev.*, **78**, 581, 340A. NO
436. Bernstein, H. J., *J. Chem. Phys.*, **18**, 1514L. NOCl
437. Bersohn, R., *J. Chem. Phys.*, **18**, 1124L. Th. quad. coupling, three nuclei
438. Birnbaum, G., *Phys. Rev.*, **77**, 144L. NH<sub>3</sub> dispersion
439. Bleaney, B., and J. H. N. Loubser, *Proc. Phys. Soc.*, **63A**, 483. NH<sub>3</sub>, CH<sub>3</sub>Cl, CH<sub>3</sub>Br, high pressures
440. Bragg, J. K., T. C. Madison, and A. H. Sharbaugh, *Phys. Rev.*, **77**, 148L. *Errata*: 571L. CH<sub>2</sub>CFCI
441. Burkhalter, J. H., R. S. Anderson, W. V. Smith, and W. Gordy, *Phys. Rev.*, **79**, 651; *Phys. Rev.*, **77**, 152L (1950); **79**, 224A. O<sub>2</sub> fine structure
442. Casimir, H. B. G., *Ned. Tijdschr. Natuurk.*, **16**, 198. Th. h.f.s.
443. Castle, J. G., Jr., and R. Beringer, *Phys. Rev.*, **80**, 114L. NO<sub>2</sub>
444. Coester, F., *Phys. Rev.*, **77**, 454. Stark-Zeeman th.
445. Coles, D. K., *Advances in Electronics*, **2**, 299. Review
446. Coles, D. K., W. E. Good, and R. H. Hughes, *Phys. Rev.*, **79**, 224A. CH<sub>3</sub>CN
447. Cornwell, C. D., *J. Chem. Phys.*, **18**, 1118L. C<sub>2</sub>H<sub>3</sub>Br, B<sub>2</sub>H<sub>5</sub>Br
448. Crain, C. M., *Rev. Sci. Instr.*, **21**, 456. Atmosphere refractive index
449. Crawford, B. L., Jr., and D. E. Mann, *Ann. Rev. Phys. Chem.*, **1**, 151. Review
450. Culshaw, W., *Proc. Phys. Soc.*, **B63**, 939. Michelson interferometer
451. Epprecht, G. W., *Z. angew. Math. Phys.*, **1**, 138. Dielectric constants of gases
452. Eshbach, J. R., R. E. Hillger, and C. K. Jen, *Phys. Rev.*, **80**, 1106; *Phys. Rev.*, **78**, 339A. S<sup>33</sup> nuclear magnetic moment
453. Essen, L., and K. D. Froome, *Proc. Phys. Soc.*, **B64**, 862. Dielectric constants of gases
454. Fletcher, E. W., and S. P. Cooke, *Cruft Laboratory O.N.R. Rept.*, 64. Frequency standard
455. Freymann, M. R., *L'Onde électrique*, **30**, 416. Review
456. Geschwind, S., H. Minden, and C. H. Townes, *Phys. Rev.*, **78**, 174L; *Phys. Rev.*, **79**, 226A. OCSe nuclear properties
457. Gilliam, O. R., C. M. Johnson, and W. Gordy, *Phys. Rev.*, **78**, 140. 2- to 3-mm spectroscopy
458. Girdwood, B. M., *Can. J. Research*, **28**, 180. CH<sub>3</sub>OH
459. Goldstein, J. H., and J. K. Bragg, *Phys. Rev.*, **78**, 347A. Asymmetric molecules with quad. coupling
460. Good, W. E., *Proc. Natl. Elec. Conf.*, **6**, 29. Techniques
461. Gordy, W., H. Ring, and A. B. Burg, *Phys. Rev.*, **78**, 512; *Phys. Rev.*, **75**, 1325A. BH<sub>3</sub>CO
462. Gordy, W., and J. Sheridan, *Phys. Rev.*, **79**, 224A. Methyl mercuric halides
463. Grabner, L., and V. Hughes, *Phys. Rev.*, **79**, 819. KF mol. beams

464. Griffing, V., *J. Chem. Phys.*, **18**, 744.
465. Hartz, T. R., and A. van der Ziel, *Phys. Rev.*, **78**, 473L. Power saturation  
Square-wave double modulation
467. Henry, A. F., *Phys. Rev.*, **80**, 396; **79**, 213A. O<sub>2</sub> Zeeman th.
468. Henry, A. F., *Phys. Rev.*, **80**, 549. NO Zeeman h.f.s.
469. Herman, R. C., and W. H. Shaffer, *J. Chem. Phys.*, **18**, 1207. Vibration-rotation  
X<sub>2</sub>Y<sub>2</sub>Z<sub>2</sub> molecules
470. Hershberger, W. D., and L. E. Norton, *J. Franklin Inst.*, **249**, 359. Stabilization servo theory
471. Herzberg, G., *Spectra of Diatomic Molecules*, D. Van Nostrand Company, Inc., New York.
472. Holstein, T., *Phys. Rev.*, **79**, 744L. Th. pressure broadening
473. Howard, R. R., and W. V. Smith, *Phys. Rev.*, **77**, 840L. Pressure broadening, temperature dependence
474. Howard, R. R., and W. V. Smith, *Phys. Rev.*, **79**, 128; 225A. Collision diameters
476. Hughes, V., and L. Grabner, *Phys. Rev.*, **79**, 314. RbF mol. beams
477. Hughes, V., and L. Grabner, *Phys. Rev.*, **79**, 829. Diatomic molecule theory, mol. beams
478. Jones, L. C., *Phys. Rev.*, **77**, 741A. Pressure broadening
479. Jones, L. H., J. N. Shoolery, R. G. Shulman, and D. M. Yost, *J. Chem. Phys.*, **18**, 990L. HNCO
480. Kessler, W., H. Ring, R. Trambarulo, and W. Gordy, *Phys. Rev.*, **79**, 54. CH<sub>3</sub>CN, CH<sub>3</sub>NC
481. Kisliuk, P., and C. H. Townes, *Phys. Rev.*, **78**, 347A; *J. Chem. Phys.*, **18**, 1109. PCl<sub>3</sub>, AsCl<sub>3</sub>
482. Kisliuk, P., and C. H. Townes, *J. Research Natl. Bur. Standards*, **44**, 611. Table microwave lines
483. Klages, G., *Experientia*, **6**, 321. Review
- 483a. Kusch, P., and A. G. Prodell, *Phys. Rev.*, **79**, 1009. H.f.s. in H and D
484. Lamb, W. E., Jr., and R. C. Retherford, *Phys. Rev.*, **79**, 549. Atomic H fine structure
485. Lamb, W. E., Jr., and M. Skinner, *Phys. Rev.*, **78**, 539. Fine structure He<sup>+</sup>
486. Lamont, H. R. L., *Wave Guides*, 3d ed., Methuen & Co., Ltd., London.
488. Lide, D. R., and D. K. Coles, *Phys. Rev.*, **80**, 911L. CH<sub>3</sub>SiH<sub>3</sub> internal rotation
489. Loubser, J. H. N., and J. A. Klein, *Phys. Rev.*, **78**, 348A. ND<sub>3</sub> mm waves
490. Low, W., and C. H. Townes, *Phys. Rev.*, **80**, 608; **79**, 198A. Nuclear masses
491. Low, W., and C. H. Townes, *Phys. Rev.*, **79**, 224A. OCS, OCSe Fermi resonance
492. Lyons, H., *J. Appl. Phys.*, **21**, 59L. Frequency dividers
493. Maier, W., *Z. Elektrochem.*, **54**, 521. Review
494. Margenau, H., and S. Bloom, *Phys. Rev.*, **79**, 213A. Th. pressure broadening
495. Margenau, H., and A. Henry, *Phys. Rev.*, **78**, 587. Th. NO
496. Matlack, G., G. Glockler, D. R. Bianco, and A. Roberts, *J. Chem. Phys.*, **18**, 332. CH<sub>3</sub>Cl
497. McAfee, K. B., Jr., *Phys. Rev.*, **78**, 340A. NO<sub>2</sub>
498. Minden, H. T., J. M. Mays, and B. P. Dailey, *Phys. Rev.*, **78**, 347A. CH<sub>3</sub>SiF<sub>3</sub>
499. Mizushima, M., *Research Chem. Phys.*, **29**, 25. Th. pressure broadening
500. Morgan, H. W., G. W. Keilholtz, W. V. Smith, and A. L. Southern, *O.R.N.L. Rept.* Y-621. ClCN isotopic analysis
501. Mulliken, R. S., *J. ACS*, **72**, 4493. Th. chemical binding
502. Murphy, J., and R. C. Raymond, *J. Appl. Phys.*, **21**, 1064. Dielectric constants of gases



503. Nielsen, H. H., *Phys. Rev.*, **77**, 130.
- 503a. Nethercot, A. H., Ph.D. Thesis, University of Michigan.
504. Nethercot, A. H., and C. W. Peters, *Phys. Rev.*, **79**, 225A.
505. Nielsen, H. H., *Phys. Rev.*, **78**, 296L.
506. Nielsen, H. H., *Phys. Rev.*, **78**, 415.
507. Nierenberg, W. A., *Phys. Rev.*, **80**, 1102L.
509. Pietenpol, W. J., J. D. Rogers, and D. Williams, *Phys. Rev.*, **78**, 480L.
510. Pierce, J. R., *Physics Today*, **3**, 24.
511. Pierce, J. R., *Travelling Wave Tubes*, D. Van Nostrand Company, Inc., New York.
512. Pryce, M. H. L., *Phys. Rev.*, **77**, 136.
513. Rainwater, J., *Phys. Rev.*, **79**, 432.
514. Ramsey, N. F., *Phys. Rev.*, **78**, 221.
515. Ramsey, N. F., *Phys. Rev.*, **78**, 699.
516. Rogers, J. D., H. L. Cox, and P. G. Braunschweiger, *Rev. Sci. Instr.*, **21**, 1014.
517. Rouse, A. G., A. V. Bushkovitch, L. C. Jones, C. A. Potter, and W. F. Sullivan, *Phys. Rev.*, **78**, 347A.
518. Senatore, S. J., *Phys. Rev.*, **78**, 293L.
519. Sharbaugh, A. H., *Rev. Sci. Instr.*, **21**, 120.
520. Sharbaugh, A. H., B. S. Pritchard, and T. C. Madison, *Phys. Rev.*, **77**, 302.
521. Sharbaugh, A. H., B. S. Pritchard, V. G. Thomas, J. M. Mays, and B. P. Dailey, *Phys. Rev.*, **79**, 189L.
522. Sharbaugh, A. H., V. G. Thomas, and B. S. Pritchard, *Phys. Rev.*, **78**, 64L.
523. Shaull, J. M., *Proc. IRE*, **38**, 6.
524. Sheridan, J., and W. Gordy, *Phys. Rev.*, **77**, 292L.
525. Sheridan, J., and W. Gordy, *Phys. Rev.*, **77**, 719L.
526. Sheridan, J., and W. Gordy, *Phys. Rev.*, **79**, 224A.
527. Sheridan, J., and W. Gordy, *Phys. Rev.*, **79**, 513.
528. Shulman, R. G., B. P. Dailey, and C. H. Townes, *Phys. Rev.*, **78**, 145; **75**, 472A.
529. Shulman, R. G., and C. H. Townes, *Phys. Rev.*, **77**, 421L; **78**, 347A.
530. Shulman, R. G., and C. H. Townes, *Phys. Rev.*, **77**, 500; **75**, 1318A.
531. Simmons, J. W., and W. E. Anderson, *Phys. Rev.*, **80**, 338.
532. Simmons, J. W., W. E. Anderson, and W. Gordy, *Phys. Rev.*, **77**, 77. *Errata*: **86**, 1055 (1952).
533. Simmons, J. W., and W. O. Swan, *Phys. Rev.*, **80**, 289L.
534. Smith, D. F., M. Tidwell, and D. V. P. Williams, *Phys. Rev.*, **77**, 420L.
535. Smith, D. F., M. Tidwell, and D. V. P. Williams, *Phys. Rev.*, **79**, 1007L.
536. Smith, W. V., and R. R. Howard, *Phys. Rev.*, **79**, 132; **76**, 473A.
537. Smythe, W. R., *Static and Dynamic Electricity*, 2d ed., McGraw-Hill Book Company, Inc., New York.
- CH<sub>3</sub>CN, CH<sub>3</sub>NC  
l doubling  
Mm-wave spark generator  
NH<sub>3</sub> infrared line widths  
l-doubling OCS, HCN  
Centrifugal stretching  
H.f.s. mol. beams  
Asymmetric tops  
Review mm waves  
Th. resonant modulation  
Th. nuclear quad.  
Mol. quad. moment  
"Chemical" effects, magnetic h.f.s.  
Frequency measurement  
Pressure broadening and shift  
POF<sub>3</sub>  
Stark spectrograph  
CF<sub>3</sub>Br  
GeH<sub>3</sub>Br, SiH<sub>3</sub>Br  
SiH<sub>3</sub>F  
Frequency standards  
CF<sub>3</sub>Br, CF<sub>3</sub>I, CF<sub>3</sub>CH  
SiF<sub>3</sub>H, SiF<sub>3</sub>CH<sub>3</sub>,  
SiF<sub>3</sub>Cl, SiF<sub>3</sub>Br  
CH<sub>3</sub>CCBr  
NF<sub>3</sub>  
Dipole moments  
OCS, HCN l-type doubling transitions  
OCS Stark effect  
CH<sub>3</sub>Cl, CH<sub>3</sub>Br, CH<sub>3</sub>I,  
ICN centrifugal distortion  
HCN  
CH<sub>3</sub>Br  
BrF  
BrCl  
Mol. quad. moments

538. Southern, A. L., H. W. Morgan, G. W. Keilholtz, and W. V. Smith, *Phys. Rev.*, **78**, 629A. Isotopic analysis
539. Sternheimer, R., *Phys. Rev.*, **80**, 102. Theory quad. coupling
- 539a. Takahashi, I., A. Okaya, T. Ogawa, and T. Hashi, *Mem. College Science, Univ. Kyoto, A*, **26**, 113. Microwave spectrometer
540. Tomassini, M., *Nuovo Cimento*, **7**, 1.  $\text{NH}_3$
541. Torkington, P., *J. Chem. Phys.*, **18**, 407. Internal rotation
542. Townes, C. H., and B. P. Dailey, *Phys. Rev.*, **78**, 346A. Quad. coupling and ionic character
543. Trambarulo, R., and W. Gordy, *Phys. Rev.*, **79**, 224A.  $\text{CD}_3\text{NC}$ ,  $\text{CD}_3\text{CN}$
544. Trambarulo, R., and W. Gordy, *J. Chem. Phys.*, **18**, 1613.  $\text{CH}_3\text{CCH}$
545. Unterberger, R. R., R. Trambarulo, and W. V. Smith, *J. Chem. Phys.*, **18**, 565L.  $\text{CHCl}_3$
546. Weiss, M. T., M. W. P. Strandberg, R. B. Lawrance, and C. C. Loomis, *Phys. Rev.*, **78**, 202.  $\text{B}^{10}$  spin
547. Wells, A. F., *Structural Inorganic Chemistry*, Clarendon Press, Oxford.
548. Westenberg, A. A., and E. B. Wilson, Jr., *J. ACS*, **72**, 199.  $\text{CHCCN}$
549. Whiffen, D. H., *Quart. Rev.*, **4**, 131. Review rotation spectra
550. Williams, J. Q., and W. Gordy, *J. Chem. Phys.*, **18**, 994. Tertiary butyl halides
551. Williams, J. Q., and W. Gordy, *Phys. Rev.*, **79**, 225A.  $\text{CHBr}_3$ ,  $\text{PBr}_3$
552. Wilson, E. B., Jr., *Faraday Soc. Discussion*, **9**, 108. Review

## 1951

553. Amble, E., *Phys. Rev.*, **83**, 210A. Trioxane
554. Anderson, R. S., C. M. Johnson, and W. Gordy, *Phys. Rev.*, **83**, 1061.  $\text{O}_2$  2.5 mm
555. Anderson, W. E., J. Sheridan, and W. Gordy, *Phys. Rev.*, **81**, 819.  $\text{GeF}_3\text{Cl}$
556. Anderson, R. S., W. V. Smith, and W. Gordy, *Phys. Rev.*, **82**, 264L.  $\text{O}_2$  line widths
557. Anderson, W. E., R. Trambarulo, J. Sheridan, and W. Gordy, *Phys. Rev.*, **82**, 58.  $\text{CF}_3\text{CCH}$
- 557a. Aslakson, C. I., *Trans. Am. Geophys. Union*, **32**, 813. Velocity of microwaves
- 557b. Barrow, R. F., et al., *Données spectroscopiques concernant les molécules diatomiques*, Hermann & Cie, Paris.
558. Beringer, R., and J. G. Castle, Jr., *Phys. Rev.*, **81**, 82.  $\text{O}_2$
559. Birnbaum, G., *Phys. Rev.*, **82**, 110L. Atmospheric refractive index
560. Birnbaum, G., S. J. Kryder, and H. Lyons, *J. Appl. Phys.*, **22**, 95. Dielectric constant gases
561. Burkhard, D. G., and D. M. Dennison, *Phys. Rev.*, **84**, 408.  $\text{CH}_3\text{OH}$
- 561a. Carlson, R. O., C. A. Lee, and B. P. Fabricand, *Phys. Rev.*, **85**, 784.  $\text{TlCl}$
562. Coles, D. K., W. E. Good, J. K. Bragg, and A. H. Sharbaugh, *Phys. Rev.*, **82**, 877.  $\text{NH}_3$  Stark
- 562a. Collins, T. L., A. O. Nier, and W. H. Johnson, Jr., *Phys. Rev.*, **84**, 717. Masses near  $A = 40$
563. Cornwell, C. D., *O.N.R. Rept.*, Iowa State, Jan. 1, 1951.  $\text{C}_2\text{H}_5\text{Br}$
564. Costain, C. C., *Phys. Rev.*, **82**, 108L.  $\text{NH}_3$
565. Crable, G. F., and W. V. Smith, *J. Chem. Phys.*, **19**, 502L.  $\text{SO}_2$

566. Cunningham, G. L., Jr., A. B. Boyd, R. J. Myers, W. D. Gwinn, and W. I. LeVan, *J. Chem. Phys.*, **19**, 676.
567. Dayhoff, E. S., *Rev. Sci. Instr.*, **12**, 1025L.
568. DeHeer, J., *Phys. Rev.*, **83**, 741.
- 568a. Deutsch, M., *Phys. Rev.*, **82**, 455L.
569. Dickinson, W. C., *Phys. Rev.*, **81**, 717.
570. Essen, L., and K. D. Froome, *Proc. Phys. Soc. B*, **64**, 862.
571. Ewen, H. I., and E. M. Purcell, *Phys. Rev.*, **83**, 881A; *Nature*, **168**, 356.
572. Freymann, R., *Physica*, **17**, 328.
- 572a. Friedburg, H., and W. Paul, *Naturwiss.*, **38**, 159.
573. Geschwind, S., Thesis, Columbia University.
574. Geschwind, S., and R. Gunther-Mohr, *Phys. Rev.*, **81**, 882L; **82**, 346A.
575. Geschwind, S., R. Gunther-Mohr, and C. H. Townes, *Phys. Rev.*, **81**, 288L; **82**, 343A.
- 575a. Gobau, G., *Proc. IRE*, **39**, 319.
576. Gokhale, B. V., and M. W. P. Strandberg, *Phys. Rev.*, **84**, 844L; **82**, 327A.
577. Gokhale, B. V., H. R. Johnson, and M. W. P. Strandberg, *Phys. Rev.*, **83**, 881A.
- 577a. Good, W. E., D. K. Coles, G. R. Gunther-Mohr, A. L. Schawlow, and C. H. Townes, *Phys. Rev.*, **83**, 880A.
578. Gordy, W., *J. Chem. Phys.*, **19**, 792.
579. Gorter, C. J., *Physica*, **17**, 169.
580. Goszini, A., *Nuovo Cimento*, **8**, 361.
581. Grabner, L., and V. Hughes, *Phys. Rev.*, **82**, 561.
582. Greenhow, C., and W. V. Smith, *J. Chem. Phys.*, **19**, 1298.
583. Gunther-Mohr, G. R., S. Geschwind, and C. H. Townes, *Phys. Rev.*, **81**, 289L.
585. Hedrick, L. C., *Rev. Sci. Instr.*, **22**, 537L.
586. Hill, R. M., and W. V. Smith, *Phys. Rev.*, **82**, 451L.
587. Hillger, R. E., and M. W. P. Strandberg, *Phys. Rev.*, **83**, 575; **82**, 327A.
588. Honerjäger, R., *Naturwiss.*, **38**, 34.
589. Hughes, R. H., *Instruments*, **24**, 1352.
590. Hughes, R. H., W. E. Good, and D. K. Coles, *Phys. Rev.*, **84**, 418; **77**, 741A (1950).
591. Hurd, F. K., and W. D. Hersberger, *Phys. Rev.*, **82**, 95L.
592. Jen, C. K., *Phys. Rev.*, **81**, 197.
593. Jen, C. K., *Physica*, **17**, 378.
594. Johnson, C. M., W. Gordy, and R. Livingston, *Phys. Rev.*, **83**, 1249L.
595. Johnson, C. M., R. Trambarulo, and W. Gordy, *Phys. Rev.*, **84**, 1178.
- Ethylene oxide,  
ethylene sulfide  
Klystron frequency  
controller  
Theory *l* doubling  
Positronium  
"Chemical effects,"  
magnetic resonance  
Dielectric constant of  
air and constituents  
Interstellar hydrogen  
radiation  
CH<sub>3</sub>CH<sub>2</sub>Cl  
Molecular beam  
focussing  
High-resolution  
microwave  
spectroscopy  
Ge, Si, S masses  
Cl<sup>35</sup>/Cl<sup>37</sup> quad. moment  
ratio  
Surface wave  
propagation  
O<sub>2</sub> line widths  
*L* uncoupling  
NH<sub>3</sub> h.f.s.  
Quad. coupling  
interpretation  
Review r.f. spectroscopy  
Dielectric constant of  
gases  
Two-quantum  
transition-  
molecular beams  
Mol. quad. N<sub>2</sub>, O<sub>2</sub>  
Polarization of nucleus  
Square-wave generator  
Mol. quad. moments  
HDS centrifugal  
distortion  
Review  
Analytical applications  
CH<sub>3</sub>OH  
CH<sub>3</sub>SH  
Mol. magnetic moments  
Magnetic moments  
Cl<sup>36</sup> moments  
2-3 mm spectroscopy



596. Johnson, K. C., *Proc. Inst. Elec. Engrs. London*, Part III, **98**, 77. Frequency stabilization
597. Kisliuk, P., and C. H. Townes, *Phys. Rev.*, **83**, 210A. AsCl<sub>3</sub>, SbCl<sub>3</sub>
598. Koch, B., *Ergeb. exakt. Naturw.*, **24**, 222. Review techniques
599. Lamb, W. E., and R. C. Retherford, *Phys. Rev.*, **81**, 222. Atomic H fine structure
600. Lamont, H. R. L., *Physica*, **17**, 446. Frequency stabilization
601. Lawrance, R. B., and M. W. P. Strandberg, *Phys. Rev.*, **83**, 363; **78**, 347A (1950). Centrifugal distortion  
H<sub>2</sub>CO
602. Leslie, D. C. M., *Phil. Mag.*, **42**, 37. Th. pressure broadening
603. Lide, D. R., *J. Chem. Phys.*, **19**, 1605. CH<sub>3</sub>SnH<sub>3</sub>
604. Lide, D. R., Jr., and D. K. Coles, *Phys. Rev.*, **80**, 911L. CH<sub>3</sub>SiH<sub>3</sub> internal rotation
605. Logan, R. A., R. E. Cote, and P. Kusch, *Phys. Rev.*, **85**, 280. Quad. interaction-mol. beams
606. Loomis, C. C., and M. W. P. Strandberg, *Phys. Rev.*, **81**, 798. PH<sub>3</sub>, AsH<sub>3</sub>, SbH<sub>3</sub>
- 606a. Luce, R. G., and J. W. Trischka, *Phys. Rev.*, **83**, 851L; **82**, 323A. CsCl
607. Lyons, H., L. J. Rueger, R. G. Nuckolls, and M. Kessler, *Phys. Rev.*, **81**, 630; **81**, 297A. Deuterated ammonias
608. Magnuson, D. W., *J. Chem. Phys.*, **19**, 1614L. Dielectric constant UF<sub>6</sub>
609. Magnuson, D. W., *J. Chem. Phys.*, **19**, 1071L; *Phys. Rev.*, **83**, 485A. NOF, dipole moments
610. Maier, W., *Ergeb. exakt. Naturw.*, **24**, 275. Review
611. Maier, W., *Landolt-Börnstein Tabellen*, Aufl. 6, B. 1, T. 2. Tables of mol. constants
612. Margenau, H., *Phys. Rev.*, **82**, 156. Th. pressure broadening
613. Marshall, W. F., *Electronics*, **24**, 92. Frequency standard
614. Mays, J. M., and C. H. Townes, *Phys. Rev.*, **81**, 940. Ge isotopes
615. McAfee, K. B., Jr., *Phys. Rev.*, **82**, 971L. NO<sub>2</sub>
616. Miller, S. L., A. Javan, and C. H. Townes, *Phys. Rev.*, **82**, 454; **83**, 209A. O<sup>18</sup> spin
617. Millman, S., *Proc. IRE*, **39**, 1035. Mm-wave tube
618. Minden, H. T., and B. P. Dailey, *Phys. Rev.*, **82**, 338A. CH<sub>3</sub>CF<sub>3</sub>, CH<sub>3</sub>SiF<sub>3</sub>  
hindered rotation
619. Mizushima, M., *Phys. Rev.*, **83**, 94; *Physica*, **17**, 453A. Th. pressure broadening  
*Errata: Phys. Rev.*, **84**, 363.
620. Mizushima, M., and T. Ito, *J. Chem. Phys.*, **19**, 739. Th. quad. coupling  
three nuclei
621. Muller, C. A., and J. N. Oort, *Nature*, **108**, 357. Interstellar hydrogen
622. Newell, G., Jr., and R. H. Dicke, *Phys. Rev.*, **83**, 1064L; **81**, 297A. Doppler width reduction
623. Nielsen, H. H., *Physica*, **17**, 432. *l* doubling
624. Nielsen, H. H., *Revs. Mod. Phys.*, **23**, 90. Vibration-rotation  
energies
625. Nierenberg, W. A., *Phys. Rev.*, **82**, 932. Spin-orbit coupling mol.  
beams
626. Nuckolls, R. G., L. J. Rueger, and H. Lyons, *Phys. Rev.*, **83**, 880. ND<sub>3</sub>
- 626a. Post, E. J., and H. F. Pit, *Proc. IRE*, **39**, 169. Stabilized crystal  
oscillator
627. Potter, C. A., A. V. Bushkovitch, and A. G. Rouse, *Phys. Rev.*, **83**, 987; **82**, 323A. NH<sub>3</sub> pressure  
broadening
628. Pierce, J. R., *Electronics*, **24**, 66. Mm wave review
629. Poynter, R. L., *O.N.R. Rept.*, Iowa State, Jan. 1, 1951. H<sub>2</sub>CCHI
630. Ramsey, N. F., *Phys. Rev.*, **87**, 1075. Magnetic effects of  
vibration and rotation
631. Reesor, G. E., *Can. J. Phys.*, **29**, 87. Absorption in excited H

632. Rogers, J. D., W. J. Pietenpol, and D. Williams, *Phys. Rev.*, **83**, 431; **77**, 741A; **82**, 323A. NOCl
633. Rogers, J. D., and D. Williams, *Phys. Rev.*, **82**, 131A. HN<sub>3</sub>
634. Rogers, J. D., and D. Williams, *Phys. Rev.*, **83**, 210A. HCOOH
635. Rogers, T. F., *Phys. Rev.*, **83**, 881A. Line shapes
636. Roubine, E., *Rev. Tech. C.F.T.H.*, **16**, 21. Stark spectrometer
637. Rueger, L. J., H. Lyons, and R. G. Nuckolls, *Rev. Sci. Instr.*, **22**, 428L. High-temperature Stark cell
638. Sawyer, K. A., and J. D., Kierstead, *MIT Research Lab. Electronics Tech., Rept.* 188. ND<sub>2</sub>H
639. Schuster, N. A., *Rev. Sci. Instr.*, **22**, 254. Phase sensitive detector
640. Shaw, T. M., and J. J. Windle, *J. Chem. Phys.*, **19**, 1063. CH<sub>3</sub>SH
641. Sheridan, J., and W. Gordy, *J. Chem. Phys.*, **19**, 965. Trifluorosilane derivatives
642. Shimoda, K., and T. Nishikawa, *J. Phys. Soc. Japan*, **6**, 512. Atomic Na h.f.s.
643. Shimoda, K., and T. Nishikawa, *J. Phys. Soc. Japan*, **6**, 516. Zeeman spectrograph
644. Shoolery, J. N., and A. H. Sharbaugh, *Phys. Rev.*, **82**, 95L. Dipole moments OCS, HNCO, H<sub>2</sub>CO, CHF<sub>3</sub>
645. Shoolery, J. N., R. G. Shulman, W. F. Sheehan, Jr., V. Schomaker, and D. M. Yost, *J. Chem. Phys.*, **19**, 1364; *Phys. Rev.*, **82**, 323A. CF<sub>3</sub>CCH
646. Shoolery, J. N., R. G. Shulman, and D. M. Yost, *J. Chem. Phys.*, **19**, 250. HNCO, HNCS
647. Sirvetz, M. H., *J. Chem. Phys.*, **19**, 938. SO<sub>2</sub>
648. Sirvetz, M. H., *J. Chem. Phys.*, **19**, 1609. Furan
649. Smith, D. F., M. Tidwell, D. V. P. Williams, and S. J. Senatore, *Phys. Rev.*, **83**, 485A. CF<sub>2</sub>O
650. Southern, A. L., H. W. Morgan, G. W. Keilholtz, and W. V. Smith, *Anal. Chem.*, **23**, 1000. N and C isotopic determination
651. Swartz, J. C., and J. W. Trischka, *Phys. Rev.*, **88**, 1085. LiF mol. beam
652. Talley, R. M., and A. H. Nielsen, *J. Chem. Phys.*, **19**, 805. C<sub>2</sub>D<sub>2</sub> vibration-rotation
653. Townes, C. H., *J. Appl. Phys.*, **22**, 1365. Frequency stabilization
654. Townes, C. H., *Physica*, **17**, 354. Nuclear properties
655. Trischka, J., *J. Chem. Phys.*, **20**, 1811L. LiF mol. beam
656. Van Vleck, J. H., *Phys. Rev.*, **83**, 880A. Theory NH<sub>3</sub> h.f.s.
657. Van Vleck, J. H., *Revs. Mod. Phys.*, **23**, 213; *Phys. Rev.*, **82**, 320A. Coupling of angular momenta
658. Weber, J., *Phys. Rev.*, **83**, 1058L; 881A. Pressure broadening
659. Weber, J., and K. J. Laidler, *J. Chem. Phys.*, **19**, 381L. Kinetics NH<sub>3</sub>-D<sub>2</sub> exchange
660. Weber, J., and K. J. Laidler, *J. Chem. Phys.*, **19**, 1089. Kinetics NH<sub>3</sub>-D<sub>2</sub> exchange
661. Weiss, M. T., and M. W. P. Strandberg, *Phys. Rev.*, **81**, 286L; **82**, 326A. Deuteroammonias
662. Weiss, M. T., and M. W. P. Strandberg, *Phys. Rev.*, **83**, 567. Deuteroammonias
663. Wentink, T., Jr., W. S. Koski, and V. W. Cohen, *Phys. Rev.*, **81**, 948; **81**, 296A; **77**, 742A (1950). S<sup>35</sup> mass
664. Wilson, E. B., Jr., *Ann. Rev. Phys. Chem.*, **2**, 151. Review

## 1952

665. Amble, E., S. L. Miller, A. L. Schawlow, and C. H. Townes, *J. Chem. Phys.*, **20**, 192L; *Phys. Rev.*, **82**, 328A (1951). ReO<sub>3</sub>Cl
666. Anderson, P. W., *Phys. Rev.*, **86**, 809L. Th. pressure broadening

- 666a. Anderson, J. R., *Trans. Instruments and Meas. Conf., Stockholm*, **5**. Square-wave generator
667. Anderson, R. S., W. V. Smith, and W. Gordy, *Phys. Rev.*, **87**, 561. O<sub>2</sub> pressure broadening
668. *Annual Review of Nuclear Science*, Vol. I, Annual Reviews, Inc., Stanford, Calif. Review nuclear moments
669. Artman, J. O., and J. P. Gordon, *Phys. Rev.*, **87**, 227A. O<sub>2</sub> pressure broadening
- 669a. Bak, B., *Trans. Instruments and Meas. Conf., Stockholm*, **8**. Review
670. Beard, C. I., and D. R. Bianco, *J. Chem. Phys.*, **20**, 1488L. D<sub>2</sub>O
671. Beringer, R., and E. B. Rawson, *Phys. Rev.*, **86**, 607A. NO  $\Lambda$  doubling
672. Beringer, R., and E. B. Rawson, *Phys. Rev.*, **87**, 228A. Zeeman effect H
673. Beringer, R., *Ann. N.Y. Acad. Sci.*, **55**, 814. Zeeman effect  
paramagnetic gases
674. Biedenharn, L. C., J. M. Blatt, and M. E. Rose, *Rev. Mod. Phys.*, **24**, 249. Tables Racah coefficients
675. Birnbaum, G., and S. K. Chatterjee, *J. Appl. Phys.*, **23**, 220. H<sub>2</sub>O dielectric constant
- 675a. Birnbaum, G., H. E. Bussey, and R. R. Larson, *Trans. IRE Prof. Group on Antennas and Propagation*, No. 3, 74. Atmospheric refractive index
676. Bloom, S., and H. Margenau, *Phys. Rev.*, **85**, 717A. Th. pressure broadening
- 676a. Bolef, D. I., and H. J. Zeiger, *Phys. Rev.*, **85**, 799. Rb<sup>87</sup>F, Rb<sup>87</sup>Cl mol. beam
- 676b. Carlson, R. O., C. A. Lee, and B. P. Fabricand, *Phys. Rev.*, **85**, 784. TlCl, mol. beam
- 676c. Boyd, D. R. J., and H. W. Thompson, *Spectrochim. Acta*, **5**, 308. HBr (I.R.)
677. Cohen, V. W., *Ann. N.Y. Acad. Sci.*, **55**, 904. Determination moments  
radioactive nuclei
678. Costain, C. C., and G. B. B. M. Sutherland, *Phys. Chem.*, **56**, 321. Th. inversion
- 678a. Deutsch, M., and S. C. Brown, *Phys. Rev.*, **85**, 1047. Positronium
679. Duchesne, J., *J. Chem. Phys.*, **20**, 1804. Th. quad. coupling
- 679a. Duchesne, J., *Nuovo Cimento*, **9**, Suppl. 3, 270. Comparison I.R. and  
microwaves
680. Dailey, B. P., *Ann. N.Y. Acad. Sci.*, **55**, 915. Survey hindered  
rotation
681. Eshbach, J. R., R. E. Hillger, and M. W. P. Strandberg, *Phys. Rev.*, **85**, 532. Magnetic moment S<sup>23</sup>
682. Eshbach, J. R., and M. W. P. Strandberg, *Phys. Rev.*, **85**, 24; **82**, 327A. Mol. *g* factors
683. Eshbach, J. R., and M. W. P. Strandberg, *Rev. Sci. Instr.*, **23**, 623. Zeeman effect apparatus
- 683a. Essen, L., and K. D. Froome, *Nuovo Cimento*, **9**, Suppl. 3, 277. Refractive index of air
684. Fristrom, R. M., *J. Chem. Phys.*, **20**, 1; *Phys. Rev.*, **85**, 717A. SO<sub>2</sub>F<sub>2</sub>
685. Froome, K. D., *Proc. Roy. Soc.*, **213**, 123. Microwave  
measurement of *c*
686. Frosch, R. A., and H. M. Foley, *Phys. Rev.*, **88**, 1337. Mol. magnetic h.f.s.
687. Gabriel, W. F., *Proc. IRE*, **40**, 940. Frequency stabilization
688. Geschwind, S., G. R. Gunther-Mohr, and G. Silvey, *Phys. Rev.*, **85**, 474; **83**, 209A. O<sup>17</sup> in OCS
689. Geschwind, S., *Ann. N.Y. Acad. Sci.*, **55**, 751. Survey high resolution
690. Ghosh, S. N., R. Trambarulo, and W. Gordy, *J. Chem. Phys.*, **20**, 605; *Phys. Rev.*, **87**, 172A. CHF<sub>3</sub>, CHCl<sub>3</sub>, CH<sub>3</sub>CF<sub>3</sub>



691. Gilbert, D. A., *Phys. Rev.*, **85**, 716A.  
 692. Golay, M. J. E., *Proc. IRE*, **40**, 1161.  
 693. Gordy, W., *Physics Today*, **7**, 5.  
 694. Gordy, W., *Ann. N.Y. Acad. Sci.*, **55**, 774.  
 695. Hardy, W. A., G. Silvey, and C. H. Townes, *Phys. Rev.*, **85**, 494L; **86**, 608A.  
 695a. Harrick, N. J., and N. F. Ramsey, *Phys. Rev.*, **88**, 228.  
 696. Hawkins, N. J., V. W. Cohen, and W. S. Koski, *J. Chem. Phys.*, **20**, 528L.  
 696a. Hogan, C. L., *Bell System Tech. J.*, **31**, 1.  
 697. Hrostowski, H. J., R. J. Myers, and G. C. Pimentel, *J. Chem. Phys.*, **20**, 518L.  
 698. Hughes, J. V., and H. L. Armstrong, *J. Appl. Phys.*, **23**, 501.  
 699. Hughes, R. H., *Phys. Rev.*, **85**, 717A.  
 700. Hughes, R. H., *Ann. N.Y. Acad. Sci.*, **55**, 872.  
 701. Ince, C. R. S., *J. Appl. Phys.*, **23**, 1408L.  
 702. Javan, A., and A. V. Grosse, *Phys. Rev.*, **87**, 227A.  
 703. Javan, A., and C. H. Townes, *Phys. Rev.*, **86**, 608A.  
 704. Jen, C. K., J. W. B. Borghausen, and R. W. Stanley, *Phys. Rev.*, **85**, 717A.  
 705. Jen, C. K., *Ann. N.Y. Acad. Sci.*, **55**, 822.  
 706. Johnson, C. M., and D. M. Slager, *Phys. Rev.*, **87**, 677L.  
 707. Johnson, H. R., *Phys. Rev.*, **85**, 764A.  
 708. Johnson, H. R., and M. W. P. Strandberg, *J. Chem. Phys.*, **20**, 687; *Phys. Rev.*, **82**, 327A.  
 709. Johnson, H. R., and M. W. P. Strandberg, *Phys. Rev.*, **85**, 503L.  
 710. Johnson, H. R., and M. W. P. Strandberg, *Phys. Rev.*, **86**, 811L.  
 711. Jones, L. C., A. V. Bushkovitch, C. A. Potter, and A. G. Rouse, *Phys. Rev.*, **87**, 227A.  
 712. Kagarise, R. E., H. D. Rix, and D. H. Rank, *J. Chem. Phys.*, **20**, 1437.  
 712a. Karplus, R., and A. Klein, *Phys. Rev.*, **86**, 257.  
 712b. Kisliuk, P., Thesis, Columbia University.  
 713. Kisliuk, P., and G. A. Silvey, *J. Chem. Phys.*, **20**, 517.  
 714. Kisliuk, P., and C. H. Townes, *Natl. Bur. Standards Circ.* 518.  
 715. Kivelson, D., and E. B. Wilson, Jr., *J. Chem. Phys.*, **20**, 1575; *Phys. Rev.*, **87**, 214A.  
 716. Klein, J. A., J. H. N. Loubser, A. H. Nethercot, and C. H. Townes, *Rev. Sci. Instr.*, **23**, 78.  
 716a. Kolsky, H. G., T. E. Phipps, N. F. Ramsey, and H. B. Silsbee, *Phys. Rev.*, **87**, 395.  
 717. Kojima, S., K. Tsukada, S. Hagiwara, M. Mizushima, and T. Ito, *J. Chem. Phys.*, **20**, 804.  
 718. Lamb, W. E., and R. C. Retherford, *Phys. Rev.*, **86**, 1014.  
 719. Lamont, H. R. L., and E. M. Hickin, *Brit. J. Appl. Phys.*, **3**, 182.  
 720. Lide, D. R., *J. Chem. Phys.*, **20**, 1761.  
 721. Lide, D. R., *J. Chem. Phys.*, **20**, 1812L.; *Erratum*, **21**, 571 (1953).
- Cl<sup>36</sup> in CH<sub>2</sub>Cl  
 Mm waves  
 Elementary review  
 Mm waves  
 Se<sup>79</sup> in OCSe  
 R.F. spectrum of H<sub>2</sub>  
 POF<sub>3</sub>, PSF<sub>3</sub>  
 Applications of ferrites  
 Pentaborane  
 Dielectric constant air  
 O<sub>3</sub>  
 Chemical analysis  
 Atomic clock  
 MnO<sub>3</sub>F  
 ICN h.f.s. anomalies  
 Mol. *g* factor  
 Survey Zeeman effects  
 OCS pressure  
   broadening  
 Th. spectrograph  
 CH<sub>2</sub>CO  
 Beam spectrometer  
 Wall-collision  
   broadening  
 Pressure broadening  
 I.R. spectrum HCN  
 Theory positronium  
 Halides of N, P, As, Sb;  
   CH<sub>3</sub>HgCN, P(CN)<sub>3</sub>  
 CF<sub>3</sub>SF<sub>5</sub>  
 Tables microwave  
   spectra  
 Th. centrifugal  
   distortion asymmetric  
   rotor  
 Techniques 1 to 3 mm  
 H<sub>2</sub> and D<sub>2</sub> R.F.  
   spectrum  
 CHBr<sub>3</sub>  
 Fine-structure H  
 Frequency stabilization  
   microwave lines  
 Intensity slightly  
   asymmetric rotor  
 CH<sub>3</sub>NH<sub>2</sub>

722. Lide, D. R., Jr., *J.ACS*, **74**, 3548; *Phys. Rev.*, **87**, 227A.  $\text{CH}_2\text{F}_2$
- 722a. Logan, R. A., R. E. Cote, and P. Kusch, *Phys. Rev.*, **86**, 280.  $eqQ$  in alkali halides
723. Lord, R. C., and R. E. Merrifield, *J. Chem. Phys.*, **20**, 1348. Rotation-vibration symmetric rotors
724. Lyons, H., *Ann. N.Y. Acad. Sci.*, **55**, 831. Frequency standards
725. Magnuson, D. W., *J. Chem. Phys.*, **20**, 229. Dielectric constant  $\text{ClF}_3$
726. Massey, J. T., and D. R. Bianco, *Phys. Rev.*, **85**, 717A.  $\text{H}_2\text{O}_2$
727. Mays, J. M., and B. P. Dailey, *J. Chem. Phys.*, **20**, 1695.  $\text{XYH}_3$  molecules
728. Mays, J. M., *Ann. N.Y. Acad. Sci.*, **55**, 789. Survey high temp., free radicals
729. Miller, S. L., L. C. Aamodt, G. Dousmanis, C. H. Townes, and J. Kraitchman, *J. Chem. Phys.*, **20**, 1112; *Phys. Rev.*, **82**, 327A.  $\text{CH}_3\text{Cl}$ ,  $\text{CH}_3\text{Br}$ ,  $\text{CH}_3\text{I}$
730. Minden, H. T., *J. Chem. Phys.*, **20**, 1964. Statistical weights  $\text{CH}_3\text{CF}_3$
- 730a. Mockler, R., J. H. Bailey, and W. Gordy, *Phys. Rev.*, **87**, 172A.  $\text{HSiCl}_3$ ,  $\text{CH}_3\text{SiCl}_3$
731. Morgan, H. W., and J. H. Goldstein, *J. Chem. Phys.*, **20**, 1981L.  $\text{CH}_2\text{CHCN}$
732. Myers, R. J., and W. D. Gwinn, *J. Chem. Phys.*, **20**, 1420.  $\text{CH}_2\text{Cl}_2$
733. Nethercot, A. H., J. A. Klein, and C. H. Townes, *Phys. Rev.*, **86**, 798L.  $\text{HCN}$
734. Nethercot, A. H., J. A. Klein, J. H. N. Loubser, and C. H. Townes, *Nuovo Cimento*, **9**, Suppl. 3, 358. 1 to 2 mm
735. Nielsen, H. H., *J. Chem. Phys.*, **20**, 1955. I.R. structure  $\text{AsH}_3$
736. Nielsen, H. H., *J. Chem. Phys.*, **20**, 759L. I.R. structure  $\text{PH}_3$ ,  $\text{AsH}_3$ ,  $\text{SbH}_3$
737. Nuckolls, R. G., and L. J. Rueger, *Phys. Rev.*, **85**, 731A. Lock-in detector
- 737a. Prodell, A. G., and P. Kusch, *Phys. Rev.*, **88**, 184. Atomic H h.f.s. mol beam
738. Rank, D. H., *J. Chem. Phys.*, **20**, 1975L. I.R. mol. constants
739. Rank, D. H., R. P. Ruth, and J. L. Vander Sluis, *Phys. Rev.*, **86**, 799L. I.R. microwave measurement  $c$
- 739a. Rawson, E. B., and R. Beringer, *Phys. Rev.*, **88**, 677L. Atomic oxygen, Zeeman effect
740. Rogers, J. D., and D. Williams, *Phys. Rev.*, **86**, 654A. H.f.s.  $\text{HN}_3$
741. Rueger, L. J., and R. G. Nuckolls, *Rev. Sci. Instr.*, **23**, 635. Stark cell
742. Schwarz, R. F., *Phys. Rev.*, **86**, 606A; Thesis, Harvard University. Molecular  $g$  factors
743. Sheridan, J., and W. Gordy, *J. Chem. Phys.*, **20**, 591.  $\text{CF}_3\text{Br}$ ,  $\text{CF}_3\text{I}$ ,  $\text{CF}_3\text{CN}$
744. Sheridan, J., and W. Gordy, *J. Chem. Phys.*, **20**, 735.  $\text{CH}_3\text{CCBr}$ ,  $\text{CH}_3\text{CCI}$
745. Silvey, G., W. A. Hardy, and C. H. Townes, *Phys. Rev.*, **87**, 236A.  $\text{TeCS}$
746. Simmons, J. W., and J. H. Goldstein, *J. Chem. Phys.*, **20**, 122; *Phys. Rev.*, **83**, 485A (1951).  $\text{CD}_3\text{Cl}$ ,  $\text{CD}_3\text{Br}$ ,  $\text{CD}_3\text{I}$
747. Sinton, W. M., *Phys. Rev.*, **86**, 424L. Mm solar radiation
748. Smith, D. F., and D. W. Magnuson, *Phys. Rev.*, **87**, 226A.  $\text{NO}_2\text{F}$
- 748a. Smith, E. K., Jr., and S. Weintraub, *N.B.S. Rept.*, 1938. Refractive index of air
- 748b. Smith, W. V., *Ann. N.Y. Acad. Sci.*, **55**, 891. Survey pressure broadening

749. Sternheimer, R., *Phys. Rev.*, **86**, 316; 595A. Th. magnetic h.f.s.  
 750. Stitch, M. L., A. Honig, and C. H. Townes, *Phys. Rev.*, **86**, 607A. KCl, TiCl  
 751. Stitch, M. L., A. Honig, and C. H. Townes, *Phys. Rev.*, **86**, 813L. NaCl, CsCl  
 752. Strandberg, M. W. P., *Ann. N.Y. Acad. Sci.*, **55**, 808. Centrifugal distortion  
 753. Swartz, J. C., and J. W. Trischka, *Phys. Rev.*, **88**, 1085; **86**, 606A. LiF molecular beams  
 754. Tetenbaum, S. J., *Phys. Rev.*, **86**, 440; **82**, 323A. BrCN 6 mm  
 755. Tetenbaum, S. J., *Phys. Rev.*, **88**, 772. OCS, N<sub>2</sub>O 6 mm  
 755a. Thompson, H. W., R. L. Williams, and H. J. Callo- HI (I.R.)  
 man, *Spectrochim. Acta*, **5**, 311.  
 756. Townes, C. H., *Ann. N.Y. Acad. Sci.*, **55**, 745. Brief survey  
 757. Townes, C. H., and B. P. Dailey, *J. Chem. Phys.*, **20**, Th. quad. coupling  
 35. solids  
 758. Twiss, R. Q., *S.E.R.L. Tech. J.*, **2**, 10. Mm-wave generation  
 758a. Van den Bosch, J. C., and F. Bruin, *Nuovo Cimento*, Spectrometer  
**9**, Suppl. 3, 238.  
 758b. Van den Bosch, J. C., and F. Bruin, *Nuovo Cimento*, Interferometers  
**9**, Suppl. 3, 245.  
 759. Van Kranendonk, J., Thesis, Amsterdam. Th. pressure broadening  
 760. Wang, T. C., C. H. Townes, A. L. Schawlow, and Ratio Cl<sup>35</sup>/Cl<sup>37</sup>  
 A. N. Holden, *Phys. Rev.*, **86**, 809. quadrupole  
 760a. Warner, A. W., *Proc. IRE*, **40**, 1030. Quartz-crystal  
 oscillators  
 761. Weatherly, T. L., and D. Williams, *Phys. Rev.*, **87**, l doubling HCN, DCN  
 517; with Y. Ting, **83**, 210A (1951); with E. R. Manring, **85**, 717A (1951).  
 762. Weatherly, T. L., and D. Williams, *J. Chem. Phys.*, Acetone  
**20**, 755L.  
 762a. Weston, R. E., Jr., and M. H. Sirvetz, *J. Chem. Phys.*, Vibration frequency  
**20**, 1820. PH<sub>2</sub>D, PHD<sub>2</sub>  
 763. Wilcox, W. S., and J. H. Goldstein, *J. Chem. Phys.*, Pyrrole  
**20**, 1656.  
 763a. Wilcox, W. S., J. H. Goldstein, and J. W. Simmons, Vinyl cyanide  
*Phys. Rev.*, **87**, 172.  
 764. Williams, Q., J. T. Cox, and W. Gordy, *J. Chem. Phys.*, CHBr<sub>3</sub>  
**20**, 1524.  
 765. Williams, Q., J. Sheridan, and W. Gordy, *J. Chem. Phys.*, POF<sub>3</sub>, PSF<sub>3</sub>, POCl<sub>3</sub>,  
**20**, 164. PSCl<sub>3</sub>  
 766. Wilson, E. B., Jr., *Ann. N.Y. Acad. Sci.*, **55**, 943. Survey mol. structure  
 from microwave  
 spectroscopy  
 767. Zeiger, H. J., and D. I. Bolef, *Phys. Rev.*, **85**, 788. TiCl mol. beam  
 768. Zieman, C. M., *J. Appl. Phys.*, **23**, 154L. Dielectric constants  
 gases

## 1953

- 768a. Abragam, A., and J. H. Van Vleck, *Phys. Rev.*, **92**, Th. O Zeeman effect  
 1448.  
 769. Anderson, F., J. R. Andersen, B. Bak, O. Bastiensen, (CH<sub>3</sub>)<sub>3</sub>CF  
 E. Risberg, and L. Smedvik, *J. Chem. Phys.*, **21**,  
 373L.  
 769a. Arendale, W. F., and W. H. Fletcher, *J. Chem. Phys.*, CH<sub>2</sub>CO  
**21**, 1898.  
 770. Artman, J. O., and J. P. Gordon, *Phys. Rev.*, **90**, O<sub>2</sub> pressure broadening  
 338A.  
 771. Bak, B., J. Bruhn, and J. Rastrup-Andersen, *J. SiD<sub>3</sub>F*  
*Chem. Phys.*, **21**, 752L.



772. Bak, B., J. Bruhn, and J. Rastrup-Andersen, *J. Chem. Phys.*, **21**, 753L.  $\text{SiD}_3\text{Cl}$
- 772a. Bak, B., L. Hansen, and J. Rastrup-Andersen, *J. Chem. Phys.*, **21**, 1612.  $\text{CH}_3\text{CCCF}_3$
- 772b. Bak, B., and J. Rastrup-Andersen, *J. Chem. Phys.*, **21**, 1305. Pyridine
- 772c. Barrow, R. F., and Caunt, A. D., *Proc. Roy. Soc. A*, **219**, 120. Alkali halides (U.V. spectrum)
773. Beers, Y., and S. Weisbaum, *Phys. Rev.*, **91**, 1014L. HDO
- 773a. Bedard, F. D., J. J. Gallagher, and C. M. Johnson, *Phys. Rev.*, **92**, 1440.  $\text{D}_0$  for CO
774. Benedict, W. S., N. Gailar, and E. K. Plyler, *J. Chem. Phys.*, **21**, 1301.  $\text{D}_2\text{O}$  (I.R.)
775. Benedict, W. S., N. Gailar, and E. K. Plyler, *J. Chem. Phys.*, **21**, 1302. HDO (I.R.)
776. Benesch, W., and T. Elder, *Phys. Rev.*, **91**, 308. Pressure broadening
777. Bird, R., and Richard C. Mockler, *Phys. Rev.*, **91**, 222A. CS
778. Birnbaum, G., *J. Chem. Phys.*, **21**, 57.  $\text{H}_2\text{O}$  dispersion mm. wavelengths
779. Birnbaum, G., and A. A. Maryott, *Phys. Rev.*, **92**, 270; **89**, 895A.  $\text{ND}_3$  high pressure
780. Birnbaum, G., and A. A. Maryott, *J. Chem. Phys.*, **21**, 1774.  $\text{NH}_3$  pressure broadening
781. Bloom, S., and H. Margenau, *Phys. Rev.*, **90**, 791. Th. pressure broadening
- 781a. Brossel, J., B. Cagnac, and A. Kastler, *Compt. rend.*, **237**, 984. Atomic Zeeman effect
- 781b. Braunstein, R., and J. W. Trischka, *Phys. Rev.*, **90**, 348A. LiF I-J interaction
782. Burke, B. F., and M. W. P. Strandberg, *Phys. Rev.*, **90**, 338A. Zeeman effect asymmetric rotor
- 782a. Burkhard, D. G., *J. Chem. Phys.*, **21**, 1541. Th. hindered rotation
- 782b. Burrus, C. A., and W. Gordy, *Phys. Rev.*, **92**, 1437. NO and DI
783. Burrus, C. A., and W. Gordy, *Phys. Rev.*, **92**, 274.  $\text{H}_2\text{S}$
- 783a. Chang, T. S., and D. M. Dennison, *J. Chem. Phys.*, **21**, 1293. Centrifugal distortion  $\text{CH}_3\text{Cl}$
- 783b. Cox, H. L., Jr., *Rev. Sci. Inst.*, **24**, 307. Lock-in amplifier
784. Cox, J. T., P. B. Peyton, Jr., and W. Gordy, *Phys. Rev.*, **91**, 222A.  $\text{CH}_3\text{F}$ ,  $\text{CH}_3\text{CCH}$
785. Crawford, H. D., *J. Chem. Phys.*, **21**, 2099L.  $\text{D}_2\text{O}$
786. Culshaw, W., *Proc. Phys. Soc. London*, **B66**, 597. Fabry-Perot interferometer
787. Dailey, B. P., *Phys. Rev.*, **90**, 337A. Cyclopropyl chloride
788. Danos, M., and S. Geschwind, *Phys. Rev.*, **91**, 1159. Wall-collision broadening
789. Danos, M., S. Geschwind, H. Lashinsky, and A. Van Trier, *Phys. Rev.*, **92**, 828L. Microwave Cerenkov effect
790. Dayhoff, E. S., S. Triebwasser, and W. E. Lamb, *Phys. Rev.*, **89**, 106. H fine structure
791. Dehmelt, H. G., *Phys. Rev.*, **91**, 313. Quad. coupling sulfur
792. Dicke, R. H., *Phys. Rev.*, **89**, 472. Th. line width
793. Ditchfield, C. R., *Proc. Inst. Elec. Engrs. London*, Part III, **68**, 365. Mm-wave crystal mixer
794. Dousmanis, G. C., T. M. Sanders, C. H. Townes, and H. J. Zeiger, *J. Chem. Phys.*, **21**, 1416. HNCS
795. DuMond, J. W. M., and E. R. Cohen, *Revs. Mod. Phys.*, **25**, 691. Atomic constants
796. Erlandsson, G., *Arkiv. Fysik.*, **6**, Paper 45, 477; **7**, Paper 17, 189. Fluorobenzene

- 796a. Erlandsson, G., *Arkiv. Fysik.*, **6**, 69.  
 796b. Erlandsson, G., *Arkiv. Fysik.*, **6**, 491.  
 797. Essen, L., *Proc. Phys. Soc.*, **66B**, 189.  
 798. Essen, L., *Proc. Inst. Elec. Engrs. London*, Part III, **100**, 19.  
 799. Fabricand, B. P., R. O. Carlson, C. A. Lee, and I. I. Rabi, *Phys. Rev.*, **91**, 1403.  
 800. Ferguson, R. C., and E. B. Wilson, Jr., *Phys. Rev.*, **90**, 338A.  
 801. Ferigle, S. M., and A. Weber, *Am. J. Phys.*, **21**, 102.  
 803. Ghosh, S. N., R. Trambarulo, and W. Gordy, *J. Chem. Phys.*, **21**, 308; *Phys. Rev.*, **87**, 172A.  
 804. Goldman, I. I., *Doklady Akad. Nauk SSSR*, **88**, 241.  
 804a. Gordy, W., *J. chim. phys.*, **50**, C114.  
 805. Gordy, W., W. V. Smith, and R. F. Trambarulo, John Wiley & Sons, Inc., New York.  
 805a. Gozzini, A., and E. Polacco, *Compt. rend.* **237**, 1497.  
 806. Gorter, C. J., *Experimenta*, **9**, 161.  
 806a. Hardy, W. A., G. Silvey, C. H. Townes, B. F. Burke, M. W. P. Strandberg, G. W. Parker, and V. W. Cohen, *Phys. Rev.*, **92**, 1532.  
 807. Harrick, N. J., R. G. Barnes, P. J. Bray, and N. F. Ramsey, *Phys. Rev.*, **90**, 260.  
 808. Hawkins, W. B., and R. H. Dicke, *Phys. Rev.*, **91**, 1008L.  
 809. Hedrick, L. C., *Rev. Sci. Instr.*, **24**, 565.  
 811. Hicks, B. L., T. E. Turner, and W. W. Widule, *J. Chem. Phys.*, **21**, 564L.  
 812. Hill, R. M., and W. Gordy, *Phys. Rev.*, **91**, 222A.  
 813. Hollander, J. M., I. Perlman, and G. T. Seaborg, *Revs. Mod. Phys.*, **25**, 469.  
 814. Honig, A., M. L. Stitch, and M. Mandel, *Phys. Rev.*, **92**, 901.  
 814a. Huggins, M. L., *J.A.C.S.*, **75**, 4123.  
 815. Hughes, R. H., *J. Chem. Phys.*, **21**, 959.  
 816. Hughes, V., G. Tucker, E. Rhoderick, and G. Weinreich, *Phys. Rev.*, **91**, 828.  
 817. Ivash, E. V., and D. M. Dennison, *J. Chem. Phys.*, **21**, 1804; *Phys. Rev.*, **89**, 895A.  
 818. Javan, A., G. Silvey, C. H. Townes, and A. V. Grosse, *Phys. Rev.*, **91**, 222A.  
 819. Jen, C. K., D. R. Bianco, and J. T. Massey, *J. Chem. Phys.*, **21**, 520.  
 820. Johnson, R. D., R. J. Myers, and W. D. Gwinn, *J. Chem. Phys.*, **21**, 1425L.  
 821. Jones, L. C., A. V. Bushkovitch, C. A. Potter, and A. G. Rouse, *Phys. Rev.*, **89**, 895A.  
 821a. Keller, F. L., and A. H. Nielsen, *Phys. Rev.*, **91**, 235.  
 822. Kendrick, W. M., and T. E. Turner, *Ballistic Research Lab. Rept.* 660.  
 823. King, W. C., and W. Gordy, *Phys. Rev.*, **90**, 319.
- CH<sub>3</sub>OH, CH<sub>3</sub>NO<sub>2</sub>  
 HCOOH  
 Refractive index H<sub>2</sub>O,  
 air, O<sub>2</sub>, N<sub>2</sub>, H<sub>2</sub>, D<sub>2</sub>, He  
 Refractive index  
 atmosphere  
 KBr  
 SOF<sub>2</sub>  
 Rotation-vibration  
 polyatomic molecules  
 Dipole moments NF<sub>3</sub>,  
 PF<sub>3</sub>, POF<sub>3</sub>, HCN,  
 CH<sub>3</sub>CN, CH<sub>3</sub>NC,  
 CH<sub>3</sub>F, CH<sub>3</sub>CCH,  
 SiF<sub>3</sub>H  
 Th. quad. coupling  
 H<sub>2</sub>O  
 Microwave  
 spectroscopy  
 Dielectric constant  
 gases  
 Review  
 OCSe<sup>79</sup>  
 H<sub>2</sub>, D<sub>2</sub>  
 Na atoms  
 Frequency standards  
 Th. asymmetric rotors  
 O<sub>2</sub> temperature  
 dependence of line  
 widths  
 Isotopes table  
 CsF, CsCl, CsBr  
 Electronegativities  
 O<sub>3</sub>  
 He atom  
 CH<sub>3</sub>OH  
 Mn<sup>55</sup>, Re<sup>185</sup>, Re<sup>187</sup>  
 quad. moments  
 D<sub>2</sub>O  
 Ethylenimine  
 Pressure broadening  
 DBr IR spectrum  
 Spectrograph  
 OCS mm wave

824. Kisliuk, P., and S. Geschwind, *J. Chem. Phys.*, **21**, 828. AsF<sub>3</sub>
825. Kivelson, D., *J. Chem. Phys.*, **21**, 536. Th. asymmetric rotor
826. Kivelson, D., and E. Bright Wilson, Jr., *J. Chem. Phys.*, **21**, 1229; *Phys. Rev.*, **90**, 338A. Th. centrifugal distortion
827. Kivelson, D., and E. Bright Wilson, Jr., *J. Chem. Phys.*, **21**, 1236. Th. mol. parameters from rotational constants
- 827a. Klein, J. A., and A. H. Nethercot, *Phys. Rev.*, **91**, 1018L. DI
828. Klinger, H. H., *J. Franklin Inst.*, **256**, 353. Review radio astronomy
829. Klinger, H. H., *J. Franklin Inst.*, **256**, 129. Review microwaves
830. Kompfner, R., *Proc. I.R.E.*, **41**, 1602. Mm-wave tube
831. Kraitchman, J., *Am. J. Phys.*, **21**, 17-24. Th. mol. structure determination
832. Krishnaji, and P. Swarup, *J. Sci. Ind. Research*, **12B**, 1-3. NH<sub>3</sub> pressure broadening
833. Krishnaji, and P. Swarup, *Z. Physik.*, **136**, 374. NH<sub>3</sub> dispersion
- 833a. Krishnaji, and P. Swarup, *J. Appl. Phys.*, **24**, 1525. Absorption in gases
834. Kusch, P., *Phys. Rev.*, **29**, 268. LiCl Li quad. interaction
835. Lee, C. A., B. P. Fabricand, R. O. Carlson, and I. I. Rabi, *Phys. Rev.*, **86**, 607A; **91**, 1395. KCl
836. Livingston, R., B. M. Benjamin, J. T. Cox, and W. Gordy, *Phys. Rev.*, **92**, 1271. I<sup>131</sup> spin, quad. mom.
837. Loubser, J. H. N., *J. Chem. Phys.*, **21**, 2231L. CH<sub>3</sub>COOH
838. Luce, R. G., and J. W. Trischka, *J. Chem. Phys.*, **21**, 105. CsCl mol. beams
839. McCulloh, K. E., and G. F. Pollnow, *J. Chem. Phys.*, **21**, 2082L. Pyridine
840. Meier, R., *Ann. Physik*, **12**, 26. Sub-mm waves
841. Miller, S. L., and C. H. Townes, *Phys. Rev.*, **90**, 537. O<sup>17</sup> and O<sup>18</sup> in O<sub>2</sub>
842. Miller, S. L., C. H. Townes, and M. Kotani, *Phys. Rev.*, **90**, 542; **86**, 607A (1952). Magnetic h.f.s. O<sub>2</sub>
843. Mizushima, M., *Phys. Rev.*, **91**, 222A. Th. O<sub>2</sub>
844. Mizushima, M., *J. Chem. Phys.*, **21**, 1222; *Phys. Rev.*, **91**, 464A. Th. allene-type molecules
845. Mizushima, M., *J. Chem. Phys.*, **21**, 539. Stark effect asymmetric rotor h.f.s.
846. Mizushima, M., and P. Venkateswarlu, *J. Chem. Phys.*, **21**, 705; *Phys. Rev.*, **89**, 896A. Rotation-vibrational dipole moment
847. Mockler, R. C., J. H. Bailey, and W. Gordy, *J. Chem. Phys.*, **21**, 1710. H SiCl<sub>3</sub>, CH<sub>3</sub>SiCl<sub>3</sub>, (CH<sub>3</sub>)<sub>3</sub>SiCl
848. Mockler, R. C., and W. Gordy, *Phys. Rev.*, **91**, 222A. (CH<sub>3</sub>)<sub>3</sub>SiCl
849. Motz, H., W. Thon, and R. N. Whitehurst, *J. Appl. Phys.*, **24**, 826. Microwave generation
850. Muller, N., *J. ACS*, **75**, 860. CH<sub>2</sub>FCI
851. Nethercot, A. H., and A. Javan, *J. Chem. Phys.*, **21**, 363; and (with C. H. Townes) *Phys. Rev.*, **87**, 226A (1952). C<sub>3</sub>H<sub>13</sub>Cl, C<sub>3</sub>H<sub>13</sub>Br
852. Nielsen, H. H., *J. Chem. Phys.*, **21**, 142. Th. XY<sub>2</sub> molecules
853. Nishikawa, T., and K. Shimoda, *J. Phys. Soc. Japan*, **8**, 426. NH<sub>3</sub> inversion spectrum
854. Nuckolls, R. G., L. J. Rueger, and H. Lyons, *Phys. Rev.*, **89**, 1101. ND<sub>3</sub> inversion
- 854a. Obi, S. Y., T. Ishidzu, S. Yanagawa, Y. Tanabe, and M. Sato, *Ann. Tokyo Astron. Observatory*, **3**, 89. Tables Racah coefficients
855. Ochs, S. A., R. E. Cote, and P. Kusch, *J. Chem. Phys.*, **21**, 459. NaCl mol. beam



- |   |                                      |
|---|--------------------------------------|
| 855a. Ogata, K., and H. Matsuda, <i>Phys. Rev.</i> , <b>89</b> , 27.  | Masses of light atoms                |
| 856. Posener, D. W., and M. W. P. Strandberg, <i>J. Chem. Phys.</i> , <b>21</b> , 1401L.  | HDO                                  |
| 856a. Potok, H. N., <i>J. Brit. Inst. Radio Engrs.</i> , <b>13</b> , 490.   | Mm-wave spark generators             |
| 856b. Ramsey, N. F., <i>Phys. Rev.</i> , <b>89</b> , 527L.  | Pseudo quad. effect                  |
| 857. Ramsey, N. F., in <i>Experimental Nuclear Physics</i> , John Wiley & Sons, Inc., New York.   | Review nuclear moments               |
| 858. Ramsey, N. F., <i>Phys. Rev.</i> , <b>91</b> , 303.  | Interactions between nuclei          |
| 859. Reich, H. J., P. F. Ordung, H. L. Krauss, and J. G. Skalnicky, <i>Microwave Theory and Techniques</i> , D. Van Nostrand Company, Inc., New York. |                                      |
| 859a. Robinson, G. W., and C. D. Cornwell, <i>J. Chem. Phys.</i> , <b>21</b> , 1436.  | Th. quadrupole h.f.s. two nuclei     |
| 859b. Robinson, G. W., <i>J. Chem. Phys.</i> , <b>21</b> , 1741.  | CCl <sub>2</sub> O                   |
| 860. Rowen, J. H., <i>Bell System Tech. J.</i> , <b>32</b> , 1333.  | Ferrite microwave applications       |
| 861. Sanders, T. M., A. L. Schawlow, G. C. Dousmanis, and C. H. Townes, <i>Phys. Rev.</i> , <b>89</b> , 1158L.  | OH radical                           |
| 862. Satomura, S., <i>Mem. Inst. Sci. Ind. Research, Osaka Univ.</i> , <b>10</b> , 34.  |                                      |
| 863. Scheibe, A., <i>Z. angew. Phys.</i> , <b>5</b> , 307.  | Review time standards                |
| 864. Sharbaugh, A. H., G. A. Heath, L. F. Thomas, and J. Sheridan, <i>Nature</i> , <b>171</b> , 87.   | SiH <sub>3</sub> I                   |
| 865. Shimoda, K., and T. Nishikawa, <i>J. Phys. Soc. Japan</i> , <b>8</b> , 133; <b>8</b> , 425.  | Methylamine                          |
| 866. Sirvetz, M. E., and R. E. Weston, <i>J. Chem. Phys.</i> , <b>21</b> , 898.   | PHD <sub>2</sub> , PH <sub>2</sub> D |
| 867. Smith, D. F., <i>J. Chem. Phys.</i> , <b>21</b> , 609; <i>Phys. Rev.</i> , <b>86</b> , 608A.   | ClF <sub>3</sub>                     |
| 868. Smith, E. K., and S. Weintraub, <i>J. Research Natl. Bur. Standards</i> , <b>50</b> , 39.  | Dielectric constant air              |
| 870. Solimene, N., and B. P. Dailey, <i>Phys. Rev.</i> , <b>91</b> , 464A.  | CH <sub>3</sub> SH                   |
| 871. Strandberg, M. W. P., <i>Microwave Spectroscopy</i> , John Wiley & Sons, Inc., New York.   |                                      |
| 872. Sverdlov, L. M., <i>Doklady Akad. Nauk SSSR</i> , <b>88</b> , 249.   | Th. isotope shifts                   |
| 874. Tate, P., and M. W. P. Strandberg, <i>Phys. Rev.</i> , <b>91</b> , 464A.   | High-temp. spectrometer              |
| 875. Trambarulo, R., S. N. Ghosh, C. A. Burrus, and W. Gordy, <i>J. Chem. Phys.</i> , <b>21</b> , 851; <i>Phys. Rev.</i> , <b>91</b> , 222A.          | O <sub>3</sub>                       |
| 876. Triebwasser, S., E. S. Dayhoff, and W. E. Lamb, <i>Phys. Rev.</i> , <b>89</b> , 98.  | Fine-structure H                     |
| 877. Turner, T. E., V. C. Fiora, W. M. Kendrick, and B. L. Hicks, <i>J. Chem. Phys.</i> , <b>21</b> , 564; <i>Phys. Rev.</i> , <b>90</b> , 338A.      | Ethylenimine                         |
| 877a. Turner, T. E., B. L. Hicks, and G. Reitwiesner, <i>Report 878, Ballistics Research Laboratory</i> , Aberdeen, Md.                               | Asym. rotor tables                   |
| 878. van den Bosch, J. C., and F. Bruin, <i>Physica</i> , <b>19</b> , 705.  | Cavity wavemeter                     |
| 879. Van Kranendonk, J., Thesis, Amsterdam.   | Th. pressure broadening              |
| 880. Van Vleck, J. H., in <i>Quantum-mechanical Methods in Valence Theory</i> , <i>Nat. Acad. Sci.</i> , 117.   | Th. pressure broadening              |
| 881. Venkateswarlu, P., R. C. Mockler, and W. Gordy, <i>Phys. Rev.</i> , <b>91</b> , 222A; <i>J. Chem. Phys.</i> , <b>21</b> , 1713.                  | GeHCl <sub>3</sub>                   |
| 882. Warner, A. W., <i>Bell Labs. Record</i> , <b>31</b> , 205.   | Quartz-crystal oscillators           |
| 883. Weber, J., <i>Trans. Inst. Radio Engrs. Prof. Group on Electron Devices</i> , <b>3</b> , 1.  | Amplification of microwaves          |

884. Weber, D., S. and S. Penner, *J. Chem. Phys.*, **21**, 1503. NO, HCl, HBr line widths
885. Weinreich, G., and V. Hughes, *Phys. Rev.*, **90**, 377A. He<sup>3</sup> mol. beam
886. Weisbaum, S., Y. Beers, and G. Herrmann, *Phys. Rev.*, **90**, 338A. HDO
- 886a. Wessel, G., and H. Lew, *Phys. Rev.*, **92**, 641. Molecular beam detector
887. White, R. L., *Phys. Rev.*, **91**, 1014L. DCCCl, DCN deuteron quad. coupling
888. White, R. L., and C. H. Townes, *Phys. Rev.*, **92**, 1256. SiD<sub>3</sub>F h.f.s.
889. Wilcox, W. S., K. C. Brannock, W. DeMore, and J. H. Goldstein, *J. Chem. Phys.*, **21**, 563L. Ethylenimine
891. Yergin, P. F., W. E. Lamb, Jr., E. Lipworth, and R. Novick, *Phys. Rev.*, **90**, 377A. Fine-structure He<sup>+</sup>
- 1954**
892. Aamodt, L. C., P. C. Fletcher, G. Silvey, and C. H. Townes, *Phys. Rev.*, **94**, 789A. OCSe<sup>76</sup>
- 892a. Althoff, K., and H. Kruger, *Naturwiss.*, **41**, 368. Cs h.f.s. P<sub>1</sub> state
- 892b. Artman, J. O., and J. P. Gordon, *Phys. Rev.*, **96**, 1237. O<sub>2</sub>
- 892c. Autler, S. H., and C. H. Townes (to be published). High frequency Stark effects
893. Bak, B., L. Hansen, and J. Rastrup-Andersen, *J. Chem. Phys.*, **22**, 565L; **22**, 2013. Pyridine
894. Baird, D. H., and G. R. Bird, *Rev. Sci. Instr.*, **25**, 319. Meas. of intensities
895. Barnes, R. G., and W. V. Smith, *Phys. Rev.*, **93**, 95. Quad. coupling constants atoms
896. Barnes, R. G., P. J. Bray, and N. F. Ramsey, *Phys. Rev.*, **94**, 893. Magnetic moment of H<sub>2</sub>
- 896a. Bassov, N. G., and A. M. Prokhorov, *J. Exp. Theor. Phys.*, *U.S.S.R.*, **27**, 431. Mol. beams techniques
897. Sterzer, F., *J. Chem. Phys.*, **22**, 2094L. CF<sub>3</sub>I
898. Beringer, R., and M. A. Heald, *Phys. Rev.*, **95**, 1474. Atomic H
899. Beringer, R., E. B. Rawson, and A. F. Henry, *Phys. Rev.*, **94**, 343. NO
900. Bernstein, R. B., F. F. Cleveland, and F. L. Voelz, *J. Chem. Phys.*, **22**, 193. IR spectrum CH<sub>3</sub>I
901. Bird, G. R., *Rev. Sci. Instr.*, **25**, 324. Meas. of intensities
902. Bird, G. R., *Phys. Rev.*, **95**, 1686L. CH<sub>3</sub>Cl saturation
903. Bird, G. R., and C. H. Townes, *Phys. Rev.*, **94**, 1203. Quad. coupling of S
904. Birnbaum, G., and A. A. Maryott, *Phys. Rev.*, **95**, 622A. Absorption in compressed gases
905. Birnbaum, G., A. A. Maryott, and P. F. Wacker, *J. Chem. Phys.*, **22**, 1782L. CO<sub>2</sub>, high pressure
906. Birnbaum, G., and A. A. Maryott, *J. Chem. Phys.*, **22**, 1457L. NH<sub>3</sub>, line width versus T
907. Bruin, F., *Proc. K. Ned. Akad. Wetensch. B*, **56**, 515. Interferometers
908. Burke, B. F., M. W. P. Strandberg, V. W. Cohen, and W. S. Koski, *Phys. Rev.*, **93**, 193. S<sup>35</sup> magnetic moment
- 908a. Burkhard, D. G., and J. C. Irvin, *Tech. Rep. 2, University of Colorado*. Th. hindered motions
909. Burrus, C. A., A. Jache, and W. Gordy, *Phys. Rev.*, **95**, 299A and *Phys. Rev.*, **95**, 706. PH<sub>3</sub>
910. Burrus, C. A., and W. Gordy, *Phys. Rev.*, **93**, 897. Mm waves OCS
911. Collier, R. J., *Phys. Rev.*, **95**, 1201. HCN *l*-doubling
- 911a. Collins, T. L., W. H. Johnson, Jr., and A. O. Nier, *Phys. Rev.*, **94**, 398. Mass spectra
912. Cornwell, C. D., and R. L. Poynter, *J. Chem. Phys.*, **22**, 1257L. Vinyl iodide



913. Cox, J., W. J. Thomas, and W. Gordy, *Phys. Rev.*, **95**, 299A. CH<sub>3</sub>Cl
- 913a. Daly, R. T., Jr., and J. H. Holloway, *Phys. Rev.*, **96**, 539L. Ga<sup>69</sup>, Ga<sup>71</sup> octupole moments
- 913b. Dehmelt, H. G., *Phys. Rev.* (to be published). Atomic P
- 913c. Dailey, B. P., and C. H. Townes, *J. Chem. Phys.* (to be published). Th. quadrupole coupling
914. DeMore, B. B., W. S. Wilcox, and J. H. Goldstein, *J. Chem. Phys.*, **22**, 876. Pyridine
915. Douglas, A. E., and C. K. Møller, *J. Chem. Phys.*, **22**, 275. IR spectrum N<sub>2</sub>O
916. Dousmanis, G. C., *Phys. Rev.*, **94**, 789A. OD
- 916a. Dousmanis, G. C., *Phys. Rev.* (to be published). NO h.f.s.
917. Erlandsson, G. *J. Chem. Phys.*, **22**, 563L. Cyclopentenone
918. Erlandsson, G., (private communication, to be published). Fluorobenzene
- 918a. Erlandsson, G., *Ark. Fys.*, **8**, 341. Chlorobenzene
919. Erlandsson, G., *J. Chem. Phys.*, **22**, 1152L. Benzonitrile
920. Farrands, J. L., and J. Brown, *Wireless Engr.*, **31**, 81. Interferometer for mm waves
921. Feeny, H., H. Lackner, P. Moser, and W. V. Smith, *J. Chem. Phys.*, **22**, 79. Press. broad. linear mols.
922. Ferguson, R. C., *J. ACS*, **76**, 850. F<sub>2</sub>OS
923. Foley, H. M., R. M. Sternheimer, and D. Tycko, *Phys. Rev.*, **93**, 734. Th. quad. coupling
924. Gallagher, J. J., F. D. Bedard, and C. M. Johnson, *Phys. Rev.*, **93**, 729. NO
- 924a. Geschwind, S., G. R. Gunther-Mohr, and C. H. Townes, *Rev. Mod. Phys.*, **26**, 444. Mass determinations
925. Gordon, J. P., H. J. Zeiger, and C. H. Townes, *Phys. Rev.*, **95**, 282L; thesis, Columbia Univ. (1955). NH<sub>3</sub> h.f.s.; molecular oscillator
926. Gordy, W., *J. Chem. Phys.*, **22**, 1276L. Th. quad. coupling and chemical bonds
- 926a. Gordy, W., *J. Phys. Radium*, **15**, 521. Mm. wave spectroscopy
- 926b. Gordy, W., *J. Chem. Phys.*, **22**, 1470L. Theory quad. coupling
927. Gordy, W., and C. A. Burrus, *Phys. Rev.*, **93**, 419. DBr
928. Gordy, W., and J. Sheridan, *J. Chem. Phys.*, **22**, 92. CH<sub>3</sub>HgCl, CH<sub>3</sub>HgBr
929. Gross, E. P., *Phys. Rev.*, **94**, 1424A. Th. press. broadening
930. Gunther-Mohr, G. R., R. L. White, A. L. Schawlow, W. E. Good, and D. K. Coles, *Phys. Rev.*, **94**, 1184; *Phys. Rev.*, **83**, 880A (1951). NH<sub>3</sub> h.f.s.
931. Gunther-Mohr, G. R., C. H. Townes, and J. H. Van Vleck, *Phys. Rev.*, **94**, 1191. NH<sub>3</sub> h.f.s.
- 931a. Gunton, R. C., J. F. Ollom, and H. N. Rexroad, *J. Chem. Phys.*, **22**, 1942L. (CH<sub>3</sub>)<sub>3</sub>SiF
- 931b. Hardy, W. A., P. Fletcher, and V. Suarez, *Rev. Sci. Inst.*, **25**, 1135L. Stark cell
932. Hardy, W. A., and G. Silvey, *Phys. Rev.*, **95**, 385. TeCS
- 932a. Heald, M. A., and R. Beringer, *Phys. Rev.*, **96**, 645. N
933. Heath, G. A., L. F. Thomas, and J. Sheridan, *Trans. Faraday Soc.*, **50**, 779. F<sub>2</sub>HSi
934. Heath, G. A., L. F. Thomas, and J. Sheridan, (private communication, to be published). C<sub>8</sub>H<sub>4</sub> (penta-1:3-Diyne)
- 934a. Hecht, K. T., and D. M. Dennison (private communication). Hindered torsional motions
935. Heineken, F. W., and F. Bruin, *Physica*, **20**, 350. Microwave refractive index of gases



936. Heitler, W., *The Quantum Theory of Radiation*, 3d ed., Oxford University Press, London.
937. Hill, R. M., and W. Gordy, *Phys. Rev.*, **93**, 1019.
938. Honig, A., M. Mandel, M. L. Stitch, and C. H. Townes, *Phys. Rev.*, **93**, 953A; **96**, 629.
939. Hrostowski, H. J., and R. J. Myers, *J. Chem. Phys.*, **22**, 262.
940. Ishiguro, E., and S. Koide, *Phys. Rev.*, **94**, 350.
941. Ito, T., Y. Tanabe, and M. Mizushima, *Phys. Rev.*, **93**, 1242.
942. Jaccarino, V., J. G. King, R. A. Satten, and H. H. Stroke, *Phys. Rev.*, **94**, 1798L.
943. Jache, A., G. Blevins, and W. Gordy, *Phys. Rev.*, **95**, 299A.
- 943a. Javan, A., and A. Engelbrecht, *Phys. Rev.*, **96**, 649.
- 943b. Jen, C. K., *Am. J. Phys.*, **22**, 553.
944. Johnson, C. M., D. M. Slazer, and D. D. King, *Rev. Sci. Instr.*, **25**, 213.
945. Kambe, K., and J. H. Van Vleck, *Bull. Am. Phys. Soc.*, **29**, 10.
946. King, W. C., and W. Gordy, *Phys. Rev.*, **93**, 407.
947. Kisliuk, P., *J. Chem. Phys.*, **22**, 86.
948. Kivelson, Daniel, *J. Chem. Phys.*, **22**, 904.
- 948a. Kivelson, D., *J. Chem. Phys.*, **22**, 1733.
949. Klinger, H. H., *Introduction to Microwaves and Their Scientific Application*, S. Hirzel, Stuttgart.
- 949a. Kojima, T., and T. Nishikawa, *J. Chem. Soc. Japan* (to be published).
- 949b. Kojima, S., and K. Tsukada, *J. Chem. Phys.*, **22**, 2093L.
950. Kraitchman, J. A., and B. P. Dailey, *Phys. Rev.*, **94**, 788A.
- 950a. Kraitchman, J. A., and B. P. Dailey, *J. Chem. Phys.*, **22**, 1477.
951. Krishnaji and P. Swarup, *J. Chem. Phys.*, **22**, 568.
952. Krishnaji and P. Swarup, *J. Chem. Phys.*, **22**, 1456L.
- 952a. Kusch, P., *J. Chem. Phys.*, **22**, 1203.
953. Kusch, P., and T. G. Eck, *Phys. Rev.*, **94**, 1799.
954. Lide, D. R., Jr., *Phys. Rev.*, **94**, 788A; *J. Chem. Phys.*, **22**, 1613L.
955. Lide, D. R., Jr., *J. Chem. Phys.*, **22**, 1577.
- 955a. Liuima, F. A., A. V. Bushkovitch, and A. G. Rouse, *Phys. Rev.*, **96**, 434.
956. Lovell, R. J., and E. A. Jones, *Phys. Rev.*, **95**, 300A.
957. Lotspeich, J. F., and Ali Javan, *Phys. Rev.*, **94**, 789A.
958. Low, W., *Phys. Rev.* (to be published).
- 958a. Mandel, M., and A. H. Barrett (to be published).
959. Massey, J. T., C. I. Beard, and C. K. Jen, *Phys. Rev.*, **95**, 622A.
960. Massey, J. T., and D. R. Bianco, *J. Chem. Phys.*, **22**, 442.
- 960a. Matricon, M., and Bonnet, *J. Phys. Radium*, **15**, 647.
961. McCulloh, K. E., and G. F. Pollnow, *J. Chem. Phys.*, **22**, 681.
- O<sub>2</sub> Zeeman effect and  $\Delta\nu$   
Alkali halides
- Pentaborane
- H<sub>2</sub>, magnetic properties  
Th. line width
- I<sup>127</sup> nuclear octupole  
moment  
AsH<sub>3</sub>
- MnO<sub>3</sub>F, ReO<sub>3</sub>Cl  
Rotational magnetic  
moments
- Mm-wave harmonic  
generators
- O Zeeman effect
- Mm waves, OCS,  
CH<sub>3</sub>F, H<sub>2</sub>O  
Group V trihalides
- SO<sub>2</sub>  
Hindered motions
- CH<sub>3</sub>SH
- CHBr<sub>3</sub>
- C<sub>2</sub>H<sub>6</sub>F
- eqQ for methyl halides
- CH<sub>3</sub>Br, high pressure  
Temp. dependence  
NH<sub>3</sub> absorption
- KClFeCl<sub>2</sub>, KBrFeBr<sub>2</sub>  
g. factor
- In<sup>115</sup> octupole moment  
CH<sub>3</sub>NH<sub>2</sub>
- Benzonitrile  
Press. broadening
- COF<sub>2</sub>  
ReO<sub>3</sub>F  
Fermi resonance
- TlCl  
HDO<sub>2</sub>
- H<sub>2</sub>O<sub>2</sub>
- Ethylamine
- Pyridine

962. Mizushima, M., *Phys. Rev.*, **94**, 789A; *Phys. Rev.*, **94**, 569. Th. NO h.f.s.
963. Mizushima, M., and R. M. Hill, *Phys. Rev.*, **93**, 745. O<sub>2</sub>
964. Morgan, H. W., and J. H. Goldstein, *J. Chem. Phys.*, **22**, 1427. C<sub>2</sub>H<sub>2</sub>I
965. Muller, N., *J. ACS*, **75**, 860. CH<sub>2</sub>ClF
966. Nielsen, H. H., *J. Chem. Phys.*, **22**, 1383. IR spectrum PH<sub>3</sub>
967. Ogg, R. A., Jr., and J. D. Ray, *J. Chem. Phys.*, **22**, 147. Si<sup>29</sup> spin
- 967a. Osipov, B. D., *J. Exp. Theor. Phys., U.S.S.R.*, **27**, 115. NH<sub>3</sub> dispersion
968. Peter, M., and M. W. P. Strandberg, *Phys. Rev.*, **95**, 622A. OCS
- 968a. Prokhorov, A. M., and A. I. Barchukov, *J. Exp. Theor. Phys., U.S.S.R.*, **26**, 761. Absorption measurements
969. Posener, D. W., and M. W. P. Strandberg, *Phys. Rev.*, **95**, 374. H<sub>2</sub>O
- 969a. Ramsey, N. F., *Nuclear Moments*, John Wiley & Sons, Inc., New York.
970. Rogers, T. F., *Phys. Rev.*, **95**, 622A. H<sub>2</sub>O in atm.
971. Sanders, T. M., Jr., A. L. Schawlow, G. C. Dousmanis, and C. H. Townes, *J. Chem. Phys.*, **22**, 245. OH
- 971a. Sanders, T. M., Jr., G. C. Dousmanis, and C. H. Townes (to be published). OH and OD
972. Satomura, S., *Inst. Sci. and Ind. Res., Memoirs*, **10**, 34. Review microwaves
973. Schatz, P. N., *J. Chem. Phys.*, **22**, 755L. Th. quad. coupling
- 973a. Sheridan, J., and Thomas, L. F., *Nature*, **174**, 798L. Methyl-cyanoacetylene
974. Sherrard, E. I., L. F. Thomas, and J. Sheridan (private communication, to be published). CH<sub>3</sub>CN, CH<sub>3</sub>NC, CH<sub>3</sub>F
975. Shimoda, K., *J. Phys. Soc., Japan*, **9**, 378; **9**, 558; **9**, 567. NH<sub>3</sub> frequency standard
976. Shimoda, K., T. Nishikawa, and T. Itoh, *J. Chem. Phys.*, **22**, 1456L; *J. Phys. Soc. Japan*, **9**, 974. CH<sub>3</sub>NH<sub>2</sub>
977. Slayton, G. R., J. W. Simmons, and J. H. Goldstein, *Phys. Rev.*, **95**, 299A; *J. Chem. Phys.*, **22**, 1678. Vinylene carbonate
978. Solimene, N., and B. P. Dailey, *Phys. Rev.*, **94**, 789A; *J. Chem. Phys.*, **22**, 2042. 1,1 Difluoroethane
- 978a. Solimene, N., and B. P. Dailey, *J. Chem. Phys.* (to be published). CH<sub>3</sub>SH
979. Sternheimer, R. M., *Phys. Rev.*, **95**, 736. Quad. screening theory
980. Sterzer, F., *Phys. Rev.*, **94**, 1410A. CH<sub>3</sub>I quad. transitions
981. Strandberg, M. W. P., *Microwave Spectroscopy*, Methuen & Co., Ltd., London; John Wiley & Sons, Inc., New York.
982. Strandberg, M. W. P., and H. Dreicer, *Phys. Rev.*, **94**, 1393. Beam absorption spectrometer
- 982a. Strandberg, M. W. P., H. R. Johnson and J. R. Eshbach, *Rev. Sci. Instr.*, **25**, 776. Microwave spectrometers
983. Strandberg, M. W. P., and M. Tinkham, *Phys. Rev.*, **95**, 623A. Th. O<sub>2</sub>
- 983a. Swarup, P., *J. Sci. Ind. Res.*, **13B**, 311. Ethyl chloride absorption
984. Swarup, P., *J. Sci. Ind. Res.*, **13B**, 389. Temp. dependence of absorption
985. Takashashi, I., A. Okaya, and T. Ogawa, *J. Inst. Elec. Commun. Engrs. Japan*, **35**, 462. Frequency measurement
986. Tannenbaum, E., R. D. Johnson, R. J. Myers, and W. D. Gwinn, *J. Chem. Phys.*, **22**, 949L. CH<sub>3</sub>NO<sub>2</sub>
987. Tate, P. A., and M. W. P. Strandberg, *J. Chem. Phys.*, **22**, 1380. KCl, NaCl
988. Tate, P. A., and M. W. P. Strandberg, *Rev. Sci. Instr.*, **25**, 956. High temp. spectrograph

- 988a. Thomas, L. F., E. I. Sherrard, and J. Sheridan (private communication, to be published).  $\text{CH}_3\text{CN}$ ,  $\text{CH}_3\text{CCH}$
989. Thomas, W. J. O., J. T. Cox, and W. Gordy, *J. Chem. Phys.*, **22**, 1718.  $D_J$ ,  $D_{JK}$ , methyl halides
990. Tinkham, M., and M. W. P. Strandberg, *Phys. Rev.*, **95**, 622A; thesis, M.I.T.  $\text{O}_2$
991. Trambarulo, R., and P. M. Moser, *J. Chem. Phys.*, **22**, 1622L.  $\text{HCOOH}$
992. Trambarulo, R., H. Lackner, P. Moser, and H. Feeny, *Phys. Rev.*, **95**, 622A. Press. broadening  $\text{BrCN}$
993. Trischka, J. W., and R. Braunstein, *Phys. Rev.*, **96**, 968.  $\text{RbCl}$  (mol. beam)
994. Van Winter, C., *Physica*, **20**, 274. Th. asymmetric rotor
995. Wagner, R. S., and B. P. Dailey, *J. Chem. Phys.*, **22**, 1459L.  $\text{C}_2\text{H}_5\text{Cl}$
996. Weissman, H. B., R. B. Bernstein, S. E. Rosser, A. G. Meister, and F. F. Cleveland, (private communication, to be published). IR spectrum  $\text{CH}_3\text{Br}$
997. Westerkamp, J. F., *Phys. Rev.*, **93**, 716.  $\text{HCN}$   $l$ -doubling
- 997a. Weinstein, R., M. Deutsch, and S. C. Brown, *Phys. Rev.* (to be published). Positronium
998. White, R. L., *Phys. Rev.*, **94**, 789A.  $eqQ$  in  $\text{DCN}$ ,  $\text{HCN}$ ,  $\text{DCCl}$
- 998a. White, R. L., *J. Chem. Phys.* (to be published).  $\text{N}^{14}$  coupling in  $\text{HCN}$
999. White, R. L., *Bul. Am. Phys. Soc.*, **20**, 11; thesis, Columbia Univ. I-J interactions
1000. Wilcox, W. S., J. H. Goldstein, and J. W. Simmons, *J. Chem. Phys.*, **22**, 516. Vinyl cyanide
- 1000a. Wilson, E. B., Jr., C. C. Lin, and D. R. Lide (to be published). Th. hindered rotation
1001. Wolfe, P. N., and Dudley Williams, *Phys. Rev.*, **93**, 360A.  $\text{O}_3$



## AUTHOR INDEX

- Aamodt, L. C., 54, 55  
 Almy, G. M., 186  
 Anderson, P. W., 347, 355, 357, 359, 363, 365, 366, 370  
 Anderson, R. S., 184, 367, 368, 442  
 Artman, J. O., 184, 368, 464  
 Autler, S. H., 279, 281-283, 439
- Bacher, R. F., 141, 143  
 Baird, D. H., 400  
 Barchukov, A. I., 445  
 Bardeen, J., 165, 168, 170  
 Barker, E. F., 39, 305, 308, 309  
 Barlow, H. M., 410  
 Barnes, R. G., 227  
 Barriol, J., 252  
 Bartunek, P. F., 39  
 Bassov, N. G., 429  
 Beam, R. E., 410  
 Becker, G. E., 439  
 Bedard, F. D., 192, 206, 207, 246  
 Beers, Y., 146, 443  
 Benedict, W. S., 107  
 Bennett, W. S., 484  
 Beringer, R., 145, 146, 199, 200, 246, 297-299, 368, 392, 410, 438, 442, 456  
 Bernstein, M. J., 454  
 Bersohn, R., 173  
 Bethe, H. A., 130, 141, 143  
 Betz, O., 127, 128  
 Biedenharn, L. C., 167, 173  
 Bird, G. R., 238, 446, 497  
 Birnbaum, G., 347, 375, 467  
 Blatt, J. M., 167, 173  
 Bleaney, B., 310, 344, 346, 347, 361-363, 370, 373, 392, 435, 438  
 Blockinzew, D., 273  
 Bloom, S., 352  
 Bohr, N., 11  
 Born, M., 5, 375  
 Bragg, J. K., 92, 109, 160, 161, 164, 244, 361  
 Brandt, W. H., 188  
 Breit, G., 141, 144  
 Bronwell, A. B., 410  
 Brouwer, F., 252
- Brown, S. C., 130  
 Budó, A., 185, 187, 188, 299  
 Burkhalter, J. H., 184, 442  
 Burkhard, D. G., 324, 326, 329, 331, 333, 334  
 Burrus, C. A., 192, 207, 246  
 Bushkovitch, A. V., 364
- Candler, A. C., 115  
 Carlson, R. O., 430  
 Carrara, N., 96  
 Carter, R. L., 484  
 Casimir, H. B. G., 61, 136, 227, 228  
 Castle, J. G., 200, 297-299, 438, 442  
 Chang, T. S., 78  
 Chatterjee, S. K., 467  
 Christy, A., 189  
 Coates, R. J., 463, 484  
 Coester, F., 290, 296  
 Coles, D. K., 42, 154, 220, 223, 312, 324, 333, 361, 414, 469  
 Collins, G. B., 405  
 Condon, E. U., 22, 62, 115, 145, 172, 176, 184, 260, 271  
 Cooke, S. P., 484  
 Cooley, J. P., 452, 455  
 Coon, J., 193  
 Cornwell, C. D., 447  
 Costain, C. C., 307, 310, 313  
 Crawford, F. H., 15, 289  
 Crawford, M. F., 143  
 Cross, P. C., 83, 91, 92, 94, 97, 100, 109, 254, 557  
 Cullen, A. L., 410  
 Culshaw, W., 464
- Dailey, B. P., 154, 225, 230, 235-237, 265, 473, 486  
 Danos, M., 374, 429  
 Davis, L., 143  
 Dayhoff, E. S., 129, 130, 475  
 Dean, L. B., Jr., 368  
 Debye, P., 338, 339, 342  
 Dehmelt, H. G., 145, 146

- Dennison, D. M., 72, 78, 86, 94, 105, 302, 304, 305, 308-310, 312, 313, 317-319, 321, 324-329, 333, 334  
 Deutsch, M., 130  
 Dicke, R. H., 337, 434, 435, 448, 449  
 Dickinson, W. C., 212  
 Dieke, G. H., 87  
 Dirac, P. A. M., 126  
 Dousmanis, G., 54, 55, 190-192, 200, 205, 227, 246, 448, 613  
 Dreicer, H., 337, 429  
 Drinkwater, J. W., 127  
 Dunham, J. L., 9, 11  
 Dushman, S., 447  
  
 Eck, T. G., 142  
 Edson, W. A., 410  
 Engelbrecht, A., 73  
 Engler, N., 643  
 Erlandsson, G., 527  
 Eshbach, J. R., 293, 294, 442  
 Essen, L., 467  
 Ewen, H. I., 146  
  
 Fabricand, B. P., 430  
 Fano, V., 260-262  
 Feeny, I. H., 369  
 Feld, B. T., 96, 143, 162  
 Fermi, E., 118  
 Fletcher, E. W., 484  
 Fock, V., 118  
 Foley, H. M., 195, 198, 199, 203, 204, 211, 215, 225, 227, 228, 232, 299, 354, 357, 366, 367  
 Fristrom, R. M., 400  
 Fröhlich, H., 339  
 Froome, K. D., 467  
 Frosch, R. A., 195, 198, 199, 203, 204, 215, 299  
  
 Gabriel, W. F., 477  
 Gallagher, J. J., 192, 206, 207, 246  
 Galloway, W. C., 477  
 Garcia de Quevedo, J. L., 484  
 Geschwind, S., 45, 47, 60, 139, 140, 374, 414, 419, 425, 429  
 Gilbert, C., 187  
 Gilliam, O. R., 442, 456, 464  
 Ginsburg, N., 105  
 Glagolewa-Arkadiewa, A., 452  
 Gobau, G., 400  
 Gokhale, B. V., 184, 368  
 Golay, M. J. E., 456  
 Golden, S., 92, 109, 161, 254, 255, 271  
 Goldman, I. I., 227  
 Goldstein, J. H., 244  
  
 Good, W. E., 154, 220, 223, 310, 312, 333, 361, 421  
 Gordon, A. R., 101  
 Gordon, J. P., 184, 220-222, 368, 429, 432, 433  
 Gordy, W., 156, 184, 192, 207, 237, 246, 310, 368, 400, 414, 416, 418, 442, 456, 457, 459, 460, 462, 464, 473  
 Goudsmit, S. A., 115, 121, 125, 141, 143  
 Green, A. E. S., 643  
 Greenhow, C., 365  
 Griesheimer, R. N., 393  
 Grotrian, W., 127  
 Gunther-Mohr, G. R., 45, 47, 60, 62, 139, 140, 202, 220-224, 429  
 Gwinn, W. D., 164, 334  
  
 Haase, T., 127, 128  
 Hadley, L. N., 310  
 Hagiwara, S., 173  
 Hainer, R. M., 83, 91, 92, 94, 97, 100, 254, 557  
 Hamilton, D. R., 402, 403  
 Hartree, D. A., 118  
 Hartz, T. R., 418  
 Heald, M. A., 145, 146  
 Hebb, M. H., 182  
 Hecht, T., 324, 325, 327-329  
 Hedrick, L. C., 420, 471, 472  
 Heer, F. de, 81  
 Heitler, W., 341  
 Henderson, R. S., 192, 193, 220  
 Henry, A. F., 199, 200, 246, 299  
 Herman, H., 484  
 Hershberger, W. D., 416, 484  
 Herzberg, G., 7, 9, 22, 27, 29, 50, 75, 80, 84, 115, 177, 314, 323, 613  
 Hicks, B. L., 89, 527  
 Hicks, E. M., 484  
 Hill, A. G., 146, 443  
 Hill, E. L., 186, 289  
 Hill, R. M., 184, 365  
 Hillger, R. E., 109, 310, 312, 442  
 Hogan, C. L., 401  
 Holden, A. N., 42, 140, 171, 484, 485  
 Hollander, J. M., 643  
 Holstein, T., 352  
 Honig, A., 16, 444  
 Horie, H., 167  
 Horsfall, R. B., 186  
 Houston, W. V., 127  
 Howard, J. B., 106  
 Howard, R. R., 348, 357, 363-365, 367, 368  
 Huggins, M. L., 237  
 Hughes, H. K., 252  
 Hughes, R. H., 42, 418, 421, 423, 486, 495, 497

- Hund, F., 177-180, 185, 188-190, 197,  
199, 200, 204, 246  
Husten, B. F., 467
- Ingersoll, J. G., 368  
Irvin, J. C., 331  
Ishidzu, T., 167  
Ito, T., 173  
Ivash, E. V., 333
- Jablonski, A., 348  
Jaccarino, V., 142  
Jauch, J. M., 259  
Javan, A., 73, 162, 244, 306  
Jen, C. K., 289, 293, 294, 436, 439, 442  
Johnson, C. M., 184, 192, 206, 207, 246,  
366, 456, 457, 459, 464  
Johnson, H. R., 337, 429, 430  
Johnson, J. B., 407  
Johnson, R. D., 334  
Jorgensen, T., Jr., 15
- Kahan, T., 464  
Kalugina, A., 452  
Karplus, R., 130, 278, 342, 373  
Keilholtz, G. W., 486, 495  
Kellogg, J. M. B., 203, 216, 430, 431  
Kemble, E. C., 61  
Kessler, M., 418  
King, D. D., 457, 459  
King, G. W., 83, 91, 92, 94, 97, 100, 254,  
557  
King, J. G., 142  
King, W. C., 459, 460, 462  
Kisliuk, P., 489, 491  
Kistiakowsky, G. B., 87  
Kivelson, D., 88, 106, 108, 109  
Klein, A., 130  
Klein, J. A., 346, 370, 454-459, 462  
Knight, G., 96, 162  
Knipp, J. K., 402  
Knudsen, M., 374  
Koehler, J. S., 317-319, 321, 333  
Kojima, S., 173  
Kompfner, R., 405  
Kraitchman, J., 54, 55, 162, 522  
Kramers, H. A., 343  
Kraus, H. L., 410  
Kronig, R. de L., 5, 343  
Kuhn, H., 349, 352  
Kuper, J. B. H., 402  
Kusch, P., 142, 145-147  
Kyhl, R. L., 154, 267, 310, 396, 418, 421,  
429, 473
- Lackner, H., 367, 369  
Lamb, W. E., Jr., 128-130, 252, 337, 440,  
441  
Lamont, H. R. L., 368, 391, 410, 484  
Lassettre, E. W., 368  
Lawrance, R. B., 109, 146, 429  
Lebedew, P., 452  
Lee, C. A., 430  
Lengyel, B. A., 464  
Leslie, D. C. M., 361  
Lew, H., 431  
Lewitzky, M., 452  
Lide, D. R., 97, 324, 331  
Lin, C. C., 324  
Lindholm, E., 354  
Lines, A. W., 454  
Livingston, R., 442  
London, F., 349, 352  
Loomis, C. C., 429  
Lorentz, H. A., 338, 339, 344-347, 354, 492  
Lotspeich, J., 306, 522  
Loubser, J. H. N., 346, 347, 370, 392, 454-  
459, 462  
Low, W., 225, 259, 261, 264  
Lyons, H., 399, 419, 428, 444, 467, 477,  
481, 484, 485
- McAfee, K. B., Jr., 193, 201, 202, 418,  
421, 423, 441  
McDermott, N. M., 517  
Mack, J. E., 643  
Madison, T. C., 310, 447  
Mandel, M., 444  
Manning, M. F., 305-307, 309  
Margenau, H., 299, 343, 347, 352, 353,  
362, 363, 366, 367  
Maryott, A. A., 347, 375  
Mays, J. M., 443-445, 448  
Meacham, L. A., 469  
Mecke, R., 90  
Meng, C. Y., 368  
Merritt, F. R., 42, 171, 273, 274, 484, 485  
Miller, S. L., 54, 55, 183, 185, 200  
Millman, S., 405, 430, 431, 454  
Minden, H. T., 73  
Mizushima, M., 82, 173, 184, 261, 362,  
363, 367  
Montgomery, C. C., 438, 467, 470, 473  
Moreno, T., 410  
Morgan, H. W., 486, 495  
Morse, P. M., 71  
Moser, P., 369  
Mott, N. F., 3, 118, 304  
Muller, C. A., 146  
Mulliken, R. S., 178, 181, 182, 189  
Mumford, W. W., 395  
Myers, R. J., 164, 334



- Nethercot, A. H., 346, 370, 371, 452, 454-459, 462  
 Nevin, T. E., 188  
 Newell, G., Jr., 337, 434, 435  
 Newton, R. R., 306, 309  
 Nicholls, E. F., 452  
 Nielsen, A. H., 27, 29, 34, 80  
 Nielsen, H. H., 31, 33, 78, 79, 108, 312, 313, 318  
 Nierenberg, W. A., 263  
 Nishikawa, T., 146, 438, 443  
 Norton, L. E., 484  
 Nuckolls, R. G., 399, 419, 423, 444  
  
 Obi, S. Y., 167  
 Oort, J. N., 146  
 Oppenheimer, J. R., 5  
 Ordnung, P. F., 410  
  
 Page, L., 134  
 Pasternack, S., 127  
 Pauling, L., 3, 5, 8, 22, 38, 65, 115, 121, 125, 229, 237, 239  
 Pekeris, C. L., 7  
 Penrose, R. P., 310, 344, 361-363, 370, 373, 392, 435, 438  
 Perlman, I., 643  
 Peters, C. N., 371  
 Pierce, J. R., 404, 405, 452, 453  
 Pietenpol, W. J., 89  
 Pippard, A. B., 464  
 Pit, H. F., 469  
 Placzek, G., 72, 73  
 Pollard, E. C., 382, 410, 425  
 Poss, H. L., 643  
 Post, E. J., 469  
 Potter, C. A., 364  
 Pound, R. V., 408, 425, 476, 477, 484  
 Pritchard, B. S., 447  
 Prodell, A. G., 145-147  
 Prokhorov, A. M., 429, 445  
 Purcell, E. M., 146  
  
 Rabi, I. I., 144, 203, 216, 263, 430  
 Racah, G., 141, 167  
 Ragan, G. L., 399  
 Rainwater, J., 225  
 Ramsey, N. F., 137, 142, 146, 203, 212, 216, 430, 432  
 Randall, H. M., 78, 86, 105  
 Rapaport, H., 410  
 Rawson, E. B., 145, 199, 200, 246  
 Ray, B. S., 84  
 Reesor, G. E., 128  
 Reich, H. J., 410  
  
 Reitwiesner, G., 89, 527  
 Retherford, R. C., 128, 129, 337  
 Rice, F. O., 447  
 Rice, K. K., 447  
 Richards, P. I., 373  
 Richardson, O., 127  
 Richter, E., 458  
 Rideout, V. C., 477  
 Roberts, A., 146, 443  
 Rogers, J. D., 89  
 Rohrbaugh, J. H., 452, 455  
 Rose, M. E., 167, 173  
 Rouse, A. G., 364  
 Rowen, J. H., 401  
 Rueger, L. J., 399, 419, 423, 444  
  
 Sandeman, I., 11  
 Sanders, T. M., 190-192, 200, 202, 205, 448  
 Sanderson, R. T., 447  
 Sarbacher, R. I., 410  
 Sato, M., 167  
 Satten, R. A., 142  
 Schawlow, A. L., 140, 143, 190, 191, 200, 202, 205, 220, 223, 448  
 Schiff, L. I., 213  
 Schlapp, R., 183  
 Schmid, R., 299  
 Schomaker, V., 241  
 Schutz, P. N., 235  
 Schwarz, R., 294, 295  
 Schwinger, J., 342, 373  
 Seaborg, G. T., 643  
 Segré, E., 643  
 Shaffer, W. H., 31, 79  
 Sharbaugh, A. H., 265, 294, 310, 361, 403, 418, 420, 421, 447  
 Shaul, J. M., 470  
 Sheng, H. E., 305, 308, 309  
 Shepherd, W. G., 404  
 Shimoda, K., 146, 438, 443, 485  
 Shortley, G. H., 22, 62, 115, 145, 172, 176, 184, 260  
 Shulman, R. G., 34, 265, 266  
 Silvey, G., 429  
 Simmons, J. W., 156, 310, 456, 473  
 Sirvetz, M. H., 105, 109, 400  
 Skalnicky, J. G., 410  
 Skilling, H. H., 410  
 Skinner, M., 129  
 Slager, D. M., 366, 457, 459  
 Slater, J. C., 118, 386, 410  
 Slawsky, Z. I., 78  
 Slotnick, M., 263  
 Smith, A. G., 156, 456  
 Smith, D. F., 370  
 Smith, W. V., 77, 184, 227, 348, 357, 363-365, 367-369, 442, 456, 484, 486, 495

- Smythe, W. R., 22, 377  
 Sneddon, I. N., 3, 118, 304  
 Snyder, H. S., 373  
 Solimene, N., 522  
 Southern, A. L., 486, 495  
 Spitzer, L., 352  
 Steacey, E. W. R., 447  
 Sternheimer, R. M., 227, 228, 232, 643  
 Stevenson, D. P., 241  
 Stitch, M., 444  
 Strandberg, M. W. P., 109, 154, 183, 184, 267, 293, 299, 310, 312, 314, 315, 337, 368, 418, 421, 429, 430, 442, 473  
 Stroke, H. H., 142  
 Sturtevant, J. M., 382, 410, 425  
 Sutherland, G. B. B. M., 307  
 Sverdlov, L. M., 90  
  
 Tanabe, Y., 167  
 Tannenbaum, E., 334  
 Tear, J. D., 452  
 Teller, E., 72, 73  
 ter Haar, D., 8  
 Terman, F. E., 391, 470  
 Tetenbaum, S. J., 244  
 Thomas, L. H., 118, 121, 306, 309  
 Tinkham, M., 183, 289, 299  
 Tolansky, S., 337, 429  
 Torrey, H. C., 407, 409, 461  
 Townes, C. H., 34, 42, 45, 47, 54, 55, 60, 62, 139, 140, 165, 168, 170, 171, 183, 185, 190-192, 200, 202, 205, 220-222, 224, 225, 230, 235-238, 244, 259, 261, 264-266, 273, 274, 279, 281-283, 310, 344-346, 361, 370, 373, 405, 414, 429, 432, 433, 444, 448, 454-459, 462, 478, 481, 485, 489, 491  
 Triebwasser, S., 129, 130  
 Tsukada, K., 173  
 Tuller, W. G., 477  
 Turner, T. E., 89, 527  
 Tycko, D., 228, 232  
  
 Uhlenbeck, G. E., 302, 304, 305  
  
 Van der Ziel, A., 418  
 Van Vleck, J. H., 62, 154, 176, 182, 186, 189, 190, 192, 193, 202, 211, 220-222, 224, 339, 342-347, 356, 368, 370, 473  
  
 Venkateswarlu, P., 82  
 Volkov, A., 367  
  
 Wacker, P. F., 375  
 Walchli, H. E., 643  
 Walker, R. M., 385  
 Wang, S. C., 86, 87  
 Wang, T. C., 140  
 Warner, A. W., 470  
 Waters, W. A., 447  
 Watson, G. N., 319  
 Watts, R. J., 418  
 Weber, J., 364  
 Weber, L. R., 86, 105  
 Weingarten, I. R., 347, 439  
 Weinstein, R., 130  
 Weiss, M. T., 314, 315, 429  
 Weisskopf, V. F., 339, 342-347, 354, 356, 370  
 Weizel, W., 178  
 Wentink, T., 267, 312, 418, 421, 429  
 Wessel, G., 431  
 Wesson, L. G., 613  
 Westerkamp, J. F., 34  
 Weston, R. E., 109  
 White, H. E., 115, 123, 125  
 White, R. L., 216, 220, 223, 244, 429  
 Whitmer, C. A., 407, 409, 461  
 Whittaker, E. T., 319  
 Wick, G. C., 17  
 Williams, D., 89, 418  
 Williams, R. C., 127  
 Williams, W. E., 127  
 Wills, A. P., 134  
 Wilson, E. B., Jr., 3, 5, 8, 22, 38, 65, 73, 106, 108, 109, 115, 154, 254, 255, 271, 313, 331, 418, 421, 423, 473  
 Wind, M., 410  
 Wright, N., 78  
  
 Yanagawa, S., 167  
 Young, L. B., 392  
  
 Zabel, C. W., 143  
 Zacharias, J. R., 143, 203, 216  
 Zaffarano, F. P., 477  
 Zeiger, H. J., 220-222, 429, 432, 433  
 Zemplén, J., 299





## SUBJECT INDEX

In addition to subject headings, this index contains the more important symbols used and all molecules mentioned in the text and tables. Molecules are listed alphabetically according to their empirical formulas by the following procedures:

1. All empirical formulas beginning with a given letter are listed at the end of the alphabetical section for that letter.

2. Symbols for the elements in the empirical formula for a molecule are in alphabetical order except that within a molecular formula:

- a. C for carbon precedes all other symbols. This groups organic compounds together.

- b. In organic compounds, H precedes all other symbols except C.

- c. Isotopes are not distinguished, so that D (for deuterium) is regarded as H for purposes of listing.

3. All molecules with formulas of the form  $X_nY$  precede those of the form  $X_{n+1}YZ$ , etc.

To aid in identification, in some cases the usual chemical formula or the name of a compound is given in parentheses. The names are not usually given separate entries. Greek letters are listed as if spelled out.

A (argon), 364–366

A, rotational constant, 48, 50, 83, 613–642

Absorption cells, high temperature, 443–445

outgassing, 498

for reactive materials, 447, 448, 498

resonant cavity, 435–439, 498

Stark modulation, 264–266, 418, 419, 498

untuned cavity, 439–441

waveguide, 264, 266, 411–415, 424, 443–446, 462, 463, 497, 498

for analysis, 497, 498

reflections in, 415, 445, 446, 496, 497

windows, 444, 447

Zeeman modulation, 424

Absorption intensity (see Intensity of absorption)

Abundance of isotopes, 495, 643–648

Accidentally symmetric rotor, 49, 50, 52, 92, 155

Alkali atom energy levels, 119, 120

$\alpha$ , attenuation, 412–414, 436, 437, 440, 441, 445, 446

minimum detectable, 412–415, 437

$\alpha$ , fine-structure constant, 123

$\alpha_s$ , diatomic molecule, 9–16, 613–642

$\alpha_s$ , linear molecule, 25–30, 33, 39–42, 45–47, 613–642

symmetric-top, 79, 613–642

Ammonia ( $\text{NH}_3$ ) (see  $\text{H}_3\text{N}$ )

absorption-frequencies table, 311, 312

Amplifiers, lock-in, 421–424

modulation-frequency, 420–424

Analysis, chemical, 486–498

equipment, 497, 498

qualitative, 488–492

quantitative, 492–497

Anharmonicity of potential, 15, 16, 27–29, 107

Astronomical sources of microwaves, 146–148, 448–450

Asymmetric rotor, centrifugal distortion, 105–109

energy levels, 83–92, 522–556

hindered torsional motions, 324–335

intensities and selection rules, 92–102, 557–612

inversion, 314–315

matrix elements, 92–102

quadrupole coupling, 241–245

- Asymmetric rotor, quadrupole hyperfine structure, 159–164  
   slightly asymmetric, 83–89, 522–526  
   Stark effect, 254, 255, 257, 259–261  
   wave functions, 93–96  
   Zeeman effect, 293–296  
 Atomic clocks, 466, 477–485  
 Atoms, fine structure, 120–124, 126–130  
   hyperfine structure, 126, 130–148  
   masses, 643–648  
   microwave absorption by, 127, 130  
   selection rules and intensities, 118, 124–126, 128, 129, 145–148  
 Attenuation, units, 384  
   waveguide, 383–385  
 Attenuators, waveguide, 397–401, 463  
 A (argon), 364–366  
 AsCl<sub>3</sub>, 53, 173, 242, 614  
 AsF<sub>3</sub>, 52, 53, 79, 614  
 AsH<sub>3</sub>, 53, 242, 307, 614  
  
 B, rotational constant, 2, 9–18, 48, 50, 83, 613–642  
 B<sub>e</sub>, diatomic molecule, 9–18  
   linear molecule, 25–30, 33, 38, 39, 41, 44, 45  
 b<sub>o</sub>, 84  
 b<sub>p</sub>, 84  
 Backward wave tubes, 405, 406, 452–454  
 Bibliography, 649–682  
 Bohr magneton, 120  
 Bolometers, 409, 410, 439, 440  
 Bond angle, effects of hybridization, 237, 238  
 Born-Oppenheimer approximation, 5, 174  
 Boundary conditions, diatomic molecule, 8  
 Breit-Rabi equation, 144  
 Bridge, microwave, 425–427, 429  
 BF<sub>3</sub>, 65, 69  
 B<sub>2</sub>BrH<sub>5</sub>, 110, 614  
 B<sub>5</sub>H<sub>9</sub>, 59, 614  
 BrCl, 236, 615  
 BrCs (CsBr), 14, 615  
 BrF, 13, 14, 236, 615  
 BrF<sub>3</sub>Si (SiF<sub>3</sub>Br), 55, 615  
 BrGeH<sub>3</sub> (GeH<sub>3</sub>Br), 55, 615  
 BrH (HBr), 236  
 BrH<sub>3</sub>Si (SiH<sub>3</sub>Br), 55, 615  
 BrK (KBr), 14, 236, 615  
 BrLi (LiBr), 14, 236, 615, 616  
 BrNa (NaBr), 14, 236, 616  
 BrRb (RbBr), 14, 616  
 Br<sub>2</sub>FeK (KBrFeBr<sub>2</sub>), 294  
 Br<sub>3</sub>P (PBr<sub>3</sub>), 53, 616  
  
 C, rotational constant, 48, 50, 83, 613–642  
 C<sub>I</sub>, 216–224  
 Casimir's function, 151, 499–516  
 Cavity resonators, 390–394, 435–439, 466–468  
   coupling to waveguide, 392–394, 436–439, 468  
   spectrographs, 435–443  
   tuning plungers, 399  
 Centrifugal distortion, asymmetric rotor, 105–109  
   diatomic molecule, 9–11  
   linear molecule, 25, 29, 32, 33  
   symmetric rotor, 77–79  
 Chemical analysis, 486–498  
   equipment, 497, 498  
   qualitative, 488–492  
   quantitative, 492–497  
 Chemical effects on nuclear resonance, 211, 212  
 Cl isotopes, mass ratio, 15, 46  
 Clock, atomic, 466, 477–485  
 Conjugated bonds, 27  
 Coriolis forces, 29–31  
 Correspondence-principle approximation, 91  
 Covalent bonds, 228–241  
   bond angle, 238  
   multiple bonds, 238–241  
   radii, 237–241  
 Crystal, quartz, frequency standards, 468–474  
 Crystal detectors, 407–410, 456–458  
   impedance, 407, 420, 421  
   mounts, 409, 456–458  
   noise, 407, 408  
 Crystal harmonic generators, 409, 458–462  
 CBrF<sub>3</sub> (CF<sub>3</sub>Br), 55, 616  
 CBrN (BrCN), 29, 30, 244, 367, 498, 616, 617  
 CClF<sub>3</sub> (CF<sub>3</sub>Cl), 55, 617  
 CCIN (ClCN, cyanogen chloride), 15, 29, 30, 170, 171, 217–219, 235, 364, 365, 495, 617  
 CCl<sub>2</sub>O (COCl<sub>2</sub>, phosgene), 617  
 CCl<sub>4</sub>, 363  
 CF<sub>3</sub>I, 55, 617  
 CF<sub>4</sub>, 82  
 CF<sub>3</sub>S (CF<sub>3</sub>SF<sub>5</sub>), 58, 322, 323, 335  
 CHBr<sub>3</sub> (CBr<sub>3</sub>H), 55, 173, 617  
 CHClF<sub>2</sub>, 617  
 CHCl<sub>3</sub> (CCl<sub>3</sub>H), 55, 363, 364, 617, 618  
 CHF<sub>3</sub> (CF<sub>3</sub>H), 55, 618  
 CHN (HCN), 29, 30, 34, 217, 244, 364, 365, 618  
 CHNO (HNCO), 110, 618  
 CHNS (HNCS), 110, 618, 619

- $\text{CH}_2\text{Br}_2$ , 619  
 $\text{CH}_2\text{Cl}_2$ , 103, 104, 110, 364, 619  
 $\text{CH}_2\text{F}_2$ , 104, 110, 619  
 $\text{CH}_2\text{O}$ , 102, 104, 109, 110, 619  
 $\text{CH}_2\text{O}_2$  ( $\text{HCOOH}$ ), 620  
 $\text{CH}_3\text{BO}$  ( $\text{BH}_3\text{CO}$ ), 58, 79, 620  
 $\text{CH}_3\text{Br}$ , 55, 620, 621  
 $\text{CH}_3\text{BrHg}$  ( $\text{CH}_3\text{HgBr}$ ), 56, 62, 621  
 $\text{CH}_3\text{Cl}$ , 46, 54, 55, 65–69, 78, 79, 88, 218, 235, 236, 263, 363, 621  
 $\text{CH}_3\text{ClHg}$  ( $\text{CH}_3\text{HgCl}$ ), 56, 621, 622  
 $\text{CH}_3\text{Cl}_3\text{Si}$  ( $\text{CH}_3\text{SiCl}_3$ ), 57, 622  
 $\text{CH}_3\text{F}$ , 55, 294, 622  
 $\text{CH}_3\text{F}_3\text{Si}$  ( $\text{CH}_3\text{SiF}_3$ ), 57, 323, 622  
 $\text{CH}_3\text{HgI}$ , 56, 622  
 $\text{CH}_3\text{I}$ , 55, 79, 155, 236, 622, 623  
 $\text{CH}_3\text{NO}$ , 335  
 $\text{CH}_3\text{NO}_2$ , 323, 324, 334, 335, 623  
 $\text{CH}_4\text{O}$  ( $\text{CH}_3\text{OH}$ ), 111, 294, 300, 302, 315, 323, 324, 333, 334, 623  
 $\text{CH}_4\text{S}$  ( $\text{CH}_3\text{SH}$ ), 111, 323, 623  
 $\text{CH}_5\text{N}$  ( $\text{CH}_3\text{NH}_2$ ), 323, 324, 623  
 $\text{CH}_6\text{Si}$  ( $\text{CH}_3\text{SiH}_3$ ), 57, 323, 324, 624  
 $\text{CH}_6\text{Sn}$  ( $\text{CH}_3\text{SnH}_3$ ), 57, 323, 624  
 $\text{CIN}$  ( $\text{ICN}$ ), 29, 30, 157–159, 244, 245, 624  
 $\text{CO}$ , 13, 14, 365, 624  
 $\text{COF}_2$ , 624  
 $\text{COS}$  ( $\text{OCS}$ ), 26, 28–30, 35–37, 39–43, 46, 47, 153, 154, 217–219, 242, 267, 268, 273, 274, 292, 294, 364–367, 369, 462, 624, 625  
 $\text{COSe}$  ( $\text{OCSe}$ ), 30, 46, 217, 219, 292, 294, 625  
 $\text{CO}_2$ , 28, 35, 364, 365, 375, 488  
 $\text{CS}$ , 14, 217, 626  
 $\text{CS}_2$ , 364, 365  
 $\text{CSSe}$  ( $\text{SCSe}$ ), 30, 626  
 $\text{CSTe}$  ( $\text{SCTe}$ ), 30, 626  
 $\text{C}_2\text{F}_3\text{N}$  ( $\text{CF}_3\text{CN}$ ), 57, 626  
 $\text{C}_2\text{HCl}$  ( $\text{HCCCl}$ ), 30, 626, 627  
 $\text{C}_2\text{H}_2$ , 365  
 $\text{C}_2\text{H}_2\text{ClF}$  ( $\text{CH}_2\text{CFCl}$ ), 627  
 $\text{C}_2\text{H}_2\text{F}_2$  ( $\text{H}_2\text{CCF}_2$ ), 104, 111, 627  
 $\text{C}_2\text{H}_2\text{O}$  ( $\text{H}_2\text{C}_2\text{O}$ , ketene), 104, 111, 627  
 $\text{C}_2\text{H}_3\text{Br}$  (vinyl bromide), 627  
 $\text{C}_2\text{H}_3\text{Cl}$  (vinyl chloride), 242, 244, 627  
 $\text{C}_2\text{H}_3\text{Cl}_3$  ( $\text{CH}_3\text{CCl}_3$ ), 323  
 $\text{C}_2\text{H}_3\text{F}_3$  ( $\text{CH}_3\text{CF}_3$ ), 57, 301, 303, 315–323, 627  
 $\text{C}_2\text{H}_3\text{HgN}$  ( $\text{CH}_3\text{HgCN}$ ), 57  
 $\text{C}_2\text{H}_3\text{I}$  (vinyl iodide), 628  
 $\text{C}_2\text{H}_3\text{N}$  ( $\text{CH}_3\text{CN}$ , methyl cyanide), 56, 628  
 $\text{C}_2\text{H}_3\text{N}$  ( $\text{CH}_3\text{NC}$ , methyl isocyanide), 56, 628  
 $\text{C}_2\text{H}_3\text{NS}$  ( $\text{CH}_3\text{NCS}$ , methyl isothiocyanate), 111, 629  
 $\text{C}_2\text{H}_3\text{NS}$  ( $\text{CH}_3\text{SCN}$ , methyl thiocyanate), 111, 629  
 $\text{C}_2\text{H}_4$  (ethylene), 322, 365  
 $\text{C}_2\text{H}_4\text{F}_2$  ( $\text{CH}_3\text{CHF}_2$ ), 323, 629  
 $\text{C}_2\text{H}_4\text{O}$  (ethylene oxide), 112, 629  
 $\text{C}_2\text{H}_4\text{S}$  (ethylene sulfide), 112, 629  
 $\text{C}_2\text{H}_5\text{Cl}$  (ethyl chloride), 629, 630  
 $\text{C}_2\text{H}_5\text{N}$  (ethylenimine), 112, 630  
 $\text{C}_2\text{H}_6$  ( $\text{CH}_3\text{CH}_3$ , ethane), 323, 365  
 $\text{C}_2\text{H}_6\text{O}$  [ $(\text{CH}_3)_2\text{O}$ ], 323, 630  
 $\text{C}_3\text{HF}_3$  ( $\text{F}_3\text{CCCH}$ ), 57, 79, 630  
 $\text{C}_3\text{HN}$  ( $\text{HCCCN}$ ), 30, 630  
 $\text{C}_2\text{H}_3\text{O}_2$  (vinylene carbonate), 630  
 $\text{C}_3\text{H}_3\text{Br}$  ( $\text{CH}_3\text{CCBr}$ ), 56, 630, 631  
 $\text{C}_3\text{H}_3\text{I}$  ( $\text{CH}_3\text{CCI}$ ), 56, 79, 631  
 $\text{C}_3\text{H}_3\text{N}$  (vinyl cyanide), 112, 631  
 $\text{C}_3\text{H}_4$  ( $\text{CH}_3\text{CCH}$ ), 56, 294, 631  
 $\text{C}_3\text{H}_4$  (allene), 82  
 $\text{C}_3\text{H}_5\text{Cl}$  (cyclopropyl chloride), 631  
 $\text{C}_3\text{H}_6\text{O}$  [ $(\text{CH}_3)_2\text{CO}$ , acetone], 632  
 $\text{C}_3\text{H}_6\text{O}_3$  (trioxane), 59, 632  
 $\text{C}_3\text{H}_9\text{ClSi}$  [ $(\text{CH}_3)_3\text{SiCl}$ ], 59, 632  
 $\text{C}_3\text{H}_9\text{FSi}$  [ $(\text{CH}_3)_3\text{SiF}$ ], 632  
 $\text{C}_3\text{N}_3\text{P}$  [ $\text{P}(\text{CN})_3$ ], 58, 632  
 $\text{C}_4\text{H}_4$  (vinylacetylene), 632  
 $\text{C}_4\text{H}_4\text{O}$  (furan), 632  
 $\text{C}_4\text{H}_5\text{N}$  (pyrrole), 112, 632  
 $\text{C}_4\text{H}_9\text{Br}$  [ $(\text{CH}_3)_3\text{CBr}$ ], 58, 632  
 $\text{C}_4\text{H}_9\text{Cl}$  [ $(\text{CH}_3)_3\text{CCl}$ ], 58, 632  
 $\text{C}_4\text{H}_9\text{I}$  [ $(\text{CH}_3)_3\text{CI}$ ], 58, 632  
 $\text{C}_4\text{H}_{10}\text{O}$  [ $(\text{C}_2\text{H}_5)_2\text{O}$ , diethyl ether], 632  
 $\text{C}_5\text{H}_4\text{O}$  ( $\text{CH}_3\text{CCCCH}$ ), 632  
 $\text{C}_5\text{H}_5\text{N}$  (pyridine), 112, 633  
 $\text{C}_5\text{H}_8\text{O}$  ( $\text{COCH}_2\text{CH}_2\text{CH}_2\text{CH}_2$ ), 633  
 $\text{C}_6\text{H}_5\text{Br}$  (bromobenzene), 633  
 $\text{C}_6\text{H}_5\text{Cl}$  (chlorobenzene), 633  
 $\text{C}_6\text{H}_5\text{F}$  (fluorobenzene), 113, 633  
 $\text{C}_6\text{H}_6$  (benzene), 488  
 $\text{C}_7\text{H}_5\text{N}$  (benzonitrile), 633  
 $\text{C}_8\text{H}_{13}\text{Br}$ , 59, 633  
 $\text{C}_8\text{H}_{13}\text{Cl}$ , 59, 633  
 $\text{Cl}$  (atom), 235  
 $\text{ClCs}$  ( $\text{CsCl}$ ), 14, 15, 236, 633  
 $\text{ClF}$ , 13, 14, 217, 234–236, 242, 633  
 $\text{ClF}_3$ , 113, 498, 634  
 $\text{ClF}_3\text{Ge}$  ( $\text{GeF}_3\text{Cl}$ ), 55, 79, 634  
 $\text{ClF}_3\text{Si}$  ( $\text{SiF}_3\text{Cl}$ ), 55, 634  
 $\text{ClGeH}_3$  ( $\text{GeH}_3\text{Cl}$ ), 55, 60, 218, 634  
 $\text{ClH}_3\text{Si}$  ( $\text{SiH}_3\text{Cl}$ ), 55, 60, 218, 242, 634  
 $\text{ClI}$  ( $\text{ICl}$ ), 13, 14, 15, 235, 236, 242, 634, 635  
 $\text{ClIn}$  ( $\text{InCl}$ ), 232–234  
 $\text{ClK}$  ( $\text{KCl}$ ), 13, 14, 15, 236, 635  
 $\text{ClNO}$  ( $\text{NOCl}$ ), 89, 635  
 $\text{ClNa}$  ( $\text{NaCl}$ ), 14, 233–235, 635  
 $\text{ClO}_2$ , 149, 174, 193, 201, 202, 448  
 $\text{ClO}_3\text{Re}$ , 55, 635  
 $\text{ClRb}$  ( $\text{RbCl}$ ), 14, 236, 635



- ClTi (TiCl), 217, 234–236, 242, 635  
 Cl<sub>3</sub>FeK (KClFeCl<sub>2</sub>), 294  
 Cl<sub>3</sub>GeH (GeCl<sub>3</sub>H), 635, 636  
 Cl<sub>3</sub>SiH (SiCl<sub>3</sub>H), 636  
 Cl<sub>3</sub>OP (PCl<sub>3</sub>O), 55, 636  
 Cl<sub>3</sub>P (PCl<sub>3</sub>), 52, 53, 88, 636  
 Cl<sub>3</sub>PS (PCl<sub>3</sub>S), 55, 636  
 Cl<sub>3</sub>Sb (SbCl<sub>3</sub>), 53, 636  
 Cs (atom), 146  
 CsF, 14, 217, 218, 636  
 CsI, 14, 636
- D*, diatomic molecule, 7, 9, 613–642  
   linear molecule, 25, 29, 613–642  
*D*, *D<sub>J</sub>*, *D<sub>K</sub>*, symmetric top, 78, 79, 613–642  
*D<sub>e</sub>*, diatomic molecule, 9–14  
 Δ states, 175  
 Δ*ν*, atomic fine-structure splitting, 121–123, 127, 141, 143  
 Δ*ν*, line-breadth parameter, 19, 24, 76, 77, 101, 102, 128, 146, 147, 336–375, 492–494  
 Detectors, microwave, crystal, 407–410, 456–458  
   millimeter wave, 455–458  
   thermal, 409, 410, 439, 440, 455, 456  
 Diatomic molecule, centrifugal distortion, 9–11  
   energy levels, 4, 5, 9–11  
   frequencies of rotational transitions, 3  
   intensities and selection rules, 18–24  
   matrix elements, 19–24  
   wave functions, 4, 6  
 Dielectric constant of absorbing gas, 339–344, 481  
 Dipole moment, electric, 19–24, 52, 73, 74, 77, 82, 93, 94, 132, 248–250, 264–268  
   due to degenerate vibrations, 82  
   measurement, 264–268  
   sign, 296  
   table, 613–642  
   variation with vibrational state, 268  
 Dipole moment matrix element, 20–24, 34–35, 74, 92–102, 557–612  
 Dirac theory of hydrogen atom, 126, 127  
 Directional couplers, 394–397  
 Discriminator, microwave cavity, 475–477  
 Dispersion at microwave line, 339–344, 414, 443, 481  
 Dissociation energy, 7  
 Distances, internuclear, 7, 12, 40–42, 53, 55–59, 109–114, 237–241, 613–642  
 Doppler broadening, 336–338, 427–435  
 Double bonds, 238–241  
 Double modulation, 416–418, 465  
 Dunham's coefficients, 9–13
- Eckart conditions, 108  
 Electronegativity, 236–238  
 Electronic angular momentum, coupling cases, 177–180  
   notation, 174, 175  
   <sup>1</sup>Σ molecules, 207–224  
   (See also *L*; Paramagnetic molecules; *S*)  
 Electronic effects, on mass measurements, 15–18, 212–215  
   on rotational energy, 212–215  
 Ellipsoid of inertia, 48  
 Energy levels, asymmetric rotor, 83–92, 105–109, 522–556  
   atom, 115–124, 126–146  
   diatomic molecule, 4, 5, 9–11  
   hydrogen atom, 116, 118, 126–130, 146–148  
   linear molecule, 25–40  
   quadrupole hyperfine structure, 150–173, 499–516  
   rigid rotor, 527–556  
   symmetric rotor, 50, 51, 62, 66–69  
 Exchange energy, 229  
 Eulerian angles, 60, 61
- F, 138, 140, 176  
*f* (fraction of molecules), asymmetric rotor, 100–105  
   atom, 145, 146  
   diatomic molecule, 19, 20  
   symmetric rotor, 74–76  
 Fabry-Perot interferometer, 464  
 Fermi resonance, 35–40, 253  
 Fine structure, atoms, 120–130  
   intensity, 499–516  
   inversion, 307–315  
 Forbidden lines, Stark effect, 269–273  
 Foreign gas broadening, 363–366  
 Frequencies of rotational transitions,  
   diatomic molecule, 3, 4  
   linear molecule, 32, 33  
   symmetric rotor, 52, 78  
 Frequency control, 474–485  
   by microwave cavity, 475–477  
   by microwave line, 477–482  
   by standard oscillator, 474, 475  
 Frequency differences, measurement of, 473, 474  
 Frequency measurement, 391–395, 399, 463, 464, 466–474  
 Frequency standards, 466, 468–485  
   microwave lines, 477–485

- Frequency standards, nuclear quadrupole resonance, 485  
 quartz crystal, 468-473  
 $\text{FH}_3\text{Si}$  ( $\text{SiH}_3\text{F}$ ), 46, 55, 636  
 $\text{FK}$  ( $\text{KF}$ ), 217  
 $\text{FLi}$  ( $\text{LiF}$ ), 217, 218, 636  
 $\text{FMnO}_3$  ( $\text{MnO}_3\text{F}$ ), 55, 637  
 $\text{FNO}$  ( $\text{NOF}$ ), 113, 637  
 $\text{FNO}_2$  ( $\text{NO}_2\text{F}$ ), 113  
 $\text{FO}_3\text{Re}$  ( $\text{ReO}_3\text{F}$ ), 55, 637  
 $\text{FRb}$  ( $\text{RbF}$ ), 217, 218  
 $\text{F}_2\text{OS}$  (thionyl fluoride), 113, 637  
 $\text{F}_2\text{O}_2\text{S}$  ( $\text{F}_2\text{SO}_2$ ), 113  
 $\text{F}_3\text{HSi}$  ( $\text{SiF}_3\text{H}$ ), 55, 60, 637  
 $\text{F}_3\text{N}$  ( $\text{NF}_3$ ), 52, 53, 67, 637  
 $\text{F}_3\text{OP}$  ( $\text{POF}_3$ ), 55, 637, 638  
 $\text{F}_3\text{P}$  ( $\text{PF}_3$ ), 53, 638  
 $\text{F}_3\text{PS}$  ( $\text{PF}_3\text{S}$ ), 55, 638
- $g$  factor, electron spin, 145  
 molecular, 286, 290-296  
 nuclear, 141  
 $g_J$ , 286, 290-296  
 $\gamma$ , absorption intensity, asymmetric rotor, 101, 102  
 atom, 124-126, 128, 129, 145-148  
 diatomic molecule, 19-24  
 symmetric rotor, 73-77
- Golay cell, 456
- H (atom), 115-118, 126-130, 146-148  
 Harmonic generators, 409, 410, 458-462, 470-473  
 Harmonic oscillator approximation, 92  
 Harmonics of microwave generators, 454, 455  
 Hindered motions, 300-335  
 torsional, asymmetric rotor, 324-335  
 potential barrier, 300-302, 318, 320, 322-324, 327-331, 333-335  
 selection rules, 331-333  
 symmetric rotor, 300-303, 315-324, 331-333  
 wave functions, 318, 319  
 (See also Inversion)
- Hund's coupling cases, (a), 177-180  
 (b), 178, 180, 182-185  
 (c), 178-180, 185  
 (d), 179, 180, 185  
 (e), 179
- Hybrid T, 396, 397  
 Hybridization of bonds, 229, 231, 232, 234-240  
 Hydrogen (atomic), 115-118, 126-130, 146-148  
 Hyperfine doubling, 205, 221-224
- Hyperfine structure, atoms, 126, 130-148  
 electric hexadecapole, 133  
 electric quadrupole, 131-140, 149-173, 499-516  
 asymmetric rotor, 159-164  
 intensities, 151-154, 172, 499-516  
 interpretation of coupling constants, 225-245  
 linear molecule, 150-154, 499-516  
 symmetric top, 154-159, 499-516  
 two or more nuclei, 164-173  
 intensities of components, 151-154, 172, 499-516  
 magnetic dipole, 140-148, 194-224  
 atoms, 140-148  
 coupling schemes, 196-199  
 I·J interaction, 194, 215-224  
 interpretation of coupling constants, 245-247  
 $\Lambda$  doublets, 203-207  
 molecules, 194-224  
 with electronic angular momentum, 199, 200  
 $\text{NH}_3$ , 221-224  
 nonlinear molecules, 200-202, 219-224  
 nonlinear  $^1\Sigma$  molecules, 219-224  
 magnetic octupole, 142  
 Zeeman effect, 143-145, 289, 290
- Hypergeometric function, 62  
 $\text{HBr}$ , 14, 638  
 $\text{HCl}$ , 13  
 Helium, 364-366  
 $\text{HI}$ , 13, 14, 217, 236, 638  
 $\text{HN}_3$ , 114, 638  
 $\text{HO}$  ( $\text{OH}$ ), 178, 186, 190-192, 205, 207, 246, 448, 639  
 $\text{H}_2$ , 203, 217, 218, 292, 294, 364  
 $\text{H}_2\text{O}$ , 49, 102, 104, 105, 109, 294-296, 345, 346, 498, 639  
 $\text{H}_2\text{O}_2$ , 323, 639  
 $\text{H}_2\text{S}$ , 109, 114, 294, 639  
 $\text{H}_3\text{N}$  ( $\text{NH}_3$ ), 49, 52, 53, 65-69, 74, 77-79, 104, 205, 217, 220-224, 242, 250, 259, 292, 294, 300-315, 344-347, 353, 360-366, 368, 370, 432-434, 479, 483, 484, 495, 498, 640  
 $\text{H}_3\text{P}$  ( $\text{PH}_3$ ), 52, 53, 78, 79, 109, 307, 640, 641  
 $\text{H}_3\text{Sb}$  ( $\text{SbH}_3$ ), 53, 641
- I, 131-133, 140, 142, 153-155, 176  
 $I_A$ , 48, 50, 83  
 $I_B$ , 48, 50, 83  
 $I_C$ , 48, 50, 83  
 $I_\infty$ , 12, 41  
 I·J interaction, 194, 215-224  
 linear molecule, 216-219

- Intensities, atoms, 124–126
- Intensity of absorption, 339–344, 369–373, 464, 465, 492–496, 499–516
  - absolute, 343
  - asymmetric rotor, 92–102, 557–612
  - atom, 124–126, 128, 129, 145–148
  - diatomic molecule, 18–24
  - fine structure, 124–126, 499–516
  - hyperfine structure, 151–154, 172, 499–516
  - integrated, 343, 344, 492
  - linear molecule, 25
  - peak, 24, 77, 101, 102, 342, 492–495
  - Stark effect, 255–258, 269–273
  - symmetric rotor, 73–77
  - temperature dependence, 24, 369, 370
- Interferometers, microwave, 464
- Intermolecular forces, 348–350, 359–368
  - dipole-dipole, 349, 359, 360, 366–368
  - dipole-induced dipole, 349, 360
  - dipole-quadrupole, 349, 364, 365, 368
  - Keesom alignment, 349, 367, 368
  - quadrupole-induced dipole, 349, 360, 365, 366
  - short-range, 349, 368
- Internuclear distances, 7, 12, 40–42, 53, 55–59, 109–114
- Inversion, 65–71, 74, 75, 77, 220–224, 250, 259, 300–315
  - asymmetric forms of ammonia, 314, 315
  - energy levels, 64–69, 300–303
  - fine structure, 307–315
  - frequencies of transitions, 67–69, 300–315
  - magnetic hyperfine structure, 220–224
  - potential barrier, 65–67, 300–310
  - Stark effect, 250, 259
  - symmetry with respect to, 65–69
  - wave functions, 70, 303–305
- Ionic character of bonds, 234–241
- Isolator, 401
- Isotope abundance, 643–648
- Isotope analysis, 495
- Isotope masses, 643–648
  - ratios, 11, 14–18, 42–47, 55, 60
- IK (KI), 14, 236, 641
- ILi (LiI), 14, 236, 641
- INa (NaI), 14, 236, 641
- IRb (RbI), 14, 641
  
- $J_a$ , 176
- Johnson noise, 407, 412–414
  
- $K$ , 50, 83, 84
- $K_1$ ,  $K_{-1}$ , 84
  
- $\kappa$  (Ray's asymmetry parameter), 84
- Keesom alignment forces, 349, 367, 368
- Klystrons, 402–406, 452–455
- Kramers-Kronig relations, 343
  
- $L$ , 123, 175–179
- $L$  uncoupling, 15, 17, 182
- $l$ , orbital quantum number (atoms), 116
- $l$ -type doubling, 31–35, 79–82, 159, 613–642
  - Stark effect, 254
- Laguerre polynomials, 8, 32, 116
- Lamb shift, 126–130
- $\Lambda$ , 175
- $\Lambda$  doubling, 180, 188–192, 289
  - Zeeman effect, 289
- Larmor's theorem, 210
- Legendre polynomials, 22, 116
- Line shape, high pressure, 345–347, 370, 371
  - Lorentz, 338, 345, 418
  - Van Vleck-Weisskopf, 339–347, 418
  - (*See also* Line width)
- Line width, 336–375, 427–435
  - collision with walls, 374, 375, 427
  - Doppler, 336–338, 427–435
  - measurement, 418
  - modulation, 425, 427, 428
  - natural, 336, 337
  - oscillator fluctuations, 427, 428
  - pressure dependence, 336, 338–371, 427, 492–494
  - saturation, 371–373, 427, 428
  - temperature dependence, 368–370
- Linear molecule, centrifugal distortion, 25, 29, 32, 33
  - energy levels, 25–40
  - frequencies of rotational transitions, 32, 33
  - intensities, 25
  - quadrupole hyperfine structure, 150–154, 499–521
  - Stark effect, 248, 250–257
  - wave functions, 25
- Lock-in amplifier, 421–424
- Lorentz line shape, 338, 345, 418
  
- $m$ , magnetic quantum number (atoms), 116
- Magic T, 396, 397
- Magnetic hyperfine structure, atoms, 140–148
  - coupling schemes, 196–199
  - $I \cdot J$  interaction, 194, 215–224
  - interpretation of coupling constants, 245–247



- Magnetic hyperfine structure,  $\Lambda$  doublets, 203–207  
   molecules, 194–224  
     with electronic angular momentum, 199, 200  
    $\text{NH}_3$ , 221–224  
   nonlinear molecules, 200–202, 219–224  
 Magnetic moment, molecular, 286–296  
   measurement, 442  
   origin, 290–292  
   sign, 288, 289  
 Magnetron, Bohr, 120  
   nuclear, 141  
 Magnetrons, 405–406, 452–455  
 Maser, 432–444, 482, 483, 485  
 Masses, nuclear, 11, 14–18, 42–47, 55, 60, 643–648  
 Mathieu's equation, 319  
   approximation for asymmetric rotor, 92  
 Matrix elements, asymmetric rotor, 92–102, 557–612  
   atom, 124, 145  
   diatomic molecule, 19–24  
    $l$ -type doubling, 34  
   quadrupole hyperfine structure, 156, 157, 164, 172, 173  
   symmetric rotor, 74  
 Maxwell's equations, 376, 377  
 Michelson interferometer, 464  
 Microwave generators, 401–407, 432–434, 451–455  
 Millimeter waves, 451–465  
   generators, 451–462  
   grating spectrograph, 463  
   propagation, 462, 463  
   spectrographs, 463–465  
   waveguide, 462, 463  
 Modulation, broadening, 427, 428  
   high-frequency, 273–283  
   resonant, 279–283  
   source (double), 416–418, 465  
   Stark, 264–266, 273–283, 418–424, 464, 465, 485  
   Zeeman, 425, 438, 485  
 Molecular beam measurements, 216, 429–434  
 Molecular constants, 613–642  
 Moments of inertia, determination of, 40–42, 53  
 Multiple bonds, 238–241  
  
 N, 176–179  
 N (atom), 146  
 $n$ , principal quantum number, 116, 119, 120  
 Natural line width, 336, 337  
  
 Noise, bolometers, 410  
   crystal detectors, 407, 408, 414–416, 425  
   oscillator, 404, 405, 414, 415  
   thermal, 407, 412–414  
 Noise figure, 414, 415  
 Nonpolar gases, absorption by, 375  
 Nonpolar molecules, transitions induced by electric field, 271–273  
 Normal coordinates, 26  
 Normal modes, 26  
 Nuclear magneton, 141  
 Nuclear moments, electric hexadecapole, 133  
   electric quadrupole, 133–140, 149–173, 643–648  
   existence of, 142  
   magnetic dipole, 140–146, 643–648  
   magnetic octupole, 142  
 Nuclear polarization, 138–140  
 Nuclear-properties table, 643–648  
 Nuclear spin, 131–133, 140, 142, 153–155, 176, 643–648  
   effect on intensities, 69–73, 102–105  
 N (atom), 146  
 NO, 14, 149, 174, 192, 199, 200, 206, 207, 246, 247, 297–299, 365, 448, 641  
 NO<sub>2</sub>, 104, 149, 174, 193, 201, 448, 641  
 NO<sub>2</sub>F (nitryl fluoride), 641  
 N<sub>2</sub>, 364, 365, 488  
 N<sub>2</sub>O, 29, 30, 42, 47, 242, 294, 365, 641  
 Na (atom), 146  
  
 O, 176–179  
 Oblate symmetric top, 51, 83, 522–526  
 $\Omega$ , 176, 179, 180  
 $\omega_e$ , diatomic molecule, 9–16  
 Oscillators, microwave, 401–407, 451–455  
   stabilization, 428  
 O<sub>2</sub>, 149, 174, 183–185, 200, 246, 247, 299, 364–366, 368, 483, 642  
 O<sub>2</sub>S (SO<sub>2</sub>), 104, 109, 294, 364, 642  
 O<sub>3</sub>, 114, 294, 642  
  
 P (atom), 146  
 $P$  branch, 99, 557–612  
 $P_x$ ,  $P_y$ ,  $P_z$ , 50, 83  
 $p_r$  electron, 238, 240, 244, 247  
 $p_\sigma$  electron, 233, 234, 238, 240, 242, 244  
 Paramagnetic molecules, 174–193  
   Hund's coupling cases, 177–180  
   notation, 175, 176  
   rotational energy levels, 180–193  
   Zeeman effect, 284–290  
 Phase-sensitive detector, 421–424  
 $\Pi$  states, 175, 187, 189–192, 203–207, 246, 285

- $\pi$  components in Zeeman effect, 287
  - Planar molecules, 52, 102
  - Polarization, magnetic, 211, 212
    - of molecule by electric field, 250
  - Positronium, 130
  - Potential, interatomic, 5-7, 27-29, 65-67, 300-310
    - Morse, 7
  - Potential barrier, hindered torsional motions, 300-302, 318, 320, 322-324, 327-331, 333-335
    - inversion, 65-67, 300-310
  - Pound stabilizer, 475-477, 484
  - Pressure broadening, 336, 338-371
    - frequency shifts, 355, 370, 371
    - high pressure, 345-347, 370, 371
    - impact theory, 338-347, 349-371
    - intermolecular forces, 348-350, 359-368
    - line shape, 338-347, 370, 371
    - statistical theory, 349-355, 362, 363
  - Pressure-induced absorption, 375
  - Principal axes, 48, 49
  - Principal moments of inertia, 48
  - Prolate symmetric top, 51, 83, 522-526
  - Propagation of microwaves in matter, 377-379
  - Pseudo quadrupole effect, 185, 211
  - Pure precession hypothesis, 214
  - P (atom), 146
- 
- $Q$ , figure of merit, 391, 392
  - $Q$ , quadrupole moment, 133-140, 225, 643-648
  - $Q$  branch, 99, 557-612
  - $q$ , electric field gradient, 137, 138, 225, 228-245
    - calculation of, in a molecule, 232-245
    - screening by closed shells, 231, 232
  - $q_J$ , 137, 138, 150, 154, 159, 226-228
  - $q_l$ , 33, 34, 613-642
  - Quadrupole coupling, 131-140, 149-173, 225-247, 613-642
    - asymmetric molecules, 241-245, 613-642
    - atoms, 131-140, 228-230
    - with bond asymmetry, 160-164, 241-245
    - molecules, 228-245, 613-642
  - Quadrupole hyperfine structure, 131-140, 149-173, 499-521
    - asymmetric rotor, 159-164
    - intensities, 151-154, 172, 499-516
    - interpretation of coupling constants, 225-245
    - linear molecule, 150-154
    - Quadrupole hyperfine structure, second-order, 157-159, 517-521
      - symmetric top, 154-159
      - two or more nuclei, 164-173
    - Quadrupole moment, molecular, 364-366, 368
      - nuclear, 133-140, 149-173, 643-648
    - Quantum defect,  $\sigma$ , 120
    - Quenching of orbital momentum, 175  
    - $R$  branch, 99, 557-612
    - $r_e$ , 7, 12, 40-42
    - $(r^{-3})_{Av}$ , 121-123, 141, 195, 196, 217-219, 226, 228, 245
    - Racah coefficients, 167
    - Radicals, free, 174, 178, 186, 190-192, 205-207, 246, 447, 448
      - detection, 447, 448
    - Radii, covalent bonds, 237-241
    - Ray's asymmetry parameter,  $\kappa$ , 84
    - Reduced mass, 6, 306
    - Refractive index of air, 467, 468
    - Resonance, of bond types, 234, 239
      - rotational, 360-362, 366, 367
    - Resonant modulation, 279-283
    - Rotation-vibration interaction, 9-16, 25-42, 45-47, 60, 79-82, 613-642
    - Rotor, rigid, 3, 25, 50-52, 527-556
    - Rydberg constant, 116  
    - $S$ , 123, 176-179
    - $S$ , transition strength, 97-99, 557-612
    - Saturation, 371-373, 427, 428
    - Schomaker-Stevenson rule, 240, 241
    - Second-order hyperfine structure energies, 157-159, 517-521
    - Selection rules, asymmetric rotor, 92-100
      - atoms, 118, 124-126
      - diatomic molecule, 18, 21-23
      - hindered torsional motions, 331-333
      - $l$ -type doubling, 34
      - quadrupole hyperfine structure, 151-152
      - Stark effect, 250
      - symmetric rotor, 52
      - Zeeman effect, 287-289, 296
    - $\Sigma$ , 176, 177
    - $\Sigma$  states, 175, 182, 185, 189, 207-224, 246, 284
    - $\sigma$  components in Zeeman effect, 287
    - Skin depth, 378
    - Slightly asymmetric rotor, energy levels, 83-89, 522-526
    - Slip effect, electronic, 17, 213, 214, 218, 224, 291



- Spark generators, millimeter waves, 451, 452
- Spectrographs, microwave, bridge, 425–427, 429  
     choice of modulation frequency, 425  
     free radicals, 447, 448  
     gas handling, 446, 447  
     general principles, 1, 411, 412  
     high- and low-temperature, 443–445  
     high-resolution, 427–435  
     intensity and line-shape measurement, 439–441, 445, 446  
     millimeter waves, 463–465  
     modulation-frequency amplifier, 420–424  
     molecular beam, 429–434, 444, 445  
     radiometers, 448–450  
     resonant cavity, 435–443  
     source modulation, 416–418  
     Stark modulation, 264–266, 418–424, 429  
     Stark wave, 434–435  
     superheterodyne detection, 425–429  
     ultimate sensitivity, 412–416, 437  
     waveguide reflections in, 415, 417, 418, 427, 445, 446  
     Zeeman effect, 424, 441–443  
     Zeeman modulation, 424
- Spectroscopic stability, 344
- Spherical tops, 51
- Spin, nuclear, 131–133, 140, 142, 153–155, 176, 643–648
- Spin-spin interaction, 202, 203
- Spin uncoupling, 185–188
- Spin wave functions, 70, 71, 102, 103
- Square-wave modulation, 418–420
- Stabilization of oscillators, 474–485  
     by absorption lines, 477–482  
     by cavity resonator, 475–477  
     by standard oscillator, 474, 475
- Stark effect, 175, 248–283  
     almost degenerate levels, 250, 252–254  
     asymmetric rotors, 254, 255, 257, 259–261  
     first-order, 249, 253, 254, 259, 277, 278  
     fourth-order, 252  
     with hyperfine structure, 258–264  
     intensities, 255–258, 269–273  
     *l*-type doubling, 254  
     linear molecules, 248, 250–257  
     rapidly varying fields, 273–283  
     resonant modulation, 279–283  
     second-order, 249–252, 259–261, 273–277  
     selection rules, 250, 269, 270  
     symmetric rotor, 249, 253, 254, 259, 277, 278  
     with Zeeman effect, 296
- Stark modulation, 264–266, 273–283, 418–424, 464, 465, 485
- Stark waveguide cell, construction, 264–266, 441–447  
     field distribution, 264–266
- Statistical weights, 72, 73, 102–105
- Structure, asymmetric rotors, 109–114, 613–642  
     diatomic molecules, 12–14, 613–642  
     linear molecules, 29, 42, 613–642  
     symmetric rotors, 53–59, 613–642
- Surface wave transmission, 400
- Symmetric rotor, accidentally, 49, 50, 52, 92, 155  
     centrifugal distortion, 77–79  
     energy levels, 50, 51, 62, 66–69  
     frequencies of rotational transitions, 52, 67–69, 77–82  
     hindered torsional motions, 300–303, 315–324, 331–333  
     intensities and selection rules, 52, 73–77  
     matrix elements, 74  
     quadrupole hyperfine structure, 154–159, 499–521  
     Stark effect, 249, 253, 254, 259, 277, 278  
     wave functions, 60–71  
     Zeeman effect, 293, 294
- Symmetry, asymmetric rotor, 92–105  
     symmetric rotor, 62–73
- $\tau = K_{-1} - K_1$ , 84
- Temperature, of astronomical sources, 147, 148  
     effect of, on intensities, 24, 369, 370  
     on line width, 368, 369
- Transformation coefficients, 167, 168
- Transition strength, asymmetric rotor, 97–99, 557–612
- Traveling-wave tubes, 405, 406, 452–454
- $U_p$ , 239–243
- Units, attenuation, 384  
     electromagnetic, 376, 377
- Valence bond approximation, 27
- van der Waals forces, 348
- Van Vleck–Weisskopf line shape, 339–347, 418
- Vector model, 120–124
- Vibration, effect on energy levels, diatomic molecules, 5–17  
     linear molecules, 25–47  
     symmetric rotors, 79–82
- Vibration-frequencies table, 613–642



- Vibration modes, linear molecule, 26  
symmetric rotor, 79, 80
- Wave functions, asymmetric rotor, 93-96  
diatomic molecule, 4, 6  
hindered torsional motion, 318, 319  
hydrogen atom, 115-118  
inversion, 70, 303-305  
*l*-type doubling, 32  
linear molecule, 25  
spin, 70, 71, 102, 103  
symmetric rotor, 60-71
- Waveguides, 379-401, 462, 463  
attenuation, 383-385  
attenuators, 397, 401, 463  
characteristic impedance, 386-388  
cutoff wavelength, 380  
directional couplers, 394-397  
ferrite devices, 400, 401  
fields, 381-383  
guide wavelength, 380  
impedance matching, 387-389  
isolator, 401  
joints, 397, 398  
millimeter waves, 462, 463  
miscellaneous types, 399, 400  
optimum length, 414  
plungers, 399  
reflections, 386-389, 415, 417, 418, 445, 446
- Waveguides, windows, 398, 399  
Wavemeters, 391-395, 399, 466-468
- $x_e$ , diatomic molecule, 9, 11
- $Y_{ij}$ , diatomic molecule, 9-11, 15, 16
- $Z_{eff}$ , 120
- Zeeman effect, 143-145, 209-212, 284-299  
asymmetric rotor, 293-296  
atoms, 143-145  
with circular polarization, 288, 289  
with hyperfine structure, 143-145, 289, 290  
with  $\Lambda$  or  $K$  doubling, 289  
measurement, 441-443  
paramagnetic molecules, 284-290  
 $\pi$  components, 287  
selection rules, 287-289, 296  
 $^1\Sigma$  molecules, 209-212, 284, 290-296  
 $\sigma$  components, 287  
with Stark effect, 296  
symmetric rotor, 293, 294  
transitions between components, 144, 145, 296-298  
weak fields, 284-286
- Zeeman modulation, 425, 438, 485
- Zero-point vibrations, 9-18, 25-30, 33, 38, 39, 41, 44, 45, 54



